IMPERIAL INSTITUTE
OF
AGRICULTURAL RESEARCH, PUSA.

PROCEEDINGS

OF THE

ROYAL SOCIETY OF LONDON

SERIES A

CONTAINING PAPERS OF A MATHEMATICAL AND
PHYSICAL CHARACTER.

VOL. CXXXVI.

LONDON:
PRINTED FOR THE ROYAL SOCIETY AND SOLD BY
HARRISON AND SONS, LTD., ST. MARTIN'S LANE,
PRINTERS IN ORDINARY TO HIS MAJESTY.

JUNE, 1932.

LONDON:
HARRISON AND SONS, LTD., PRINTERS IN ORDINARY TO HIS MAJESTY,
ST. MARTIN'S LANE.

CONTENTS.

SERIES A. VOL. CXXXVI.

No. 829.—May 2, 1932.

PAGE

On the Influence of Hydrogen on the Pyrolysis of Ethane and Ethylene near 600°.—Part I. By M. W. Travers, F.R.S. and L. E. Hockin 1

The Band Spectrum of Nitrogen Sulphide (NS). By A. Fowler, F.R.S., and C. J. Bakker. (Plate 1) 28

Notes on the Theory of Radiation. By C. G. Darwin, F.R.S. 36

The Phenomena of Superconductivity with Alternating Currents of High Frequency. By J. C. McLennan, F.R.S., A. C. Burton, A. Pitt and J. O. Wilhelm. (Plate 2) 52

The Determination of the Heat of Dissociation of Fluorine and of the Latent Heat of Vaporisation of Lithium. By M. S. Desai. Communicated by M. N. Saha, F.R.S. 76

Crystallography of the Simpler Quinones. By W. A. Caspari. Communicated by F. G. Donnan, F.R.S. 82

On the Torsion of Cylinders of Symmetrical Section. By W. J. Duncan. Communicated by R. V. Southwell, F.R.S. 95

Quantum Analysis of the Rotational Structure of the First Positive Bands of Nitrogen (N_2). By S. M. Naudé. Communicated by A. Fowler, F.R.S. (Plates 3 and 4) 114

Mobility of Positive Alkali Ions in Argon, Neon and Helium. By A. M. Tyndall and C. F. Powell. Communicated by A. P. Chattock, F.R.S. 145

On a Determination of the Pitot-Static Tube Factor at Low Reynolds Numbers, with Special Reference to the Measurement of Low Air Speeds. By E. Ower and F. C. Johansen. Communicated by L. Bairstow, F.R.S. 153

Some Special Solutions of the Equations of Axially Symmetric Gravitational Fields. By T. Lewis. Communicated by G. A. Schott, F.R.S. 176

On the Action of Tuned Rectangular Frame Aerials when receiving Short Waves. By L. S. Palmer. Communicated by E. V. Appleton, F.R.S. 193

The Formation of Superlattices in Alloys of Iron and Aluminium. By A. J. Bradley and A. H. Jay. Communicated by W. L. Bragg, F.R.S. (Plate 5) 210

On the Nature of X-Rays. By J. A. Wasastjerna. Communicated by W. L. Bragg, F.R.S. 233

The Atomic Heat of Bismuth at Higher Temperatures. By L. G. Carpenter and T. F. Harle. Communicated by A. C. Egerton, F.R.S. 243

Dipole Moments and Molecular Structure. Part I—A simple Resonance Method for the Measurement of Dielectric Constants. By J. W. Smith. Communicated by F. G. Donnan, F.R.S. 251

a 2

PAGE

Dipole Moments and Molecular Structure. Part II.—The Trichlorides of the Elements of Group V. By J. W. Smith. Communicated by F. G. Donnan, F.R.S. 256

Theoretical Intensities in the Spectrum of H_2. By W. C. Price. Communicated by O. W. Richardson, F.R.S. 264

The Atomic Scattering Power of Iron for Various X-Ray Wave-Lengths. By A. J. Bradley and R. A. H. Hope. Communicated by W. L. Bragg, F.R.S. (Plate 6) 272

The Collision of Slow Electrons with Atoms. I.—General Theory and Elastic Collisions. By H. S. W. Massey and C. B. O. Mohr. Communicated by R. H. Fowler, F.R.S. 289

A Thyratron "Scale of Two" Automatic Counter. By C. E. Wynn-Williams. Communicated by Lord Rutherford, F.R.S. 312

Investigations with a Wilson Chamber. I.—On the Photography of Artificial Disintegration Collisions. By P. M. S. Blackett and D. S. Lees. Communicated by Lord Rutherford, F.R.S. (Plates 7 and 8) 325

Further Investigations with a Wilson Chamber. III.—The Accuracy of the Angle Determination. By P. M. S. Blackett and D. S. Lees. Communicated by Lord Rutherford, F.R.S. (Plate 9) 338

The Ranges of the α-Particles from the Radioactive Emanations and "A" Products and from Polonium. By W. B. Lewis and C. E. Wynn-Williams. Communicated by Lord Rutherford, F.R.S. 349

Studies of Gas-Solid Equilibria. Part IV.—Pressure-Concentration Equilibria between Ferric Oxide Gels and (*a*) Water, (*b*) Ethyl Alcohol, (*c*) Benzene, directly determined under Isothermal Conditions. By B. Lambert and A. G. Foster. Communicated by F. Soddy, F.R.S. 363

The Quantum Mechanics of Electrochemistry.—II. By R. W. Gurney. Appendix by R. H. Fowler, F.R.S. 378

The Association of γ-Rays with the α-Particle groups of Thorium C. By C. D. Ellis, F.R.S. 396

The γ-Rays from Actinium Emanation and their Origin. By Lord Rutherford, O.M., F.R.S., and B. V. Bowden 407

The Mechanism and Molecular Statistics of the Reaction $CuSO_4.5H_2O = CuSO_4.H_2O + 4H_2O$. By B. Topley. Communicated by F. G. Donnan, F.R.S. 413

The Artificial Production of Nuclear γ-Radiation. By H. C. Webster. Communicated by J. Chadwick, F.R.S. 428

Relativistic Quantum Mechanics. By P. A. M. Dirac, F.R.S. 453

No. 830.—June 1, 1932.

Discussion on the Structure of Atomic Nuclei. Opening Address by Lord Rutherford, F.R.S. 735

Ship Waves: their Variation with certain Systematic Changes of Form. By T. H. Havelock, F.R.S. 465

PAGE

Molecular Structure and Physical Properties of Prussic Acid. Part I.—Refractive Dispersion of Prussic Acid and its Homologues. By T. M. Lowry, F.R.S., and S. T. Henderson 471

A Note on the Theory of Rectification. By A. H. Wilson. Communicated by R. H. Fowler, F.R.S. 487

Radio Transmission Problems Treated by Phase Integral Methods. By T. L. Eckersley. Communicated by W. H. Eccles, F.R.S. 499

A Theory of Some Electron-levels in H_2. By J. K. L. MacDonald. Communicated by R. H. Fowler, F.R.S. 528

The Reproducibility and Rate of Coagulation of Stearic Acid Smokes. By H. S. Patterson and W. Cawood. Communicated by R. Whytlaw-Gray, F.R.S. 538

The Motion of Electrons in the Static Fields of Hydrogen and Helium. By J. McDougall. Communicated by R. H. Fowler, F.R.S. 549

Electron Polarisation. By G. O. Langstroth. Communicated by O. W. Richardson, F.R.S. 558

Ionic Diamagnetic Susceptibilities. By W. R. Angus. Communicated by F. G. Donnan, F.R.S. 569

The Diamagnetic Susceptibilities of some Beryllium Compounds. By W. R. Angus and J. Farquharson. Communicated by F. G. Donnan, F.R.S. 579

Fine Structure in the Arc Spectra of Bromine and Iodine. By S. Tolansky. Communicated by O. W. Richardson, F.R.S. (Plate 10) 585

The Anomalous Scattering of α-Particles by Hydrogen and Helium. By H. M. Taylor. Communicated by R. H. Fowler, F.R.S. 605

Experiments with High Velocity Positive Ions. (i) Further Developments in the method of obtaining High Velocity Positive Ions. By J. D. Cockcroft and E. T. S. Walton. Communicated by Lord Rutherford, F.R.S. (Plate 11)........ 619

On some Close Collisions of Fast β-Particles with Electrons, Photographed by the Expansion Method. By F. C. Champion. Communicated by Lord Rutherford, F.R.S. (Plates 12 and 13) 630

On the Polarisation of Electrons by Scattering. By E. G. Dymond. Communicated by Lord Rutherford, F.R.S. 638

On the Photographic Action of Slow Electrons. By R. Whiddington, F.R.S., and J. E. Taylor. (Plate 14) 651

The Nature of the Interaction between Gamma-Radiation and the Atomic Nucleus. By L. H. Gray and G. T. P. Tarrant. Communicated by Lord Rutherford, F.R.S. 662

The Existence of a Neutron. By J. Chadwick, F.R.S. 692

The Collisions of Neutrons with Nitrogen Nuclei. By N. Feather. Communicated by J. Chadwick, F.R.S. (Plates 15 and 16) 709

Attempts to Detect the Interaction of Neutrons with Electrons. By P. I. Dee. Communicated by J. Chadwick, F.R.S. (Plates 17–19) 727

Index 763

PROCEEDINGS OF
THE ROYAL SOCIETY.

Section A.—Mathematical and Physical Sciences.

On the Influence of Hydrogen on the Pyrolysis of Ethane and Ethylene near 600°.—*Part* I.

By Morris W. Travers, F.R.S., and L. E. Hockin, B.Sc.

(Received January 12, 1932.)

I. *Introduction.*

It is well known that when ethane is heated to the neighbourhood of 600° in silica apparatus, the equilibrium represented by the equation

$$C_2H_6 \rightleftharpoons C_2H_4 + H_2,$$

is approached very rapidly. We have confirmed this result, and have obtained accurate values for the equilibrium constant at 590° and 610°. As we shall show presently, this reaction is accompanied by other reactions which involve the condensation of both ethane and ethylene independently, with formation of methane and of a product which is mainly benzene, though we are not actually interested in the final product. It appears that though hydrogen takes part in only the ethane-ethylene-hydrogen reaction, it has indirectly a profound influence on the rates at which the other reactions take place. Further, it seems that the silica surface does not act as a catalyst, though, again, the fact that the reaction vessels are of silica, and the pretreatment to which they are subjected, has great influence in determining the course of the reactions. This investigation has been carried out with the object of studying the kinetics of these reactions.

II. *Method of Investigation.*

Now, mainly on account of the complex character of the reactions, and also on account of the fact that hydrocarbons are formed which readily condense, it was not possible to adopt the method of measuring the changes of pressure of the gas at constant volume, which is commonly employed for following the course of gaseous reactions. Our method involved the heating of definite quantities of the pure gases in sealed silica tubes to a definite temperature, for varying periods, and making a complete analysis of the contents of each tube.

The gas analyses involved the determination of hydrogen, methane, ethane, ethylene, and the higher hydrocarbons together as condensate. Investigation showed that the quantities of acetylene and three-carbon hydrocarbons produced were negligible. As it was not convenient to use tubes of over 45 c.c. capacity, the pressures employed were higher than usual. Most of the experiments were carried out at 0·025 gram mols. of the gas, corresponding to 0·05 gram atoms of carbon per litre, the pressure at 590° being close to 2 atmospheres. The advantages of working at low pressures have been discussed from the theoretical standpoint by others, and cannot be overlooked. As will appear later, however, simplification may be misleading, and only an elaborate investigation can bring out such facts as we have to put forward.

The ethane was obtained from zinc diethyl, by enclosing a 1-gram tube in a sheath of copper foil, and crushing it under water below a bell jar. The gas was treated with bromine till brown, and then with caustic potash; it was then purified by condensation in a bulb cooled in liquid air, and finally subjected to fractional distillation from a bulb cooled with solid CO_2 and alcohol. The gas was redistilled shortly before use, and the ethane recovered from individual experiments was discarded, and was not used for further work.

The reaction tubes were made from clear silica glass tubing of 20 mm. internal diameter, a 30-cm. length making two tubes. Stems of thick-walled silica tubing, of about 3 mm. internal diameter, were sealed to them, fig. 1, and drawn down to capillary dimensions for sealing after filling with the gas. The stem, including the capillary, which was replaced after each experiment, was altogether 20 mm. long, and was formed near the open end into a bulb, which was packed with silk fabric, to prevent fragments of rubber from the connecting tube to the filling apparatus, or other foreign matter, from entering the reaction tube.

The filling apparatus, fig. 2, needs little description. The reaction tube was attached at A. B led to a Töpler pump through a drying tube containing P_2O_5. After exhausting, the cock C was turned so as to fill the capillary tube above it with mercury. A measured quantity of gas was then admitted through the syphon E, and completely condensed in the reaction tube, which was cooled with liquid air. If hydrogen was also introduced, after admitting the ethane and condensing it, hydrogen was admitted, and then mercury was allowed to enter through the cock F and to rise to a mark on the apparatus just below the bulb D, which was filled with silver and gold leaf, to retain traces of mercury.

The pretreatment of the reaction tubes will be dealt with later.

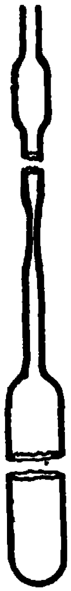

Fig. 1.

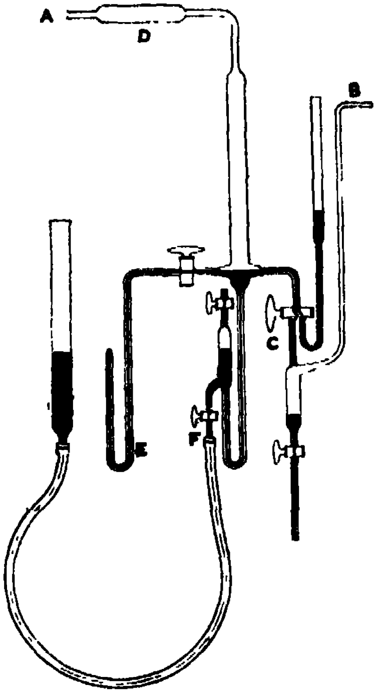

Fig. 2.

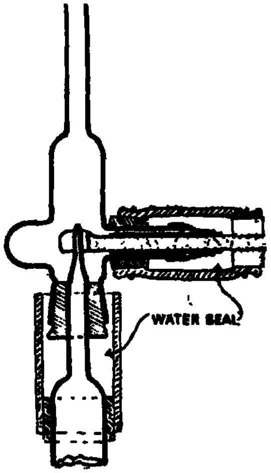

Fig. 3.

It is usual to remove the contents of such reaction tubes by breaking the point inside a piece of thick-walled rubber tubing, but this method often leads to loss of the gas, through puncturing of the rubber tubing, and may also involve the contamination of the reaction tube with traces of rubber. The apparatus shown in fig. 3 was used in our experiments with hardly a single failure. The stem of the reaction tube passed through the rubber stopper so that the point could be broken off by the steel fork, shown in section, which was operated from without the apparatus. Entry of air was prevented by water seals.

The investigation called for accuracy in analysis unattainable by ordinary methods. In the first place the contents of the tube were separated into three *fractions, by cooling the tube with liquid air, breaking off the point,* pumping off and collecting the gas given off, then changing the liquid air for solid CO_2 and alcohol, and pumping off and collecting a second fraction of gas. The condensate remained in the tube. By again condensing the second fraction in liquid air, exhausting, repeating the process a second time, and adding the small quantity of gas removed to the first fraction, very complete separation of the gaseous product into fractions containing methane and hydrogen, and ethane and ethylene, respectively, was accomplished. The method of analysis was that worked out in this laboratory, and described by Broom.* All volume measurements were made with dry gas. Hydrogen and methane were separated by oxidation of the hydrogen by copper oxide at 290°, and measuring the volume of the dry gas before and after treatment. The determination of the ethylene involved the treatment of the gas over mercury with a drop of water, and then with a drop of bromine, so that the gas became brown. A few drops of strong potash solution were then introduced. The residual ethane was allowed to pass into the Töpler pump through a U-tube cooled in solid CO_2 and alcohol, to condense vapour of ethylene dibromide, which would pass through a tube containing P_2O_5, and make the apparent volume of the ethane too large. In conducting this analysis it was important to boil out the liquid in the reaction apparatus after removing the ethane and before introducing the ethane-ethylene mixture. When very accurate results were required, the methane or the ethane was burned completely to CO_2 by introducing the gas into a silica tube containing copper oxide heated to about 500°, and determining the quantity of CO_2 exactly. In this way it was possible to prove that no other gas than methane or ethane was present in the gas under examination.

The tube furnace consisted of a block of Hadfield's H.R. Era steel, 300 mm. long and 100 mm. diameter, with three holes of 3·5 cm. diameter drilled symmetrically through its length, and a hole of 10 mm. diameter through the axis. The cylinder was covered with a layer of asbestos, and was wound with 22 gauge nichrome wire. In the central tube was an auxiliary heater for adjusting temperature, consisting of a length of 24 gauge nichrome wire passing backwards and forwards through small-bore silica tubing. The furnace was insulated with Moler diatomite bricks, and was shielded from draughts. The power was supplied from a motor-generator set, with a contant voltage regulator. Temperatures were measured by a platinum platinum-rhodium thermocouple, with a Cambridge Instrument Company's indicator, and could be kept constant to within 1 degree for any length of time by operating the fine adjustment by hand occasionally.

---

* 'J. Soc. Chem. Ind.,' vol. 47, T., p. 276 (1928).

III. *Experiments with Ethane. Series I.*

We did not expect to encounter any difficulty in obtaining results which would, at least, be reproducible, but our first experiments entirely disillusioned us. Using a single reaction tube, treating it in a manner which was apparently identical, after burning out the residue from the previous experiment, and sealing on a new stem, filling it with the same gas and heating it for the same period, the analysis of the products showed that the course of the reaction was rarely closely similar in different experiments, and often widely different. Every possible method of pretreating the tubes was tried. In different series, the tubes were preheated for different times and to different temperatures. In other series, special methods were used for drying out the tubes before admitting the gas. Every care was taken to prevent the admission of solid impurities, or of mercury vapour. We may say that the results of some series of experiments showed such regularity that we were inclined to accept them as having a definite significance, but the results of different series differed so markedly that we were forced to the conclusion that the apparent regularity was entirely fortuitous.

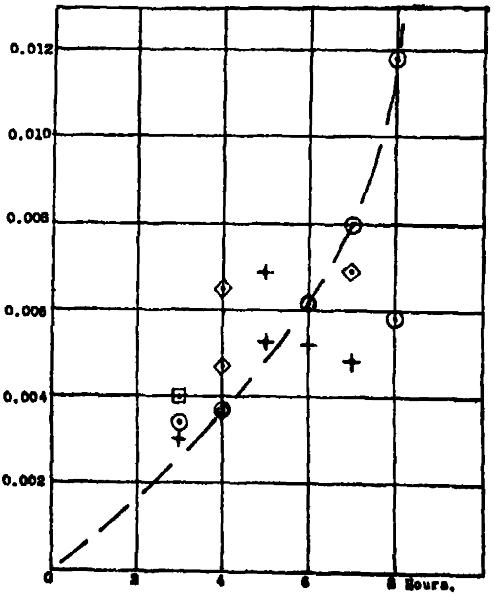

Fig. 4.—Formation of condensate in tubes 11, 12, 14 and 15.

The nature of the irregularities to which we have referred is indicated by fig. 4, which represents the rates of formation of condensate, which is found to give the clearest indication of the course followed by the reaction, determined with four different reaction tubes.

While carrying on experiments with the simple type of reaction tube which we have described, other experiments were carried out in which tubes containing two or three test-tube-like inner tubes of silica glass were used. It was thus possible to increase the area of silica glass of identical character in contact with the gas. Several of these "large-surface" tubes were made. With one of these tubes (LSB) series of results at 0·01 and 0·025 gram molecules per litre of ethane were carried out. The results are set down in Table I, and in the graphs in fig. 5.

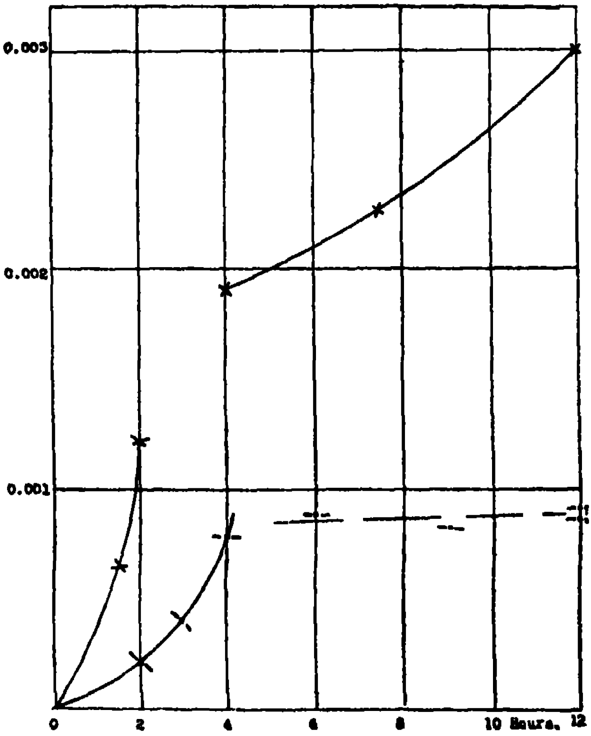

Fig. 5.—Formation of condensate in large-surface tubes.
(Initial concentration 0·025 —·—, 1/10 scale.)

In all the experiments carried out with these large-surface tubes the same sharp break in the graphs (fig. 5) representing the rate of formation of condensate is found, and in graphs representing the rate of disappearance of ethane or the rate of formation of methane, the same change of rate is indicated. Another fact which is of importance is that the rate of formation of condensate obtained with different large surface tubes was always nearly the same, and represented, generally, the lower limiting values of the erratic results obtained with the simple tubes.

Table I.

(Contents of tube in gram atoms C or H per litre.)

Time, hours.	C_2H_6.	C_2H_4.	H_2.	CH_4.	Condensate.
Tube LSB. $t = 590°$. Initial concentration of ethane 0·01 gm. mol./litre.					
1½	0·01556	0·00294	0·00296	0·00075	0·00065
2	0·01484	0·00226	0·00316	0·00129	0·00121
4	0·01386	0·00228	0·00362	0·00196	0·00190
7½	0·01238	0·00212	0·00322	0·00323	0·00227
12	0·01016	0·00192	0·00338	0·00492	0·00300
Tube LSB. $t = 590°$. Initial concentration of ethane 0·025 gm. mol./litre.					
2	0·03918	0·00480	0·00440	0·00487	0·00215
3	0·03472	0·00396	0·00490	0·00704	0·00428
4	0·02474	0·00302	0·00441	0·01433	0·00791
6	0·02436	0·00248	0·00472	0·01424	0·00890
9	0·02206	0·00238	0·00468	0·01725	0·00831
12	0·02196	0·00208	0·00498	0·01723	0·00863
12	0·02094	0·00222	0·00508	0·01764	0·00920

Certain other facts may also be referred to now. When a number of experiments had been carried out with a particular tube, and variable results had been obtained for the rate of formation of condensate and of hydrogen for identical time periods, it was found that the quantity of condensate varied in inverse proportion to the quantity of hydrogen in the tube.

The observation which led us finally to the solution of the difficulty arising out of the impossibility of obtaining reproducible results with the plain reaction tubes was a curious one. After some 500 experiments, the results of which are not recorded, had been carried out, a fresh series were started with reaction tubes made from a new consignment of silica tubing. The results were more erratic than ever, and the only difference in the tubing was that it was thinner than usual. Reviewing the previous results, it became clear that the variation in the results, and particularly in the extent to which the rates of reaction were generally above the lower limits obtained with the large-surface tubes, was in same way connected with the thickness of the silica. The thick tubes gave less erratic results than the thin tubes. We knew that hydrogen had a considerable influence on the course of this reaction, and also that it diffused into and through silica at 600°; so that though the loss in our experiments was insufficient to interfere with quantitative relationships, there must clearly be some connection between this phenomenon and the peculiar results which we had observed. We determined therefore to try the effect of protecting the outside of the tube by an outer tube, the space between the two tubes being filled with hydrogen; our idea at that time being to make sure that the material of the silica was saturated with hydrogen. In the meantime, we undertook some experiments in which a reaction tube with walls about 4 mm. thick was used, and which was heated, while full of hydrogen, to 600° for 15 hours (overnight) before each experiment.

We had in our minds the fact that we were dealing with chain reactions, which were in some way initiated by hydrogen atoms, produced either in or on the walls of the tube. The suggestion that hydrogen adsorbed on the walls of a silica tube is dissociated to a greater extent than the hydrogen in the gaseous phase has been made very frequently, but it seemed to be thermodynamically impossible that the effect produced in or on the solid phase could in any way influence the concentration of the hydrogen atoms in the gaseous phase. Some source of the activation energy must be postulated.

Now both hydrogen and oxygen diffuse through the walls of a silica tube at high temperatures, the former rapidly, the latter slowly. The walls of silica tube exposed to the air outside, and to an atmosphere of hydrogen inside, must be a region in which the gases can come into contact and react. Some reaction between the oxygen and the hydrogen molecules may be supposed to provide the energy of formation of hydrogen atoms, which pass into the atmosphere inside the tube, and can exist there for a measurable period of time. Whether the process of activation takes place on the inner surface, or in the body of the wall of the tube cannot be discussed now. The quantity of hydrogen disappearing in this process need be relatively very small, compared to the quantity of the products formed in the chain reactions initiated in this way, so that it would not affect the stoichiometric relationships as determined by the analyses. We may also point out here that it is probable that the reactions so initiated are not identical with those arising in absence of the disturbing influences now being discussed.

IV. *Experiments with Ethane. Series II.*

For these experiments two reaction tubes were made from the same piece of silica glass tubing, with walls of 4 mm. thick. One of these thick-walled tubes, TWA, was heated to 600° while full of air, and was then exhausted, cooled, and filled with ethane as usual. The other was heated to 600° for about 15 hours (overnight) while full of hydrogen, and was then exhausted, cooled, and filled with ethane. After each experiment, the tube was burned out as usual, by heating it in the furnace to 600° for about an hour, and then the routine was repeated as above. The results of the experiments are set down in Table II, and are represented by the graphs in figs. 6 and 7.

Table II.—$t = 590°$. Initial concentration of ethane 0·025 gm. mol./litre. Contents of tubes in gram atoms C or H per litre.

Serial.	Time, hours.	C_2H_6.	C_2H_4.	H_2.	CH_4.	Condensate.
		Tube TWB pretreated with hydrogen.				
8	½	0·04418	0·00416	0·00466	0·00095	0·00071
5	1	4176	452	542	221	151
6	2	3738	354	596	543	364
4	3	3278	334	544	846	542
7	4	3154	316	599	954	576
12	4	3266	322	602	886	526
9	5	3016	286	584	1075	623
1	5	3206	308	572	922	564
3	6½	2880	262	594	1194	684
11	6½	2822	312	578	1212	654
2	8	2606	282	620	1350	762
		Tube TWA not pretreated with hydrogen.				
3	3	0·03524	0·00386	0·00576	0·00704	0·00386
8	4	3278	332	614	927	463
1	5	2860	290	582	1207	643
7	6½	2178	298	520	1656	868
2	8	—	—	598	1408	—
5	8	2402	300	552	1511	787
6	8	2250	240	534	1634	876

It will be observed that the graphs representing the rates of reaction in the tube which was pretreated with hydrogen bear a marked similarity to those representing the rates of reaction in the large-surface tubes, fig. 5. In this case also the concentration of the hydrogen appears to attain a maximum, and then to remain sensibly constant. The results obtained with the tube which had not been pretreated with hydrogen may be described as *erratic*, but not to the same results as those obtained generally with the thin-walled tubes, fig. 4.

Experiments were then carried out at 570° and at 610°, and the results as set down in Table III.

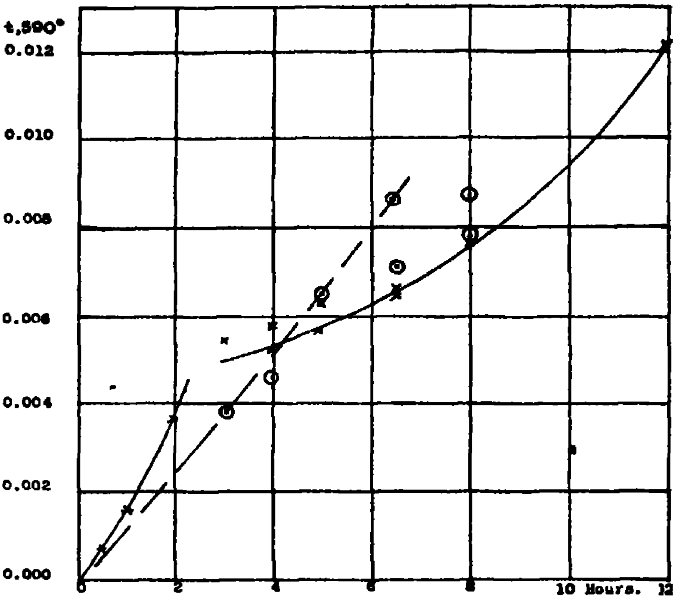

FIG. 6.—Formation of condensate in reactubes A and B.

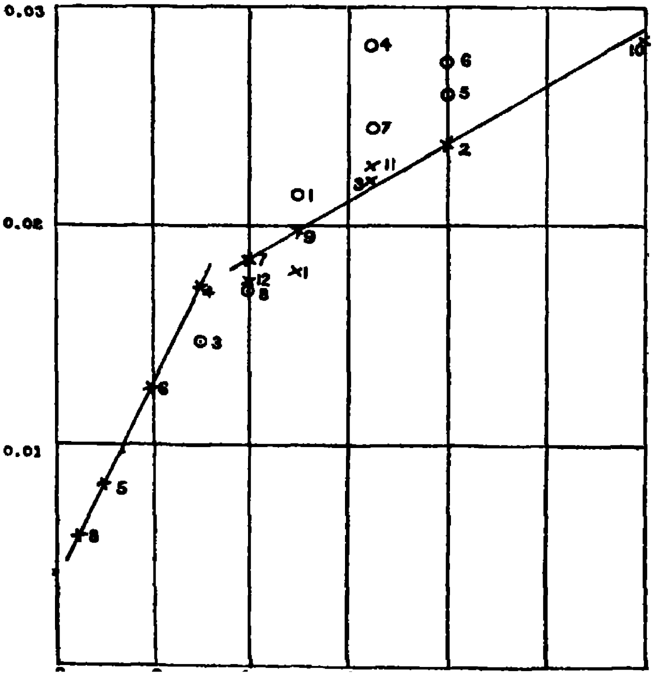

FIG. 7.—Disappearance of ethane. Tube A = ⊙; Tube B = ×.

Table III.—Tube TWB. Initial concentration of ethane 0·025 gm. mol./litre. Contents of tube in gram atoms C or H per litre.

Serial.	Time, hours.	C_2H_6.	C_2H_4.	H_2.	CH_4.	Condensate.
			Temperature 570°.			
15	1	0·04566	0·00338	0·00370	0·00068	0·00028
16	1½	0·04802		0·00428	0·00115	0·00083
17	2	0·04292	0·00354	0·00444	0·00188	0·00166
13	4	0·04020	0·00356	0·00486	0·00377	0·00243
14	6	0·03676	0 00304	0·00474	0·00660	0·00360
			Temperature 610°.			
18	1	0·03588	0·00472	0·00626	0·00614	0·00325
19	2	0·02744	0·00398	0·00687	0·01165	0·00693
20	4	0·01454	0·00246	0·00538	0·02193	0·01107
21	6	0·01432	0·00214	0·00628	0·02196	0·01158

It was noticed that in successive later experiments, not now recorded, the tube appeared to continue to take up considerable quantities of hydrogen, but no measurements were made of the volumes absorbed. This may account for the fact that when a thick-walled reaction tube has been in use for some time it requires somewhat drastic treatment before it is possible to obtain what we have termed *erratic* results with it.

In concluding this section of the work, two further experiments were carried out. A piece of the thin-walled silica tubing, from which reaction tubes had been made which gave erratic results, was enclosed in an outer silica tube, through which the capillary stem passed, so that it could be filled with ethane as usual. The space between the tubes was filled with hydrogen, and the tube was subjected to the 15-hour preheating with hydrogen before filling with ethane. Also, one of the large-surface tubes already described was pretreated with hydrogen before filling with ethane.

The results of these experiments, given in Table IV, indicate that the rate of the reaction is only very slightly greater in the case of the large-surface tube, and the double-walled tube, than in the case of the thick-walled tube, but the difference is so small as to be attributable to experimental error, arising from the cooling of the furnace when the thick-walled tube is introduced. We believe that the effect of increase in surface is actually negligible. Since the inner linings of the large-surface tube were

Table IV.—$t = 590°$. Initial concentration of ethane 0·025 gm. mol./litre.

Serial.	Time, hours.	C_2H_6.	C_2H_4.	H_2.	CH_4.	Condensate.
Double-walled reaction tube with hydrogen in space between tubes.						
1	2	0·03458	0·00410	0·00560	0·00682	0·00410
2	3½	0·03104	0·00338	0·00622	0·00986	0·00572
3	5	0·02988	0·00290	0·00566	0·01506	0·00666
Large-surface tube pretreated with hydrogen.						
1	1½	0·03834	0·00442	0·00574	0·00427	0·00297
2	2	0·03586	0·00410	0·00600	0·00613	0·00391
3	5	0·02866	0·00324	0·00616	0·01145	0·00665

not more than 3 or 4 mm. apart when the tube lay in the furnace, the effect of dimensions, within these limits, must also be negligible. We shall discuss the results of these experiments with ethane and offer an explanation of them later (p. 24).

V. *Experiments with Equilibrium Mixtures of Ethane-Ethylene-Hydrogen.*

Our experiments having failed to lead to any satisfactory explanation of the peculiar breaks in the graphs, we decided to attempt to simplify the chemical aspect of the problem by starting with mixtures of ethane, ethylene, and hydrogen, corresponding to equilibrium conditions at 590°. The value of the ratio $P_{C_2H_4} \times P_{H_2}/P_{C_2H_6}$ (atmospheres) was found from the mean of a large number of observations, mainly from the ethane side, to be 0·0235, and this number was used in calculating the composition of the equilibrium mixtures. Later, it appeared more probable that the true value was 0·0245 (p. 23), but the error in this connection is unimportant. Mixtures of ethane and ethylene, sufficient for a number of experiments, were made up in exactly known proportions. A volume corresponding to 0·025 gram molecule per litre in the reaction tube was measured out (except in Series V, when half the quantity was used), and condensed in the reaction tube; tube TWB was used throughout. A quantity of hydrogen, in such excess of the quantity corresponding to the equilibrium mixture as would make proper allowance for the gas in the stem and dead space, was then introduced, and the bulb was sealed, the gas remaining in the stem being pumped off and measured, so that the exact quantity of gas in the reaction tube was known. The experiments were not easy to carry out. The subsequent treatment of the tube was as usual. The results are set down in Table V.

Table V.—Experiments with Equilibrium Mixtures.

Time, hours.	C_2H_6 fd.	C_2H_4 fd.	CH_4.	H_2 *t*.	H_2 fd.	Condensate.
Series I. C_2H_6 *t* 0·04626 ; C_2H_4 *t* 0·00374.						
1	0·04302	0·00370	0·00238	0·00826	0·00758	0·00090
2	0·04116	0·00324	0 00407	0·00808	0·00744	0·00153
Series II. C_2H_6 *t* 0·04550 ; C_2H_4 *t* 0·00450.						
1	0·04146	0·00410	0·00304	0·00672	0·00680	0·00140
1½	0·04024	0 00398	0·00384	0·00676	0·00656	0·00194
2	0·03976	0·00376	0·00424	0·00678	0·00676	0·00224
3	0·03620	0·00352	—	0·00680	—	—
3½	0·03418	0 00352	0·00783	0·00676	0·00702	0·00427
4	0·03240	0·00342	0·00923	0·00678	0·00688	0·00445
Series III. C_2H_6 *t* 0·04456 ; C_2H_4 *t* 0·00544 (C_2H_4 equal to H_2).						
¾	0·04180	0·00472	0·00194	0·00536	0·00562	0·00157
1	0·04056	0·00464	0·00276	0·00540	0·00572	0·00204
1½	0·03780	0·00448	0 00453	—	0·00584	0·00319
3	0·03350	0·00380	0·00786	0·00538	0·00596	0·00484
4	0·03152	0·00358	0·00921	0·00550	0·00616	0·00569
5¾	0·02688	0·00306	0·01274	0·00542	0·00588	0·00732
Series IV. C_2H_6 *t* 0·04326 ; C_2H_4 *t* 0·00674.						
1	0·03898	0·00524	0·00298	0·00440	0·00512	0·00280
2	0·03558	0·00452	0·00551	0·00452	0·00572	0·00439
4½	0·02954	0·00372	0·00996	0 00446	0·00594	0·00678
Series V. C_2H_6 *t* 0·02124 ; C_2H_4 *t* 0·00376.						
1	0·02006	0·00324	0·00094	0·00378	0·00390	0·00076
2	0·01890	0·00298	0·00177	0·00388	0·00406	0·00135
3	0·01716	0·00270	0·00317	0·00380	0·00432	0·00197
4	0·01636*	0·00258*	0·00367	0·00384	0·00432	0·00239
5	0·01550	0·00240	0·00431	0·00386	0·00438	0·00279
Series VI. C_2H_6 *t* 0·04175 ; C_2H_4 *t* 0·00825.						
1	0·03798	0·00532	0·00316	—	0·00444	0·00354
2	0·03448	0·00424	0·00579	0·00350	0·00532	0·00549
3½	0·02978	0·00358	0·00923	0·00352	0·00540	0·00741

* Calculated from $C_2H_6 + C_2H_4$ and equilibrium constant.

If we now make the assumption, which the whole of our experiments appear to justify fully, that the hydrogen enters directly only into the reaction represented by the equation,

$$C_2H_6 \rightleftharpoons C_2H_4 + H_2,$$

it is possible to make the following analysis of the process :—

(i) (H_2 found − H_2 taken) = ΔH_2 = quantity of ethylene formed from ethane during the reaction period.

(ii) (C_2H_4 taken − C_2H_4 found) = ΔC_2H_4.

(iii) $\Delta H_2 + \Delta C_2H_4$ = total ethylene converted into condensate, or into condensate and methane.

The total condensate formed from the ethane and ethylene is determined from the results of the primary analyses. If we subtract from the values of the total condensate the corresponding sum of $\Delta H_2 + \Delta C_2H_4$, we should, on the assumption that the total carbon in the ethylene which has disappeared appears as carbon in the condensate, obtain values representing condensate formed direct from ethane. This involves a further assumption that, when the ethylene forms condensate, the hydrogen goes to form methane through some secondary reaction involving ethane, and possibly involving at the same time the utilisation of the energy of the primary process, and the ending of a chain. There is no chemical evidence for accepting the first of the two alternatives put forward under (iii), but if we adopt it we seem to be led to a set of conclusions which are simpler than those resulting from the adoption of the alternative, that part of the ethylene goes to benzene, and part to methane, though we have evidence that this does take place when pure ethylene undergoes condensation.

Assuming then that the whole of the carbon in the ethylene which disappears appears as carbon in the condensate, and knowing from the primary analyses the rate of formation of total condensate, we obtain the rate of formation of condensate from the ethane directly. As the graphs in figs. 8 to 11 show, the rate of formation of condensate from ethane is represented by a straight line. This may, of course, be purely fortuitous, and of such misleading relationships we have good reason to beware. We do not believe that it really indicates that the process which it represents is a simple one, and certainly it does not suggest that the adsorption has anything whatever to do with it.

In figs. 8 to 12, the graphs represent: A, the formation of hydrogen or ethylene from ethane; B, the disappearance of ethylene as condensate; C, the formation of total condensate; D, the formation of condensate from ethylene; and E, the formation of condensate from ethane. In dealing with the experimental results we shall, for convenience, use the expressions (H_2), (C_2H_4), etc., to represent concentrations in gram atoms carbon or hydrogen per litre, and reckon time in hours. We shall use the terms ΔH_2, ΔC_2H_4 as above; and C_{total}, C_{ethane}, $C_{ethylene}$, are used to represent quantities of condensate in gram atoms carbon per litre. The rates of reaction have been determined graphically from the curves, no alternative method being, under the circumstances, possible.

Why we have calculated the values of the function $(dC_{ethylene}/dt)/(C_2H_4)^4$ will be explained later.

Series I.—It is somewhat unfortunate that we have first to refer to these results, for we are here entering into a region where the rate of formation of condensate from ethylene becomes negligible, and the rate of formation of condensate from ethane decreases, while another reaction also sets in, which yields methane as a sole product. From the experimental results we find that after 2 hours the change in the hydrogen concentration is —0·00064, and the change in the ethylene concentration is —0·00050, which almost exactly compensate one another. We can assume then that $dC_{ethylene}/dt$ is zero, or nearly so, and that the values of C_{total} and C_{ethane} are identical, the value of

$$dC_{ethane}/dt = 0{\cdot}0008$$

in gram-molecule-litre-hours.

Series II.—The following data are derived directly from the experimental results:—

Table VI.

Time (hours):	1.	1½.	2.	3.	3½.	4.
ΔH_2	0·00008	—0·00020	0·00008	—	0·00026	0·00010
ΔC_2H_4	0·00040	0·00052	0·00074	0·00098	0·00098	0·00108
$C_{ethylene}$	0·00048	0·00032	0·00074	0·00098	0·00098	0·00118
C_{total}	0·00140	0·00194	0·00224	—	0·00447	0·00495
C_{ethane}	0·00092	0·00162	0·00142	—	0·00323	0·00377

Now though the value of C_{total} is the difference between the total ethane and ethylene taken, and the sum of the products of analysis, the errors generally average out, so that the experimental points lie on a continuous curve. If we now assume that the graph of the rate of formation of C_{ethane} is a straight line, we can obtain smoothed interpolated values of C_{ethylene}, and use these for plotting the graph from which the rate dC_{ethylene}/dt is obtained. The following are the smoothed results :—

Table VII.

Time (hours) :	1.	1½.	2.	2½.	3.	4.
C_{total}	0·00140	0·00205	0·00268	0·00328	0·00386	0·00498
C_{ethane}	0·00092	0·00140	0·00188	0·00234	0·00282	0·00376
C_{ethylene}	0·00048	0·00065	0·00080	0·00094	0·00104	0·00123
$(dC_{\text{ethylene}}/dt) \times 10^4$	3·95	—	2·78	—	2·02	—
$(dC_{\text{ethylene}}/dt) \times 10^{-4}/(C_2H_4)^4$	1·40	-	1·40	—	1·29	--
$(aC_{\text{ethane}}/dt)d \times 10^4 = 9{\cdot}4$	—	—	—	--	---	—

The data are represented by the graphs in fig. 8.

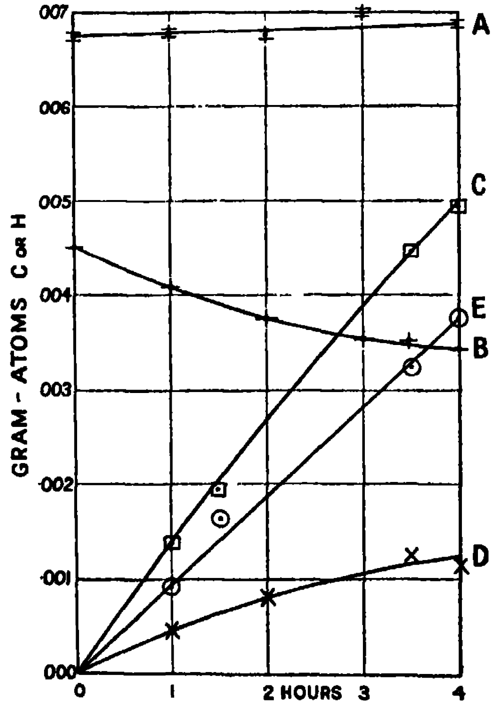

Fig. 8.—Equilibrium Mixture II.

Series III.—In this case the data were more numerous, and the following calculations are based upon the experimental results directly :—

Table VIII.

Time (hours) :	¾.	1.	1½.	3.	4.	5¾.
ΔH_2	0 00026	0·00032	0·00042	0·00058	0·00066	0·00046
ΔC_2H_4	0·00072	0·00080	0·00096	0·00164	0·00186	0·00238
$C_{ethylene}$	0·00098	0·00112	0·00138	0·00222	0·00252	0·00284
C_{total}	0·00157	0·00204	0 00319	0·00484	0·00569	0·00732
C_{ethane}	0·00059	0 00092	0·00181	0·00262	0·00317	0·00448
$(dC_{ethylene}/dt) \times 10^4$	—	6·6	5·8	4·1	2·85	—
H_2	—	0·00573	0·00584	0·00595	0·00595	—
C_2H_4	—	0·00464	0·00440	0·00380	0·00350	—
$(dC_{ethylene}/dt) \times 10^{-6}/(C_2H_4)^4$		1·42	1 60	1·96	1·90	-
$(dC_{ethane}/dt) \times 10^4 — 7·8$	—	-	—	—	—	·

The results are represented by the graphs in fig. 9.

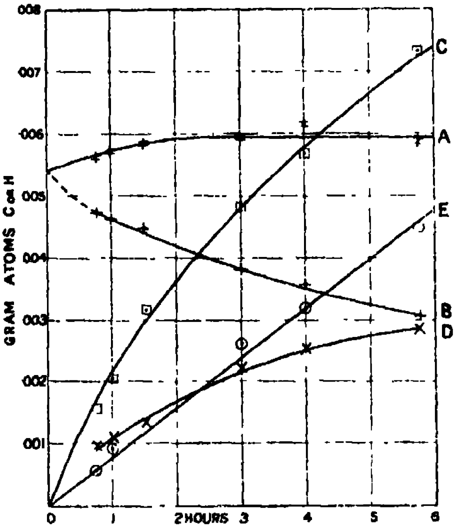

Fig. 9.—Equilibrium Mixture III.

Series IV.—The experimental results were dealt with in the same manner as those in Series II. The following is the analysis of the actual experimental data :—

Table IX.

Time (hours) :	1.	2.	4½.
ΔH_2	0·00072	0·00120	0·00594
ΔC_2H_4	0·00150	0·00222	0·00302
$C_{ethylene}$	0·00222	0·00342	0·00450
C_{total}	0·00280	0·00439	0·00678
C_{ethane}	0·00058	0·00087	0·00228

The following are the smoothed results :—

Table X.

Time (hours) :	1.	2.	3.	4.
C_{ethane} .	0·00050	0·00100	0·00150	0·00200
C_{total} .	0·00280	0·00439	0·00555	0·00645
$C_{ethylene}$.	0·00230	0·00339	0·00405	0·00445
(H_2) .	0·00512	0·00572	0·00590	—
(C_2H_4) .	0·00525	0·00454	0·00408	—
$(dC_{ethylene}/dt) \times 10^4$.	14·5	8·7	4·8	—
$(dC_{ethylene}/dt) \times 10^{-6}/(C_2H_4)^4$	1·93	2·05	1·64	—
$(dC_{ethane}/dt) \times 10^4 = 5{\cdot}0$.	—	—	—	—

The results are represented by the graphs in fig. 10.

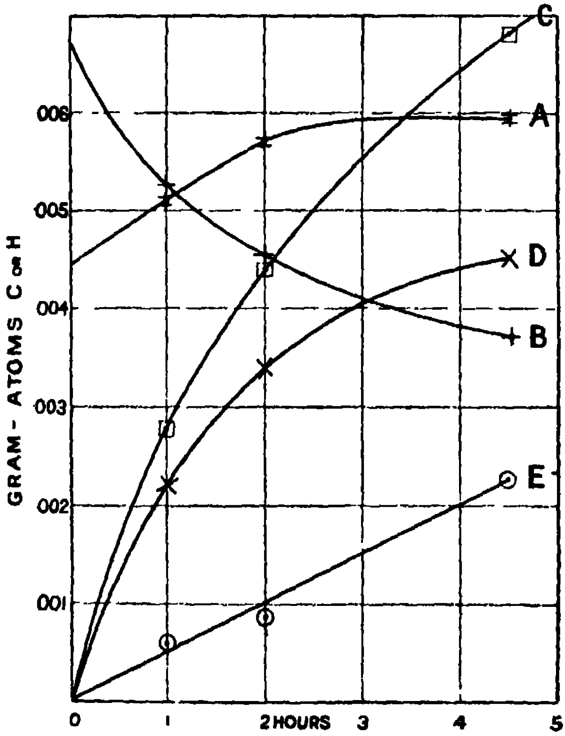

Fig. 10.—Equilibrium Mixture IV.

Series V.—In this series alone the initial concentration of the ethane-ethylene mixture was 0·0125 gram molecules per litre, or one-half of the concentration in the other series. It will be seen later, fig. 13, that the rates of formation of condensate from ethane and from ethylene fall into line with the observed rates in the other series.

The results were treated in the same manner as those of the Series II and IV.

Table XI.

Time (hours):	1.	2.	3.	4.	5.
ΔH_2	0·00012	0·00018	0·00052	0·00048	0·00052
ΔC_2H_4	0·00052	0·00078	0·00106	0·00118	0·00136
Cethylene	0·00064	0·00096	0·00158	0·00166	0·00188
Ctotal . .	0·00076	0·00135	0·00197	0·00239	0·00279
Cethane	0·00012	0·00039	0·00039	0·00073	0·00091

The following are the smoothed results :—

Table XII.

Time (hours) :	1.	2.	3.	4.	5
Cethane	0·00018	0·00037	0·00055	0·00073	0·00091
Ctotal	0·00076	0·00138	0·00191	0·00238	0·00279
Cethylene	0·00058	0·00101	0·00136	0·00165	0·00188
$(d\text{C}_{\text{ethylene}}/dt) \times 10^4$. . .	4·80	3·82	3·07	2·57	—
C_2H_4	0·00330	0·00295	0·00270	0·00250	0·00240
H_2	0·00395	0·00405	0·00415	0·00430	0·00440
$(d\text{C}_{\text{ethylene}}/dt) \times 10^{-6}/(C_2H_4)^4$	4·05	3·1	5·8	6·6	—
$(d\text{C}_{\text{ethane}}/dt) \times 10^4 = 4·8$	—	—	—	—	—

The results are represented by the graphs in fig. 11.

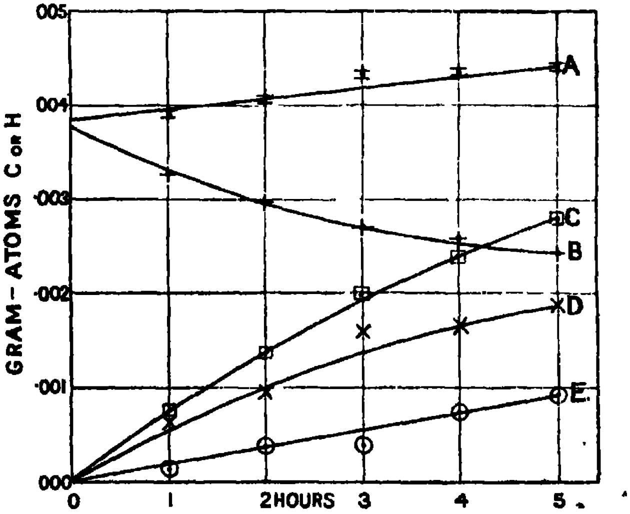

FIG. 11.—Equilibrium Mixture V.

Series VI.—It seems that in this region the conditions are such that condensate is no longer formed from the ethane direct, but only from the ethylene.

Table XIII.

Time (hours):	1.	2.	$3\frac{1}{2}$.
ΔH_2	0·00094	0·00182	0·00192
ΔC_2H_4	0·00293	0·00588	0·00659
C_{ethylene}	0·00387	0·00583	0·00659
C_{total}	0·00354	0·00549	0·00741

It will be seen that the sum of ΔH_2 and ΔC_2H_4 is, for the two shorter time periods, greater than the amount of the total condensate. As the rapid increase in the hydrogen concentration in this region is materially affecting the course of the reaction as it proceeds, it is not possible to make much of the data. Approximate values for the functions which we have used have been calculated from the graph for C_{total} — time, for 1 and 2 hours.

Table XIV.

Time (hours):	1.	2.
$(dC_{\text{ethylene}}/dt) \times 10^4$	2·825	1·575
$(dC_{\text{ethylene}}/dt) \times 10^{-6}/(C_2H_4)^4$	3·5	4·9
H_2	0·00440	0·00530
C_2H_4	0·00532	4·00424

The results are represented by the graphs in fig. 12.

VI. *Discussion of the Results.*

Stoichiometric relationships may, as this investigation shows, be entirely misleading; but the method of analysis which we have applied to our data appears to lead to results which are so closely related that they cannot be merely fortuitous, even if our conclusions are incorrect. It appears that when ethane is heated to the neighbourhood of 600° three processes are involved—

(i) The reversible ethane-ethylene-hydrogen reaction.

(ii) The formation of benzene and methane from ethane alone.

(iii) The formation of benzene and methane from ethylene and ethane.

The stoichiometric relationships in these reactions are discussed later (p. 25).

Hydrogen takes part as a reactant only in the reversible process. It seems to be quite certain that the last two reactions are related; and that the relation between them is due to some action of the hydrogen, depending on its concentration.

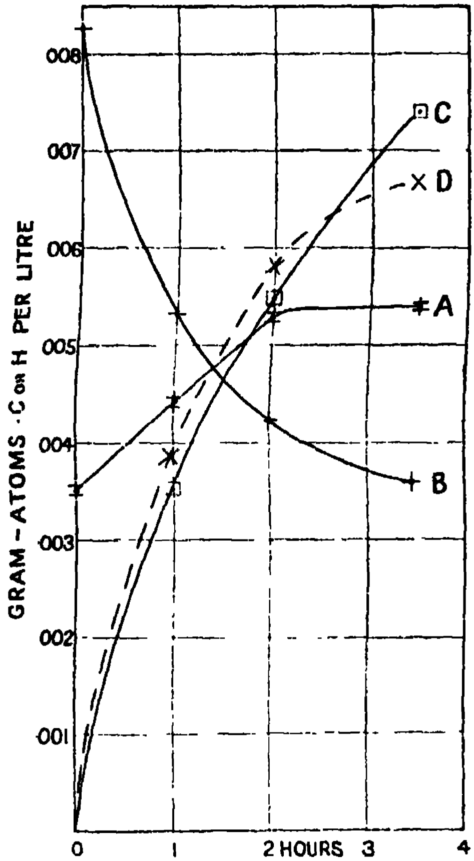

Fig. 12.—Equilibrium Mixture VI.

Study of figs. 8 to 12 shows that the graphs E are straight lines. Further study of the problem indicates that they might be slightly curved, for, as we shall show directly, the rate of formation of condensate from ethane depends only upon the hydrogen concentration. If the graphs E were perfectly linear, the rate of formation of benzene from ethane would depend only on the initial concentration of the hydrogen, and in this case we could only conclude that it was determined by some condition set up instantaneously in the silica at the beginning of each experiment, which is not impossible. But if we plot the rates of formation of benzene from ethane, given by the slopes of the graphs E, against the initial hydrogen concentration in each series, we obtain the graph A in fig. 13. This graph includes the result for Series V in which the concentration was one-half of the concentrations in the remaining series, confirming the fact that the rate of formation of benzene from ethane is quite independent of the ethane concentration. It will also be noted that in the Series VI no benzene was formed from ethane, and the point on the ordinate corresponding to Series VI lies just below that at which the graph A cuts the ordinate. Also, as we shall show later (p. 24) no benzene is produced from the ethane, when the pure gas is heated, till some hydrogen has been formed by the reversible process, so that the existence of a limit of hydrogen concentration below which benzene is not produced from ethane seems to be fully established. Also, we have found that when a comparatively small quantity of hydrogen is added to ethane, and the mixture is heated, no condensate at all is formed, but only methane, so that the existence of an upper limit is established, and the return of the graph A to the ordinate at a point of higher hydrogen concentration is confirmed. All the experimental facts in this connection seem to fall into line. The investigation of these processes at higher concentrations of hydrogen forms the subject of a separate research, which has been in progress for some time.

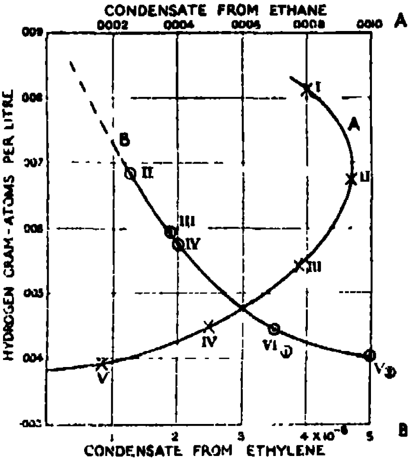

Fig. 13.

The rate of formation of benzene from ethylene might be related both to the ethylene concentration and to the ethane concentration, as it appears that both ethane and ethylene take part in the process (p. 23), of which we are probably only studying the first stage. Pease* states that the condensation of pure ethylene is bimolecular, but his experimental conditions are not comparable with ours. We could find no such relationship ; but, suspecting that we were dealing with a chain reaction, we were not surprised to find that the function

$$[10^{-6} \times d\,(\mathrm{C_{ethylene}})/dt]/(\mathrm{C_2H_4})^4,$$

calculated for short time periods for the different series, varied regularly with the hydrogen concentration. The relationship is, of course, empirical. The values of this function plotted against the hydrogen concentrations give the graph B in fig. 13. This shows, what the individual results show less distinctly, that the rate of formation of benzene from ethylene becomes very small when the hydrogen concentration is such that the rate of formation of benzene from ethane reaches a maximum. In this region a fourth process, which results in the formation of methane as a sole product, sets in, and, for this reason, the analysis of experimental results begins to be really difficult. As the concentration of the hydrogen falls to the lower limit at which the rate of formation of benzene from ethane alone becomes zero, the rate of formation of benzene from ethylene and ethane becomes very large. There seems to be a very close analogy between the phenomenon which we observe here, and the phenomena associated with the combustion of phosphorus, which have been studied by Semenoff and his school.

We will now discuss the reversible ethane-ethylene-hydrogen reaction. The value of the equilibrium constant,

$$\mathrm{K}_t = \mathrm{P_{H_2}} \times \mathrm{P_{C_2H_4}}/\mathrm{P_{C_2H_6}},$$

from the results of a very large number of experiments mainly from the ethane side, and at a concentration of 0·025 gram molecules per litre, was found to be 0·0235 (atmospheres) at 590°, and four experiments with equilibrium mixtures (Series V) at a concentration of 0·0125, also from the ethane side, gave values 0·0223, 227, 241, 241, mean 0·0233. Experiments at higher hydrogen concentrations, when the mixture undergoes less chemical change, appear to lead to the conclusion that the value is not less than 0·0245, and probably very close to that value. The value at 610° was found to be 0·033.

A very great deal depends upon the assumption that hydrogen takes part as a reactant only in the reversible ethane-ethylene-hydrogen process. It is impossible to give definite proof of the validity . . . . either of this assumption, or of the further assumption that hydrogen does not act as a catalyst, but only as a reactant in this process. Attempts have been made to calculate the values of the velocity constants in the reversible reaction from the experimental data, with a view to justifying the latter assumption; but, as the changes in the concentrations of the ethane and ethylene in the gas are due to the complex condensation reactions, it has only been possible to obtain semi-quantitative results, useless for this purpose. Since, however, the values of the equilibrium constant, obtained in cases in which the hydrogen content of the gas differed very considerably, varies by amounts not greater than experimental error, it is clear that hydrogen does not influence the rate at which equilibrium is approached to an extent equal to that to which it affects the condensation reactions, and probably does not influence it at all.

---

* 'J. Amer. Chem. Soc.,' p. 1158 (1930) ; p. 613 (1931).

It must follow that the processes which lead to the formation of benzene and methane must be initiated entirely independently from the activation processes in the reversible reaction.

It is now possible to offer some explanation of the results of the experiments with pure ethane described in Section IV. Since no condensate is formed from ethane till the hydrogen concentration has exceeded the lower critical limit, none is formed during the first interval of the reaction period. At first only hydrogen and ethylene are formed. We will take the results in Tables II and III for the experiments at 590° and 610°, those at 570° involving too little change over the early period to be useful, and treat them as we have treated the experimental results with the ethane-ethylene-hydrogen equilibrium mixtures.

Table XV.

	Temperature 610°.		Temperature 590°.		
Time (hours):	1.	2.	½.	1.	2.
$\Delta H_2 + \Delta C_2H_4$	0·00154	0·00289	0·00050	0·00090	0·00242
C_{total}	0·00325	0·00693	0·00071	0·00151	0·00364
C_{ethane}	0·00171	0·00404	0·00021	0·00061	0·00122
H_2	0·00626	0·00687	0·00966	0·00542	0·00596

The results plotted in fig. 14 show that, as might be expected, no condensate is formed from ethane during a short interval. Our results also explain why it is that the process of condensation comes to a stop after a second interval. The break in the graphs is due to the fact that as the hydrogen concentration increases, the rate of formation of condensate from ethylene decreases more rapidly than the rate of formation of condensate from ethane increases (*vide* fig. 11)..

The change in the concentration of the hydrogen, the effect of which cannot be considered quantitatively, adds an additional complication which makes it impossible to use the data which we are discussing for the calculation of the critical increments of the reactions.

VII. *Stoichiometric Relationships between Condensate Formation and Methane Formation.*

It seems to have been generally assumed that the process of condensation of ethane necessarily involved the formation of ethylene as a first step, and that methane and hydrogen were more or less casual products of side reactions. This view is incorrect. Though no reactions such as we are studying can proceed without a trace of side reaction, the results which have been discussed make it quite clear that there must be stoichiometrical connection between the rates of formation of the condensates and the rate of formation of methane.

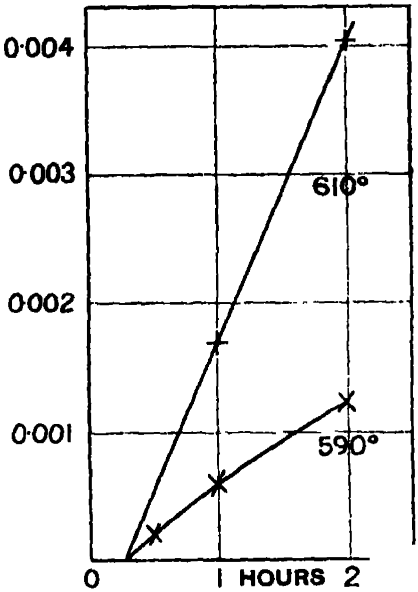

Fig. 14.

The formation of a $(CH)_n$ product from ethylene, together with methane can be represented stoichiometrically by

$$3nC_2H_4 = 4\,(CH)_n + 2nCH_4.$$

We believe that this reaction takes place when ethylene and hydrogen are heated, at least during the first short period. When much ethane is present the stoichiometric relationship is represented by

$$nC_2H_4 + nC_2H_6 = 2\,(CH)_n + 2nCH_4.$$

The formation of benzene and methane from ethane is represented by an equation much less simple than the latter—

$$3nC_2H_6 = 2\,(CH)_n + 4nCH_4.$$

If these last two relationships hold good the ratio

(C in condensate)/(C in methane)

should be unity in the case of ethylene and 1/2 in the case of ethane.

In Series VI, when practically only ethylene forms condensate, the ratio is 0·00354/0·00311 for 1 hour, and 0·00549/0·00547 for 2 hours, both of which are reasonably close to unity. In Series I the ratio for the 1 and 2 hour periods is in both cases 1/2·6. As we have pointed out, we are here entering a region where another process sets in, increasing the production of methane. More information is obtained by analysing the results of an intermediate series, thus, from Series III, we have :—

Table XVI.

Time (hours) :	1.	2.
C_{ethylene}	0·00112	0·00222
C_{ethane}	0·00092	0·00262
$(C_{\text{ethylene}} + 2C_{\text{ethane}})$	0·00296	0·00746
CH_4	0·00276	0·00786

The agreement is reasonably good.

VIII. *Summary and Conclusions.*

In this paper we have described a series of experiments with ethane, and with ethane-ethylene-hydrogen mixtures, heated in sealed silica tubes to temperatures near 600°. A technique which is to a certain extent new, and which is suited to investigations of this kind, has been developed, and is described in some detail. The reactions have been studied in much greater detail, and with a higher degree of accuracy than is usual.

We have studied a source of error which arises when reactions, in which hydrogen is a reactant or resultant, are carried out in thin-walled silica apparatus. We have assigned a cause to the phenomenon involved, and have shown how the resulting errors may be avoided. We believe that this phenomenon has no influence on the main reactions referred to below.

We show that there are three reactions involved :—

(i) The reversible ethane-ethylene-hydrogen reaction.

(ii) A reaction which results in the formation of benzene and methane from ethane alone.

(iii) A reaction which results in the formation of benzene and methane from ethylene and ethane.

The reversible ethane-ethylene-hydrogen reaction appears to be independent of the two other reactions, except in so far as it proceeds in one direction or in the other, so as to maintain a condition approaching equilibrium, as ethane or ethylene is removed from the system in the processes resulting in the formation of benzene and methane. It is also independent of the hydrogen concentration, except in so far as hydrogen is a reactant. The reversible reaction is being studied further in an independent investigation.

The processes which lead to the formation of benzene differ in that the process starting from ethane is endothermic, and therefore, if regarded as a chain reaction at all, will only proceed for one or two *links*, before the activation energy will be exhausted. This fact is probably connected with the simple relationship, the apparently *zero order* relationship, which represents the rate of reaction. On the other hand, the first stage of formation of benzene from ethylene, is obviously exothermic, so that a small amount of activation energy results in the conversion of a very large quantity of material. The complicated character of the process is indicated by the complex form of the expression used to represent the rate of formation of benzene. At low hydrogen concentrations the process bears a similarity to that observed in the case of the oxidation of phosphorus, where, on the one side of a limiting critical concentration of a component, the reaction proceeds slowly, and on the other side very fast. In this case the hydrogen is a catalyst only in the reaction which shows this acceleration, and is a reactant only in the ethane-ethylene-hydrogen reaction, which does not show it.

Further discussion of the results must await the completion of the investigation at higher hydrogen concentrations, and at other temperatures.

In conclusion, we wish to convey our thanks to the Imperial Chemical Industries, Limited, for their generous contribution to the cost of this research, and to the Department of Scientific and Industrial Research for a grant which enabled one of us to take part in it.

The Band Spectrum of Nitrogen Sulphide (NS).

By A. Fowler, D.Sc., F.R.S., Yarrow Research Professor of the Royal Society, and C. J. Bakker, Ph.D.

(Received January 20, 1932.)

(Plate 1.)

Introductory.

The present investigation had its origin in an observation by one of us that in a vacuum tube containing sulphur vapour with an impurity of nitrogen, there appeared a previously unrecorded band spectrum which bore a striking resemblance to that of nitric oxide (NO). As only sulphur and nitrogen were known to be present, this similarity suggested that the new spectrum might be due to nitrogen sulphide (NS), since oxygen and sulphur have the same number of valence electrons. This supposition appears to be fully confirmed by the further experiments which have been made and by the vibrational analysis of the bands. The principal members of both sets of bands occur in the ultra-violet and nearly in the same region. It will be convenient first to give a brief account of the bands of nitric oxide.

The Bands of Nitric Oxide.

The principal bands of NO are well known from their occurrence in air vacuum tubes; they were long ago named the "Third Positive Bands of Nitrogen" by Deslandres,* who, nevertheless, considered that the presence of both nitrogen and oxygen was necessary for their production. These bands were observed by Fowler and Strutt (now Lord Rayleigh)† to appear in the spectrum of the nitrogen afterglow, and the opinion was expressed that nitrogen alone was capable of producing them. Subsequent work by Lewis‡ and by Strutt,§ however, supported the view that the bands were produced only when both nitrogen and oxygen were present. During the present investigation, also, it has been found that the bands in question do not occur in vacuum tubes containing nitrogen when oxygen has been completely removed. These experimental results are in agreement with the conclusion derived from analyses of the band structure that the bands originate in the diatomic molecule NO.

---

* 'C. R. Acad. Sci. Paris,' vol. 101, p. 1256 (1885).

† 'Proc. Roy. Soc.,' A, vol. 85, p. 377 (1911).

‡ 'Phil. Mag.,' vol. 25, p. 826 (1913).

§ 'Proc. Roy. Soc.,' A, vol. 93, p. 254 (1917).

The general appearance of the NO spectrum as it occurs in an air vacuum tube is illustrated in Plate 1, spectrum *b*. It will be seen that the "Third Positive" bands appear with double-double heads and are degraded towards shorter wave-lengths. These were designated the "γ bands" by Fowler and Strutt in their account of the spectrum of the nitrogen afterglow, and this designation has since been widely adopted.

Another system of bands, designated the "β bands" by Fowler and Strutt, appears rather feebly in the air vacuum tube, but becomes very prominent in the nitrogen afterglow spectrum, as shown in Plate 1, spectrum *a*. The β bands are doublets and are degraded towards the red; in the afterglow they can be traced well into the visible spectrum.*

A third system of bands of NO was first recognised by Knauss,† with active nitrogen as source, and was named by him the "δ system" of NO. These bands are degraded towards shorter wave-lengths, and are similar in appearance and separations to the γ bands. The approximate wave-lengths given by Knauss were 1913, 1987, 2062, 2142, 2229 and 2320 A. More accurate wave-lengths for three of the bands were afterwards given by R. Schmid.‡

Still another system of bands of NO, incompletely observed in absorption by Leifson§ has been designated the "ε system" by Birge.|| Leifson's wave-lengths for these are 1877·2, 1799·6, 1729·7 and 1666·6 A.

Structure of NO *spectrum.*

The orderly arrangement of the γ bands was first shown by Deslandres,¶ but has been indicated more completely by M. Guillery** in connection with her rotational analyses of some of the bands. The structure of this spectrum, however, has not yet been presented with the completeness and accuracy which is desirable.

It results from the work of Mulliken†† and others that the γ-bands represent transitions $A\,^2\Sigma \rightarrow X\,^2\Pi$ (see fig. 1), the wider separation corresponding with the two Π levels, and the narrower ones representing the heads of different branches. The (0, 0) band is at λ 2269 and appears strongly in the absorption

---

* Johnson and Jenkins, 'Phil. Mag.,' vol. 2, p. 621 (1926).

† 'Phys. Rev.,' vol. 32, p. 422 (1928).

‡ 'Z. Physik,' vol. 59, p. 42 (1930).

§ 'Astrophys. J.,' vol. 63, p. 73 (1926).

|| 'Int. Crit. Tables,' vol. 5, p. 409 (1929).

¶ 'C. R. Acad. Sci. Paris,' vol. 139, p. 584 (1904).

** 'Z. Physik,' vol. 42, p. 121 (1927).

†† 'Phys. Rev.,' vol. 28, p. 493 (1926).

spectrum of NO at ordinary temperatures, together with other members of the ($v' \rightarrow 0$) progression.

The origins of the γ-bands are represented by the following formulæ given by Schmid*:—

$$\nu_0 = 44199 + (2358 \cdot 0v' - 16 \cdot 3v'^2) - (1892 \cdot 12v'' - 14 \cdot 424v''^2),$$
$$\nu_0 = 44079 + (2358 \cdot 0v' - 16 \cdot 3v'^2) - (1891 \cdot 98v'' - 14 \cdot 454v''^2).$$

Accurate measurements and rotational analyses of several of the β bands have been made by Jenkins, Barton and Mulliken.† These bands correspond with transitions $B\,^2\Pi_{3/2} \rightarrow X\,^2\Pi_{3/2}$ and $B\,^2\Pi_{1/2} \rightarrow X\,^2\Pi_{1/2}$, and the heads are represented approximately by the following formulæ given by Johnson and Jenkins:—

$$\nu_{\text{head}} = \left.\begin{matrix}45394 \cdot 6 \\ 45485 \cdot 0\end{matrix}\right\} + (1029v' - 7 \cdot 5v'^2) - (1889 \cdot 05v'' - 13 \cdot 96v''^2).$$

More accurate formulæ, involving higher powers of v' and v'' have been given by Jenkins, Barton and Mulliken. The separation $B\,^2\Pi_{3/2} - B\,^2\Pi_{1/2}$ is not observed directly, but is deduced from the observed $\Delta\nu = 124$ of the γ system and $\Delta\nu = 91$ of the β system. The (0, 0) bands of this system, the calculated positions of which are λλ 2202·2 and 2197·8, have not been observed either in absorption or in emission.

The δ system of NO is attributed to transitions from a higher $^2\Sigma$ level (c in fig. 1) to the final levels $X\,^2\Pi$, the bands having the same separations and vibrational levels as the γ system. The (0, 0) band has its least refrangible head near λ 1910 (ν 52340) and has been observed in the absorption spectrum of NO by Leifson. It has also been observed as a strong absorption band by R. Curry and J. Rankine at the Imperial College. The plates obtained by the latter observers also exhibit the ($v' \rightarrow 0$) progression of the γ system and several members of the ($v' \rightarrow 0$) progression in the β system, beginning with $v' = 2$.

The transitions involved in the production of the NO bands are indicated in fig. 1, which is drawn to scale with the doublet separations enlarged ten times. Corresponding transitions in NS are also shown in this diagram. The designations of the various levels for NO are in accordance with those of Mulliken‡ and Weizel.§

---

* 'Z. Physik,' vol. 64, p. 84 (1930).

† 'Phys. Rev.,' vol. 30, p. 150 (1927).

‡ 'Chem. Rev.,' vol. 6, p. 524 (1929).

§ "Bandenspektren," p. 364 (Leipzig, 1931).

Production of NS *Bands.*

Compounds of nitrogen and sulphur are highly explosive, and in these preliminary experiments it was accordingly considered sufficient to produce the NS bands by passing uncondensed discharges through a mixture of nitrogen and sulphur vapour. The discharge tube was of an ordinary end-on type, made of Pyrex glass and provided with quartz windows ; the capillary had a diameter of about 2 mm. and the electrodes were of aluminium. A small well, projecting below one of the wider parts of the tube, served to contain the sulphur, and the supply could be replenished through a ground-in stopper vertically above the well. The tube was exhausted by a three-stage mercury vapour pump, backed by a Hyvac pump, a liquid air trap being interposed to prevent mercury from entering the discharge tube and to protect the pumps from sulphur.

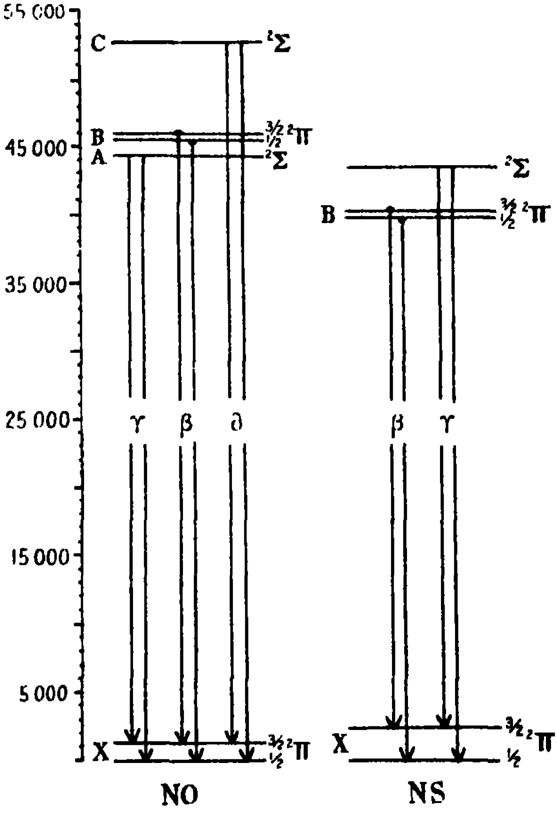

FIG. 1.

In order to obtain the NS bands in this way it is essential to "clean" the discharge tube thoroughly. The presence of even a very little oxygen, in conjunction with the nitrogen, suffices to bring out strongly the γ bands of NO, which lie in the same region of the spectrum and would obscure the bands of NS. It was found sufficient to use commercial nitrogen, dried by passage over P_2O_5.

The final cleaning of the discharge tube was then accomplished by passing a gentle stream of the dried nitrogen through it for several hours while the discharge was passing. The pressure of the gas was regulated in such a manner that the second positive nitrogen bands appeared very strongly as observed with a hand spectroscope. After trial exposures had shown the absence of the γ bands of NO, the sulphur was gently heated by a Bunsen flame. The conditions were found to be most favourable for the appearance of the NS bands when the second positive nitrogen bands and the bands of sulphur appeared to be of about equal intensity as observed visually.

Photographs for the present investigation were taken with small quartz spectrographs, and wave-lengths were obtained by means of copper arc comparison spectra. No great precision can be claimed for the measurements, but they appear to be sufficiently accurate for a preliminary vibrational analysis of the bands.

It should be remarked that the bands of sulphur, which extend from the visible into the ultra-violet,* appear strongly as far as the head at λ 2829, but no further, so that the region more refrangible than this is left clear for the spectrum of NS. The second positive bands of nitrogen end with the pair of heads at λλ 2820 and 2814. Numerous photographs were obtained in which there were no traces of NO bands.

Description of NS *Bands.*

The NS bands, as obtained in the way described above, are illustrated in Plate 1, spectrum *c*, from which it will be observed that the most prominent bands correspond closely in appearance with the γ and β bands of NO. It will accordingly be convenient to give the same names to corresponding systems in both spectra.

As in NO, the γ system presents bands with double-double heads, degraded to the violet, but the separations are greater in NS than in NO and successive bands are closer together.

---

* Fowler and Vaidya, 'Proc. Roy. Soc.,' A, vol. 132, p. 310 (1931).

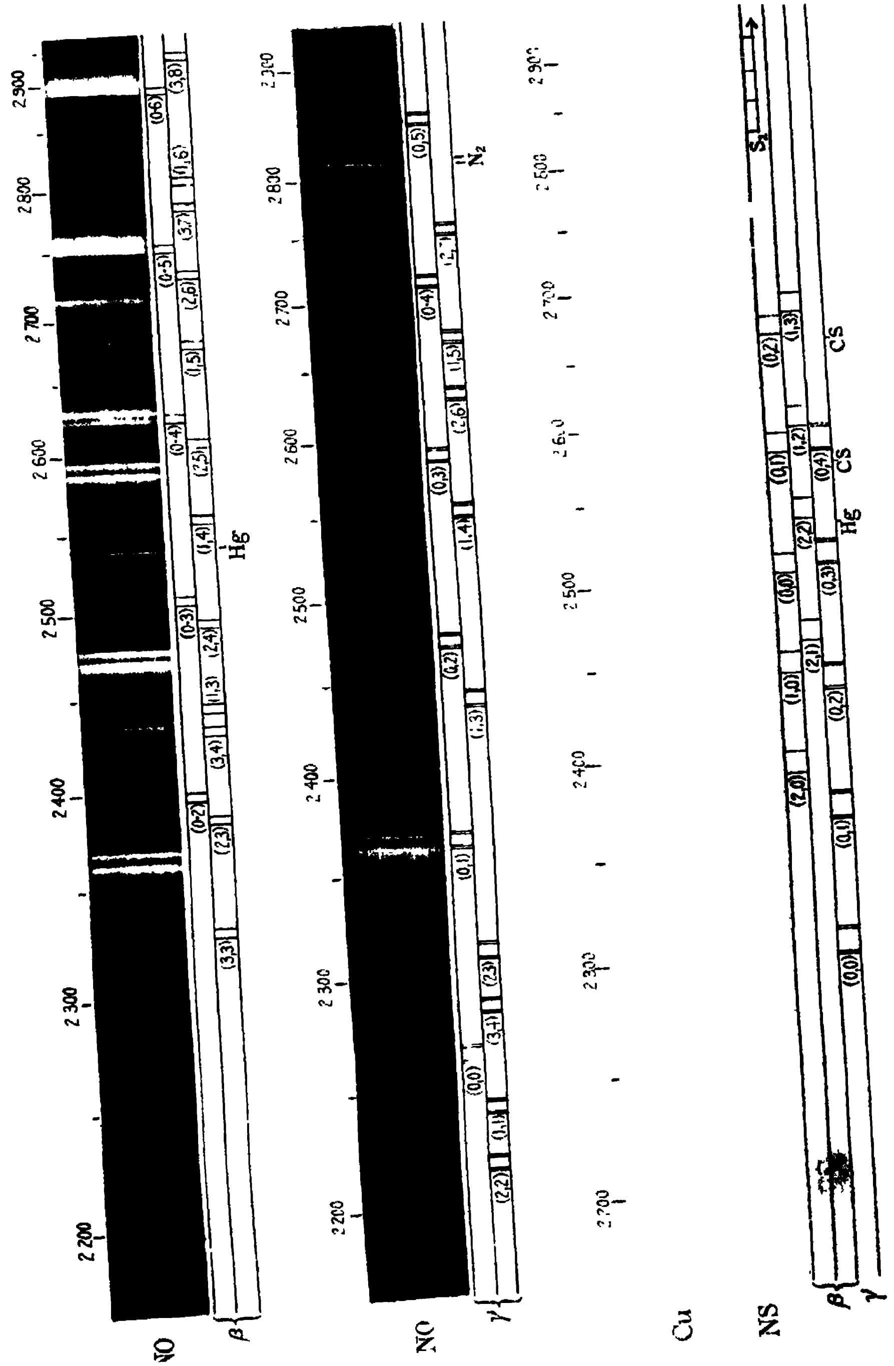
NO
β
NO
γ
Cu
NS
β
γ
Hg
CS
N₂
S₂
2 900
2 800
2 700
2 600
2 500
2 400
2 300
2 200
(0-6)
(3,8)
(1,6)
(3,7)
(0-5)
(2,6)
(1,5)
(0-4)
(2,5)
(1,4)
(0-3)
(2,4)
(1,3)
(3,4)
(0-2)
(2,3)
(3,3)
(0,5)
(2,7)
(0-4)
(1,5)
(2,6)
(0,3)
(1,4)
(0,2)
(1,3)
(0,1)
(2,3)
(3,4)
(0,0)
(1,1)
(2,2)
(0,2)
(1,3)
(0,1)
(1,2)
(0,4)
(2,2)
(0,0)
(0,3)
(2,1)
(1,0)
(0,2)
(2,0)
(0,1)
(0,0)

The pairs of bands forming the β system of NS are also more widely separated than those of NO and not so far apart.

The photographs of NS show, in addition, a number of bands, degraded to the red, which do not appear to belong to the β system, and have no counterpart in NO. The strongest of these are at wave-lengths 2762·0, 2744·5, 2715·2, 2655·6, 2634·2, 2557·3, 2400·2 and 2387·3. Their intensities appear to have a constant relation to those of the β bands, but it is not yet certain that they are due to NS.

In some of the photographs, including the one reproduced, Plate 1, there are two fairly strong heads of bands, degraded to the red, at wave-lengths 2575·9 and 2662·3. These are due to carbon monosulphide, as found by a careful comparison with photographs of the spectrum of this substance taken by L. C. Martin* and with the measurements of W. Jevons.† Besides the main heads, the first of which is double, some of the adjacent heads on their less refrangible sides are also shown feebly when the principal heads are strong. Independent evidence of the presence of small impurity of carbon is afforded by the occurrence of the CN band at λ 3883.

The γ *Bands of* NS.

Details of the γ band-heads which have so far been traced are shown below :—

v' \ v''	0		1		2		3		4
0	43142 (10) 43166 (10)	*1202* *1204*	41940 (10) 41962 (10)	*1187* *1189*	40753 (5) 40773 (5)	*1172* *1173*	39581 (3) 39600 (3)		
	224		*222*		*222*		*223*		
	43367 (8) 43389 (8)	*1204* *1206*	42162 (10) 42183 (10)	*1187* *1189*	40975 (4) 40994 (4)	*1171* *1170*	39804 (3) 39824 (3)	*1161* *1160*	38643 (1) 38664 (1)

The numbers in parentheses, to the right of the wave-numbers, represent estimated intensities.

The vibrational quantum numbers have been assigned by analogy with the γ system of NO. In NO the (0, 0) band at λ 2269 is clearly indicated as such by the absorption spectrum, and by the fact that it is the obvious termination of the $(0 \rightarrow v'')$ progression. There is no evidence at present from the absorption spectrum in the case of NS, but since the photographs extend far enough to have exhibited an additional band if it had been present, the bright band of which the first head is at ν 43142 may reasonably be taken to be the (0, 0) band.

---

* 'Proc. Roy. Soc.,' A, vol. 89, p. 127 (1913).

† 'Proc. Roy. Soc.,' A, vol. 117, p. 351 (1928).

There are some indications of faint bands which may represent the $(1 \rightarrow v'')$ progression, but further work is necessary to establish them with certainty.

The above heads are represented approximately by the following formulæ :—

$$^2\Sigma \rightarrow X\,^2\Pi_{3/2} : \ \nu_{\text{head}} = \left.\begin{matrix}43142\\43166\end{matrix}\right\} - (1212v'' - 8v''^2)$$

$$^2\Sigma \rightarrow X\,^2\Pi_{1/2} : \ \nu_{\text{head}} = \left.\begin{matrix}43367\\43389\end{matrix}\right\} - (1212v'' - 8v''^2).$$

As will appear from what follows, the $^2\Sigma$ level lies above B $^2\Pi$ in NS, and it is not certain with which of the two $^2\Sigma$ levels in NO it corresponds.

The β *Bands of* NS.

The β system of NS has been more completely observed than the γ system. Since both have the same final levels, the assignment of vibrational quantum numbers follows simply from the Δν of the γ system. All the bands which have been identified are included in the following scheme :—

v' \ v''	0		1		2		3
0	39694 (8)	*1202*	38493 (6)	*1191*	37302 (4)		
	186		*183*		*183*		
	39880 (8)	*1204*	38676 (5)	*1191*	37485 (3)		
	933				*933*		
	945				*947*		
1	40627 (7)	*1203*	+	*1189*	38235 (4)	*1173*	37062 (5)
	198				*197*		*194*
	40825 (6)	*1203*	+	*1190*	38432 (3)	*1176*	37256 (4)
	922				*921*		
	925				*924*		
2	41549 (4)	*1203*	40346 (3)	*1190*	39156 (3)		
	201		*200*		*201*		
	41750 (4)	*1204*	40546 (3)	*1189*	39357 (2)		

These band heads may be approximately represented by the following formulæ :—

$$B\,^2\Pi_{3/2} \rightarrow X\,^2\Pi_{3/2} : \ \nu_{\text{head}} = 39694 + (938\cdot5v' - 5\cdot5v'^2) - (1212\cdot25v'' - 7\cdot75v''^2)$$

$$B\,^2\Pi_{1/2} \rightarrow X\,^2\Pi_{1/2} : \ \nu_{\text{head}} = 39880 + (956\cdot5v' - 10\cdot5v'^2) - (1212\cdot25v'' - 7\cdot75v''^2).$$

As in NO, the separation of the B $^2\Pi$ levels is the difference between the separation of the X $^2\Pi$ levels and the observed separations of the β bands; that is, for NS, approximately $224 - 186 = 38$.

If the quantum numbers have been correctly assigned, the β system of NS differs from that of NO in the occurrence of the (0, 0) and other bands of low quantum numbers which have not been observed in NO. The intensity distribution in NS thus appears to be quite different from that in NO. Johnson and Jenkins's Table III (*loc. cit.*) indicates a wide-open Condon parabola for NO, with its maximum at about $v'' = 8$, whilst in NS the parabola appears to be a rather narrow one having its axis roughly in the direction of the diagonal. The difference in intensity distribution, however, is in general accordance with expectation, since in NO the ratio of w''_e to w'_e is about 1·9, whilst in NS it is about 1·25.

The (1, 1) band of NS appears to be entirely absent.

Classified Bands of NS.

λ (intensity).	γ bands ($v'v''$).	β bands ($v'v''$).
2697·40 (5)	—	37062 (1, 3)
2683·35 (4)	—	37256 (1, 3)
2680·05 (4)	—	37302 (0, 2)
2667·00 (3)	—	37485 (0, 2)
2614·60 (4)	—	38235 (1, 2)
2601·25 (3)	—	38432 (1, 2)
2597·15 (6)	—	38493 (0, 1)
2587·00 (1)	38643 } (0, 4)	—
2585·60 (1)	38664 }	
2584·80 (5)	—	38676 (0, 1)
2553·10 (3)	—	39156 (2, 2)
2540·10 (2)	—	39357 (2, 2)
2525·70 (3)	39581 } (0, 3)	—
2524·50 (3)	39600 }	
2518·50 (8)	—	39694 (0, 0)
2511·55 (3)	39804 } (0, 3)	—
2510·30 (3)	39824 }	
2506·75 (8)	—	39880 (0, 0)
2477·80 (3)	—	40346 (2, 1)
2465·60 (3)	—	40546 (2, 1)
2460·70 (7)	—	40627 (1, 0)
2453·05 (5)	40753 } (0, 2)	—
2451·85 (5)	40773 }	
2448·75 (6)	—	40825 (1, 0)
2439·75 (4)	40975 } (0, 2)	—
2438·65 (4)	40994 }	
2406·05 (4)	—	41549 (2, 0)
2394·45 (4)	—	41750 (2, 0)
2383·63 (10)	41940 } (0, 1)	—
2382·40 (10)	41962 }	
2371·10 (10)	42162 } (0, 1)	—
2369·90 (10)	42183 }	
2317·19 (10)	43142 } (0, 0)	—
2315·94 (10)	43166 }	
2305·17 (8)	43367 } (0, 0)	—
2304·03 (8)	43389 }	

Summary.

A spectrum of bands attributed to nitrogen sulphide (NS) has been obtained by passing uncondensed discharges through tubes containing nitrogen and sulphur vapour. The spectrum is strikingly similar to that of nitric oxide (NO) and appears in nearly the same (ultra-violet) region. Two systems of bands, corresponding with the well-known γ and β bands of NO, are clearly shown. In NS the doublet separations are larger, and the separations of successive bands smaller, than in NO.

DESCRIPTION OF PLATE.

a.—Nitrogen afterglow, showing γ and β bands of NO strongly. (For 0·2 ... *read* 0, 2 ...)

b.—Air vacuum tube; γ bands strong, β bands weak.

c.—Vacuum tube containing nitrogen and sulphur vapour. (The bands at λ 2576 and λ 2662 are due to an impurity of CS.) Copper arc comparison.

Notes on the Theory of Radiation.

By C. G. Darwin, F.R.S.

(Received January 22, 1932.)

It will probably be agreed that among all the recent developments of the quantum theory, one of the least satisfactory is the theory of radiation. The present paper is intended as a preliminary to a new line of attack on the subject. It was begun some time ago, but owing to lack of success in carrying it to a conclusion, its publication has been much delayed. In the meantime other papers have appeared,* which in some respects follow the same train of thought. The authors of these works have carried their methods further in some directions than I have attempted, but there is still perhaps room for the discussion of a number of questions from the rather different point of view adopted here.

1. The main principle of the present work is the idea that, since matter and light both possess the dual characters of particle and wave, a similar mathematical treatment ought to be applied to both, and that this has not yet been

---

* Landau and Peierls, 'Z. Physik,' vol. 62, p. 188 (1930); Oppenheimer, 'Phys. Rev.,' vol. 38, p. 725 (1931).

done as fully as should be possible. Whereas we have a fairly complete calculus for dealing with the behaviour of any number of electrons or atoms, for photons the existing processes are much less satisfactory. The central difficulty, which makes it hard to apply the ordinary methods of wave mechanics to light, is the fact that (at least according to our present ideas) photons can be created and annihilated, and to represent this in a wave system we have to be able to think of a medium suddenly coming into existence and then going out again, when the light that it was carrying is absorbed. Such behaviour is a grave difficulty in the way of allowing us to think of the photon as a wave, and tends to make us think with more favour of its particle aspect, until we recall that after all it is quite unlike any known particle to come into existence and later to disappear without trace. The theories at present current, such as that of Heisenberg and Pauli,* avoid these difficulties because they are mainly formal generalisations of the classical theory; this frees them from the above difficulties, but they pay for it in being highly abstract, and, as it has turned out, rather unsuccessful.

The guiding idea adopted here was that for the present one should set aside difficulties of creation and annihilation, and should see to it that in cases where the photon can be endowed with some measure of individuality, its general description should follow the lines which have been so successful for the electron. In particular the Compton effect, at its discovery, was regarded as a simple collision of two bodies, and yet the detailed discussion at the present time involves the idea of the annihilation of one photon and the simultaneous creation of one among an infinity of other possible ones. We would like to be able to treat the effect as a two-body problem, with the scattered photon regarded as the same individal as the incident, in just the way we treat of the collisions of electrons. Also we must include in our account of it all the associated phenomena of the effect; in a good theory the change of wave-length of the light, the velocity of recoil of the electron, the association of the directions of the two and their simultaneity will all be represented at once. It was with a view to finding ways of describing all these features of the Compton effect that I discussed, now nearly three years ago, the collision of two material particles in the wave mechanics.† That work contributed little new to the wave theory of matter, but it was the result of an investigation as to how all the phenomena of the Compton effect could be represented together, and this investigation clearly showed that the configuration space of the two bodies would yield the description so perfectly that it could hardly be right to look further. It seemed therefore right to apply a similar method to the Compton effect, treating the collision of photon and electron by the same method as is used in the wave mechanics for two material particles. It will be seen that this is very like the work of Landau and Peierls (*loc. cit.*), and it is immediately clear that the method will yield qualitatively all the features of the Compton effect. The trouble begins when we try to make the theory exact, for this demands a relativistically invariant theory of two bodies, which hardly exists yet. In view of this difficulty, and also of the complicated calculations necessary to relate the work with the formulæ of Klein and Nishina,* I shall not in the present note attempt to discuss the exact form of the interaction of a photon and an electron. Simpler questions in this connection are dealt with in the present work, and I hope to return to the question of the interaction in a later communication.

---

* 'Z. Physik,' vol. 56, p. 1 (1929), and vol. 59, p. 168 (1930).

† 'Proc. Roy. Soc.,' A, vol. 124, p. 375 (1929). Among other things a rather complicated problem was discussed in which the particles were made to collide twice over. In relativistic processes it is dangerous to think of simultaneity in different places, and the point of this problem was that it avoided this danger and yet implied the simultaneity.

We must recognise that the present idea involves rather a radical change in our conception of electromagnetic waves. In the theory of Heisenberg and Pauli (*loc. cit.*) the electric force of such a wave is regarded as an observable quantity, but here we treat it as of the nature of the unobservable ψ of the wave mechanics. Consequently we abandon the idea of identifying the electric force of a light wave with a static electric force, or even with the force in wireless waves. This is unavoidable, but it is made plausible by the consideration that observable electric forces always arise from millions of electrons, and wireless waves always involve millions of photons, and that it is reasonable to demand a mastery of the behaviour of a single photon before proceeding to discuss that of a large number. Moreover it is certainly in accordance with fact that for light waves, just as for electron waves, it is the intensity that is observed, while the amplitude of the light wave is just as unobservable as the ψ of an electron. We shall therefore abandon entirely the quasi-classical view that a light wave shakes an electron to and fro, and so causes it to emit light by virtue of its acceleration ; with the appropriate modifications this is the method of consideration prevalent at present. Instead we shall consider electron and photon as two bodies, and shall find their mutual potential, though only in incomplete form in the present paper.

2. Our first task is to throw the description of the unperturbed photon into a form acceptable to the wave mechanics. In doing this we have to accom-

---

* 'Z. Physik,' vol. 52, p. 853 (1929).

modate the facts of polarisation, and so must start with some form of the electromagnetic equations, but we have to consider which of them is suitable. Thus we might choose for our variables either the electric or magnetic forces or both, or the potentials, or even such other types as the components of the Hertzian vector, but with the aims of the present work there could be no doubt as to which should be chosen. The equations of the spinning electron involve differentials of the first order in the time, so if we wish to combine an electron with a photon in a single system of equations we must have the photon's equations also of the first order in the time. This means that we do not want the potentials, but must use some combinations of the electric and magnetic forces. If we only needed to consider the unperturbed photon it would be possible to combine the six quantities, E, H into four independent ones $E_x + iE_y$, E_z, etc., which exactly satisfy Dirac's equations with m zero; but it is inadvisable to do this, because it conceals the actual vector character of the electric force of a light wave, as exhibited by the polarisation of scattered light. It is simplest to face a certain amount of redundancy and to make use of the six components of E, H, as our wave functions.

We submit the ordinary electromagnetic equations to the process which may be regarded as the fundamental process of all wave motions, the problem of finding the condition of the medium at any time in terms of arbitrary initial conditions. This is a well-known process and it will suffice merely to quote the result. Consider a radiation field in free space, supposing that at $t = 0$ the values of E and H are given everywhere. We shall denote vectors by a subscript, and shall make use of the ordinary summation convention (over the three space dimensions) for duplicate subscripts. The initial field is then E_α^0, H_α^0, but the six quantities are not independent on account of the divergence relations

$$\frac{\partial E_\alpha^0}{\partial x_\alpha} = 0, \quad \frac{\partial H_\alpha^0}{\partial x_\alpha} = 0, \tag{2.1}$$

and so they really only involve four arbitrary functions. In introducing Fourier integrals we shall increase the resemblance to the wave of an electron by writing the quantum in (denoting by h the quantum divided by 2π) even though in fact it plays no part in the work. We derive six functions $A_\alpha^0(p)$, $B_\alpha^0(p)$ of the three variables p_β given by

$$\begin{aligned} E_\alpha^0(x) &= \int A_\alpha^0(p)\, e^{ip_\beta x_\beta/h}\, dp^{(3)} \\ H_\alpha^0(x) &= \int B_\alpha^0(p)\, e^{ip_\beta x_\beta/h}\, dp^{(3)} \end{aligned} \tag{2.2}$$

where $dp^{(3)}$ is short for $dp_x\, dp_y\, dp_z$; and A^0, B^0 can be explicitly determined by inversion of the Fourier integrals. Now take

$$\left.\begin{aligned} A_\alpha(p) &= \tfrac{1}{2}\{A_\alpha^0(p) - [p, B^0]_\alpha/w\} \\ B_\alpha(p) &= \tfrac{1}{2}\{B_\alpha^0(p) + [p, A^0]_\alpha/w\} = [p, A]_\alpha/w, \end{aligned}\right\} \qquad (2.3)$$

where w is the positive square root of p_β^2. On account of (2.1) we have

$$p_\alpha A_\alpha = 0. \qquad (2.4)$$

Then the solution of our problem is

$$\left.\begin{aligned} E_\alpha(x, t) &= \int A_\alpha(p)\, e^{i(p_\beta x_\beta - wct)/h}\, dp^{(3)} + \int A_\alpha^*(p)\, e^{-i(p_\beta x_\beta - wct)/h}\, dp^{(3)} \\ H_\alpha(x, t) &= \int B_\alpha(p)\, e^{i(p_\beta x_\beta - wct)/h}\, dp^{(3)} + \int B_\alpha^*(p)\, e^{-i(p_\beta x_\beta - wct)/h}\, dp^{(3)}, \end{aligned}\right\} \qquad (2.5)$$

where as usual A_α^* is conjugate to A_α.

Now compare this with the corresponding process for the spinning electron. If the four components of ψ are chosen initially quite arbitrarily, so that their real and imaginary parts constitute eight real arbitrary functions, then the values at other times will depend on two Fourier integrals involving respectively

$$\exp i\,[p_\beta x_\beta \mp wct]/h,$$

where $w = \sqrt{(m^2c^2 + p_\beta^2)}$. This is, of course, the well-known fact that negative energy cannot be avoided in the description of the spinning electron, if complete generality is to be attained. If we want to have only positive energy we must leave four of the eight real functions adjustable; it is a matter of indifference whether we choose two of the four ψ's as arbitrary complex functions and determine the other two from them, or whether we regard the real parts of all four as given and deduce the imaginary parts from them.

Returning to the photon, if we admit the existence of imaginary solutions, then we have in fact assigned eight functions, the six real functions for E^0 and H^0, reduced to four by (2.1), and the corresponding imaginary parts defined to be zero. To represent the propagation of the disturbance we must again use two sets of terms with exponents of both signs. The fact that the electromagnetic equations can be put in a real form implies that a completely real solution can be found, but if we regard the exponential type of solution as the right primitive solution, then we must regard the real solution as a superposition of two primitive ones of equal amplitude, one with positive frequency and the other with negative.

Now the energy of material particles of all kinds is described in the quantum theory by means of the frequency of their expansion in exponentials, and we would like to be able to regard the energy of a photon as on the same footing. It would seem natural then to regard an electromagnetic wave, written in the usual real form, as the superposition of two waves, one with positive energy and momentum and the other with both negative. For an actual light wave it would seem natural to exclude the wave of negative energy, and to take as our wave the first term in (2.5). In the case of the electron Dirac* has made an attempt to justify the exclusion of negative energy with the help of the exclusion principle and of an infinite number of electrons of negative energy. We cannot, of course, invoke the same idea here because of the different statistics of photons, nevertheless Dirac's theory does not seem to have turned out very well. So we must, I think, exclude the negative energy in both cases for the same reason —that is to say, nobody knows how or why. It might be thought that we are increasing the troubles of the quantum theory by introducing a new case of negative energy, but it is usually found that the best hope of resolving a deep difficulty is to extend its application as widely as possible.

It should be noticed that the suppression of the second term in (2.5) leads to one significant difference. When a harmonic wave is represented by real quantities, it involves a factor cos ϕ where the phase $\phi = (px - wct)/h$. For the intensity this is squared, and then averaged, yielding $\frac{1}{2}$, but there is in addition a term in $\frac{1}{2}\cos 2\phi$, and in all ordinary waves, such as water waves or sound waves, there is a real pulsation in the pressure exerted by the wave, of frequency twice that of the wave. Classical theory indicates that the same should be true for the momentum of light waves, but the general trend of the quantum theory points the other way. Imagine an experiment in which a mirror is mounted with a spring, so that it can vibrate along the normal to its face. When the mirror is reflecting light of frequency ν, adjust the spring so that it will vibrate with frequency 2ν; then if the term in $\cos 2\phi$ is present the mirror will be thrown into resonance. Now when we consider the actual mechanism of reflection, we may think this experiment conceived in too macroscopic a manner, but it is easy to see what modification will fit it into the quantum theory. For interaction between two waves of phases ϕ and ϕ' we shall have a chance depending on $e^{i(\phi-\phi')}$, and the analogue of the term in $\cos 2\phi$ will be a term depending on $e^{i(\phi+\phi')}$. To make this term display its effect we should need to make the system interact with a further system possessing phase nearly equal to $\phi + \phi'$. It seems very improbable that such interaction would occur, but if it does it would be explained in the language of the quantum theory by saying that our first system has jumped to negative energy. So once again it seems that we have reason to reject the second term in (2.5).

---

* 'Proc. Roy. Soc.,' A, vol. 126, p. 360 (1930).

3. We will now consider certain dynamical properties of the photon, especially those connected with its polarisation, and compare them with the corresponding quantities for the electron. With a view to this comparison we first give certain properties of a wave packet of light, treated classically, and afterwards we shall develop the same results by methods analogous to those used for the electron.

Suppose that we have a field of radiation given by the real parts of

$$\left.\begin{aligned} \mathrm{E}_\alpha &= \int \mathrm{A}_\alpha(p)\, e^{\iota(p_\beta x_\beta - wct)/h}\, dp^{(3)} \\ \mathrm{H}_\alpha &= \int [(p/w),\, \mathrm{A}]_\alpha\, e^{\iota(p_\beta x_\beta - wct)/h}\, dp^{(3)} \end{aligned}\right\} \qquad (3.1)$$

The divergence relation requires that A should satisfy

$$p_\alpha \mathrm{A}_\alpha = 0. \qquad (3.2)$$

The ensuing calculations depend only on Fourier integrations and need not be shown in detail; in the course of them the pulsating terms of octave frequency are rejected as usual. The following results are obtained :—

(i) The energy

$$\left.\begin{aligned} \mathrm{W} &= \int \frac{1}{8\pi}(\mathrm{E}_\alpha{}^2 + \mathrm{H}_\alpha{}^2)\, dx^{(3)} \\ &= \pi^2 h^3 \int |\mathrm{A}_\alpha|^2 dp^{(3)} \end{aligned}\right\} \qquad (3.3)$$

(ii) The momentum

$$\left.\begin{aligned} \mathrm{P}_\alpha &= \int \frac{1}{4\pi c}\,[\mathrm{E},\, \mathrm{H}]_\alpha\, dx^{(3)} \\ &= \frac{\pi^2 h^3}{c}\int \frac{p_\alpha}{w}\,|\mathrm{A}_\beta|^2 dp^{(3)}. \end{aligned}\right\} \qquad (3.4)$$

This result is general; for a wave packet $\mathrm{A}_\alpha = 0$ except for p near some definite value and hence $\mathrm{P}_\alpha = \mathrm{W}p_\alpha/wc$.

(iii) The motion of the packet can be studied by finding how its centre of gravity moves. Then

$$\bar{x}_\beta \mathrm{W} = \int x_\beta \frac{1}{8\pi}(\mathrm{E}_\alpha{}^2 + \mathrm{H}_\alpha{}^2)\, dx^{(3)}.$$

The reduction is a little more complicated, but is done by writing $x_\beta \, e^{ip_\gamma x_\gamma/h}$ as $\frac{h}{i}\frac{\partial}{\partial p_\beta} e^{ip_\gamma x_\gamma/h}$ and integrating by parts. The result is

$$\overline{x}_\beta \, \mathrm{W} = \pi^2 h^3 \int dp^{(3)} \left\{ ct \, \frac{p_\beta}{w} \, |\mathrm{A}_\alpha|^2 + ih\mathrm{A}_\alpha{}^* \frac{\partial \mathrm{A}_\alpha}{\partial p_\beta} \right\}. \tag{3.5}$$

The centre of gravity therefore travels with velocity c along the direction given by the momentum P; the second term gives its initial position.

(iv) The angular *momentum* about an axis through the *origin* is given by

$$\mathrm{M}_\beta = \int \left[x, \frac{1}{4\pi c} [\mathrm{E}, \mathrm{H}] \right]_\beta dx^{(3)}.$$

This can be reduced to

$$\frac{\pi^2 h^3}{c} \int dp^{(3)} \left\{ ih \left[\mathrm{A}_\alpha{}^* \frac{\partial \mathrm{A}_\alpha}{\partial p}, \frac{p}{w} \right]_\beta + \frac{ih}{w} [\mathrm{A}, \mathrm{A}^*]_\beta \right\}. \tag{3.6}$$

If we take the special case of a wave packet, we see that the first term represents $[\overline{x}, \mathrm{P}]_\beta$ which is the *angular momentum of a particle of momentum* P, moving with the centre of gravity of the packet. The second term is intrinsic momentum and may be written as

$$\frac{\mathrm{W}}{cw} \frac{\int ih \, [\mathrm{A}, \mathrm{A}^*] \, dp^{(3)}}{\int (\mathrm{A}, \mathrm{A}^*) \, dp^{(3)}}. \tag{3.7}$$

If we quantise we write $\mathrm{W} = wc$. We then see that a photon can have intrinsic momentum about its direction of motion ranging between $\pm h$ the extreme values corresponding to circular polarisation.

This angular momentum is analogous to the spin of the electron, but we should observe that the analogy is imperfect, because we have only got one quantity instead of two, since the momentum of the photon is always about the line of its motion. The polarisation of the light is incompletely described by the angular momentum, whereas the axis of spin of an electron completely describes its polarisation. It is possible, of course, for the case of the photon, to establish a geometrical correspondence so that the specification of a direction in space should yield not only the ellipticity of the light, but also the axes of the ellipse, but such a correspondence is purely conventional and without dynamical significance. This is natural when we consider that the electromagnetic equations for free space are symmetrical between the electric and magnetic forces, so that we can never hope to get a discrimination between them, until we introduce a perturbation (say an electron) which is unsymmetrical in its reaction to electric and magnetic forces.

We now apply the methods of quantum theory to the same problem. The wave function ψ has six components E_x, E_y, E_z; H_x, H_y, H_z, which we denote by $\psi_1, \ldots, \psi_6$, taken in this order. Here there is one peculiar feature which does not usually occur in quantum processes, and this is that the six components are restricted by the two divergence relations. If we keep in mind the differential equations to which the quantum processes are equivalent, we shall run no danger from this. The six curl equations of the electromagnetic field can be derived from a Hamiltonian

$$\mathfrak{H} = c\,(\beta_x p_x + \beta_y p_y + \beta_z p_z), \tag{3.8}$$

where $p_x = -ih\partial/\partial x$, etc., as usual, and the β's are the matrices

$$\beta_x = \begin{pmatrix} \cdot & \cdot & \cdot & \cdot & \cdot & \cdot \\ \cdot & \cdot & \cdot & \cdot & \cdot & 1 \\ \cdot & \cdot & \cdot & \cdot & -1 & \cdot \\ \cdot & \cdot & \cdot & \cdot & \cdot & \cdot \\ \cdot & \cdot & -1 & \cdot & \cdot & \cdot \\ \cdot & 1 & \cdot & \cdot & \cdot & \cdot \end{pmatrix}, \quad \beta_y = \begin{pmatrix} \cdot & \cdot & \cdot & \cdot & \cdot & -1 \\ \cdot & \cdot & \cdot & \cdot & \cdot & \cdot \\ \cdot & \cdot & \cdot & 1 & \cdot & \cdot \\ \cdot & \cdot & 1 & \cdot & \cdot & \cdot \\ \cdot & \cdot & \cdot & \cdot & \cdot & \cdot \\ -1 & \cdot & \cdot & \cdot & \cdot & \cdot \end{pmatrix}, \quad \beta_z = \begin{pmatrix} \cdot & \cdot & \cdot & \cdot & 1 & \cdot \\ \cdot & \cdot & \cdot & -1 & \cdot & \cdot \\ \cdot & \cdot & \cdot & \cdot & \cdot & \cdot \\ \cdot & -1 & \cdot & \cdot & \cdot & \cdot \\ 1 & \cdot & \cdot & \cdot & \cdot & \cdot \\ \cdot & \cdot & \cdot & \cdot & \cdot & \cdot \end{pmatrix}. \tag{3.9}$$

The equations are then

$$\mathfrak{H}\psi = ih\,\frac{\partial\psi}{\partial t}. \tag{3.10}$$

The stationary states are given by taking all components proportional to $\exp i\,(p_x x + p_y y + p_z z - wct)/h$. The result is a six-rowed determinant which reduces to

$$w^2\,(w^2 - p_x^2 - p_y^2 - p_z^2)^2 = 0. \tag{3.11}$$

The solutions $w = 0$ represent static electric and magnetic fields, derivable from potentials; they are to be excluded as having nothing to do with a photon. Actually they are excluded by the relations $div\, \mathrm{E} = 0$, $div\, \mathrm{H} = 0$, which cannot be derived from the Hamiltonian though their time-differentials can. We shall also exclude the negative values of w yielded by the second factor of (3.11), as discussed earlier.

We can now derive many results like those for the electron, but in general they are more troublesome, because the β's have not the simple commutation rules of the α's of Dirac; in particular they have no reciprocals. In fact, the required relations are only easily found by using ordinary vector methods and then translating them. In this way we can show that, provided $w \neq 0$,

$$(\beta_x p_x + \beta_y p_y + \beta_z p_z)^2 = p^2, \tag{3.12}$$

so that each component of ψ satisfies $\Box^2\psi = 0$. We may also mention another relation which will be used later. If we form the six-rowed matrix

$$\gamma_z = \beta_x\beta_y - \beta_y\beta_x \tag{3.13}$$

we can verify by matrix multiplication that

$$\beta_x\gamma_z - \gamma_z\beta_x = \beta_y, \quad \beta_y\gamma_z - \gamma_z\beta_y = -\beta_x, \quad \beta_z\gamma_z - \gamma_z\beta_z = 0. \tag{3.14}$$

As in the case of the electron we have a current function derived from the equation

$$\frac{\partial}{\partial t}(\psi^*\psi) + \frac{\partial}{\partial x}(c\psi^*\beta_x\psi) + \frac{\partial}{\partial y}(c\psi^*\beta_y\psi) + \frac{\partial}{\partial z}(c\psi^*\beta_z\psi) = 0. \tag{3.15}$$

By substituting for ψ in terms of E and H we see that the components $c\psi^*\beta\psi$ are simply the Poynting vector associated with the electromagnetic energy $\psi^*\psi$. So, too, we can work out the momentum $P_x = \int \psi^* p_x \psi \, dx^{(3)}$, but it will be observed that though the integral comes out the same as (3.4), the integrand is not the same; this will make an important difference for the angular momentum. We can also work out the centre of gravity of a packet, and show that it travels with the speed of light.

The system of either an electron or a photon in free space is unduly simple in that there are two separate theorems of conservation of angular momentum. There is first the angular momentum of a particle moving with the centre of gravity, and there is also the intrinsic momentum, and each is conserved separately. In Dirac's theory of the electron the angular momentum, as formally defined, is of the first type, and in order to get the general conservation and not merely the uninteresting first type of it, he had to impose a spherically symmetrical perturbing force. We have worked out the angular momentum on classical principles and have got both types together, and it should be noticed that this was because in effect we did have a perturbing force, since the classical formula for the momentum of radiation is derived by considering the interaction with matter. We will now attack the same question in the manner of Dirac, and obtain the same result as before.

We suppose that a spherically symmetrical perturbation Q acts on the photon, so that

$$\mathfrak{H} = c(\beta_x p_x + \beta_y p_y + \beta_z p_z) + Q. \tag{3.16}$$

Using the quantum definition of angular momentum we have

$$\mathrm{M}'_z = \int \psi^* (xp_y - yp_x)\, \psi\, dx^{(3)}. \tag{3.17}$$

The time differential of this is reduced with the help of (3.10) and its conjugate to

$$\frac{d\mathrm{M}'_z}{dt} = \int \psi^* \left[c\beta_x p_y - c\beta_y p_x - x\frac{\partial \mathrm{Q}}{\partial y} + y\frac{\partial \mathrm{Q}}{\partial x} \right] \psi\, dx^{(3)}.$$

The last two terms vanish on account of the symmetry of Q; to deal with the first two, consider

$$\mathrm{M}''_z = -\int \psi^* ih\gamma_z \psi\, dx^{(3)}, \tag{3.18}$$

where γ_z is given by (3.13). Then with the help of (3.14), we obtain

$$\frac{d\mathrm{M}''_z}{dt} = \int \psi^* \left[c\beta_y p_x - c\beta_x p_y \right] \psi\, dx^{(3)}.$$

Thus we have

$$\frac{d}{dt}(\mathrm{M}'_z + \mathrm{M}''_z) = 0,$$

and the quantity conserved is

$$\mathrm{M}_z = \int \psi^* \left[xp_y - yp_x - ih\gamma_z \right] \psi\, dx^{(3)}. \tag{3.19}$$

If we write out γ_z and replace ψ by E, H, we find that this is exactly the same as (3.6).

It should perhaps be remarked that though we have spoken of the angular momentum as having any values between $\pm h$, this is not contrary to the statement of Dirac† that plane polarised light is to be regarded as having equal probabilities of being light with eigenvalues $\pm h$ and not as having angular momentum zero. To reconcile the two statements it is only necessary to think of the analogy of the spinning electron; in one sense it may only have angular momentum either $\frac{1}{2}h$ or $-\frac{1}{2}h$ along the z axis, but in another we may say that it has no angular momentum along z if it is pointing along x. It is merely a question of whether we think of the particle as simultaneously in two stationary states, or insist that it shall be in only one.

4. We have discussed the angular momentum of the photon and have obtained an expression for it of broadly the same character as that of the electron. It is now proper to point out that this angular momentum suffers

† "Quantum Mechanics," p. 131.

from just the same disability as does that of the electron. In both cases the momentum is divisible into two parts which we may call respectively the external, due to the motion of the centre of gravity, and the intrinsic, due to the polarisation, but the division is really quite artificial and dynamically meaningless. This fact was shown by Bohr,* as far as concerns the magnetic moment of the electron, and it is only a trifling extension to apply it to the angular momentum. The ensuing argument deals with angular momentum in general; it is nothing but a simple application of the principle that no experiment interpreted according to classical ideas can yield the quantum, and it must, I think, be familiar to many, though I can give no citation.

By the type of argument with which the uncertainty principle has made us familiar, it is easy to show that no experiment can ever reveal the intrinsic momentum of a photon or free electron. In order to know it we should have to know what allowance to make for the external momentum, and this requires a knowledge of the line of motion. Suppose that we want the intrinsic momentum about the axis of z. Then we try to reduce as low as possible the external momentum about this axis, and this we may do by sending the particle along the z-direction through a small hole at the origin. Then if b is the radius of the hole, diffraction will introduce a transverse linear momentum of order h/b, and as the particle may pass through anywhere at distance less than b from the axis, it clearly may have external momentum anything up to h in amount. This is sufficient to mask the intrinsic momentum. Moreover, the same result is true for atoms or molecules, when allowance is made for the possibility that they may carry several quanta of momentum; in this case our measure will refuse to tell us in exactly which quantised state the atom is.

It may be well to elaborate the argument a little further. In conformity with the general principles of resolving power we know that no system of lenses, etc., can be better than the small hole considered, but there is another device that needs closer examination. Suppose that we intend to measure the momentum by absorbing the particle in a body that is free to turn. We might take this body as of very small size and at a large distance from the hole defining the incident particle's path. Consider the momentum about the axis joining the centre of the hole to that of the absorber. Then, though the particle may emerge from the hole with any external momentum up to h, yet it will only strike the absorber if its external momentum about this axis is very small, and we might think that we could isolate the intrinsic momentum in this way. The fallacy, however, is the same as that which asserts that we can know the path of a particle and its momentum as accurately as we like by choosing a particle that has gone through two small holes one after the other; we can observe when this happens, but it is useless for knowing what will happen to the particle later. In the present case we must suppose that we can measure the change in angular momentum of the absorber, and to observe the intrinsic momentum given to it by our particle we must measure the momentum to accuracy better than h; but this we can never do, since the absorber will itself have uncertain external momentum of order h, and that no matter how massive it may be. It is a rather striking example of the duality of the quantum theory, that one aspect insists that every system always has angular momentum an exact multiple of the quantum, while the other insists that it can never be possible to measure the angular momentum of any system to the nearest quantum; indeed it is really this second fact that allows us to make the first assertion without fear of contradiction.

---

* 'Proc. Roy. Soc.,' A, vol. 124, p. 440 (1929).

Although the angular momentum of the free electron or photon is a single quantity not to be separated into two parts, yet it is, of course, possible to do statistical experiments from which the intrinsic momentum can be inferred. Thus if a beam of circularly polarised light is collimated as accurately as possible, each of its photons will have intrinsic momentum h in the same sense, though their external momenta will range between $\pm h$. If N of these photons are absorbed at a surface, the surface should acquire angular momentum $(N \pm \sqrt{N})h$ and the uncertainty becomes insignificant when N is large. It is not, of course, to be expected that the angular momentum should be practically observed, for it will only give rise to the very small couple produced by multiplying the force due to the radiation pressure by an arm equal to a wave-length of the light.

There are certain points about the angular momentum of radiation that should be noticed, though they are not so fundamental as the preceding. We may recall that long ago Rubinowitz* discussed the question in connection with the change of an atom's azimuthal quantum number. If we take the classical problem of an electron describing a small circle, we find that in addition to the terms in $1/r$ the electric force at a distance has others in λ/r^2, and this means that the wave front of the emitted radiation faces not exactly away from the origin, but from a point about a wave-length away from it. The same is true for the Poynting vector. This, of course, does not matter, since the origin of a source of light is always indefinite to a wave-length, but it is contrary to what we expect at first sight of a particle. It implies that the photon which is to carry away the energy and angular momentum from an atom of radius 10^{-8} cm. starts its life outside the atom at a distance 10^{-5} cm. away.

---

* 'Phys. Z.,' vol. 19, p. 441 (1918).

It is also interesting to consider whether the phenomenon of emission can be described regarding the photon as a pure particle. The atom is to lose angular momentum h about the z axis by the emission of a single photon of linear momentum $2\pi h/\lambda$ in an arbitrary direction. The intrinsic momentum of a photon is always directed along its direction of motion ; let m be its magnitude. Let θ, ϕ, give the direction of motion of the photon and let ξ, η, 0, be its birthplace in the equator. Then we easily see that the three conditions of angular momentum can only be satisfied if

$$\left.\begin{aligned} m &= h\cos\theta \\ \xi &= \lambda\sin\theta\sin\phi/2\pi \\ \eta &= -\lambda\sin\theta\cos\phi/2\pi \end{aligned}\right\}, \qquad (4.1)$$

The polarisation of the photon if it goes into the direction θ is just such as is indicated in the classical theory and confirmed by observation in the Zeeman effect. As far as it goes this is satisfactory, but its scope is limited, because we must also consider the quadrupole emission where $2h$ of momentum is lost in a single photon. The same argument now would give $m = 2h\cos\theta$ and even though for this type of quadrupole there is not much emission in high latitudes, still there is some, which would give to m inadmissible values greater than h. For quadrupole emission the pure particle concept is a failure.

5. We now consider the perturbation of a photon. This may be due either to the refraction of a medium (of any type of anisotropy) or, as in the case we shall study here, it may be an electron. We only consider the case where the momentum of the photon is insufficient to move the electron perceptibly, and shall only consider the first approximation. The photon is perturbed by a potential Q, a function of position ; Q is in general a matrix of 36 components, but we may take all but 9 of them as zero, as the following considerations show. When the momentum and energy of a photon are given, the magnetic components can be expressed in terms of the electric. Thus suppose that $u\,(p)$ represents the six components of the solution

$$u\,(p)\,e^{i(p_\beta x_\beta - wct)/h}, \qquad (5.1)$$

then u_4 can be expressed in terms of u_1, u_2, u_3 with the help of p and w. The amplitude of the scattered wave will in the usual way depend on

$$\int u^*\,(p')\,\mathrm{Q}u\,(p)\,e^{i(p_\beta - p'_\beta)x_\beta/h}\,dx^{(3)}, \qquad (5.2)$$

and in this it is possible to replace u_4, etc., on both sides of Q by u_1, etc., that is to say, to transfer all the other components of Q to the first nine. In doing so we, of course, have to introduce p and p' into Q and so we must be ready to regard it as possibly involving differential operators. It should be noted that the possibility of reducing Q to nine members depends on the exclusion of negative energy; with given p, the magnetic components are only uniquely expressed in terms of the electric, provided that w is also given. In our present problem there is no danger of the energy changing sign, and so we need only regard Q as consisting of the nine electric-electric members.

The best method of solving the perturbation problem is by means of the Green function. It is easily verified in the present case that for a ψ proportional to $e^{-iwct/h}$ the wave equation can be written as

$$\left.\begin{aligned} \mathrm{E}_\alpha(x) &= \mathrm{E}_\alpha{}^0(x) - \frac{1}{4\pi wc}\int dx'^{(3)}\,\frac{e^{iwr/h}}{r}\left\{\frac{\partial^2}{\partial x'_\alpha\,\partial x'_\beta}\mathrm{Q}'_{\beta\gamma}\mathrm{E}'_\gamma + \frac{w^2}{h^2}\mathrm{Q}'_{\alpha\gamma}\mathrm{E}'_\gamma\right\} \\ \mathrm{H}_\alpha(x) &= \mathrm{H}_\alpha{}^0(x) + \frac{i}{4\pi hc}\int dx'^{(3)}\,\frac{e^{iwr/h}}{r}\,[\mathrm{curl}\,(\mathrm{Q}'\mathrm{E}')]_\alpha \end{aligned}\right\}. \tag{5.3}$$

Here E^0, H^0, is any solution of the unperturbed equation, $r = \sqrt{(x_\alpha - x'_\alpha)^2}$ and Q', E' represent the values of the respective quantities at the point x'. This is exact, but we can approximate by substituting E^0 for E under the integral sign and expanding r. Then incident wave

$$\mathrm{E}_\alpha = \mathrm{A}_\alpha\, e^{ip_\beta x_\beta/h} \tag{5.4}$$

yields scattered wave in direction p'

$$\mathrm{E}'_\alpha = \frac{1}{4\pi}\,\frac{e^{iwr_0/h}}{r_0 wc}\int dx'^{(3)}\; e^{-ip'_\gamma x'_\gamma/h}\,\{p'_\alpha p'_\beta \mathrm{Q}'_{\beta\delta}\mathrm{A}_\delta - w^2\mathrm{Q}'_{\alpha\delta}\mathrm{A}_\delta\}. \tag{5.5}$$

This is the form that we shall actually need, but it is of course, quite easy to go on in the ordinary way and show that the scattered wave has amplitude proportional to (5.2).

We want to find what form of Q will give the scattering which is actually caused by an electron, in fact, the Thomson scattering. According to the classical formulæ the incident wave

$$\mathrm{E}_\alpha = \mathrm{A}_\alpha\, e^{i(p_\beta x_\beta - wct)/h} \tag{5.6}$$

gives rise to a scattered wave

$$\mathrm{E}'_\alpha = \frac{e^2}{mc^2}\,\frac{1}{w^2}\{p'_\alpha p'_\beta \mathrm{A}_\beta - w^2\mathrm{A}_\alpha\}\frac{e^{iw(r-ct)}}{r}. \tag{5.7}$$

If we compare this with (5.5) we see that the solutions can be identified if

$$Q_{11} = Q_{22} = Q_{33} = 4\pi \frac{e^2}{mc^2} \frac{h^2 c}{w} \delta(x_1)\, \delta(x_2)\, \delta(x_3)\,, \tag{5.8}$$

while the other components all vanish. Here δ is the singular function of Dirac. This form of Q is much the simplest, but is by no means unique. We could, for example, make the first three components of ψ mean dielectric displacement instead of electric force; this would annul Q_{11}, etc., and introduce Q_{41}, etc., in place, thus undoing again the simplification made above.

It should be noticed that Q is an "improper" expression, since we cannot replace w in it by a time differentiation. This, of course, means that there is no first order differential equation which can yield the observed scattered wave. That does not matter, for in a fuller theory the electron would be free, and the mc^2 in the coefficient would then be replaced by the energy of the electron; so even if the w had not occurred in the denominator, the fuller theory would involve an improper expression. As a matter of fact, the product of w and mc^2 is admirably suited to turn into a relativistic invariant. It should also be observed that the infinity of δ in (5.8) prevents the carrying out of any higher approximations. As far as the present work goes the photon must not have wave-length much less than 10^{-8} cm., or it would set the electron in motion; and so we may imagine the singular function replaced by any function with a single peak much narrower than this, and we could carry the approximation further with such a function, though it would not be significant to do so. If the theory is extended to cover the Compton effect, the restriction on the singular function becomes much more severe, but even in that case we cannot claim to have any data for distances less than, say, 10^{-12} cm. Thus the singularity at the origin is only an approximation to a state of affairs about which we have no experimental evidence. From the other side of the question, it should be noticed that the classical calculation of (5.7) is itself an approximation, worked by supposing that the electron's radiation is negligible during the calculation of its own motion. The higher approximations of the classical theory are merely constructed out of general dynamical principles, and it will be easier to apply such general principles (with the appropriate modifications) through the quantum theory direct, rather than by means of a laborious translation of the classical forms.

Summary.

The general aim of the work was to apply the methods of wave mechanics to the single photon, following out as far as possible the process which has succeeded for the electron.

The usual real form of electromagnetic waves implies the presence of two waves of equal amplitude, but respectively of positive and negative energy and momentum, and it is suggested that the latter should be rejected.

The polarisation of light is connected with its angular momentum in a way resembling the spin of the electron. The separation of angular momentum into two parts, one external, due to the motion of the centre of gravity, and the other intrinsic, is shown to be conventional; no experiment can divide it in this way, and since the external momentum is always uncertain to h, the intrinsic momentum of a photon is unobservable. Certain features of the radiation of an atom are considered.

The perturbation of the photon by an electron is considered and the energy of perturbation is given for the case of Thomson scattering.

The Phenomena of Superconductivity with Alternating Currents of High Frequency.

By J. C. McLennan, F.R.S., A. C. Burton, A. Pitt, and J. O. Wilhelm.

(Received February 8, 1932.)

[Plate 2.]

In a previous paper* the authors described experiments on the resistance of lead to currents having the high frequency of 10^7 per second. In these experiments no evidence was found of an abrupt change of resistance corresponding to the phenomenon of superconductivity that appears with direct currents when the critical temperature of 7·2° K. is passed, and it was pointed out that the partial silvering of the vacuum flasks that contained the lead coil was a source of error.

In a set of new experiments† to be described below unsilvered flasks were used, but the same technique of measurement was adopted. It was found that there was an abrupt decrease of the high frequency resistance at a temperature which appeared to be slightly lower than that characteristic of the transition to superconductivity with direct currents. Experiments with tin instead of lead showed a similar result. The transition temperature was progressively lowered as the frequency was increased. The behaviour of tantalum was investigated also, and this metal, too, showed a depression of the critical temperature for high frequency currents.

---

* 'Phil. Mag.,' vol. 12, p. 707 (1931).

† Preliminary notes on these experiments were published in 'Nature,' vol. 128, p. 1004 (1931), and 'Trans. Roy. Soc. Canada,' section III, p. 191 (1931).

Method.

The principle of the method employed in all the experiments was the same as that described in the paper referred to. A brief sketch of this method is here given.

A resonant circuit was constructed, consisting of a coil of wire wound on a fibre former in series with a condenser which was mounted on the same former. The entire electrical circuit was made of the metal under investigation. The resonator used in the first experiments with lead is shown in fig. 1, Plate 2. The lead plates of the condenser were kept at the proper distances by fibre washers on the central fibre spindle. This resonator, C, fig. 2, was contained in the Dewar flask E, in which the liquid helium was produced at the liquefier L. T, the helium thermometer, gave the temperature of the helium gas that circulated in the space D and round the coil. High frequency currents were induced in the latter by an oscillator below—of which A and B represent the plate and grid coils respectively.

The magnitude of the currents induced in the coil was measured by their reaction upon the oscillations in the generator, as indicated by the plate current of the latter. The frequency of the oscillator was varied over a small range extending to each side of the natural frequency of the resonator, and the values of the plate current observed. The curve obtained with no coil present in the flask, but with otherwise identical conditions, was subtracted from the curves first obtained. "Resonance curves" resulted, from which the high frequency resistance of the metal could be deduced for the different temperatures.

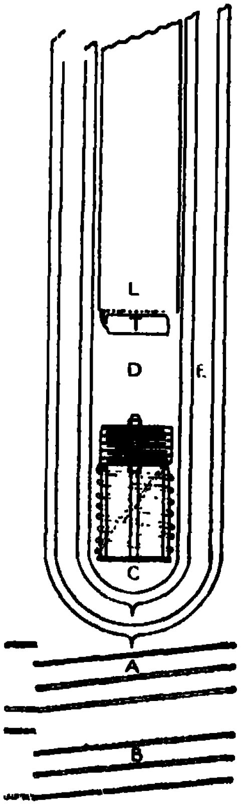

Fig. 2.

A simple treatment of the theory is as follows. Let the oscillatory current in the coil of the generator be i_1. Then the induced e.m.f. in the resonator coil will be $-M\frac{di_1}{dt}$, where M is the mutual inductance between the two. This e.m.f. will produce a current in the coil given by

$$i_2 = \frac{-M\frac{di_1}{dt}}{\sqrt{R'^2 + \left(\omega L - \frac{1}{\omega C}\right)^2}}$$

where R′, L, C are respectively the high frequency resistance, inductance, and capacity of the coil. At resonance the impedance is due to resistance only as $\left(\omega L - \frac{1}{\omega C}\right)$ becomes zero, and $i_2 = -\frac{M}{R'}\frac{di_1}{dt}$.

There will be an induced e.m.f. in the generator coil due to this current given by

$$e = -M\frac{di_2}{dt} = \frac{M^2}{R'}\frac{d^2 i_1}{dt^2} = -\frac{M^2\omega^2}{R'}i_1. \tag{1}$$

By the use of a grid leak and condenser in the circuit of the generator, the average plate current was made to serve as an indication of the total amplitude of the oscillations. The conditions of operation were such that the change in the plate current was proportional to the oscillating e.m.f., e, producing it. This was proved by a calibration experiment described in the previous paper. We have, then,

$$\Delta I_p \propto -\frac{M^2\omega^2}{R'}i_1, \tag{2}$$

or, the change in plate current due to the reaction of the resonator upon the generator, at the point of resonance, is proportional to 1/R′.

$$R' \alpha \frac{1}{p}, \tag{3}$$

where p is the height of the "peak" of the resonance curve. Changes in the high frequency resistance of the metal of the resonator can therefore be followed by observations of the magnitude of the resonance peaks.

The presence of metallic screening is equivalent to the effect of a second circuit in the neighbourhood of that of the resonator, having, say, a mutual inductance with it of M_s. Solution of the differential equations, which are very similar to those dealt with in the theory of the transformer, shows that it has the effect both of lowering the reactance, and of increasing the resistance of the resonator. If X_s, R_s are the reactance and resistance of the second circuit, equivalent to the screening, the reactance of resonator circuit is effectively decreased by $\frac{\omega^2 M_s^2 X_s}{X_s^2+R_s^2}$ while the resistance is increased by $\frac{\omega^2 M_s^2 R_s}{X_s^2+R_s^2}$. The latter quantity we may call the "induced resistance," and the height of the resonance curve gives, not the true resistance of the resonator, but the sum of R' and this "induced resistance." At very low temperatures the true resistance, R', may become very small compared to the induced resistance due to neighbouring conductors, and the height of the resonance peaks then becomes very insensitive to the changes in the resistivity of the metal of the coil. If, as will usually be the case, the screening is very far from resonance with the oscillations, its reactance X_s will be, at low temperatures, much greater than its resistance R_s. In this case the induced resistance to which it gives rise becomes approximately proportional to R_s. We have then the paradox that the peak, at the resonance with the coil, measures the resistance not of the coil, but of the screening in its neighbourhood. Thus it may be seen how the partial silvering of the helium flasks was able to mask completely the changes in the resistance of the lead, and how the peaks could continue to decrease below the superconducting point, as the resistance of the silvering decreased.

The existence of this additive "induced" resistance imposes a limitation on the use of the method, as the coil can never be infinitely far from any conducting circuit, the coils of the generator itself being necessarily coupled to it. The limitation to its use is greater at the higher frequencies, the induced resistance varying as the square of the frequency. Even if the resistance in the superconducting state were truly zero, the induced resistance would prevent an observation to that effect. Care was therefore taken to have all conducting bodies as far removed from the resonator as possible. The nearest metallic object was the helium thermometer T, which was some 18 cm. above the top of the coil.

The great advantage of the method, compared to others that might be suggested, is that the whole of the circuit of the resonator is cooled in the helium flask, and that there is no metal present other than that being investigated. Theoretically, it would be more desirable to keep the frequency of the oscillations fixed while the resonator was tuned across the resonance point. This, however, was not practicable, and since the tuning was very sharp indeed, the variation demanded to obtain the resonance curves in practice was very small. But the fact that the frequency was varied introduces a peculiarity into the results when superconductivity is reached; this phenomenon will be discussed later.

Apparatus.

The oscillator, circuit of which is shown in fig. 3, was of the tuned plate regenerative type, in which a UX. 112A vacuum tube was used. It was essential that, when the frequency was varied over the required range by means of the variable condenser connected in parallel with the plate coil A, there should be no abrupt or irregular changes in the amplitude of the oscillations. To this end the resonance frequency of the grid circuit was made much less than that of the oscillating circuit by using a large capacity for the grid condenser. It was found that any form of choke in the circuit introduced parasitic oscillations, but by careful screening of the leads it was possible to dispense with its use. The numerical values given in the diagram are for the oscillator of wave-length 26 metres, other wave-lengths were obtained by substituting coils of greater inductance for A and B. The total plate current was read by the milliammeter M, and small changes in its value, produced by the reaction of the resonator, were indicated by the galvanometer G, the normal plate current through which was balanced by a potentiometer device. The oscillator was enclosed in an earthed copper screen and connected by screened leads to the batteries and galvanometer, which were contained in an earthed metal box. In this way freedom from interference and from the effects of body capacity was satisfactorily obtained. To ensure steadiness the voltage across the filament was kept at 5 volts for at least 4 hours before a run was made. In the later experiments it was found that the resonance peaks were so sharp that finer adjustment of capacity than that provided by the 50 MMF. condenser was needed, and a variable condenser of approximately 1 MMF. was connected in parallel with the former.

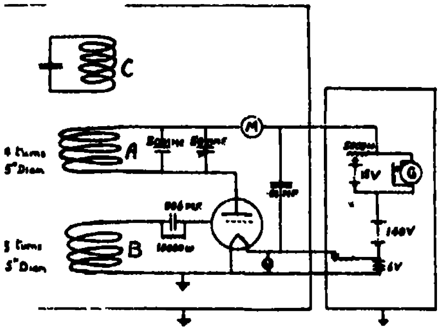

Circuit Diagram.

FIG. 3.

Results with Lead.

The resonance curves obtained at different temperatures with the lead coil, whose dimensions were, diameter 4 cm., height 5 cm., are shown in fig. 4. They were taken at repeated intervals of time until their constancy indicated that the coil had reached a steady temperature, equal to that of the helium thermometer T. Changes in the readings of the latter were rapidly followed, especially at the lower temperatures, by changes in the magnitude of the resonance peaks, indicating that there was little lag in the temperature of the coil behind that of the thermometer. The progressive shift of the resonance to higher frequencies as the temperature was lowered was due to the change in capacity of the lead condenser by contraction on cooling. In the later experiments with tin and tantalum, this shift was compensated by a shift in the opposite direction of comparable amount, when the liquid helium covered the condenser plates; its dielectric constant being 1·04.

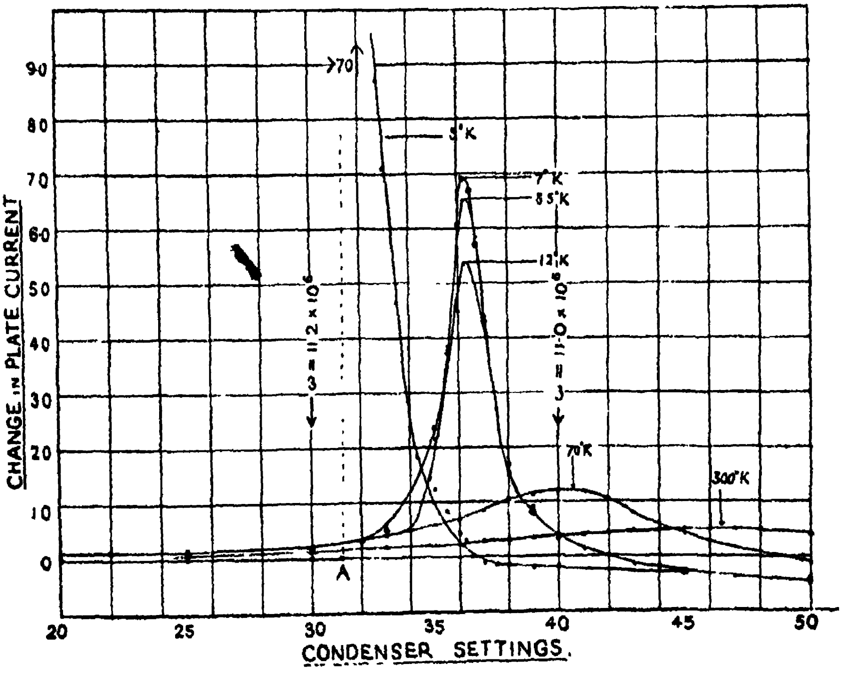

Fig. 4.

The peaks regularly increased as the temperature was lowered, great care being exercised in the observations as the normal superconducting temperature of 7·2° K. was approached. The coil was kept for some time at 7° K., and it was seen that there was, so far, no indication of an abrupt change in the resistance. It was thought that the result of the experiment would prove to be the same as that obtained with the partially silvered flasks, and accordingly the temperature was lowered until the helium thermometer indicated a temperature of 5° K. It was a few minutes after this that an abrupt change in the peaks occurred, and the resonance curve took the form shown in the figure. The resonance was now too sharp for the magnitude of the peak to be obtained accurately, but it was certainly greater than 10 times the peak for 7° K., and sufficient, momentarily, to throw the generator out of oscillation. A pronounced asymmetry appeared, the curve falling abruptly to the point A on the diagram, as the curve was obtained by increasing the frequency, *i.e.*, by decreasing the capacity from the right-hand side of the diagram towards the left. When the curve was traced in the opposite direction, *i.e.*, with progressively decreasing frequency, no resonance could be found. As the supply of helium was exhausted, no further observations could be taken at the time, but they sufficed to show that, in contradiction to the previous results with partially silvered flasks, there was superconductivity for currents of the frequency of 11 million per second. There was definite indication that the temperature at which the phenomenon appeared was below 7° K., while with direct currents, an experiment with the same coil showed that the critical temperature was the usual one of 7·2° K.

From equation (3), the ratio of the high frequency resistance at any temperature to that at room temperature, is equal to the inverse ratio of the corresponding peaks.

$$\frac{R'}{R'_0} = \frac{P_0}{P}. \tag{4}$$

The values of this ratio calculated from the resonance curves are given in the second column of Table I. For comparison with the values of the ratio R/R_0 obtained in direct current experiments, a correction has to be made for the "skin effect," which at high frequencies tends to confine the currents to the surface of the conductor. The high frequency resistance is greater than the direct current resistance of the same wire; the ratio of the two, R'/R, being a function of the quantity x, which is given by

$$x = \pi d \sqrt{\frac{2\mu\omega}{1000\rho}},$$

where

d = diameter of wire = $0{\cdot}030$ cm.

μ = magnetic permeability = 1 for lead,

ω = frequency = $1{\cdot}1 \times 10^7$.

ρ = specific resistivity, for direct currents, in microhm-cm.

= $24{\cdot}9$ (by direct measurement for the wire).

The adequate treatment of the case of the coils of the experiment is quite beyond mathematical analysis, and for lack of any better formula, that for a straight wire may be used. The ratio R′/R for a wire in the form of a coil will be considerably greater. Tables of the ratio R′/R for the straight wire are given in Bureau of Standards Circular No. 74, p. 300, *et seq.* For a given value of x they give the value of $f(x) = \mathrm{R}'/\mathrm{R}$. As the temperature is lowered, the resistivity ρ decreases and x, and therefore $f(x)$, increases.

At any temperature we have $\mathrm{R}' = \mathrm{R} \,.\, f(x)$.

At room temperature, $\mathrm{R}'_0 = \mathrm{R}_0 f(x_0)$, therefore

$$\frac{\mathrm{R}'}{\mathrm{R}'_0} = \frac{\mathrm{R}}{\mathrm{R}_0} \times \frac{f(x)}{f(x_0)}. \tag{5}$$

The result of skin effect is then, that the high frequency resistance does not decrease as rapidly as does the direct current resistance. To deduce the values of R/R_0 from the observed values of $\mathrm{R}'/\mathrm{R}'_0$, a method of successive approximation is used. Starting from an assumed value of R/R_0 (equal to ρ/ρ_0), the value of x, which is equal to $x_0 \,.\, \sqrt{\frac{\rho_0}{\rho}}$ is calculated; from it the quantity $f(x)$ and thus $\frac{f(x)}{f(x_0)}$. When the experimental value of $\mathrm{R}'/\mathrm{R}'_0$ is divided by this last quantity, a better value is obtained for the ratio R/R_0 than that used as a starting point. The process quickly leads to the values of R/R_0 which, when the skin effect correction is made, will yield the experimental values of $\mathrm{R}'/\mathrm{R}'_0$. For values of x greater than 10, $f(x)$ is very nearly proportional to x, *i.e.*, for two temperatures 1 and 2 for which this is true

$$\frac{\mathrm{R}'_1}{\mathrm{R}'_2} = \frac{\mathrm{R}_1}{\mathrm{R}_2} \times \frac{x_1}{x_2} = \frac{\mathrm{R}_1}{\mathrm{R}_2} \times \sqrt{\frac{\rho_2}{\rho_1}} = \sqrt{\frac{\mathrm{R}_1}{\mathrm{R}_2}}.$$

i.e.,

$$\frac{\mathrm{R}_1}{\mathrm{R}_2} = \left[\frac{\mathrm{R}'_1}{\mathrm{R}'_2}\right]^2 = \frac{p_2^2}{p_1^2}. \tag{6}$$

This relation is probably true, with close approximation, for the values at the lowest temperatures of the experiments, even if the formula used for the skin effect ratio, R′/R, is not applicable.

The resulting values of R/R_0 are given in the third column of Table I, and may be compared with those found for direct currents, given in the last column.

Table I.

Temperature, degrees K.	High frequency.		Direct current (Onnes), R/R_0.
	R'/R'_0.	R/R_0.	
300	1 00	1·00	1·00
70	0·41	0·21	0·21
12·5	0·091	0 013	0·0080
8·5	0·076	0·009	0·0018
7	0·072	0·008	0·0010
(5)	<0·01	<0·0001	0·00000

It will be seen that the values for 70° K. are in close agreement, but that there is an increasing discrepancy at temperatures below about 20° K. It is not known whether this is due to the inadequacy of the formulæ used to deal with the case, or to some real difference between the resistivity to high frequency and to direct currents. The permeability has been assumed to be unity throughout, and this may not be true at the lowest temperatures.

Experiments with Tin.

The observations with lead made it desirable to investigate whether there was a real difference between the temperatures at which superconductivity appeared with the high frequency currents and with direct currents. In view of difficulties in the accurate measurement of temperature between the boiling points of helium and of hydrogen, it was decided to study tin instead of lead, as the critical temperature of the former lies just below the boiling point of helium. The whole resonator would then be immersed in the liquid helium at the temperatures of greatest interest to the research, and these temperatures could be adjusted and observed with accuracy from the value of the vapour pressure of the helium. The sensitivity of this method is such that a change of one-tenth of a degree Kelvin corresponds closely to a change of vapour pressure of 50 mm. of mercury in the range of temperature of the experiments.

Tin wire was drawn, from strips cut from a sheet of block tin, to a diameter of 0·06 cm. This was wound on a fibre former, identical with that used for the lead coil, the ends of the wire being soldered, using tin as the soldering metal, to the two sets of tin plates mounted on the fibre spindle above the coil.

The way in which the resonance curves behaved as the temperature was lowered can be seen from Table II—the second column of which gives the ratio of the observed peaks. The latter must be large enough at room temperature and at 65° K. to permit of numerical comparison, and yet not so great at the lowest temperatures as to invalidate equation (2). Therefore, after curves had been obtained at 65°, others were taken at the same temperature and at all the lower temperatures with less coupling between resonator and generator. The ratio of the peaks taken at the same temperature with the different couplings allows the peaks at the lower temperatures to be compared with that at room temperature. This procedure was followed in all the later experiments.

Table II.

Temperature, degrees K.	High frequency.		Direct current, R/R_0.
	R'/R'_0.	R/R_0.	
300	1·00	1·00	1·00
65	0·436	0·21	0·21
15	0·18	0·038	—
8·5	0·12	0·021	—
7·5	—	—	0·0022
4·2	0·095	0·0102	0·0020

Owing to the low resistance of the tin coil, the peaks at the low temperatures were exceedingly sharp, practically the whole of the observable resonance curve being included in the range of the smaller, 1 MMF., condenser. As they became sharper, the curves showed a peculiarity that is illustrated in the right-hand graph of fig. 5. The curves followed a different course according as the peak was approached from the side of lower or from that of higher frequency. The two peaks thus obtained, A with increasing frequency, B with decreasing frequency, were of different magnitude and differed slightly as to the frequency of resonance. This phenomenon of "delayed" resonance is found with an iron cored coil,* and in that case is due to the dependence of the inductance upon the current. From the equation

$$I = \frac{E}{\sqrt{R^2 + \left(\omega L - \frac{1}{\omega C}\right)^2}}$$

---

* Morecroft, "Experimental Radio Engineering," pp. 57–60.

impossible to keep the system accurately enough at the resonance point. It was possible, however, to see quite definitely that the resistance continued to fall, as the pressure was further decreased, from the sharpness and character of the resonance peaks. Finally a point was reached where no further change was observed and the curves had the character shown in the left-hand graph of fig. 5, in which it should be noted that the vertical scale is twice that of the right-hand graph. With increasing frequency there was scarcely any change in plate current until the sudden " kick " of the galvanometer at the point A indicated that the resonance had been passed, while with decreasing frequency the curve rose as if to a peak similar to those at the higher temperatures, became flat, and suddenly reached resonance as shown at B. The extreme sharpness of resonance in the superconducting state is shown by the fact that the peaks lie completely within a fraction of one division of the scale of the small condenser, one division of which represents a change in frequency of only 0·004 per cent. The change from curves of the one type to those of the other was complete in a range of pressure from 435 mm. to 405 mm., representing a change of temperature of 0·06° K. The coil was then allowed to warm up to above the critical temperature by increasing the pressure over the helium, and a second set of observations was taken at temperatures decreasing by small steps. In this way there was obtained three values of the pressure, at which the abrupt change set in, which agreed to within 1 mm. of pressure, and with less accuracy three values of the pressure at which no further change was observable.

The resistance of the same coil of tin for direct currents was measured by attaching potentiometer leads to the two sets of plates of the condenser. The values of R/R_0 are plotted against the pressures of helium vapour in fig. 6. It will be seen that the resistance begins to fall abruptly at a pressure of 485 mm., and has vanished at a pressure of 450 mm. The corresponding pressures found with the currents of frequency $1 \cdot 14 \times 10^6$ were 435 and 405, that is, superconductivity did not begin to appear with the high frequency currents until a temperature was reached that was lower than that at which it was complete in the case of direct currents. A definite depression of the critical temperature for high frequency currents was thus indicated. The temperatures corresponding to the above pressures were obtained by the empirical formula given by Keesom.* For $T > 2 \cdot 190$ K.

$$\log_{10} \text{P cm.} = - \frac{3 \cdot 024}{T} + 2 \cdot 208 \log_{10} T + 1 \cdot 217.$$

---

* 'Commun. Phys. Lab. Univ. Leiden,' vol. 202, p. 36 (1929).

These temperatures are, for direct currents, 3·76° K. and 3·70° K.; for currents of frequency 1·14 × 10^6, 3·67° K. and 3·61° K.; a depression of corresponding points of 0·09° K.

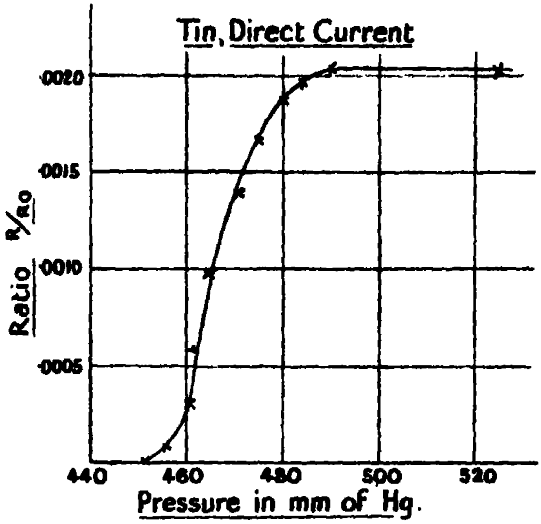

Fig. 6.

Experiments with other Frequencies.

By removing some of the tin plates of the condenser of the resonator, the latter was made to have a natural frequency of about 1·6 × 10^7, corresponding to a wave-length of 18·7 metres. The wave-length of the generator was correspondingly lowered by reducing the number of turns of copper wire in the plate and grid coils. As it was evident that more conclusive results would be obtained the greater the resistance of the coil of the resonator, the latter was wound partly non-inductively, so as to increase the resistance without a corresponding increase in inductance.

The pressures found for the "starting point" and the "vanishing point" were in this case 425 and 396 mm. respectively; which were slightly lower than those obtained with the lower frequency. The initial point was obtained with certainty, but it was difficult to fix as definitely the final point at which no further change took place. The corresponding temperatures were 3·65 and 3·59° K. respectively.

As it was apparent that the experimental difficulties for higher frequencies than this were very great, an experiment at a frequency of 0·645 × 10^7 per second (wave-length 46·5 metres) was next carried out. It had also to be shown that the apparent depressions of the critical temperature observed did

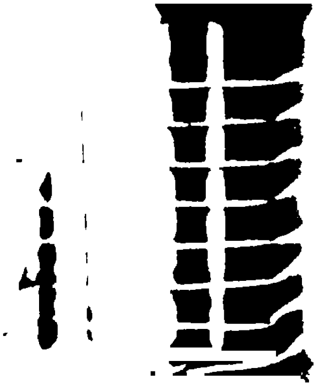

not arise from a difference between the temperature of the coil and the surrounding liquid helium, due to the heating of the former by the high frequency currents in the surface of the tin wire. The facts that no increased boiling of the helium in contact with the coil could be observed when the currents in it were increased to resonance, and that changes in the pressure of the helium vapour could be followed without any noticeable lag by the observations of the resonance peaks, were evidence against this view. There remained the possibility, however, that the effect was a manifestation of the Silsbee effect, in which the current through the superconductor produces, by its own magnetic field, a depression of the critical temperature. The currents in the high frequency experiments were of small magnitude compared to those used in the direct current experiment with the same coil, but the different distribution of the currents (skin effect) might make them sufficient to produce such a depression.

That these could not be the explanation of the phenomena was proved in the experiment with 46·5 metre waves. When the critical pressures had been found, the coupling between the resonator and generator was made less by lowering the latter, and then making a redetermination. In all, five determinations were made, in which the magnitudes of the peaks just before the superconducting point, were proportional to the numbers 1·85, 2·50, 2·80, 3·60 and 5·20. The pressures found for the point at which superconductivity started agreed among themselves to within 2 mm. of pressure, and showed no correlated progressive change. The pressure at which the final point was reached, however, showed a little change, becoming higher as the coupling was decreased. The pressures and corresponding temperatures for this frequency are included in Table III.

From (1), eliminating M

$$i_2 = -\frac{M\omega j i_1}{R'},$$

therefore

$$M^2\omega^2 = \frac{i_2^2 R'^2}{i_1^2}$$

and

$$e = -\frac{M^2\omega^2}{R'} i_1 = -\frac{R'}{i_1}[i_2]^2,$$

i.e., the square of the current in the resonator is proportional to the height of the resonance peak, when the coupling M is changed. The current in the tin coil in the experiment had therefore been changed in the ratio of 1 : $\sqrt{2\cdot 8}$ without observed change in the depression; although the heat generated by the current in the coil changed in the ratio of the square of that current, *i.e.*, 1 : 2·8. The possibility of the Silsbee effect as an explanation was at the same time ruled out.

There remained the question whether the depression was a true frequency effect, or whether it was connected with the skin effect, which was different for the different frequencies. The experiment was therefore repeated using a wire of smaller diameter, which would have a smaller skin effect, but at the same frequency as one of the previous experiments. Some commercially extruded tin wire of diameter 0·06 cm. was obtained, and it was found possible by careful cold drawing to reduce this to a diameter of 0·038 cm. The former was wound with this and the capacity was adjusted until the resonator had a natural frequency very close to that of the first experiment, with a wave-length of 27 metres. The critical pressure obtained was identical with that found with the thicker wire at approximately the same frequency, namely, 435 mm. In the few ideal cases, both of straight wires and of coils, that can be dealt with mathematically, the skin effect ratio is approximately proportional to the diameter of the wire. Since, when the diameter was changed in the ratio of 1 : 1·6 no change in the critical temperature was produced, the depression cannot be directly connected with the skin effect, but must be a function of the frequency of the currents alone.

The effect of decreasing the coupling, upon the pressure found for the final point, was carefully investigated. It was found that although the initial point was unchanged when the coupling was made less, the final point was

Table III.—Results of Experiments with Tin.

Wave-length.	Frequency $\omega \times 10^7$.	Starting point.		Vanishing point.	
		Pressure.	Temperature.	Pressure.	Temperature.
metres.		mm.	° K.	mm.	° K.
∞ (D.C.)	0	485	3·770	450	3·700
144 (diameter 0·038)	0·208	460	3·720	424	3·66
46·5 (diameter 0·060)	0·645	441	3·680	422	3·65
27·2 (diameter 0·038)	1·10	435	3·665	408	3·61
26·5 (diameter 0·060)	1·14	435	3·665	405	3·61
18·7 (diameter 0·060)	1·61	425	3·650	396	3·59

dependent upon it. When the coupling was sufficiently small, the end point became independent of the coupling, at a pressure of 408 mm. The "starting points" given in Table III are therefore to be relied upon, whilst the "vanishing points" are not to be given the same importance.

The results of an experiment with waves of 144 metres complete the table. For this frequency the coil of the resonator was of the thinner wire, wound upon a former that was a little longer than those used for the lower frequencies. The coil consisted of two layers, each of 28 turns of diameter 3·5 cm., length 6 cm., separated by fibre spacing strips. The condenser mounted above had 10 plates of tin.

Finally, the direct current resistance of the thinner tin wire was measured and its behaviour was found to be identical with that of the specimen of greater diameter.

The results for the different frequencies are shown in the graph, fig. 7, in which the pressures, and corresponding temperatures, at which the superconductivity started and "finished" are plotted against the frequency of the currents in the metal. The points on the lower curve, as has been explained,

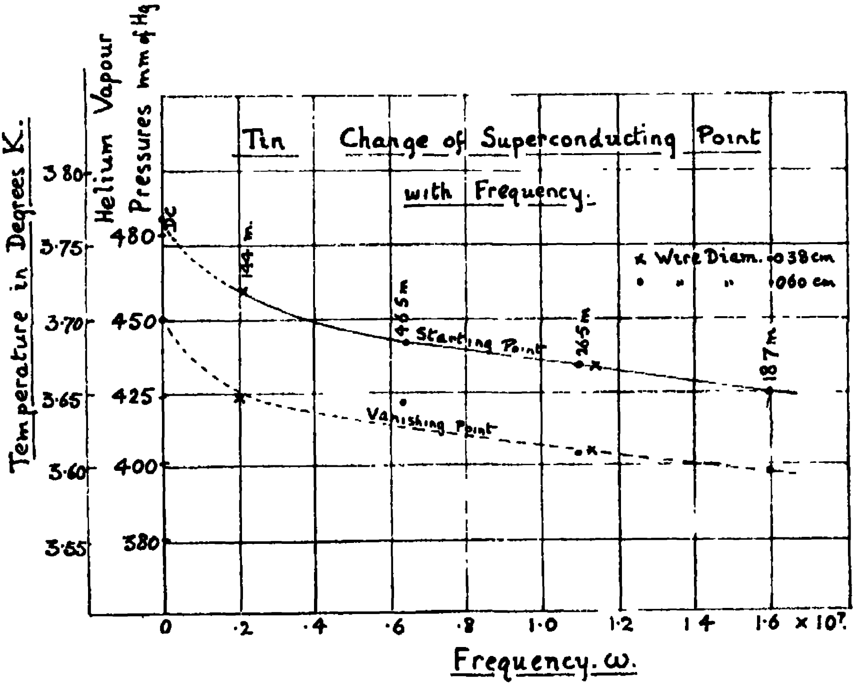

FIG. 7.

have a greater experimental error than those of the upper curve, which were reproducible to within a millimetre of pressure, or to one-five-hundredth of a degree Kelvin.

The pronounced asymmetry between the two resonance peaks obtained in the superconducting state, shown in the left-hand graph of fig. 5, can now be given an explanation. Suppose the metal is at such a temperature that, for a frequency represented by a vertical line drawn in the centre of the diagram, superconductivity is complete. For frequencies greater than this, *i.e.*, lying to the left-hand side of this line, superconductivity would not be complete. If then we approach the resonance point from the right-hand side of lower frequencies, there is complete superconductivity throughout the curve and the symmetrical curve giving the sharp resonance peak at A is obtained. Approaching from the left-hand side of higher frequency, however, we have incomplete superconductivity, and at B we reach superconductivity and the point of resonance together. It was also found, as would be predicted, that where there was any difference observable in the point at which the two peaks A and B, of the right-hand graph, begin to change, the one at the lower frequency, B, first showed the approach of superconductivity.

Experiments with Tantalum.

In order to establish whether this frequency disturbance of superconductivity was a property of superconductors in general, experiments with other metals were considered. Tantalum fulfilled best the conditions for accurate measurement, as its critical temperature, for direct currents, is about 4·38° K., which may be obtained by raising the vapour pressure over liquid helium to 900 mm. of mercury.

The frequency of $1 \cdot 14 \times 10^7$ was used, as this had given the most easily reproducible results in the experiments with tin. Pure tantalum was available in the form of wire, of diameter 0·0254 cm., and the condenser plates were cut from a sheet of tantalum of thickness 0·043 cm. As it was not possible to solder the ends of the coil to the condenser plates, and as spot-welding was found to be unsatisfactory as well as difficult, a different construction for the condenser was adopted from that illustrated in fig. 1, Plate 2. The interleaved, kidney-shaped plates, of which there were five, were mounted, two on one side, three on the other, on two brass pillars. They were separated and spaced by washers cut from the same tantalum plate and the ends of the tantalum wire coil were twisted beneath them on the pillars. When pressure was applied by screwing down nuts on the brass pillars, the plates were held rigidly in good electrical contact with the ends of the coil. As the coefficient of expansion of brass is greater than that of tantalum and the latter has great powers of elastic recovery, this contact remained good as the coil was cooled to the low temperatures. The impedance of two surfaces in close contact at high frequencies is in any case negligibly small, even if the ohmic resistance between them is considerable.

The resistance of the tantalum resonator at room temperature was greater than that of the tin coils that were used, as the diameter of the wire was much less. The resistance also decreased much less than that of the tin as the temperature was lowered, the ratio R/R_0 for direct currents, just above the superconducting point, being 0·07 instead of 0·002 for tin and 0·001 for lead. For these reasons the resonance curves at the low temperatures were much less sharp than formerly, and showed none of the peculiarities that have been discussed and are illustrated in fig. 5. Quantitative measurements of the fall of the resistance as superconductivity set in could then be made to a much greater accuracy, although the sharpness of resonance when superconductivity was complete finally rendered measurement of the peak impossible.

The progress of the measurements is shown in Table IV and illustrated in fig. 8. The values of R/R_0, corrected for skin effect, for pressures less than 917 mm., were calculated using equation (6). The abrupt fall of resistance did not begin until a pressure was reached only just greater than the atmospheric pressure, and to reach the point where the superconducting state was complete the pressure over the helium had to be reduced below that of the atmosphere.

Table IV.—Tantalum. ω 11·4 × 10^6.

Temperature ° K.	Pressure, mm. Hg.		Peak p, in cm. scale.		R'/R'_0.	R/R_0.
300	—	—	2·20	—	1·00	1·00
70	—	—	3·75	—	0·54	0·305
70	—	—	1·15	—	0·27	0·094
12·5	—	—	2·45	—	0·27	0·094
7·0	—	—	2·25	—	0·295	0·110
4·40	917	—	3·40	—	0·24	0·079
4·355	877	—	3·40	—	—	0·079
4·34	858	—	3·40	—	—	0·079
4·305	838	—	3·30	—	—	0·086
4·27	817	—	3 25	—	—	0·088
4·25	—	805	—	1·30	—	0·087
4·25	—	799	—	1·35	—	0·081
4·25	797	—	3·30	—	—	0·086
4·245	—	794	—	1·35	—	0·081
4·235	—	785	—	1·30	—	0·087
4·225	—	778	—	1·40	—	0·075
4·22	777	—	3·50	—	—	0·074

Table IV—continued.

Temperature °K.	Pressure. mm. Hg.		Peak p. in cm. scale.		R'/R'_0.	R/R_0.
4·22	—	773	—	1·50	—	0·069
4·21	—	769	—	1·55	—	0·061
4·20	765	765	3·70	1·60	—	0·0655
4·195	758	—	3·80	—	—	0·061
4·19	—	753	—	2·00	—	0·037
4·18	745	—	4·90	—	—	0·036
4·18	—	744	—	2·10	—	0·033
4·165	735	—	5·45	—	—	0·027
4·15	725	—	6·35	—	—	0·0195
4·15	—	724	—	2·90	—	0·017
4·135	715	—	7·40	—	—	0·014
4·135	—	714	—	3·40	—	0·005
4·12	705	—	Too sharp	—	—	—

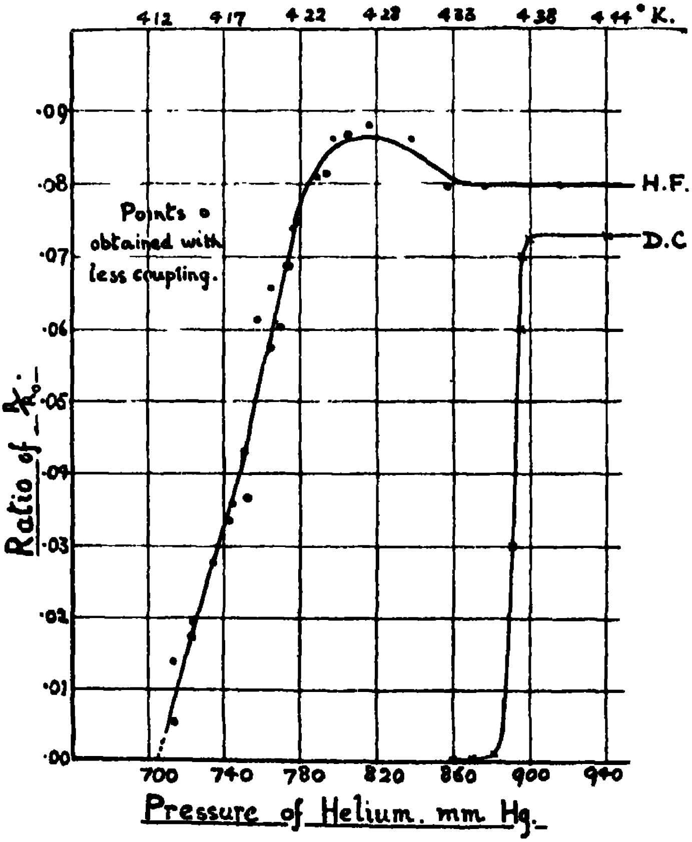

Fig. 8.

The results of an experiment with direct currents with the same coil are given in Table V, and the curve is drawn on the same graph, fig. 8. The fall in resistance was very abrupt and indicated that the sample of tantalum wire was of very high purity compared with those investigated by Onnes.*

Table V. —Tantalum. D.C.

Pressure, mm. Hg.	Kelvin temperature.	R/R_0.
	°	
-	300	1·000
—	85	0·322
	11	0·0726
-	7	0·0725
904	—	0·0726
900	4·38	0·0726
897		0·0700
896	—	0·0600
892	4·37	0·0200
888	-	0·0200
882	4·36	0·0100
871	—	0·0030
860	4·34	0·0020
858	-	0·000

There is a very definite depression of the critical temperature, amounting to about 0·22° K., *corresponding to a shift in the vapour pressure from* 900 *mm. to* 800 mm. The apparent rise in the resistance to high frequency currents just before the fall to superconductivity may be due to experimental error, which is much greater in this region, where the peaks are small, than for the smaller values of the resistance corresponding to larger peaks. The transition to the superconducting state is not nearly so abrupt as it is with the direct currents.

Discussion of Results.

The *experiments have established, first, that for currents of frequency* 10^7 per second there is an abrupt fall in the resistance of a superconductor corresponding to the abrupt disappearance of resistance for direct currents, when the temperature falls below a critical value. The methods of measurement and the complications that are unavoidable with these high frequencies made it impossible to find how nearly zero the high frequency resistance became in the superconducting state, but it fell to a value certainly less than, in the case of lead, one-hundredth of its original value within a range of temperature of a fraction of a degree Kelvin. Results of some reliability were obtained, for tantalum, *for the way in which the resistance decreased after the critical* temperature was reached, and it was found that the slope of the curve was much less than for the direct currents, *i.e.*, the transition to superconductivity was not so abrupt.

---

* See Meissner, 'Z. Physik,' vol. 61, p. 191 (1930).

Secondly, it has been established that the critical temperature at which the phenomenon occurs is lower for the high frequency currents than for direct currents in the same specimen.

The experiments with different amounts of coupling of the generator to the tin resonator coils proved that this depression of the critical temperature was not dependent upon the magnitude of the high frequency currents in the metal, and was therefore attributable neither to the heating of the coil above the surrounding helium nor to the effect of the magnetic field of the currents. Experiments with wires of different sizes but with the same frequency showed that the depression was not a direct function of the skin effect. It must then be a *function of the frequency of the currents in the metal alone.*

Further, the amount of the depression of the temperature increases with increase of frequency in the manner shown by the graph, fig. 7. Though the curve is continued by the dotted line to reach the axis of zero frequency at an oblique tangent, it might be expected that the true tangent at the axis would be horizontal, the departure beginning at some frequency of the order of 10^6 or less. It would be desirable to settle this point experimentally, but the depression of temperature would in either case be so small in this region that a definite conclusion would be difficult to obtain.

The curve appears to become linear at the higher frequencies, and if the extrapolation to the zero of the temperature scale be made on this supposition a frequency of the order of 10^9 is reached. This is true even if a parabolic law is fitted to the experimental points. The conclusion, if this extrapolation is justified, is that for frequencies greater than this, which corresponds to a wave-length of the order of 30 cm., the superconducting state does not exist. In support of this is the fact that no evidence of an abrupt change corresponding to superconductivity has been observed with light waves, experiments so far having given a negative result.*

The disturbance of the superconducting point by frequency of the applied field must then be added, with its theoretical implications, to the other known disturbing effects that change the critical temperature, as that of a magnetic field, of tension, and of alloying with foreign metals.

---

* McLennan, Hunter and McLeod, 'Proc. Roy. Soc. Canada,' 3, vol. 24, p. 3 (1930). Some unpublished work done in this laboratory on the absorption of light in lead films at the superconducting temperature.

All "orientation" effects, that is, phenomena which involve vector quantities, are considerably modified in high frequency fields provided the frequency is sufficiently high. A well-known example is the dielectric constant, which rapidly diminishes in value for high frequency fields, falling, in the case of water, from the value 80 for fields of frequency up to 10^7 per second, to (the square of the refractive index) 1·8, for the frequency of light waves. The frequency at which the modification becomes considerable is that whose time period is comparable with the "relaxation time" associated with the phenomenon. The work of Debye and his associates has yielded much information as to the magnitude of this quantity in polar liquids, but of the corresponding quantity for solids little is known. In the case of ice, the experimental evidence shows that the relaxation time is of the order of 10^{-6} second at 0° C., and that it rapidly increases as the temperature is lowered.* It might be expected that the corresponding relaxation for a metal lattice at very low temperatures would be comparable to an oscillation period lying well within the radio-frequency range.

The corresponding decrease in the magnetic permeability as the frequency is increased has recently been established by the experiments of Arkadiew† and Wien.‡ In this case the modification does not become appreciable until a frequency corresponding to a wave-length of 5 metres is reached, *i.e.*, the relaxation time is of the order of 10^{-8} seconds.

The introduction of high frequency fields instead of static fields usually modifies the mathematic analysis by the introduction of a factor $\frac{1}{1 + j\omega\tau}$, where ω is the frequency and τ the relaxation time, *i.e.*, of an amplitude factor $\frac{1}{(1 + \omega^2\tau^2)}$ together with a phase difference. If inertia has to be considered as well as frictional forces, the factor takes the form

$$\frac{1}{[(1 - a\omega^2)^2 + \omega^2\tau^2]^{\frac{1}{2}}}.$$

In a recent theory, due to L. V. King,§ which develops the theory of J. J.

---

* Errara, 'J. Phys.,' 6, vol. 5, p. 304 (1924); J. Granier, 'C. R. Acad. Sci., Paris,' vol. 179, p. 1314 (1924); Debye and Wintsch, (Debye) "Polar Molecules," p. 102, para. 20, *et seq.*

† 'Ann. Physik,' vol. 11, p. 406 (1931).

‡ 'Ann. Physik,' vol. 11, p. 423 (1931).

§ Not yet published.

Thomson,[*] the superconducting state is connected with the existence of a permanent state of dielectric polarisation in the metal lattice, as would be predicted from the ordinary equations for the polarisation under an applied field, if the polarisability became great enough with fall of temperature. In this state the internal field of the oriented dipoles is sufficient to hold them so oriented against the tendency of thermal agitation to re-orient them at random. It seems to us that with higher frequency fields, with the introduction of a factor such as given above, the polarisability becomes less, and a lower temperature has to be reached before the condition for permanent polarisation is fulfilled. The simple theoretical treatment, however, does not give for the variation with frequency the form of the curve found experimentally.

It is of interest to make the analogy between superconductivity and piezoelectric phenomena, such as occur in quartz. Perrier[†] found that the piezoelectric properties observable at room temperature disappeared quite suddenly when the temperature was raised above the critical point of 580° C. He concluded at the time that there was a transformation exactly analogous to the loss of ferro-magnetism at the Curie point, in which the spontaneous magnetic polarisation of the microstructures disappears. Quartz is a dielectric, but it has a small conductivity, which is many hundreds of times greater along the axis of polarisation than in directions at right angles. A similar type of phenomenon occurring at low temperatures in a metal, in which we have the additional factor of the existence of free electrons, might give superconductivity. The later X-ray measurements show, however, that a small change in the crystal structure of quartz takes place at the critical temperature which is sufficient to explain the facts of piezo-electricity, and that the hypothesis of spontaneous polarisation seems to be disposed of. There has been no evidence of a connection between superconductivity and crystal structure.

The analogy of superconductivity with ferromagnetism and of the superconducting critical temperature with the Curie point, is given additional emphasis by these experiments, for in 1914 J. R. Ashworth[‡] found that an alternating field produced a lowering of the Curie point. Confirmatory experiments have not been reported. It is to be hoped that superconductivity will prove to have an explanation along similar lines to the theory of ferromagnetism, in which case much of the work of Heisenberg might be taken over into the new field. When results have been obtained for more metals than the three already investigated, a correlation between the magnetic disturbance and the frequency disturbance of the critical point may be possible. At present we know that the latter effect is greater in tantalum than in tin, and probably greater in lead than in either. The magnetic disturbance is greater in lead than in tin; that of tantalum has not been investigated.

---

[*] 'Phil. Mag.,' vol. 30, p. 192 (1915).

[†] 'Arch. Sci. phy. nat.,' vol. 41, p. 493 (1916).

[‡] 'Phil. Mag.,' vol. 27, p. 357 (1914); "Nature," vol. 12, p. 1003 (1931).

The data so far obtained are far too incomplete to justify any attempt at a quantitative explanation, but a new road of attack upon the fundamental problem of superconductivity seems to be opened up by the discovery of the frequency disturbance.

Summary.

In the experiments described in this paper it was found that with currents of frequency $1 \cdot 1 \times 10^7$ per second a coil of lead wire showed an abrupt loss of resistance, of relatively large amount, at a temperature that appeared to be slightly lower than the critical temperature 7·2° K. characteristic of the transition to superconductivity, found for the same wire with direct current.

In a series of repeated experiments with a coil of tin wire, drawn to a diameter of 0·3 mm., it was found that with direct currents the resistance of the coil began to decrease abruptly at 3·76° K. and disappeared completely at 3·70° K. Experiments with the same coil with currents of frequency $1 \cdot 1 \times 10^7$ per second gave for the corresponding temperatures 3·67° K. and 3·61° K., *i.e.*, superconductivity did not begin to appear until a temperature was reached that was below the one at which it was complete in the case of the direct current experiments. Further experiments with higher frequencies revealed depressions of the critical transition temperature increasing in amount with the frequency. Extrapolation of the transition temperature-frequency curve, which appeared to be linear for the higher frequencies, gave 10^9 per second for the frequency corresponding to 0° K.

With tantalum wires results were obtained similar in character to those found with wires of tin and of lead. Experiments with tin wire coils showed that the observed depression of the critical temperature was not dependent upon the magnitude of the high frequency currents in the coils and was therefore attributable neither to the heating of the coils above the temperature of the surrounding liquid helium, nor to the effect of the magnetic field of the currents. Experiments with wires of different sizes made with currents of the same frequency showed that the depression of the transition temperature was not a direct function of the skin effect. It would appear then to be a function of the frequency of the current in the metal alone.

The conclusion is drawn that polarisation and orientation phenomena are involved in the production of the superconducting state in metals. This electrical state, it is pointed out, appears in part at least to be somewhat analogous to the saturated magnetic state obtainable with ferromagnetic metals.

In conclusion, we should like to record our appreciation of the valuable help rendered in this investigation by the skilful glass-blower of the laboratory, Mr. R. H. Chappell.

The Determination of the Heat of Dissociation of Fluorine and of the Latent Heat of Vaporisation of Lithium.

By Manohar S. Desai, M.Sc., Research Scholar, Department of Physics, Allahabad University, India.

(Communicated by M. N. Saha, F.R.S.—Received October 19, 1931).

The heats of dissociation of chlorine,* bromine,† and iodine‡ have been determined by thermal methods and estimated to be 58·9, 45·2 and 35·2 kilo-cals. respectively. But no data are yet known concerning the heat of dissociation of fluorine. It is very difficult to subject fluorine to the same treatment as Cl_2, Br_2 and I_2 (*i.e.*, heating to a high temperature in a sealed quartz bulb) owing to its extreme chemical reactivity, and hence no direct method of determining the heat of dissociation of fluorine has yet been devised.

In the present paper I have determined it indirectly by interpretation of the absorption spectra of alkali fluorides (for the present only NaF and KF).

A short theory of the experiment is given below.

Theory.

Kratzer's theory of a diatomic molecule has been reconsidered by Born and Franck§ for a molecule nearing dissociation. According to these authors, all ionic compounds, particularly the halides of alkalies, when in a vaporised state possess a region of continuous absorption beginning from a long wave-length limit. When light of this wave-length falls on an alkali-halide molecule, the electron passes over from the halogen to the metal ion, causing splitting of the compound into two neutral atoms according to the equation

---

* Henglein, 'Z. anorg. Chem.,' vol. 123, p. 137 (1922).

† Bodenstein and Cramers, 'Z. Electrochem.,' vol. 22, p. 327 (1916).

‡ Bodenstein and Starck, 'Z. Electrochem.,' vol. 16, p. 910 (1910).

§ 'Z. Physik,' vol. 31, p. 411 (1925).

$$\mathrm{NaCl} + h\nu = \mathrm{Na} + \mathrm{Cl},$$

and when dissociation takes place light is absorbed continuously because the two atoms can separate from each other with any amount of kinetic energy.

By using these arguments of Franck a method has been evolved for determining the heat of dissociation from the absorption spectra of the alkali fluorides in the gaseous state.

If R denotes the heat required for dissociating 1 gm. atom each of M and F, we have

$$\mathrm{R\ (in\ kilo\text{-}cals.)} = \mathrm{N}\frac{h\nu}{\mathrm{J}}. \qquad (1)$$

R may be denoted as the " atomic heat of dissociation," which is short for the " heat of dissociation of the molecule into its constituent atoms."

R can be obtained from the known thermo-chemical data about the heat of formation of solid MF out of solid M and F_2; with the aid of a Born cycle.*

Thus we obtain

$$[\mathrm{M}] + \tfrac{1}{2}\mathrm{F}_2 = [\mathrm{MF}] + \mathrm{Q}_{\mathrm{MF}}$$

now

$$[\mathrm{M}] = \mathrm{M} - \mathrm{L}_{\mathrm{M}}.$$

[ ] denotes the solid state, M denotes the gaseous state, and L_M is the heat of evaporation of M.

$$\mathrm{F}_2 = 2\mathrm{F} - \mathrm{D}_{\mathrm{F}_2}.$$

D_{F_2} denotes the heat of dissociation of F_2.

$$[\mathrm{MF}] = \mathrm{MF} - \mathrm{L}_{\mathrm{MF}},$$

L_{MF} is the heat of evaporation of MF. Then from thermo-dynamical considerations it can be shown that

$$\mathrm{R} = \mathrm{Q} + \mathrm{L}_{\mathrm{M}} + \tfrac{1}{2}\mathrm{D}_{\mathrm{F}_2} - \mathrm{L}_{\mathrm{MF}}. \qquad (2)$$

R can be obtained from the equation (1), and we have

$$\tfrac{1}{2}\mathrm{D}_{\mathrm{F}_2} = \mathrm{R} - [\mathrm{Q} + \mathrm{L}_{\mathrm{M}} - \mathrm{L}_{\mathrm{MF}}]. \qquad (2')$$

The Experiment.

Anhydrous NaF and KF were vaporised inside a vacuum furnace and their absorption spectra photographed by passing a beam of continuous light through the vapour.

---

* Fowler, " Statistical Mechanics," p. 255.

The furnace used was the vacuum graphite furnace of this laboratory, see fig. 1.

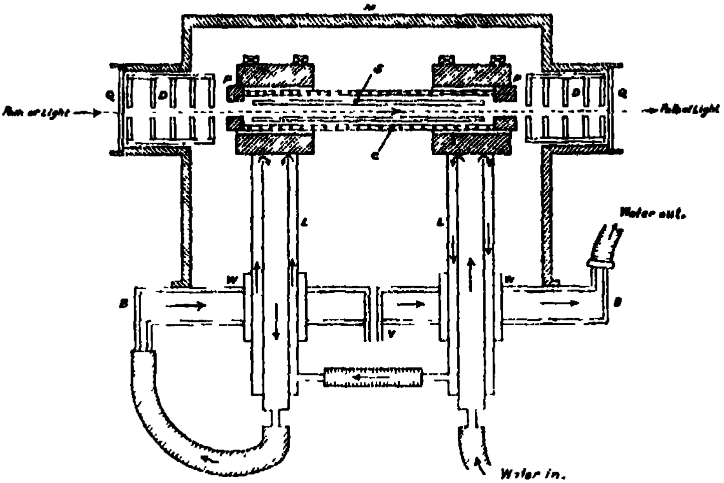

FIG. 1.

B, water-cooled brass base. M, cast-iron mantle sealed vacuum tight over B by means of a sealing mixture. QQ, quartz windows cooled by water jackets (not shown in the figure) and sealed by means of shellac to M. LL, two double-walled iron tubes, cooled by a water current, and insulated from the base by rubber washers WW. V, brass tube connecting the furnace to vacuum pump and nitrogen cylinder; LL carry iron heads with cylindrical holes. C, Acheson graphite tube, about 2 mm. thick and about 10 cm. long, which is placed between the iron heads, and fixed to these by iron collars. A packing of copper foils is used for good contact. LL are connected by means of thick copper leads (1 sq. in. in cross-section) to the terminals of a soldering low tension transformer. This gives a maximum of about 1000 amp. at a pressure of 10 volts. The transformer is fed from an A.C. generator (50 ~ 100 volts, 100 amp.). When such a high current is passed through C, it becomes white hot. An insulated iron mantle (not shown in the figure) is put round C to prevent extra loss of energy by radiation. The halide is placed inside the silica tube S. As the substance evaporates too rapidly *in vacuo*, the furnace was filled with nitrogen at about 50 cm. pressure. Under these conditions a good mass of vapour was obtained inside the tube. To prevent contamination of the quartz plates QQ by condensation of vapour, a number of brass diaphragms DD were inserted at each end between P and Q.

The spectrum was photographed by means of a Hilger E_2 quartz spectroscope. The time of exposure was 2–3 minutes with fairly wide slits. The source of continuous light was an underwater spark worked by a 16-inch induction coil, and a large kerosine oil condenser (made of tin and glass plates). A copper arc was used for comparison.

For sodium fluoride the absorption became noticeable at about λ 2370, and for potassium fluoride at about λ 2240.

Discussion of Experimental Results.

We have

$$\tfrac{1}{2}D_{F_2} = R - [Q + L_{Na} - L_{NaF}], \tag{2'}$$

and for NaF we have $\lambda = 2370$ Å.U., and KF we have $\lambda = 2240$ Å.U.

It can be shown that if we divide 286,000 by the value of λ (expressed in Å. units) we get the quantity R in kilo-cals. The data, in Table I, for the other quantities are taken from Landolt and Börnstein's tables.*

Table I.

Fluorides.	Q.	L_M.	L_{MF}.	Boiling point in ° C.
LiF	120	—	55	1676
NaF	111	26	56	—
KF	109	24	42	1504
RbF	108	16·3	40	1352
CsF	107	15·5	35	1254

NOTE.—It may be noted here that the values of L_M given in the above table are not taken directly from Landolt and Börnstein's tables, but are calculated from the vapour pressure data for the metals (given in these tables) according to the equation

$$L = R\frac{T_1 T_2}{T_1 - T_2} \log_e \frac{P_1}{P_2}, \tag{3}$$

where R is the constant 1·985, P_1 and P_2 are the vapour pressures of the metal at the absolute temperatures T_1 and T_2, and L is the latent heat of vaporisation of the metal.

The values of L thus calculated for alkali metals are given in the column 4 of the table and are made use of in the calculation of D_{F_2}. No vapour pressure data are available for lithium.

Calculations.

(1) *Sodium Fluoride.*

$$\lambda_{obs} = 2370 \text{ Å.U.}$$

$$R = \frac{286000}{2370}$$

$$= 120 \text{ kilo-cals.}$$

therefore

$$\tfrac{1}{2}D_{F_2} = 120 - (111 + 26 - 56)$$

$$= 120 - 81$$

$$= 39 \text{ kilo-cals.}$$

or

$$D_{F_2} = 78 \text{ kilo-cals.} \tag{A}$$

---

* Landolt and Börnstein, "Physikatish-Chemische Tabellen," 3rd ed., Berlin (1923).

(2) *Potassium Fluoride.*

$$\lambda_{obs} = 2240 \text{ Å.U.}$$

$$R = \frac{286000}{2240}$$

$$= 128 \text{ kilo-cals.}$$

therefore

$$\tfrac{1}{2}D_{F_2} = 128 - (109 + 24 - 42)$$

$$= 37 \text{ kilo-cals.}$$

or

$$D_{F_2} = 74 \text{ kilo-cals.} \qquad (B)$$

It appears therefore that the heat of dissociation of fluorine is

$$76 \pm 2 \text{ kilo-cals.} \qquad (I)$$

It may be remarked that it is very difficult to determine the exact stage at which the absorption just begins, for the intensity fades very gradually and the values are rather uncertain to the extent of about 10–15 Å.U. But the results obtained may be considered correct within the limits of the experimental errors, since a change of 10–15 Å.U. in λ involves a change of 1–2 kilo-cals. in the final results.

The Latent Heat of Vaporisation of Lithium.

Further experiments were carried out on the absorption spectrum of LiF. The absorption was found to be continuous and began from λ 2160; hence we find that the value of R for LiF is 132·4 kilo-cals.

The latent heat of vaporisation of lithium is not yet known, as there are practically no measurements of its vapour pressure. But making use of the formula (2)

$$R = Q + \tfrac{1}{2}D_{F_2} + L_{Li} - L_{(LiF)},$$

and using the value of $D_{F_2} = 76$ kilo-cals. obtained above, we find

$$L = 29 \cdot 4 \text{ kilo-cals.}$$

This is a very likely value, as can be seen from the following arguments. The vapour-pressure of sodium has been determined very carefully by Ladenburg and Thiele* between the temperatures 614° A. and 771° A. They find that the pressure in millimetres is given by the empirical formula

$$\log p_{Na} = -\frac{26077}{4 \cdot 573 \times T} - 1 \cdot 178 \log T + 11 \cdot 329, \qquad (4)$$

---

* 'Z. phys. Chem.,' vol. 7, p. 167 (1930).

here 26077 cals. represent the latent heat of vaporisation of Na. 1·178 represents the specific heat term (atomic), and 11·329 includes the chemical constant given by the formula

$$C = -1\cdot588 + 3/2 \log M, \qquad (5)$$

where M is the atomic weight.

As sodium and lithium are very similar in nature and in their properties, their specific heat terms would be nearly the same, hence the vapour pressure of lithium should be given approximately by the formula

$$\log p_{Li} = -\frac{29400}{4\cdot573 \times T} - 1\cdot178 \log T + 10\cdot554. \qquad (6)$$

The last term 10·554 is obtained by deducting (3/2 log 23/7) from the corresponding term in the sodium formula, as the chemical constant of Li is less than that of Na by this amount.

The boiling point of lithium, as recorded in Landolt and Börnstein's tables is 1400° C. or 1673° A. Putting T = 1673 in (6), we obtain p_{Li} at 1673° A, to be 828 mm. We obtain the theoretical value of p_{Li}, viz., 760 mm., if we put $L_{(Li)}$ 29570 instead of 29400 cals. The agreement is therefore as good as can be expected.

Thus the latent heat of vaporisation of lithium cannot differ much from that of the value obtained by this method, viz.,

$$29\cdot4 \text{ kilo-cals.} \qquad \text{(II)}$$

Summary.

In the present paper, the absorption spectra of the fluorides of potassium and sodium in the vapour state have been obtained. The absorption is continuous and begins gradually from an ill-defined long wave-length limit as in the case of other alkali halides. Using Born and Franck's (*loc. cit.*) equation

$$h\nu = R = Q + \tfrac{1}{2}D_{F_2} + L_M - L_{MF},$$

where R = atomic heat of dissociation obtained from the long wave-length limit of absorption, we find D_{F_2} (since the other quantities are known) to be 76 ± 2 kilo-cals.

In the second section of the paper, the absorption spectrum of LiF has been investigated. Using Born and Franck's equation and the value of D_{F_2} obtained in the first part, the latent heat of evaporation of lithium has been calculated as 29·4 kilo-cals. per gram atom.

Acknowledgment.

My sincere thanks are due to Professor M. N. Saha, F.R.S., for his valuable guidance throughout the work.

Crystallography of the Simpler Quinones.

By W. A. Caspari.

(Communicated by F. G. Donnan, F.R.S.—Received October 24, 1931.)

The hydrocarbons benzene, naphthalene, and anthracene each yield an ortho- and a para-quinone, all of which are solid at ordinary temperatures. In general, the para-quinones are stable and easier to prepare than the ortho-quinones; chemical interest has settled chiefly about benzoquinone and ordinary (meso-) anthraquinone, and these are the only members of the series of which the crystal morphology has been well studied. In the present investigation, crystals of all the quinones concerned (except orthobenzoquinone, which is exceedingly unstable) have been prepared and described, the dimensions and symmetry of their unit cells have been worked out, and crystal structures have been assigned as far as possible. The β-angles of the monoclinic crystals have been derived from the X-ray data alone.

The X-ray spectrograms were obtained with copper radiation, pinhole beams and photographic plates being used for the most part. The spectrometer, which was constructed in the laboratory workshop, was of a simple type adaptable to either rotation or oscillation photographs as desired. The somewhat volatile crystals of benzoquinone and 1-4 naphthoquinone were covered, during photography, with gelatine capsules.

In setting up crystal structures, once the unit cells and space-groups were known, the well-established principle of the approximate constancy of atomic domains (or diameters) has been applied, and also the equally well-established fact that in rotation-photographs the layer-lines alternate in intensity, when the cell-face, normal to the axis of rotation, is interleaved by a plane of similar density. Further, it has been taken for granted that the shapes of molecules, as built into the cell, are much the same as the shapes of their structural formulæ as written by organic chemists; this again has been so frequently confirmed in the X-ray examination of organic crystals that there can be little question of its general validity. With complicated organic molecules like those of the present series, it might be premature to draw conclusions from refined intensity-measurements and considerations of structure factor, especially since the fundamental theory of scattering from electrons is not yet firmly established in all respects.

Benzoquinone crystallises in the holohedral group of the monoclinic system. Its habit is too well known to need illustration; the principal faces are (001), (110), and $(20\bar{1})$, the crystals are elongated along b and somewhat tabular upon (001), there is a first-rate cleavage along $(20\bar{1})$, and the crystals show a high degree of plasticity. According to Hintze* the axial ratio is 1·035 : 1 : 1·7100, with $\beta = 101^\circ\ 0'$. As will be gathered from the X-ray results given below, the relative length of the c axis should be divided by two, and planes $(1kl)$, as written in the older literature, should be replaced by $(2kl)$.

Well-formed crystals were easily obtained by the evaporation of benzene or acetone solutions of the freshly steam-distilled substance. X-ray analysis by the rotation and oscillation methods showed the unit cell of the crystal to be as follows:—

$$a = 7{\cdot}08\ \text{Å}.$$

$$b = 6{\cdot}79$$

$$c = 5{\cdot}80$$

$$\beta = 101^\circ\ 0',$$

from which it may be calculated that the unit cell contains the substance of two chemical molecules and that the specific gravity of the crystal is 1·310.

In all the photographs, specially intense reflections were noted from (001), (110), and $(20\bar{1})$, of which the last named was much the strongest. Reflections from a total of 32 planes were identified, among which there were no systematic (hkl) halvings. In the $(h0l)$ series, however, comprising (001), (002), (003), (200), (201), $(20\bar{1})$, (202) and $(20\bar{2})$, none but planes with even h were represented. The b plane appeared only in its second order (020). The unit cell therefore has the symmetry of space-group C_{2h}^5, for which four asymmetric lattice-units are required; and since the cell contains only one molecule beside the primary, the benzoquinone molecule must possess a symmetry of its own, in this case a centre of symmetry. The second molecule, then, is a rotated-reflected molecule and stands in the middle of four primary molecules, all in the (001) plane. So far as molecules are concerned, the crystal is built up exactly like those of naphthalene,* of diphenyl† or of the even-carbon aliphatic acids of the adipic acid series.‡

---

* Groth, 'Chem. Kryst.,' vol. 4, p. 140.

As to the position of the atoms in the unit cell some guidance is provided, in the first place, by the dimensions of the molecule itself. We may start from the assumption, which has been shown to hold good in the crystal structure of a number of benzenoid and naphthalenic substances, that the carbon atoms are arranged in a hexagonal ring. A benzene or benzoquinone molecule would then be 3–4 Å. across the ring and about 2 Å. thick, without allowing for the hydrogen (diameter about 1·0 Å.) and oxygen (diameter about 1·4 Å.) atoms which jut across space between one ring and the next. It is clear then, to begin with, that the quinone molecules cannot lie with the hexagon ring flat upon the (001) plane (interplanar distance 5·7 Å.) or the (110) plane (distance 4·85 Å.), since thereby wide empty gaps would be produced together with overcrowding in the layers. They might conceivably lie upon (010) or (100), at distances of 3·4–3·5 Å.; but it will be shown later that the molecules are in all probability flat upon (201).

Crystal structure must, *inter alia*, account for crystal habit, and conversely any evidence from habit must be of value in elucidating structure. Now the majority of organic crystals are bounded by pinacoids and by the simplest prismatic and domal forms; this is an obvious consequence of the superior reticular densities of these faces, which in turn follow from the usual types of crystal structure. When, however, there is exceptional development of so peculiar a face as $(20\bar{1})$, the cause must be sought in some factor other than reticular density. Where a molecule has a shape far removed from compactness and has outstanding fields of force, or active spots, concentrated at one or more regions of its contour, the plane in which a great number (per unit surface) of these active spots lie will be a face of great adsorbent power, consequently, according to modern views of crystal growth, a slow-growing face, and consequently one of the more highly developed faces of the actual crystal. In the benzoquinone molecule there are clearly active spots around the oxygen atoms, that is, at two opposite corners of the hexagon ring; in the crystal the prominence of (20Ī) would therefore appear to be due to a concentration of oxygen atoms upon this face. Such a concentration is effected if the line joining the two oxygen atoms lies in (201), but not if the hexagon rings lie flat upon (100).

---

* Bragg, 'Proc. Phys. Soc.,' vol. 34, p. 33 (1921).

† Hengstenberg and Mark, 'Z. Krystallog.,' vol. 70, p. 283 (1929).

‡ Caspari, 'J. Chem. Soc.,' p. 3235 (1928).

The question whether the hexagon rings lie flat upon (201) or, alternatively, upon (010), was answered by the results of rotation-photographs about the 20Ī–010 axis. These showed very clear alternations of intensity in successive layer-lines, whereas those about *b* showed normal decrease in intensity. But with molecules like benzene, naphthalene, or anthracene, pronounced alternating intensity will seldom be found when the breadth or length of the molecule is in line with the rotation axis, because fluctuations of material density along the line of the axis will be all but obliterated; whereas if the flat side lies normal, or nearly so, to the axis, there will be fairly abrupt alternations of density. It may be concluded, therefore, that the benzoquinone molecules lie in (201), and the unit cell takes the final form shown in fig. 1. Here the cell is projected upon (010), the molecules being indicated diagrammatically as sections vertically across the plane of the ring, with oxygen atoms at each end. The molecules in dotted contours lie half-way across the cell above and below the plane of the paper. It is seen that (20Ī) faces are well filled with oxygen atoms, there being 1 in 10·5 sq. Å. as against 1 in 39·4 sq. Å. in the (100) face; hence the preponderating development of the former.

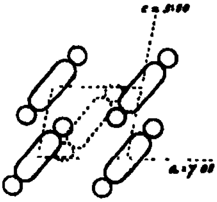

FIG. 1.

1-2 *Naphthoquinone.*—The substance is very prone to oxidation, and it was not found possible to prepare useful crystals by deposition from any kind of solvent. A method which proved successful, however, was slow sublimation *in vacuo*. The crystals so obtained were needles elongated along *c* and bounded by (100), (001), and sometimes (010); they are of a deep orange colour, contrasting markedly with the pure yellow of the para-quinones; they cleave readily along (110) and are almost as plastic as benzoquinone. X-ray analysis gave the following results:—

$$a = 3{\cdot}84 \text{ Å}.$$

$$b = 8{\cdot}10$$

$$c = 13{\cdot}40$$

$$\beta = 118^\circ\ 40',$$

whence the unit cell is found to contain two molecules, and the specific gravity is calculated to be 1·450. Among 26 reflections identified, the most intense were from (100), (011), (112), (110) and (102), in the order named. There are no systematic halvings in the (*hkl*) series, but (*h*0*l*) is halved when *l* is odd; the planes found were (002), (004), (100), (102) and $(10\bar{4})$. A moderately strong reflection is given by (010) and weaker ones by (020), (030) and also (040). Since, from the chemical formula, the molecule can only be regarded as asymmetrical, the two-molecule cell must have hemihedral symmetry, and the substance must crystallise in the domal subdivision of the monoclinic system, space-group C_s^2, although there are no visible evidences of hemihedrism.

For the structure of the 1-2 naphthoquinone crystal, the governing factor is clearly the very short *a* dimension, which corresponds to a spacing between planes of 3·37 Å. From the approximate figures for the dimensions of the benzene ring, it follows that the molecules must lie flat in (100) and that the cell may be treated as two-dimensional in that plane. The *b* dimension of the cell (8·01 Å.) is much the same as the *c* of the well-known naphthalene cell (8·69 Å.) which represents the length of the naphthalene double hexagon. Lastly, the *c* dimension of the present cell is not much longer than the overall length of two benzene rings. The primary molecules may therefore be placed as in fig. 2, when the cell is projected upon the *bc* or (100) plane.

The position of the reflected molecules, vertically in line, or nearly so, with the primary molecules as shown, follows from the fact that (010) is not interleaved; not only do odd orders of (010) appear, but layer-lines in the *b* axis photograph decrease normally in intensity.

1–4 *Naphthoquinone.*—Good crystals were procured by slow evaporation of benzene solutions of the freshly recrystallised substance. They are bounded by (110) and (012), with small occasional developments of (001), $(10\bar{1})$, and (100), and are somewhat elongated along *c*. There are no well-marked cleavages. The crystals are not notably plastic.

The X-ray results with 1-4 napthoquinone were :—

$$a = 13{\cdot}50 \text{ Å.}$$

$$b = 7{\cdot}74$$

$$c = 8{\cdot}25$$

$$\beta = 121^\circ\ 10'.$$

Four molecules make up the unit cell; the calculated specific gravity of the crystal is 1·422.

Reflections from 39 planes were identified, among which those from (002), (110), and (012) were of conspicuous intensity. No halvings in the (*hkl*) series were apparent, but the (*h*0*l*) reflections observed were (002), (200), (400), $(20\bar{2})$, $(40\bar{2})$, (101), $(10\bar{3})$, $(30\bar{1})$, and no others, in all of which $h + l$ is even. The only orders of (010) represented were the second and fourth. These data point to a cell of space-group C_{2h}^5, with a reflected-rotated molecule almost in the spatial centre of the cell. The *c* axis photograph shows a strongly marked alternation of intensity in the layer-lines, so that the (001) planes are evidently interleaved.

The crystal structure of the isomeric 1-2 naphthoquinone, together with that of naphthalene, is of assistance in interpreting that of the present substance. The cell-lengths 13·4 Å. in the former and 13·5 Å. in its present isomer correspond to two benzene hexagons side by side, and it remains to decide whether the long dimension of the naphthoquinone molecule lies along *b* (7·74 Å.) or *c* (8·25 Å.). Comparing the present cell, as before, with that of naphthalene,

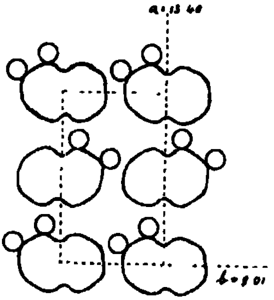

Fig. 2.

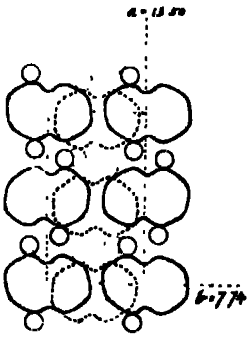

Fig. 3.

it is seen that *c* approximates more nearly to the naphthalene-length than *b*, whence an orientation of the naphthoquinone molecules lengthwise along *c* and flat upon (010) would be indicated. On the other hand, this arrangement would leave rather a wide space (3·8 Å.) between layers of molecules on the flat. The alternating layer-lines about the *c* axis, again, point rather to molecules lying flat upon (001). The balance of evidence being on the whole in favour of the latter alternative, the unit cell is drawn up, provisionally, as in fig. 3, where it is projected upon the *ab* or (001) plane. Molecules with dotted contours are situated half-way across the cell, above and below the plane of the paper. The short spacing of 7·74 Å. is not, indeed, easily reconciled with molecules end to end lengthwise, and it may be that they are somewhat tilted against (001), possibly towards (012), which is an actual crystal face.

1–2 *Anthraquinone* was prepared, together with the isomeric para-quinone, from α-anthrol by the method of Dienel.* The crude quinones were purified by sublimation. The 1–2 isomer was obtained in deep orange acicular crystals by slow evaporation of ethyl acetate solutions. The only faces noted were (110), (100) and (011), elongation being taken as along the c axis. The crystals are brittle, but show no plane of cleavage.

Two possible unit cells presented themselves, the one with the smaller β (102° 50′) having $a = 8 \cdot 90$ Å., $b = 11 \cdot 56$ Å., and $c = 9 \cdot 30$ Å. A better interpretation of crystal structure, however, can be made from the following cell:—

$$a = 11 \cdot 41 \text{ Å.}$$

$$b = 11 \cdot 56$$

$$c = 9 \cdot 30$$

$$\beta = 130^\circ\ 30',$$

whence four molecules per cell and a specific gravity of 1·480 may be calculated. Of reflections from 30 planes noted, those from (002), (110), and (022) were the most intense. The only ($h0l$) planes represented were (002), (200), (201), and ($20\bar{2}$); no halvings in the (hkl) series; no odd orders of (010). The crystal therefore belongs to space-group C_{2h}^5, and a molecule lies in the middle of (001).

A clue to the general orientation of the molecules is afforded by comparing the unit cell with that of anthracene, which is bimolecular and has $a = 8 \cdot 50$ Å., $b = 6 \cdot 02$ Å., and $c = 11 \cdot 18$ Å., with $\beta = 125^\circ\ 0'$. According to Bragg† the triple hexagon rings here lie flat, or nearly so, in (010) and c is the overall length of the molecule. Now in the 1–2 anthraquinone cell the length of the molecule, which must be much the same as that of anthracene, will lie either along the a axis (11·41 Å.) or the b axis (11·56 Å.); for the present there is no evidence to decide between the two. Assuming, by analogy with anthracene, the a position as the more probable, the cell will have its molecules flat in (010), but there will be four layers of molecules normal to b instead of two as in anthracene. The diagrammatic appearance of the cell, in projection upon (010), will then be as in fig. 4. Underneath the primary molecules are rotated molecules in dotted outlines half-way across the cell above and below the plane of the paper; the reflected and reflected-rotated molecules (these latter omitted in the figure) in the middle are one-quarter and three-quarters of the way across. The position of the molecules as shown expresses the fact that only the *a* axis rotation photographs have an intensity-distribution definitely precluding any interleaving of the (100) planes.

---

* 'Ber. deuts. chem. Ges.,' vol. 39, p. 930 (1906).

† 'Proc. Phys. Soc.,' vol. 35, p. 167 (1923).

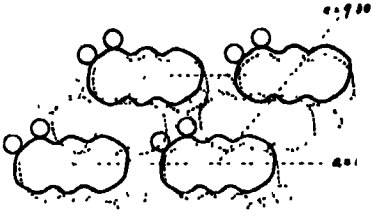

FIG. 4.

1–4 *Anthraquinone.*—This substance was found to be dimorphous. The crystals deposited from ethyl acetate solution are of tabular habit, whilst from alcohol or benzene an acicular modification settles out. When acetone solutions are allowed to evaporate slowly, both kinds are formed side by side. Both are yellow like 1–4 naphthoquinone, and of brittle consistency.

Tabular Modification.—The crystals have (001) much developed; the bounding faces are (100), (010), and (10$\bar{6}$); no cleavage was observed. The unit cell was found to be

$$a = 4{\cdot}19 \text{ Å.}$$
$$b = 5{\cdot}81$$
$$c = 19{\cdot}62$$
$$\beta = 101^\circ\ 30',$$

which gives two molecules to the cell and a specific gravity of 1·477. Among reflections from 27 planes identified, (100), (120), (002), and (014) were the strongest; the base appeared in all even orders up to (008). No (*hkl*) halvings; besides (001) there occurred (100), (202), (104), and (10$\bar{6}$); (0*k*0) as (020) only. The space-group is thus the hemihedral one C_s^2, as in the case of 1–2 naphthoquinone, and there is a reflected molecule in the middle of the (100) face.

In so narrow a cell the long dimension of the molecules, at an overall length of a fraction over 11 Å., can only be accommodated in a line not much inclined to the *c* axis; but if they lay actually along *c*, there would be a gap of about 8 Å. between consecutive molecules. The diagonal of half the cell, however, corresponding to (102), works out at 11·55 Å., which is approximately the length of a molecule. On placing anthraquinone molecules, accordingly, flat upon the (102) plane, we have $b = 5\cdot81$ Å. for the breadth of the molecule and $3\cdot53$ Å. for the distance between planes of molecules all on the flat. These dimensions agree with the approximate overall breadth and thickness of a benzene ring. Projected upon the *bc* or (010) plane, then, the cell appears as in fig. 5. Intensities of layer-lines on the rotation photographs are in harmony with this disposition of the molecules: those about *a* and *b* show decided non-alteration, whilst in that about *c* intensities are much the same up to the sixth layer-line, and (004) is stronger than (002).

Acicular Modification.—This would appear to correspond to the needles in which 1–4 anthraquinone is described as crystallising in the organic chemistry literature. The forms observed were (110) bounded by (001), and no others; imperfect cleavage along (001). The unit cell was found to be

$$a = 13\cdot82 \text{ Å.}$$

$$b = 9\cdot54$$

$$c = 7\cdot31$$

$$\beta = 100° \ 50',$$

and therefore contains four molecules, the calculated specific gravity of the crystal being $1\cdot461$. The strongest reflections, among 26 identified, were from (200) and (012). The *c* axis rotation photograph has pronounced alternation of intensity in the layer-lines. No general *hkl* or *h0l* halvings could be detected; (010) appeared only as (020) and (040). The space-group to be assigned to the crystal is therefore C_{2h}^{2}.

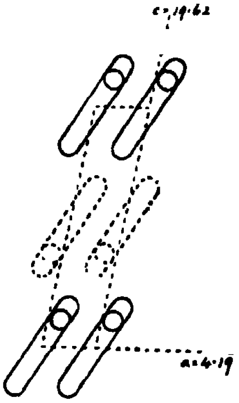

Fig. 5.

From the character of the *c* axis photograph, the unit cell is evidently two-storied along *c*; the flat of the molecules may be taken as lying in or near (001), of which half the spacing is $3\cdot65$ Å. There must be a reflected molecule half-way along *b*; but the *b* cell-side ($9\cdot54$ Å.) is too short to accommodate two breadths of a molecule or one anthracene-length. The inference, then, is that the molecules are tilted about the *a* axis and lie in some such plane as (011), of which the spacing, namely $5\cdot72$ Å., corresponds to a benzene-ring breadth. The long dimension of the molecules thus comes to lie along *a*; since $13\cdot82$ Å. is considerably in excess of an anthracene-length, it is probable that two coplanar molecules are not in direct contact along *a*, but are interconnected through the molecule lying below. In projection upon the *bc* or (100) plane, the structure of the unit cell appears as in fig. 6; the dotted molecules are approximately half down the cell along *a*; the molecules in full lines have their oxygen-bearing ends all pointing towards the reader and the dotted ones have them all pointing in the opposite sense.

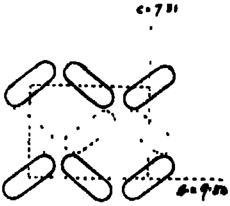

FIG. 6.

Meso-anthraquinone.—This well-known substance crystallises, unlike most anthracene derivatives, in the orthorhombic system. Angle-measurements by Fels* led to the axial ratio $a : b : c = 0\cdot8004 : 1 : 0\cdot1607$, and these figures agree with the axial lengths now found.

On slow-grown crystals from toluene or chloroform solution the forms observed were (110), (100), and (001), *c* being the axis of elongation; a fairly good cleavage was noted along (001). X-ray analysis yielded the following data:—

$$a = 19\cdot65 \text{ Å}.$$
$$b = 24\cdot57$$
$$c = 4\cdot00.$$

There are therefore eight molecules in the cell, and the specific gravity of the crystal is 1·432. Since the cell is rather more complicated than those dealt with above, the reflections identified are set out in the accompanying table.

The (*hkl*) planes are evidently halved when $h + k$ is odd. It follows that the lattice underlying the crystal is Γ'_0, a molecule identical in orientation with the corner molecules lying in the centre of the (001) cell-side. A holohedral cell built up on the Γ'_0 lattice requires 16 asymmetrical molecules, whereas only eight are here present. There is some difficulty, however, in accepting a holohedral structure of the cell. The anthraquinone molecule in that case would have to contribute an element of symmetry of its own; and the only elements compatible with the formula of anthraquinone are either a centre or a dyad axis passing lengthwise through the three rings, *i.e.*, parallel to the long dimension of the molecule. Now a dyad axis would preclude the placing of the molecule in a line with *c*, owing to the shortness of the cell in that direction; but if the dyad axis of a molecule is to lie in line with *a* or with *b*, either all *h0l* or all *hk0* reflections, or both, would have to be halved.† The table of reflections shows that neither of these general halvings obtains. Hence,

---

* Groth, 'Chem. Kryst.,' vol. 5, p. 442.

† Astbury and Yardley's classification, 'Phil. Trans.,' vol. 224, p. 235 (1924).

Reflections from Meso-Anthraquinone Crystal.

Rotation axis *a*.				Rotation axis *b*.				Rotation axis *c*.			
Plane.	Intensity.	Spacing.		Plane.	Intensity.	Spacing.		Plane.	Intensity.	Spacing.	
		Observed.	Calculated.			Observed.	Calculated.			Observed.	Calculated.
040	Strong	6·20	6·14	400	Very weak	4·92	4·91	220	Strong	7·70	7·67
080	Weak	3·09	3·07	401	Moderate	3·08	3·10	040	Strong	6·19	6·14
0120	Very weak	2·06	2·04	800	Very weak	2·44	2·45	440	Strong	3·86	3·83
111	Moderate	3·85	3·87	111	Moderate	3·84	3·87	080	Weak	3·09	3·07
151	Weak	3·07	3·06	311	Strong	3·36	3·38	480	Weak	2·62	2·60
230	Strong	7·65	7·67	511	Weak	2·78	2·79	840	Moderate	2·31	2·28
260	Weak	5·78	3·77	220	Strong	7·65	7·67	0120	Weak	2·05	2·04
221	Strong	3·51	3·54	221	Strong	3·52	3·54	880	Weak	1·93	1·92
311	Strong	3·36	3·38	620	Weak	3·13	3·16	111	Strong	3·86	3·87
331	Moderate	3·14	3·15	331	Moderate	3·13	3·15	221	Very strong	3·56	3·54
390	Very weak	2·54	2·52	531	Very weak	2·63	2·65	311	Very strong	3·39	3·38
440	Moderate	3·82	3·83	731	Weak	2·20	2·21	331	Moderate	3·17	3·15
401	Weak	3·11	3·10	440	Moderate	3·82	3·83	441	Weak	2·78	2·75
480	Weak	2·60	2·60	441	Very weak	2·75	2·77	461	Weak	2·47	2·47
530	Weak	3·54	3·54	840	Moderate	2·26	2·28	481	Weak	2·21	2·19
531	Very weak	2·63	2·65	151	Weak	3·03	3·06	661	Very weak	2·10	2·13
551	Weak	2·43	2·43	551	Very weak	2·40	2·43	681	Very weak	1·94	1·95
620	Moderate	3·16	3·16	751	Very weak	2·06	2·08	422	Moderate	1·82	1·83
661	Weak	2·15	2·13	260	Moderate	3·74	3·77	442	Moderate	1·78	1·77
750	Weak	2·45	2·43	261	Very weak	2·74	2·75	462	Weak	1·70	1·69
731	Very weak	2·23	2·21	860	Weak	2·12	2·11	662	Weak	1·58	1·57
751	Weak	2·09	2·08	480	Weak	2·59	2·60				
840	Strong	2·26	2·28								

although there is no morphological evidence of hemihedrism, the crystal would appear to be orthorhombic-bisphenoidal, with an asymmetric molecule, and to belong to one of the Q space-groups, either Q^5 or Q^6. Since there is no evidence that (001) is halved, the space-group Q^6 may be assigned to the crystal.

For the orientation of the molecules in the unit cell, it is significant, first of all, that neither (001) nor any of its orders are represented in the reflections; (001) therefore cannot be well filled with atoms, as would be expected if the molecules lay flat on (001). At the same time, it hardly seems doubtful that the centres of all the molecules in the cell are coplanar in (001), since the rotation photographs about *c* have layer-lines diminishing in intensity in a typically normal way, so that interleaving appears to be precluded. As to the lengthwise direction of the molecules, the cell dimension $b = 24 \cdot 57$ Å. is little more than two anthracene-lengths; so that the long dimension of the molecule may be placed along *b*. The symmetry conditions of the unit cell then require that the molecules shall lie as in fig. 7; they must lie, approximately at least, with their long dimensions parallel to *b*. This diagrammatic representation is not, however, to be taken as implying that the molecules lie flat in (001). Apart from the reason given above, the *c* spacing of 4·0 Å. appears somewhat excessive for such a stratification. Moreover, the overall width of a molecule (4·6 Å. at widest, containing carbon atoms only) would entail too close a fit laterally as compared with one-quarter of *a*, namely 4·91 Å., even when the dovetailing shown in fig. 7 is taken into account. The molecules, then, must be supposed to be slightly tilted out of the (001) plane. It is even possible that they might

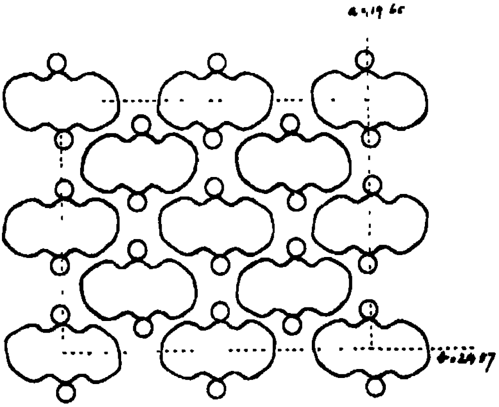

Fig. 7.

lie in the (311) plane (spacing 3·38 Å.) or the (221) plane (spacing 3·54 Å.), both of which give rise to remarkably intense reflections. Whatever tilting there be, the centres of all the molecules remain coplanar in (001), in accordance with the evidence from the *c* axis photographs. It may be added that the layer-line intensities of the *a* and *b* photographs indicate that (100) and (010) are interleaved, as would follow from the structure shown in fig. 7. Incidentally, it is seen that, if the reasoning applied above to benzoquinone be correct, (100) should be developed on the anthraquinone crystal rather than (010), owing to the oxygen atoms lying in the former plane; and such is indeed the case.

A survey of the foregoing data and structures reveals no regularities or general characteristics for quinones as a class. It had been surmised that there might be some homology between naphthoquinone and anthraquinone comparable to the well-known homology between naphthalene and anthracene; but no such connection is apparent. The "active spots" about the oxygen atoms in the molecules would appear to govern the mutual position of the molecules and to bring about a different structure for each substance. A point of some interest is that where the effect of the active spots is relatively great, either through their unsymmetrical position in the molecule or through smallness of the molecule (1–2 naphthoquinone, benzoquinone), the tendency is towards unit cells of few molecules, whereas large molecules with symmetrically disposed active spots group themselves to polymolecular cells and consequently, in the case of meso-anthraquinone, lead to higher symmetry in the crystal.

All the above structures agree well with a set of approximate overall dimensions (including the hydrogen atoms) for the simple, double, and triple benzene ring, namely, thickness about 3·6 Å., breadth 5·5–6·0 Å., length of naphthalene 8·0–8·7 Å., length of anthracene 11·2–11·5 Å. These dimensions appear in the unit cell when the molecules are side by side, but not when two molecules are linked by a third one lying in another plane.

The writer wishes to express his indebtedness to Imperial Chemical Industries, Ltd., for permission to publish this work. Some of the measurements were carried out in the Davy-Faraday Laboratory of the Royal Institution, to which body he is obliged for facilities accorded.

On the Torsion of Cylinders of Symmetrical Section.

By W. J. Duncan, D.Sc., A.M.I.Mech.E.

(Communicated by R. V. Southwell, F.R.S.—Received October 27, 1931.)

§ 1. *Introduction and Summary.*—Several methods are already known for the approximate solution of the St. Venant torsion problem for cylinders of arbitrary sectional form.* In the present investigation the object is to obtain a solution by calculation directly from the equation to the boundary of the section.

In many technical problems the section of the cylinder is thin, *i.e.*, the ratio of breadth to length is small, and particular interest therefore attaches to methods which are specially adapted to such cases. Accordingly the method suggested here is to expand the solution in ascending powers of a "thickness parameter"; and the solution is applicable to the family of boundaries which are obtained by variation of the parameter. Hitherto the method has only been applied to solid sections having an axis of symmetry, and the boundaries of the family are accordingly orthogonal projections of one another.†

In a few simple cases, such as the ellipse, the method readily yields the exact solution, but in general the coefficient of the *n*th power of the thickness parameter cannot be given explicitly. These coefficients are, however, obtained by a simple process of successive derivation, and examples indicate that for sections whose fineness ratio is not less than about five, a very few terms in the expansion suffice for practical requirements. No proof of the convergence of the general solution is advanced, but a criterion is established which permits the assignment of definite limits to the error in the approximation at any stage. Moreover, it is shown that, provided the boundary is smooth,‡ the percentage error in the approximation necessarily tends to zero as the thickness is reduced. Thus the solutions obtained are certainly applicable to very thin sections.

Several cases are worked out, and a cubic oval closely resembling an aerofoil section is treated in some detail as an example of method.

§ 2. *Formal Statement of the Problem.*—The problem considered is the torsion of a cylinder in the special case first treated in a general manner by St. Venant, namely, that in which the stresses are independent of the co-ordinate z measured parallel to the generators of the cylinder. The construction of the St. Venant theory need not be considered here, but it will be convenient to have a *résumé of the principal results and formulæ for easy reference.*[*]

---

* Reference to some of these methods are given in the Appendix.

† *Note added 15th February,* 1932.—Applications to the torsion of unsymmetrical cylinders and tubes, and to the flexure of cantilevers will be described in a paper which will appear shortly in the Rep. and Mem. Aero. Res. Ctee.

‡ Sharp angles on the axis of symmetry at the ends of the section are not excluded.

The complete solution can be made to depend on the determination of a shearing stress function Ψ which has a constant value on the boundary of the section and satisfies the differential equation[†]

$$\nabla^2\Psi + 2 = 0 \tag{1}$$

everywhere within the section. If μ is the rigidity of the isotropic material of the cylinder and τ is the twist per unit length, then the shearing stresses on the section are given by

$$X_z = \mu\tau \frac{\partial \Psi}{\partial y}, \tag{2}$$

and

$$Y_z = -\mu\tau \frac{\partial \Psi}{\partial x}, \tag{3}$$

while all the other stress components are zero. It follows from equations (2) and (3) that any contour of constant Ψ is a line of shearing stress and a possible boundary for the section. Further, when the boundary value of Ψ is chosen as zero, the torsional stiffness of the cylinder is given by

$$C = 2\mu \iint \Psi \, dx \, dy. \tag{4}$$

Since Ψ is not related in any way to the position of the axis of twist, it follows that the stresses and the stiffness are independent of the position of this axis. Let the origin be on the axis of twist and let

$$\psi = \Psi + \tfrac{1}{2}(x^2 + y^2). \tag{5}$$

Then by equation (1), ψ is a harmonic function and there is a conjugate function ϕ related to ψ by the equations

$$\frac{\partial \phi}{\partial x} = \frac{\partial \psi}{\partial y}, \tag{6}$$

$$\frac{\partial \phi}{\partial y} = -\frac{\partial \psi}{\partial x}. \tag{7}$$

---

[*] The formulæ of this section are for the most part as given in Love's "Mathematical Theory of Elasticity," 2nd edition, chap. XIV.

[†] Throughout the paper ∇^2 stands for the two-dimensional operator $\partial^2/\partial x^2 + \partial^2/\partial y^2$.

The components of displacement then are :

$$u = -\tau yz, \tag{8}$$

$$v = \tau zx, \tag{9}$$

$$w = \tau\phi. \tag{10}$$

All the strain components vanish except e_{zx} and e_{yz}, and these are given by the equations

$$e_{zx} = \tau\frac{\partial\Psi}{\partial y}, \tag{11}$$

$$e_{yz} = -\tau\frac{\partial\Psi}{\partial x}. \tag{12}$$

In view of the foregoing résumé it is clear that the problem under consideration can be expressed formally as follows : "Find a function Ψ which satisfies the differential equation (1) and vanishes on a specified boundary having OX as an axis of symmetry."

The process which it is proposed to use in the determination of Ψ is explained in the next section.

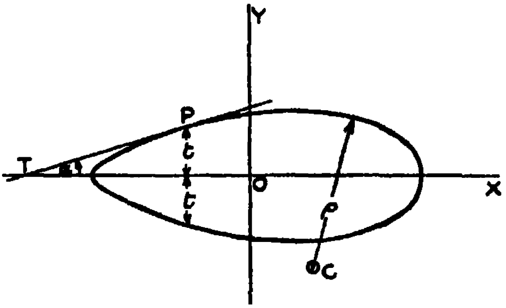

FIG. 1.

§ 3. *Determination of the Shearing Stress Function.*—The half thickness t of the section (see fig. 1) is some known function of x, and its derivatives are supposed to be continuous. Particular interest attaches to the case where t is everywhere small, and it will sometimes be convenient to write

$$t = \theta T, \tag{13}$$

where θ is a thickness parameter, independent of x, and T is an assigned function of x. The intention is to obtain a solution correct to a specified power of θ.

On account of the symmetry of the section only even powers of y can occur in the expression for Ψ. For a reason which will become apparent later it will be convenient to assume as a solution

$$\Psi = t^2 - y^2 + \sum_1^\infty (t^{2n} - y^{2n}) f^n(x). \tag{14}$$

This function vanishes on the boundary, and it only remains to find the functions* f^n so that the differential equation (1) shall be satisfied. Now

$$\begin{aligned} \nabla^2\Psi + 2 = D^2t^2 + D^2 \sum_1^\infty t^{2n} f^n(x) - \sum_1^\infty y^{2n} D^2 f^n(x) \\ - \sum_1^\infty 2n(2n-1)\, y^{2n-2} f^n(x) = 0, \end{aligned} \tag{15}$$

where D stands for d/dx. First, equate to zero the coefficient of y^2 and of the higher powers of y:

$$f^2(x) = -\frac{1}{4\cdot 3} D^2 f^1(x) = -\frac{2}{4\,!} D^2 f^1(x),$$

$$f^3(x) = -\frac{1}{5\cdot 6} D^2 f^2(x) = +\frac{2}{6\,!} D^4 f^1(x),$$

and, in general

$$f^n(x) = \frac{2(-1)^{n-1}}{(2n)\,!} D^{2n-2} f^1(x). \tag{16}$$

The superscript may now be omitted from $f^1(x)$, and on substitution from (16) the expression on the right-hand side of (15) becomes

$$D^2t^2 + 2D^2 \sum_1^\infty \frac{(-1)^{n-1} t^{2n}}{(2n)\,!} D^{2n-2} f(x) - 2f(x) = 0.$$

Hence $f(x)$ must satisfy the infinite differential equation

$$f(x) = D^2 \left\{ \tfrac{1}{2}t^2 + \frac{t^2}{2\,!} f(x) - \frac{t^4}{4\,!} D^2 f(x) + \frac{t^6}{6\,!} D^4 f(x) + \text{etc.} \right\}. \tag{17}$$

Now introduce the thickness parameter θ from equation (13). Then

$$f(x) = D^2 \left\{ \tfrac{1}{2}\theta^2 T^2 + \frac{\theta^2 T^2}{2\,!} f(x) - \frac{\theta^4 T^4}{4\,!} D^2 f(x) + \text{etc.} \right\}. \tag{18}$$

Evidently the expression for $f(x)$ must contain the second and higher even powers of θ. For sections so thin that θ^2 can be neglected, $f(x)$ is zero. A suffix notation will be used to indicate the highest power of θ retained in any approximate expression. For example $f_{2n+1}(x)$ means that approximation to

---

* The n in f^n is a mere ordinal superscript, not an index.

$f(x)$ which is correct up to the $(2n+1)$th power of θ inclusive (but it is to be observed that the highest power which appears explicitly is the $2n$th, since $f(x)$ is an even function of θ). In accordance with this notation

$$f_1(x) = 0. \tag{19}$$

The next approximation to $f(x)$ arises from the first term only on the right of (18), for the remaining terms contain the fourth or higher powers of θ. Hence

$$f_3(x) = \tfrac{1}{2}\mathrm{D}^2 t^2. \tag{20}$$

In order to condense the expressions for the higher approximations a single symbol will be used for t^2, thus

$$t^2 = \eta. \tag{21}$$

To obtain $f(x)$ correct to the fifth power of θ it is only necessary to retain the first two terms in (18), and to substitute $f_3(x)$ for $f(x)$ in the second. Hence

$$f_5(x) = \mathrm{D}^2\left\{\tfrac{1}{2}\eta + \frac{\eta}{2\,!}f_3(x)\right\}, \tag{22}$$

$$= \tfrac{1}{2}\mathrm{D}^2\eta + \tfrac{1}{4}\mathrm{D}^2\eta\mathrm{D}^2\eta, \tag{23}$$

where D^2 operates on the complete product to the right of itself. It is easy to see that the general relation corresponding to (22) is

$$f_{2n+1}(x) = \mathrm{D}^2\left\{\tfrac{1}{2}\eta + \frac{\eta}{2\,!}f_{2n-1}(x) - \frac{\eta^2}{4\,!}\mathrm{D}^2 f_{2n-3}(x) + \dots + \frac{(-1)^n\eta^{n-1}}{(2n-2)\,!}\mathrm{D}^{2n-4}f_3(x)\right\}. \tag{24}$$

Application of the formula (24) leads successively to the results

$$f_7(x) = \tfrac{1}{2}\mathrm{D}^2\eta + \tfrac{1}{4}\mathrm{D}^2\eta\mathrm{D}^2\eta + \tfrac{1}{8}\mathrm{D}^2\eta\mathrm{D}^2\eta\mathrm{D}^2\eta - \tfrac{1}{48}\mathrm{D}^2\eta^2\mathrm{D}^4\eta, \tag{25}$$

$$\begin{aligned} f_9(x) = {} & \tfrac{1}{2}\mathrm{D}^2\eta + \tfrac{1}{4}\mathrm{D}^2\eta\mathrm{D}^2\eta + \tfrac{1}{8}\mathrm{D}^2\eta\mathrm{D}^2\eta\mathrm{D}^2\eta + \tfrac{1}{16}\mathrm{D}^2\eta\mathrm{D}^2\eta\mathrm{D}^2\eta\mathrm{D}^2\eta \\ & - \tfrac{1}{48}\mathrm{D}^2\eta^2\mathrm{D}^4\eta - \tfrac{1}{96}\mathrm{D}^2\eta\mathrm{D}^2\eta^2\mathrm{D}^4\eta - \tfrac{1}{96}\mathrm{D}^2\eta^2\mathrm{D}^4\eta\,\mathrm{D}^2\eta + \tfrac{1}{1440}\mathrm{D}^2\eta^3\mathrm{D}^6\eta, \end{aligned}$$

and so on. It will be noted that the new terms in each approximation are homogeneous and of degree $2n$ in both D and t.

Upon substitution of the values of the functions $f^n(x)$ from (16) in (14) it is found that the typical approximation to the stress function is *

$$\Psi_{2n+1} = t^2 - y^2 + (t^2 - y^2)f_{2n-1}(x) - \frac{2}{4\,!}(t^4 - y^4)\mathrm{D}^2 f_{2n-3}(x) + \dots + \frac{2(-1)^{n-2}}{(2n-2)\,!}(t^{2n-2} - y^{2n-2})\mathrm{D}^{2n-4}f_3(x). \tag{27}$$

---

* Clearly y is of the first degree in θ, for $y = \theta\zeta$, where $|\zeta| \ngtr \mathrm{T}$ (see equation (13)).

The first few approximations are

$$\Psi_3 = t^2 - y^2, \tag{28}$$

$$\Psi_5 = (t^2 - y^2)(1 + \tfrac{1}{2}D^2t^2), \tag{29}$$

and

$$\Psi_7 = (t^2 - y^2)\{1 + \tfrac{1}{2}D^2t^2 + \tfrac{1}{4}D^2t^2D^2t^2\} - \tfrac{1}{24}(t^4 - y^4)D^4t^2. \tag{30}$$

The approximations to the function ψ are obtained at once from the corresponding approximations to Ψ by means of equation (5). In order to derive the approximations to ϕ it is necessary to observe that differentiation with respect to y reduces the degree in θ of a function by unity. Hence equations (6) and (7) yield

$$\frac{\partial \phi_{2n}}{\partial x} = \frac{\partial \psi_{2n+1}}{\partial y}, \tag{31}$$

and

$$\frac{\partial \phi_{2n}}{\partial y} = \frac{\partial \psi_{2n-1}}{\partial x}. \tag{32}$$

Upon substitution of the known approximations to ψ and integration the following results are obtained :—

$$\phi_2 = -xy, \tag{33}$$

$$\phi_4 = -xy - yDt^2, \tag{34}$$

$$\phi_6 = -xy - y\{Dt^2 + \tfrac{1}{2}Dt^2D^2t^2\} + \frac{y^3}{3!}D^3t^2, \tag{35}$$

$$\begin{aligned}\phi_8 = -xy - y\{Dt^2 + \tfrac{1}{2}Dt^2D^2t^2 + \tfrac{1}{4}Dt^2D^2t^2D^2t^2 - \tfrac{1}{24}Dt^4D^4t^2\} \\ + \frac{y^3}{3!}\{D^3t^2 + \tfrac{1}{2}D^3t^2D^2t^2\} - \frac{y^5}{5!}D^5t^2,\end{aligned} \tag{36}$$

and so on.

§ 4. *Geometrical Interpretation of the Approximation* Ψ_5 .—For really slender sections the approximate stress function Ψ_5 is sufficiently accurate for all practical purposes. As an example, the error in Ψ_5 for an elliptic section of fineness ratio 10 is 1 part in 10^4, while even for a fineness ratio of 5 the error is only 0·16 per cent.* On account of the usefulness of this particular approximation it is of interest to express it in terms of the simple geometrical properties of the boundary ; this may also assist in the application to boundaries of empirical form.

Let α be the inclination of the tangent to the boundary to OX (see fig. 1) and ρ the radius of curvature of the boundary (taken positive when the boundary is convex outwards as in fig. 1). Then

---

* For boundaries other than elliptic the approximation is probably not quite so good.

$$\tfrac{1}{2}D^2t^2 = tD^2t + (Dt)^2$$
$$= -\frac{t\sec^3\alpha}{\rho} + \tan^2\alpha.$$

Hence equation (29) becomes

$$\Psi_5 = (t^2 - y^2)\left(1 - \frac{t\sec\alpha}{\rho}\right)\sec^2\alpha. \tag{37}$$

§ 5. *Relation of the Present Solution to the Standard Functional Solution.*—To make clear this relation write

$$f(x) = D^2g(x). \tag{38}$$

Then equation (17) becomes

$$D^2\left\{\tfrac{1}{2}t^2 - g(x) + \frac{t^2}{2\,!}D^2g(x) - \frac{t^4}{4\,!}D^4g(x) + \text{etc.}\right\} = 0. \tag{39}$$

Since, by equation (38), $g(x)$ is arbitrary to a linear function of x, the expression inside the bracket in (39) can be equated to zero without loss of generality. Hence

$$t^2 = 2\left\{1 - \frac{t^2}{2\,!}D^2 + \frac{t^4}{4\,!}D^4 + \text{etc.}\right\}g(x)$$
$$= 2\cos tD\,.\,g(x)$$
$$= (e^{itD} + e^{-itD})\,.\,g(x)$$
$$= g(x + it) + g(x - it). \tag{40}$$

Also from equations (14) and (16)

$$\Psi = t^2 - y^2 + 2\sum_1^\infty (t^{2n} - y^{2n})\frac{(-1)^{n-1}}{(2n)\,!}D^{2n-2}f(x), \tag{41}$$
$$= t^2 - y^2 - 2\left\{1 - \frac{t^2}{2\,!}D^2 + \frac{t^4}{4\,!}D^4 + \text{etc.}\right\}g(x)$$
$$+ 2\left\{1 - \frac{y^2}{2\,!}D^2 + \frac{y^4}{4\,!}D^4 + \text{etc.}\right\}g(x)$$
$$= t^2 - y^2 - g(x + it) - g(x - it) + g(x + iy) + g(x - iy)$$
$$= g(x + iy) + g(x - iy) - y^2, \tag{42}$$

on account of equation (40). This is the standard solution of the differential equation (1) for the case of symmetry about OX. The condition that Ψ vanishes on the boundary is expressed by equation (40).

§ 6. *Discussion of the Errors in the Approximations to the Shearing Stress Functions.*—While numerical examples indicate that the successive approximations to the stress function converge rapidly towards the true value (see §§ 8, 9, 10), at least for thin sections, it is nevertheless true that no proof of the convergence of the approximations has been given. It is therefore very desirable to establish a rule for the delimitation of the error in the approximation at any stage.

In the discussion use will be made of the following theorem :—

Lemma.—If z vanishes on a closed curve α, and if $\nabla^2 z$ is everywhere positive (negative) within α, then z is everywhere negative (positive) within α.

For, suppose that z is positive at some point P within α. Then there must be some closed contour β (possibly coincident with α itself) surrounding P on which z vanishes, and within which z is everywhere positive. Apply Green's theorem to the contour β :—

$$\iint\left\{\left(\frac{\partial z}{\partial x}\right)^2+\left(\frac{\partial z}{\partial y}\right)^2+z\nabla^2 z\right\}dx\,dy=\int z\frac{\partial z}{\partial \nu}\,ds=0. \qquad (43)$$

But by hypothesis the integrand is everywhere positive within β. Hence z cannot be positive at any point within α.

In terms of the well-known membrane analogue of torsion the theorem merely states that if a membrane bounded by a plane curve is everywhere loaded downwards, then the displacement will be everywhere downwards, which is sufficiently obvious.

Let Ψ' be one of the approximations to Ψ. Then Ψ' vanishes on the boundary and

$$\nabla^2\Psi' = -2+\epsilon, \qquad (44)$$

where ϵ is in general a function of x and y. If ϵ were actually zero, it would follow from the uniqueness theorem that $\Psi'=\Psi$. Suppose next that ϵ is a finite constant. Then if

$$\Psi'' = \frac{2}{2-\epsilon}\,\Psi', \qquad (45)$$

it follows that

$$\nabla^2\Psi'' = -2,$$

and that

$$\Psi'' = \Psi. \qquad (46)^*$$

---

* As an example, for the ellipse $t^2=\frac{b^2}{a^2}(a^2-x^2)$,

$$\Psi_2=(t^2-y^2),\quad\text{and}\quad \nabla^2\Psi_2=-2\left(1+\frac{b^2}{a^2}\right).$$

Hence
$$\Psi=\frac{a^2}{a^2+b^2}\Psi_2$$
(*cp.* equation (59)).

Lastly, if ϵ is variable, let ϵ_1 and ϵ_0 be its maximum and minimum values within the section. Define Ψ'_1 by the conditions that it vanishes on the boundary and satisfies the equation

$$\nabla^2\Psi'_1 = -2 + \epsilon_1. \tag{47}$$

Since ϵ_1 is a constant

$$\Psi'_1 = \frac{2-\epsilon_1}{2}\Psi. \tag{48}$$

Also $\nabla^2(\Psi'_1 - \Psi') = \epsilon_1 - \epsilon \geqslant 0$. Therefore by the lemma $\Psi' \geqslant \Psi'_1$ everywhere. Similarly, if Ψ'_0 is defined by the conditions that it vanishes on the boundary and satisfies the equation

$$\nabla^2\Psi'_0 = -2 + \epsilon_0, \tag{49}$$

then

$$\Psi'_0 = \frac{2-\epsilon_0}{2}\Psi, \tag{50}$$

and $\Psi' \leqslant \Psi'_0$ everywhere.

Hence, finally

$$\left(1 - \frac{\epsilon_1}{2}\right)\Psi \leqslant \Psi' \leqslant \left(1 - \frac{\epsilon_0}{2}\right)\Psi. \tag{51}$$

Thus upper and lower limits to the error in the approximation Ψ' can be assigned whenever ϵ_1 and ϵ_0 have been calculated. In this connection it is worthy of note that the error ϵ in the value of $\nabla^2\Psi'_{2n+1}$ must be of degree $2n$ in θ. For the coefficients of all the powers of θ vanish when the complete infinite series for Ψ' is substituted in the expression $\nabla^2\Psi' + 2$. Now the lowest power of θ in $\nabla^2(\Psi' - \Psi'_{2n+1})$ is the $2n$th, since the double differentiation with respect to y reduces the degree in θ by 2. Hence $\nabla^2\Psi'_{2n+1} + 2$ contains no power of θ lower than the $2n$th. But it obviously can contain no higher power, and it is therefore of degree $2n$, or is zero. The coefficient of θ^{2n} in ϵ is an expression involving T and its derivatives with respect to x (see equation (13)). Provided that, as postulated, the derivatives of T are all continuous, the coefficient of θ^{2n} must be finite. Hence θ can always be chosen sufficiently small to render ϵ less than any arbitrarily assigned small quantity.

§ 7. *First Example: t^2 a Linear Function of x.*—Suppose that

$$t^2 = ax + b^2. \tag{52}$$

Then by (20) $f_2(x) = 0$, and by successive application of (24) all the higher approximations to $f(x)$ vanish. Hence $f(x)$ is zero and

$$\Psi' = \Psi'_2 = t^2 - y^2, \tag{53}$$

which is obviously correct.

Since (52) cannot represent a closed boundary the solution (53) is only of limited applicability as regards torsion. The solution will hold for a thin parallel strip except near the ends, and in the neighbourhood of the vertex of the parabola in the case of a boundary composed of a parabolic arc and some other curve.

§ 8. *Second Example : t^2 a Quadratic Function of x.*—Let $D^2t^2 = \text{constant} = 2\gamma$, say. Then equation (26) gives

$$f_9(x) = \gamma + \gamma^2 + \gamma^3 + \gamma^4. \tag{54}$$

This suggests that $f_{2n+1}(x)$ is a constant, namely, $\sum_{m=1}^{m=n} \gamma^m$. An inductive proof of this will now be given.

Suppose that the formula holds for $f_{2n-1}(x)$, and therefore also for all the approximations of lower order. Since these functions f are all constants, equation (24) gives

$$\begin{aligned} f_{2n+1}(x) &= D^2 \left\{ \tfrac{1}{2}t^2 + \frac{t^2}{2!} f_{2n-1}(x) \right\} \\ &= \gamma + \gamma \sum_{m=1}^{m=n-1} \gamma^m = \sum_{m=1}^{m=n} \gamma^m. \end{aligned} \tag{55}$$

The formula is correct for $n = 4$, and it is therefore true in general. Also, provided that $|\gamma| < 1$, the series is convergent and

$$f(x) = \sum_{m=1}^{n=\infty} \gamma^m = \frac{\gamma}{1-\gamma}. \tag{56}$$

Also by (27),

$$\begin{aligned} \Psi &= (t^2 - y^2)(1 + f(x)) \\ &= \frac{t^2 - y^2}{1-\gamma}. \end{aligned} \tag{57}$$

It can be immediately verified that this expression satisfies the differential equation (1) for all values of γ.

The most important case included in the present example is the elliptic boundary given by

$$t^2 = \frac{b^2}{a^2}(a^2 - x^2), \tag{58}$$

where a and b are respectively the semi-major and semi-minor axes. Equation (57) here becomes

$$\Psi = \frac{a^2b^2 - b^2x^2 - a^2y^2}{a^2 + b^2}. \tag{59}$$

Another example is provided by the infinite wedge for which

$$t^2 = m^2x^2, \tag{60}$$

and

$$\Psi = \frac{m^2x^2 - y^2}{1 - m^2}. \tag{61}$$

The formula (61) will be applicable to a thin finite wedge except in the vicinity of the base, but for finite wedges of wide angle the formula will only hold near the vertex, since the "interference" due to the base will then be propagated far into the section. Some examples will make this clear. For the equilateral triangle the exact solution is

$$\Psi = \tfrac{1}{2}\left(1 - \frac{x}{a}\right)(x^2 - 3y^2). \tag{62}$$

Near the vertex Ψ is nearly equal to

$$\Psi' = \frac{x^2 - 3y^2}{2}, \tag{63}$$

which agrees with (61) when $m = 1/\sqrt{3}$. It will be seen that here the percentage error in Ψ' is proportional to the distance from the vertex. Again

$$\Psi = \{(3 + \sqrt{8})\,y^2 - x^2\}\left\{\frac{x^2}{a^2} - \frac{y^2}{(3 + \sqrt{8})\,a^2} - \frac{1}{2 + \sqrt{8}}\right\} \tag{64}$$

is the exact solution for a wedge of total vertical angle 45°, and having as base a hyperbolic arc whose asymptotes are inclined at 135°. Near the vertex, where x and y are small, this agrees with (61) when $m = \tan 22\tfrac{1}{2}° = \dfrac{1}{\sqrt{3 + \sqrt{8}}}$. Another relevant example is provided by Greenhill's solution for the sector of a circle. The formulæ are cumbrous and will not be quoted.*

It is worth noting that for a slightly tapered wedge, the expression (61) differs very little from the approximation $\Psi_3 = (t^2 - y^2)$. Thus, if the vertical angle is 10°, $m = \tan 5°$, and the error in Ψ_3 is only about ¾ per cent.

§ 9. *Third Example: t^2 a Cubic Function of x.*—It has not hitherto been found possible to obtain the exact solution when t^2 is a cubic in x, but the expression for the approximation Ψ_9 has been obtained and applied to a particular oval resembling an aerofoil. The error in Ψ_9 is shown to be less than 1 part in 1000 for an oval of fineness ratio 6·5.

---

* Love, "Mathematical Theory of Elasticity," p. 307 (2nd edition).

Let the equation to the boundary be

$$t^2 = \frac{\theta^2}{a}(x^3 + bx^2 + c^2x + d^3), \tag{65}$$

where θ is the thickness parameter and a, b, c, d are lengths. By equation (25)

$$\begin{aligned} f_7(x) = {} & \frac{\theta^2}{a}(3x + b) + \frac{\theta^4}{a^2}(18x^2 + 12bx + b^2 + 3c^2) \\ & + \frac{\theta^6}{a^3}\{180x^3 + 180bx^2 + 3x(13b^2 + 21c^2) + b^3 + 15bc^2 + 18d^3\}. \end{aligned} \tag{66}$$

Hence equation (27) gives

$$\begin{aligned} \Psi_9 &= (t^2 - y^2)(1 + f_7(x)) - \frac{2}{4!}(t^4 - y^4)\,\mathrm{D}^2 f_5(x) \\ &= (t^2 - y^2)\left[\begin{aligned} & 1 + \frac{\theta^2}{a}(3x+b) + \frac{\theta^4}{a^2}(18x^2+12bx+b^2+3c^2) \\ & + \frac{\theta^6}{a^3}\{180x^3+180bx^2+3x(13b^2+21c^2)+b^3+15bc^2+18d^3\} \end{aligned}\right] \\ & \qquad - \frac{3\theta^4}{a^2}(t^4 - y^4). \end{aligned} \tag{67}$$

As a particular case consider the oval whose equation is

$$\left(\frac{t}{a\theta}\right)^2 = \frac{x}{a}\left(1 - \frac{x}{a}\right)^2. \tag{68}$$

The "chord" of this oval is a, the maximum ordinate occurs at one-third chord from the nose and is given by

$$t_{\text{max.}} = \frac{2a\theta}{\sqrt{27}}.$$

Hence the fineness ratio is $\sqrt{27}/4\theta$. There is a node at the tail and the inclinations of the tangents there to the centre line are $\pm \tan^{-1}\theta$. The curve is shown accurately drawn* in fig. 2 for the case where $\theta = 1/5$.

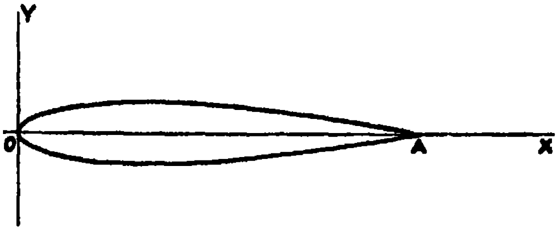

Fig. 2.

---

* The curve of course extends to the right beyond the node, but these branches irrelevant from the present point of view.

For the oval (68) the constants b, c, d have the values $b = -2a$, $c = a$, $d = 0$. Hence (67) becomes

$$\Psi_9 = (t^2 - y^2)\left[1 + \theta^2\left\{3\left(\frac{x}{a}\right) - 2\right\} + \theta^4\left\{18\left(\frac{x}{a}\right)^2 - 24\left(\frac{x}{a}\right) + 7\right\} + \theta^6\left\{180\left(\frac{x}{a}\right)^3 - 360\left(\frac{x}{a}\right)^2 + 219\left(\frac{x}{a}\right) - 38\right\}\right] - \frac{3\theta^4}{a^2}(t^4 - y^4). \qquad (69)$$

The real meaning of the formula (69) will best be made clear by an application to calculate Ψ_9 on the centre line of the section at eleven evenly spaced positions extending from nose to tail. Table I gives a summary of the results of the calculations, and serves to illustrate several interesting points. In the first place, although the numerical multipliers of the powers of (x/a) in the coefficient of θ^6, for example, are large numbers, the coefficient itself is not large.* The convergence is least rapid at the blunt nose, and is very rapid near the widest part of the section where both Ψ itself and the stresses are greatest. At the sharp tail the expression for Ψ_9 agrees with that for a wedge of the same angle (compare last line of Table I with results for wedge given in § 8).

Table I.—Values of Ψ_9 on Centre-line of Cubic Oval.

Value of (x/a).	Value of (Ψ_9/t^2).	Successive approximations to value of (Ψ_9/t^2) for $\theta = 1/5$.			
		First.	Second.	Third.	Fourth.
0	$1 - 2\theta^2 + 7\theta^4 - 38\theta^6$	1·0	0·92	0·9312	0·928768
0·1	$1 - 1{\cdot}7\theta^2 + 4{\cdot}78\theta^4 - 19{\cdot}763\theta^6$	1·0	0·932	0·939648	0·938383
0·2	$1 - 1{\cdot}4\theta^2 + 2{\cdot}92\theta^4 - 7{\cdot}544\theta^6$	1·0	0·944	0·948672	0·948189
0·3	$1 - 1{\cdot}1\theta^2 + 1{\cdot}42\theta^4 - 0{\cdot}281\theta^6$	1·0	0·956	0·958272	0·958254
0·4	$1 - 0{\cdot}8\theta^2 + 0{\cdot}22\theta^4 + 3{\cdot}088\theta^6$	1·0	0·968	0·968352	0·968550
0·5	$1 - 0{\cdot}5\theta^2 - 0{\cdot}5\theta^4 + 3{\cdot}625\theta^6$	1·0	0·98	0·9792	0·979432
0·6	$1 - 0{\cdot}2\theta^2 - 0{\cdot}92\theta^4 + 2{\cdot}392\theta^6$	1·0	0·992	0·990528	0·990681
0·7	$1 + 0{\cdot}1\theta^2 - 0{\cdot}98\theta^4 + 0{\cdot}451\theta^6$	1·0	1·004	1·002432	1·002461
0·8	$1 + 0{\cdot}4\theta^2 - 0{\cdot}68\theta^4 - 1{\cdot}136\theta^6$	1·0	1·016	1·014912	1·014839
0·9	$1 + 0{\cdot}7\theta^2 - 0{\cdot}02\theta^4 - 1{\cdot}307\theta^6$	1·0	1·028	1·027968	1·027884
1·0	$1 + \theta^2 + \theta^4 + \theta^6$	1·0	1·04	1·0416	1·041664

---

* This is, of course, related to the fact that the coefficients of the powers of θ are functions of (x/a) which all have the maximum possible number of real roots, all lying in the range $0 - 1$. The roots of the successive functions separate one another.

The errors in Ψ_9 will now be investigated by the aid of the rule established in § 6. Equation (69) yields

$$\begin{aligned} \epsilon &= \nabla^2\Psi_9 + 2 \\ &= \theta^8\left\{5310\left(\frac{x}{a}\right)^4 - 14160\left(\frac{x}{a}\right)^3 + 13212\left(\frac{x}{a}\right)^2 - 4944\left(\frac{x}{a}\right) + 584\right\} \\ &\qquad - \frac{\theta^6 y^2}{a^2}\left\{1080\left(\frac{x}{a}\right) - 720\right\}. \quad (70) \end{aligned}$$

Since y is to be regarded as of degree 1 in θ, ϵ is of degree 8 in θ, as it should be (see § 6). It is now necessary to find the absolute maximum and absolute minimum values of ϵ for points in the section. This requires :—

(1) Determination of the stationary values of ϵ *within* the section.

(2) Determination of the stationary values of ϵ upon the boundary.

(3) Determination of the values of ϵ at the two ends of the boundary.

(1) It is found that the only stationary values within the section occur on the centre line. The abscissæ and corresponding values of ϵ are :—

$0\cdot347522a$ and $-55\cdot372\theta^8$ (true minimum)
$0\cdot712766a$ and $+15\cdot28\theta^8$ (true maximum)
$0\cdot939712a$ and $-4\cdot53\theta^8$ (minimax).

(2) The abscissæ and values of the stationary values of ϵ on the boundary are :—

$0\cdot400789a$ and $-8\cdot513\theta^8$ (minimum)
$0\cdot671212a$ and $+13\cdot343\theta^8$ (maximum)
$0\cdot927999a$ and $-5\cdot700\theta^8$ (minimum).

(3) The values of ϵ at the ends of the boundary are :—

$+584\theta^8$ at the nose ($x = 0$)
$+2\theta^8$ at the tail ($x = a$).

Hence

$$\epsilon_1 = +584\theta^8,$$
$$\epsilon_0 = -55\cdot37\theta^8,$$

and equation (51) gives, if $\theta = 1/5$,

$$0\cdot999253\Psi < \Psi_9 < 1\cdot0000708\Psi,$$

or

$$\left.\begin{aligned} \Psi &> 0\cdot999929\Psi_9 \\ &< 1\cdot00074\Psi_9 \end{aligned}\right\}. \qquad (71)$$

It will be noted that the comparatively large positive values of ϵ only occur near the nose; this accords with the fact that the convergence of the solution is least rapid in that region (see Table I). Over most of the section the approximation will be considerably better than the inequalities (71) would suggest. Also there are four contours crossing the section from side to side upon which ϵ vanishes. There are accordingly five regions in the section in each of which ϵ has the sign opposite to that in the neighbouring region or regions. The membrane analogy shows that the oppositely signed errors in $\nabla^2\Psi'_9$ will to a considerable extent neutralise one another in their influence on Ψ'_9.

The stiffness of the cylinder will be calculated by the formula (4). In the integration of Ψ'_9 throughout the section integrals of the following type occur :—

$$\mathrm{I}_n = \iint (t^2 - y^2)\left(\frac{x}{a}\right)^n dx\, dy. \tag{72}$$

$$= \tfrac{4}{3}\int_0^a t^3 \left(\frac{x}{a}\right)^n dx\, dy$$

$$= \tfrac{4}{3}\, a^4\theta^3 \int_0^1 \xi^{(2n+3)/2}(1-\xi)^3\, d\xi$$

$$= \frac{128 a^4\theta^3}{(2n+5)(2n+7)(2n+9)(2n+11)}. \tag{73}$$

Also

$$\iint (t^4 - y^4)\, dx\, dy = \tfrac{8}{5}\int_0^a t^5 \,.\, dx = \frac{4096 a^6\theta^5}{5\,.\,7\,.\,9\,.\,11\,.\,13\,.\,17}. \tag{74}$$

Hence from (4) and (69)

$$\mathrm{C}_{10} = \frac{256\mu a^4\theta^3}{3465}\left(1 - \frac{11}{13}\theta^2 + \theta^4 - \frac{379}{221}\theta^6\right). \tag{75}$$

When $\theta = 1/5$ the successive approximations to the bracketed expression in (75) are

1·0

0·966154

0·967754

0·967644.

To complete the investigation of the cubic oval it only remains to examine the shearing stresses. Now interest is really confined to the greatest value of the resultant shear stress, and by Boussinesq's theorem this must occur on the boundary. Let F be the resultant shear stress on the boundary. Then from (2), (3) and (69)

$$F = \mu\tau a\theta\left(1 - \frac{x}{a}\right) Y\sqrt{Z}, \tag{76}$$

where

$$Y = 1 + \theta^2\left\{3\left(\frac{x}{a}\right) - 2\right\} + \theta^4\left\{18\left(\frac{x}{a}\right)^2 - 24\left(\frac{x}{a}\right) + 7\right\}$$
$$+ \theta^6\left\{174\left(\frac{x}{a}\right)^3 - 348\left(\frac{x}{a}\right)^2 + 213\left(\frac{x}{a}\right) - 38\right\}, \tag{77}$$

and

$$Z = 4\left(\frac{x}{a}\right) + \theta^2\left(1 - \frac{3x}{a}\right)^2. \tag{78}$$

After considerable reduction it is found that the abscissæ of the points on the boundary where F is stationary are given by the roots of the following equation where ξ is written for (x/a) :—

$$\begin{aligned} S(\xi) \equiv 12\xi - 4 &+ \theta^2(96\xi^2 - 96\xi + 16) \\ &+ \theta^4(666\xi^3 - 1110\xi^2 + 510\xi - 50) \\ &+ \theta^6(7560\xi^4 - 17640\xi^3 + 13704\xi^2 - 3864\xi + 256) = 0. \end{aligned} \tag{79}$$

Denote the root of (79) which lies within the range 0 to 1 by α, and adopt the suffix notation to indicate the highest power of θ retained. Then clearly

$$\alpha_1 = 1/3, \tag{80}$$

so that the maximum stress occurs at the widest part of the section when θ is very small. This is clearly universally true,* and the supposed rule (suggested by Boussinesq) that the greatest stress occurs at the point on the boundary nearest the centroid is completely refuted. The next and succeeding approximations to α will be obtained by Newton's method. Thus†

$$S(\alpha_1)_3 = -\frac{16}{3}\theta^2,$$

and

$$S'(\alpha_1)_3 = 12.$$

Hence

$$\alpha_3 = \alpha_1 - \frac{S(\alpha}{S'(}$$
$$= \tfrac{1}{3} + \frac{4\theta^2}{9}. \tag{81}$$

---

* Subject to the proviso that the thickness changes smoothly with x as postulated in § 3.

† $S(\alpha_r)_m$ means the value of $S(\alpha_r)$ with powers of θ up to and including the mth retained.

Next

$$S(\alpha_3)_5 = \frac{64\theta^4}{9}.$$

Hence

$$\alpha_5 = \alpha_3 - \frac{S(\alpha_3)_5}{S'(\alpha_1)_3}$$

$$= \tfrac{1}{3} + \frac{4\theta^2}{9} - \frac{16\theta^4}{27}. \qquad (82)$$

Lastly

$$S(\alpha_5)_7 = -\frac{944\theta^6}{27},$$

and

$$\alpha_7 = \alpha_5 - \frac{S(\alpha_5)_7}{S'(\alpha_1)_3}$$

$$= \tfrac{1}{3} + \frac{4\theta^2}{9} - \frac{16\theta^4}{27} + \frac{236\theta^6}{81}. \qquad (83)$$

In any given case the maximum stress can be obtained from (76) and (83).

§ 10. ***Fourth Example*****:** ***Lenticular Section*** $t^2 = b^2(1 + \cos x/a)$.—The lenticular section shown in fig. 3 will be very briefly considered as an example of the cases where t^2 is given as a transcendental function of x.

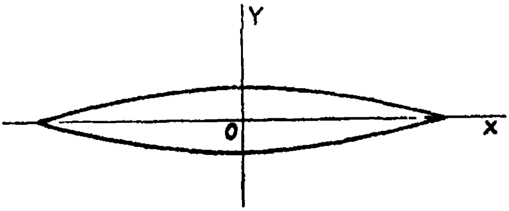

Fig. 3.

The equation to the boundary is

$$t^2 = b^2\left(1 + \cos\frac{x}{a}\right) \qquad (84)$$

or

$$t = \sqrt{2}b\cos\frac{x}{2a}, \qquad (85)$$

Hence equation (25) gives

$$f_7(x) = -\tfrac{1}{2}\frac{b^2}{a^2}\cos\frac{x}{a} + \tfrac{1}{4}\frac{b^4}{a^4}\left(\cos\frac{x}{a} + 2\cos\frac{2x}{a}\right)$$

$$-\frac{1}{192}\frac{b^6}{a^6}\left(41\cos\frac{x}{a} + 224\cos\frac{2x}{a} + 207\cos\frac{3x}{a}\right). \qquad (86)$$

Also by equation (27)

$$\Psi_9 = (t^2 - y^2)\left[\begin{array}{l} 1 - \frac{1}{2}\frac{b^2}{a^2}\cos\frac{x}{a} + \frac{1}{4}\frac{b^4}{a^4}\left(\cos\frac{x}{a} + 2\cos\frac{2x}{a}\right) \\ \qquad - \frac{1}{192}\frac{b^6}{a^6}\left(41\cos\frac{x}{a} + 224\cos\frac{2x}{a} + 207\cos\frac{3x}{a}\right)\end{array}\right]$$

$$- \frac{(t^4 - y^4)}{24a^2}\left[\frac{b^2}{a^2}\cos\frac{x}{a} - \frac{1}{2}\frac{b^4}{a^4}\left(\cos\frac{x}{a} + 8\cos\frac{2x}{a}\right)\right] - \frac{(t^6 - y^6)}{720a^4}\frac{b^2}{a^2}\cos\frac{x}{a}. \quad (87)$$

For instance, at the centre of the section where Ψ_9 is obviously a maximum

$$\Psi_9 = 2b^2\left(1 - \frac{b^2}{2a^2} + \frac{2}{3}\frac{b^4}{a^4} - \frac{114}{45}\frac{b^6}{a^6}\right). \quad (88)$$

The length of the section is $2\pi a$ and the total breadth is $2\sqrt{2}b$. Hence, if $b/a = 1/3$ as in the figure, the fineness ratio is 6·66, and the successive approximations to the value of $\Psi_9/2b^2$ are :—

1·0
0·9444
0·9527
0·9498.

APPENDIX.

Some Methods for the Solution of the St. Venant Torsion Problem for Arbitrary Boundaries.

(1) An experimental method for the approximate determination of the stress function Ψ, based on the soap bubble analogy first pointed out by L. Prandtl, has been developed by G. I. Taylor and A. A. Griffith.* The authors show that with care the method is capable of an accuracy of the order of 1 per cent.

(2) A purely graphical method, based on a process of repeated contour integration, is given by L. Bairstow and A. J. Sutton Pippard.† The order of accuracy appears to be about the same as in the soap-bubble method.

(3) J. Orr proposes an arithmetical process of successive approximation.‡ In this method, which is an adaptation of a process devised by A. Thom, the

---

* 'Proc. Instn. Mech. Eng. Lond.,' p. 755, December, 1917.

† 'Proc. Inst. Civil Eng.,' vol. 214, p. 291 (1921–22).

‡ 'Proc. Roy. Soc.,' A, vol. 131, p. 30 (1931) and 'Aero. Res. Ctee. Rep. and Mem. No. 1393.'

section of the cylinder is divided into small squares, and roughly estimated values of Ψ are assigned. The values of Ψ at the centres of the squares are then calculated by the approximate formula

$$\begin{aligned}\Psi_M &= \tfrac{1}{4}(\Psi_A + \Psi_B + \Psi_C + \Psi_D) - \tfrac{1}{8}S^2\nabla^2\Psi \\ &= \tfrac{1}{4}(\Psi_A + \Psi_B + \Psi_C + \Psi_D + S^2),\end{aligned}$$

where A, B, C, D are the corners of the square, M is its centre, and S the side. The centre values are then used to recalculate the corner values by means of the same formula, and the process is repeated until the values cease to change. Examples given in the paper show that the method is useful, more especially for sections of very irregular form.

(4) Another purely arithmetical method is based on the theorem of W. Ritz. This theorem asserts that the integral U is stationary for small variations of Ψ which vanish on the boundary, where

$$U = \iint\left\{\tfrac{1}{2}\left(\frac{\partial\Psi}{\partial x}\right)^2 + \tfrac{1}{2}\left(\frac{\partial\Psi}{\partial y}\right)^2 - 2\,\Psi\right\}dx\,dy.$$

The theorem can be proved at once by forming δU and application of Green's theorem, and it is the direct analytical expression of the fact that the total potential energy in the soap-bubble analogue must be stationary for equilibrium. In the application of the theorem, an analytical function Ψ is chosen which vanishes on the boundary and contains a number of disposable parameters or functions. The parameters or functions are then determined so as to render U stationary. It is quite clear that the success of this method depends very much on the choice of the assumed function Ψ, and it is very necessary that the resulting approximate solution should be tested by the method given in § 6 of the present paper. The method has been applied to sections bounded by parabolic arcs by L. C. Leibenzon in a paper entitled "Calculation of Torsional Stresses in Propeller Blades" (No. 65 of the 'Transactions of the Central Aero-Hydrodynamical Institute,' Moscow, 1924).

Quantum Analysis of the Rotational Structure of the First Positive Bands of Nitrogen (N_2).[*]

By S. M. Naudé, M.Sc., Ph.D., Senior Lecturer in Physics, University of Capetown, South Africa.

(Communicated by A. Fowler, F.R.S.—Received November 24, 1931.)

[Plates 3 and 4.]

I. *Introduction.*

The greenish-yellow afterglow of active nitrogen was first described by Lewis.[†] Two decades have passed since Fowler and Strutt[‡] showed that this afterglow was due to a selective excitation of a few green, yellow and red bands belonging to the first positive system of the nitrogen molecule (N_2). Recent work[§] on active nitrogen indicates that the selective excitation is due to metastable nitrogen atoms giving up their energy to metastable nitrogen molecules in state A,[||] the final state of the first positive bands, thus leading to the selective excitation of certain specific vibrational levels in state B,[||] the initial state of the first positive bands. The molecule then returns to state A, at the same time emitting the bands which constitute the afterglow.

From the rotational analysis of the second positive nitrogen bands by Lindau,[¶] and Hulthèn and Johansson,[**] it is known that state B corresponds to a $^3\Pi$ state, the second positive bands having their final state in common with the initial state of the first positive bands.[||] No definite information has been found concerning the electronic configuration of the nitrogen molecule which gives rise to state A. This can be obtained by making a detailed analysis of the rotational structure of the first positive nitrogen bands.

The first positive nitrogen bands extend from λ 5032 to λ 10500. From an analysis of the bands lying in the region between λ 5032 and λ 8903 Birge[††] obtained the first vibrational analysis. By extending the analysis to the bands having a wave-length greater than λ 8900, Poetker* showed that Birge's analysis was fundamentally correct, but that the quantum numbers in the lower vibrational state should be diminished by one and that the origin of the system should be shifted to 9518·6 cm.$^{-1}$. The vibrational formula for this system of bands becomes, according to Birge,†

---

[*] A preliminary account of this work was published in the 'Phys. Rev.,' vol. 38, p. 372 (1931).

[†] 'Astrophys. J.,' vol. 20, p. 49 (1904).

[‡] 'Proc. Roy. Soc.,' A, vol. 85, p. 377 (1911), *et seq.*

[§] G. Cario and J. Kaplan, 'Z. Physik,' vol. 58, p. 769 (1929).

[||] R. T. Birge, 'Phys. Rev.,' vol. 23, p. 294 (1924); see also H. O. Kneser, 'Ergebn. Exakt. Naturw.,' vol. 8, p. 245 (1929).

[¶] 'Z. Physik,' vol. 26, p. 343 (1924).

[**] 'Z. Physik,' vol. 26, p. 308 (1924).

[††] "Molecular Spectra in Gases," p. 135.

$$\nu = 9518 \cdot 6 + (1718 \cdot 40\, v' - 14 \cdot 437\, v'^2) - (1446 \cdot 46\, v'' - 13 \cdot 929\, v''^2). \quad (1)$$

Beyond a description of the appearance of the individual bands,‡ very little was known about their rotational structure. A few branches were found by Birge and his collaborators. After the author had started the present work, Professor Birge kindly sent him some of the material obtained in the course of their investigations which was based on plates taken by himself.§ As was anticipated, it proved advisable to obtain new data with an instrument having a larger resolving power than that used by Birge.

II. *Apparatus and Procedure.*

The rotational analysis of the first positive bands is complicated owing to the overlapping of adjacent bands. Various investigators‖ have studied the selective excitation of these bands. Since a selective excitation of only a few bands would facilitate the analysis considerably, a preliminary investigation of the most favourable conditions of excitation was first carried out with a 1½ metre concave grating. Various mixtures of pure helium, neon and argon with pure nitrogen, which was prepared by heating sodium azide *in vacuo,* were studied in differently designed discharge tubes. In every case the intensity of the selectively excited bands was so much weakened compared with their intensity in a discharge through pure nitrogen, that it would have been impossible to photograph them under large dispersion. For the same reason the use of the selective excitation in the active nitrogen afterglow was out of the question. Finally, a very powerful discharge in pure nitrogen was adopted, but instead of attempting an analysis of the more strongly developed bands, as was done by Birge and his collaborators, the main attention was directed towards the weaker bands where the overlapping of adjacent bands was necessarily less.

---

* 'Phys. Rev.,' vol. 30, p. 812 (1927).

† 'Intern. Crit. Tables,' vol. 5, p. 409 (1929).

‡ Von der Helm, 'Z. Wiss. Phot.,' vol. 8, p. 405 (1910).

§ 'Astrophys. J.,' vol. 39, p. 50 (1914).

‖ *Vide* H. O. Kneser, 'Ergebn. Exakt. Naturw.,' vol. 8, p. 245 (1929).

The positive column of a discharge in an inverted Π-tube of Pyrex glass (see fig. 1), which was constructed with large aluminium electrodes capable of carrying 1·6 amps. and which could be water-cooled, was used as source. The current was supplied by a 5 KW. transformer having a peak voltage of 6600. During exposures only 0·8 amp. was sent through the tube, giving a current density of 1·6 amp. per cm.² in the positive column of the discharge. The pressure of the nitrogen in the discharge tube was about 3 mm.

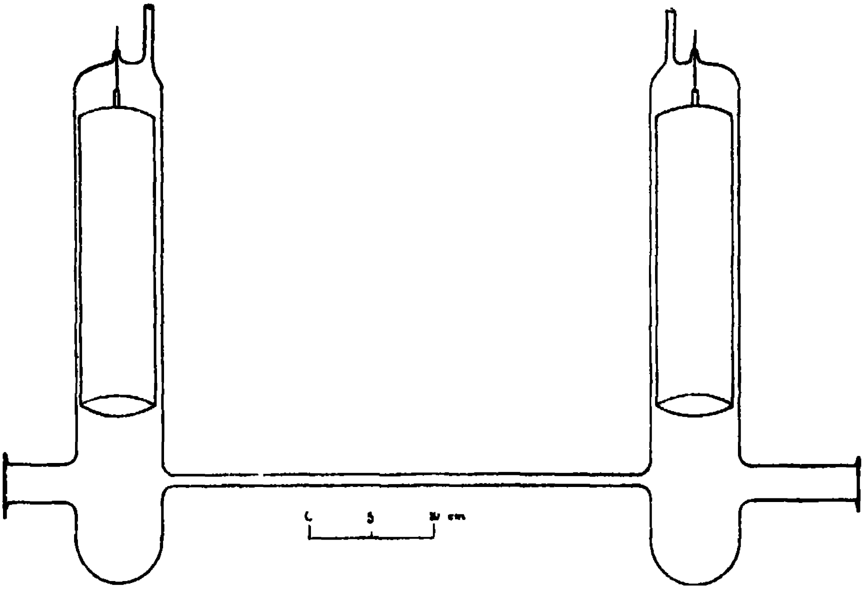

Fig. 1.—Discharge Tube.

The discharge was photographed end on in the third and second orders of the Paschen mounting of the 21-foot Rowland grating of the University of Chicago. The dispersion thus obtained amounted to about 0·7 A. per millimetre in the third order and about 1·3 A. per millimetre in the second. The time of exposure in the third order varied from 8 to 12 hours, and from 2 to 4 hours in the second order. Ilford special rapid panchromatic plates were used.

The following bands, 4-1 with head at λ 6788 A.; 5-2, λ 6705 A.; 6-3, λ 6623 A.; 5-1, λ 6127 A.; 6-2, λ 6070 A.; and 7-3, λ 6013 A., have been measured against neon standards* both in the third and second orders of the 21-foot grating. After an exposure with pure nitrogen in the discharge tube had been made, the nitrogen was pumped out, neon was passed into the tube, and the comparison spectrum was taken. In this way a shift of the comparison spectrum relative to the nitrogen spectrum owing to a shift of the source could be avoided. The neon could be pumped out and stored in a flask after it had been purified by circulating it through a charcoal trap cooled with liquid air.

---

* Burns, Meggers and Merrill, 'Bureau of Standards,' No. 329, p. 765 (1918).

The measurements were accurate to 0·003 mm., which corresponds to an accuracy of 0·002 A. or 0·005 cm.$^{-1}$ in the case of sharp lines of the third order plates. On measuring out the plates, however, it was found that the neon standard lines were too far apart to give the above accuracy throughout the regions investigated, and it was decided to take new plates with the iron arc spectrum for comparison. Owing to external circumstances this could not be carried out, but the experimental error was reduced to a minimum by the following method :—A third order equation was passed through the neon standards, and with this equation the wave-lengths of imaginary points 1 mm. apart on the plate were calculated. These wave-lengths were converted into wave-numbers using Kayser's "Schwingungszahlen" tables. The dispersion in wave-numbers for each millimetre interval was now known, and the wave-numbers of lines lying in these millimetre intervals were found by interpolation. Thus the wave-numbers of lines relative to one another may attain an accuracy of 0·01 cm.$^{-1}$ in the case of sharp lines, whereas 0·05 cm.$^{-1}$ will be the maximum error for fuzzy lines. The resolving power obtained in the third order amounted to about 180,000, which is 80 per cent. of the value expected theoretically. Even with this resolving power some lines could not be resolved.

Since the 5-2 band has its initial state in common with the final state of the 2-5 band of the second positive nitrogen bands analysed by Lindau,* an analysis of the 5-2 band was first attempted and thereafter that of the 6-3 band, which is more strongly developed than the 5-2 band. Before proceeding further with the analysis of the 6-3 band, the Δ_2F values for the $v' = 5$ vibrational level of the 5-2 band were tested for agreement with those of the $v'' = 5$ level of the second positive 2-5 (λ 3942 A.) band of Lindau.

III. *The Structure of the Bands.*

The first positive bands of nitrogen are degraded towards the violet. When photographed under small dispersion they appear to have four or five heads, of which three are very conspicuous and the others somewhat weaker. On the plates taken with the 21-foot grating having a large resolving power, only the three strong heads can still obviously be recognised as heads (*cf.* Plates 3 and 4).

---

* 'Z. Physik,' vol. 26, p. 361 (1924).

On first attempting an analysis of the 5-2 band, two strong branches belonging to the least refrangible head were observed. These two series clearly had the appearance of Q and R branches, of which the consecutive lines had alternating intensities. No corresponding strong branch having the form of an ordinary P branch could be found.

Before attempting the analysis of complex band structures it is very desirable to have an approximate idea of the type of structure to be expected, *i.e.*, multiplicity, number of branches, etc. This can be predicted in most cases by studying the most likely electronic configurations and what states result from these according to Wigner and Witmer.* This information combined with the empirical data was of great help in starting the present analysis. Thus the initial state of the first positive bands is known to be a $^3\Pi$ state (*cf.* Section 1). The final state is in all probability a $^3\Sigma$ or a $^3\Delta$ state. The alternating intensities of the two observed branches conform with a $^3\Pi \rightarrow {}^3\Sigma$ but not with a $^3\Pi \rightarrow {}^3\Delta$ transition. Furthermore, the observed two branches would also correspond to the main P and Q branches of the $^3\Pi_0 \rightarrow {}^3\Sigma$ transition, but in that case another strong R branch having the appearance of an S branch should be observed.

Owing to a considerable Λ-type doubling in the $^3\Pi_0$ state (as will be seen below) the location of the R branch caused some difficulty. By assuming the observed two branches to be P and Q branches and neglecting the effect due to the Λ-type doubling, it was possible to calculate the wave-numbers of the R branch lines from the P and Q lines according to the simple relation

$$R(J) - Q(J) = Q(J+1) - P(J+1).$$

The points marking the positions of these fictitious R branch lines were marked on an enlargement (1 A. = 1 cm.). Strong lines were observed which for large J values were separated by approximately constant amounts from these marks. These lines were extended backwards towards the head (by making use of the second wave-number difference between consecutive lines of the same branch being approximately constant) and proved to be the R branch having the form of an S branch. Two further groups of three branches belonging to the other two strong heads were observed. The nine strong branches starting from the red end of the band had consecutively the appearance of Q, R, S; P, Q, R; and O, P, Q branches. The three groups of three strong branches clearly belonged to the three strong heads, and those having the appearance of O and P branches in the last group formed the weaker heads observed under small dispersion.

---

* 'Z. Physik,' vol. 51, p. 859 (1928).

The branches in each of the above groups were assumed to be P, Q and R branches, respectively. The quantities $\Delta_2 F_i' = R_i(J) - P_i(J)$ for the 5-2 band could now be calculated and were found to agree within experimental error with the quantities $\Delta_2 F''_i = R_i(J-1) - P_i(J+1)$ determined from Lindau's data on the 2-5 band of the second positive system (*cf.* Table I). The values of J given in Table I are determined as described in Section VIII. In comparing Lindau's $\Delta_2 F$ values with those obtained from the present data, it must be borne in mind that Lindau's band lines were measured only approximately from an enlargement on a screen,* so that the fact that no systematic increase occurs in the difference between his $\Delta_2 F$ values and those given here, is enough proof that the $\Delta_2 F$ values agree.

The analysis was now extended to the better developed 6-3 band where similarly nine strong branches were found. Owing to the greater intensity of the 6-3 band, the branches could be followed to larger J values and up to the head in most cases. A total of 26 branches was observed in the 6-3 band and 24 in the 5-2 band. All the favourably situated branches showed alternating intensities of the consecutive lines. The strong lines and practically all the weak lines of the 6-3 band are included in the above-mentioned 26 branches. The remaining weak lines may be due to the overlapping of branches of the adjoining bands and the weaker bands of higher vibrational quantum numbers.

The structure of the band is exactly that predicted if one assumes a $^3\Pi \rightarrow {}^3\Sigma$ transition with the $^3\Pi$ state conforming to Hund's case *a* for the lower J values. In this case 27 branches are expected, of which 9 are very strong and a few are expected to be very weak. The other branches have medium intensity. The twenty-seventh branch which has not been observed in the 6-3 band is unfavourably situated since it partly overlaps the 7-4 band. The three groups of three strong branches can now be identified as P_1, Q_1, R_1; P_2, Q_2, R_2; and P_3, Q_3, R_3 branches, and are the main branches belonging to the transitions $^3\Pi_{\text{low}} \rightarrow {}^3\Sigma$, $^3\Pi_{\text{med}} \rightarrow {}^3\Sigma$, and $^3\Pi_{\text{high}} \rightarrow {}^3\Sigma$ where low, med. and high mean low, medium and high frequencies. Fig. 2 gives a schematic representation of the theoretically expected transitions. The transitions giving the strong branches are represented by heavy lines, those giving the lines of medium intensity by thinner lines and the weak branches by dotted lines. The notation used agrees with

---

* 'Z. Physik,' vol. 25, p. 247 (1924).

Table I.—Comparison of $\Delta_2F'_i = R_i(J) - P_i(J)$ obtained from the first positive 5-2 band with $\Delta_2F''_i = R_i(J-1) - P_i(J+1)$ obtained from the second positive 2-5 band (λ 3942) of Lindau.

J.	$^3\Pi_{\text{low}}$.		$^3\Pi_{\text{med}}$.		$^3\Pi_{\text{high}}$.	
	Author. $\Delta_2F'_{1b}(J) = R_1(J) - P_1(J)$.	Lindau. $\Delta_2F''_1(J) = R_1(J-1) - P_1(J+1)$.	Author. $\Delta_2F'_{2b}(J) = R_2(J) - P_2(J)$.	Lindau. $\Delta_2F''_2(J) = R_2(J-1) - P_2(J+1)$.	Author. $\Delta_2F'_{3b}(J) = R_3(J) - P_3(J)$.	Lindau. $\Delta_2F''_3(J) = R_3(J-1) - P_3(J+1)$.
3	—	—	—	—	—	23·2
4	—	—	27·16	—	—	29·8
5	—	—	33·27	33·4	36·62	36·4
6	—	—	39·51	39·5	42·99	42·9
7	—	—	45·87	45·5	49·41	49·3
8	—	—	51·83	51·8	55·85	55·7
9	54·69	—	57·85	57·8	62·25	61·8
10	60·59	60·4	64·02	63·9	68·63	68·5
11	66·48	66·7	70·28	70·1	75·01	74·8
12	72·46	72·6	76·48	76·4	81·30	81·1
13	78·50	78 5	82·60	82·6	87·55	87·3
14	84·47	84·5	88·68	88·6	93·72	93·6
15	90·52	90·4	94·88	94·8	100·03	99·8
16	96·50	96·3	101·04	100·9	106·21	106·0
17	102·49	102·6	107·15	107·1	112·42	112·2
18	108·47	108·3	113·25	113·1	118·64	—
19	114·48	—	119·40	119·2	124·84	124·6
20	120·51	120·4	125·51	125·3	131·01	130·8
21	126·57	126·5	131·61	131·6	137·28	137·1
22	132·57	132·9	137·65	137·8	—	143·3
23	138·63	—	143·82	143·6	—	149·2
24	144·62	144·7	149·85	149·9	—	155·3
25	150·64	150·7	155·90	156·0	—	161·5
26	156·57	156·6	—	162·1	—	167·9
27	162·54	162·6	—	167·8	—	—
28	—	168·6	—	—	—	—

that given in the "Report on Notation for Spectra of Diatomic Molecules."* The validity of the assignment of $^3\Pi_{\text{low}}$, $^3\Pi_{\text{med}}$ and $^3\Pi_{\text{high}}$ as $^3\Pi_0$, $^3\Pi_1$ and $^3\Pi_2$ will be discussed in Section VI.

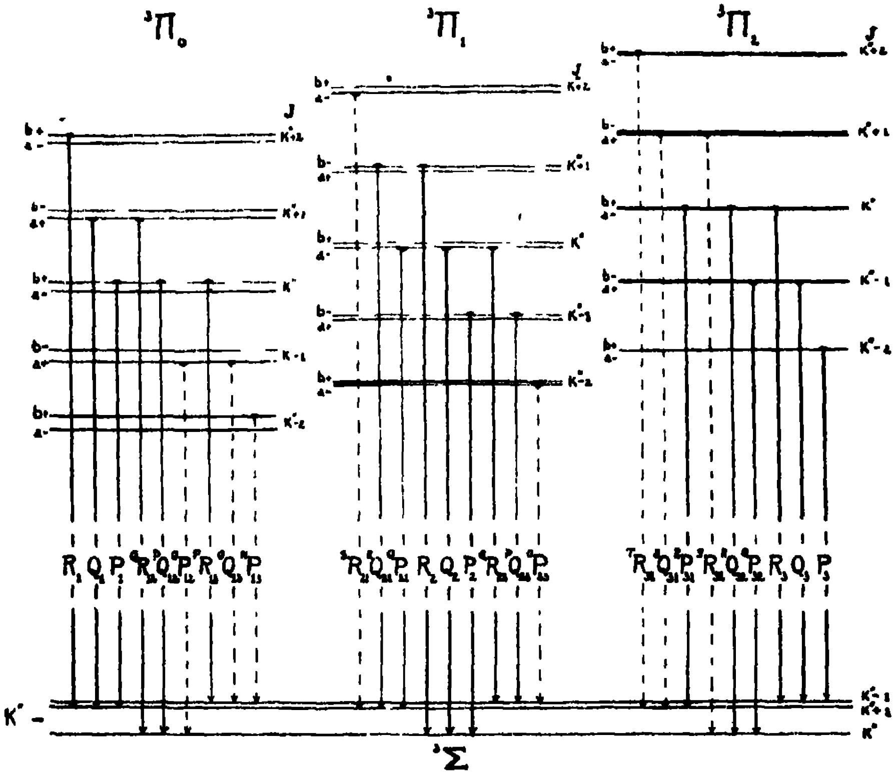
$^3\Pi_0$
$^3\Pi_1$
$^3\Pi_2$
J
b+
a−
K+2
K+1
K
K−1
K−2
R_1 Q_1 P_1 $^QR_{12}$ $^PQ_{12}$ $^OP_{12}$ $^PR_{13}$ $^OQ_{13}$ $^NP_{13}$
$^SR_{21}$ $^RQ_{21}$ $^QP_{21}$ R_2 Q_2 P_2 $^QR_{23}$ $^PQ_{23}$ $^OP_{23}$
$^TR_{31}$ $^SQ_{31}$ $^RP_{31}$ $^SR_{32}$ $^RQ_{32}$ $^QP_{32}$ R_3 Q_3 P_3
K′
K′−1
K′+1
$^3\Sigma$

FIG. 2.—A schematic representation of the structure of the rotational energy levels in the initial $^3\Pi$ state and the final $^3\Sigma$ state of the first positive bands of nitrogen, and of the transitions which are expected.

IV. *Data.*

Since the structure of a $^3\Pi \rightarrow {}^3\Sigma$ transition offers so many possibilities of testing all the combination differences of the rotational levels, it is unnecessary to analyse bands having the same initial or final vibrational quantum numbers. The 6-3 and 5-2 bands further give us the opportunity to determine the variation of the molecular constants with consecutive vibrational quantum numbers and therefore the analyses of these two bands are given here.

In Tables II, III, IV and V, VI, VII the wave-numbers and intensity data of the first positive nitrogen bands, 6-3 and 5-2, are given. The wave-numbers

---

* R. S. Mulliken, 'Phys. Rev.,' vol. 36, p. 611 (1930).

Table II.—Wave-numbers of the lines in the 6-3 band belonging to the $^3\Pi_0 \rightarrow {}^3\Sigma$ transition.

J.	R_1.	Q_1.	P_1.	$^QR_{12}$.	$^PQ_{12}$.	$^OP_{12}$.	$^PR_{13}$.	$^OQ_{13}$.	$^NP_{13}$.
1	—	15096·84 (3)^2	—	15097·90 (1)^1	15095·33 (2)^3	—	15093·56 (5)^2	15084·96 (0·5)^2	—
2	15108·18 (2)^3	96·84 (3)^2	15094·33 (1)^3	15100·84 (3)^2	95·33 (2)^3	15086·77 (1)^1	93·79 (3)^1	82·50 (0)^1	15080·01 (0)^1
3	—	99·68 (0·5)^1	94·18 (1)^3	03·58 (2)^2	95·33 (2)^3	84·07 (1)^1	93·93 (3)^1	79·90 (0)^1	—
4	—	15102·40 (5)^2	94·18 (1)^3	06·89 (2)^1	95·45 (2)^2	81·40 (0)^1	94·18 (1)^1	77·39 (0)^1	68·84 (0·5)^3
5	25·10 (0)^1	05·72 (2F)^2	94·33 (1)^3	10·02 (1)^1	95·69 (3)^2	78·87 (1)^1	94·33 (1)^3	74·98 (0·5)^3	63·44 (0·5)^2
6	30·92 (5)^3	08·86 (5)^1	94·50 (5)^1	13·31 (2)^1	95·75 (3)^2	76·38 (1)^1	94·56 (5)^2	72·47 (0)^1	—
7	36·72 (1)^2	12·07 (3)^1	94·56 (5)^2	16·57 (2)^2	95·93 (2)^1	73·94 (2)^1	94·87 (3)^1	70·16 (0·5)^3	52·70 (2)^1
8	42·85 (4)^2	15·37 (6)^1	94·72 (3)^1	19·99 (0·5)^1	96·26 (2)^2	71·60 (1)^1	95·40 (2)^2	67·88 (2)^3	47·19 (0·5)^1
9	49·10 (1)^2	18·78 (5)^2	95·01 (3)^1	23·56 (1)^1	96·84 (3)^2	69·37 (1)^1	96·16 (2)^2	—	—
10	55·51 (3)^1	22·36 (8)^3	95·69 (5)^2	27·22 (0·5)^3	97·56 (2)^1	67·28 (0·5)^1	97·02 (2)^1	—	37·21 (0·5)^3
11	62·02 (2)^1	26·05 (3)^2	96·38 (2)^1	31·13 (1)^1	98·45 (4)^1	65·30 (3)^1	—	61·99 (0)^1	—
12	68·75 (3)^1	29·89 (6)^1	97·24 (4)^1	35·11 (0·5)^1	99·47 (6)^1	63·44 (1)^2	15099·26 (0 5)^1	60·30 (0·5)^2	27·55 (0)^1
13	75·67 (3)^2	33·87 (6)^2	98·27 (2)^1	39·25 (1)^1	15100·65 (3)^2	61·76 (2)^2	15100·65 (3)^2	58·90 (3)^3	—
14	82·72 (3)^1	38·06 (10)^4	99·47 (6)^2	43·65 (0·5)^1	02·04 (1)^1	60·29 (1)^2	02·22 (0·5)^1	57·49 (0·5)^2	—
15	90·00 (2)^1	42·42 (4)^1	15100·84 (3)^2	48·16 (1)^1	03·58 (2)^2	58·90 (3)^3	03·89 (1)^1	56·37 (0·5)^3	—
16	97·44 (5)^1	46·96 (10)^1	02·40 (5)^2	52·91 (1)^3	05·31 (1)^1	57·74 (0·5)^1	05·83 (2F)^1	55·40 (0)^1	—
17	15205·10 (2)^3	51·72 (5)^2	04·10 (2)^1	57·85 (1)^1	07·26 (2)^1	56·77 (1)^1	07·99 (0)^1	54·69 (0·5)^3	—
18	12·95 (3)^1	56·66 (6)^1	06·05 (5)^3	—	09·43 (1)^1	56·03 (0 5)^1	10·35 (1)^1	54·04 (0·5)^2	—
19	21·04 (2)^1	61·75 (8)^4	08·19 (2)^2	68·40 (2)^1	11·77 (2)^1	55·47 (1)^1	—	—	—
20	29·33 (4)^1	67·13 (6)^1	10·54 (4)^1	73·90 (1)^2	14·32 (0·5)^1	55·02 (0)^1	15 80 (0)^1	—	—
21	37·88 (2)^1	72·68 (6)^2	13·14 (2)^1	79·72 (0·5)^1	17·17 (3)^2	54·95 (0·5)^2	17·57 (4)^2	—	—
22	46·58 (3)^1	78·50 (8)^2	15·91 (3)^1	85·66 (3)^3	20·10 (0)^1	54·95 (0·5)^2	—	—	—
23	55·48 (1)^1	84·47 (5)^3	18·94 (2)^1	91·94 (0·5)^3	23·35 (0·5)^1	55·26 (0·5)^1	—	—	—
24	64·76 (2)^2	90·74 (5)^3	22·13 (3)^2	—	26·85 (0)^1	55·87 (0·5)^2	—	—	—
25	74·17 (1)^1	97·21 (2)^1	25·61 (1)^1	15205·10 (2)^3	30·48 (2)^2	56·58 (0)^1	—	—	—
26	83·85	15203·89 (5)^2	29·28 (2)^1	—	34·45 (0)^1	57·49 (0·5)^2	—	—	—
27	Overlaps 7-4 band from J = 26	10·84 (4)^2	33·24 (3)^3	—	—	58·60 (2)^3	—	—	—
28	—	17·96 (3)^1	37·39 (2)^2	—	—	59·81 (3)^3	—	—	—
29	—	25·35 (2)^2	41·84 (2)^2	—	—	61·19 (0)^1	—	—	—
30	—	32·99 (2)^1	46·41 (1)^1	—	—	—	—	—	—
31	—	40·94 (1)^1	51·21 (5)^3	—	—	—	—	—	—
32	—	49·20 (4)^2	—	—	—	—	—	—	—
33	—	57·76 (5)^2	—	—	—	—	—	—	—
34	—	66·36 (3)^2	—	—	—	—	—	—	—

are arranged in the various branches as borne out by the analysis. The quantum numbers are given in terms of the total angular quantum number J since the rotational quantum number K has no definite meaning in Hund's case *a*. The values of J were determined from the analysis as described in Section VIII. Even with the large resolving power used here the structure of the bands, especially in the neighbourhood of the heads, is very intricate. Consequently blends of two, or in some cases more, lines are relatively frequent and thus the same wave-number often occurs more than once in the tables. The superscript following the number in brackets indicates the number of lines to which the particular wave-number has been assigned. The number in brackets gives a visual estimate of the intensity of the observed line made during the measurement of the plate. The relative intensity of lines holds only for lines close together. F indicates a broad, fuzzy line, whereas *d* indicates that the line gave signs of being double, but still could not be measured as two components. In a few cases the breadth of the fuzzy lines could be measured and in such cases the most suitable wave-number falling within the limits of the fuzzy line was chosen in the analysis.

On Plates 3 (*a*), (*b*), and 4 (*c*), (*d*) an enlargement of the 6-3 band made from a third order plate is given.

V. *Interpretation of the Data.*

It has been stated in Section III above that the first positive nitrogen bands are in all probability due to a $^3\Pi \rightarrow {}^3\Sigma$ transition where the $^3\Pi$ state conforms to Hund's case *a* for the lower J values. This interpretation will now be further investigated.

The rotational levels of a $^3\Pi$ state conforming to case *a* are given by

$$T = T_e + G + A\,\Lambda\Sigma + B_v\,[J\,(J+1) - \Omega^2 + \bar{G}^2 + S_{\text{perp}}{}^2] \\ + \Phi_i\,(\Sigma, J) + D_v J^2 (J+1)^2 + \dots \quad (2)$$

$T_e + A\,\Lambda\Sigma$ can be considered as representing the electronic energy, the different values of Σ (T_e and Λ remaining fixed) giving the components of the molecular multiplet according to

$$\Omega = \Lambda + \Sigma = \Lambda + S, \quad \Lambda + S - 1, \dots, \quad |\Lambda - S|. \quad (3)$$

In the present case $\Lambda = 1$ and $S = 1$, and consequently $\Omega = 2$, 1 and 0, thus giving the three components of the triplet, $^3\Pi_2$, $^3\Pi_1$, and $^3\Pi_0$. Every vibrational level now has three components which belong to the molecular multiplet, and every component has its own set of rotational levels. The

Table III.—Wave-numbers of the lines in the 6-3 band belonging to the ${}^3\Pi_1 \rightarrow {}^3\Sigma$ transition.

J.	${}^{S}R_{21}$.	${}^{R}Q_{21}$.	${}^{Q}P_{21}$.	R_2.	Q_2.	P_2.	${}^{Q}R_{23}$.	${}^{P}Q_{23}$.	${}^{O}P_{23}$.
0	—	—	—	15139·08 (0·5)^{1}	—	—	15133·87 (6)^{3}	15130·92 (5)^{4}	—
1	15144·38 (0)^{3}	15138·29 (1)^{1}	—	42·13 (2)^{2}	15136·50 (0·5)^{2}	15133·49 (2)^{1}	35·10 (0·5)^{3}	29·08 (0·5)^{2}	—
2	50·10 (1)^{1}	41·06 (0·5)^{1}	15135·49 (1)^{1}	45·49 (1)^{1}	36·72 (1)^{3}	30·70 (3)^{1}	35·7 (0·5)^{1}	26·71 (1F)^{3}	15121·12 (0)^{1}
3	56·46 (2)^{1}	44·38 (0)^{3}	—	49·10 (1)^{2}	37·28 (2)^{2}	28·23 (1)^{1}	36·56 (1)^{2}	24·46 (1)^{3}	15·65 (2)^{3}
4	63·09 (4)^{3}	47·95 (1)^{1}	36·09 (1)^{1}	52·92 (1)^{3}	38·08 (10)^{4}	25·95 (3)^{1}	37·65 (1)^{1}	22·57 (3)^{1}	10·74 (3)^{1}
5	69·94 (0·5)^{1}	51·74 (5)^{3}	36·95 (0·5)^{1}	56·87 (1)^{1}	39·10 (2)^{2}	24·01 (1)^{2}	39·14 (1)^{2}	20·88 (3)^{2}	06·05 (5)^{3}
6	77·13 (3)^{2}	55·74 (1)^{1}	37·97 (10)^{4}	61·30 (1)^{3}	40·57 (1)^{2}	22·30 (8)^{2}	40·74 (2)^{1}	19·45 (5)^{2}	01·64 (3)^{2}
7	84·55 (5)^{3}	60·11 (3F)^{3}	39·42 (2)^{2}	65·91 (1)^{1}	42·18 (2)^{3}	20·88 (3)^{3}	42·65 (2)^{1}	18·26 (2)^{1}	15097·47 (2)^{1}
8	92·05 (1)^{3}	64·69 (4)^{1}	40·97 (1)^{1}	70·73 (1)^{2}	44·04 (1)^{1}	19·69 (1)^{2}	44·75 (2)^{3}	17·32 (4)^{1}	93·56 (5)^{2}
9	15200·05 (6)^{1}	69·55 (3)^{1}	42·85 (4)^{2}	75·84 (3)^{1}	46·18 (5)^{2}	18·78 (5)^{2}	47·19 (2)^{2}	16·65 (2)^{1}	89·97 (1)^{1}
10	08·28 (2)^{1}	74·64 (2)^{1}	45·00 (1)^{1}	81·20 (1)^{1}	48·56 (2)^{1}	18·06 (1)^{2}	49·79 (1)^{1}	16·18 (4)^{3}	86·55 (2)^{1}
11	16·62 (1)^{1}	80·01 (1)^{3}	47·37 (0·5)^{1}	86·88 (5)^{2}	51·21 (5)^{2}	17·60 (4F)^{3}	52·71 (0)^{1}	16·07 (2)^{1}	83·43 (2)^{2}
12	25·35 (2)^{2}	85·66 (3)^{3}	50·02 (1)^{2}	92·74 (1)^{1}	54·12 (2)^{1}	17·50 (4F)^{1}	55·86 (1)^{1}	16·18 (4)^{2}	80·54 (1)^{1}
13	34·44 (0·5)^{1}	91·53 (1)^{1}	52·92 (1)^{3}	98·91 (2)^{1}	57·31 (4)^{1}	17·60 (4F)^{3}	59·36 (0)^{1}	16·52 (2)^{2}	77·90 (0·5)^{1}
14	43·60 (6)^{2}	97·70 (8)^{2}	56·11 (1)^{1}	15205·42 (2)^{2}	60·76 (3)^{2}	17·90 (1)^{1}	63·09 (4)^{3}	17·18 (3)^{2}	75·58 (2)^{1}
15	53·09 (1)^{1}	15204·13 (2)^{1}	59·55 (0·5)^{1}	12·01 (3)^{1}	64·45 (5)^{3}	18·57 (3)^{1}	66·92 (3)^{3}	18·06 (2)^{2}	73·46 (0·5)^{1}
16	62.88 (1)^{1}	10·84 (4)^{2}	63·27 (1F)^{2}	18 99 (2)^{1}	68·31 (4F)^{3}	19·45 (5)^{3}	71·22 (1)^{1}	19·24 (3)^{3}	71·66 (1)^{1}
17	72·85 (0)^{1}	17·77 (1)^{1}	67·20 (6)^{2}	26·21 (3)^{1}	72·68 (6)^{3}	20·64 (3)^{1}	75·67 (3)^{2}	20·70 (3)^{2}	70·06 (0)^{3}
18	83·08	25·02 (1)^{1}	71·44 (1)^{3}	33·71 (1)^{1}	77·13 (3)^{3}	22·13 (3)^{2}	80·48 (0)^{1}	22·36 (8)^{2}	68·84 (0·5)^{2}
19	93–55	32·54 (0·5)^{1}	75·91 (0·5)^{1}	41·48 (2)^{1}	81·88 (5)^{1}	23·79 (2)^{1}	85·47 (0)^{1}	24·42 (1)^{3}	67·88 (2)^{3}
20	Overlaps 7-4 band from J = 18	40·30 (1)^{1}	80·67 (0)^{1}	49·46 (1F)^{1}	86·88 (5)^{2}	25·81 (1)^{1}	90·74 (5)^{3}	26·6 (1)^{2}	67·08 (1)^{2}
21	—	47·27 (0)^{1}	85·66 (3)^{3}	57·76 (5)^{2}	92·15 (5)^{1}	28·00 (1)^{1}	—	29·08 (0·5)^{2}	66·42 (0)^{1}
22	—	56·56 (1)^{2}	90·95 (2F)^{2}	66·21 (1F)^{1}	97·70 (8)^{2}	30·48 (2)^{2}	15202·10 (0·5)^{1}	31·84 (0·5)^{1}	—
23	—	—	—	75·07	15203·50 (3)^{2}	33·24 (3)^{2}	—	34·88 (0·5)^{1}	—
24	—	—	—	84·03	09·54 (2)^{1}	36·28 (0·5)^{2}	—	—	—
25	—	—	—	93·22	15·83 (3)^{1}	39·59 (2)^{1}	—	—	—
26	—	—	—	Overlaps 7-4 band from J = 23	22·39 (5)^{2}	43·09 (1)^{1}	—	—	—
27	—	—	—	—	29·24 (3)^{1}	46·76 (1)^{2}	—	—	—
28	—	—	—	—	36·29 (5)^{2}	50·84 (1)^{3}	—	—	—
29	—	—	—	—	43·65 (6)^{3}	—	—	—	—
30	—	—	—	—	51·26 (2)^{1}	—	—	—	—
31	—	—	—	—	59·08 (1)^{1}	—	—	—	—
32	—	—	—	—	67·18 (0)^{1}	—	—	—	—
33	—	—	—	—	75·58	—	—	—	—

Table IV.—Wave-numbers of the lines in the 6-3 band belonging to the $^3\Pi_2 \rightarrow {}^3\Sigma$ transition.

J.	$^TR_{31}$.	$^SQ_{31}$.	$^RP_{31}$.	$^SR_{32}$.	$^RQ_{32}$.	$^QP_{32}$.	R_3.	Q_3.	P_3.
1	—	—	—	15176·66 (2F)^3	—	—	—	—	—
2	—	—	—	81·55 (0)^1	15170·96 (0)^1	—	15171·44 (1)^3	15161·30 (0·5)^3	—
3	—	—	—	86·66 (0·5)^1	72·90 (1)^1	15162·84 (0)^1	73·90 (0·5)^2	60·56 (0)^1	15150·02 (1)^3
4	—	—	—	91·98 (1)^3	75·38 (2)^1	62·02 (2)^3	76·72 (2F)^2	60·20 (3)^2	—
5	—	15190·74 (5)^3	15174·15 (0·5)^1	97·83 (0·5)^1	78·21 (2)^1	61·67 (8)^4	79·63 (1)^2	60·04 (1)^1	43·45 (0·5)^1
6	—	96·61 (1)^2	77·1 (3)^3	15203·89 (5)^1	81·11 (1)^1	61·50 (0·5)^1	82·97 (3)^1	60·20 (3)^3	40·57 (1)^3
7	—	—	80·01 (1)^3	10·39 (2)^1	84·47 (5)^3	61·60 (8)^4	86·73 (1)^1	60·76 (3)^2	38·00 (10)^4
8	—	15209·20 (0·5)^1	83·28 (0·5)^1	17·30 (1)^1	88·20 (1)^1	62·23 (1)^1	90·90 (2)^1	61·75 (8)^4	35·87 (2)^1
9	15248·46 (0·5)^1	16·07 (0·5)^1	87·08 (1)^2	24·48 (2)^2	92·32 (3)^1	63·20 (1F)^3	95·37 (2)^1	63·09 (4)^3	34·08 (2)^1
10	—	—	—	32·15 (1)^1	96·82 (1)^1	64·45 (5)^2	15200·24 (5)^1	64·82 (6)^1	32·66 (2)^1
11	—	30·96 (1)^2	95·58 (0·5)^1	40·13 (2)^1	15201·66 (2)^1	66·25 (0·5)^1	05·42 (2)^2	66·92 (3)^3	31·66 (4)^3
12	—	38·95 (0·5)^1	15200·55 (1)^2	48·32 (0·5)^1	06·85 (1)^1	68·35 (2F)^3	10·99 (5)^1	69·33 (6)^1	30·96 (5)^4
13	—	47·10 (2)^1	05·66 (0)^1	56·96 (1)^1	12·39 (2)^1	70·73 (1)^2	16·85 (2)^1	72·05 (3)^1	30·58 (4)^3
14	—	55·74 (1)^1	11·22 (0·5)^1	65·94 (0·5)^2	18·24 (1)^1	73·45 (0·5)^1	23·02 (4)^1	75·14 (5)^1	30·64 (4)^3
15	—	64·76 (2)^3	17·06 (0)^1	75·07	24·45 (1)^1	76·60 (2F)^3	29·51 (1)^1	78·50 (8)^2	30·92 (5)^4
16	—	73·86 (0)^1	23·24 (0·5)^1	Overlaps 7-4 band from J = 15.	30·97 (0·5)^1	80·01 (1)^3	36·29 (5)^2	82·25 (5)^1	31·61 (4)^2
17	—	83·37	29·72 (0)^1	—	37·73 (1)^1	83·66 (0)^1	43·41 (2)^1	86·28 (3)^1	32·61 (2)^1
18	—	92·20	36·50 (0·5)^1	—	44·82 (0)^1	87·67 (0)^2	50·78 (3)^1	90·57 (5)^2	33·87 (6)^3
19	—	Overlaps 7-4 band from J = 17.	43·65 (6)^3	—	52·20 (0·5)^1	91·94 (0·5)^3	58·45 (1)^1	95·15 (2)^1	35·41 (1)^3
20	—	—	51·01 (3)^1	—	59·90 (0)^1	96·61 (0·5)^2	66·36 (3)^2	99·97 (6)^3	37·28 (2)^2
21	—	—	—	—	67·79 (0·5)^1	15200·46 (0·5)^2	74·61	15205·10 (2)^3	39·42 (2)^2
22	—	—	—	—	Overlaps 7-4 band.	—	83·08	10·67 (3)^1	41·84 (2)^2
23	—	—	—	—	—	—	91·87	16·39 (1)^1	44·57 (1)^1
24	—	—	—	—	—	—	Overlaps 7-4 band from J = 21.	22·39 (5)^2	47·58 (2)^1
25	—	—	—	—	—	—	—	28·69 (1)^1	50·84 (1)^3
26	—	—	—	—	—	—	—	35·27 (2)^1	54·42 (1)^1
27	—	—	—	—	—	—	—	42·11 (1)^1	58·29 (1)^1
28	—	—	—	—	—	—	—	49·20 (4)^2	62·37 (1)^1
29	—	—	—	—	—	—	—	56·56 (1)^2	66·72 (0·5)^1
30	—	—	—	—	—	—	—	64·21 (1)^1	71·44 (1)^3
31	—	—	—	—	—	—	—	72·14 (0·5)^2	76·33 (0)^1
32	—	—	—	—	—	—	—	80·28	—
33	—	—	—	—	—	—	—	88·70 Overlaps 7-4 band from J = 32.	—

Table V.—Wave-numbers of the lines in the 5-2 band belonging to the $^3\Pi_0 \rightarrow {}^3\Sigma$ transition.

J.	R_1.	Q_1.	P_1.	$^QR_{12}$.	$^PQ_{12}$.	$^OP_{12}$.	$^PR_{13}$.	$^OQ_{13}$.	$^SP_{13}$.
1	—	—	—	—	14911·85 (2)^2	—	—	—	—
2	—	14914·39 (0·5)^1	—	14918·23 (1)^1	12·05 (1)^2	—	—	—	—
3	—	17·10 (1)^1	14910·95 (1F)^1	21·11 (0·5)^1	12·20 (2)^2	—	—	—	—
4	—	20·01 (2)^1	11·04 (1F)^1	24·22 (0)^1	12·43 (1)^2	—	—	—	—
5	—	23·05 (2)^1	11·29 (1)^1	27·28 (3F)^2	12·66 (3)^2	14896·75 (0·5)^1	—	—	—
6	—	26·12 (3)^1	11·5 (2)^1	30·55 (1)^1	12·85 (3)^1	93·18 (0)^1	14911·65 (2F)^2	—	—
7	—	29·40 (2)^1	11·65 (2F)^2	33·87 (2)^2	13·06 (1)^2	90·70 (0·5)^1	12·05 (1)^2	—	—
8	14960·79 (0·5)^1	32·74 (4)^1	11·85 (2)^2	37·32 (2)^2	13·33 (2F)^2	88·35 (0)^1	12·43 (1)^2	14884·48 (0)^1	—
9	66·89 (1)^1	36·17 (4)^2	12·20 (2)^2	40·94 (1)^1	13·85 (2F)^1	85·92 (1)^2	13·06 (1)^2	82·32 (0)^1	—
10	73·25 (4*d*)^2	39·71 (6F)^2	12·66 (3)^2	44·60 (2)^2	14·54 (1)^1	83·75 (0)^1	13·99 (0·5)^1	—	—
11	79·81 (1)^1	43·44 (3)^1	13·33 (2F)^2	48·50 (1)^1	15·40 (2)^1	81·86 (1)^1	15·00 (0)^1	—	—
12	86·65 (4F)^2	47·30 (10)^2	14·19 (4)^1	52·55 (1)^1	16·36 (3)^2	—	—	—	—
13	93·68 (2)^1	51·34 (2)^1	15·18 (1)^1	56·72 (1)^1	17·54 (1F)^1	78·15 (1)^1	17·50 (1)^1	75·10 (1)^2	—
14	15000·83 (3)^2	55·54 (5)^1	16·36 (3)^2	61·07 (1)^2	18·87 (0)^1	76·52 (0·5)^1	18·87 (0)^1	—	—
15	08·19 (2)^1	59·91 (3)^2	17·67 (1)^1	65·69 (0·5)^1	20·42 (1)^1	75·10 (1)^1	20·63 (0·5)^1	72·25 (0)^1	—
16	15·70 (5F)^2	64·48 (5)^2	19·20 (2)^1	70·43 (0·5)^1	22·11 (0)^1	73·85 (0)^1	—	—	—
17	23·39 (2F)^2	69·25 (2)^1	20·90 (1)^1	75·42 (0)^1	24·04 (0·5)^1	72·83 (0·5)^1	—	—	—
18	31·31 (3)^1	74·19 (5)^1	22·84 (3)^1	80·62 (0·5)^1	26·18 (3)^1	72·06 (0)^1	—	—	—
19	39·44 (1)^1	79·36 (2)^2	24·96 (1F)^1	—	28·48 (0)^1	71·36 (0)^1	—	—	—
20	47·79 (3)^2	84·74 (3)^2	27·28 (3F)^2	—	30·98 (0)^1	70·92 (0·5)^1	—	—	—
21	56·39 (1)^2	90·35 (2)^1	29·82 (1)^1	—	33·75 (0·5)^1	70·70 (1F)^1	—	—	—
22	65·15 (3)^1	96·13 (4)^1	32·58 (2)^1	—	36·67 (0·5)^2	—	—	—	—
23	74·16 (2)^1	15002·11 (2F)^2	35·53 (1F)^1	—	39·71 (6F)^2	—	—	—	—
24	83·39 (2)^2	08·40 (3)^1	38·77 (2)^2	—	—	—	—	—	—
25	92·83 (1)^2	14·89 (1)^1	42·19 (0·5)^1	—	—	—	—	—	—
26	15102·45	21·61 (3)^2	45·88 (2)^1	—	—	—	—	—	—
27	12·35	28·56 (1)^1	49·81 (2)^2	—	—	—	—	—	—
28	Overlaps 6-3 band from J = 26.	35·75 (1)^1	53·97 (1)^1	—	—	—	—	—	—
29	—	43·17 (2)^1	58·34 (2)^2	—	—	—	—	—	—
30	—	50·81 (2)^2	62·96 (0)^1	—	—	—	—	—	—
31	—	58·69 (3)^2	—	—	—	—	—	—	—
32	—	66·86 (2)^2	72·94 (0)^1	—	—	—	—	—	—
33	—	75·18 (0·5)^1	—	—	—	—	—	—	—
34	—	83·78 (1)^1	—	—	—	—	—	—	—
35	—	92·61 (0·5)^1	—	—	—	—	—	—	—

Table VI.—Wave-numbers of the lines in the 5-2 band belonging to the ${}^3\Pi_1 \to {}^3\Sigma$ transition.

J.	${}^{S}R_{21}$.	${}^{R}Q_{21}$.	${}^{Q}P_{21}$.	R_2.	Q_2.	P_2.	${}^{Q}R_{12}$.	${}^{P}Q_{12}$.	${}^{O}P_{12}$.
2	—	—	—	—	—	—	14952·83 (2)^2	—	—
3	—	—	—	—	14954·38 (0)^1	—	53·90 (2)^2	14941·65 (0·5)^1	—
4	—	—	—	14970·36 (0)^2	14955·37 (0·5)^2	14943·20 (0)^1	55·05 (1F)^2	39·71 (6F)^2	—
5	14977·62 (1F)^2	14969·20 (3)^2	—	74·42 (0·5)^1	56·51 (0·5)^1	41·15 (0)^1	56·35 (0)^1	37·93 (1)^2	—
6	94·76 (1F)^2	73·25 (4*d*)^2	14955·37 (0·5)^2	78·87 (0·5)^1	57·85 (0·5)^1	39·36 (0)^1	58·06 (0·5)^1	36·45 (2)^1	14918·41 (1)^1
7	15002·41 (2F)^2	77·70 (1F)^2	56·68 (1)^2	83·60 (1)^2	59·52 (1)^1	37·93 (1)^2	59·91 (3)^2	35·24 (1)^1	14·19 (4)^2
8	10·27 (1)^1	82·42 (2F)^1	58·34 (2)^2	88·50 (0·5)^1	61·38 (1)^1	36·67 (0·5)^1	62·08 (0·5)^1	34·24 (3)^2	10·18 (0·5)^1
9	18·23 (2)^2	87·31 (1)^1	60·12 (0)^1	93·61 (1)^1	63·51 (2)^2	35·70 (1)^1	64·48 (5)^2	33·48 (1)^1	—
10	26·40 (0·5)^2	92·40 (6)^2	62·31 (0·5)^1	99·00 (1)^1	65·92 (1)^1	34·98 (0·5)^2	67·16 (1)^1	33·06 (2)^1	—
11	35·05 (1*d*)^2	97·82 (1)^1	64·70 (1)^1	15004·79 (2)^2	68·60 (3)^1	34·46 (2)^1	70·08 (0·5)^1	32·8 (3F)^2	14899·82 (0·5)^1
12	43·92 (0·5)^1	15003·59 (2)^1	67·35 (0·5)^2	10·72 (0·5)^1	71·52 (1)^1	34·24 (3)^2	73·32 (4*d*)^2	32·93 (3)^2	96·78 (1)^1
13	53·05 (0·5)^1	09·51 (1)^1	70·36 (0·5)^2	16·95 (1)^1	74·72 (3)^1	34·35 (1)^1	76·76 (0·5)^1	33·27 (1)^1	94·05 (0·5)^2
14	62·33 (0·5)^1	15·75 (5F)^2	73·52 (3*d*)^2	23·39 (2F)^2	78·19 (2)^2	34·71 (1)^2	80·45 (2F)^2	33·87 (2)^2	91·70 (1)^1
15	71·90 (0·5)^1	22·22 (0)^1	76·94 (0)^1	30·19 (2)^1	81·90 (4)^2	35·31 (1)^1	84·49 (0)^1	34·76 (1)^2	—
16	81·82 (0)^1	28·95 (4F)^2	80·70 (0·5)^1	37·21 (1)^2	85·89 (2)^1	36·17 (4)^2	88·72 (0·5)^1	35·92 (0·5)^1	87·64 (1)^1
17	91·87 (0·5)^1	35·98 (1)^1	84·73 (3)^2	44·47 (2)^1	90·15 (4)^2	37·32 (2)^2	93 22 (0·5)^1	37·37 (2)^2	86·00 (1)^1
18	15102·23 (0·5)^1	43·27 (1)^1	88·90 (0)^1	52·02 (1)^1	94·66 (2)^1	38·77 (2)^2	98·00	39·00 (1)^1	84·70 (1)^1
19	12·83	50·81 (2)^2	—	59·81 (3F)^2	99·42 (3)^1	40·41 (1)^1	Overlaps 6-3 band from J = 18.	42·94 (0·5)^1	—
20	23·82	58·60 (3F)^2	—	67·88 (2)^2	15004·45 (3)^2	42·37 (1)^1	—	43·20 (1)^2	82·80 (1)^1
21	34·90	66·66 (0)^1	—	76·21 (2)^1	09·77 (3)^1	44·60 (2)^2	—	45·69 (0)^1	82·30 (0)^1
22	Overlaps 6-3 band from J = 18.	74·98 (0)^2	—	84·73 (3)^2	15·30 (1)^2	47·08 (1)^1	—	—	—
23	—	83·61 (0·5)^1	—	93·63	21·12 (2)^1	49·81 (2)^2	—	—	—
24	—	92·40 (0·5)^2	—	15102·68	27·17 (1)^1	52·83 (2)^1	—	—	—
25	—	—	—	12·01	33·52 (3)^1	56·11 (1)^1	—	—	—
26	—	—	—	Overlaps 6-3 band from J = 23.	40·10 (1)^1	59·69 (0)^1	—	—	—
27	—	—	—	—	46·94 (3)^1	63·51 (2)^2	—	—	—
28	—	—	—	—	54·04 (1)^2	—	—	—	—
29	—	—	—	—	61·39 (2)^1	—	—	—	—
30	—	—	—	—	69·02 (3)^2	—	—	—	—
31	—	—	—	—	76·78 (1)^1	—	—	—	—
32	—	—	—	—	84·96 (0·5)^2	—	—	—	—
33	—	—	—	—	92·40 (0·5)^2	—	—	—	—

Table VII.—Wave-numbers of the lines in the 5-2 band belonging to the ${}^3\Pi_2 \rightarrow {}^3\Sigma$ transition.

J.	${}^TR_{31}$.	${}^SQ_{31}$.	${}^RP_{31}$.	${}^SR_{32}$.	${}^RQ_{32}$.	${}^QP_{32}$.	R_3.	Q_3.	P_3.
2	—	—	—	—	—	—	14988·72 (0)^2	14978·18 (2)^2	—
3	—	—	—	—	—	—	91·42 (0)^1	77·81 (1)^1	14967·35 (0·5)^2
4	—	—	—	15009·77 (3)^2	14993·01 (0)^1	14979·36 (2)^2	94·20 (1)^1	77·46 (2)^2	63·74 (0)^1
5	—	15008·58 (3)^2	—	15·60 (5F)^2	95·74 (1)^1	79·01 (2)^2	97·20 (0·5)^1	77·31 (1)^1	60·58 (1)^1
6	—	14·39 (0·5)^1	14994·55 (2F)^2	21·61 (3)^2	98·7 (1F)^2	78·80 (1)^2	15000·60 (2)^1	77·46 (2)^2	57·61 (0·5)^1
7	—	—	—	28·38 (2)^2	15002·11 (2F)^2	79·01 (3)^2	04·45 (3F)^2	78·04 (2)^1	54·99 (2F)^2
8	—	27·17 (1)^2	15000·83	35·33 (0·5)^1	05·88 (0·5)^1	79·36 (2)^2	08·58 (3)^1	79·01 (2)^2	52·73 (2)^2
9	—	34·16 (0)^1	04·74 (2F)^2	42·73 (1)^1	10·03 (2)^1	80·41 (2F)^2	13·15 (1)^1	80·35 (2F)^2	50·9 (1F)^2
10	—	41·53 (0)^1	08·81 (0)^1	50·43 (0·5)^1	14·62 (0·5)^1	81·90 (4)^2	18·06 (2)^1	82·12 (5)^1	49·43 (2)^1
11	—	—	13·37 (0·5)^1	58·45 (2)^1	19·52 (1)^2	83·59 (1)^2	23·34 (2F)^2	84·23 (2)^1	48·33 (2)^1
12	—	—	18·27 (1)^2	66·86 (3)^2	24·74 (0·5)^1	85·65 (0·5)^1	28·93 (4F)^2	86·65 (4F)^2	47·63 (2F)^2
13	—	—	23·59 (0)^1	75·58 (2)^2	30·37 (2)^1	88·04 (1)^1	34·85 (2F)^2	89·42 (2)^1	47·30 (10)^2
14	—	—	29·17 (0·5)^1	—	36·25 (0·5)^1	90·88 (0·5)^1	41·07 (3)^1	92·49 (6F)^2	47·35 (10)^2
15	—	—	35·10 (0d)^1	93·93	42·50 (1)^1	93·94 (1)^1	47·63 (1)^1	95·93 (2)^1	47·6 (2F)^2
16	—	—	41·28 (0·5)^1	Overlaps 6-3 band.	49·00 (0·5)^1	97·40 (0·5)^1	54·46 (2)^1	99·65 (5)^1	48·25 (2)^1
17	—	—	47·79 (3)^2	—	55·87 (1)^2	15001·05 (0·5)^1	61·58 (2)^1	15003·68 (2)^1	49·16 (1)^1
18	—	—	54·69 (0·5)^1	—	63·01 (0)^1	—	69·02 (3)^2	08·00 (4)^1	50·38 (2)^1
19	—	—	61·76 (2)^2	—	70·42 (0)^1	—	76·78 (1)^1	12·64 (2)^1	51·94 (1)^1
20	—	—	69·24 (0·5)^1	—	78·12 (0)^1	—	84·73 (3)^2	17·54 (3)^1	53·79 (2)^2
21	—	—	77·05 (0)^1	—	—	—	Overlaps 6-3 band.	22·73 (2)^1	55·94 (0·5)^1
22	—	—	84·96 (0·5)^2	—	—	—	—	28·20 (4)^2	58·34 (2)^2
23	—	—	93·32	—	—	—	—	33·96 (1)^1	61·07 (0)^2
24	—	—	Overlaps 6-3 band from J = 22.	—	—	—	—	40·01 (3F)^1	64·06 (0·5)^1
25	—	—	—	—	—	—	—	46·30 (1)^1	—
26	—	—	—	—	—	—	—	52·89 (2)^1	—
27	—	—	—	—	—	—	—	59·81 (3F)^2	—
28	—	—	—	—	—	—	—	67·08 (1)^2	—
29	—	—	—	—	—	—	—	—	—

rotational levels in each set are again double owing to Λ-type doubling with two values of $\Phi_i(\Sigma, J)$ for each value of Σ and J, $\Phi_a(\Sigma, J)$ and $\Phi_b(\Sigma, J)$. $B_v\bar{G}^2$ usually is very small and is inseparable from $T_e + G$ in the analysis. When the conditions are not purely case *a*† (as is the case here presumably for high J values), B_v depends on Σ according to

$$B_{v, \Sigma^*} = B_v (1 \pm 2B_v/A\,\Lambda), \tag{4}$$

i.e., for $\Sigma = 0$, $B^* = B_v$; for $\Sigma = \pm 1$, $B^* = B_v (1 \pm 2B_v/A)$.

$$\left.\begin{aligned} S^2_{\text{perp}} - \Omega^2 = S^{*2} - \Sigma^2 - \Omega^2 &= S(S+1) - \Sigma^2 - \Omega^2 \\ &= 2 - 1 - 0 = 1 \text{ for } {}^3\Pi_0 \\ &= 2 - 0 - 1 = 1 \text{ for } {}^3\Pi_1 \\ &= 2 - 1 - 4 = -3 \text{ for } {}^3\Pi_2 \end{aligned}\right\}. \tag{5}$$

The variable part of the rotational energy for each component can thus be given as

$$\left.\begin{aligned} F'_{ia} &= B'_v J(J+1) + \Phi'_a(\Sigma, J) + D'_v J^2 (J+1)^2 + \ldots \\ F'_{ib} &= B'_v J(J+1) + \Phi'_b(\Sigma, J) + D'_v J^2 (J+1)^2 + \ldots \end{aligned}\right\}. \tag{6}$$

F'_1, F'_2 and F'_3 give the rotational levels for the three components ${}^3\Pi_{\text{low}}$, ${}^3\Pi_{\text{med}}$ and ${}^3\Pi_{\text{high}}$.

The lines of the R_{ib}, Q_{ib} and P_{ib} branches are now given by :—

$$R_{ib}(J) = \nu_e + \nu_v + F'_{ib}(J+1) - F''_i(J) \tag{7}$$

$$Q_{ib}(J) = \nu_e + \nu_v + F'_{ib}(J) - F''_i(J) \tag{8}$$

$$P_{ib}(J) = \nu_e + \nu_v + F'_{ib}(J-1) - F''_i(J), \tag{9}$$

and similarly the R_{ia}, Q_{ia}, P_{ia} lines can be obtained. Hence

$$\Delta_2 F'_{ib}(J) = R_{ib}(J) - P_{ib}(J) = F'_{ib}(J+1) - F'_{ib}(J-1), \tag{10}$$

i.e.,

$$\Delta_2 F'_{ib}(J) = 2(B'_v + 2D'_v) + 4(B'_v + 3D'_v)J + 12D'_v J^2 + 8D'_v J^3. \tag{11}$$

The experimental values corresponding to equation (11) for the $v' = 5$ level of the 5-2 band should agree with the rotational term differences

$$\Delta_2 F''_{ib}(J) = R_{ib}(J-1) - P_{ib}(J+1) = F''_{ib}(J+1) - F''_{ib}(J-1)$$

obtained from the 2-5 second positive bands for the level $v'' = 5$. This was shown to be the case within the experimental error in Table I.

---

† *Cf.* E. L. Hill and J. H. van Vleck, 'Phys. Rev.,' vol. 32, p. 250 (1928).

In Table VIII the $\Delta_2 F'_{ia}$ and $\Delta_2 F'_{ib}$ of the 6-3 band for all three components of the $^3\Pi$ state are given.

Beyond the agreement with the 2-5 second positive combination differences, equation (11) does not allow any further testing of the term differences within each component of the triplet. In order to obtain further proof of the validity of the assignment, the $\Delta_1 F'$ values must be studied, but here due consideration must be given to the Λ-type doubling. The following term differences can be tested for agreement :—

$$\begin{aligned}\Delta_1 F'_{1ba}(J) &= F'_{1b}(J+1) - F'_{1a}(J) = R_1(J) - Q_1(J)\\ &= {}^PQ_{12}(J+1) - {}^OP_{12}(J+1) = {}^PR_{13}(J) - {}^OQ_{13}(J).\end{aligned} \qquad (12)$$

$$\begin{aligned}\Delta_1 F'_{1ab}(J) &= F'_{1a}(J) - F'_{1b}(J-1) = Q_1(J) - P_1(J)\\ &= {}^QR_{13}(J-1) - {}^PQ_{12}(J-1) = {}^OQ_{13}(J) - {}^NP_{13}(J).\end{aligned} \qquad (13)$$

$$\begin{aligned}\Delta_1 F'_{2ba}(J) &= F'_{2b}(J+1) - F'_{2a}(J) = {}^RQ_{21}(J+1) - {}^QP_{21}(J+1)\\ &= R_2(J) - Q_2(J) = {}^PQ_{23}(J+1) - {}^OP_{23}(J+1),\end{aligned} \qquad (14)$$

$$\begin{aligned}\Delta_1 F'_{2ab}(J) &= F'_{2a}(J) - F'_{2b}(J-1) = {}^SR_{21}(J-1) - {}^RQ_{21}(J-1)\\ &= Q_2(J) - P_2(J) = {}^QR_{23}(J-1) - {}^PQ_{23}(J-1),\end{aligned} \qquad (15)$$

$$\begin{aligned}\Delta_1 F'_{3ba}(J) &= F'_{3b}(J+1) - F'_{3a}(J) = {}^TR_{31}(J) - {}^SQ_{31}(J)\\ &= {}^RQ_{32}(J+1) - {}^QP_{32}(J+1) = R_3(J) - Q_3(J),\end{aligned} \qquad (16)$$

$$\begin{aligned}\Delta_1 F'_{3ab}(J) &= F'_{3a}(J) - F'_{3b}(J-1) = {}^SQ_{31}(J) - {}^RP_{31}(J)\\ &= {}^SR_{32}(J-1) - {}^RQ_{32}(J-1) = Q_3(J) - P_3(J).\end{aligned} \qquad (17)$$

Samples of the rotational term differences corresponding to equations (12) to (17) are given for $v' = 6$, $^3\Pi_0$, $^3\Pi_1$ and $^3\Pi_2$ in Tables IX, X and XI, respectively. It will be seen that the agreement is well within the experimental error, which may be expected to be as large as 0·1 cm.$^{-1}$ in cases where the branch lines are blends of two or more lines. Three similar tables for $v' = 5$, $^3\Pi_0$, $^3\Pi_1$ and $^3\Pi_2$ may be readily constructed from Tables V, VI and VII, but, in order to economise space, they are not given here.

The rotational levels of the final $^3\Sigma$ state can be represented by

$$T_i = T_e + G + F''_i, \qquad (18)$$

i.e.,

$$T_i = T_e + G + B''_v K(K+1) + f''_i(K, J-K) + D''_v K^2(K+1)^2 + \ldots, \qquad (18\text{A})$$

where J is the total angular quantum number, its values being $J = K + S$,

Table VIII.—$\Delta_2 F'$ values in the $^3\Pi$ states of the $v' = 6$ vibrational level.

J.	A. $^3\Pi_0$ state.		B. $^3\Pi_1$ state.			C. $^3\Pi_2$ state.	
	$\Delta_2 F'_{1b}$ (J).	$\Delta_2 F'_{1a}$ (J).	$\Delta_2 F'_{2a}$ (J).	$\Delta_2 F'_{2b}$ (J).	$\Delta_2 F'_{2a}$ (J).	$\Delta_2 F'_{3a}$ (J).	$\Delta_2 F'_{3b}$ (J).
	$R_1(J) - P_1(J)$.	$^QR_{12}(J) - {}^OP_{12}(J)$.	$^SR_{21}(J) - {}^QP_{21}(J)$.	$R_2(J) - P_2(J)$.	$^QR_{23}(J) - {}^OP_{23}(J)$.	$^SR_{32}(J) - {}^QP_{32}(J)$.	$R_3(J) - P_3(J)$.
1	—	—	—	8·64	—	—	—
2	13·85	14·07	14·61	14·79	14·58	—	—
3	—	19·51	—	20·87	20·91	23·82	23·88
4	25·06	25·49	27·00	26·97	26·91	29·96	—
5	30·77	31·15	32·99	32·86	33·09	36·16	36·18
6	36·42	36·93	39·16	39·00	39·10	42·39	42·40
7	42·16	42·63	45·13	45·03	45·18	48·79	48·73
8	48·13	48·39	51·08	51·04	51·19	55·07	55·03
9	54·09	54·19	57·20	57·06	57·22	61·28	61·29
10	59·82	59·94	63·28	63·14	63·24	67·70	67·58
11	65·64	65·83	69·25	69·28	69·28	73·88	73·76
12	71·51	71·67	75·33	75·24	75·32	79·97	80·03
13	77·40	77·49	81·52	81·31	81·46	86·23	86·27
14	83·25	83·36	87·49	87·52	87·51	92·49	92·38
15	89·16	89·26	93·54	93·44	93·46	98·47	98·59
16	95·04	95·17	99·61	99·54	99·56	—	104·68
17	101·00	101·08	105·65	105·57	105·61	—	110·80
18	106·90	—	111·64	111·58	111·64	—	116·91
19	112·85	112·93	117·64	117·69	117·59	—	123·04
20	118·79	118·88	—	123·65	123·66	—	129·08
21	124·74	124·77	—	129·76	—	—	135·19
22	130·67	130·71	—	135·73	—	—	141·24
23	136·54	136·68	—	141·83	—	—	147·30
24	142·63	—	—	147·75	—	—	—
25	148·56	148·52	—	153·63	—	—	—
26	154·57	—	—	—	—	—	—

Table IX.—$\Delta_1 F'_1$ values in the $^3\Pi_0$ state of the $v' = 6$ vibrational level.

J.	$\Delta_1 F'_{1ba}(J) = F'_{1b}(J+1) - F'_{1a}(J)$.			$\Delta_1 F'_{1ab}(J) = F'_{1a}(J) - F'_{1b}(J-1)$.		
	$R_1(J) - Q_1(J)$.	$^PQ_{12}(J+1) - {}^OP_{12}(J+1)$.	$^PR_{13}(J) - {}^OQ_{13}(J)$.	$Q_1(J) - P_1(J)$.	$^QR_{12}(J-1) - {}^PQ_{12}(J-1)$.	$^OQ_{13}(J) - {}^NP_{13}(J)$.
1	—	8·56	8·60	—	—	—
2	11·34	11·26	11·29	2·51	2·57	2·49
3	—	14·05	14·03	5·50	5·51	—
4	—	16·82	16·79	8·22	8·25	8·55
5	19·38	19·37	19·35	11·39	11·44	11·54
6	22·06	21·99	22·09	14·36	14·33	—
7	24·65	24·66	24·71	17·51	17·56	17·46
8	27·48	27·47	27·52	20·65	20·64	20·69
9	30·32	30·28	—	23·77	23·73	—
10	33·15	33·15	—	26·67	26·72	—
11	35·97	36·03	—	29·67	29·66	—
12	38·86	38·89	38·96	32·65	32·68	32·75
13	41·80	41·75	41·75	35·60	35·64	—
14	44·66	44·68	44·73	38·59	38·60	—
15	47·58	47·57	—	41·58	41·61	—
16	50·48	50·49	—	44·56	44·58	—
17	53·38	53·40	—	47·62	47·60	—
18	56·29	56·30	—	50·61	50·59	—
19	59·29	59·30	—	53·56	—	—
20	62·20	62·22	—	56·59	56·63	—
21	65·20	65·15	—	59·54	59·58	—
22	68·08	68·09	—	62·59	62·55	—
23	71·01	70·98	—	65·53	65·56	—
24	74·02	73·90	—	68·61	68·59	—
25	76·96	76·96	—	71·60	—	—
26	79·96	—	—	74·61	74·62	—
27	—	—	—	77·60	—	—
28	—	—	—	80·57	—	—
29	—	—	—	83·51	—	—
30	—	—	—	86·58	—	—
31	—	—	—	89·73	—	—

Table X.—$\Delta_1 F'_2$ values in the $^3\Pi_1$ state of the $v' = 6$ vibrational level.

J.	$\Delta_1 F'_{2ba}(J) = F'_{2b}(J+1) - F'_{2a}(J)$.			$\Delta_1 F'_{2ab}(J) = F'_{2a}(J) - F'_{2b}(J-1)$.		
	$^RQ_{21}(J+1) - {}^QP_{21}(J+1)$.	$R_2(J) - Q_2(J)$.	$^PQ_{23}(J+1) - {}^OP_{23}(J+1)$.	$^SR_{21}(J-1) - {}^RQ_{21}(J-1)$.	$Q_2(J) - P_2(J)$.	$^QR_{23}(J-1) - {}^PQ_{23}(J-1)$.
1	5·57	5·63	5·59	—	3·01	2·95
2	—	8·77	8·81	6·09	6·02	6·02
3	11·86	11·82	11·83	9·04	9·05	8·99
4	14·79	14·84	14·83	12·08	12·13	12·10
5	17·77	17·77	17·81	15·14	15·09	15·08
6	20·69	20·73	20·79	18·26	18·27	18·26
7	23·72	23·73	23·76	21·39	21·30	21·29
8	26·70	26·69	26·68	24·44	24·35	24·39
9	29·64	29·66	29·63	27·36	27·40	27·43
10	32·64	32·64	32·64	30·50	30·50	30·54
11	35·64	35·67	35·64	33·64	33·61	33·61
12	38·61	38·62	38·62	36·61	36·62	36·64
13	41·59	41·60	41·60	39·69	39·71	39·68
14	44·58	44·66	44·60	42·91	42·86	42·84
15	47·57	47·56	47·58	45·90	45·88	45·91
16	50·57	50·58	50·64	48·96	48·86	48·86
17	53·58	53·53	53·52	52·04	52·04	51·98
18	56·63	56·58	56·54	55·08	55·00	54·97
19	59·63	59·60	59·52	58·06	58·09	58·12
20	62·61	62·58	62·66	61·01	61·07	61·05
21	65·61	65·61	—	—	64·15	64·14
22	—	68·51	—	—	67·22	—
23	—	—	—	—	70·26	70·26
24	—	—	—	—	73·26	—
25	—	—	—	—	76·24	—
26	—	—	—	—	79·30	—
27	—	—	—	—	82·48	—
28	—	—	—	—	85·45	—

Table XI.—$\Delta_1 F'_3$ values in the $^3\Pi_2$ state of the $v' = 6$ vibrational level.

J	$\Delta_1 F'_{3ba}(J) = F'_{3b}(J+1) - F'_{3a}(J)$.			$\Delta_1 F'_{3ab}(J) = F'_{3a}(J) - F'_{3b}(J-1)$.		
	${}^{T}R_{31}(J) - {}^{S}Q_{31}(J)$.	${}^{R}Q_{32}(J+1) - {}^{Q}P_{32}(J+1)$.	$R_3(J) - Q_3(J)$.	${}^{S}Q_{31}(J) - {}^{R}P_{31}(J)$.	${}^{S}R_{32}(J-1) - {}^{R}Q_{32}(J-1)$.	$Q_3(J) - P_3(J)$.
2	—	10·06	10·14	—	—	—
3	—	13·36	13·34	—	10·59	10·54
4	—	16·54	16·52	—	13·76	—
5	—	19·61	19·59	16·59	16·60	16·59
6	—	22·87	22·77	19·51	19·62	19·63
7	—	25·97	25·97	—	22·78	22·76
8	—	29·12	29·15	25·92	25·92	25·88
9	32·39	32·37	32·28	28·99	29·10	29·01
10	—	35·41	35·42	—	32·16	32·16
11	—	38·50	38·50	35·38	35·33	35·26
12	—	41·66	41·66	38·40	38·47	38·37
13	—	44·79	44·80	41·44	41·47	41·47
14	—	47·85	47·88	44·52	44·57	44·50
15	—	50·96	51·01	47·70	47·70	47·58
16	—	54·07	54·04	50·62	50·62	50·64
17	—	57·15	57·13	53·65	—	53·67
18	—	60·26	60·21	56·70	—	56·70
19	—	63·29	63·30	—	—	59·74
20	—	66·33	66·39	—	—	62·69
21	—	—	69·51	—	—	65·68
22	—	—	72·41	—	—	68·83
23	—	—	75·48	—	—	71·82
24	—	—	—	—	—	74·81
25	—	—	—	—	—	77·85
26	—	—	—	—	—	80·85
27	—	—	—	—	—	83·82
28	—	—	—	—	—	86·83
29	—	—	—	—	—	89·84
30	—	—	—	—	—	92·77
31	—	—	—	—	—	96·81

$K + S - 1, \ldots, K - S$. S is the resultant electronic spin. Since $S = 1$ for a triplet state $J = K + 1$, K and $K - 1$. Due to the three values of J we shall as a rule have three closely spaced energy states for each value of K. These energy states are designated by F_1, F_2 and F_3 corresponding to $J = K+1$, $J = K$ and $J = K - 1$, respectively.

As Kramers† showed, $f_i(K, J - K)$ for $^3\Sigma$ states consists of two parts, one of which is due to the interaction of the resultant electronic spin S^* with the rotational angular momentum K^* and is equal to

$$\tfrac{1}{2}\gamma\,[J(J+1) - K(K+1) - S(S+1)] = \tfrac{1}{2}\gamma\,[J(J+1) - K(K+1) - 2], \quad (19)$$

while the other part is due to the interaction of the individual spins of the electrons and is given by $w_i(K, J - K)$.

$f_i(K, J - K)$ now becomes:

$$f_i(K, J - K) = \tfrac{1}{2}\gamma\,[J(J+1) - K(K+1) - 2] + w_i(K, J - K). \quad (20)$$

Kramers showed that $w_i(K, J - K)$ has the following values for the three values of J:

$$J = K + 1, \qquad w_1 = -\,\varepsilon\,[1 - 3/(2K+3)] \quad (21)$$

$$J = K, \qquad w_2 = +\,2\varepsilon \quad (22)$$

$$J = K - 1, \qquad w_3 = -\,\varepsilon\,[1 + 3/(2K-1)] \quad (23)$$

$f_i(K, J - K)$ then is:

$$J = K + 1, \qquad f_1 = -\,\varepsilon\,[1 - 3/(2K+3)] + \gamma K \quad (24)$$

$$J = K, \qquad f_2 = +\,2\varepsilon - \gamma \quad (25)$$

$$J = K - 1, \qquad f_3 = -\,\varepsilon\,[1 - 3/(2K-1)] - \gamma(K+1). \quad (26)$$

Now

$$\Delta_2 F''_i(J) = R_i(J-1) - P_i(J+1) = F''_i(J+1) - F''_i(J-1). \quad (27)$$

Substituting in equation (27) for F_i according to equations (18), (24), (25) and (26), and neglecting terms in ε/K for moderate and large values of K, since ε is usually small:

$$J = K + 1, \quad \Delta_2 F''_1(J-1) = 2\,(B''_v + 2D''_v + \gamma) + 4\,(B''_v + 3D''_v)\,K + 12D''_vK^2 + 8D''_vK^3, \quad (28)$$

$$J = K, \quad \Delta_2 F''_2(J) = 2\,(B''_v + 2D''_v) + 4(B''_v + 3D''_v)\,K + 12D''_vK^2 + 8D''_vK^3, \quad (29)$$

$$J = K - 1, \quad \Delta_2 F''_3(J+1) = 2\,(B''_v + 2D''_v - \gamma) + 4\,(B''_v + 3D''_v)\,K + 12D''_vK^2 + 8D''_vK^3. \quad (30)$$

---

† 'Z. Physik,' vol. 53, p. 422 (1929).

The following rotational term differences in the final state can now be tested for agreement:

$$\begin{aligned}\Delta_2 F''_1(J) &= F''_1(J+1) - F''_1(J-1) = R_1(J-1) - P_1(J+1)\\ &= {}^{S}R_{21}(J-1) - {}^{Q}P_{21}(J+1) = {}^{T}R_{31}(J-1) - {}^{R}P_{31}(J+1), \qquad (31)\end{aligned}$$

$$\begin{aligned}\Delta_2 F''_2(J) &= F''_2(J+1) - F''_2(J-1) = {}^{Q}R_{12}(J-1) - {}^{O}P_{12}(J+1)\\ &= R_2(J-1) - P_2(J+1) = {}^{S}R_{32}(J-1) - {}^{Q}P_{32}(J+1) \qquad (32)\end{aligned}$$

$$\begin{aligned}\Delta_2 F''_3(J) &= F''_3(J+1) - F''_3(J-1) = {}^{P}R_{13}(J-1) - {}^{N}P_{13}(J+1)\\ &= {}^{Q}R_{23}(J-1) - {}^{O}P_{23}(J+1) = R_3(J-1) - P_3(J+1). \qquad (33)\end{aligned}$$

In Table XII, A, B and C, the $\Delta_2 F''_1$, $\Delta_2 F''_2$ and $\Delta_2 F''_3$ values for $v'' = 3$ are given. The values in each of the sections A, B and C should agree within experimental error, which seems to be the case. Similar tables giving the corresponding values for the level $v'' = 2$ may readily be constructed from the data in Tables V, VI and VII.

VI. *Fine Structure of the* $^3\Pi$ *State due to* Λ*-type Doubling.*

So far it has been assumed tentatively that the transitions $^3\Pi_{\text{low}} \rightarrow {}^3\Sigma$, $^3\Pi_{\text{med}} \rightarrow {}^3\Sigma$ and $^3\Pi_{\text{high}} \rightarrow {}^3\Sigma$ correspond to $^3\Pi_0 \rightarrow {}^3\Sigma$, $^3\Pi_1 \rightarrow {}^3\Sigma$ and $^3\Pi_2 \rightarrow {}^3\Sigma$, *i.e.*, that the triplet Π state is normal. Two methods are available for distinguishing a normal from an inverted triplet. Firstly, the missing lines near the origin should give some information. Since the lines become very weak in the neighbourhood of the origin, and owing to the overlapping of the various branches in these regions, blends between lines are very frequent for low J values, and consequently this method cannot be applied here. Another criterion may be obtained by studying the magnitude of the Λ-type doubling.

The Λ-type doubling can be obtained from Tables IX to XI by building the differences $\Delta\nu_{iab}$ as follows:

$$2\Delta\nu_{iab}(J+\tfrac{1}{2}) = \Delta\nu_1 F'_{iba}(J) - \Delta\nu_1 F'_{iab}(J+1). \qquad (34)$$

These differences are given in Table XIII. Although there are some signs of systematic differences between the values for $v' = 6$ and $v' = 5$, the general trend is the same: $\Delta\nu_{1ab}$ decreasing from a large value (2·52 for J = 6·5) to 1·15 for J = 25·5; $\Delta\nu_{2ab}$ decreasing from − 0·15 for J = 5·5 to − 0·96 for J = 26·5 and $\Delta\nu_{3ab}$ increasing from − 0·03 for J = 5·5 to $\Delta\nu_{3ab}$ = 0·28 for J = 24·5. The $\Delta\nu$ values given here are only absolute values and hence the positive and negative signs given have only a relative meaning.

Table XII.—$\Delta_2 F''_i$ values in the $^3\Sigma$ state of the $v'' = 3$ vibrational level.

J.	A. $\Delta_2 F''_1(J) = F_1(J+1) - F_1(J-1)$.		B. $\Delta_2 F''_2 = F_2(J+1) - F_2(J-1)$.			C. $\Delta_2 F''_3(J) = F_3(J+1) - F_3(J-1)$.	
	$R_1(J-1) - P_1(J+1)$.	$^SR_{21}(J-1) - {}^QP_{21}(J+1)$.	$^QR_{12}(J-1) - {}^OP_{12}(J+1)$.	$R_2(J-1) - P_2(J+1)$.	$^SR_{32}(J-1) - {}^QP_{32}(J+1)$.	$^QR_{23}(J-1) - {}^OP_{23}(J+1)$.	$R_3(J-1) - P_3(J+1)$.
1	—	—	—	8·38	—	12·75	—
2	—	—	13·83	13·90	13·82	19·45	—
3	14·00	14·01	19·44	19·54	19·53	24·96	—
4	—	19·51	24·81	25·09	24·99	30·51	30·45
5	—	25·12	30·51	30·62	30·48	36·01	36·15
6	30·54	30·52	36·08	35·99	36·23	41·67	41·63
7	36·20	36·16	44·71	41·61	41·66	47·18	47·10
8	41·71	41·70	47·20	47·13	47·19	52·68	52·65
9	47·16	47·05	52·71	52·67	52·85	58·20	58·24
10	52·72	52·68	58·26	58·24	58·23	63·76	63·71
11	58·27	58·26	63·78	63·70	63·80	69·25	69·28
12	63·75	63·70	69·37	69·28	69·40	74·81	74·84
13	69·28	69·24	74·82	74·84	74·87	80·28	80·35
14	74·83	74·89	80·35	80·34	80·36	85·90	85·93
15	80·32	80·33	85·91	85·97	85·93	91·43	91·41
16	85·90	85·89	91·39	91·37	91·43	96·86	96·90
17	91·39	91·44	96·88	96·86	Overlaps 7-4 band.	102·38	102·42
18	96·91	96·94	102·38	102·42	—	107·79	108·00
19	102·41	102·41	—	107·90	—	113·40	113·50
20	107·90	107·89	113·45	113·48	—	119·05	119·03
21	113·42	—	118·95	118·98	—	—	124·52
22	118·94	—	124·46	124·52	—	—	130·04
23	124·45	—	129·79	129·93	—	—	135·50
24	129·87	—	135·36	135·48	—	—	141·03
25	135·48	—	—	140·94	—	—	—
26	140·93	—	146·50	146·46	—	—	—
27	146·46	—	—	—	—	—	—

Table XIII.—Λ-type doubling.

J.	$\Delta\nu_{1ab}$.		$\Delta\nu_{2ab}$.		$\Delta\nu_{3ab}$.	
	$v' = 6$.	$v' = 5$.	$v' = 6$.	$v' = 5$.	$v' = 6$.	$v' = 5$.
2·5	3·03	—	—	—	—	—
3·5	2·90	—	−0·12	—	—	—
4·5	2·70	—	−0·13	—	—	−0·05
5·5	2·68	—	−0·15	−0·15	−0·03	−0·03
6·5	2·52	2·52	−0·23	−0·23	−0·01	+0·02
7·5	2·27	2·31	−0·32	−0·26	+0·02	0·03
8·5	2·00	2·06	−0·28	−0·31	0·03	0·08
9·5	1·87	2·00	−0·35	−0·33	0·05	0·07
10·5	1·75	1·84	−0·43	−0·44	0·08	0·02
11·5	1·74	1·73	−0·49	−0·53	0·05	0·04
12·5	1·65	1·63	−0·49	−0·45	0·05	0·07
13·5	1·64	1·60	−0·54	−0·58	0·10	0·11
14·5	1·59	1·61	−0·64	−0·64	0·13	0·10
15·5	1·55	1·54	−0·66	−0·67	0·10	0·12
16·5	1·49	1·52	−0·69	−0·73	0·17	0·12
17·5	1·42	1·43	−0·72	−0·76	0·10	0·14
18·5	1·40	1·38	−0·72	−0·78	0·22	0·14
19·5	1·36	1·35	−0·73	−0·81	0·24	0·16
20·5	1·34	1·32	−0·70	−0·84	0·30	0·19
21·5	1·32	1·26	−0·77	−0·88	0·34	0·20
22·5	1·31	1·22	−0·80	−0·89	0·34	0·20
23·5	1·26	1·22	—	−0·94	0·29	0·21
24·5	1·19	1·21	—	−0·92	0·34	0·22
25·5	1·18	1·15	—	−0·95	—	—
26·5	1·18	1·10	—	−0·96	—	—
27·5	1·18	1·04	—	—	—	—
28·5	—	1·00	—	—	—	—

The theory for the Λ-type doubling in triplet states either conforming to Hund's case *a* or case *b* has been given by Hill and van Vleck.[*] According to Mulliken[†] one would expect for a normal $^3\Pi$ state conforming to case *a* that the Λ-type doubling would be fairly large and remain constant in the $^3\Pi_0$ state, would increase proportional to J (J + 1) in the $^3\Pi_1$ state, and would be very small in the $^3\Pi_2$ state. For $^3\Pi$ states conforming to case *b*, on the other hand, the Λ-type doubling would be of moderate width and proportional to K (K + 1) in all three components of the multiplet. As is clear from Table XIII, the observed doubling does not correspond to either of the cases. Probably we have case *a* for small J values, because the doubling $\Delta\nu_{1ab}$ is relatively large as one expects for a case *a* $^3\Pi_0$ state, $\Delta\nu_{2ab}$ increases and $\Delta\nu_{3ab}$ is small. The fact that $\Delta\nu_{1ab}$ definitely decreases and $\Delta\nu_{3ab}$ increases slightly is probably due to a transition from case *a* for the lower J values to case *b* for larger J values. The results therefore, agree best with the theory if one assumes the $^3\Pi$ state is normal, and conforms to Hund's case *a* for lower J values and goes over to case *b* for higher J values.

---

[*] 'Phys. Rev.,' vol. 32, p. 250 (1928); see also J. H. van Vleck, 'Phys. Rev.,' vol. 33, p. 467 (1929).

[†] 'Rev. Mod. Phys.,' vol. 3, p. 145 (1931).

VII. *Spin Fine Structure of the* $^3\Sigma$ *State.*

The spin fine structure of the $^3\Sigma$ state can be obtained directly from the empirical data by determining the values corresponding to the differences between equations (13), (14) and (15). Thus:

Equation (14) — equation (13):

$$\Delta f_{21} = 2\varepsilon - \gamma + \varepsilon(1 - 3/2K + 3) - \gamma K$$
$$= 3\varepsilon(2K + 2/2K + 3) - \gamma(K + 1). \quad (35)$$

Equation (14) — equation (15):

$$\Delta f_{23} = 2\varepsilon - \gamma + \varepsilon(1 - 3/2K - 1) + \gamma(K + 1)$$
$$= 3\varepsilon(2K/2K - 1) + \gamma K. \quad (36)$$

Now

$$\begin{aligned}\Delta f_{21}(K) &= {}^{Q}R_{12}(J) - Q_1(J+1) = {}^{P}Q_{12}(J) - P_1(J+1)\\ &= R_2(J) - {}^{R}Q_{21}(J+1) = Q_2(J) - {}^{Q}P_{21}(J+1)\\ &= {}^{S}R_{32}(J) - {}^{S}Q_{31}(J+1) = {}^{R}Q_{32}(J) - {}^{R}P_{31}(J+1) \qquad (37)\end{aligned}$$

$$\begin{aligned}\Delta f_{23}(K) &= {}^{P}Q_{12}(J) - {}^{P}R_{13}(J-1) = {}^{O}P_{12}(J) - {}^{O}Q_{13}(J-1)\\ &= Q_2(J) - {}^{Q}R_{23}(J-1) = P_2(J) - {}^{P}Q_{23}(J-1)\\ &= {}^{R}Q_{32}(J) - R_3(J-1) = {}^{Q}P_{32}(J) - Q_3(J-1). \qquad (38)\end{aligned}$$

In fig. 3 the average experimental values of Δf_{12} and Δf_{32} for the vibrational level $v'' = 3$ are plotted against K. The corresponding values for the $v'' = 2$ level are not given since in most cases these values coincide with the given values. The drawn-out curve represents the curve given by the calculated values where $\varepsilon'' = -0{\cdot}433$ and $\gamma'' = -0{\cdot}003$. It will be seen that the graph represents the experimental values within experimental error. The determination of the Δf values becomes less certain in the neighbourhood of the heads, but for large J values, Kramers' theory seems to explain the observed fine structure of the $^3\Sigma$ state in N_2 very well.

The fine structure of the $^3\Sigma$ state has been studied in the molecules O_2,*

---

* R. S. Mulliken, 'Phys. Rev.,' vol. 32, p. 880 (1928); H. A. Kramers, 'Z. Physik,' vol. 53, p. 422 (1929); W. Lochte-Holtgreven and G. H. Dieke, 'Ann. Physik,' vol. 3, p. 937 (1929).

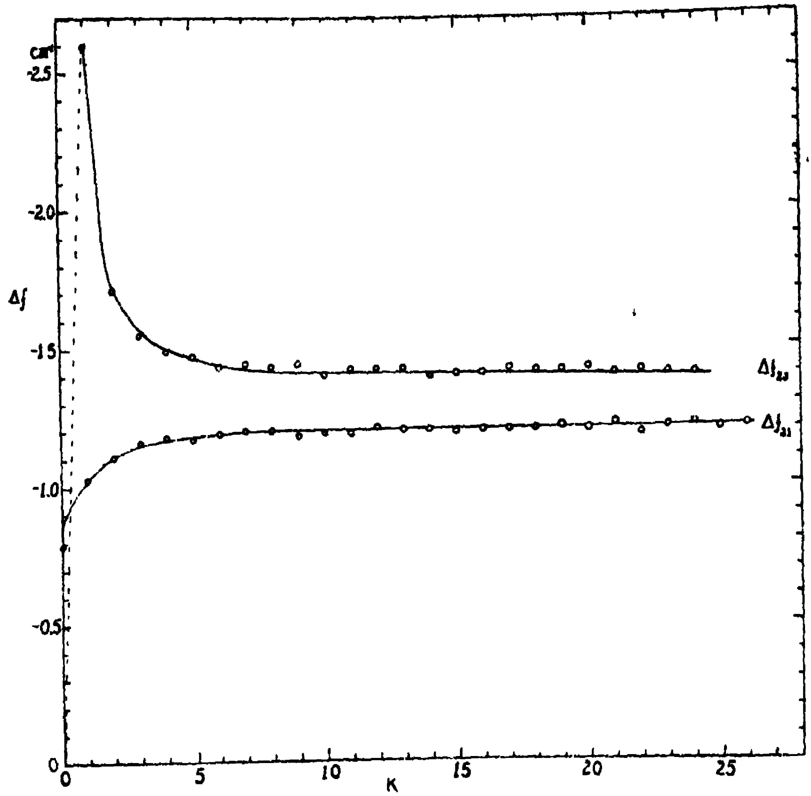

FIG. 3.—Graphs showing the average observed separations of the triplets in the final $^3\Sigma$ state. The circular points represent the averaged intervals in the $v'' = 3$ level corresponding to equations (37) and (38). The drawn graphs represent the theoretical curves corresponding to equations (35) and (36) where $\varepsilon = -0\cdot433$ and $\gamma = -0\cdot003$.

PH* and S_2.† If one compares the diagrams of the fine structure of the $^3\Sigma$ states in these molecules corresponding to fig. 3, it is clear that N_2 provides an interesting case where γ is so small that the Δf_{21} and Δf_{23} curves do not cross, but have an approximately constant separation for moderate values of K. For moderate K values, therefore, the effect due to the interaction of the resultant electronic spin with the rotational angular momentum is approximately equal and opposite to the effect due to the interaction of the individual spins of the electrons.

Further, it is also interesting to note that for every K value, the level for which $J = K$ lies below those for which $J = K + 1$ and $J = K - 1$ as indicated in fig. 2. In this respect the $^3\Sigma$ state also differs from the $^3\Sigma$ states in O_2 and PH. In the case of S_2 we cannot decide with certainty since only $(\epsilon' - \epsilon'')$ could be found from the analysis, the S_2 bands being due to a $^3\Sigma \rightarrow {}^3\Sigma$ transition. This inversion in the $^3\Sigma$ state of N_2 is due to ϵ having a negative value, ϵ being positive in both the other cases.

---

* R. W. B. Pearse, 'Proc. Roy. Soc.,' A, vol. 129, p. 328 (1930).

† S. M. Naudé and A. Christy, 'Phys. Rev.,' vol. 37, p. 490 (1931).

VIII. *The Molecular Constants.*

From the rotational analysis of the first positive bands the molecular constants of the N_2 molecule in the initial $^3\Pi$ and the final $^3\Sigma$ state can be determined.

The constant A in equation (2) which determines the separation of the components of the triplet is of considerable interest. Equation (6) must, however, be taken into consideration when A is determined. Owing to the large Λ-type doubling in the $^3\Pi$ state, the spin fine structure in the $^3\Sigma$ state, as well as the fact that the lines become very weak and overlap very much near the heads, the position of the origins of the three components could only be determined approximately. Thus the following values were found: the separation of the origins of the $^3\Pi_0 \rightarrow {}^3\Sigma$ and $^3\Pi_1 \rightarrow {}^3\Sigma$, $\Delta\nu_{12} \simeq 42$ cm.$^{-1}$, and the separation of the origins of the $^3\Pi_1 \rightarrow {}^3\Sigma$ and $^3\Pi_2 \rightarrow {}^3\Sigma$ components $\Delta\nu_{23} \simeq 37$ cm.$^{-1}$; giving as total separation of the $^3\Pi_0 \rightarrow {}^3\Sigma$ and $^3\Pi_2 \rightarrow {}^3\Sigma$ components $\Delta\nu_{13} \simeq 79$ cm.$^{-1}$. Consequently $A \simeq 39{\cdot}5$ cm.$^{-1}$.

The values of B'^*_v can be found from equation (12) by plotting the $\Delta_2 F'_i$ values given in Tables VII and I against J, the slope giving us $4B'^*_v$. The $\Delta_2 F'_i$ values are, however, affected by the Λ-type doubling, as can be seen if one compares the $\Delta_2 F_{ia}$ and $\Delta_2 F_{ib}$ values. This can be overcome partly by plotting the average of the $\Delta_2 F'_{ia}$ and $\Delta_2 F'_{ib}$ values, but in the $^3\Pi_0$ state where the Λ-type doubling is large, the B'^*_v value thus obtained may still be slightly erroneous. From B'^*_v the value of B'_v can be found according to equation (4), but the B'_v values thus obtained from the $^3\Pi_0$, $^3\Pi_1$ and $^3\Pi_2$ states do not agree. The value of B'_v in the $^3\Pi_1$ state is therefore taken as B'_v. B'_e, α'_e and r'_e can be determined with the help of the following equations:

$$\alpha_e = (B_0 - B_v)/v \tag{39}$$

$$B_e = B_0 + \tfrac{1}{2}\alpha_e, \tag{40}$$

and

$$r_e^2 = \frac{27{\cdot}66 \times 10^{-40}}{\mu B_e} \tag{41}$$

Since the extrapolation from B'_4 and B'_5 to B'_0 is large the values of B'_e and r'_e will only be approximately correct.

The values of B''_v can be obtained from equations (28), (29) and (30). Since γ is small, these three equations give almost identical values of B''_v, and hence, only the averaged value of B''_v is given. From the values for $v'' = 3$ and $v'' = 2$ the constants B''_e, α''_e and r''_e are obtained according to equations (39), (40) and (41). These constants are tabulated in Table XIV.

The values of $r'_e = 1 \cdot 20 \times 10^{-8}$ cm. and $r''_e = 1 \cdot 289 \times 10^{-8}$ cm. are in good agreement with the values $r'_0 = 1 \cdot 21$ and $r''_0 = 1 \cdot 28 \times 10^{-8}$ cm. obtained from Morse's empirical formula.*

The values of D'_e and D''_e given in Table XIV could be obtained from the formula $D_e = -4B_e^3/\omega_e^2$ and agrees within experimental error with the values obtained from equations (11), (28), (29) and (30).

From equations (28), (29) and (30) the value of the total angular quantum number J could be determined. These values of J are given in Tables I to XIII above.

IX. *Discussion.*

As can be seen from Tables II to VII and on Plates 3 and 4, the consecutive lines in every favourably situated branch have alternating intensities in the ratio of approximately two to one. This agrees very well with the value of this ratio obtained by van Wijk† in the first negative bands of N_2^+ and in the second positive bands of N_2 and indicate that the nitrogen nucleus has unit internal momentum.

From Tables II to VII it is evident that the rotational levels of the $^3\Sigma$ state having odd K values have greater statistical weight than those having even K values, since the lines terminating on these levels are approximately twice as intense as those having even K values. From this fact and the fact that the entire wave-function must be symmetrical, it may be concluded that the final state is either $^3\Sigma_g^-$ or $^3\Sigma_u^+$. The initial $^3\Pi$ state which combines with the final state will then be either $^3\Pi_u$ or $^3\Pi_g$. Which of these states actually exists can only be determined by considering the electronic configurations of the N_2 molecule and the states corresponding to these electronic configurations which are most likely to exist in the N_2 molecule.

In Section VI it was inferred from the Λ-type doubling that the $^3\Pi$ state is normal. By studying Lindau's analysis of the 2-5 second positive band, it at first appears that an inverted $^3\Pi$ state both in the initial and final states agrees with the missing lines given by him. If the J values of the present analysis

---

* 'Phys. Rev.,' vol. 34, p. 57 (1929).

† 'Z. Physik,' vol. 59, p. 313 (1930).

Table XIV.—The Molecular Constants.

	B_v*. (cm.$^{-1}$.)	B_v. (cm.$^{-1}$.)	B_e, α_e, r_e.	D_e, ϵ and γ. (cm.$^{-1}$.)
$^3\Pi_0$ $v' = 6$	1·477	—		
$v' = 5$	1·500	—	$\alpha'_e = 0·023$ cm.$^{-1}$ $B'_e \simeq 1·66$ cm.$^{-1}$ $r'_e \simeq 1·20 \times 10^{-8}$ cm.	$D'_e = -6·2 \times 10^{-6}$
$^3\Pi_1$ $v' = 6$	1·514	1·514		
$v' = 5$	1·537	1·537		
$v' = 0$	—	1·652 (extrapolated)		
$^3\Pi_2$ $v' = 6$	1·559			
$v' = 5$	1·582			
$^3\Sigma$ $v'' = 3$	—	1·395	$\alpha''_e = 0·013$	$\epsilon'' = -0·433$
$v'' = 2$	—	1·408	$B''_e = 1·440_5$	$\gamma'' = -0·003$
$v'' = 0$	—	1·434 (extrapolated)	$r''_e = 1·289 \times 10^{-8}$ cm.	$D''_e = -5·5 \times 10^{-6}$

are substituted in his analysis according to Table I, and it is noticed that the R_3 and P_3 lines having wave-numbers 25372·9 and 25358·8 cm.$^{-1}$ as given by him, are also assigned as P_3 and P_2 lines, the missing lines in Lindau's analysis will also be in agreement with a normal $^3\Pi$ state. In this case some lines belonging to the R_1 and P_1 branches having lower J values should yet be found to exist. Certain anomalies which were pointed out by Mulliken,* in case the $^3\Pi$ state were inverted, consequently disappear. The result that the $^3\Pi$ state is normal agrees with the conclusion reached by Mulliken (*loc. cit.*) in his discussion of Lindau's data on the second positive bands.

X. *Summary.*

The emission spectrum of the first positive nitrogen (N_2) bands has been obtained by means of a powerful discharge in pure nitrogen in a water-cooled, inverted H-tube, the plates being taken in the third order of a 21-foot concave grating giving a dispersion of 0·7 A. per millimetre. The following bands have been studied: 5·2 (λ 6705 A.) and 6-3 (λ 6623 A.). Each band consists of three groups of nine branches, of which three in each group are prominent. The structure agrees with a $^3\Pi \rightarrow {}^3\Sigma$ transition, the $^3\Pi$ state probably conforming to Hund's case *a* for the lower J values and going over to case *b* for higher J values. From the Λ-type doubling it is concluded that the $^3\Pi$ state is normal. The consecutive lines of the branches show alternating intensities in the ratio 2 to 1 approximately, thus indicating that the nitrogen nucleus has unit internal angular momentum. The rotational levels of the $^3\Sigma$ state having odd

---

* 'Phys. Rev.,' vol. 33, p. 509 (1929).

K values were found to have greater statistical weight and thus the $^3\Sigma$ state is either $^3\Sigma_g^-$ or $^3\Sigma_u^+$. The spin fine structure of the $^3\Sigma$ state agrees closely with the theory of Kramers if the constants $\epsilon'' = -0{\cdot}433$ and $\gamma'' = -0{\cdot}003$.

The molecular constants obtained from the analysis are :—

$$B''_e = 1{\cdot}440 \text{ cm.}^{-1},\ \alpha''_e = 0{\cdot}013 \text{ cm.}^{-1},\ r''_e = 1{\cdot}289 \times 10^{-8} \text{ cm.},$$
$$D''_e = -5{\cdot}5 \times 10^{-6} \text{ cm.}^{-1} \text{ and } B'_e \simeq 1{\cdot}66 \text{ cm.}^{-1},\ \alpha'_e = 0{\cdot}023 \text{ cm.}^{-1},$$
$$r'_e \simeq 1{\cdot}20 \times 10^{-8} \text{ cm.},\ D'_e = -6{\cdot}2 \times 10^{-6} \text{ cm.}^{-1}.$$

The experimental part of this work was carried out at the Ryerson Physical Laboratory, University of Chicago. The author wishes to express his appreciation to Professor R. S. Mulliken for suggesting this problem and for his interest and advice in connection with this work, and to Dr. W. Weizel for helpful suggestions. The author also wishes to thank Professor R. T. Birge for consenting to his taking up the problem which Professor Birge and his collaborators had worked on for several years, and for submitting some of the lower dispersion data obtained by them.

DESCRIPTION OF PLATES.

PLATES 3 (*a*), (*b*), and 4 (*c*), (*d*) show an enlargement of the 6-3 band made from the original third order plate. The various branches are marked by lines drawn opposite the lines on the picture. The scale is given in wave-numbers. The plates overlap slightly and the branches may be followed from the smaller wave-numbers on Plate 3 (*a*), through (*b*), (*c*) and (*d*). The most refrangible strong head of the 7-4 band is visible on Plate 4 (*d*). In the branches which form heads, the branch lines having lower J values and leading up to the heads are indicated by vertical lines hanging from the horizontal lines, and the branch lines beyond the heads are indicated by vertical lines standing on the horizontal lines. The assignment of the various branches is given alternately on the right and on the left.

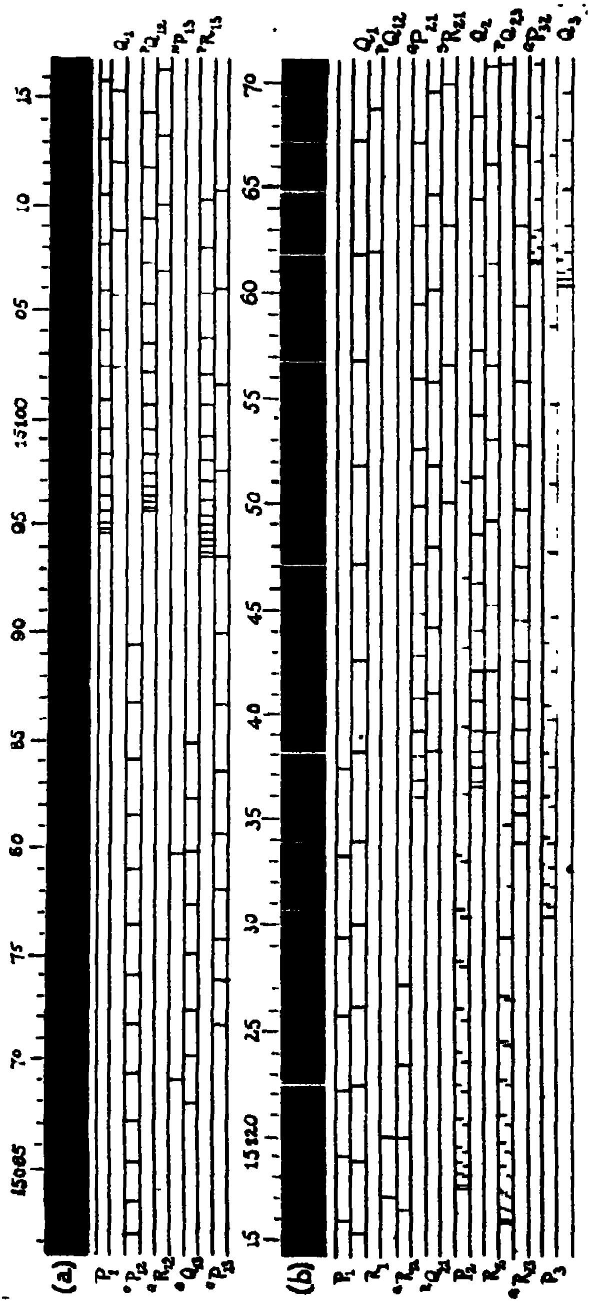
(a)
(b)
15
10
05
15100
95
90
85
80
75
70
15085
70
65
60
55
50
45
40
35
30
25
15120
15
P₁
Q₁
P₁₂
Q₁₂
R₁₂
P₁₃
Q₁₃
R₁₃
R₁
Q₂₁
P₂₁
R₂₁
P₂
Q₂
R₂
Q₂₃
R₂₃
P₃₂
P₃
Q₃

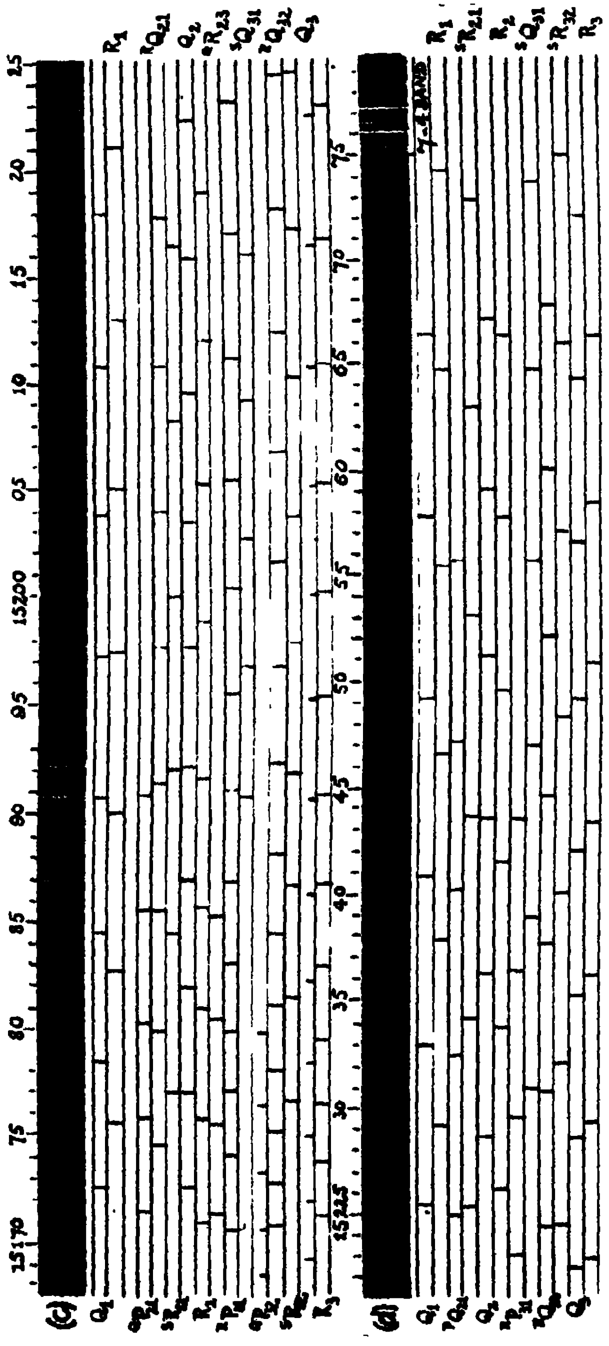
(c)
(d)
15170
15200
15225
Q₁
R₁
Q₂
R₂
Q₃
R₃

Mobility of Positive Alkali Ions in Argon, Neon and Helium.

By A. M. Tyndall and C. F. Powell.

(Communicated by A. P. Chattock, F.R.S.—Received November 25, 1931.)

In a previous paper* we described the application of new methods of measuring the mobility of ions to the case of positive ions of helium moving through helium gas. We also gave an example of the profound effect of traces of impurities in giving rise to groups of ions moving at speeds different from that of helium ions. This result is contrary to those obtained in many earlier investigations on the mobility of ions produced in one gas and measured in another. It was found that such ions could not be distinguished in their mobility from an ion of the gas in which the measurements were made. This is explained by the fact that, judged by present standards, the gas in all these early experiments was very impure and the ions consisted of clusters of polar molecules. Moreover, except in the case of the radio-active recoil atoms investigated by Rutherford and by Franck, which have a low ionisation potential, the conditions were often favourable for a transfer of charge from the original ion to some other atom or molecule, so that even the core of the cluster may not have been that of the original ion. In the determination of the mobility of different ions in a gas, the positive ions may be produced from Kunsman sources of the alkalies or alkaline earths, or from a glow discharge in a gas containing small amounts of known impurities. The present paper describes the results obtained in argon, neon and helium by the first method using ions of sodium, potassium, rubidium and cæsium.

Experimental.

Reference must be made to previous papers for details of the method by which the mobility of an ion is deduced from the position of a sharp peak in an electrometer current-frequency curve.

In working with Kunsman sources it is necessary to employ some cooling device in order to prevent the hot platinum strip carrying the Kunsman mixture from heating the gas in the measuring chamber. Otherwise there will be not only a serious rise in the temperature of the gas as a whole, but also a large temperature gradient of uncertain distribution along the path of the ions. Thus in some recent experiments on the mobility of positive sodium ions in nitrogen and hydrogen, Loeb* found that the temperature of an electrode, coplaner with the hot source, sometimes rose to 200° C. and that the mean temperature of the gas was as much as 80° C. This involved large corrections in determining a value for the mobility of the ions and left the final result uncertain to about 10 per cent. Such uncertainties would have been very serious in the present work as the difference in mobility, between sodium and potassium ions in helium, is only 4 per cent.

---

* 'Proc. Roy. Soc.,' A, vol. 134, p. 125 (1931).

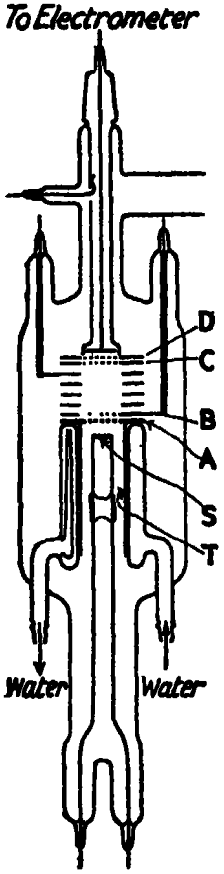

Fig. 1.

The experimental tube employed is shown in fig. 1. It is similar in principle to that shown in fig. 1 of our previous paper except that the old plate, A, is replaced by a heavy pierced copper plate, A, welded to a copper tube, T. A water jacket, J, fitting closely round it keeps the copper cool. Three Kunsman sources, one of which is shown at S, are mounted side by side in the copper tube 2 or 3 mm. from the copper plate. To test the efficiency of the cooling system a thermo-junction was inserted immediately above the plate, B. The rise in temperature of the gas when a source was heated to a bright yellow heat was 4° C. We concluded that the maximum rise in temperature during any experiment was never more than 3° C. and in general was less than 1° C. This is of the same order as the fluctuations in room temperature and both these sources of error, leading to corrections of probably less than 1 per cent., have been ignored.

We are indebted to Mr. Luang Brata for the preparation of the Kunsman sources. They were made by mixing together 93 per cent. precipitated ferrous oxide, 5 per cent. alumina and 2 per cent. of the alkalies in the form of the nitrate or hydrate. These chemicals were the best analytical reagents procurable commercially. The mixture was heated to redness in air and then ground in an agate mortar, the process being repeated several times. The mixture was reduced in hydrogen in bulk and each source was individually reduced again after insertion in the apparatus.

The argon was of a high grade of purity supplied to us by the G.E.C. Research Laboratory. The neon contained 2 per cent. of helium. The helium was obtained from thorianite. Each gas was purified before admission to the apparatus although the ionisation potentials of the alkalies are low so that elaborate precautions, which must be taken when the positive ions are produced by a glow discharge in a rare gas, were unnecessary. The gas was never so impure that the alkali ions changed in mobility owing to the formation of complex ions by collisions with impurities.

---

* 'Phys. Rev.,' vol. 38, p. 549 (1931).

The curves shown in this paper were taken in the third order with the alternating potentials out of phase. In other words, the ions crossed the measuring apparatus in a time equal to two and a half periods of the peak frequency of the alternating fields. Fig. 2 is an example of the resolving power which was obtained. Curve A was taken with a potassium source in neon. Curve B is a peak due to sodium ions in the same gas plotted on a larger current scale to show the accuracy with which the peak frequency can be determined.

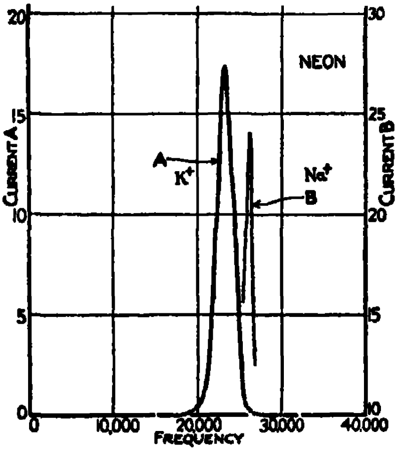

Fig. 2.

Results.

The first results obtained were very illuminating and may be illustrated by some experiments in argon. Three sources of sodium, potassium and rubidium were mounted side by side so that they could be used in turn in the same specimen of gas. Measurements were taken after each source had been heated to redness *in vacuo* for a few hours and the gas then admitted. Starting with sodium, it was found that all three sources gave the same type of curve consisting of two peaks at mobilities 2·34 and 2·74. The curves for the sodium source are shown in fig. 3, A. It was quite clear that we were not dealing with a pure source of ions, firstly because of the existence of two peaks instead of one, and secondly because it was impossible to believe that ions of rubidium (atomic weight 79) and of sodium (atomic weight 23) would travel at the same rate in argon (atomic weight 39). Now the emission of ions from a Kunsman source at a given temperature depends upon the ionisation potential of the

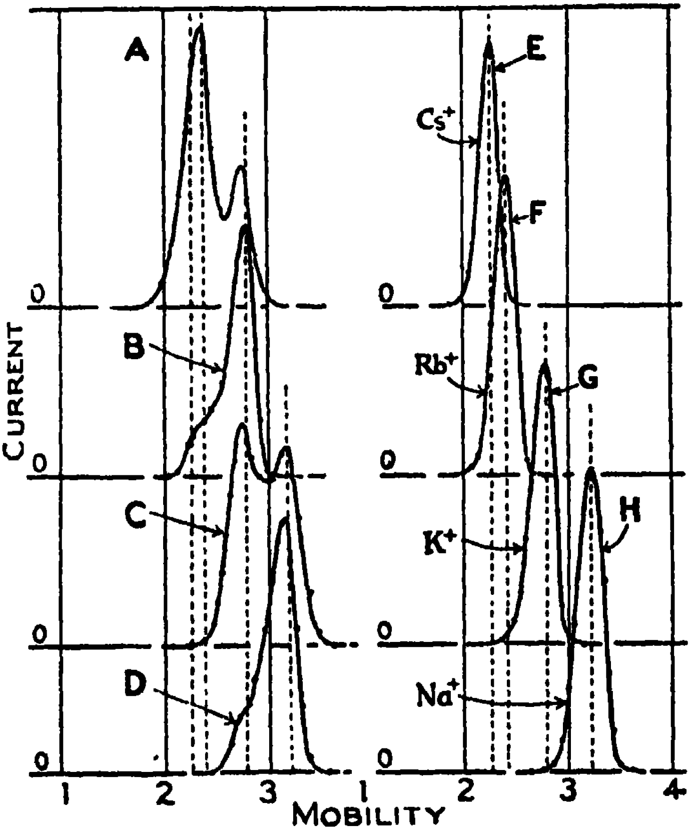

FIG. 3.

alkali. If a source contains small quantities of heavier alkalies, present as impurities, then the fraction that they contribute to the total emission will be far in excess of that appropriate to their concentration. It therefore seemed possible that the first peaks we obtained were due not to sodium but to rubidium and potassium present in the sodium source in traces. We were able to confirm this in the following manner. After heating the source *in vacuo* for about 6 hours with the field applied to remove the ions continuously, both these peaks disappeared and were replaced by a single peak at a higher mobility. Current frequency readings, taken every 2 hours during this run, are shown in fig. 3, A–D. Curve A shows the two peaks obtained before this treatment and attributed to rubidium and potassium respectively. B, taken 2 hours afterwards, shows that in that interval nearly all the rubidium had gone. C, obtained after another 2 hours, shows a new peak at mobility 3·18, which in D, at the conclusion of the run, is the only one remaining. We may assume that this is the true peak due to sodium ions as further heating left it unchanged.

The correctness of these deductions was confirmed by experiments with the other Kunsman sources. A cæsium source never gave more than the one peak shown in fig. 3, E. The rubidium source after continuous heating gave F and that of potassium G. H is another curve for sodium. The vertical dotted lines in curves A to D mark the positions of the several maxima of the curves E to G and in accordance with our analysis the three for rubidium, potassium and sodium show a close coincidence with the peaks given by the sodium source during its process of ageing.

The behaviour of the sodium source illustrates the remarkable sensitiveness of the method in detecting traces of the heavier alkalies. The alkali in this case was Kahlbaum's best analytical soda and any rubidium or potassium in it was almost certainly undetectable chemically. Other observers have found that a sodium source will emit potassium ions, but we are able to make a more detailed analysis because we require a much smaller emission from the source than is necessary for work involving magnetic analysis, where only a very small fraction of the ions passes through the defining slits. Also, in our method, the analysis of the ions takes at most 15 minutes.

The sensitivity of the method may also be gauged from another observation. Two Kunsman sources were mounted in the apparatus side by side about 3 mm. apart, one of cæsium and the other giving potassium ions. After some continuous use of the potassium source a single run of the cæsium source of about 15 minutes' duration was made in order to obtain the position of the cæsium peak. When on the completion of this run the potassium source was used again, it was found to give nothing but cæsium ions. Presumably cæsium metal had evaporated from the hot strip and condensed on the adjoining cold source because after the latter had been heated for about 10 minutes the supply of cæsium ions ceased and the potassium peak reappeared. It is clear from these experiments that some care is necessary in the interpretation of results obtained with Kunsman sources when a mass analysis by a magnetic field is not available.

In Table I are summarised the results obtained from the various sources in argon, neon and helium. The pressures in argon varied from 9 to 11, in neon from 17 to 23, and in helium from 24 to 51 millimetres of mercury. The "main" field in which the ions moved was 70 volts/centimetre throughout the experiments. We had previously shown that the mobility of helium ions in helium was inversely proportional to the pressure and independent of the field over a wide range. We have found no evidence to the contrary for these alkali ions over the range of "E/p" at which we worked, and we have therefore reduced all the results to normal pressure.

Table I.

Gas.	Mobility of ion (cm./sec./volt/cm.).			
	Sodium.	Potassium.	Rubidium.	Cæsium.
gon .	3·21	2·77	2·37	2·23
on . . .	8·87	7·88	7·08	6·49
lium	23·1	22·3	20·9	19·2

In consequence of the presence of 2 per cent. of helium in the neon, it is calculated that the observed mobilities in this gas are too high by about 1 per cent. The values inserted in the table have, therefore, been corrected by this amount. In most cases the numbers are means of four or five determinations with an extreme difference of less than 2 per cent.

Discussion of Results.

We can now compare these results with such information as is available from theoretical data. On the assumption that the ion, of mass M, and the molecules of the gas, of mass m, are elastic spheres and that there is an inverse fifth power attractive field between them due to the polarisation of the molecules, Langevin deduced the following formula for the mobility, K.

$$K = \frac{A}{\sqrt{\rho(D-1)}} \cdot \left[1 + \frac{m}{M}\right]^{\frac{1}{2}},$$

where ρ is the density of the medium and D is its dielectric constant.

A is a function of the sum of the radii of the ion and the molecule of the gas and of the polarisability of the molecules. Its value is governed by the relative importance of the attractive field and of elastic collisions in determining the path of the ion through the gas. For strong attractive forces, A tends to a limiting value. If, therefore, we take the case of ions moving in a highly polarisable gas we might expect the variation of mobility with mass to approach that given by the expression,

$$K \propto [1 + m/M]^{\frac{1}{2}}.$$

If we replace the elastic spheres by point centres of force with a superposed attractive force due to polarisation, the same conclusion will follow provided that the effect of the polarisation force is large compared with that of any others. With a gas of low polarisability, however, we may expect that the size of the elastic spheres, or its equivalent in fields of force, cannot be neglected and that a deviation from the simple mass relation, of amount increasing with the size of the ion, will occur.

Now the relative values of the polarisability of argon, neon and helium are approximately 8, 2 and 1 respectively, so that if there were any deviation from the simple mass relation with increase of mass of the ion, it should be least in argon and greatest in helium. In fig. 4 the full lines are curves in which the ratio of the mobilities of the alkali ions to that of sodium, deduced on the assumption that $K \propto (1 + m/M)^{\frac{1}{2}}$, is plotted with the mass of the ion. The experimental values are shown as circles. It will be seen that in argon the mass relation is obeyed very exactly. There is some deviation from it in neon and still more in helium. The deviation is moreover in the direction which the theory would lead one to expect.

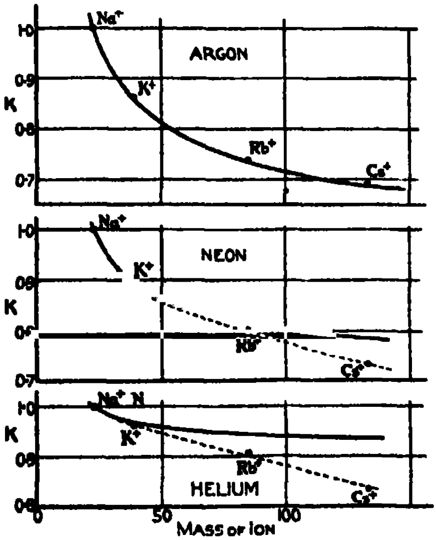

Fig. 4.

We must await further development of the theory of the motion of ions in terms of fields of force between ions and molecules before rigid quantitative tests can be applied. In the meantime an experimental study of other ions which may be produced by glow discharge in various gases containing small quantities of known impurities should give results of interest and investigations on these lines are now proceeding.

Summary.

The mobilities of positive ions of sodium, potassium, rubidium and cæsium have been measured in argon, neon and helium. In each gas the mobility decreases with increase of mass of the ion. In argon the mobilities range from 3·21 cm./sec./volt/cm. for sodium ions to 2·23 for cæsium. The corresponding figures for neon are 8·87 and 6·49 and for helium 23·1 and 19·2.

In argon the variation of the mobility K with the mass of the ion M is given by the relation $K \propto (1 + m/M)^1$, where m is the mass of an argon atom. In neon the fall in mobility with increase in mass of the ion is slightly greater than that given by this expression. This deviation is still more marked in helium. Theoretical considerations suggest that the simple mass relation should apply in the ideal case of a highly polarisable medium and in this respect it is significant that the polarisability of argon is approximately four times that of neon and eight times that of helium.

We are indebted to the Colston Research Society of the University of Bristol for a grant in aid of the work and to Mr. Luang Brata for assistance in the experiments.

On a Determination of the Pitot-Static Tube Factor at Low Reynolds Numbers, with Special Reference to the Measurement of Low Air Speeds.[*]

By E. Ower, B.Sc., A.C.G.I., and F. C. Johansen, M.Sc., A.M.I.Mech.E.

(Communicated by L. Bairstow, F.R.S.—Received November 26, 1931.)

§ 1. *Introduction.*

1.1. Of the numerous instruments that have been devised for the measurement of the speed of flowing gases, the pitot-static combination alone has proved itself suitable for use as a standard. It owes its superiority in this respect mainly to the fact that its calibration factor has been found to be constant over a large range of Reynolds number and is affected only by mechanical damage of a kind that can easily be detected by cursory inspection. A single calibration therefore endures throughout the life of the instrument. For this reason the combined pitot-static tube, in one or other of a few types differing only in unimportant details, has been universally adopted as a standard and, although in many circumstances other apparatus or instruments may be more conveniently used for measuring gas-flow, the calibration of such apparatus or instruments has always ultimately to be referred to pitot-static measurements.

1.2. The construction of a pitot-static tube will be clear from fig. 3 (*a*). It consists of two coaxial tubes A and B arranged over part of their length with their axes parallel to the direction of motion of the flowing gas. This portion of the instrument is known as the " head," while the " stem " comprises those parts of the tubes perpendicular to the head. The stem is generally considerably longer than the head for convenience in mounting the instrument in the required position without interfering with the flow past the head. Tube A is open to the stream only at its end C, which must be arranged to face the motion, while tube B is sealed from tube A entirely and from the stream except at the series of small orifices shown at D. Provision is made at the other ends of the tubes in the stem to connect each to one side of a differential manometer. There is then no flow through the tubes and it is found that if the shapes and proportions of the head are properly chosen, the pressure acting at the aperture C is the total head in the stream (that is the velocity head plus the static pressure), while that at the orifices D is very nearly equal to the static pressure. The differential head indicated by the manometer is thus substantially equal to the velocity head. An empirical calibration factor allows for any discrepancy between the static pressure and the pressure at the static orifices D.

---

[*] Work done at the National Physical Laboratory for the Aeronautical Research Committee.

1.3. In the form usually employed, the relation between the differential pitot-static pressure p, the mass density of the gas ρ, and the speed of flow v is

$$K \cdot p = \tfrac{1}{2}\rho v^2, \tag{1}$$

where K is the pitot-static factor which has to be determined by calibration. In 1912 this factor was determined at the N.P.L.* over a range of air speed of 20 to 60 feet per second† for a form of pitot-static tube which has since been adopted as the British standard. Over this range of air speed the value of the factor K was found to be unity within the observational accuracy, and subsequent (unpublished) experiments in water showed that this value persisted, without appreciable change, up to rates of flow equivalent to air speeds of the order of 250 feet per second.

1.4. No direct calibration of the British standard has hitherto been made for air speeds of less than 20 feet per second, nor are the writers aware that any low speed calibration has been undertaken for other types of pitot-static tube. There is no *a priori* justification for the assumption that the factor will retain its value of unity for the lower speeds. Indeed, consideration of the real nature of the pressure at the static holes—the resultant of the suction due to the flow past the mouth of the tube and the upstream pressure due to the presence of the stem‡—suggests the possibility of scale effect, while general aerodynamic experience further suggests that the region in which scale effect is most likely to make itself felt, if at all, is that of low Reynolds numbers,§ *i.e.*, precisely that range of air speeds for which no calibration exists.

1.5. This argument applies only to the static side of the instrument. As regards the total-head side, some work by Miss Barker‖ has shown that the total head is accurately measured by a pitot-tube down to a Reynolds number of 30, the linear dimension here being the *radius* of the mouth of the tube. For the British standard, therefore, it follows from this work that there is no scale effect on the total-head side above an air speed of 0·65 feet per second under ordinary atmospheric conditions. Hence any scale effect found between air speeds of 20 and 0·65 feet per second may be attributed to the static tube.

---

* Bramwell, Relf and Fage, 'Aero. Res. Com. R. and M., No. 71,' 1912, "On a determination on the whirling arm of the pressure velocity constant for a pitot (velocity head and static pressure) tube; and on the absolute measurement of velocity in aeronautical work."

† Unless otherwise stated, air speeds referred to in general terms throughout this paper relate to air under average atmospheric conditions.

‡ Ower and Johansen. See 'Aero. Res. Com. R. and M., No. 981,' 1925, "The design of pitot-static tubes."

§ The Reynolds number for the pitot-static tube is defined as the product vd/ν, where v is the speed of the fluid, d is the external diameter of the static tube (B, fig. 3, *a*) and ν is the coefficient of kinematic viscosity of the fluid.

‖ 'Proc. Roy. Soc.,' A, vol. 101, p. 435 (1922).

1.6. Speeds of this order of magnitude are of little importance in general aerodynamic work, nor is their accurate measurement usually necessary in the qualitative experimental investigations of fluid motion often conducted at low Reynolds numbers. But for the calibration of low speed anemometers and similar instruments, for which there is a considerable demand, the provision of a reliable low speed standard is very desirable, and in view of the outstanding advantages of the pitot-static tube it was decided to extend the calibration of the British standard to a speed of 2 feet per second. This limit was fixed as it was about the lowest speed for which the pressure could be read to an accuracy of 1 per cent. with the new sensitive manometer available (see § 2.1 and § 3.4).

§ 2. *General Considerations affecting the Choice of Method.*

2.1. The ideal method of conducting a fundamental calibration of the instrument would be to cause it to move in a straight path at a known speed through still air, and to measure the pressure difference set up at the total-head and static orifices. Little consideration is needed to realise the very grave objections to this method on the score of both expense and experimental difficulty. It was therefore decided to adopt a method similar to that previously employed for calibrations at the higher speeds at the N.P.L. and elsewhere. Here the pitot-static tube is mounted on the end of an arm rotating about a central axis, generally vertical, so that the instrument moves in a circular path at a measurable speed relative to the ground. Unfortunately, this speed is not the same as the air speed of the instrument, for the motion sets up a rotary movement or " swirl " of the air, and the true air speed is the difference between the ground speed and the swirl speed. It is in the accurate measurement of the swirl speed that the major difficulty of all calibrations on a whirling arm lies. In the present instance, also, there was the additional difficulty of measuring with sufficient accuracy the very small pressure differences set up by the instrument at low air speeds* ; but this was successfully overcome by the development of a specially sensitive manometer responding to a differential head of less than 0·00001 inch of water.*

---

* At 2 feet per second, for example, the pressure difference is equivalent to a head of about 0·001 inch of water.

§ 3. *Apparatus.*

3.1. Sketches of the apparatus appear in figs. 1 and 2. Briefly, it comprised means for moving the pitot in a circular path totally enclosed by an annular wooden tunnel of 2 feet square section and about 50 inches mean radius. Thus the pitot was shielded from draughts in the room, whose influence can be very disturbing at low speeds. The pitot protruded vertically downwards into the tunnel through an annular slit in the roof at the mean radius, the slit being closed everywhere, except at the point of entry of the pitot, by means of a rubber seal, lubricated with glycerine, whose details will be apparent from fig. 2. Outside the tunnel, the pitot was attached to the end of one of the four braced radial arms whose inner ends were anchored to the outer rotating portion of the specially designed central oil seal (A in fig. 1), by whose agency the pressures acting at the total-head and static orifices of the moving pitot were transmitted through rubber tubing to the stationary manometer alongside the tunnel. Lateral bracing for the four arms was furnished by the wooden ring (E in fig. 2) connecting their outer ends, while additional vertical stiffening was provided by the strips of tinplate F fastened all round both edges of the ring.

3.2. The drive was effected by means of the electric motor (B in fig. 1) through a belt and pulley system, the final member being the large wooden pulley C carried by the rotating portion of the seal. Provision was made for continuous indication of the speed of the driving motor in order that any tendency for the speed to creep during the few minutes occupied in taking an observation could be detected instantly and corrected by means of suitable rheostat control. For this purpose a simple A.C. generator D was used, consisting of a fixed coil wound on an iron core and placed between the limbs of a permanent horseshoe magnet rotated through a claw coupling at the speed of the driving motor shaft. The alternating current from the coil was led to an electrodynamometer, consisting of a moving and a fixed coil in series, the deflection of the former being observed by means of the usual optical system adopted for reflecting mirror galvanometers. This arrangement proved extremely sensitive to small changes of motor speed, well within the limits required over the whole speed range. The speed of the rotating ring itself (and hence that of the pitot over the ground) was separately measured, at low speeds directly by means of a stop-watch and at the higher speeds by means of a recording chronograph.

---

* See Ower, 'Phil. Mag.,' vol. 10, p. 544 (1930).

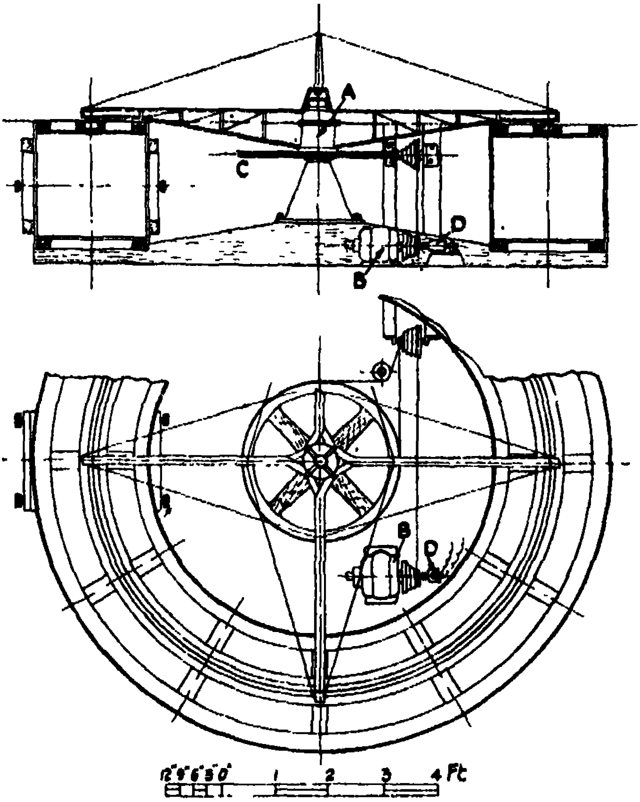

FIG. 1.—Annular tunnel.

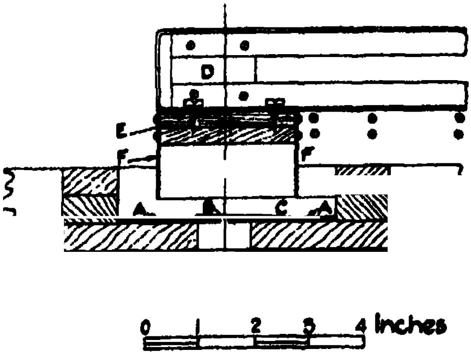

FIG. 2.—Detail of rubber seal in roof of tunnel. AA, strips of thick sheet rubber nailed to roof of tunnel. B, strips of thin sheet rubber stuck to thick strips at C. D, arm for carrying pitot.

3.3. Mention may here be made of the means adopted for reducing the unsteadying effect on the manometer of such pressure fluctuations inside the tunnel as could occur on a gusty day. Owing mainly to the fact that the damping of the total-head orifice to the passage of a pressure wave is less than that of the static orifices, a pressure impulse in the tunnel, although acting simultaneously at the total-head and static orifices, produces an oscillation in the manometric liquid which may seriously impair the accuracy of the pressure measurement. This difficulty was overcome by introducing into the rubber tube connecting the total-head tube to the manometer a piece of glass capillary tubing in order to increase the damping of the total-head side. With static and total-head connections made to the manometer, the length of the capillary was adjusted until a small artificially produced pressure, simultaneously applied to both sides of the pitot-static tube, gave rise to the minimum disturbance in the manometer. As a result of this expedient, and of the special design of the oil seal, the fluctuations of pressure encountered during readings were always small and insufficient to render difficult the taking of accurate observations.

3.4. Two different manometers were used, one for speeds above about 15 feet per second and the other for lower speeds. The former was a 13-inch Chattock gauge of the ordinary type, although somewhat improved in mechanical details. It was calibrated on a tilting table before use. The manometer employed for speeds below 15 feet per second was the new sensitive instrument to which reference has already been made. Its geometrical constants had been previously determined by the Metrology Department of the N.P.L. During the course of the investigation, when, as will later be seen, the pitot-static factor at low speeds was found to drop sharply, it was thought desirable to make a direct check of the accuracy of this manometer. For this purpose use was made of apparatus belonging to the Engineering Department, which enabled a very small known pressure difference to be applied to the manometer. The pressure difference was produced by the difference in weight of two air columns of measurable and equal height, one at the temperature of melting ice and the other at room temperature. In the actual test the air in both columns was carefully dried in order that its density could be accurately calculated from a knowledge of the temperature and pressure. With the warm column at a temperature of about 19° C. a pressure difference of $0 \cdot 00242_4$ grms. per cm.^{2} was applied to the manometer. The corresponding pressure difference observed on the latter was $0 \cdot 00243_4$ grms. per cm.^{2}, which was the mean of three readings agreeing within 1 per cent. Hence a steady differential pressure of this low order could be measured to an accuracy of 0·4 per cent., and it should be noticed that in magnitude it was about equal to the differential pitot-static pressure at an air speed of 2 feet per second.

§ 4. *Range of the Investigation and Experimental Details.*

4.1. The British standard pitot-static tube was calibrated over the range of true air speed from about 1·6 to 23·8 feet per second. In addition, a somewhat less thorough calibration was made of a tube having a hemispherical nose and of a copy of the standard instrument constructed to a scale of 0·535 to 1. Drawings of the standard head and that with the hemispherical nose are given in fig. 3, *a* and *b*, respectively. The latter instrument had been designed from the data given in R. and M., No. 981,* to have a constant of unity above 20 feet per second. The small scale copy of the standard was tested in order to provide some check of the results obtained during the main calibration.

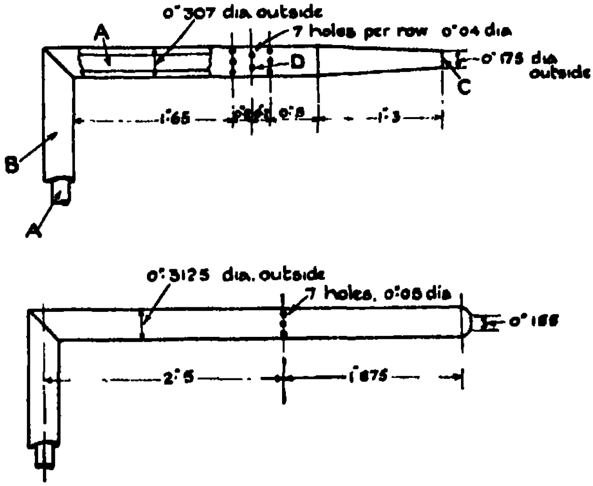

FIG. 3.—(*a*) Standard head; (*b*) Head with hemispherical nose.

4.2. The methods of testing the three instruments were similar and the following description, which relates to the standard, will suffice as an indication of the experimental procedure. The instrument was mounted in the tunnel with the stem vertical and the head horizontal and tangential to the circular path at the central row of static holes. The radius of the path, measured to the axis of the head at the static holes, was approximately 50 inches, and, as the mouth of the total-head tube is 2 inches forward of the central row of holes, it follows that the local angle of yaw at the mouth of the total-head tube was about 2½°. Some work by R. Jones and the late J. R. Pannell* showed that the total-head tube registers correctly up to an angle of yaw of more than 10°, so that no error was caused by the small local yaw inevitable in the setting chosen for this calibration. Confirmatory tests were, in fact, made, in which the tangential point was midway between the central row of static holes and the mouth, but no difference could be detected in the pressure observed at a given translational speed. Another possible source of error resulting from the setting, namely, that the radii of the axis of the tube at the static holes and at the mouth are slightly different, is examined in Appendix II and shown to be negligibly small.

---

* See earlier reference.

4.3. The following was the procedure in taking a complete observation at each speed. The arm was set in motion and its rate of rotation was adjusted until rough timing with the stop-watch showed that the pitot was travelling at approximately the speed desired. The motor speed was then maintained constant, by means of the electrical speed indicator already mentioned, and the arm was allowed to make the number of revolutions (see § 5.3) requisite for the growth of the swirl to its steady value. When the full swirl was established, simultaneous observations were made of the pitot-static pressure and of the arm speed, the duration of the observation being sufficient to enable the speed to be measured to an accuracy well within 0·1 per cent.

4.4. After a satisfactory run the connections of the pitot-static tube to the two chambers of the oil seal were interchanged and a second set of observations was made at the same speed as before. The object of this procedure was mainly to eliminate from the final result any pressure set up in the system by the rotation of the moving parts of the seal. Such pressures would depend only on the rate of rotation and hence the mean of the pitot-static pressures observed with connections direct and reversed was free from errors due to this cause. Despite the fact that usually no systematic difference was observed between the two pressure observations, this process of interchanging the connections was adopted throughout the investigation as it provided two results for each speed which served as a check on each other.

4.5. When the two sets of observations at each speed were completed, wet- and dry-bulb temperatures of the air in the tunnel were noted in order to enable the value of ρ to be calculated. The remaining quantity—the barometric pressure—necessary for the determination of ρ was obtained from the Metrology Department, who kindly took barometric observations for this purpose at frequent intervals on those days on which the calibration was in progress.

---

* 'Aero. Res. Com. R. and M., No. 445,' 1918, "The design of a sensitive yawmeter."

4.6. Finally, it should be noted that a correction to the measured radius was applied at the higher speeds to allow for the centrifugal deflection of the pitot head. This was found by measurement to amount to about 0·05 inches at an arm speed of 29 feet per second. Below 18 feet per second this correction was, however, negligible, being equivalent to less than 0·1 per cent. of the square of the speed.

§ 5. *Measurement of the Swirl.*

5.1. The arrangements made for the determination of ground speed and of pressure permitted, without undue difficulty, an accuracy of the order of 0·1 per cent. in the measurement of each of these quantities down to a speed of about 7 feet per second. Below this limit the accuracy of pressure determination was reduced, although that of speed was maintained. The accuracy of the final calibration therefore hinged upon the precision of the swirl measurement, and this presented the most troublesome problem of the whole investigation. Various fruitless methods of measuring, or, alternatively, of eliminating, the swirl were tried and abandoned. Finally, it was decided that the use of the hot-wire anemometer offered the only reasonable prospect of success, and a technique was developed which gave satisfactory results. The hot-wire was first calibrated on the rotating arm itself, and was then removed from the arm and mounted in a suitable stationary position in the tunnel to measure the swirl set up by the pitot (see below, § 5.4).

5.2. The wires used were platinum, about 0·7 inch in length and 0·001 or 0·002 inch in diameter, both sizes being employed at different times in the measurements. They were welded to short lengths of stouter platinum wire soldered to the supports, which consisted of tapered brass wire attached to an ebonite base, and were used also to make electrical connection with the Wheatstone bridge circuit. A sketch of the wire appears in fig. 4, *b*, while fig. 4, *a*, shows the measuring circuit. The wire is run at constant temperature (*i.e.*, at constant resistance), so that when it is in motion relatively to the air the current through it has to be increased by an amount depending on the speed. The scheme of operation is therefore to balance the Wheatstone bridge by adjusting the external current with the aid of suitable rheostats. When the bridge galvanometer G_1 indicates balance the potential drop across the wire is observed by means of the potentiometer P and its galvanometer G_2.

5.3. The relation between the potential drop in the wire and the relative air speed was obtained by attaching the hot-wire instrument to the rotating arm and moving it through the air inside the tunnel at known speeds covering the swirl range. In every case the corresponding potentiometer reading was obtained within two revolutions of the arm, and, as it was found that about 150 revolutions of the arm were necessary to establish the swirl due to the pitot-static tube at its full steady value, it was assumed that no appreciable error was made by taking the arm speed at the proper radius as being the true air speed of the wire during calibration. Confirmation of this assumption was provided by check pressure measurements of the swirl (§ 5.5).

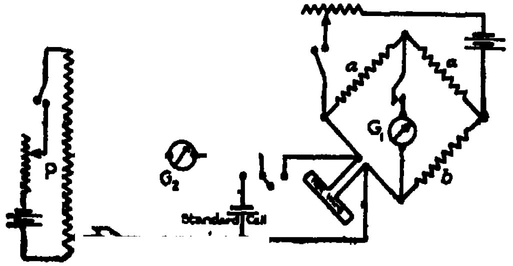

Fig. 4.—(*a*) Electrical Connections for Hot Wire Anemometer.

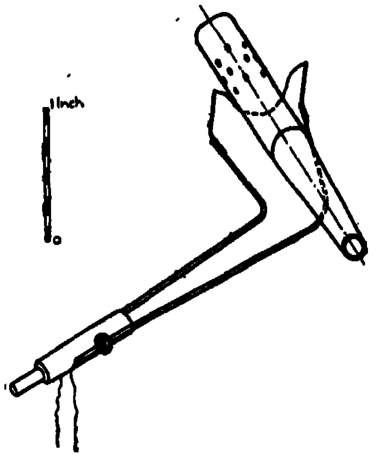

Fig. 4.—(*b*) Sketch of Hot Wire Anemometer. In position relative to pitot head.

5.4. After a wire had been calibrated it was removed from the arm and fixed in the tunnel so that it came as close as possible to the actual path of the pitot head. The smallest clearance between the wire and the head as it passed was rather less than 0·05 inch. Tests carried out to find whether, provided the wire was reasonably close to the path, there was any difference in the swirl measured with the wire in different attitudes with respect to the pitot head, failed to reveal any such difference whether the wire was vertical or horizontal. A slight increase in clearance also produced no perceptible change. Generally, the wire was bent into a shallow open loop whose two ends were in an approximately horizontal line perpendicular to the path of the pitot (see fig. 4, *b*). In this attitude the wire more or less enclosed the head from below as it passed, and the clearance could be reduced to quite a small amount without risk of fouling due to the centrifugal deflection of the pitot-head.

5.5. Altogether three determinations of swirl were made for the standard instrument, one for the hemispherical pitot, and one for the small-scale copy of the standard, the range being generally from 0·1 to 3 feet per second. Fig. 5 shows the results obtained for the standard pitot and its copy. With regard to the curve for the standard, it will be seen that satisfactory agreement was obtained between the three entirely distinct sets of measurements, which were made with different hot wires and at intervals of many weeks. On the same figure three check measurements, made by means of total-head and static readings taken with the moving pitot itself, are plotted, and it will be seen that they fully justify the confident acceptance of the hot-wire values.

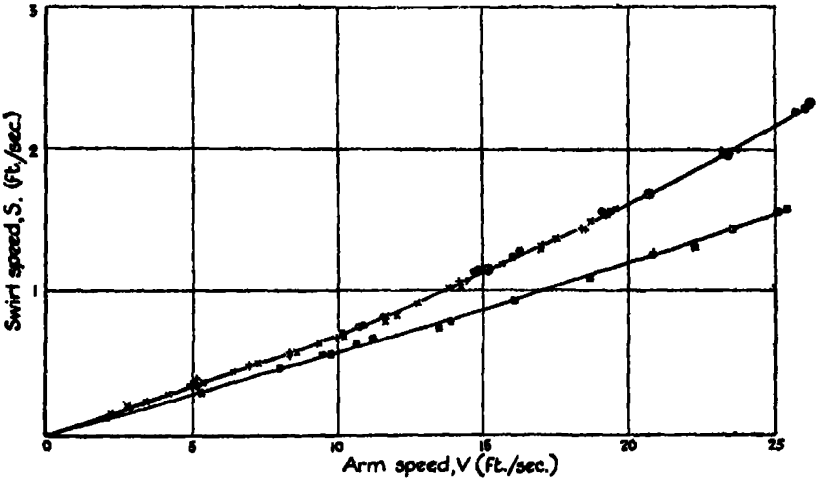

FIG. 5.—Swirl for Standard Pitot-static Tube and Small-scale Copy. Standard tube: ⊙ Results obtained 6.10.30; + Results obtained 10.11.30; × Results obtained 23.2.31; ⊕ Check values obtained by pressure measurement. ⊡ Small-scale copy of standard.

5.6. It should be noted that in these check observations total-head and static readings were observed separately, the former by means of the sensitive manometer and the latter, with the exception of that at 15·1 feet per second with the Chattock gauge. At the two higher speeds (20·7 and 26·2 feet per second) the check is direct, since the value of the pitot-static factor K is known from the calibration of 1912 to be unity, but the static reading at 15·1 feet per second has been corrected in accordance with the value of K taken from the final mean calibration curve for the standard pitot given in fig. 6. The value of K at this speed is $1 \cdot 003_5$ and it follows from equation (1) that the true static pressure s in the orbit of the pitot is given by

$$s = p_s - \frac{0 \cdot 0035}{1 \cdot 0035} \cdot \tfrac{1}{2}\rho V^2, \qquad (2)$$

where p_s is the static pressure reading.

5.6. In considering the probable accuracy of the accepted values of the swirl at any speed it is necessary to bear in mind the fact that the swirl was only about 7 per cent. of the arm speed, so that an error of 1 per cent. on the swirl was equivalent to less than 0·1 per cent. of the true air speed. It is considered that values of the swirl taken from a carefully drawn mean curve, such as that shown in fig. 5, were accurate to about 3 per cent. at the lowest speeds and to well within 1 per cent. at the highest. The equivalent accuracy on air speed thus ranges from about 0·2 per cent. to less than 0·1 per cent. In view of the fact that the lowest value of the swirl was only 0·113 feet per second at 1·729 feet per second ground speed, the percentage accuracy is not regarded as unsatisfactory. This matter is further discussed in §§ 7.1 and 7.2 in relation to the overall accuracy of the calibration.

5.7. An analysis of the swirl results presents certain features of interest which are considered in Appendix I. It is there shown that the swirl due to the small pitot can be fairly closely predicted by calculation from the values measured for the standard.

§ 6. *Discussion of Results.*

6.1. Tables I, II and III contain respectively the results of the observations made with the standard, with the small-scale copy of the standard, and with the hemispherical-nose instrument. The results are also plotted in figs. 6 and 7 (p. 167) against Reynolds number vd/ν (v = air speed, d = external diameter of total-head tube = 0·307 inch, ν = coefficient of kinematic viscosity of air). A scale of air speed for dry air at a temperature of 15° C. and 760 mm. pressure is also included; in fig. 6 it relates only to the standard instrument, and not to the small-scale copy.

6.2. As the investigation was mainly concerned with the standard tube, for which the results obtained were considerably more numerous than for the other two instruments, the major part of this discussion will be devoted to consideration of the results for the standard. Examination of the data for this instrument, plotted in fig. 6, shows that above a Reynolds number R of about 2300

Table I.—Values of K ($= \frac{1}{2}\rho V^2/p$) for standard pitot-static tube. $v =$ air speed, $p =$ differential pitot-static pressure.

Observation No.	Date.	Observed air speed v, ft./sec.	Reynolds number vd/ν.	K.
1*	6.10.30	23·60	$37 \cdot 5 \times 10^2$	$0 \cdot 998_5$
2*	6.10.30	17·75	28·2	$1 \cdot 001_2$
3*	7.10.30	21·32	33·9	$0 \cdot 998_4$
4*	7.10.30	23·80	37·9	$0 \cdot 999_1$
5*	20.10.30	13·96	21·9	$1 \cdot 007_4$
6*	20.10.30	17·40	27·3	$1 \cdot 001_3$
7*	20.10.30	21·66	34·0	$0 \cdot 999_1$
8*	20.10.30	23·32	36·5	$0 \cdot 997_8$
9	11.11.30	9·35	14·9	$1 \cdot 016_6$
10	11.11.30	10·78	17·1	$1 \cdot 014_4$
11	11.11.30	13·27	21·1	$1 \cdot 011_6$
12	5.3.31	1·88	3·0	$0 \cdot 993_9$
13	5.3.31	1·62	2·6	$0 \cdot 959_5$
14	5.3.31	2·77	4·4	$1 \cdot 000_4$
15	5.3.31	4·00	6·4	$1 \cdot 003_0$
16	9.3.31	2·94	4·7	$1 \cdot 015_8$
17	9.3.31	4·08	6·6	$1 \cdot 014_2$
18	9.3.31	5·85	9·4	$1 \cdot 008_5$
19	11.3.31	5·57	8·9	$1 \cdot 009_8$
20	11.3.31	7·69	12·2	$1 \cdot 013_4$
21	11.3.31	3·73	5·9	$1 \cdot 015_6$
22	11.3.31	1·80	2·8	$0 \cdot 985_3$
23	11.3.31	10·64	16·8	$1 \cdot 015_7$
24	11.3.31	14·02	22·2	$1 \cdot 007_8$
25	16.3.31	1·62	2·5	$0 \cdot 975_7$
26	16.3.31	1·89	3·0	$0 \cdot 995_3$
27	16.3.31	2·99	4·7	$1 \cdot 009_3$
28	16.3.31	3·89	6·1	$1 \cdot 022_6$
29	16.3.31	5·95	9·4	$1 \cdot 011_4$
30	16.3.31	4·76	7·5	$1 \cdot 007_8$
31	19.3.31	4·53	7·0	$1 \cdot 028_7$
32	19.3.31	3·80	5·9	$1 \cdot 021_8$
33	20.3.31	4·95	7·6	$1 \cdot 024_8$
34	20.3.31	3·79	5·8	$1 \cdot 017_1$
35	20.3.31	5·73	8·8	$1 \cdot 014_1$
36	20.3.31	6·51	10·0	$1 \cdot 011_4$
37	21.3.31	2·33	3·6	$0 \cdot 999_3$
38	21.3.31	7·36	11·4	$1 \cdot 004_2$
39	25.3.31	7·18	11·4	$1 \cdot 003_5$
40	27.3.31	8·86	14·2	$1 \cdot 003_8$
41	28.3.31	10·86	17·3	$1 \cdot 004_8$
42	28.3.31	13·41	21·4	$1 \cdot 004_6$
43	30.3.31	11·19	17·9	$1 \cdot 005_0$
44	30.3.31	14·74	23·7	$1 \cdot 004_5$
45	14.4.31	13·34	21·2	$1 \cdot 005_1$
46	14.4.31	11·58	18·4	$1 \cdot 005_8$
47	14.4.31	7·75	12·3	$1 \cdot 000_6$
48	14.4.31	5·77	9·2	$0 \cdot 997_2$
49	15.4.31	5·71	8·8	$0 \cdot 999_6$
50	15.4.31	5·71	8·8	$0 \cdot 998_9$
51	15.4.31	3·75	5·9	$0 \cdot 995_4$
52	15.4.31	7·62	12·0	$1 \cdot 001_5$
53	16.4.31	3·78	6·0	$1 \cdot 001_4$
54	16.4.31	10·75	16·9	$1 \cdot 004_5$
55	17.4.31	1·90	3·0	$0 \cdot 958_9$
56	17.4.31	1·90	3·0	$0 \cdot 960_4$
57	17.4.31	1·89	3·1	$0 \cdot 945_9$
58	21.4.31	2·84	4·5	$0 \cdot 988_9$
59	22.4.31	8·32	13·0	$1 \cdot 010_5$
60	23.4.31	4·66	7·3	$1 \cdot 021_7$
61	23.4.31	7·26	11·4	$1 \cdot 011_4$
62	23.4.31	11·31	17·6	$1 \cdot 010_3$
63	23.4.31	14·40	22·2	$1 \cdot 003_2$
64	24.4.31	14·39	22·0	$1 \cdot 004_5$

with 18-inch Chattock manometer; sensitive manometer used in all

Table II.—Values of K for 0·535 to 1 scale copy of standard tube.

v, ft./sec.	vd/ν.	K.
16·69	14·3 × 10^3	0·997$_8$
19·15	16·4	0·999$_0$
22·82	19·8	1·003$_6$
24·87	21·5	1·004$_6$
27·03	23·4	1·005$_2$
18·47	15·6	1·005$_7$
19·66	16·6	1·002$_5$
16·90	14·3	1·001$_6$
14·74	12·5	1·002$_2$
13·24	11·2	1·001$_7$
11·32	9·6	0·993$_7$
9·57	8·1	0·992$_2$
1·95	1·6	0·958$_0$
2·05	1·7	0·956$_9$
1·75	1·5	0·960$_4$
2·86	2·4	0·970$_4$
3·81	3·2	0·968$_2$
4·68	3·9	0·983$_3$
5·46	4·6	0·987$_6$
6·86	5·7	0·998$_4$
7·54	6·3	0·988$_3$
8·47	7·1	0·985$_9$
10·52	8·8	0·980$_5$

Table III.—Values of K for Hemispherical-nose Pitot-static Tube.

v, ft./sec.	vd/ν.	K.
21·90	35·6 × 10^3	1·003$_4$
17·87	29·0	1·001$_0$
13·29	21·4	1·008$_9$
8·93	14·3	1·006$_2$
6·42	10·3	0·999$_1$
4·47	7·3	0·999$_6$
3·63	6·0	0·980$_7$
3·12	5·1	0·964$_3$
1·84	3·0	0·949$_2$
1·83$_5$	3·0	0·939$_9$

($v \simeq 14{\cdot}5$ feet per second), they fall on a single curve which gives a value for K of 0·999 at the highest Reynolds numbers reached in these experiments ($v \simeq 24$) and so agrees, to 0·1 per cent., with the value above 20 feet per second established by the calibration of 1912. As the value of R decreases so that of K grows, reaching 1·004 at R = 2300. Below this value of R the points become progressively more scattered as the value of R falls, but there is a general tendency for K to increase somewhat down to a value of R of about 700 ($v \simeq 4$). As R is further decreased the value of K drops sharply, the beginning of the drop being associated with the greatest scattering of the observed points.

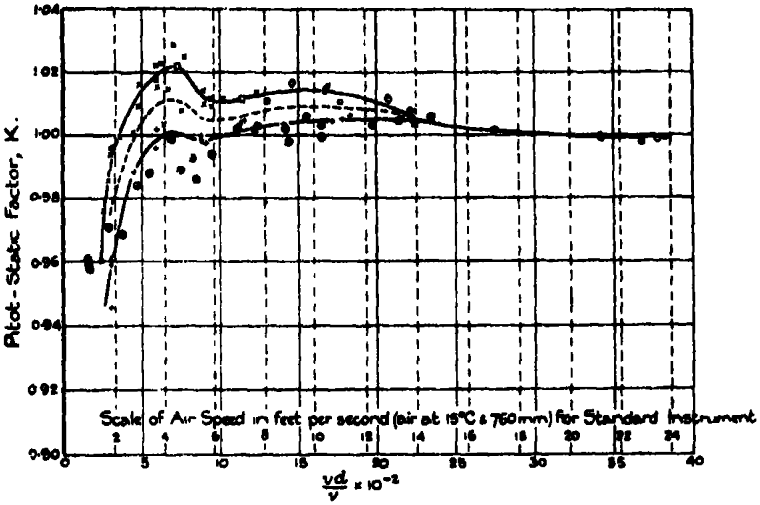

Fig. 6.—Pitot-static Factor for Standard Instrument and Small-scale Copy of Standard.

Points for Standard Instrument
- ⊙ Observations 1 to 8 taken with Chattock gauge.
- ◈ Observations 9 to 11 taken with sensitive manometer.
- × Observations 12 to 37 taken with sensitive manometer.
- + Observations 38 to 58 taken with sensitive manometer.
- ⊡ Observations 59 to 64 taken with sensitive manometer.

Points for small-scale copy shown thus ⊕.

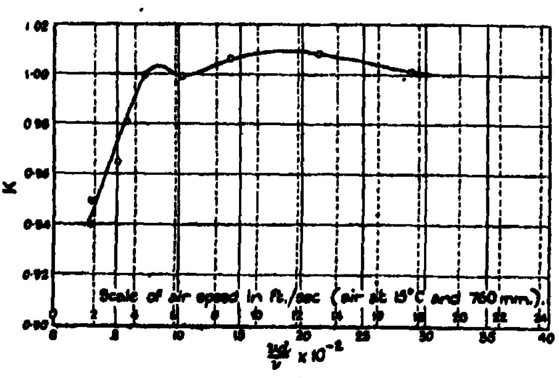

Fig. 7.—Pitot-static Factor for Hemispherical-nose Instrument.

6.3. The range R = 500 to R = 2300 appears to be a range of transition between two types of flow, each of which prevails at one end of the range. The phenomenon appears, in fact, strongly reminiscent of the critical transitional range between the turbulent and streamline *régimes* of flow in smooth pipes.

In both cases a scattering of parameters characteristic of the flow appears when they are plotted against Reynolds number within the region of transition. But whereas in pipe flow the points are distributed at random over a band, in the case of the pitot-static tube they appear definitely to tend to group themselves about one or other of two curves. Inspection of fig. 6 shows that, except in the neighbourhood of R = 600 to 800, very few of the results for the standard instrument lie between the two curves drawn in full lines below R = 2300, at which value of R the two curves converge into a single curve.

6.4. It is noteworthy, also, that the results as successively obtained were not distributed indiscriminately between the two curves. On the contrary, for a considerable period, values would be obtained which lay consistently on one curve, and then a sudden unaccountable change would occur and the next set of results would favour the other curve. This will be clear from consideration of Table I in conjunction with fig. 6. Thus, with reference only to the results obtained with the sensitive manometer, observations Nos. 9, 10 and 11 (Table I) taken on November 11, 1930, fell on the upper curve. Another series, Nos. 12 to 37 inclusive, dating from March 5 to March 21, 1931, also fell on the upper curve. Then a change took place; the next observation, No. 38, taken on the same date as No. 28, lay on the lower curve, together with all the succeeding observations up to No. 58, taken at various times between March 21 and April 21, 1931. Observation No. 59, taken on April 22, returned to the upper curve, as did all those up to and including No. 64, the last observation, taken on April 24, 1931.

6.5. Although this behaviour is difficult to explain, it is, to some extent, analogous to the kind of results often obtained in the measurement of the drag of a streamline body in a wind tunnel. Over a certain sensitive range of Reynolds number the values of drag plotted against speed generally fall consistently on a single curve on one occasion, but a different curve may be found when an attempt is made to repeat the observations. This effect is now attributed to differences in the degree of turbulence present in the air stream. Some such effect may have existed in the pitot calibration, for the swirl was set up mainly by the cylindrical stem of the instrument, and a cylinder is notoriously liable to cause unsteadiness in the flow pattern of a fluid streaming past it. Nevertheless, the reason why the pitot-static factor K seems to favour two definite values, and no others, at a given speed within the transition range is still obscure.

6.6. While the scattering of the points between R = 500 and R = 2300 ($v \simeq 3$ and 14 respectively) is of academic interest as indicating an unstable *régime* transitional between two types of flow, it is not serious from a practical point of view. A dotted curve has been drawn in fig. 6 to represent the mean of the two curves derived from the observations. Over the range $R = 500$ to 2300 values of K taken from the mean curve nowhere deviate by more than 1 per cent. from corresponding values on either of the observed curves, and this maximum deviation is not reached until R has fallen to 700 ($v \simeq 4\frac{1}{2}$). It follows that, with the aid of this mean curve, the standard pitot-static tube can be used to measure air speed to an accuracy of $\pm 0\cdot5$ per cent. down to a speed of 3 feet per second under ordinary atmospheric conditions. At a speed of 6 feet per second the accuracy has increased to about $\pm 0\cdot3$ per cent., and it further increases with rising speed.

6.7. The results for the small-scale copy of the standard in the main substantiate the lower curve obtained with the standard. There are small discrepancies in what appears for the standard also to be the region of most unstable flow, viz., between $R = 700$ and $R = 1000$; otherwise the agreement is reasonably good when the comparison is made on a Reynolds number base. Two points in the neighbourhood of $R = 1500$ are rather off the curve, but it should be noted that the accuracy obtained with this small instrument was not as good as that possible with the standard. For some reason both swirl and pressure observations exhibited a degree of unsteadiness which rendered the readings more open to error. The main characteristics of the results do, however, support the general type of scale effect found with the standard. Whether points corresponding to the upper curve would have been obtained had work with this instrument been prolonged, it is not possible to say. It is relevant to state, however, that had only the 21 observations, Nos. 38 to 58, been available for the standard the existence of the upper curve would not have been suspected. Only 23 observations were made with the small copy of the standard.

6.8. The few observations made with the hemispherical-nose instrument, shown graphically in fig. 7, again exhibit the same main features of a rise in K to a maximum value at about $R = 1800$, followed by a decrease at lower values of R culminating in a sharp drop at about $R = 700$.

§ 7. *Accuracy of the Results.*

7.1. As has already been stated, the arrangements made for the measurement of speed allowed an accuracy of about $0\cdot1$ per cent. to be achieved. The errors possible in the swirl determination (see § 5.6) reduced the overall accuracy on the calculated value of the air speed to about $0\cdot2$ per cent. at the higher speeds and 0·3 per cent. at the lower end of the range. As regards pressures, these could be observed with the Chattock gauge between speeds of 17 feet per second and 26 feet per second to limits of 0·2 per cent. and 0·1 per cent. respectively.* Below 17 feet per second the sensitive manometer was used, and this enabled pressures to be observed to well within 0·1 per cent. at 15 feet per second while the accuracy at 2 feet per second was about 1 per cent. The maximum error in any one observation of K is twice the error on speed (since K is a function of v^2) plus the error on pressure. Values of the maximum error calculated in this way are given in Table IV.

Table IV.—Estimated Maximum Error of a Single Observation of K. (Error assumed in the measurement of any single quantity = 0·1 per cent.)

Air speed, feet per second.	Maximum error per cent.	Manometer used for pressure observations.
26	0·4	13-inch Chattock
17	0·5	13-inch Chattock
15	0·4	Sensitive manometer
10	0·5	
6	0·6	
4	0·8	
2	1·6	

7.2. The errors in the mean curves drawn through the numerous observations are naturally much smaller than the maximum errors shown in the above table, and had only one calibration curve been obtained for the standard instrument below 15 feet per second, instead of the two actually found, the calibration would certainly have enabled the instrument to be used to measure air speed to an accuracy of 0·1 per cent. down to 5 feet per second and to about 0·3 per cent. at 2 feet per second; for the error made on a speed measurement by assuming a certain value of K is only half the error in K.

§ 8. *Summary of Conclusions, and Recommendations.*

8.1. There is a scale effect at low Reynolds numbers on the static tube of a pitot-static combination, which becomes apparent at a considerably higher value of the Reynolds number than that at which the scale effect on the total-head tube begins. As a consequence, the factor of the British standard instrument departs at low air speeds from its value of unity previously found to hold at speeds above 20 feet per second for air under ordinary atmospheric conditions. The factor increases slowly with reduction of speed below about 18 feet per second, where its value is unity. A maximum is reached, having a mean value of 1·009, at 10 feet per second. Thereafter the mean factor decreases to 1·005 at 6 feet per second, rises to 1·011 at about 4½ feet per second, and then drops rapidly, passing through a value of unity at 3 feet per second.

---

* This high order of accuracy, despite the comparatively low readings on the Chattock gauge, was possible because the pressure remained very steady during an observation.

8.2. Mean values of K at different speeds are summarised in Table V. The use of these values will enable air speed to be measured with the standard instrument to an accuracy of ± 0·5 per cent. down to 3 feet per second. In the measurement of an unknown low air speed the procedure will be to calculate the speed approximately from the observed differential pressure on the assumption that K = 1, and then to substitute the value of K corresponding to the approximate speed thus obtained and to recalculate. A second approximation will be unnecessary in view of the small variation of K.

Table V.—Mean Values of K for Standard Pitot-static Tube.

Air speed (15° C. and 760 mm.) ft./sec.	Mean K.
2	0·980
4	1·011
6	1·005
8	1·008
10	1·009
12	1·008
14	1·005
16	1·002
18	1·001
20	1·000
22	0·999
24	0·999

8.3. The assumption that K is equal to unity at all speeds down to 3 feet per second will in no case involve an error exceeding 1 per cent. on speed, and for most practical purposes this will probably be good enough. But it is always desirable for the accuracy of a standard instrument against which other instruments are calibrated to be considerably higher than that demanded of the latter. Hence the variations of K found for the standard pitot-static tube, although relatively small, are not unimportant if the instrument is to become the standard at the N.P.L. for the calibration of low speed anemometers.

8.4. It would be unwise in making such calibrations to rely on values of K taken from the mean curve below 4 feet per second where the change with speed is rapid. It has therefore been suggested that an accurate copy of the standard instrument be constructed to twice the scale and used as the low speed standard. This will delay the onset of the steep fall of the curve to a speed of 2 feet per second. Such a pitot-static tube, together with the sensitive manometer, will provide a satisfactory low speed standard with which a speed of 2 feet per second can be measured to within ± 1 per cent.

§ 9. *Acknowledgments.*

9.1. The writers desire to record their appreciation of the able assistance rendered by Mr. A. F. Brown during the major part of the investigation, and by Mr. C. A. Culverhouse in the design and erection of the apparatus.

APPENDIX I.

Analysis of Swirl Measurements.

Since the standard pitot and its small-scale model were arranged to project into the tunnel for the same distance (roughly 7 inches) below the roof it is possible to compare their respective swirls on a quantitative basis.

In the first place, an interesting example of the law of similarity is afforded by the results. It is best seen when the swirl is expressed as a percentage of the ground speed v_g of the pitot and is plotted against the quantity $v_g\, d/d_s$, where d and d_s are respectively the external diameters of the static tubes of the instrument to which the values relate and of the standard. For the latter the ratio d/d_s is, of course, unity, while for the small-scale copy it is 0·535. This plotting is equivalent to plotting against Reynolds number since both instruments were tested in air at sufficiently nearly the same temperature and pressure. The curves of fig. 8 have been obtained in this manner and it will be seen that both show a marked discontinuity in the same range of abscissæ. It is evident, therefore, that the swirl is related to the type of flow past the instrument.

It is interesting, also, to see how closely the swirl for one instrument can be predicted from the measured values for the other. In steady motion, the drag of the pitot due to its travel through the air in the tunnel is balanced by the frictional drag exerted by the swirl on the walls of the tunnel. If it is assumed that the swirl is caused entirely by the stem of the pitot inside the tunnel, which is probably very nearly true, this equilibrium condition may be expressed by the equation

$$K_D\, \rho l d (v_g - s)^2 = C \rho s^2, \tag{3}$$

where K_D is the drag coefficient of the stem, l is the length of stem inside the tunnel, d is the diameter of the stem, s is the swirl speed in the orbit of the pitot, and C is a coefficient expressive of the friction on the walls and also of the fact that the swirl at the walls is probably less than the swirl in the orbit.

From (3), if suffix 1 denotes the standard and suffix 2 the small copy, the following relation is obtained between the swirl speed and the pitot diameter when the condition that $l_1 = l_2$ is inserted :—

$$\frac{K_{D_2} C_1 s_1^2 (v_g - s_2)^2}{K_{D_1} C_2 s_2^2 (v_g - s_1)^2} = \frac{d_1}{d_2} = 1{\cdot}87, \tag{4}$$

from which s_2 can be calculated in terms of s_1 if the ratios K_{D_1}/K_{D_2} and C_1/C_2 are known.

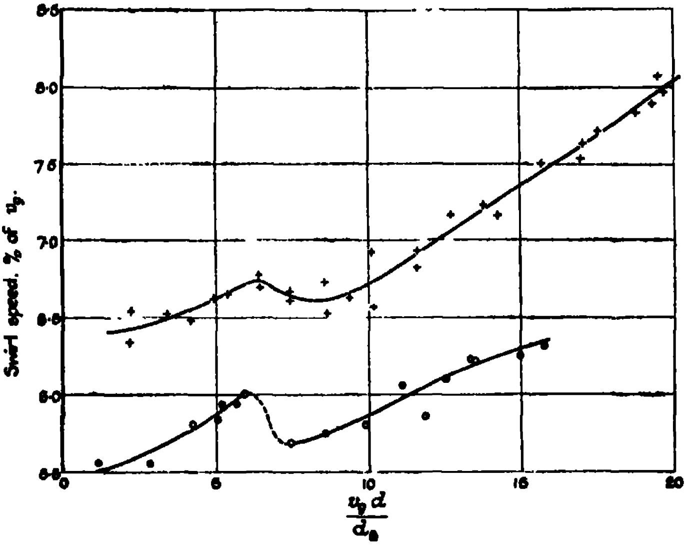

FIG. 8.—Swirl Speed as a Percentage of the Ground Speed of the Pitot. + Standard instrument; ⊙ Small-scale copy. v_g = ground speed of pitot (ft./sec.); d = diameter of pitot; d_s = diameter of standard.

Now $K_{D_1} \neq K_{D_2}$ on account of the scale effect on cylinders. Also, it cannot be assumed that $C_1 = C_2$. The values of K_D will depend upon the value of $(v_g - s)d/\nu$ and since s is only a small percentage of v_g, it will be sufficiently close to assume K_D to depend upon $v_g d/\nu$. Values of K_{D_1} and K_{D_2} at the appropriate pitot speeds can then be obtained from the curves for infinitely long cylinders given in 'Aeronautical Research Committee R. and M., No. 102.'* Although the pitot stems do not approach infinite length, it is only the ratio of K_{D_2} to K_{D_1} that enters into (4), and the assumption that the drag coefficients are in the same ratio as those for infinite cylinders of the same diameters cannot be far from the truth.

---

* Relf, "Discussion of the results of measurements of the resistance of wires, with some additional tests on the resistance of wires of small diameter" (1914).

As regards values of C_1 and C_2, since no data are available for curved pipes of square section, all that can be done is to calculate approximate values at the equivalent Reynolds numbers on the basis of Stanton's and Pannell's* results for smooth straight pipes. As with the coefficients K_D, only the ratio of C_1 to C_2 occurs in (4), so that the errors due to this approximation will not be as great as if absolute values of C_1 and C_2 were required.

Values of s_1, the swirl for the standard, have been taken from the mean swirl curve at values of v_g of 5, 10, 15, 20 and 25 feet per second, and have been used to calculate s_2 by the aid of (4), the coefficients K_D and C being estimated in the manner described. The results of the calculations are given in the following table, and it will be seen that they are in fair agreement with the measured values of s_2, although systematically rather lower.

v_g feet per sec.	s_1 feet per sec.	s_2 (calc'd.) feet per sec.	s_2 (obs'd.) feet per sec.
5	0·33	0·25	0·28
10	0·67	0·51	0·50
15	1·10	0·79	0·85
20	1·60	1·13	1·19
25	2·17	1·50	1·54

Appendix II.

Estimation of the Error due to Neglect of the Inequality of the Radii of the Static Holes and the Mouth of the Total-head Tube.

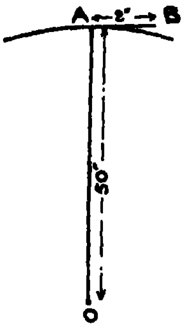

Let A represent the position of the static holes and B that of the mouth of the total-head tube. O is the centre of rotation. The distance AB is 2 inches in the standard tube while OA, the radius of the track, was about 50 inches.

Let S be the swirl speed, V_A the peripheral speed of the static holes, and V_B the peripheral speed of the mouth of the total-head tube. Both V_A and V_B are speeds relative to the ground.

The resultant pressure in the mouth of the total-head tube is the sum of the velocity head at that point, the centrifugal pressure due to the rotation, and the atmospheric pressure, *i.e.*,

---

* 'Phil. Trans.,' A, vol. 214, p. 199 (1914).

$$P_1 = \tfrac{1}{2}\rho (V_B - S)^2 - \tfrac{1}{2}\rho V_B^2 + \pi.$$

Similarly the pressure in the static tube at A is

$$P_2 = \pi - \tfrac{1}{2}\rho V_A^2.$$

Hence the true differential pressure is

$$P_1 - P_2 = \tfrac{1}{2}\rho\, [(V_B - S)^2 - (V_B^2 - V_A^2)],$$

so that, if K is the pitot-static factor as defined by equation (1), § 1.2 of the main text,

$$K = \tfrac{1}{2}\rho\, \frac{[(V_B - S)^2 - (V_B^2 - V_A^2)]}{P_1 - P_2}.$$

In the actual tests, the assumption is made that $V_A = V_B$ and K is calculated from the equation

$$K = \frac{\tfrac{1}{2}\rho\, (V_A - S)^2}{P_1 - P_2}.$$

Hence

$$\frac{\text{True K}}{\text{Calculated K}} = \frac{(V_B - S)^2 - (V_B^2 - V_A^2)}{(V_A - S)^2}.$$

Now $V_B^2 = \frac{2504}{2500} V_A^2$, and we may take S as equal to $0 \cdot 07\ V_A$, so that

$$\frac{\text{True K}}{\text{Calculated K}} = 0 \cdot 99987$$

That is, the error due to the assumption that $V_A = V_B$ amounts only to 0·013 per cent., and this is negligibly small in relation to the experimental accuracy, which was of the order of 0·1 per cent. on an individual observation.

Some Special Solutions of the Equations of Axially Symmetric Gravitational Fields.

By T. Lewis, M.Sc., Aberystwyth.

(Communicated by G. A. Schott, F.R.S.—Received November 26, 1931.)

Introduction.

The problem of axially symmetric fields was first treated by Weyl,* who succeeded in obtaining solutions for a static field in terms of the Newtonian potential of a distribution of matter in an associated canonical space. He also solved the more general problem involving the electric field. Levi Civita,† by slightly different methods, obtained solutions differing from those of Weyl in one respect, and discussed fully the case in which the field is produced by an infinite cylinder. R. Bach‡ has discussed the special case of two spheres and has calculated their mutual attraction. Bach also considered the field of a slowly rotating sphere, and obtained approximate solutions, taking the Schwarzchild solution as his zero-th approximation. The same field was discussed earlier by Leuse and Thirring,§ who considered the linear terms, only, in the gravitational equation. Kornel Lanczos|| has also considered a special case of stationary fields and applied the results to cosmological problems. The more general case of gravitational fields produced by matter in stationary rotation has been treated by W. R. Andress¶ and E. Akeley.** Both these authors obtain approximate solutions of the general problem, and the latter treats at length the field of a rotating fluid.

The object of this paper is to present some special, but exact, solutions which the author obtained some years ago and, also, two methods of successive approximation for obtaining solutions of a more general type, which behave in an assigned manner at infinity and on a surface of revolution enclosing the rotating matter to which the field is due. Our solutions include as special cases the solutions of Weyl, Levi Civita and others which pertain to static fields. Also, the approximate solutions for stationary fields obtained by Leuse

---

* 'Ann. Physik,' vol. 54, p. 117 (1917).

† 'R. Acc. Lincei,' 5, vol. 28, p. 101 (1919).

‡ 'Mat. Z.,' vol. 13, p. 134 (1922).

§ 'Phys. Z.,' vol. 19, p. 156 (1918).

|| 'Z. Physik,' vol. 21, p. 73 (1924).

¶ 'Proc. Roy. Soc.,' A, vol. 126, p. 592 (1930).

** 'Phil. Mag.,' vol. 11, p. 322 (1931).

and Thirring, Bach and Andress are contained in our solutions when appropriate choice of boundary conditions is made and higher order terms are neglected.

The special feature of this paper is the simplification of the gravitational equations which results on the introduction of canonical co-ordinates. This is always admissible in space free of matter. In order to illustrate the advantage gained by working with canonical co-ordinates we express Andress' approximate equations in these co-ordinates and show that, to the approximation considered by him, they are equivalent to our equations. No loss of generality is involved in the use of canonical co-ordinates, which are connected with any other co-ordinates preserving the normal form of the line element by a transformation of the type

$$r + iz = \phi\,(x_1 + ix_2).$$

In fact, the canonical co-ordinates serve to remind one of the degree of arbitrariness involved in our solutions.

We do not concern ourselves with the problem of finding the gravitational field inside matter. Certain stresses, t_{ik}, of non-gravitational origin, are necessary to maintain the steady rotation of the field producing matter, so we will assume that inside matter the gravitational potentials have any reasonable values which are continuous on the surface, and regard the equations

$$\mathrm{R}_{ik} - \tfrac{1}{2}g_{ik}\mathrm{R} = -\,(\mathrm{T}_{ik} + t_{ik}),$$

as equations to determine the t_{ik} (T_{ik} being the components of the energy-momentum tensor).

The gravitational equations will be derived from a *Variational Principle* after the manner of Weyl. The latter's work was criticised by Levi Civita on the grounds that he did not make full use of the principle. Weyl based his calculation of the *action function* on a normal form of the line element and thereby obtained a set of equations which are not complete, though certainly compatible with the complete set. In order to avoid this difficulty we shall base our calculation of the *action function* on a non-normalised line element and show that it can be normalised without violating the gravitational equations. The possibility of introduction of canonical co-ordinates is immediately suggested by the form of our equations.

Exact solutions will be given in the case of the field due to an infinite rotating cylinder in the canonical space, and, to illustrate one method of approximation in the general case, the field of a rotating sphere will be worked out to a second order of approximation.

§ 1. *The Hamiltonian Function and Gravitational Equations.*

The field will depend upon two variables x_1 and x_2, $x_1 = 0$ being the axis of symmetry of the field. x_0 will be interpreted as time co-ordinate and x_3 as an angular variable varying from 0 to 2π. The fundamental quadratic form may be written

$$ds^2 = f dx_0^2 - \{e^{\mu} dx_1^2 + e^{\nu} dx_2^2 + l dx_3^2\} - 2m dx_0 dx_3, \tag{1.1}$$

in which ν will be put equal to μ after the gravitational equations have been deduced. The effect of the rotation is represented mainly by the last term.

With the usual notation we find that

$$-g = r^2 e^{\mu+\nu}, \quad \text{where} \quad r^2 = fl + m^2, \tag{1.2}$$

and

$$g^{00} = r^{-2} l, \quad g^{11} = -e^{-\mu}, \quad g^{22} = -e^{-\nu}, \quad g^{33} = -r^{-2} f, \quad g^{03} = -r^{-2} m.$$

The only 3-index symbols which concern us are the following:

$$\left\{ {00 \atop 1} \right\} = \tfrac{1}{2} e^{-\mu} f_1, \left\{ {11 \atop 1} \right\} = \tfrac{1}{2} \mu_1, \left\{ {22 \atop 1} \right\} = -\tfrac{1}{2} e^{-\mu+\nu} \nu_1, \left\{ {33 \atop 1} \right\} = -\tfrac{1}{2} e^{-\mu} l_1, \left\{ {03 \atop 1} \right\} = -\tfrac{1}{2} e^{-\mu} m_1,$$
$$\left\{ {00 \atop 2} \right\} = \tfrac{1}{2} e^{-\nu} f_2, \left\{ {11 \atop 2} \right\} = -\tfrac{1}{2} e^{\mu-\nu} \mu_2, \left\{ {22 \atop 2} \right\} = \tfrac{1}{2} \nu_2, \left\{ {33 \atop 2} \right\} = -\tfrac{1}{2} e^{-\nu} l_2, \left\{ {03 \atop 2} \right\} = -\tfrac{1}{2} e^{-\nu} m_2,$$

where the suffix 1 denotes differentiation with respect to x_1 and 2 with respect to x_2.

The action function from which the field equations are derived differs from $R\sqrt{-g}$ by the divergence of a function of the gravitational potentials and their derivatives. It is G, defined by

$$2G = \left\{ {ik \atop r} \right\} \frac{\partial}{\partial x_r} (g^{ik} \sqrt{-g}) - \left\{ {ir \atop r} \right\} \frac{\partial}{\partial x_k} (g^{ik} \sqrt{-g}).$$

Inserting the above expressions for the 3-index symbols we obtain, finally,

$$2G = e^{-(\mu-\nu)/2} \left(\frac{f_1 l_1 + m_1^2}{r} + 2 r_1 \nu_1 \right) + e^{(\mu-\nu)/2} \left(\frac{f_2 l_2 + m_2^2}{r} + 2 r_2 \mu_2 \right). \tag{1.3}$$

The gravitational equations are the necessary and sufficient set of conditions for a stationary value of the integral

$$\int G dx$$

for arbitrary small variations of the g_{ik} which vanish on the boundary of the region of integration.

On carrying out the variation and putting $\nu = \mu$ the following equations are obtained :—

$$2r_{22} + (r_1\mu_1 - r_2\mu_2) + \frac{1}{2r}\{(f_1l_1 + m_1^2) - (f_2l_2 + m_2^2)\} = 0. \tag{1.4}$$

$$-2r_{11} + (r_1\mu_1 - r_2\mu_2) + \frac{1}{2r}\{(f_1l_1 + m_1^2) - (f_2l_2 + m_2^2)\} = 0, \tag{1.5}$$

$$\frac{\partial}{\partial x_1}\left(\frac{f_1}{r}\right) + \frac{\partial}{\partial x_2}\left(\frac{f_2}{r}\right) + \frac{f}{2r}\left\{\frac{[f,l]+[m,m]}{r^2} + 2\nabla^2\mu\right\} = 0, \tag{1.6}$$

$$\frac{\partial}{\partial x_1}\left(\frac{l_1}{r}\right) + \frac{\partial}{\partial x_2}\left(\frac{l_2}{r}\right) + \frac{l}{2r}\left\{\frac{[f,l]+[m,m]}{r^2} + 2\nabla^2\mu\right\} = 0, \tag{1.7}$$

$$\frac{\partial}{\partial x_1}\left(\frac{m_1}{r}\right) + \frac{\partial}{\partial x_2}\left(\frac{m_2}{r}\right) + \frac{m}{2r}\left\{\frac{[f,l]+[m,m]}{r^2} + 2\nabla^2\mu\right\} = 0 \tag{1.8}$$

where

$$[\phi,\psi] \equiv \phi_1\psi_1 + \phi_2\psi_2,$$

and

$$\nabla^2 = \frac{\partial^2}{\partial x_1^2} + \frac{\partial^2}{\partial x_2^2}$$

§ 2. *The Compatibility of our Equations and Introduction of Canonical Co-ordinates.*

We notice that the last three equations are invariant with respect to a transformation of the type

$$x_1 + ix_2 = \phi\,(x_1' + ix_2').$$

Again, subtracting (1.5) from (1.4) yields a simple equation involving r only, namely,

$$r_{11} + r_{22} = 0. \tag{2.1}$$

Hence, if z be the conjugate of r, we can make the following identification

$$r + iz = x_1 + ix_2. \tag{2.2}$$

This equation defines our canonical co-ordinates. The equations (1.4) and (1.5) now become identical.

Multiplying (1.6) by l, (1.7) by f, (1.8) by $2m$, and adding, we get, in virtue of (1.2)

$$\frac{\partial}{\partial r}\left(\frac{(r^2)_1}{r}\right) + \frac{\partial}{\partial z}\left(\frac{(r^2)_2}{r}\right) - \frac{1}{r}\{[f,l] + [m,m]\} + 2r\,\nabla^2\mu = 0.$$

But

$$\frac{\partial}{\partial r}\left(\frac{(r^2)_1}{r}\right) + \frac{\partial}{\partial z}\left(\frac{(r^2)_2}{r}\right) \equiv 0.$$

Hence

$$\nabla^2 \mu = \frac{1}{2r^2}\{[f, l] + [m, m]\}. \tag{2.3}$$

The remaining equations now become

$$\mu_1 = -\frac{1}{2r}\{f_1 l_1 + m_1^2 - (f_2 l_2 + m_2^2)\}, \tag{2.4}$$

$$f_{11} + f_{22} - \frac{f_1}{r} = -\frac{f}{r^2}\{[f, l] + [m, m]\}, \tag{2.5}$$

$$l_{11} + l_{22} - \frac{l_1}{r} = -\frac{l}{r^2}\{[f, l] + [m, m]\}, \tag{2.6}$$

$$m_{11} + m_{22} - \frac{m_1}{r} = -\frac{m}{r^2}\{[f, l] + [m, m]\}. \tag{2.7}$$

The last three equations are not independent. If f and l, for example, have been found (1.2) determines m which will satisfy (2.7) identically.

We also notice that when f, l, m have been determined, μ can be found from (2.3) and (2.4). But instead of the latter equation it is convenient to use another equation which has been calculated separately, namely, the one

$$R_{12} = 0.$$

(This equation could have been obtained by including a term $g_{12}\, dx_1\, dx_2$ in our quadratic form and putting $g_{12} = 0$ after variation of G.)

In canonical co-ordinates the equation is

$$\mu_2 = -\frac{1}{2r}\{f_1 l_2 + f_2 l_1 + 2m_1 m_2\}. \tag{2.8}$$

If (2.5)–(2.7) are taken into account, one easily verifies that $\mu_{12} - \mu_{21} = 0$, and that (2.3) is a consequence of (2.4) and (2.8). We can therefore write

$$\mu = -\int \frac{1}{2r}\{f_1 l_1 + m_1^2 - (f_2 l_2 + m_2^2)\}\, dr + \frac{1}{2r}\{f_1 l_2 + f_2 l_1 + 2m_1 m_2\}\, dz. \tag{2.9}$$

Thus the determination of f, l, m completely determines μ except for an additive constant, and it follows that μ cannot assume an arbitrarily assigned value on the boundary.

§ 3. *Transformation of Equations* (2.5)–(2.7).

One can always find a linear transformation of the differentials of the co-ordinates such that the fundamental quadratic form (1.1) transforms into

$$ds^2 = F\, dt'^2 - \{e^{\mu}(dr^2 + dz^2) + L\, d\theta^2\}.$$

In general, this transformation is purely local, *i.e.*, non-integrable. For example, let

$$dx_0 = dt = dt' \cosh u - d\theta' \sinh u, \quad d\theta = dx_3 = d\theta' \cosh u - dt' \sinh u, \tag{3.1}$$

$$f = \mathrm{F} \cosh^2 u - \mathrm{L} \sinh^2 u, \quad l = \mathrm{L} \cosh^2 u - \mathrm{F} \sinh^2 u,$$

$$m = \tfrac{1}{2} (\mathrm{L} - \mathrm{F}) \sinh 2u. \tag{3.2}$$

It follows that

$$fl + m^2 = \mathrm{FL} = r^2. \tag{3.3}$$

This relation suggests the substitutions

$$\mathrm{F} = r e^{-\lambda}, \quad \mathrm{L} = r e^{\lambda}. \tag{3.4}$$

The action function now becomes

$$\mathrm{G} = \frac{1}{2r} - \tfrac{1}{2} r [\lambda, \lambda] + 2r \sinh^2 \lambda \, [u, u] + [r, \mu],$$

and variation gives the following equations for λ and u :—

$$\frac{\partial}{\partial r}\left(r \frac{\partial \lambda}{\partial r}\right) + \frac{\partial}{\partial z}\left(r \frac{\partial \lambda}{\partial z}\right) + 2r \sinh 2\lambda \, [u, u] = 0, \tag{3.5}$$

$$\frac{\partial}{\partial r}\left(r \sinh^2 \lambda \frac{\partial u}{\partial r}\right) + \frac{\partial}{\partial z}\left(r \sinh^2 \lambda \frac{\partial u}{\partial z}\right) = 0, \tag{3.6}$$

A special set of solutions suggests itself at once, namely,

$$u = \text{constant}, \quad \lambda = \log r - 2\psi, \tag{3.7}$$

where ψ is the Newtonian potential of an arbitrary axially symmetric distribution of matter in the canonical space (r, z, θ). It follows that F and L are identical with the f and l found by Weyl in the static case. Our f and l are linear combinations of Weyl's, with constant coefficients. They admit of a very simple interpretation—the observer in the canonical space (r, z, θ) is using a system of reference which rotates with constant angular speed to describe the static field of the canonical space (r', z', θ').

§ 4. *Special Solutions involving Functional Relation between λ and u.*

It is possible to obtain solutions of (3.5) and (3.6) on the assumption that u is a function of λ. It is easily verified that the condition for this is

$$\frac{d^2u}{d\lambda^2} + 2 \frac{du}{d\lambda} \coth \lambda - 2 \left(\frac{du}{d\lambda}\right)^3 \sinh 2\lambda = 0. \tag{4.1}$$

The general solution of this equation is

$$u = u_0 + \tfrac{1}{2}\log\frac{\cosh\lambda \mp \sqrt{k^2\sinh^2\lambda + 1}}{\sinh\lambda} \tag{4.2}$$

where u_0 and k are arbitrary constants, and k^2 need not be positive. Let us now put

$$\psi = \int^u \sinh^2\lambda\, du = \pm\tfrac{1}{2}\int^\lambda \frac{\sinh\lambda\, d\lambda}{\sqrt{k^2\sinh^2\lambda + 1}}.$$

Equation (3.6) shows that ψ satisfies the equation for a Newtonian potential in the canonical space, namely,

$$\psi_{11} + \psi_{22} + \psi_1/r = 0. \tag{4.3}$$

Integration of the expression for ψ gives

$$\psi = \pm\frac{1}{2k}\log\left(k\cosh\lambda + \sqrt{k^2\sinh^2\lambda + 1}\right), \tag{4.4}$$

Solving this equation for $\cosh\lambda$ we get

$$\left.\begin{aligned} \cosh\lambda &= \frac{1}{2k}\{e^{\pm 2k\psi} - (1-k^2)\,e^{\mp 2k\psi}\} \\ \text{and}\qquad \sqrt{k^2\sinh^2\lambda + 1} &= \tfrac{1}{2}\{e^{\pm 2k\psi} + (1-k^2)\,e^{\mp 2k\psi}\} \end{aligned}\right\}. \tag{4.5}$$

We can substitute these expressions in (4.2) and thus find u, and then find f, l, m from the formulæ (3.2) and (3.4). The calculation, however, which is long and tedious, will not be given here. But one can verify directly that

$$f = r(\alpha_1^2 e^{\psi} - \gamma_1^2 e^{-\psi}),\quad l = r(-\alpha_2^2 e^{\psi} + \gamma_2^2 e^{-\psi}),$$
$$m = r(-\alpha_1\alpha_2 e^{\psi} + \gamma_1\gamma_2 e^{-\psi}) \tag{4.6}$$

satisfy equations (2.5), (2.6) and (2.7), where the constants satisfy the equation

$$\alpha_1\gamma_2 - \alpha_2\gamma_1 = 1, \tag{4.7}$$

and ψ is any function which is a formal solution of (4.3). But since f, l, m must be real, ψ cannot be complex—it must be real or purely imaginary.

We notice that if ψ is a function of r only, the solutions (4.6) are the most general solutions, for they involve four arbitrary constants, the fourth being contained in ψ, which is now of the form

$$\psi = -k\log r/r_0, \tag{4.8}$$

where both k and r_0 are arbitrary. (r_0, however, plays no essential rôle, for it can be absorbed in the constants $(\alpha_1, \alpha_2, \gamma_1, \gamma_2)$ without violating (4.7)).

In this special case

$$\mu_1 = -\frac{1}{2r}(f, l, + m_1{}^2) = -\frac{1}{2r}(1 - r^2\psi_1{}^2) = \frac{k^2 - 1}{2r},$$

which, on integration, gives

$$\mu = \tfrac{1}{2}(k^2 - 1)\log r + \text{constant}, \tag{4.9}$$

k is not necessary real. The solutions corresponding to an imaginary k will be given separately.

It is convenient to introduce new constants defined by the formulæ

$$\alpha_1 = \kappa\beta_1, \quad \gamma_1 = \kappa\omega\beta_2, \quad \alpha_2 = \kappa\omega\beta_2{}^{-1}, \quad \gamma_2 = \kappa\beta_1{}^{-1}, \quad 1 - k = \epsilon \tag{4.10}$$

where $\kappa = (1 - \omega^2)^{-\frac{1}{2}}$.

The expressions (4.6) and (4.9) can now be written in the form

$$f = \kappa^2(\beta_1{}^2 r^\epsilon - \omega^2\beta_2{}^2 r^{2-\epsilon}), \quad l = \kappa^2(\beta_1{}^{-2} r^{2-\epsilon} - \omega^2\beta_2{}^{\;2} r^\epsilon),$$

$$m = \kappa^2\omega(\beta_2{}^2 r^{2-\epsilon} - \beta_1{}^2 r^\epsilon)\,\beta_1{}^{-1}\beta_2{}^{-1} \tag{4.11}$$

$$e^\mu = (r/r_0)^{-\epsilon(2-\epsilon)/2}. \tag{4.12}$$

When $\omega = 0$, these solutions reduce to those discussed by Levi Civita, *i.e.*, those characteristic of the gravitational field of an infinite cylinder in the canonical space. The modification of the field due to the stationary rotation of the cylinder is thus represented by the terms involving ω, which is of zero dimensions and may be regarded as a measure of the angular velocity of rotation. ϵ is of zero dimensions and proportional to the mass per unit length of cylinder. β_1 is of zero dimensions and very nearly equal to unity and β_2 is the reciprocal of a length—Newtonian theory gives no indication of its magnitude.

One of the most interesting effects of the rotation is to disturb the radial character of the field. It can be shown from the equations of motion that, in general, a particle started at rest anywhere in the field will not move radially, as in the corresponding static field. (The exceptional case is given by $\omega = 1$, which makes κ infinite.) This result is consistent with Einstein's fundamental hypothesis that a gravitational field is equivalent to an acceleration field. In our case, the forces derived from the ω^2 terms in f and l are analogous to centrifugal forces, and the forces derived from m correspond to Coriolis forces of the classical theory of rotating axes.

The more general solutions (4.6) allow for a variation of the density of the cylinder as z varies, but they are essentially solutions associated with an *infinite* cylinder.

If we write $i\psi$ for ψ in (4.6), the corresponding f, l, m are still formal solutions of the gravitational equations. We easily verify that these solutions are real provided

$$\alpha_1^2 - \gamma_1^2, \quad \alpha_2^2 - \gamma_2^2, \quad \alpha_1\alpha_2 - \gamma_1\gamma_2 \text{ are real}$$

and

$$\alpha_1^2 + \gamma_1^2, \quad \alpha_2^2 + \gamma_2^2, \quad \alpha_1\alpha_2 + \gamma_1\gamma_2 \text{ imaginary.}$$

These conditions are satisfied if we introduce new real constants defined by

$$\sqrt{2}\alpha_1 = a_1 + ib_1, \quad \sqrt{2}\gamma_1 = b_1 + ia_1, \quad \sqrt{2}\alpha_2 = a_2 + ib_2, \quad \sqrt{2}\gamma_2 = b_2 + ia_2.$$

The new constants are arbitrary except for the condition

$$a_1b_2 - a_2b_1 = 1. \tag{4.7$'$}$$

The solutions may now be written

$$r^{-1}f = (a_1^2 - b_1^2)\cos\psi - 2a_1b_1\sin\psi, \quad -r^{-1}l = (a_2^2 - b_2^2)\cos\psi$$
$$- 2a_2b_2\sin\psi, \quad -r^{-1}m = (a_1a_2 - b_1b_2)\cos\psi - (a_1b_2 + a_2b_1)\sin\psi. \tag{4.6$'$}$$

If ψ is a function of r only, it is of the form

$$\psi = -k'\log(r/\nu_0), \tag{4.8$'$}$$

and

$$\mu_1 = -\frac{1}{2r}(1 + r^2\psi_1^2) = -\frac{k'^2+1}{2r}.$$

It follows that

$$\mu = -\tfrac{1}{2}(k'^2 + 1)\log r + \text{constant}. \tag{4.9$'$}$$

These solutions are interesting because there are no corresponding, real solutions of the static problem, *i.e.*, the constants a and b cannot be chosen so as to make m vanish everywhere.

The space-time defined by these solutions is entirely without resemblance to space-time, empty of matter, ordinarily available to physical exploration. Its deviation from *flat* space-time could be demonstrated without exploring very large tracts of it. If these solutions have any applications at all, it must be to the fields of vast astronomical distributions of matter. The discussion of such fields is safer in the hands of astronomers.

Some further special solutions of (3.5) and (3.6) may be obtained by assuming λ to be a function of r only and that

$$u = v(r) + az,$$

where a is a constant.

λ and v satisfy the differential equations

$$\frac{d}{dr}\left(r\frac{d\lambda}{dr}\right) + 2r \sinh 2\lambda\,(k^2/r^2 \sinh^4 \lambda + a^2) = 0$$

$$\frac{dv}{dr} = k/r \sinh^2 \lambda.$$

When a is zero, the solutions of these equations reduce to those already discussed. The equation for λ may be solved by a method of successive approximation, but as the solutions obtained in this way do not appear to have any obvious application they will not be pursued. A more general solution obtained by successive approximations is given in the next paragraph.

§ 5. *Approximate Solutions satisfying given Boundary Conditions.*

If we multiply (2.5) by l, (2.6) by $-f$, and add, we obtain the equation

$$\frac{\partial}{\partial r}\left\{\frac{1}{r}(lf_1 - fl_1)\right\} + \frac{\partial}{\partial z}\left\{\frac{1}{r}(lf_2 - fl_2)\right\} = 0.$$

Introducing new functions defined by the equations

$$2\psi = \log l/f, \qquad \tau = m/r, \tag{5.1}$$

the above equation becomes

$$\psi_{11} + \psi_{22} + \psi_1/r = \frac{2\tau}{1-\tau^2}[\tau, \psi]. \tag{5.2}$$

The equation for τ is obtained by writing τr for m in (2.7). It is

$$\tau_{11} + \tau_{22} + \tau_1/r - \tau/r^2 = -\frac{\tau}{r^2}\{[f, l] + [m, m]\}, \tag{5.3}$$

where

$$f = r\sqrt{1-\tau^2}\,e^{-\psi}, \qquad l = r\sqrt{1-\tau^2}\,e^{\psi}. \tag{5.4}$$

Provided m and the differential coefficients of f are small quantities, equations (5.2) and (5.3) are forms suitable for obtaining solutions by successive approximations. The first approximations are got by neglecting the right-hand sides. They are

$$\psi_0 = \log r - 2V, \qquad \tau = \tau_0, \tag{5.5}$$

where V is the Newtonian potential of an arbitrary, axially symmetrical distribution of matter in the canonical space (r, z, θ), and τ_0 is the coefficient of

$\sin\theta$ in the expansion of $\phi(r, z, \theta)$, which is a second arbitrary Newtonian potential. It is of the form

$$\phi = \phi_0(r, z) + \tau_0 \sin\theta + \sum^{\infty} \phi_n \sin n\theta + \text{cosine terms}.$$

Each term of the expansion is a solution of Laplace's equation.

It will be assumed that all the matter producing the field is enclosed by a surface of revolution S and that on this surface f, l, m assume assigned values, while at infinity $f \to 1$, $l \to r^2$, $m \to 0$, that is, the metric approaches that of the *Special Theory of Relativity*.

We can always determine ψ_0 and τ_0 such that these conditions are satisfied.*

If we write

$$\psi' = \psi - \psi_0, \qquad \tau' = \tau - \tau_0, \tag{5.6}$$

ψ' and τ' are small quantities of the second order which vanish on S and at infinity. They satisfy the differential equations

$$\psi'_{11} + \psi'_{22} + \psi'_1/r = \frac{2\tau}{1-\tau^2}[\tau, \psi], \tag*{(5.2)$'$}$$

$$\tau'_{11} + \tau'_{22} + \tau'_1/r - \tau'/r^2 = -\frac{\tau}{r^2}\{[f, l] + [m, m]\}. \tag*{(5.3)$'$}$$

Approximate solutions of these equations can be obtained if on the right-hand sides quantities of order higher than the second are neglected, τ_0 and the differential coefficients of f being treated as small.

To this order, the right-hand side of (5.2)$'$ is

$$\rho_0 = 2\tau_0\tau_{01}/r, \tag{5.7}$$

and the right-hand side of (5.3)$'$, by means of (5.4) and (5.5)

$$\sigma_0 = -4\tau_0 V_1/r. \tag{5.8}$$

It is convenient to introduce the functions

$$\phi' = \tau' \sin\theta, \quad \sigma'_0 = \sigma_0 \sin\theta. \tag{5.9}$$

We have now to find functions ψ' and ϕ' which vanish on S and at infinity and satisfy the Poisson equations

$$\nabla^2\psi' = \rho_0, \quad \nabla^2\phi' = \sigma_0'.$$

The problem may be regarded as a purely geometric one and can be solved with the aid of Green's function, *i.e.*, a function $G(x, y, z;\ x', y', z')$, which vanishes on S and at infinity, and satisfies Laplace's equation at all points except (x', y', z'), where it behaves like $1/4\pi\sqrt{(x-x')^2+\ldots}$. In terms of this function

---

* Dirichlet's problem for space.

$$\left.\begin{aligned}\psi' &= -\int G(x, \ldots, x', \ldots)\, \rho_0(x', \ldots)\, dx' \ldots \\ \phi' &= -\int G(x, \ldots, x', \ldots)\, \sigma_0'(x', \ldots)\, dx' \ldots\end{aligned}\right\}, \qquad (5.10)$$

where the region of integration is the space bounded by S and the sphere at infinity.

Approximations of higher order can be obtained by similar processes.

Using the expressions (5.4) for f and l, one easily verifies the relations

$$f_1l_1 + m_1^2 = 1 - r^2\{(1-\tau^2)\,\psi_1^2 - \tau_1^2/(1-\tau^2)\},$$

$$f_2l_2 + m_2^2 = -r^2\{(1-\tau^2)\,\psi_2^2 - \tau_2^2/(1-\tau^2)\},$$

$$f_1l_2 + f_2l_1 + 2m_1m_2 = -2r^2\{(1-\tau^2)\,\psi_1\psi_2 - \tau_1\tau_2/(1-\tau^2)\}.$$

If we substitute these expressions in (2.9) and neglect terms of order higher than the second, and bear in mind the equations satisfied by V and ψ', we get, eventually,

$$\mu + 2V - \psi' = \int \tfrac{1}{2}r\{4(V_1^2 - V_2^2) - \tau_0^2/r^2 - (\tau_{01}^2 - \tau_{02}^2)\}\, dr + \tfrac{1}{2}r\{8V_1V_2 - 2\tau_{01}\tau_{02}\}\, dz. \qquad (5.11)$$

Another method of approximation is available when S has certain forms. This method will be illustrated by an example in § 7.

§ 6. *Andress' Equations in Canonical Co-ordinates.*

In the second part of his paper Andress deduces the approximate equations of the stationary field with axial symmetry on the basis of the quadratic form

$$ds^2 = -e^\lambda(dx^2 + dr^2) - r^2e^{-\rho+\epsilon} + e^{\rho+\epsilon}\,dt^2 + 2r\tau\, d\theta\, dt, \qquad (6.1)$$

and the final forms of his differential equations are*

$$\tau_{11} + \tau_{22} + \tau_2/r - \tau/r^2 = 0, \qquad (6.2)$$

$$\nabla^2(\rho + \epsilon) = -\tau_1^2 - (\tau_2 + \tau/r)^2, \qquad (6.3)$$

$$\epsilon_{11} + \epsilon_{22} + 2\epsilon_2/r = -(\tau_1^2 + \tau_2^2 + \tau\tau_2/r + \tau^2/r^2), \qquad (6.4)$$

---

* *Loc. cit.*, pp. 601, 602. In (6.5), Andress' (5.44), he has ϵ instead of $-\epsilon$ on the left-hand sides. But it is clear from his equations (2.11)–(2.14) and (5.11), (5.12) and (5.16) that $-\epsilon$ is correct. There are other minor misprints in the indices of the last equation.

$$\left.\begin{aligned}\frac{\partial}{\partial r}(\lambda+\rho-\varepsilon) &= \tfrac{1}{2}r\,(\rho_2{}^2-\rho_1{}^2) - r\,(\varepsilon_{11}-\varepsilon_{22}) \\ &\qquad - r\tau\,(\tau_{11}-\tau_{22}-\tau_2/r) - \tfrac{1}{2}r\,(\tau_1{}^2-\tau_2{}^2+\tau^2/r^2) \\ \frac{\partial}{\partial x}(\lambda+\rho-\varepsilon) &= r\rho_1\rho_2 + 2r\varepsilon_{12} + r\tau_1(\tau_2+\tau/r) + 2r\tau\tau_{12}\end{aligned}\right\}, \qquad (6.5)$$

where the suffix 1 means differentiation with respect to x and 2 with respect to r.

Comparing (6.1) with (1.1) of this paper we get

$$f = e^{\rho+\varepsilon}, \quad l = r^2 e^{-\rho+\varepsilon}, \quad m = -r\tau, \quad \mu = \lambda.$$

It follows from (5.1) that

$$2\psi = \log l/f = 2\log r - 2\rho \qquad (6.6)$$

and

$$fl + m^2 = r^2\,(e^{2\varepsilon} + \tau^2). \qquad (6.7)$$

In virtue of the existence of canonical co-ordinates we can write

$$e^{2\varepsilon} + \tau^2 = 1, \qquad (6.8)$$

i.e., we can identify r and x with the canonical co-ordinates without changing the form of (6.1). The relation (6.8) does not follow accurately from Andress' equations on account of his neglecting all but linear terms in (6.2).

However, to the order of approximation considered by Andress, we can write, in virtue of (6.8),

$$\varepsilon = -\tfrac{1}{2}\tau^2. \qquad (6.9)$$

On substituting this expression for ε in (6.4) we find that the latter is identically satisfied in virtue of (6.2). Making the same substitution in (6.3) it reduces to

$$\nabla^2\rho = -\frac{2\tau\tau_2}{r}, \qquad (6.10)$$

which is identical with the equation satisfied by ψ' of this paper when higher order terms are neglected.

The equations (6.5) reduce to

$$\begin{aligned}\frac{\partial}{\partial r}(\lambda+\rho) &= \tfrac{1}{2}r\,(\rho_2{}^2-\rho_1{}^2) + \tfrac{1}{2}r\,(\tau_1{}^2-\tau_2{}^2) - \tau^2/2r, \\ \frac{\partial}{\partial x}(\lambda+\rho) &= r\rho_1\rho_2 - r\tau_1\tau_2\end{aligned} \qquad (6.11)$$

These last equations are equivalent to (5.11) of this paper if $(2V - \psi')$ is written for ρ and μ for λ on the left-hand sides and $2V$ for ρ and τ_0 for τ on the right-hand sides. The solution of (6.10) actually given by Andress is a particular one—the Poisson Integral. He omits the complementary function 2V which is necessary to make the solution reduce to his solution for the static case for a vanishing τ.

We thus see that the use of canonical co-ordinates greatly simplifies the differential equations to be solved. If we consider any transformation of co-ordinates which preserves the normal form of $e^{\mu}(dr^2 + dz^2)$, the expressions for f, l, m are obtained by direct substitution in the expressions for these potentials in the canonical system, and e^{μ} must be multiplied by the modulus of the transformation. When discussing the static case Andress actually introduces canonical co-ordinates by putting $\nu = -\rho$. In the stationary case, however, it is not so easy to spot canonical co-ordinates unless one proceeds from the *variational principle.*

§ 7. *The Field of a Rotating Sphere.*

Green's function is known for a spherical surface, but the integrations involved in the calculation of second order terms are very cumbersome, and labour is saved by using another method. We will show how to calculate second order terms in ψ, but the calculation for the second order terms in τ will not be given in detail. The method is essentially the same in the two cases, though the differential equations involved are different.

It is convenient to use spherical polar co-ordinates associated with the canonical space. They are defined by the transformation

$$x = \mathrm{R} \sin \theta' \cos \theta, \quad y = \mathrm{R} \sin \theta' \sin \theta, \quad z = \mathrm{R} \cos \theta', \quad r = \mathrm{R} \sin \theta'. \tag{7.1}$$

The first approximations in this case may be written

$$\left.\begin{aligned} \mathrm{V} &= -\frac{\kappa \mathrm{M}}{\mathrm{R}} + \sum_{n=1}^{\infty} \mathrm{A}_n \mathrm{P}_n (\cos \theta')/\mathrm{R}^{n+1} \\ \tau_0 &= \frac{\mathrm{B}_1 \sin \theta'}{\mathrm{R}^2} + \sum_{n=2}^{\infty} \mathrm{B}_n \mathrm{P}_n{}^1 (\cos \theta')/\mathrm{R}^{n+1} \end{aligned}\right\}. \tag{7.2}$$

$-\kappa\mathrm{M}/\mathrm{R}$ is the ordinary Newtonian potential for a spherically symmetrical distribution of matter. We will assume that the distribution in the canonical space deviates but slightly from spherical symmetry and that the angular speed is not too great. This amounts to assuming that the A_n are small quantities of the second order. We also assume, for simplicity, that the B_n ($n = 2, 3, \ldots$) are of the second order. The A_n and B_n have been chosen so as to satisfy boundary conditions on the surface of the sphere. As these boundary conditions do not affect the determination of terms of higher order, we need not limit ourselves to any particular set of boundary values.

Hence, disregarding all terms other than the dominant ones, we find that, by (5.7)

$$\rho_0 = 2\tau_0\tau_{01}/r = 2B_1^2(1-3\sin^2\theta')/R^6. \tag{7.3}$$

It is required to find a solution of the equation (5.2)′, which becomes

$$\frac{\partial}{\partial R}\left(R^2\frac{\partial\psi'}{\partial R}\right)+\frac{1}{\sin\theta'}\frac{\partial}{\partial\theta'}\left(\sin\theta'\frac{\partial\psi'}{\partial\theta'}\right)=2B_1^2(1-3\sin^2\theta')/R^4. \tag{7.4}$$

The right-hand side of this equation can be written in the form

$$\rho_0 = \Sigma\, k_n P_n(\cos\theta')/R^4, \tag{7.3$'$}$$

where

$$k_0 = -2B_1^2, \quad k_2 = 4B_1^2,$$

and all the other k_n are zero.

We can find a particular solution of (7.4) of the form

$$\Sigma\, f_n P_n(\cos\theta'),$$

where f_n satisfies the differential equation

$$\frac{d}{dR}\left(R^2\frac{df_n}{dR}\right)-n(n+1)f_n = k_n/R^4.$$

This equation has a particular integral

$$k_n/R^4\{12-n^2-n\}.$$

It follows that

$$B_1^2(-1+4P_2(\cos\theta'))/6R^4 \tag{7.5}$$

is a particular solution of (7.4).

But on the sphere $R = a$ (a is not to be confused with the gravitational radius) ψ' is zero. Hence to (7.5) one must add a term of the type

$$\frac{C_1}{R}+\frac{C_2P_2(\cos\theta')}{R^3}.$$

Substituting boundary conditions we find, ultimately, that

$$\psi' = B_1^2\left\{\frac{1}{a^3}-\frac{1}{R^3}+4\left(\frac{1}{R^3}-\frac{1}{aR^2}\right)P_2(\cos\theta')\right\}\Big/6R. \tag{7.6}$$

Again, putting in their values for the dominant terms in (5.11), we get

$$\mu + 2\mathrm{V} - \psi' = \int \frac{r}{2}\left\{\frac{4\kappa^2\mathrm{M}^2(r^2 - z^2)}{\mathrm{R}^6} - \frac{\mathrm{B}_1{}^2(5r^4 - 11r^2z^2 + 2z^4)}{\mathrm{R}^{10}}\right\} dr$$

$$+ \frac{r}{2}\left\{\frac{8\kappa^2\mathrm{M}^2rz}{\mathrm{R}^6} + \frac{6\mathrm{B}_1(z^2 - 2r^2)\,rz}{\mathrm{R}^{10}}\right\} dz$$

$$= -\kappa^2\mathrm{M}^2r^2/\mathrm{R}^4 + \mathrm{B}_1{}^2\{-r^2/2\mathrm{R}^6 + 9r^4/8\mathrm{R}^8\}. \tag{7.7}$$

To the same order, we get from (5.8) and (7.2)

$$\sigma_0 = -4\mathrm{B}_1\kappa\mathrm{M}\sin\theta'/\mathrm{R}^5\,; \tag{7.8}$$

and equation (5.3)′ for τ' may be written

$$\frac{\partial}{\partial\mathrm{R}}\left(\mathrm{R}^2\frac{\partial\tau'}{\partial\mathrm{R}}\right) + \frac{1}{\sin\theta'}\frac{\partial}{\partial\theta'}\left(\sin\theta'\frac{\partial\tau'}{\partial\theta'}\right) - \frac{\tau'}{\sin^2\theta'} = -4\mathrm{B}_1\kappa\mathrm{M}\sin\theta'/\mathrm{R}^3. \tag{7.9}$$

This equation has a particular solution of the form

$$k\sin\theta'/\mathrm{R}_3.$$

Evaluating the constant and adding a solution of the homogeneous equation, we finally get a function satisfying (7.9) and vanishing on the surface of the sphere and at infinity. It is

$$\tau' = -\mathrm{B}_1\,\kappa\mathrm{M}\sin\theta'\left(\frac{1}{\mathrm{R}^3} - \frac{1}{a\mathrm{R}^2}\right). \tag{7.10}$$

It is assumed that both B_1 and $\kappa\mathrm{M}$ are small. Approximations of higher order can be obtained in an analogous manner. The solutions will proceed in powers of $\kappa\mathrm{M}$ and B_1. At no stage do we introduce a singularity other than the original one at $\mathrm{R} = 0$, so there should be no difficulty about convergence, provided the above-named constants are small.

Disregarding A_1, B_2, etc., the values of f, l, m, as far as second order terms, are obtained by expanding (5.4) and putting in the expressions for V, ψ', τ_0 and τ'. These values are

$$\left.\begin{aligned} f &= 1 - \frac{2\kappa\mathrm{M} + \mathrm{B}_1{}^2/6a^3}{\mathrm{R}} + \frac{2\kappa^2\mathrm{M}^2}{\mathrm{R}^2} + \frac{2\mathrm{B}_1{}^2\mathrm{P}_2(\cos\theta')}{3a\mathrm{R}^3} \\ &\qquad - \frac{\mathrm{B}_1{}^2(1 + 2\mathrm{P}_2(\cos\theta'))}{6\mathrm{R}^4} \\ r^{-2}l &= 1 + \frac{2\kappa\mathrm{M} + \mathrm{B}_1{}^2/6a^3}{\mathrm{R}} + \frac{2\kappa^2\mathrm{M}^2}{\mathrm{R}^2} - \frac{2\mathrm{B}_1{}^2\mathrm{P}_2(\cos\theta')}{3a\mathrm{R}^3} \\ &\qquad - \frac{\mathrm{B}_1{}^2(1 - 2\mathrm{P}_2(\cos\theta'))}{2\mathrm{R}^4} \\ r^{-2}m &= \frac{\mathrm{B}_1\sin\theta'}{\mathrm{R}^2}\{(1 + \kappa\mathrm{M}/a) - \kappa\mathrm{M}/\mathrm{R}\} \end{aligned}\right\}. \tag{7.11}$$

If squares and products of κM and B_1 are neglected, the form (1.1) becomes

$$ds^2 = \left(1 - \frac{2\kappa M}{R}\right) dt^2 - \left\{\left(1 + \frac{2\kappa M}{R}\right)(dr^2 + dz^2 + r^2 d\theta^2)\right\} - \frac{2B_1 r^2}{R^3}\, d\theta\, dt.$$

This approximation is identical with the form obtained by Leuse and Thirring, and with Bach's first approximation. These authors write $-\kappa \frac{4}{5} Ml^2 w$ for B_1, *i.e.*, they assume B_1 to be proportional to the angular momentum.

If we examine the coefficient of 1/R in the first two of equations (7.11), we notice that at a sufficiently great distance from the sphere the effect of the rotation is to increase the effective mass of the sphere by $B_1{}^2/12\kappa a^3$.

We also notice that τ_0 is proportional to the magnetic potential of a uniformly magnetised sphere. The effect of this term on the motion of a material particle is analogous to the effect of a Coriolis force.

One cannot expect our second order terms to fit with the second order terms obtained by Bach. For, in fact, they do not represent the field of the same distribution of matter. A sphere in Bach's space is not a sphere in the canonical space. Weyl has shown, in the static case, that the canonical co-ordinates are connected with the co-ordinates of the Schwarzchild space by the transformation

$$r + iz = r' + iz' - \frac{(a/2)^2}{r' + iz'},$$

where a is the *gravitational radius* of the particle, in this case. The particle is transformed into a uniform rod of length $2a$ in the canonical space. Since the transformation involves the square of a (or κM), the first approximations of Bach are necessarily contained in our first approximations when boundary conditions are suitably chosen.

[*Note.*—When the field in question is due to a large body there is no comparison between the gravitational radius and the ordinary radius. For example, the gravitational radius of the sun is about 1·47 kilometres and the gravitational radius of the earth only 5 millimetres. Hence there is no danger of our method of approximation leading to a singularity of the gravitational potentials outside matter.]

My thanks are due to Professor Schott for the interest he has taken in this work and for many valuable suggestions.

On the Action of Tuned Rectangular Frame Aerials when receiving Short Waves.

By L. S. PALMER, M.Sc., Ph.D., Professor of Physics, The University College, Hull.

(Communicated by E. V. Appleton, F.R.S.—Received December 1, 1931.)

I. *Introduction.*

Some preliminary experiments in 1927 showed that the maximum current produced by the incidence of short wireless waves on a tuned rectangular frame aerial was very critically dependent on the dimensions of the frame. An increase or decrease in the width or height of the frame by only a few centimetres might change the current many hundred fold, such current variations being quite independent of the tuning. Furthermore the reduction of current caused by, say, a decrease in the frame width could be compensated by an increase in the frame height and *vice versa*, but the changes in dimensions were not equal in magnitude, neither was their product a constant. In fact, the maximum current depended on the shape of the frame and also varied irregularly with the area. For a given wave-length there were certain critical areas for maximum current, and doubling the area of a frame did not quadruple the current (as when receiving long waves) but the current was reduced to one of negligible magnitude, although the frame was kept properly tuned.

It was found that these anomalous effects could be explained by taking into consideration, not only the action of the passing wave, but also the mutual action between the currents flowing in adjacent parts of the frame. In order to do this, it is convenient to consider the current in any limb as the resultant of two component currents; namely a "direct" component due to the incidence of the wave on the particular limb, and an "indirect" component due to the effects of the currents in adjacent limbs. These two components will, in general, differ in phase and amplitude, and the problem reduces to the determination of those conditions which tend to produce the maximum resultant current.

It seems reasonable to suppose that, with a tuned rectangular frame, the resultant currents in opposite limbs tend, at any instant, to be π out of phase with each other, and any condition which promotes the establishment of this phase relation must reduce the apparent impedance of the frame. These conditions are determined in the following section.

II. *Theory of the Action of a Tuned Rectangular Receiving Frame.*

It is convenient to simplify the problem by discussing the effect of a plane polarised wave incident on a tuned rectangular frame. Let the plane of the frame be in the direction of wave propagation and let this direction make an angle γ with the side AB of the frame (fig. 1).

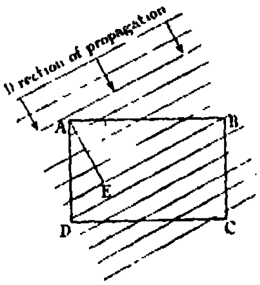

Fig. 1.

Then if the transmitter be distant at least several wave-lengths from the receiving frame, the phase difference of the e.m.fs. produced by the wave in the sides AD and BC will depend only on their *effective* distance apart, which, from the figure, is seen to be AE; that is, AB cos γ. Since the frame is tuned, this distance will also determine the phase angle between the "direct" current components in AD and BC; the required phase difference being

$$2\pi \mathrm{AB} \cos \gamma / \lambda = a \cos \gamma, \tag{1A}$$

where $a = 2\pi \mathrm{AB}/\lambda$, λ being the wave-length.

Similarly the "direct" current components produced in AB and CD will differ in phase by

$$2\pi \mathrm{AD} \sin \gamma / \lambda \quad \text{or} \quad a' \sin \gamma, \tag{1B}$$

where $a' = 2\pi \mathrm{AD}/\lambda$.

We have next to determine the phase difference between the "indirect" current components; that is, the phase difference between a current in AD, for example, and the current it produces in BC. This is best done by considering the case of two tuned Hertzian antennæ situated along AD and BC respectively. Suppose the current in AD at any instant be given by

$$\mathrm{I} = \mathrm{I}_0 \sin \omega t.$$

Then we have to determine the phase of the current I′ in BC produced by I when the two antennæ are AB (= W) cm. apart. The electric moment of AD is $-\int \mathrm{I}_0 \sin \omega t \, dt$, which results in a field at BC such that the electric vector E of the field is given by

$$\mathrm{E} = -\mathrm{AI}_0 \left\{ \frac{1}{\mathrm{W}^3} \cos(\omega t - a) + \frac{1}{v\mathrm{W}^2} \frac{d}{dt} [\cos(\omega t - a)] + \frac{1}{v^2 \mathrm{W}} \frac{d^2}{dt^2} [\cos(\omega t - a)] \right\},$$

where A is a constant, v is the velocity of the electromagnetic waves in the medium, and $a = 2\pi W/\lambda$. Hence

$$E = -\frac{AI_0}{W^3}[a^2 + (1 - a^2)^2]^{\frac{1}{2}} \sin [\omega t - (a - \phi + \pi/2)]$$

$$= E_0 \sin [\omega t - (a - \phi + \pi/2)],$$

where $\phi = \tan^{-1} a/(1 - a^2)$.

E_0 is a monotonic function of a, and when E_0 is assumed to be constant for the purpose of facilitating the solution of the equation, the results prove to be such as to justify the assumption for approximate purposes.

This e.m.f. produces or reflects a current I′ in BC which, since the antennæ are supposed to be tuned, will be in phase with E. Hence the phase difference between the current I in AD and that produced by it in BC a distance W away is given by the expression

$$(a - \phi + \pi/2). \tag{2A}$$

Similarly antennæ lying along AB and CD will produce currents in each other which differ in phase by

$$(a' - \phi' + \pi/2), \tag{2B}$$

where $a' = 2\pi AD/\lambda$ or $2\pi H/\lambda$ and $\phi' = \tan^{-1} a'/(1 - a'^2)$.

Since AD and AB are perpendicular they will not influence each other. Thus, when the two pairs of parallel antennæ are present together in the form of a frame, each pair will experience "indirect" or reflected currents which will differ in phase by the amount given in expression (2A) or (2B).

The resultant frame current will be the vector sum of the "direct" components differing in phase by $a \cos \gamma$ and $a' \sin \gamma$, and the "indirect" components differing in phase by $(a - \phi + \pi/2)$ and $(a' - \phi' + \pi/2)$. If the amplitudes of the components are independent of a (or a') then the resultant current will be a maximum when the *total* phase differences (θ_W and θ_H, say) between the currents in opposite sides of the frame are equal to π. That is, when

$$\theta_W = a (1 + \cos \gamma) - \phi + \pi/2 = \pi, \tag{3A}$$

and when

$$\theta_H = a' (1 + \sin \gamma) - \phi' + \pi/2 = \pi. \tag{3B}$$

And the solutions of these equations in terms of a (or W/λ) and a' (or H/λ) will give the critical frame dimensions for which the resultant currents in the opposite sides of the frame differ by π and are therefore a maximum.*

---

* With the first signs minus (or $\gamma = 180°$), other critical widths arise, but these are not discussed in the present paper.

It is readily seen that when the transmitter is situated a distance from the frame very great compared with the dimensions of the frame, then the amplitude of the "direct" current components is independent of a (or a') and only dependent on the transmitter constants, the distance between the transmitter and the frame and the angle γ at which the waves descend upon the aerial. It has also been stated above that E_0 may be assumed constant, and hence I' or the "indirect" current component is also sensibly independent of a (or a'). Therefore the solutions of equations (3) will give the values of frame width W and of frame height H for which the frame current is a maximum.

These equations reduce to the transcendental equations :—

$$\tan a(1 + \cos\gamma) = (a^2 - 1)/a \tag{4A}$$

and

$$\tan a'(1 + \sin\gamma) = (a'^2 - 1)/a'. \tag{4B}$$

In the case when $\gamma = 0$ and the electric vector of the wave is parallel to AD, the solutions of the equations are

$$a = 2\cdot05, \quad 3\cdot75, \quad 5\cdot35, \quad \text{etc.},$$

and

$$a' = 4\cdot45, \quad \text{etc.},$$

leading to values of W (or $a\lambda/2\pi) = 0\cdot33\lambda$, $0\cdot60\ \lambda$, $0\cdot85\ \lambda$, etc., and of H (or $a'\lambda/2\pi) = 0\cdot71\ \lambda$, etc.

There is an ambiguity in these solutions arising from the fact that they include values of a and a' for both maximum and minimum currents, but experiments show that odd solutions give maximum current conditions and even solutions give minimum current conditions.

Thus we conclude that a frame of height $0\cdot71\ \lambda$ and of width either $0\cdot33\ \lambda$ or $0\cdot85\ \lambda$ will have an abnormally large current circulating round it when its plane is in the direction of wave propagation and its sides are parallel to the electric vector of the wave.

Now the early preliminary experiments showed that if these critical widths were altered, then the large current could still be maintained by suitably readjusting the height of the frame. This fact can be explained by extending the foregoing theory as follows :—

Suppose the frame width be *increased* so that the phase difference between the currents in the two sides be no longer equal to π. Let the new phase difference be $(\pi + \psi)$, say. Then

$$\theta_W = a(1 + \cos\gamma) - \phi + \pi/2 = \pi + \psi, \tag{5A}$$

and the new width may be considered to have acted as an added inductance producing the additional and undesirable phase lag ψ. Now if the height be *decreased* just sufficiently to produce a phase lead of $(\pi - \psi)$ in the currents in the top and bottom of the frame, then the effect is similar to introducing a capacity of sufficient magnitude to compensate for the inductive effect of the increased width. Thus

$$\theta_H = a'(1 + \sin\gamma) - \phi' + \pi/2 = \pi - \psi, \tag{5B}$$

and the *total* reactance effect due to θ_W and θ_H is the same as before, but the solutions of these new equations result in frames of quite different dimensions depending on the value of ψ substituted in the equations.

The frame dimensions (that is, values of W/λ and H/λ) for different values of ψ and γ can be calculated from the reduced transcendental equations :—

$$\tan\left[a(1 + \cos\gamma) - \psi\right] = (a^2 - 1)/a \tag{6A}$$

and

$$\tan\left[a'(1 + \sin\gamma) + \psi\right] = (a'^2 - 1)/a'. \tag{6B}$$

This has been done graphically for values of γ equal to 0°, 15°, 30°, 45°, 60°, 75° and 90°, and for sufficient values of ψ to get the complete curves shown in figs. 2 and 3. Fig. 2, for which $\gamma = 0°$, is included in fig. 3 but is shown separately for convenience of discussion.

The co-ordinates of a point on any one of the graphs give the dimensions of a frame which will have maximum current produced in it when the angle of incidence γ of the wave is that corresponding to the particular graph. This follows because for every point on any graph the lag (or lead) resulting from a given value of W/λ is just compensated by an equal lead (or lag) resulting from the corresponding value of H/λ.

The points A and A′ in fig. 2 give the dimensions of the frames mentioned above, for which $\gamma = 0$ and $\psi = 0$; whilst for points B and B′, $H/\lambda = W/\lambda$ and the frames are square. Only two graphs are shown for each value of γ because calculations were not made for values of W exceeding two wave-lengths. It follows that for a frame of any height less than one wave-length there are, in general, at least two critical widths for which the current will be a maximum, whilst for a height of about 0·8 λ, for example, there are more than two critical widths less than one wave-length. These are indicated by the points C′ in fig. 3. The possibility of these additional critical widths is confirmed by the presence of the subsidiary peak in the experimental curve for H = 7 metres in fig. 6. Similarly for a width of about half a wave-length there may be the additional critical heights indicated by the points C in fig. 2.

Since both the height and the width have critical values depending on the wave-length, it follows that the area of the frame will also be critically dependent on the wave-length. By calculating the values of HW/λ^2 for different points on any given graph it may be shown that the frame of maximum area is not necessarily that for which H equals W. For example, in the case when $\gamma = 0$, the maximum frame areas are $0\cdot24\ \lambda^2$ and $0\cdot72\ \lambda^2$ and these occur for $H = 0\cdot6\lambda$, $W = 0\cdot4\ \lambda$, and $H = 1\cdot22\ \lambda$, $W = 0\cdot6\ \lambda$ respectively; whilst for $\gamma = 45°$ the maximum areas are only $0\cdot15\ \lambda^2$ and $0\cdot50\ \lambda^2$ when $H = W = 0\cdot39\ \lambda$ and $0\cdot72\ \lambda$ respectively. Only in this case do the frames of maximum area happen to be square. The reduction in the maximum critical area as γ changes from 0° to 45° indicates that if a correctly proportioned frame be rotated

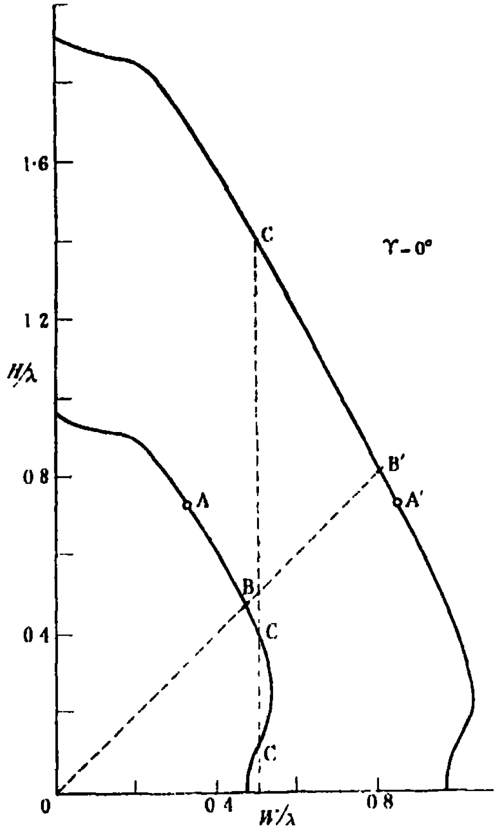

Fig. 2.

through 45° about an axes *perpendicular* to its plane, the signal strength will change although the frame dimensions remain constant.

Again, since the critical areas decrease as the critical frame dimensions diverge from the values deduced above, it follows that the maximum frame

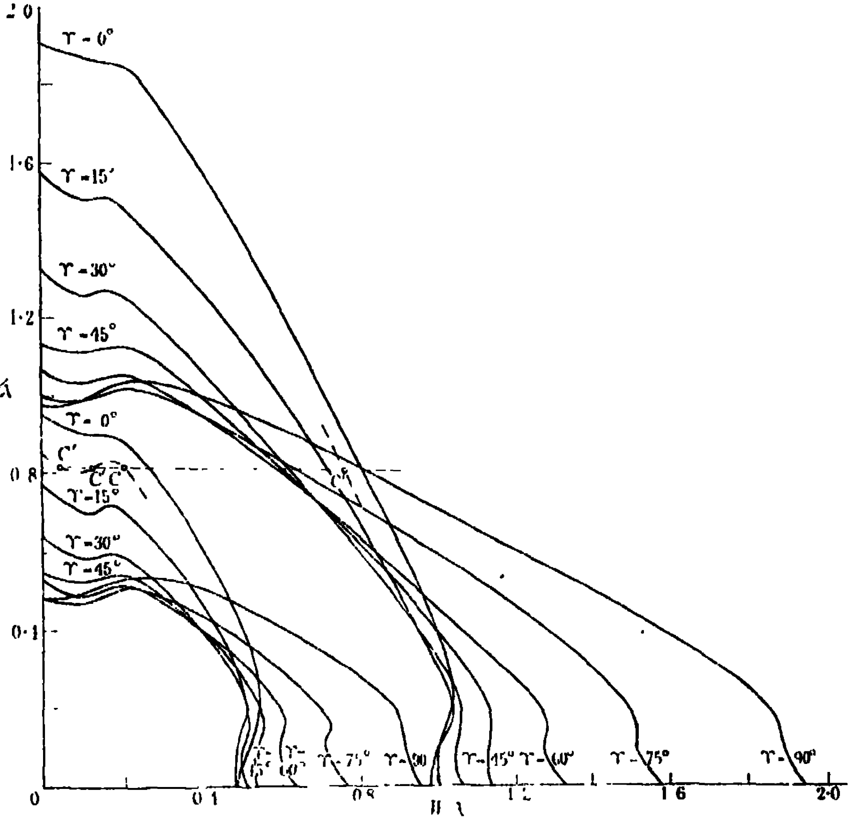

Fig. 3.

currents will also decrease as the dimensions of the frame diverge from these values. In other words, long narrow frames or short wide frames, even when of correct critical dimensions, will have comparatively small currents circulating in them. The curves shown in fig. 6 tend to confirm this conclusion.

The foregoing theory was tested experimentally and the practical work and results are outlined in the following section.

III. *Experimental Investigation.*

Since the foregoing theory applies to frames comparable in dimensions with the wave-length, it is necessary to work with short waves in order that the frame shall not be too unwieldy. A transmitter was therefore used which was capable of radiating on wave-lengths from 7·54 to 8·80 metres. The power of the transmitter was sufficient for the received current in the frame aerial to be measured by a vacuum thermojunction and microammeter.

The frame was made from bare flexible stranded copper wire which passed over four insulators, two of which were in the form of insulated metal drums round which surplus wire could be wound or from which wire could be unwound according to the size of the frame in use. The sides of the frame were vertical and the top and bottom were horizontal. The height of the frame could be varied by lowering or raising a horizontal beam along which the two top insulators could be moved. The two lower insulators moved along a fixed horizontal beam placed about 5 feet above the ground. The horizontal movements of the insulators enabled the width of the frame to be varied. The actual movements were accomplished mechanically by pulling cords attached to trolleys on which the insulators were fixed. Arrangements were made to ensure that the surplus wire, when small frames were in use, was automatically wound on the drums which formed the lower pair of insulators. The whole frame was supported on two 60-foot scaffold poles erected 30 feet apart.

In order to tune so large an inductance to the short waves it was necessary to shunt the frame with a very small coil across which a tuning condenser reading up to 0·0005 μF was connected. The vacuum thermojunction and microammeter were inserted in series with the condenser. This method of tuning is particularly convenient because it ensures that the variation of frame dimensions changes the total circuit inductance by an almost negligible amount. It was not found practicable at this stage to vary the angle γ at which the radiation was incident on the frame. Rough measurements with a tilting aerial method similar to that used by Smith-Rose and Barfield* showed that γ was probably less than 10°. There was an appreciable horizontal component of the electric vector indicating that the wave was elliptically polarised in the plane of propagation. This fact has important bearings on the results and is referred to in the discussion below. The elliptical polarisation of the wave was to be expected because the conductivity of the ground is not perfect and it was unfortunately not practicable to raise the frame high up in the air.

In order to ensure that the direction of propagation was in the plane of the frame, the lines of the magnetic component of the field of the transmitter were plotted on a plan of the locality, and the transmitter was moved about until the lines of the magnetic field, which passed between the scaffold poles, were everywhere perpendicular to the line joining them. The direction of the lines of the magnetic field was determined by carrying a portable frame aerial about the ground and measuring with a compass the orientation of the frame when the received current was a minimum.

---

* 'Proc. Roy. Soc.,' A, vol. 107, p. 587 (1925).

When these preliminary experiments were concluded, a series of measurements of the frame current were made on wave-lengths of 7·54, 8·65 and 8·80 metres. The procedure adopted was to take a set of resonant current readings as the width of the frame was first gradually decreased and then gradually increased, the height remaining constant. These measurements were repeated for heights ranging from 1 to 8 metres. In all cases the frame was kept tuned to the particular wave-lengths in use. Some typical results are shown in fig. 6 for a wave-length of 8·65 metres. On one or two occasions the width was fixed and the height continuously varied, but this method was less convenient because it necessitated the employment of two assistants to operate the moving horizontal beam carrying the top wire of the frame. The two methods of manipulation gave results in complete agreement as may be seen by comparing the current values of the points A in figs. 4 and 5. Fig. 4 shows the current readings plotted against the frame widths for a constant height of 3 metres, and fig. 5 is a graph of current readings plotted against the heights for a constant width of 4 metres.

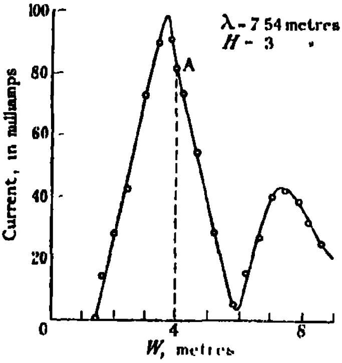

FIG. 4.

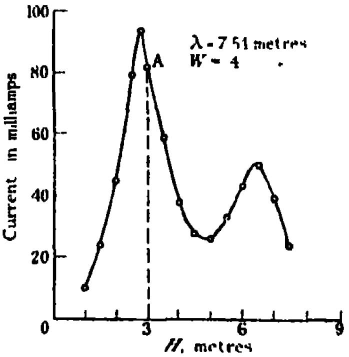

FIG. 5.

IV. *Discussion of Results.*

The chief points arising from a consideration of fig. 6 are :—

(i) There are, in general, for each value of H two critical values of W less than one wave-length for which the current is a maximum ;

(ii) The positions of the peaks move towards higher values of W as H gets smaller; and

(iii) The smallest peak current values occur for long and narrow or short and wide frames, that is, the smallest peaks occur on the curves for H = 8 metres and H = 1 metre.

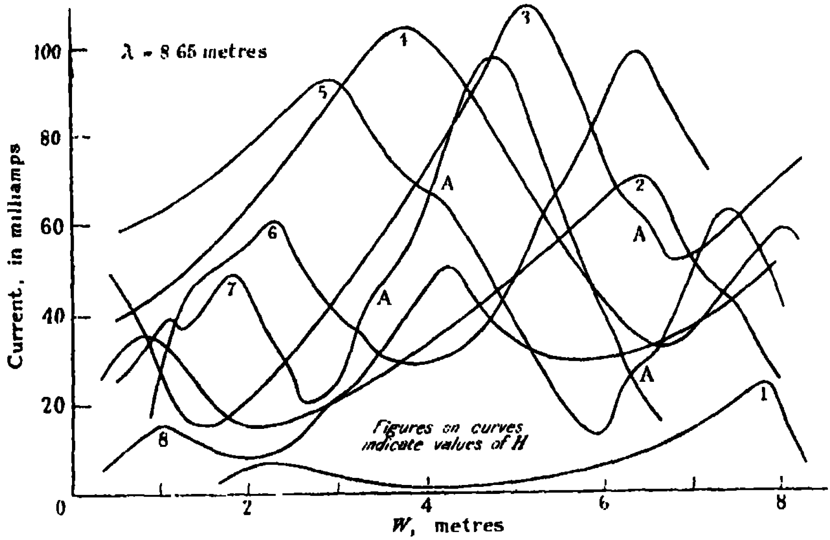

Fig. 6.

The first point follows directly from figs. 2 and 3, and the points A and A′ in the former figure are examples which have already been considered from the theoretical standpoint. A more critical test of the theory is the appearance on the curve for H = 7 metres in fig. 6 of a subsidiary peak. When H = 7, H/λ = 0·81, and by reference to the dot and dash curves of fig. 3 it may be seen that at least one such subsidiary peak ought to occur at this value of H/λ if γ lies somewhere between 0° and 15°. These peaks are indicated by the points of intersection C′, and the second and third of these correspond roughly with the positions of the first two peaks of the graph for H = 7 in fig. 6. In view of the theoretical importance of such subsidiary peaks a separate series of measurements was undertaken to verify their presence on other wavelengths. These measurements were made during the summer weather and a subsidiary peak was again found but it occurred for a value H/λ equal to 0·78, indicating a slightly greater value of γ and a consequent decrease in the earth's electrical conductivity upon which the value of γ depends. Unfortunately, it was not possible with the frame in use to determine whether or not a further subsidiary peak existed correspondingly to the first point C′ in fig. 3. In any case the theory is less reliable for such small values of W.

It is shown below by an independent deduction from all the graphs in fig. 6 that γ is probably about 8°.

Assuming this to be the value for the inclination of the electric vector of the wave and taking the wave frequency f to be 34·7 megacycles (for $\lambda = 8{\cdot}65$ metres), a value of the earth's conductivity σ may be calculated from the modified formula due to Zenneck and used by Smith-Rose and McPetrie,* namely

$$\sigma = f/4 \tan^2 \gamma = 4{\cdot}4 \,.\, 10^8 \text{ e.s.u.}$$

This value, for the boulder clay soil near Hull, seems to be somewhat lower than the values obtained by Smith-Rose and McPetrie for waves of similar frequency at Slough. But, in view of the fact that the above value of 8° for γ has been obtained by a very indirect method (see p. 207), it cannot be considered as reliable. Nevertheless it is an interesting additional test of the general theory of the action of a frame aerial upon which it has been based.

The minor fluctuations at points A in fig. 6 are not accounted for by the present theory, but I understand that J. A. Ratcliffe, by taking into consideration re-radiation to and fro between parallel portions of the frame, can account for the presence of such inflections. We are not, however, concerned with these in the present problem of determining the conditions for maximum frame current.

The second point, namely, that as W increases H decreases for the peak values of the current, indicates that, at least qualitatively, the variations in the critical shape of the frame are in accordance with the foregoing theory. But it remains to see whether these peak values of H and W do actually lie on one or other of the theoretical curves drawn in fig. 3. By taking the coordinates of the positions of the peaks from graphs such as those shown in fig. 6 and plotting the values of H/λ against W/λ the points were found to lie as shown in fig. 7 and not to coincide with any one of the theoretical curves of fig. 3. If we now place a trace of fig. 3 on fig. 7 we find the unexpected result that all the experimental points lie close to the envelope of the theoretical curves. To facilitate this comparison the relevant theoretical curves have been redrawn on fig. 7.

The explanation of this seems to depend on the fact that the wave is elliptically polarised. Hence there will always be some component of the electric vector for every value of γ between 0° and 90°. With a very tall narrow frame (point A on fig. 7) the effect of the horizontal component of the electric vector will be practically negligible because the horizontal wires of the frame are of very small dimensions; whilst the vertical component of the electric field will readily influence the long vertical sides of the frame. Hence point A lies near the graph for $\gamma = 0°$. A similar argument for a flat wide frame leads to the conclusion that the horizontal component is alone operative and hence point B lies near the theoretical curve for $\gamma = 90°$. The frame of more equal dimensions will be affected by both components and hence will have peak current positions on the theoretical graphs for intermediate values of γ. Thus we may account for the fact that the whole series of points taken from sets of graphs similar to those in fig. 6 are all found to lie along the envelope of the curves of fig. 3.

---

* 'Proc. Phys. Soc.,' vol. 43, p. 592 (1931).

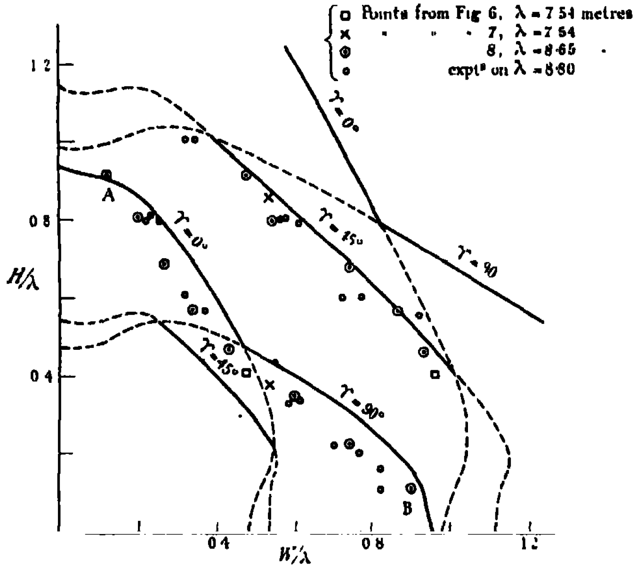

Fig. 7.

In view of the very great difficulties of the experiments it is thought that the greater divergence between the experimental values for the frames of larger areas and the theoretical curves is due to some error of measurement peculiar to the larger frames. Although the error has not yet been definitely located, the discrepancy does not seem to affect the validity of the general theory of the action of a frame aerial which has been discussed in the second section.

The third point, concerning the small maximum currents produced in long thin frames, is a result which has already been deduced when discussing the theory on p. 198. It was there anticipated that the largest currents would be produced in those frames for which the height was not greatly different from the width. This followed because such frames, although not exactly square, except when $\gamma = 45°$, had a greater area than the long narrow or wide flat frames, even though the respective frame dimensions in each case were such that the current tended to be a maximum.

Besides the three points mentioned at the beginning of this section, a fourth, but less obvious conclusion, can be deduced from the graphs of fig. 6. This conclusion can best be seen by tabulating the current values for frames of the same area but of different dimensions. These data can be obtained by considering a given area (say 10, 12, 14, etc., square metres) and calculating the values of W which, when multiplied by the values of H in fig. 6 (namely 1 to 8) will give the particular area under consideration. Then, from the graph corresponding to each particular value of H, the current value for the appropriate width can be read. This procedure can be repeated for the several selected areas. The data so obtained from the graphs of fig. 6 are recorded in

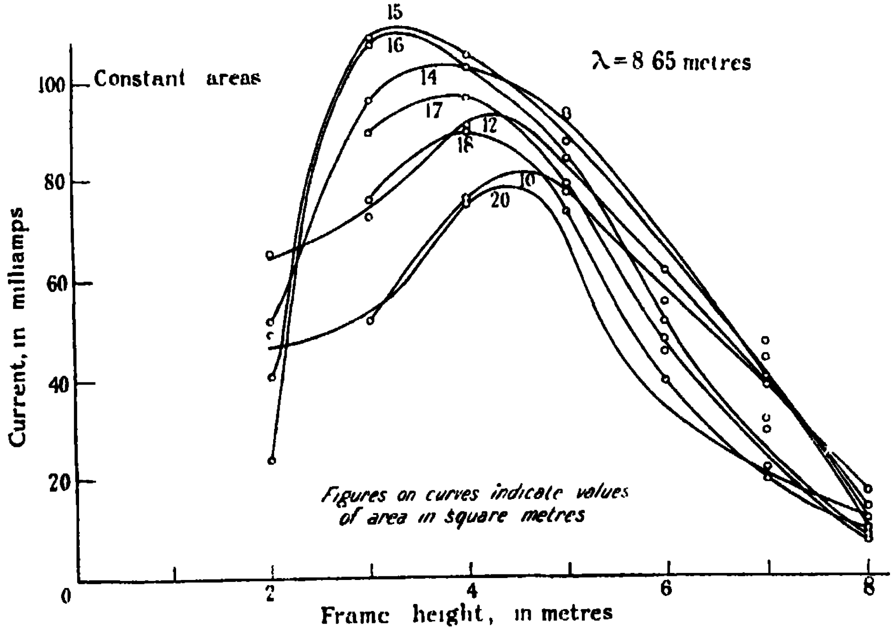

FIG. 8.

Table I, and the resulting curves in fig. 8 show how the current varies as a frame of fixed area changes its shape. From this figure we see that there are optimum dimensions for each area; and, what is most important, there is one

Table I.

Area in Square metres. →	10.		12.		14.		15.		16.		17.		18.		20.	
H metres. ↓	W calculated.	Current from fig. 6.	W calculated.	Current from fig. 6.	W calculated.	Current from fig. 6.	W calculated.	Current from fig. 6.	W calculated.	Current from fig. 6.	W calculated.	Current from fig. 6.	W calculated.	Current from fig. 6.	W calculated.	Current from fig. 6.
1	10·0	—	12·0	—	14·0	—	15·0	—	16·0	—	17·0	—	18·0	—	20·0	—
2	5·0	49	6·0	66	7·0	52	7·5	41	8·0	24	8·5	—	9·0	—	10·0	—
3	3·3	52	4·0	73	4·7	97	5·0	109	5·3	108	5·7	90	6·0	76	6·7	52
4	2·5	77	3·0	91	3·5	103	3·75	105	4·0	103	4·25	97	4·5	90	5·0	76
5	2·0	78	2·4	95	2·8	93	3·0	94	3·2	88	3·4	80	3·6	74	4·0	68
6	1·7	52	2·0	56	2·3	62	2·5	56	2·7	48	2·8	46	3·0	40	3·3	34
7	1·4	39	1·7	48	2·0	44	2·1	40	2·3	32	2·4	29	2·6	20	2·9	22
8	1·25	14	1·5	10	1·75	9	1·9	8	2·0	8	2·1	9	2·25	10	2·5	12

particular area which is better for reception (when of the optimum dimensions) than any smaller or *larger* area. This is more clearly seen by plotting the maximum possible currents (*i.e.*, the peak values of the curves in fig. 8) against the corresponding areas. The result is shown in fig. 9 where the peak occurs for an area of about 0·21 λ^2 (or 15·5 square metres for $\lambda = 8·65$ metres).

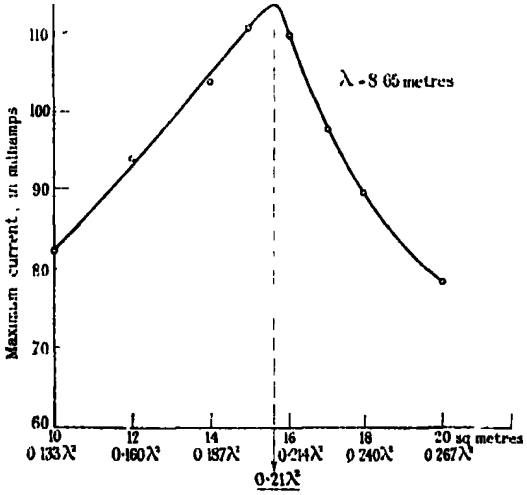

Fig. 9.

The foregoing theory predicted a value lying between 0·15 λ^2 and 0·24 λ^2 depending on the value of the angle γ. If the theory be correct we may conclude from fig. 3 and the data on p. 198 that the value of 0·21 λ^2 corresponds to an angle γ of about 8°. This value of γ is determined by a very indirect method, but is of the same order as the rough preliminary measurement made with a tilting aerial and referred to in Section III. It also lies within the limits of 0° and 15° deduced from the presence of the subsidiary peak on the graph for $H = 7$ in fig. 6.

V. *Conclusion.*

The main principle which has been developed in Section II and tested by the experiments described in Section III may now be summarised. In the same sense that the phase lead due to the capacity of an oscillating circuit may be annulled by an equal phase lag due to the inductance of the circuit with a resulting maximum or resonant circuit current; so a phase lead (or lag) due to the width of a frame aerial may be annulled by an equal phase lag (or lead) due to the height of the frame, with a resulting maximum frame current.

The word "tuning" is invariably used for the first process and therefore it cannot be used for the second process which is entirely different. It appears that a new term is desirable to describe the process of adjusting the dimensions of a frame aerial in order to obtain maximum current. To this end it is tentatively suggested that the word "formatising" (from the Latin *formare*—to form or to shape) be used when referring to this particular process. We may then conveniently speak of a "tuned" and "formatised" frame aerial or of one which has been "tuned" but has not been "formatised." Such a frame would be "tuned" but "deformatised." "Formatisation" may be defined as the process of obtaining maximum frame aerial current by the adjustment of the frame dimensions.

Thus it appears that the resonant current which circulates in a tuned frame aerial under the influence of an electromagnetic wave is not necessarily the maximum current that can be produced by the incident wave. By formatising the frame by a proper adjustment of the height H and the width W the current may be increased to a very much larger value.

The conditions for a tuned formatised frame in the plane of wave propagation are given by the odd solutions of the equations

$$\tan[a(1+\cos\gamma)-\psi] = (a^2-1)/a$$

and

$$\tan[a'(1+\sin\gamma)+\psi] = (a'^2-1)/a',$$

where $a = 2\pi W/\lambda$, $a' = 2\pi H/\lambda$, ψ is any arbitrary phase angle and γ the angle of incidence of the wave. Finally, we conclude that the maximum areas of a tuned formatised frame vary respectively from $0 \cdot 15\ \lambda^2$ and $0 \cdot 50\ \lambda^2$ when $\gamma = 45°$ to $0 \cdot 24\ \lambda^2$ and $0 \cdot 73\ \lambda^2$ when $\gamma = 0°$ and $90°$.

Summary.

(1) To explain certain observed peculiarities in the behaviour of a tuned rectangular frame aerial when influenced by an electromagnetic wave comparable in length with the frame dimensions, the wave is considered to cause a frame current which can be resolved into a "direct" current component due to the primary action of the wave and an "indirect" current component due to the field of the current in adjacent parts of the frame.

This treatment leads to the conclusion that the resultant current is dependent on the dimensions of the frame, on the wave-length and on the angle of incidence of the wave.

(2) A theory is developed from which it is concluded that for each particular height of the frame less than one wave-length there are at least two critical widths for which the frame current will be a maximum; that is, there are at least two critical areas for which the current will be a maximum and any variation of these areas will result in very great decrease of signal strength.

(3) The resonant current which circulates in a tuned frame aerial under the influence of an electromagnetic wave is not necessarily the maximum current that can be produced in the frame by the incident wave. By a proper adjustment of the height and width of the frame the current may be increased to a very much larger value.

(4) The word "formatising," as distinct from "tuning," is suggested as appropriate for describing this process of adjusting the dimensions or form of a frame aerial.

(5) Experiments on 7·54, 8·65 and 8·80 metres were carried out with a tuned frame capable of expanding and contracting in either or both dimensions.

(6) The observed data lead indirectly to a determination of the conductivity of the ground which was found to be about $4 \cdot 4 . 10^8$ e.s.u. for a wave-length of 8·65 metres.

(7) The experimental results show that the maximum frame current only results when the frame is both tuned and formatised. The formatising conditions determined by experiment approximate to the conditions given by the odd solutions of the theoretical equations

$$\tan [a(1 + \cos \gamma) - \psi] = (a^2 - 1)/a$$

and

$$\tan [a'(1 + \sin \gamma) + \psi] = (a'^2 - 1)/a'.$$

I should like to take this opportunity of expressing my thanks to the Board of Scientific and Industrial Research for a grant enabling me to utilise the services of Mr. L. L. K. Honeyball in carrying out the experimental work, and to Mr. Honeyball for the ingenuity he displayed in devising the mechanism of the expanding frame and for the skill he showed in the construction of the short-wave oscillator.

The Formation of Superlattices in Alloys of Iron and Aluminium.

By A. J. Bradley, Ph.D , and A. H. Jay, B.Sc.

(Communicated by W. L. Bragg, F.R.S.—Received December 5, 1931.)

[Plate 5.]

The crystal structures of metallic elements or alloys are built up of individual atoms arranged according to a regular pattern. In the case of a metallic element, such as aluminium, all the atoms being alike, the structure is usually very simple, and all positions are equivalent. In the case of an alloy, geometrical theory would require atoms of different kinds to be sorted out into different sets of positions. For example, in the alloy AlSb, as in NaCl, the atoms as a whole are situated on a simple cubic lattice, but the two sorts of atoms are distributed at alternate positions.

There are many alloys which do not behave according to the geometrical theory, and unlike atoms occupy positions which should strictly be occupied by atoms of identical character. In some cases the atoms are distributed entirely at random, but in others there is a partial approach towards an ordered arrangement. On the whole, each type of atom has its appropriate place in the lattice, but, owing to one element being in excess, it partially takes the place of the other.

This tendency to ordered arrangement is sometimes influenced by the previous heat treatment of the alloy. For example, when prepared in the usual way alloys of gold and copper of whatever composition have their atoms distributed entirely at random. A powder photograph of such an alloy is indistinguishable from a photograph of pure copper or pure gold except for a slight difference in dimensions, and X-ray analysis fails to indicate that two metals are present.

Johansson and Linde* have shown that if CuAu alloys of certain compositions are annealed for several days at about 300° C. the structure slowly changes. Consider, for example, an alloy the composition of which corresponds to the formula Cu_3Au. When first prepared this alloy was face-centred cubic like pure copper or gold and the atoms were distributed at random, but after the above heat treatment it was found that the atoms were regularly arranged. Regarding copper and gold as equivalent, the structure was still face-centred cubic, but a detailed study of the powder photographs showed that the atoms of gold now occupied positions at the corners of a simple cubic lattice. The copper atoms occupied the remaining positions of the face-centred cubic lattice (centres of cube faces). A structure of this kind is usually termed a superlattice (überstruktur).

---

* 'Ann. Physik,' vol. 78, p. 439 (1925).

The present paper describes an example of this phenomenon which presents some novel features, and an attempt has been made to determine the extent to which atoms of different kinds are segregated into different sets of positions.

1. GENERAL ACCOUNT OF X-RAY RESULTS.

An X-ray powder photograph examination has been made of alloys of iron and aluminium containing 0–50 atomic per cent. Al corresponding to the range Fe–FeAl. It has been shown that this portion of the Al-Fe system cannot as formerly be regarded simply as a solid solution phase, but that it has in fact many extremely interesting features.

The peculiarities exhibited by these alloys are of two kinds, namely in lattice spacings and in atomic distribution. A detailed account of the changes in lattice dimensions will be published shortly. The present paper deals with the remarkable changes in the mode of distribution of the iron and aluminium atoms.

Throughout the whole range of solid solutions studied here the atoms are arranged in the body-centred cubic lattice which is characteristic of α iron, and the most prominent lines in the powder photograph are due to this lattice. In addition there is in certain ranges a segregation of the aluminium atoms into definite positions of the lattice resulting in the partial or complete formation of a "superlattice." This superlattice is shown by the appearance on the film of additional lines which cannot be ascribed to the body-centred lattice.

The present paper describes a careful quantitative study of these lines, and throws considerable light on the successive stages by which the superlattice is built up.

Up to 18 atomic per cent. Al the body-centred cubic lattice of α-Fe still exists, aluminium atoms replacing iron atoms at random. Beyond 18 per cent. Al there are differences in the behaviour of quenched and annealed alloys. In the case of the annealed alloys an ordered state is gradually attained as the proportion of Al increases, aluminium and iron atoms being sorted out into definite positions. Alloys quenched from above 600° C. remain in the random state up to 25 per cent. Al. Beyond this point there is a sudden change, and henceforth both annealed and quenched alloys have some measure of ordered arrangement.

There are two main types of structure with ordered arrangement present in these alloys. The first is present only in certain annealed alloys and is most closely attained at the composition Fe_3Al. The second is present in a wide range of both quenched and annealed alloys and in its ideal form corresponds to the formula FeAl.

2. PREPARATION OF ALLOYS.

With the exception of two alloys, all the specimens used in the present research were prepared by melting electrolytic iron and aluminium of 99·96 per cent. purity in a high frequency induction furnace, under a low pressure of hydrogen. The composition of each alloy was checked by chemical analysis, the aluminium, silicon and carbon content being determined. Two alloys (24 per cent. atomic Al and 27·6 per cent. atomic Al) were prepared from materials of a lower degree of purity and were melted in air. On analysis these alloys were found to contain 13·4 per cent. Al, 0·38 per cent. Si and 0·04 per cent. C in one case, and 15·6 per cent. Al, 0·10 per cent. Si and 0·05 per cent. C in the other case. With these exceptions, the silicon content was negligible and the C content was in each case about 0·05 per cent.

After preparation each alloy was allowed to cool in the furnace. It was then heated for 24 hours at 900° C. to promote homogeneity and slowly cooled, and next reduced to powder form in readiness for the X-ray photograph. The alloys are for the most part very tough and only in the case of the alloy with 50 per cent. Al was it possible to crush the specimen into powder; in other cases drillings or filings were obtained. The specimens were in each case homogeneous single phase alloys so that it was possible to separate out the small fragments by sieving without fear of obtaining an unrepresentative specimen. This is necessary in order to produce satisfactory photographs.

Further heat treatment was carried out on the powdered specimens. The drillings, filings or ground materials being in a cold worked state are very responsive to heat-treatment and so a further prolonged heating at high temperatures is not necessary. The alloys were heated up to 750° C. for 1 hour, then either quenched or slowly cooled. Quenching was carried out from both 600° C. and 700° C. The annealing process consisted in slowly cooling the alloy in the furnace. The maximum rate of cooling was about 50° C. per hour, but in the range 600°–450° the rate of cooling was about 30° C. per hour. The temperature was not held at any given point, as we were unaware of the existence of a definite transformation temperature. The results of recent measurements, communicated to us by Dr. C. E. Sykes, show that the conductivity which is greater in the annealed than in the quenched state, is not appreciably affected by slowing up the rate of cooling beyond this point, The alloys are therefore likely to be in a fully annealed condition. The effect of different conditions of annealing is being further studied. The present results merely describe the effect on the alloy of a type of heat treatment which was the same in every case.

3. METHODS.

Powder photographs were taken of the whole series of alloys, in the quenched and annealed states. All the photographs which had extra lines, in addition to the lines for a body-centred cube, were carefully photometered. In order to obtain reliable photometric measurements it was essential to obtain films as perfect as possible. Streaky lines do not give reliable measurements, and it was therefore necessary to sieve the material in order to remove large particles. The sieve used for this purpose was 250 mesh per lineal inch (spaces of 0·005 cm.). The specimen was in addition continuously rotated during the exposure.

In an investigation of this kind, where the number of films is very great, it would be a somewhat lengthy process to measure accurately each line on every film. For not only the practical, but also the arithmetical work involved would be unnecessarily lengthy. It was found to be sufficient to analyse completely the photograph of the structure FeAl and then to use the measured intensities of certain " key " lines on the other films as an index of the extent to which an ordered arrangement had been attained.

The complete analysis was made with an alloy containing 50 per cent. Al, corresponding to the formula FeAl. The film was photometered very carefully, using every possible precaution, and the results so obtained are probably very reliable. The measurements of blackening were taken by means of a Cambridge microphotometer, designed by Dobson.* They were then converted into intensity values by means of a calibration curve, obtained from a series of graduated blackenings added to the film after the exposure of the specimen. To get this blackening scale a rotating sector wheel was used. The intensity measurements were next plotted for various points along the film and an integrated value of the intensity of each line was obtained by determining the area under the curve and above the base line of general blackening.

---

* 'Proc. Roy. Soc.,' A, vol. 104, p. 248 (1923).

The investigation was carried out in the following stages :—

(*a*) A powder photograph of FeAl using Mo Kα radiation, was photometered, fig. 1, Plate 5. The atomic scattering factors of Fe and Al for Mo radiation are known with considerable accuracy. The factor for Al determined experimentally by James, Brindley and Wood* and by Bearden† agrees to within 0·35 unit with that calculated for Hartree's‡ electron distribution in the aluminium atom ; while the factor for iron may be calculated for the Thomas-Fermi electron distribution, as it is known that this distribution gives a good representation in the case of so heavy an element. Using these atomic scattering factors, it is possible to verify from the line intensities that the alloy of composition FeAl has a cæsium chloride structure in which *all* cube corners are occupied by iron atoms and *all* cube centres by aluminium atoms. It is important to ascertain that this segregation of the atoms is complete and not partial, and this necessitated the use of Mo radiation for which the atomic scattering factors are known.

(*b*) A powder photograph of the same alloy FeAl was made with Fe radiation, and photometered, fig. 1, Plate 5. This is necessary *in order that the atomic scattering factor of Fe for Fe radiation may be determined.* This factor is abnormal because the scattered radiation has a wave-length so near that of the iron absorption edge. In a further investigation by Bradley and Hope,§ the FeAl crystal structure is used to examine this effect in greater detail.

The lines corresponding to an even sum of indices (110, 200, 220, 222) have a structure factor $f_{\text{Fe}} + f_{\text{Al}}$, whereas those with an odd sum of indices have a structure factor $f_{\text{Fe}} - f_{\text{Al}}$. The structure factor f_{Al} for iron radiation is not abnormal ; it has the same value as for Mo rays and is accurately known. Hence the measurements of both types of lines on the film enable us to deduce f_{Fe} for iron radiation K_α and K_β.

Certain values of f_{Fe} and f_{Al}, for lines of the FeAl structure, are given in the following table. The values of f_{Fe} for K_β are more influenced by the neighbourhood of the absorption edge than those for K_α. The influence consists in a reduction below the normal value ; this is obvious in the table.

(*c*) In other alloys, varying in composition between pure iron and FeAl our object is an accurate measurement of the extent to which aluminium atoms have replaced iron atoms in an orderly way.

---

* 'Proc. Roy. Soc.,' A, vol. 125, p. 401 (1929).

† 'Phys. Rev.,' vol. 29, p. 20 (1927).

‡ Waller and Hartree, 'Proc. Roy. Soc.,' A, vol. 124, p. 119 (1929).

§ 'Proc. Roy. Soc.,' A, vol. 136, p. 272 (1932).

Table I.—"f" Values for Fe and Al with Fe, K_α and K_β Radiation in FeAl.

(hkl)	(100)	(110)	(111)	(200)	(210)	(211)
$\sin\theta/\lambda$	0·172	0·245	0·298	0·346	0·386	0·424
K_α radiation—						
Fe	18·3	-	13·5	–	11·1	—
Al	9·2		7·4	—	6·3	—
K_β radiation—						
Fe	-	13·2	-	10·2	—	8·3
Al	-	8·1	--	6·8	--	6·0
Mo radiation—						
Fe	19·6	16·8	15·0	13·8	12·7	11·8
Al	9·3	8·2	7·5	6·8	6·3	5·8

The powder photograph of each alloy shows the lines of the cubic body-centred structure, which have values of hkl whose sum is even. Whatever the distribution of Al and Fe atoms amongst the points of this lattice, such reflections have a full contribution due to all atoms working together. Hence *the structure factor for these lines is known.* It depends only on the composition of the alloy and the values of f_{Fe} and f_{Al} which have already been determined.

In addition, lines due to the superlattice appear, fig. 1, Plate 5. They arise from the segregation of the aluminium atoms into favoured positions. The effective structure factors which produce these lines may be measured by comparing their intensities with those of the body-centred lattice, which form a standard.

As explained above, it is only necessary to measure a few lines on each film in order to discover how the aluminium atoms are distributed. In the case of alloys which are a partial approximation towards the FeAl type, for instance, this approximation is indicated by the strength of the lines 100, 111, 210. In measuring their structure factors it is inconvenient and inaccurate to match them against K_α lines due to 110, 200, 211 since these are so very much stronger. We therefore took as standards for calibration the K_β lines with indices 110, 200, 211 which are more nearly of the same intensity as the faint lines due to the superlattice. The "f" values for these standards are given in the table.

For example, suppose it is desired to find the extent to which aluminium atoms in a given alloy have been segregated into positions at cube centres, a process which is complete in the FeAl structure. This can be done by comparing a pair of lines such as K_α 100 and K_β 110. The extent of segregation can be measured by the structure factor $F_{\alpha\,(100)}$, which owes its existence to a difference between cube corners and cube centres. For a random distribution $F_{\alpha\,(100)}$ is zero since cube corners and centres are on the average indistinguishable. For the perfect FeAl structure, $F_{\alpha\,(100)} = f_{Fe} - f_{Al}$, the difference in atomic scattering factors for the (100) reflection and K_α radiation. Let

$F_{\beta\,(110)}$ be the structure factor for the lines whose indices have an even sum; this factor ranges from 2Fe to Fe + Al according to the composition of the alloy. We can write

$$\frac{F_{\alpha\,(100)}}{F_{\beta\,(110)}} = K\sqrt{\frac{I_{\alpha\,(100)}}{I_{\beta\,(110)}}},$$

when $I_{\alpha\,(100)}$, $I_{\beta\,(110)}$ are the photometered intensities of the lines.

The point to note is that K is a constant, for a given pair of lines, throughout the whole series of alloys, and that it depends upon the angles of diffraction of the two lines, upon the number of co-operating planes, and upon the relative strength of K_α and K_β rays. The lattice spacing is so nearly the same throughout the range that the factors depending upon angle vary very slightly, and the other factors are, of course, constant, hence we can measure K for some one alloy (FeAl in this case) and use it for all other alloys. Thus F for a superlattice line can be obtained by comparing its intensity with that of a neighbouring K_β line of the body-centred lattice.

The type of superstructure represented by Fe_3Al gives other lines, but the same process can be carried out. To sum up, the comparison of a few faint superlattice lines with our calibrated standard K_β lines enables us to obtain a quantitative estimate of the extent to which an ordered arrangement has been attained.

4. Alloys of the FeAl Type.*

(A) *Pure FeAl.*

Table II.

Line, Σh^2.	*hkl.*	Int.	θ (obs.).	$\sin^2\theta$.	$\frac{\sin^2\theta}{\Sigma h^2}$.	"*a*" in Å. lattice spacing.
10 β	(310)	m	72·74	0·91197	0·09120	2·9024
8 α_2	(220)	m	70·63	0·88999	0·11125	2·9021
α_1		ms	70·30	0·88637	0·11080	2·9021
8 β	—	w-m	58·68	0·72980	0·09122	2·9021
6 α_2	(211)	s	54·80	0·66772	0·11129	2·9018
α_1		vs	54·63	0·66495	0·11083	2·9019
5 α	(210)	w-m	48·17	0·5552	0·11104	2·901
6 β	—	m	47·73	0·5476	0·09126	2·901
4 α	(200)	s	41·82	0·4446	0·11115	2·900
4 β	—	w-m	37·22	0·3659	0·09147	2·898
3 α	(111)	w-m	35·30	0·3339	0·1113	2·898
2 α	(110)	vvs	28·19	0·2232	0·1116	2·894
2 β	—	s	25·37	0·1836	0·0918	2·893
1 α	(100)	ms	19·55	0·1120	0·1120	2·889
				Value of "*a*" Extrapolated to $\theta = 90°$		2·903

---

* A. Westgren, 'Z. Metallk.,' vol. 11, p. 1 (1930); 'Metallwirtschaft,' vol. 45, p. 919 (1930).

A photograph of the alloy containing 50 per cent. Al taken with Mo radiation is shown in fig. 1, Plate 5. This alloy corresponds exactly to the formula FeAl. The β lines were filtered out by means of a zircon screen, so that the photograph gives only the lines due to the K_α radiation of Mo. It is clear that the reflections fall into two sets, odd lines being on the whole much weaker than even lines. The latter are due to the fundamental body-centred cube, the former to the sorting out of the iron and aluminium atoms. The photograph with Fe radiation is more complicated owing to the presence of β lines. The results of the measurements of this film are shown in Table II.

The results of the intensity measurements for alloys quenched from 600° C. and also from 700° C. are given in Table III and shown graphically in fig. 2.

(B) *Quenched Alloys of the FeAl Type.*

Table III.—Photometer Measurements. Alloys quenched from 600° and 700° C.

Composition atomic per cent. Al.	Intensity ratios. Alloy quenched from 600° C.		Intensity ratios. Alloy quenched from 700° C.	
	$I_{(100)\alpha}/I_{(110)\beta}$.	$I_{(111)\alpha}/I_{(200)\beta}$.	$I_{(100)\alpha}/I_{(110)\beta}$.	$I_{(111)\alpha}/I_{(200)\beta}$.
27·6	0·14	0·25	0·14	0·22
31·2	0·19	0·32	0·18	0·32
34·0	0·24	0·39	0·24	0·43
40·8	0·34	0·59	0·35	0·59
44·6	0·41	0·70	0·47	0·72
50·0	—	– –	0·52	0·91

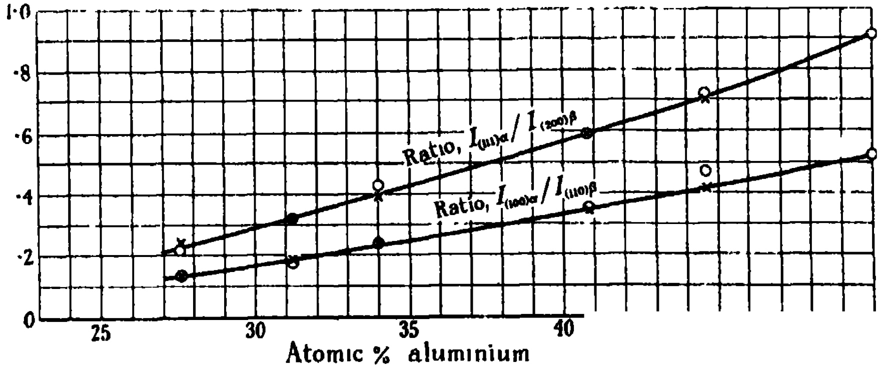

Fig. 2.—Intensity Ratios. ⊙ = quenched 700° C. × = quenched 600° C.

The results are appreciably the same. The table gives the ratios of the intensities of the faint superlattice lines and the β lines of the body-centred cube. In the graph the intensity ratios are plotted against the compositions of the alloys, and it is seen that the intensity values lie on a smooth curve which is virtually a straight line. Values read off from these curves were used to calculate the proportions of the Al and Fe atoms in alloys of various compositions.

(C) *Interpretation of Intensity Curves.*

Deduction of F Values for Odd Reflections.—The CsCl type of structure has two atoms per unit cell. The co-ordinates of the two structurally equivalent positions which may be designated as a and b are :-

a	....	0 0 0
b	....	$\frac{1}{2}$ $\frac{1}{2}$ $\frac{1}{2}$

Let A and B represent the scattering powers of atoms in a and b positions respectively. Then the scattering factor is

$$\mathrm{A} + \mathrm{B}e^{i\phi} = \mathrm{A} + \mathrm{B}\cos(h + k + l)\pi.$$

Reflections are of two kinds :—

Case I. $(h + k + l)$ odd. Expression becomes A — B.

Case II. $(h + k + l)$ even. Expression becomes A + B.

For convenience we shall write :—

$$\mathrm{A} + \mathrm{B} = \mathrm{F}x.$$

$$\mathrm{A} - \mathrm{B} = \mathrm{F}y.$$

The intensity of an even reflection is thus proportional to $\mathrm{F}x^2$, whereas that of an odd reflection is proportional to $\mathrm{F}y^2$. For example,

$$(\mathrm{A} + \mathrm{B})\,(110)\beta = \mathrm{F}_{(110)\,\beta}$$

$$(\mathrm{A} - \mathrm{B})\,(100)\,\alpha = \mathrm{F}_{(100)\,\alpha}.$$

Of the two atoms in the unit cell let the composition be such that a fraction p is aluminium and hence $2 - p$ are iron.

$$\mathrm{F}_{(110)\,\beta} = \{p f_{\mathrm{Al}} + (2 - p) f_{\mathrm{Fe}}\}\,(110)\beta.$$

Knowing p, we can readily calculate $\mathrm{F}_{(110)\,\beta}$. The values for $\mathrm{F}_{(110)\,\beta}$ are given in the second column of Table IV. From the equation

$$\frac{\mathrm{F}_{(100)\,\alpha}}{\mathrm{F}_{(110)\beta}} = \mathrm{K}\sqrt{\frac{\mathrm{I}_{(100)\,\alpha}}{\mathrm{I}_{(110)\,\beta}}},$$

we can then calculate $\mathrm{F}_{(100)\alpha}$ for each alloy. The results are given in column 4.

Table IV.

Composition of alloy. Atomic per cent. Al.	Fx calculated for $(110)\beta$.	Observed ratio, $I_{(100)\alpha} : I_{(110)\beta}$.	Fy for $(100)\,\alpha$ deduced from observations.
50	21·3	0·53	9·1
45	21·8	0·425	8·3
40	22·3	0·335	7·6
35	22·8	0·25	6·7
30	23·3	0·17	5·65
25	23·85	0·11	4·65

The determination of A and B, which are respectively the scattering powers of the atoms in the a and b positions, requires a knowledge of Fx and Fy for the same value of $\sin\theta/\lambda$. We have found Fy for the (100) reflection, $\sin\theta/\lambda = 0\cdot172$. We now require the value of Fx at the same angle. This is easily calculated from the composition of the alloy in the manner previously explained. From Fx and Fy we may then calculate A and B since

$$A = \frac{Fx + Fy}{2} \qquad B = \frac{Fx - Fy}{2}.$$

The values so obtained are given in Table V.

Table V.

Composition of alloy. Atomic per cent. Al.	Fx calculated for (100).	Fy experimental for (100).	A.	B.	Per cent. Al in b position.	Total per cent. Al from atomic composition.
50	27·5	9·1	18·3	9·2	50	50
45	28·4	8·3	18·35	10·03	45·5	45
40	29·3	7·6	18·45	10·85	41	40
35	30·2	6·7	18·45	11·75	36	35
30	31·1	5·65	18·37	12·72	30·5	30
25	32·0	4·65	18·32	13·67	25·5	25

It will be seen from Table V that for the alloy containing 50 per cent. Al, corresponding to the formula FeAl, the values of A and B agree precisely with the "f" values of iron and aluminium for the appropriate value of $\sin\theta/\lambda$, see Table I. This merely serves as a check, since these values were used originally to calculate K. The other results are purely experimental in origin and are extremely interesting. The values of A are constant, within the limits of experiment and agree extremely well with the value (18·3) for pure iron.

This proves conclusively that, for every quenched alloy ranging from 25 per cent. Al to 50 per cent. Al, the position *a* is entirely occupied by iron atoms. As regards B, the values show a gradual increase from 9·2 per cent. for pure FeAl, to 13·67 per cent. corresponding to the composition Fe_3Al. These values may now be used in order to obtain a check on the amount of aluminium in the *b* positions.

Let x represent the fraction of the total number of atoms occupying *b* positions which are Al. Then B, the total scattering power of all atoms occupying *b* positions, is given by:—

$$B = xf_{Al} + (1 - x)f_{Fe}$$

where f_{Al} is the scattering power of an Al atom and f_{Fe} is the scattering power of an Fe atom. Hence

$$x = \frac{f_{Fe} - B}{f_{Fe} - f_{Al}}.$$

The proportion of Al so calculated is expressed in Table V as a percentage of the total composition of the alloy. It will be seen that within the limits of experimental error the amount of aluminium in *b* positions agrees with the total Al content.

(D) *Discussion of Results for Quenched Alloys of the FeAl Type.*

The results show without ambiguity that at a point just beyond 25 per cent. Al, *a* atoms are all iron and *b* atoms are half iron and half aluminium. Further, between this composition and that corresponding to 50 per cent. Al, the addition of aluminium occurs by a simple replacement of the iron atoms in the *b* positions by aluminium atoms, until at 50 per cent. all the *b* atoms are aluminium. The *a* atoms are entirely unaffected by the addition of aluminium.

The extremely simple nature of the solution and the excellent agreement of the experimental data provide a good check on the soundness of the method, and suggest that satisfactory results may be obtained in the more complicated problem of the annealed alloys of the Fe_3Al type.

5. THE Fe_3Al TYPE OF STRUCTURE.

A. *Experimental—Annealed Alloys.*

The series of annealed alloys from 24 per cent. Al to 50 per cent. Al gives photographs with extra lines, which indicate that in each case there is some measure of ordered arrangement. From 40 per cent. Al to 50 per cent. Al these extra lines may be interpreted in exactly the same way as in the case of the quenched alloys, but from 24 per cent. Al to 35 per cent. Al it is necessary to assume that the size of the unit cell is increased.

Table VI.—Fe_3Al, 25 per cent. Al annealed.

Line Σh^2.	Indices.	Int.	θ (obs.).	$\sin^2\theta$.	$\frac{\sin^2\theta}{\Sigma h^2}$.	Lattice spacing in Å.
$40\ \beta$	(620)	m	73·52	0·91952	0·022988	5·7810
$32\ \alpha_2$	(440)	m	71·33	0·89749	0·028047	5·7800
$32\ \alpha_1$		ms	70·96	0·89360	0·027925	5·7808
$27\ \alpha$	(511) (333)	vw	60 34	0·75519	0·02797	5·780
$32\ \beta$	—	w-m	59 07	0·73572	0·022991	5·7806
$24\ \alpha_2$	(422)	s	55·14	0·67329	0·028054	5·7794
$24\ \alpha_1$		vs	54·95	0·67020	0·027925	5·7808
$20\ \alpha$	(420)	vvw	48·44	0 5596	0·02798	—
$24\ \beta$	—	m	47 99	0·5521	0·02300	—
$19\ \alpha$	(331)	vvw	46·84	0·5318	0·02798	—
$16\ \alpha$	(400)	s	42 01	0·4479	0·02799	—
$16\ \beta$	—	w-m	37·38	0·3686	0·02304	—
$12\ \alpha$	(222)	vvw	35·44	0 3362	0·02802	—
$11\ \alpha$	(311)	vw	33·72	0·3082	0·02801	
$8\ \alpha$	(220)	vvs	28·27	0·2243	0·02804	—
$8\ \beta$	—	s	25·44	0·1845	0·02307	—
$4\ \alpha$	(200)	w-m	19·57	0·1122	0·02805	
$3\ \alpha$	(111)	m	16·86	0·0841	0·02804	—

This will be seen from Table VI, which gives the lines for an alloy containing 25 per cent. Al, a composition which corresponds closely to the formula Fe_3Al.* The new unit cell consists of eight body-centred cubes placed side by side, see drawing, fig. 3.

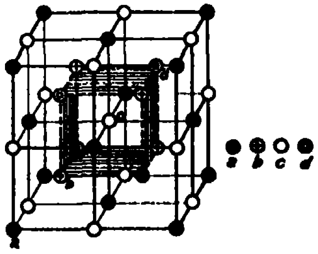

FIG. 3.—Fe_3Al Type of Structure.

In this way the length of the cube edge is doubled. The larger unit is a face-centred cube, since it gives only those reflections for which the indices *h*, *k*, *l*, are either all odd or all even. Since there are 16 atoms in the new unit cube it is clear that they must fall into four sets of face-centred cubic positions. These sets will be distinguished as *a*, *b*, *c* and *d* positions. The drawing shows *a*, *b*, *c*, *d* atoms differently shaded.

---

* For Cu_3Al, E. Persson, 'Z. Physik,' vol. 57, p. 115 (1929), and Fe_3Si, G. Phragmen, 'Stahl und Eisen,' vol. 45, p. 299 (1925).

A remarkable feature of the photographs of the annealed alloys is the way in which the intensities of the extra lines vary from one specimen to another. This variation is readily visible to the eye, and makes the photometer measurement of the photographs of the annealed alloys even more interesting than those of the quenched alloys. The details of these measurements are shown in Table VII. It will be seen that the extra lines fall into two series, which behave quite differently. One series is present throughout the range, the intensities gradually increasing as the aluminium content increases. This includes lines (200) and (222). If they alone were present the unit cell need not be doubled, since they correspond to planes (100), (111) of the simple cell. The other series includes planes (111) and (311), which cannot be explained by the simple cell. The intensities of this series increase to a maximum with increasing aluminium content and then steadily diminish until finally they disappear at 40 per cent. Al, when every observed reflection can again be ascribed to the simple cell. The results are shown graphically in figs. 4 and 5.

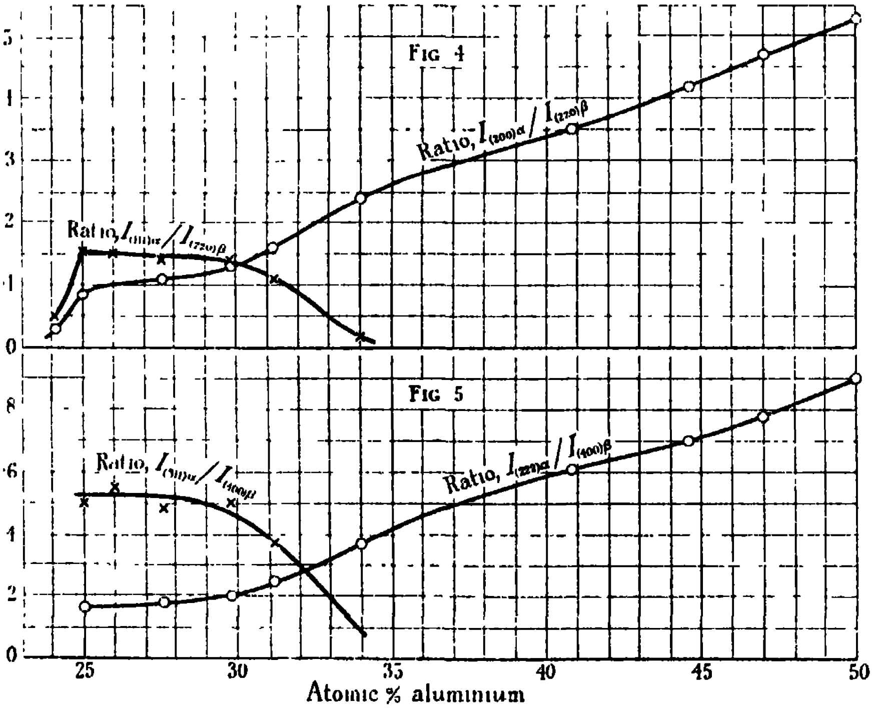

FIGS. 4 and 5.—Intensity Ratios of Annealed Alloys.

Table VII.—Photometer Measurements. Annealed Alloys.

Composition. Atomic per cent. Al.	Intensity ratios.			
	$I_{(111)\alpha}/I_{(220)\beta}$.	$I_{(200)\alpha}/I_{(220)\beta}$.	$I_{(311)\alpha}/I_{(400)\beta}$.	$I_{(222)\alpha}/I_{(400)\beta}$.
24·1	0·05	0·03	—	—
25·0	0·155	0·085	0·50	0·16
26·0	0·15	—	0·55	—
27·6	0·14	0·11	0·48	0·18
29·8	0·14	0·13	0·50	0·20
31·2	0·11	0·16	0·37	0·25
34·0	0·02	0·24	—	0·37
40·8	—	0·35	—	0·61
44·6	—	0·42	—	0·70
47·0	—	0·47	—	0·78
50·0	—	0·53	—	0·90

B. *Interpretation of the Intensity Changes.*

(i) *Formulæ for Structure Factors.*—In order to explain the presence of all the extra lines on the X-ray photographs of the annealed alloys, we have in some cases to assume the existence of a larger unit containing 16 atoms per unit cell. These atoms fall into four sets of structurally equivalent positions. The co-ordinates are :—

a	....	0 0 0	½ 0 ½	0 ½ ½	½ ½ 0
b	....	¼ ¼ ¼	¾ ¼ ¾	¼ ¾ ¾	¾ ¾ ¼
c	....	½ ½ ½	0 ½ 0	½ 0 0	0 0 ½
d	....	¾ ¾ ¾	¼ ¾ ¼	¾ ¼ ¼	¼ ¼ ¾

the structure factor for the unit cell is therefore

$$\begin{aligned}F &= \Sigma A e i\phi \\ &= \{1 + \Sigma e^{\pi i(h+k)}\}\{A + Be^{\frac{\pi i(h+k+l)}{2}} + Ce^{\pi i(h+k+l)} + De^{\frac{3\pi i(h+k+l)}{2}}\},\end{aligned}$$

where A, B, C, D, are the mean atomic scattering factors for positions *a*, *b*, *c*, *d*, respectively.

It can be shown that the above formula leads to three special cases, and that no other reflections may occur.

Case I. *h*, *k*, *l*, all odd.

This case includes—

Σh^2	....	3	11	19
hkl	....	(111)	(311)	(331)

$$F = 4\{A - C) \pm i\,(B - D)\},$$

where $i = \sqrt{-1}$.

Case II. h, k, l, all even, $\frac{h+k+l}{2}$ odd.

This case includes—

Σh^2	....	4	12	20
hkl	....	(200)	(222)	(420)

$$F = 4\,\{(A - B) + (C - D)\}.$$

Case III. $\frac{h+k+l}{2}$ even.

This case includes—

Σh^2	....	8	16	24
hkl	....	(220)	(400)	(422)

$$F = 4\,(A + B + C + D).$$

In order to make the structure factors comparable with those of the FeAl type, it is more convenient to refer F to the smaller unit, so that we have :—

(1) h, k, l, all odd $\quad F = \tfrac{1}{2}\,\{(A - C) \pm i(B - D)\}$

(2) $\frac{h+k+l}{2}$ odd $\quad F = \tfrac{1}{2}\,\{(A - B) + (C - D)\}$

(3) $\frac{h+k+l}{2}$ even $\quad F = \tfrac{1}{2}\,(A + B + C + D).$

We shall, in the first place, confine our attention to reflections of types (2) and (3) in order to fix the allotment of atoms as between positions *a* and *c* on the one hand and *b* and *d* on the other hand. Afterwards we shall use reflections of class (1), in order to distinguish atoms in *a* from atoms in *c*, and atoms in *b* from atoms in *d*.

(ii) *Determination of the Relative Amounts of Iron and Aluminium in positions* (*a*, *c*) *and* (*b*, *d*).—The alloys which exhibit the Fe_3Al type of structure range from 24 per cent. to 35 per cent. Al. The relative intensities of lines (200) α and (220) β can be read off from the curve given in fig. 4 for the annealed alloys. These values are used in order to determine the F values for the (200) planes, in the manner previously described.

The expression

$$F_y = K\,F_x\sqrt{\alpha/\beta}$$

is used for this purpose as already shown, and K again has the value 0·587. The results are shown in Table VIII.

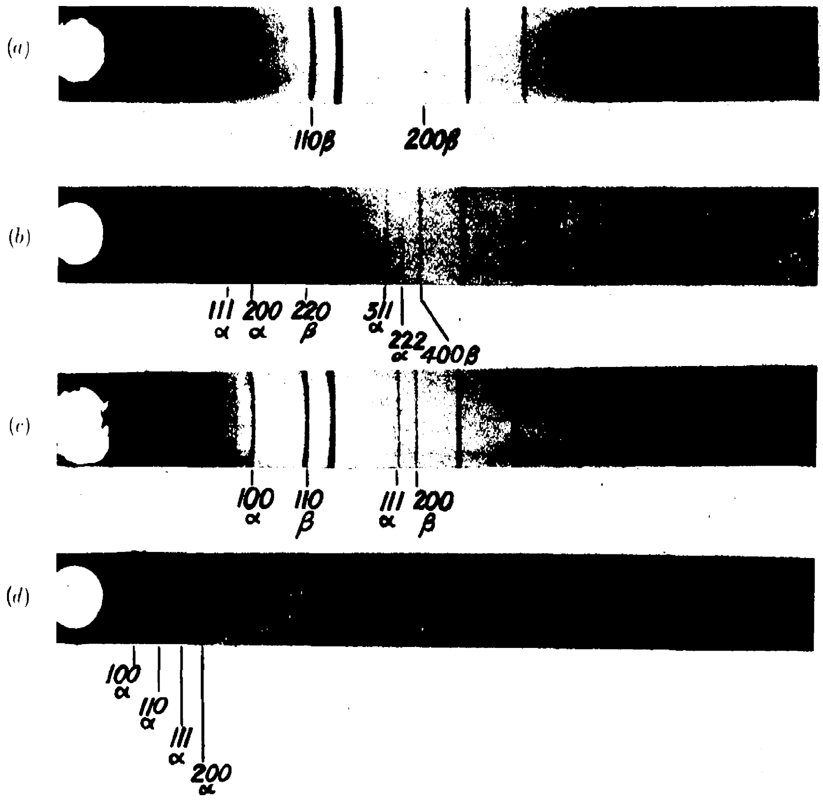

Fig. 1.—X-Ray Powder Photographs of Iron-Aluminium Alloys.

(*a*) Pure Iron. Fe Kα and Kβ radiation.
(*b*) Fe_3Al Type. Fe Kα and Kβ radiation.
(*c*) FeAl Type. Fe Kα and Kβ radiation.
(*d*) FeAl Type. Mo Kα radiation.

(*Facing p.* 224.)

Table VIII.

Atomic composition, per cent Al.	Fx calculated for $(220)_\beta$.	Observed ratio. $(200)_a : (220)_\beta$.	Fy for $(200)_a$ deduced from observations.
24	23·9	0·03	2·4
25	23·85	0·085	4·08
30	23·34	0·14	5·12
35	22·83	0·25	6·7

The scattering powers of the (*a*, *c*) and (*b*, *d*) positions are found by substituting the values of Fx and Fy at the same value of sin θ/λ, in the expressions

$$A + C = \frac{Fx + Fy}{2}$$

$$B + D = \frac{Fx - Fy}{2}$$

We arbitrarily select the position *b* as containing the most aluminium atoms. The values of (A + C) and (B + D) so found are given in the following table :—

Table IX.

Composition of alloy. Atomic per cent. Al.	Fx calculated for (200).	Fy experimental for (200).	A + C.	B + D.	Per cent. Al in *a*, *c* positions.	Per cent. Al in *b*, *d*, positions.
24	32·1	2·4	17·25	14·85	5·5	19
25	32·0	4·08	18·04	13·96	1·5	23·5
30	31·1	5·12	18·11	12·99	1·0	29
35	30·2	6·7	18·45	11·75	0·0	35·5

The values of A + C are seen to be less than the value for pure iron (18·3) in the case of the first three alloys. This indicates that *a* and *c* positions are not entirely filled by iron atoms. These positions correspond to *a* positions in the simpler structure of the quenched alloys. In that case, the value of A agreed to within 0·1 of the value of "*f*" for pure iron (18·3). The close agreement was taken as proof that no aluminium atoms occupied *a* positions. For the annealed alloys, on the contrary, the suggestion is that *a* and *c* positions are not entirely filled by iron atoms, except at higher Al contents, and the question arises whether the difference might be explained by the presence of greater experimental errors in the case of the annealed alloys. But it seems unlikely that experimental errors should be all in one direction in the case of the annealed alloys, and so much greater than in the case of the quenched alloys (see figs. 4 and 5). It therefore seems more probable that the difference is a genuine effect, which may be explained by an imperfect segregation of the aluminium atoms from (*a*, *c*) positions.

Using the values deduced from (A + C) and (B + D) the mean atomic scattering factors of the (*a*, *c*) and (*b*, *d*) groups, it is possible to calculate the mode of distribution of the atoms in these groups.

The formula is

$$x = \frac{f_{\mathrm{Fe}} - (\mathrm{A} + \mathrm{C})}{f_{\mathrm{Fe}} - f_{\mathrm{Al}}}$$

where x is the fraction of the atoms in *a* and *c* which are aluminium, f_{Fe}, f_{Al} are the scattering powers of iron and aluminium and (A + C) is the total scattering power of all atoms in (*a*, *c*) positions. A similar formula applies to the (*b*, *d*) atoms.

The results of these calculations are given in Table IX. This table gives the amounts of aluminium in (*a*, *c*) and (*b*, *d*) positions respectively. The sum of these values is, of course, equal to the total Al content of the alloy as given in the first column of the table.

It will be seen from Table IX that, except for the alloy containing 24 per cent. Al, the amount of aluminium in the (*a*, *c*) positions is very small, indicating that nearly all the aluminium has segregated into positions (*b*, *d*). The values found for the alloy containing 24 per cent. Al are particularly interesting. It may be seen from the films, that the extra lines which are produced by the segregation of the atoms, are far stronger on the photograph of the 25 per cent. alloy than on that of the 24 per cent. alloy. Yet when the results are worked out quantitatively we see that even in the case of the 24 per cent. alloy, more than 75 per cent. of the aluminium atoms are placed in (*b*, *d*) positions. This shows that a visual inspection alone is likely to prove misleading, and emphasises the importance of accurate quantitative results.

(iii) *Determination of the Relative Amounts of Iron and Aluminium in each of the positions a, b, c, d.*—So far we have made no attempt to distinguish *a* atoms from *c* atoms, or *b* atoms from *d* atoms. For this purpose we need to consider the data from lines with odd indices. The intensity data have already been given in Table VII, but in order to make use of the values there given we must first deduce from them the values of F*y*, which is in this case the structure factor for a plane with odd indices. This can be done as before, using the formula

$$\frac{Fy}{Fx} = K\sqrt{\frac{I_\alpha}{I_\beta}},$$

Fx has the same value as before but K is different.

The determination of K is not so simple as in the previous example. There are no experimental data from the FeAl alloy which are applicable, since odd reflections of the large cube do not occur in the FeAl type of structure. We may however deduce a value of K by indirect means. From a consideration of the θ factor, absorption factor and number of co-operating planes for FeAl we calculate the ratio $\alpha : \beta$ of the $(111)\alpha$ reflection to the $(220)\beta$ reflection, for a fictitious structure factor equal to $(f_{Fe} - f_{Al})$. The ratio $\alpha : \beta$ so calculated may then be used to calculate K provided that we put $Fy = (f_{Fe} - f_{Al})$. The values of K so found were 0·435 for $(111)\alpha$, and $(220)\beta$, and 0·219 for $(311)\alpha$ and $(400)\beta$. Substituting these values of K in the above formula, we may now deduce the value of Fy for any given composition. Values so obtained are given in Table X.

Table X.

Composition Atomic per cent. Al.	Fx calculated for $(220)\beta$.	K calculated for $(111)\alpha$, $(220)\beta$.	Observed ratio $(111)\alpha : (220)\beta$.	Fy for $(111)\alpha$ deduced from observations.
(1) 24	23·9	0·435	0·05	2·3
25	23·85	0·435	0·155	4·1
30	23·34	0·435	0·13	3·65
35	22·83	0·435	0·02	1·4

Composition. Atomic per cent. Al.	Fx calculated for $(400)\beta$.	K calculated for $(311)\alpha$, $(400)\beta$.	Observed ratio $(311)\alpha : (400)\beta$.	Fy for $(311)\alpha$ deduced from observations.
(2) 25	18·7	0·219	0·525	2·97
30	18·36	0·219	0·45	2·7

The results given in Table IX have shown that the amount of aluminium in the (a, c) positions is small compared with that in the (b, d) positions. Since the intensity of lines of odd indices depends on the expression

$$(A - C)^2 + (B - D)^2$$

it is clear that the small amount of aluminium in a and c positions has no appreciable effect on the intensities of these lines. Thus we may make use of the intensities of lines of odd indices in order to fix the atomic distribution in *b* and *d* positions, without reference to positions *a* and *c*. We may therefore write

$$Fy \mathrel{\hat{=}} (B - D).$$

In order to evaluate B and D separately we require to know the value of (B + D), which we may write F*z*. It is necessary to calculate the value of F*z* for the same value of $\sin\theta/\lambda$ as F*y*. We then have

$$B = \frac{Fz + Fy}{2}, \qquad D = \frac{Fz - Fy}{2}$$

Table XI gives the values of F*z* calculated from the total composition of *b* and *d* groups as already determined, and the values of B and D calculated from F*z* and F*y*.

Table XI.

Composition Atomic per cent. Al.	Reflecting plane.	F*z* calculated.	F*y* deduced from observations.	D.	B.	Aluminium content of	
						d positions.	*b* positions.
						per cent.	per cent.
24	(111) *a*	15·3	2·3	8·8	6·5	3·5	15·5
25	(111) *a*	14·5	4·1	9·3	5·2	0·75	23
	(311) *a*	10·9	2·97	6·93	3·95	0·5	23
30	(111) *a*	13·55	3·65	8·6	4·95	4·5	24·25
	(311) *a*	10·25	2·7	6·47	3·78	4·0	24·75
34	(111) *a*	12·55	1·4	6·97	5·57	13·0	21·0

From the scattering factors B and D it is possible to calculate the aluminium content of positions *b* and *d* individually, in the manner described previously. The result of this determination is given in the last two columns of Table XI. The results, as in previous tables, are expressed as percentages of the total atomic composition of the alloy, and each position contains 25 per cent. of the total number of atoms in the alloy.

The complete atomic distribution is given in Table XII. In order to fix the distribution in groups *a* and *c* an assumption must be made which cannot be tested experimentally. The most reasonable assumption is that the aluminium atoms are equally divided between groups *a* and *c*. The structure is in this case holohedral, with centres of symmetry at B and D.

Table XII.—Atomic Distribution in Alloys of the Type Fe_3Al.

Atomic per cent. Al.	Percentage distribution of aluminium atoms.			
	a.	*b.*	*c.*	*d.*
24	2·75	15·5	2·75	3·5
25	0·75	23 0	0·75	0·5
30	0·5	24·5	0·5	4·5
34	0·0	21·0	0·0	13·0

C. *Discussion of the Results for the Annealed Alloys of the Fe_3Al Type.*

The results indicate that up to 25 per cent. Al the majority of the aluminium atoms go into the *b* position, while the remainder are distributed at random in *a, c, d* positions. In alloys between 25 per cent. Al and 30 per cent. Al the *b* position becomes gradually more saturated with aluminium atoms, while the remainder of the aluminium atoms go more and more into the *d* position. Alloys with higher aluminium content have no aluminium in *a* and *c* positions, but *b* and *d* gradually get more equal in composition until when equality is attained between the aluminium contents of *b* and *d*, there ceases to be any difference between annealed and quenched alloys.

6. GRAPHICAL EXPRESSION OF RESULTS.

The atomic distribution found for alloys of the Fe_3Al type is given in Table XII. The results for alloys of the FeAl type have not been tabulated, but a complete picture of the atomic distribution for all compositions for both annealed and quenched alloys is given by the graphs of atomic distribution in fig. 6. Here the percentage of aluminium atoms found in each of the four structurally equivalent positions of the Fe_3Al type is plotted against the percentage composition of the alloy.

For the quenched alloys and the annealed alloys other than those of the Fe_3Al type, there are strictly only two sets of positions *a* and *b*; *a* atoms may be regarded as corner atoms and *b* atoms as centre atoms of a unit cube. However, in order to make the results comparable with those from the Fe_3Al type, it is advantageous to refer them all to the larger unit containing 16 atoms, fig. 3. In passing along a cube diagonal in a given direction one encounters in succession *a, b, c, d* atoms. In the simpler structure *a* and *c* are of the same kind, as are also *b* and *d*.

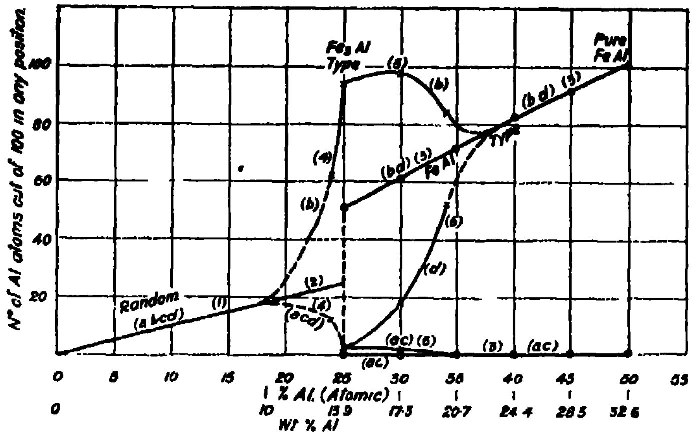

Between 18 atomic % Al & 40 atomic % Al the straight lines refer to quenched alloys only & the curved lines to annealed alloys only. In the other part of the diagram the data refers to both quenched & annealed alloys

FIG. 6.—Distribution of Aluminium Atoms between four positions *a, b, c, d,* of fig. 3.

The curves of atomic distribution are divided into a number of well-marked portions :—

A. *Annealed and Quenched Alloys.*

0 to 18·5 per cent. Al.

In this range the iron and aluminium atoms are distributed at random, so that the aluminium contents of *a, b, c, d* are equal. Hence the distribution curve of the aluminium atoms is represented by a single straight line for both quenched and annealed alloys. This line is common to all four positions.

B. *Alloys Quenched from* 600° *and* 700° *C.*

18·5 per cent. to 25 per cent. Al.

The atomic distribution is still random. The curve B is a continuation of A.

C. *Quenched from* 600° *and* 700° *C.*

25 per cent. to 50 per cent. Al.

The atoms are partially arranged throughout this region. There is an abrupt transition from the random arrangement at 25 per cent. Al, which is represented by the vertical line showing the point at which line B splits up into two branches. The lower branch of C represents the fact that *a* and *c* positions are now solely occupied by iron atoms, while the upper branch shows that the amount of aluminium in *b* and *d* positions steadily increases, until every *b* and *d* position is occupied by aluminium at a composition corresponding to the formula FeAl.

D. *Alloys Annealed by Slow Cooling.*

18·5 per cent. to 25 per cent. Al.

At some point the random distribution which exists up to 18 per cent. Al begins to change over to an ordered arrangement. This process does not take place suddenly like the change in the quenched alloys at 25 per cent., but it is difficult to say precisely where it begins, as the intensities of the extra lines are extremely faint until the arrangement is nearly complete. Certainly at 24 per cent. Al the process is well under way, and in view of the lattice spacing data, which we hope to publish later, it is not likely that it begins before 18 per cent. Al. Whether the change to an ordered arrangement begins gradually at 18 per cent. Al or more suddenly at, say, 22 per cent., we cannot tell, but the lattice spacing data suggest that the former is more likely, and we have therefore indicated this possibility by dotted lines. These lines indicate that the bulk of the aluminium content is being sorted out into position *b*, the amount of aluminium in *a*, *c*, *d* gradually sinking, until at the composition corresponding to Fe_3Al there is an almost perfect atomic arrangement. 23 out of 25 aluminium atoms are sorted into *b* positions, leaving only 2 Al atoms distributed between *a*, *c* and *d* positions.

E. *Annealed Alloys.*

25 per cent. to 50 per cent. Al.

The amount of Al in the *b* position slowly rises to a maximum at about 30 per cent. Al. when almost all the *b* positions are filled by Al. Simultaneously the amount of Al in position *d* increases rapidly. This increase continues still more rapidly up to beyond 35 per cent.Al at the expense of the Al content of the other three positions. The Al in positions *a* and *c* gradually sinks to zero, while that in position *b* falls slowly towards the value of the Al in position *d*. Ultimately, somewhere between 35 per cent. Al and 40 per cent. Al, the curves for positions *b* and *d* come together, and merge into a single curve identical with that for the quenched alloys in this range.

SUMMARY.

(1) A quantitative examination has been made of the intensities of the lines of a series of powder photographs of alloys of iron and aluminium in the range Fe — FeAl.

(2) All the alloy structures are primarily based on a simple body-centred cubic lattice like that of α iron, but a detailed examination of alloys in the annealed and quenched states gave widely differing results.

(3) Alloys quenched from 600° C. and above show a random distribution of atoms up to 25 atomic per cent. Al. Between 25 per cent. and 26 per cent. Al there is an abrupt change in structure, and cube centres differ in composition from cube corners. The intensity measurements show that in the quenched alloys with ordered arrangement one set of positions is occupied only by iron atoms, but the other set contains iron and aluminium atoms in varying proportions depending on the alloy composition.

(4) Annealed alloys with less than 18 per cent. Al have a random distribution, and from 40 per cent. to 50 per cent. Al they have the FeAl type of structure exactly like the quenched alloys in this range. At intermediate compositions a new type of structure appears which is of the type Fe_3Al.

(5) In the Fe_3Al arrangement the Al atoms lie on a face-centred cubic lattice forming a superlattice with dimensions twice as great as those of the small body-centred cube.

(6) Intensity measurements have been used in order to follow out in a detailed manner the process of the building up and decay of the Fe_3Al structure. There is no precise composition at which the Fe_3Al structure can be said to begin or end, and the structure is not completely realised even at the theoretical composition.

Our thanks are due particularly to Dr. C. Sykes, of Research Department, Metropolitan-Vickers Electrical Company, Ltd., for drawing our attention to the anomalies which he had found in the physical properties of the iron aluminium system, and for suggesting that an X-ray investigation of the crystal structure of this system would show corresponding anomalies in the lattice.

Our thanks are also due to the British & Dominions Feralloy Company, Ltd., for supplying us with specially prepared alloys of iron and aluminium, which enabled us to carry out the work and for permission to publish it. We thank Captain J. W. Bampfylde of the above Company for analysing the samples used.

One of us (A.J.B.) has also to thank Mr. A. P. M. Fleming, C.B.E., Director-Manager, Research and Education Departments, for his interest and encouragement in the work and for permission to publish it.

We are indebted to Professor W. L. Bragg, F.R.S., for his kind interest in the work, which was carried out in the Physical Laboratories of the University of Manchester. One of us (A.H.J.) was in receipt of a grant from the Department of Scientific and Industrial Research.

On the Nature of X-Rays.

By Jarl A. Wasastjerna, Helsingfors University.

(Communicated by W. L. Bragg, F.R.S.—Received December 8, 1931.)

§ 1. Einstein's* statistical-thermodynamic calculations of the random variations of the radiation density constitute the ground upon which the light quantum hypothesis was originally based. According to these calculations such a variation of the radiation energy prevails—superposed above the fluctuations caused by the interferences calculated according to the classical theory—as if the radiation consisted of mutually independently mobile quanta $h\nu$ of energy. According to Einstein, Maxwell's theory correctly renders mean time values, which alone have been directly observable, as proved by the complete agreement between theory and experiment in optics; but Maxwell's theory leads to laws respecting the thermic properties of radiation which are incompatible with the entropy-probability relation. After the wave-mechanical theory of de Broglie and Schrödinger had been generally accepted, the idea concerning the statistical character of the wave-field—already presented by Einstein in 1905—has, of course, been taken up again by Born in a more general way.

As is well known, Bohr and Heisenberg have tried to conquer the difficulties to which the radiation theory has led by a radical change in our conception of energy.

According to Bohr every idea which we can form of the radiation phenomenon consists only of a construction which in a more or less convenient way summarises our experiences regarding the statistical connection between certain real elementary processes, separated from each other in regard to space as well as time. We can only state that mutually linked elementary processes take place, whereas the real linking mechanism cannot as a matter of fact be brought into concordance with our conception of space and time. Bohr's conception agrees closely with a way of putting the matter, suggested by Ritz amongst others, with retarded functions, and the same objections may be raised in both cases. Thus, considered philosophically, in Bohr's case all problems connected with the nature of the radiation are eliminated as meaningless but yet, on account of the statistical, irrational linking between the elementary processes, considered in Bohr's theory, that theory leads to the same variations —possible to state in principle—as Einstein's light quantum hypothesis.

---

* A. Einstein, 'Ann. Physik,' vol. 17, p. 132 (1905); vol. 20, p. 199 (1906); 'Phys., Z.,' vol. 10, p. 185 (1909); vol. 10, p. 817 (1909).

Considering how important for our entire present mode of physical reasoning is the conception of a propagation of energy with definite velocity, it appears as if it were most practical, in any case provisionally, to sum up the experimental results by assuming localisation of energy as to space and time.* This will give us a clear idea of the position held by the observed phenomena in the entire complex, affected by the Bohr and Heisenberg theory. At the same time this will also, as it were, automatically allow us later on to adopt without difficulty an interpretation compatible with Bohr's standpoint.

Thus we will start by assuming that the energy is actually propagated with definite velocity from point to point in the field of radiation. In other respects the radiation mechanism may be considered as unknown.

§ 2. When the intensity of a radioactive α- or β-radiation is measured by the ionisation produced in an absorbing gas, we know that certain probability variations occur, that is to say the Schweidler variations, which are characteristic of the radioactive disintegration processes, and simultaneously exhibit the corpuscular nature of the α- and β-radiation. These variations, which are closely related to the density variations, according to Einstein characteristic of black body radiation, have been established by Meyer and Regener,† Kohlrausch,‡ and Geiger,§ and they have been carefully investigated by Ernst,‖ Muszkat and Wertenstein¶ and by Borman.** The Schweidler variations have been studied by means of various differential methods, the principle of which may be applied likewise when investigating the variations which, according to the light quantum hypothesis, are to be expected in the case of the ionisation effects caused by X-rays.

Similar experiments (for γ-rays) were proposed by v. Schweidler†† as early as 1910 and they have actually been carried out by E. Meyer,‡‡ Laby and

---

* J. A. Wasastjerna, 'Soc. Sci. fenn. Comm. Phys.-Math.,' vol. 5, No. 19 (1930).

† E. Meyer and E. Regener, 'Verh. deuts. phys. Ges.,' vol. 10, p. 1 (1908); 'Ann. Physik,' vol. 25, p. 757 (1908).

‡ K. W. F. Kohlrausch, 'SitzBer. Akad. Wiss. Wien,' vol. 115, p. 673 (1906).

§ H. Geiger, 'Phil. Mag.,' vol. 15, p. 539 (1908).

‖ A. Ernst, 'Ann. Physik,' vol. 48, p. 877 (1915).

¶ A. Muszkat and L. Wertenstein, 'J. Phys. Radium,' vol. 2, p. 119 (1921).

** E. Borman, 'SitzBer. Akad. Wiss. Wien,' vol. 127, p. 2347 (1918).

†† 'Phys. Z.,' vol. 11, p. 225 and p. 614 (1910).

‡‡ 'Ber. deuts. phys. Ges.,' vol. 32, p. 647 (1910); 'Jahrb. Rad. Elektr.,' vol. 7, p. 279 (1910); 'Phys. Z.,' vol. 11, p. 1022 (1910); 'Phys. Z.,' vol. 13, p. 73 and p. 253 (1912); 'Ann. Physik,' vol. 37, p. 700 (1912).

Burbidge,[*] and Burbidge.[†] These experiments, which have been discussed by Campbell[‡] and Buchwald[§] did not yield any unambiguous results, amongst other reasons because the random variation of the ionisation effect of one single ray in this case by far exceeded the variation of the number of γ-rays passing the diaphragm. Analogous experiments with X-rays (Campbell) were abandoned on account of the great experimental difficulties involved.

§ 3. In the laboratory for applied physics at the Helsingfors University detailed investigations[||] were carried out during the years 1928–1930 into the variations which are characteristic of the radiation emitted from the anticathode in an X-ray tube. Further, the variations of the intensity of a radiation which had traversed an absorbing layer were investigated, as well as the corresponding variations of a beam formed by interference.

The experimental arrangement was as follows: A Coolidge tube was operated by means of a high voltage battery comprising 21,600 cells. The radiation energy within a given solid angle was measured by means of ionisation. The ionisation current was led to a direct current amplifier, worked by means of electron valves, constructed for the purpose. The amplifying factor was $7 \cdot 75 \, . \, 10^6$. The amplified current was registered photographically by means of a mirror galvanometer of the Deprez-d'Arsonval type. The film, 50 cm. wide, was carried forward at a speed of 1 cm. per second.

In almost all the experiments a differential method was applied. Two ionisation chambers, filled with a strongly absorbing gas (CH_3Br) were subjected to radiation. The results obtained may be summarised as follows :—

The radiation energy absorbed during the time Δt causes a mean ionisation Q which is subject to random variations ΔQ. The variations ΔQ follow the Gauss law of error. The amount of the mean square variation $\overline{(\Delta Q)^2}$ is, independently of the length of the time interval, given by the equation

$$\overline{(\Delta Q)^2}/Q = 0 \cdot 83 \times 10^{-16} \text{ Coulombs.} \qquad (1)$$

The variations cannot be referred to variations in the intensity of the total radiation nor can they emanate from variations in the position of the focal spot of the cathode rays. Besides, the variations ΔQ, occurring simultaneously in both ionisation chambers, are quite independent of each other. (The mean square variation is additive.)

---

[*] T. H. Laby and P. W. Burbidge, 'Nature,' vol. 87, p. 144 (1911); 'Proc. Roy. Soc.,' A, vol. 86, p. 333 (1912)

[†] P. W. Burbidge, 'Proc. Roy. Soc.,' A, vol. 89, p. 45 (1913).

[‡] N. R. Campbell, 'Phys. Z.,' vol. 11, p. 826 (1910); vol. 13, p. 73 (1912).

[§] E. Buchwald, 'Ann. Physik,' vol. 39, p. 41 (1912).

[||] J. A. Wasastjerna, 'Acta. Soc. Sci. fenn. nova Serie,' A, vol. 1, No. 7 (1928), and vol. 2, No. 1 (1930).

If the energy of the radiation absorbed per time unit were constant, these results would either indicate that the ionisation can vary considerably even in the case of constant absorption, or else, that the saturation current during constant ionisation is able to show the variation in question.

As we know, ionisation is a consequence of a secondary β-radiation. The knowledge we have of the ionising properties of the α- and β-radiation as well as of the variations connected with the corpuscular radiation, exclude the possibility of the first-mentioned alternative. The deviation from the mean effect would be of a different kind, and actually of a much smaller order of magnitude than the observed variations ΔQ.

The second alternative may likewise be excluded. It might, certainly, be possible that the ionisation *current* should vary during a short interval Δt even when the ionisation is constant, in consequence of the variations in the course of the β-particles which certainly occur. If the ionisation is produced in the vicinity of the electrode the ionisation current rises, in the opposite case it falls. This would be a consequence of the limited velocity of the ions. In this case it would necessarily follow that on a variation effect appearing during a given time interval there would appear an effect of opposite sign during the following interval or intervals. From our investigations it is evident, however, that the mean square variation is characterised by the remarkable property $\overline{(\Delta Q)^2}/\Delta t = \text{const.}$, which means that the effect observed during a given time interval Δt in no way determines the nature of the effects which are to be expected during the following time intervals.

The variations observed may, on the other hand, be explained completely by the light quantum hypothesis. According to this hypothesis the mean ionisation Q would be subject to random variations which must obey the Gauss law of errors. According to the theory of probability the magnitude of these variations would, for the actual distribution of spectral energy, be given by the equation

$$(1/h) \,.\, (\overline{(\Delta Q)^2}/Q) = 1{\cdot}30 \times 10^{10} \text{ Coulomb erg.}^{-1} \text{ sec.}^{-1}, \qquad (2)$$

which is independent of the length of the time interval.

The magnitude of an energy quantum is determined by equations (1) and (2). We then obtain

$$h = 6{\cdot}4 \times 10^{-27} \text{ erg. sec.}$$

This value of h agrees fairly well with the value of Planck's constant ($h = 6 \cdot 55 \times 10^{-27}$) theoretically calculated.

Our results may briefly be summarised in the following manner. If the amount of energy E, which during the time Δt is transmitted by radiation in the frequency range ν, $\nu + d\nu$ from the focal spot of the cathode in the X-ray tube into the gas present in an ionisation chamber, is divided by the product $h\nu$, and if the quotient obtained in this way is denoted by $E/h\nu = n$, the variations Δn appearing, will follow the Gauss law of errors, while the mean square variation $\overline{(\Delta n)^2}$ is given by the variation formula

$$\overline{(\Delta n)^2} = n,$$

known from the probability calculus of Poisson.

It might appear that the observed variations could be produced by the absorption mechanism without there necessarily being any variations of the amount of energy passing the diaphragm per time unit. This is, however, not the case.

We assume that the energy is at every moment localised as to space, and it follows then that through the diaphragm aperture of an ionisation chamber there passes during each time interval Δt on an average a given amount of energy which, independently of the structure of the radiation field, may be denoted as $n_0 \, . \, h\nu$. The mean square variation may be denoted as $\overline{(\Delta n_0)^2} \, . \, (h\nu)^2$. The absorption may take place as quanta of the magnitude $h\nu$, the absorption process being considered as a chance phenomenon, the probability of which is proportional to the radiation intensity in the neighbourhood of the point considered. Every amount of energy $h\nu$ which is released by absorption at a point A is definitely abstracted from the primary radiation field, the mean intensity of which has been lowered to a corresponding degree. The fraction of the incident radiation energy which on an average is absorbed by the gas, may be denoted as p. During the time Δt an amount of energy $pn_0h\nu = nh\nu$, will on an average be absorbed by the gas. Its mean square variation may be denoted as $\overline{(\Delta n)^2} \, . \, (h\nu)^2$. It is due partly to the variations of the incident radiation energy (suffix 1) and partly to the variations of the absorbed fraction of the incident radiation energy, consequently to the absorption mechanism (suffix 2). According to Bernouilli's theorem for $\overline{(\Delta n)^2}$ we obtain the equation

$$\overline{(\Delta n)^2} = [p^2 \, \overline{(\Delta n_0)^2}]_1 + [n_0 p \, (1 - p)]_2 = [p^2 \, \overline{(\Delta n_0)^2}]_1 + [n \, (1 - p)]_2. \quad (3)$$

If the fraction absorbed is small ($p \simeq 0$, $(1 - p) \simeq 1$) the equation (3) changes into Poisson's law

$$\overline{(\Delta n)^2} \simeq [n]_2, \quad (3\text{A})$$

independently of the value of $\overline{(\Delta n_0)^2}$. Consequently, if the absorbed fraction is small the variations which are regulated by the mechanism of the absorption process (suffix 2) will dominate. Thus experiments carried out with a low absorption percentage cannot be used as a basis for any considerations concerning the nature of the radiation. This case is encountered in the investigations of E. Meyer, T. H. Laby and P. W. Burbidge on similar variations, brought about by means of radioactive γ-radiation.

If, on the contrary, $p \simeq 1$ and $(1-p) \simeq 0$, the equation (3) changes into the equation (3B)

$$\overline{(\Delta n)^2} \simeq [p^2 \overline{(\Delta n_0)^2}]_1 \simeq [\overline{\Delta n_0}]_1^2, \tag{3B}$$

which means that the variations observed in the case of complete absorption are identical with those of the incident radiation energy, and independent of the mechanism of the absorption process. It is perfectly clear that the variations which are due to the discontinuous character of the absorption process disappear in the case of complete absorption, as then every quantity of energy which enters the ionisation chamber will sooner or later be absorbed. Each amount $h\nu$ can be absorbed at one single point only and not in another as well. Every absorption process which takes place in a given layer of the gas hereby reduces the energy of the radiation field, and thereby also lowers the probability of an absorption in the subsequent layers in such a way that the total variation, due to the mechanism of the absorption process, disappears.

It is, however, evident from our investigations that the variations which correspond to Poisson's law, remain even in the case of complete absorption. As in this case $n = n_0$, and according to the experiments $\overline{(\Delta n)^2} = n$, it follows from (3B)

$$\overline{(\Delta n_0)^2} = n_0. \tag{4}$$

Thus our experimental results cannot depend on absorption taking place in quanta. As a matter of fact, the experiments mentioned do not throw any light on the mechanism of the absorption process.

When, however, we assume a localisation, as to space and time, of the radiation energy in the radiation field, which involves that the diaphragm aperture of the ionisation chamber during each time interval Δt is traversed by a certain amount of energy, defined in each single case, then we may conclude that these energy quantities vary according to the probability laws of Gauss and Poisson, in which case a unit of energy ϵ appears which has been found to be identical with a light quantum $h\nu$.

§ 4. Let the radiation emitted from the anticathode of an X-ray tube within a given solid angle ω traverse an absorbing layer. This layer, during the time Δt, will be on the average struck by an amount of energy E. The mean square variation may be denoted as $\overline{(\Delta E)^2}$. According to the above-mentioned experimental results $\overline{(\Delta E)^2}$ may then be calculated according to the formula

$$\overline{(\Delta E)^2} = \overline{(\Delta n_0)^2} \cdot (h\nu)^2 = n_0(h\nu)^2 = Eh\nu.$$

Thus, the equation

$$\overline{(\Delta E)^2}/E = h\nu \tag{5}$$

is identical with the variation law of Poisson. The relative mean variation

$$\overline{[\Delta E]}/E = \sqrt{\overline{(\Delta E)^2}}/E$$

may be calculated to be

$$\overline{[\Delta E]}/E = \sqrt{h\nu/E}. \tag{6}$$

On an average the layer absorbs the fraction p of the incident radiation energy, while on an average the fraction q penetrates the layer. In this case $E' = q \cdot E$, and its mean square variation $\overline{(\Delta E')^2}$ may be observed. If the absorption is continuous, so that an identical fraction p is absorbed from each amount of energy, the equation

$$[\Delta E']/E' = \overline{[\Delta E]}/E \tag{7}$$

is valid. If, on the contrary, the absorption is discontinuous, which means that p varies independently of E, we may write

$$\overline{[\Delta E']}/E' > \overline{[\Delta E]}/E.$$

The following formula applies generally :

$$\overline{(\Delta E')^2} = q^2\,\overline{(\Delta E)^2} + E^2\,\overline{(\Delta q)^2} = (1-p)^2\,\overline{(\Delta E)^2} + E^2\,\overline{(\Delta p)^2}, \tag{8}$$

where $\overline{(\Delta p)^2}$ characterises the mechanism of the absorption process. A continuous absorption would give $\overline{(\Delta q)^2} = \overline{(\Delta p)^2} = 0$. Consequently, the formula (7) is found to be a special case of formula (8).

Let us now consider the optical phenomena in the strict sense of the word. During the time Δt the optical system will on an average be hit by the energy amount E. Its mean square variation may be denoted as $\overline{(\Delta E)^2}$. As an example we may take an interference phenomenon. A beam formed by interference encounters a small surface σ, which, during the time Δt, is on an average traversed by a fraction g of the radiation E. We are then able to observe

$E'' = qE$ and its mean square variation $\overline{(\Delta E'')^2}$. If the interference is continuous, *i.e.*, in conformity with the classical wave theory, the same equation

$$\overline{[\Delta E'']}/E'' = \overline{[\Delta E]}/E \tag{9}$$

is valid here also.

If the phenomenon is discontinuous, we write

$$\overline{[\Delta E'']}/E'' > \overline{[\Delta E]}/E, \tag{10}$$

in which case again

$$\overline{(\Delta E'')^2} = q^2\,\overline{(\Delta E)^2} + E^2\,\overline{(\Delta q)^2}. \tag{11}$$

Our series of experiments, comprising thousands of Δt, have shown that Poisson's law holds good with a great degree of accuracy, both in the case of radiation which has penetrated an absorbing layer, and in the case of a beam produced by interference.

As the variation law of Poisson is valid both before and after the absorption, the values of the mean square variation $\overline{(\Delta E)^2}$ and $\overline{(\Delta E')^2}$ satisfy the equation

$$\overline{(\Delta E')^2}/E' = \overline{(\Delta E)^2}/E = h\nu. \tag{12}$$

According to formula (8) we may write in general

$$\overline{(\Delta E')^2} = q^2\,\overline{(\Delta E)^2} + E^2\,\overline{(\Delta q)^2}. \tag{13}$$

The absorption mechanism may be characterised by the mean square variation $\overline{(\Delta p)^2} = \overline{(\Delta q)^2}$ derived from these equations (12)-(13)

$$\overline{(\Delta p)^2} = \overline{(\Delta q)^2} = pq\,(h\nu/E). \tag{14}$$

Furthermore, as ΔE and $\Delta E'$ follow Gauss's law, the distribution of $\Delta p = -\Delta q$ must also obey the same law. The random variations Δp must therefore be assumed to be due to an absorption of some kind of energy elements E/n_0 where n_0 is an unknown though finite number, which process is governed by chance. Thus every incident energy element will either disappear in the absorbing layer (case A), or penetrate the same (case B).

Consequently, one of the cases A, B must necessarily arise so soon as the absorbing layer is encountered by the energy element E/n_0. The probability p applies to the first case, the probability of q to the second one, so that $p + q = 1$. This choice between A and B is repeated n_0 times.

Any combination of the cases A, B, comprising n_0 elements and occurring A n' times, B n'' times, leads up to a probability product of n_0 factors, of which n' are equal to p and n'' equal to q, so that $p^{n'}\,q^{n''}$ will be the ensuing product.

There are, however, as many combinations of this kind as the permutations given by n_0 elements—of which n' are of one kind, and n'' of another, *i.e.*,

$$n_0\,!/n'\,!\;n''\,!$$

As a probability of $p^{n'}\,q^{n''}$ applies to every arrangement of this kind, the total probability that the cases A, B should reoccur in the numbers $n'\,n''$ is represented by

$$\mathrm{W}\,(\mathrm{A}^{n'}\,\mathrm{B}^{n''}) = (n_0\,!/n'\,!\;n''\,!)\,.\,p^{n'}\,q^{n''}.$$

The mean value of a magnitude depending on chance is equal to the sum of its single values multiplied by their corresponding probabilities. Thus, if we write

$$n' - n_0 p = n_0\,(p + \Delta p) - n_0 p = n_0 \Delta p,$$

then

$$n_0^{\,2}\,\overline{(\Delta p)^2} = \sum_{n'=n_0}^{0} (n' - n_0 p)^2\,(n_0\,!/n'\,!\;n''\,!)\,p^{n'}\,q^{n'} = n_0 pq,$$

from which

$$\overline{(\Delta p)^2} = pq\,(1/n_0). \tag{15}$$

If we compare the theoretical formula (15) with the experimentally established formula (14) we find

$$n_0 = \mathrm{E}/h\nu \quad \text{and} \quad \mathrm{E}/n_0 = h\nu. \tag{16}$$

Thus when the absorbing layer is struck by the energy element $h\nu$, one of the cases A, B must necessarily occur. The energy element will either be absorbed or transmitted. ***Absorption is caused by a kind of elementary processes, governed by chance, the primary radiation field in the case of each elementary process of this kind loosing an amount of energy of the magnitude of $h\nu$.***

As already pointed out above, the mean square variations $\overline{(\Delta \mathrm{E}'')^2}$ and $\overline{(\Delta \mathrm{E})^2}$ which occur in interference experiments are likewise governed by Poisson's law, and thus satisfy the equation

$$\overline{(\Delta \mathrm{E}'')^2}/\mathrm{E}'' = \overline{(\Delta \mathrm{E})^2}/\mathrm{E} = h\nu. \tag{17}$$

The relation between the energy of the incident, homogeneous radiation and the radiation, which—owing to an interference process—becomes deviated into a given direction is represented by $1/q$. If we introduce the expression $(1 - p) = q$ the formulæ (13)–(14) still remain valid. The random variations Δq must be assumed to be due to the deviation of direction of each separate energy element E/n_0 in the interference phenomenon being accidental. Every incident quantity of energy E/n_0 will thereby either be deviated in the prescribed direction (case B) or not be so (case A). A probability of q applies in the first case, a probability p in the second. The formulæ (15)-(16) are therefore also still valid with respect to interference.

Consequently, an interference phenomenon is composed of elementary processes, governed by chance. In each elementary process of this kind the direction of propagation of an energy element $h\nu$ *changes in a definite manner.*

Summary.

If we assume that radiation energy is localised as to space and time, being propagated from point to point in the radiation field, from which follows that every surface element in the radiation field during each time interval t, $t + \Delta t$ is traversed by a quantity of energy defined in each case, we are able to conclude, from the experimentally proved variations of the ionisation effects of the radiation—

(1) that the radiation consists of energy elements $h\nu$;

(2) that the absorption is brought about by distinct elementary processes, whereby the primary radiation field in the case of each elementary process of this kind looses an amount of energy of the magnitude $h\nu$;

(3) that the interference phenomena are made up of elementary processes governed by chance. In every elementary process of this kind the direction of propagation of an energy element $h\nu$ changes in a definite manner.

If, however, with Bohr and Heisenberg, we abandon the claim of a localisation of the energy as to space and time, and instead adopt the view that the energy is in fact not really defined within finite spheres of space and time, but as it were virtually distributed over the entire field of radiation, then the experimental results will imply a quantitative statement of the very variation effects which, according to the above theory, characterise the irrational, non-causal coupling of quantum-processes.

The Atomic Heat of Bismuth at Higher Temperatures.

By L. G. CARPENTER and T. F. HARLE, University College, Southampton.

(Communicated by A. C. Egerton, F.R.S.—Received December 9, 1931.)

Introduction.

The thermal capacity of metallic bismuth has been investigated by a number of experimenters.* Though the true specific heat from absolute zero up to air temperatures is known from measurements made with the vacuum calorimeter by Keesom and Ende, and by Anderson, from air temperatures up to the melting point we have only mean specific heats, determined over considerable ranges of temperature, while of the true specific heat of the liquid and its variation with temperature nothing reliable is known.

In order to use a vacuum calorimeter at temperatures much above room temperature it is necessary to evolve a design employing materials which have satisfactory electrical, mechanical and thermal properties at the temperatures in question. Such a calorimeter has been successfully developed, and the present paper describes its construction and gives the results of measurements made by means of it on bismuth, over a temperature range of 30° to 370° C.

Experimental Details.

In this vacuum calorimeter the same platinum coil was used to supply heat electrically and to measure the rise of temperature produced.

The calorimeter A, fig. 1, which was closed by a screw-on cap B, consisted of a thin cylinder of mild steel of length 8 cm. and diameter 5 cm. On this was wound the coil C, consisting of 370 cm. of 38 S.W.G. platinum, blackened with carbonised bakelite varnish, actual contact being prevented by the interposition of asbestos spacing pieces D of as small area as possible. The asbestos was very carefully freed from electrolytic impurities by washing in distilled water, and was an excellent electrical insulator at high temperatures.

Surrounding the coil, but not actually touching it, was a sheet of thin silver foil E, polished on its outer and blackened on its inner surface, and held in position and in thermal contact with the steel wall of the calorimeter by short steel pillars F. The outer surface of the steel calorimeter was also blackened, so that the blackened coil was enclosed in the annular space between blackened steel and blackened silver. The whole was enclosed in an outer case of silver foil G, polished on both surfaces and connected both thermally and mechanically by means of steel pillars H to the steel wall of the calorimeter. J and K denote the leads to the coil and the compensating leads usual in platinum thermometry. The calorimeter was suspended by platinum wires which are not shown in fig. 1.

---

* *Vide* Landolt-Börnstein's Tables (1923 Edition), p. 1248, and the 2nd Supplement (1931), p. 1169, where the data of Dewar, Richards and Jackson, Giebe, Ewald, Schimpff, Jaeger and Diesselhorst, Magnus, Schübel, Iitaka, Person, Keesom and Ende, Awbery and Griffiths, Umino, and Anderson are given.

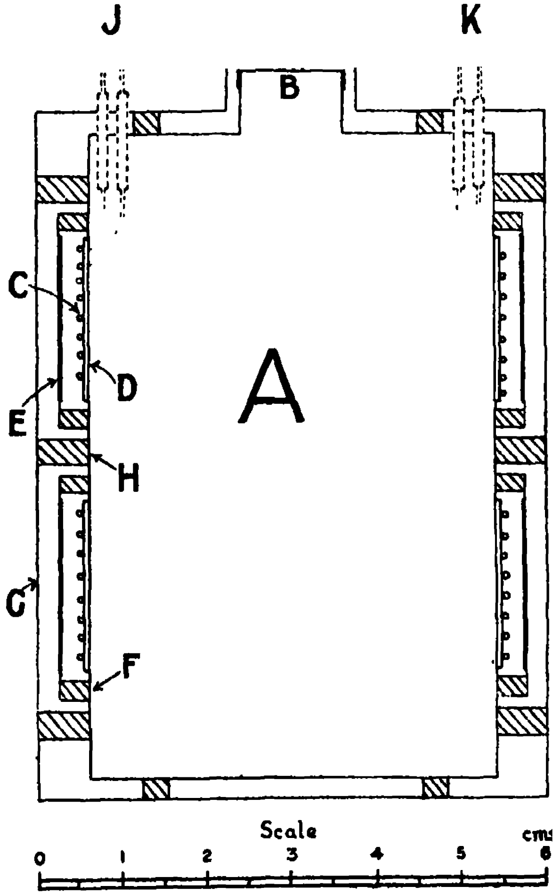

Fig. 1.

The calorimeter was suspended inside a vertical copper cylinder, closed top and bottom, and silver-plated within, the whole being enclosed in a pyrex tube which was exhausted by means of a mercury vapour pump. For measurements above room temperature the pyrex tube was placed within a tubular thermostatically controlled electric furnace.

The heat, developed electrically in the platinum coil, was transferred in part directly to the blackened wall of the calorimeter by radiation, and in part by radiation to the inner blackened surface of the silver shield E and thence by conduction down the pillar F to the calorimeter.

The essential points of the design were (*a*) that the coil made effective thermal contact with the calorimeter by radiation, (*b*) the outer silver foil which controls the heat loss was maintained at definite and known temperatures, and (*c*) that the high electrical insulation and freedom from mechanical strain of the coil necessary for accurate platinum thermometry were insured. It was, of course, necessary to make correction for the heat lost during the time the current was flowing and during the subsequent period when the coil was regaining thermal equilibrium with the calorimeter, and for that part of the heat developed in the leads which does not enter the calorimeter.

These corrections, a general discussion of the design of high temperature calorimeters, and a more detailed description of the present calorimeter will be given elsewhere.* It may, however, be mentioned here that the most important correction, viz., that for loss of heat during the time of input and during the subsequent time in which the coil was re-attaining thermal equilibrium with the calorimeter was 5 per cent. of the heat input at air temperatures, and 8 per cent. at 370° C., the greater rate of loss at the higher temperature being partly compensated by its shorter duration.

The total mass of bismuth was 1337·9 grams, and the thermal capacity of the empty calorimeter was 40 per cent. of the bismuth it contained. The calorimeter was calibrated as a resistance thermometer at the ice point, the steam point and the melting point of bismuth, assuming the latter to be 271·0° C.† The resistance measurements were made with a Callendar-Griffiths bridge, which could measure a maximum of 52 ohms. The resulting restriction of the maximum temperature of working to about 380° C. was not, however, inherent in the calorimeter, which may be used up to at least 500° C.

Results.

The heat capacity of the empty calorimeter was first determined over the temperature range 30° to 370° C. and a smooth curve drawn through the individual points which were 14 in number. No individual point deviated from the curve by more than 2/3 per cent.

---

* 'Proc. Phys. Soc.,' vol. 44 (1932).

† Landolt-Börnstein's Tables, p. 329 (1923 edition).

The calorimeter was filled *in vacuo* with melted bismuth, and the heat capacities again determined over the whole temperature range. From the individual values of the heat capacity of the full calorimeter were subtracted the values for the empty calorimeter at the same temperatures as read from the smooth curve mentioned above. The resulting values converted to molar heat capacities (using M = 209·0) are given in Table I and, with the exception of those above 9 calories per mole (which cannot conveniently be included on account of difficulties of scale) have been plotted in fig. 2.

Table I.

Absolute temperature.	C_p.	Absolute temperature.	C_p.
305·9 solid	6·207	536·4 solid	9·318
306·5 ,,	6·140	537·9 ,,	10·73
372·5 ,,	6·353	538·5 ,,	11·85
373·0 ,,	6·356	539·4 ,,	13·47
427·5 ,,	6 563	540·0 ,,	14·97
428·4 ,,	6·566	540·8 ,,	20·51
477·9 ,,	6·686	541·4 ,,	25·96
478·6 ,,	6·661	545·6 liquid	7·217
505·1 ,,	6·792	546·2 ,,	7·200
505·8 ,,	6 841	558·0 ,,	7·172
520·8 ,,	7 100	558·6 ,,	7·190
521·7 ,,	7·103	576·8 ,,	7·148
522·4 ,,	7·093	577 6 ,,	7·203
523·1 ,,	7·195	600·2 ,,	7·119
534·7 ,,	9·040	601·2 ,,	7·076
535·4 ,,	9·618	643·1 ,,	6·971
535·8 ,,	8·973	644·1 ,,	6·995

Table II.

Absolute temperature.	C_1	
300 solid	6 15	6·08
350	6·31	6·22
400	6·46	6·35
450	6·60	6·48
500	6·73	6·60
540	6·83	6·70

In fig. 2 the best smooth curve has been drawn through the individual points. The rapidly increasing rise above 500° abs. is due to the presence of a small amount of impurity in the bismuth. The curve has, therefore, been extrapolated to the melting point as shown by the broken line. The justification for this procedure will be given later. In order to exhibit on a convenient scale our data in relation to previous work, the observations of the other experimenters mentioned in the introduction* have been plotted in fig. 3, and our own curve from 300° abs. upwards has been replotted from fig. 2. Our work appears to be in excellent agreement with that of Anderson, the only other observer who has made accurate measurements of the true specific heat, and we estimate that it is not in error by more than ½ per cent.

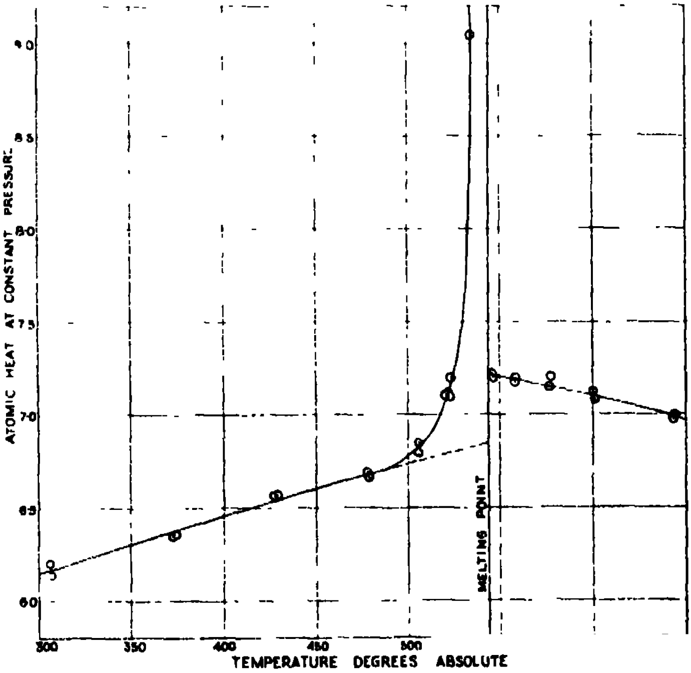

Fig. 2.

The Purity of the Bismuth and the Specific Heat near the Melting Point.

The bismuth was obtained from Messrs. Adam Hilger, and was the purest obtainable at the time of purchase. Spectrographic analysis gave :—

Pb, 0·01 per cent. by weight,
Ag, 0·002 per cent. by weight,
and very minute traces of Na, Mg, Ca, Fe, Ni, Sn and Th.

---

* Awbery and Griffiths have pointed out that their original paper (' Proc. Phys. Soc.,' A, vol. 38, p. 378 (1926)) contains an arithmetical slip, and hence the two points plotted to represent their results have been recalculated from their total-heat temperature data.

The amount of lead, which was the most important impurity present, was confirmed chemically by Mr. G. H. Jeffery, to whom our grateful thanks are due. We are also indebted to Dr. R. S. Hutton, who very kindly had a spectrographic analysis made for us at the laboratories of the British Non-Ferrous Metals Research Association. The total amount of impurity may be taken as of the order of 0·014 atomic per cent.

Van't Hoff's equation connecting molar proportion of impurity and depression of freezing point may be used to calculate the apparent specific heat due to premature melting in a slightly impure solid, provided that the impurity does not separate out appreciably in the form of a solid solution. Alternatively, the equilibrium diagram for the binary system in question may be used if it is known, and it can be shown that the apparent specific heat at any temperature should be inversely proportional to the square of the interval between that temperature and the melting point of the pure solid.

In the present case ΔC_p, the difference at T° abs. between the ordinates of the full and broken line curves in fig. 2 is given very closely by the expression

$$\Delta C_p = \frac{152}{(544 \cdot 1 - T)^2}, \qquad (1)$$

where 544·1 is the absolute melting temperature of pure bismuth, and the constant 152 corresponds to 0·023 atomic per cent. of impurity. The agreement of this figure with that determined by analysis (viz., 0·014 atomic per cent.) may, in view of the difficulty of quantitative analysis of such small amounts of impurity, be considered as satisfactory. The very large increase in apparent specific heat in the neighbourhood of the melting point, caused by the relatively small amount of impurity, emphasises the importance in work of this kind of using substances of the highest purity.

The Atomic Heat at Constant Volume.

C_v, the atomic heat at constant volume has been calculated from C_p, the observed atomic heat at constant pressure, by means of the relation

$$C_p - C_v = \frac{\alpha^2 VT}{\kappa}, \qquad (2)$$

where α is the coefficient of cubical expansion, V the atomic volume, T the absolute temperature and κ the compressibility. The most reliable determination of α is probably that of Roberts* who found that its value was $4 \cdot 02 \times 10^{-5}$ from 0° to 240° C., and that from 240° C. to the melting point it rapidly decreases, anticipating the large change of volume that takes place on melting. This latter effect, however, he attributes to the presence of impurity, and α has therefore been taken as constant right up to the melting point.

---

* 'Proc. Roy. Soc.,' A, vol. 106, p. 385 (1924).

Since V does not vary by more than about 1 per cent. from air temperature to the melting point, it has been taken as 21·3 (*i.e.*, 209/9·8) over the whole temperature range. Bridgman's values of the compressibility have been used since they are probably the most reliable, and are in good agreement with other observers. He gives $\kappa = 29{\cdot}17 \times 10^{-7}$ cm.^{2}/kgm. at 30° and $29{\cdot}89 \times 10^{-7}$ cm.^{2}/kgm. at 75° C. As the exact form of the compressibility-temperature curve is not known it has been assumed to be linear, and appropriate values of κ read off at each temperature.

The values of C_v have been inserted on fig. 3 and given in Table II. together

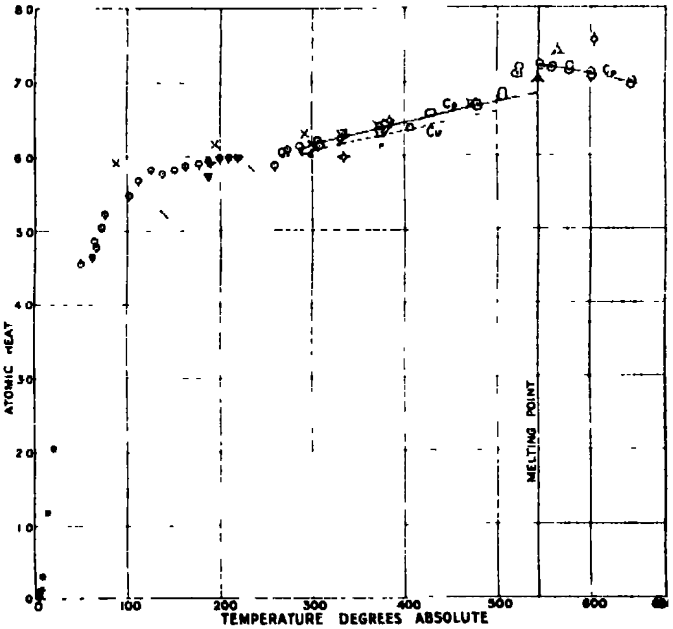

Fig. 3.

♀	Anderson.	▣	Magnus.
⌘	Awberry and Griffiths.	◊	Person.
⊙	Dewar.	⸝	Richards and J
⸜	Ewald.	▽	Schimpff.
×	Giebe.	⸝	Schübel.
▲	Iitaka.	✦	Umino.
△	Jaeger and Diesselhorst.	⊙	Authors.
✳	Keesom and v.d Ende.		

with the values of C_p read off our smooth curve in fig. 2. C_v for the liquid has not been calculated as the necessary data are lacking.

Discussion of Results.

It is evident from fig. 3 that C_v exceeds the Debye maximum of 3R at all temperatures above about 260° abs., and that at the melting point this excess amounts to over 10 per cent.* Since the contribution of free electrons to the atomic heat (as calculated on the basis of Fermi-Dirac statistics) is unlikely to be more than 2 or 3 per cent., it seems reasonable to attribute the major portion of the effect to anharmonic oscillations.

Born and Brody† worked out a theory of the anharmonic oscillator, taking into account terms in the potential energy up to and including the fourth power of the displacements. It follows from their theory that at high temperatures the deviation of C_v from 3R should be a linear function of the absolute temperature, and that the linear high temperature part of the C_v curve should, when extrapolated back to $T = 0$, cut the axis of C_v at 3R.

The variation of C_v with temperature for solid bismuth, as shown in fig. 3, is very nearly linear above about 300° abs., but when extrapolated back the intercept on the C_v axis is only about 5·3. It is not possible to attribute this to experimental error, as our value at 300° abs. is in very good agreement with other observers, and hence, taking it as correct, it would be necessary to reduce the value at the melting point from 6·7 to 6·2 in order to make the curve extrapolate back to 3R at $T = 0$. An experimental error of this magnitude is, however, extremely unlikely.

The value of C_p for the liquid decreases with increase of temperature, as indeed is usual, and the curve appears to be slightly convex upwards.

In conclusion, we should like to express our thanks to Professor H. Stansfield, in whose laboratory this work has been carried out, for his kind interest and support.

---

* A similar phenomenon, though much less marked, has been examined and discussed in the case of mercury. *Vide* 'Phil. Mag.,' vol. 10, p. 249 (1930), and vol. 12, p. 511 (1931).

† 'Z. Physik,' 2, vol. 6, p. 132 (1921).

Dipole Moments and Molecular Structure. Part I.—A simple Resonance Method for the Measurement of Dielectric Constants.

By JOHN WILLIAM SMITH, B.Sc., Ph.D., the Sir William Ramsay Laboratories of Physical and Inorganic Chemistry, University College, London.

(Communicated by F. G. Donnan, F.R.S.—Received December 12, 1931.)

Numerous types of resonance methods for the measurement of dielectric constants have been described by different investigators. That detailed in the present communication has no claim to originality, but it is a simple, whilst at the same time reliable, form, which has proved to be very useful for the measurement of the dielectric constants of dilute solutions for the purpose of dipole moment determination.

A fairly powerful oscillator is used, enabling the valveless resonance circuit to be some distance removed from it, whilst still receiving ample " pick-up " for the measurements. Resonance in the pick-up circuit is detected by means of a low-resistance thermo-junction, introduced directly into the circuit. The resistance thus introduced does not damp the oscillation unduly. The very small conductivity of the solvent liquids employed does not produce any appreciable error owing to the current resonance not occurring at the same tuning capacity as the voltage resonance.*

Apparatus.

The Oscillator.—Oscillations are generated by means of a circuit of the form shown diagrammatically in fig. 1, the values of the components being as indicated. A quartz crystal, Q, connected between the grid and the anode of the valve V_1 is used to control the frequency of the oscillations. The anode coil consists of the primary winding of a high frequency transformer, T_1, specially designed to give a suitable input to the grid of the valve V_2. The secondary winding of the transformer is tuned. Under these conditions the valve V_1 will oscillate over a small range of capacity in the condenser C_1, and the oscillations set up are of constant frequency, viz., the natural frequency of vibration of the quartz crystal Q. A high tension of about 90 volts is used on the valve V_1, this being obtained from a constant-voltage battery supply. The non-earthed end of the secondary coil from the transformer T_1 is connected through a low capacity condenser to the grid of valve V_2, of the large

---

* *Cf.* Kniekamp, 'Z. Physik,' vol. 51, p. 92 (1928).

Mullard D.O. 40 type. The plate coil of this valve is again the primary coil of the high frequency transformer T_2, the secondary coil of which is tuned. A neutralising coil is also wound on this transformer, and is connected as shown

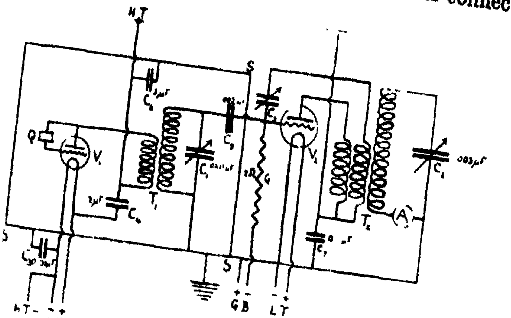

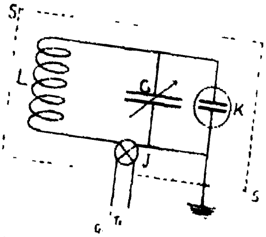

FIG. 1 above. FIG. 2 below.

through the small neutralising condenser, C_3, with the grid of valve V_2. The other connections are as shown in the diagram. A high tension of about 700 volts, and a grid bias of about −36 volts have been found to be about correct for operating this circuit. The high tension is generated by means of a direct-current generator, and this has proved to be quite satisfactory without employing any smoothing choke. The whole of the primary oscillator is enclosed in an earthed metal screen, S, S, the connections, when necessary, passing through small bushed holes in the screen. The amplifying circuit can be readily neutralised by connecting a Moullin voltmeter across the secondary coil of transformer T_2, and completing all connections of the circuit as in use, with the exception of the low tension of the first valve. The position of the condenser C_3 can then be found such that no oscillation is set up by the second valve, whatever be the value of the condenser C_2. With the circuit neutralised in this way, it has been found that if a wavemeter be tuned to the frequency of the oscillator, no change in frequency can be detected on turning either condenser C_1 or C_2 slightly away from its optimum position for maximum output. Actually, however, the condensers C_1 and C_2 are maintained in a constant position whilst the oscillator is in use. A large sheet of metal brought near to the oscillator also causes no detectable change in the frequency, the only effect being that if brought sufficiently close it may modify the capacities in the circuit to such an extent that the circuit ceases to oscillate. Many test experiments have been carried out to detect any variation in frequency during prolonged running of the oscillator, or during intermittent running, but in each case it has been found that there is no change whatever under such circumstances, so far as can be detected. The characteristic frequency of the quartz crystal Q was measured by the National Physical Laboratory as 1,227,282 ± 20 cycles per second.

The Resonance Circuit.—The pick-up circuit employed is of the form shown in fig. 2. The coil L has an inductance of about 280 μH, and is wound on a tube of "Keramot" (a loaded ebonite), which had been cut longitudinally into three sections and mounted on bakelite end pieces. Using a length : diameter ratio of about 1 : 1·37 for the coil, this arrangement renders its inductance almost invariant with temperature.* The coil was wound firmly with 18 gauge bare copper wire in a spiral notch which had been cut in the tube. The condenser C is a Sullivan Standard Variable Air Condenser, which is screened and the screen connected to the moving plates. The range of the instrument is from about 50 to 260 μμF, and this is divided into 180 scale divisions, a vernier enabling measurements to be made to 0·05 scale divisions or about 0·06 μμF. The moving vanes of this condenser are connected to earth and are also connected to the coil through the primary heating wire of a low-resistance vacuum thermo-junction (resistance 1·26 ohms). The other vanes of the condenser are connected directly to the other end of the inductance coil. The liquid condenser is connected in parallel across the variable condenser, the ends of the leads from each condenser dipping into mercury cups. All connections are made with very stout wires to avoid any variation in inductance and capacity. The liquid cell, the form of which will be described later, is immersed in a water thermostat, which is earthed, and the outer plate of the condenser is connected to the earthed terminal of the variable condenser.

The whole of the resonance circuit is enclosed in an electrostatic screen, consisting of wires 1½ inches apart running round the apparatus on a square framework, being bonded at one end and free at the other. The base and lid are of similar design, and the whole is earthed. This screen does not diminish very greatly the amount of "pick-up" on the resonance circuit. The secondary (couple) terminals, of the thermo-junction are connected through two Wearite

---

* 'Experimental Wireless,' vol. 6, p. 543 (1929).

" heavy-duty " chokes to a Moll galvanometer. The sensitivity of the galvanometer can be varied by varying the current passed through the magnet coil.

The resonance curve obtained is very sharp, and the position of the peak is unaltered when a large sheet of metal is brought close to the outside of the screen. The frequency of the oscillator is not " pulled " when the condenser of the resonance circuit is tuned through the frequency of the oscillator.

The Liquid Condenser.—The test condenser is of the Sayce and Briscoe type.* The outer surface of the inner tube, and the inner surface of the outer tube are silvered very heavily. Connection is made to the plates by means of pieces of platinum foil fused to the respective surfaces, and connected to platinum wires which pass into the interior of the inner tube, and into a side tube sealed to the outer tube, respectively. The platinum wire in the inner tube is covered with mercury, into which dips a rigid rod which passes up the centre of the tube. The other end of the rod is bent twice at right angles, and is arranged to fit into a mercury cup in an ebonite block attached to the top of the thermostat in which the condenser is immersed. The lead from the outer plate is also rigid, and drops similarly into another mercury cup. A stand holds the test condenser in the thermostat in a uniform manner. Repeated tests have shown that the error produced by the continuous displacement and replacement of the vessel is not detectable by any change in the tuning capacity on the variable condenser. The lead from the outer condenser plate is, of course, connected to the earthed side of the resonance circuit, whilst the thermostat case is earthed.

After silvering the appropriate surfaces of the condenser, the inside was dried by washing two or three times with pure, dry alcohol, and then several times with pure, dry ether. Dry air was then drawn through the vessel for some time. The equivalent parallel resistance of the condenser when heavily silvered and well dried out is very low.

Experimental Procedure.

No attempt has been made to utilise this system for absolute measurements of dielectric constants. Since it is required only to measure the dielectric constants of solutions differing comparatively little from the pure solvents, relative values only are required. The resonance point of the circuit with the condenser filled with dry air is first determined. The resonance point is then obtained again with the pure dry solvent. From these measurements, using standard values of the dielectric constant of the solvent, the "zero" point can be determined. For if the capacity required in the tuning condenser be C_1 with air in the dielectric cell, and C_2 with the pure solvent in the cell, and if ε be the dielectric constant of the solvent, then the "zero" capacity, *i.e.*, the capacity which would be required with the leads, but without the condenser, is given by

---

* 'J. Chem. Soc.,' vol. 127, p. 315 (1925).

$$C_0 = C_1 + \frac{C_1 - C_2}{\varepsilon - 1} = \frac{C_1\varepsilon - C_2}{\varepsilon - 1}.$$

Then, if C_x be the capacity of the condenser at resonance with any solution in the liquid condenser, the dielectric constant of this solution will be given by

$$\varepsilon_x = \frac{C_0 - C_x}{C_0 - C_1}.$$

The actual resonance point is determined by tracing the resonance curve over a range of 0·5–1·0° of scale on either side of the maximum, the condenser being set to each vernier division in turn, and the galvanometer reading taken in each case. This is much more accurate than setting the condenser to give the maximum deflection and then reading off the position.

Summary.

A simple resonance method suitable for measuring the dielectric constant of solutions is described. Details are given of the construction and operation of the apparatus.

In conclusion, the author desires to express his great indebtedness to the Department of Scientific and Industrial Research for a Senior Grant, during the tenure of which this work was carried out; to Dr. R. W. Lunt and Mr. A. L. M. Sowerby, of this laboratory, for many valuable suggestions, and especially to Professor F. G. Donnan, for the deep interest which he has shown in this work.

Dipole Moments and Molecular Structure. Part II.—*The Trichlorides of the Elements of Group V.*

By John William Smith, B.Sc., Ph.D., the Sir William Ramsay Laboratories of Physical and Inorganic Chemistry, University College, London.

(Communicated by F. G. Donnan, F.R.S.—Received December 12, 1931.)

Although numerous investigators have carried out measurements of the dipole moments of the commoner organic compounds, few references are to be found to analogous data for inorganic compounds. The latter are confined almost exclusively to those substances which can be investigated in the gaseous state. The present series of investigations were commenced, therefore, with a view to applying the method of dilute solutions to the measurement of the dipole moments of such inorganic compounds as are soluble in non-polar solvents, and to relating the dipole moments of analogous groups of compounds to their molecular structures.

The first series of measurements to be made, and those described in this paper, were upon the trichlorides of phosphorus, arsenic and antimony. Of these, measurements had been recorded only with respect to antimony trichloride* when this investigation was carried out. More recently, measurements of the dipolar moments of all three compounds have been recorded by Bergmann and Engel.† but their experimental results show much greater discrepancies among one another than do those of the author. Werner used both benzene and ethyl ether as solvents for the antimony trichloride, finding a considerable difference between the values obtained in the two cases. Bergmann and Engel used carbon tetrachloride as solvent for the phosphorus and arsenic trichlorides and benzene for the antimony trichloride. In the present investigation, benzene has been used as the solvent for all three compounds.

Experimental.

Preparation of Materials.—The benzene used was the British Drug Houses "Extra Pure for Molecular Weight Determinations" grade. This did not contain detectable amounts of thiophene. It was dried over sodium wire, recrystallised twice, dried again, and then fractionally distilled. It was then dried thoroughly with sodium wire, which was renewed periodically until no further trace of hydrogen was evolved, and the sodium retained its metallic

---

* O. Werner, 'Z. Anorg. Chem.,' vol. 181, p. 154 (1929).

† 'Phys. Z.,' vol. 32, p. 507 (1931); 'Z. phys. Chem.,' B, vol. 13, p. 232 (1931).

The chlorides were purified by distilling them three times in a high vacuum; on dissolving in the dry benzene they showed no trace of cloudiness, such as would have been produced if any of the products of hydrolysis were present.

The solutions of these pure compounds in dry benzene showed practically no action on the silver films forming the plates of the liquid condenser.

Experimental Results.—The results obtained are set out in the tables below. The dielectric constants (ε) were measured by the method described in Part I, Hartshorn and Oliver's value of 2·2725 for the dielectric constant of benzene at 25°* being taken as a standard value. The densities (ρ) were measured accurately to four significant figures by means of a pyknometer. The total polarisation (P) for each solution was calculated according to the modified form of the Clausius-Mosotti equation

$$P = \frac{\varepsilon - 1}{\varepsilon + 2} \cdot \frac{M_1 f_1 + M_2 f_2}{\rho},$$

where f_1 and f_2 are the mol fractions of the solute and solvent respectively, and M_1 and M_2 their molecular weights, respectively. Now this polarisation, P, is equal to $P_1 f_1 + P_2 f_2$, where P_1 and P_2 are the total polarisations of the solute and solvent respectively. From the known values of f_1, f_2 and P_2, the value of P_1 could therefore be calculated. The values of P_1 for different concentrations were plotted against f_1, and the curve produced extrapolated to zero concentration of the solute. This yielded the value of the polarisation of the solute at infinitely great dilution.

The polarisation thus determined may be regarded as the sum of three terms, P_0, P_E, and P_A.† The first, the orientation polarisation, is due to the permanent dipoles, whilst the second and third, the electronic and atomic polarisations, are due to electronic and atomic displacement respectively. The two latter are proportional only to the polarisability, and are invariant with temperature, whereas the former is proportional to the square of the dipole moment (μ) and inversely proportional to the absolute temperature. It is necessary, therefore, to determine P_0 before the dipole moment can be calculated. For this purpose three distinct methods have been used.

(i) Since the electronic and atomic polarisations are invariant with temperature, whereas the orientation polarisation is inversely proportional to the absolute temperature, the equation $P = P_E + P_A + P_O$ can be written in the form

---

* 'Proc. Roy. Soc.,' A, vol. 123, p. 664 (1929).

† Ebert, 'Z. phys. Chem.,' vol. 113, p. 1 (1924).

$$P = A + B/T,$$

where $A = P_E + P_A$ and $B = 4\pi N\mu^2/9kT$. N being the Avogadro number and k Boltzmann's constant. Consequently, if the total polarisations are measured at two different temperatures, the value of B can be calculated, and therefore the value of μ. ($\mu = 0{\cdot}0127\sqrt{B} \times 10^{-18}$.) In the present series of experiments, the polarisations were measured at 25° and 40°.

(ii) The total polarisation measured for optical frequencies gives only P_E. This can be calculated according to the Lorenz-Lorentz equation

$$n^2 - 1 \quad \frac{M}{\rho},$$

where n, M and ρ are the refractive index, molecular weight and density respectively of the pure polar compound. In accordance with the suggestion of Debye,[*] n is referred to the D line of sodium. Subtracting this value of P_E from the total polarisation gives an approximate value of P_0. This method of calculation neglects P_A, the value of which is small.

(iii) It is assumed by Ebert (*loc. cit.*) that the polarisation calculated from the dielectric constant of the pure polar compound in the solid state gives the value of $P_E + P_A$, which will be the same for both the solid and liquid states. The veracity of this assumption is rather open to question, but if it be true approximately, the value of P_0 can evidently be determined from the total polarisation at one temperature and the dielectric constant and the density of the substance in the solid state.

In the succeeding tables the vertical columns refer to different solutions, which are arranged in increasing order of concentration.

Phosphorus Trichloride.

Temperature 25° C.

	Benzene.	I.	II.	III.	IV.	V.
f_1	0	0·0245	0·0637	0·1201	0·1670	0·2030
$M_1f_1 + M_2f_2$	78	79·46	81·79	85·16	87·94	90·08
ρ	0·8738	0·8899	0·9164	0·9548	0·9872	1·0105
ϵ	2·2725	2·318	2·389	2·484	2·560	2·609
$P_1f_1 + P_2f_2$	26·59	27·25	28·25	29·52	30·48	31·12
P_2f_2	26·59	25·94	24·90	23·40	22·15	21·20
P_1f_1	—	1·31	3·35	6·12	8·31	9·92
P_1	—	53·4	52·6	50·9	49·9	48·8

Whence extrapolated value of P_1 for $f_1 = 0$ is 54·0.

---

[*] "Polar Molecules," p. 43 (1929).

Temperature 40° C.

	Benzene.	I.	II.	III.	IV.	V.
f_1	0	0·0245	0·0637	0·1201	0·1670	0·2030
$M_1f_1 + M_2f_2$	78	79·46	81·79	85·16	87·94	90·08
ρ	0·8575	0·8730	0·8989	0·9368	0·9677	0·9900
ϵ	2·243	2·283	2·350	2·440	2·510	2·553
$P_1f_1 + P_2f_2$	26·64	27·26	28·26	29·48	30·43	31·04
P_2f_2	26·64	25·98	24·94	23·44	22·19	21·24
P_1f_1	—	1·28	3·30	6·04	8·24	9·80
P_1	—	52·2	51·6	50·3	49·3	48·2

Extrapolated value of P_1 for $f_1 = 0$ is 53·2 c.c.

Calculating the dipole moment from the change in the polarisation with change in temperature, we have

$$P_{25^\circ} = 54\cdot0 \text{ c.c.} \qquad P_{40^\circ} = 53\cdot2 \text{ c.c.}$$

Whence

$$B = 0\cdot8 \times 298 \times 313/15 = 4973$$

and

$$A = 37\cdot3 \text{ c.c.}$$

and therefore

$$\mu = 0\cdot0127 \times \sqrt{4973} \times 10^{-18}$$
$$= 0\cdot90 \times 10^{-18} \text{ e.s.u.}$$

From the above 25° polarisation data, and optical data, we have the following:—

n_{18° for liquid PCl_3 (sodium D line) = 1·51215,
Density of liquid PCl_3 at 18° = 1·579.

Whence from the Lorenz-Lorentz equation $P_E = 26\cdot15$ c.c. Hence

$$P_O = 54\cdot0 - 26\cdot15 = 27\cdot9 \text{ c.c.}$$
$$B = 27\cdot9 \times 298 = 8{,}314,$$

and therefore

$$\mu = 1\cdot16 \times 10^{-18} \text{ e.s.u.}$$

Arsenic Trichloride.

Temperature 20° C.

	Benzene.	I.	II.	III.	IV.	V.
f_1	0	0·0285	0·0450	0·0513	0·0632	0·0743
$M_1f_1 + M_2f_2$	78	80·95	82·66	83·31	84·54	85·69
ρ	0·8738	0·9106	0·9315	0·9399	0·9554	0·9680
ϵ	2·2725	2·480	2·605	2·656	2·740	2·814
$P_1f_1 + P_2f_2$	26·59	29·39	30·92	31·52	32·48	33·36
P_2f_2	26·59	25·83	25·39	25·23	24·91	24·61
P_1f_1	—	3·56	5·53	6·29	7·57	8·75
P_1	—	125·0	122·9	122·4	119·7	117·7

Extrapolated value of P_1 for $f_1 = 0$ is 128·2.

Temperature 40° C.

	Benzene.	I.	II.	III.	IV.	V.
f_1	0	0·0285	0·0450	0·0513	0·0632	0·0743
$M_1f_1 + M_2f_2$	78	80·95	82·66	83·31	84·54	85·69
ρ	0·8575	0·8944	0·9152	0·9230	0·9378	0·9512
ϵ	2·243	2·438	2·551	2·594	2·673	2·747
$P_1f_1 + P_2f_2$	26·64	29·33	30·78	31·32	32·30	33·15
P_2f_2	26·64	25·89	25·45	25·29	24·96	24·67
P_1f_1	—	3·44	5·33	6·03	7·34	8·48
P_1	—	120·3	118·3	117·6	116·1	114·1

Extrapolated value of P_1 for $f_1 = 0$ is 123·6.

Calculating the dipole moment from the temperature coefficient of the polarisation, we have

$$P_{25^\circ} = 128\cdot2 \text{ c.c.} \qquad P_{40^\circ} = 123\cdot6 \text{ c.c.}$$

Whence

$$B = 4\cdot6 \times 298 \times 313/15 = 28{,}600$$

$$A = 32\cdot3 \text{ c.c.}$$

$$\mu = 2\cdot15 \times 10^{-18} \text{ e.s.u.}$$

If the 25° polarisation data be employed and combined with the optical data for the pure arsenic trichloride, we have the following :—

$n_{15\cdot8^\circ}$ $AsCl_3$ for sodium D line $= 1\cdot60395$

Density liquid $AsCl_3$ at 15·8° = 2·016.

From which

$$P_E = 30\cdot96 \text{ c.c.}$$

Therefore

$$P_0 = 97\cdot2 \text{ c.c. at } 25^\circ \text{ C.}$$

and

$$B = 28{,}965.$$

From which

$$\mu = 2\cdot17 \times 10^{-18} \text{ e.s.u.}$$

If, instead of the optical data for the pure liquid arsenic trichloride, Bergmann and Engel's optical data for arsenic trichloride solutions be employed, one obtains that $P_E = 30\cdot2$ c.c., $B = 29{,}200$, and $\mu = 2\cdot17 \times 10^{-18}$ e.s.u.

Antimony Trichloride.

Temperature 25° C.

	Benzene.	I.	II.	III.	IV.	V.
f_1	0	0·00460	0·00676	0·00821	0·01215	0·01445
$M_1f_1 + M_2f_2$	78	78·71	79·00	79·23	79·80	80·15
ρ	0·8738	0·8817	0·8856	0·8881	0·8951	0·8992
ϵ	2·2725	2·377	2·425	2·460	2·546	2·588
$P_1f_1 + P_2f_2$	26·59	28·09	28·77	29·21	30·32	30·84
P_2f_2	26·59	26·46	26·41	26·36	26·27	26·21
P_1f_1	—	1·63	2·36	2·84	4·05	4·63
P_1	—	354·4	349·1	347·5	333·6	320·4

Extrapolated value of P_1 for $f_1 = 0$ is 368 c.c.

Temperature 40° C.

	Benzene.	I.	II.	III.	IV.	V.
f_1	0	0·00460	0·00676	0·00821	0·01215	0·01445
$M_1f_1 + M_2f_2$	78	78·71	79·00	79·23	79·80	80·15
ρ	0·8575	0·8656	0·8694	0·8719	0·8791	0·8830
ϵ	2·243	2·340	2·389	2·417	2·494	2·534
$P_1f_1 + P_2f_2$	26·64	28·08	28·72	29·15	30·18	30·71
P_2f_2	26·64	26·51	26·46	26·41	26·32	26·26
P_1f_1	—	1·57	2·26	2·74	3·86	4·45
P_1	—	341·3	334·3	334·1	317·7	307·9

Extrapolated value of P_1 for $f_1 = 0$ is 354 c.c.

Calculating the value of the dipole moment from the temperature coefficient of the polarisation, we have

$$P_{25^\circ} = 368 \text{ c.c.} \qquad P_{40^\circ} = 354 \text{ c.c.}$$

Whence

$$B = 14 \times 298 \times 313/15 = 87{,}040$$

and

$$A = 76 \text{ c.c.}$$

Whence $\mu = 0\cdot0127 \times 10^{-18} \times \sqrt{87040} = 3\cdot75 \times 10^{-18}$ e.s.u.

From measurements of the refractive indexes of solutions of antimony trichloride in benzene, Bergmann and Engel (*loc. cit.*) found the value of P_E for antimony trichloride at infinite dilution to be 31·5 c.c.

Hence at 25°,

$$P_0 + P_A = 336 \text{ c.c.}$$

From which

$$B = 100{,}100 \quad \text{and} \quad \mu = 4\cdot02 \times 10^{-18} \text{ e.s.u.}$$

Lastly, if we assume that the value of $P_E + P_A$ is the same for both the solid and liquid states, we have the following data; dielectric constant in the solid state is 5·4 at 18° C.,* density solid at 18° = 3·06. (In the absence of any accurate value of the density at this temperature this is an estimated value only.)

Whence

$$P_E + P_A = 44{\cdot}0 \text{ c.c.}$$

therefore

$$P_0 \text{ at } 25° = 368 - 44 = 324 \text{ c.c.}$$

This gives

$$B = 96{,}530 \quad \text{and} \quad \mu = 3{\cdot}93 \times 10^{-18} \text{ e.s.u.}$$

Discussion of Results.—As has been seen previously, the actual values obtained for the dipole moments vary somewhat according to the method of calculation. The temperature range over which the change of polarisation has been measured is not sufficiently wide to lead to extremely accurate results, but it is interesting to note that in each case the figure obtained from the change of the polarisation with temperature is the lowest. The results are summarised below, and are compared with the corresponding values found by Werner and by Bergmann and Engel.

	PCl_3.	$AsCl_3$.	$SbCl_3$.
Temperature coefficient of polarisation	0·90 × 10^{-18}	·15 × 10^{-18}	3·75 × 10^{-18}
Polarisation at 25° and refractivity	1·16	·17	4·02
Polarisation at 25° and polarisation in the solid state			3·93
Werner			3·64 in benzene 3·90 in ether
Bergmann and Engel	0·80	1·97	4·06

Thus the dipole moments in this series of compounds increase with increasing atomic weight of the central atom. This is exactly the reverse of the progression observed with the corresponding series of hydrides, as is shown in the following table:—

		NH_3	1·48 × 10^{-18}
PCl_3	0·90 × 10^{-18}	PH_3	0·55
$AsCl_3$	2·15	AsH_3	0·15
$SbCl_3$	3·75		

---

* Schlundt, 'J. Phys. Chem.,' vol. 13, p. 669 (1909).

The values for ammonia, phosphine, and arsine are taken from the results of Watson.* The increase in the case of the chlorides is associated with the rapidly increasing electropositive character of the central atom. This would be expected to increase the dipole moment in the case of the chlorides, and to diminish the moment in the case of the hydrides.

Summary.

Using the method described in Part I of this series, the dielectric constants and densities of a series of dilute solutions of phosphorus trichloride, arsenic trichloride, and antimony trichloride in benzene have been measured at 25° and at 40°. From the results obtained the electric moments of these molecules have been calculated. The values increase with increasing atomic weight of the Group V element, this being the reverse of the order observed in the case of the hydrides.

In conclusion, the author desires to express his deep indebtedness to the Department of Scientific and Industrial Research for a Senior Award, during the tenure of which this work was carried out, and especially to Professor F. G. Donnan, F.R.S., for the interest which he has shown in these researches.

---

* 'Proc. Roy. Soc.,' A, vol. 117, p. 43 (1927).

Theoretical Intensities in the Spectrum of H_2.

By W. C. PRICE, B.Sc., University College of Swansea.

(Communicated by O. W. Richardson, F.R.S.—Received December 22, 1931.)

For electronic vibrational transitions in which only the lower vibrational quantum number varies, the relative intensities in emission are given by a series whose principal term is

$$\nu^4_{n'n''}\, \mathrm{I}^2_{n'n''},$$

where

$$\mathrm{I}_{n'n''} = \int \mathrm{F}'_{n'}\, \mathrm{F}''_{n''}\, dr. \quad \text{and} \quad \mathrm{F} = \mathrm{P}r.$$

Here r is the nuclear separation, and P has its usual meaning, as in Kronig's text-book. Thus to this accuracy the calculated intensities depend only on the nature of the wave-functions F that are used. These in their turn depend on the potential energy functions U of the electronic states concerned. Davidson* discusses various potential energy formulæ and their eigenfunctions. The formulæ will here be applied to those bands in the visible spectrum whose structure is sufficiently regular to enable the necessary constants to be specified accurately. In all cases numerical intensity measurements are available for comparison.

The Harmonic Oscillator.—The eigenfunctions are well known. For the $2p\,^1\Sigma$ state of hydrogen they are shown in fig. 1. It will be seen that they extend over a considerable range of r. If ξ is $(r - r_0)/r_0$, the functions, even for the smallest n's, are appreciable at $\xi = \pm 0 \cdot 5$. The harmonic potential formula is $\mathrm{U} = 2 \cdot 871\, \xi^2$ volts and is thus the first term of the experimentally determined formula†;

$$\mathrm{U}\,(2p\,^1\Sigma) = 2 \cdot 871\, (\xi^2 - 1 \cdot 605\, \xi^3 + 2 \cdot 54\, \xi^4 - \ldots). \qquad (1)$$

(It should be remarked that the U's throughout this paper are defined so as to be zero at their minima.) The corresponding harmonic formula for $3d\,^1\Pi_b$ is $\mathrm{U} = 5 \cdot 365\, \xi^2$, the experimental series being‡

$$\mathrm{U}\,(3d\,^1\Pi_b) = 5 \cdot 365\, (\S^2 - 1 \cdot 966\, \xi^3 + 3 \cdot 05\, \xi^4 - \ldots). \qquad (2)$$

---

* 'Proc. Roy. Soc.,' A, vol. 135, p. 459 (1932).

† See O. W. Richardson and P. M. Davidson, 'Proc. Roy. Soc.,' A, vol. 125, p. 23 (1929). The spectroscopic constants, which are usually given in terms of the old mechanics, must, of course, be converted to their values on the wave mechanics.

‡ This state shows rotational uncoupling, and is considered theoretically in a paper by Davidson, not yet published. The constants here used are based on this work.

The values of the intensities can be found either by algebraic integration, as has been done by Hutchisson,* or by graphical integration, which is the method used in this paper for the more complex types of eigenfunctions. In Table I, the intensity for the transition $(0' - 0'')$ is made 286 for comparison with the experimental measurements of Kapuscinski and Eymers.† Q3 lines are used throughout the table, and the calculated intensity of the first maximum in each row is made to agree with the experimental value.

Table I.—Intensities for $3d\,{}^1\Pi_b \rightarrow 2p\,{}^1\Sigma$.

n'' n'	0.	1.	2.	3.	
0	286	95	29·1	9·1	Measurement.
	286	182·2	28·5	1·01	Harmonic.
	286	135·8	39·7	9·55	New eigenfunctions.
	286	131·5	31·02	5·0	Morse.
	286	132·0	34·0	9·8	Morse modified.
1	375	35·4	159·0	56	Measurement.
	375	66·6	440	163	Harmonic.
	375	30·1	126·0	81	New eigenfunctions.
	375	82·8	210·2	90·7	Morse.
	375	48·0	130·0	67	Morse modified.
2	75·2	395	3·4	61	Measurement.
	573·0	395	9·8	725·0	Harmonic.
	120·6	395	4·41	84·1	New eigenfunctions.
	144·3	395	4·43	172	Morse.
	107	395	1·0	83	Morse modified.
3	—	102	142	29·3	Measurement.
	50·7	102	7·74	27·5	Harmonic.
	1·14	102	144	21	New eigenfunctions.
	0·8	102	134·2	0·2	Morse.
	0·5	102	167	16	Morse modified.

The agreement with the experimental intensities is not good; but for the other functions in this paper, all of which should represent U more accurately, the results are much better.

The Morse Function.‡—This is one of the best known attempts to obtain a readily quantised U formula, valid over a large range of r. The formula is

$$U = D(1 - e^{-ar_0\xi})^2 \tag{3}$$

$$= Da^2r_0^2(\xi^2 - ar_0\xi^3 + \tfrac{7}{12}a^2r_0^2\xi^4 - \ldots), \tag{4}$$

---

* 'Phys. Rev.,' vol. 36, p. 410 (1930), and vol. 37, p. 45 (1931).

† 'Proc. Roy. Soc.,' A, vol. 122, p. 58 (1929).

‡ 'Phys. Rev.,' vol. 34, p. 57 (1929). Its validity is discussed by Davidson, *loc. cit.*

where

$$D = h\omega_0^2/4x\omega_0 \quad \text{and} \quad a^2 = 2\pi^2 M\omega_0^2/D.$$

The energies are

$$E/h = (n + \tfrac{1}{2})\,\omega_0 - x\omega_0\,(n + \tfrac{1}{2})^2. \tag{5}$$

If the dissociation energy D is known, and the experimental $\omega_n : n$ curve is nearly linear up to the dissociation point, either of two values of $x\omega_0$, not very different, can be used in the above expressions. One will make the curve go accurately to the experimental D; the other will give the energies very accurately for the smaller n's. For the $2p\,^1\Sigma$ state of hydrogen the curvature of the $\omega_n : n$ graph is appreciable. For ω_0 the "experimental" value (obtained by assuming higher powers of $(n + \frac{1}{2})$ in the energy formula) has been used; and here, as in $3d\,^1\Pi_b$, $x\omega_0$ has been given a value which gives a good general agreement with the observed energy levels. The experimental B_0 has been used, so that the coefficient of ξ^2 in (4), being determined by B_0 and ω_0, will be the same as in the U's given previously. We find for (4)

$$U(2p\,^1\Sigma) = 2\cdot 87\,(\xi^2 - 0\cdot 94\,\xi^3 + 0\cdot 514\,\xi^4 - \ldots)$$
$$U(3d\,^1\Pi_b) = 5\cdot 365\,(\xi^2 - 1\cdot 64\xi^3 + 1\cdot 57\xi^4 - \ldots).$$

The constant to which the $2p\,^1\Sigma$ curve goes is very nearly the experimental D.

The Modified Morse Function.—Davidson (*loc. cit.*) suggests a modification in which the constants D and a are chosen so that the coefficients of ξ^2 and ξ^3 in (4) have their "experimental" values. Usually, of course, the curves do not go to the correct D's, nor do they give the correct values for E. They should, however, give the first few eigenfunctions in the region of $\xi = 0$ more correctly than the unmodified U's; though in the present cases, as Davidson observes, the argument from which this conclusion is drawn may only be valid when n is very small. The U's are

$$U(2p\,^1\Sigma) = 2\cdot 871\,(\xi^2 - 1\cdot 605\,\xi^3 + 1\cdot 503\,\xi^4 - \ldots)$$
$$U(3d\,^1\Pi_b) = 5\cdot 365\,(\xi^2 - 1\cdot 966\,\xi^3 + 2\cdot 245\,\xi^4 - \ldots).$$

The Anharmonic Oscillator.—The eigenfunctions have been given by Hutchisson (*loc. cit.*). They are approximate solutions for the experimental U(ξ) series. They are themselves series in powers of a parameter $\sqrt{\kappa}$, which for hydrogen is rather large, about $\frac{1}{8}$. In practice only three terms of the series are considered, and they are determined by B_0 and the terms of the U(ξ) series as far as ξ^4. Since only three terms in the eigenfunctions are considered, they may not at large $|\,\xi\,|$, behave like the true solutions of the U(ξ) series, whether it is terminated at ξ^4 or not. It must be remembered also that a terminating $U(\xi)$ series cannot represent a molecular U at a distance from the minimum.

Some New Eigenfunctions.—A direct solution of the wave equation, corresponding to a U whose expansion can have any desired coefficients for ξ^2 and ξ^3, has been given by Davidson (*loc. cit.*). The expansions are

$$U\,(2p\,{}^1\Sigma) = 2\cdot871\,(\xi^2 - 1\cdot605\,\xi^3 + 2\cdot11\,\xi^4 - \ldots)$$
$$U\,(3d\,{}^1\Pi_b) = 5\cdot365\,(\xi^2 - 1\cdot966\,\xi^3 + 2\cdot91\,\xi^4 - \ldots).$$

These certainly resemble the experimental series, but at large r the first U goes to infinity approximately as r to the $\frac{2}{3}$. The second U, by chance, is practically identical with Kratzer's function $k\,(1 - 1/\rho)^2$, which is a special case of these U's, and which goes to a constant value as r goes to infinity; the present U goes to infinity as a very small fractional power of r. The general expression for this power is $(2a + 4)$, where a is the coefficient of ξ^3 inside the bracket, and is a negative quantity (between $-1\frac{1}{2}$ and -2 in the hydrogen states).

Comparison.—As may be seen from Table I, the results of the harmonic oscillator show the general defect that the calculated values of the second maxima in the intensity rows are too high. The unmodified Morse results are better, though the same defect is found to a lesser degree. The modified Morse and the new eigenfunctions, in both of which U has the "experimental" coefficient for ξ^3, give fairly concordant results, and give, on the whole, the best agreement with the experimental intensities. It must be remembered, of course, that the expression for the intensities, given at the start of the paper, is itself an approximation.

It will be seen that, in comparison with the "simple harmonic" curves, all the others are stretched out towards the region of greater r (*i.e.*, the roots and turning values are displaced to greater values of r); at the same time the maximum magnitude in the region of great r are increased, while those in the region of small r are diminished.*

The graphs illustrate a general deduction made by Davidson,† that if $\sqrt{\kappa}$ is a small fraction, the eigenfunctions for small n are determined with considerable accuracy, in the range where they are large, by B_0 and the coefficients

---

* Correspondingly in the old quantum theory the nuclei swing with greater amplitude outward (from the equilibrium position) than inward; and they spend a greater time in the outward range than in the inward.

† *Loc. cit.*, Section 2.

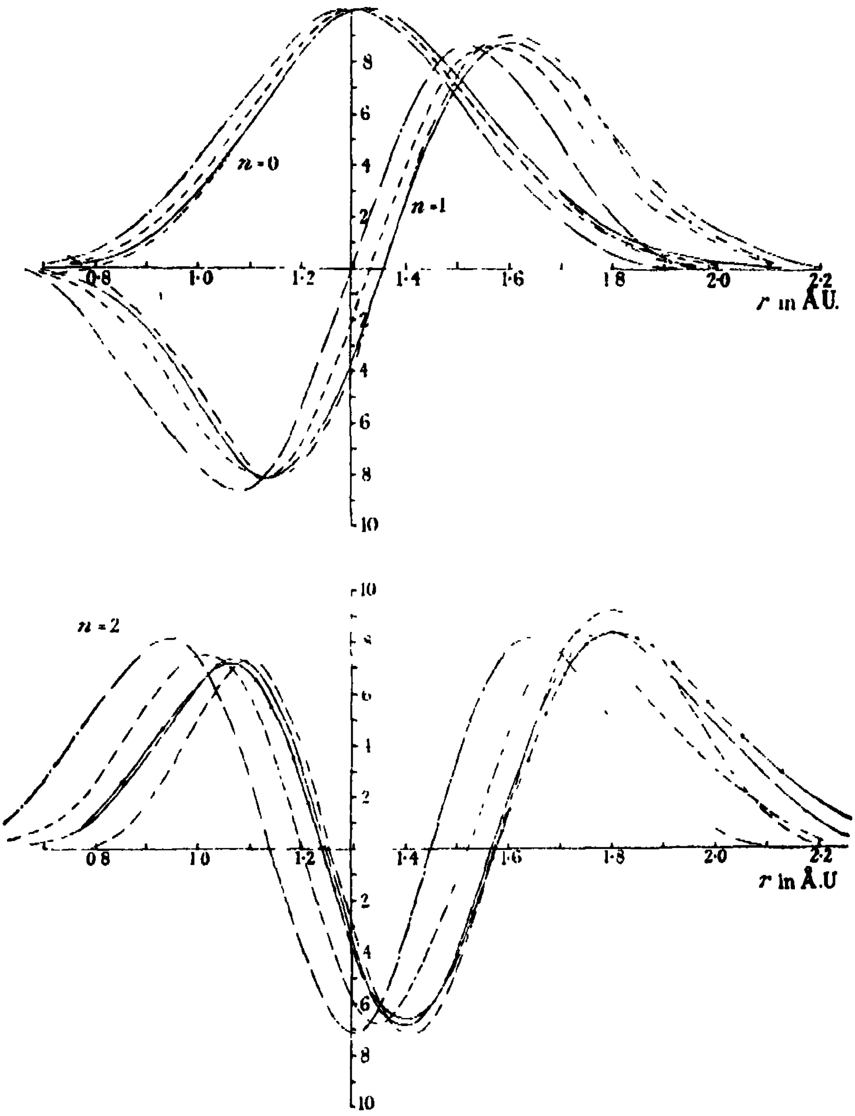

Fig. 1.—Eigenfunctions for $2p\,^1\Sigma$. For convenience the curves are all normalised in such a way that the amplitude of the $n = 0$ harmonic is 10. The axes intersect at r_0.

——‖—— Harmonic functions.
———— New Eigenfunctions.
— · — · — · — Perturbed functions.
— — — — — Morse.
——o—— Morse, modified.

of ξ^2 and ξ^3 in the expansion for the particular one of these U's which we are employing; and that the departure from the harmonic curve is proportional to the coefficient of ξ^3. The curves show to what extent all this is true when $\sqrt{\kappa}$ has the large value $\frac{1}{5}$. Thus it will be seen that at $n = 0$ and $n = 1$ the unmodified Morse curve, for which the coefficient of ξ^3 is $-0 \cdot 94$, lies intermediate between the harmonic curve and the others, for all of which the coefficient is $-1 \cdot 6$. In these n's the curves for the modified Morse and the new eigenfunctions are so close together that a single line has been drawn for them. At $n = 2$ these two curves are still very close together, and the anharmonic oscillator curve departs from them in a way which is connected with the impossible behaviour of anharmonic curves at a distance from the centre (they frequently have the wrong sign, giving the wrong number of nodes). Actually at $n = 2$, and for this large $\sqrt{\kappa}$, the expansion as far as $\sqrt{\kappa}$ terms is inadequate near $\xi = 0$; in fact for this n the $\sqrt{\kappa}$ term vanishes at that point so that the curves would all coincide with the harmonic if later terms were neglected.* Nevertheless the agreement between the modified Morse and the new eigenfunctions is still good throughout the range, the different behaviour of their U's at large r evidently affecting them little.

Before leaving the singlet bands it may be remarked that the relative intensities (experimental) in Table 1 are practically the same from whatever rotational level we take the data. This, indeed, is to be expected, since the F's are very slightly affected by changing the rotational quantum number. It may be remarked also that the bands to $2p\,{}^1\Sigma$ from $3d\,{}^1\Pi_a$ and $3d\,{}^1\Sigma$ are similar in intensity distribution to those from $3d\,{}^1\Pi_b$ which we have considered. This presumably means that the U curves are much the same in the Π and Σ upper states, as indeed we should expect theoretically.

The System $3p\,{}^3\Pi \rightarrow 2s\,{}^3\Sigma$. (*The* α *bands*).—Here the r_0's of the two states are close together, and the U curves are very similar in shape. Thus, as would be expected, the intensities are of the type known as "diagonal." Quite fair results are obtained from the "simple harmonic" calculation; if the anharmonic oscillator is used the effects of the perturbation terms tend to cancel out. Some of the experimental intensities in Table II are represented by question marks, indicating that measurements have not been made so far into the red. The experimental intensities given are an average of the values for $m = 1, 2$ and 3, the obviously blended lines being omitted, and the intensity

---

* The departure of the anharmonic curve from the harmonic at this point is due, of course, to the κ term, which for this n has here its maximum value, determined more by the coefficient of ξ^3 than of ξ^4.

Table II.—Intensities for $3p\,{}^3\Pi \rightarrow 2s\,{}^3\Sigma$.

n' \ n''	0.	1.	2.	3.	
0	100	?	—	–	Measurement.
	(10)	(0)	—	—	Eye estimate.
	100	4	0	0	Harmonic.
	100	4·13	0	0	New eigenfunctions.
1	23	98	?	—	Measurement.
	(9)	(10)	(8)	–	Eye estimate.
	17	98	8	0	Harmonic.
	20	98	8·3	0	New eigenfunctions.
2	2·5	36	86	?	Measurement.
	(1)	(10)	(10)	(6)	Eye estimate.
	0·04	35·5	86	13	Harmonic.
	3·8	38·8	86	9·5	New eigenfunctions.
3	0	5·3	40	60	Measurement.
	(0)	(4)	(10)	(10)	Eye estimate.
	0	0·04	40	52	Harmonic.
	0	4·1	40	71·4	New eigenfunctions.

at (0′ — 0″) being brought up to 100. The figures in brackets are the eye estimates of Gale, Monk and Lee.*

The new eigenfunctions for these states correspond to the potential formulæ

$$U\,(2s\,{}^3\Sigma) = 6\cdot36\,(\xi^2 - 1\cdot626\,\xi^3 + 2\cdot21\,\xi^4 - \ldots)$$

$$U\,(3p\,{}^3\Pi) = 5\cdot70\,(\xi^2 - 1\cdot56\xi^3 + 2\cdot1\xi^4 - \ldots).$$

Thus they differ considerably from the "harmonic" functions; but the tables only differ markedly in the weaker intensities (2′ — 1″), (3′ — 2″), and it is here that the more accurate functions justify themselves by predicting the correct intensities where the "harmonic" values are far too small.

The System $4p\,{}^3\Pi \rightarrow 2s\,{}^3\Sigma$. (*The* β *bands.*)—The U of the upper state is practically the same as in the α bands; hence the same F's can be used without much error, the only change necessary being in the ν^4 factor. The results are shown in Table III. More experimental intensities are available in this system than in the α system, and the extra values agree quite well with the calculations. Much of the strength in the line (0 — 1″), *m* = 1, (1 (Q)) is required in the singlet system. If we take the *m* = 1 line of the R bands, whose relative intensities are usually much the same as in the Q bands, we find (0′ — 0″) : (0′ — 1″) = 100 : 4·23, which is very close to the predicted ratio 100 : 5.

---

* 'Astrophys. J.,' vol. 67, p. 89 (1928).

Table III.—Intensities for $4p\,^3\Pi \rightarrow 2s\,^3\Sigma$.

n' \ n''	0.	1.	2.	3.	
0	100	about 5	—	—	Average measurement.
	100	5	0	00	New eigenfunctions.
1	17·2	94	13	—	Average measurement.
	16·4	94	9·4	0	New eigenfunctions.
2	—	17	60	21	Average measurement.
	1·7	18	60	9·2	New eigenfunctions.
3	—	—	16	32	Average measurement.
	00	1·47	15·9	32	New eigenfunctions.

Corresponding calculations have also been made with the old quantum theory—Condon's original theory in its quantitative form. Certain arbitrary assumptions have to be made. The method fails in two important respects; firstly it limits the number of transitions possible, and secondly it does not predict the intensities at all well. The central minimum in the rows is not nearly small enough relative to the two maxima.

In conclusion, I should like to thank Dr. Davidson for suggesting this problem and for his interest and encouragement.

Summary.

Theoretical intensities in the band spectrum of hydrogen are calculated for sets of lines differing only in their lower vibrational quantum number. Several types of eigenfunctions are used. The agreement with experiment is good, and some theoretical points are illustrated by means of the eigenfunctions.

The Atomic Scattering Power of Iron for Various X-Ray Wave-Lengths.

By A. J. BRADLEY, Ph.D., and R. A. H. HOPE, B.Sc.

(Communicated by W. L. Bragg, F.R.S.—Received December 23, 1931.)

[PLATE 6.]

1. *Introduction.*

Calculations of f, the atomic scattering factor of an element for X-rays, have hitherto been made on the assumption that the value of f for a given value of $\sin\theta/\lambda$ is independent of wave-length. This assumption is only justified when the frequency of the X-rays is much greater than the characteristic frequency of any of the energy levels in the scattering atom. This condition is realised when a hard radiation such as Mo Kα is used in order to investigate crystals containing only light elements, such as aluminium. Under these conditions it has been found that absolute determination of f made experimentally give results in excellent agreement with theory.*

In many investigations, however, we are dealing with an entirely different set of conditions. For example, investigations of alloys are usually carried out with Cr, Fe or Cu radiation. Often the alloys contain Cr, Mn, Fe, Co, Ni, Cu or Zn, and the K absorption edge for each of these elements is near the wave-length of the radiation employed. Under these circumstances the conditions postulated by the simple theory no longer hold. Dispersion terms must now be introduced into the scattering formula, and we get an effect which may in some degree be compared with the anomalous dispersion of light.

We should therefore anticipate that, on plotting values of f for a given value of $\sin\theta/\lambda$ against λ, a sudden change in the f value would be encountered in the neighbourhood of the absorption edge.

Experiments to test this phenomenon have been made by various investigators. Mark and Szillard† investigated rubidium bromide using strontium and bromine radiations. Later Miss Armstrong‡ in an investigation of the scattering powers of copper and iron, using molybdenum and copper radiations,

---

* James, Brindley and Wood, ' Proc. Roy. Soc.,' A, vol. 125, p. 401 (1929).

† ' Z. Physik.,' vol. 33, p. 688 (1925); Kallmann and Mark, ' Naturwiss.,' p. 648 (1926); ' Ann. Physik.,' vol. 82, p. 585 (1927); Bethe, ' Z. Physik.,' vol. 40, p. 653 (1927); Kronig and Kramers, ' Z. Physik.,' vol. 48, p. 174 (1928).

‡ ' Phys. Rev.,' vol. 34, p. 931 (1929).

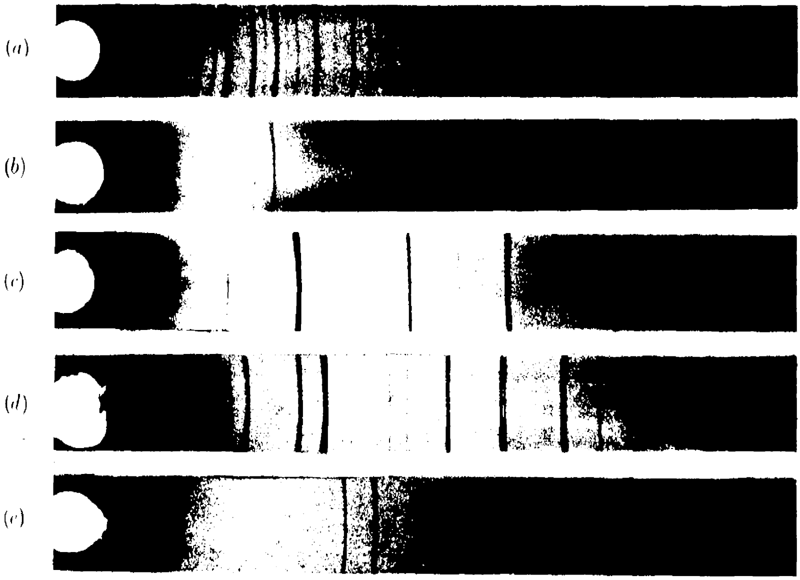

Fig. 1.—X-Ray Powder Photograph of FeAl using different radiations.

(*a*) Molybdenum.	Kα radiation.
(*b*) Copper.	Kα and Kβ radiations.
(*c*) Cobalt.	Kα and Kβ radiations.
(*d*) Iron.	Kα and Kβ radiations.
(*e*) Chromium.	Kα and Kβ radiations.

found the effect very clearly marked. In this investigation the ionisation method was used in order to determine the relative intensities of reflection from different planes of the powdered crystals. The values were then normalised by comparison with the (220) reflection of NaCl, using the absolute value determined by James and Firth* for Mo radiation. The quantitative results of these experiments rested on the assumption that the strength of the (220) reflection of NaCl was the same for Cu as for Mo. This assumption has since been justified by the results obtained by Wyckoff and others. It has been shown conclusively that the value of *f* is independent of wave-length so long as the frequency of the radiation is much greater than that of the absorption edge.

A difficulty in experiments of the above type is that the determination of the absolute values of *f* requires an extremely accurate knowledge of the absorption coefficient of the powder block. An attempt to overcome this difficulty was made by Wyckoff† in an investigation of the scattering powers of nickel and oxygen using NiO. Wyckoff made ionisation measurements on the powdered oxide with molybdenum, copper and nickel Kα radiations. The results were standardised by comparison with the (220) reflection of NaCl. The validity of the Ni values was checked by comparing the oxygen values for different wave-lengths, which should be identical with one another. However, the oxygen curves for the different radiations do not exactly superimpose; although crossing at a certain value of sin θ/λ, they have distinctly different slopes. This makes the precise quantitative value of his results somewhat uncertain, though there is no doubt of the general effect.

The scattering power of nickel shows a decided drop at the absorption edge. Wyckoff's results are given below, for sin $\theta/\lambda = 0\cdot3 \times 10^{-8}$ A.:—

sin $\theta/\lambda \times 10^{-8}$	*f* (Mo Kα)	*f* (Cu Kα)	*f* (Ni Kα)
0·300	16·03	13·57	14·87

It appears from these results that the scattering power falls to its lowest value for Cu radiation, but rises again for Ni radiation. More recently G. A. Morton‡ has investigated the scattering power of Cu and O in cuprous oxide, using Cu radiation. His work confirms the previous results of Miss Armstrong on the scattering power of metallic copper, the Cu *f* curves agreeing within the limits of experimental error. The oxygen curve agrees with that found by Wyckoff from NiO.*

---

* 'Proc. Roy. Soc.,' A, vol. 117, p. 62 (1927).

† 'Phys. Rev.,' vol. 35, p. 583 (1930).

‡ 'Phys. Rev.,' vol. 38, p. 41 (1931).

During a recent X-ray investigation of the iron-aluminium system, it was found that an iron-aluminium alloy, consisting of 32·6 per cent. Al with the composition FeAl, has a structure of the body-centred cubic type in which iron atoms occupy the positions at the cube corners, and aluminium atoms at the centres, or *vice versa.*

It is evident that from such a structure we shall get sum and difference spectra in which the scattered waves from iron and aluminium atoms add or subtract according as $(h + k + l)$ is even or odd, where h, k, l, are the indices of the reflection. From such a set of spectra it is easy to get a set of relative values for the scattering of iron and of aluminium. Using the aluminium values as a basis for normalisation, a set of absolute f values for iron can be obtained. Thus it is evident that the accuracy of the f curve so obtained depends only on the validity of the aluminium curve used as the basis for normalisation. The theoretical f curve of aluminium deduced by Hartree's method has been shown by James, Brindley and Wood (*loc. cit.*) to be a true representation of the scattering power of aluminium. This method of normalising from the aluminium f curve has the advantage that the comparison is made in only one crystal, so that there is no uncertainty from the application of the absorption factor.

2. (*a*) *Preparation of the Alloy.*

In order that the alloy should be obtained in as pure a state as possible it was prepared in a high frequency induction furnace. The alloy was made from electrolytic iron and aluminium 99·6 per cent. pure, to the composition 32·6 per cent. aluminium.

An alumina lined crucible was used in order to prevent any reaction of the metals with the material of the crucible, and the metals were melted together under a small pressure of hydrogen. The fullest possible precautions were taken to make a homogeneous alloy free from pinholes. The metals were carefully weighed out in the correct proportions and there was no furnace loss. On examining the alloy it was found to consist, throughout its entire volume, of a homogeneous mass of almost perfectly formed minute crystals.

A number of these crystals were selected and, on account of the brittle nature of the alloy, were ground in an agate mortar. The powder obtained was so fine that it passed through the 380 mesh per linear inch sieve by simply being dropped on to it. The alloy grains thus sieved were used in the investigations. On account of the extreme fineness of these particles it was hoped that extinction effects would be negligible. The powder was heated up to 750° C., kept there for 1 hour to remove strain, and then slowly cooled to room temperature, the whole process taking 8 to 10 hours.

---

* 'Phys. Rev.,' vol. 36, p. 1116 (1930).

(*b*) *Photographic Technique.*

X-ray powder photographs were taken, using six different radiations. Fig. 1, Plate 6, shows the photographs obtained with the five radiations employed. These were Mo, Cu, Co, Fe and Cr. In the cases of Co and Cr the anticathode was made by the electro-deposition of the metals in question on a copper base. With the exception of molybdenum the radiation was unfiltered, and each photograph contains both $K\alpha$ and $K\beta$ lines, but only the former were used. The lines are crowded together so closely on the molybdenum photograph that it was deemed necessary to filter out the β radiation and a zirconia screen was used for the purpose.

After the exposure had been made a calibration scale was added to each film, using the same radiation, and the film was developed for a constant time at a constant temperature. Care was taken to ensure even development, a special developing dish being designed for this purpose.

Each photograph was carefully photometered, using a Cambridge microphotometer. A null method is used which gives direct readings of the blackening of the film. The readings were taken at regular intervals and the values converted into intensities by means of the calibration curves The intensity values were next plotted against the distance along the film. The integrated value of each reflection was obtained by adding up the areas of the peaks above the background of general radiation. In some cases the slope of the peaks was so great that a correction had to be introduced for slit width. This is, however, a simple matter, the correction being at the most about 1 or 2 per cent.

(*c*) *Absorption Correction.*

By means of the above technique a series of relative intensities was obtained. They were corrected for absorption by Claassen's* method, the following experimental procedure being adopted. Each of the five photographs was taken with the same specimen. The dimensions of the specimen were found with a microscope. The Canada balsam was then dissolved away and the powder carefully weighed. From these values a determination of μR was made, and the correction could be applied. (μ is the mean absorption coefficient of the powder used allowing for dilution by the Canada balsam, and R is the radius of the powder rod.) The formula is

---

* 'Phil. Mag.,' vol. 9, p. 57 (1930).

$$\mu R = \frac{\mu}{\rho} \cdot \frac{m}{\pi R l},$$

where

μ/ρ = mass absorption coefficient.

l = length of powder rod.

m = mass of FeAl in powder rod.

The approximate value of μ/ρ was obtained by means of Jönsson's* tables.

The absorption data for each photograph are summarised below.

Table I.

$R = 0 \cdot 025$ cm. $l = 0 \cdot 334$ cm. $m = 0 \cdot 0011$ gm.

Radiation.	μ/ρ for Al.	μ/ρ for Fe.	μ/ρ for FeAl.	μR.
Mo Kα	5·3	38·3	27·5	1·13
Cu Kα	48·7	324·0	233·9	9·63
Co Kα	72·6	55·8	61·3	2·52
Fe Kα	92·8	72·8	79·3	3·26
Cr Kα	149·0	114·6	125·4	5·16

The value of the absorption factor A for a given value of μR depends upon the angle of reflection. It may be calculated according to Claassen's method for a given angle. In practice it is most convenient to calculate values of A for a series of values of μR and interpolate at the desired value of μR. This procedure is carried out for each of the values of the glancing angle, $\theta = 0°$, $22\frac{1}{2}°$, $45°$, $67\frac{1}{2}°$, $90°$. Values for intermediate angles are obtained by graphical interpolation.

The method of applying the correction is illustrated by a detailed account for the Mo radiation given in Table II.

The second column of this table gives the mean of the observed intensity values of the two lines on either side of the film. These values are purely relative and must ultimately be reduced to an absolute scale. Before this can be done it is necessary to allow for those factors, namely, the number of

---

* Uppsala Universitets Arsskrift, 1928.

Table II.—Photometer Measurements from FeAl. (Mo Kα Radiation).

Line *hkl*.	Relative intensity (I).	Absorption factor (A).	Planar factor (*p*).	θ factor $\frac{1+\cos^2 2\theta}{\sin^2\theta\cos\theta}$	F relative.	
					h + *k* + *l* odd.	*h* + *k* + *l* even.
100	1074	16·48	6	134	8·98	—
110	6628	16·59	12	63·7	—	22·8
111	260	16·71	8	42·1	6·72	—
200	1036	16·82	6	30·7	—	18·3
210	343	16·94	24	23·9	5·94	—
211	2029	17·05	24	19·6	—	15·9
220	585	17·30	12	14·2	—	14·1
300, 221	148	17·41	30	12·4	4·78	—
310	659	17·55	24	10·8	—	12·0
311	87	17·70	24	9·7	4·59	—
222	147	17·89	8	8·65	—	10·9
320	42	18·01	24	7·85	3·52	—
321	616	18·15	48	7·25	—	9·87
400	48	18·50	6	6·15	—	8·33
410, 322	42	18·70	48	5·6	2·88	—
411, 330	243	18·85	36	5·25	—	8·27
331	17	18·98	24	4·9	2·76	—
420	124	19·12	24	4·6	—	7·68

co-operating planes, absorption factor and angular factor, which vary for different lines on the film.

We may write

$$I = K\,\frac{1+\cos^2 2\theta}{\sin^2\theta\cos\theta}\,p\,A\,F^2,$$

where

I is the observed relative intensity.

θ is the glancing angle, and $\frac{1+\cos^2 2\theta}{\sin^2\theta\cos\theta}$ is the angular factor.

F is the structure factor.

p is the number of co-operating planes and A is the absorption factor.

K is a factor which is the same for all the lines on the same film.

Table II gives the appropriate values of $1+\cos^2 2\theta/\sin^2\theta\cos\theta$, *p* and A, leading to the series of relative F values.

(*d*) *Reduction of F Values.*

Photographs of FeAl using five different radiations were photometered, and for each radiation a series of relative F values was obtained. These values, being on a relative scale, must be made absolute before they can be used to determine the atomic scattering factor for iron. The process may be followed through in detail for the case of Mo radiation, for which the relative F values are shown in Table II.

The F values fall into two sets :—

(1) Odd planes, *e.g.*, (100), (111), (210) for which $F = f_{Fe} - f_{Al}$.

(2) Even planes, *e.g.*, (110), (200), (211) for which $F = f_{Fe} + f_{Al}$.

On plotting these values against the corresponding values of $\sin \theta/\lambda$, we get two curves of the kind shown in figs. 2 to 6. It is a simple matter to deduce from these curves a relative Al f curve.

In order to normalise we change the scale until the observed f curve for Al coincides with a standard Al curve. To apply this method correctly we should have to know the absolute value of fAl in FeAl at room temperature. We cannot use the f values obtained for other crystals without reckoning with the difference in temperature factor. This factor has the effect of changing

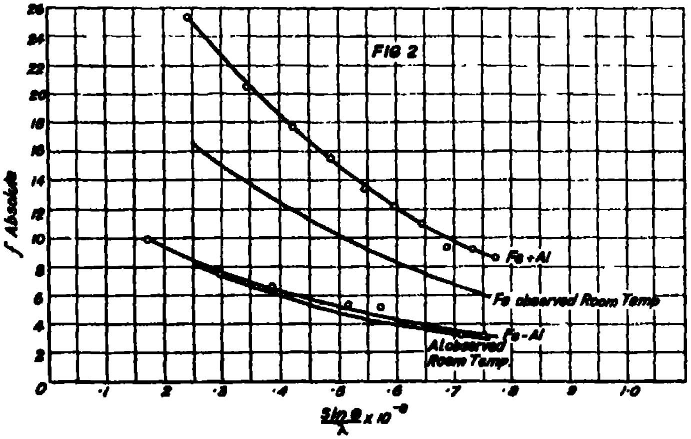
FIG 2

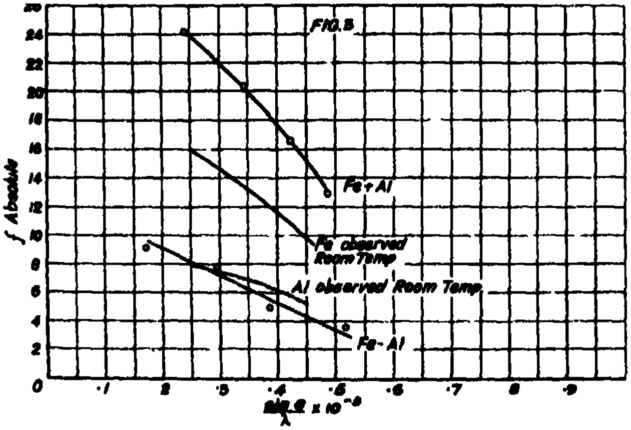
FIG. 3

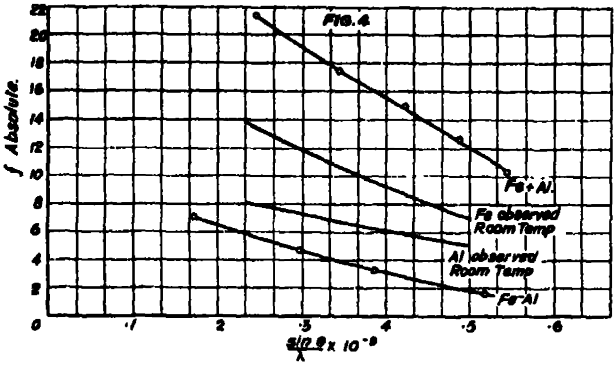

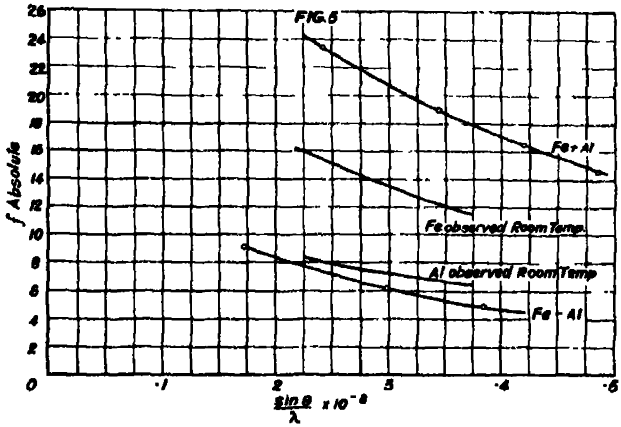

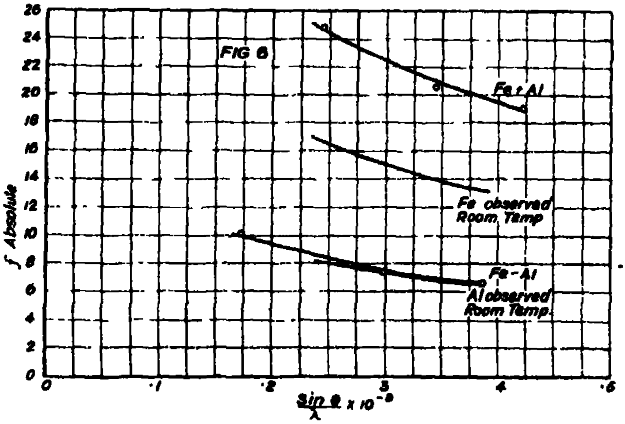

FIGS. 2–6.—Absolute *f* curves at room temperature. Fig. 2, Mo Kα; fig. 3, Cu Kα; fig. 4, Co Kα; fig. 5, Fe Kα; fig. 6, Cr Kα.

the slope of the *f* curve. The simplest way to make the comparison is to reduce our measurements to absolute zero. We may then compare the observed

f curve for Al directly with the f curve deduced by Hartree's method. The Hartree f curve is directly applicable to the theoretical condition of absolute zero and absence of zero-point energy, and has received ample experimental corroboration by the work of James, Brindley and Wood (*loc. cit.*) and of Bearden.*

The normalisation of our results thus involves the determination of two factors: (1) an empirical proportionality factor which fixes the absolute scale of the results; (2) the temperature factor which fixes the slope of the curves. In making the experimental f curve for Al obtained with Mo radiation coincide with the Hartree f curve, we fix both these factors:—

Let

$x =$ observed relative f value at room temperature.

$f =$ absolute f value at room temperature.

$f_0 =$ absolute f value at 0° A. in the absence of zero-point energy.

Then we may write

$$x = Cf = Cf_0\, e^{-B(\sin\theta/\lambda)^2},$$

where C is an empirical proportionality factor and B represents the temperature factor.

The evaluation of B and C may be carried out graphically. Taking logarithms we have

$$(\log x - \log f_0) = \log C - 0{\cdot}4343\, B\left(\frac{\sin\theta}{\lambda}\right)^2.$$

On plotting $(\log x - \log f_0)$ against $(\sin\theta/\lambda)^2$ we get a curve from which it is easy to deduce the values of B and C, since the C term is a constant, whereas the B term varies rapidly.

In the case of Mo radiation, it was found that

$$C = 1{\cdot}11 \qquad B = 0{\cdot}45.$$

The value of B deduced from Mo radiation is also valid for the other radiations. It is only necessary to evaluate the empirical factor C in each case.

3. *Comparison of f Values for different Radiations.*

(*a*) *f Curves at Room Temperature.*—Applying the appropriate value of the normalising factor C deduced in the manner described in the previous section, we obtain a series of F values for different planes of FeAl. These values, shown in Table III, are the observed values at room temperature recalculated to the absolute scale.

---

* 'Phys. Rev.,' vol. 29, p. 20 (1927).

Table III.—Observed Absolute F Values from FeAl using five different Radiations.*

Line *hkl.*	$\sin\theta/\lambda \times 10^{-8}$.	Mo K*a*.	Cu K*a*.	Co K*a*.	Fe K*a*.	Cr K*a*.
100	0·1725	9·97	9·12	7 1	9·1	10·1
110	0·244	25·3	24 1	21·4	23·3	24·8
111	0·2985	7·45	7 8	4·7	6·1	7·4
200	0·345	20·5	20·4	17·5	18·9	20·5
210	0·386	6·6	4 99	3·4	4·8	6·7
211	0·422	17·65	16 6	15·0	16·4	19·0
220	0·487	15·6	12·9	12·7	14 6	—
300, 221	0·517	5·3	3 5	1·63	—	—
310	0·545	13·3	—	10·4	—	—
311	0·572	5·1	—	—	—	—
222	0·598	12·1	—	—	—	—
320	0·622	3·9	—	—	—	—
321	0·645	10·9	—	—	—	—
400	0·689	9·25	—	—	—	—
410, 322	0·711	3·2	—	—	—	—
411, 330	0·731	9·2	—	—	—	—
331	0·751	3 05	—	—	—	—
420	0·771	8·5	—	—	—	—

It is not possible within the limits of the present paper to give an account of the detailed methods employed in order to remove possible sources of error in these results. The technique is likely to give very accurate results, except possibly in the case of Cu radiation. Here there is considerable difficulty. The large value of the absorption coefficient (see Table I) weakens the lines, while the great amount of secondary radiation from the specimen produces a strong background. The contrast is too small for a high degree of accuracy to be attained. The results from Cu must therefore be taken with some caution.

The cobalt and iron films had very clear backgrounds in proportion to the strength of the lines, and the results obtained from these films are probably extremely accurate. The results from molybdenum and chromium will also be very good, but a few individual weak lines may be slightly out. But errors in individual readings are likely to be eliminated by the graphical treatment now to be described, and this is especially true for molybdenum where there are many points.

---

* Some slight arithmetical errors were noticed which necessitated an alteration in Table III and in fig. 6. These changes were made at the time the proofs were corrected. They do not influence the final results in figs. 2 and 12.

The experimental f values given in Table III are plotted against $\sin\theta/\lambda$ in figs. 2 to 6. The curves drawn through these points are the f curves for (Fe + Al) and (Fe − Al) respectively; from them are deduced absolute f curves for aluminium and iron: these are also shown in figs. 2 to 6. They are, however, valid only for the crystal FeAl at room temperature and have no general application. They cannot be compared with theoretical values until the temperature correction has been introduced.

(*b*) *f Curves Reduced to Absolute Zero.*—The f curves for Fe and Al shown in figs. 2 to 6 are corrected for temperature effect by means of the factor B already determined. The corrected f curves are shown in figs. 7 to 11, from which the values given in Tables IV and V were obtained.

Table IV.—Experimental f_0 Values for Aluminium for Various Wave-lengths.

$\sin\theta/\lambda \times 10^{-8}$.	0·3	0·4.	0·5	0·6.	0·7.
Hartree (calc.)	7·75	6·6	5·5	4·5	3·7
Mo Kα	7·7	6·5	5·45	4·5	3·75
Cu Kα	7·7	6·55		—	—
Co Kα	7·7	6·6	5·5	—	—
Fe Kα	7·65	6·6	—	—	
Cr Kα	7·7	—	—	—	—

Table V.—Experimental f_0 Values for Iron for Various Wave-lengths.

$\sin\theta/\lambda \times 10^{-8}$.	0·3.	0·4.	0·5.	0·6.	0·7.
Thomas (calc.)	15·6	13·4	11·7	10·2	8·9
Mo Kα	15·6	13·0	11·3	9·8	8·4
Cu Kα	15·1	12·5	—	—	—
Co Kα	12·5	10·2	8·0	—	—
Fe Kα	14·1	11·5	—	—	—
Cr Kα	15·6	—	—	—	—

(*c*) *Discussion of figs.* 7–11.—The observed f curves are now under suitable conditions for comparison with the theoretical f curves. Only one aluminium f curve is shown in each figure. This is the Hartree curve, calculated by the method of self consistent fields, which was used as the basis of normalisation. The observed f curve for Al is indicated by crosses, as the differences are too small for a second Al curve to be drawn. The precise agreement in the case of Mo radiation (fig. 7) is an inevitable consequence of the method of normalisation, since the observed values have been made to fit the theoretical curve in both magnitude and slope.

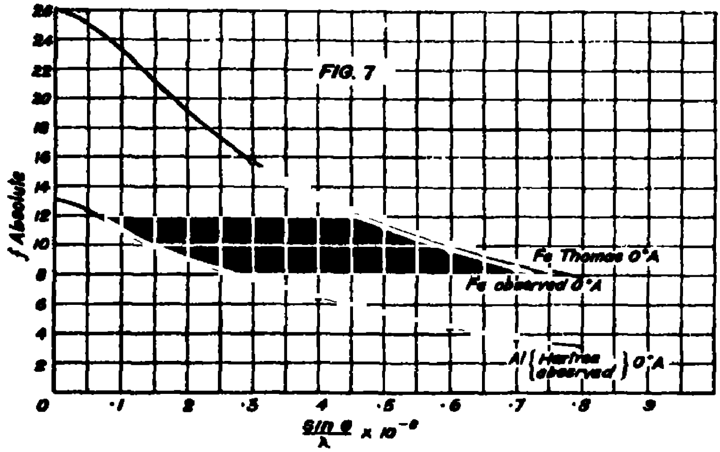
FIG. 7

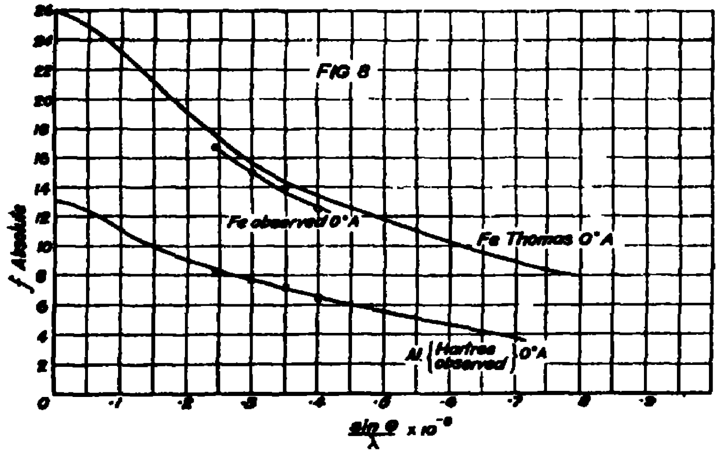
FIG 8

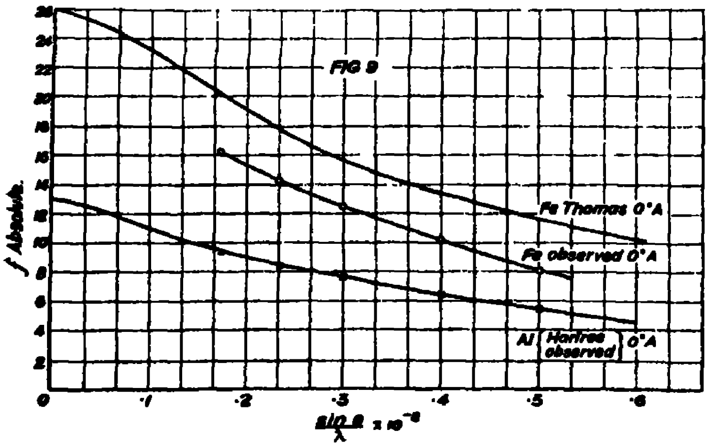
FIG 9

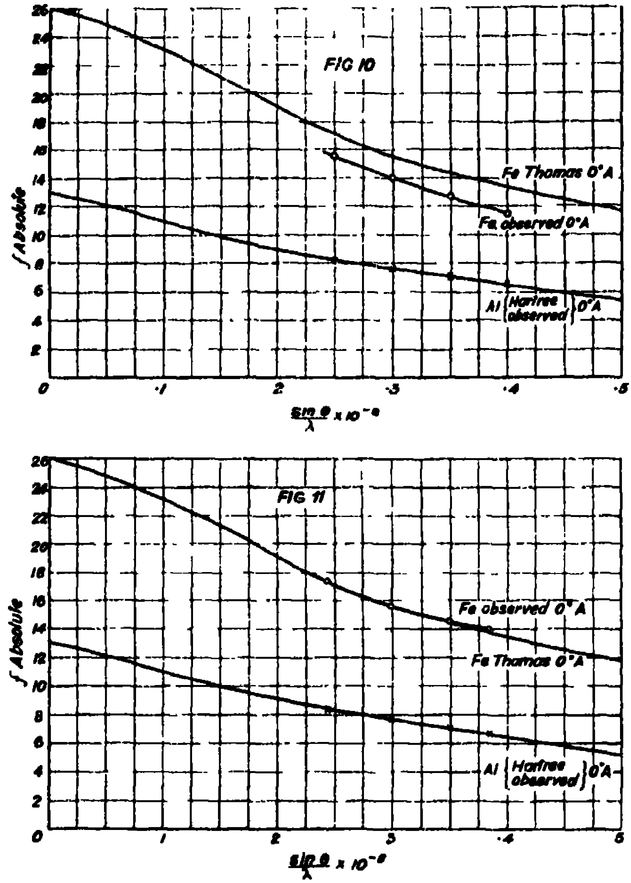

Figs. 7-11.—Absolute f curves corrected for temperature factor. Fig. 7, Mo Kα; fig. 8, Cu Kα; fig. 9, Co Kα; fig. 10, Fe Kα; fig. 11, Cr Kα.

In all other cases the Al f curve is of great importance for the purpose of testing the experimental technique. The scale of the observed f values is again arbitrary, but the slope is determined only by the experimental data, including the temperature factor deduced from the Mo results. The cobalt film is the only other which gives readings at values of sin θ/λ large enough to be affected by the temperature factor. The experimental points for cobalt radiation given in fig. 8 lie exactly on the Hartree curve. This shows that the value of B (the temperature factor) determined from the Mo film is accurate.

The temperature factor is of less importance for Fe and Cr radiations, and the observed f values for aluminium may be used as a check on the accuracy of the photometric method and of the absorption correction. Owing to the large value of λ, the results for chromium radiation are confined to a small range of sin θ/λ values so that the temperature effect is almost negligible. On the other hand, the absorption coefficient is large, and the variation in the absorption factor is further increased by the wide range of angles investigated. The good agreement affords a satisfactory check on this factor.

The results for copper are confined to a small range of angles. Owing to the difficulties introduced by the lack of contrast it was not possible to photometer more than a certain number of inner lines on the copper film, and within these limits the temperature factor is of minor importance. The agreement is very satisfactory considering the difficulties involved in measuring the (Fe—Al) lines on this film.

The agreement at all angles between the observed *f* value for aluminium and the calculated Hartree *f* curve for aluminium for all five radiations may be taken as a most satisfactory confirmation of the accuracy of the experimental technique, and suggests that confidence may be placed in the experimental *f* curves for iron. The latter were made absolute for each radiation using the factors B and C deduced from the corresponding Al curves. So that the validity of each Fe curve depends on the validity of the corresponding Al curve.

The figs. 7 to 11 give, in addition to the Hartree Al curve, two *f* curves for iron. The lower curve is in each case the observed *f* curve normalised in the manner just indicated. The upper curve is a theoretical *f* curve for iron calculated by James and Brindley* according to the Thomas-Fermi† method. Sometimes the two curves overlap and the observed values may then be detected by the circles. It is of great interest to compare the observed and calculated curves in each case, and it will be seen that whereas in some cases they are very close, in others there is a wide difference. This is because the calculated curve makes no allowance for the resonance effect at the absorption edge, which reduces the scattering power of iron with certain radiations.

The molybdenum results (fig. 7) show that for values of sin θ/λ between 0·2 and 0·3 the experimental curve agrees precisely with the theoretical curve. This result is not unexpected, because the frequency of Mo radiation is well above the critical absorption frequency for iron. It confirms our choice of the alloy FeAl for the investigation, showing that the iron and aluminium atoms are completely sorted out into centres and corners of the unit cube respectively.

---

* 'Z. Krist.,' vol. 78, p. 470 (1931); 'Phil. Mag.,' vol. 12, p. 81 (1931).

† L. H. Thomas, 'Proc. Camb. Phil. Soc.,' vol. 23, p. 542 (1927). E. Fermi, 'Z. Physik,' vol. 48, p. 72 (1928).

It will be noted that at values of sin θ/λ beyond 0·3 the observed f curve shows a slight falling off when compared with the Thomas-Fermi curve. The difference reaches a maximum value of 0·4 units and may probably be accounted for by uncertainties in the method of calculation used to obtain the theoretical values.

For copper, cobalt, and iron radiations we have an interesting series of results. It will be seen that in each case the experimental f curve falls decidedly below the Thomas-Fermi curve. It is clear that these results are influenced by the proximity of the absorption edge. The values for copper, fig. 8, are apparently about 0·5 below those for molybdenum. We cannot be quite sure of the validity of this result on account of the difficulties involved in photometering a film which shows so little contrast, and it would be well not to stress the importance of the fact that the copper values are below the molybdenum.

The results for cobalt, fig. 9, are very striking. Referring back to fig. 4, it will be seen that the (Fe — Al) curve falls rapidly, indicating that the scattering power of iron is decreasing much more rapidly than that of aluminium. Turning to fig. 9, it is seen that the rapid fall in the (Fe — Al) curve is due to the fact that the iron curve is, throughout the whole range of angles under investigation, far below the Thomas-Fermi curve. The difference appears to increase with increasing angle, but if we compare the iron curve for Co radiation with that for Mo radiation (see Table V) we see that the difference is constant within the limits of experiment for sin θ/λ 0·3, 0·4, 0·5. The mean difference is about 3·0.

The values for iron radiation, fig. 10, are intermediate between the cobalt and molybdenum values. The difference between the Mo and Fe values is the same as sin $\theta/\lambda = 0{\cdot}3$ and 0·4, and is equal to 1·5.

The Fe f curve, chromium radiation, fig. 11, is most interesting. It is surprising to find that the f curve is identical within the limits of experiment with the Thomas-Fermi curve. The large value of the wave-length permits only a small range of values of sin θ/λ to be investigated, but within this range the results are also identical with those obtained with Mo radiation. This result is most important, as it shows that the f curve for iron has the same value on either side of the absorption edge; a fact which has not hitherto been established.

Referring to Table V, it will be seen that in general the differences in f

with different wave-lengths are constant at all angles. This is a most striking fact. It is therefore possible to plot the f values obtained for any given value of $\sin \theta/\lambda$, and the results will be typical of the whole series. The resulting curve is shown in fig. 12.

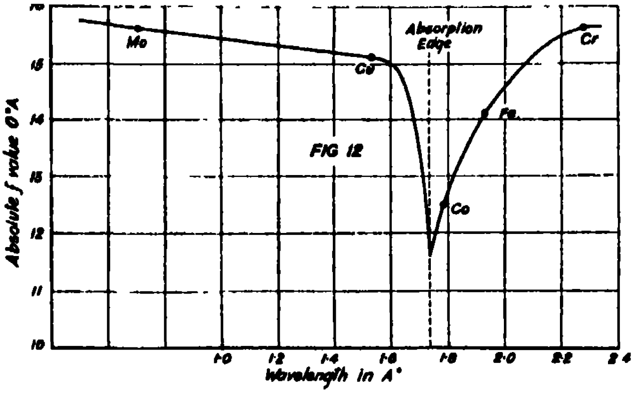

FIG. 12.—Variation of atomic scattering power with wave-length for $\sin \theta/\lambda = 0{\cdot}3$.

Fig. 12 shows the experimental values of f_0 (absolute zero) for iron for $\sin \theta/\lambda = 0{\cdot}3$, plotted against the wave-length of the radiation. The graph shows a big drop in f in the neighbourhood of the absorption edge (indicated by a dotted line). The f values fall from molybdenum on the one side, and rise to chromium on the other, with a minimum at cobalt, the results for iron coming between those of chromium and cobalt. It would be interesting to get the values for manganese in order to complete this portion of the curve. On the short wave-length side the results are less satisfactory. An attempt was made to obtain data from a nickel anticathode, but owing to the large absorption coefficient and the dense blackening of the film, no satisfactory measurements could be made. For the same reason the results with copper radiation are difficult to obtain. It is hoped in the future to modify the technique in order to obtain satisfactory results for Ni, Cu and Zn.

Summary.

(1) An experimental investigation has been made of the atomic scattering factor of Fe using X-rays of different wave-lengths. Powder photographs of the alloy FeAl were made with Mo, Cu, Co, Fe and Cr radiations, and the intensities of the lines were measured photometrically.

(2) The reflections are of two types, Fe + Al and Fe — Al. It was therefore possible to deduce relative f curves for Fe and Al. By reducing the Al f

curve to the same scale as Hartree's f curve for Al, and introducing a temperature factor, the observations were made absolute.

(3) By this means absolute values of the atomic scattering factors of Fe and Al were obtained for different values of sin θ/λ. It was found that the f curves for Al overlap almost exactly at all angles; this provides a check on the accuracy of the method.

(4) The Fe f values for each radiation were compared with the f values calculated by James and Brindley, using the Thomas method. For Mo and Cr radiation the observed results agree closely with theory between sin $\theta/\lambda = 0 \cdot 2$ and $0 \cdot 3$. For larger angles the observed values for Mo fall very slightly below the calculated values (about 0·3 units).

(5) The f values for Cu, Co and Fe radiations are considerably less than the Thomas values. The difference in f for two radiations is almost independent of the angle of reflection.

(6) The f values fall in the following sequence: Mo and Cr, Cu, Fe, Co. The value for Cu is about 0·5 units, for Fe about 1·5, and for Co about 3 units below that of Mo and Cr.

(7) The results indicate that away from the absorption edge the Thomas formula is applicable to Fe, but in the neighbourhood of the absorption edge the scattering power falls off. The effect is very important at large angles where the f value for Fe is, in proportion, much more seriously diminished than at small angles.

We desire to thank Professor W. L. Bragg, F.R.S., for his kind interest in the work. One of us (A.J.B.) is also indebted to Mr. A. P. M. Fleming, C.B.E., Director-Manager, Research and Education Departments, Metropolitan-Vickers Electrical Co., Ltd., for his interest in the work, and permission to publish it.

[*Note added in proof, February* 19, 1932.—Since this work was communicated, a paper has appeared by R. Glocker and K. Schäffer, 'Z. Physik,' vol. 73, p. 289 (1931), dealing with the same problem but by a different method. The scattering factor for iron was determined by using a mixture of the powdered metals. The results differ considerably from those given in the present paper.]

The Collision of Slow Electrons with Atoms. I.—General Theory and Elastic Collisions.

By H. S. W. Massey, B.A., M.Sc., Senior 1851 Exhibitioner, Trinity College, Cambridge, and C. B. O. Mohr, B.A., M.Sc., Trinity College, Cambridge, 1851 Exhibitioner, University of Melbourne.

(Communicated by R. H. Fowler, F.R.S.—Received December 23, 1931.)

Introduction.

An outstanding defect of the old quantum theory was its inability to treat the phenomena occurring in the collision of electrons with atoms, and Born's theory* showed how the new quantum mechanics was capable of removing this defect. The original theory of Born was a method of successive approximations to the solution of the wave equation representing the colliding systems, and could be applied to both elastic and inelastic collisions. In its actual applications, which could be worked out to the first approximation, the theory fell far short of expectations. The Ramsauer effect,† the most interesting phenomenon exhibited in the elastic scattering of electrons, could not be explained, and in the field of inelastic collisions, it failed to provide a means of explaining the excitation of levels of a term system which does not combine with the ground state system, *e.g.*, the excitation of the triplet lines of helium. These failures are, of course, failures of the theory in its first approximation.‡

The first approximation in Born's method of successive approximations neglected the disturbance of the electron waves by the field of the scatterer, and also the possibility of exchange of electrons between the atoms and the colliding beam. The neglect of both these effects becomes important for low velocity impacts, and it was clear that the Ramsauer effect, which is only observed for low velocity electrons, could only be explained by more accurate theory. The question was whether both effects, the distortion of the electron waves by the atomic field, and the exchange of electrons was important, or only one of them.

Oppenheimer§ first pointed out the neglect of exchange in the simple theory, and showed that its inclusion, owing to the Pauli principle, led to the possibility of interference effects between exchanged and incident electron waves, a phenomenon which should produce maximum effect in the case of atoms with closed shells. As the Ramsauer effect is most prominent in these cases, the suggestion was that exchange was the cause of this effect.

---

* 'Z. Physik,' vol. 38, p. 803 (1926).

† *Vide* Kollath, 'Z. Physik,' vol. 31, p. 985 (1930).

‡ When the velocity of the incident electron is less than the orbital velocity of the atomic electrons, Born's series of approximations does not converge though it may be asymptotic.

§ 'Phys. Rev.,' vol. 32, p. 361 (1928).

Oppenheimer did not carry the theory beyond the stage of general results and, meanwhile, Faxen and Holtsmark* developed a method of calculating the scattering of electron waves by a given static field, following methods similar to those used by Rayleigh in his treatment of the scattering of sound waves by obstacles. This method disregarded the effect of exchange, just as Oppenheimer neglected the distortion of the incident waves, but it seemed that in this case the neglect was justified, for the application of Faxen and Holtsmark's method to argon† gave a very good representation of the observed cross section, and also of the angular distributions of the scattered electrons as measured by Bullard and Massey.‡ It thus appeared that exchange was of no importance, and this idea would seem to be justified by a recent paper by Morse and Allis§ in which Faxen and Holtsmark's theory was used for a simple atomic model, enabling results to be obtained for all atoms by suitable adjustment of parameters. They then found that they could explain the observed cross sections of all the elements investigated, both in magnitude and in form of variation with velocity of the incident electrons, using this method.

When, however, one considers the application of the theory to inelastic collisions in connection with the observations, a difficulty at once arises. The application of Oppenheimer's theory to the calculation of the probability of excitation of triplet terms of helium, as made by us in a previous paper,‖ gives results in fair agreement with experiment, which shows that triplet excitation by electrons of low velocity is as probable as, or more so, than that of the corresponding singlets, and is comparable with the probability of elastic scattering. Now the triplet terms can only be excited by electron exchange, as a rearrangement of spins must take place, and so we have direct experimental evidence that electron exchange is an important phenomenon at low velocities. How is this result to be reconciled with the theory of the Ramsauer effect ? This difficulty is further accentuated by the fact that the theory of Paper I, which deals fairly successfully with the inelastic collisions, would indicate a large exchange effect for elastic collisions in helium and hydrogen.

---

* 'Z. Physik,' vol. 45, p. 307 (1927).

† 'Z. Physik,' vol. 55, p. 437 (1929).

‡ 'Proc. Roy. Soc.,' A, vol. 130, p. 579 (1931).

§ 'Z. Physik,' vol. 70, p. 567 (1931).

‖ 'Proc. Roy. Soc.,' A, vol. 132, p. 605 (1931). This paper will be frequently referred to later as Paper I.

It is clear, then, that in order to resolve the difficulties, a theory must be developed which takes account of both the distortion of the electron waves by the atomic field, and also of the possibility of exchange, and in this paper we have developed a method which must be regarded as a first step in this direction, accurate where exchange effects are not too large. Instead of using plane waves as a first approximation, as was done in Paper I, we make use of waves distorted by the potential field of the atom as the first approximation. On substitution in the integral equations of the scattering problem, numerical quadrature suffices to give the required second approximation. In this way the effect of distortion is included in the calculation of the exchange effect. As the first approximation neglects the effect of exchange, this theory will not give accurate results where the exchange is actually large, but it will certainly give the exchange effect correctly when it is small.

In this paper the theory is applied to electron collisions in hydrogen and helium. Calculations were first carried out using the Allis-Morse model as a first approximation, but just as they were completed, the wave functions of the motion in the field of the hydrogen atom and in the Hartree* field of helium were made available by the calculations of MacDougall.† The calculations were repeated, using these wave functions, and the final results differ only in detail from those obtained with the Allis-Morse wave functions.

For the elastic scattering we predicted in Paper I that exchange effects should particularly manifest themselves in the angular distribution of the scattered electrons, a minimum appearing below 70 volts and moving in to smaller angles as the electron velocity is diminished, finally giving a distribution showing an increase of scattering with angle. Later experimental investigations by E. C. Bullard and one of us (H. S. W. M.)‡ have revealed peculiarities in the angular distributions occurring below 10 volts, in the existence of a minimum at small angles, and it appeared that this was probably the exchange effect. The present improved calculations make this immensely more probable, as the result of allowing for the distortion of the incident waves is to make the exchange effect fall off more rapidly than before with increasing velocity of the incident waves, so the anomalous angular distributions should now occur below 15 volts, in good agreement with experiment. The peculiar form of the angular distributions at higher voltages—falling at first sharply with angle and then becoming very flat—is also explained satisfactorily by the new theory. This agreement with experiment is of special interest in view of the failure of the theory of Faxen and Holtsmark to explain the angular distributions if exchange be neglected. In general it appears that exchange and distortion act in opposite directions for atoms with closed shells, and nearly cancel each other's effect except at quite low velocities. This is the probable explanation of the apparent validity of the Born first approximation under conditions where it would be expected to fail. However, the new calculations do not show how it is that the Ramsauer effect may be explained without consideration of exchange, rather do they make this appear more remarkable than before. The extension of the calculations to lithium may throw more light on this.

---

* 'Proc. Camb. Phil. Soc.,' vol. 24, p. 89 (1928).

† In course of publication.

‡ 'Proc. Roy. Soc.,' A, vol. 133, p. 637 (1931).

Besides the more obvious applications of the new method to elastic collisions, we have used the distorted waves to calculate inelastic collision probabilities.* It appears that plane waves represent a fairly satisfactory approximation for use in calculating these probabilities down to very low velocities if exchange is included. This will be discussed more fully in a paper to follow this, where further detailed calculations in connection with inelastic collisions will be described.

We will now proceed to the detailed account of the method and its application, and to a complete discussion of the results.

SECTION I.—THEORY OF COLLISIONS.

§ 1. *General Theory.*

Let us consider an electron wave incident on an atomic system, the aggregate of whose co-ordinates we denote by r_a, those of the incident electron being (r, θ, ϕ). The wave equation of the complete system is

$$\left[-\frac{h^2}{8\pi^2 m}\nabla^2 - \mathrm{H}_a(r_a) - (\mathrm{E}_0 + \tfrac{1}{2}mv^2) + \mathrm{V}(r, r_a)\right]\Psi = 0, \tag{1}$$

where E_0 is the energy of the atom in the initial state, v the velocity of the incident electrons, and H_a the Hamiltonian of the atomic system.

Now we may expand Ψ in the form

$$\Psi = \Sigma_n \psi_n(r_a)\,\mathrm{F}_n(r), \tag{2}$$

---

* The distortion of the outgoing wave is relatively more important than that of the incoming, and this effect will be discussed in a subsequent paper.

where $\psi_n(r_a)$ is a wave function of the atom in the nth state with energy E_a^n and satisfies the equation

$$\{H_a(r_a) - E_a^n\}\,\psi = 0. \tag{3}$$

Substituting this in equation (1) and using the relation (2) we obtain the equation

$$\Sigma_n\left[-\frac{h^2}{8\pi^2 m}\nabla^2 - (E - E_a^n)\right]\psi_n F_n = -V\Psi.$$

where E has been written for $E_0 + \frac{1}{2}mv^2$.

If we now multiply by $\bar{\psi}_n$ and integrate over all co-ordinate space of the atomic electrons, we obtain at once the equation

$$\left[-\frac{h^2}{8\pi^2 m}\nabla^2 - (E - E_a^n)\right]F_n = -\int V\Psi\bar{\psi}_n\,dv_a, \quad n = 0, 1, \ldots. \tag{4}$$

This equation may now be converted into an integral equation by means of Green's theorem, as we may treat the right-hand side just as if it were a known function of (r, 0, ϕ). This gives

$$F_n = A_n e^{ik_n n\ r} - \frac{2\pi m}{h^2}\iint V(r', r_a)\,\Psi\bar{\psi}_n\frac{e^{ik_n|\mathbf{r}-\mathbf{r}'|}}{|\mathbf{r}-\mathbf{r}'|}\,dv_a\,dv', \tag{5}$$

where

$$k_n^2 = \frac{8\pi^2 m}{h^2}(E - E_a^n),$$

representing an incident plane wave and a scattered spherical wave; k_n is such that $k_n h/2\pi m$ denotes the velocity of the scattered electron after exciting the atom to the nth state. As we start with a plane wave, $e^{ik\mathbf{n}_0\cdot\mathbf{r}}$ only, we have

$$A_n = 0, \quad n \neq 0,$$

and the asymptotic expansion for F_n becomes

$$F_n \sim \frac{e^{ik_n r}}{r}f_n(\theta, \phi), \tag{6}$$

where

$$f_n(\theta.\ \phi) = -\frac{2\pi m}{h^2}\iint V(r', r_a)\,\Psi(r', r_a)\,\bar{\psi}_n(r_a)\,e^{-ik_n\mathbf{n}_1\cdot\mathbf{r}'}\,dv'\,dv_a, \tag{7}$$

$\mathbf{n}_1$ being a unit vector in the direction of observation. We have thus thrown the differential equation into a series of integral equations which give solutions of the correct asymptotic form.

§ 2. *Introduction of Exchange.*

Since the solution we have considered is a complete one, the question arises as to how exchange can be included in such a solution. Exchange is included because Ψ contains in its asymptotic expansion terms which correspond to $\psi_n(r_a)$ being a wave function of the continuous spectrum, and of such an energy that $F_n(r)$ corresponds to negative energy of the incident electron, *i.e.*, terms representing outgoing waves in the space of the atomic electrons; these terms correspond to the exchanged electrons. A method of calculating the exchange terms based on this method is not of any practical value, and we accordingly use the following method.

Suppose we designate a particular atomic electron by r_1, and determine the probability of its being an outgoing wave after the collision. Denote the aggregate of co-ordinates of the remainder of the atomic electrons and the incident electron by r_b. Then we have, as before, the wave equation

$$\left[-\frac{h^2}{8\pi^2 m}\nabla_1{}^2 - H_b(r_b) - E + V(r_1, r_b)\right]\Psi = 0.$$

Let us now expand Ψ in the form

$$\Psi = \Sigma_n G_n(r_1)\,\psi_n(r_b), \tag{8}$$

where $\psi_n(r_b)$ is the nth atomic wave function with the incident electron in place of electron 1.

We find, by an exactly similar method of calculation as for the F's,

$$G_n \sim \frac{e^{ik_n r_1}}{r_1}\,g_n(\theta, \phi), \tag{9}$$

where

$$g_n(\theta, \phi) = -\frac{2\pi m}{h^2}\iint V(r_1, r_b)\,\Psi\bar{\psi}_n(r_b)\,e^{-ik_n\mathbf{n}_1\cdot\mathbf{r}_1'}\,dv_1'\,dv_b, \tag{10}$$

giving the amplitude of the outgoing waves in r_1 space in the form of an integral. It is important to note that the interaction energy is now $V(r_1, r_b)$, instead of $V(r, r_a)$ as it was taken to be in Paper I using Dirac's method of variation of parameters in which it is not clear which perturbation energy must be used. To the approximation used in Paper I both potentials give practically the same results.

§ 3. *Methods of Approximation.*

Further calculation must consist of approximate methods of solution of the integral equations. These consist in appropriate initial choice of the function

Ψ. The first approximation (used in Paper I) is simply that due to Born of taking $F_n = 0$, and $F_0 = e^{ik\mathbf{n}_0\cdot\mathbf{r}}$, the incident plane wave, but this will not be valid for low velocities where the distortion of the incident wave is large. We make, then, the following assumptions :—

(*a*) The inelastic collision probabilities are small compared with the elastic.

(*b*) The probability of exchange in elastic collisions is small.

We then have $F_n = 0$, $n \neq 0$, $G_n = 0$ for all n, as initial approximation. This makes

$$\Psi = F_0(r)\,\psi_0(r_a) \tag{11}$$

as zero order approximation.

We have, then, substituting the value for Ψ in the expressions (5) and (9)

$$F_n = -\frac{2\pi m}{h^2}\iint V(r', r_a)\,F_0(r')\,\psi_0(r_a)\,\bar{\psi}_n(r_a)\,\frac{e^{ik_n|\mathbf{r}-\mathbf{r}'|}}{|\mathbf{r}-\mathbf{r}'|}\,dv'\,dv_a. \tag{12}$$

$$G_n = -\frac{2\pi m}{h^2}\iint V(r', r_b)\,F_0(r')\,\psi_0(r_a)\,\bar{\psi}_n(r_b)\,\frac{e^{ik_n|\mathbf{r}_1-\mathbf{r}'|}}{|\mathbf{r}_1-\mathbf{r}'|}\,dv'\,dv_a, \tag{13}$$

giving

$$f_n(\theta, \phi) = -\frac{2\pi m}{h^2}\iint V(r', r_a)\,F_0(r')\,\psi_0(r_a)\,\bar{\psi}_a(r_a)\,e^{ik_n\mathbf{n}\cdot\mathbf{r}}\,dv'\,dv_a, \tag{14}$$

$$g_n(\theta, \phi) = -\frac{2\pi m}{h^2}\iint V(r_1', r_b)\,F_0(r')\,\psi_0(r_a)\,\bar{\psi}_n(r_b)\,e^{ik_n\mathbf{n}\cdot\mathbf{r}'}\,dv'\,dv_a. \tag{15}$$

Returning to (4), we have the differential equation for F_0, viz.,

$$\left[-\frac{h^2}{8\pi^2 m}\nabla^2 - (E_r - E_0^0)\right]F_0 = -\int V(r', r_a)\,\Psi\,\psi_0(r_a)\,dv_a,$$
$$= -V_{00}F_0 \tag{16}$$

on substituting the approximation (11) for Ψ, where V_{00} is the static potential of the atomic field acting on the electron. This equation may be solved for F_0, either for an actual atomic field by numerical integration, or for an approximate atomic field chosen to make the equation exactly soluble. In the latter case, we may use F_0 as calculated for the approximate field, and obtain a better approximation by substitution in (12) with $n = 0$. A test of the accuracy of the approximate field is that the resultant F_0 should not differ greatly from the original.

Having obtained the solution F_0 of (16), we substitute in the formulæ for f_n and g_n, the evaluation of these being then only a matter of quadratures.

If the exchange effect is small, this method will give accurate results, as condition (*b*) will not then be violated. However, if the exchange term G_0

calculated as above, is large, then it is clear that an exact calculation of G_0 would also show it to be large, though not necessarily of the same magnitude, for if it were not large, the approximate calculation would be accurate and give the actual small value of G_0. The method thus suffices to show when the exchange effect is small, though it will not be accurate when the exchange is large.

If the exchange is large compared with the non-exchange term, another method of approximation must be used to give accurate results; the following method shows how this may be done. We suppose G_0 is large compared with the difference of F_0 from a plane wave, and again neglect the effect of the inelastic collisions to a first approximation. We have, without approximation

$$\left[-\frac{h^2}{8\pi^2 m}\nabla_1^2-(E-E_0^0)\right]G_0=-\int V(r_1,r_b)\,\Psi\,\bar{\psi}_0(r_b)\,dv_b, \qquad (17)$$

and we now take

$$\Psi=e^{ik\mathbf{n}_0\cdot\mathbf{r}}\,\psi_0(r_a)+G_0(r_1)\,\psi_0(r_b), \qquad (18)$$

giving

$$\left[-\frac{h^2}{8\pi^2 m}\nabla_1^2-(E-E_0^0)\right]G_0=-G_0\int V(r_1,r_b)\,\psi_0(r_b)\,\bar{\psi}_0(r_b)\,dv_b$$

$$-\int V(r_1,r_b)\,\psi_0(r_a)\,\bar{\psi}_0(r_b)\,e^{ik\mathbf{n}_0\cdot\mathbf{r}}\,dv_b. \qquad (19)$$

Thus we have an equation for G_0 of the form

$$[\nabla^2+a+f(r)]\,G_0=g(r),$$

the solution of which may be obtained if the solution of

$$[\nabla^2+a+f(r)]\,G_0=0,$$

is known. This is actually the same equation as that for F_0 above, and so its solution may be obtained. The labour of calculation in this method is much greater, as double numerical integration is required to complete the computations, so in the present paper the calculations have been confined to the previous approximation where exchange is taken as small. Later, the application of the above theory will be worked out to apply where exchange effects are large.

The remaining approximation, of considering the inelastic collisions as having a small effect, is certainly not justified at electron voltages near a resonance potential, and corresponds to the effect of polarisation of the atom by the electron waves. It can also be taken into account approximately by calculating F_n and G_n in the manner described above, and substituting the solutions in the expression

$$\Psi = \Sigma F_n(r)\,\psi_0(r_a). \tag{20}$$

On substitution in (5) and (9), we obtain a series of approximations which includes the polarisation effect. This also has not been carried through completely, but will be included in a later paper.

§ 4. *Inclusion of Symmetry Characteristics.*

So far we have considered a general atom, but for simplicity we shall now consider the case of hydrogen, and show how the final formula, with the correct combination of F and G, is arrived at. Denoting the two electrons concerned by suffixes 1 and 2, we have two solutions $\Psi(r_1, r_2)$, $\Psi(r_2, r_1)$, of the differential equation for the scattering. The complete solution will be a symmetric or antisymmetric linear combination of them, viz.,

$$\Psi = \Psi(r_1, r_2) \pm \Psi(r_2, r_1), \tag{21}$$

corresponding respectively to the two electrons having the same or opposite spin. If we now compute the ratio of the scattered current to the incident we write

$$\Psi = \psi_0(r_1)\,e^{ikz_1} \pm \psi_0(r_2)\,e^{ikz_1} + \Psi_s(r_1, r_2) \pm \Psi_s(r_2, r_1), \tag{22}$$

where Ψ_s represents scattered waves, and has the asymptotic form

$$\Psi_s(r_1 r_2) \sim \Sigma_n \left\{\frac{e^{ik_n r_1}}{r_1} f_n(\theta_1\,\phi_1)\,\psi_n(r_2) + g_n(\theta_2\phi_2)\,\frac{e^{ik_n r_2}}{r_2}\,\psi_n(r_1)\right\}.$$

Calculating the ratio of the scattered to incident currents, using the usual quantum mechanical formula for current density, gives two cross sections

$$\Sigma_n \frac{k_n}{k}\,|f_n(\theta_1) \pm g_n(\theta_1)|^2, \tag{23}$$

according as the electron spins are parallel or antiparallel.

If, now, we are dealing with an unpolarised beam, the antisymmetric cross-section must receive a weight three times that of the symmetric,* just as in the spectrum of helium where the antisymmetric states, the triplets, have a weight 3 compared with the singlets. Therefore we have for the intensity of scattering of unpolarised electrons by hydrogen atoms

$$I(\theta)\sin\theta\,d\theta = \Sigma_n \frac{k_n}{k}\,\tfrac{1}{4}\{|f_n + g_n|^2 + 3\,|f_n - g_n|^2\}. \tag{24}$$

---

* Mott, 'Proc. Roy. Soc.,' A, vol. 125, p. 222 (1929).

In the case of a two-electron system we have, denoting the extra atomic electron by a suffix 3, an elementary solution which has the asymptotic form

$$\Psi(r_1r_2r_3) \sim \psi_0(r_2r_3)\,e^{ikz_1} + \Sigma_n\left\{\psi_n(r_2r_3)\frac{e^{ik_nr_1}}{r_1}f_n(\theta_1) + \psi_n(r_1r_2)\frac{e^{ik_nr_3}}{r_3}g_n(\theta_3)\right.$$
$$\left. + \psi_n(r_3r_1)\frac{e^{ik_nr_2}}{r_2}g_n(\theta_2)\right\}, \quad (25)$$

the two atomic electrons being initially in the symmetrical ground state. For this case, we have only to take the wave function

$$\Psi(r_1r_2r_3) + \varepsilon\Psi(r_3r_1r_2) + \varepsilon^2\Psi(r_2r_3r_1), \quad (26)$$

where $\varepsilon^3 = 1$.

Proceeding as before, we find for the cross section

$$I(\theta)\sin\theta\,d\theta = \Sigma_n\frac{k_n}{k}\left|f_n(\theta) - g_n(\theta)\right|^2\sin\theta\,d\theta. \quad (27)$$

The same formula will hold for each pair of electrons in a closed shell, and represents complete interference of the incident and exchanged electron waves.

Let us now proceed to the detailed calculation for hydrogen and helium. These follow very closely those of Paper I, the only difference being in the use of the distorted wave function F_0 instead of the plane wave $e^{ik\mathbf{n}_0\cdot\mathbf{r}}$. We will accordingly discuss briefly the wave function F_0 used. As we will not be further concerned with inelastic collisions we will, in what follows, use F to denote F_0.

§ 5. *The Distorted Wave Function.*

This wave function is the solution of the differential equation

$$\left[\nabla^2 + \left(k^2 - \frac{8\pi^2m}{h^2}V\right)\right]F = 0, \quad (28)$$

where V, the potential of the static field of the atom concerned, is a function of r only. Expanding F in the form

$$F = \Sigma F_n(r)\,P_n(\cos\theta), \quad (29)$$

gives

$$\frac{d^2}{dr^2}(rF_n) + \left\{k^2 - \frac{8\pi^2mV}{h^2} - \frac{n(n+1)}{r^2}\right\}(rF_n) = 0. \quad (30)$$

The solution of this equation will have the asymptotic form

$$\frac{C_n}{kr}\sin(kr - \tfrac{1}{2}n\pi + \delta_n), \quad (31)$$

where δ_n is a phase constant which determines the scattering, so

$$F \sim \Sigma \frac{C_n}{kr} \sin\left(kr - \tfrac{1}{2}n\pi + \delta_n\right) P_n(\cos\theta). \tag{32}$$

For our purposes, we require this solution normalised to represent a plane wave of unit amplitude, and the corresponding scattered wave. Using the expansion*

$$e^{ikr\cos\theta} = \sqrt{\frac{\pi}{2kr}}\,\Sigma\, i^n (2n+1) J_{n+\frac{1}{2}}(kr) P_n(\cos\theta), \tag{33}$$

and representing the scattered spherical wave by

$$\frac{e^{ikr}}{r} \sum_n g_n P_n(\cos\theta),$$

we see that

$$\sum_n c_n \sin\left(kr - \tfrac{1}{2}n\pi + \delta_n\right) P_n(\cos\theta) = \sum_n i^n (2n+1) \sin\left(kr - \tfrac{1}{2}n\pi\right) P_n(\cos\theta) + \sum_n g_n e^{ikr} P_n(\cos\theta). \tag{34}$$

Equating the coefficients of $\sin(kr - \frac{1}{2}n\pi) P_n(\cos\theta)$ and $\cos(kr - \frac{1}{2}n\pi) P_n(\cos\theta)$ on both sides of equation (34) gives

$$c_n = i^n (2n+1) e^{i\delta_n}. \tag{35}$$

We thus have

$$F = \Sigma (2n+1) i^n e^{i\delta_n} F_n(r) P_n(\cos\theta), \tag{36}$$

where F_n satisfies the equation (30) and has the asymptotic form

$$F_n \sim \frac{\sin\left(kr - \frac{1}{2}n\pi + \delta_n\right)}{kr}. \tag{37}$$

For actual atoms V is too complicated a function to enable F to be obtained analytically, but it may always be obtained by numerical integration of the differential equation. This has been done by MacDougall for hydrogen and helium, the results being in course of publication. Before these results were made available, the functions obtained by Allis and Morse† for the motion of electrons in a model atomic field were used. The field was given by

$$\begin{aligned} V &= Ze^2\left(\frac{1}{r} - \frac{1}{r_0}\right) \qquad r < r_0. \\ &= 0 \qquad\qquad\qquad\quad\; r > r_0. \end{aligned}$$

---

* Watson, "A Treatise on the Theory of Bessel Functions," Cambridge, p. 368 (1922).

† 'Z. Physik,' vol. 70, p. 567 (1931).

They found that the resulting solution for F, which may be obtained in terms of Whittaker functions, gives a good representation of the scattering cross sections as measured by Ramsauer and others, the constants Z and r_0 being adjusted to be in close accord with values deduced from Slater's rules.*

SECTION II.

§ 6. *Calculation of Elastic Cross Sections for Hydrogen and Helium.*

We shall now give the calculation of f_0 and g_0 using the distorted wave functions for the initial electron.

For such light atoms as hydrogen and helium, the wave function of the incident electron differs appreciably from the plane wave

$$e^{ikr\cos\theta} = \sqrt{\frac{\pi}{2kr}}\sum_n i^n (2n+1)\,\mathrm{J}_{n+\frac{1}{2}}(kr)\,\mathrm{P}_n(\cos\theta) \tag{38}$$

only for $n = 0$; it is thus often convenient in the calculations simply to correct the results obtained in Paper I using plane waves for F by allowing for the difference betewen F and $\sqrt{\frac{\pi}{2kr}}\,\mathrm{J}_{\frac{1}{2}}(kr)$. If the complete function $\Sigma \mathrm{F}_n \mathrm{P}_n(\cos\theta)$ is used, there is no need to calculate f_0 by a further integration because the function F satisfies the integral equation

$$\mathrm{F}(r) = -\frac{2\pi m}{h^2}\iint \mathrm{V}(r'_1 r_a)\,\mathrm{F}(r')\,\psi_0(r_a)\,\overline{\psi_0}(r_a)\,\frac{e^{ik|\mathbf{r}-\mathbf{r}'|}}{|\mathbf{r}-\mathbf{r}'|}\,dv'\,dv_a, \tag{39}$$

and so the asymptotic expression obtained by substituting the complete function $\Sigma\,\mathrm{F}_n\mathrm{P}_n(\cos\theta)$ in (39) will be just that of F itself. Actually, however, we assume only F_0 to be different from a plane wave and calculate the integral on that basis; the resulting expression will then include the effect of higher values of n. When using only approximate functions for F, this procedure is, of course, necessary in order to obtain the accuracy required. This was done when the calculations were first carried out with the Allis-Morse functions, and continued when the calculations were repeated using MacDougall's functions.

As the wave function for the ground state of hydrogen is simply

$$\frac{1}{(\pi a_0^3)^{\frac{1}{2}}}\,e^{-(r_1/a_0)},$$

---

* 'Phys. Rev.,' vol. 36, p. 57 (1930).

and since we take the Hylleraas approximate function

$$\frac{\mu^3}{\pi a_0^3} e^{-\mu(r_1+r_2)/a_0},$$

where $\mu = 1\cdot69$, for the ground state of helium, we see that the number of electrons of velocity $kh/2\pi m$ which are scattered between angles θ and $\theta + d\theta$ by atoms of hydrogen and helium respectively, is given by $\mathrm{I}(\theta) \sin\theta\, d\theta$, where

$$\mathrm{I}(\theta) = 2\pi\{\tfrac{1}{4}|f+g|^2 + \tfrac{3}{4}|f-g|^2\}$$

for hydrogen,

$$= 2\pi|f-g|^2$$

for helium.

Here, for hydrogen

$$\left.\begin{aligned} f &= \frac{2me^2}{a_0^3 h^2}\iint\left(\frac{1}{r_2}-\frac{1}{r_{12}}\right) e^{-(2r_1/a_0)}\, e^{-ik\mathbf{n}_1\cdot\mathbf{r}_2}\, \mathrm{F}(r_2)\, dv_1\, dv_2 \\ g &= \frac{2me^2}{a_0^3 h^2}\iint\left(\frac{1}{r_2}-\frac{1}{r_{12}}\right) e^{-(r_1+r_2)/a_0}\, e^{-ik\mathbf{n}_1\cdot\mathbf{r}_2}\, \mathrm{F}(r_1)\, dv_1\, dv_2 \end{aligned}\right\} \quad (40)$$

for helium*

$$\left.\begin{aligned} f &= \frac{2me^2\mu^6}{\pi a_0^6 h^2}\iiint\left(\frac{2}{r_3}-\frac{1}{r_{23}}-\frac{1}{r_{13}}\right) e^{-2\mu(r_1+r_2)/a_0}\, e^{-ik\mathbf{n}_1\cdot\mathbf{r}_3}\, \mathrm{F}(r_3)\, dv_1\, dv_2\, dv_3 \\ g &= \frac{2me^2\mu^6}{\pi a_0^6 h^2}\iiint\left(\frac{2}{r_3}-\frac{1}{r_{23}}-\frac{1}{r_{13}}\right) e^{-\mu(2r_1+r_2+r_3)/a_0}\, e^{-ik\mathbf{n}_1\cdot\mathbf{r}_3}\, \mathrm{F}(r_2)\, dv_1\, dv_2\, dv_3 \end{aligned}\right\}. \quad (41)$$

Writing

$$\left.\begin{aligned} \int\left(\frac{1}{r_2}-\frac{1}{r_{12}}\right) e^{-(2\lambda r_1/a_0)}\, e^{-ik\mathbf{n}_1\cdot\mathbf{r}_2}\, \mathrm{F}(r_2)\, dv_1\, dv_2 &= \mathrm{J}_1(\lambda) \\ \int\left(\frac{1}{r_2}-\frac{1}{r_{12}}\right) e^{-\lambda(r_1+r_2)/a_0}\, e^{-ik\mathbf{n}_1\cdot\mathbf{r}_2}\, \mathrm{F}(r_1)\, dv_1\, dv_2 &= \mathrm{E}_1(\lambda) \\ \frac{a_0^3}{\lambda^3}\int \mathrm{F}(r)\, e^{-\lambda r}\, dv \int\left(\frac{1}{r_2}-\frac{1}{r_{12}}\right) e^{-\lambda(2r_1+r_2)/a_0}\, e^{-ik\mathbf{n}_1\cdot\mathbf{r}_2}\, dv_1\, dv_2 &= \mathrm{E}_2(\lambda) \end{aligned}\right\}, \quad (42)$$

$$\frac{2me^2\lambda^3}{a_0^3 h^2} = c(\lambda),$$

we have

$$\mathrm{I}(\theta) = c(1)^2\{|\mathrm{J}_1(1)+\mathrm{E}_1(1)|^2 + 3\,|\mathrm{J}_1(1)-\mathrm{E}_1(1)|^2\}$$

for hydrogen,

$$= c(\mu)^2\,|2\mathrm{J}_1(\mu)-\mathrm{E}_1(\mu)-\mathrm{E}_2(\mu)|^2 \quad (43)$$

for helium.

---

* In Paper I a factor of 4 was omitted in the expression for f for helium in formula (45).

It therefore remains to calculate J_1, E_1, and E_2 in detail, which we will now proceed to do.

1. *Calculation of* J_1. --As

$$F(r_1) = e^{i\delta_0} F_0(r_1) + \sqrt{\frac{\pi}{2kr}} \sum_n i^n (2n+1) J_{n+\frac{1}{2}}(kr_1), \tag{44}$$

we see that

$$J_1 = \iint \left(\frac{1}{r_2} - \frac{1}{r_{12}}\right) e^{\frac{-2\lambda r_1}{a_0}} \left\{ e^{ik(\mathbf{n}_0 - \mathbf{n}_1).\mathbf{r}_2} - e^{-ik\mathbf{n}_1.\mathbf{r}_2} \left(\frac{\sin kr_2}{kr_2} - e^{i\delta_0} F_0(r_2)\right)\right\} dv_1 \, dv_2. \tag{45}$$

This gives finally

$$J_1 = B - D_r + iD_i. \tag{46}$$

where B is just the value given by the Born formula, viz.,

$$B = \frac{\pi^2}{\lambda^3} \frac{2\lambda^2 + k^2 \sin^2 \frac{1}{2}\delta,}{(\lambda^2 + k^2 \sin^2 \frac{1}{2}\delta)^2}$$

and

$$\left.\begin{aligned} D_r &= 16\pi^2 \int_0^\infty \int_0^{r_1} \left(\frac{1}{r_2} - \frac{1}{r_1}\right) e^{\frac{-2\lambda r_1}{a_0}} \frac{\sin kr_2}{kr_2} \left(\frac{\sin kr_2}{kr_2} - \cos \delta_0 F_0(r_2)\right) r_1^2 r_2^2 \, dr_1 \, dr_2 \\ D_i &= 16\pi^2 \int_0^\infty \int_0^{r_1} \left(\frac{1}{r_2} - \frac{1}{r_1}\right) e^{\frac{-2\lambda r_1}{a_0}} \frac{\sin kr_2}{kr_2} \sin \delta_0 F_0(r_2) r_1^2 r_2^2 \, dr_1 \, dr_2. \end{aligned}\right\} \tag{47}$$

represent the effect of distortion.

From the table of F_0 given by McDougall, the integration of D_r, D_i, may then be carried out numerically.

2. *Calculation of* E_1.—Using the series (36) for F we find, following the methods described in Paper I,

$$E_1 = \sum_{n=0}^{\infty} E_1^n P_n(\cos\theta), \tag{48}$$

where

$$E_1^0 = \frac{16\pi^2 e^{i\delta_0}}{\lambda^3 k} \int_0^\infty \int_0^{r_1} r_1 (r_1 - r_2) e^{-\lambda(r_1+r_2)/a_0} \sin kr_2 F_0(r_1) \, dr_1 \, dr_2, \tag{49}$$

$$E_1^n = \frac{8\pi^2}{\lambda^3 k} \int_0^\infty \int_0^\infty \gamma_n(r_1 r_2) e^{-\lambda(r_1+r_2)/a_0} J_{n+\frac{1}{2}}(kr_1) J_{n+\frac{1}{2}}(kr_2) r_1^{3/2} r_2^{3/2} \, dr_1 \, dr_2,$$

$$\left.\begin{aligned} \gamma_n(r_1 r_2) &= \frac{r_1^n}{r_2^{n+1}} \qquad r_2 > r_1 \\ &= \frac{r_2^n}{r_1^{n+1}} \qquad r_1 > r_2 \end{aligned}\right. \tag{50}$$

The terms (50) are just those given in formulæ (38) and (45) of Paper I, but E_1^0 must be calculated numerically from tables of F_0.

3. *Calculation of* E_2.—It is easy to see that E_2 is independent of angle, and reduces to the form

$$E_2 = e^{i\delta_0} \frac{16\pi^3}{\lambda^3} \frac{15\lambda^2 + k^2}{(9\lambda^2 + k^2)^2} \int_0^\infty F_0(r)\, e^{-\mu r} r^2\, dr. \tag{51}$$

For helium we may then write the complete exchange effect in the form,

$$2\,(E_r + iE_i),$$

where

$$\left.\begin{aligned} E_r &= \tfrac{1}{2}(E_1^0 + E_2)\cos\delta_0 + \tfrac{1}{2}\sum_{n=1}^{\infty} E_1^n P_n(\cos\theta) \\ E_i &= \tfrac{1}{2}(E_1^0 + E_2)\sin\delta_0 \end{aligned}\right\}. \tag{52}$$

Substituting the expressions obtained for f and g we see that $I(\theta)$ is of the form

$$4\,\{(B - D_r - E_r)^2 + (D_i - E_i)^2\}. \tag{53}$$

the terms denoted by D representing the effect of distortion of the incident wave, those denoted by E the effect of exchange. We have a similar form for hydrogen, but as the scattering by a hydrogen atom is of no practical interest we will discuss shortly what result we would expect for molecular hydrogen.

Case of Molecular Hydrogen.—The scattering of electrons by atomic hydrogen cannot be observed experimentally, so it is of interest to extend the above methods to represent approximately the case of molecular hydrogen. To do this, we assume that the only difference from the scattering by two hydrogen atoms is given by the alteration of the symmetry properties due to the presence of two electrons. We thus take the scattered intensity from molecular hydrogen as given by

$$2\,|f - g|^2,$$

where f and g have just the values calculated for atomic hydrogen. Some justification for this is provided by the results obtained by us* for the elastic scattering by the molecule using Born's formula only, in which it was shown that the deviation of the scattered intensity from that of two hydrogen atoms was inappreciable.

We will now proceed to the discussion of the results of the calculations.

§ 7. *Discussion of Results.*

As stated in the introduction, the primary reason for carrying out these calculations was to see if exchange effects could really be neglected, as seemed so from the work of Allis and Morse on the Ramsauer effect. In the notation of the preceding section, this would mean that E_r and E_i could be neglected in comparison with D_r and D_i. In fig. 1 the real quantities D_r and E_r are illustrated on the one hand, and the imaginary D_i and E_i on the other. It will be seen that below 20 volts the exchange effect can clearly not be neglected, and up to 50 volts it exerts an appreciable influence on the scattering, especially through the term $E_1{}^1$ at the higher voltages. In fig. 2 the exchange effect calculated with and without the distorted incident wave functions are compared. It is seen that the effect of the distortion is to make the exchange effect fall off more sharply than before. The explanation of this in general terms seems to be that, when plane waves are used, the two functions

---

* 'Proc. Roy. Soc.,' A, vol. 135, p. 258 (1932).

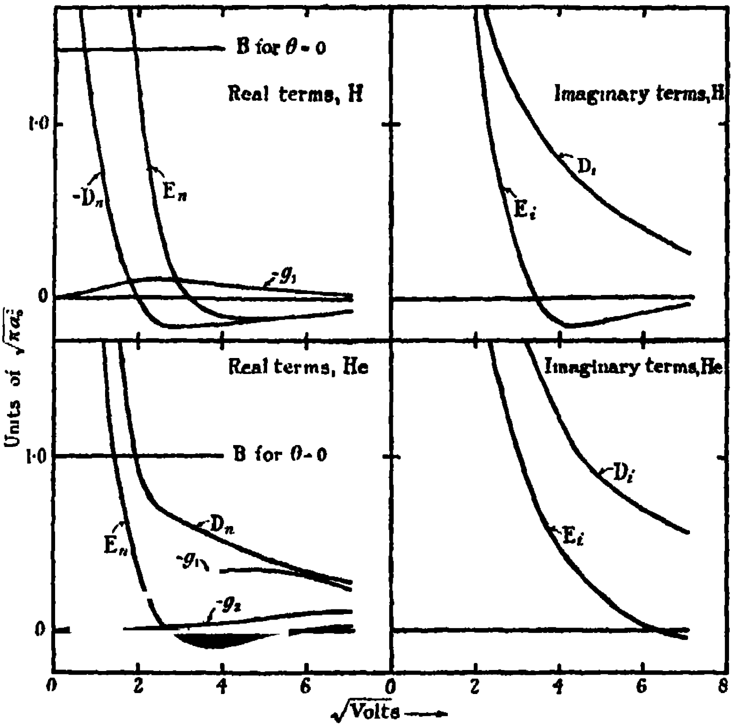

Fig. 1.—Illustrating relative magnitude of different terms in the scattering of electrons in helium and hydrogen. B gives Born's formula for zero angle of scattering, E_r E_i the real and imaginary first order terms due to exchange, D_r, D_i the real and imaginary terms due to distortion, g_1, g_2 the second and third order exchange terms (both real).

$$e^{ik\mathbf{n}_0 \cdot \mathbf{r}}, \qquad F(r),$$

are in phase everywhere, as they both represent plane waves of the same wave-length and phase, whereas the distortion of F (r) removes this coherence effect, and accordingly reduces the contribution due to exchange.

It is now fitting to consider comparison with experiment. The experimental evidence is of two kinds: experiments of Ramsauer's type where the total cross section $Q = \int I(\theta) \sin\theta \, d\theta$ is measured as a function of velocity, and those in which the angular distribution $I(\theta)$ of the scattered electrons is measured at a fixed velocity of impact. In Paper I, using the plane wave approximation, we showed that when the exchange term g becomes comparable with f, interference effects become prominent owing to the form $|f - g|^2$ for the intensity of scattering. As a result, a minimum appears in the angular distribution at a certain voltage, and moves to smaller angles with decrease of velocity, eventually disappearing to leave an angular distribution in which there is an increase of scattering with angle. Experiments by E. C. Bullard and one of us (H. S. W. M.) showed later that such effects do occur in helium at voltages of 10 volts and less, and these results were confirmed by Ramsauer and Kollath, who showed also that similar effects occur in hydrogen below 5 volts. This seemed to be definite evidence of the effect of the exchange term g, but owing to the use of plane waves in Paper I, a voltage of 70 volts was obtained as the point at which the peculiarities should appear. A reference to fig. 1 indicates how the improved theory of this paper shows that the exchange effect falls off much more rapidly with velocity than was obtained on the simpler theory of Paper I, and the detailed calculations show that the present theory predicts

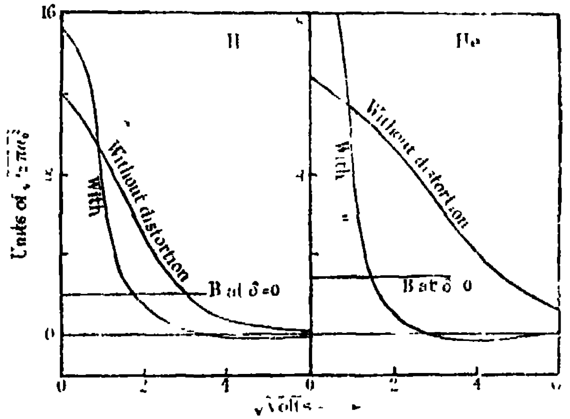

FIG. 2.—Illustrating effect of distortion of the incident wave on the calculation of exchange effects. B gives the limit of the Born formula for zero angle of scattering for comparison.

the appearance of these exchange effects below 15 volts in helium and 5 volts in hydrogen in complete agreement with experiment. As the exchange effect is comparable with the distortion at these voltages, one must not expect exact agreement with experiment, for one of the assumptions of the theory is that the effect of exchange is small compared with distortion. Nevertheless, fig. 3 which compares the calculated low voltage angular distributions in helium and molecular hydrogen with the experimental shows the close similarity of the calculated and experimental curves. The experimental results for helium are those of Bullard and Massey, and for hydrogen, Bullard and Massey, and Ramsauer and Kollath.

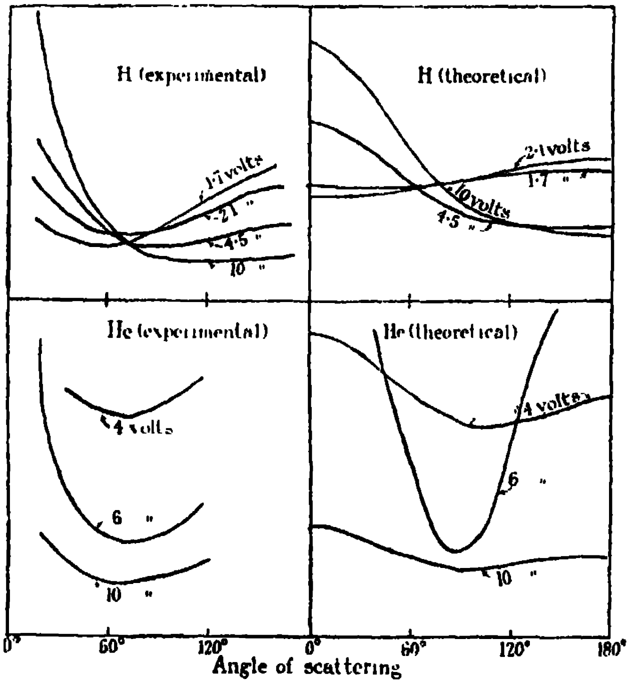

FIG. 3.—Comparison of observed and calculated angular distributions for scattering of low voltage electrons in hydrogen and helium. The experimental results for hydrogen are for H_2, the theoretical for 2H with symmetry relations for 2 electrons.

In order to show that the Faxen-Holtsmark theory fails to give any indication of the observed curves in fig. 4, the curves obtained by this theory (in which E_r, E_t are assumed zero) are compared with those calculated from our theory, and with the experimental curves.

Finally, to show that no reasonable change of initial field will make the Faxen-Holtsmark curves any more satisfactory, curves calculated from Allis and Morse's field, which is considerably different from the actual helium field, are also given.

We will now shortly explain how the calculations lead to the form of curves shown. The angular distribution $I(\theta)$ is given by

$$I(\theta) = 4\{(B - D_r - E_r)^2 + (D_i - E_i)^2\}^2.$$

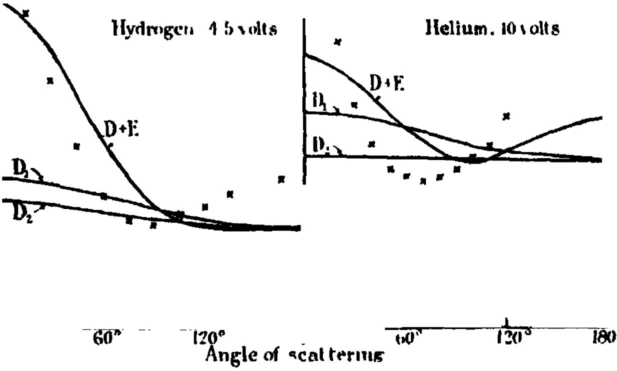

Fig. 4.—Illustrating importance of electron exchange for low voltage collisions. + + represent observed angular distributions. D_1 is the curve calculated, using Allis and Morse's distorted waves and neglecting exchange. D_2 is the curve calculated, using McDougall's distorted waves and neglecting exchange. D + E is the curve calculated, including both distortion and exchange.

Using the forms (47) and (52) for these quantities we see that

$$I(\theta) = [\Sigma a_n P_n(\cos\theta)]^2 + b^2, \tag{54}$$

where

$$\left.\begin{aligned} a_0 &= 2\{B_0 - D_r - \tfrac{1}{2}(E_1{}^0 + E_2)\cos\delta_0\} \\ a_n &= 2\{(B_n - \tfrac{1}{2}E_1{}^n)\} \\ b &= D_i - \tfrac{1}{2}(E_1{}^0 + E_2)\sin\delta_0 \end{aligned}\right\}. \tag{55}$$

Born's formula being supposed expanded in the form

$$B = \Sigma B_n P_n(\cos\theta).$$

The series (54) converges rapidly for low velocities. We note also that the terms a_n are all positive and have the same sign as B_0 (see fig. 1). If, then, a_0 is positive there will be a uniform decrease of scattering with angle, as is the case for higher velocity impact when only B_0 and D_r above, are important. When the expression changes sign, which it will do when the exchange terms become large and positive, the angular distribution will first show minima and then an increase of scattering with angle. On examining the magnitude of the various terms illustrated in fig. 1, we can see in this way how the angular distribution of fig. 3 occurs. To describe the effect shortly, one must consider the scattered intensity as broken up into that due to scattered waves of different orders. The effect of exchange is to produce at a certain voltage—owing to interference, as it were, of the incoming wave and outgoing exchange wave—a considerable decrease in the contribution in the zero order term, so producing angular distributions which oscillate much more with change of angle than would otherwise be the case.

At intermediate voltages where the zero order term of the exchange contribution is not sufficiently large to produce minima, we see by reference to fig. 1 that the angular distributions will show a " background " at large angles of scattering due to the term b^2. The effect of exchange now becomes most prominent in the second order term a_1, at these voltages. As a consequence of this increase of this term the expression $[\Sigma a_n P_n (\cos \theta)]^2$ of (54) decreases more rapidly with angle than would be the case if $E_1{}^n$ were neglected. As a result, the theory predicts angular distributions which at first fall steeply with increasing angle and then become very flat. This flat part occurs when b^2 becomes large compared with $[\Sigma a_n P_n (\cos \theta)]^2$. Referring to the experimental results of Bullard and Massey, one finds that this behaviour is observed, as is illustrated in fig. 5. Actually, the calculated curves in this figure do not

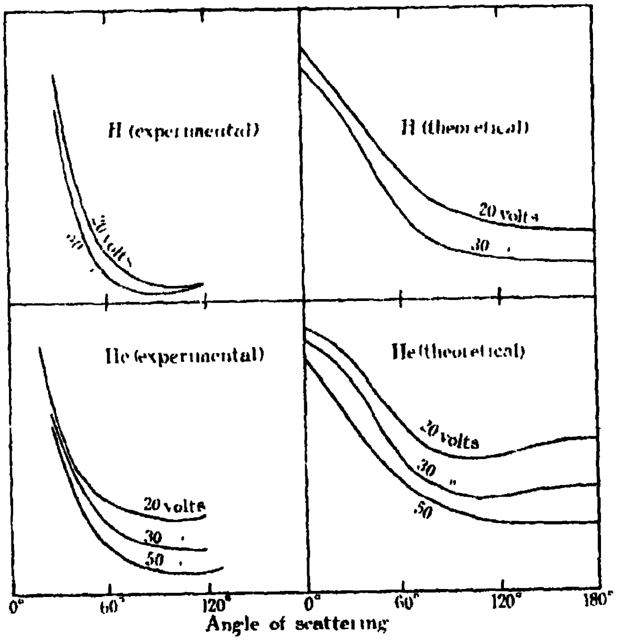

Fig. 5.—Comparison of observed and calculated angular distributions for scattering of higher voltage electrons in hydrogen and helium.

agree quantitatively with the observations, but this is not surprising in view of the fact that these curves are very sensitive to slight changes in the constants used, a slight change in the phase δ_0 making a considerable difference to the calculations.

It remains to consider the total cross sections. In fig. 6 the calculated and observed cross sections for hydrogen and helium are compared with the experimental. The agreement with the hydrogen curve obtained by Normand is surprisingly good, and, as predicted in Paper I, the minimum observed at 1 volt seems to be definitely due to the effect of exchange. In view of the fact that there is a considerable disagreement between the experimental results at low voltages in hydrogen, and as the theory ceases to be accurate when exchange is large, this agreement may be fortuitous, but it is likely that the main features should appear as they do. For helium the minimum which the calculations would indicate at 5 volts is not found experimentally, but as stated above, the theory is inaccurate at these low voltages,* and the effect of polarisation must always be apparent at such a minimum position.

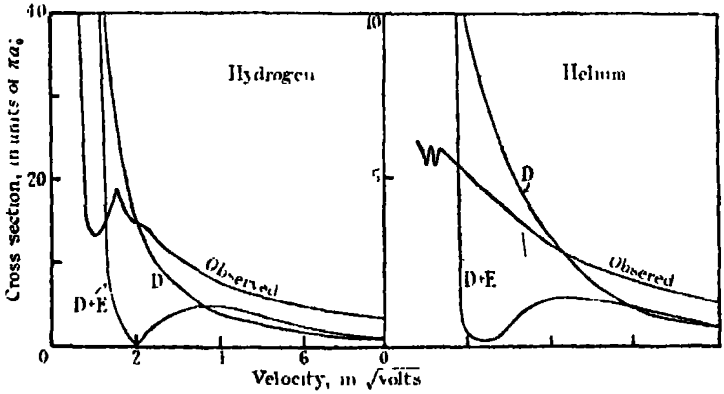

Fig. 6.—Calculated and observed cross sections. D denotes that calculated, using distorted waves only. D + E denotes that calculated, using distortion and exchange. Observed curve is for the total cross section as obtained by Normand.

In order to improve the theory, it is necessary to take account of the polarisation of the incident electrons. The polarisation field is not by any means a simple one, and arises from the interaction of the inelastically scattered wave with the elastic. As the field corresponding is complex, it would seem that any attempt to bring it into account by modifying the static field of the atom has no physical significance. In order to calculate the effect of these inelastic collisions, it is necessary to calculate the intensity of the inelastically scattered waves by means of the integral equations (14) and (15), and then substitute them in the expression for the complete wave function Ψ of the system atom + incident electron, and recalculate the various integrals for f_n, g_n, etc. This is being done, and the results will be published later.

---

* The occurrence of such a marked minimum is due to the same phase factor $e^{i\delta_0}$ occurring in both the exchange and directly scattered waves. In an exact theory this would not be the case. The angular distributions are much less sensitive to such changes in phase than the total cross sections.

As the exchange effect seems to be of greatest importance at very low voltages, the method given in § 3, equation (19), must be used to give results for these cases. Calculations on these lines are proceeding also.

The extension of the calculations to lithium will be of interest, as experimental investigations of the scattering by this atom, although difficult, can be carried out. Apart from this atom, the calculations would be of such complexity as to be prohibitive, though for certain voltage regions it may be possible to carry them out.

It would appear, then, that the inclusion of exchange is really necessary to give the effects observed in scattering experiments, although its effect first becomes important at much lower voltages than was supposed in Paper I The experimental evidence in its favour is considerable. It is important to point out here that as the angular distribution of the scattered electrons is of the form

$$|\Sigma_n h_n P_n (\cos \theta)|^2$$

it is always possible, by adjusting the atomic field used, to obtain the experimental results without considering exchange. For helium and hydrogen the adjustment of the field required for this purpose would be considerable, but for heavier atoms this may not be the case, and agreement obtained with experiment neglecting exchange may really be of no physical significance. By proceeding according to the method of this paper, the actual processes occurring are clearly differentiated, and no attempt has been made at any stage to alter the constants in any way whatever, though such adjustments would doubtless have made the agreement much closer.

Inelastic Collisions.—Calculations have been carried out for the $1S - 2\,^1S$ and $1S - 2\,^3S$ excitation probabilities using the new theory, and the difference from the calculation of Paper I is not very great. This appears to be a general feature of the inelastic collisions. The important correction to Born's formula seems to be due to exchange rather than distortion of the incident wave.* In a paper to follow this very shortly, a complete account will be given of the calculation of excitation probabilities for hydrogen and helium carried out to a considerably greater degree of accuracy than in Paper I.

---

* See, however, footnote on p. 3.

It is a pleasure to express our thanks to Drs. Allis and Morse for providing the material with which the detailed calculations of the above paper were first carried out. We also gratefully acknowledge the value of the many discussions we have had with them and with Mr. N. F. Mott.

Summary.

The theory of collisions of slow electrons with atoms has been developed in which the zero approximation is not a plane wave but the wave representing the motion of the electron in the static field of the atom concerned. Using this method the elastic scattering of slow electrons in hydrogen and helium is considered in detail, and the effect of electron exchange included in the calculations throughout. It is found that exchange does not become very important until lower voltages than obtained on Born's theory, using the plane wave as first approximation. At lower voltages it is shown that strong interference effects occur between the incident and exchanged electron waves, giving peculiar angular distributions of the scattered electrons. These effects are experimentally observed.

A theory valid for the case of large exchange is also given but not worked out in detail.

A Thyratron " Scale of Two " Automatic Counter.

By C. E. Wynn-Williams, Ph.D., Clerk-Maxwell Scholar.

(Communicated by Lord Rutherford, O.M., F.R.S.—Received December 23, 1931)

Introduction.

In a previous paper[*] the author discussed a method of using thyratrons for high-speed automatic counting of physical events which are repeated very rapidly. It was shown that a group of, say, four or five thyratrons associated with a mechanical counting meter can be made to record continuously occurrences of events separated by time intervals which are very much shorter than the time required by the mechanical meter to effect its own changes of dial readings. This is made possible by the development of a special " thyratron ring " circuit which enables the " inertialess relay " characteristics of the individual thyratrons to be utilised to the greatest advantage. By using in the circuit a sufficient number of thyratrons, the counting speed can be made independent of the mechanical inertia of the recording mechanism and dependent only on the electrical characteristics of the circuit.

The method, as pointed out in the paper, can be used for the recording of any physical event the occurrence of which can be made to apply a voltage impulse to the thyratron counting ring. The means of doing this are various, the choice of a suitable one being dependent upon individual experimental conditions. For the recording of an optical event, for example, the required voltage impulse might be applied to the thyratrons by means of a photoelectric cell used in conjunction with a suitable valve amplifier.

A counting ring of this kind, consisting of four thyratrons, has been employed with success in the Cavendish Laboratory for high-speed counting of α-particles.[†] In this case the ionisation currents due to the individual α-particles are linearly amplified by means of valves until a sufficiently large voltage impulse is obtained to operate the thyratron ring. The high counting speed which this arrangement makes possible, and the advantage which it offers for work of this kind, can best be realised if the " resolution " which a single thyratron can effect when used as a simple relay in conjunction with a mechanical meter, is compared with that which can be effected when the thyratron is replaced by a " ring " circuit of, say, five thyratrons.[‡] With the single thyratron, two particles arriving within 1/25th second would have been recorded as a *single particle*, since the mechanism of the meter requires 1/25th second to operate. With the "*ring*" circuit, however, as many as five particles could follow one another in rapid succession within a total time of 1/25th second, and still be individually recorded. Moreover, two particles separated by as little as 1/500th second could be "resolved" and correctly recorded.

---

[*] Wynn-Williams, 'Proc. Roy. Soc.,' A, vol. 132, p. 295 (1931).

[†] Rutherford, Wynn-Williams and Lewis, 'Proc. Roy. Soc.,' A, vol. 133, p. 351 (1931).

[‡] See fig. 4, p. 302, of the author's earlier paper.

The counting circuits described in the previous paper, while extremely effective in practice, suffer from the disadvantage of being somewhat complicated in their construction. For this reason they may not appeal as convenient for general counting purposes. Since the paper was published, however, the writer has been able to develop a new type of circuit. This, while very stable and reliable in action, and possessing all the qualities of high "resolving power" and counting speed that characterise the "ring" type of circuit, is very much simpler in its construction and needs no critical adjustments. In addition, it has the great convenience that, as it does not require separate heating of the cathodes of the thyratrons, and separate accumulators, all current supplies can be taken from the laboratory mains. Moreover, it can be shown that its counting efficiency, for the same number of thyratrons, is higher than that of the ring type of circuit when the number of thyratrons is greater than four. As will be shown later in the paper, a "resolution" of the order of 1/1250th second can be obtained without difficulty.

The new type of circuit has, therefore, important practical advantages, and will be found more suitable and convenient for general counting purposes than the "ring" type. For this reason an account of it and a discussion of its characteristics and operation are given here.

Principle of Operation.

The principle of the method of counting employed in the new type of circuit is that of arranging several units of two thyratrons in cascade so as to reduce the rate of counting by a factor of two per unit, until the final counting rate is sufficiently slow to enable a mechanical meter to be used. For most purposes, two or three such units (*i.e.*, four or six thyratrons) should suffice. Under these conditions, the speed reductions would be respectively, $2^2 = 4$, and $2^3 = 8$ times. Each of the individual units of two thyratrons (fig. 1) is virtually a "two-thyratron ring" of the type previously described. As pointed out on p. 304 of the earlier paper, however, when a thyratron ring contains only *two* thyratrons, the connections can be very much simplified, and certain disadvantages associated with the "priming" operation automatically disappear. It may also be recalled that in the earlier paper, attention was drawn to the similarity between this two-thyratron circuit and a circuit possessing similar characteristics which had previously been described by Hull.*

Characteristics of a Single Unit.

The circuit connections of a single unit are shown in fig. 1. It will be observed that the circuit is quite symmetrical. For simplicity the cathode heating currents and anode currents are shown as being derived from batteries, while the "impulses" are applied from the secondary winding of a transformer through the grid condensers C_A and C_B. The impulses arise from changes of current in the transformer primary winding occasioned by the events it is desired to count.

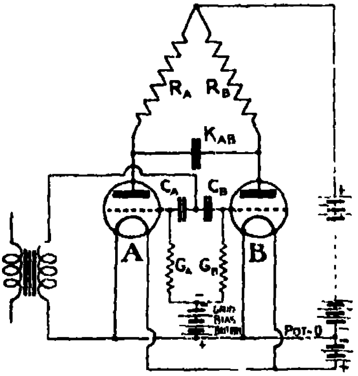

Fig. 1.—Circuit diagram of a single two-thyratron unit

Suppose that the steady bias potential applied to both grids by the grid bias battery through the grid resistances G_A and G_B is slightly more negative than the critical negative potential required to prevent arcs from striking in the thyratrons, and that there is *initially* an arc in *one* thyratron, say, A. It is characteristic of the circuit that if a series of positive voltage impulses slightly greater in magnitude than the excess negative bias are simultaneously applied to both grids, the arc will be "transferred" alternatively from A to B and from B to A. The striking of an arc in one thyratron consequent upon the arrival of an impulse at the grid results in a sudden drop of its anode potential from a value of, say, + 220 volts, to a value of + 15 volts. The resulting negative potential surge which is transmitted through the condenser K_{AB} to the anode of the other thyratron causes the arc in that thyratron to be extinguished.† As the time required to strike the arc is extremely small, being of the order of a few microseconds, a circuit of this kind can be made to respond to impulses which are repeated extremely rapidly.

---

* 'Gen. Elec. Rev.,' vol. 32, p. 398, fig. 41 (1929).

† A full account of the characteristic properties and numerous applications of thyratrons has been published by Hull, 'Gen. Elec. Rev.,' vol. 32, pp. 213 and 390 (1929). A brief explanation of the action of a thyratron was also given in the author's earlier paper (*loc. cit.*). The particular thyratrons used for this work (Mazda Type B.T.1 Thyratrons) are described in 'J. Sci. Inst.,' vol. 8, p. 296 (1931).

Thus, assuming that the arc is initially in thyratron A, and numbering the successive impulses applied from the transformer, Nos. 1, 2, 3, 4, 5, 6, –, –, it is evident that the arc will be transferred from A to B by impulses Nos. 1, 3, 5, 7, –, and back again from B to A, by impulses Nos. 2, 4, 6, 8, –. In this way, thyratrons A and B each respond to *one half* the total number of applied impulses, the one, A, responding to the even numbered impulses, and the other, B, to the odd.

Cascade Arrangement of Units.—Suppose a second similar counting unit of two thyratrons, C and D is coupled to the first (in a manner described later) so that whenever *one* thyratron of the first unit (say thyratron A) arcs, an impulse is transmitted to the second unit CD, but no such impulse is transmitted when the other thyratron (B) arcs. This is represented diagrammatically in fig. 2. It is clear that an alternation of the arcs in thyratrons C and D will occur each time thyratron A strikes, but not when the arc is struck in thyratron B. Thyratrons C and D will therefore each be made to arc half the number of times A has been made to arc, which, in turn, is numerically equal to half the total number of impulses originally applied to the first unit AB. From this it will be seen that one thyratron, say C, will respond to those impulses whose numbers are represented by a multiple of four, while the other thyratron, D, will respond to those whose numbers are represented by a multiple of four, plus or minus two.

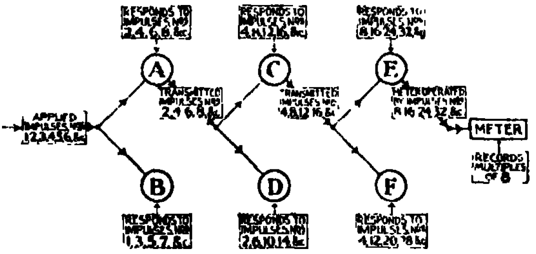
RESPONDS TO IMPULSES NOS 2,4,6,8,&c
RESPONDS TO IMPULSES NOS 4,8,12,16,&c
RESPONDS TO IMPULSES NOS 8,16,24,32,&c
A
C
E
TRANSMITTED IMPULSES NOS 2,4,6,8,&c
TRANSMITTED IMPULSES NOS 4,8,12,16,&c
METER OPERATED BY IMPULSES NOS 8,16,24,32,&c
APPLIED IMPULSES NOS 1,2,3,4,5,6,&c
METER
RECORDS MULTIPLES OF 8
B
D
F
RESPONDS TO IMPULSES NOS 1,3,5,7,&c
RESPONDS TO IMPULSES NOS 2,6,10,14,&c
RESPONDS TO IMPULSES NOS 4,12,20,28,&c

FIG. 2.—Cascade arrangement of three two-thyratron units.

Proceeding on these lines, a third similar unit of two thyratrons, EF, can be coupled to thyratron C, so that thyratron E will respond to those impulses whose numbers are represented by a multiple of eight, while thyratron F responds to those whose numbers are represented by a multiple of eight, plus or minus four. If necessary, still more units could be added. It will be obvious that the cycle of events in such an arrangement repeats itself after 2^n impulses have been applied, where n is the number of two-thyratron units.

Three units can therefore be used for counting up to 2^3, or 8, after which the cycle is repeated.*

Addition of a Counting Meter.—By coupling a mechanical meter to one of the thyratrons in the final unit, say E, the total number of cycles, or multiples of eight, can be counted. Then, from the reading of this meter and the combination of the three luminous arcs which at any moment are distributed among the three units AB, CD and EF, the total number of voltage impulses recorded by the circuit up to that moment can be determined. This number will be given by eight times the meter reading plus a certain number ranging from 0 to 7 indicated by the arc combination according to the following code, the letters of which indicate the thyratrons which contain the arcs at the moment :—

ACE = 0 BCE = 1 ADE = 2 BDE = 3

ACF = 4 BCF = 5 ADF = 6 BDF = 7

The succession of events and the arc combinations that arise in the course of a complete cycle can be made out from fig. 3. The succession of groups in the figure represents the changes which take place in the positions of the arcs in the thyratrons as successive impulses are applied to the first unit AB, an arrow indicating that the arc in the unit where it occurs has changed its position in the direction indicated. In following the various changes, it will be observed that :—

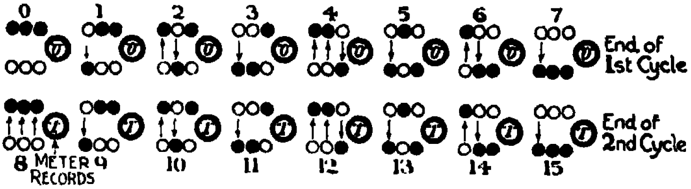

FIG. 3.—Arc combination corresponding to various phases of two complete cycles. • = arcing thyratron. ○ = extinguished thyratron. Ⓝ = meter reading. Arrows indicate direction of alternation of arc.

(1) There is always an arc in one, and *only* one, of the two thyratrons of any unit (initially in A, C and E).

(2) Successive voltage impulses applied to unit AB cause the arc in that unit to alternate between A and B.

---

* It is evident that the counting efficiency of such a system is higher than that of a thyratron ring if the number of thyratrons exceeds four. A cycle in a ring of $2n$ thyratrons is repeated after $2n$ impulses. In the present circuit, however, by using n pairs of thyratrons (*i.e.*, $2n$ thyratrons) 2^n impulses may be recorded before the cycle is repeated.

(3) While a shift of the arc from A to B (downwards in fig. 3) does not affect the arc in unit CD, its return to A (upward in fig. 3) causes the position of the arc in CD to change, and similarly for the action of the arc in CD on that in EF.

It will be noted that after every eighth impulse, the meter reading changes, and the arcs occupy their initial positions and are ready for the next cycle.

"*Scale of Two*" *Notation.*—An examination of the diagram shows that while the arc in unit AB changes its position with every impulse, the arc in unit CD changes with every second impulse, and that in unit EF, with every fourth impulse. The units can, therefore, be regarded as having recording significances of 1, 2 and 4 respectively. From this, one can deduce a simple method of reading off the numbers between 0 and 7 corresponding to the various arc combinations. This consists of ignoring thyratrons A, C and E, and assigning recording values of 1, 2 and 4 respectively to thyratrons B, D and F, and adding together the numbers indicated by the arcs in these thyratrons. Fig. 4 represents the first 15 natural numbers recorded in this way.

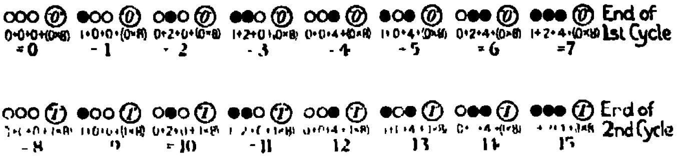

FIG. 4.—Recording of natural numbers as a "scale of two" notation by three units and a meter.

Arc in thyratron B indicates......... 1 2^0.
Arc in thyratron D indicates......... 1 × 2^1.
Arc in thyratron F indicates......... 1 × 2^2.
Number N on meter dial indicates N × 2^3.

The circuit as thus arranged is really the simplest possible example of an arrangement which was suggested on p. 309 of the author's earlier paper, but which had not then been tried experimentally. It may be described, perhaps, as a "thyratron dial meter," since each of the three units of two thyratrons is virtually a dial which, according to the thyratron in it that contains the luminous arc, registers "0" or "1" of the recording value of the unit. Taking the three units and their thyratrons in the order AB, CD, EF, "0" is indicated by the arcing of the first thyratron in each (A, C and E) and "1" by the arcing of the second (B, D and F). Hence, as the recording, or group, values of the "dial" units are, respectively, 2^0 or 1, 2^1 or 2, and 2^2 or 4, and since the meter indicates the total number of groups of 2^3 or 8, the counting is carried out according to a "scale of two," the three thyratron dials recording "units," "twos" and "fours" and the meter "eighths," instead of units, tens, hundreds, and thousands.

There is no theoretical limit to the number of units which could be employed. In practice, however, whenever possible, it is more economical to use a mechanical meter than a thyratron unit. Only as many thyratron units, therefore, should be employed as are necessary to ensure that the mechanical meter can follow alternations of the arcs in the final unit comfortably. The "resolution" of the whole system is then governed by the rapidity with which alternations of arcs can take place in the *first* unit. This depends only upon the electrical characteristics of the first unit as a whole, which, being to a certain extent under control, can be chosen for maximum efficiency.

Practical Arrangements.

The counting circuit at present in use is illustrated in fig. 5. For simplicity, the cathode heating circuit and anode batteries, etc., are omitted. The circuit is seen to consist of three two-thyratron units similar to that shown in fig. 1, with a mechanical meter coupled to the last unit. As regards the mode of coupling the various units with one another, it will be remembered that on p. 309 of the writer's previous paper the possibility of using a valve form of coupling is suggested in a footnote. Owing to the simplicity of the present two-thyratron units, however, the latter may be linked together in the simplest possible manner by connecting the input side of the grid condensers in the second and third units respectively to the anodes of one of the thyratrons in

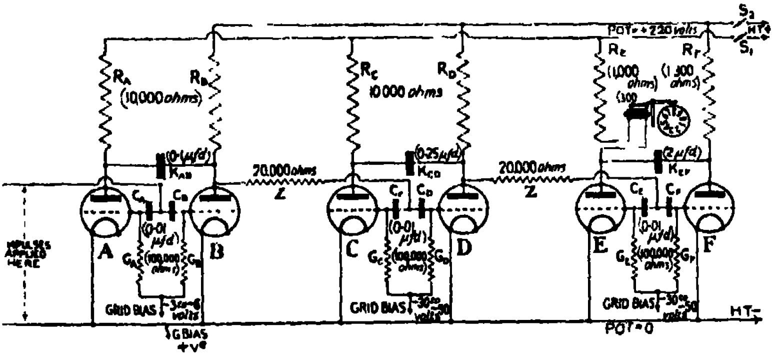

Fig. 5.—Circuit diagram of cascade arrangement of three two-thyratron units.

the preceding first and second units, through high resistances (Z) as shown.* The impulses are then transmitted from one unit to the next as follows.

Assuming that there is initially an arc in A, when B strikes the anode potential of B drops suddenly from say, +220 volts to +15 volts, and a negative potential surge is transmitted through the condenser K_{AB} to the anode of A, thus extinguishing A. A similar negative surge is also transmitted through the condensers C_C and C_D to the grids of thyratrons C and D ; since, however, the surge is *negative* in sign, thyratrons C and D will not respond to this impulse. When, on the other hand, thyratron A strikes, as before, a negative surge is first transmitted to the anode of B, causing B to be extinguished. The extinction of the arc in B is immediately followed by a very rapid exponential *rise* in the anode potential of B, of the order of double the magnitude of the applied anode potential (*i.e.*, in this case, about 400 volts), and so a very large *positive* impulse is now transmitted through condensers C_C and C_D to the grids of thyratrons C and D. This impulse causes the arc in one thyratron (C or D) to be transferred to the other in the manner already described in the case of thyratrons A and B. Thus, a *positive* impulse is transmitted from the first unit to the second when thyratron B is extinguished (or in other words, when A arcs) but not when B arcs. In a similar way positive impulses are transmitted from the second unit CD to the third unit EF, when thyratron C arcs, but *not* when D arcs.

It will be realised that the magnitudes of the impulses applied to the second and third units are in no way dependent upon the magnitudes of the impulses originally applied to thyratrons A and B in the first unit, but depend only upon the characteristics of the thyratrons and their associated circuits, and upon the applied anode voltages. This is a very great advantage, for while some slight initial adjustment might possibly be necessary to ensure that thyratrons A and B were matched so as to respond equally well to an applied impulse of given magnitude, a much cruder adjustment suffices for thyratrons C, D, E and F, and delicate adjustments can therefore be completely eliminated. The large impulses applied to these thyratrons have a further advantage in that a much greater margin of safety can be allowed in choosing the values of the negative grid bias potential to be applied to thyratrons C, D, E and F ; for comparison it may be observed that, whereas the bias applied to A and B is usually between —3 and —6 volts, that applied to C, D, E and F is of the order of —30 to —50 volts. In passing it may be mentioned that the process of determining the values of the bias to be applied is merely a simple "trial and error" experiment occupying a few minutes. With a "ring" circuit, on the other hand, the process of adjusting the ring so that all thyratrons respond equally well to a given impulse occasionally proves to be an extremely delicate operation, though, of course, experimental conditions may very often be such that the ring need not be very critically adjusted. The present circuit, on account of the greater margin of safety, is found to be very stable and reliable in operation from day to day, and to require very little attention indeed.

---

* The object of the resistances Z is to reduce the tendency of the second and third units to react back and disturb conditions in the first and second units with which they are connected. Under certain conditions, however, it is found that they may be omitted (*i.e.*, —$Z = 0$) without affecting the operation of the circuit.

The connection of the counting meter for this type of circuit is very much simpler than in the case of a ring circuit; the magnet winding of the meter is simply connected in series with the anode resistance of thyratron E, and the anode circuit of thyratron F is made symmetrical with that of E. The meter is then actuated when E strikes. Telephone call meters suitably modified to work at high speed are used for the purpose.* The remaining components consist of high quality commercial wireless apparatus.

Choice of Time-Constant.†

In order to reduce the anode currents and increase the life of the thyratrons, the anode resistances should, where possible, be made large. The "extinguishing" condenser K_{AB} should be made as small as possible in order that the resolution of the first unit should be high. In other words, thyratron B must be ready to strike again as soon as possible after its extinction consequent upon the striking of thyratron A. The same remarks apply to units CD and EF, though of course, since these units have to count at mean rates of one-half and one-quarter that of unit AB, they may have correspondingly longer time-constants, thus increasing the safety margin.

It was concluded theoretically that unit AB should fail to resolve impulses unless they were separated by time intervals rather greater than 0·7 RK. For it can be shown that after the negative surge from the striking thyratron has extinguished the arc in the other, the anode potential of the extinguished thyratron, though rising exponentially with time constant RK, does not rise above the minimum value for which an arc can be maintained until a time

---

* Referred to as "Message Recorder" Type 4007 J, obtainable from the Standard Telephone & Cable Company.

† In what follows, the product of the anode resistance R and the capacity K will be referred to as the "time-constant."

$T = RK . \log_e 2$, or $0 \cdot 69$ RK seconds after the extinction. During this period, the extinguished thyratron can be regarded as "dead" to an applied impulse.

A simple experiment showed that this conclusion was justified. Pairs of impulses whose time separation could be varied were applied to the circuit, while the value of RK for the first unit was varied. It was found that the minimum time of separation of impulses which could be counted separately (*i.e.*, "resolved") was approximately proportional to the time-constant RK over the range of values tried, and that this minimum time of separation was of the order of 0·7 to 0·8 RK, which is of the same order of magnitude as the theoretical minimum possible value. As it was desired merely to determine very generally the effect of varying the time-constant upon the resolution and the approximate practical value of the constant of proportionality, no attempt was made to attain high accuracy in the timing in this experiment.

While it is desirable to use as low a time-constant as possible, a practical limit is set by the fact that if RK is made too small, the extinction processes may become somewhat uncertain. With the particular apparatus and thyratrons used, this uncertainty was encountered when RK was made rather less than $0 \cdot 5 \times 10^{-3}$ seconds. It must be observed, however, that this practical limit might possibly depend upon individual circumstances, and that it might be still lower under different conditions. Reference to fig. 5 will show that R and K for the first unit are respectively 10,000 ohms and 0·1 μfd. giving a value of $RK = 10^{-3}$ seconds. This value was chosen as being reasonably low, and at the same time ensuring certainty of operation of the first unit. According to the factor given above, this unit should therefore resolve pairs of impulses with time separations of about 1/1400th to 1/1250th second, which are much shorter than are usually encountered in the research for which the circuit is at present being used. Should the necessity arise, however, it should be possible to make the apparatus respond to still shorter time intervals. In the case of units CD and EF, the larger time-constants have been chosen to increase the margin of safety.

Current Supplies.

Owing to the absence of critical adjustments and the large margin of safety which can be allowed in biasing the thyratrons, small fluctuations of anode potential do not seem to affect the working of the apparatus. The necessary potential for the anodes can therefore be taken, very conveniently, from the laboratory 220-volt D.C. mains, regardless of whether the latter are connected to accumulators or to a dynamo. If it is anticipated that high frequency surges are likely to be carried along the mains to the apparatus, it might be advisable to incorporate a smoothing circuit between the mains and the thyratrons; so far, however, the present apparatus has operated satisfactorily without such a filter.

Since the cathodes are all at a common potential, they can derive their heating current from a common supply, and A.C. from a transformer can be used to supply the necessary 6 or 7 amperes at 2 volts required by each thyratron, the centre of the secondary winding being connected to the high-tension supply negative terminal. As mentioned in the earlier paper, the use of A.C. for directly heated cathodes is attended by the slight disadvantage that there is a periodic variation in the critical striking potential of $\sqrt{2}$ volts at double the A.C. frequency. Usually, however, this is not a very great drawback compared with the advantages gained by the use of A.C. for cathode heating. It may be eliminated, of course, by employing indirectly heated thyratrons for the first unit, or by using D.C. for cathode heating.

The grid bias potentials are all supplied from a common battery, thyratrons A and B being biased to just below their critical potentials, while the remaining thyratrons are heavily biased to increase the margin of safety. The characteristics of the first two thyratrons will usually be sufficiently similar for the same bias to be applied to both. If better matching is required, a 2-volt potentiometer can be incorporated in the grid circuit of one thyratron for finer control.* In the case of the remaining thyratrons this is entirely superfluous.

The superiority of the present circuit over the ring circuit is evident when it is realised that the "priming" operation of the ring circuit (upon which the principle of that circuit depends) necessitates the use of (*a*) independent current supplies from separate transformer windings for *every* thyratron, or alternatively, indirectly heated thyratrons, (*b*) separate 30 to 50 volt grid bias batteries for every thyratron, (*c*) a steady anode potential supply from accumulators, and (*d*) rather careful adjustments of potentials.

It is interesting to note the ease with which the first unit of the present circuit can be isolated from the rest of the apparatus should this prove desirable. If necessary, the first unit thyratrons may have their cathodes heated from an accumulator, and derive their comparatively small anode currents from a separate accumulator battery to ensure steadiness, while the remainder of the thyratrons derive their supplies from the common laboratory mains.

---

* See also p. 308 of the author's earlier paper (*loc. cit.*) and p. 352 of the paper by Rutherford, Wynn-Williams and Lewis (*loc. cit.*).

Additional Conveniences.

One or two practical details, which have been found to be extremely useful in increasing the ease of operating the counting circuit, may be briefly mentioned :—

(*a*) In starting up the apparatus, the sudden application of anode potential to all the thyratrons may cause both thyratrons of one unit to arc simultaneously. This can be avoided by the use of two anode switches S_1 and S_2 (fig. 5) which are closed separately.

(*b*) After a count, it is desirable to return the arcs to thyratrons A, C and E (corresponding to "0"). This may be done rapidly by means of a triple contact key or relay which momentarily connects the grids of thyratrons A, C, E to their cathodes, *in that order.*

(*c*) Observations may be more conveniently taken at a distance from the thyratrons if the meter leads are extended, and a "repeater" consisting of three commercial neon lamps ("Osglim" lamps) are used. The latter have their anodes and cathodes connected in parallel with those of thyratrons A, C and E, and glow when respectively thyratrons B, D and F are arcing, but are extinguished when arcs strike in A, C and E, since they are short circuited by these arcs. The neon lamps then function as the "1," "2" and "4" dials corresponding to fig. 4. The first unit is made symmetrical by means of an additional lamp connected across thyratron B. The use of the neon lamps has another advantage in that the glowing lamp connected across an extinguished thyratron tends to maintain a steady potential between the anode and cathode of that thyratron despite small fluctuations in the supply voltage.

(*d*) When a long series of rapid counts is to be made, conversion of the meter and thyratron readings into corresponding natural numbers can be rapidly effected by reference to a simple table in which the natural numbers are simply written in order in eight columns, as shown below.

Meter reading.	Combination of arcs in thyratrons B, D, F.							
	– – – = 0	B – – = + 1	– D – = + 2	B D – = + 3	– – F = + 4	B – F = + 5	– D F = + 6	B D F = + 7
0	0	1	2	3	4	5	6	7
1	8	9	10	11	12	13	14	15
2	16	17	18	19	20	21	etc.	etc.

The above table could be modified for any number of units; with four units, AB, CD, EF, and GH, for example, the values of thyratrons B, D, F and H are "1," "2," "4" and "8," while the meter records multiples of "16."

Summary.

A new type of automatic counting circuit is described whereby several units of two thyratrons are arranged in cascade to form what might be termed a "thyratron dial meter." This meter can be used to record the occurrence of physical events according to a notation on a "scale of two." Since there are no moving parts associated with the thyratrons, the time of response of the circuit is governed only by its electrical characteristics. Events can therefore be recorded at extremely high rates, two events separated by as little as 1/1250th second, or even less, being "resolved" and separately registered by the counting circuit.

To a certain extent, the circuit resembles the "thyratron ring" counting circuit previously described by the author, since both circuits utilise to the greatest advantage the "inertialess relay" characteristic of the thyratron. The present circuit, however, operates in a different manner, and has many advantages over the ring circuit. These include:—

(1) All current supplies can be derived from the common laboratory mains.
(2) An entire absence of delicate adjustments.
(3) Large margins of safety, ensuring stability and reliability.
(4) Simplicity of construction.
(5) Only *two* thyratrons need be matched, and the impulses to be counted need be applied only to these two thyratrons.
(6) When the number of thyratrons exceeds four, the counting efficiency exceeds that of a ring containing an equal number of thyratrons.

The circuit has been fully tested, and is at present in use for the automatic counting of α-particles. Practical details are given of the various values of the components required for its construction.

The writer has much pleasure in expressing his thanks to Lord Rutherford for his encouragement and interest in the work, and for granting facilities for carrying out the experimental tests in the Cavendish Laboratory. He also desires to record his gratitude to the British Thomson Houston Company, Rugby, for a gift of six Mazda Type BT.1 Thyratrons. These were employed in the apparatus, and enabled the necessary tests to be made.

Investigations with a Wilson Chamber. I.—On the Photography of Artificial Disintegration Collisions.

By P. M. S. Blackett and D. S. Lees.

(Communicated by Lord Rutherford, F.R.S.—Received December 23, 1931.)

[Plates 7 and 8.]

Introduction.

The work of photographing by the Wilson method the artificial disintegration of elements has been continued. In the earlier work,* about 400,000 tracks of alpha particles in nitrogen were photographed and eight collisions were observed in which a proton was ejected and the alpha particle captured. This process was shown to correspond to the formation of a then unknown isotope of oxygen O_{17}. Recently this isotope has been discovered spectroscopically in the atmosphere.† Four more collisions of the same type have been observed by Harkins‡ and his co-workers.

There are two main objectives in such investigations. It is important to discover if the disintegration of elements other than nitrogen takes place also with the capture of the alpha particle, or whether disintegration without capture can occur. The Wilson method is the only *direct* method of doing this, since it is only thus that the motion of all the particles involved in the collision can be observed.

It is also important to decide whether the process of disintegration by capture takes place with a definite energy change. This question can be investigated more easily by other methods, if assumptions as to the nature of the collisions are made. But the directness of the evidence provided by the Wilson method to some extent atones for its inevitable paucity.

An automatic Wilson chamber of 16 cm. diameter was used in conjunction with a double camera taking two photographs on two cinema films at right angles. The lenses were tilted in such a way that the whole plane of the chamber was in sharp focus on both films. This method makes it possible to work with much wider beams of alpha particles than with the original type of apparatus. Full descriptions of the automatic apparatus§ and of the theory and design of the camera have been published.* The condition for obtaining the maximum number of "resolved" collisions has also been discussed.

---

* Blackett, 'Proc. Roy. Soc.,' A, vol. 107, p. 349 (1925).

† Giauque and Johnston, 'Nature,' vol. 123, p. 831 (1929).

‡ 'Z. Physik,' vol. 50, p. 97 (1928); 'Phys. Rev.,' vol. 35, p. 809 (1930).

§ Blackett, 'J. Sci. Inst.,' vol. 6, p. 184 (1929).

The obvious elements to investigate, other than nitrogen, would be boron, fluorine and phosphorus, all of which disintegrate readily and can be obtained in gaseous compounds. While experiments were undertaken to overcome the technical difficulties involved in working with these elements, it was decided to photograph tracks in argon. This is technically easy to do and some early measurements of Rutherford and Chadwick† by the scintillation method gave some hope that the yield of disintegration collisions was not too small to be observed photographically.

Accordingly some 750,000 tracks in a mixture of 50 per cent. argon, 10 per cent. oxygen, and 40 per cent. hydrogen were photographed using a source of thorium B + C. In addition some 350,000 tracks in a mixture of 50 per cent. nitrogen, 45 per cent. hydrogen and 5 per cent. oxygen were also photographed, in order to extend our knowledge of the nitrogen disintegration process.

The oxygen was added to the gas to make the tracks fine, and the hydrogen to increase their length, so as to separate them more widely from each other and so to increase the number of resolved tracks, that is, those that are not obscured by their neighbours.

The result of the work was disappointing. Among the 750,000 tracks in the argon mixture, no collision was observed that could possibly be attributed to the disintegration of argon. The only two inelastic collisions found amongst the tracks in the argon-oxygen mixture appeared to be due to the disintegration of nitrogen or oxygen atoms. The measurements were not sufficiently exact to distinguish between these possibilities. However, the evidence that oxygen does not disintegrate at all, obtained by other methods, is sufficiently strong to conclude that the gas mixture must have contained an appreciable amount of nitrogen.‡

Among the 350,000 tracks in the nitrogen mixture two disintegration collisions were found. Both these are of the same type as the eight obtained in the earlier work. Little fresh information has thus been obtained from the million new tracks photographed.

The great advantage of the new camera and larger chamber can be seen from the following figures. In the earlier work, to obtain 400,000 tracks,

---

* Blackett, 'Proc. Roy. Soc.,' A, vol. 123, p. 613 (1929).

† 'Proc. Phys. Soc. Lond.,' vol. 36, p. 417 (1924).

‡ The argon from the cylinder was not analysed. It was supposed to be 99 per cent. purity.

23,000 photographs were required, averaging 18 tracks a photograph. In the recent work, 1,100,000 tracks have been obtained on 18,000 photographs, averaging 60 tracks a photograph. In addition the new tracks are all in perfect focus, which was not true previously of those at the extreme sides of the beam. If a track image is said to be resolved, when no other track lies within a distance of twice its width,* then the fraction of the images of the disintegration collision resolved in the new work is 63 per cent., compared with 19 per cent. in the earlier work.

The new camera requires a smaller intensity of illumination, owing to the smaller magnification used (1/5 compared with 1/2); against this must be set the slightly detrimental effect of the film grain on the appearance, but not on the measurability, of the photographs.

Still greater efficiency would have been obtained by using the gas under investigation at reduced pressure instead of diluted with hydrogen.

The small yield of disintegration collisions with the nitrogen mixture is to be attributed partly to chance, partly to the fact that the tracks were not photographed as close to the source as before, and partly to the policy of diluting the nitrogen with hydrogen (*loc. cit.*, p. 627), in order to increase the yield of *resolved* tracks at the expense of the total number.

The Dynamics of the Collision.

Consider a collision in which an alpha particle of mass M is captured by a nucleus of mass m_0, with the ejection of a proton of mass m_p, and with the formation of a new nucleus of mass m_n. Then if momentum is conserved during the collision we have

$$m_p v_p = \mathrm{MV} \sin w / \sin (\psi + w) \tag{1}$$

$$m_n v_n = \mathrm{MV} \sin \psi / \sin (\psi + w), \tag{2}$$

where V, v_p, v_n are the initial velocity of alpha particle, and the final velocities of the proton and nucleus. The angles ψ and w are the angles of projection of the proton and nucleus. If V is known from the distance of the collision from the source, v_p and v_n can be calculated from (1) and (2) using the observed values of ψ and w.

An independent determination of all these velocities, since these are related by (1) and (2), can be obtained by the measurement of the range R_n of the nucleus, by using the relation between the range and velocity of these particles.

---

* 'Proc. Roy. Soc.,' A, vol. 123, p. 032 (1929).

For it has been shown previously how the range-velocity relation of any isotope such as O_{17} may be estimated.* This method also allows the ambiguity, usually present when using a thorium B + C source, as to whether the particle concerned was one of the 8·6 or 4·8 cm. groups, to be settled.

The nature of the disintegrated nucleus, if this is in doubt, can be decided by comparing the observed R_n with the calculated value, assuming in turn the various possible nuclei, or, by what amounts to the same method, by calculating the atomic number of the new nucleus from its range and momentum.

If the ejected proton track ends in the chamber, so that its range R_p can be measured, another independent determination of v_p and so of V and v_n can be made.

The energy Q released during the capture process is given in terms of the kinetic energies E_α, E_p and E_n of the alpha particle before collision, and the proton and nucleus after the collision by

$$-Q = E_\alpha - E_p - E_n, \tag{3}$$

which with (1) and (2) gives

$$Q = -\tfrac{1}{2}MV^2\left\{1 - \frac{M}{m_p}\,\frac{\sin^2 w}{\sin^2(\psi + w)} - \frac{M}{m_n}\,\frac{\sin^2\psi}{\sin^2(\psi + w)}\right\}. \tag{3A}$$

Of the two observed angles w is less accurately measurable than ψ since the track due to the new nucleus is short and rather wobbly, while the track of the proton is straight and fine. Since, further, E_p is usually considerably larger than E_n, the accuracy of the determination of Q depends mainly on the accuracy of the measurement of w. The actual expression for the error in Q due to an error δw in w is found from (3A) to be

$$\Delta Q = m_p v_p^2\left\{\cot w - \cot(\psi + w)\left(1 + \frac{m_p}{m_n}\,\frac{\sin^2\psi}{\sin^2 w}\right)\right\}\delta w. \tag{4}$$

It has been shown in Paper 3 that the error in w is to be taken as about 1 degree. If this is done the error in Q for a typical nitrogen disintegration collision is about 300,000 volts.

The Disintegration Collisions.

In Table I are given the measurements of the four best of the original eight disintegration collisions (tracks 1, 2, 3 and 5), together with the four new collisions (9, 10, 11 and 12) and one photographed by Harkins and Shadduck (*loc. cit.*).

---

* 'Proc. Roy. Soc.,' A, vol. 107, p. 314 (1925).

The original eight collisions have all been critically re-examined and re-measured and it was decided that only the four mentioned above were technically good enough to give significant values for the energy change. Track No. 3 had been previously wrongly assigned to an 8·6 cm. particle.

Table 1.—Nitrogen Disintegration Collisions.

	Measured quantities.				Calculated quantities.					
	1	2	3	4	5	6	7	8	9	10
Track	ψ.	w.	R_s.	R_n.	R_a.	$v_a \times 10^{-8}$	$v_p \times 10^{-8}$	$v_n \times 10^{-8}$	R_n/R_n'.	R_p.
	°	°	mm.	mm.	mm.	cm./sec.	cm./sec.	cm./sec.		cm.
1	41·5	20·8	23·2	2·25	59·5	18·3 (18·3)	29·2	3·22 (3·23)	1·13	27·2
2	62·2	29·0	14·7	2·94	68·0	19·1 (20·0)	37·4	3·97 (4·15)	1·17	64
3	65·3	20·8	6·8	2·52	37·5 S	15·7 (16·8)	22·9	3·36 (3·60)	1·22	12·1
5	84·1	22·4	25·2	3·42	57·5	18·1 (19·5)	29·6	4·42 (4·75)	1·21	28·4
9	111·8	13·2	58·7	2·78	24·0	13·4 (12·9)	14·6	3·57 (3·43)	1·09	3·0 obs. >3·5
10	67·7	18·6	26·9	2·60	55·8	18·0 (14·9)	(19·0)	3·92 (3·25)	0·91	6·7
11	107·1	18·0	21·7	3·00	22·6 S	13·1 (13·3)	19·9	3·60 (3·66)	1·15	7·7
12	27·0	13·8	15·1	1·50	29·2 S	14·4 (12·9)	19·6	2·34 (2·10)	0·97	7·3
H & S	118·5	15·3	26	4·3	62	18·6 (17·8)	26·4	5·32 (5·10)	1·07	19·4

The ranges are given in millimetres of air at 760 mm., 15° C.

Numbers 1, 2, 3, 5 are from the earlier work.
Numbers 9, 10, 11, 12 are from the new work.
Number H & S is by Harkins and Shadduck.
Numbers 9 and 10 were taken in an argon-oxygen mixture, in which nitrogen must have been present as an impurity.

Among the 750,000 new tracks from thorium B + C in the argon mixture only two inelastic collisions were found, both corresponding clearly to the capture of an alpha particle and the ejection of a proton. For the reasons mentioned it is assumed that these two collisions represent the disintegration of nitrogen nuclei. These tracks are numbered 9 and 10.

Columns 1 and 2 give the angles ψ and w of projection of the proton and the O_{17} atom. Columns 3 and 4 give the distance R_s from the source to the collision and the length R_n of the track of the O_{17} atom. Column 5 gives the residual range of the alpha particle before the collision, obtained by subtracting R_s from 82·7 or 44·3 mm. These were the measured mean ranges in the chamber of the particles forming the 8·6 and 4·8 cm. groups. The reduction in range is to be attributed to a dirty source. The ranges given are equivalent ranges at 760 mm. and 15° C. For track number 9 there is no ambiguity about the group to which the alpha particle belongs, since $R_s > 4\cdot8$ cm., so that the alpha particle must have been an 8·6 cm. particle. Number 10 is also attributed to the same group (see below).

Column 6 gives the velocity of the alpha particle before the collision obtained from the ranges in column 5. The letter S in column 5 denotes that the track was assigned to the 4·8 cm. group, those not marked being assigned to the 8·6 cm. group.

Columns 7 and 8 give the values of v_p and v_n obtained from equation (1) and (2). Column 9 gives the ratio of the observed range R_n of the new nucleus to the range R'_n of a nitrogen nucleus of the same velocity. Column 10 gives the range of the proton calculated from v_p, using data given in a paper by one of us.* In brackets in column 8 is given the value of v_n obtained from R_n, assuming a value for the ratio R_n/R'_n of 1·14. In brackets in column 6 is the corresponding value of V_α.

A new determination of the relation between the range and velocity of nitrogen and argon atoms has been made.† The following are the results relevant to the present discussion.

Range (mm. air) at 760 mm. 15° C.	1	2	3	4	5
	cm./sec.	cm./sec.	cm./sec.	cm./sec.	cm./sec.
Velocity of nitrogen atoms	$1\cdot65\times10^8$	$2\cdot88\times10^8$	$4\cdot10\times10^8$	$5\cdot35\times10^8$	$6\cdot60\times10^8$
Velocity of argon atoms	$1\cdot40\times10^8$	$2\cdot10\times10^8$	$2\cdot75\times10^8$	—	—

It has been shown previously‡ that the ratio R_n/R'_n should be about 1·14 if the new nucleus is an O_{17} atom. For track No. 9 the observed ratio is 1·09, which is in good agreement with expected value. For No. 10 the ratio is 0·91. This low value can be explained if the velocity of the alpha particle was less than that calculated from the distance from the source. There were always found in the beam some particles which had considerably less than the full range of the groups. These were probably produced by a dirty source. It is reasonable to attribute the discrepancy to this cause, and to take, therefore, for the initial velocity of the alpha particle the lower value obtained from R_n, shown in brackets in column 6.

---

* Blackett, 'Proc. Roy. Soc.,' A (*in the press*).

† Blackett and Lees, 'Proc. Roy. Soc.,' A, vol. 134, p. 658 (1931).

‡ Blackett, 'Proc. Roy. Soc.,' A, vol. 107, p. 349 (1925).

It is impossible to attribute either of these two collisions (9 and 10) to the disintegration of argon, as the recoil atoms of atomic number 43 would be then expected to travel only 1·35 and 1·40 mm., while actually the observed lengths are 2·78 and 2·60. Since the gas mixture was supposed to contain only argon and oxygen, one would conclude that these two tracks represent the disintegration of oxygen. However, the evidence from other methods that oxygen does not disintegrate, together with the fact that these two tracks are quantitatively and qualitatively similar to the undoubted nitrogen disintegration collisions, makes it very probable that there was actually a considerable amount of nitrogen in the chamber. These two tracks are therefore assumed to represent nitrogen disintegration collisions.

The track (9) is reproduced on Plate 7 and is interesting in that almost the whole length of the proton track appears in the photograph. One can judge from the appearance of the proton track that it would end only a short distance outside the field of view. The observed length of a little greater than 3·5 cm. is in very good agreement with the calculated length of 3·0 cm. when account is taken of the fact that the range depends approximately on the cube of the velocity. Taking, as is nearly true, R_p as experimentally observed, we obtain, using equation (1), an independent determination of V_a in close agreement with the other two independent determinations. In no other collision photographed can this be done. The chance that R_p is small enough to end in the chamber, and further that the track lies near enough to the horizontal plane to do so, is very small.

The second track (No. 10) is poor technically. The photograph provides, however, an immediate proof, additional to that given by R_n, that the struck nucleus is not argon. For its track is deflected at one point through about 35° without however producing a visible spur. This can only occur when a particle strikes another atom considerably heavier than itself; for instance when an O_{17} atom strikes an argon atom.

The measurements of the two disintegration collisions Nos. 11 and 12 found among the 350,000 tracks in the nitrogen mixture are given also in Table I. Both are exactly of the type previously found and are certainly to be attributed to the formation of O_{17} from nitrogen. Both collisions are attributed to 4·8 cm. particles. One photograph of No. 11 is reproduced on Plate 8 (photograph No. 1).

The mean of the values of R_n/R'_n for all the tracks except Nos. 10 and 12 is 1·13, which is in good agreement with the estimated value of 1·14. The closeness of the agreement is fortuitous as the uncertainties both in the measurements and in the theoretical estimation are large. The low values for Nos. 10 and 12 are to be attributed to the alpha particles having a smaller initial velocity than that calculated from their distance from the source.

The Energy Change.

In Table II, column 3, is shown the energy change Q in millions of volts, calculated from (3). The initial energy E_α of the alpha particles is also given. The values of V_α used are the means of those in column 6, Table I, that is the

Table II.—Energy Change during Disintegration Collisions.

1.	2.	3.	4.	5.
Track.	E_α $\times 10^{-6}$ volts.	Q $\times 10^{-6}$ volts.	Difference from mean.	ΔQ from (4).
1	7·10	−1·63	0·36	0·33
2	8·07	+0·94	(2·21)	0·46
3	5·67	−1·69	0·42	0·25 (0·28)
5	7·50	−0·90	0·37	0·45
9	3·64	−1·41	0·14	0·23
10	4·71	−1·85	0·58	0·28 (0·48)
11	3·70	−0·41	0·86	0·32
12	3·93	−1·45	0·18	0·22 (0·28)
H & S	7·03	−0·83	0·44	0·71
	Mean	−1·27 ± 0·13	Mean 0·42	Mean 0·39

Track No. 2 is excluded from the averages of columns 3 and 4.

mean of the values deduced from R_s and R_n; except for No. 10, where, owing to the large discrepancy, the value obtained from R_n has been adopted.

In the last column is given the probable error ΔQ calculated from (4), assuming a probable error of 1° in w. This value for the probable error of w is derived from the results of the measurements of a number of elastic collisions. The work is described in detail in Paper III. There is also to be considered the error in Q due to the error in V_a. This latter can be taken as about half the difference between the energies corresponding to the values in column 6. For all the tracks, except 10 and 12, this error is quite small compared with that due to the error in w. For the two cases where the errors are comparable, the errors have squared and added. The values so obtained are shown in brackets underneath the values obtained from (4).

DISCUSSION OF RESULTS.

The Energy Change.

Chadwick, Constable and Pollard[*] have recently examined the disintegration of nitrogen by an electrical counting method. They find evidence of only a single group corresponding to a loss of energy of 1·3 million volts. The earlier experiments of Rutherford and Chadwick by the scintillation method gave 1·4 million volts.

A discussion by Bothe[†] of these results, together with some earlier work by Bothe and Franz,[‡] gives support for the assumption that the main disintegration process with nitrogen occurs with an absorption of energy of $1 \cdot 0 \times 10^6$ volts.

The average value of Q for all the nine tracks under consideration is $-1 \cdot 0$ million volts, with a mean deviation from the mean of 0·6. Thus the results as a whole can only be considered as in agreement with those obtained by the electrical method, if the average error of Q for a single track is as high as 0·6 million volts, that is considerably greater than the average value of 0·39 for the estimated individual errors (column 5).

If we exclude No. 2, we are left with eight tracks and for these the mean value of Q is $-1 \cdot 27$ million volts, with a mean difference from the mean of 0·42 (column 4). This corresponds to a probable error of a single determination of 0·36, which is in close agreement with the value of 0·39 obtained quite independently by assuming a probable error of 1° in the angle w. The probable error of the mean value of Q is $0 \cdot 845 \times 0 \cdot 36/\sqrt{8} = 0 \cdot 13$ million volts. The eight tracks of this group have therefore values of Q which show a spread of just the amount to be expected in view of the estimated errors in the angles.

---

[*] 'Proc. Roy. Soc.,' A, vol. 130, p. 463 (1931).

[†] 'Z. Physik,' vol. 51, p. 613 (1928).

[‡] 'Z. Physik,' vol. 49, p. 1 (1928).

Returning to track No. 2, for which $Q = + 0 \cdot 94$ million volts, we find that the angle ψ has a value about 7° larger than that which corresponds to the mean Q of the main group. Though the photograph is not very good, owing to the proximity of other tracks, there would be little justification for assuming ψ to be as much in error as this, were it not for the fact that, did such collisions really exist, they would surely have been detected by the scintillation and electrical methods; for this collision gives a proton of range 63 cm., while the maximum range found by Rutherford and Chadwick for alpha particles of the same velocity was 40 cm.

It is always difficult to draw any certain conclusion from a single track owing to the possibility that the recoil atom may have been deflected from its initial direction by making a subsequent nuclear collision within a short distance of the collision which set it in motion. For instance, there is a 1 in 200 chance that an O_{17} nucleus of velocity 4×10^8 cm. per second will make an elastic deflection with a nitrogen nucleus of more than 7°, while travelling the first 2/10 mm. of its track. If this occurred with track No. 2, the event would escape notice in the photograph and so might result in the large value of ψ which is observed. An additional reason to believe that this high value of Q is false is to be found in the weakness of the γ-rays when nitrogen is bombarded by the alpha particles from polonium.* For such a high value of Q would indicate a lower energy level into which it is to be expected that all the other newly formed nuclei would eventually fall with the emission of γ-rays.

One concludes therefore that the evidence of these tracks points to the existence of only one energy level; the alpha particle must be bound into a level $1 \cdot 27 \pm 0 \cdot 13 \times 10^6$ volts higher than the level out of which the proton is ejected.

This result is in disagreement with the conclusions of Urey,† and of Harkins and Gans,‡ in a recent discussion of the earlier data. In both cases an error of 10 minutes of arc was assumed for w, whereas it is now demonstrated in Paper III that the error is much greater, in fact about 1°. The spread of the values of Q can now be explained without the hypothesis of more than one level.

---

* Bothe and Becker, 'Z. Physik,' vol. 66, p. 289 (1930).

† 'Phys. Rev.,' vol. 37, p. 923 (1931).

‡ 'Phys. Rev.,' vol. 37, p. 1671 (1931).

The mass equivalent of the energy change Q is 0·00133 ± 0·00013 in atomic weight units, so the mass of the O_{17} atom should be 14·0083 + 4·0022 — 1·0078 + 0·0013 = 17·0040. This calculation has, however, little value, as the error of 0·0028 given by Aston for his determination of the mass of the nitrogen atom is more than twice the energy corresponding to Q.

The Appearance of Different Types of Collision.

It is of interest to demonstrate the difference between disintegration collisions and ordinary elastic collisions by plotting a point for each collision corresponding to the values of ψ and w (the direction of the tracks of the proton and new nucleus respectively) in the first case, and a point corresponding to the values of ϕ and 0 (the deflection of the alpha particle and the direction of the struck nucleus) in the second case. This is done in fig. 1.

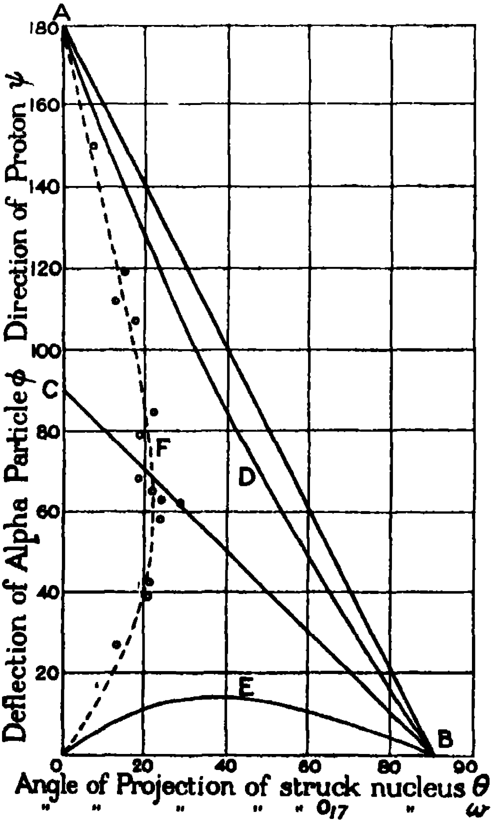

FIG. 1.—⊙ Twelve nitrogen disintegration collisions. ● Two nitrogen disintegration collisions (Harkins).

For an elastic collision we have

$$\frac{m_0}{\mathrm{M}} = \frac{\sin\phi}{\sin(2\theta+\phi)},$$

where M is the mass of the alpha particle and m_0 that of the nucleus. For elastic collision with a very heavy nucleus ($m_0 = \infty$), $2\theta + \phi = \pi$, and points representing such collisions lie on the line AB. For $m_0 = \mathrm{M}$, as for the collision of an alpha particle with a helium atom $\theta + \phi = \pi/2$ and the points lie on BC. For $m_0 = 3\cdot5\,\mathrm{M}$, as for the elastic collision of an alpha particle with a nitrogen nucleus, the points lie on the line ADB. For $m_0 = \mathrm{M}/4$, as for the collision of an alpha particle with a hydrogen nucleus, the points lie on OEB.

For a disintegration collision with capture of the alpha particle the points lie on such a curve as AFO. This corresponds to the collision of a 3·95 cm. alpha* particle with a nitrogen nucleus, with the ejection of a proton and with a loss of kinetic energy $1\cdot40 \times 10^6$ volts. ($\mathrm{Q} = -1\cdot4 \times 10^6$ volts.) It thus corresponds roughly to the single group observed.

To obtain this curve we require an expression for w in terms of V, Q and ψ. This is found from (3) to be

$$\cos(2w - \chi) = \left(\frac{\mathrm{M}}{m_p} + 2\,\frac{\mathrm{M}}{m_n}\sin^2\psi - 1 - \frac{\mathrm{Q}}{\mathrm{E}_a}\right)\Big/(\mathrm{A}^2 + \mathrm{B}^2)^{\frac{1}{2}},$$

where

$$\tan\chi = \mathrm{B}/\mathrm{A},$$

and

$$\mathrm{A} = \mathrm{M}/m_p - (1 + \mathrm{Q}/\mathrm{E}_a)\cos 2\psi,$$

$$\mathrm{B} = (1 + \mathrm{Q}/\mathrm{E}_a)\sin 2\psi.$$

The points corresponding to the measured value of ψ and w for 14 tracks are given in the diagram. Two of these are by Harkins and are shown as full circles. It must be noted that the points would not lie exactly on the curve, even if Q had the above value for each, since the initial energy E_a of the alpha particle differs from track to track. A larger energy loss ($\mathrm{Q} < 1\cdot4 \times 10^6$ volts), or a smaller value of E_a will shift the point to the left of the drawn curve. It will be noticed that in only four of the tracks is the proton ejected at an angle greater than 90°.

The Yield of Collisions.

Assuming that the two doubtful collisions were in fact with nitrogen, the yield can be obtained as follows.

---

* Energy $5\cdot33 \times 10^6$ volts.

The effect of the dilution of the nitrogen with about the same volume of hydrogen is to reduce the chance of a collision with a nitrogen atom by about 25 per cent.* The 350,000 tracks in the nitrogen mixture gave therefore an effective number of 260,000. Assuming that the argon really contained 20 per cent. of nitrogen (this is the utmost that can be assumed), the 750,000 tracks reduce to 120,000 effective tracks in nitrogen, giving altogether a total of 380,000 effective tracks.†

The yield therefore works out at four disintegration collisions in 380,000 tracks or about 11 a million. This is of the same order as the generally accepted yield for complete absorption of 7 cm. particles in nitrogen. Taking the two tracks in the argon mixture alone the yield is 2 in 60,000, which is very high and would be higher still if a smaller content of nitrogen were assumed.

The occurrence of the three tracks Nos. 9, 11 and 12, for which $R\alpha$ has the values 24, 23 and 29 mm., is remarkable. In fact, some support might be derived from these results for the hypothesis of the existence of a selective excitation of nitrogen by particles of about 2·6 cm. range.

Summary.

(1) The experiments on the photography of disintegration collisions have been continued; 750,000 tracks were taken in an argon-oxygen-hydrogen mixture, and 350,000 in a nitrogen-oxygen-hydrogen mixture.

(2) Four more capture disintegration collisions were found, two in each group; the two in the argon mixture being certainly not due to the disintegration of argon. These have been attributed to nitrogen, assumed to be present as an impurity.

(3) The method and accuracy of the determination of the energy charge is discussed, and the results for the four new tracks, the four best of the old, and one of Harkins are given. Eight of these give a mean energy loss of 1·27 ± 0·13 million volts in complete agreement with the results obtained by other methods. One gives a gain of energy, but it is not considered possible to uphold this result against those of other methods, in which such collisions are not found.

We are indebted to the Department of Scientific and Industrial Research both for a grant to one of us (D.S.L.) and for grants for apparatus.

---

* Blackett, 'Proc. Roy. Soc.,' A, vol. 123, p. 628 (1929).

† The 4·8 cm. tracks were photographed from about 3·8 cm. residual range to their ends; the 8·6 cm. tracks from about 7·6 cm. to 1·0 cm. from their ends.

We wish to thank Mr. J. S. Barnshaw, of King's College, for assistance with the trigonometrical calculations.

DESCRIPTION OF PLATES.

PLATE 7.

Photograph of the ejection of a proton from a nitrogen nucleus by an alpha particle of residual range 2·4 cm. Range of proton 3·5 cm. The source was thorium B + C and the end of the 4·8 cm. group of alpha particles can be seen on the photograph. This track is No. 9 of Table I.

PLATE 8.

No. 1.—Another nitrogen disintegration collision (No. 11, Table I).

Nos. 2 and 3.—A pair of photographs of a very nearly head-on and elastic collision of a fast alpha particle with a nitrogen nucleus. The deflection of the alpha particle is about 175°.

No. 4.—An elastic collision of a fast alpha particle with an argon nucleus.

Nos. 5 and 6.—A pair of photographs of an elastic collision of a fast alpha with a hydrogen nucleus. The alpha particle is deflected through about 5°.

Further Investigations with a Wilson Chamber. III.—*The Accuracy of the Angle Determination.*

By P. M. S. BLACKETT and D. S. LEES.

(Communicated by Lord Rutherford, F.R.S.—Received December 23, 1931.)

[PLATE 9.]

I.—The question of the precision of the determination of the angles of forked tracks is of considerable importance, in particular owing to the possibility of determining nuclear energy levels from Wilson photographs. In an earlier paper* some experiments were described in which an artificial track consisting of a bent glass fibre was photographed in different positions. The average error of determination of the angle was found to be 10 minutes of arc. This error was attributed to the lack of perfect adjustment of the camera. That the error of measuring actual tracks could be nearly as small as this was shown by measurements of three collisions in which the difference between the calculated and expected mass ratios was consistent with a probable error

---

* Blackett, 'Proc. Roy. Soc.,' A, vol. 103, p. 62 (1923).

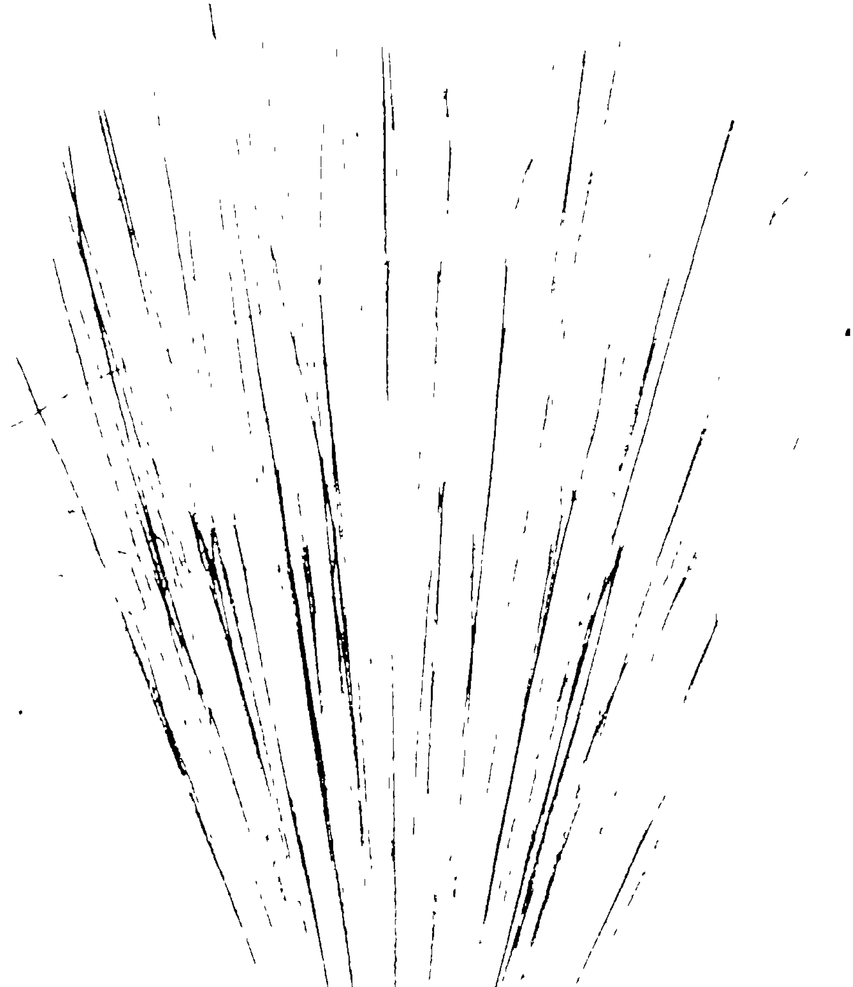

(*Facing p.* 338.)

1

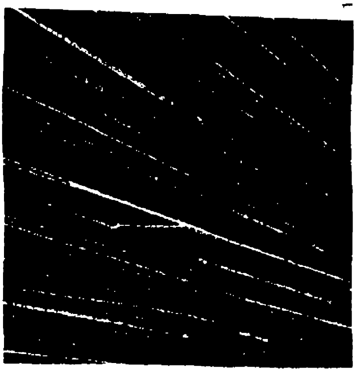

2

3

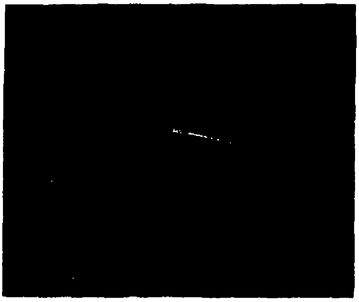

4

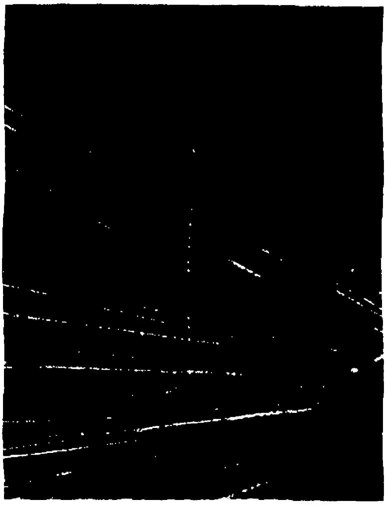

5

6

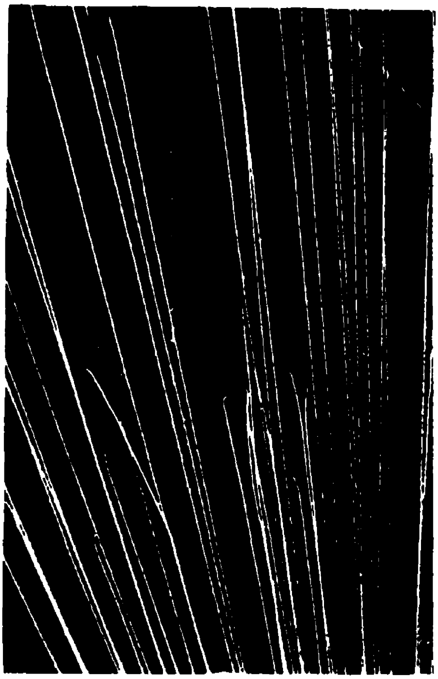

1

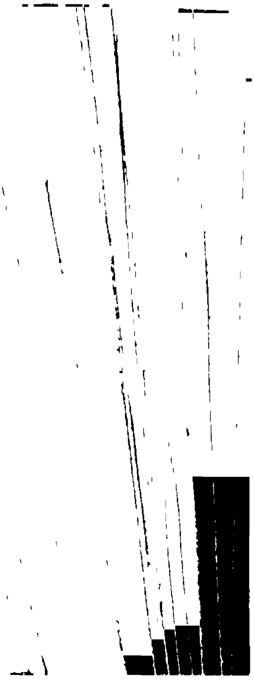

2

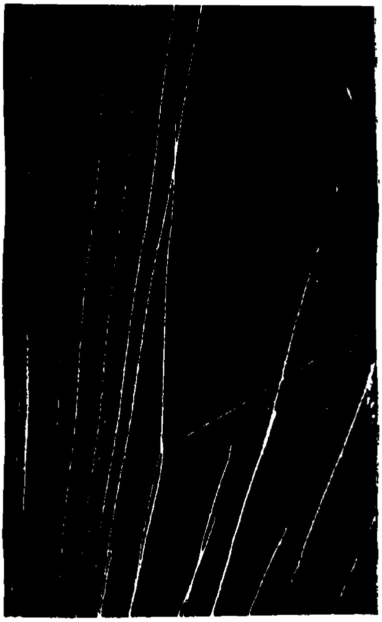

3

of about 10 minutes of arc for the angle measurements. Only such forks were used for these calculations of the mass ratio, for which the three arms appeared unusually straight and for which the test for coplanarity was accurately satisfied. Subsequently two collisions with hydrogen nuclei were described in which the error of the angles was held to be as low as 6 minutes of arc. It was pointed out at the time that many tracks did not, in fact, satisfy these conditions, but sufficient data were not then available for a statistical analysis of the distribution of calculated mass ratios, from which a reliable estimation of the probable error of measurement of an *average* fork could be made. Since then a great many more photographs have been taken with a larger chamber and an improved camera* and such a statistical test is now possible.

To test the camera itself five photographs were taken of two black lines ruled on a card. The angles calculated from the photographs were :—

°	′		°	′	
40	0				
39	52	mean	39	54	Mean difference from true value 5′.
39	52				
39	56	measured directly	39	49	
39	51				

These results make it probable that the new camera is more accurate than the old. This can be attributed to its method of construction which allows greater accuracy of adjustment. The camera errors may, therefore, be taken to be of the order of 5 minutes of arc, except of course for tracks so placed that the trigonometrical calculations become nearly or completely indeterminate. [NOTE.—Three cameras are necessary if a determinate answer is required for all possible directions of a track.] Having measured a photograph of a collision one wants to know the total error, that is, the difference between the measured angle and the actual angle between the paths of the particles immediately after the collision. This error depends on the camera errors, the distortion due to the chamber and possibly on the change of direction of the tracks due to subsequent nuclear collisions. The method of estimating the errors of the angular measurements of the actual tracks is based on the assumption that the collisions are elastic. From the relation

$$\beta = M\alpha/Mn = \sin(2\theta + \phi)/\sin\phi,$$

giving the mass ratio in terms of the angle of projection θ of the struck nucleus and the angle of deflection ϕ of the alpha particle, we obtain for the error $\delta\beta$ due to errors in the angles,

---

* Blackett, 'Proc. Roy. Soc.,' A, vol. 123, p. 613

$$\delta\beta_\theta = 2\beta \cot(2\theta + \phi)\, \delta\theta, \tag{1}$$

$$\delta\beta_\phi = \beta\, [\cot(2\theta + \phi) - \cot\phi]\, \delta\phi. \tag{2}$$

The most suitable tracks for accurate measurement are the close collisions of fast alpha particles with hydrogen or helium nuclei. For then both parts of the track after the collision are fine and straight.

Table I gives the results of the measurements of 16 such collisions of fast alpha particles with hydrogen nuclei. The measured values of ϕ and θ, the calculated values of M_n/M_α, and the difference of the latter from their mean are given for each track.

Table I.

No.	ϕ.	θ.	$\dfrac{M_n}{M_\alpha}$	Difference from mean.	δx minutes of arc.
	° ′	° ′			
1	14 53	42 22	0·2605	0·0074	25
2	14 39	42 10	0·2561	30	10
3	11 45	21 44	0·2479	52	15
4	13 31	49 8	0·2517	14	4
5	13 40	28 4	0·2518	13	5
6	11 6	58 29	0·2445	86	19
7	14 28	44 43	0·2563	32	10
8	14 16	37 13	0·2465	66	24
9	11 58	20 24	0·2504	43	22
10	11 31	21 20	0·2462	69	21
11	14 39	33 13	0·2561	30	11
12	13 20	54 0	0·2675	144	37
13	11 24	21 1	0·2461	40	21
14	13 26	27 29	0·2494	37	13
15	14 18	30 20	0·2558	27	9
16	14 37	35 52	0·2528	3	1
		Mean .	0·2531 ± 0·0011	Mean ..	15·5′
		True value	0·2517	Probable error	13′

The mean value of the mass ratio for the 16 tracks is 0·2531, whereas the true value is known to be 0·2517. The mean deviation from the mean is 0·0051 and consequently the probable error of the arithmetic mean is $0 \cdot 845/\sqrt{16}$ times this, that is 0·0011. So the difference 0·0014 between the observed value and the true value is somewhat more than the probable error.

As the two tracks after the collision are both nearly equally straight and easy to measure, the errors of the two angles can be taken as equal. The total error $\Delta\beta$ in β is then obtained by adding the squares of the errors (1) and

(2). For each track then, $\delta x = \delta\theta = \delta\phi$ can be calculated from the observed value of $\Delta\beta$. These values are given in the last column of Table I. The mean of these values is 15·5 minutes, giving a probable error of 13 minutes of arc. The reason why this average error is greater than the older estimate of 10 minutes lies in the selection of the forks to be measured. In the present work the 16 forks were selected by their apparent suitability for accurate measurement.* Once selected, they were all retained as part of the data, however poorly they satisfied the test for coplanarity. Some of the forks with the larger errors would have been excluded on this ground as definitely distorted in some way, if, for instance, the object had been to verify the accuracy with which the energy is conserved. But as the present object was to find the probable error of an observation of any fork, which, though well defined, is otherwise taken at random, no such exclusions were made. It is also possible that greater distortions occur in a large chamber such as was used in the present experiments, than in the original small one.

A further test is afforded by a group of 33 collisions of alpha particles with hydrogen, which were selected for the range velocity determination of the projected H-particles.† It is to be expected that the angle measurements would be less accurate than in the first group as the alpha particles were on the whole quite slow and the average length of the particle tracks was only a few millimetres. The average value of $Mn/M\alpha$ of the 33 tracks was 0·2529, with a mean difference from the mean of 0·0136 and so with a probable error of the mean of 0·0020. The actual difference between the mean value and the true value is 0·0012. For these tracks the errors of the two angles are certainly not equal. The track of the alpha particle after the collision was usually fairly long and straight but the track of the H-particle was generally short and often distinctly curly. So θ certainly could not be measured as accurately as ϕ. As a rough guess at the relative magnitude of the errors, we will take $\delta\theta = 2\delta\phi$. Then the total error of β is obtained by adding the squares of weighted particle errors. In this way it is found that the probable error of ϕ is 24 minutes and of θ is 48 minutes of arc. These are, as was to be expected, markedly greater than the errors of the first group considered.

A third group of 13 collisions of alpha particles with nitrogen and oxygen atoms gave values for the errors, with the same assumption of double accuracy for ϕ, of 25 minutes for ϕ and 50 minutes for θ.

It is this group of tracks which resemble most closely the disintegration tracks in nitrogen.* The track of the O_{17} atoms is very similar to those of nitrogen atoms in elastic collisions and so one may assume the error in ω to be not very different from that in θ. It is likely, however, to be somewhat greater as the elastic collisions studied were selected as suitable for measurement from a large number, whereas the disintegration collisions are far too scarce to allow much selection. It is therefore reasonable to assume that the error in ω is about 60 minutes of arc. It is this error which governs almost entirely the determination of the energy balance at a disintegration collision. The error in ψ is taken as one-half that in ω.

---

* Only a fraction of the total number of available forks was measured.

† 'Proc. Roy. Soc.,' A, vol. 134, p. 658 (1931).

The following table gives a summary of the determination of probable errors $\Delta\phi$ and $\Delta\theta$:—

Type of collision.	How selected.	Number.	$\Delta\phi$ Probable error, minutes of arc.	$\Delta\theta$ Probable error, minutes of arc.
Hydrogen	Selected for $Mn/M\alpha$ determination	16	13	13
Hydrogen	Selected for range-velocity determination	33	24	48
Nitrogen and oxygen	,,	13	25	50
Nitrogen disintegration collisions	—	—	$\Delta\psi = 30$ estimated	$\Delta\omega = 60$ estimated

It will be noticed that the mean values of $Mn/M\alpha$ for the two groups of hydrogen collisions (0·2531 and 0·2529), are both high. This corresponds to the angles ϕ and θ being about 5 minutes of arc too large, so that the characteristic point on such a diagram as the figure of Paper I, lies above the theoretical curve. As the measurements on the test tracks were also 5 minutes too large, one may suspect a small consistent error in the camera.† If the angles really were too great, it would indicate a gain of energy on collision, a very improbable result. Actually we may attribute the divergence to camera errors and conclude that the collisions are elastic within the experimental error.‡ Among the 1,300,000 tracks recently photographed, no evidence has been obtained of any inelastic collisions between alpha particles and oxygen, nitrogen or argon atoms, other than the nitrogen disintegration collisions. But no systematic study of all these collisions has been made. It would be necessary to measure many hundreds in order to be able to say definitely that any apparently inelastic collision could not be explained by the assumption of a subsequent nuclear collision or other accidental distortion.

---

* Blackett, 'Proc. Roy. Soc.,' A, vol. 107, p. 349 (1925).

† It is also possible to attribute such consistently large values for the angles to the distortion of the whole track, if the particle enters the chamber before the expansion is complete ('Proc. Roy. Soc.,' A, vol. 103, p. 77 (1923)).

‡ Blackett and Hudson, *loc. cit.*

II. *The Calculation of the Angles.*—In a former paper* the geometrical theory has been given of the calculation of the angles of a fork from measurements of the two images. An alternative presentation of the exact theory will now be given. This is simpler and leads to formulæ which are more convenient for numerical work. The method is equally applicable to the old type of camera with its lenses parallel to the image planes and to the new type with tilted lenses.

Let L′ and L″ be the centres of the two lenses, and O′ and O″ the feet of the perpendiculars from L′ and L″ on to the two image planes Y′O′Z′ and X″O″Z″. Construct axes O′X′, O′Y′, O′Z′ and O″X″, O″Y″, O″Z″ in the image space, and correspondingly the axes OX, OY, OZ, in the object space (fig. 1). Let A′B′ in the plane Y′O′Z′, and A″B″ in the plane X″O″Z″ be the two images of a line AB in the object space. Then AB and A′B′ and L′ must be coplanar; so also must be AB, A″B″ and L″.

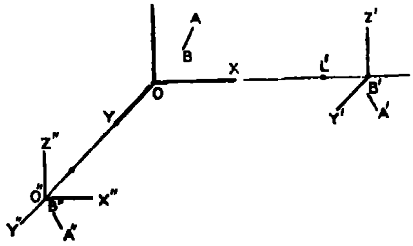

FIG. 1.

Let A′B′ cut O′Y′ at the point (OY′O) and O′Z′ at (OOZ′). Then the required plane passes through these two points and the centre of the lens (—*v*00) where O′L′ = O″L″ = *v* = the image distance, so that its equation referred to the axes O′X′, OY′, OZ′ is

$$-\frac{x'}{v}+\frac{y'}{Y'}+\frac{z'}{Z'}=1,$$

or referred to the axes OX, OY, OZ,

$$-\frac{x}{v}+\frac{y}{Y'}+\frac{z}{Z'}=-\frac{u}{v}, \tag{1}$$

where u = OL′ = OL″ = object distance.

---

* Blackett, 'Proc. Roy. Soc.,' A, vol. 103, p. 63 (1923).

In a similar way the equation of the plane through A''B'' and L'' referred to OX, OY, OZ, is

$$\frac{x}{\mathrm{X}''} - \frac{y}{v} + \frac{z}{\mathrm{Z}''} = -\frac{u}{v}. \tag{2}$$

The line AB is the intersection of these two planes and so has direction cosines λ, μ, ν, given by

$$\frac{\lambda}{-v^2 \cot b + \mathrm{Z}''v} = \frac{\mu}{-v^2 \cot a + \mathrm{Z}'v} + \frac{\nu}{\mathrm{Z}'\mathrm{Z}'' - v^2 \cot a \cot b} \tag{3}$$

where

$$\left.\begin{aligned} \tan a &= -\mathrm{X}''/\mathrm{Z}'' \\ \tan b &= -\mathrm{Y}'/\mathrm{Z}' \end{aligned}\right\}. \tag{4}$$

If α and β are the angles between OZ and the rectangular projection of AB on ZOX and ZOY, then

$$\left.\begin{aligned} \tan \alpha &= \lambda/\nu \\ \tan \beta &= \mu/\nu \end{aligned}\right\}. \tag{5}$$

If $(x'z')$ and $(y''z'')$ are the co-ordinates on the two photos of the image of any point on AB, then using (4) we have

$$\left.\begin{aligned} \mathrm{Z}' &= z' - y' \cot b \\ \mathrm{Z}'' &= z'' - x'' \cot a \end{aligned}\right\}. \tag{6}$$

From (5), using (3) and (6), we find

$$\left.\begin{aligned} \tan \alpha &= (\tan a + \varepsilon_1 \tan b - \varepsilon_3 \tan a \tan b)/(1 - \gamma) \\ \tan \beta &= (\tan b + \varepsilon_2 \tan a - \varepsilon_4 \tan a \tan b)/(1 - \gamma) \end{aligned}\right\} \tag{7}$$

where

$$\gamma = (\varepsilon_1 - \varepsilon_3 \tan a)(\varepsilon_2 - \varepsilon_4 \tan b), \tag{8}$$

and

$$\begin{aligned} \varepsilon_1 &= x''/v \\ \varepsilon_2 &= y'/v \\ \varepsilon_3 &= z''/v \\ \varepsilon_4 &= z'/v \end{aligned} \tag{9}$$

The angle ϕ between any two lines is given in terms of the directions (α, β) $(\alpha'\beta')$ of their projections by

$$\cos^2 \phi = \frac{(\tan \alpha \tan \alpha' + \tan \beta \tan \beta' + 1)^2}{(\tan^2 \alpha + \tan^2 \beta + 1)(\tan^2 \alpha' + \tan^2 \beta' + 1)} \tag{10}$$

In (9) the co-ordinates x'', y', z'', z', refer to the images of the point of intersection of the two lines.

These equations are exact. When a collision lies at the origin O, the co-ordinates are zero and $\alpha = a$, $\beta = b$. When the angles α and β equal $\pi/2$, the method breaks down, as is obvious it must. In other cases the required value of ϕ is given as a function of measured angles with the co-ordinates of the collision entering as correcting terms. For the camera used $v = 11 \cdot 0$ cm., and the mean value of ε_1 and ε_2 is about 0·17 and of ε_3 and ε_4 about 0·05. Thus, for a track for which all the angles are small, say less than 40°, the value of γ varies little from 0·022, and the main correcting terms are the second in the numerators of (7), so that we have the approximate formulæ

$$\left.\begin{aligned} \tan\alpha &= 1 \cdot 02\,(\tan a + \varepsilon_1 \tan b) \\ \tan\beta &= 1 \cdot 02\,(\tan b + \varepsilon_2 \tan a) \end{aligned}\right\}. \tag{7A}$$

It is easy to construct a special type of slide rule to carry out the evaluations in (7A) and this method is used in all work which does not require an accuracy greater than, say, 2°, such as the statistical work on helium collisions recently described by Blackett and Champion.* To the same accuracy the calculation of ϕ from (10) is done graphically on the surface of a sphere.

Returning to the exact method, it is easy to see from (7) or (7A) the order of accuracy required in the co-ordinate measurements to obtain a given accuracy in the calculated angles. Suppose, for instance, that a and b are equal and small, then the error in α due to an error of 1/5 mm. in x'' is 6 minutes of arc; this is of the same order as the probable error of an angle determination. The advantage of this method *for the accurate determination of the angles* of alpha particle tracks, over the Pulfrich method of stereometry as used by Skobelzyn for β-ray tracks is clear.† It is quite easy to determine the direction of a line image 1 mm. long to 10 minutes of arc, by setting a fine cross wire along it. But to attain this accuracy of angle determination by measuring the co-ordinates of the end points, requires an error of less than 3/1000 mm. in the co-ordinate measurements. It might be possible to attain this accuracy on isolated point images, but it is quite impossible on most actual tracks.

III. *The Exact Measurement of Length.*—The method of calculating the lengths of tracks from measurements of two rectangular projections has been given in a previous paper.‡ The refinements necessary to take into account the fact that the actual photographs are not rectangular projections will now be given.

---

* 'Proc. Roy. Soc.,' A, vol. 130, p. 380 (1931).

† Skobelzyn, 'Z. Physik,' vol. 65, p. 773 (1930).

‡ Blackett, 'Proc. Roy. Soc.,' A, vol. 103, p. 65 (1923).

Let XYZ be the co-ordinates of a point in the object space. Then the co-ordinates (xz_x) (yz_y) of the two images* are given by

$$\left.\begin{aligned} \frac{x}{v} &= -\frac{X}{u-Y}, \quad \frac{y}{v} = -\frac{Y}{u-X} \\ \frac{z_x}{v} &= -\frac{Z}{u-Y}, \quad \frac{z_y}{v} = -\frac{Z}{u-X} \end{aligned}\right\}, \tag{11}$$

where u and v are the object and image distances from the lens. From these we obtain

$$\left.\begin{aligned} X &= \quad mx(1+\varepsilon_2)/(1-\varepsilon_1\varepsilon_2) \\ Y &= -my(1+\varepsilon_1)/(1-\varepsilon_1\varepsilon_2) \\ Z &= -mZ_x(1+\varepsilon_2)/(1-\varepsilon_1\varepsilon_2) = -mZ_y(1+\varepsilon_1)/(1-\varepsilon_1\varepsilon_2) \end{aligned}\right\} \tag{12}$$

when as before $\varepsilon_1 = x/v$, $\varepsilon_2 = y/v$ and $m = u/v$ and equals the reciprocal of the magnification. These equations give the rectangular co-ordinates of a point in terms of the four measured image co-ordinates.

The actual distance D between any two points (XYZ) and (X′Y′Z′) in the chamber is given by

$$D^2 = \{(X-X')^2 + (Y-Y')^2 + (Z-Z')^2\}. \tag{13}$$

It is not, however, the actual distance in the chamber which is usually required but rather what may be called the reduced range in air at N.T.P., that is the length the part of the track would have in the gas if the total pressure of the gas were so chosen as to make the length of the track of a standard alpha particle equal to its standard range R_0 in air at 15° C. and 760 mm.†

Let R be the reduced range of the part of the track under consideration, for instance of one arm of a forked track, then by the above definition

$$\frac{R}{R_0} = \frac{D}{D_0}, \tag{14}$$

---

* The two images are now distinguished by the suffixes x and y, and the two ends of a track by dashes.

† If the differential stopping power of the gas relative to air is constant along the range, then the reduced range equals the air equivalent range, that is the actual range of the particle, between the given velocity limits, in air at N.T.P. When the stopping power varies along the range the two are different (‘Proc. Roy. Soc.,’ A, vol. 134, p. 658 (1931)). In the photographs described either a polonium or a thorium (B + C) source were used. In the first case $R_0 = 3 \cdot 87$ and in the second 4·79 cm., since the 8·6 cm. alphas went right through the chamber and so could not be used as the standard tracks.

where D is the actual length in the chamber of the part of the track considered and D_0 is the actual length of the standard full range alpha particle respectively.

Now let L_0 be the length of the *image* of a full range standard track which lies in the middle of the beam and so is parallel to OZ. Then for such a track

$$x = y = x' = y',$$

and so

$$\varepsilon_1 = \varepsilon_2 = \mu \quad \text{(say)},$$

and since now

$$L_0 \quad Z_x - Z'_x = Z_y - Z_y{}',$$

we have from (12)

$$D_0 = m L_0 \frac{1 + \mu}{1 - \mu^2}. \tag{15}$$

In (14) we substitute D_0 from (15) and D from (12) and (13) and so obtain

$$R = \frac{R_0}{L_0} \frac{1 - \mu^2}{1 + \mu} \left[\left\{ \frac{x(1 + \varepsilon_2)}{1 - \varepsilon_1 \varepsilon_2} - \frac{x'(1 + \varepsilon'_2)}{1 - \varepsilon'_1 \varepsilon'_2} \right\}^2 + \{\ldots\}^2 + \{\ldots\}^2 \right]^{\frac{1}{2}}.$$

Now since the product $\varepsilon_1 \varepsilon_2$ varies less than 0·4 per cent. over the whole field, we can cancel all the terms $(1 - \varepsilon_1 \varepsilon_2)$, etc., with $(1 - \mu^2)$ so that we obtain

$$R = \frac{R_0}{L_0} \frac{1}{1 + \mu} [(x - x')^2 + (y - y')^2 + (z - z)^2]^{\frac{1}{2}}, \tag{16}$$

where

$$X = x(1 + y/v),$$

$$Y = y(1 + x/v),$$

$$Z = z_x(1 + y/v) = z_y(1 + x/v),$$

and similarly for X′, Y′, Z′.

These give the reduced range of any part of a track, whose end points are defined on the two photographic images by the co-ordinates (xz_x, yz_y) and $(x'z_x', y'z_y')$. Neither the pressure, temperature, composition or stopping power of the gas are required, nor the magnification of the camera, but only the length L_0 of the image of a centrally placed standard alpha ray track whose standard range is R_0.

Summary.

The accuracy of the angular measurements of forked tracks is estimated by studying various types of collision. For 16 fast hydrogen collisions the probable errors of ϕ and θ are estimated to be 13 minutes of arc. For 33 collisions of slower alpha particles with hydrogen atoms, selected for the determination of the range velocity curves, the errors are 24 minutes and 48 minutes of arc. For 13 nitrogen collisions the errors are 25 minutes and

50 minutes of arc. It is estimated from these results that the probable errors of the angles ψ and w of a nitrogen disintegration track are about 30 minutes and 60 minutes of arc.

An exact method of calculating the angles from the photograph, which is analytically simpler than that used previously, is given in Section 2.

A new and precise method of obtaining the reduced lengths of the tracks, which allows for the fact that the images are not orthogonal projections, is described in Section 3.

We wish to thank Mr. J. S. Barnshaw, of King's College, for his assistance with the trigonometrical calculations. We are also indebted to the Department of Scientific and Industrial Research for a grant to one of us (D.S.L.) and for apparatus.

PLATE 9.

DESCRIPTION OF THE PHOTOGRAPHY OF ELASTIC COLLISION OF ALPHA PARTICLES WITH HYDROGEN NUCLEI.

No. 1.—The contrast between the long and fine track of the H-particle and the shorter and thicker track of the alpha particle is very marked.

No. 2.—A similar photograph.

Nos. 3 and 4.—Two photographs of the same track.

The Ranges of the α-Particles from the Radioactive Emanations and "A" Products and from Polonium.

By W. B. Lewis, B.A., and C. E. Wynn-Williams, Ph.D., Clerk-Maxwell Scholar.

(Communicated by Lord Rutherford, O.M., F.R.S.—Received December 23, 1931.)

The analysis of groups of α-particles by new counting methods has been described in previous papers,* in which details have been given of the examination of the α-particles emitted by radium-C and -C′, thorium-C and -C′, and actinium-C and -C′, including the long range particles. The methods have the advantage that any appreciable inhomogeneity of a group of α-particles is readily detected, and moreover, the mean range of a group may be directly measured with a high degree of precision.

The experiments have now been extended to an examination of the α-particles emitted by the emanations and " A " products of the three radioactive series, and by polonium. The examination of these α-ray groups is not only of great interest from the point of view of the radioactive transformations, but also for the possible connection with the emission of γ-rays.

The method of experiment adopted was similar to that previously described. The groups of α-particles were analysed by means of the differential ionisation chamber connected to a valve amplifier. The counting was done by an automatic counter employing thyratrons. The results are obtained in the form of straggling curves, by the shape of which the homogeneity of each α-particle group may be tested, and from the position of which the mean range is directly determined.

Of the six α-ray elements, viz., radon, radium-A, thoron, thorium-A, actinon and actinium-A, which we have examined in the present experiments, all are found to emit a single homogeneous group of α-particles with the exception of actinon, which emits two well-marked groups. The homogeneity of the α-rays from radium-A has previously been shown by Rosenblum† using the magnetic deflection method, and Mme. Irène Curie* has shown that the α-rays from actinium-A are also homogeneous by the expansion chamber method.

---

* Rutherford, Ward and Wynn-Williams, 'Proc. Roy. Soc.,' A, vol. 129, p. 211 (1930); Wynn-Williams and Ward, 'Proc. Roy. Soc.,' A, vol. 131, p. 391 (1931); Rutherford, Ward and Lewis, 'Proc. Roy. Soc.,' A, vol. 131, p. 684 (1931); Wynn-Williams, 'Proc. Roy. Soc.,' A, vol. 132, p. 295 (1931); Rutherford, Wynn-Williams and Lewis, 'Proc. Roy. Soc.,' A, vol. 133, p. 351 (1931).

† 'C. R. Acad. Sci., Paris,' vol. 190, p. 1124 (1930).

The mean ranges of all the groups observed have been carefully measured. In order to compare the values obtained with the "extrapolated" ionisation ranges of the α-rays found directly by other observers, the differences to be expected between the mean and extrapolated ranges have been deduced and applied. It seems desirable in the future to use the mean range of the α-particles in air, which is directly measured by the new methods, rather than the extrapolated range, which has a rather indefinite interpretation. Moreover, since measurements have now been made of all the α-particle groups for which data from velocity measurements are available, it has been possible to construct an experimental curve relating mean range with velocity. By interpolating on this curve, the velocity of any group of α-particles may be obtained from the mean range.

Experimental Procedure.

As already mentioned, the experimental procedure was similar to that described in earlier papers. For the experiments with the emanations and "A" products, however, it was not possible to use the normal type of source consisting of a deposit on a polished metal disc. The source was therefore contained in a small brass capsule of the form shown in fig. 1. A small quantity of an emanating preparation was wrapped in a roll of fine cigarette paper and placed in the recess. The capsule was then sealed up with wax, so that the emanation could not escape. Some of the emanation, after diffusion through the paper, passed into the narrow space 0·4 mm. wide between the central

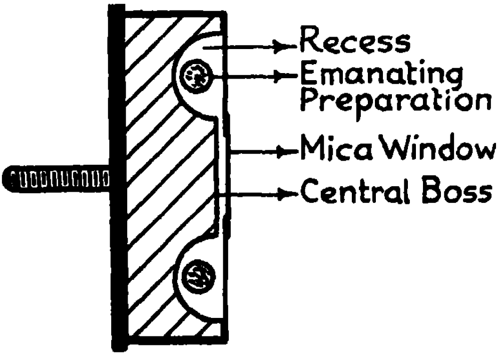

FIG. 1.—(Scale :—About twice actual size.)

---

* 'C. R. Acad. Sci., Paris,' vol. 192, p. 1102 (1931).

boss and the thin mica window. Some of the α-particles resulting from disintegrations in this space passed through the mica window and could be analysed in the normal way. The α-particles from the active deposit which settled on the surfaces of the boss and the mica were also present at the same time. Thus the groups of α-particles from the " A," " C " and " C′ " products could also be examined.

In the case of radon, owing to its long half value period, of 3·8 days, it was not necessary to enclose the emanating substance in the capsule. The radon was admitted through a glass tube sealed to the back of the capsule. When, by trial, it was found that a sufficient quantity had been admitted, the glass tube was drawn off and sealed.

(*a*) *Actinon and Actinium-A.*—The straggling curve obtained from the experiments with an actinium preparation in the capsule is shown in fig. 2. (The actual points obtained are shown as open circles.) This curve comprises the groups of α-particles from actinon, actinium-A and actinium-C.

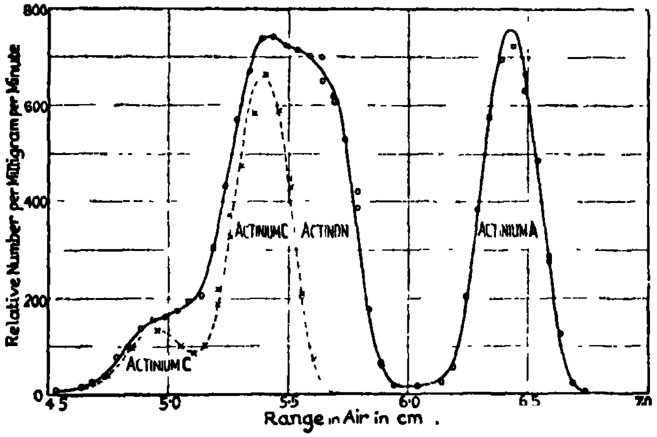

FIG. 2.

The actinium preparation was afterwards removed from the capsule, and the α-particles from the actinium-C remaining were analysed. The points obtained corrected for the decay of the actinium-C are indicated by crosses in fig. 2. The broken line curve fitted to these points is of the form determined in our previous experiments with actinium-C,* very slightly modified to take account of the finite depth of the source due to the form of the capsule. By subtracting this curve from the points shown as open circles, the points shown in fig. 3 are obtained. These therefore represent the groups of α-particles from actinon and actinium-A.

---

* Rutherford, Wynn-Williams and Lewis (*loc. cit.*).

From the accepted scheme of transformations in the actinium series, it is to be expected that the same total number of particles should be included in the groups ascribed to each of the three elements actinon, actinium-A and actinium-C, since under the experimental conditions the substances were approximately in radioactive equilibrium. The branch product actinium-C′ gives rise to such a relatively small number of α-particles (1/310 of the number from actinium-C) that its presence may be neglected.

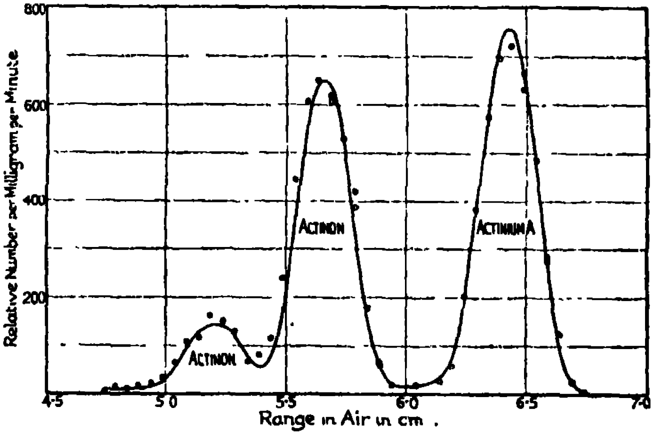

Fig. 3.

Since the curve fitted to the long range group in fig. 3 corresponds to the same number of particles as included in the two actinium-C groups, it is to be supposed that this long range group includes all the α-particles from actinium-A, and further that it is a homogeneous group of α-particles. The two shorter range groups are therefore to be attributed to actinon. It will be seen that the curve fitted to these two groups is almost exactly similar in form to that for the α-particles from actinium-C, and differs only in a slightly greater separation between the groups, the numbers in corresponding groups being the same. The curve does not fit the points quite as well as usual, but owing to the difficult nature of the experiment the discrepancy is within the experimental error.

The presence of the short range group from actinon and its approximate magnitude have been verified in additional experiments with other similar sources. It was found that the group was present immediately after filling the capsule before the groups from actinium-C had grown to more than one-fifth of the equilibrium magnitude. Further, in the same experiment it was verified that the numbers in the long range group from actinon were markedly less than the numbers in the actinium-A group. This has also been found from a separate determination of the combined straggling curve for all the groups.

We conclude that the α-rays from actinium-A form a single homogeneous group, but that the α-rays from actinon are complex, and consist of two groups which appear to be closely analogous to the groups from actinium-C. In both cases the number of particles in the group of shorter range is approximately 19 per cent. of the number in the larger group. The difference of energy between the two groups is estimated to be $3 \cdot 49 \times 10^5$ electron-volts for actinon, and $3 \cdot 54 \times 10^5$ electron-volts for actinium-C, values which are indistinguishable under the limits of experimental error.

(*b*) *Thoron and Thorium-A.*—For the measurements of the thoron and thorium-A ranges, a small quantity of a radiothorium preparation was substituted for the actinium in the capsule. The source was thus exactly similar to the actinium source, but owing to the slower rate of growth of thorium-C (half value period of thorium-B = 10·6 hours) it was possible to adopt a somewhat simpler method of experiment. The general form of the straggling curve showing the thoron, thorium-A, thorium-C and -C′ ranges was first determined by a preliminary experiment with another similar capsule. The main experiment was then carried out using the original capsule in order to obtain as accurate a check as possible on the scale of ranges, by means of a comparison of the ranges of the groups from thorium-C′ and actinium-C with the values previously determined.

In the experiment, the ranges where the α-particles from thorium-C were to be expected were explored immediately after filling the capsule, before the thorium-C had grown to an appreciable amount; the rest of the straggling curve was explored later. The curve obtained is shown in fig. 4 and appears to consist of two homogeneous groups containing equal numbers of particles. For the purpose of fixing the scale of ranges, and checking the numbers in the groups, the thorium-C′ peak was examined after the thorium-C had grown to the equilibrium amount. In this way it was verified that the curves (which are of the calculated shape) fitted to the groups from thoron and thorium-A (fig. 4) correspond to a number of particles which is 100/65 of the number in the thorium-C′ group, as expected from the scheme of transformations in the thorium series.

(*c*) *Radon and Radium-A.*—In this case the experiment was straightforward as the number of α-particles from radium-C is relatively so small (1/4000 of

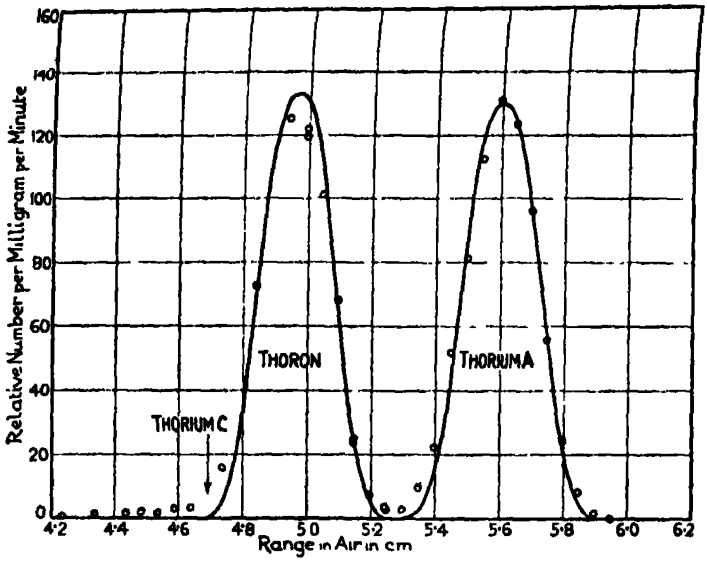

Fig. 4.

the number in the radium-C′ group). The two groups from radium-A and radon are shown in fig. 5, and it will be seen that both groups correspond to

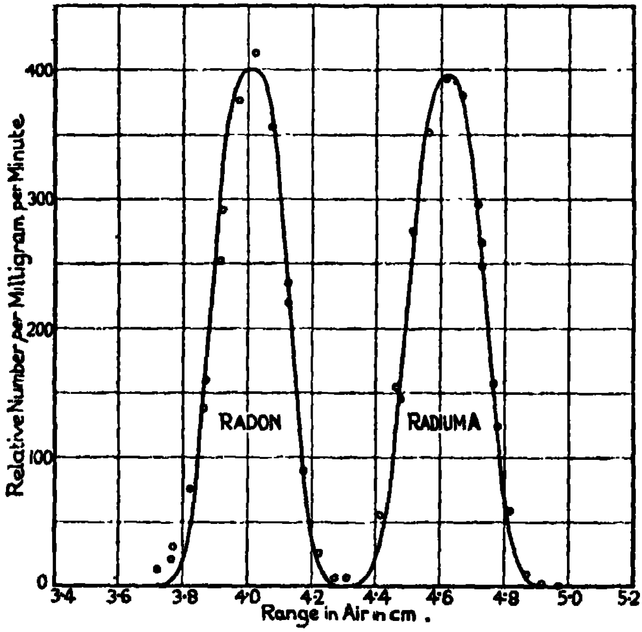

Fig. 5.

the same number of particles, and that each appears to be a homogeneous group. The scale of ranges was fixed by the radium-C′ peak, which was also examined and found to correspond to the same number of particles. A separate experiment was made to determine the difference between the radium-C′ and thorium-C′ ranges. In this experiment, in order to eliminate sources of error as far as possible, thorium-C and radium-C sources were obtained on the same source disc at the same time. The thorium active deposit was first obtained by a short exposure to the emanation; the disc was then left overnight so that, for convenience, the thorium-C would be decaying with the period of thorium-B during the experiment. The radium-C was obtained by collecting radium-B on the same source by the recoil method. A check experiment was made under exactly similar conditions to obtain the rise and decay of radium-C on such a source.

(*d*) *Polonium.*—The polonium source was prepared by a special method by which a very clean source can be obtained. A drop of a solution containing polonium was placed on the centre of a polished nickel disc. Sufficient polonium was deposited from this drop in about half a minute, after which time the disc was plunged into a large vessel of water to free it from the remaining solution. The source was then washed in alcohol and dried. The polonium was thus confined to a small spot in a deposited layer so thin that it could only just be detected by eye under good illumination. The straggling curve obtained from this source agreed very well with the calculated shape, and, as would be expected for a clean source, the " tail " on the short range side was very slight.

Corrections and Accuracy.

It is of great importance to consider in detail the accuracy with which the mean ranges may be measured, so the exact procedure will be described. In the straggling curves shown the number of α-particles per minute counted are plotted as ordinates against the total equivalent air path from the source to the effective centre of the ionisation chamber. The numbers are reduced to correspond to the emission from the source within a standard solid angle, and to a strength of source arbitrarily chosen as standard. The total equivalent air path consists of the actual path in air reduced to 760 mm. and 15° C., together with the air equivalent of the absorption of the mica window (4 mm.), the collodion film (3 mm.) and the gold foils of the ionisation chamber (0·8 mm.). The position of the effective centre of the ionisation chamber is known, from the " chamber characteristic " described in an earlier paper, to be very close to the back of the central foil, and to vary by only a few hundredths of a millimetre by changing the " effective slit width " (also explained in the same paper) which depends upon the size limits of the ionisation surges counted; allowance is made for this variation where necessary. The experiments were carried out at atmospheric pressure and room temperature, and the correction to 760 mm. and 15° C. was always less than 2·5 per cent.

The correction of the barometer mercury column to 0° C. and to the value of g at latitude 45°, and the allowance for the humidity of the air have been made in one combined correction, which is by no means negligible. It was thought that the variations in this correction would be negligible, but it appears that the accuracy with which the mean ranges of experimental curves may be located is just sufficiently great to warrant a correction for the variations. For the purpose of this combined correction, an average temperature of 16° C. has been assumed, and the normal humidity has been taken as 75 per cent. of saturation at that temperature. An addition of 0·5 mm. has been made to the reduced barometric height at Cambridge (latitude 52·2°) to obtain the height of the column at latitude 45°. The combined correction reduces the observed ranges in the proportion 1·0048 : 1.

Reference has been made to the operation of fixing the scale of ranges from a standard range; this is necessary as the stopping powers of the collodion film and micas used were not known with great accuracy. Values were therefore assigned such that the mean range of the 8·6 cm. particles from thorium-C′ would be 8·533 cm., which is the value assumed in our previous work. The accuracy of all our values of mean ranges depends both upon the accuracy of this standard mean range, which might be in error by 0·010 cm., and also on the accuracy with which relative measurements of ranges are made. It has been found that these measurements are repeated within 0·005 cm. in the case of isolated groups. For groups (such as the actinon groups) which have not yet been obtained clear from other groups, an accuracy of more than 0·015 cm. cannot be claimed. This accuracy of repetition of range measurements refers to similar sources prepared by the same procedure. Defective conditions of the surface on which the source is deposited can produce a diminution in the observed range. The present series of measurements involve only comparisons of ranges from essentially similar sources, so that such errors should be entirely eliminated, with the possible exception of the polonium source. From the appearance of the source disc and the shape of the straggling curve obtained it is probable that the error, even in this case, is less than 0·010 cm. In addition to these possible errors, the question of systematic errors must be raised. It is believed that these are negligible when two small corrections, viz., the "secant effect" correction and the mica stopping power correction have been applied. The secant effect correction arises from the fact that the aperture of the ionisation chamber is of finite size, so that particles from a point source entering at the edge of the aperture over the ionisation chamber will have travelled a greater distance than those which enter at the centre of the aperture. The aperture used was 0·85 cm. in diameter, so the correction is very slight for long range particles, but amounts to 0·010 cm. in the case of polonium.

Secondly, the stopping power of the mica cannot be assumed to be the same for particles of all ranges, though the observations of Braddick for Briggs,[*] and also of Harper and Salaman[†] show that the variation of stopping power with range is slight. An experiment was therefore carried out to determine approximately the magnitude of the effect. Measurements of the apparent range of the 8·6 cm. particles were made with a mica of 1·5 cm. stopping power close to the source, and with the mica 4 cm. from the source. It was concluded that the difference in the apparent range in the two cases was 0·025 cm. That is to say, if the stopping power of the mica is 1·500 cm. for particles of mean range 3·9 cm., it is 1·525 cm. for particles of range 7·9 cm. (the range being the equivalent range in air measured from the centre of the mica). For the purpose of the correction which has to be applied to our measurements of range, it has been assumed that the stopping power of mica varies linearly with the range between these limits. Since the mica used in the range determinations was only of 4 mm. stopping power, the correction to be applied never amounted to more than 0·006 cm. It may be mentioned that no corresponding correction is necessary for the collodion film, since this was kept at a fixed distance from the ionisation chamber, and therefore at the same mean distance from the end of the α-particle range under examination.

Difference between Mean and Extrapolated Ranges.

The differences between mean and extrapolated ranges have been deduced by many writers, but unfortunately there is considerable disagreement between the results obtained. For example, the difference for the 7 cm. range from radium-C′ has been found by Briggs (*loc. cit.*) to be 0·6 mm. and by Gamow[‡] to be 1·16 mm. Formerly we have employed the difference ($\rho_m\sqrt{\pi}/2$ — 0·3 mm.) deduced by F. A. B. Ward. In this expression ρ_m is the straggling coefficient determined by Briggs* for mica, and $\rho_m \sqrt{\pi}/2$ is the difference between the mean and the extrapolated range which would be determined by the counting method using a single ionisation chamber, or by the scintillation method. We believe that this correction is accurate for the longer ranges, but is rather too small for short ranges. The correction necessary to convert mean ranges to extrapolated ionisation ranges and *vice versa* has been recalculated by one of us (W. B. L.) in greater detail, and it was found that the difference $0 \cdot 8\rho - 0 \cdot 06$ mm. (where ρ is the straggling coefficient for air) is accurate over a greater range. This value has therefore been employed in this paper. We have taken ρ to be $0 \cdot 896\ \rho_m$, so that for the $8 \cdot 6$ cm. group from thorium-C′ $\rho = 1 \cdot 20$ mm., a value which best fits the straggling curve we obtain.

---

[*] Briggs, 'Proc. Roy. Soc.,' A, vol. 114, p. 341 (1927).

[†] Harper and Salaman, 'Proc. Roy. Soc.,' A, vol. 127, p. 175 (1930).

[‡] Gamow, "Atomic Nuclei and Radioactivity" (Oxford University Press).

The method by which the difference $0 \cdot 8\rho - 0 \cdot 06$ mm. has been deduced is as follows. Three calculations have been made for $\rho = 0 \cdot 5$, $1 \cdot 0$ and $2 \cdot 0$ mm. (ρ for a range of $3 \cdot 8$ cm. is $0 \cdot 62$ mm. and for a range of $11 \cdot 5$ cm. is $1 \cdot 46$ mm.). For $\rho = 1 \cdot 0$ mm. the pure straggling curve is of the form shown in fig. 6. The straggling curve obtained by counting all particles stopping within a band $0 \cdot 1$ mm. wide is almost indistinguishable from this. Let y_x be the ordinate of this curve at a distance x from the mean range. The ionisation in a chamber of depth $0 \cdot 1$ mm. at an average distance z from the mean range (see fig. 6) is then $\mathrm{I} = \sum_{x=z}^{x=\infty} y_x \mathrm{I}_{x-z}$, where I_{x-z} is the ionisation produced by an α-particle in $0 \cdot 1$ mm. at an average distance $x - z$ from the end of its track. The summation is to be made for intervals of x of $0 \cdot 1$ mm.

This calculation has been carried out using values of I_{x-z} taken from the data obtained by Feather and Nimmo,† and for values of z at $0 \cdot 1$ mm. intervals. The same has been done for $\rho = 0 \cdot 5$ mm.; since, however, $0 \cdot 1$ mm. is in this case as much as $\frac{1}{5}\ \rho$, the result is not quite so accurately determined. For $\rho = 2 \cdot 0$ mm., the calculations have been made for values of z at $0 \cdot 2$ mm. intervals. The resulting curves of I plotted against z, which should correspond with the Bragg ionisation curves, are shown in fig. 7. Assuming that the straight portions of these curves are fairly long, these have been extended to determine the extrapolated range in the normal manner. It is believed that the result is as accurate as the determinations of the extrapolated range warrant. The correction $0 \cdot 8\rho - 0 \cdot 06$ mm. fits the three cases calculated within the limits of error incurred in drawing the straight line for the extrapolation, which is about 0·003 cm.

---

* Briggs, 'Proc. Roy. Soc.,' A, vol. 114, p. 313 (1927). It should be noted that the quantity ρ, which we term the straggling coefficient and which is expressed in millimetres, is the quantity which Briggs denotes by $\rho_s x$ where ρ_s is a true straggling *coefficient* without physical dimensions. To obtain the straggling coefficient for ranges greater than 7 cm. we have extrapolated the curve given by Briggs as described in a previous paper (Rutherford, Ward and Lewis, *loc. cit.*).

† 'Proc. Camb. Phil. Soc.,' vol. 24, p. 139 (1928).

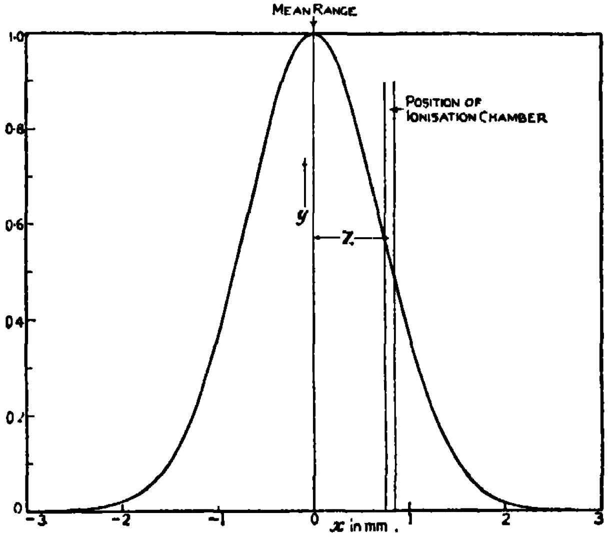

Fig. 6.

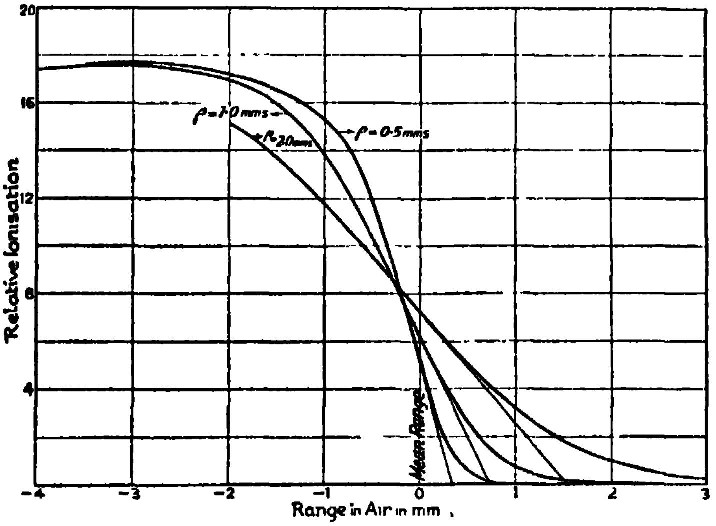

Fig. 7.

The main application of the above calculation is in deciding on the value to be adopted for the standard mean range of the α-particles from thorium-C′.

The value chosen (8·533 cm.) is such that the extrapolated ranges calculated from the mean ranges we have determined for thorium-C′, radium-C′ and (with less weight) thorium-C and polonium, differ by a minimum amount from the most accurate absolute determinations of these extrapolated ranges. An approximate determination of the absolute value of the mean range of the thorium-C′ α-particles with our apparatus gave the value 8·52 cm.; we consider it unlikely that this value should be in error by as much as 0·04 cm., so that there is a real disagreement with the low value $8{\cdot}48_7$ suggested by Gamow (*loc. cit.*).

Velocities and Energies of α-particles.

The velocities and energies of the α-particles given in the table below have been deduced by the method described in a previous paper,* except that a new curve showing the departure from Geiger's law $V^3 = kR$ has been drawn, fig. 8. This curve differs from that previously given owing to the inclusion of fresh velocity and range data and to the use of mean ranges instead of extrapolated ranges. In this curve the correction

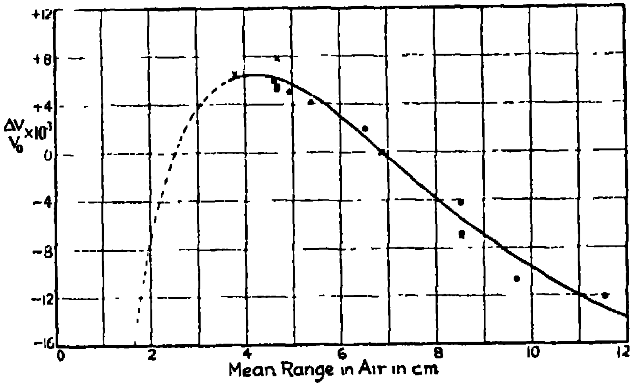

FIG. 8.

● Rosenblum; ○ Briggs. × Laurence.

$$\frac{\Delta V}{V_0} = \frac{V}{V_0} - \left(\frac{R}{R_0}\right)^{1/3}$$

is shown plotted against range. V_0 and R_0 are the velocity and mean range of the α-particles from radium-C′, which are taken as a standard. The points represent the values of $\Delta V/V_0$ calculated from the velocity measurements of

---

* Rutherford, Ward and Lewis (*loc. cit.*).

I. Curie, Briggs, Laurence and Rosenblum,* and the values of the mean ranges which we have determined. It will be noticed that the form of the curve is very uncertain owing to the disagreement in the velocity measurements.

Table.†

	Mean range (cm. of air at 760 mm. and 15° C.)	Straggling coefficient ρ in mm.	Extrapolated ionisation range (cm. of air at 760 mm. and 15° C.)	Velocity in terms of V_0.	Energy of α-particle (electron-volts $\times 10^{-6}$).	Energy of disintegration (electron-volts $\times 10^{-6}$).
Actinon (short)	5·203	0·81	5·262	$0\cdot916_7$	$6\ 45_5$	$6\cdot57_5$
Actinon (long)	5·655	0·87	5·718	$0\cdot941_3$	$6\cdot80_4$	$6\cdot93_1$
Actinium-A	6·420	0·96	6·491	$0\cdot979_3$	$7\cdot36_7$	$7\cdot50_7$
Actinium-C (short)	4·947	0·78	5·003	$0\cdot902_0$	$6\cdot24_9$	$6\cdot37_0$
Actinium-C (long)	5·392	0·83	5·453	$0\cdot927_3$	$6\cdot60_3$	$6\cdot73_1$
Actinium-C′	6·518	0·97	6·590	$0\cdot983_5$	$7\cdot43_6$	$7\cdot58_9$
Thoron	4·967	0·78	5·023	$0\cdot903_3$	$6\cdot26_5$	$6\cdot38_1$
Thorium-A	5·601	0·86	5·664	$0\cdot938_4$	$6\cdot76_4$	$6\cdot89_1$
Thorium-C (mean)	4·693	0·74	4·746	$0\cdot886_6$	$6\cdot03_9$	$6\cdot15_5$
Thorium-C′	8·533	1·20	8·623	$1\cdot069_3$	$8\cdot78_6$	$8\cdot95_7$
Radon	4·014	0·65	4·060	$0\cdot842_4$	$5\cdot44_9$	$5\cdot54_9$
Radium-A	4·620	0·73	4·673	$0\cdot882_3$	$5\cdot97_6$	$6\cdot09_9$
Radium-C′	6·870	1·02	6·945	$1\ 000_0$	$7\cdot68_3$	$7\cdot82_9$
Polonium (Radium-F)	3·805	0·62	3·848	$0\cdot827_4$	$5\cdot25_7$	$5\cdot35_9$

The velocities given in the table are calculated from the relation

$$\frac{V}{V_0} = \frac{\Delta V}{V_0} + \left(\frac{R}{R_0}\right)^{1/3}$$

where $\Delta V/V_0$ is obtained from the curve of fig. 8. It may be noted that the accuracy with which V/V_0 is obtained by interpolation on this curve does not depend on the accuracy of the absolute values of the mean ranges, and is independent of systematic errors in the ranges.

---

* I. Curie, 'C. R.,' vol. 175, p. 220 (1922); Briggs, 'Proc. Roy. Soc.,' A, vol. 118, p. 549 (1928); Laurence, 'Proc. Roy. Soc.,' A, vol. 122, p. 543 (1929); Rosenblum, 'C. R.,' vol. 190, p. 1124 (1930); Rosenblum, 'C. R.,' vol. 193, p. 848 (1931); Curie and Rosenblum, 'C. R.,' vol. 193, p. 33 (1931). M. Rosenblum informs us that the value of the ratio α *Ra* C′/α *Ra* A is 1·133(8), the value 1·335(8) given in the reference 'C. R.,' vol. 190, quoted above, is a misprint. The other ratios published are all correct.

† The values given in the above table should be taken as correct in cases where they differ from our previously published values. The altered values do not depend on new measurements, but arise from the application of a systematic correction derived from the humidity and standard barometer corrections which previously were omitted. The extrapolated ranges, velocities and energies may again be different owing to the revised derivations discussed in the text. The values given for thorium-C refer to the weighted mean of the two main groups of the complex range.

The values given for the velocities and energies must be regarded as provisional, as more accurate velocity data are expected to be available in the near future. There may be a considerable systematic error in the values given amounting to possibly 1 part in 1000 in the velocity, due to error in drawing the curve of fig. 8.

Discussion.

We have seen that the complexity in the case of the groups of α-particles from actinon is very analogous to the complexity of the α-particles from actinium-C, both with regard to the relative numbers and energies of the α-particles in the two groups. This similarity suggests a recurring characteristic of the nucleus, which, if it extended throughout the series, would involve a similar complexity of the α-particles from radio-actinium and protactinium. I. Curie (*loc. cit.*) has shown that the α-particles from radio-actinium are complex, apparently consisting of two groups of equal numbers, differing in energy by $2 \cdot 8 \times 10^5$ electron volts. The homogeneity of the α-rays from actinium-A suggests that it is not a case of branching of the series, and it might be expected that the complexity is associated with γ-ray emission in some such way as suggested by Gamow.*

Summary.

Measurements by the new counting methods of the mean ranges in air of α-ray groups have been extended to the α-particles emitted by radon, radium-A, thoron, thorium-A, actinon and actinium-A, and the range from polonium has been remeasured.

With the exception of actinon, each of the elements appears to emit a single homogeneous group of α-rays. The α-rays from actinon, however, appear to consist of two groups closely analogous both in relative numbers and in energy difference to the two groups emitted by actinium-C, discussed in previous papers.

As before, the ranges have been measured relative to the mean range of the main group of α-particles from thorium-C′ (taken as 8·533 cm.) as a standard. The manner in which this standard value is derived from absolute measurements of the extrapolated ionisation ranges made by other observers is discussed.

---

* 'Nature,' vol. 126, p. 397 (1930).

Following a suggestion that the mean ranges should be adopted in future in place of the extrapolated ranges, an experimental curve is given connecting the mean range with the initial velocity of the α-particle groups, based on the available velocity data and our measurements of mean range. By interpolation on this curve, the velocities, and hence the energies, of the α-ray groups have been determined. The accuracy of these velocities would not be affected by systematic errors in our range measurements, though such errors affect the true form of the curve.

We wish to express our thanks to Lord Rutherford for his advice and direction throughout the course of the work, which forms a continuation of the earlier work on the analysis of α-rays done in collaboration with him. We also wish to thank Mr. B. V. Bowden for assisting with some of the observations and Mr. G. R. Crowe for preparing the sources and assisting in the experiments. We are indebted to the Department of Scientific and Industrial Research for a grant to one of us (W. B. L.).

Studies of Gas-Solid Equilibria. Part IV.—*Pressure-Concentration Equilibria between Ferric Oxide Gels and* (a) *Water,* (b) *Ethyl Alcohol,* (c) *Benzene, directly determined under Isothermal Conditions.*

By BERTRAM LAMBERT and ALEXANDER GRAHAM FOSTER.

(Communicated by F. Soddy, F.R.S.—Received December 31, 1931.)

In this part of the work attempts have been made to determine the pressure-concentration equilibria between ferric oxide gel and water, making use of exactly the same procedure as that employed in Parts II and III,* and using ferric oxide gel from the same batch as that employed in Parts I and II.*

A serious difficulty was encountered owing to the liberation of a small quantity of gas from the activated and evacuated gel when the concentration of water in the system was brought near to saturation. The presence of a gas (as distinct from water vapour) in the system made itself evident—usually quite suddenly—by a very marked slowing-down of the rate at which water vapour could be transferred by evaporation from the water reservoir to the gel system. The pressure of this gas could, after some time, be estimated by the height to which mercury rose into the "cut-off" from the mercury reservoir. The largest pressure recorded in this way showed the presence of approximately 4 c.c. (at N.T.P.) of gas in the system.

---

* Part I, 'Proc. Roy. Soc.,' A, vol. 117, p. 183 (1927); Part II, 'Proc Roy. Soc.,' A, vol. 122, p. 497 (1929); Part III, 'Proc. Roy. Soc.,' A, vol. 134. p. 246 (1931).

Attempts were made to get over the difficulty by saturating the gel with water vapour (at 60° and at 70° C.), removing this water as far as possible by distillation *in vacuo* without altering the temperature, and then finally completing the evacuation at the original activation temperature of 148° C. After several repetitions of this treatment a small quantity of gas was still given off by the gel when it was subsequently nearly saturated with water.

The difficulty has not been encountered in parallel experiments with the same batch of ferric oxide gel and (*a*) benzene, or (*b*) ethyl alcohol. In the benzene-ferric oxide gel system (*vide* Part II) and the ethyl alcohol-ferric oxide gel system (*vide infra*), the purity of the gaseous phases has been convincingly shown, throughout many consecutive experiments, by the fact that the equilibrium pressures at saturation are identical with the vapour pressures of the pure liquids themselves.

There is no doubt that the activated and evacuated ferric oxide gel can be made to take up either benzene vapour or ethyl alcohol vapour until it is saturated, and then be made to lose the absorbed vapour, without causing—even after many repetitions of these processes—the liberation of any gas from the gel. When, however, water vapour is added to the gel, under precisely the same conditions, small quantities of gas are invariably liberated.

Similar experiments with silica gel and (*a*) water, (*b*) ethyl alcohol, (*c*) benzene (*vide* Parts II and III), have shown that the absorption of these vapours does not result in the liberation of gas from that gel.*

A final attempt was made to get over the difficulty by allowing the evacuated gel to take up water vapour (until it was about two-thirds saturated) and then heating the water-laden gel for several hours at 148° C. before again evacuating. This drastic treatment of the ferric oxide gel did not prevent the liberation of a small quantity of gas when the water content of the gel was subsequently raised nearly to saturation.

---

* It was thought possible that this peculiarity of the water-ferric oxide gel system might be explained by assuming that the gel, on account of its basic character, contained carbon dioxide which was not removed by the process of activation and evacuation, but was liberated by the action of the absorbed water under the conditions of our experiments.

It has not been found possible to remove the gas from the sealed system and analyse it, but attempts to show the presence of carbon dioxide in the system have led to negative results.

The use of this "*water-treated*" ferric oxide gel in later experiments on the ethyl alcohol-ferric oxide gel system, and the comparison of the results with those obtained in parallel experiments with the *original* gel, showed, however, *that a very marked change had been brought about in the absorptive powers of the gel by the "water-treatment" described above.*

Pressure-concentration equilibria have been determined for the ethyl alcohol-ferric oxide gel system using (1) the original gel and (2) the "water-treated" gel.

Pressure-concentration equilibria have also been determined for the benzene-ferric oxide gel system, using this new form of the gel, and the results have been compared with those obtained for the same system when the original gel was employed (*vide* Part II).

It has not been found possible—because of the difficulties described above—to obtain reliable pressure-concentration isothermals for the water-ferric oxide gel system.

The System Water-Ferric Oxide Gel.

Four experiments were carried out on this system—the first at 60° C., the second and third at 70° C., and the fourth (on the "water-treated" gel) at 60° C. In no case could an experiment be completed owing to the liberation of gas from the gel when its water-content had been raised to about two-thirds of the saturation value.

It is obvious that no great reliance can be placed on the results obtained. Since, however, no appreciable amount of gas was liberated from the gel until its water-content approached saturation, the plotting (in fig. 1) of the early results obtained in each of the four experiments affords some indication of the shape of the "ascending" pressure-concentration isothermals for the system. The figure also shows a shift, in successive experiments, of the pressure-concentration isothermals towards the pressure axis.

Curves II and III (70° C.) and curve I (60° C.) are drawn from results obtained with the original gel; the dotted curve IV (60° C.) is drawn from results obtained with the "water-treated" gel.

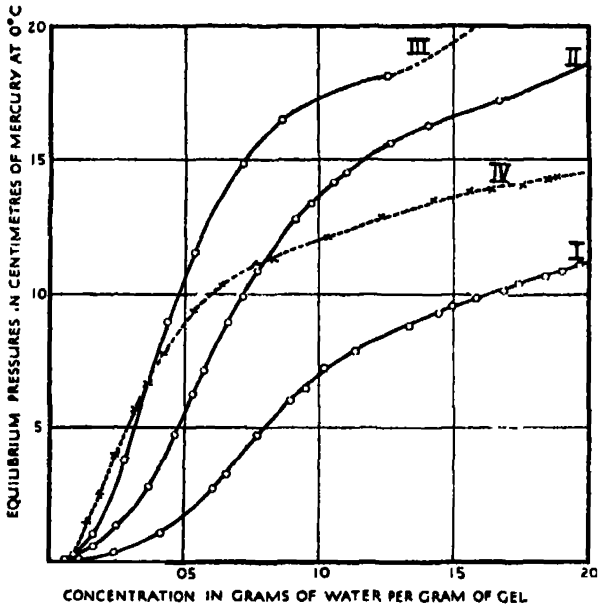

FIG. 1.—Pressure-concentration equilibrium curves for water-ferric oxide gel system determined isothermally. Temperature 60° C., curves I and IV; temperature 70° C., curves II and III.

The System Ethyl Alcohol-Ferric Oxide Gel.

Pressure-concentration equilibria for this system have been determined with *two* kinds of ferric oxide gel—the original gel (from the same batch as that used in Parts I and II) and the " water-treated " gel referred to above.

In the early stages of the experiments with the " water-treated " gel the results obtained were very irregular; reliable and repeatable results were only obtained after the alcohol-content of the gel had been raised (to saturation) and reduced many times. Eventually, however, the system " settled down " and a long series of experiments, at different temperatures, gave results which were reproducible—both for " ascending " and " descending " equilibrium points—over the whole concentration range.

Seven successive experiments were carried out in the following order: (1) at 70° C., (2) at 60° C., (3) at 50° C., (4) at 40° C., (5) at 50° C., (6) at 60° C., (7) at 70° C. Two separate and independent experiments were thus done at 50° C., 60° C., and 70° C. At each of these temperatures the equilibrium points—both " ascending " and " descending "— showed a high degree of reproducibility. The equilibrium points obtained in the separate experiments at the same temperature all fell on the same isothermal curve; there was no trace of shift in the curves and the gaseous phase remained pure throughout, as shown by the coincidence of the equilibrium pressures at saturation with the vapour pressures of pure alcohol.

Note.—The vapour pressures of pure alcohol are given in Part III.

The results obtained in the experiments at 40° C., 50° C., and 60° C. are given in Table I below.

Equilibrium pressures are expressed in centimetres of mercury at 0° C. and the alcohol-content of the gel is given in grams of alcohol per gram of gel.

Table I.—System Ethyl Alcohol-Ferric Oxide "Water-treated" Gel.

Experiment at 60° C.

No.	Concentration of alcohol.	Pressure.	No.	Concentration of alcohol.	Pressure.
1	0·0141	1·670	15	0·1636	34·85
2	0·0227	14·15	16	0·1626	34·04
3	0·0335	23·60	17	0·1614	33·61
4	0·0412	26·80	18	0·1536	33·30
5	0·0520	29·40	19	0·1482	33·15
6	0·0620	30·63	20	0·1350	32·86
7	0·0709	31·37	21	0·1216	32·58
8	0·0760	31·69	22	0·1074	32·19
9	0·0837	32·13	23	0·0916	31·79
10	0·0965	32·66	24	0 0791	31·30
11	0·1113	33·07	25	0·0550	29·28
12	0·1305	33·55	26	0·0442	27·62
13	0·1501	33·89	27	0·0280	19·72
14	0·1595	34·25			

" Ascending " points 1 to 15. " Descending " points 16 to 27.

Experiment at 50° C.

No.	Concentration of alcohol.	Pressure.	No.	Concentration of alcohol.	Pressure.
1	0·1700	22·19	12	0·0302	13·35
2	0·1665	22·12	13	0·0196	4·43
3	0·1640	21·16	14	0·0267	11·78
4	0·1580	20·90	15	0·0352	15·37
5	0·1434	20·69	16	0·0484	17·96
6	0·1260	20·48	17	0·0617	19·22
7	0·1052	20·19	18	0·0801	20·11
8	0·0824	19·77	19	0·0986	20·62
9	0·0642	18·95	20	0·1183	20·91
10	0·0585	18·54	21	0·1360	21·17
11	0·0512	17·89	22	0·1564	21·41

" Descending " points 1 to 13. " Ascending " points 14 to 22.

Table I.—(Continued).

Experiment at 40° C.

No.	Concentration of alcohol.	Pressure.	No.	Concentration of alcohol.	Pressure.
1	0·1625	12·84	11	0·0385	9·68
2	0·1547	12·60	12	0·0520	11·05
3	0·1311	12·40	13	0·0700	11·84
4	0·0925	12·00	14	0·0902	12·27
5	0·0748	11·72	15	0·1054	12·48
6	0·0472	10·40	16	0·1395	12·78
7	0·0320	8·30	17	0·1518	12·84
8	0·0235	5·40	18	0·1637	13·00
9	0·0202	2·81	19	0·1740	13·52
10	0·0312	8·30			

" Descending " points 1 to 9. " Ascending " points 10 to 19.

In the parallel experiments with the *original* gel, irregularity of behaviour was again noticed in the early stages, but the system required a much shorter time to " settle down " and give reproducible values.

A complete experiment at 60° C. was carried out with this gel and almost complete results were obtained in an experiment at 70° C., before an accident caused a break in the apparatus. The results obtained at the two temperatures are, however, considered sufficient to show the behaviour of the system since the shape of the isothermal is the same for the two temperatures.

The results obtained in these two experiments are given below in Table II.

Table II.—System Ethyl Alcohol-Ferric Oxide " Original " Gel.

Experiment at 60° C.

No.	Concentration of alcohol.	Pressure.	No.	Concentration of alcohol.	Pressure.
1	0·0153	0·080	13	0·2123	31·45
2	0·0270	0·150	14	0·2131	35·06
3	0·0437	0·250	15	0·2203	35·30
4	0·0508	0·740	16	0·2101	26·86
5	0·0572	1·665	17	0·2025	23·74
6	0·0621	3·445	18	0·1850	22·98
7	0·0738	9·560	19	0·1719	22·53
8	0·1095	19·560	20	0·1599	22·25
9	0·1329	22·080	21	0·1436	21·87
10	0·1599	23·865	22	0·1258	21·16
11	0·1831	25·29	23	0·0848	15·15
12	0·2050	27·82			

" Ascending " points 1 to 15. " Descending " points 16 to 23.

Table II.—(Continued).

Experiment at 70° C.

No.	Concentration of alcohol.	Pressure.	No.	Concentration of alcohol.	Pressure.
1	0·1104	31·21	10	0·2131	51·45
2	0·1299	34·44	11	0·2088	41·34
3	0·1527	36·83	12	0·1989	36·89
4	0·1723	38·80	13	0·1893	36·41
5	0·1894	40·46	14	0·1785	36·00
6	0·1993	41·81	15	0·1625	35·56
7	0·2057	43·24	16	0·1496	35·12
8	0·2123	50·78	17	0·1313	34·07
9	0·2165	54·31	18	0·2119	49·70

" Ascending " points 1 to 9 and 18. " Descending " points 10 to 17.

The purity of the gaseous phase—the complete absence of gas other than alcohol vapour—in all these experiments with alcohol and the two kinds of ferric oxide gel, is evident from the fact that, when the systems are saturated, the equilibrium pressures are identical with the vapour pressures of pure ethyl alcohol.

In fig. 2 the results of the experiments at 60° C. are plotted ; the isothermal A shows the results obtained with the original gel and the isothermal B those obtained with the " water-treated " gel.

The shapes of the isothermals are typical of the ethyl alcohol-ferric oxide gel systems when the two kinds of gel are used.

The System Benzene-Ferric Oxide " Water-treated " Gel.

The marked difference between the pressure-concentration isothermals obtained with the two kinds of ferric oxide gel and ethyl alcohol suggested the determination of the pressure-concentration equilibria between benzene and the new " water-treated " gel so that a comparison could be made with the results already obtained (*vide* Part II) with the original gel.

Complete experiments were carried out at 40° C., 50° C., and 60° C. The results are given in Table III (p. 371).

In these experiments (as in all our experiments on the equilibria between benzene and gels) the system settled down immediately and gave equilibrium pressures with a very high degree of reproducibility both on the " ascending " and " descending " isothermals ; there was, again, a complete absence of the uncertainty of behaviour associated with the early stages of all the experiments on the equilibria between ethyl alcohol and gels.

The purity of the gaseous phase of the system was maintained throughout, as shown by the identity of the equilibrium pressures, at saturation, with the vapour pressures of pure benzene. (The vapour pressures of pure benzene, at various temperatures, are given in Part I.)

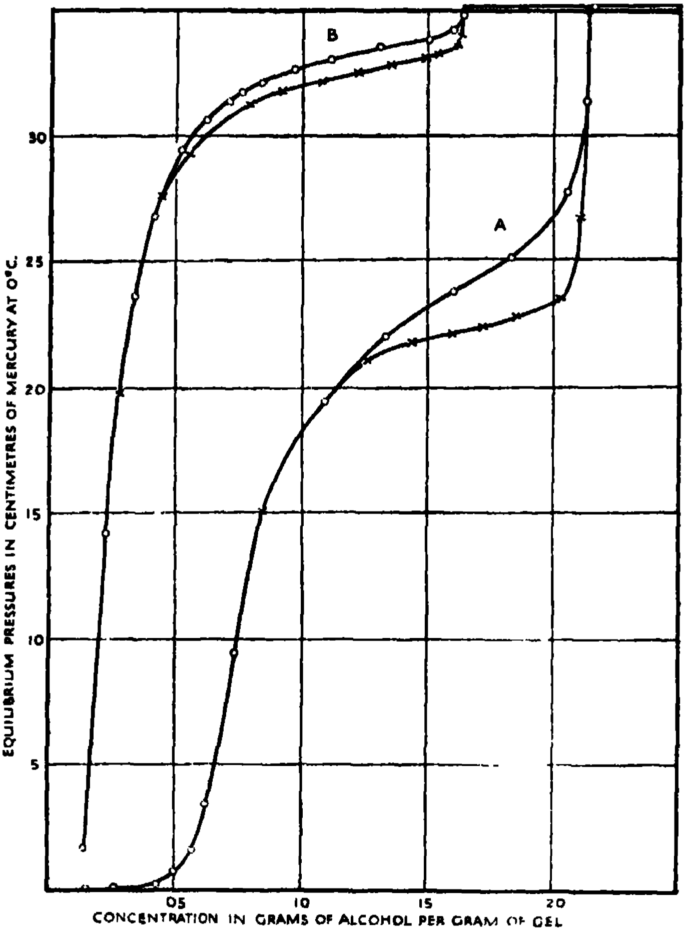

FIG. 2.—Pressure-concentration equilibrium curves for alcohol-ferric oxide gel systems determined isothermally at 60° C. A, isothermal for original ferric oxide gel; B, isothermal for "water-treated" ferric oxide gel. "Ascending" points are marked thus, O. "Descending" points are marked thus, ×.

The results of the experiments at 40° C., and 50° C., are plotted in fig. 3 (see p. 372). Alongside these isothermals for the benzene-ferric oxide "water-treated" gel system are drawn, for purposes of comparison, the corresponding isothermals for the benzene-ferric oxide "original" gel system (*vide* Part II).

Table III.—System Benzene-Ferric Oxide "Water-treated" Gel.

Experiment at 60° C.

No.	Concentration of benzene.	Pressure.	No.	Concentration of benzene.	Pressure.
1	0·0041	1·25	15	0·1422	84·08
2	0·0175	11·22	16	0·1247	33·38
3	0·0295	19·16	17	0·1004	32·65
4	0·0453	26·47	18	0·0825	31·72
5	0·0635	30·49	19	0·0610	30·31
6	0·0842	32·67	20	0·0492	26·71
7	0·1005	33·66	21	0·0357	22·08
8	0·1178	34·37	22	0·0285	18·55
9	0·1342	34·84	23	0·0250	16·12
10	0·1478	35·14	24	0·0206	13·00
11	0·1597	35·61	25	0·0161	9·57
12	0·1755	38·39	26	0·0132	7·15
13	0·1850	38·85	27	0·0095	4·13
14	0·1625	34·82	28	0·0142	8·11

"Ascending" points 1 to 13 and 28. "Descending" points 14 to 27.

Experiment at 50° C.

No.	Concentration of benzene.	Pressure.	No.	Concentration of benzene.	Pressure.
1	0·1810	27·11	16	0·0110	3·66
2	0·1760	25·50	17	0·0175	7·215
3	0·1682	24·32	18	0·0255	11·62
4	0·1599	24·025	19	0·0367	15·87
5	0·1485	23·76	20	0·0415	17·36
6	0·1360	23·44	21	0·0576	20·40
7	0·1163	22·91	22	0·0810	22·36
8	0·1001	22·56	23	0·0950	23·13
9	0·0850	21·98	24	0·1082	28·57
10	0·0679	20·87	25	0·1195	23·88
11	0·0505	18·68	26	0·1319	24·12
12	0·0398	16·46	27	0·1475	24·42
13	0·0303	13·20	28	0·1603	24·69
14	0·0240	10·40	29	0·1775	26·70
15	0·0068	1·49	30	0·1830	27·15

"Descending" points 1 to 15. "Ascending" points 16 to 30.

Table III.—(Continued.)

Experiment at 40° C.

No.	Concentration of benzene.	Pressure.	No.	Concentration of benzene.	Pressure.
1	0·1780	18·27	19	0·1135	15·83
2	0·1745	16·47	20	0·1340	16·09
3	0·1630	16·14	21	0·1480	16·30
4	0·1506	15·94	22	0·1680	16·70
5	0·1340	15·64	23	0·1820	18·27
6	0·1140	15·36	24	0·1760	16·67
7	0·1020	15·05	25	0·1645	16·17
8	0·0900	14·80	26	0·1529	15·91
9	0·0775	14·44	27	0·1396	15·75
10	0·0640	13·59	28	0·1231	15·45
11	0·0452	11·80	29	0·1079	15·17
12	0·0263	7·80	30	0·0967	15·01
13	0·0212	5·92	31	0·0828	14·62
14	0·0346	10·10	32	0·0231	6·67
15	0·0458	12·46	33	0·0148	3·75
16	0·0595	13·77	34	0·0125	2·92
17	0·0740	14·67	35	0·0060	0·74
18	0·0902	15·26			

"Descending" points 1 to 13 and 24 to 35. "Ascending" points 14 to 23.

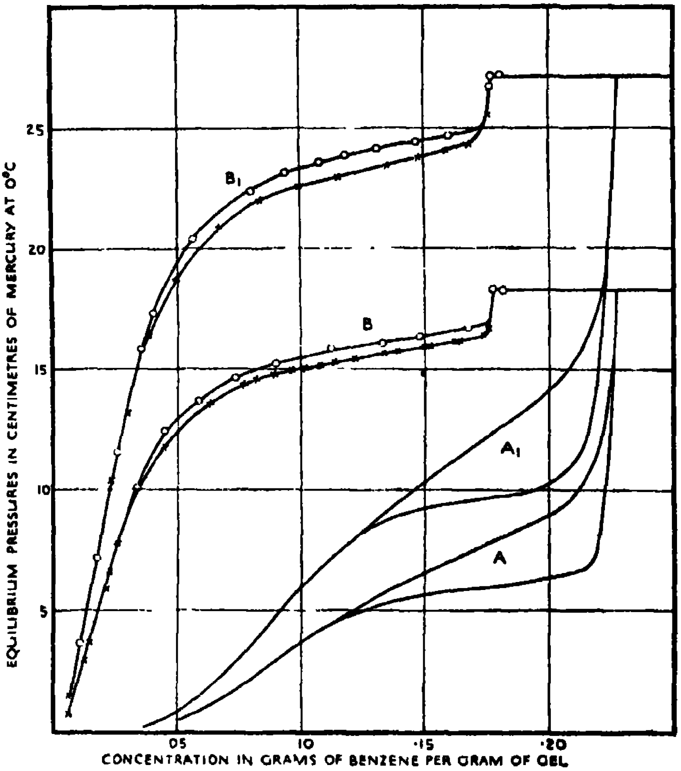

Fig. 3.—Pressure-concentration equilibrium curves for benzene-ferric oxide gel systems determined isothermally. 40° C. isothermals: original gel, curve A; "water-treated" gel, curve B. 50° C. isothermals: original gel, curve A_1; "water-treated" gel, curve B_1. "Ascending" points are marked thus, O. "Descending" points are marked thus, X.

In fig. 4 the comparative pressure-concentration isothermals (at 60° C.) are plotted for the systems :—

(*a*) Benzene-ferric oxide " original " gel.

(*b*) Benzene-ferric oxide " water-treated " gel.

(*c*) Ethyl alcohol-ferric oxide " original " gel.

(*d*) Ethyl alcohol-ferric oxide " water-treated " gel.

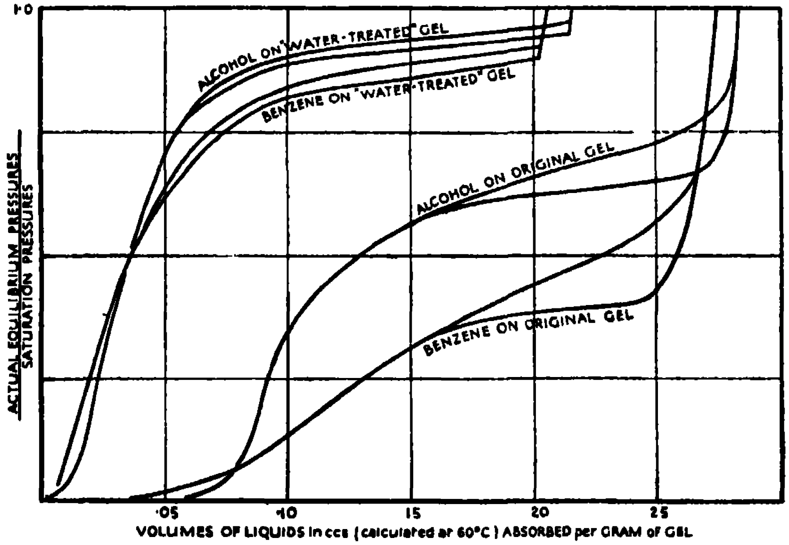

FIG. 4.—Comparative pressure-concentration isothermals for systems (*a*) alcohol-ferric oxide gel and (*b*) benzene-ferric oxide gel, using original and " water-treated " gels, in which actual equilibrium pressures/saturation pressures are plotted against volumes of liquid in cubic centimetres (calculated at 60° C.) absorbed by 1 gram of gel.

The actual equilibrium pressures have been reduced to the same pressure scale by dividing these pressures by the saturation pressures in each case; the relative pressures so obtained have been plotted against the volumes of the liquids absorbed per gram of gel (these volumes being calculated at 60° C.).

The results which have now been obtained from studies of the equilibrium relations between (1) silica gel, (2) ferric oxide gel (two kinds) and the vapours of benzene and of ethyl alcohol permit of the following general conclusions being drawn :—

(*a*) Each of the gels—the silica gel and the two kinds of ferric oxide gel—considered by itself, exercises its absorptive power in essentially the same manner towards both benzene and alcohol.

There is no really marked difference in shape between the benzene and the alcohol isothermals for the same gel, and the absorptive capacity of each gel (taking the volumes of liquid absorbed at saturation) is always slightly greater for alcohol than it is for benzene. The absorptive capacity of the "water-treated" ferric oxide gel is over 20 per cent. less than that of the original ferric oxide gel both for benzene and for alcohol.

(*b*) There are, however, very striking differences between the isothermals for the silica gel systems and those for the ferric oxide gel systems. These differences can be seen very clearly by considering, side by side, the *comparative* pressure-concentration isothermals for the two systems—graph V (Part III) and fig. 4 above.

The isothermals for the silica gel systems rise very slowly from the pressure axis as the concentration of absorbed vapour increases: they are of a simple type throughout their whole course and are never convex to the pressure axis; they are completely reversible over the whole range of concentration, both "ascending" and "descending" points falling on the same smooth curve; *they show no trace of hysteresis.*

The isothermals for the ferric oxide gel systems rise much more rapidly from the pressure axis as the concentration of absorbed vapour increases, and they are much less simple in character. In the systems involving the use of the original ferric oxide gel, the isothermals are convex to the pressure axis over a wide range of concentrations and, in the systems involving the use of the "water-treated" ferric oxide gel the isothermals are, over almost the complete range, markedly convex to the pressure axis. Although all these isothermals are quite definitely reversible over a considerable range at low concentration and again, to a less extent, over a range of concentration near to saturation, there is an intermediate concentration range over which the systems are not reversible. Over this range the equilibrium pressures on the "ascending" isothermal are always higher than those on the "descending" isothermal and *an hysteresis region is invariably shown.*

Both types of isothermal—the simple type characteristic of the silica gel systems and the more complicated type characteristic of the ferric oxide gel systems—represent real equilibrium conditions; they are, throughout their whole range, definitely repeatable and reproducible for both "ascending" and "descending" equilibrium points.

The hysteresis shown by all the isothermals of the ferric oxide gel systems (both with alcohol and with benzene) is, then, a real equilibrium phenomenon. The purity of the gaseous phase—as shown by the exact coincidence of the equilibrium pressures at saturation with the vapour pressures of the pure liquids themselves—in all the experiments, shows quite conclusively that the hysteresis does not arise from faulty technique.

It has been suggested that hysteresis in the pressure-concentration isothermals obtained from the study of solid-vapour (or non-permanent gas) systems, is due to the presence of permanent gases in the systems investigated. Now all inorganic gels, possessing a high absorptive power, contain water and permanent gases which are not removed by the activation process. This can be demonstrated quite clearly by using an automatic Topler (or Sprengel) pump for evacuation during the activation process. A gel which has been activated by being heated, *in vacuo*, at its proper activation temperature, for a sufficient length of time, can be kept at that same temperature without giving off any gas; if the temperature be raised 10°, sufficient gas is given off to make itself evident in the fall-tube of the Topler pump; further increases of temperature will cause the evolution of more and more gas (along with water) from the gel and will lead to the lowering, and eventual destruction, of the absorptive power of the gel.

The silica and ferric oxide gels used in all our experiments were activated by prolonged heating at 148° C., *in vacuo*, and must, therefore, have contained the water and permanent gases not removable by this treatment.

That this residual permanent gas is not displaced by absorbed benzene or alcohol (at temperatures up to 70° C.) is shown by the purity of the gaseous phase in all the experiments with these vapours.

The uncertainty of behaviour of both gels during the early stages of the experiments with alcohol, and the necessity for a "settling down" period before reproducible results could be obtained, seem to indicate that the absorbed alcohol may be affecting the residual water of the gel; but, if water is displaced from the gel, the amount is insufficient to be detected by its influence on the gaseous phase.

Note.—It is to be remembered that absorbed water vapour displaces the residual permanent gas from ferric oxide gel, although it does not displace it from the silica gel. This point is dealt with later.

It seems to be clear, then, that the hysteresis phenomena which are found in the pressure-concentration isothermals of the ferric oxide gel systems (with benzene and with alcohol), and are absent in the corresponding silica gel systems, cannot be due solely to the presence of permanent gas in the systems.

(*c*) There are marked differences between the gels in connection with their powers to retain absorbed vapours. This is clearly seen from a comparison of the equilibrium pressures in systems at corresponding concentration.

When half-saturated with benzene at 50° C.—

Silica gel has an equilibrium pressure about 1/80th the saturation pressure;

Ferric oxide "original" gel has an equilibrium pressure 1/4th the saturation pressure;

Ferric oxide "water-treated" gel has an equilibrium pressure 6/7th the saturation pressure.

So lightly is the absorbed vapour retained by the "water-treated" ferric oxide gel that almost all of it can be distilled off isothermally at 60° C.

It is interesting to note that when silica gel and ferric oxide gel are used as substitutes for active charcoal, in the production of high vacua, the higher retentivity of the silica gel is strikingly illustrated.*

A satisfactory comparison between the gels in their behaviour towards water is unfortunately not possible because of the peculiar behaviour of the ferric oxide gels referred to above.

Note.—The amount of permanent gas "locked up" in an activated and evacuated gel is quite considerable.

During successive experiments with the same sample of ferric oxide gel and water, the total volume of residual permanent gas liberated by the gel was approximately equal to the volume of the gel itself; this sample of gel had previously been heated for more than 100 hours in a high vacuum, with an efficient mercury-vapour pump running.

The fact that absorbed water liberates permanent gas from ferric oxide gels and not from silica gel, under the same conditions of experiment, is another indication of the difference between the structures of the two gels.

The experiments carried out on the water-silica gel system (*vide* Part III) show quite clearly that that gel exercises its absorptive power towards water in a manner quite different from the way in which it behaves towards benzene and alcohol.

The water-silica gel isothermals, with their small hysteresis region and their rapid rise from the concentration axis, might be considered as transitionary in character between the simple type obtained in benzene (or alcohol)-silica gel systems and the more complicated types obtained in the ferric oxide gel systems.

---

* *Vide* "Report of the Oxygen Research Committee," H.M. Stationery Office, p. 51 (1923).

The extremes of type of pressure-concentration isothermal for solid-vapour systems would seem to be represented by the benzene-silica gel isothermal and the benzene-ferric oxide " water-treated " gel isothermal; the former, which is concave throughout to the pressure axis, showing the behaviour of a gel of high retentivity, the latter, which is almost entirely convex to the pressure axis, showing the behaviour of a gel with a low retentivity.

Neither layer theories of adsorption nor theories involving the conception of condensation within fine capillaries, can, of themselves, afford a satisfactory explanation of these experimental results. It seems probable that an explanation will have to be sought in a combination of the conceptions of layer adsorption and condensation, associated with proper consideration of (*a*) the diameters of the vapour molecules and (*b*) the sizes of the capillaries.

Summary.

(1) Attempts have been made to determine the pressure-concentration equilibria between ferric oxide gel and water; but the absorption of water by the gel resulted in the liberation of small quantities of permanent gas from the gel and prevented complete results being obtained.

(2) Attempts to prevent the liberation of gas from the gel by heating it in water vapour at 148° C., resulted in the production of a new kind of gel with a very low retentive power.

(3) Complete pressure-concentration equilibria have been determined for the systems :—

(*a*) Ethyl alcohol-ferric oxide " original " gel.
(*b*) Ethyl alcohol-ferric oxide " water-treated " gel.
(*c*) Benzene-ferric oxide " water-treated " gel.

(4) Comparative pressure-concentration isothermals for all the ferric oxide gel systems (with alcohol and with benzene on each kind of gel) have been drawn.

(5) Hysteresis phenomena and the different types of pressure-concentration isothermals obtainable in gel-vapour systems are discussed.

Some of the apparatus used in this work was purchased out of a grant made by Imperial Chemical Industries, Ltd.; this assistance is acknowledged with much gratitude.

The Quantum Mechanics of Electrochemistry.—II.

By R. W. Gurney, Ph.D. Cambridge, Lecturer in Manchester University.

(Communicated by R. H. Fowler, F.R.S.—Received January 4, 1932.)

One of the few physical controversies of the nineteenth century that still smoulder is that regarding the relation between metallic contact potential and the electromotive force of any voltaic cell. While the dispute as to the physical facts themselves is now almost extinct, the dispute as to the interpretation of these facts remains. In a recent paper,* which will be referred to as Part I, the author has made a first application of quantum mechanics to such problems of electrochemistry. Instead of dealing with the problems of widest significance, the special problem of "overpotential" was there analysed, in order to show that the new method was capable of giving definite results where other methods had been less successful. In the present paper the general question of the voltaic cell will be considered, including electrode potentials, the meaning of solution pressure, the rôle of contact potential, and of chemical energy.

At the beginning of the century it was still uncertain whether the Volta contact potential difference between two metals was due to some intrinsic property of the metals, or to an adventitious surface layer of moisture or gas. But in 1906 Einstein† proclaimed the intrinsic nature of the potential difference as being approximately equal to the difference between the photoelectric work functions characteristic of the two metals

$$(\phi_1 - \phi_2) = \varepsilon\mathfrak{V}. \tag{1}$$

Though this relation is not exact, at room temperature and below it differs from the precise relation by a negligible amount. A few years after Einstein's work, when the thermionic phenomena had made the metallic work functions more familiar, there was no longer any doubt among physicists as to the intrinsic nature of the Volta contact potential difference, often amounting to more than two volts. It is therefore somewhat surprising to find that in 1930 in the recent volume 8 of the Ostwald-Drucker "Handbuch der Allgemeinen Chemie," the 10 pages devoted to the Volta p.d. are exclusively occupied with the ancient argument that it is mainly a spurious effect due to a layer of moisture or gas. The same view is put forward in volume 3 of the 1930 edition of Jellinek's "Lehrbuch der Physikalischen Chemie," which has recently been described as "undoubtedly the most important and authoritative treatise on physical chemistry of the time."* Thanks mainly to the work of Langmuir† and of Butler,‡ chemical opinion is in some quarters more progressive: "Although there is no agreement as to the rôle of the metal contact potential in the total e.m.f. of a cell, it is now generally accepted that the hypothetical 'solution pressure' of a metal is closely connected with its thermionic work function."§

---

* 'Proc. Roy. Soc.,' A, vol. 134, p. 137 (1931).

† 'Ann. Physik,' vol. 20, p. 203 (1906).

In any cell with electrodes of dissimilar metals one cannot close the circuit without obtaining the ordinary Volta contact p.d. at the metal-metal junction in the external circuit (the introduction of an intermediate metal, of course, leaves the p.d. unchanged). It has long been known that the electrochemical order of the elements is the same, or almost the same, as that of the Volta series, as if it were the unavoidable dry metal-metal contact in the external circuit which determines the e.m.f. of the cell. The controversy turns upon the difficulty of reconciling this with another experimental fact—that for any cell the product of the observed e.m.f. and the electronic charge is approximately equal to the heat evolved when solution of the metal takes place as an ordinary test-tube reaction.

Now a chemical change such as $CuSO_4aq + Zn \rightarrow ZnSO_4aq + Cu$, carried out as a test-tube reaction, does not appear to be connected with any electrical Volta p.d.; hence the parallelism between the chemical series and the Volta series appears to be merely fortuitous, or else spurious. The only method of reconciling the contending views would be to prove that by some concealed relation the heat evolved in the test-tube reaction is itself determined by the Volta p.d. characteristic of the reacting metals. If the proof of this unsuspected relation could be obtained, then certainly the controversial deadlock would disappear. The required proof is obtained in § 2.

The subject has often been obscured by the ambiguous use of the term "electrode potential." When a metal is dipped into an electrolyte, there is a definite p.d. set up between the liquid and the electrode, and this p.d. is known as an electrode potential. On the other hand, when a cell is formed of two dissimilar half-cells, the contribution made by each to the e.m.f. of the cell is known as the electrode potential of the half-cell, and is often denoted by the symbol π. To avoid this confusion, we shall use the term "interface potential" to specify the actual p.d. at any metal-liquid interface. If two particular half-cells, containing electrodes of different metals, happen to have identical interface potentials, they will not have the same electrode potentials, owing to the difference in the contribution to the metal-metal p.d. As in Part I, the interface potentials will be denoted by V. We will give a precise definition of electrode potential as follows. Let the given half-cell be coupled with a standard half-cell; then on closing the external circuit a current will in general flow unless a certain reverse e.m.f. has been introduced into the external circuit. The value π of this opposed e.m.f. required to prevent a current from flowing is defined as the electrode potential of the half-cell, referred to the standard half-cell.

---

* "Nature," p. 958, December 5, 1931.

† 'Trans. Amer. Electrochem. Soc.,' vol. 29, p. 125 (1916).

‡ 'Phil. Mag.,' vol. 48, p. 927 (1924).

§ Glasstone, "The Electrochemistry of Solutions," p. 321 (1930).

The mechanism of the Volta metal-metal p.d. has been made clearer by the Sommerfeld theory of metals, which has given us a theoretical derivation of the metallic work-function.* On this basis Frenkel† has recently pointed out that a metal-metal contact may be treated in quantum mechanics as a narrow potential barrier. Let A in fig. 1 represent the usual simple potential energy of an electron along a straight line drawn through a metal; and let B represent the potential energy in some other metal of the same valency but of higher work-function. The horizontal lines indicate the electron levels occupied at ordinary low temperatures. On bringing the metals into "contact," the electrons in the higher levels of A immediately make transitions through the potential barrier into B, leaving a positive charge on the surface of A. This positive charge modifies the potential energy in B, creating new local electron levels into which the transferred electrons can fit.‡ The negative charge of the transferred electrons will conversely modify the potential energy in A, causing the local disappearance of some electron-levels, thereby leaving

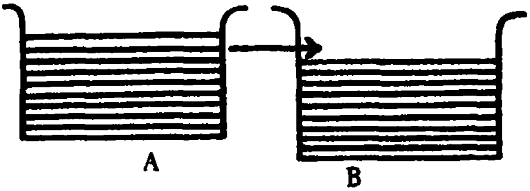

FIG. 1.

---

* Eckart, 'Z. Physik,' vol. 47, p. 38 (1928).

† Frenkel, 'Phys. Rev.,' vol. 36, p. 1604 (1930).

‡ Compare Lennard-Jones, 'Trans. Faraday Soc.' (*in course of publication*).

the positive cores of surface atoms of A incompletely neutralised. The whole then comes to equilibrium as in fig. 2. After equilibrium has been attained, any fast electron can still make a spontaneous transition through the potential barrier to a level of equal energy in the other metal; and the important point to be noticed is that no work is done in this transfer, in spite of the intense field between the metals. Throughout the discussion it will be convenient to bear in mind that it is the " noble " metals, silver, copper, etc., which have large work functions, and so become negative with respect to the baser metals.

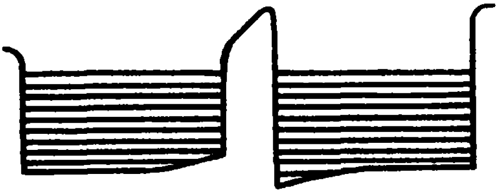

FIG. 2.

§ 1. *Deposition and Solution of Ions.*

Suppose that we have an assembly of similar atoms (or molecules) one of which is a negative ion. The popular idea is that one particular ion bears a negative charge exactly $-\epsilon$. But in quantum theory the wave function representing the surplus electron has an amplitude of non-zero value in the interior of every other atom in the assembly, and it is this wave function when integrated over all space which is normalised to be equal to exactly $-\epsilon$. On every atom the charge will therefore be $\eta\epsilon$, where $-1 < \eta < 0$. In the same way a positive ion situated among similar neutral atoms will receive contributions from the wave functions of the neutral atoms, and will bear a charge $\eta\epsilon$, where $0 < \eta < 1$. These considerations cease to be trivial at distances of atomic dimensions. When, for example, two atoms are united to form a diatomic molecule, they participate jointly in the valence electrons; and if this participation is unequal the molecule has a permanent electric moment. For many such polar molecules the distance apart of the two atoms is known, and then the moment may be described by saying that one of the two atoms bears a charge $+\eta\epsilon$ and the other a charge $-\eta\epsilon$. Thus, for example, the value of η for the HCl molecule is 0·16.

These considerations have been introduced in order to apply them to the solution and deposition of metal ions at a metal surface. In the Sommerfeld theory of metals the valence electrons are all quasi-free electrons, the atoms of the lattice being ions; but all participate equally in the free electrons. When an ion is removed from a metal surface its participation falls rapidly to zero, and work has to be done in separating the positive and negative charges. From another point of view work has to be done against the forces of the mirror-image attraction. The potential energy curve for a metallic ion along a line perpendicular to the metal surface is therefore of the form given in fig. 3. The horizontal lines indicate the vibration levels of a surface ion about its position of equilibrium on the surface of the lattice. The same potential energy curve applies, of course, whether the ion in fig. 3 is moving from left to right or from right to left, *i.e.*, whether we are removing ions from the lattice or bringing up fresh ions and adding them to the lattice. The curve only differs from that already given in fig. 3 of Part I, for a non-metallic ion,

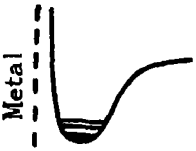

FIG. 3.

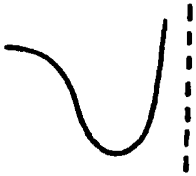

FIG. 4.

in that there it was assumed that the participation was small enough to be

We have next to consider the potential energy of an ion in the neighbourhood of a water molecule. This has already been done in fig. 5*a* of Part I for the special case where the ion is a proton; and for metallic ions the curve will be of the same general form, the depth of its potential minimum corresponding to the value of the hydration energy of the ion. The curve is given in fig. 4, where the vertical line on the right represents the centre of gravity of an H_2O molecule. When we have an H_2O molecule at some distance from a metal surface, the potential energy of an ion along a line between them is, of course, obtained by joining together the curves of figs. 3 and 4. When an electrode is dipping into an aqueous electrolyte there is water in contact with the surface, and the curves of figs. 3 and 4 overlap, giving a resultant of the form of fig. 5. The H_2O molecule will, of course, be subject to thermal agitation, but for the moment we will consider it fixed. The ion has two alternative positions of equilibrium with an extremely small potential barrier between. Although the probability of an atom making a transition through a potential barrier is in general negligible, this is not so when the barrier is small enough.

In fig. 5 let the dotted line through C represent the centre of gravity of the H_2O molecule. We have two cases to consider :—

(1) Let the dotted line through B represent the surface of the metal. A surface ion of the lattice, vibrating in the level AB will be represented by a wave-function which will leak into BC, indicating a probability of transition to a level of equal energy, *i.e.*, solution of the ion, leaving the level AB vacant.

(2) Conversely, let us start with an ion in solution in the region BC, and let the dotted line through A now be the position of the metal surface, the surface-ions of the lattice being to the left of A. The vacant region AB now indicates a possible position of equilibrium for an ion to be deposited. The ion in BC will be represented by a wave-function which will leak into AB, indicating a probability of deposition of the ion on to the metal lattice. The contrasted types of transitions in which deposition and solution of the ion takes place may be called *d*-transitions and *s*-transitions, respectively; and the initial configurations which give rise to them may be called *d*-situations and *s*-situations. The potential energy curve is by definition the same whether we are considering transitions from left to right or from right to left.

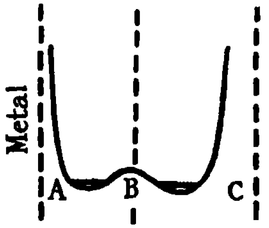

FIG. 5.

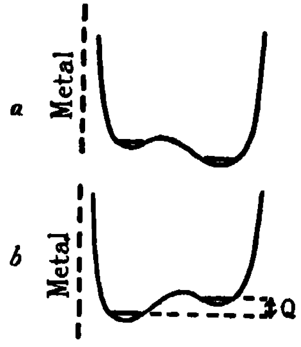

FIG. 6.

In the above we have been dealing tacitly with a special case where the two values of potential minimum are approximately at the same level. For most elements, however, the curve will have the form of either fig. 6, *a* or *b*. Since at ordinary low temperatures the ions are concentrated in their lowest vibration levels, solution of ions is almost impossible in fig. 6, *b*, *i.e.*, it is only possible from exceptionally high vibration levels, and deposition of ions is almost impossible in fig. 6, *a*. The situation is in fact quite analogous to that of electrons in fig. 1 above. On dipping into water a metal whose levels are of the form of fig. 6, *a*, ions make transitions into solution, leaving the metal negatively charged, and setting up a static potential difference, as do the electrons in fig. 2 above. The negative charge on the metal is distributed uniformly over the surface by the motion of the free electrons. On dipping a metal whose levels are of the form of fig. 6, *b* into a solution of one of its salts, ions from the latter will make transitions on to the surface, charging the metal positively. In each case the initial curve of fig. 6, *a* or *b*, has now to be compounded with a curve representing an interface potential V, positive or negative, or rather the potential energy $m\epsilon V$, where $m\epsilon$ is the charge on the ion. And a moment's reflection shows that the sign of the p.d. is in each such as to bring the system to equilibrium, *i.e.*, to bring fig. 6 towards the form of fig. 5. From the ease with which a current of either sign will flow we know that transitions take place readily in either direction. The standard condition to which fig. 6 was supposed to refer is that when there is no electrical double layer at the surface, and this is taken as the definition of $V = 0$. An expression for the equilibrium conditions will be deduced in § 3. The European convention with regard to the sign of electrode potentials is to take the potential of the electrolyte as the zero of potential. We must take the same sign for the interface potentials, so that V will be negative when the metal is negative with respect to the liquid.

Consider the surface of the lattice of a metal crystal at absolute temperature T. The distribution of the surface ions in their vibration levels will be given by the Boltzmann law, so that the fraction of the total number that are in a level of energy U will be given by an expression containing the factor $\exp\{(U_m{}^0 - U)/kT\}$, where $U_m{}^0$ is the energy of the lowest quantum level of a metallic surface ion. Taking the same view of the ions in solution as was taken in Part I, the distribution of the ions will involve a similar factor $\exp\{(U_s{}^0 - U)/kT\}$. The quantities $U_m{}^0$ and $U_s{}^0$ have characteristic values for each element. Now suppose that an ion in the level $U_s{}^0$ in fig. 6, *b* makes a transition through the barrier and falls into the vacant level $U_m{}^0$; an amount of energy Q, equal to $(U_s{}^0 - U_m{}^0)$, characteristic of the element, will be given out as heat. This is what will happen in the absence of any interface potential. If an arbitrary interface potential V exists, bringing the levels of fig. 6 nearer together or further apart, the heat evolved will depend on the difference of the levels so modified, *i.e.*, the heat evolved will be equal to $(Q - \epsilon V)$ for a monovalent ion, or $(Q - m\epsilon V)$ for an ion of valency *m*. Similarly the heat evolved on solution of an ion will be $-(Q - m\epsilon V)$. This value applies to transitions between the two ground levels; but at ordinary low temperatures the ions are so concentrated near the ground levels that the average value $(\overline{Q} - m\epsilon V)$ will scarcely differ appreciably from the former.

Before applying these ideas to the Volta p.d. controversy in § 2, it will be convenient to have in view some definite type of cell. The point at issue is fully represented in the simplest type of bimetallic cell, and until the controversy is resolved it will be well to restrict attention to this type—two half-cells each consisting simply of a metal dipping into a dilute solution of one of its salts, the small liquid junction p.d. being eliminated by one of the usual methods. The e.m.f. of such a cell depends to some extent upon the relative concentration of the two solutions and on temperature. But even when the e.m.f. is extrapolated to absolute zero of temperature, the limiting value of the e.m.f. of this simple fundamental type of cell does not usually differ from the value at room temperature by as much as 0·1 volt. This approach to constancy suggests that the total e.m.f. could be expressed as the sum of two or more terms, the principal and largest term being really characteristic of the two metals and independent of concentration and temperature. Dealing first with concentration, we know that when the values of the two concentrations are very disparate, the cell will behave partly as a concentration cell, a considerable balance of purely osmotic work being done, thereby contributing a small supplementary e.m.f. over and above the e.m.f. possessed by the cell when the concentrations are comparable. The sign of this supplementary e.m.f. depends merely on whether it is the ions of the positive or negative metal which have the higher concentration; and its value does not depend at all on the pair of metals involved, but is the same for any pair of metals of given valency. Hence if we wish to arrive at an e.m.f. which is really characteristic of the two metals, this adventitious e.m.f. must be segregated and expressed by an additional term. This separation is made possible by the fact that the supplementary e.m.f., like the e.m.f. of any concentration cell will be proportional to the absolute temperature, vanishing at absolute zero. This supports the idea that it is in the value extrapolated to zero temperature that we may look for an e.m.f. which is really characteristic of the two metals. In the mechanism outlined above this amounts to treating the ions and electrons as all in their lowest levels.

§ 2. *Resolution of the Volta p.d. Controversy.*

The parallelism of the Volta series applies not only to the chemical series obtained from the e.m.fs. of aqueous cells, but also from non-aqueous cells.

For when cells are made up using as solvent some liquid such as methyl alcohol instead of water, the surprising fact is found that in every case the e.m.f. has almost the same value as with the corresponding aqueous solution.* This, however, ceases to be remarkable when it is realised that what has been carefully measured in each case is merely the metal-metal p.d. in the external circuit, slightly modified by the interface potentials, indicating that it is not the chemical energy which determines the value of the e.m.f.

This paradox is easily resolved by the aid of the processes represented in figs. 5 and 6. Taking for example the system ($CuSO_4aq + Zn$), consider a zinc surface where zinc ions are making transitions from the lattice into solution. If V_z is an arbitrary interface potential at the surface, the heat evolved per ion dissolved is $-(\bar{Q}_z - 2\epsilon V_z)$. The general case will be treated in § 3 ; here we are primarily interested in the limiting value at zero temperature which is obtained by replacing $\bar{Q}_z$ by its value Q_z. Again, if V_c is an arbitrary interface potential at a copper surface where copper ions are being deposited, the heat evolved per ion deposited is $(Q_c - 2\epsilon Z_c)$. Hence when zinc displaces copper from a solution, whatever be the values of V_z and V_c, the total heat of reaction will be equal to

$$2\epsilon (V_z - V_c) + (Q_c - Q_z). \qquad (4)$$

Let us now fix our attention upon a particular particle of dissolving zinc which has a growing film of copper on part of its surface ; as the zinc goes into solution the copper grows by deposition. Let S be any point in the electrolyte near the edge of the copper film, and C any point in the film. Since the electrolyte is a good conductor, any difference of potential between the points C and S will be equal to whatever interface potential V_c there happens to be at the liquid-copper interface. Similarly if Z is any neighbouring point in the zinc, the difference of potential between the points Z and S will be just V_z. Hence the difference $(V_z - V_c)$ is seen to be equal to the potential difference between the points Z and C. Now the potential energy of an electron along the line ZC will have the form of fig. 2 ; and since the electronic transitions are much more rapid than the ionic, the p.d. between the metals will be held steadily to the value $\mathfrak{B}_{cz}$ throughout the reaction, as is clear from fig. 2. Though we are able to leave the values of V_z and V_c arbitrary, their difference is controlled by the electrons, and we may substitute for $(V_z - V_c)$ in (4). We find that the heat of reaction measured calorimetrically will be equal to

$$2\epsilon\mathfrak{B}_{cz} + (Q_c - Q_z). \qquad (5)$$

---

* Buckley and Hartley, 'Phil. Mag.,' vol. 8, p. 320 (1929).

This is the value per divalent ion; the value per electronic charge transferred will be half of this. For any pair of metals 1 and 2, whose ionic valencies are respectively m_1 and m_2, the heat of reaction per electronic charge will be

$$\varepsilon \mathfrak{V}_{12} + \left(\frac{Q_1}{m_1} - \frac{Q_2}{m_2}\right). \tag{6}$$

Since the second term is usually small compared with the first, we find that the heat of chemical change in a test-tube reaction is governed by the value of the intrinsic Volta p.d. characteristic of the reacting elements.

§ 3. *Derivation of Interface and Electrode Potentials.*

The next step is to use the process of figs. 5 and 6 to describe and evaluate the equilibrium at the metal-liquid interface of an electrode, the equilibrium for which Nernst introduced the idea of "solution pressure." Since the adverse calculations of Lehfeldt in 1899 the hypothetical solution pressure has usually been regarded as without physical reality. But the arguments urged on either side have been mostly irrelevant, since both critics and defenders, with the exception of Butler, have alike confused interface potential with the much larger total electrode potential. Butler* was successful in giving an elementary kinetic theory picture of the equilibrium. A discussion of the general case from the point of view of statistical mechanics is given below by Mr. Fowler as an appendix to the present paper.

Here we shall show that figs. 5 and 6 provide a way of visualising the equilibrium. Its dependence on concentration and on temperature will be seen most simply by treating the vibration levels as one-dimensional, assuming no change of specific heat on solution or deposition of an ion. Let the composition of the solution into which the metal is dipping be M_s mols of a salt of the metal added to M_w mols of water, or other solvent, and let the ratio M_s/M_w be defined as the concentration c in theoretical units. Consider next the surface ions of the metal lattice; we shall suppose that owing to the interaction of neighbouring molecules all energies above the ground level are possible vibration levels, instead of a discrete set. Taking as usual the potential of the electrolyte as the zero of potential, if there is an interface potential V, of the total number of lattice ions per unit area of the surface a fraction

$$F(U)\,dU = \frac{1}{kT}\cdot\exp\{(U_m{}^0 + m\varepsilon V - U)/kT\}\,dU \tag{7}$$

---

* 'Trans. Faraday Soc.,' vol. 19, p. 729 (1924).

will be in levels between U and U + dU, all values of U being possible between ($U_m{}^0 + m\epsilon V$) and infinity. If N_w is the number of water molecules in contact with unit area of the surface, a fraction $N_w F(U)\,dU$ will provide s-situations associated with the eigenvalue U. Similarly the number of d-situations per unit area associated with the value U will be given by

$$\frac{N_s}{kT}\,.\,\exp\{(U_s{}^0 - U)/kT\}\,dU, \tag{8}$$

where N_s/N_w is the concentration of the solution in the layer in contact with the electrode ; this may differ by a certain factor from the concentration in the body of the solution, but it will be shown below that this factor cancels itself out. For equilibrium the number of d-situations multiplied by the probability of a d-transition must be equal to the number of s-situations multiplied by the probability of an s-transition. Let the ratio of the latter probability to the former be β, which will be a factor of the order of unity. Then detailed balancing requires that

$$N_w \exp\{(U_m{}^0 + m\epsilon V - U)/kT\} = \beta N_s \exp\{(U_s{}^0 - U)/kT\}, \tag{9}$$

that is to say

$$\beta c = \exp\{(m\epsilon V + U_m{}^0 - U_s{}^0)/kT\}. \tag{10}$$

Hence the interface potential at any temperature T is given by

$$V = V_0 + \frac{kT}{m\epsilon}\log\beta c, \tag{11}$$

where V_0, the characteristic limiting value at zero temperature is $(U_s{}^0 - U_m{}^0)/m\epsilon$, which is the same as $Q/m\epsilon$. If $\mathfrak{V}_{st}$ is the Volta contact p.d. between the electrode and some standard metal, the total electrode potential of the half-cell will be given by

$$\begin{aligned}\pi &= \mathfrak{V}_{st} + V\\ &= \mathfrak{V}_{st} + \frac{Q}{m\epsilon} + \frac{kT}{m\epsilon}\log\beta c.\end{aligned} \tag{12}$$

The e.m.f. of a cell formed by coupling two half-cells of electrode potentials π_1 and π_2, being given by $\mathfrak{E} = \pi_1 - \pi_2$, the maximum work done per electronic charge flowing round the circuit will, since $\mathfrak{V}_{13} - \mathfrak{V}_{23} = \mathfrak{V}_{12}$, be given by

$$\mathfrak{E}\epsilon = (\pi_1 - \pi_2)\epsilon = \epsilon\mathfrak{V}_{12} + \left(\frac{Q_1}{m_1} - \frac{Q_2}{m_2}\right) + kT\left(\frac{1}{m_1}\log\beta_1 c_1 - \frac{1}{m_2}\log\beta_2 c_2\right). \tag{13}$$

As T tends to zero the last term drops out, and it will be seen that the expression becomes identical with equation (6), which was deduced as the limiting value of the heat evolved in a test-tube reaction.

It was mentioned above that the concentration of the solution in the boundary layer may not be the same as the value c in the body of the liquid. If we write $N_s/N_w = gc$, this will add a term $(kT/m\varepsilon)\log g$ on the right-hand side of equation (11). But if an ion is deposited on the surface, its place in the boundary layer is taken by another ion from the body of the solution, so that we are really transferring an ion from the body of the solution to the metal, or *vice versa*, and the work done must be independent of the concentration of the boundary region. In dissolving ions the work required to take an ion from the boundary layer to the body of the solution is just $-(kT/m\varepsilon)\log g$, which cancels out the other term.

§ 4. *Activity Coefficients.*

Closer examination shows that in the argument from which (10) was derived there is a defect, so it would not be expected that (12) would accurately represent the experimental facts, even in very dilute solution; nor indeed does it. The potential energy of an ion in the neighbourhood of a water molecule has the form of fig. 4 because it polarises and distorts the water molecule, obtaining mutual negative potential energy. Further, the lattice ion of fig. 5 finds for itself a possible level in the solution because it is allowed to polarise the adjacent molecule of solvent, giving rise to an attraction or binding. This binding, which is the hydration or solvation of the ion, has been treated by several authors; it has been pointed out by Sack* that the solvent molecules adjacent to the ion will become electrically "saturated," that is, incapable of further polarisation. Now in counting up the number of s-situations per unit area of the interface we treated all solvent molecules as free molecules, whereas clearly solvent molecules which are already saturated by positive ions in solution, or partially saturated beyond a certain degree, will not provide s-situations, and must be subtracted. Thus in (9) N_w must be replaced by $(N_w - pN_s)$ where p is the number of solvent molecules put out of action by one ion. Hence in (10) c must be replaced by $c/(1 - pc)$, which in very dilute solution may be written ce^{pc}. And from (11) the actual solution will provide the same interface potential as would an ideal solution of strength fc instead of c, where

$$\log f = pc. \tag{14}$$

From consideration of the interface transitions one is thus led directly to the idea of "activity coefficients" which were introduced long ago from thermodynamic reasoning into all processes involving heat of dilution. And in equations (11) to (13) the concentration c must now be replaced by the activity $a = fc$. Other things being equal, the value of p will clearly be greater, the higher the charge borne by the ion. Hückel* proposed the theoretical formula

---

* 'Phys. Z.,' vol. 27, p. 206 (1926); Debye, "Polar Molecules," chap. 6.

$$\log f = \mathrm{A}c - \frac{\mathrm{B}\sqrt{c}}{1 + \mathrm{C}\sqrt{c}}, \tag{15}$$

where again A increases with the valency of the ion. It will be noticed that whereas f tends to unity at infinite dilution, β which multiplies c in (12) does not.†

In all the expressions so far the concentration has been given in absolute units. The method of expressing the concentration of aqueous solutions most used by chemists is to give the number of mols of solute added to 55·5 mols of water. Hence the concentration in practical units c' is equal to $55 \cdot 5c$. We can now write down an expression for the electrode potential of a half-cell at unit activity and 25° C. Putting fc' equal to unity, we obtain

$$\pi_0 = \mathfrak{V}_{st} + \frac{\mathrm{Q}}{m\varepsilon} + 298\,\frac{k}{m\varepsilon}\log\frac{\beta}{55 \cdot 5}. \tag{16}$$

The practical standard referred to some chosen standard half-cell will be the difference between two such expressions.

§ 5. *Conclusion.*

The prolonged failure to agree upon the rôle played by the Volta p.d. has been due to the difficulty of visualising the processes. We may therefore conclude by pointing out how figs. 1 to 6 give an insight into their physical nature. Dealing first with an electrode on open circuit, we may say that in very dilute solution the number of *d*-situations is so small compared with the number of *s*-situations that equilibrium can only be obtained if most of the *s*-situations are put out of action. What is needed is that the lattice ground-level be slightly lower than the other ground level, for then *s*-transitions will only be possible from exceptionally high lattice levels, as in fig. 6, *b*. Even a small difference between the levels will suffice to put out of action a large fraction of the *s*-situations, and this is what is needed for equilibrium in dilute solution. The sign of the interface potential required to bring about this equilibrium may be positive for some metals and negative for others, since the characteristic initial potential energy curve for V = 0 may for some elements have the form of fig. 6, *a*, and for others that of fig. 6, *b*. But we are led to the result that the equilibrium form of the curve will be approximately the same for all elements.

---

* 'Phys. Z.,' vol. 26, p. 119 (1925).

† See Appendix.

When now we close the external circuit, fig. 2 shows how the electronic levels of the baser metal are lowered relative to those of the noble metal; and the important point is that when the levels of a metal are lowered on an electronic diagram, they are raised on the positive ion diagram, and *vice versa*. Hence on closing the external circuit of a cell, the ionic levels of the base metal are thrown into the form of fig. 6, *a*, and those of the noble metal into the form of fig. 6, *b*. This modification of the interface potentials is permanent, since the state represented by fig. 2 lasts as long as the circuit remains closed. There is therefore a continuous solution of the base metal and deposition of the noble metal, until finally the relative concentration would adjust itself to the interface potentials. The Nernst theory of "solution pressure" attempted to account for this behaviour of any two metals in the Electrochemical Series by ascribing to the baser metal a higher intrinsic tendency to throw ions into solution. On the contrary, it seems to be the electrons at the metal-metal junction which are responsible, the order of the metals being that of the Volta Series.

APPENDIX.

A Note on the Statistical Theory of the e.m.f. of a Reversible Cell and the Verification of the Gibbs-Helmholtz Equation.

By R. H. Fowler, F.R.S.

(Received January 4, 1932.)

The model proposed by Mr. Gurney, in the paper to which this note is appended, appears to be susceptible of a more exact discussion than Mr. Gurney has attempted, from the point of view of statistical mechanics. Using the same model and so far as possible the same notation, we shall attempt to give a general expression for the electromotive force $\mathfrak{E}$ of a reversible cell and for the dependence of the interface potential on the concentration of the metal ions in the solution, and to verify that $\mathfrak{E}$ obeys the Gibbs-Helmholtz equation.

From the point of view of the equilibrium theory of statistical mechanics we may consider the equilibrium of the metallic ions between two phases, the metal and the body of the solution, ignoring the local properties of the surface layer, where, however, the conditions must be and may be assumed to be such that the surface layer itself is a third phase also in equilibrium. The surface layer in general is, however, an electrical double layer and *the long range effects* of this must be included in the form of the interface potential. The main problem is then one of the equilibrium of a solid and an "atmosphere" of one of its constituents; the other constituent (the electrons) may be ignored. The atmosphere of metallic ions in Gurney's model is, however, of a special type. They are not effectively free, but are to be thought of as attached to water molecules or groups of water molecules. Thus the partition function for an "atmospheric" ion is not of the form $V^*f(T)$, where V^* is the volume freely available to the atmosphere. If there were one water molecule available for the ion, the partition function for the atmospheric ion would be of the form $w(T)$, say, where

$$w(T) = \sum_0^\infty \varpi_j e^{-E_j/kT}. \tag{A1}$$

E_j, ϖ_j are the energies and weights of the vibrational states of the hydrated ion, $w(T)$ is strictly the extra factor which the partition function for the hydrated ion possesses over and above the partition function for an ordinary water molecule. Free, unhydrated states of the ion would possess so much more energy that they can be ignored altogether. If there are W water molecules available as hosts for the ion, then its partition function as an atmospheric ion is to a first approximation simply

$$Ww(T), \tag{A2}$$

as if all the weights of all its states were increased by a factor W. This approximation, of course, neglects the fact that the water molecules are close together, so that levels in neighbouring molecules will interact and split into separate levels instead of remaining degenerate. The $w(T)$ of (A2) is thus not strictly the $w(T)$ of (A1), but we shall ignore the difference here. In any case the *form* of (A2) is correct.

After these preliminaries we may proceed at once to assert that the equilibrium number of dissolved ions is given by the general "vapour pressure" formula

$$\bar{N} = W\frac{w(T)}{\kappa(T)}, \tag{A3}$$

where $\kappa(T)$ is the corresponding partition function for an ion in the metal.†

---

† For example, Fowler, 'Statistical Mechanics,' p. 117 and § 5.9 (Cambridge, 1929).

The arguments by which (A3) is established for an ordinary vapour-solid equilibrium are exactly repeatable here.

Formula (A3) contains all that we require, though some care is needed in the interpretation. In the first place if $\overline{\text{N}}$ is really small compared with W, W in Gurney's model is strictly the number of water molecules in the body of the solution and therefore $\overline{\text{N}}/\text{W} = c$. This will be modified later to extend crudely to values of c not so very small. Again, the lowest energy value, E_0, for the hydrated ion is Gurney's $\text{U}_0{}^s$, and the lowest energy value for the ion in the metal, referred to the same standard energy zero, is Gurney's $\text{U}_0{}^m + m\epsilon\text{V}$, where V is the interface potential and m the valency of the ion. Thus we may write

$$w(\text{T}) = e^{-\text{U}_0{}^s/k\text{T}}\, w'(\text{T}), \tag{A3.1}$$

where

$$w'(\text{T}) \sim \varpi_0 \qquad (\text{T} \to 0);$$

and also

$$\kappa(\text{T}) = e^{-(\text{U}_0{}^m + m\epsilon\text{V})/k\text{T}}\, \kappa'(\text{T}), \tag{A3.2}$$

where

$$\kappa'(\text{T}) \sim \rho_0 \qquad (\text{T} \to 0),$$

ρ_0 being the weight of the lowest vibrational state of the ion in the crystal. Combining these interpretations with (A3) and taking logarithms we find

$$k\text{T}\left\{\log c - \log \frac{w'(\text{T})}{\kappa'(\text{T})}\right\} = m\epsilon\text{V} + \text{U}_0{}^m - \text{U}_0{}^s, \tag{A4}$$

which is the completed form of Gurney's formula (10).

Various points of interest arise out of (A4). In the first place if $\overline{\text{N}}/\text{W}$ is not very small, one can correct for a type of saturation effect just as Gurney does in § 4. If each ion in solution puts out of action on the average p water molecules, the W in (A2) becomes effectively $\text{W}(1 - pc)$ and the c in (A4) is replaced by $c/(1 - pc)$. The statistical argument is unaffected. There is nothing to add to § 4 on this point.

In the second place we notice that (A4) can be written

$$\text{V} = \frac{\text{U}_0{}^s - \text{U}_0{}^m}{m\epsilon} + \frac{k\text{T}}{m\epsilon}\log\left\{\frac{c}{1 - pc}\,\frac{\kappa'(\text{T})}{w'(\text{T})}\right\}, \tag{A5}$$

corresponding to Gurney's (11). Unlike an activity coefficient (such as $1/(1 - pc)$ which is a rudimentary form of one) $w'(\text{T})/\kappa'(\text{T})$ may or may not tend to unity at infinite dilution—it is in fact superficially at least independent of c. When $\text{T} \to 0$, $\kappa'(\text{T})/w'(\text{T}) \to \rho_0/\varpi_0$, which need not *a priori* be equal to unity, though from the nature of our model, which suggests for the states of the ion those of a simple vibrator either in the crystal or the water-complex, it is extremely likely that in fact $\rho_0/\varpi_0 = 1$. For a more general model this might not hold. If we may regard both $w'(\mathrm{T})$ and $\kappa'(\mathrm{T})$ as approximately partition functions for a Planck vibrator, then when $k\mathrm{T} \gg h\nu$, where $h\nu$ is the average separation of the energy levels of the vibrator, we shall have approximately

$$w'(\mathrm{T}) \backsim \frac{k\mathrm{T}}{h\nu_s}, \qquad \kappa'(\mathrm{T}) = \frac{k\mathrm{T}}{h\nu_m};$$

in these formulæ ν_s and ν_m refer to the vibrator in the solution and the metal respectively. For such a model, even for ordinary temperatures, we should have

$$\mathrm{V} = \frac{\mathrm{U}_0{}^s - \mathrm{U}_0{}^m}{m\varepsilon} + \frac{k\mathrm{T}}{m\varepsilon}\log\left\{\frac{c}{1-pc}\,\frac{\nu_s}{\nu_m}\right\}, \qquad \text{(A6)}$$

and again ν_s/ν_m need not be equal to unity. With other assumptions as to the nature of the sets of states of the ion in the metal and the solution, we get other but similar formulæ over which we need not delay here.

We must now use (A4) to obtain a formula for $\mathfrak{E}$, the electromotive force of a cell such as those contemplated in § 1. We shall neglect fine adjustments at the metal-metal contact; and therewith the Peltier heat effect at that contact, assuming as in Gurney's discussion that when contact is made equilibrium requires the adjustment of the tops of the occupied electron levels to exactly equal energies. It is easy to generalise the argument and to include formally the Peltier effect at the metal-metal contact if desired, but it is an effect of exactly the same nature as the electrode-solution effects which we are about to discuss, and its inclusion adds nothing to the argument.

The e.m.f. was defined as the reverse of that p.d. which must be inserted between the electrodes in the outer circuit to prevent any flow of current when the circuit is closed. It is therefore the reverse of that p.d. required to bring the tops of the occupied electron levels to equal energies. On open circuit the tops of the occupied electron levels would differ by $\varepsilon\mathfrak{V}_{12}$, where $\mathfrak{V}_{12}$ is the true contact p.d., if it were not for the interface potentials, and these levels actually differ by

$$\varepsilon\,(\mathfrak{V}_{12} + \mathrm{V}_1 - \mathrm{V}_2).$$

Therefore

$$\begin{aligned}\mathfrak{E} &= -\,\mathfrak{V}_{12} + \mathrm{V}_2 - \mathrm{V}_1,\\ &= -\,\mathfrak{V}_{12} + \frac{(\mathrm{U}_0{}^s)_2 - (\mathrm{U}_0{}^m)_2}{m_2\varepsilon} + \frac{k\mathrm{T}}{m_2\varepsilon}\log\left\{c_2\,\frac{\kappa'_2(\mathrm{T})}{w'_2(\mathrm{T})}\right\}\\ &\qquad - \frac{(\mathrm{U}_0{}^s)_1 - (\mathrm{U}_0{}^m)_1}{m_1\varepsilon} - \frac{k\mathrm{T}}{m_1\varepsilon}\log\left\{c_1\,\frac{\kappa'_1(\mathrm{T})}{w'_1(\mathrm{T})}\right\}. \qquad \text{(A7)}\end{aligned}$$

This is the general formula for $\mathfrak{E}$. We find at once on partial differentiation with respect to T that

$$\mathfrak{E} - \mathrm{T}\frac{\partial \mathfrak{E}}{\partial \mathrm{T}} = -\mathfrak{B}_{12} + \frac{(\mathrm{U}_0{}^s)_2 - (\mathrm{U}_0{}^m)_2}{m_2\varepsilon} - \frac{k\mathrm{T}^2}{m_2\varepsilon}\frac{d}{d\mathrm{T}}\left[\log\frac{\kappa'_2(\mathrm{T})}{w'_2(\mathrm{T})}\right]$$
$$- \frac{(\mathrm{U}_0{}^s)_1 - (\mathrm{U}_0{}^m)_1}{m_1\varepsilon} + \frac{k\mathrm{T}^2}{m_1\varepsilon}\frac{d}{d\mathrm{T}}\left[\log\frac{\kappa'_1(\mathrm{T})}{w'_1(\mathrm{T})}\right]. \quad \text{(A8)}$$

Consider now the average energy $\overline{\mathrm{E}}$ of an ion in the metal or in the solution when the interface potential is V. By the well-known general formula of statistical mechanics

$$\overline{\mathrm{E}} = k\mathrm{T}^2\frac{\partial}{\partial \mathrm{T}}\log f(\mathrm{T}), \quad \text{(A9)}$$

where $f(\mathrm{T})$ is the corresponding partition function. Thus for ions of type 1 we find, using (A3.1) and (A3.2), that

$$\overline{\mathrm{E}_1{}^s} = (\mathrm{U}_0{}^s)_1 + k\mathrm{T}^2\frac{d}{d\mathrm{T}}[\log w'_1(\mathrm{T})],$$
$$\overline{\mathrm{E}_1{}^m} = (\mathrm{U}_0{}^m)_1 + m_1\varepsilon \mathrm{V}_1 + k\mathrm{T}^2\frac{d}{d\mathrm{T}}[\log \kappa'_1(\mathrm{T})].$$

Thus when ions of type 1 go into solution the average heat $\overline{\mathrm{Q}_1}$ given out per ion dissolving is equal to

$$\overline{\mathrm{Q}_1} = \overline{\mathrm{E}_1{}^m} - \overline{\mathrm{E}_1{}^s}$$
$$= (\mathrm{U}_0{}^m)_1 - (\mathrm{U}_0{}^s)_1 + m_1\varepsilon \mathrm{V}_1 + k\mathrm{T}^2\frac{d}{d\mathrm{T}}\left[\log\frac{\kappa'_1(\mathrm{T})}{w'_1(\mathrm{T})}\right].$$

Similarly for ions of type 2 going into solution

$$\overline{\mathrm{Q}_2} = (\mathrm{U}_0{}^m)_2 - (\mathrm{U}_0{}^s)_2 + m_2\varepsilon \mathrm{V}_2 + k\mathrm{T}^2\frac{d}{d\mathrm{T}}\left[\log\frac{\kappa'_2(\mathrm{T})}{w'_2(\mathrm{T})}\right].$$

Thus the heat given out when one gram-equivalent of ions of type 1 goes into solution and displaces one gram-equivalent of ions of type 2, which are thereupon deposited, the whole process being isothermal, is

$$\mathrm{Q} = \frac{\overline{\mathrm{Q}_1}}{m_1\varepsilon} - \frac{\overline{\mathrm{Q}_2}}{m_2\varepsilon}$$
$$= (\mathrm{V}_1 - \mathrm{V}_2) + \frac{(\mathrm{U}_0{}^m)_1 - (\mathrm{U}_0{}^s)_1}{m_1\varepsilon} + \frac{k\mathrm{T}^2}{m_1\varepsilon}\frac{d}{d\mathrm{T}}\left[\log\frac{\kappa'_1(\mathrm{T})}{w'_1(\mathrm{T})}\right]$$
$$- \frac{(\mathrm{U}_0{}^m)_2 - (\mathrm{U}_0{}^s)_2}{m_2\varepsilon} - \frac{k\mathrm{T}^2}{m_2\varepsilon}\frac{d}{d\mathrm{T}}\left[\log\frac{\kappa'_2(\mathrm{T})}{w'_2(\mathrm{T})}\right]. \quad \text{(A10)}$$

But, as already pointed out by Gurney, under the calorimetric conditions in which the Q of such a reaction is measured, we must have $V_1 - V_2 = -\mathfrak{V}_{12}$, and therefore on combining (A8) and (A10) we verify that

$$\mathfrak{E} - T\frac{\partial \mathfrak{E}}{\partial T} = Q,$$

the Gibbs-Helmholtz equation.

The Association of γ-Rays with the α-Particle groups of Thorium C.

By C. D. Ellis, F.R.S.

(Received January 20, 1932.)

As a result of the experiments of Rutherford, Ward and Lewis,* it is now generally accepted that the emission of γ-rays from radioactive bodies is associated with the transitions of α-particles between stationary states in the nucleus. Direct evidence for the existence of these excited states in the case of radium C′ is obtained from the several groups of long range α-particles which have been detected.

Rosenblum† has found that thorium C also emits several groups of α-particles, and the existence of a corresponding number of nuclear α-particle states can be safely inferred, which should also give rise to γ-radiation. This case was first discussed by Gamow,‡ who pointed out that there was an essential difference here from radium C′. In the latter body the extra α-particle states all have energy greater than the normal, and emission of the corresponding long range α-particles is a rare phenomenon, of the order of one long range particle for a million normal α-particles. The case of radium C′ appears to be accounted for satisfactorily by the assumption of two alternative processes, either internal nuclear switch or α-emission from the excited state, the relative frequencies of occurrence depending on the ratio of the transition probabilities. With thorium C, however, the most intense α-particle group is not the one of lowest energy, and the groups only vary in intensity by a factor of one hundred instead of one million as with radium C′. The assumption of *alternative* processes of

---

* 'Proc. Roy. Soc.,' A, vol. 131, p. 684 (1931).
† 'J. Physique,' vol. 1, p. 438 (1930).
‡ Gamow, 'Nature,' vol. 126, p. 396 (1930).

γ- and α-emission would lead to values for the ratio of the transition probabilities for the two processes which are absolutely incompatible with what is known about the orders of magnitude of the probabilities of α-particle emission and radiation switch. Gamow therefore proposed that the thorium C nucleus is initially formed with its α-particles all in the ground state and that disintegration could sometimes occur in such a way as to leave the product nucleus excited. Rosenblum* gives the following data for the velocities and relative intensities of the groups from thorium C.

Table I.—α-Particle Groups from Thorium C.

I. Relative velocity.	II. Intensity.	III. Energy of α-particle volts $\times 10^{-6}$.	IV. Total energy liberated volts $\times 10^{-6}$.	V. Energy difference volts $\times 10^{-5}$.
1·0034	0·74	6·056	6·172	0
1·0000	0·22	6·015	6·131	—0·41
0·9758	0·022	5·727	5·837	—3·35
0·9640	0·004	5·590	5·697	—4·75
0·9624	0·015	5·571	5·678	—4·94

The energies of the α-particles corresponding to these velocities have been calculated from the ratio of the squares of the velocities, the energy corresponding to velocity 1·0000 being taken as $6{\cdot}015 \times 10^6$ volts. However, when α-particles of this energy are emitted there will be a corresponding recoil of the residual atom, and the total energy liberated by the nucleus will be the sum of the energy of the α-particle and the energy of the recoil atom. To obtain this quantity, the values in column III need to be multiplied by $(1 + m/\mathrm{M})$, where m and M are the masses of the α-particle and recoil atom respectively, viz., 4 and 208. The correcting factor is therefore 1·0192. Column IV shows the deficit of energy of the other modes of disintegration compared to that of the first, and according to Gamow's hypothesis these values should represent the positive energy excesses of a set of excited states of the product nucleus thorium C″, as shown in column V and in fig. 1. Previous writers on this subject have not taken the recoil energy into account and have therefore obtained different values for the energies of the excited states, but there seems no doubt that the present procedure is the correct one. Gamow concluded that the evidence at that time did show that γ-rays of energies corresponding to this level system were emitted by sources of thorium $C + C''$, and was able to make out a sound *a priori* case for his hypothesis.

---

* 'J. Physique,' vol. 1, p. 438 (1930).

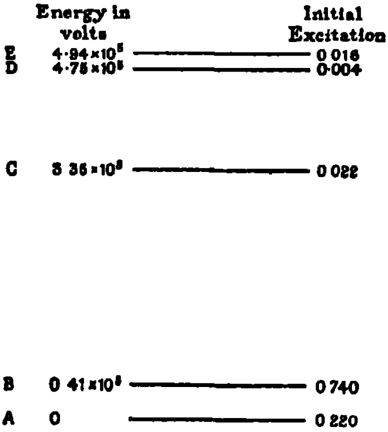

Fig. 1.

I discussed this hypothesis in some detail in a paper* at the recent Volta Conference, and concluded on the basis of the evidence then available that while there was no striking experimental proof of the correctness of the hypothesis, there was also nothing against it.

The more obvious methods of testing the hypothesis are inconclusive. For example, since the energy differences of the nuclear levels are deduced from the difference of two large α-particle energies, it is not possible to test the theory merely by seeing whether γ-rays of exactly the correct energies are emitted. The energies of the γ-rays are found from those of the β-ray groups in the natural β-ray spectrum, but there are so many weak groups in this region of the thorium $C + C''$ spectrum that, within the rather large tolerance that must be allowed, groups corresponding sufficiently with many of the calculated transitions could be found. A better test was found to be to compare the relative intensities of the α-particle sub-groups and the corresponding β-ray lines, and using some recent measurements I had made I found on the whole evidence in favour of Gamow's views. A slightly modified level scheme† which he had also proposed was found not to be satisfactory, since the level system now included a γ-ray which was too intense in relation to the α-particle groups. As, however, I pointed out on that occasion, the only satisfactory test of this hypothesis was to verify that γ-rays of the correct energies were emitted immediately after the α-particle disintegration of thorium C.

---

* In the course of publication.

† Gamow, 'Atomic Nuclei and Radioactivity,' Clarendon Press, 1931. Chap. III, s. 2, p. 66, Table Vc.

The scheme of transformation in which this body is concerned is shown in fig. 2. All our detailed knowledge of the γ-rays by means of β-ray spectra has been obtained by using sources of thorium C in company with its products, and it is not therefore known to which body the β-ray groups should be assigned.

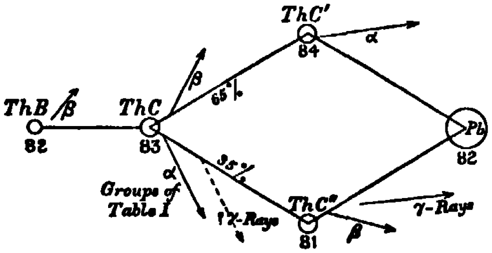

FIG. 2.

However, thorium C″ can be prepared free from other products by recoil from thorium C, and, although it is a short-lived body with a period of only 3·1 minutes, simple electroscope measurements had shown that it emitted powerful γ-rays corresponding closely in penetrating power to those from a source of thorium (C + C′ + C″). It had therefore always been assumed in the past that all the γ-rays, and hence also the β-ray groups, were due to the disintegration of thorium C″, but if Gamow's hypothesis is correct, some of the γ-rays should arise after the disintegration of thorium C. A source of pure thorium C″ prepared by recoil should not therefore show these γ-rays or the associated β-ray groups, since from such a source one would obtain only those radiations emitted after the thorium C″ disintegration.

At the time of the Volta Conference I had only made some preliminary experiments, but I reported that the crucial β-ray groups did not appear to be given by thorium C″ sources. I have since confirmed this work, and the results appear to support Gamow's theory in detail.

§ 2. *Experimental.*

The object of the following experiments is to decide whether the γ-rays that could arise from the set of levels shown in fig. 1 are emitted immediately after the α-disintegration of thorium C. The next table shows the energies of the β-ray groups that would occur by conversion in an atom of atomic number 81, the L_1 level being used for the first two transitions and the K level for the remainder. The energies, Hρ values and intensities of groups of approximately the right energies found in the *combined* emission of thorium C and thorium C″ are shown in column IV.

The values of Hρ and energy given here are based on some new measurements I have made, and differ slightly from previous values. These experiments are not quite finished and some small alterations in the values may yet have to be made, but these values are sufficiently accurate for the present case, where no attempt at criticism is being based on exact agreement in the energies. The values for the intensities of the groups which are quoted have been also determined in the course of this work.

Table II.

I.	II.	III.	IV.		
			β-ray groups found from Th . C + C″.		
Transition see fig. 1).	Energy volts × 10^{-5}.	Resulting β-ray group volts × 10^{-5}.	Energy volts × 10^{-5}.	Hρ.	Number of electrons per disintegration.
E—D	0·188	0·035	—	—	—
B—A	0·417	0·264	0·252	543	0·21
D—C	1·404	0·553	—	—	—
E—C	1·592	0·741	—	—	—
C—B	2·931	2·080	2·06	1673	2·6 × 10^{-2}
C—A	3·348	2·497	2·47	1861	0·6 × 10^{-2}
D—B	4·335	3·484	3·53	2319	0·2 × 10^{-2}
E—B	4·523	3·672	3·73	2400	0·2 × 10^{-2}
D—A	4·752	3·901	3·93	2480	0·09 × 10^{-2}
E—A	4·940	4·089	—	—	—
Chief changes introduced by using revised levels.					
C—B	2·76	1·91	1·92	1609	14·6 × 10^{-2}
C—A	3·16	2·31	2·38	1819	0·08 × 10^{-2}

Under the heading of " revised levels " are shown the two important alterations in the table which occur if Gamow's second set of levels is used. In this case he adjusted the energies of the levels slightly to give a better fit with the β-ray evidence instead of taking the energy differences directly from the α-particle measurements.

While the agreement between the energies is not good, it is not so poor as to count against the hypothesis, since the values used in columns II and III are obtained from the difference of two α-particle energies. It may be noted that an error of one in a thousand in the latter would give an error of $\pm 0{\cdot}06 \times 10^5$ volts in the values of column II.

If Gamow's hypothesis is correct, the β-ray groups shown in column IV should be emitted immediately after the α-disintegration of thorium C, and therefore should not be found in the β-ray spectrum of thorium C″ prepared by recoil. It is convenient to adopt the terminology "of the β-ray groups of thorium C . C″" to mean those actually emitted from a thorium C″ nucleus which has been left excited by the preceding thorium C disintegration. Such groups would in practice only be found from a source of thorium C and not from one of thorium C″, which would give the thorium C″ . Pb groups. It will be seen that the strongest groups concerned in this discussion are those of Hρ 543, and 1673, or, if the revised levels are used, Hρ 1609. While I found that Hρ 1609 was emitted by thorium C″ . Pb, the other two lines, Hρ 543 and 1673 are not. It would therefore appear that the revised level system is not an improvement and cannot be accepted, but that in its original form Gamow's hypothesis is strongly confirmed by experiment.

The method of measuring the thorium C″ . Pb β-ray spectrum was to prepare a source of thorium C″ *in situ*.

The usual type of semicircular focussing apparatus in vacuum was used and the arrangement of the source is shown in fig. 3. A was a small plate 3 × 8 mm. activated with thorium (B + C), the strength of the source being usually equivalent in γ-ray activity to about 5 mg. of radium. Some of the recoil atoms of thorium C″ ejected from A impinged on the plate B, and gave there a source placed in the correct position under the slit S to furnish a β-ray

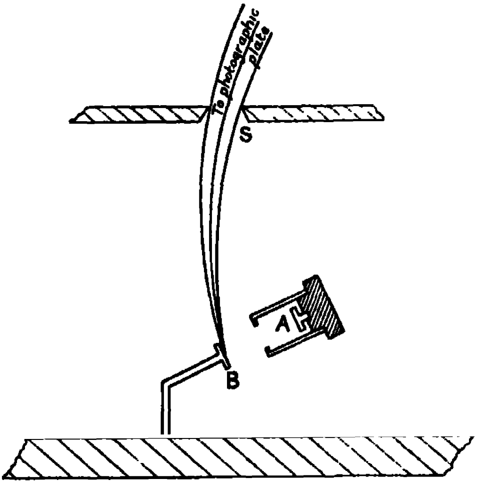

Fig. 3.

spectrum of the usual type. It will be seen that the main source A was enclosed in a tube which prevented any β-rays from getting directly to the photographic plate. The solid angle for collection of the recoil atoms provided by this arrangement was small and exposures of 15 to 25 hours were necessary to obtain photographs of the lines in the thorium C″ . Pb spectrum. There was little difficulty, however, in giving such long exposures, since a large permanent magnet* was employed to give the necessary magnet fields, and the vacuum was maintained by a charcoal tube immersed in liquid air. No attention was therefore necessary to the apparatus, and in fact the exposure was usually carried out over night.

To test out the apparatus, a photograph of the β-rays in the region 2500–3500 Hρ was first taken, and the two strong lines Hρ 2628 and Hρ 2914† were obtained. This was satisfactory, since these two β-ray groups are associated with the γ-rays of energy $5 \cdot 17$ and $5 \cdot 90 \times 10^5$ volts which are known to be emitted by thorium C″. Attention was then turned to two regions, the one including Hρ 1609, the other Hρ 543, and a series of photographs taken of each. In every case the line Hρ 1609 showed up strongly, whereas Hρ 543 was present on some photographs but not on others. It seemed at once likely that the phenomenon of aggregate recoil was complicating matters, and that under these conditions of recoil in vacuum some thorium B and thorium C was being carried across to the receiving plate B. A proof that this was occurring was furnished by two photographs in which the strong thorium B line Hρ 1398 was present as well as the line Hρ 1609. It was then clear that it was not sufficient merely to look for the presence or absence of a line, and that the problem could only be solved satisfactorily by comparing the relative intensities of the lines obtained by the recoil method with those obtained when a normal source of thorium (B + C + C″) was used. For example, my results in the region Hρ 1300 to Hρ 2100 are shown in Table III. The first three columns show the Hρ values, usual accepted origin, and relative photographic intensities of the stronger lines in this region and of certain weaker lines mentioned in Table II. The last column shows the intensities of the lines found on the recoil photograph. These plates were carefully photometered, but since the three weaker lines were faint, the intensities given are subject to the large uncertainty shown. It will be noticed that the thorium B line Hρ 1398, which is 55 times as strong as Hρ 1609 in the direct photographs, is only one-fifth as strong in the recoil photograph. Its occurrence to this

---

* Cockcroft, Ellis, and Kershaw, 'Proc. Roy. Soc.,' A, vol. 135, p. 628 (1932).

† Old values Hρ 2622 and 2914.

Table III.

$H\rho$.	Origin.	Relative photographic intensities from source of Th (B+C+C″).	Relative photographic intensities from recoil source.
1398	B	200	About 1
1459	B	0·4	—
1483	C or C″	0·7	0·7 to 1·3
1492	C or C″	0·07	—
1609	C or C″	3·6	5
1673	C or C″	0·7	—
1707	B	6·6	—
1767	B	25	—
1819	C or C″	0·02	—
1825	B	6·2	—
1839	B	1·7	—
1861	C or C″	0·15	—
1939	C or C″	0·7	0·7 to 1·3
1999	C or C″	0·15	—
2045	B	0·75	—

abnormally small extent can only be accounted for by concluding that a certain amount of thorium B was carried across to the receiving plate by aggregate recoil. On the other hand, the three lines Hρ 1483, Hρ 1609 and Hρ 1939 appear in about their correct relative intensities, and there is therefore a strong presumption that these are true recoil lines and come from thorium C″ . Pb.

There are two ways by which we can support this conclusion. The first is to verify that the absolute intensities of the lines are of the correct order of magnitude to be accounted for by the recoil. The efficiency of the recoil under these conditions was measured by carrying out the experiment exactly as usual, and when the apparatus had been properly evacuated for about an hour, air was let in rapidly, the receiver B was removed, and its activity measured by an electroscope. Taking the main source of thorium (B + C) as unity, I found on the recoil source about 2×10^{-3} of thorium C″ about $0 \cdot 1 \times 10^{-3}$ of thorium C, and traces of thorium B. Now in arbitrary units of photographic density I find that the intensity of Hρ 1609 by recoil is about 3×10^{-4} per milligram-minute of thorium (B + C) exposure, whereas direct it is about 2×10^{-1}, giving a ratio of about $1 \cdot 5 \times 10^{-3}$ for the total recoil efficiency in good agreement with that found by direct measurement.

A further proof that the line Hρ 1609 does come from the thorium C″ prepared by recoil is obtained by determining the intensity of this line on the recoil photographs relative to the intensities of the two lines Hρ 2628 and 2914 also obtained by recoil. We can be sure on independent evidence that the two latter lines are due to thorium C″ . Pb, so that if this is also true of Hρ 1609 the relative intensities of these lines from recoil photographs should be the same as from direct photographs. That this is the case can be seen from the following short table.

Table IV.

Line.	Hρ 1609.	Hρ 2628.	Hρ 2914.
Relative intensities—			
Direct .	2×10^{-1}	1×10^{-1}	$0{\cdot}8 \times 10^{-1}$
Recoil ..	3×10^{-4}	$1{\cdot}9 \times 10^{-4}$	$1{\cdot}3 \times 10^{-4}$
Ratio of intensities	$0{\cdot}66 \times 10^{3}$	$0{\cdot}53 \times 10^{3}$	$0{\cdot}6 \times 10^{3}$

In fact, taking into account the difficulties of photometering weak lines on a strong background, the agreement is rather better than would often be obtained in this type of work.

These experiments have therefore proved definitely that of the lines shown in Table III, Hρ 1483, 1609, and 1939 come from thorium C$''$. Pb. This shows that the revised set of levels proposed by Gamow (lower portion of Table II) are not correct, since it requires Hρ 1609 to come from thorium C . C$''$. However, Gamow's original scheme (upper portion of Table II) included instead the line Hρ 1673, and reference to Table III will show that this line was *not* obtained on the recoil photographs, although in the direct photographs it is of the same intensity as two lines Hρ 1483 and Hρ 1939, which were found by recoil. This is the first piece of strong evidence in favour of the hypothesis, but the crucial evidence must depend on the low energy line Hρ 543, which will now be discussed. In all seven experiments were made to photograph this line by recoil; on four of them were faint indications of the line, on three of them no sign of the line could be seen. Even on the photographs where the line was present the intensity per unit exposure varied greatly in a manner quite different from that of the lines previously discussed. However, I think the matter is settled quite definitely by applying the same criteria as in the previous cases. I find in direct photographs, using a source of thorium (B + C + C$''$) that Hρ 543 is about five times as strong as Hρ 1609, whereas in that recoil photograph where it was strongest Hρ 543 was at the most one-third as strong as Hρ 1609 for equal exposures. Therefore in the most favourable case there is a discrepancy of a factor of 15, and in three photographs, on two of which I place particular weight, there was no sign of the line. It would appear therefore that this line does come from thorium C . C$''$, a result in agreement with Gamow's hypothesis. It is interesting to note that its occurrence in certain photographs would be accounted for by just the amount of aggregate recoil found to occur in the control experiment.

Meitner and Phillips* have also started experiments on this same subject, and in a preliminary note in the 'Naturwissenschaften' state that they have found that this line Hρ 543 is emitted by thorium C″ . Pb in disagreement with Gamow's hypothesis. I cannot see any obvious reason for this disagreement, but it is clear that there are many factors to be taken into consideration in interpreting the results of this type of experiment, and the decision which conclusion is correct can only be reached later after a detailed criticism of all details. I shall therefore continue the present discussion on the basis of the experiments described in this paper, which appear to be in favour of Gamow's view.

It is important to note that the values of the energies of the γ-rays deduced from the β-ray data do support their association with this level system. For example (see Table II) the energy of the transition C—A and C—B *as obtained from the β-ray lines* (column IV) are $3 \cdot 32 \times 10^5$ and $2 \cdot 91 \times 10^5$ volts, and their difference agrees well with that for the measured value of the low frequency γ-ray $0 \cdot 405 \times 10^5$ volts as required by the level system. The same is true of the transitions D—A and D—B due to the γ-rays whose measured energies are $4 \cdot 78 \times 10^5$ and $4 \cdot 38 \times 10^5$ volts, giving again a difference in good agreement with that of the γ-ray $0 \cdot 405 \times 10^5$ volts.

It is therefore justifiable to use the β-ray lines to give the energy values of the excited α-particle states, since they can be measured with much greater accuracy than the difference of the α-particle energies can be determined. The values obtained in this way for the energies of the excited states of the thorium C″ nucleus are shown in Table V, and also the energies of the α-particle groups associated with their excitation, after making allowance as before for the effect of recoil. These values have been obtained by taking the energy of the most intense group of α-particles to be $6 \cdot 015 \times 10^6$ volts.

With the proof of the correctness of Gamow's picture of the mechanism of emission of the γ-rays in the case of thorium C, we have reached a definite stage in understanding the origin of the γ-rays of radioactive substances. We have now sufficient proof of the association of γ-rays with excited nuclear α-particle states to make it reasonable to conclude that all the γ-rays of radioactive bodies arise in this way. It is possible to obtain evidence about the α-particles in the nucleus from several different lines of work, and we may hope to see a rapid accumulation of data on the subject.

---

* 'Naturwiss,' December 11, p. 1007 (1931).

Table V.—Values for the Energies of the α-particle Groups from Thorium C and for the excited states of Thorium C″ revised by data from the β-ray spectrum.

Energy of excited states of Th . C″ in excess of that of the ground state (in volts × 10^{-6}).	Energy of α-particle group from thorium C (in volts × 10^{-6}).		Number of α-particles in group and also number of excitations of corresponding excited state per Th . C . C″ disintegration.
	Calculated.	Measured.	
0	6·056	6·056	0·22
0·406	6·015	6·015	0·74
3·32	5·730	5·727	0·022
4·78	5·587	5·590	0·004
4·99	5·566	5·591	0·016

There are many points of interest that rise from consideration of the detailed information we now possess about the excited states of the thorium C″ nucleus, but it would appear best to deal with these separately on another occasion.

I would like to express my indebtedness to Lord Rutherford for his interest in this work and for many helpful discussions.

Summary.

Experiments have been carried out to ascertain whether certain γ-rays known to be emitted as the result of the disintegration of either thorium C or thorium C″ actually arise from thorium C, as predicted by certain theoretical considerations of Gamow. These γ-rays are found to be emitted immediately after the disintegration of thorium C in agreement with the theory. This provides a further proof of the connection of the γ-rays with excited α-particle states in the nucleus and enables a comprehensive view to be taken of the whole problem of γ-ray emission of radioactive bodies.

I wish gratefully to acknowledge grants from the Caird Fund of the Royal Society, and also from the Government Grant Committee for the purchase of the radio-thorium used in this work and for the construction of the large permanent magnet.

My thanks are due to Mr. R. Cole for his assistance in carrying out the experiments.

The γ-Rays from Actinium Emanation and their Origin.

By Lord RUTHERFORD, O.M., F.R.S., and B. V. BOWDEN, B.A.

(Received January 21, 1932.)

As a result of recent experiments, evidence is accumulating that the penetrating γ-rays from radioactive substances have their origin not in the movement of electrons but in the transitions of α-particles in an excited nucleus. Strong evidence in support of this view was obtained by Rutherford, Ward and Lewis* from their analysis of the groups of long range α-particles from radium C′, and a more detailed discussion of the results was given by Rutherford and Ellis.† This problem of the origin of the γ-rays can be attacked in another direction from a consideration of the so-called fine structure shown by the groups of α-particles emitted by certain radioactive substances. In particular, Rosenblum‡ found that the transformation of thorium C was accompanied by the appearance of five homogeneous groups of α-particles. In explanation of these results, Gamow§ suggested that γ-rays should be emitted as a result of such a complex transformation, the energies of the individual γ-rays corresponding to the differences of energies between the α-particles in the various groups. Unfortunately it is a difficult matter to give a decisive answer on this important question.

In a recent paper, Ellis‖ concludes that the experimental evidence is in support of Gamow's theory, but on the other hand, Meitner¶ as a result of her investigations, has expressed a contrary opinion. It is thus of much importance to examine all methods of obtaining evidence on this question.

On Gamow's theory, all transformations which give more than one group of α-particles must give rise to γ-rays. In the simplest case, when two groups of α-particles only are observed, the energy of the γ-ray should be equal to the difference in energy of the α-particles in the two groups, and the number of γ-rays emitted should be equal to the number of α-particles in the lower velocity group. For example, both actinium C and actinium X have been shown to emit two groups of α-particles, and thus should emit γ-rays, the energy of which can be calculated. Though γ-rays of about the right energy have been deduced from the β-ray spectra, it is unfortunately difficult to be certain from which radioactive body they originate.

---

* 'Proc. Roy. Soc.,' A, vol. 131, p. 684 (1931).

† 'Proc. Roy. Soc.,' A, vol. 132, p. 667 (1931).

‡ 'C. R. Acad. Sci., Paris,' vol. 188, p. 1401 (1929), and vol. 190, p. 1124 (1930).

§ "Nature," vol. 126, p. 397 (1930), and "Atomic Nuclei and Radioactivity," Clarendon Press, p. 63 (1931).

‖ 'Proc. Roy. Soc.,' A vol. 136 p. 396 (1932).

¶ 'Naturwiss,' December, 1931.

In the course of their investigations on the complexity of the α-rays from various radioactive bodies, Lewis and Wynn-Williams* informed us that the α-rays from actinium emanation (actinon) were complex, consisting of two groups differing in energy by about $3 \cdot 5 \times 10^5$ volts. About 16 per cent. of the α-particles were emitted in the lower velocity group. Allowing for the energy of recoil, the transformation of actinon should thus be expected to give rise to powerful γ-rays of energy about $3 \cdot 56 \times 10^5$ volts. It will be seen that this new observation afforded a method of testing the general correctness of Gamow's theory by experiments of a simple kind.

The experimental arrangement is shown in the figure. A steady current of air passed over the actinium preparation in A, through the large stopcock S into a metal box B, the upper part of which was covered with a sheet of mica.

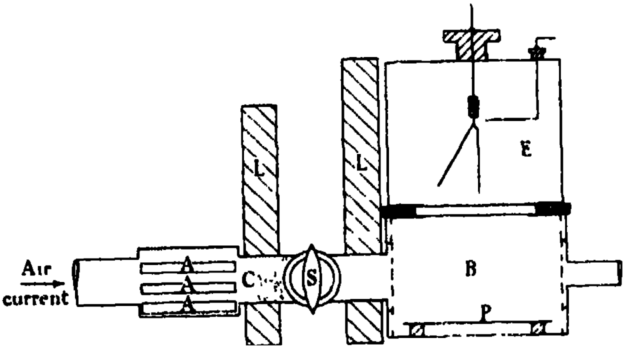

A β-ray electroscope E was placed above the mica to determine the effect of any β- or γ-radiation emitted from the emanation and its products. Any active deposit initially present with the emanation was removed from the air stream by a thick plug of glass wool at C. The rate of flow of the air current was adjusted so that on an average the emanation remained about 10 seconds in the box before removal by the current of air, so that the greater part of the emanation was transformed in the box. On turning on the air current, an immediate effect was observed in the electroscope, showing that the emanation or its product actinium A (period 1/500 second) emitted some β-rays. The effect in the electroscope increased slowly with time owing to the diffusion to the walls of a small part of the active deposit from the emanation transformed in the box. In order to estimate the magnitude of this β-ray activity compared with that due to the active deposit in equilibrium with the emanation an insulated metal plate P was charged to a potential of —200 volts, in order to collect the products of decay of the emanation, viz., actinium (B + C + C′), on its surface. Under these conditions, the introduction of the emanation gave the same initial effect as that obtained without the field, but the β-ray activity rose rapidly due to the β-rays emitted from the actinium (B + C + C′), reaching a maximum after about 3 hours: The initial effect due to the emanation was about 2 per cent. of the effect of the active deposit when in equilibrium with the emanation. Under the experimental conditions, the β-rays had to pass through mica, etc., equivalent to about 12 cm. of air in stopping power, and the effect in the electroscope became very small when sufficient absorbers were introduced to stop the β-rays. In order to test for the presence of γ-rays, a Geiger-Muller* tube counter was used in place of the electroscope. Instead of counting the number of throws of a string electrometer, the total current passed through the counter was collected in a condenser of about 0·5 mF. capacity for a definite interval varying from 20 seconds to a minute, and the condenser was then discharged through a ballistic galvanometer. This in practice proved a simple and convenient method of measuring the number of discharges in the tube counter. In order to reduce the effect in the counter due to the γ-rays emitted directly from the actinium preparation, suitable lead screens L were interposed. The thickness of the brass walls of the counter (1 mm.) was sufficient to absorb all the β-rays, and any soft γ-rays arising from the emanation.

---

* 'Proc. Roy. Soc.,' A, vol. 136, p. 349 (1932).

On passing the emanation through the box without the electric field, a marked γ-ray effect was immediately observed which increased only slightly with time. When the active deposit was collected on the plate there was a more noticeable increase, the γ-ray effect ultimately (after about 3 hours) reaching about 2½ times that due to the emanation itself. These experiments thus showed clearly that the emanation (or actinium A) emitted a weak β-radiation and a strong γ-radiation comparable with that arising from its subsequent γ-ray emitting products, actinium (B + C + C′). Before these observations, it had been supposed that the emanation emitted only α-rays. The small β-ray effect is to be ascribed to the internal conversion of the γ-rays in their escape from the nucleus, and is of the order of magnitude to be expected from this cause.

---

* We are indebted to Mr. Occhialini for the loan of a counter in good working order, constructed by him.

In order to determine the penetrating power of the γ-rays emitted by the emanation, sheets of lead or brass were interposed between the box and the counter. On account of the smallness of the effect it was difficult to determine the absorption curve with accuracy, but the observations indicated that the absorption by lead was exponential, with a value of $\mu/\rho = 0{\cdot}4$, the γ-rays being half absorbed in a thickness of 1·5 mm. lead. The absorption coefficient in brass was determined over a smaller range and is less accurate, the value of μ/ρ being 0·08.

It is difficult to fix the energy of the individual γ-rays from this value of the absorption coefficient, since the experimental arrangement employed in its determination was unsuitable for a direct estimation of the various factors (such as scattering, photo-electric effect, etc.) involved, and the strength of the actinium preparation was too small to allow a determination of the absorption under conditions more suitable for calculation. An estimate of the energy of the γ-ray can best be made by comparison of the absorption coefficients of γ-radiations of known maximum frequency made under comparable conditions. For example, Rutherford and Richardson* found that the less penetrating component of the γ-radiations from radium B gave a value of μ/ρ of 0·41 in lead. From the analysis given by Ellis, it is known that there are present two strong γ-rays of energies about 300,000 and 350,000 volts, which must in the main control this absorption coefficient. In addition Jaeger† has determined the absorption coefficient of X-rays of different frequencies in lead. Taking account of his data, and combining our observations of the absorption coefficients in lead and in brass, we estimate that the energy of transformation of the γ-rays from the emanation is about 350,000 volts, and this is of about the magnitude to be expected from the observed difference in energy of disintegration of the two groups of α-particles, viz., 356,000 volts. On the other hand, calculation from the data given by L. H. Gray,‡ gives a value of about 306,000 volts for the quantum energy.§ Considering the difficulties of an accurate estimate, the agreement is as close as could be expected, in view of the possibility that the transitions may not be as simple as has been assumed in the calculations.

---

* 'Phil. Mag.,' vol. 25, p. 722 (1913).

† 'Z. Physik,' vol. 69, p. 565 (1931).

‡ 'Proc. Camb. Phil. Soc.,' vol. 27, p. 103 (1931).

§ We are indebted to Mr. L. H. Gray for his help in these calculations.

A more definite test of the agreement of theory and experiment might be made if the quantum energy of the γ-rays could be directly determined in the ordinary way by means of the magnetic spectrum. Such an experiment would be very difficult and require much more intense sources of actinium emanation than were available in our experiments. Since preparations of actinium X produce the emanation immediately, the β-ray spectrum of this body should normally show a strong line due to the emanation, of energy about 350,000 volts. Owing to the escape of the emanation from the source of actinium X under experimental conditions, it is difficult to estimate the intensity to be expected for the emanation line in the γ-ray spectrum. It should be noted that the energy of the γ-ray from the emanation should be nearly the same as that of the γ-ray arising from the complex α-ray transformation of actinium C, since the differences of energy between the respective groups are about the same, a γ-ray of about this energy (350,000 volts) has actually been observed and has been ascribed to actinium $(B + C + C')$. Further experiments are required to throw light on this interesting question.

It should be pointed out that, while for simplicity we have spoken of the γ-rays from the actinium emanation, the γ-rays on Gamow's theory are supposed to arise from a transition in the subsequent product actinium A a very short interval after the emission of the α-particle from the emanation. It would be more correct to speak of the γ-ray arising from the transformation actinon-actinium A. It is impossible to conclude from these experiments whether the γ-radiation is emitted from actinon or from actinium A, but since no evidence of complexity of the α-rays of actinium A has been observed, it is natural to conclude that the γ-rays are connected with the transformation of the emanation itself. In general our experiments afford strong corroborative evidence of the correctness of Gamow's theory that γ-rays should be a necessary accompaniment of fine structure in the α-rays emitted from a radioactive substance. The intensity of the γ-rays and their energies are of the right order of magnitude to be expected from this theory. The experiments also afford support for the view that γ-rays have their origin in α-ray transformations in an excited nucleus.

The experiments of Lewis and Wynn-Williams (*loc. cit.*) have not shown any observable complexity in the α-rays from thorium or radium emanations. We should consequently not expect to observe any strong γ-radiation from either of these two bodies. In the case of radium emanation, the experiments of Slater* show that, if this body emits γ-rays at all, it does so in exceedingly small quantity (of the order of 1/6000 of that emitted by the active deposit in equilibrium with the emanation). We have ourselves made experiments with the emanation of thorium. A minute γ-ray effect of the order of 1/10,000 of that due to the thorium C″ in equilibrium with it was noted, but it is difficult to give a decisive proof whether the small effect observed is due directly to the emanation or to a trace of active deposit carried into the testing vessel with the emanation. Further experiments on this point are in progress.

---

* 'Phil. Mag.,' vol. 42, p. 904 (1921).

Summary.

Following the discovery of Lewis and Wynn-Williams that the actinium emanation emits two distinct groups of α-particles, evidence has been obtained that the transformation actinon-actinium A is accompanied by weak β-rays and strong γ-rays. From the measurement of the penetrating power of the γ-rays, it is concluded that the energy of the γ-rays is of the right order to be expected from the difference of energies of the α-particle groups (of 350,000 volts). These experiments afford strong confirmatory evidence that the γ-rays have their origin in transitions of α-particles in an excited nucleus, and are in agreement with the general view suggested by Gamow that γ-rays must accompany all transformations where more than one group of α-particles is emitted.

In conclusion we wish to express our thanks to Mr. G. R. Crowe for his help in making the measurements.

The Mechanism and Molecular Statistics of the Reaction $CuSO_4 . 5H_2O = CuSO_4 . H_2O + 4H_2O$.

By B. Topley, M.A.

(Communicated by F. G. Donnan, F.R.S.- Received October 13, 1931.)

§ 1. *Introduction.*

It has been suggested in previous papers* that a reaction localised in the interfacial zone between two solid phases could be considered from a molecular-kinetic point of view in the following general way.

Since the reactions have temperature coefficients of the normal exponential form, it is a natural supposition that the rate is determined by the attainment of a critical energy in some bond or structure, the breaking of which leads to the re-arrangement of the ions and molecules in its immediate neighbourhood, followed (in a dissociation reaction) by escape of molecules of the gaseous product. In the case of simple dissociations, such as carbonates and salt hydrates, the reaction is naturally endothermic, and it seems very unlikely that any kind of "chain" reaction would spread in the solid, except in the limited sense that the breaking of one bond in, for example, the hydrate $CaCO_3 . 6H_2O$, might obviously lead to the loss of all six water molecules.

The general fact that these reactions take place more readily where the two solids are in contact than at the free surface of the reactant solid is qualitatively attributed to the imposition on the reaction zone of a force field by the second solid, produced practically in molecular contact with the first by the reaction itself. According to the special nature of the reaction the second solid phase might act in one or both of two ways. It might act simply as an "acceptor" for the dis-arranged lattice constituents in the vicinity of the broken bond, thus preventing the broken unit of the lattice from reforming its original configuration. Another, and with dissociation reactions probably more important function, is that the force field exerted in the interfacial zone by the solid product is equivalent to an adsorption potential acting on the molecules of the gaseous product. This acts in the direction of lowering the minimum energy required for whatever unit act *initiates* the re-arrangement of ions and molecules which in its totality constitutes the completed chemical reaction.

It is usually found that the solid product is in a very finely divided state; nevertheless, a process of recrystallisation or aggregation must take place to some extent in the layers left behind by the continuous movement of the interface through the reactant crystal.* This process is sometimes rapid in comparison with the reaction rate, and sometimes much slower.†

---

* Topley and Hume, 'Proc. Roy. Soc.,' A, vol. 120, p. 211 (1928); Spencer and Topley, 'J. Chem. Soc.,' vol. 124, p. 2633 (1929); Spencer and Topley, 'Trans. Faraday Soc.,' vol. 27, p. 94 (1931); Topley and Smith, 'Nature,' vol. 128, p. 290 (1931).

This conception of the mechanism led to the expression‡

$$\text{Rate} = C \, . \, \nu \, . \, e^{-\frac{A}{RT}}, \tag{1}$$

where C is a constant computed from the interface area and the composition and density of the reactant solid, and A is empirically determined in the usual way. The factor ν represents the frequency associated with the vibration responsible for initiating the decomposition, and is introduced on the grounds that the rate at which a given linkage can acquire energy (become activated) is proportional to ν, since this is the frequency with which it can change its energy. The order of magnitude of ν was assumed to be that of atomic frequencies and taken as 5×10^{12}.

Applied to the dissociation of the metastable $CaCO_3 . 6H_2O$ into calcite and liquid water (Topley and Hume, *loc. cit.*), this equation gives a value entirely of the wrong order, about 10^{20} times too small. Kassel, discussing this result in detail in a paper on "Reactions with very high temperature coefficients,"§ concludes that the reaction must be complex, and has analysed the consequences of assuming that there are a series of steps of the type

$$AB_3 \rightleftharpoons B + AB_2 \rightleftharpoons 2B + AB \rightarrow 3B + A,$$

B in this case representing liquid water which is present throughout the reaction. By postulating for each partial reaction a rate and a temperature coefficient which entails no difficulty about the possible rate of activation, the very large total temperature coefficient can be accounted for.‖

---

* The physical condition of the product and the influence of this upon the dynamic equilibrium in a dissociating system were very clearly discussed twenty years ago by J. R. Partington, 'J. Chem. Soc.,' vol. 99, p. 466 (1911).

† Topley and Hume, *loc. cit.*; and Spencer and Topley, *loc. cit.*

‡ Substantially the same expression has recently been derived by Bradley, 'Phil. Mag.,' vol. 12, p. 290 (1931).

§ 'J. Amer. Chem. Soc.,' vol. 51, p. 1136 (1929).

‖ It is not, however, really essential to the argument to assume the transient formation, even to an undetectable extent, of definite intermediate hydrates; the presence of liquid water makes possible an effect similar to that described in connection with the reaction $Ag_2CO_3 \rightarrow Ag_2O + CO_2$ in the presence of CO_2 below the dissociation pressure (Spencer and Topley, 'J. Chem. Soc.,' vol. 124, p. 2633 (1929)). In fact, a marked decrease in the rate when external pressure is applied to the Water + $CaCO_3 . 6H_2O$ system, observed by Hume and the author, makes this seem more probable.

Another metastable hydrate, $KHC_2O_4 . \frac{1}{2}H_2O$ recently studied by Hume and Colvin* exhibits an absolute rate and temperature coefficient of the same order as $CaCO_3 . 6H_2O$. But in this case the decomposition took place under conditions such that the water-vapour was removed immediately. Here the application of Kassel's suggestion, in the form that definite lower hydrates having a transient life intervene, is difficult, and the alternative view involving an adsorption layer in the interface cannot be reconciled with the fact that the rate is not appreciably reduced in the presence of moderate water vapour concentrations.

The reaction $Ag_2CO_3 \rightarrow Ag_2O + CO_2$, when the carbon dioxide is effectively removed so that the maximum rate is realised,† is in reasonably good agreement with equation (1). But since the reaction was measured in the presence of a small amount of water vapour, it is a possibility that part of the interface is occupied by water vapour adsorbed in the reaction zone to an extent which would be a function of temperature and might therefore seriously affect the temperature coefficient: moreover, there is the possibility of the intermediate formation of silver hydroxide.

There seemed to be no satisfactory data available for examining the relationship between reaction velocity and its temperature coefficient for reaction in solids. Accordingly, Mr. M. L. Smith and the author measured the reaction $CuSO_4 . 5H_2O = CuSO_4 . H_2O + 4H_2O$ with special reference to the influence of temperature and of small pressures of water vapour, and the elimination of disturbing effects caused by the increasing thickness of the solid product.‡ During the progress of this work and since its completion, three other experimental researches have been published dealing with the same reaction.§ From these and earlier studies more qualitative and quantitative information is now available about this reaction than any other of the same type. The numerical agreement obtained by different workers measuring the rate of dehydration of pentahydrate crystals of widely different sizes shows the satisfactory reproducibility of the results.

The reaction as it has been measured in practice is physically a composite one, in that the interface moves parallel to the original faces of an anisotropic crystal. But the rate does not differ in different directions by more than 10 per cent. (Garner and Tanner, *loc. cit.*). This difference would only be important in the present discussion through its possible effect upon the temperature coefficient. It has been found, however, that the velocity is very sensitive to temperature (about a threefold increase for 10°), but there is no appreciable change in the slope of the line log (Rate) $v.$ $1/T$ during a 100-fold increase in total rate (Smith and Topley, *loc. cit.*) between 0° and 43°. It follows that since the rates parallel to different faces are nearly the same at an intermediate temperature, the relative contributions to the total rate must remain much the same over the range investigated.

---

* 'Proc. Roy. Soc.,' A, vol. 125, p. 635 (1929).

† Spencer and Topley, *loc. cit.*, 'J. Chem. Soc.'

‡ 'Proc. Roy. Soc.,' A, vol. 134, p. 224 (1931).

§ Garner and Tanner, 'J. Chem. Soc.,' vol. 125, p. 47 (1930); Hume and Colvin, 'Proc. Roy. Soc.,' A, vol. 132, p. 548 (1931); Kohlschütter and Nitschmann, 'Z. phys. Chem.,' Bodenstein Festival vol., p. 494 (1931).

Some points about the general mechanism of this particular reaction are discussed in § 2, and in § 3 a statistical mechanical theory is attempted on the lines of equation (1) above.

§ 2. *General Mechanism of the Reaction* $CuSO_4 . 5H_2O = CuSO_4 . H_2O + 4H_2O$.

The rate of dehydration of crystals of $CuSO_4 . 5H_2O$ in air at atmospheric pressure has been studied by Rae[*] and especially by Crowther and Coutts.[†] The latter worked at 100° for the dehydration as far as monohydrate, the last molecule requiring 220°. Under these conditions the rate passes through a series of maxima and minima, the minima occurring at the compositions of the lower hydrates; this was interpreted in terms of Langmuir's[‡] well-known reasoning from the requirements of the phase rule in a heterogeneous dissociation.

Below 50°, the decomposition in a vacuum proceeds to the stage of the monohydrate, the rate of decomposition of this being negligible in comparison. There is no sign of the formation of the trihydrate. With very small partial pressure of water vapour,[§] the rate is considerably decreased, but otherwise the behaviour is the same. With larger pressures (but still much less than the equilibrium pressure in the penta-hydrate system) the decomposition curve begins to show an inflexion corresponding to formation of trihydrate. At 56°, Garner and Tanner (*loc. cit.*), using comparatively large crystals in a high vacuum, again obtained the trihydrate, which decomposed more slowly than the pentahydrate.

---

[*] 'J. Chem. Soc.,' vol. 109, p. 1229 (1916).

[†] 'Proc. Roy. Soc.,' A, vol. 106, p. 215 (1924).

[‡] 'J. Amer. Chem. Soc.,' vol. 38, p. 2221 (1916).

[§] Hume and Colvin, *loc. cit.*, and Smith and Topley, *loc. cit.*

These, at first sight, rather contradictory observations on the conditions under which the trihydrate appear are explicable when considered in the light of the recent examination by Kohlschütter and Nitschmann (*loc. cit.*) of the Debye X-ray diagrams of the decomposition product before and after heating. These authors found that the monohydrate obtained in the decomposition of the pentahydrate in vacuum at 20° or 40° was completely amorphous, but it changed to a sharply crystalline state on heating to 100° (to a slight extent even at 60°), or if prepared at 100°. Also a sample of pentahydrate partially dehydrated in dry air at 45° gave a weak diagram of the trihydrate together with residual pentahydrate.

The experiments of Hume and Colvin (*loc. cit.*) led them also to the view that the amorphous product first formed tends to aggregate into its characteristic lattice; they assumed that the reaction in the interface between the pentahydrate and the solid product was always the formation of the trihydrate in an amorphous condition. They say, " This will possess two tendencies, namely to aggregate and to decompose. Whether one or the other will predominate depends on the surrounding conditions. Aggregation and slow nucleation account for the persistence in mixtures of hydrates of a hydrate which is metastable under the vapour tension conditions of the environment."

There is, however, no definite evidence that the trihydrate is the first product of the reaction in the interface. Kohlschütter and Nitschmann lay emphasis upon the opposite conclusion drawn from their observation that the amorphous monohydrate is found in vacuum at low temperatures, whilst a *partially* dehydrated pentahydrate crystal gives a sharp trihydrate diagram after heating in a closed tube to 100°. They consider that the trihydrate is produced by a reaction between pentahydrate and monohydrate. But since this latter change cannot be an interface reaction, and must proceed through dehydration of the pentahydrate into the vapour phase followed by rehydration of the monohydrate, this leaves open the question of the first and temporary product.

We cannot at present decide whether the first product consists of trihydrate in a highly dispersed condition or monohydrate in a highly dispersed condition; in either case a subsequent reaction is possible in the reaction zone itself, giving monohydrate or trihydrate respectively.

We shall assume that the constitution of the pentahydrate is $[Cu \,.\, 4H_2O]^{++}$ $[SO_4 \,.\, H_2O]^{=}$ and the monohydrate $[Cu]^{++}$ $[SO_4 \,.\, H_2O]^{=}$. We are not concerned with the splitting off of the last water molecule. The Cu^{++} ion in the pentahydrate is regarded as linked to four water molecules by definite bonds having a characteristic vibration frequency. In these terms we may write the alternative possibilities for the series of steps (omitting the relatively stable hydrated anion) as follows:—

$$\begin{tikzcd}
& {[Cu\,.\,4H_2O]^{++}} \arrow[dl, shift right, "A"'] \arrow[dr, shift left, "D"] & \\
{\{Cu^{++}+4H_2O\}} \arrow[ur, dotted, shift right] \arrow[d, "B"'] \arrow[rr, dotted, shift right] & & {\{Cu\,.\,2H_2O^{++}+2H_2O\}} \arrow[ul, dotted, shift left] \arrow[ll, shift right, "C"'] \arrow[d, "E"] \\
{[Cu]^{++}+4(H_2O)_g} & & {[Cu\,.\,2H_2O]^{++}+2(H_2O)_g}
\end{tikzcd}$$

In this scheme $[\quad]^{++}$ indicates that the ion forms part of a definite compound with $[SO_4\,.\,H_2O]^{--}$, and that it is no longer in the reaction zone, which is probably only a few molecular diameters thick, fig. 1, but has definitely become part of the final product. The curl brackets $\{\quad\}$ indicate the nature of the mixed ions and molecules in the reaction zone, that is, momentarily in an entirely un-coordinated state and about to undergo one of the re-arrangements shown by the arrows. The subscript "g" means that the water molecule has diffused out of the reaction zone. The dotted arrows are the reverse reactions which depend upon the presence of some water molecules in the reaction zone, which may be either molecules which have not had time to diffuse away, or molecules added from the gas phase.

The alternatives for monohydrate formation are A — B, or D — C — B, with C and B rapid in comparison with E. Antecedent to these steps there is, of course, the thermal activation of the original cation which controls the rate.

The trihydrate will be formed under conditions which accelerate the change E *relative to the net rate of* C. In the presence of a small concentration of water vapour the total reaction rate is greatly diminished, mainly through reversal of either A or D, and if a sufficient concentration of water vapour is present the net forward rate of C is so far decreased, assuming mechanism D—E, or the net rate of the reverse of C, assuming A—C—E, is so far increased, that B becomes slower than E. Hume and Colvin (*loc. cit.*) find that with certain water vapour concentrations the final product is a mixture of monohydrate and trihydrate.

Now if we may suppose that the aggregation of amorphous to micro-crystalline trihydrate is accelerated by rise of temperature in the same way as found by Kohlschütter and Nitschmann for the monohydrate, then Garner and Tanner's observation that the *trihydrate* is the main product of the decomposition in vacuum at 56°, instead of the monohydrate as at lower temperatures, becomes comprehensible.

In looking for an explanation of the suddenness with which the trihydrate becomes the product isolated (the change occurs in a range of less than 10°), we must bear in mind that the rate of production of water molecules from the pentahydrate "core" increases rapidly with temperature; so also does the concentration of water molecules in the reaction zone, in contact with all except the outermost layers of the solid product, as a result of the "impedance" effect (Smith and Topley, *loc. cit.*). The increase is only a relative one, the actual concentration remaining always small, even inside the comparatively large crystals used by Garner and Tanner, because the actual rate of production of water vapour is always small (*ca.* 10^{-1} mgm. per cm.^{2} per minute). Now any amorphous trihydrate formed, either by mechanism D or by A followed by the reverse of C, will be greatly stabilised by very small concentrations of water vapour in contact with it, just as the pentahydrate is at slightly lower temperatures. A combination of these circumstances with the increased rate of aggregation at 56° makes possible the formation of micro-crystalline trihydrate. Once formed, this material is presumably more stable than the amorphous substance, and may have its life-period lengthened through the circumstance that each minute crystal requires the formation of a nucleus and its growth. This is in agreement with the fact that Crowther and Coutts' (*loc. cit.*) curves for the decomposition of the trihydrate formed and aggregated at 100° show the characteristic auto-acceleration, the exceptionally slow nucleation in this case being due to the inhibiting effect of water vapour held back by the presence of air at atmospheric pressure. In Garner and Tanner's experiment the nucleation occurred rapidly (in vacuum) as soon as the decomposition of the pentahydrate was over; but the fact that the break in the velocity-composition curve for 56° occurred close to the composition $CuSO_4 . 3H_2O$ shows how effectively the decomposition of the trihydrate was held up as long as the pentahydrate core remained.

§ 3. *Kinetic Theory of the Mechanism.*

Between 0° and 43° the rate of the reaction $CuSO_4 . 5H_2O = CuSO_4 . H_2O + 4H_2O$ is expressed by (Smith and Topley, *loc. cit.*)

$$\log_{10} K = 12 \cdot 112 - \frac{3982}{T},$$

(K = mgm. H_2O lost per square centimetre of the interface per minute).

This refers to the limiting rate when the water molecules diffuse out of the reaction zone so quickly that the reverse reactions indicated in the scheme above play no part. The temperature coefficient is thus a function of the activation process only and it becomes possible to enquire whether a simple mechanism of the type outlined in § 1 can provide an adequate rate of activation.

When a water molecule is lost by direct escape from the surface of the pentahydrate into a vacuum, the simplest view of the process is that the molecule has acquired by chance an energy of vibration outwards in excess of the critical amount required just to elongate the bond between it and the Cu^{++} ion to a point at which the restoring force is reduced to zero through the rapidly increasing deviation from Hooke's law. We assume that the reaction advances through the solid by contributions of a similar kind scattered at random in the plane of the reaction zone; but the critical energy for dissociation is modified by the ionic field of the solid reaction product.

The diagrams assist a more detailed discussion of this hypothesis. Fig. 1

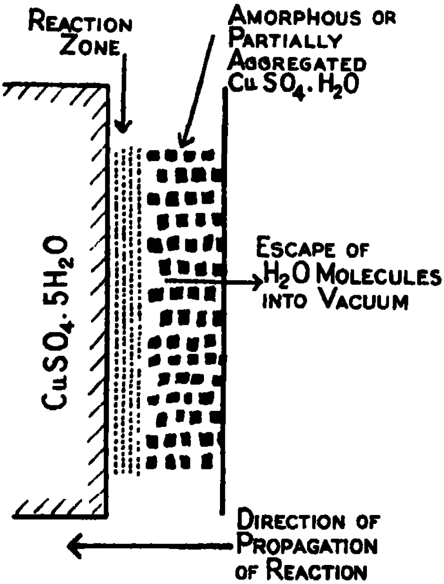
REACTION ZONE
AMORPHOUS OR PARTIALLY AGGREGATED CuSO4.H2O
CuSO4.5H2O
ESCAPE OF H2O MOLECULES INTO VACUUM
DIRECTION OF PROPAGATION OF REACTION

FIG. 1.

illustrates the conception of the reaction zone containing the disordered ions and molecules in process of rapid re-arrangement to the monohydrate. It must be supposed that the $[Cu . 4H_2O]^{++}$ ion after "activation," *i.e.*, loss of *one* H_2O molecule, is an unstable structure and immediately loses either one more or three more, according to whether mechanism D—C—B or A—B is assumed to follow. The consequences are the same for our present purpose, because all the subsequent steps leading finally to the loss of $4H_2O$ per unit out of activation are sufficiently rapid to prevent any important concentration of water molecules being built up in the reaction zone. The monohydrate forms a pseudomorph of the original crystal, and since it has a molecular volume just less than one-half that of the pentahydrate, the layers through which the water vapour escapes must have a porous structure somewhat as shown.

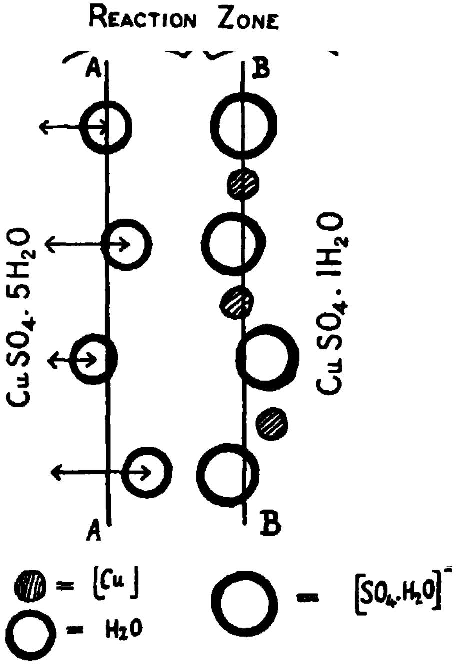

FIG. 2.

Fig. 2 represents a small element of the pentahydrate side of the reaction zone. The equilibrium positions of the centres of the H_2O molecules with which we are concerned are in the plane AA. (We shall assume in the numerical calculation that for each $[Cu . 4H_2O]^{++}$ ion in the interface only two H_2O molecules are in a position to oscillate directly out into the reaction zone, the other two being screened off by the Cu^{++} ion.) These attached molecules are considered as dipoles oriented and further polarised by the Cu^{++} ion, oscillating as a whole with their positive ends towards the nearest $[SO_4H_2O]^-$ in the adjacent layer of the solid product. The plane BB contains the equilibrium positions about which the centres of these anions oscillate. There must, of course, be some electrostatic interaction between the H_2O dipole and other ions surrounding the particular Cu^{++} ion to which it is regarded as attached by a definite linkage. But there will be a total resultant restoring force in the H_2O molecule when oscillating in the interfacial zone, and for practical purposes we shall treat this as a linkage between the H_2O molecule and the Cu^{++} ion only. We shall also neglect any change of position of the Cu^{++} ions with respect to the plane AA, because it does not appear that taking it into account in the calculations which follow would alter the general result.

On this view the absolute rate of reaction (molecules per square centimetre per second) is given by

$$K_a = 4 . n . \nu . \phi(T). \tag{2}$$

where n is the number of H_2O molecules per square centimetre in the plane AA, ν is the frequency of the periodic motion towards BB, and $\phi(T)$ is the temperature-dependent function giving the probability that any particular vibration fulfils the condition for "activation." The precise form of $\phi(T)$ depends upon the working hypothesis made about the action of the solid product in facilitating activation.

Case A.—The overlapping attractions of ions of the plane BB produce an attractive field of force effectively uniform in planes parallel to BB in that part of the reaction zone which contains the vibration of the H_2O molecule from the plane AA. The force curve of such an attraction is illustrated as $b'b$A in fig. 3. Curve Aaa' is the restoring force of the $Cu^{++} \longleftrightarrow H_2O$ bond, qualitatively drawn to represent a vibration approximately harmonic up to the

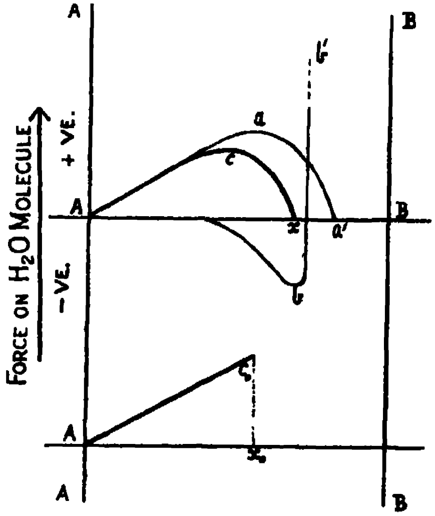

FIG. 3.

point *a*, then changing rapidly to the point of dissociation *a′*. The resultant force obtained by adding the two curves is A*cx*.

Replacing the area A*cx* by the equal area Ac_0x_0 representing a harmonic vibration up to the point x_0 at which the restoring force suddenly vanishes, the condition for activation becomes simply that the molecule shall exceed a critical displacement in the direction AB :

$$x > x_0.$$

The chance that this condition is satisfied in any one vibration is

$$\phi_A = e^{-Fx_0^2/2kT} \tag{3}$$

where k is Boltzmann's constant and F is the force constant for the equivalent harmonic oscillator. This follows at once from the fact that the fulfilment of $x > x_0$ merely requires that the oscillator shall have an energy greater than $\frac{1}{2}Fx_0^2$.

Case B.—Instead of the general attractive field (equivalent to an adsorption potential which is not fluctuating with the thermal agitation of the ions in the plane BB), we shall consider also the alternative possibility that the dissociation process is assisted by a strong attraction localised in a narrow region round the surface of each $[SO_4 . H_2O]^=$ ion of the plane BB.

In the limit this would reduce to an interaction between the $[SO_4 . H_2O]^-$ ion and the polarised water molecule which remains zero until a critical nearness of their centres was reached, when it suddenly becomes large.

Thus the mechanism suggested in case B is that when a molecule of H_2O from the plane AA enters the hypothetical strong local field round an anion from the plane BB, it remains attached to the latter, thereby severing its connection with the Cu^{++} ion and becoming adsorbed on to the monohydrate.

Further consideration of the rate of reaction in this (extreme) case, in which activation occurs exclusively when the positive pole of the H_2O dipole oscillates to within a critical separation from the centre of the anion, requires that the amplitude of thermal vibration of the anions be taken into account. In fig. 4 *d* is the separation of the two equilibrium planes. The displacement of the H_2O molecule is x (taken positive from AA towards BB), and that of the anion is y taken positive in the opposite direction. The positive pole of the H_2O is distant *e* from the centre of mass of the molecule, and *b* is the range of the attractive field of the anion, measured from its centre of mass.

In any vibration the H_2O molecule is activated and therefore contributes to the reaction only if its amplitude x_0 carries it within a distance $d-e-b=c$, fig. 4, of the opposite anion. The anions have varying displacements (y) normal to the reaction zone and on both sides of the plane BB. These displacements correspond at any moment to the distribution of potential energy among the anions considered as simple oscillators; since on the average this distribution is maintained, we may for simplicity treat them as fixed in their places with this distribution of displacements.

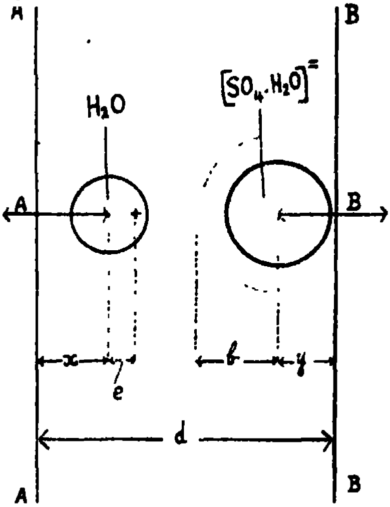

FIG. 4.

The condition for activation is then:

$$x + y \geqslant c.$$

For the probability ϕ_B that any vibration is an activated one we have:

$$\left.\begin{array}{l}\text{Contribution to } \phi_B\\ \text{from anions lying}\\ \text{between } y \text{ and}\\ \quad y + dy\end{array}\right\} \quad \left.\begin{array}{l}\text{Probability that}\\ \text{an anion lies}\\ \text{between } y \text{ and}\\ \quad y + dy\end{array}\right\} \times \left\{\begin{array}{l}\text{Probability that an}\\ H_2O \text{ molecule ex-}\\ \text{ceeds } \tfrac{1}{2}F_x(c - y)^2\\ \text{in total energy}\end{array}\right.$$

$$= \tfrac{1}{2}\sqrt{\left(\frac{2F_y}{\pi kT}\right)}\, e^{-F_y y^2/2kT} \,.\, dy \times e^{-F_x(c-y)^2/2kT},$$

where F_y, F_x are the force constants of the anion and the H_2O molecule, respectively.

Therefore

$$\phi_B = \tfrac{1}{2}\sqrt{\left(\frac{2F_y}{\pi kT}\right)}\, e^{-F_x c^2/2kT} \int_{-\infty}^{+\infty} e^{-\frac{1}{2kT}\left\{y^2 - 2\frac{F_x}{F_x+F_y} . cy + \frac{F_x}{F_x+F_y} c^2\right\}(F_x+F_y)}\, dy$$

$$\phi_B = \sqrt{\left(\frac{F_y}{F_x + F_y}\right)}\, e^{-\frac{F_x F_y}{F_x+F_y} . c^2/2kT}. \tag{4}$$

The slightly different mechanisms (A) and (B) therefore both lead to the same form of relationship between absolute reaction velocity and its temperature coefficient; they differ only by the factor $\sqrt{\frac{F_y}{F + F_y}}$, which must be roughly $1/\sqrt{2}$.

Taking mechanism (B) the rate of reaction becomes:

$$K_{calc} = \frac{4}{\sqrt{2}} n \,.\, \nu \,.\, e^{-\frac{\varepsilon_0}{kT}} \tag{5}$$

and

$$\frac{d\,ln\,K_{exp}}{dT} = \frac{\varepsilon_0}{kT^2} = \frac{d\,ln\,K_{calc}}{dT}$$

where

$$\varepsilon_0 = \frac{F_x F_y}{2(F_x + F_y)}.$$

Comparison with Experiment.—The experimental value of the reaction velocity, in molecules per square centimetre per second, is

$$ln\,K_{exp} = 68 \cdot 55 - 9170/T \Big]_{T = 273° \text{ Abs.}}^{T = 310° \text{ Abs}}$$

The appropriate value of *n*, calculated from the molecular volume of $CuSO_4 . 5H_2O$ on the assumption of a uniform distribution of copper sulphate pentahydrate molecules throughout the crystal, is $6 \cdot 16 \times 10^{14}$.

It is difficult to estimate ν at all closely. Bradley,* assuming that the H_2O molecule is bound to the Cu^{++} ion electrostatically only, calculates for a rigid H_2O dipole an oscillation frequency of $(5 \pm 2) \times 10^{12}$. If, on the other hand, the H_2O molecule is considered to be attached to the central ion by a co-ordinate linkage, a rough estimate of the frequency is possible by comparison with other shared-electron bonds which have been studied by infra-red methods. Bailey and Cassie† and also Dadieu and Kohlrausch‡ find that in a number of compounds the force constants of single linkages group themselves round 7×10^5 dynes cm.$^{-1}$. In the compounds in question the heats of dissociation for the single linkages were of the order of 70,000 calories. Taking into consideration the much lower energy of linkages in the present case, it is clear that the frequency will be somewhat less than the value $2 \cdot 4 \times 10^{13}$ which corresponds for the oscillating water molecule to $F_x = 7 \times 10^5$ dyne cm.$^{-1}$.

---

* 'Phil. Mag.,' vol. 12, p. 290 (1931).

† 'Proc. Roy. Soc.,' A, vol. 132, p. 236 (1931).

‡ 'Mhft. Chem.,' vol. 55, p. 201 (1930).

Thus in either case it seems reasonable to assume the value $\nu = 5 \times 10^{12}$ sec.$^{-1}$. This makes $h\nu/kT$ equal to 0·8, and justifies the assumption of equipartition in equations (3), (4) and (6).

With these values of n and ν and the experimental value of ε_0, equation (5) gives

$$\left.\begin{array}{ll} & K_{calc} = 2\cdot8 \times 10^{14} \\ \text{whereas} & K_{exp} = 1\cdot8 \times 10^{16} \end{array}\right\} \text{molecules per square centimetre per second.}$$

Thus the calculated rate is about 65 times too small in case B and about 45 times too small in case A.

Case C.—The possibility of taking into account more Internal Energy Terms.—The reactant complexes are

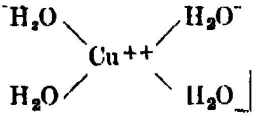

If we consider them as molecules composed of four linear oscillators coupled together through the central ion we have† for the probability of a total energy exceeding η_0

$$\phi c = \frac{1}{3!}\left(\frac{\eta_0}{kT}\right)^3 e^{-\frac{\eta_0}{kT}} \qquad (6)$$

and

$$\frac{d \ln \phi_c}{dT} = \frac{\eta_0 - 3kT}{kT^2} = \frac{\varepsilon_0}{kT^2}.$$

The feature essential to any acceptable mechanism, that the function of the Solid$_1$ — Solid$_2$ interface in promoting the dissociation reaction must be accounted for, is preserved in this case also, because only the H_2O molecules capable of vibrating outwards into the reaction zone are taken to be susceptible of activation to the point of breaking their linkage, the activation energy being lowered for them by the presence of the solid product to the value which accounts for the observed rate.

Using the simpler picture of the non-oscillating attractive field of the solid product, the rate of reaction becomes

$$K_{calc} = \frac{4}{3!} \cdot 6\cdot16 \times 10^{14} \cdot \nu^* \cdot \left(\frac{\eta_0}{kT}\right)^3 e^{-\frac{\eta_0}{kT}} \qquad (7)$$

with

$$\frac{\eta_0}{k} = 9170 + 3T = 10055 \text{ at } 22° \text{ C}^1.$$

---

† Fowler, "Statistical Mechanics" (1931).

In this expression ν^* is the frequency with which all or nearly all the energy of the four coupled oscillators finds its way into any one of them. This must be less than $\nu = 5 \times 10^{12}$, and depends upon the strength of the coupling exerted through the central ion. The value of ν^* required to make $K_{calc.}$ in (7) agree with the experimental value is 8×10^{11}, which is about one-sixth of the value of ν itself.

The mechanism discussed in this section is obviously at best only a very rough picture. The assumption of Hooke's law up to a point at which the force suddenly vanishes cannot be a very adequate conception of the behaviour of a chemical linkage, although it is perhaps nearer the truth in a solid reaction (in virtue of the increasing attraction exerted by the solid product as the water molecule approaches) than when a bond breaks inside an activated molecule in a gas.

It should be remarked that any error in the experimental value (Smith and Topley, *loc. cit.*) of ε_0 which forms the basis of the numerical calculation is likely to have given too large rather than too small a value, although it is not thought that ε_0 is seriously in error.

The conclusions which we draw from these calculations is that the mechanism discussed is a possible one for this reaction, although it requires a very high rate of internal re-arrangement of energy inside the complexes—a rate which would seem to approach the highest value which is at all feasible.

Summary.

Suggestions about the function of the solid product in promoting the type of reaction which involves the dissociation of one pure solid phase into another pure solid phase and a gas are reviewed.

The possible intermediate steps in the dehydration of $CuSO_4 . 5H_2O$ to the monohydrate, and the factors governing the appearance of the trihydrate instead of the monohydrate as the product of the reaction in vacuum, are discussed.

A more detailed statistical-mechanical interpretation of the relationship connecting absolute reaction velocity and its temperature coefficient is attempted, by means of a model which takes account of the actual conditions in the reaction zone. It appears that it is just possible to account for the observed rate, if four degrees of freedom in the complex cations are taken into account, and regarded as strongly coupled through the central Cu^{++} ion; in addition, a very rapid redistribution of energy inside the activated complexes is required.

The author is indebted to Professor R. H. Fowler, F.R.S., for his friendly criticism and advice in connection with § 3 of this paper.

ERRATA.

In a preceding paper on "The Reaction $CuSO_4 . 5H_2O = CuSO_4 . H_2O + 4H_2O$" ('Proc. Roy. Soc.,' A, vol. 134, p. 244):—

p. 224. "$S_1 . nH_2O$" *should read* "$S_1 . n_1H_2O$."

p. 237. Table II, column 2. "0·122" *should read* "0·722."

p. 238. Fig. 2. On the axis of ordinates, "0·5" *should read* "$\bar{1}{\cdot}5$," and "$\bar{1}{\cdot}5$" *should read* "$\bar{2}{\cdot}5$."

p. 241. Table V, last column, "correction" *should read* "corrected."

p. 245. "0·250" *should read* "0·025."

The Artificial Production of Nuclear γ-Radiation.

By H. C. Webster, M.Sc. (Melbourne), Clare College, Cambridge.

(Communicated by J. Chadwick, F.R.S.—Received January 19, 1932.)

§ 1. *Introduction.*

The study of the γ-radiations emitted by atomic nuclei has greatly increased in interest and importance in recent years owing to the theories connecting these radiations with the intimate structure of the nuclei. Many attempts have been made to excite atomic nuclei to radiation by external stimulation, mainly by bombardment with the α-, β-, or γ-rays emitted by radioactive bodies. The first evidence of the artificial stimulation of nuclear γ-radiation was obtained by Slater in 1921,* who found that a small amount of penetrating γ-radiation was produced when the elements tin and lead were bombarded by the α-particles emitted from radon. The experiments were very difficult on account of the rapid growth of radium B and C, but the consistency of the results, control experiments with paper substituted for lead, and the absorption coefficients of the radiations, all indicated that the results were trustworthy. Slater estimated that the fraction of the radon α-particles passing through the ead which produced γ-radiation was of the order 1 in 6000; in the case of tin this fraction was about 1 in 12000. Subsequent experiments by other investigators, including the present writer, using polonium α-particles instead of radon α-particles, showed definitely the absence of effects of this order of magnitude. Since polonium α-particles have only slightly less energy than radon α-particles, the observations are very difficult to reconcile. Later in this paper a possible explanation of this discrepancy will be suggested.

---

* 'Phil. Mag.,' vol. 43, p. 904 (1921).

Two years ago the writer obtained evidence, which will be mentioned later, of the production of penetrating γ-radiations when aluminium was bombarded by polonium α-particles, and Bothe and Becker* have definitely established the production of nuclear γ-radiation in several of the lighter elements by α-particle bombardment. The effects are, however, in every case of a much smaller intensity than those found by Slater. The amount of radiation observed is indeed so small that very strong sources of polonium are essential, and on this account the writer has only recently been able to make a detailed study of the radiations.

The results confirm in many respects and amplify those obtained by Bothe and Becker. In particular they show that the radiations from different elements vary very greatly in penetrating power; some have energies of a few hundred thousand volts, while others have energies of several million electron volts. The latter are thus of greater energy than any γ-rays so far known to be emitted from the radioactive elements. It will appear in the course of the discussion that, while in some cases the radiations can be connected with the process of the artificial disintegration of the nucleus accompanied by the release of a proton, in the more striking cases it must be assumed that a hitherto unsuspected process is taking place, the formation of a new nucleus by the capture of the α-particle with the release of energy only in the form of radiation.

§ 2. *Methods of Measurement.*

Two methods have been used in the experiments to be described—Geiger-Müller tube-counters and high-pressure ionisation chambers. It is appropriate to examine at this stage the relative advantages of the two methods.

In the present experiments, since secondary γ-radiations of very small intensity were investigated, it was obviously desirable to choose the method which gave the greater ratio between the effect due to the secondary radiation and that due to cosmic radiation and primary γ-radiation from the source.

---

* 'Z. Physik,' vol. 66, p. 289 (1930).

There are two factors to be considered—the variation of the sensitivity of the apparatus with quantum energy, and the relation between the theoretically desirable and the practically convenient size and shape of the apparatus. In the earlier experiments the "background" consisted chiefly of cosmic radiation. In this case consideration of the first factor indicated the ionisation chamber as preferable. As regards the second factor, however, simple considerations show that a very small measuring apparatus, placed close to the source, was desirable and this was much more nearly attainable, without technical inconvenience, with the counter than with the high-pressure ionisation chamber. This more than compensates for the advantage due to the first factor.

In the later measurements, on the other hand, it was found that with the larger quantities of polonium available the primary γ-radiation constituted the major part of the background with counters and an appreciable part with the high-pressure ionisation chamber used. *Under these conditions there is* little to choose theoretically between the two methods and the ionisation chamber was therefore used, on account of its greater technical convenience and reliability.

§ 3. *Experiments with Counters.*

The results of the earlier experiments with counters are not of much importance, on account of the small amount of polonium available. Suffice it to say that by means of a counter of the annular type, with the source of α-particles and the materials to be bombarded placed inside the inner cylinder, evidence was obtained of a secondary γ-radiation from aluminium. The numerical estimate was 9·0 quanta per million bombarding α-particles, with a statistical mean error of 2·4 per million, and a factor of uncertainty in the absolute value of at least 10. Less conclusive evidence was obtained of secondary γ-radiations from boric acid, paracyanogen, and copper. Tin and lead were assumed to give no secondary γ-radiation, since the minimum total effect was observed when these elements were bombarded.

The hollow counter method, while the most sensitive, is inconvenient for the measurement of the absorption coefficients of the radiation. Hence in the later experiments, when larger quantities of polonium were available, two or three small counters were used, of internal diameter about 1 cm., and length 2 cm. The absorbers used were cut from lead sheet several centuries old, and thus of small radioactivity. The counting apparatus was operated by a thyratron,* and the voltage applied to the case of the counter was produced by a high-tension set operated from A.C. mains, with a special stabilising device, described in another paper.*

---

* De Bruyne and Webster, 'Proc. Camb. Phil. Soc.,' vol. 27, p. 113 (1931).

The polonium and the materials to be bombarded were contained in the apparatus shown in fig. 1. The base of the apparatus was of brass, and the top of pyrex glass. The polonium was deposited on a silver button, which was screwed into a brass plug, which fitted into the conical hole A. The materials to be bombarded were attached to the wheel B, which could be rotated by means of the ground joint C. The apparatus was evacuated during observations, so that the bombarding α-particles possessed their full range.

The polonium was deposited from a solution of radium (D + E + F) in half normal hydrochloric acid. No trace of β-ray activity could be observed with a β-ray electroscope, so that the amount of radium (D + E) impurity must have been very small.

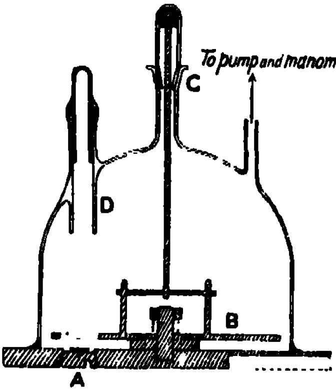

FIG. 1.

A hole, diameter 1·5 cm., was drilled in the wheel in such a position that it could be brought vertically above the polonium. It was assumed that with this arrangement the observed γ-radiation consisted, apart from the natural effect, entirely of primary γ-radiation from the source. It is to be noted that, with this arrangement, the neighbouring portions of the brass wheel, and the glass top of the apparatus, were all bombarded by α-particles. It is, however, justifiable to assume that these have no appreciable secondary γ-radiation, since in no case was a total γ-ray intensity observed less than that observed when the hole on the wheel was vertically above the source.

With this apparatus the secondary γ-radiations from beryllium, boron and fluorine were detected, and the absorption in lead roughly examined. Corrections had to be applied on account of the finite time of operation of the counting mechanism† and a slow change in the sensitivity of the counters. The results are summarised in Table I.

The numbers of quanta were estimated by comparison with a radium standard placed at a measured distance from the counters, and may be in error by a factor of 10.

---

* Webster, 'Proc. Camb. Phil. Soc.,' vol. 28, p. 121 (1932).

† *Cf.* Bothe and Becker, *loc. cit.*

Table I.

Element giving γ-radiation.	Absorption coefficient in lead in cm.$^{-1}$.	Number of quanta per million α-particles (for pure element).
Be	$0\cdot36 \pm 0\cdot1$	~ 100
B	$<0\cdot5$	~ 6
F (CaF_2)	~ 1	~ 9

§ 4. *Experiments with High-pressure Ionisation Chambers.*

Two chambers were used in these experiments. The first was kindly lent by Dr. Gray and has already been described by him.* The second was similar, except that a cavity was cut in one end, as shown in fig. 2, to facilitate observations on the softer radiations. The minimum thickness of this end was 5 mm.

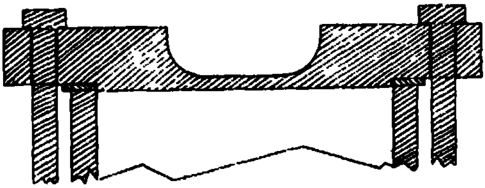

FIG. 2.

The chamber was pumped to over 95 atmospheres pressure. The pressures during the experiments were between 80 and 95 atmospheres. The rate of leakage, as determined by the rate of change in the ionisation current produced by a radium standard placed in a standard position, was about 0·1 per cent. per diem. The subsidiary apparatus for the chamber was similar to that of Gray. The chamber was mounted so that the lead-in to the insulated electrode was at the bottom.

The apparatus containing the polonium and materials to be bombarded, as described in the preceding section, was supported at various distances above the chamber, the polonium being roughly on the axis of the chamber. Room was allowed for the insertion of a limited amount of absorbing material between the bombardment apparatus and the ionisation chamber.

In the later experiments a different polonium source was used. The polonium was here deposited on platinum foil which was sealed across the end of a glass tube. The deposition was carried out electrolytically from a solution in tenth normal nitric acid of radium (D + E + F). Examination for β-rays indicated traces of radium E, probably in equilibrium with radium D impurities. The source was supported in two ways; in the first it was attached to a glass tube, which was passed through the tube D (fig. 1), and waxed in position. With this arrangement the γ-ray quanta were investigated which were emitted in the forward direction, *i.e.*, in roughly the same direction as the α-particles producing them. In the second arrangement the source was attached to a brass cap, the flange of which fitted over the hole A, so that portion of the cap projected up into the hole. With this arrangement the radiation emitted in the backward direction was investigated.

---

* L. H. Gray and G. T. P. Tarrant (*in course of publication*).

All measurements were made in the way described by Gray, except that the case of the chamber was always positively charged. As the measurements of the intensities of the γ-radiations involved the measurement of the difference between two ionisation currents, not of the absolute values, reversal of the field was unnecessary. In order to minimise errors due to fluctuations in the intensity of cosmic radiation, insulation leakage, etc., measurements were made in the following order. Denote by (*a*) the arrangement under which either the hole in the wheel, or a substance considered to give no secondary γ-radiation, was adjacent to the polonium, and by (*b*), (*c*), (*d*), . ., the arrangement under which the materials (*b*), (*c*), (*d*) respectively were adjacent to the polonium. Then observations were made in the order (*a*), (*b*), (*c*), (*d*), (*a*), . ., or, if only one "active" material was under examination, in the order (*a*), (*b*), (*b*), (*a*), ... The mean error of a series of observations was determined from the mean errors in the times for the collection of a given charge, computed in the usual way, viz.,

$$\varepsilon = \sqrt{\frac{\Sigma (\mathrm{T} - \bar{\mathrm{T}})^2}{n(n-1)}},$$

where T is the observed time, $\bar{\mathrm{T}}$ the mean time, and n the number of observations. In some of the experiments the amount of γ-radiation was very small and the measurements were correspondingly difficult. In such cases the statistical error of an observation was sometimes rather large, as may be seen from an inspection of the experimental curves (*cf.* figs. 3 and 6). In addition to the observations on the secondary γ-radiations, the primary radiation of polonium was investigated. For this purpose the first polonium source, which was free from radium (D + E) impurities, was used. Determinations were made of the difference in ionisation current produced by complete removal of the apparatus containing the polonium.

Secondary γ-radiations were observed with several substances. The absorption of these radiations in lead was investigated, lead absorbers cut from sheet metal about 2 mm. thick being used. In certain cases it was found impossible to obtain a reliable estimate of the frequency of the radiation from the absorption coefficient in lead alone. In these cases the absorption in iron was therefore

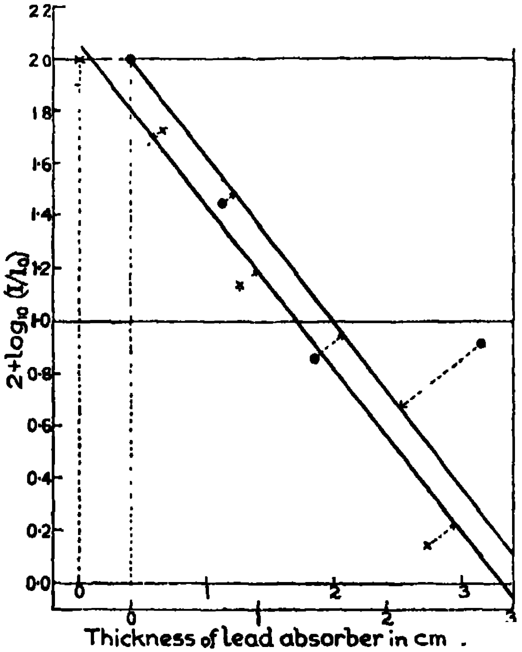

Fig. 3.—Absorption of lithium γ-radiation. ⊗ "Forward" radiation. × "Backward" radiation.

also investigated, and, in two cases, the absorption in aluminium also. These last determinations were, however, not of great value, since the lightness of the aluminium and the small amount of space available for absorbers made the measurement of the absorption coefficient considerably less accurate than with iron. The aluminium and iron absorbers were in the form of discs, of various thicknesses. The thickness of all absorbers was determined by weighing. Some of the absorption curves obtained are illustrated in figs. 3 to 7, and the measurements of absorption coefficients are collected in columns 5 to 7 of Table II. The limits of error given there are calculated from the mean errors in the observations, determined as described above. In some cases there was definite evidence of non-homogeneity of the radiation. In the separation into components, however, a very wide choice was possible on account of the inferior accuracy of the measurements (see, *e.g.*, fig. 6). The latitude of choice chiefly affects the softer components, so that only very rough

Table II.

Substance bombarded.	Element responsible for the γ-radiation emitted.	Range of α-particles in centimetres of normal air.	Whether radiation observed in backward or forward direction.	Absorption coefficients in units of cm.^{-1}.			Quantum energy in millions of electron-volts.	Number of quanta per million α-particles (for the pure element).
				Lead.	Iron.	Aluminium.		
Paraffin wax	H	3·9	*f*	0·5 (assumed)	—	—	2·0 (assumed)	0·1 ±1·2
Li + LiOH	Li	3·9	*b*	1·4 ±0·2	—	—	0·6 ±0·1	30 ±6
Li + LiOH	Li	3·9	*f*	1·4 ±0·2	—	—	0·6 ±0·1	30 ±3
Be	Be	3·9	*b*	{0·28 ±0·02	0·157 ±0·012	0·071 ±0·023	5·7 ±1	30 ±0·2
				~1·7	—	—	~0·5	~30
Be	Be	3·6	*b*	0·30 ±0·02	—	—	4·9 ±1	24 ±0·3
Be	Be	2·7	*b*	0·29 ±0·06	—	—	5·2 ±2	7 ±0·4
Be	Be	2·1	*b*	0·34 ±0·15	—	—	~4	3 ±0·5
Be	Be	3·9	*f*	{0·22 ±0·015	0·137 ±0·006	0·046 ±0·004	6·6 ±0·5	31 ±0·4
				~2·2	—	—	~0·4	~30
B	B	3·9	*b*	0·30 ±0·06	—	—	4·8 ±2	2 ±0·2
B	B	3·9	*f*	{0·19 ±0·06	0·12 ±0·05	—	7·8 ±2	2 ±0·2
				~1	—	—	0·7	4 ±1
C_2N_2	C	3·9	*f*	1 (assumed)	—	—	0·7 (assumed)	−0·7 ±2·2
	N	3·9	*f*	1 ”	—	—	0·7 ”	−0·8 ±2·5
CaF_2	F	3·9	*b*	0·7 ±0·2	—	—	1·1 (<2, >0·8)	8 ±2
			f	0·55 ±0·10	—	—	2·0 ±0·5	7 ±1
NaOH	Na	3·9	*f*	1·6 ±0·3	—	—	0·5 ±0·2	14 ±2
Mg	Mg	3·9	*b*	0·3 (assumed)	—	—	5 (assumed)	0·3 ±0·4
Mg	Mg	3·9	*f*	0·3 ±0·2	—	—	~5	0·5 ±0·2
Al	Al	3·9	*b*	0·4 (assumed)	—	—	3·0 (assumed)	0·5 ±0·5
Al	Al	3·9	*f*	0·40 ±0·06	—	—	3 ±1	1·4 ±0·2
—	Po	—	—	{0·8 ±0·1	—	—	1·0 ±0·1	11·8 ±0·7
				2·5 ±0·5	—	—	0·4 ±0·1	~13

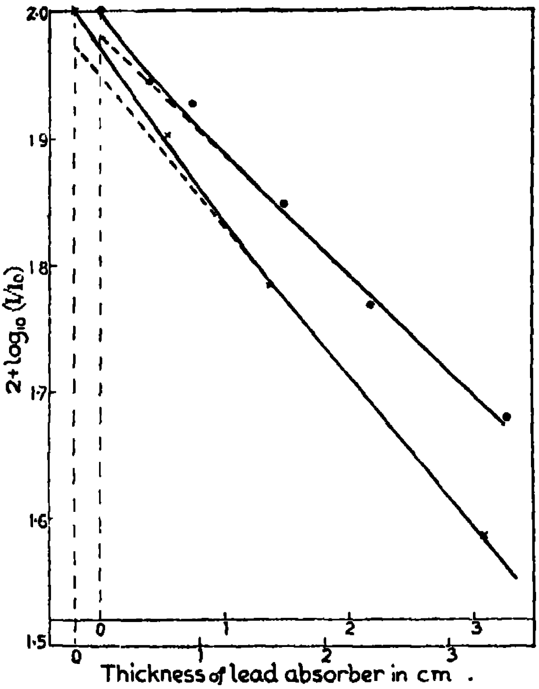

FIG. 4.—Beryllium γ-radiation (3·9 cm. α-particles). × "Backward" radiation. ⊗ "Forward" radiation.

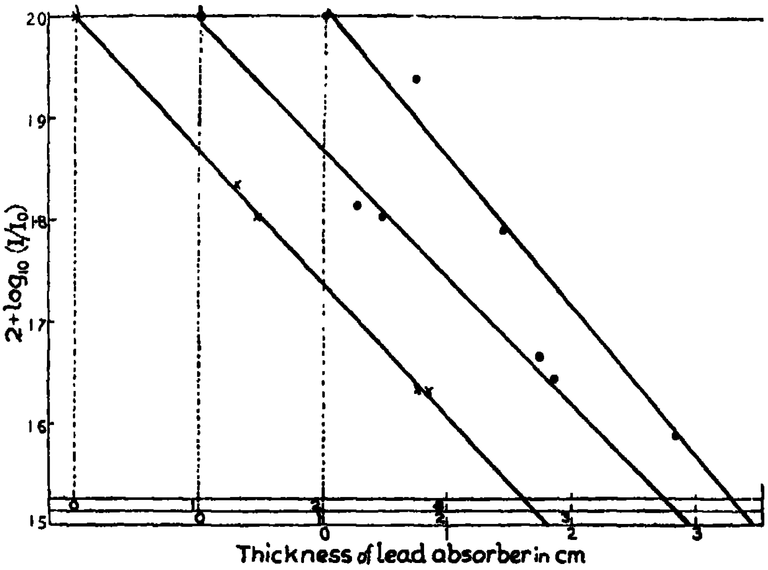

FIG. 5.—Radiation from beryllium (backward). × 3·6 cm. α-particles. ⊗ 2·7 cm. α-particles. ⊙ 2·1 cm. α-particles.

estimates of the absorption coefficients of these could be obtained. In addition to the results given in the table, it should be mentioned that searches for secondary γ-radiations from nickel, copper, brass, tin and platinum gave negative results.

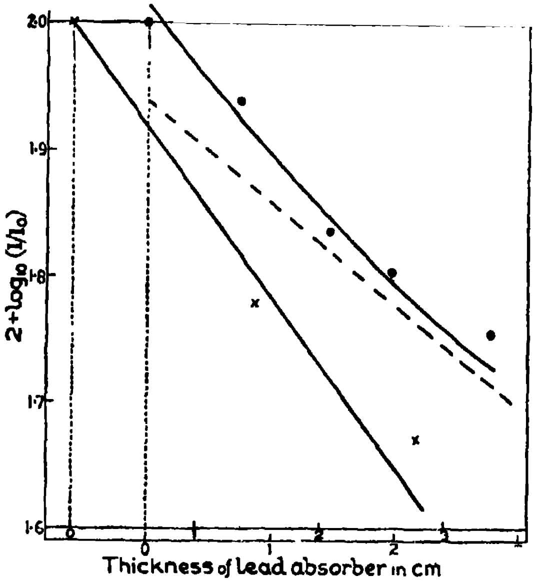

Fig. 6.—Boron γ-radiation. × "Backward" radiation. ⊗ "Forward" radiation.

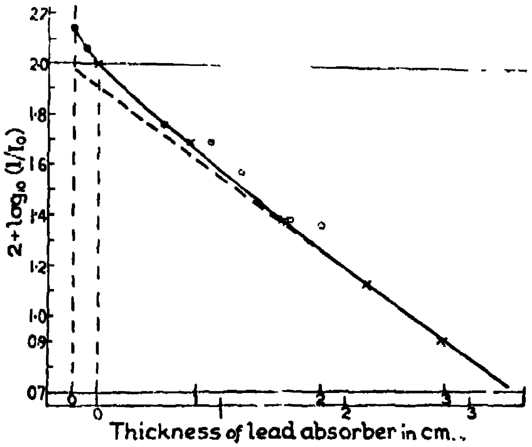

Fig. 7.—Polonium γ-radiation. × Present experiments. ⊙ Bothe and Becker's points.

[N.B.—As a rough allowance for different experimental conditions, 0·2 cm. absorber in Bothe and Becker's arrangement is assumed to correspond with no absorber in the writer's.]

§ 5. *The Quantum-energies of the Radiations.*

Due to the proximity of the source of γ-radiation to the ionisation chamber (necessary on account of the weak intensity of the radiations), the measured absorption coefficients are subject to certain corrections. In the first place, some of the γ-radiation entering the chamber passed obliquely through the absorbers, and hence the measured absorption coefficient tended to be higher than the true value. Secondly, the normal definition of absorption coefficient requires that any radiation scattered by the absorbers, even through a small angle, should not be permitted to enter the measuring chamber. In the present experiments a large fraction of the scattered radiation entered the chamber, so that, on this account, the measured absorption coefficient tended to be lower than the true value.

The magnitudes of these corrections were determined theoretically. For simplicity the problem was somewhat idealised. The radiation was assumed to be emitted from a point source situated on the axis of the chamber, and the ionisation produced along a given ray was assumed proportional to the length of path in the gas and to the scattering absorption coefficient in the gas. The calculations for obliquity were carried out by the standard method,* scattered radiation being neglected.

The calculation of the "scattering" correction was more difficult. The corrections could, indeed, be calculated for primary radiation proceeding along the axis of the chamber. For primary radiation entering the chamber obliquely, however, an exact calculation was impracticable. General considerations suggest that the corrections will be rather smaller than with the axial radiation under similar conditions. A further complication arises from the fact that as the absorber thickness increased the scattering correction became smaller due to the "degraded" radiation approaching equilibrium with the primary. It was finally decided to calculate the corrections for axial radiation and an "average" value of the absorber thickness. The calculated corrections are thus probably of the right order of magnitude, but rather too high.

The calculations were carried out for iron absorbers for a series of quantum energies. The amount of radiation scattered in a thin section of the absorber separated from the interior of the chamber by 5 cm. of iron was calculated from the Klein-Nishina formula and thence the ratio between the ionisation produced in the chamber by this scattered radiation and that produced by the undeviated beam, twice scattered radiation being neglected.

---

* *Cf.* Kohlrausch, "Radioaktivität," p. 69, Akad. Verges, Leipzig (1928).

In Table III are given the differences between the effective total scattering coefficients (σ') per extra-nuclear electron, calculated in this way, and the true scattering coefficients (σ). By graphical interpolation it was now possible to determine the quantum energy of any radiation once the value of σ' was known.

Table III.

Quantum energy in millions of electron-volts.	2·04.	4·09.	6·13.	8·18.	10·22.
$(\sigma - \sigma') \times 10^{27}$	24·7	18 5	14·7	13·4	11·8

In the case of the softer secondary γ-radiations, the quantum energies were actually deduced directly from a curve connecting the absorption coefficients in lead with the quantum energies calculated by Gray* from consideration of all existing data concerning the absorption of γ-radiation in that element. In these cases the accuracy of the measurement was always low (on account of the weak intensity of the radiations), and since, in addition, the scattering correction was small compared with the total absorption coefficient, it could justifiably be neglected. The obliquity correction was calculated as before.

For the harder γ-radiations, the determination of the frequencies was complicated by the nuclear absorption effect reported by Tarrant,† Chao,‡ and others, the variation of which with frequency is not known. The absorption coefficient may thus be divided into three parts, the effective scattering coefficient σ', the photoelectric coefficient, and the nuclear absorption coefficient. The photoelectric coefficient could be deduced with sufficient accuracy for the present purpose by extrapolation from regions in which it is known The values of the nuclear coefficients are known for the 2·6 million electron-volt radiation of thorium C″. To obtain the values for other quantum energies, it was assumed that the ratio of the nuclear coefficients for iron and lead is independent of the quantum energy. There is no real justification for this assumption, but some assumption was necessary, and this appeared to be the most satisfactory. With this assumption the measurements of the absorption coefficients in lead and iron sufficed to determine the quantum energies, for the difference in the absorption coefficients per electron, corrected for the photoelectric coefficients, gave directly the difference in nuclear absorption per extra-nuclear electron. The quantum energies thus deduced are given in column 8 of Table II. The values of the nuclear absorption coefficients, per extra-nuclear electron, obtained in this way are given in Table IV. The values for the 2·6 million electron-volt radiation are those obtained by Tarrant.*

---

* 'Proc. Camb. Phil. Soc.,' vol. 27, p. 103 (1931).

† 'Proc. Roy. Soc.,' A, vol. 128, p. 345 (1930).

‡ 'Proc. Nat. Acad. Sci.,' vol. 16, p. 431 (1930).

Table IV.

Quantum energy in millions of electron-volts.	Nuclear absorption coefficients per extra-nuclear electron × 10^{37}.		
	Aluminium.	Iron.	Lead.
2·6	5·3	9·2	34·5
5·7	—	10 ± 4	37 ± 13
6·6	2 ± 5	7 ± 2	25 ± 8
7·8	—	~6	~22

In some cases the absorption coefficients in lead only were measured; the values of the nuclear absorption coefficients for these radiations were obtained by interpolation.

The fact that reasonable and consistent values were obtained for the nuclear absorption coefficients is evidence against the suggestion that the ionisation observed was produced not by electromagnetic radiations but by high-speed corpuscles consisting, *e.g.*, of a proton and an electron in very close combination. If this suggestion were correct it should be possible to detect the corpuscles by means of the expansion chamber. Mr. Champion has kindly taken 50 expansion-chamber photographs, with the chamber adjusted for β-ray tracks, beryllium bombarded by polonium α-particles being placed near the chamber. Only one track was observable, and the position of this showed that it could not possibly have been due to a corpuscle originating in the beryllium. Calculations showed that if the corpuscles produced 10 ions per centimetre of track, about 10 tracks altogether would have been expected in the photographs taken. Thus it is justifiable, for the present at any rate, to assume the secondary radiations to be electromagnetic in nature. This point is interesting in view of the suggestion that cosmic radiation may consist of protons,[*] or neutrons, and the usefulness of the conception of neutrons[†] in accounting for astrophysical and nuclear phenomena.

---

* 'Proc. Roy. Soc.,' A, vol. 135, p. 223 (1932).

§ 6. *The Absolute Efficiencies of the Processes of Production of the γ-Radiations.*

For the determination of these quantities it was necessary to determine firstly, the absolute rate of emission of γ-ray quanta from the bombarded materials, and, secondly, the rates of incidence of the α-particles. The first measurement was made in the following way: A source of thorium active deposit was standardised in terms of radium by means of a standard γ-ray electroscope. It was then allowed to decay for some time, so that a source of known, and convenient, strength was obtained. This was placed near the ionisation chamber, in the position normally occupied by the bombarded materials. The positions of the bombarded materials were actually slightly different in different experiments, but allowance could easily be made for this. The radiation from the thorium was filtered by lead absorbers so that the only component of the thorium (B + C) γ-radiation reaching the chamber in appreciable amount was the $2 \cdot 6 \times 10^6$ electron-volt radiation. Now it follows from Shenstone and Schlundt's[‡] estimates of the number of 8·6 cm. α-particles emitted per second from " 1 mgm. equivalent " of thorium C that about $1 \cdot 4 \times 10^7$ quanta of energy $2 \cdot 6 \times 10^6$ electron-volts were emitted per second per " milligram equivalent " with the source used in the present experiments. (The assumption is involved that one such quantum is emitted per atom of thorium C″ disintegrating.) Hence, making due allowance for the difference in quantum energies, the number of quanta in the secondary γ-radiations could be estimated from the ionisation currents produced. In making this allowance it was assumed that the ionisation was proportional to the quantum energy and the calculations were carried out along the lines outlined in connection with the obliquity correction, no account being taken of " degraded " radiation. It is interesting to note that from the thorium (B + C) results can be deduced a rough value for the mean loss of energy by secondary electrons per pair of ions. With the first chamber (100 atmospheres pressure) the value was about 150 electron-volts per ion pair and with the second chamber (90 atmospheres) about 115 electron-volts. These abnormally high values are in qualitative agreement with the results of Broxon[§] and others.[||]

---

[*] H. Geiger, 'Proc. Roy. Soc.,' A, vol. 132, p. 334 (1931).

[†] *Cf.* Langer and Rosen, 'Phys. Rev.,' vol. 37, p. 1579 (1931).

[‡] 'Phil. Mag.,' vol. 43, p. 1038 (1922).

[§] 'Phys. Rev.,' vol. 37, p. 1320 (1931).

[||] *Cf.* H. A. Erikson, 'Phys. Rev.,' vol. 27, p. 473 (1908).

In determining the numbers of quanta of the secondary radiations it was, of course, necessary to know the absorption coefficients in iron and in the compressed gas. In many cases the absorption coefficient in lead only was known experimentally, the others were deduced from this, assuming the photo-electric absorption coefficient per electron proportional to the cube of the atomic number, and the nuclear absorption coefficients in the same ratios as those holding for the $2 \cdot 6 \times 10^6$ electron-volt radiation of thorium C″.

With regard to the rate of incidence of α-particles, I am indebted to Dr. Chadwick for measurements of the strength of the polonium source, obtained by direct counts of the numbers of α-particles emitted in a known small angle. The fractions of the α-particles emitted by the polonium which fell on the materials bombarded, in the present experiments, were calculated from the geometry, and the values are therefore rather rough in view of the small distances between the polonium and the bombarded materials. In some cases it was impossible to use the free elements for bombardment, and chemical compounds had therefore to be employed. Allowance was made for this in calculating the efficiency of the production of γ-radiation, using the known stopping powers of the atoms concerned. In the case of lithium the metal was used, but this was covered with a layer of hydroxide of variable and uncertain thickness. The appropriate factor therefore lay between 1 and 3. A very rough estimate was made of the effective value.

The final values for the efficiency of γ-ray production are given in column 9 of Table II. The limits of error given represent merely the statistical errors of the observations. The factor of uncertainty in the absolute values is difficult to assess, but it may be as large as 2. In the case of lithium it is, of course, larger.

§ 7. *The Efficiencies of Production of the Secondary γ-Radiations as a Function of the Energy of the α-Particles.*

The effect of varying the range of the α-particles on the intensity of secondary γ-radiation was investigated for beryllium, boron, and lithium. For this purpose the material to be bombarded was fixed vertically above the polonium by mounting on a brass rod which passed through the tube D (fig. 1). Between the polonium and the secondary radiator moved a brass wheel in which were drilled four holes, diameter 1·5 cm., which could be brought in turn between the polonium and the secondary radiation. Three of the holes were covered with absorbing screens of known stopping power for α-particles. The residual range of the α-particles could be further adjusted by introducing air or CO_2 into the apparatus. The intensity of secondary γ-radiation was measured by the difference in ionisation current produced by moving the wheel into a position such that no α-particles reached the secondary radiator. It was assumed that the brass gave no secondary γ-radiation, which was justified by control experiments.

The results are illustrated in fig. 8. It will be noted that the intensity appears to be zero in all cases for α-particles of residual range less than about 1 cm., corresponding to about 1½ million electron-volts energy.

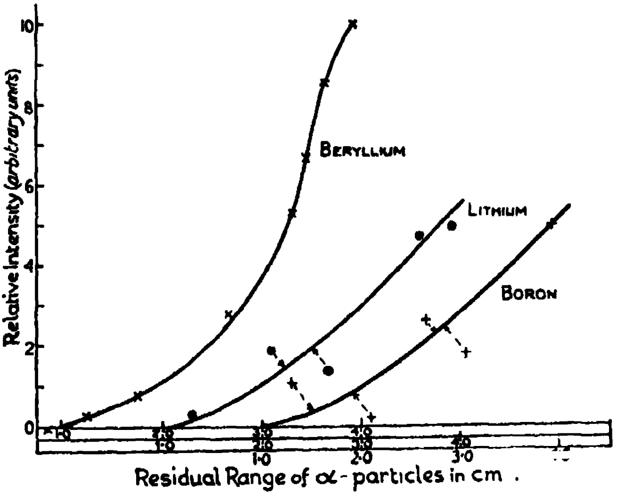

Fig. 8.—Efficiency of production as a function of the residual range of α-particles.

The γ-radiation investigated in these experiments, with comparatively thick layers of bombarded material, was produced by collisions in which the α-particles had *any* energy between about 1½ million electron-volts, and the energy corresponding to the maximum residual range. By differentiating the curves of fig. 8, the intensity of γ-radiation produced per centimetre of path was obtained, roughly, as a function of the residual range. Owing, however, to the small distance between the polonium and the secondary radiator, the length of path of the α-particles before entering the secondary radiator, and hence, in general, their residual range, varied considerably for different parts of the source and secondary radiator. On this account the differential coefficient represents rather an effective average value of the intensity for α-particle ranges varying between certain limits. It was, however, possible to obtain roughly the relative probability of production of γ-radiation by a collision as a function of the energy of the α-particle at collision. The results obtained are illustrated in fig. 9.

On account of the inferior accuracy in the other cases, the curves for beryllium alone are significant. The decrease in the efficiency of production with increasing energy above 4·7 million electron-volts, shown by fig. 9, is interesting, if a genuine effect. An attempt was made to verify it by direct experiment. For this purpose thin films of beryllium were prepared by distilling the meta *in vacuo*, on to a copper sheet. A special vacuum furnace was constructed, the beryllium being placed in the trough formed by a strip of molybdenum, bent to have a V-shaped section. The molybdenum was heated with a current of the order of 200 amps, the electrodes being water-cooled. The films obtained were estimated from the intensity of the secondary γ-radiation to have stopping powers of the order of 0·2 mm. of normal air.

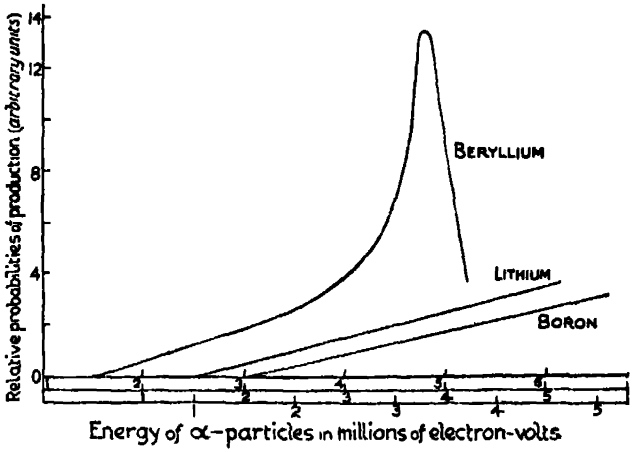

Fig. 9.—Relative probabilities of production of γ-radiation per collision as functions of energy of α-particle on collision.

The results obtained are illustrated in fig. 10, in which the lower curve corresponds to observations of the radiation in the backward direction, while the upper curve corresponds to some observations in the forward direction. In the latter case the beryllium film, with its copper backing, was mounted on the ordinary wheel, and the residual range varied by means of the pressure of gas in the apparatus. In neither case can any evidence of decrease in intensity with increasing residual range be observed. This was perhaps due to the beryllium being too close to the polonium. It would possibly have been more satisfactory to use a thicker film of beryllium at a greater distance from the polonium.

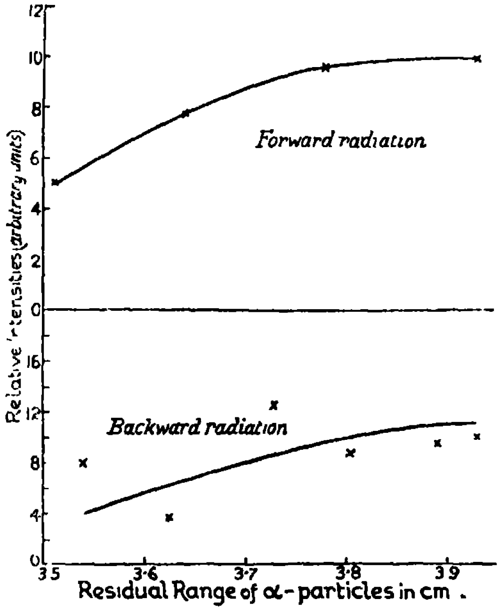

FIG. 10.—Radiation from thin films of beryllium.

§ 8. *Theoretical Interpretation of the Radiations.*

All of the secondary γ-radiations observed can probably be accounted for in terms of one or other of the following four processes :—

(1) An inelastic collision takes place between the α-particle and the nucleus, without capture of the α-particle. The energy lost by the α-particle is radiated as a quantum, as in the production of continuous X-radiation by electron impact.

(2) The same process occurs, save that the energy lost by the α-particle excites the nucleus, which later returns to its normal state, with emission of γ-radiation.

(3) The α-particle is captured by the nucleus, a new normal nucleus being formed, and the surplus energy is at the same time radiated as a quantum.

(4) The α-particle is captured by the nucleus, a proton is emitted with part of the available energy, leaving the new nucleus in an excited state. Subsequently a transition to the normal state takes place, with emission of a γ-ray quantum.

Nearly all the secondary γ-radiations observed can probably be accounted for in terms of processes (3) and (4). If, however, the indications, obtained in the earlier counter experiments, of the existence of soft radiations from paracyanogen and copper, are correct, these radiations must probably be ascribed to one or other of the first two processes. *A priori*, one would not expect the first process to occur, since no continuous X-radiation appears* to be produced by collisions between α-particles and extra-nuclear electrons. Beck† has considered the second process theoretically in some detail. The order of magnitude predicted by him is about 10^{-2} of that detectable in the present experiments, but calculations of nuclear processes cannot be expected to predict even orders of magnitude.

The quantum energies of the radiations produced by process (3) can be computed theoretically if the mass defects of the initial and final nuclei are known. Let M, M′, be the masses of the initial and final nuclei, m that of the α-particle, $h\nu$ the energy of the quantum emitted, u the initial velocity of the α-particle, v' the final velocity of the struck nucleus, θ, φ the angles between the direction of motion of the quantum, and struck nucleus, respectively, and the initial direction of the α-particle. Then for the conservation of momentum and energy

$$(h\nu/c)\sin\theta = \mathrm{M}'v'\sin\phi$$

$$mu = \mathrm{M}'v'\cos\phi + (h\nu/c)\cos\theta$$

$$\tfrac{1}{2}mu^2 + (\mathrm{M} + m)c^2 = \tfrac{1}{2}\mathrm{M}'v'^2 + \mathrm{M}'c^2 + h\nu,$$

using the usual approximation to the relativistic expression for the kinetic energy. Eliminating v' and φ from these equations, one obtains

$$h\nu = [(m + \mathrm{M} - \mathrm{M}')c^2 + \tfrac{1}{2}(1 - m/\mathrm{M}')mu^2]/[1 - (mu/\mathrm{M}'c)\cos\theta + h\nu/2\mathrm{M}'c^2].$$

An approximate calculation shows that the second and third terms in the denominator are always small compared with unity, and may therefore be neglected. The numerator is readily computable if the mass defects are known. It will be noted that the quantum energy is a function of the energy of the α-particle. Consequently, since all absorption coefficients were measured for thick layers of bombarded material, and the energy of the α-particles at impact was therefore different from different parts of the bombarded material, the radiation would not, in general, be expected to be homogeneous. The inhomogeneity would, however, hardly be sufficient to produce a marked deviation from linearity in the absorption curves. The measured absorption coefficients correspond then to the effective mean quantum energies.

* Bothe and Fränz, 'Z. Physik,' vol. 52, p. 466 (1928).

† 'Z. Physik,' vol. 67, p. 227 (1931).

These can be calculated approximately for elements for which the dependence of probability of production on the residual range of the α-particles was investigated, by means of the expression

$$h\nu = (\mathrm{M} + m - \mathrm{M}')c^2 + (1 - m/\mathrm{M}')\,\overline{\mathrm{E}}$$

where

$$\overline{\mathrm{E}}\int_0^{\mathrm{R}_0}\mathrm{F}(\mathrm{R})\,d\mathrm{R} = \int_0^{\mathrm{R}_0}\mathrm{E}(\mathrm{R})\,\mathrm{F}(\mathrm{R})\,d\mathrm{R},$$

$\mathrm{F}(\mathrm{R})d\mathrm{R}$ being the probability of production by α-particles of residual range between R and R + dR, and E(R), the corresponding classical kinetic energy.

The fourth process of production of secondary γ-radiation was suggested by Chadwick, Constable and Pollard* in order to account for their measurements on the ranges of disintegration protons. They deduced from their observations that in certain cases the proton was emitted sometimes with all the available energy, and sometimes with an energy smaller than this by an amount which was independent of the energy of the α-particle. In the latter case the nucleus was left in an excited state and a transition to the normal state, with emission of a γ-ray quantum, must have occurred later. From the difference in energy between the two sets of protons, using the conservation of momentum and energy, the quantum energy can be calculated. The proton experiments also provide, in some cases, a rough estimate of the absolute probability of production of the radiation.

The radiations from the various elements will now be considered in turn. The most accurate measurements were made in the case of *beryllium.* The absorption curves show that while the radiation is probably non-homogeneous, it by no means permits a unique separation into components. The estimated limits of error for the harder components are, however, probably not far wrong. The harder components of both the " forward " and " backward " radiations would appear to be produced by capture without emission of a proton. The high quantum energy found excludes inelastic impact without capture as a possible process ; further, it is unlikely that the γ-radiation is associated with proton emission since investigations for protons from beryllium bombarded by polonium α-particles have always given negative results, whereas a comparatively large number of γ-ray quanta are emitted. Assuming that Be_9, the most plentiful of the beryllium isotopes, is responsible for the radiation, and taking the difference in mass defects of Be_9 and C_{13} to be $5 \cdot 0 \times 10^{-3}$ atomic units, the theory predicts quanta of about 7½ million electron-volts effective mean energy. The discrepancy between this result and the experimental value for the quantum energy of the radiation emitted in the forward direction—6·6 million—is not serious, for it is quite possible that too high an estimate was made of the "scattering" correction. If the scattering correction is neglected altogether a value $9 \cdot 3 \times 10^6$ electron-volts is obtained. A much more serious discrepancy with theory is, however, the difference between the radiation emitted in the backward direction and that emitted in the forward direction, for the observations were made under practically identical experimental conditions. The theory does indeed predict a slightly harder radiation in the forward direction than in the backward ($7 \cdot 6 \times 10^6$ electron-volts, as against 7·4), but this cannot possibly account for the observed difference in the absorption coefficients. It is possible, though unlikely, that the discrepancy is due to experimental errors. If the discrepancy is real it may possibly be explicable along the following lines. The radiation may be assumed to consist in each case of two components, one 7½ million electron-volts quantum energy and one of about 1 million. The difference in apparent hardness may then be considered due to different admixture of the two components. The experimental curves can, indeed, be accounted for in terms of these two components (assuming a scattering correction such that the measured absorption coefficients for the harder component of the forward radiation correspond to 7½ million electron-volts). It is, however, necessary to assume that while less of the harder radiation is emitted in the backward direction than in the forward, *more* of the softer radiation is emitted in the backward direction. It does not appear possible to obtain any theoretical justification for these assumptions.

---

* 'Proc. Roy. Soc.,' A, vol. 130, p. 463 (1931).

As regards the latter assumption, it should be remarked that the evidence concerning the softer radiation provided by the curves is of questionable value. In the first place, according to theory, the harder radiation should itself not be homogeneous, though this would not account for the whole of the departure from straight line absorption. In the second place, it is readily shown that the correction for scattered radiation entering the chamber decreases with increasing total thickness of absorber, and this would give rise to an apparent heterogeneity. These effects, however, act in the direction of strengthening the case for insistence on the second assumption.

If the softer radiation is indeed emitted non-uniformly, it cannot be due to the fourth process, which cannot conceivably have a preferred direction of emission. It is worthy of note that Kirsch* has reported the observation of disintegration protons of short range from beryllium bombarded by radium C′ α-particles, but experiments with polonium α-particles have always given negative results. The softer radiation, if real, is thus probably due to the second process.

---

* 'Erg. Exakt. Naturw.,' vol. 5, p. 165 (1926).

As regards the γ-radiations produced by bombardment of beryllium by α-particles of reduced range, all that can be said is that the experimental values agree with theory within the limits of experimental error.

The results for *boron* are less accurate than those for beryllium. The radiation in the forward direction appears to be definitely heterogeneous; the results for the backward direction are not sufficiently accurate to show whether a similar heterogeneity was present or not. It does appear, however, that, as in the case of beryllium, the radiation in the forward direction is considerably harder on the average than that in the backward direction, though the experimental error is here large enough to explain the discrepancy.

It should be mentioned that Chadwick, Constable and Pollard (*loc. cit.*), on the basis of their investigations of disintegration protons, have predicted a γ-radiation from boron of about 3×10^6 electron-volts quantum-energy. They have further shown that B_{10}, and not B_{11}, is the isotope responsible and that about 3 quanta should be emitted per million incident α-particles. It is possible that the softer radiation observed in the forward direction originates in this process. The bad agreement between the experimental estimates and the theoretical—$\mu_{Pb} = 1$ cm.$^{-1}$, instead of 0·45 cm.$^{-1}$—is not serious, in view of what has been said previously concerning softer components. The estimated number of quanta—about 4 per million α-particles—is of the right order of magnitude. If this ascription is correct, the softer radiation must be emitted uniformly in all directions so that the apparently smaller mean energy in the backward direction, if a real effect, must be due entirely to a deficiency in the harder component. The estimated relative numbers of quanta are consistent with this supposition.

The harder component is probably due to the third process. The isotope responsible is probably B_{11}, for this is the more abundant isotope, and, further, B_{10} gives so many protons that it is doubtful whether α-particle capture without proton emission is possible. The theoretical quantum energy is thus about 14 million electron-volts, using Birge's* estimate of the mass defect of N_{15}. The discrepancy with the experimental value—7·8 million—is probably due to error in the scattering correction, as with beryllium. Neglecting the scattering correction, one obtains 12·5 million electron-volts for the quantum energy.

---

* 'Phys. Rev.,' vol. 37, p. 841 (1931).

The results for fluorine, sodium, magnesium and aluminium are too inaccurate to give conclusive evidence as to the process of production. In the cases of fluorine and aluminium, Chadwick, Constable and Pollard (*loc. cit.*) have predicted γ-radiation from their results on the disintegration protons from these elements. In the case of fluorine they predict about 3 quanta per million α-particles of about 7 × 10^5 electron-volts energy. Thus, if the results of the present experiments are correct, the observed radiation (6 quanta per million α-particles of about 2 × 10^6 electron-volts energy) cannot be accounted for entirely by the disintegration changes and must be due in part to some other mode of excitation of radiation. In the case of aluminium the experimental results (1 quantum per million α-particles of about 3 × 10^6 volts energy) agree within experimental error with prediction (about 0·7 quanta per million α-particles of 2·3 × 10^6 electron-volts energy). In the case of sodium the proton experiments have not yet reached the stage when definite predictions can be made, but the general nature of the results is consistent with the observed γ-radiation (13 quanta per million α-particles, of about 5 × 10^5 electron-volts energy). Investigations have as yet revealed no protons of range longer than 18 cm. from magnesium, so that it is rather unlikely that the observed γ-radiation is associated with proton emission. The experimental results (about 0·5 quanta per million α-particles of energy of the order 5 × 10^6 electron-volts) are consistent with simple capture, but are too inaccurate to be determinative.

The soft radiation from lithium is probably not associated with proton emission since disintegration experiments have given negative results. It is impossible, however, to discriminate between the other possible processes, for the mass defects of the lithium isotopes are not sufficiently well known* for one to predict the result of simple capture with sufficient accuracy.

The primary γ-radiation from the polonium source consisted of two components. It is probable that both of these originated in the polonium itself, since no trace of β-ray activity could be observed with a β-ray electroscope. Control experiments with a solution of radium (D + E + F) in equilibrium showed that the harder component certainly originated in the polonium itself. It is unlikely that the softer component originated in radium E impurities since two absorption curves, taken on dates separated by about three months, indicated about the same proportion of softer component. Any radium E present would have been in equilibrium with radium D, so that the proportion of softer component should have increased by over 50 per cent. The absorption curves agree within the limits of experimental error with those obtained by Bothe and Becker.*

---

* *Cf.* Chadwick, Constable and Pollard, *loc. cit.*

It is interesting to note that the quantum energies of the two components—$1 \cdot 0 \times 10^6$ and 4×10^5 electron-volts—agree, within the limits of experimental error, with the energies of the two components of the anomalously scattered radiation investigated by Gray and Tarrant,† viz., $9 \cdot 2 \times 10^5$ and $4 \cdot 6 \times 10^5$ electron-volts. Gray and Tarrant have found that when hard γ-radiation is scattered, in addition to the Compton radiation, there is present radiation consisting of a mixture of these two components for *all* scattering materials. With lead in particular, the suggestion is that the incident radiation excites the nucleus, which later returns to its normal state emitting the "anomalously scattered" radiation. On the other hand, in the case of the polonium γ-radiation, one may suppose that the α-particle is sometimes emitted with less than the normal energy, leaving the residual *lead* nucleus in an excited state, with subsequent emission of γ-radiation. The two interpretations are obviously consistent.

A further interesting coincidence is that the softer component of the radiation investigated by Gray and Tarrant has approximately the same energy as the secondary radiation from lead and tin observed by Slater (*loc. cit.*). Whether this coincidence has any real significance it is difficult to say. It suggests that the phenomena observed by Slater were due to the excitation of the nucleus by inelastic collisions with the α-particles, followed by a cascade of small quantum jumps, each giving rise to a quantum of radiation. Several quanta must be postulated to account for the large intensity observed by Slater. That radon α-particles were able to excite lead, while polonium α-particles of only slightly less energy were unable to do so, is probably understandable when one considers that the maximum energy of the polonium α-particles corresponds to an excitation potential of the lead nucleus. It is, however, difficult to understand Slater's results for tin, since one would expect, *a priori*, a smaller excitation potential for the nucleus of this element.

The negative result obtained when paraffin wax was bombarded is of some interest, since Atkinson's‡ theory of the synthesis of matter involves the building-up of nuclei by the addition of protons and electrons to helium nuclei. Atkinson assumes that the chance of capture of a proton which entered a helium nucleus would be nearly unity. Each capture would be expected to give rise to a quantum of γ-radiation. Thus if helium were bombarded by high-speed protons, or conversely, if hydrogen were bombarded by α-particles, one would expect to observe γ-radiation. If the radius of the α-particle is taken as $4 \cdot 5 \times 10^{-13}$ cm., the number of direct hits per million α-particles would, on classical theory, be about 600 for pure hydrogen, and hence the absence of detectable γ-radiation suggests 10^{-3} as the upper limit of possible capture per encounter.

---

* 'Z. Physik,' vol. 66, p. 307 (1930).

† *Unpublished.*

‡ 'Astrophys. J.,' vol. 73, pp. 250, 308 (1931).

§ 9. *Summary.*

The production of nuclear γ-radiation by bombardment with α-particles has been observed for the elements Li, Be, B, F, Na, Mg, Al. Negative results were obtained with H, C, N, Ni, Cu, Sn. Two methods of measurement were used, Geiger-Müller tube-counters and high-pressure ionisation chambers, and the relative advantages of each are discussed. By measurements of the absorption coefficients in lead, and in some case also in iron, the quantum energies of the radiations could be deduced from the Klein-Nishina formula. The absorption coefficients had to be corrected for obliquity, and for "degraded" radiation entering the measuring vessel. The magnitude of the Tarrant nuclear absorption coefficient had to be estimated by comparison of the absorption coefficients in lead and iron. The deduced quantum energies ranged from about 8 million electron-volts for boron, to 0·5 million for sodium.

The absolute efficiencies of production of the various radiations were determined from the ionisation currents observed, the apparatus being standardised by means of a source of thorium (B + C) of known strength. They range from about 0·5 quanta per million α-particles for magnesium to about 30 quanta for beryllium. In addition, the way in which the efficiency of production varies with the residual range of the α-particles was investigated. The processes probably responsible for the radiations are discussed; some appear to be due to the capture of an α-particle by a nucleus without proton emission, others are probably due to a secondary process following proton emission, others may arise from inelastic collisions without capture. The relation between the primary γ-radiation of polonium and the "anomalously scattered" radiation investigated by Gray and Tarrant is discussed and an attempt made to explain the results of Slater on the production of secondary γ-radiation in tin and lead by radon α-particles.

In conclusion, I should like to express my warmest thanks to Lord Rutherford and Dr. J. Chadwick for their advice and encouragement during this work. To Dr. Chadwick I am also indebted for the preparation of the polonium sources, from material kindly given by Dr. Burnam and Dr. West, of the Kelly Hospital, Baltimore, U.S.A. My thanks are also due to Professor Stratton for permission to carry out these experiments, free from radioactive contamination, at the Solar Physics Observatory, Cambridge. I also desire to thank the 1851 Commissioners for a Scholarship, during the tenure of which these experiments were commenced, and which indirectly rendered their completion possible.

Relativistic Quantum Mechanics.

By P. A. M. Dirac, F.R.S., St. John's College, Cambridge.

(Received March 24, 1932.)

§ 1. *Introduction.*

The steady development of the quantum theory that has taken place during the present century was made possible only by continual reference to the Correspondence Principle of Bohr, according to which, classical theory can give valuable information about quantum phenomena in spite of the essential differences in the fundamental ideas of the two theories. A masterful advance was made by Heisenberg in 1925, who showed how equations of classical physics could be taken over in a formal way and made to apply to quantities of importance in quantum theory, thereby establishing the Correspondence Principle on a quantitative basis and laying the foundations of the new Quantum Mechanics. Heisenberg's scheme was found to fit wonderfully well with the Hamiltonian theory of classical mechanics and enabled one to apply to quantum theory all the information that classical theory supplies, in so far as this information is consistent with the Hamiltonian form. Thus one was able to build up a satisfactory quantum mechanics for dealing with any dynamical system composed of interacting particles, provided the interaction could be expressed by means of an energy term to be added to the Hamiltonian function.

This does not exhaust the sphere of usefulness of the classical theory. Classical electrodynamics, in its accurate (restricted) relativistic form, teaches us that the idea of an interaction energy between particles is only an approximation and should be replaced by the idea of each particle emitting waves, which travel outward with a finite velocity and influence the other particles in passing over them. We must find a way of taking over this new information into the quantum theory and must set up a relativistic quantum mechanics, before we can dispense with the Correspondence Principle.

A preliminary attack on the question of relativistic quantum mechanics has been made through the solution of the problem of a single charged particle moving in a specified classical field. For the treatment of this problem it is essential to use Schrödinger's form of quantum mechanics, according to which the motion of the particle is described by a wave function involving the space and time co-ordinates in a symmetrical manner. The solution is satisfactory from the point of view of the Correspondence Principle, although it involves a difficulty owing to the appearance of possible negative energy values for the particle. The difficulty is not due to a misuse of classical information and will not concern us here.

The extension of this wave-function method to two or more particles can easily be made so long as we keep to the idea of a given classical field in which the particles are moving. The resulting theory is logically satisfactory, but is, of course, incomplete, as it gives no interaction between the particles. It becomes necessary then to abandon the idea of a given classical field and to have instead a field which is of dynamical significance and acts in accordance with quantum laws.

An attempt at a comprehensive theory on these lines has been made by Heisenberg and Pauli.* These authors regard the field itself as a dynamical system amenable to Hamiltonian treatment and its interaction with the particles as describable by an interaction energy, so that the usual methods of Hamiltonian quantum mechanics may be applied. There are serious objections to these views, apart from the purely mathematical difficulties to which they lead. If we wish to make an observation on a system of interacting particles, the only effective method of procedure is to subject them to a field of electromagnetic radiation and see how they react. Thus the rôle of the field is to provide a means for making observations. *The very nature of an observation requires an interplay between the field and the particles.* We cannot therefore suppose the field to be a dynamical system on the same footing as the particles and thus something to be observed in the same way as the particles. The field should appear in the theory as something more elementary and fundamental.

Again, the field equations are always linear and thus of the form typical of the wave equation of quantum theory. This suggests deep-lying connections and possibilities for simplification and unification which are entirely lacking in the Heisenberg-Pauli theory.

---

* 'Z. Physik,' vol. 56, p. 1, and vol. 59, p. 168 (1929).

In the present paper a scheme is proposed which gives the interplay between particles and field apparently correctly and in a surprisingly simple manner. Full use is made of all the information supplied by the classical theory. The general ideas are applicable with any kind of simple harmonic wave transmitting the interaction between particles and providing the means of observation of particles (*e.g.*, with longitudinal waves like sound waves) and not merely for the electromagnetic case, though presumably only the latter is of interest in atomic theory.

§ 2. *Relativistic Observations.*

A definite advance in the relativistic theory of the interaction of two electrons is contained in a recent paper by Möller,* where it is shown that in the calculation of the mutual scattering of two colliding electrons by Born's method of approximation, one may describe the interaction with retarded potentials and use relativistic ideas throughout, without getting any ambiguity in the scattering coefficient to the first order of approximation. This lack of ambiguity is ground of presumption of the correctness of the result. When, however, one tries to apply similar methods to the higher approximations or to more general problems, one meets very definitely with ambiguities.

The method by which Moller obtained his result may be compared with the methods of the Correspondence Principle in use before the introduction of Heisenberg's matrix theory, for calculating Einstein's A and B coefficients from classical models. In certain cases the result obtained was unambiguous (usually those cases for which the result was zero) and was then presumed to be correct. In general, however, there was ambiguity, so that one could get no reliable accurate result.

This analogy suggests that it would be useless to try to extend Möller's method by setting up rules to provide a definite interpretation for ambiguous quantities. Any attempts in this direction would be just as futile as the attempts made in the pre-Heisenberg epoch to calculate Einstein's A's and B's from some sort of mean of classical quantities referring to the initial and final states. One ought to proceed on quite different lines, namely by following the methods introduced by Heisenberg in 1925, which have already met with such great success for non-relativistic quantum mechanics.

---

* 'Z. Physik.' vol. 70, p. 786 (1931).

Heisenberg put forward the principle that one should confine one's attention to observable quantities, and set up an algebraic scheme in which only these observable quantities appear. Strictly speaking, it is not the observable quantities themselves (the Einstein A's and B's) that formed the building stones of Heisenberg's algebraic scheme, but rather certain more elementary quantities, the matrix elements, having the observable quantities as the squares of their moduli. The extra phase quantities introduced in this way are essential.

Let us see what are the corresponding quantities in relativistic theory. To make a relativistic observation on a system of particles we must, as mentioned in the introduction, send in some incident electromagnetic radiation and examine the scattered radiation. The numerical quantity that we observe is thus the probability of occurrence of a certain radiative transition process. This process may be specified by the intensities of the various monochromatic components of the ingoing and of the outgoing fields of radiation. (We shall ignore the purely mathematical difficulty that the total number of these components is an infinity of a high order.) The phases must not be specified together with the intensities, as this would violate well-established quantum principles.

In non-relativistic quantum mechanics the probability of occurrence of any transition process is always given as the square of the modulus of a certain quantity, of the nature of a matrix element or simply a transformation function, referring to the initial and final states. It appears reasonable to assume that this will still be the case in relativistic quantum mechanics. Thus the relativistic observable quantities, which are always transition probabilities, will all appear as the squares of the moduli of certain quantities. These quantities, which we shall refer to as probability amplitudes, will then be the building stones analogous to Heisenberg's matrix elements. We should expect to be able to *set up an algebraic scheme involving only the probability amplitudes and to translate the equations of motion of relativistic classical theory directly into exact equations expressible entirely in terms of these quantities.*

The information that classical theory supplies is thus to be used to give relations between the probability amplitudes of *different* physical processes, rather than to enable one to calculate a particular one of them. Only in very special cases, of which Möller's paper provides an example, is it possible to evaluate a relativistic transition probability without at the same time evaluating a whole series of them, referring to all the possible ways in which the particles under consideration can react with the radiation field.

A point of special importance about the building stones of the new theory is that each of them refers to one field of ingoing waves and one field of outgoing waves, or to one initial field of a transition process and one final field. Quantities referring to two initial fields, or to two final fields, are not allowed. This shows a departure from the theory of Heisenberg and Pauli, according to which, if one is given any quantity referring to one initial field and one final field, one can obtain from it a quantity referring to two initial fields, or to two final fields, by a straightforward application of the transformation theory of quantum mechanics. The Heisenberg-Pauli theory thus involves many quantities which are unconnected with results of observations and which must be removed from consideration if one is to obtain a clear insight into the underlying physical relations.

§ 3. *Equations of Motion.*

We shall now consider in detail the question of how the information contained in classical electrodynamics can be taken over into the quantum theory. We meet at once with the difficulty that the classical theory itself is not free from ambiguity.

To make the discussion precise, let us suppose we have a single electron interacting with a field of radiation and consider the radiation resolved into *ingoing* and *outgoing* waves. The classical problem is, given the ingoing radiation and suitable initial conditions for the electron, determine the motion of the electron and the outgoing radiation. The classical equations which deal with this problem are of two kinds, (i) those that determine the field produced by the electron (which field is just the difference of the ingoing and outgoing fields) in terms of the variables describing the motion of the electron, and (ii) those that determine the motion of the electron. Equations (i) are quite definite and unambiguous, but not so equations (ii). The latter express the acceleration of the electron in terms of field quantities at the point where the electron is situated and these field quantities in the complete classical picture are infinite and undefined.

In the usual approximate treatment of the problem one takes for these field quantities just the contributions of the ingoing waves. This treatment is necessarily only approximate, since it does not take into account the reaction on the electron of the waves it emits. We should expect in an accurate treatment, that the field determining the acceleration of the electron would be in some way associated with both the ingoing and outgoing waves. Classical attempts have been made to improve the theory by assuming a definite structure for the electron and calculating the effect on one part of it of the field produced by the rest, but such methods are not permissible in modern physics.

We must recognise at this point that we have reached the limit of classical electromagnetic theory. We have quite definite equations for determining the motion of the electron in terms of field quantities, but we cannot interpret these field quantities in the usual classical picture and the most we can say about them is that they are related in some non-classical way to two fields, namely, those of the ingoing and of the outgoing waves. Further advance can be made only by introducing quantum ideas.

Let us make the assumption that *the passage from the field of ingoing waves to the field of outgoing waves is just a quantum jump performed by one field.* This assumption is permissible on account of the fact, discussed in the preceding section, that all the quantities in relativistic quantum mechanics are of the nature of probability amplitudes referring to one ingoing field and one outgoing field, so that we may associate, say, the right-hand sides of the probability amplitudes with ingoing fields and the left-hand sides with outgoing fields. In this way we automatically exclude quantities referring to two ingoing fields or to two outgoing fields and make a great simplification in the foundations of the theory.

The significance of the new assumption lies in the fact *that the classical picture from which we derive our equations of motion must contain no reference to quantum jumps.* This classical picture must therefore involve just one field, a field composed of waves passing undisturbed through the electron and satisfying everywhere Maxwell's equations for empty space. With this picture the equations of motion for the electron are perfectly definite and unambiguous. There are no equations of motion for the field, as the field throughout space-time is pictured as given. Thus the interaction between electron and field is introduced into the equations in only one place.

The quantisation of the equations of motion derived from this picture may conveniently be carried out in two stages. Let us first quantise only the variables describing the electron. We then get just the usual quantum theory of the motion of an electron in a given classical field, with the difference that in the present case the field must necessarily be resolvable into plane waves and must therefore contain nothing of the nature of a Coulomb force. We have a Schrödinger equation of the form

$$F\psi = 0,$$

where the operator F is, neglecting spin

$$F = \left(ih\frac{\partial}{\partial t} + eA_0\right)^2 - \left(ihc\frac{\partial}{\partial x} - eA_x\right)^2 - \ldots - m^2c^4. \qquad (1)$$

It should be remembered that the wave-function ψ involves not only the variables x, y, z, t describing the electron, but also a large number of parameters describing the field, which parameters may conveniently be taken to be the intensities J and phases w of the various Fourier components of the field. The potentials A occurring in F are likewise functions, not only of the variables x, y, z, t describing the momentary position of the electron, but also of the parameters J and w.

In the second stage of the quantisation we assume that the J's and w's occurring in ψ and the A's are not numerical, but are operators satisfying the usual quantum conditions governing the intensities and phases of the Fourier components of the electromagnetic field in empty space. The new wave equation obtained in this way is to be treated on the same lines as the previous one. In particular, it may be used to determine matrix elements associated with electron jumps. Each such matrix element will now be a function of the non-commuting J's and w's, so that, when we take a representation of the J's and w's, it becomes a set of quantities, each referring to two states of the field as well as the two electronic states, and thus being of the nature of the probability amplitudes of § 2.

For the problem of the interaction of two electrons, we require a wave-function ψ which is a function of the variables x_1, y_1, z_1, t_1 and x_2, y_2, z_2, t_2 describing the two electrons and of one set of J's and w's describing one field. This ψ must satisfy the two wave equations

$$F_1\psi = 0, \qquad F_2\psi = 0. \tag{2}$$

where F_1 is the operator obtained from F by substituting $\partial/\partial t_1$, etc., for $\partial/\partial t$, etc., and taking for the A's their values at the point x_1, y_1, z_1, t_1, and similarly for F_2. These two wave equations describe completely the relations between the two electrons and the field. No terms of the type of a Coulomb interaction energy are required in the operators of the wave equations. The interaction of the two electrons is due to the motions of both being connected with the same field. This interaction manifests itself mathematically through the fact that, if we take a wave function ψ_1, a function only of x_1, y_1, z_1, t_1 and the J's and w's, satisfying

$$F_1\psi_1 = 0, \tag{3A}$$

and a second wave-function ψ_2, a function only of x_2, y_2, z_2, t_2 and the J's and w's, satisfying

$$F_2\psi_2 = 0, \tag{3B}$$

then neither of the products $\psi_1\psi_2$ and $\psi_2\psi_1$ will satisfy both the wave equations (2). The solution of equations (2) is an essentially different and more complicated problem than the solution of (3A) and (3B).

§ 4. *Interaction between Two Particles in One Dimension.*

It may seem rather surprising that a theory in which all the fields are resolvable into plane waves can give anything of the nature of the usual electrostatic forces between electrons. We shall therefore illustrate by a simple example the fact that these forces really are contained in our wave equations. We shall take the case of two particles moving in a field in one-dimensional space and shall proceed to solve equations (2), making various approximations that are permissible when we are not interested in relativistic effects.

Suppose the field to be describable by a potential function V satisfying the wave equation

$$\frac{\partial^2 V}{\partial x^2} - \frac{1}{c^2}\frac{\partial^2 V}{\partial t^2} = 0,$$

and the classical expression for the energy to be

$$H = \frac{1}{8\pi}\int\left\{\left(\frac{\partial V}{\partial x}\right)^2 + \frac{1}{c^2}\left(\frac{\partial V}{\partial t}\right)^2\right\} dx.$$

If we resolve V into its Fourier components, thus

$$V = \int_{-\infty}^{\infty} \{a_\nu e^{i\nu(t+x/c)} + b_\nu e^{i\nu(t-x/c)}\}\, d\nu, \tag{4}$$

the expression for the energy will go over into

$$H = \frac{1}{c}\int_0^{\infty} \nu^2 \{a_\nu a_{-\nu} + b_\nu b_{-\nu}\}\, d\nu. \tag{5}$$

Let us now see what are the Poisson bracket relations between the Fourier coefficients a and b. These relations must be chosen such that the quantities $a_\nu e^{i\nu t}$, $b_\nu e^{i\nu t}$, considered as dynamical variables, satisfy equations of motion of the Hamiltonian form with the Hamiltonian function (5), thus

$$\frac{d}{dt}(a_\nu e^{i\nu t}) = [a_\nu e^{i\nu t}, H]$$

or

$$i\nu a_\nu = [a_\nu, H],$$

and similarly for b_ν. It is easily verified that we must have

$$[a_\nu, a_{\nu'}] = [b_\nu, b_{\nu'}] = ic/\nu \,.\, \delta(\nu + \nu')$$

$$[a_\nu, b_{\nu'}] = 0.$$

In the quantum theory these relations become

$$\left.\begin{aligned} a_\nu a_{\nu'} - a_{\nu'} a_\nu = b_\nu b_{\nu'} - b_{\nu'} b_\nu = - hc/\nu \,.\, \delta(\nu + \nu') \\ a_\nu b_{\nu'} - b_{\nu'} a_\nu = 0 \end{aligned}\right\} . \tag{6}$$

We now introduce two particles, of masses m_1 amd m_2 and "charges" ϵ_1 and ϵ_2, and suppose the interaction of each with the field can be described by an interaction energy equal to its charge multiplied by the value of V at the point where it is situated. Thus, if we neglect the relativistic variation of mass with velocity, we have the two wave equations

$$\left\{ih\frac{\partial}{\partial t_1} + \frac{h^2}{2m_1}\frac{\partial^2}{\partial x_1{}^2} - \epsilon_1 \mathrm{V}(x_1 t_1)\right\}\psi = 0,$$

$$\left\{ih\frac{\partial}{\partial t_2} + \frac{h^2}{2m_2}\frac{\partial^2}{\partial x_2{}^2} - \epsilon_2 \mathrm{V}(x_2 t_2)\right\}\psi = 0.$$

By putting $t_1 = t_2 = t$, we can reduce these to the one wave equation

$$\left\{ih\frac{\partial}{\partial t} + \frac{h^2}{2m_1}\frac{\partial^2}{\partial x_1{}^2} + \frac{h^2}{2m_2}\frac{\partial^2}{\partial x_2{}^2} - \epsilon_1 \mathrm{V}(x_1 t) - \epsilon_2 \mathrm{V}(x_2 t)\right\}\psi = 0. \tag{7}$$

We shall proceed to obtain a solution of this equation in the form of a power series in the ϵ's. Thus we put

$$\psi = \psi_0 + \psi_1 + \psi_2 + \cdots$$

where

$$\left\{ih\frac{\partial}{\partial t} + \frac{h^2}{2m_1}\frac{\partial^2}{\partial x_1{}^2} + \frac{h^2}{2m_2}\frac{\partial^2}{\partial x_2{}^2}\right\}\psi_0 = 0 \tag{8}$$

$$\left\{ih\frac{\partial}{\partial t} + \frac{h^2}{2m_1}\frac{\partial^2}{\partial x_1{}^2} + \frac{h^2}{2m_2}\frac{\partial^2}{\partial x_2{}^2}\right\}\psi_1 = \{\epsilon_1 \mathrm{V}(x_1 t) + \epsilon_2 \mathrm{V}(x_2 t)\}\psi_0 \tag{9}$$

$$\left\{ih\frac{\partial}{\partial t} + \frac{h^2}{2m_1}\frac{\partial^2}{\partial x_1{}^2} + \frac{h^2}{2m_2}\frac{\partial^2}{\partial x_2{}^2}\right\}\psi_2 = \{\epsilon_1 \mathrm{V}(x_1 t) + \epsilon_2 \mathrm{V}(x_2 t)\}\psi_1. \tag{10}$$

We take as the solution of (8)

$$\psi_0 = e^{ip_1 x_1/h}\, e^{ip_2 x_2/h}\, e^{-i\mathrm{W}t/h}\, \delta_{\mathrm{J}0},$$

where

$$\mathrm{W} = \frac{p_1{}^2}{2m_1} + \frac{p_2{}^2}{2m_2}, \tag{11}$$

representing a state for which the particles have the momenta p_1 and p_2, and all the J's, *i.e.*, the intensities of the Fourier components of the field, vanish. Now the operator $\varepsilon_1 V(x_1 t) + \varepsilon_2 V(x_2 t)$ occurring on the right-hand sides of (9) and (10), if expressed as a matrix in a representation in which the J's are diagonal, would contain only matrix elements referring to transitions in which just one of the J's changes by one quantum. It follows that ψ_1 must consist of a sum of terms each referring to a state of the field in which just one oscillation is excited by one quantum. Similarly ψ_2 must consist of a sum of terms each referring either to a two-quantum or to a zero-quantum state of the field. The latter are the ones that interest us here, as they may be compared with the terms that would arise from the insertion of an interaction energy between the two particles into the operator of the wave equation (7).

We can obtain the solution of equation (9) by expanding the right-hand side in terms of its Fourier components by means of (4) and dividing each component by the number to which the operator on the left-hand side of (9) is equivalent when it operates on that component. This gives

$$\begin{aligned}\psi_1 = \varepsilon_1 \int_{-\infty}^{\infty} \Bigg\{ & \frac{a_\nu e^{i\nu(t+x_1/c)}}{W - h\nu - (p_1 + h\nu/c)^2/2m_1 - p_2^2/2m_2} \\ & + \frac{b_\nu e^{i\nu(t-x_1/c)}}{W - h\nu - (p_1 - h\nu/c)^2/2m_1 - p_2^2/2m_2} \Bigg\} d\nu . \\ + \varepsilon_2 \int_{-\infty}^{\infty} \Bigg\{ & \frac{a_\nu e^{i\nu(t+x_2/c)}}{W - h\nu - p_1^2/2m_1 - (p_2 + h\nu/c)^2/2m_2} \\ & + \frac{b_\nu e^{i\nu(t-x_2/c)}}{W - h\nu - p_1^2/2m_1 - (p_2 - h\nu/c)^2/2m_2} \Bigg\} d\nu . \psi_0\end{aligned}$$

If we use (11) and also neglect terms like $p_1/m_1 c$, $h\nu/m_1 c^2$ compared with unity, as is permissible when we are not interested in relativistic effects, this reduces to

$$\begin{aligned}\psi_1 \doteq & -\frac{\varepsilon_1}{h} \int_{-\infty}^{\infty} \{a_\nu e^{i\nu(t+x_1/c)} + b_\nu e^{i\nu(t-x_1/c)}\} \frac{d\nu}{\nu} . \psi_0 \\ & -\frac{\varepsilon_2}{h} \int_{-\infty}^{\infty} \{a_\nu e^{i\nu(t+x_2/c)} + b_\nu e^{i\nu(t-x_2/c)}\} \frac{d\nu}{\nu} . \psi_0\end{aligned} \tag{12}$$

When we substitute this value for ψ_1 in the right-hand side of (10) and also substitute for V its expansion given by (4), we obtain an expression consisting of an operator, which is a homogeneous quadratic function of the a's and b's, operating on ψ_0. We must evaluate that particular part of the expression that refers to the unexcited state of the field. Only those terms of the operator involving products like $a_\nu a_{-\nu}$ or $b_\nu b_{-\nu}$ will contribute anything to that part. To obtain the contribution of a term involving $a_\nu a_{-\nu}$, we observe that, for $\nu > 0$, a_ν and $a_{-\nu}$ are like the quantities $p + iq$ and $p - iq$ respectively in the problem of the simple harmonic oscillator. Thus $a_\nu a_{-\nu}$, with $\nu > 0$, is proportional to twice the energy of the corresponding oscillation (without zero-point energy) so that it gives no contribution when multiplied into ψ_0. The first of the quantum conditions (6) now shows that, to get the contribution from a term involving $a_{-\nu}a_\nu$ with $\nu > 0$, we must count $a_{-\nu}a_\nu$ as equal to $hc/\nu \, . \, \delta(\nu - \nu')$. In the same way we find that we must count $b_\nu b_{-\nu} = 0$ and $b_{-\nu}b_\nu = hc/\nu \, . \, \delta(\nu - \nu')$ with $\nu > 0$.

The term on the right-hand side of (10) arising from the product of $\epsilon_2 V(x_2 t)$ with the first of the terms for ψ_1 in (12) may be written

$$-\frac{\epsilon_1\epsilon_2}{h}\int_{-\infty}^{\infty} d\nu' \{a_{-\nu'} e^{-i\nu'(t+x_2/c)} + b_{-\nu'} e^{-i\nu'(t-x_2/c)}\}$$
$$\times \int_{-\infty}^{\infty}\frac{d\nu}{\nu}\{a_\nu e^{i\nu(t+x_1/c)} + b_\nu e^{i\nu(t-x_1/c)}\} \, . \, \psi_0.$$

That part of it referring to the unexcited state of the field is, by the foregoing rules

$$-\frac{\epsilon_1\epsilon_2}{h}\int_0^\infty d\nu'\int_0^\infty \frac{d\nu}{\nu}\frac{hc}{\nu}\delta(\nu-\nu')\{e^{-i\nu'(t+x_2/c)}e^{i\nu(t+x_1/c)} + e^{-i\nu'(t-x_2/c)}e^{i\nu(t-x_1/c)}\} \, . \, \psi_0$$
$$= -2\epsilon_1\epsilon_2 c\int_0^\infty \frac{d\nu}{\nu^2}\cos\nu(x_1-x_2)/c \, . \, \psi_0.$$

The coefficient of ψ_0 here differs only by an infinitely great constant (independent of x_1 and x_2) from

$$2\epsilon_1\epsilon_2 c\int_0^\infty\frac{d\nu}{\nu^2}\{1-\cos\nu(x_1-x_2)/c\} = \pi\epsilon_1\epsilon_2|x_1-x_2|.$$

The other terms on the right-hand side of (10) may be dealt with in the same way and give for the complete part referring to the unexcited state of the field

$$\{2\pi\epsilon_1\epsilon_2|x_1-x_2|+K\}\psi_0, \qquad (13)$$

where K is an infinite constant.

Equation (10) with expression (13) on its right-hand side is just what we should get if we were solving the wave equation

$$\left\{ih\frac{\partial}{\partial t}+\frac{h^2}{2m_1}\frac{\partial^2}{\partial x_1^2}+\frac{h^2}{2m_2}\frac{\partial^2}{\partial x_2^2}-2\pi\epsilon_1\epsilon_2|x_1-x_2|-K\right\}\psi=0,$$

by a method of approximation through expansion in powers of $\epsilon_1\epsilon_2$. Thus our wave-equation (7) contains implicitly an interaction between the particles, expressible approximately by the interaction energy $2\pi\epsilon_1\epsilon_2|x_1 - x_2|$. This interaction energy agrees numerically with what we should expect from a one-dimensional electrostatic theory. There is, however, a mistake in sign, as it gives an attractive force between like charges.

Summary.

A quantum theory is proposed in which the interaction between particles takes place by means of vibrations of an intervening medium transmitted with a finite velocity. The fundamental relations involve only quantities having observational significance, account being taken of the fact that an act of observation necessarily involves an interplay between particles and field. A detailed solution of a one-dimensional problem is given in order to show that forces of electrostatic nature are implicitly contained in the theory.

[*Note added, April 20th.*—It has been pointed out to me by Professor Heisenberg that the sign of the interaction energy given by the above calculation is really quite correct, since with the one-dimensional, longitudinal waves there used the classical theory also requires an attractive force between like charges.]

Ship Waves: their Variation with certain Systematic Changes of Form.

By T. H. HAVELOCK, F.R.S.

(Received February 24, 1932.)

1. The following paper is an examination, by analysis and by curves, of a single definite problem in wave profiles. Consider a ship model, of great draught, in which at some point in the form, at bow, stern or shoulders, for example, there is a sharp corner giving a sudden change of slope of the horizontal lines of the model. What is the effect on the wave profile of replacing this sudden change by a gradual change of slope of the same total amount, but distributed uniformly over any given length of the ship's form? Apart from direct applications, the problem is suggested by certain other considerations. In comparing theoretical and experimental resistance curves, I suggested some years ago* an indirect effect of the friction belt along the sides of the ship in that it may be equivalent to smoothing out the lines of the model, especially towards the stern. From an examination of interference effects with experimental models, it has been estimated that the effective length of the model is roughly 8 per cent. greater than the actual length, and this may probably be ascribed to some such frictional effect. The present paper deals with wave profiles since measurements of surface elevation are now becoming available, though the main results so far are for a simple model with straight lines and sharp corners; such a form simplifies the calculations but no doubt introduces other complications in practice, and a small correction for the smoothing effect of a friction belt would not be likely to account for the remaining differences between calculation and observation. It must be noted, moreover, that there are other approximations in the theory, apart from the neglect of fluid friction, but these need not be discussed here.

For these reasons no attempt has been made to apply the results of the present paper directly to experimental data, but it is hoped that the progressive series of curves will be of interest in showing the changes in profile due to successive changes of form of a definite kind.

2. The general analysis will be quoted from a recent paper,† to which reference may be made for further detail, and the expressions will then be adapted to the particular problem.

---

* 'Proc. Roy. Soc.,' A, vol. 110, p. 233 (1926).

† 'Proc. Roy. Soc.,' A, vol. 135, p. 1 (1932).

Take O in the free surface, with Ox in the direction of motion and Oz vertically upwards; and let u be the velocity of the model. We consider first a distribution of horizontal doublets in the plane $y = 0$, extending from the free surface down to a great depth, and we take the moment M per unit area to be a function of x only. Further, we suppose that the distribution of M is confined to a finite range in x, is continuous within this range, and is zero at the two limits of the range.

The surface elevation along the median line $y = 0$ is given by

$$\zeta = \frac{4}{\pi u} \Sigma \left\{ \left| \mathrm{M}'(x) \right|_r^s \mathrm{F}(x - x_{rs}) + \int \mathrm{M}''(h) \, \mathrm{F}(x - h) \, dh \right\}, \tag{1}$$

where the summation covers all points of sudden change in the gradient of M, and the integrals extend over the ranges of continuous variation of gradient. The function F is defined for positive and negative values of its argument by

$$\left. \begin{aligned} \mathrm{F}(q) &= -\frac{\pi}{2\kappa_0} \mathrm{Q}_0(\kappa_0 q) \\ \mathrm{F}(-q) &= -\frac{\pi}{2\kappa_0} \mathrm{Q}_0(\kappa_0 q) + \frac{2\pi}{\kappa_0} \mathrm{P}_0(\kappa_0 q), \end{aligned} \right\}, \tag{2}$$

with $q > 0$, and $\kappa_0 = g/u^2$.

We have also, for positive values of p,

$$\left. \begin{aligned} \mathrm{P}_0(p) &= -\frac{\pi}{2} \int_0^p \mathrm{Y}_0(p) \, dp \\ \mathrm{Q}_0(p) &= \frac{\pi}{2} \int_0^p \{\mathrm{H}_0(p) - \mathrm{Y}_0(p)\} \, dp \end{aligned} \right\}, \tag{3}$$

in the usual notation for Struve and Bessel functions.

One of the approximations of the theory lies in the connection between the form of the ship and the equivalent distribution of doublets in the median plane $y = 0$. For a ship model, of infinite draught, whose horizontal half-section is given by $y = f(x)$, the usual approximation amounts to taking

$$\mathrm{M}'(x) = (u/2\pi) f'(x). \tag{4}$$

With this relation, the surface elevation along $y = 0$ is given by

$$\zeta = \frac{2}{\pi^2} \Sigma \left\{ \left| f'(x) \right|_r^s \mathrm{F}(x - x_{rs}) + \int f''(h) \, \mathrm{F}(x - h) \, dh \right\}. \tag{5}$$

Here x, and h, are positive in the direction from stern to bow, x_{rs} being the position of any sharp corner in the form of the model. With this convention the discontinuities in $f'(x)$ at stern and bow are both positive; at an intermediate sharp corner, say, at a shoulder, the discontinuity would usually be negative. Along the curved lines of the model $f''(h)$ is negative, except for hollow lines where the form is concave outwards and where $f''(h)$ is positive. Thus, knowing the character of the function F, the expression (5) gives a general idea of the contributions of the various parts of the form. These possibilities are illustrated in fig. 1, which represents a half section of a model by a horizontal plane; or, to be more exact, the diagram gives the distribution

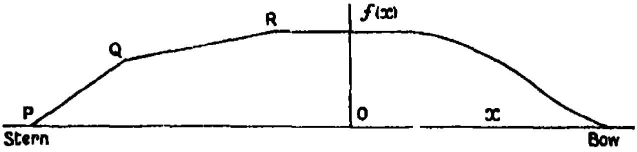

Fig. 1.

of doublets which is approximately equivalent to a model of this form. The figure also indicates the conventions for direction which are adopted throughout this paper.

3. We now isolate one particular feature for examination separately. It should, however, be noted that the function Q defined in (3) increases without limit as its argument becomes greater, though the expression (5) for the model as a whole remains finite everywhere. Therefore there is a certain artificiality, as regards that part of the disturbance, in applying the expressions to an isolated element of the form; but that may be allowed for, and in any case the method gives the differences made by changes in any particular element.

Consider a point on the model, given by $x = x_1$, where the lines of the model are straight lines meeting at a finite angle, for example, P, Q, or R in fig. 1. Let C be the discontinuity in $f'(x)$ at that point; that is, C is the difference of slope of the lines forward and aft of that point. Then, from (2) and (5), the contribution of this element to the surface elevation is

$$\begin{aligned} \zeta_1 &= \frac{2C}{\pi^2} F(x - x_1) \\ &= (4C/\pi\kappa_0)\{-\tfrac{1}{4}Q_0(\kappa_0 q_1) + P_0(\kappa_0 q'_1)\}, \end{aligned} \tag{6}$$

where $q_1 = x - x_1$ and $q'_1 = x_1 - x$. Further, we may use (6) for all values of x with the convention that P_0 is to be taken zero for negative values of its argument, and that $Q_0(-p) = Q_0(p)$. Now suppose that the same change of slope is carried out uniformly in a given range; that is, suppose the sharp corner replaced by a parabolic arc extending from $x = x_2$ to $x = x_3$, the point x_1 lying within this range. Considering the effect of this by itself apart from any other changes, we see from (5) that the corresponding contribution to the surface elevation is now

$$\zeta_{23} = \frac{2C}{\pi^2 (x_3 - x_2)} \int_{x_2}^{x_3} F(x-h)\, dh. \tag{7}$$

We shall use the notation

$$Q_1(p) = \int_0^p Q_0(p)\, dp, \tag{8}$$

$$P_0^{-1}(p) = 1 + P_1(p) = \int_0^p P_0(p)\, dp. \tag{9}$$

After evaluating (7) for points in advance of x_3, between x_2 and x_3, and in the rear of x_2, we find that we may express (7) in a single expression for all values of x, namely

$$\zeta_{23} = \frac{4C}{\pi\kappa_0^2 (x_3 - x_2)} \{ -\tfrac{1}{4} Q_1(\kappa_0 q_2) + \tfrac{1}{4} Q_1(\kappa_0 q_3) - P_0^{-1}(\kappa_0 q'_2) + P_0^{-1}(\kappa_0 q'_3) \}, \tag{10}$$

with $q_2 = x - x_2 = -q'_2$, $q_3 = x - x_3 = -q'_3$, and with the convention that P_0^{-1} is zero for negative values of its argument, while Q_1 is anti-symmetrical so that

$$Q_1(-p) = -Q_1(p).$$

The expression (6) is, of course, the limiting value of (10) when $x_3 - x_2$ is small and the points x_2 and x_3 ultimately coincide with the point x_1.

Numerical values of the functions may be calculated from their definitions as integrals, or from suitable series; for example, using the expansion of H_0 as a power series, we have

$$Q_0(p) = P_0(p) + \frac{p^2}{2} - \frac{p^4}{1^2 . 3^2 . 4} + \frac{p^6}{1^2 . 3^2 . 5^2 . 6} - \dots \tag{11}$$

$$Q_1(p) = P_0^{-1}(p) + \frac{p^3}{2 . 3} - \frac{p^5}{1^2 . 3^2 . 4 . 5} + \frac{p^7}{1^2 . 3^2 . 5^2 . 6 . 7} - \dots . \tag{12}$$

4. The special object in view is a comparison of the relative values of (6) and (10). The quantity C may be either positive or negative, and x_1 may be at any point between x_2 and x_3. But to make the problem definite in the first place, we suppose C negative and take $x_3 = x_1$ and $x_2 < x_1$; thus we are considering a sharp-angled shoulder on the model, such as Q or R in fig. 1, with the smoothing out entirely to the rear of that point. This process, if

carried out on an actual model, would no doubt involve other changes which would have to be considered in a theory capable of taking exact account of actual dimensions; but meantime we may isolate the effect of this particular change.

For convenience we consider separately the effect on the local disturbance and on the wave motion to the rear. Taking the former, we see from (6) and (10) that the difference amounts to replacing $\frac{1}{4} Q_0 (\kappa_0 q_1)$ by

$$\frac{1}{4\kappa_0 (q_2 - q_1)} \{Q_1 (\kappa_0 q_2) - Q_1 (\kappa_0 q_1)\}. \tag{13}$$

This can be shown in a form applicable to various velocities and to various ranges of $x_2 - x_1$ by graphing the quantity

$$\frac{1}{4k} \{Q_1 (p + k) - Q_1 (p)\} \tag{14}$$

on a base p, for several values of k. These curves are shown in fig. 2.

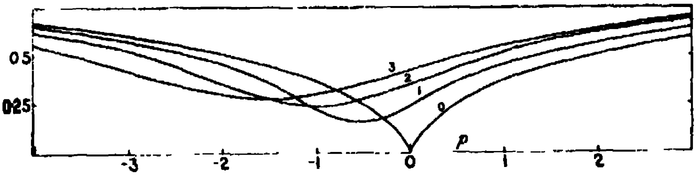

FIG. 2.—Curves of $\{Q (p + k) - Q_1 (p)\}/4k$ for different values of k.

In applying these curves to actual distances along the ship model, we note that $p = \kappa_0 x = gx/u^2$, where u is the velocity; and similarly $k = gd/u^2$, where d is the range over which the original sudden change in slope has been distributed. Thus the relative importance of the effects depends upon the ratio gd/u^2, or upon the ratio of d to λ, the wave-length of straight water waves for velocity u. In the diagram, $k = 0$ denotes the curve for the sharp corner; the bow of the model is to the right of the diagram and the stern to the left. Apart from the general smoothing effect, the chief point to notice in these curves is the raising of the profile forward of the point in question and a lowering to the rear of it. This is due to taking the range d entirely to the rear of the original sharp corner. If, on the other hand, the corner is taken at the middle of the range d in each case, by a suitable relative displacement of the curves, it is easily seen that the smoothing of the corner does not make any appreciable difference to the local disturbance except within the range d itself.

Turning now to the wave portion of the surface elevation, the change from (6) to (10) consists in replacing $-P_0(\kappa_0 q'_1)$ by

$$\frac{1}{\kappa_0(q'_1 - q'_2)}\{P_0^{-1}(\kappa_0 q'_2) - P_0^{-1}(\kappa_0 q'_1)\}. \tag{15}$$

In fig. 3 curves have been drawn for the quantity

$$\{P_0^{-1}(p-k) - P_0^{-1}(p)\}/k, \tag{16}$$

on a base p, for several values of k.

There are several points of interest in these curves. Since $k = d/2\pi\lambda$, the relative effect of smoothing out a sharp corner over a given range is less the smaller the ratio of d to λ, as might be expected. In the curves for the smaller values of k, although there is some diminution of amplitude, the more noticeable effect is the displacing of the troughs and crests to the rear, an effect which would increase the apparent interference length of the model. For the larger values of k, from about $k = 2$, there is a pronounced lessening of the amplitudes.

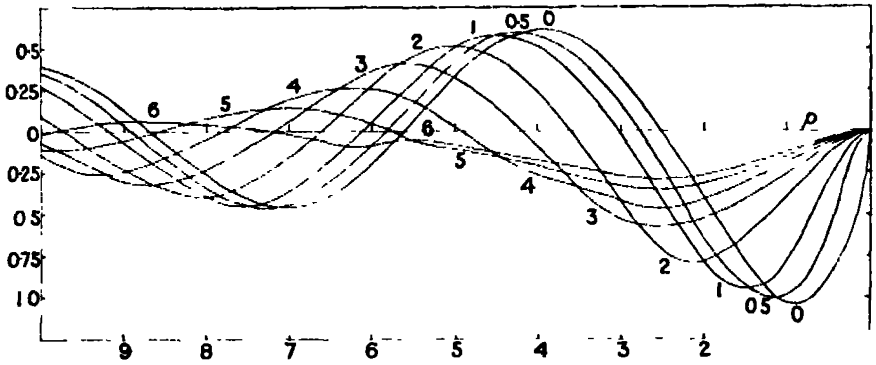

FIG. 3.—Curves of $\{P_0^{-1}(p-k) - P_0^{-1}(p)\}/k$ for different values of k.

On the convention already described, in calculating these curves from (16) the first term is zero until after $p = k$, and hence within the range k, the curve is simply the value of $-P_0^{-1}(p)\,.\,/k$. This quantity has a first maximum numerically, at about $p = 2\cdot54$, and this may be observed in the curves for $k = 3, 4, 5, 6$. Further, in the curves for the higher values, the effect of later maxima of the same quantity may be noticed; for instance, with $k = 6$ the range of continuous variation of slope is practically equal to the effective wavelength, and so subsidiary interference phenomena of this nature are obtained.

By displacing the curves to right or left we could examine the case when the smoothing of the lines takes place partly in front of the corner; and for a positive discontinuity the curves may be inverted. We may thus obtain, for example, some idea of the effect of smoothing out the lines of a sharp-angled stem, whether actually or by the equivalent effect of a friction belt.

Summary.

An examination, by analysis and by curves, of the changes in wave profile produced by replacing a sudden change of slope in the lines of a model by a continuous variation of the same total amount uniformly distributed over a given length of the model.

Molecular Structure and Physical Properties of Prussic Acid. Part I.—Refractive Dispersion of Prussic Acid and its Homologues.

By T. M. Lowry, F.R.S., and S. T. Henderson, Ph.D.

(Received February 26, 1932.)

The structure of prussic acid has been a subject of constant interest ever since Gautier,* by his discovery of the *iso*cyanides provided an alternative formula for the acid. In general, opinion has leaned towards the view that the free acid is a cyanide rather than an *iso*cyanide. In particular, Wade† regarded its relatively unobjectionable physiological properties as evidence of a cyanide structure; but evidence of an *iso*cyanide structure has been found by Peratoner and Palazzo‡ in the conversion of the acid into methyl *iso*cyanide by the action of diazomethane. A possible compromise may be found in the suggestion, already made in Butlerow's classical paper "Ueber Isodibutylen,"§ that prussic acid may be an example of reversible isomeric change, as represented by the scheme

$$\begin{array}{ccccc} CH_3 . C \equiv N & \longleftarrow & H . C \equiv N \rightleftharpoons H . N = C\langle & \longrightarrow & CH_3 . N = C\langle \\ \text{Methyl cyanide.} & & \text{Prussic acid.} & & \text{Methyl } \textit{iso}\text{cyanide.} \end{array}$$

---

* 'Ann. Chim. Phys.,' vol. 17, p. 103 (1869).

† 'J. Chem. Soc.,' vol. 81, p. 1596 (1902).

‡ 'Rend. Acc. Lincei,' vol. 16, ii, pp. 432, 501 (1907).

§ 'Liebig's Ann.,' vol. 189, p. 44 (1877).

The two forms of the acid differ from one another only in the point at which a proton is attached to an anion, which is identical for the cyanides and *iso*cyanides,* as represented by the following electronic formulæ

$$\begin{array}{ccccc} \mathrm{H:C:::N:} & \rightleftharpoons & \overset{+}{\mathrm{H}} + \mathrm{:\overset{-}{C}:::N:} & \rightleftharpoons & \mathrm{:\overset{-}{C}:::\overset{+}{N}:H} \\ \text{Hydrogen} & & \text{Common} & & \text{Hydrogen} \\ \text{cyanide.} & & \text{anion.} & & \textit{iso}\text{cyanide.} \end{array}$$

or

$$\mathrm{H.C\equiv N} \rightleftharpoons \overset{+}{\mathrm{H}} + \overset{-}{\mathrm{C}}\mathrm{\equiv N} \rightleftharpoons \overset{-}{\mathrm{C}}\mathrm{\equiv}\overset{+}{\mathrm{N}}\mathrm{.H}$$

Unlike the alkyl-derivatives, therefore, the ionised metallic salts exist only in one form, which can be described equally well as cyanide or *iso*cyanide.

Butlerow postulated that the reversible isomeric change of the two forms of prussic acid (unlike that of the *iso*dibutylenes) could proceed *in the absence of a catalyst.* In view of the unusual character of the isomerism, which involves an $\alpha\beta$ migration of a proton, *without any secondary re-arrangement of valency electrons*, this contention may be still valid, in spite of the fact that, in prototropic changes involving an $\alpha\gamma$-migration, it has been demonstrated repeatedly during the past 30 years that a catalyst is required to promote isomeric change, even when so strong an acid as nitrocamphor is dissolved in an inert solvent. In agreement with Butlerow's hypothesis, therefore, Kurt Meyer and Hopff† were unable to effect any separation of isomers from prussic acid by the method of "aseptic distillation" which Meyer had applied successfully to ethyl acetoacetate; and, as long ago as 1869, Gautier (*loc. cit.*) failed to effect any separation by fractional crystallisation of not less than 600 grams of the liquid acid.‡

These results could be explained equally well, however, by supposing that the equilibrium is so one-sided that only a trace of a labile isomeride exists in equilibrium with a large excess of the stable isomeride; and this point of view appears to be acquiesced in very generally. Experimental support for it has been found by Usherwood§ in measurements of specific heat, which "point to the existence in hydrocyanic acid of an equilibrium in which formonitrile is by far the more important constituent," the proportion of HNC being estimated at about 0·5 per cent.; and more recently Dadieu,[*] from a comparison of the intensity of the lines of the Raman spectrum of the liquid with those of alkyl cyanides and *iso*cyanides, concluded that "the proportion of *iso*-acid might be of the order of ½ per cent."

---

* *Cf.* Lowry, 'J. Chem. Soc.,' vol. 123, p. 828 (1923).

† 'Ber. deuts. chem. Ges.,' vol. 54, p. 1709 (1921).

‡ The supposed separation of two isomeric acids by Enklaar ('Rec. trav. Chim.,' vol. 42, p. 1000 (1923), vol. 44, p. 889 (1925), vol. 45, p. 414 (1926)) has been denied by Coates, Hinkel and Angel ('J. Chem. Soc.,' p. 540 (1928)).

§ 'J. Chem. Soc.,' vol. 121, p. 1604 (1922).

A comparison of the molecular refraction of the gas ($[R_L]_D$ for HCN = 6·63, $CH_3.CN$ = 11·10, $C_2H_5.CN$ = 15·76) with his own values for the homologous cyanides led Brühl[†] to conclude that prussic acid had the cyanide structure; but the agreement of the observed with the extrapolated value was by no means complete. A similar conclusion was drawn by Meyer and Hopff (*loc. cit.*) from a comparison of their own measurements of the refractive indices of the liquid acid with earlier values for methyl and ethyl cyanides and for ethyl *iso*cyanide :—

	$[R_L]_\alpha$	$[R_L]_D$	$[R_L]_\gamma$
HCN (calculated)	6·48	6·52	6·63
HNC (calculated)	7·25		7·44
Found	6·45	6·48	6·65
HCN per cent.	−3·9		+2·4

The observed molecular refraction of the liquid acid, $[R_L]_D = 6·48$, was similar to that of the vapour, which would not be expected if either were an equilibrium mixture of labile isomerides. The value recorded agreed best "with the assumption that free prussic acid is identical with formonitrile." When compared with extrapolated values for HCN and HNC, their values for $[R_L]_\alpha$ and $[R_L]_\gamma$ correspond with small negative and positive percentages of the latter as shown in the preceding table. An opposite conclusion was reached, however, by Enklaar from a study of refractive dispersions, which gave values nearly midway between those calculated for the cyanide and *iso*cyanide.

Since no complete study of the refractive dispersion of this series of compounds has ever been made, it appeared desirable to apply to them the methods which have recently been developed for this purpose by Lowry and Allsopp.[‡] Refractive indices have therefore been determined, over a wide range of the visible and ultraviolet spectrum, for methyl and ethyl cyanides and *iso*cyanides, and for liquid prussic acid. The results are set out in Tables I to VI, and are shown graphically in figs. 1 and 2.

---

[*] 'Ber. deuts. chem. Ges.,' vol. 64, p. 358 (1931).

[†] 'Z. phys. Chem.,' vol. 16, p. 512 (1895).

[‡] 'Proc. Roy. Soc.,' A, vol. 133, p. 26 (1931).

Table I.—Refractive Indices.

Wave-length.		HCN (5 series).	CH_3CN (5 series).*	C_2H_5CN (5 series).†	CH_3NC (1 series).	C_2H_5NC (2 series).
Li	6707·86	1·25994 (+8)	1·34188 (+4)	1·36388 (−6)	1·34233 (−3)	1·36036 (+9)
Cd	6438·47	1·26028 (−1)	1·34244 (+2)	1·36453 (−1)	1·34311 (+7)	1·36099 (+2)
Zn	6362·34	1·26041 (−1)	1·34256 (−3)	1·36474 (+1)	1·34325 (0)	1·36119 (+1)
Li	6103·6	1·26098 (+6)	1·34322 (−2)	1·36544 (+2)	1·34402 (−1)	1·36203 (+6)
Na	5895·93	1·26136 (0)	1·34388 (+6)	1·36605 (+2)	1·34473 (0)	1·36271 (+4)
Hg	5790·66	1·26161 (+1)	1·34426 (+11)	1·36645 (+7)	1·34520 (+8)	1·36312 (+5)
Cu	5782·15	1·26161 (−1)	1·34426 (+9)	1·36645 (+5)	1·34514 (−1)	1·36314 (+4)
Hg	5769·60	1·26176 (+11)	1·34430 (+9)	1·36652 (+7)	1·34526 (+6)	1·36322 (+7)
Cu	5700·24	1·26185 (+3)	1·34447 (+3)	1·36672 (+4)	1·34546 (−1)	1·36348 (+6)
Ba	5535·53	1·26232 (+7)	1·34509 (+8)	1·36732 (+3)	1·34623 (+7)	1·36407 (−4)
Ag	5471·51	1·26237 (−6)	1·34520 (−4)	1·36750 (−3)	1·34644 (0)	1·36437 (−3)
Hg	5460·73	1·26247 (+1)	1·34536 (+8)	1·36767 (+9)	1·34656 (+7)	1·36451 (+6)
Cu	5220·06	1·26316 (−4)	1·34626 (0)	1·36861 (0)	1·34758 (−9)	1·36564 (+1)
Ag	5209·04	1·26320 (−4)	1·34626 (−5)	1·36864 (−2)	1·34769 (−3)	1·36568 (−1)
Cu	5153·26	1·26341 (+1)	1·34653 (−1)	1·36891 (−1)	1·34794 (−8)	1·36600 (+1)
Cu	5105·55	1·26359 (0)	1·34678 (0)	1·36915 (−1)	1·34827 (−2)	1·36625 (−2)
Cd	5085·82	1·26355 (−11)	1·34682 (−5)	1·36922 (3)	1·34839 (−1)	1·36633 (−5)
Ba	4934·10	1·26429 (+6)	1·34754 (−8)	1·37001 (−3)	1·34930 (−6)	1·36731 (+2)
Zn	4810·53	1·26473 (0)	1·34823 (−6)	1·37070 (−5)	1·35003 (−8)	1·36810 (−1)
Cd	4799·91	1·26477 (0)	1·34824 (−11)	1·37080 (−2)	1·35013 (−5)	1·36816 (−2)
Zn	4722·16	1·26502 (−10)	1·34876 (−4)	1·37126 (−3)	1·35072 (−1)	1·36871 (−2)
Zn	4680·14	1·26522 (−9)	1·34901 (−4)	1·37141 (−15)	1·35097 (−6)	1·36904 (0)
Cd	4678·15	1·26522 (−10)	1·34892 (−14)	1·37158 (0)	1·35098 (−7)	1·36904 (−1)
Li	4603·0	1·26570 (+3)	1·34949 (−5)	1·37206 (−2)	1·35163 (+1)	1·36957 (−6)
Ba	4554·04	1·26597 (+5)	1·34981 (−5)	1·37235 (−7)	1·35195 (−6)	1·37020 (+18)
Hg	4358·34	1·26700 (+2)	1·35138 (+11)	1·37405 (+15)	1·35389 (+18)	1·37193 (+19)
Mean deviation		±4·3	±5·7	±4·2	±4·7	±4·5
Mean error		−0·1	−0·2	0·0	−0·5	+2·5

* Two with a 90° prism and 3 with a 60° prism.

† One with a 90° prism and 4 with a 60° prism.

The numbers in brackets show the differences, (obs. − calc.) × 10^5, from the values calculated from the formulæ in Table VII.

Refractometer Measurements.

The visual readings were made with a Pulfrich refractometer. A 90° prism was first used to measure the refractive indices of the two cyanides, but those of prussic acid were too low to be measured in this way. A 60° prism was therefore procured and used to measure the refractive indices of the acid and of the two *iso*cyanides, as well as for additional series of measurements of the two cyanides.

The divided circle of the instrument had been provided with a much finer scale, as recommended by Geffcken and Kohner.‡ With the help of this fine adjustment, the prism was calibrated to *five* decimals, for 26 lines derived

---

‡ 'Z. phys. Chem.,' B, vol. 1, p. 456 (1927).

Table II.—Molecular Refractions.

Formula of Lorenz and Lorentz, $[R_L]_\lambda = \frac{n^2 - 1}{n^2 + 2} \cdot \frac{M}{d}$.

Wave-length.	C_2H_5NC.	C_2H_5CN.	CH_3NC.	CH_3CN.	HNC *(calc.).*	HCN *(calc.).*	$HCN \rightleftharpoons HNC$ *(obs.).*	HNC per cent.
Li 6707·86	16·410	15·672	11 602	11 046	6·794	6 420	6·435	4·0
Cd 6438·47	16·436	15 698	11 626	11 062	6·816	6·426	6·442	4·1
Zn 6362·34	16·444	15·706	11·630	11 066	6·816	6·426	6·446	5·1
Li 6103·6	16·479	15·733	11·654	11·085	6·829	6·437	6·459	5·6
Na 5895·93	16·506	15·756	11·676	11·104	6·846	6·452	6·468	4·1
Hg 5790·66	16·523	15·772	11 690	11 115	6·857	6·458	6 473	3·8
Cu 5782·15	16·524	15·772	11·688	11 115	6·852	6·458	6·473	3·8
Hg 5769·60	16 527	15·774	11·692	11·116	6·857	6 458	6·477	4·8
Cu 5700·24	16·538	15·782	11·698	11·121	6·858	6 460	6 478	4 5
Ba 5535·53	16 562	15·805	11·722	11·139	6·882	6 473	6·490	4 2
Ag 5471·51	16·574	15·812	11·728	11·143	6·882	6·474	6·491	4·2
Hg 5460·73	16·580	15·819	11·732	11·147	6 884	6 475	6·493	4 4
Cu 5220 06	16·626	15·855	11·763	11 174	6 900	6·493	6·509	3·9
Ag 5209 04	16·628	15·856	11·766	11·174	6·904	6·492	6·510	4 4
Cu 5153·26	16·641	15·866	11·774	11·181	6·907	6 496	6·515	4·6
Cu 5105·55	16·651	15·876	11·784	11 189	6·917	6·502	6·521	4·6
Cd 5085·82	16·654	15·878	11·788	11·190	6·922	6·502	6·520	4·3
Ba 4934·10	16·694	15·909	11·815	11·211	6·936	6·513	6·535	5·2
Zn 4810·53	16·726	15 935	11·838	11·231	6·950	6·527	6·545	4 3
Cd 4799·91	16·728	15·939	11·841	11·231	6·954	6·523	6·546	5 3
Zn 4722·16	16·751	15·957	11·859	11·247	6 967	6·537	6·551	3·7
Zn 4680·14	16·764	15·962	11·866	11·254	6·968	6·546	6·556	2 4
Cd 4678·15	16·764	15·969	11·867	11·251	6·970	6 533	6 556	5·3
Li 4603·0	16 786	15·988	11·886	11·268	6·986	6·548	6·567	4·3
Ba 4554·04	16·812	16·002	11·896	11·277	6·980	6·552	6·574	5·0
Hg 4358·34	16·882	16·064	11·955	11 323	7·028	6·582	6·597	3·4
							Mean	+4·3

from the arc spectra of lithium, sodium, barium, mercury, silver-cadmium and brass. These were thrown into the field of view of the refractometer by means of a constant deviation spectroscope arranged as a monochromator, so that only a small range of the spectrum was visible for any given setting of the spectroscope.

A quartz plate cut perpendicularly to the optic axis was used for the calibration, readings being taken both of the ordinary and of the extraordinary ray. The refractive indices were interpolated from Gifford's values, for the ordinary ray by means of Coode Adams' equation* corrected to 20°, and for the extraordinary ray by an appropriate modification of this equation.

As a protection against escape of prussic acid, the instrument was enclosed in a box connected with an exhaust fan, leaving only the scale and telescopes exposed. Advantage was then taken of this arrangement in order to produce

---

* 'Proc. Roy .Soc.,' A, vol. 117, p. 209 (1927).

Table III.—Molecular Refractions.

Formula of Eykman, $[R_E]_\lambda = \frac{n^2 - 1}{n + 0{\cdot}4} \cdot \frac{M}{d}$.

Wave-length.	C_2H_5NC.	C_2H_5CN.	CH_3NC.	CH_3CN.	HNC (calc.).	HCN (calc.).	$HCN \rightleftharpoons HNC$ (obs.).	HNC per cent.
Li 6707·86	35·896	34·298	25·317	24·101	14·738	13·904	13·907	0·36
Cd 6438·47	35·955	34·356	25·372	24·139	14·789	13·922	13·924	0·23
Zn 6362·34	35·974	34·375	25·381	24·146	14·788	13·917	13·931	1·61
Li 6103·6	36·054	34·438	25·435	24·191	14·816	13·944	13·960	1·84
Na 5895·93	36·118	34·492	25·485	24·235	14·852	13·978	13·980	0·23
Hg 5790·66	36·156	34·528	25·518	24·260	14·880	13·992	13·992	0·0
Cu 5782·15	36·159	34·528	25·514	24·260	14·869	13·992	13·992	0·0
Hg 5769·60	36·166	34·534	25·522	24·263	14·878	13·992	14·000	0·90
Cu 5700·24	36·190	34·552	25·536	24·277	14·882	14·002	14·005	0·34
Ba 5535·53	36·246	34·605	25·590	24·316	14·934	14·027	14·029	0·22
Ag 5471·51	36·274	34·621	25·605	24·323	14·936	14·025	14·031	0·66
Hg 5460·73	36·288	34·637	25·614	24·334	14·940	14·031	14·036	0·55
Cu 5220·06	36·394	34·721	25·685	24·394	14·976	14·067	14·071	0·44
Ag 5209·04	36·398	34·723	25·693	24·394	14·988	14·065	14·074	0·97
Cu 5153·26	36·428	34·748	25·711	24·412	14·994	14·076	14·085	0·98
Cu 5105·55	36·452	34·769	25·733	24·429	15·014	14·089	14·094	0·54
Cd 5085·82	36·459	34·775	25·742	24·432	15·025	14·089	14·092	0·32
Ba 4934·10	36·552	34·846	25·806	24·480	15·060	14·114	14·130	1·69
Zn 4810·53	36·626	34·906	25·857	24·526	15·088	14·146	14·152	0·64
Cd 4799·91	36·632	34·916	25·864	24·526	15·096	14·136	14·154	1·88
Zn 4722·16	36·684	34·957	25·905	24·561	15·126	14·165	14·168	0·31
Zn 4680·14	36·715	34·970	25·923	24·578	15·131	14·186	14·178	−0·85
Cd 4678·15	36·715	34·985	25·924	24·572	15·133	14·159	14·177	1·85
Li 4603·0	36·764	35·028	25·969	24·610	15·174	14·192	14·201	0·92
Ba 4554·04	36·824	35·054	25·991	24·631	15·158	14·208	14·216	0·84
Hg 4358·34	36·987	35·206	26·127	24·736	15·267	14·266	14·268	0·20
							Mean ..	+0·68

Table IV.—Refractive Indices of Ethyl Isocyanide at 20°

Wave-length of coincidence.	Film.	*n* obs.	(O − C) × 10^4.	Wave-length of coincidence.	Film.	*n* obs.	(O − C) × 10^4.
Fe 4282·4	*a*	1·3731	+6	Fe 3397·0	*a*	1·3857	+2
Fe 4184·9	*a*	1·3731	−4	W 3311·4	*b*	1·3868	−6
Fe 4170·9	*a*	1·3740	+3	Fe 3292·0	*a*	1·3881	+3
Fe 4132·1	*a*	1·3741	0	Fe 3227·8	*a*	1·3894	0
Fe 4014·5	*a*	1·3753	−2	Fe 3214·1	*b*	1·3895	−2
Fe 3930·3	*a*	1·3773	+8	Fe 3180·2	*b*	1·3902	−4
Fe 3883·3	*a*	1·3774	+3	Fe 3151·3	*b*	1·3916	+1
Fe 3825·9	*a*	1·3779	0	Fe 3025·6	*a*	1·3953	+1
W 3780·8	*a*	1·3783	−3	Fe 3008·1	*b*	1·3955	−2
Fe 3748·3	*a*	1·3794	+3	Fe 2981·5	*b*	1·3963	−3
Fe 3738·3	*a*	1·3792	−2	Fe 2929·1	*b*	1·3982	−2
Fe 3704·5	*a*	1·3797	−1	Fe 2904·1	*b*	1·3991	−2
Fe 3621·5	*a*	1·3809	−3	Fe 2904·1	*b*	1·3996	+3
Fe 3582·2	*a*	1·3818	−1	W 2879·4	*b*	1·4004	+2
Fe 3542·1	*a*	1·3820	−6	Fe 2739·6	*b*	1·4064	+4
Fe 3497·8	*a*	1·3827	−7	Fe 2613·8	*b*	1·4125	+2
Fe 3427·1	*a*	1·3848	0				

Mean deviation of 33 readings .... ±0·00028
Mean error .... −0·00003

Table V.—Refractive Indices of Ethyl Cyanide at 20°.

Wave-length of coincidence.	Film.	*n* obs.	(O − C) × 10^4.	Wave-length of coincidence.	Film.	*n* obs.	(O − C) × 10^4.
Fe 5001·9	*g*	1·3692	−5	Fe 3370·8	*c*	1·3852	−10
Fe 4919·0	*g*	1·3697	−4	Fe 3370·8	*c*	1·3855	−7
W 4843·8	*f*	1·3701	−4	Fe 3314·7	*g*	1·3873	0
W 4757·6	*f*	1·3711	0	Fe 3306·4	*c*	1·3865	−10
Fe 4745·8	*f*	1·3714	+2	Fe 3268·2	*g*	1·3882	−2
W 4659·9	*f*	1·3717	0	Fe 3257·6	*d*	1·3881	−4
Fe 4619·3	*f*	1·3722	+3	Fe 3254·4	*g*	1·3879	−6
Fe 4547·8	*c*	1·3731	+7	Fe 3233·1	*g*	1·3885	−5
W 4513·1	*e*	1·3727	0	Fe 3233·1	*f*	1·3890	0
Fe 4476·0	*g*	1·3731	+2	Fe 3222·1	*g*	1·3892	0
Fe 4447·7	*e*	1·3727	−5	Fe 3215·9	*f*	1·3896	+2
Fe 4442·3	*g*	1·3733	+1	Fe 3214·1	*f*	1·3894	0
Fe 4422·6	*f*	1·3735	+1	Fe 3212·0	*g*	1·3902	+7
W 4408·3	*g*	1·3731	−4	Fe 3200·0	*g*	1·3894	−3
Fe 4375·9	*g*	1·3736	−1	Fe 3197·0	*f*	1·3900	+2
Fe 4375·9	*g*	1·3740	+3	Fe 3197·0	*f*	1·3906	+8
Fe 4282·4	*g*	1·3743	−2	Fe 3171·4	*d*	1·3904	0
Fe 4191·4	*g*	1·3755	+2	Fe 3142·9	*d*	1·3917	+6
Fe 4127·6	*f*	1·3768	+9	Fe 3116·6	*d*	1·3922	0
Fe 4100·7	*c*	1·3756	−6	Fe 3083·7	*c*	1·3917	−8
Fe 4076·6	*f*	1·3762	−2	Fe 3031·6	*d*	1·3931	−7
Fe 4067·6	*c*	1·3768	+3	Fe 3025·6	*h*	1·3936	−4
Fe 4044·6	*e*	1·3771	+4	Fe 3021·1	*c*	1·3935	−6
Fe 4021·9	*g*	1·3773	+3	Fe 3021·1	*g*	1·3946	+5
Fe 3997·4	*g*	1·3772	−1	Fe 3009·6	*d*	1·3942	−2
Fe 3966·1	*g*	1·3770	−6	Fe 2981·5	*d*	1·3950	−2
Fe 3942·4	*e*	1·3780	+2	Fe 2965·3	*g*	1·3962	+5
Fe 3942·4	*f*	1·3781	+3	Fe 2960·0	*d*	1·3957	−2
Fe 3886·3	*c*	1·3781	−4	Fe 2957·4	*g*	1·3957	−3
Fe 3840·4	*f*	1·3794	+4	Fe 2950·3	*g*	1·3965	+3
Fe 3827·8	*f*	1·3789	−3	Fe 2936·9	*c*	1·3965	0
Fe 3815·8	*g*	1·3793	0	Fe 2936·9	*g*	1·3968	+3
Fe 3795·0	*g*	1·3791	−6	Mn 2933·1	*d*	1·3969	+2
Fe 3756·9	*f*	1·3798	−3	Fe 2929·1	*g*	1·3962	−6
Fe 3722·6	*g*	1·3810	+4	Fe 2923·7	*g*	1·3976	+6
Fe 3676·3	*g*	1·3813	+1	Fe 2923·3	*c*	1·3974	+4
Fe 3659·5	*c*	1·3811	−3	Fe 2912·2	*d*	1·3972	−1
Fe 3631·5	*g*	1·3817	−2	Fe 2912·2	*h*	1·3973	0
Fe 3589·1	*g*	1·3827	+2	Fe 2901·9	*g*	1·3969	−7
Fe 3545·6	*g*	1·3828	−4	Fe 2877·3	*g*	1·3987	+3
Fe 3533·1	*f*	1·3838	+4	Fe 2858·9	*h*	1·3991	+1
Fe 3529·8	*g*	1·3827	−7	Fe 2832·4	*h*	1·3997	−2
Fe 3506·5	*g*	1·3842	+4	Fe 2807·0	*h*	1·4006	−2
Fe 3489·7	*g*	1·3835	−6	Fe 2795·0	*d*	1·4012	0
Fe 3475·6	*g*	1·3845	+2	Fe 2753·3	*d*	1·4033	+5
Fe 3465·9	*g*	1·3847	+2	Fe 2737·3	*d*	1·4039	+5
Fe 3440·8	*e*	1·3851	+2	Fe 2620·4	*h*	1·4081	−2
Fe 3427·1	*g*	1·3855	+3	Fe 2577·9	*h*	1·4100	−2
Fe 3413·1	*g*	1·3853	−1	Fe 2537·2	*h*	1·4121	−1
Fe 3399·3	*g*	1·3860	+3				

Four readings omitted.

Mean deviation of 99 readings . . ±0·00033

Mean error . . . . −0·00004

Table VI.—Refractive Indices of Methyl Cyanide at 20°.

Wave-length of coincidence.	Film.	*n* obs.	(O – C) × 10^4.	Wave-length of coincidence.	Film.	*n* obs.	(O – C) × 10^4.
Fe 4957·5	*q*	1·3475	0	Fe 3582·2	*k*	1·3600	+5
W 4843·8	*m*	1·3476	–5	Fe 3576·8	*n*	1·3600	+4
W 4799·9	*k*	1·3485	+2	Fe 3556·9	*m*	1·3590	–9
W 4757·7	*o*	1·3490	+4	Fe 3541·1	*k*	1·3610	+9
Fe 4741·5	*q*	1·3481	–6	Fe 3526·5	*m*	1·3605	+1
Fe 4741·5	*k*	1·3485	–2	Fe 3476·7	*o*	1·3613	+2
Fe 4619·3	*k*	1·3493	–2	Fe 3465·9	*n*	1·3610	–3
Fe 4602·9	*q*	1·3500	+4	Fe 3450·3	*k*	1·3623	+8
Fe 4547·9	*q*	1·3502	+3	Fe 3401·5	*m*	1·3627	+4
Fe 4494·6	*m*	1·3505	+2	Fe 3370·8	*m*	1·3631	+2
Fe 4494·6	*q*	1·3505	+2	W 3311·4	*o*	1·3637	–2
Fe 4442·3	*q*	1·3507	0	Fe 3225·8	*p*	1·3662	+5
Fe 4442·3	*m*	1·3512	+5	Fe 3222·1	*n*	1·3657	0
Fe 4422·6	*n*	1·3508	0	Fe 3214·5	*k*	1·3668	+9
Fe 4367·6	*q*	1·3515	+3	Fe 3180·7	*q*	1·3665	–1
Fe 4352·7	*o*	1·3517	+3	Fe 3116·6	*o*	1·3676	–5
Fe 4337·1	*m*	1·3514	–1	Fe 3100·3	*m*	1·3686	+2
Fe 4337·1	*n*	1·3517	–4	Fe 3091·6	*n*	1·3682	–4
Fe 4294·1	*q*	1·3519	+1	Fe 3059·1	*l*	1·3697	+3
Fe 4202·0	*q*	1·3530	+4	Fe 3042·7	*l*	1·3697	–1
Fe 4191·4	*k*	1·3532	+5	Fe 2970·1	*q*	1·3719	+2
Fe 3935·8	*o*	1·3551	0	Fe 2966·9	*l*	1·3715	–3
Fe 3888·5	*m*	1·3559	+3	Fe 2936·9	*m*	1·3727	0
Fe 3859·9	*o*	1·3550	–9	Fe 2936·9	*n*	1·3730	+3
Fe 3834·2	*k*	1·3557	–5	Fe 2918·0	*p*	1·3731	–1
Fe 3815·8	*n*	1·3572	+7	Fe 2895·0	*l*	1·3733	–6
Fe 3808·7	*m*	1·3563	–3	Fe 2739·6	*l*	1·3791	+1
W 3792·8	*o*	1·3571	+3	Fe 2720·9	*l*	1·3796	–1
W 3769·9	*m*	1·3565	–5	Fe 2628·3	*l*	1·3836	+6
Fe 3733·3	*m*	1·3571	–4	Fe 2584·5	*l*	1·3855	+2
Fe 3659·5	*o*	1·3588	+3	Fe 2563·5	*l*	1·3867	+5
W 3625·4	*m*	1·3583	–6	Fe 2527·3	*l*	1·3885	+6
Fe 3594·6	*o*	1·3589	–4	Fe 2496·5	*l*	1·3897	+3
W 3592·4	*m*	1·3592	–2	Fe 2473·1	*l*	1·3916	+11

Three readings omitted.

Mean deviation of 68 readings . .	±0·00035
Mean error	+0·00008

an improved control of temperature. For this purpose a heater was inserted in the inlet duct, and operated by a spiral toluene regulator in the box, so that the instrument was bathed constantly in air at 20° ± 0·2°, and the usual effects of atmospheric cooling were thus almost completely eliminated. The liquid was contained in a totally enclosed glass cell, of the type used by Geffcken and Kohner in order to avoid changes of concentration when measuring the refractive indices of salt-solutions. Its temperature was controlled directly by an internal circulation of water from a thermostat at 20° ± 0·1°. The cell was fastened to the prism by means of " Sylca " translucent dental cement, and was clamped to the instrument by means of a brass ring. The block round the prism was also provided with the usual flow of water from the thermostat.

The better control of temperature, and the much greater accuracy of the readings on the finely divided circle, produced a remarkable improvement in the accuracy of the refractive indices throughout the visible spectrum. Thus, determinations made in this laboratory just before these improvements had been effected showed mean deviations from the dispersion-equations as follows:—

Cyclohexane	± 0·00012	(9 lines).
,, ...	± 0·00017	(21 lines).
Benzene	± 0·00016	(22 lines).

In the present experiment the mean deviations were as follows:—

HCN	± 0·00004	(26 lines).
CH_3CN	± 0·00006	,,
C_2H_5CN	± 0·00004	,,
CH_3NC	± 0·00005	,,
C_2H_5NC	± 0·00005	,,

It therefore appears that the errors of reading have been reduced to one-third and that refractive indices can now be read with a mean deviation of only half a unit in the fourth place of decimals.

The refractive indices of the five compounds at 20° are set out in Table I for 26 wave-lengths in the visible spectrum. The number of independent series of observations is indicated at the head of each column and each series included at least five readings of each line, and many more in the case of the more difficult violet lines. Table I also shows the deviations from the formulæ, given in Table VII, which were found to represent both the visual and the photographic readings within the limits of the casual errors of observation.

The molecular refractions deduced from the refractometer readings by means of the formulæ of Lorenz and Lorentz and of Eykman are set out in Tables II and III. Columns 6 and 7 of these tables show the molecular refractions of the two forms of prussic acid as calculated by extrapolation from the molecular refractions of the homologous *iso*cyanides and cyanides. The observed molecular refractions of the acid agree fairly closely throughout the spectrum with those deduced by extrapolation from the homologous cyanides, but differ widely from the values calculated from the *iso*cyanides. The molecular refractions calculated by the formula of Lorenz and Lorentz correspond with the presence of 4·3 per cent. of *iso*cyanide in the liquid, as indicated in the last column of Table II; but this is actually within the limits of accuracy of the method of extrapolation, since the molecular refractions deduced from the formula of Gladstone and Dale lie *outside* the calculated values for the two isomers, to an extent which would correspond to a concentration of *minus* 6 per cent. of *iso*cyanide. It is therefore not surprising to find that the empirical formula of Eykman* $[R] = \frac{n^2 - 1}{n + 0 \cdot 4} \frac{M}{d}$, which eliminates the effect of temperature more completely than either of the others, gives an almost complete agreement between the observed values and those extrapolated from the homologous cyanides. The apparent concentration of *iso*cyanide as indicated in the last column of Table III is thus reduced to 0·7 per cent., in close general agreement with the conclusions reached by Usherwood and by Dadieu.

These relationships are set out graphically in fig. 1, where the molecular

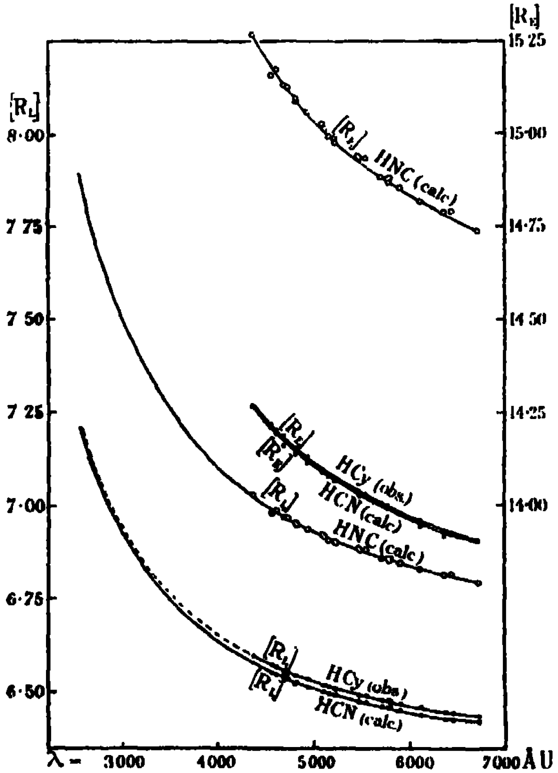

FIG. 1.—Molecular Refractions.

---

* 'Rec. trav. chim.,' vol. 14, p. 185 (1895), vol. 15, p. 52 (1896).

refractions deduced from the formula of Lorenz and Lorentz are shown in the lower part of the diagram, whilst those deduced from the formula of Eykman are shown above.

Interferometer Measurements.

The significance of refractive indices can only be judged satisfactorily from a study of complete curves of refractive dispersion. Our measurements were therefore extended into the ultra-violet by photographic observations of the interference bands formed in thin films of liquid enclosed between the quartz plates of an etalon, according to the method developed by Lowry and Allsopp (*loc. cit.*). This method enables measurements to be made almost up to the limit of transmission of light by thin films of the liquid. In practice, values were obtained over a range which extended from about 5000 Å.U. in the green-blue region of the spectrum to about 2400 Å.U. in the ultra-violet, *i.e.*, almost to the point at which the spectrum of the iron arc weakens abruptly at 2327 Å.U. The number of wave-lengths for which refractive indices can be deduced is also very large, since as many as 200 values may be read from a single exposure. Unfortunately they cannot be averaged in the same way as the refractometer readings, since each series refers to a different selection of spectrum lines; the results therefore appear to be less accurate than is really the case.

The etalon used for these measurements has already been described by Lowry and Allsopp.* The necessity for working in a draught was again made use of in order to control the temperature of the air with which the instrument was surrounded. No special difficulty was experienced in securing interference fringes from films of the homologous cyanides and *iso*cyanides, but the interference bands were not quite so sharp as usual. Methyl *iso*cyanide was not examined in this way, since the purified material was lost by explosion in the course of the refractometric work. Films of prussic acid were less easy to prepare, since the liquid boils at 26°, and there is therefore a margin of only 6° from the temperature of observation. Six films were, however, prepared and photographed, and a total of about 240 refractive indices was read off from the plates. These show a satisfactory agreement with values deduced by extrapolation from the visual readings with the refractometer, but they are spread out much more widely than the readings for the homologues, probably because it was quite impossible to control the temperature of so volatile a liquid. Three of the best series of observations are reproduced in fig. 2.

---

* 'Proc. Roy. Soc.,' A, vol. 126, p. 165 (1929), vol. 133, p. 26 (1931).

Refractive indices were determined with the help of films of the following thickness :—

Substance.	Number of readings.	Thickness of film.
C_2H_5NC	136	*a* 11·3, *b* 11·1 μ.
C_2H_5CN	271	*c* 6·0, *d* 6·0, *e* 11·0, *f* 18·7, *g* 10·5, *h* 10·4 μ.
CH_3CN	172	*k* 6·5, *l* 41·3, *m* 13·5, *n* 8·0, *o* 7·4, *p* 6·4, *q* 27·8 μ.
HCN	241	*r* 9·3, *s* 9·2, *t* 8·7, *u* 8·2, *v* 11·9, *w* 11·6 μ.

The total number of readings was so great that it is not practicable to reproduce in full the tables in which they are set out. Tables IV, V and VI therefore *show only those readings in which the centre of an interference fringe coincided* with the intersection of a spectral line by one or other of the reference lines running across the spectrum; all readings for which the wave-length had to be interpolated from those of adjacent spectrum lines have been omitted from the tables, although some of these were actually used to deduce the order of the interferences from observations in the overlap between the visual and photographic series. A few erroneous readings were detected by graphical interpolation and were not used for further calculation.

In addition to refractive indices for given wave-lengths, the tables indicate the film with which each observation was made, and show the deviations of the observed refractive indices from those calculated by means of the equations in Table VII. The mean deviations are as follows :—

$C_2H_5 . NC$	± 0·00028	(33 readings)
$C_2H_5 . CN$	± 0·00033	(99 „)
$CH_3 . CN$	± 0·00035	(68 „)

These are of similar magnitude to those recently recorded for :—

Cyclohexane	± 0·0004	(97 readings)
„	± 0·0004	(31 „)
Benzene	± 0·00031	(52 „)
„	± 0·00056	(52 „)

Fig. 2 shows the whole of the refractive indices deduced from the interferometric readings for methyl and ethyl cyanides and for ethyl *iso*cyanide. Since the order of the interference bands is deduced from the overlap between the visual and photographic readings, these necessarily form a continuous curve. An arbitrary scale of ordinates has been employed, in order to economise space and prevent overlapping, but the magnitude of this scale is constant throughout. At the top of the diagram (in spite of the smallness of the absolute values) we have shown the visual readings for prussic acid itself, together with the three series of photographic readings which approximate most closely to the mean of the series.

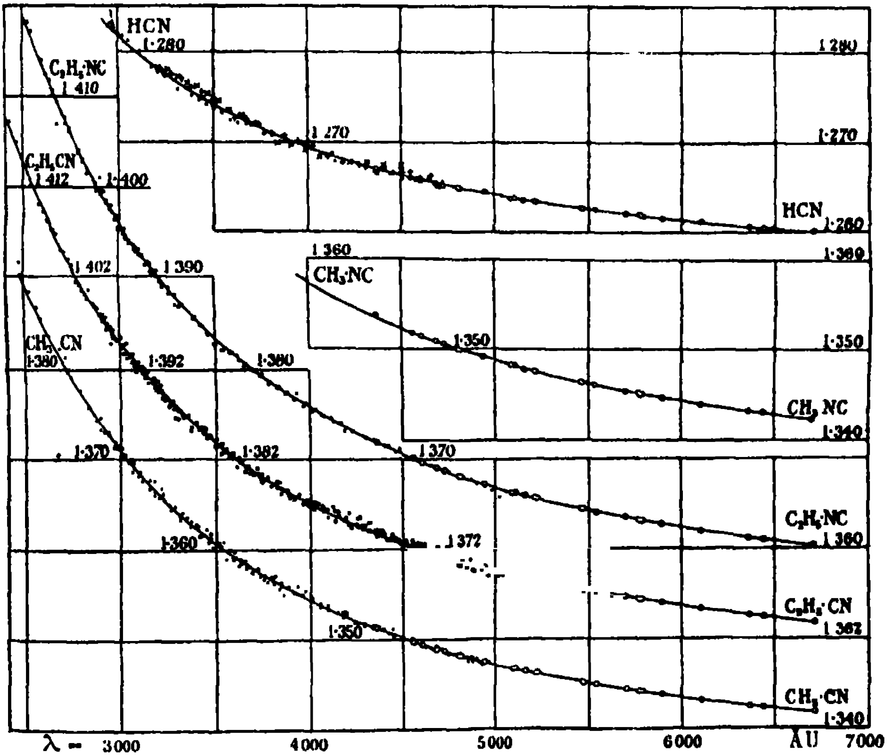

FIG. 2.—Refractive Indices. Each square represents 0·01 on the vertical scale and 500 Å.U. on the horizontal scale.

Dispersion Equations.

The equations used to represent the refractive indices are set out in Table VII.

The calculation of the constants in these equations was simplified greatly by making use in the first instance of Sellmeier's equation, since this contains only *two* arbitrary constants, which can therefore be deduced as easily as the two constants of Drude's equation for simple rotatory dispersion. The

Table VII.—*Dispersion Equations.*

	Sellmeier.	Ketteler-Helmholtz.	λ_0
C_2H_5NC	$n^2 - 1 = \frac{0 \cdot 82880\ \lambda^2}{\lambda^2 - 0 \cdot 011385}$	$n^2 = 1 \cdot 82880 + \frac{0 \cdot 009442}{\lambda^2 - 0 \cdot 011385}$	1067 Å.U.
CH_3NC	$n^2 - 1 = \frac{0 \cdot 78094\ \lambda^2}{\lambda^2 - 0 \cdot 011770}$	$n^2 = 1 \cdot 78094 + \frac{0 \cdot 009192}{\lambda^2 - 0 \cdot 011770}$	1085 Å.U.
C_2H_5CN	$n^2 - 1 = \frac{0 \cdot 84143\ \lambda^2}{\lambda^2 - 0 \cdot 009880}$	$n^2 = 1 \cdot 84143 + \frac{0 \cdot 008314}{\lambda^2 - 0 \cdot 009880}$	994 Å.U.
CH_3CN	$n^2 - 1 = \frac{0 \cdot 78296\ \lambda^2}{\lambda^2 - 0 \cdot 009880}$	$n^2 = 1 \cdot 78296 + \frac{0 \cdot 007736}{\lambda^2 - 0 \cdot 009880}$	994 Å.U.
HCN	$n^2 - 1 = \frac{0 \cdot 57476\ \lambda^2}{\lambda^2 - 0 \cdot 009565}$	$n^2 = 1 \cdot 57476 + \frac{0 \cdot 005498}{\lambda^2 - 0 \cdot 009565}$	978 Å.U.

dispersion-constants thus deduced refer to wave-lengths which are so remote that they can be introduced at once into the Ketteler-Helmholtz equation. The refractive index at infinite wave-length was also deduced from the Sellmeier equation so that the number of arbitrary constants in the Ketteler-Helmholtz equation was reduced to *one*, which could be calculated at once without difficulty. This procedure not only requires less work than is needed to deduce the three constants directly by means of three simultaneous equations, but it diminishes substantially the sensitiveness of the solutions of these equations to small experimental errors. The constants deduced in this way may therefore prove to be more precise than those deduced directly, and thus require less adjustment to make them fit the experimental data.

The equations in Table VII indicate that, whilst the dispersion of the *iso*cyanides is controlled by a characteristic frequency at 1085 to 1067 Å.U., that of the cyanides is controlled by a frequency at 994 Å.U. The frequency for prussic acid is very similar to that of the cyanides, but occurs at a rather shorter wave-length, namely 978 Å.U. The other important constants of these equations are the refractive indices for infinite wave-length. When these are used to calculate molecular refractions, as in Table VIII, the results obtained are very similar to those given by the lines of the visible spectrum, the proportions of *iso*cyanide deduced from the three formulæ being −6·2, +5·8 per cent., and 2·0 per cent. We therefore conclude that the liquid consists predominantly of hydrogen cyanide, and that, if any *iso*cyanide is present, the proportion is too small to be detected by the method now under consideration.

Table VIII.—Molecular Refractions at Infinite Wave-length.

	Gladstone–Dale.	Lorenz-Lorentz.	Eykman.
C_2H_5NC	26·175	16·081	35·137
CH_3NC	18·402	11·362	24·767
Theoretical for HNC	10·629	6·643	14·397
C_2H_5CN	25·108	15·406	33·683
CH_3CN	17·580	10·852	23·658
Theoretical for HCN	10·052	6·298	13·633
HCy	10·016	6·318	13·648
HNC (per cent.)	−6·2	+5·8	+2·0

Materials.—Prussic acid was prepared by the action of 60 per cent. H_2SO_4 on 30 per cent. KCN. The vapour was dried by calcium chloride at 30–35° and condensed to a liquid. This was redistilled twice from phosphoric oxide, the range of 0·1° being reduced to 0·05° in the second distillation. The pure acid boiled at 25·75 ± 0·05° (corr.) at 760 mm. pressure, and froze at − 13·35° ± 0·05°. Two determinations of density gave 0·6874 and 0·6878 at 20°/4°. It was prepared in quantities of about 25 c.c. and stored as a solid in a freezing-mixture of solid carbon dioxide with alcohol or ether, which was renewed after 2 or 3 days when necessary.

Acetonitrile was purified by contact with potassium hydroxide and then with calcium chloride and distilled from phosphoric oxide. Repeated fractionation of 680 c.c. through a Dufton column gave 500 c.c. boiling between 81·67° and 81·73° (corr.) at 761·5 mm. pressure; the freezing-point of the pure compound was found by means of a thermocouple to be — 44°. Two determinations of density gave 0·7825 and 0·7827 at 20°/4°.

Propionitrile was treated with a small amount of concentrated hydrochloric acid to remove possible traces of *iso*cyanide, made alkaline after 18 hours, separated from the aqueous layer, dried over calcium chloride and fractionated over phosphoric oxide. After three fractionations and one further distillation, 260 c.c. gave 180 c.c. boiling at 96·86° to 97·02° (corr.) at 752·5 mm. pressure. Two determinations of density gave 0·7827 and 0·7826 at 20°/4°.

Methyl isocyanide was prepared by mixing equal weights (about 100 grams each) of redistilled* methyl iodide and dry silver cyanide in a stout-walled bottle, which was closed quickly with a rubber stopper and fastened with wire.

---

* On one occasion, when recovered methyl iodide was used, the bottle burst about 10 minutes after mixing, leaving a tarry residue, perhaps as a result of vigorous polymerisation.

The bottle was heated slowly in a bath of water to 50° in the course of 3 hours, kept for 4 hours more at 50-60°, and cooled. The excess of methyl iodide was then poured off, and the solid product, consisting of silver iodide and the *iso*cyanide complex, AgCN, CH_3NC, was broken up, transferred to a bolt-head flask, washed with ether, warmed to expel the ether, mixed with potassium cyanide (120 gr.) and water (100 gr.) and heated in an oil bath at 100°. The oily liquid, which distilled on heating slowly to 140°, was separated from the watery layer, washed with brine and stored over quicklime. Three fractional distillations over quicklime, of a total yield of 50 c.c. (about 70 per cent. of theory), gave boiling-points ranging from 58·3–58·73°, 58·65–58·90° and 58·65–59·05° (corr.) at 758 mm. pressure. The final product (30 c.c.) had a density 0·7461, 0·7466, 0·7464, at 20°/4°. It was used 2 days later for refractometry, but was lost in a violent explosion, which took place, without flame or any visible production of carbon or tar, when resealing the glass container. The dangerous character of this endothermic compound has been mentioned by Lemoult,* but on no other occasion was anything unusual observed when sealing the *iso*cyanides in similar glass tubes.

Ethyl isocyanide was prepared by refluxing ethyl iodide (116 gr.) with dry silver cyanide (100 gr.) in a bolt-head flask of 600 c.c. capacity, under a slight excess of pressure. After 2 hours, the flask was cooled and the excess of ethyl iodide was poured off. The solid cake was washed twice with ether and dried off on the water bath. Potassium cyanide (130 gr.) and water (120 gr.) were added, and the *iso*cyanide was distilled off as before. The yield of crude *iso*cyanide was 90–95 per cent., and the recovered ethyl iodide was used again without disadvantage. *After four fractionations over quicklime through a* Dufton column, in a protected place, 100 c.c. gave 50 c.c. boiling at 78·87 to 79·19° (corr.) under 775 mm. pressure. This was sealed up over quicklime for 3 months when it became slightly yellow. When redistilled, it boiled at 78·25 to 79·16° under 771·5 mm. pressure, and its density was found to be 0·7401, 0·7414, 0·7402 at 20°/4°.

Summary.

(1) Improvements in the methods of measuring refractive indices with a refractometer are described whereby the mean deviation has been reduced to about 5 units in the fifth decimal place.

---

* 'C. R. Acad. Sci. Paris,' vol. 143, p. 902 (1906), vol. 148, p. 1603 (1909).

(2) Measurements have been made of the refractive indices of prussic acid and of the homologous methyl and ethyl cyanides and *iso*cyanides for 26 wave-lengths in the visible spectrum and over a range of wave-lengths extending to 2473 A.U. in the ultra-violet.

(3) These refractions can be expressed by equations of the Ketteler-Helmholtz type, the characteristic frequency being at 978 A.U. for prussic acid, 994 A.U. for methyl and ethyl cyanides and 1085 and 1067 A.U. for methyl and ethyl *iso*cyanides.

(4) By comparing the molecular refractions of prussic acid with those of the cyanides and *iso*cyanides it has been shown that the liquid acid consists almost exclusively of hydrogen cyanide.

A Note on the Theory of Rectification.

By A. H. Wilson, Emmanuel College, Cambridge.

(Communicated by R. H. Fowler, F.R.S.—Received January 5, 1932.)

Introduction.

1. It has long been known that certain crystal contacts will rectify alternating currents, but no entirely satisfactory theory has yet been given. The most generally accepted theory is that due to Schottky,* which has recently been discussed by van Geel.† If a metal, and a semi-conductor such as cuprous oxide or selenium, are joined together in series in such a way that the contact between them is not perfect, a large resistance is found, which varies enormously with the direction of the current. Schottky's theory assumes that, if a potential difference is created between the ends of the combination of metal and semiconductor, most of the drop in potential takes place in the transition layer between the two crystals, and electrons are drawn from one substance to the other by the high field set up. Further, owing to the differences in the inner potentials and the work functions of the two substances, the electrons are pulled out selectively, and the current-voltage curve is asymmetrical. The theory was by no means complete, the most serious objection to it being that

---

* 'Z. Physik,' vol. 14, p. 87 (1923).

† 'Z. Physik,' vol. 69, p. 765 (1931).

it did not explain why one of the components must necessarily be a semiconductor. This is not surprising, as at that time the nature of semi-conductors was unknown, but recently a theory has been proposed* which enables a start to be made on the many problems which involve semi-conductors.

When subjected to alternating current, the rectifier copper/cuprous-oxide behaves in many ways like a condenser, and the capacity of the equivalent condenser was measured by Schottky and Deutschmann.† They found that the capacity of the transition layer corresponds to a thickness of about $1 \cdot 3 \times 10^{-6}$ cm. This fact has led Schottky to doubt the adequacy of the theory. He says‡ "In any discussion of the asymmetry of the current across the transition layer, the question is met, how is it possible for an additional specific resistance to occur which is a hundred to a thousand times greater than the specific resistance of a massive oxide layer of the maximum thickness of the transition layer, while at the same time the outer oxide layer has practically the same material properties as the inner ones. If one believes that this additional resistance can be explained as a wave mechanical tunnel effect at a transition layer a few atoms thick and of unknown origin, then there is not much difficulty in interpreting the asymmetry in the current. One has only to use the wave mechanical theory of semi-conductors and assume that only a few conduction electrons are thermally excited, the majority of the electrons corresponding to the free electrons in a metal being in bound states. One can then understand qualitatively, that in one direction (from the metal to the semi-conductor) a large number of electrons can pass, while in the opposite direction only a very small current can flow. I would not care to say whether this explanation is the correct one or not, so long as it is impossible to show that the capacity of the transition layer really corresponds to an atomic thickness. . . ."

Now, although these criticisms are in the main justified, it seems as if the original Schottky theory, together with the new theory of semi-conductors, does offer a reasonable explanation of a large part of the phenomena associated with crystal detectors, which is more than can be said for any other theory yet proposed. The existence of the large additional resistance seems to demand a quantum mechanical tunnel effect as its cause. In this connection it should be kept in mind that this resistance is determined from the current-voltage curve, and is not a resistance of the ordinary type. It is in fact due to the reflexion of electrons at the transition layer, whereas the bulk resistance of a solid is due to the interaction of the electrons with the elastic vibrations. The experiment of Schottky and Deutschmann has by no means an obvious interpretation, and it is not very clear that for the purposes of the experiment the transition layer can be thought of as a condenser shunted by a resistance. To treat this question properly it would be necessary to consider the resistance of the contact as consisting of two parts. One is due to the elastic reflection of electrons at the surface of separation, and the other is the ordinary ohmic resistance due to the heat motion of the atoms. This latter resistance gives rise to a finite free path, which must determine the capacity of the layer. Unfortunately the ohmic resistance is extremely difficult to calculate, since it depends on the mean free path of electrons near the surface of a crystal, and, at the moment, surface effects can only be treated phenomenologically. At present, therefore, the possibility of answering this question, and of calculating the capacity of the transition layer must be deferred. It is, however, significant that the thickness of this layer, as determined by Schottky and Deutschmann, is of the order of the mean free path in ordinary electronic conductors.

---

* 'Proc. Roy. Soc.,' A, vol. 133, p. 458, and vol. 134, p. 277 (1931), referred to as I and II.

† 'Phys. Z.,' vol. 30, p. 839 (1929).

‡ 'Phys. Z.,' vol. 32, p. 833 (1931).

Inspite of the insufficiency of any calculations, which can be carried out at the moment, to explain all the phenomena, it still seems worth while to work out an approximate value for the apparent resistance due to the reflection of electrons at the interface, and to determine under what conditions an asymmetry in the current-voltage curve can occur. This is not really quite so simple as the statement by Schottky, quoted above, would suggest, and the correct analysis brings out quite clearly the factors involved. It is found that, with reasonable assumptions, the variation of the current with voltage and with temperature is given correctly. On the whole, it seems unlikely that a theory which can explain so many of the observed facts should be incapable of explaining the others, when it becomes possible to extend it so as to include the effect of the mean free path.

General Theory.

2.1. In any crystal rectifier there are always two contacts to consider, namely, the two at the boundaries of the semi-conductor. One of these contacts is always supposed to have a negligible rectifying effect. The justification for this is difficult to find. If the contacts are very dissimilar, then there is a rectifying effect, but, as we shall see later, the direction of easy flow is determined more by the nature of the dissimilarity than by its magnitude. For the present, however, we shall consider one contact only.

As the model of the metal we shall use that of Sommerfeld and Peierls, of which a summary is given in I, § 1.1. The valency electrons are considered as "nearly free," the mean value of the potential energy of a valency electron being E_1. To a first approximation the energy levels are given by

$$E = E_1 + \tfrac{1}{2}m\,(u^2 + v^2 + w^2), \tag{1}$$

where m is the mass of the electron, and (u, v, w) the velocity. If we take into account the deviation of the potential energy from the constant value E_1, then the energy levels are quite different for those electrons whose de Broglie wave-lengths are nearly sub-multiples of the lattice constant, but remain practically unchanged for the other electrons. This complication does not have any essential effect here, and we shall therefore use the simple formula (1) for the energy. The number of electrons per unit volume with velocity components lying in the range (du, dv, dw) is given by $n_1(uvw)du\,dv\,dw$, where n_1 is the Fermi function

$$n_1(uvw) = n_1(E) = 2\left(\frac{m}{h}\right)^3 \frac{1}{e^{\frac{E-E_0}{kT}} + 1}. \tag{2}$$

Here E_0 is an energy of the order 10 volts, and at ordinary temperatures is practically independent of the temperature.

As the model of the semi-conductor we shall use the one developed in I and II. It was there shown that at the absolute zero all the electrons are in what may be called bound states, but that at any other temperature a few electrons are thermally excited into states in which they can conduct. These electrons are, as in the case of metals, nearly free, and, if the mean value of the potential energy for these electrons is W_2, the energy levels are given by

$$E = W_2 + \tfrac{1}{2}m\,(u^2 + v^2 + w^2) \tag{3}$$

approximately, for small values of u, v, w. The distribution function depends on whether the conduction electrons are derived from impurities or not. The interesting case is when the conduction electrons are derived from impurities, the levels of the impurities having an energy W_1 $(< W_2)$. In this case the distribution function of the conduction electrons is given by

$$n_2(uvw) = 2\left(\frac{m}{h}\right)^3 B\,(kT)^{-\frac{3}{4}} \exp\{-\tfrac{1}{2}(W_2 - W_1) - \tfrac{1}{2}m\,(u^2 + v^2 + w^2)\}/kT, \tag{4A}$$

or

$$n_2(\mathrm{E}) = 2\left(\frac{m}{h}\right)^3 \mathrm{B}\,(k\mathrm{T})^{-\frac{3}{4}} \exp\{\tfrac{1}{2}(\mathrm{W}_1 + \mathrm{W}_2) - \mathrm{E}\}/k\mathrm{T}, \tag{4B}$$

which is the expression given in II, § 1, when allowance is made for the fact that we are here using the velocity components (u, v, w) instead of the more usual impulse quantum numbers (ξ, η, ζ). The constant B depends on the number of impurities ν_0 per unit volume as follows

$$\mathrm{B} = \frac{\nu_0^{\frac{1}{2}}}{2^{\frac{5}{4}}}\left(\frac{h^2}{\pi m}\right)^{\frac{3}{4}}. \tag{5}$$

It may here be remarked that for certain substances W_1 is greater than W_2. In this case the number of free electrons per unit volume is equal to ν_0, and the substance has a resistance which steadily increases with the temperature, and which increases as the substance is purified. Such semi-conductors are of little interest, and will not be considered further.

2.2. We have now to determine the equilibrium distribution when the metal and the semi-conductor are placed in contact. For simplicity we make the problem one-dimensional by considering the substances to be in contact along a plane perpendicular to the axis of x, that is, we consider the bounding surfaces to be everywhere at the same distance apart. Then the potential energy of a conduction electron is, to a first approximation, of the form given in fig. 1, the hump representing the potential energy of an electron in the gap between the two substances.

The null-point energy E_0 of the electrons in the metal, which gives the top of the Fermi distribution, and the null-point energy W_1 of the electrons in the semi-conductor are shown as dotted lines. The position of E_1 relative to W_2 is determined from the condition of equilibrium. We shall see that E_0 is approximately mid-way between W_1 and W_2.

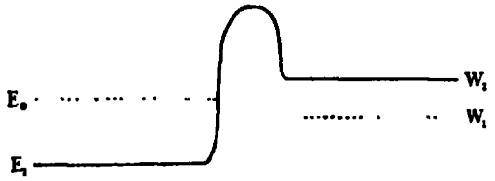

FIG. 1.

The number of electrons in the semi-conductor hitting unit area of the boundary per second with their velocities in the x direction lying between u and $u + du$ is

$$u\,du \int_{-\infty}^{\infty}\int_{-\infty}^{\infty} n_2(\mathrm{E})\,dv\,dw.$$

We change to a new variable U given by

$$\mathrm{U} = \tfrac{1}{2}mu^2.$$

The energy E is then

$$\mathrm{W}_2 + \mathrm{U} + \tfrac{1}{2}m\,(v^2 + w^2).$$

If D (E) is the transmission coefficient of the potential hump as a function of the energy, the number of electrons per unit area passing from the semi-conductor to the metal per second is

$$\frac{1}{m}\int_0^\infty d\mathrm{U}\int_{-\infty}^\infty\int_{-\infty}^\infty \mathrm{D}\,(\mathrm{E})\,n_2(\mathrm{E})\left\{1 - \tfrac{1}{2}\left(\frac{h}{m}\right)^3 n_1(\mathrm{E})\right\}dv\,dw.$$

This we shall write as

$$\frac{1}{m}\int_0^\infty d\mathrm{U}\int_{-\infty}^\infty\int_{-\infty}^\infty \mathrm{D}\,(\mathrm{W}_2+\mathrm{U})\,n_2(\mathrm{W}_2+\mathrm{U})\left\{1 - \tfrac{1}{2}\left(\frac{h}{m}\right)^3 n_1(\mathrm{W}_2+\mathrm{U})\right\}dv\,dw, \quad (6)$$

the terms $\tfrac{1}{2}m\,(v^2 + w^2)$ being omitted for simplicity of writing. The term $\{1 - \tfrac{1}{2}\,(h/m)^3\,n_1(\mathrm{E})\}$, which is characteristic of the Fermi distribution, must be inserted, since an electron can only pass into the metal if the energy level in the metal is originally unoccupied.

The number of electrons passing in the reverse direction is

$$\frac{1}{m}\int_{\mathrm{W}_2-\mathrm{E}_1}^\infty d\mathrm{U}\int_{-\infty}^\infty\int_{-\infty}^\infty \mathrm{D}\,(\mathrm{E}_1+\mathrm{U})\,n_1(\mathrm{E}_1+\mathrm{U})\left\{1 - \tfrac{1}{2}\left(\frac{h}{m}\right)^3 n_2(\mathrm{E}_1+\mathrm{U})\right\}dv\,dw, \quad (7)$$

since the transmission coefficient is zero if $\mathrm{E} < \mathrm{W}_2$, and does not depend on whether the electrons are moving from the metal to the semi-conductor or *vice versa*. Changing the variable in the last expression, we see that the resultant current from the metal is

$$\frac{\epsilon}{m}\int_0^\infty d\mathrm{U}\int_{-\infty}^\infty\int_{-\infty}^\infty \mathrm{D}\,(\mathrm{W}_2+\mathrm{U})\,\{n_1(\mathrm{W}_2+\mathrm{U}) - n_2(\mathrm{W}_2+\mathrm{U})\}\,dv\,dw, \quad (8)$$

where ϵ is the electronic charge.

So for equilibrium we must have

$$n_1\,(\mathrm{W}_2+\mathrm{U}) = n_2\,(\mathrm{W}_2+\mathrm{U}), \quad (9)$$

which on substitution in (2) and (4B) gives

$$\exp\,(\mathrm{W}_2 - \mathrm{E}_0)/k\mathrm{T} = \mathrm{B}^{-1}\,(k\mathrm{T})^{\frac{3}{4}}\exp\tfrac{1}{2}\,(\mathrm{W}_2 - \mathrm{W}_1)/k\mathrm{T}$$

approximately, or

$$E_0 = \tfrac{1}{2}(W_1 + W_2) + kT \log \{B (kT)^{-\frac{3}{2}}\}. \tag{10}$$

The last term is small, and, to the order of accuracy to which we are working, it is doubtful if we are justified in retaining it. For $T = 0$ it is, of course, zero, and for Cu_2O at ordinary temperatures, with $\nu_0 = 10^{17}$, it is a few hundredths of a volt. At first sight it seems curious that the term $\log B$ becomes infinite as ν_0 tends to zero. It must, however, be remembered that these formulæ are only correct so long as the amount of impurity present is sufficiently large to mask entirely the natural conductivity of the substance, so that for very small values of ν_0 the formulæ are no longer valid.

2.3. We now suppose a potential difference to be set up between the distant ends of the combination. The electrons near the gap will redistribute themselves until a steady state is reached. The drops in potential in the metal, the gap and the semi-conductor will then be such as to provide a uniform current throughout the system. Let the potential drop across the gap from metal to semi-conductor be V, then, if we neglect the change in the Fermi distribution due to the applied field, the effect of the field will be to change the transmission coefficient and to increase E_1 and E_0 by εV, while leaving W_2 unaltered. Actually only differences in these quantities are significant, so it is no restriction to consider W_2 as invariable. The current across the gap from the metal will then be

$$I = \frac{\varepsilon}{m}\int_0^\infty dU \int_{-\infty}^\infty \int_{-\infty}^\infty D(W_2 + U, V)\{n_1(W_2 + U, V) - n_2(W_2 + U)\}\, dv\, dw, \tag{11}$$

where

$$n_1(W_2 + U, V) = 2\left(\frac{m}{h}\right)^3 \Big/ [\exp\{W_2 + U + \tfrac{1}{2}m(v^2 + w^2) - \varepsilon V - E_0\}/kT + 1]. \tag{12}$$

Now, if εV is not extremely large and positive, we may omit the term 1 in the last expression, and we obtain for the current

$$I = \frac{2m^2\varepsilon}{h^3} B (kT)^{-\frac{1}{2}} e^{-\frac{W_2 - W_1}{2kT}}\left(e^{\frac{\varepsilon V}{kT}} - 1\right)$$
$$\int_0^\infty dU \int_{-\infty}^\infty \int_{-\infty}^\infty D(W_2 + U, V) \exp\{-U - \tfrac{1}{2}m(v^2 + w^2)\}/kT\, dv\, dw, \tag{13}$$

using the relation (10) to eliminate E_0. The integration over v and w can be carried out immediately, as the transmission coefficient does not depend on these variables, giving

$$\mathrm{I} = \frac{4\pi m\varepsilon}{h^3}\mathrm{B}\,(k\mathrm{T})^{-\frac{1}{2}}\,e^{-\frac{\mathrm{W}_2-\mathrm{W}_1}{2k\mathrm{T}}}\left(e^{\frac{\varepsilon\mathrm{V}}{k\mathrm{T}}}-1\right)\int_0^\infty \mathrm{D}\,(\mathrm{W}_2+\mathrm{U},\mathrm{V})\,e^{-\frac{\mathrm{U}}{k\mathrm{T}}}\,d\mathrm{U}. \qquad (14)$$

This is as far as we can go using only general theory. For the correctness of this equation it is only necessary to assume that the problem is one-dimensional, and that the transition layer is not large compared with the mean free path of the electrons. To proceed further we must know something about the transmission coefficient.

The Conditions for Rectification.

3.1. To calculate the transmission coefficient we must know the exact form of the potential energy in the gap. This is determined by the applied field and the space charges due to the electrons. Theoretically the problem is quite determinate, but it is so complicated that no one has yet been able to carry out the calculations, and it is necessary to resort to an approximate phenomenological theory by assuming that the potential energy is of the type given in fig. 1, without enquiring too closely into the factors which determine it.

Before proceeding to a detailed discussion of the transmission coefficient, let us examine equation (14). If D were independent of the applied voltage, then we see that the current-potential curve would be very asymmetrical, the direction of easy flow being from the metal. In this case, therefore, we have a large rectifying effect. On the other hand, the effect of the applied field on the transmission coefficient will always be such as to tend to nullify the rectifying effect. This follows from the fact that a decrease in $(\mathrm{W}_2 - \mathrm{E}_1)$ makes the potential hump bigger and decreases the transmission coefficient. Whether we get a rectifying effect or not will therefore depend on the relative sizes of the two factors involving V in equation (14).

3.2. We shall now consider some special cases, which will represent the two limits obtainable. If we particularise the potential hump by supposing that in the absence of an external field it is of a rectangular form, then we can use some calculations by Fowler,* and also by Georgeson,† who worked out a slightly more general case. We suppose the potential hump in fig. 1 to be rectangular, of height C above E_1 and of thickness l.

---

* 'Proc. Roy. Soc.,' A, vol. 122, p. 36 (1929).

† 'Proc. Camb. Phil. Soc.,' vol. 25, p. 175 (1929).

Similar calculations have recently been applied by Frenkel* to the theory of rectification by metallic contacts, and, as was to be expected, he found the effect to be extremely small. The following formulæ are quoted from his paper.

If the potential hump is small, then it is found that

$$D^*(V) = \int_0^\infty D(W_2 + U, V)\, e^{-U/kT}\, dU$$

$$= 8\sqrt{\pi}\,\frac{(kT)^{\frac{1}{2}}(W_2 - E_1)^{\frac{1}{2}}}{C}\, e^{-2\kappa l(\frac{1}{2}\epsilon V + C - W_2)^{\frac{1}{2}}} \tag{15}$$

approximately, where $\kappa^2 = 8\pi^2 m/h^2$, provided

$$e^{-2\kappa l(C - W_2)^{\frac{1}{2}}} \gg e^{-(C - W_2)/kT}. \tag{16}$$

If, on the other hand, the hump is large, and condition (16) is satisfied with the sign of the inequality reversed, then

$$D^*(V) = kT\, e^{-(\frac{1}{2}\epsilon V + C - W_2)/kT}. \tag{17}$$

In these two limiting cases we have the following approximate expressions for the current.†

$$I = P(kT)^{\frac{1}{2}}\, e^{-\frac{W_2 - W_1}{2kT}}\left(e^{\frac{\epsilon V}{kT}} - 1\right) e^{-\frac{\epsilon V}{kT_1}} \tag{18}$$

and

$$I = Q(kT)^1\, e^{-[C - \frac{1}{2}(W_1 + W_2)]/kT}\left(e^{\frac{\epsilon V}{2kT}} - e^{-\frac{\epsilon V}{2kT}}\right) \tag{19}$$

respectively, where

$$P = 32\pi^{\frac{1}{2}} m\epsilon h^{-3}\, C^{-1}(W_2 - E_1)^{\frac{1}{2}}\, B \exp\{-2\kappa l(C - W_2)^{\frac{1}{2}}\}, \tag{20}$$

$$Q = 4\pi m\epsilon h^{-3}\, B, \tag{21}$$

$$kT_1 = 2(C - W_2)^{\frac{1}{2}}/\kappa l. \tag{22}$$

From the condition (16) we see that the current is given by (18) provided $kT_1 \gg 4kT$. At any given temperature we therefore have I proportional to

$$e^{\alpha\frac{\epsilon V}{kT}} - e^{-(1-\alpha)\frac{\epsilon V}{kT}}, \tag{23}$$

where α is independent of V and lies between 1 and $\frac{1}{2}$. Actually α can never be exactly unity, but when the hump is small it may be fairly close to that value.

---

* 'Phys. Rev.,' vol. 36, p. 1604 (1930).

† An expression similar to (18) has been derived by C. Wagner using different assumptions. 'Phys. Z.,' vol. 32, p. 641 (1931).

Unless α is $\frac{1}{2}$ the current-voltage curve is asymmetrical, and so, unless the hump is very large, there is a rectifying effect. It is in fact obvious that if the hump is large the problem is effectively the same as that in which two metals or two semi-conductors are in contact, and in these cases it is known that there is very little rectifying effect. The rectifying effect of metal contacts is much smaller than that calculated by Frenkel, *loc. cit.*, as he expanded I as a power series in V, stopping at the term involving V^2. The higher terms tend to cancel out the effect of the V^2 term, and for a metal contact α cannot differ much from $\frac{1}{2}$.

3.3. When we come to insert numerical values we are on very uncertain ground, the difficult quantities to assess being l and C. In order to obtain some idea of the rectifying effect of a single contact we give below the current-voltage curve, and the differential resistance curve ($R = dV/dI$ plotted against V), for what might be considered a moderately good contact, with $l = 10^{-7}$ cm., and $C - W_2 = \frac{1}{2}$ volt. With the above values we have $kT_1 = 4{\cdot}5 \times 10^{-13}$, and, since $kT = 4 \times 10^{-14}$, condition (16) is satisfied, and we have $\alpha = 0{\cdot}9$.

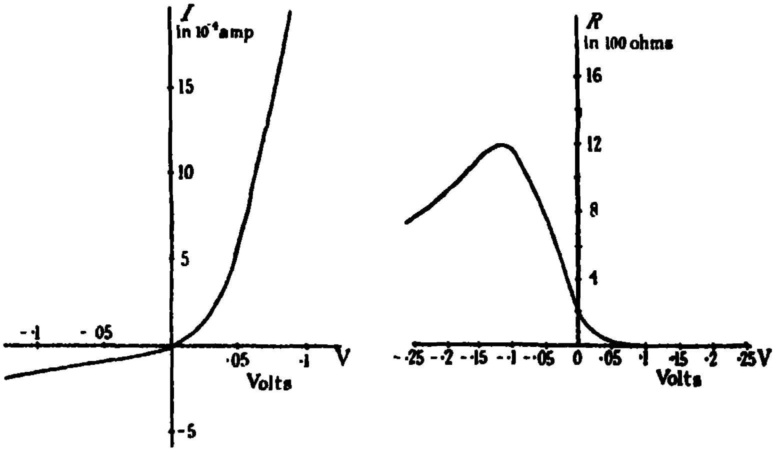

FIG. 2.

N.B.—The scales correspond to the conditions stated in the text, but are typical only, and small changes in the conditions vary them by large factors.

3.4. The problem of two contacts is much more complicated than that of only one contact, as the potential drop consists of three parts, the drops in the two gaps and the drop along the semi-conductor. It is not necessary to consider explicitly this last, which is determined by the bulk resistance of the semi-conductor, as it can be easily eliminated from the experimental results. The simplest and most usual way of doing this is to consider the differential resistance $R = dV/dI$. The bulk resistance then appears as an additive constant and is easily eliminated. Since the drops in potential in the two gaps adjust themselves so as to give the same current, the potential drop is greater across the worse contact, but the problem is complicated by the fact that when the current is in the preferred direction at one contact it is not in the preferred direction at the other contact. This complication makes it impossible to give any general rule for determining the direction of easy flow, and it is not possible to give an explicit expression for the current as a function of the total voltage. There are, however, two particular cases in which this question can at once be settled. If the two contacts have approximately the same value of α, the effective surfaces, however, being different, that is, P is different for the two contacts, then it is easily seen that the direction of easy flow is from the metal to the semi-conductor across the contact with the smaller value of P, that is, the worse contact. If, on the other hand, one contact is so bad that it has $\alpha = \frac{1}{2}$, then it exerts no rectifying effect, and the direction of easy flow is from the metal to the semi-conductor across the other, better, contact.

It seems possible that in the copper/cuprous-oxide rectifier the contact between the oxide and the mother copper is much better than the other contact, which is made by a piece of metal pressing against the external face of the oxide. Now the seat of the rectification is the transition layer between the copper and the oxide, and we must therefore suppose that the combination makes an efficient rectifier because the copper/cuprous-oxide contact is so much more perfect than the external one.* It is not possible to decide whether this view is to be preferred to the more usual one, that the copper/cuprous oxide junction is the bad one, since the important quantities l and C are quite unknown. Further, a better theory of the transmission coefficient will have to be developed before quantitative tests can be applied to the theory. We can, however, say that, unless $(C - W_2)$ is very small, the ordinary hypothesis probably fits the facts better, since a large value of $(C - W_2)$ and an α nearly equal to $\frac{1}{2}$ would give an enormous resistance in the gap. That $(C - W_2)$ is not large may be inferred from the fact that the gap resistance has approximately the same temperature variation as the bulk resistance of the semi-conductor, which is proportional to

$$T^{\frac{3}{4}} e^{-\frac{W_2 - W_1}{2kT}}.$$

The evidence is not conclusive, since different specimens of cuprous oxide have conductivities which vary by factors of 10. In order to show the modification which can be introduced by the presence of a second contact, the current-voltage curve is given for a pair of contacts, the separate current-voltage characteristics being

---

* This suggestion is due to R. H. Fowler.

$$I = 10^{15}\,\varepsilon\left(e^{0\cdot 9\frac{\varepsilon V}{kT}} - e^{-0\cdot 1\frac{\varepsilon V}{kT}}\right)$$

$$I = 10^{15}\,\varepsilon\left(e^{0\cdot 8\frac{\varepsilon V}{kT}} - e^{-0\cdot 2\frac{\varepsilon V}{kT}}\right).$$

The positive direction of the electron current is from the metal to the semiconductor at the first contact.

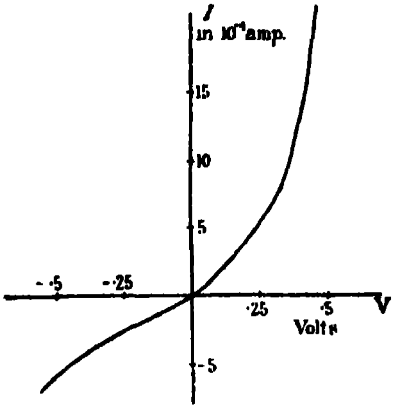

Fig. 3.

N.B.—The scales are again only typical, and small changes in the conditions vary them by large factors.

In conclusion, the theory developed here differs in several important aspects from those which have hitherto been proposed. The essential point is that it is the potential difference which causes the asymmetry in the current. The difference in potential between the two components changes the number of electrons which can pass from one component to the other, while the high field only effects the transmission coefficient, and makes the passage of the electrons easier or more difficult. The difficulties in the way of a complete theory of the transmission coefficient are considerable, but the crude theory seems adequate to explain quite a large part of the phenomena.

Radio Transmission Problems Treated by Phase Integral Methods.

By T. L. ECKERSLEY.

(Communicated by W. H. Eccles, F.R.S.—Received January 12, 1932.)

§ 1. In a recent paper* the writer has shown that there is a formal analogy between the analytical description of the transmission of electric waves through a medium of variable electronic density, and the Schroedinger wave theory of quantum dynamics; and that, as in quantum dynamics, each electrical problem is characterised by a set of proper values determined by the boundary conditions. These proper values which, in quantum dynamics, give the energy levels, in the wireless theory give a discrete set of direction cosines and attenuation factors of the various possible waves. A complete analysis of the wave equation is necessary in every case to give the accurate proper values; but in certain conditions, where the wave-length λ is so short that the phase velocity does not change appreciably (compared with c) in a wave-length, and where the radius of curvature of the rays is small compared with λ, approximate methods may be used by which the proper values may be calculated. These methods correspond with the old Bohr-Sommerfeld phase integral method of calculating the energy levels.

In particular, where transmission between two spherical shells is considered, as in the region between the earth and Heaviside layer, the proper values for the system are found to approximate closely to those found for the case where the layers are *plane* so long as the height of the layer is small compared with the radius of the earth. In the following illustration the full wave analysis is applied to the transmission between *plane* stratified layers, the existence of the proper values is demonstrated, and their relation with the approximately calculated proper values given. The results indicate clearly the nature of the transmission to be expected and the nature of the attenuation suffered by the waves for various wave-lengths and density distributions in the layer, and these results may be applied in the first approximation to the spherical case when the above limitation obtains.

In this paper complete solutions of certain simple cases of radio transmission in the region between horizontal layers are given in order to illustrate the phase integral method. In each of the cases considered the final analytical solution is the sum of the number of Eigen solutions which may be identified with those determined by the phase integral method. The first example is that of a radially symmetrical transmitter between two perfectly conducting planes. The complete analysis, using an image method and a contour integral to transform the series derived from the set of images, exhibits very clearly the set of proper solutions which can be compared with those derived by the phase integral method.

---

* 'Proc. Roy. Soc.,' A, vol. 132, p. 83 (1931).

The second is an extension of this example to the case where one of the bounding layers is not perfectly conducting and is assumed to have electrical characteristics consistent with a structure of a partially ionised atmosphere. The method for obtaining a solution, however, differs entirely from that used previously and is an extension of Sommerfeld's method of analysis of the transmission of electric waves over the surface of the earth. Here again the solution is exhibited as a series of cylindrical waves of the type

$$S_n = \sqrt{\frac{2}{\pi\gamma_n r}}\, e^{i(\gamma_n r - \pi/4)}\, F(\gamma_n, z, z_0). \tag{1}$$

In which γ_n has a finite number of discrete values derived from a characteristic equation, which is identical with the one derived by the phase integral method. A few illustrations of the nature of the characteristic waves is given, but a complete discussion would take up too much space and would hardly be justified in view of the fact that the results would not be applicable to the actual case of transmission of radio waves round the world. Measurements made by Appleton and others show that the layer can hardly be considered as sharply defined.

The above refers to the case of a sharply defined conducting layer. As a contrast a graded ionic refracting layer is considered next. This example is one in which the ionic density is proportional to the square of the height. The connection between this and the phase integral method is again considered.

The final example differs from the previous ones in that the upper conducting layer is supposed to be removed and the *diffraction* of the waves round a conducting sphere is computed by the phase integral method.

This problem has already been considered by others. In the explicit form given by G. N. Watson* and amplified by Van der Pol,† it is shown that for long waves and sufficiently high earth conductivity the diffraction formula is independent of the earth's resistivity. In the application to radio transmission phenomena on the earth's surface it is only in the broadcast range in daylight, say, from wave-lengths 150 to 1500 m., that diffraction is likely to play a predominant part; this is because it is only in this range that the reflection coefficient of the Heaviside layer is so small that the effect of this layer may be neglected. But the wave-lengths here are so short that the condition above is no longer valid, and diffraction does depend on the earth's resistivity. In practice we are faced with the problem of connecting up the Sommerfeld curves which give the field intensity in the neighbourhood of the transmitter, and which do depend in a marked manner upon the earth's resistivity with the diffraction formula valid at greater distances which apparently do not depend on the earth's resistivity.

---

* 'Proc. Roy. Soc.,' A, vol. 95, p. 546 (1919).

† 'Phil. Mag.,' vol. 38, p. 365 (September, 1919).

It will be shown that the phase integral method is in such a form that it indicates a simple method whereby the effect of the earth's resistivity on diffraction can be taken account of. A series of measurements on the 120 K.W. Broadcasting Station at Warsaw have been made to test the theory and reasonable agreement obtained.

§ 2. The first example is that of two perfectly conducting planes, which was investigated by the writer in 1924 and 1925. G. W. Kenrick* deals with the same problem, but the solution is only approximate and leaves out just those points I wish to emphasise.

The analysis in this case is based on image methods, which can best be explained with reference to fig. 1.

Let A and B be the perfect conducting planes and T the transmitter. In the region between the planes A and B the effect of the first reflection at the perfectly conducting surface is the same as that of an image at a height 2H vertically above T.

On re-reflection at the lower surface another image at —2H is produced, and finally, considering all the reflections, the electric field within the space between the two perfectly conducting planes is equal to that produced by an infinite set of images on the vertical axis through T, spaced a distance 2H apart.

If each of these is supposed to be a Hertzian doublet of equal moment to the actual transmitter, we can write down their potential as the sum of a number of terms, thus:

$$\Pi_n = \frac{A}{r_n} e^{-\frac{2\pi i r_n}{\lambda} + ipt}. \tag{2.1}$$

Then

$$\frac{\partial^2 \Pi_n}{\partial x^2} = E_n,$$

---

* 'Phil. Mag.,' vol. 6, p. 289 (1928).

the vertical electric force, and

$$\frac{\partial^2 \Pi_n}{\partial x\, \partial t} = \mathrm{H}_n,$$

the horizontal magnetic force where $r_n = r_{-n} = (x^2 + 4n^2\mathrm{H}^2)^{\frac{1}{2}}$.

r_n is the distance of the nth image from the point x under consideration, and the total electric and magnetic forces are

$$\frac{\partial^2 \Pi}{\partial x^2} \quad \text{and} \quad \frac{\partial^2 \Pi}{\partial x\, \partial t},$$

where

$$\Pi = \sum_{n=-\infty}^{n=+\infty} \Pi_n.$$

This series is very slowly convergent when the distance x is large compared with 2H, and is of little use for computation or for giving a picture of the electromagnetic forces in the region between the two planes.

The series can, however, be transformed into an integral in the following manner :—

Consider the quantity

$$\chi = \frac{1}{2\mathrm{H}} \frac{\mathrm{A}}{(1+\zeta^2)^{\frac{1}{2}}} \frac{e^{\pi i x\zeta/2\mathrm{H} - 2\pi i x(1+\zeta^2)^{1/2}/\lambda}}{\sin \pi x\zeta/2\mathrm{H}}. \tag{2.2}$$

The limit $\chi\left(\zeta - \frac{2\mathrm{H}n}{x}\right)$ where n is an integer and when $\zeta \rightarrow 2n\mathrm{H}/x$ is

$$\frac{\mathrm{A}}{\pi} \frac{e^{in\pi}}{(x^2 + 4n^2\mathrm{H}^2)^{\frac{1}{2}}} \frac{e^{-2\pi i (x^2+4n^2\mathrm{H}^2)^{1/2}/\lambda}}{\cos n\pi},$$

which by 1 and 2 is equal to Π_n/π. Thus the residue of the function χ at $\zeta = 2n\mathrm{H}/x$ is Π_n/π.

We may draw a contour in the ζ plane which encloses all the positive values of $\zeta = 2n\mathrm{H}/x$. The value of χ will be regular along this contour if we join the points $\pm i$ with a cut and draw the contour in such a way that it does not cross this cut.

Such a contour passes from 0 to i on the right of the cut, along the imaginary axis from i to $i\infty$, from $i\infty$ to $-i\infty$ by a large semicircle C, and from $-i\infty$ to 0 again by the negative part of the imaginary axis.

Then

$$\int_{\mathrm{C}} \chi\, d\zeta = 2\pi i \sum_{\text{residues}} \chi \quad \text{at} \quad \zeta = 2n\mathrm{H}/x,$$

i.e.,

$$\sum_1^n \Pi_n = \frac{1}{2i} \int_{\mathrm{C}} \chi\, d\zeta$$

and

$$\Pi = \Pi_0 + \sum_{n=1}^{n=\infty} \pi_n + \sum_{n=-1}^{n=-\infty} \Pi_n = \Pi_0 + \frac{1}{i}\int_C \chi \, d\zeta.$$

Now the integral round the contour C can be split up into two parts:

$$\frac{1}{i}\int_{-i\infty}^{+i\infty} \chi \, d\zeta + \frac{1}{i}\int_{\text{semicircle } C} \chi \, d\zeta.$$

The examination of the second term shows that so long as $\lambda > 2H$

$$\frac{1}{i}\int_{\text{semicircle}} \chi \, d\zeta \rightarrow 0,$$

and therefore

$$\Pi = \Pi_0 + \frac{A}{2iH}\int_{-i\infty}^{+i\infty} \frac{e^{i\pi x\zeta/2H - 2\pi i x(1+\zeta^2)^{1/2}/\lambda}}{(1+\zeta^2)^{1/2}\sin\frac{x\pi\zeta}{2H}}\, d\zeta, \tag{2.3}$$

this integral is convergent in these conditions, but is not uniformly so when $\lambda \rightarrow 2H$. There is thus a discontinuity in the value of Π considered as a function of λ (or H) as $\lambda \rightarrow 2H$. For values of $H > \lambda/2$ an extension of the method previously used gives rise to the following integral for Π:

$$\Pi = \Pi_0 + \frac{A}{2iH}\int_{-i\infty}^{+i\infty} \frac{e^{i(2s+1)\beta\zeta - i\gamma(1+\zeta^2)^{1/2}}}{(1+\zeta^2)^{1/2}\sin\beta\zeta}\, d\zeta, \qquad \left.\begin{aligned}\beta &= \pi x/2H \\ \gamma &= 2\pi x/\lambda\end{aligned}\right\} \tag{2.4}$$

where s is an integer such that

$$(s+1)\lambda > 2H > s\lambda, \tag{2.5}$$

i.e., s is the greatest integer less than $2H/\lambda$.

This gives the value of Π at the surface of the lower layer. At a point of height z above the lower conducting plane the value of Π is

$$\begin{aligned}\Pi = \Pi_0 &+ \frac{A}{4iH}\int_{-i\infty}^{+i\infty} \frac{e^{i(2s+1)(\beta\zeta-\phi) - i\gamma(1+\zeta^2)^{1/2}}}{(1+\zeta^2)^{1/2}\sin(\beta\zeta-\phi)}\, d\zeta, \\ &+ \frac{A}{4iH}\int_{-i\infty}^{+i\infty} f(+\phi)\,.\,d\zeta,\end{aligned} \tag{2.6}$$

where $\sin\phi = \pi z/H$.

The problem then consists entirely in evaluating these integrals.

In the simplest case, where $\lambda > 2H$, the mathematics are fairly simple. We obtain

$$\Pi = \Pi_0 + \frac{A}{x}e^{-\frac{2\pi i x}{\lambda}} + \frac{A}{iH}\int_0^1 \frac{e^{-\frac{2\pi i x}{\lambda}t}}{(1-t^2)^{\frac{1}{2}}}\, dt + Q,$$

where

$$Q = \frac{A}{H}\int_1^{\infty} \frac{\cosh\{\gamma(t^2-1)^{\frac{1}{2}} - \beta t\}}{(t^2-1)^{\frac{1}{2}}\sinh\beta t}\, dt, \tag{2.7}$$

since

$$\Pi_0 = \frac{A}{x} e^{-\frac{2\pi i x}{\lambda}},$$

$$\Pi = 2\Pi_0 + \frac{A}{iH}\int_0^1 \frac{e^{-i\gamma t}}{(1-t^2)^{\frac{1}{2}}}\, dt + Q. \tag{2.8}$$

Q represents a stationary wave term (since it does not involve i)

$$\frac{A}{iH}\int_0^1 \frac{e^{-i\gamma t}}{(1-t^2)^{\frac{1}{2}}}\, dt.$$

can be calculated immediately in terms of the standard Bessel functions. Thus

$$\frac{A}{iH}\int_0^1 \frac{e^{-i\gamma t}}{(1-t^2)^{\frac{1}{2}}}\, dt = \frac{\pi}{2}\frac{A}{iH} J_0(\gamma) + \frac{iA}{iH}\int_0^1 \frac{\sin\gamma t}{(1-t^2)^{\frac{1}{2}}}\, dt.$$

When x/λ large enough, this is

$$\frac{A}{2iH}\left(\frac{\lambda}{x}\right)^{\frac{1}{2}} e^{-i\frac{2\pi x}{\lambda} - i\frac{\pi}{4}}.$$

The main term in Π when x large, is

$$\frac{A}{2iH}\left(\frac{\lambda}{x}\right)^{\frac{1}{2}} e^{i\left(pt - \frac{2\pi x}{\lambda} - \frac{\pi}{4}\right)}$$

on introducing the periodic factor e^{ipt}.

Q is always a small quantity compared with the first term when x/H is large.

It can also be shown that at a height Z above the lower surface Π has the same value.

The solution is therefore a cylindrical wave spreading out uniformly in the space between the two layers.

There is no high angle radiation, or rather, all the high angle radiation cancels out.

We may compare this with the ray theory according to which all the high angle rays should be present.

Case where $2H > \lambda$.—In this case we have to evaluate the integral

$$\frac{A}{2iH}\int_{-i\infty}^{+i\infty} \frac{e^{i\beta(2s+1)\zeta - i\gamma(1+\zeta^2)^{1/2}}}{(1+\zeta^2)^{\frac{1}{2}}\sin\beta\zeta}\, d\zeta, \tag{2.9}$$

where s is an integer such that

$$(s+1)\lambda > 2\mathrm{H} > s\lambda.$$

By a suitable transformation this may be put in the form (apart from the stationary wave term)

$$\frac{\mathrm{A}}{2i\mathrm{H}}\int_0^1 2\sinh(2s+1)\beta(1-t^2)^{\frac{1}{2}}\,e^{-i\gamma t}\,dt/(1-t^2)^{\frac{1}{2}}\sinh\beta(1-t^2)^{\frac{1}{2}} \qquad (2.10)$$

the integrand being of the form

$$\frac{\sinh(2s+1)\chi}{(1-t^2)^{\frac{1}{2}}\sinh\chi}e^{-i\gamma t}.$$

The integral can be expanded into a finite number of terms of the form

$$\frac{\mathrm{A}}{2i\mathrm{H}}\int_0^1 \sum_{r=0}^{r=s-1} e^{-i\gamma t}\,.\cosh\frac{(2s-2r)\,\beta\,(1-t^2)^{\frac{1}{2}}}{(1-t^2)^{\frac{1}{2}}}\,dt+\frac{\mathrm{A}}{2i\mathrm{H}}\int_0^1\frac{e^{-i\gamma t}}{(1-t^2)^{\frac{1}{2}}}\,dt. \qquad (2.11)$$

Each integral is of the form

$$\int_0^1\frac{e^{\pm p(1-t^2)^{1/2}-i\gamma t}}{(1-t^2)^{\frac{1}{2}}}\,dt,$$

where $p=2\,(s-r)\,\beta$, $\gamma > p$, these integrals can be approximately evaluated in terms of Bessel functions and the final result is a series of progressive waves of the type

$$\frac{\mathrm{A}}{i\mathrm{H}}\cos 2\,(s-m)\,\phi\,\frac{\pi^{\frac{1}{2}}}{[2\gamma\sqrt{1-\beta_m{}^2}]^{\frac{1}{2}}}\,e^{-i\gamma\sqrt{1-\beta_m{}^2}+ipt-i\pi/4} \qquad (2.12)$$

where $\beta_m=(s-m)\,\lambda/2\mathrm{H}$ together with negligible stationary wave terms.

The progressive wave represents one which is travelling along a normal, the direction cosine of which (in the x direction) is $\sqrt{1-\beta_m{}^2}$, so that in the figure (1) $\cos\theta_m=\sqrt{1-\beta_m{}^2}$ or $\sin\theta_m=\pm\beta_m$. These directions are obviously such that the distance AO and BO of two adjacent paths differ by $s-m$ wave-lengths, *i.e.*, an integral number of wave-lengths; so that the waves which survive after the manifold reflections from the upper and lower reflectors are those which satisfy these conditions.

A close scrutiny of the mechanism by which these waves are produced shows that the waves from a considerable group of images are all in phase along these directions and the effects therefore all add. In other directions they cancel.

The term for which $\beta_m=0$ is the original integral for the case where $\mathrm{H} < \lambda/2$.

The total effect therefore consists of supplementary high angle rays, the direction of these being given by

$$\sin \theta_m = (s - m) \frac{\lambda}{2\mathrm{H}}, \tag{2.13}$$

where m is an integer varying from 1 to $s - 1$.

Thus where $2\mathrm{H} > \lambda$ there are only a finite number of high angle rays, $s - 1$, s being the greatest integer which makes $s\lambda < 2\mathrm{H}$. There are a finite number of proper values in this case which may be evaluated from by the phase integral method as shown in the following paragraph.

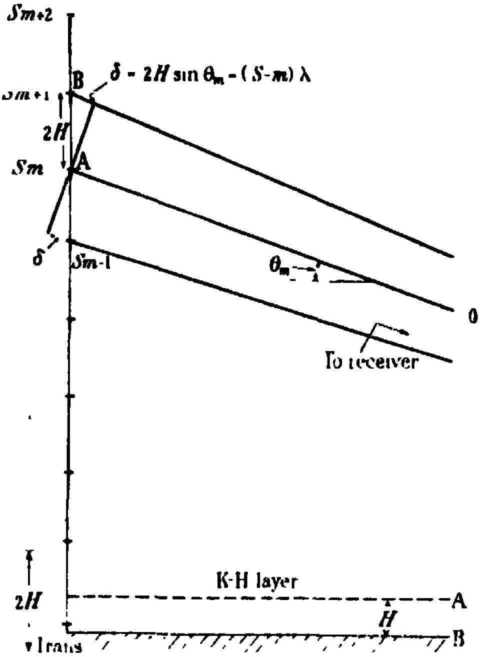

FIG. 1.—Image theory.

Phase Integral Method.—An extension of the phase integral method is applicable where the bounding layers are sharply defined.

For this we require the phase change on reflection at the sharp boundary.

Let $\delta\phi$ be this phase change so that the reflection coefficient may be put in the form

$$\rho = e^{-i\delta\phi}. \tag{2.14}$$

$\delta\phi$ may include an imaginary part which will give the amplitude change on reflection.

We have expressed the phase integral in the form,

$$\frac{2\pi i}{\lambda}\oint\sqrt{n^2-\nu_0^2/\nu^2}\,dz = 2\pi ir \tag{2.15}$$

for the case where the density gradient is purely vertical, *i.e.*, in the z direction, and where $1-\nu_0^2/\nu^2=\mu^2$, and μ is the refractive index at a height z, ν_0^2 being $Ne^2c^2/\pi m\,(1+i\alpha)$. Where N, e and m have their usual significance and $\alpha=\nu_c/\pi\nu$, ν_c being the collision frequency and ν the actual frequency of the waves considered.

In the region between the two layers N and ν_0 are zero and the contribution to the phase integral from 0 to H is

$$\frac{2\pi i}{\lambda}\int_0^{H} n\,dz$$

on reflection the contribution is $i\delta\phi$, on the negative branch H to 0 it is

$$-\frac{2\pi i}{\lambda}\int_H^{0} n\,dz,$$

so that the phase integral relation becomes in this case

$$2\,.\,\frac{2\pi i}{\lambda}\,n\mathrm{H}+i\delta\phi=2\pi ir, \tag{2.16}$$

where r is an integer.

In this case the change of phase at reflection is zero (since the change of phase at reflection from a perfect conductor is zero). Therefore

$$2n\mathrm{H}=r\lambda$$

or

$$n=\frac{r\lambda}{2\mathrm{H}} \tag{2.17}$$

where r is the same integer as that given previously.

Since n must be less than unity for any real wave, the largest value of r for which this condition holds is given by

$$r\lambda<2\mathrm{H}<(r+1)\lambda.$$

Thus the phase integral gives, by a very simple method, the characteristic direction cosines found by the more elaborate analysis which, of course, gives a much fuller account of solution, since it gives the amplitudes of the Eigen functions as well as the stationary wave terms which have to be added to the Eigen functions to give the complete solution.

§ 3. The next example is an extension of the previous one to the case where one of the planes is not perfectly conducting.

This comes nearer actuality than the former example. In a sense it may be considered to supplement Watson's analysis, which only refers to the longer waves guided round the earth by a conducting layer, *i.e.*, in which the current is in phase with the e.m.f. Although the analysis only refers to plane layers, it was shown in the previous paper (*loc. cit.*) that the proper values determined by the plane layer analysis will serve very approximately for the spherical case, and when inserted in the expression

$$\frac{}{\sqrt{2 \sin \theta}} \cos\left(\frac{2\pi n_s \theta R}{\lambda} + \pi/4\right) \qquad (3.1)$$

will give the proper function.

The analysis that follows is applicable to a much wider range of layer constants than is considered by Watson. It is not, however, to be considered as a true representation of the actual facts of transmission but rather as an illustration of the results obtained by phase integral methods.

The method of investigation used in this case differs entirely from that used in the previous one, and is based on Sommerfeld's analysis of the transmission of electric waves over the surface of the earth.

In order not to complicate further the analysis (which is already sufficiently complex) we will assume that a transmitter is situated on a perfectly conducting earth, so that we are concerned with the effect of atmospheric attenuation only.

Consider a cylindrically symmetrical point source situated half-way between the two planes 1 and 2, which are the boundaries of the conducting region.

The electromagnetic forces in the region between the horizontal plane through 0 and the upper boundary 1 will then be the same as if a perfectly conducting plane had been assumed to pass through 0 (where 0 is half-way between 1 and 2).

The source at 0 produces electric waves, the electric and magnetic forces of which can be derived from the potential function $\Pi = e^{ik_0R - ipt}/R$, where R is the radius vector from 0 to the point considered, and $k_0 = 2\pi/\lambda$, λ being the wave-length of the radiation.

If we use cylindrical co-ordinates r, θ, and z, the last representing the vertical axis, then assuming radial symmetry about 0, the electromagnetic forces will be only functions of r and z and not of θ.

Sommerfeld* has shown that the expression e^{ik_0R}/R can be put in the alternative forms

$$\int_0^\infty \frac{\lambda\, d\lambda}{\sqrt{\lambda^2 - k_0^2}}\, J_0(\lambda r)\, e^{-\sqrt{\lambda^2-k_0^2}\,z}$$

and $\qquad$ (3.2)

$$\int_0^\infty \frac{\lambda\, d\lambda}{\sqrt{\lambda^2 - k_0^2}}\, J_0(\lambda r)\, e^{+\sqrt{\lambda^2-k_0^2}\,z}$$

according as z is positive or negative.

A general solution of the radially symmetrical type of differential equation of wave propagation in a medium, the constants of which are :—

$\bar{\mu}$ = permeability
K = dielectric constant
ρ = resistivity

is given by the integral

$$\int_0^\infty \lambda\, d\lambda\, f(\lambda)\, J_0(\lambda r)\, e^{\pm\sqrt{\lambda^2-k_1^2}\,z}, \tag{3.3}$$

where $f(\lambda)$ is an arbitrary function of the parameter λ (not to be confused with the wave-length), to be chosen so as to satisfy the boundary conditions, and

$$k_1^2 = \frac{\bar{\mu} K p^2}{c^2} + \frac{4\pi i p \bar{\mu}}{\rho}, \tag{3.4}$$

$p = 2\pi$ × frequency.

In terms of the ionic theory

$$k_1^2 = \left(\frac{2\pi}{\lambda}\right)^2 - 4\pi N e^2 \Big/ m\left(1 + \frac{i\nu_e}{\pi\nu}\right) \tag{3.5}$$

so that

$$\mu = \text{refractive index} = \left\{1 - \frac{\nu_0^2}{\nu^2}\Big/(1+\alpha^2)\right\}^{\frac{1}{2}} \tag{3.6}$$

$$\rho = \frac{\nu^2}{\nu_0^2}\,\frac{2\pi_e^2}{\nu_e}\,(1+\alpha^2) \tag{3.7}$$

and

$$\frac{\rho p}{4\pi c^2} = \frac{\nu^2}{\nu_0^2}\,\frac{(1+\alpha^2)}{\alpha}, \tag{3.8}$$

where $\alpha = \nu_e/\pi\nu$, ν = wave frequency, ν_e = mean collision frequency.

Accordingly we can express the potential function in the region between the boundaries in the form

$$\begin{aligned}\Pi = \frac{e^{ik_0R}}{R} &+ A\int_0^\infty \lambda\, d\lambda\, f(\lambda)\, J_0(\lambda r)\, e^{+\sqrt{\lambda^2-k_0^2}\,z} \\ &+ B\int_0^\infty \lambda\, d\lambda\, f(\lambda)\, J_0(\lambda r)\, e^{-\sqrt{\lambda^2-k_0^2}\,z}\end{aligned} \tag{3.9}$$

---

* 'Ann. Physik,' vol. 28. p. 665 (1909).

where the two latter terms represent the effect of the multiple reflection from the boundaries of the original wave. Similarly in the media 1 and 2 the general solution applicable to this case can be expressed in the form

$$\Pi_1 = \int_0^\infty \lambda d\lambda f_1(\lambda)\, J_0(\lambda r)\, e^{+\sqrt{\lambda^2-k_1^2}\, z}$$

$$\Pi_2 = \int_0^\infty \lambda d\lambda f_1(\lambda)\, J_0(\lambda r)\, e^{-\sqrt{\lambda^2-k_1^2}\, z}.$$

The surface conditions require the continuity of E_r and H_r at the two surfaces $Z = \pm Z_0$, where $2Z_0$ is the distance between them, from which we derive

$$\begin{aligned}
\Pi_0 &= \Pi_1 && \text{at } Z = -Z_0 \\
\Pi_0 &= \Pi_2 && \text{at } Z = +Z_0 \\
\frac{1}{k_0^2}\frac{\partial \Pi_0}{\partial z} &= \frac{1}{k_1^2}\frac{\partial \Pi_1}{\partial z} && \text{at } Z = -Z_0 \\
\frac{1}{k_0^2}\frac{\partial \Pi_0}{\partial z} &= \frac{1}{k_1^2}\frac{\partial \Pi_2}{\partial z} && \text{at } Z = Z_0.
\end{aligned}$$

From this we can determine A, B, $f_1(\lambda)$, and $f(\lambda)$.

After reduction we find

$$\Pi_0 = \frac{e^{ik_0R}}{R} + \int_0^\infty \frac{\lambda d\lambda (J_0(r\lambda)).2[k_1^2}{2\sqrt{\lambda^2-k_0^2}\{k_1^2\sqrt{\lambda^2-k_0^2}\sinh\sqrt{\lambda^2-k_0^2}.z_0 + k_0^2\sqrt{\lambda^2-k_1^2}\cosh\sqrt{\lambda^2-k_0^2}.z_0\}}. \tag{3.10}$$

The solution of the problem therefore resolves itself into the examination of this rather formidable integral.

The integrand has branch points at k_0 and k_1, also poles at the zeros of

$$k_1^2\sqrt{\lambda^2-k_0^2}\sinh\sqrt{\lambda^2-k_0^2}.z_0 + k_0^2\sqrt{\lambda^2-k_1^2}\cosh\sqrt{\lambda^2-k_0^2}\,z_0 = 0. \tag{3.11}$$

The contour integral may be transformed so as to encircle the branch points and poles in the first quadrant of the complex plane of λ, and therefore depends on the residues of the functions at these points.

For this purpose, following Sommerfeld's procedure, we may express $J_0(\lambda r)$ as the sum of two parts

$$J_0(\lambda r) = \tfrac{1}{2}H_1(\lambda r) + \tfrac{1}{2}H_2(\lambda r),$$

where $H_1(x)$ and $H_2(x)$ are the Hankel Functions which when λr or x is great enough can be expressed in the forms

$$H_1(x) = \sqrt{\frac{2}{\pi x}}\, e^{i(x-\pi/4)},$$

$$H_2(x) = \sqrt{\frac{2}{\pi x}}\, e^{-i(x-\pi/4)},$$

so that the second integral in (3.10) may be expressed

$$\Pi' = \int_0^\infty \tfrac{1}{2} H_1(\lambda r)\, \phi(\lambda, z, z_0)\, d\lambda + \int_0^\infty \tfrac{1}{2} H_2(\lambda r)\, \phi(\lambda, z, z_0)\, d\lambda, \qquad (3.12)$$

where

$$\phi(z, z_0, \lambda) = \frac{\lambda . [k_1^2\sqrt{\lambda^2 - k_0^2} - k_0^2\sqrt{\lambda^2 - k_1^2}]\, 2\cosh\sqrt{\lambda^2 - k_0^2} . z}{2\sqrt{\lambda^2 - k_0^2}\,[k_1^2\sqrt{\lambda^2 - k_0^2}\sinh\sqrt{\lambda^2 - k_0^2} . z_0 + k_0^2\sqrt{\lambda^2 - k_1^2}\cosh\sqrt{\lambda^2 - k_0^2} . z_0]} . \qquad (3.13)$$

Now $H_1(x)$ tends to zero exponentially when λ is in the first quadrant and $H_2(x)$ tends to zero exponentially when λ is in the fourth quadrant.

The integral 0 to ∞ of the first term in the first quadrant can be transformed to

$$\int_0^{i\infty} + \int_{c_1} + \int_{c_2} + \Sigma \int \text{round poles} = R_1 + P + Q + S_1,$$

since the integral at ∞ is zero on account of the vanishing of $H_1(x)$ exponentially.

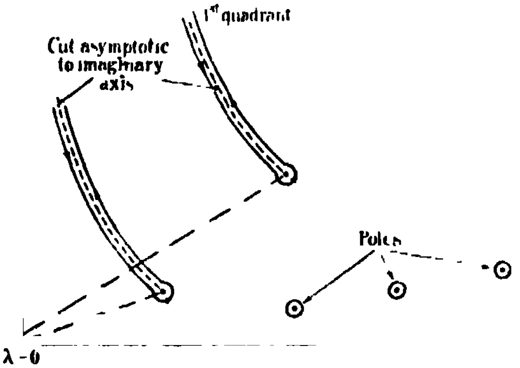

FIG. 2.

$\int_{c_1}$ and $\int_{c_2}$ are the integrals round the contours surrounding the cuts from c_1 to ∞ and c_2 to ∞, these cuts being the loci for which $\sqrt{\lambda^2 - k_0^2}$ and

$\sqrt{\lambda^2 - k_1^2}$ respectively are purely imaginary. They approach the imaginary axis asymptotically as $\lambda \to \infty$ and c_1, c_2, are the branch points of the integrand. The integral of the second term can similarly be expressed as $\int_0^{-i\infty} + \int$ round poles in the fourth quadrant $= R_2 + S_2$, say.

Now it can be shown that $R_1 + R_2$ is zero, for we have $-H_1(x) = H_2(xe^{i\pi/4})$. Put $x = (\lambda r)$, multiply both sides by $\phi(\lambda, z, z_0)$ and integrate from 0 to $i\infty$ on the positive imaginary axis, then the left-hand side becomes $-R_1$.

Make the substitution $\lambda' = \lambda e^{-i\pi}$, then the right-hand side becomes $\int_0^{-i\infty} H_2(\lambda' r)\, \phi(\lambda', z, z_0)\, d\lambda'$ along the negative imaginary axis, *i.e.*,

$$-R_1 = R_2 \quad \text{or} \quad R_1 + R_2 = 0.$$

The total integral therefore becomes

$$P + Q + S_1 + S_2.$$

S_1 and S_2 are the sum of the residues in the first and fourth quadrant of the quantities

$$\left.\begin{array}{l} \tfrac{1}{2} H_1(\lambda r)\, \phi(\lambda, z, z_0) \\ \tfrac{1}{2} H_2(\lambda r)\, \phi(\lambda, z, z_0) \end{array}\right\} \tag{3.14}$$

respectively.

The full solution then involves the determination of the roots of the equation

$$k_1^2 \sqrt{\lambda^2 - k_0^2} \sinh \sqrt{\lambda^2 - k_0^2}\, z_0 + k_0^2 \sqrt{\lambda^2 - k_1^2} \cosh \sqrt{\lambda^2 - k_0^2}\, z_0 = 0, \tag{3.15}$$

as well as the evaluation of the integrals P and Q.

In the first place it should be observed that all the contributions to S_1 and S_2 represent waves of the cylindrical type, for if λ_n is one of the solutions of (3.15) the corresponding term S_n is

$$S_n = \sqrt{\frac{2}{\pi \lambda_n r}}\, e^{i(\lambda_n r - \pi/4)}\, \phi(\lambda_n z, z_0), \tag{3.16}$$

when (λr) is great enough.

S_n considered as a function of r is of the cylindrical type $A/r\, e^{i\lambda_n r}$, where A and λ_n do not involve r, but are functions of k_0, k_1, z, and z_0, *i.e.*, the constants of the media and height of the layer.

In general P and Q which probably decrease as $1/r$ and $1/r^2$ respectively are small compared with the cylindrical terms unless these latter are highly attenuated.

We will first make a study of the cylindrical terms for which solutions of equation (3.15) are required.

We may modify this as follows :—

Let

$$(\lambda^2 - k_0^2) z_0^2 = S^2 \quad \text{or} \quad \lambda^2 = k_0^2 + S^2/z_0^2$$

then

$$(\lambda^2 - k_1^2) = k_0^2 - k_1^2 + S^2/z_0^2,$$

and substituting in (3.15) we get

$$k_1^2 S \sinh S + k_0^2 \sqrt{S^2 + (k_0^2 - k_1^2) z_0^2} \,.\, \cosh S = 0$$

or

$$\tanh^2 S = \frac{k_0^4}{k_1^4}\left(1 + \frac{k_0^2 - k_1^2}{S^2} z_0^2\right) \tag{3.17}$$

in which S is considered to be the unknown.

This is the characteristic equation which determines the proper values λ_n *for this case.*

Phase Integral Method.—For the case under consideration we require the reflection coefficient of a conducting layer for vertically polarised rays.

Following Hartree,* we may put this in the form

$$\tan \frac{\delta\psi}{2} = \left.\frac{\partial E}{dz} \middle/ kE \right]_{z=0},$$

where E is a solution of the differential equation of propagation in the reflecting layer from which we get

$$\tan \frac{\delta\phi}{2} = k \frac{\sqrt{n^2 - \nu_0^2/\nu^2}}{in}, \tag{3.18}$$

where $n = \sin\theta$ and θ is the angle that the normal to the wave surface makes with the surface of separation, and

$$k = \frac{k_0^2}{k_1^2} = \frac{1}{(1 - \nu_0^2/\nu^2)}. \tag{3.19}$$

this gives for the phase integral condition

$$2n\mathrm{H} - r\lambda = \frac{\lambda}{2\pi} \,.\, 2 \tan^{-1} k \frac{\sqrt{n^2 - \nu_0^2/\nu^2}}{n}, \tag{3.20}$$

or

$$i \tan\left(\frac{2\pi}{\lambda} n z_0 - \pi r\right) = k \sqrt{n^2 - \frac{\nu_0^2}{\nu^2}} \Big/ n,$$

---

* 'Proc. Roy. Soc.,' A, vol. 131, p. 428 (1931).

or writing z_0 for H

$$\tanh^2\left(\frac{2\pi n z_0}{\lambda i}\right) = k^2 - \frac{\nu_0^2}{\nu^2}\frac{k^2}{n^2},$$

putting S† for $2\pi n z_0/\lambda i$

$$\tanh^2 S = k^2 + \frac{k^2\nu_0^2}{\nu^2}\left(\frac{2\pi z_0}{\lambda}\right)^2\frac{1}{S^2}$$

$$\tanh^2 S = \frac{k_0^4}{k_1^4}\left(1 + \frac{(k_0^2 - k_1^2)}{S^2}z_0^2\right), \tag{3.21}$$

which is identically the same as the characteristic equation (3.17) determined by the complete analysis. The phase integral method leads to the same proper values as those determined by the full analysis. The phase integral method determines the normal cylindrical type waves but neglects the P and Q terms which, however, are small at distances large compared with z_0.

The meaning and scope of the phase integral method is exhibited very clearly by these examples. The complete determination of the roots of the characteristic equation (3.17) for all the possible ranges of values of z_0 and k_0 and k_1 would occupy too much space and would be beyond the scope of the present paper, but some of the results are tabulated below.

Table I.—Attenuation Coefficient.

Layer Constants.	Ray order 0.	1	n.
Layer acting as Conductor $\alpha \gg 1$ $\left\lvert\frac{1}{\left(\mu^2 + \frac{i4\pi c^2}{\rho p}\right)}\right\rvert = N_1$ small, also $\left(\frac{2\pi z_0}{\lambda}\right)^2\left\lvert\frac{1 - \mu^2 - \frac{i4\pi c^2}{\rho p}}{\mu^2 + \frac{i4\pi c^2}{\rho p}}\right\rvert = N_2$ small	$\frac{1}{2z_0}\left(\frac{\rho p}{8\pi c}\right)^{1/2}$	$\frac{1}{z_0}\left(\frac{\rho p}{8\pi c}\right)^{1/2}$	$\frac{1}{z_0}\left(\frac{\rho p}{8\pi c}\right)^{1/2}\frac{1}{\cos\theta_n}$
$\lvert N_1\rvert$ small $\lvert N_2\rvert$ large	$\frac{p^2\rho}{8\pi c^3}$	$\pi^{5/2}c^3/\sqrt{2}p^{5/2}\rho^{1/2}z_0^3\cos\theta_1$ $= \chi/\cos\theta_1$	$\chi/\cos\theta_n$
Layer acting by Refractive Bending: $\left(\frac{2\pi z_0}{\lambda}\right)(1 - \mu^2) = \frac{2\pi z_0}{\lambda}\left(\frac{\nu_0^2}{\nu^2}\right)$ small, also α small	$\frac{4\pi c}{\rho}$	Very large.	

---

† It is easy to show that S defined in this manner is the same quantity as S defined in Eq. (3.17).

The first column gives the electrical conditions of the layer and the second, third and fourth the attenuation coefficients for the various order rays 0, 1, *n*, etc.

The first row represents the conditions appropriate to long wave transmission where α is large. The attenuation exponent is of the " Watson " and " Austen Cohen " form, varying inversely as the square root of the wave-length and directly as the square root of the resistivity of the layer.

It is to be noted that the attenuation of the 1st to *n*th order waves, is, apart from the term $1/\cos\theta_n$ (nearly unity), just twice that of the zero order ray.

The zero order wave attenuation is the same as that found by G. N. Watson.

This condition of affairs only obtains when $4\pi c^2/\mu p$ is a large quantity and simultaneously $\left(\frac{2\pi z_0}{\lambda}\right)\frac{\rho p}{4\pi c^2}$ is small for a given resistivity ρ; this latter quantity can be made large by taking λ small enough, in which case the types of attenuation alter to those shown in the second row. The Watson–Austin Cohen type of attenuation is therefore confined to wave-lengths greater than a fixed value given by $\lambda_0^3 = (2\pi z_0)^2\,\rho/2c$. Observation shows that the Watson–Austin Cohen type of attenuation formula appears to be confined to the longer range of wave-lengths, say, $\lambda > 5$ km., though, of course, this does not necessarily imply that the layer is sharply defined.

This illustration is an idealisation of the long wave radio case, where the earth and Heaviside layers have the properties of pure conductors, *i.e.*, the currents in the conductors are in phase with the electric forces. This is, of course, the case for the earth. It also follows that in the ionised region of the atmosphere the same holds good (even in the presence of the earth's magnetic field) so long as the time period of the waves is long compared with the mean time between collision of electrons and molecules.*

§ 4. We may consider the other extreme ideal case that of ionic refraction, where the time period between collisions is very large compared with the time period of the waves, *i.e.*, where the electrons are substantially free and the ionic refraction theory obtains.

We may even dispense with the ideal condition that the layer is sharply defined and assume, for instance, that the density varies in proportion to the square of the height, and we shall again find that if λ is great enough there are no high angle rays or proper values, and with smaller wave-lengths there are only a finite number.

---

* Eckersley, 'J. Inst. Elect. Eng., Lond.,' vol. 65, p. 626 (1927).

Here we enter the field of the ionic refraction ray theory, and show that the ray theory is inadequate even here if wave-lengths are large enough.

The analysis is based on the differential equation of the waves in the medium above the earth's surface.

The differential equation is

$$\nabla^2\psi = \left(1 - \frac{\nu_0^{\,2}}{\nu^2}\right)\frac{1}{c^2}\frac{\partial^2\psi}{\partial t^2}, \tag{4.1}$$

where ψ is the vector potential,

$$\nu_0^{\,2} = \frac{\mathrm{N}_z e^2}{\pi m}c^2 \qquad \nu = \text{frequency},$$

and N_z ionic density at a height z above the earth's surface.

e — electronic charge

m - electronic mass

c = velocity of light.

N_z is a function of the height z above the earth's surface.

Assume a solution of the form

$$e^{\frac{2\pi i l x}{\lambda}}\left(\mathrm{F}(z)\right) e^{2\pi i \nu t}.$$

ψ is a function of x and z only, *i.e.*, we suppose the density is graded in the vertical direction only.

Then substituting this value for ψ in the differential equation, we get

$$\frac{\partial^2\mathrm{F}(z)}{\partial z^2} + \left\{\left(\frac{2\pi n}{\lambda}\right)^2 - \frac{4\pi^2\nu_0^{\,2}}{c^2}\right\}\mathrm{F}(z) = 0, \tag{4.2}$$

where $n^2 = (1 - l^2)$.

Now $\mathrm{N} \propto \nu_0^{\,2} \propto z^2$, *i.e.*, we assume the density is proportional to the square of the height, and therefore finally (4.2) can be written

$$\frac{\partial^2\mathrm{F}(z)}{\partial z^2} + \{\beta^2 - \gamma^2 z^2\}\mathrm{F}(z) = 0, \tag{4.3}$$

which is of the form discussed by Schroedinger in the case of the vibration of an electron.

We know that in this case F (z) is only single valued and finite at $+\infty$ for a series of so-called "proper values" of β. These are given by

$$\beta^2 = (2m + 1)\gamma, \tag{4.4}$$

γ is a measure of the gradient of N, *i.e.*,

$$N_z = \frac{m}{4\pi e^2}\gamma^2 z^2.$$

Let z_0 be the height where N = critical density N_0 corresponding to the frequency ν.

Then

$$N_0 = \frac{m}{4\pi e^2}\gamma^2 z_0^2 = \frac{\pi m}{e^2 c^2}\nu^2,$$

so that

$$\gamma^2 z_0^2 = (2\pi/\lambda)^2$$

or

$$\gamma = 2\pi/\lambda z_0.$$

The equation

$$\beta^2 = (2m + 1)\gamma$$

is now

$$\left(\frac{2\pi}{\lambda}\right)^2 n^2 = (2m + 1)\,\frac{2\pi}{z_0\lambda},$$

i.e.,

$$n^2 = (2m + 1)\,\frac{\lambda}{2\pi z_0}, \tag{4.5}$$

which gives the possible values of the direction cosines, n, of the rays.

If $\lambda > 2\pi z_0$ there is *no possible* value of m (integer) which satisfies this equation.

If $\lambda < 2\pi z_0$, m is the greatest integer which makes $(2m + 1)\,\lambda/2\pi z_0 < 1$.

There are then $m + 1$ possible rays, the corresponding values of $\cos\theta_m$ being

$$\sqrt{2m + 1}\left(\frac{\lambda}{2\pi z_0}\right)^{\frac{1}{2}}.$$

The approximate phase integral method in this case can be calculated as follows :—

The phase integral gives

$$\oint\sqrt{n^2 - \nu_0^2/\nu^2}\,dz = \oint\sqrt{n^2 - z^2/z_0^2}\,dz, \tag{4.6}$$

where z_0 has the same meaning as before.

This gives

$$2\int_{-nz_0}^{+nz_0} n^2 z_0\left(1 - \frac{z^2}{n^2 z_0^2}\right)^{\frac{1}{2}}\frac{dz}{nz_0} = r\lambda$$

or

$$n^2 = r\lambda/\pi z_0. \tag{4.7}$$

The correct wave method gives

$$n^2 = (r + \tfrac{1}{2}) \lambda/\pi z_0. \tag{4.8}$$

When r is large, which is the case where the gradient is gradual with a finite angle of elevation, the $\frac{1}{2}$ integer can be neglected in comparison with r, and the approximate method is correct within $100/2r$ per cent.

Here again we have a finite number of high angle rays. It is interesting to note that when $\lambda < 2\pi z_0$ there is *no possible* solution, in contradistinction to the case of the perfectly conducting boundaries where when $\lambda < 2z_0$ there is a solution. This is connected with the effective reversal in phase on reflection or refraction at the upper layer. Thus in the simple case of two sharply defined ionic refracting layers we can use the image theory to make this clear.

At every reflection we produce a *reversed* image, and the final effect is that of an infinite series of images alternately at a distance $2z_0$ apart. At a great distance the fields from all these cancel, *so long as* $\lambda > 2z_0$.

§ 5. *Diffraction.*—The final example is that of diffraction of electric waves round the earth's surface.

The propagation of waves in the broadcast band where in the main, and for daylight conditions, the reflection from the Heaviside layer is negligible, is mainly confined to what is generally known as the direct or surface ray. Sommerfeld has given a very comprehensive analysis of the intensity of this direct ray for relatively short distances where the earth can be considered as flat, taking into account the effect of the earth's resistivity and inductivity.

Watson, on the other hand, has considered the effect of the earth's curvature in the case of rather longer waves, and his formula is not applicable in the immediate neighbourhood of the transmitter.

He shows that with earth conductivities of 10^{-13} and with waves greater than 5 km. the effect of the earth's finite resistivity is negligible in the range considered.

For wave-lengths of the longer broadcast waves Sommerfeld's curve, which is approximately correct for short distances, passes over into Watson's curve for long distances.

The nature of the transition is naturally, as in all cases where simplifying assumptions cannot be made, difficult to compute. Also there are indications that with shorter wave-lengths and greater resistivities the Watson formula, even at the greater distance where normally it is applicable, requires modification on account of the finite conductivity of the earth. It is of importance to know for what wave-lengths and conductivities Watson's formula holds, in fact to have a criterion to determine where it breaks down. This criterion is difficult to obtain from Watson's analysis, and requires the redetermination by complicated mathematical methods of the zeros of certain functions which, in the ultimate analysis, determine the propagation constants. It was therefore thought that a more simple method of obtaining such a criterion would be afforded by the use of the approximate phase integral method.

It is shown that the transmission over the surface of a sphere is determined by an expression of the type

$$E = A \cos \{(n_s + \tfrac{1}{2})\theta - \pi/4\}/\sqrt{\sin\theta}, \tag{5.1}$$

where n_s is a root of the phase integral relation,

$$\oint \left\{1 - g(r) - n(n+1)\frac{\lambda^2}{(2\pi r)^2}\right\}^{\frac{1}{2}} dr = s\lambda, \tag{5.2}$$

where s is an integer and the integral is taken round suitable branch points of the integrand, $g(r)$ is a function which gives the deviation from unity of the refractive index of the medium (outside the sphere). In our case we may take $g(r) = 0$.

Let r_1 be the radius of the earth. Then effectively the reflection at $r = r_1$ corresponds to a branch point (with no change of phase) if the surface is a perfect conductor, but with a change of phase and amplitude depending on n if the surface is not a perfect reflector.

We may anticipate the final result (or use Watson's analysis) to show that when s is a small integer $n\lambda/2\pi r_1$ differs but slightly from unity.

The branch points occur in this integral when

$$\frac{n(n+1)\lambda^2}{(2\pi r)^2} = 1, \tag{5.3}$$

and when $r = r_1$.

Let r_0 be the value of r which satisfies (5.3), we have in effect to integrate from r_1 to r_0 round the branch point and back to r_1 again. The effect of the conducting surface at $r = r_1$ might have been taken account of by a sudden and practically discontinuous change in $g(r)$ at $r = r_1$, $g(r)$ being a function of the electrical constants of the conducting earth, being in fact $1 - \mu^2$ where μ is the complex refractive index of the earth.

It will be seen that this sudden discontinuity in $g(r)$ will produce, mathematically, a branch point at $r = r_1$ and the change of phase and amplitude at reflection will be given by the integration round this branch point.

In the region $r > r_1$ the integrand will have branch points at

$$r = \pm\sqrt{n(n+1)}\,\lambda/2\pi$$

so long as this quantity is greater than r_1. Values of n smaller than this give no branch points and give rise to a continuous spectrum, for instance divergent waves centred on $r = 0$.

The case where $\sqrt{n(n+1)}\,\lambda/2\pi > r_1$ leads to proper values which we shall find are connected with the types of wave found by G. N. Watson in his analysis of the diffraction problem.

Considering the case then in which this condition holds, and supposing the earth to be a perfect conductor, then the change of phase on reflection at $r = r_1$ will be zero, and the phase integral will be

$$2\int^{r_0}\left\{1-\frac{n(n+1)\lambda^2}{(2\pi r)^2}\right\}dr = s\lambda. \tag{5.4}$$

Make the substitution

$$\frac{n(n+1)\lambda^2}{(2\pi r)^2} = \frac{1}{z^2}, \tag{5.5}$$

i.e.,

$$r = z\,\frac{\sqrt{n(n+1)}\,\lambda}{2\pi}.$$

The phase integral relation then becomes

$$2\int_{r_1}^{r_0}\{1-1/z^2\}^{\frac{1}{2}}\,dz = s2\pi/\sqrt{n(n+1)},$$

the limits of z are

$$r = r_0 \qquad z = 1$$

$$r = r_1 \qquad z = \frac{2\pi r_1}{\sqrt{n(n+1)}\,\lambda}$$

$$= 1/k \text{ say, where } k > 1.$$

The phase integral becomes

$$2\int_{1/k}^{1}\{1-1/z^2\}^{\frac{1}{2}}\,dz = 2\pi s/\sqrt{n(n+1)},$$

z lies between $1/k$ and 1, *i.e.*, is always < 1.

We make the further substitution $z = \cos\theta$, θ will then be small and we have

$$2\int_{\cos^{-1}1/k}^{0}\{-\sin^2\theta\}^{\frac{1}{2}}\left(-\frac{\sin\theta}{\cos\theta}\right)d\theta = 2\pi s/\sqrt{n(n+1)},$$

now this is

$$-2i\int_{\cos^{-1}1/k}^{0}\left(\frac{1}{\cos\theta}-\cos\theta\right)d\theta = 2\pi s/\sqrt{n(n+1)}. \tag{5.6}$$

Each of these terms can be integrated, but since θ is small we can make an approximation straight away and put

$$1/\cos\theta = 1 + \theta^2/2, \quad \cos\theta = 1 - \theta^2/2,$$

therefore

$$-2i\int_{\cos^{-1}1/k}^{0}\theta^2\,d\theta = +2i\,\theta_1{}^3/3 = 2\pi s/\sqrt{n\,(n+1)},$$

where

$$\cos\theta_1 = 1/k$$

$$\sin\theta_1 = \sqrt{1-1/k^2} \simeq \theta_1$$

$$+2i\,\theta_1{}^3/3 = \tfrac{2}{3}i\left(1-\frac{1}{k^2}\right)^{3/2} = 2\pi s/\sqrt{n\,(n+1)}.$$

n is large so that $\sqrt{n\,(n+1)} = n + \frac{1}{2}$ very nearly. Now k is slightly > 1, let it be $1 + \xi$

$$1 - \frac{1}{k^2} = \frac{2\xi}{1+2\xi}$$

very nearly, and

$$\tfrac{2}{3}i\left(1-\frac{1}{k^2}\right)^{3/2} = \tfrac{2}{3}i\left(\frac{2\xi}{1+2\xi}\right)^{3/2} = \tfrac{2}{3}i\,(2\xi)^{3/2}$$

nearly ξ small, therefore

$$\tfrac{2}{3}i\,(2\xi)^{3/2} = 2\pi s/\sqrt{n\,(n+1)}$$

and

$$\xi = \frac{(2\pi s)^{2/3}}{2}\,(n+\tfrac{1}{2})^{-2/3}\,(3/2)^{2/3}\,e^{-\pi i/3}. \tag{5.7}$$

Now

$$k = \frac{\lambda}{2\pi r_1}\sqrt{n\,(n+1)} = 1 + \xi$$

or neglecting ξ in comparison with unity in determining $\sqrt{n\,(n+1)}$ since n is large

$$(n+\tfrac{1}{2})^{2/3} = \left(\frac{2\pi r_1}{\lambda}\right)^{2/3}$$

and

$$\xi = \frac{(2\pi s)^{2/3}}{2}\,(\tfrac{3}{2})^{2/3}\,e^{-\pi i/3}\,\frac{1}{\left(\dfrac{2\pi r_1}{\lambda}\right)^{2/3}}, \tag{5.8}$$

and $\dfrac{2\pi r_1}{\lambda}\,(\xi + 1)$, the coefficient of θ in (5.1) giving the attenuation and propagation constant is

$$x + \rho x^{1/3}\,e^{-i\pi/3}, \tag{5.9}$$

where

$$x = \frac{2\pi r_1}{\lambda}, \text{ and } \rho = \frac{(3\pi s)^{2/3}}{2}.$$

This, it will be observed, is exactly in the form given by G. N. Watson, but his values of ρ differ from ours with—

		Watson.
$S = 1$	$\rho = 2\cdot214$	$0\cdot6083$
$S = 2$	$\rho = 3\cdot514$	$2\cdot577$
$S = 3$	$\rho = 4\cdot605$	$3\cdot83$

while the values given by Watson are shown in the second column.

In plotting the values it would appear that the two values would approach each other for s large.

The phase integral method is approximate, it neglects the change of phase on integration round the branch point at $r = r_0$. Further approximation by the method of L. Brillouin[*] show that a phase change must occur here. It is however unnecessary to compute this further by this method because a comparison between Watson's and my results show immediately what this phase change must be.

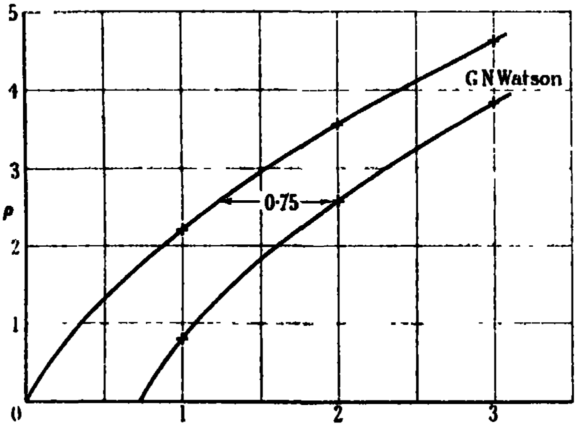

Fig. 3.

In fig. 3 the two sets of values are plotted against s. On examination it appears that the two curves through the points are identical in shape and can be fitted on each other by a lateral shift of 0·75 on my curve. This implies a phase change of $\frac{3}{4} \cdot 2\pi$ or $\frac{3}{2}\pi$ at r_0 and the true phase integral values for n are

---

[*] 'C. R. Acad. Sci. Paris,' vol. 182, p. 374 (1926), and 'J. Phys. Radium,' vol. 7, p. 353 (1926).

$$x + \rho_s x^{-1/3} e^{-\pi i/3},$$

where

$$\rho_s = \frac{[2\pi(s - \frac{3}{4})]^{2/3}}{2} (\tfrac{3}{2})^{2/3}. \tag{5.10}$$

We are now in a position to take into account the effect of the earth's resistivity.

When the earth is not perfectly conducting the phase change at reflection at the earth's surface is no longer zero, but is finite and depends on the angle of incidence of the waves. Let this angle be 90° — θ, then the phase change at reflection is

$$2 \tan^{-1} \frac{\sqrt{\sin^2\theta + \varepsilon - 1 + 2i\sigma\lambda c}}{\sin\theta(\varepsilon + 2i\sigma\lambda c)} = \chi, \tag{5.11}$$

where

ε = specific inductive capacity of the earth
σ = conductivity (e.m. units)
λ = wave-length
c = velocity of light

$2\sigma\lambda c$ is of the order 600 for $\lambda = 1$ km., ε can therefore be neglected in comparison with $2\sigma\lambda c$.

Taking this phase change at reflection into account the values of ρ_s are

$$\rho_s = (2\pi s - 3\pi/2 + \chi)^{2/3} (\tfrac{3}{2})^{2/3}/2 \tag{5.12}$$

formally the value of θ depends on n, which is the direction cosine of the normal to the wave surface.

Taking $n = \cos\theta$

$$\sin\theta = (1 - n^2)^{\frac{1}{2}} = i\sqrt{2\rho_s}\,\frac{e^{-i\pi/6}}{x^{1/3}}, \tag{5.13}$$

so that χ which depends on $\sin\theta$ is a function of ρ_s and which again depends on χ and is a function of ρ_s.

We can proceed by successive approximations when θ is small, or θ is nearly $\pi/2$.

Two extreme limits occur when the earth conductivity or the wave-length is great enough, so that $\sin\theta\sqrt{\sigma\lambda c}$ is a large enough quantity, then χ is a small angle. On the other hand, if σ and λ are small enough so that $\sin\theta\sqrt{\sigma\lambda c}$ is small

$$\left|\frac{\{\sin^2\theta + \varepsilon - 1 + 2i\sigma\lambda c\}^{\frac{1}{2}}}{\sin\theta(\varepsilon + 2i\sigma\lambda c)}\right| \text{ is large}$$

and χ tends to π.

There are therefore limiting values for ρ_s, one for long enough waves in which the earth's resistivity can be neglected and is the value obtained by Watson, and the other is the value of ρ_s putting $\chi = \pi$, which is appropriate to the case of sufficiently short waves or high resistivities. The transition between the two can be computed, as shown above, by successive approximations.

The transition values have been computed by Millington and are shown in fig. 4. The real part of the exponential factor, representing the attenuation, can be put in the form

$$e^{-\frac{\beta\phi}{\lambda^{1/3}}}. \tag{5.14}$$

ϕ is the angular separation of transmitter and receiver and λ is the wave-length in kilometres. The value for β when $\chi \rightarrow 0$ is that calculated by Watson, *i.e.*, 23·9 for $s = 1$ when, however, $\chi \rightarrow \pi$ the value of $\beta \rightarrow 53$.

In the figure the transition value of β is plotted against $\sigma^{1/2}\lambda^{5/6}$ upon which the value of β depends when r_1 is constant. It will be seen that β varies smoothly between the limits 23·9 and 53. If λ is 1 km. the transition occurs between the limits 10^{-11} and 10^{-15} of σ. Or taking σ constant 10^{-13} e.m. units, the wave-length limits are 3·7 km. and 16 m.

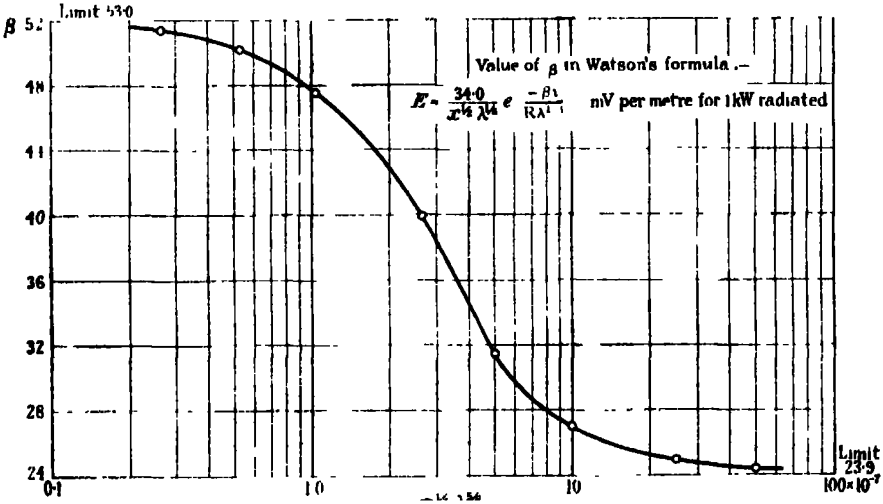

FIG. 4.—Value of β in Watson's Formula :—

$$E = \frac{34\,.\,0}{x^{1/2}\lambda^{1/6}}\, e^{\frac{-\beta x}{R\lambda^{1/3}}} \text{ in mV per metre for 1 K.W. radiated.}$$

A number of measurements of the field strength of the broadcast transmitting station at Warsaw (λ 1410 m., 100 k.w. radiated power) have been made recently at Chelmsford. During the mid-day hours 1100 to 1300 G.M.T.

the field intensity, although not quite steady, only fluctuates 20 to 30 per cent. so that the resultant field may be considered to be made up of a steady surface ray (diffracted) of a mean value 40 micro volts/m. and a reflected ray of about 20 to 30 per cent. of this.

The distance between Warsaw and Chelmsford is 1400 k.m. and quite sufficient to show marked diffraction effects. This is obvious on comparing the observed field intensity with that calculated (on Sommerfeld's theory) for a flat earth. Taking $\sigma = 10^{-13}$ the calculated value is of the order of 500 micro volts per metre, more than 10 times the observed value. The difference is due without doubt to the fact the effect of the earth's curvature over this distance is to place the receiver in the geometrical shadow, the field is entirely due to the diffraction spread from the regions outside the geometrical shadow.

We can compare the observed result with that calculated from the diffraction formula by using Van der Pol's explicit form, *i.e.*,

$$E = \frac{0\cdot5365hI}{(\sin\phi)^{1/2}\ \lambda^{7/6}}\, e^{\frac{-\beta\phi}{\lambda^{1/3}}} \tag{5. 15}$$

or

$$E = \frac{0\cdot5365}{(\sin\phi)^{\frac{1}{2}}}\, \frac{\sqrt{W}}{40\lambda^{1/6}}\, e^{-\beta\phi/\lambda^{1/3}},$$

where W is the power radiated in watts, $r_1\phi = 1400$ km. and λ is the wavelength in kilometres.

E_{obs}	E_{calc}		
	$\sigma = \infty$.	$\sigma = 10^{-12}$.	$\sigma = 10^{-13}$.
40	98	39·6	12·0

using the value of β appropriate to the value of σ heading the columns.

It will be seen that the best agreement is obtained with $\sigma = 10^{-12}$ e.m. units. Measured values of σ, the earth's conductivity, vary from about 10^{-12} to 10^{-14}.

Measurements made at Broomfield, Chelmsford, gave values $1/2 \times 10^{12}$; other measurements in England (derived from field intensity curves on the broadcast band) give values of the order of 10^{-13}. In the absence of any knowledge of the average conductivity over the route Warsaw—Chelmsford, and remembering that part of the route is over sea ($\sigma = 10^{-11}$) the agreement may be considered satisfactory.

In conclusion, I wish to acknowledge my thanks to Marconi Wireless Telegraph Company for allowing me to publish this paper.

This paper is concerned with the transmission of electromagnetic waves in the space bounded by various conducting or ionically refracting surfaces or regions. In particular, the transmission between either plane or spherically stratified layers is considered.

In a recent paper by the writer it was shown how the main characteristics of the solution of such transmission problems could be obtained from a phase integral method analogous to the Bohr-Sommerfeld phase integral method of quantum dynamics.

In the present paper certain particular problems are treated and a full wave solution is obtained and compared with the solution derived by the phase integral method.

It is found that the full solutions are characterised by a series of " Eigen functions " appropriate to the particular case considered, and as in quantum dynamics, each Eigen function is associated with a definite " proper value " which determines the generalised direction cosine and attenuation coefficient

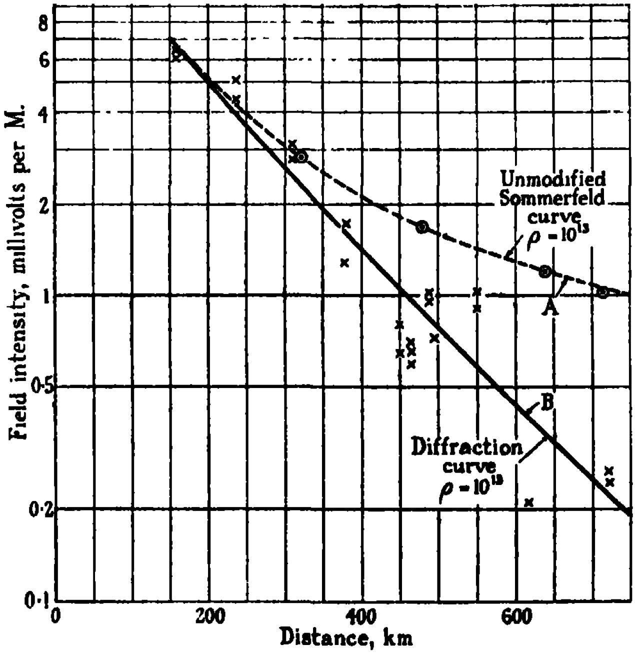

FIG. 5.—5XX Daventry Daylight Field Strength, Mid-day, July, 1931, λ = 1550 m. Normal power, 25 k.w. × = observed points.

of the electromagnetic wave. It is then shown that the phase integral method determines these proper values very simply.

The paper is designed to illustrate, by the full solution of certain examples, the meaning and scope of the phase integral method.

The solution of the transmission between plane perfectly conducting layers is first considered, and then generalised to the case of imperfectly conducting layers. Finally, the phase integral method is applied to the case of diffraction of electromagnetic waves round a semi-conducting sphere, a problem already considered by G. N. Watson. The effect of the finite conductivity of the sphere was neglected by Watson.

It is found, however, that the phase integral method is in such a form that the finite conductivity of the sphere can be taken into account.

The theory is applied to compute the field intensity produced by the 120 k.w. broadcast at Warsaw and reasonable agreement is obtained.

[*Note added in proof, April* 5, 1932.—I have recently obtained by the courtesy of Mr. Kirke, of the British Broadcasting Corporation, field intensity measurements of Daventry 5XX up to distances of 720 km. These measurements, shown in fig. 5, are in good accord with the Diffraction Formula (Curve B) with $\sigma = 10^{-13}$ and 25 k.w. radiated. The Sommerfeld curve A gives values which are considerably too high at great distances.

A Theory of some Electron-levels in H_2.

By J. K. L. MacDonald, 1851 Exhibitioner, Emmanuel College, Cambridge, England.

(Communicated by R. H. Fowler.—Received January 19, 1932.)

§ 1. *Introduction.*—Preparatory to a theoretical investigation of the Stark-effect in the hydrogen molecule, it was found necessary to undertake the present study of some excited electron levels. Suitable approximate wave functions must be determined in order to calculate the Stark-effect perturbations associated with neighbouring states. The functions must be appropriate for certain integrations in which the equilibrium nuclear separations are used.

Kemble and Zener* have employed a method which gives wave functions suitable for great inter-atomic separation. Their calculations for "equilibrium" energies show rather poor quantitative agreement with experimental values for the $2p\Pi$ states. In an unpublished study of the $2p\Sigma$ states, using the method of Kemble and Zener, the writer also found great discrepancies. Guillemin and Zener† used a variation method and obtained moderately good agreement with the experimental results for the $2p\,{}^1\Sigma$ state. A short time before the present paper was submitted for publication a paper by Hylleraas‡ appeared. In it the energy curves for 2-quantum electron levels were determined. The results arrived at by Hylleraas agree well with the experimental data which he gives. In his paper Hylleraas does not discuss the methods by which his 2-quantum wave functions are constructed from the basic $H_2{}^+$-like functions which he uses.

Two observations suggested the method of investigation followed in the present communication. Firstly, the potential energy curves for the hydrogen molecular ion and for the excited molecular levels are similar in shape and equilibrium position, and secondly, the levels of the "outer electron" are spaced as expressed by an ordinary Rydberg formula.§ Our solutions for H_2 are therefore built up from the functions associated with one electron in the normal $H_2{}^+$ state and with the other in an "n-quantum" H_1 state, together with interchanges. The most important (experimentally) nuclear separation to be considered is that of normal $H_2{}^+$, namely two atomic units, and so, to make the calculations as analytically correct as possible, by avoiding unjustified functional expansions and without making them prohibitively lengthy, the above-mentioned nuclear separation has been employed alone throughout the work.

---

* 'Phys. Rev.,' vol. 33, p. 512 (1929).

† 'Phys. Rev.,' vol. 34, p. 999 (1929).

‡ 'Z. Physik,' vol. 71, p. 739 (1931).

§ 'Trans. Faraday Soc.,' vol. 25, p. 686 (1929).

The H_2^+ fixed nucleus problem has been studied by a number of investigators. The method of Burrau,* considered by Teller,† is questionable since it is dependent upon the use of the first few terms of a rather rapidly diverging series. Wilson's‡ function is too complicated for this particular problem, while that of Morse and Stueckleberg§ is unsuitable at equilibrium separation of the protons. It has been remarked that the problem is probably insoluble in terms of a series expansion. However, the Guillemin and Zener function‖ determined by a variation method has much to recommend it analytically as well as for its simple form. This last function, namely

$$M_+(\xi, \eta, \phi) = Ce^{-\alpha D\xi} \cosh \beta D\eta,$$

(where C, α and β are constants, 2D is the nuclear separation and ξ, η and ϕ are spheroidal co-ordinates) was finally selected as the most suitable for the problem.

§ 2. *The Mathematical Problem.*—The fixed-nucleus¶ wave equation for H_2 may be expressed in atomic units (*i.e.*, length, mass, charge and energy in terms of the quantities associated with the lowest level of atomic hydrogen) as follows

$$-[\nabla_a^2 + \nabla_b^2 - E - 2(V_a + V_b + V_{ab})]\psi$$
$$= [H_a + H_b + E + 2V_{ab}]\psi = [H + E]\psi = 0.$$

We have used

$$V_a = -[(1/aA) + (1/aB)], \quad V_b = -[(1/bA) + (1/bB)], \quad V_{ab} = (1/ab),$$

"*a*" and "*b*" refer to electrons, "A" and "B" to protons, *a*A, *b*A, etc., being the corresponding separation distances between the particles. It is important to note that we are using *negative* energy units for E; thus the actual total energy equals $-Rh$E.

---

* 'K. Danske. Vidensk. Selsk. Skr.,' vol. 7, p. 14 (1927).

† 'Z. Physik,' vol. 61, p. 458 (1930).

‡ 'Proc. Roy. Soc.,' A, vol. 118, p. 617 (1928).

§ 'Phys. Rev.,' vol. 33, p. 932 (1929).

‖ 'Proc. Nat. Acad. Sci.,' vol. 15, p. 314 (1929).

¶ 'Ann. Physik,' vol. 84, p. 457 (1927), and 'Phys. Rev.,' vol. 32, p. 250 (1928).

For states with the principal quantum number " n " we build up a variation function as follows[*]

$$\begin{matrix}\text{Singlet}\\ \text{Triplet}\end{matrix}\ \psi = \sum_{l=0}^{n-1} \sum_{m=-l}^{+l} \{M_+(a)\,(nlm\,|\,b) \pm M_+(b)\,(nlm\,|\,a)\}\, C_{nlm}.$$

In this equation $M_+(a)$ is the chosen H^+_2 function associated with the energy (E_+). $M_+(a)$ satisfies the following variation equation

$$\delta\left\{\int \overline{M}_+(a)\,[H_a]\,M_+(a)\,d\tau_a\right\} = 0 \qquad d\tau_a = dx_a\,dy_a\,dz_a$$

subject to

$$\int \overline{M}_+(a)\,M_+(a)\,d\tau_a = 1$$

and

$$\int \overline{M}_+(a)\,[H_a + E_+]\,M_+(a)\,d\tau_a = 0. \tag{A}$$

Also, $(nlm\,|\,b)$ is the atomic hydrogen wave function in polar co-ordinates referred to the centre of the inter-nuclear axis.

We have

$$[\nabla^2_b - (1/n^2) + (2/b)]\,(nlm\,|\,b) = 0 = [-H_b - (1/n^2) + 2\,(1/b) + V_b)]\,(nlm\,|\,b), \tag{B}$$

where we have used " b " in $(1/b)$ as the radial co-ordinate.

We proceed to determine " E " and " C_{nlm} " from the variation equation[†]

$$\delta\int \overline{\psi}\,|H+E]\psi\,d\tau_a d\tau_b = 0 = \sum_{l_1,m_1} \sum_{l_2,m_2} \{C_{nl_1m_1}\,(nl_1m_1\,|\,H+E\,|\,nl_2m_2)\}\,\delta C_{nl_2m_2}, \tag{C}$$

where

$$(nl_1m_1\,|\,H+E\,|\,nl_2m_2) = 2\int [\overline{M}_+(a)\,\overline{(nl_1m_1}\,|\,b) \pm \overline{M}_+(b)\,\overline{(nl_1m_1}\,|\,a)] \times [H+E]\,[M_+(a)\,(nl_2m_2\,|\,b)]\,d\tau_a\,d\tau_b$$

(using the symmetry between a and b).. Now by the properties (A) and (B) above, and with $\varepsilon_{nlm} = (E - E_+ - 1/n^2)$ the expression becomes

$$2\int \{[\overline{M}_+(a)\,\overline{(nl_1m_1}\,|\,b) \pm \overline{M}_+(b)\,\overline{(nl_1m_1}\,|\,a)]\,[\varepsilon_{nlm} + 2\,(V_{ab} + V_b + 1/b)] \times M_+(a)\,(nl_2m_2\,|\,b) \quad \pm \overline{M}_+(b)\,(nl_2m_2\,|\,b)\,\overline{(nl_1m_1}\,|\,a)[H_a + E_+]\,M_+(a)\}\,d\tau_a d\tau_b.$$

---

[*] The general theory of the variation method was developed in Rayleigh's researches. Later the method was investigated by Ritz.

[†] The equation is the equivalent of the group in (A). E may be regarded as an " undetermined multiplier."

Since $M_+(a)$ is symmetrical about the inter-nuclear axis and since it as well as $(V_{ab} + V_b + 1/b)$ and $(nlm|b)$ are also symmetrical about the mid-point of the axis, therefore the above integrals vanish term by term unless $m_1 = m_2$ and $l_1 + l_2 =$ even integer.

For the cases $n = 2$ and $n = 3$, by using the above rules and equating to zero the coefficients of C_{nlm} in (C) we get the following relations for determining the energies associated with the various states listed below :—

$$\begin{array}{llll}
2s\,{}^{1,3}\Sigma: & (200|H+E|200)=0; & 3p\,{}^{1,3}\Sigma: & (310|H+E|310)=0; \\
2p\,{}^{1,3}\Sigma: & (210|H+E|210)=0; & 3p\,{}^{1,3}\Pi: & (311|H+E|311)=0; \\
2p\,{}^{1,3}\Pi: & (211|H+E|211)=0; & 3d\,{}^{1,3}\Pi: & (321|H+E|321)=0; \\
 & & 3d\,{}^{1,3}\Delta: & (322|H+E|322)=0;
\end{array}$$

$$3s\,{}^{1,3}\Sigma \text{ and } 3d\,{}^{1,3}\Sigma: \; C_{310}(300|H+E|300) + C_{320}(320|H+E|300) = 0$$

$$C_{300}(320|H+E|300) + C_{320}(320|H+E|320) = 0$$

To facilitate the calculations we set

$$\tfrac{1}{2}(nl_1m_1|H+E|nl_2m_2)/\{N(nl_1m_1)\,N(nl_2m_2)\} = (nl_1m_1|H+E|nl_2m_2)_1 \pm (nl_1m_1|H+E|nl_2m_2)_2,$$

thereby separating the "Coulomb" from the "exchange" terms. We use

$(nlm) \rightarrow$	200	210	211	300	310	311	320	321	322
$N(nlm) \rightarrow$	$1/4$	$1/4$	$\sqrt{2}/8$	$\sqrt{2}/81\sqrt{3}$	$2/81$	$\sqrt{2}/81$	$2/81\sqrt{3}$	$\sqrt{2}/243$	$\sqrt{2}/486$
$(nl\|a)_0 \rightarrow$	$(2-a)\,e^{-a/2}$	$ae^{-a/2}$		$(2a^2-18a+27)\,e^{-a/3}$	$a\,(a-6)\,e^{-a/3}$		$a^2e^{-a/3}$		

a, μ_a and ϕ_a are spherical polar co-ordinates of electron "a," and

$$(nl/a)_0 = \sqrt{2\pi}\,(nlm|a)/N\,(nlm)\;P_l^m\,(\mu_a)\,e^{im\phi_a},$$

$$P_l^m = (1-\mu^2)^{m/2}\,(d/d\mu)^m\,P_l\,(\mu).$$

Using the normalisation of the functions and the polar expansions for V_b and V_{ab}, we get the expressions below.

"Coulomb term":

$$
\begin{aligned}
(nl_1m|\mathrm{H}+\mathrm{E}|nl_2m)_1 &= \varepsilon_{nlm}\,\delta(l_1, l_2)/[\mathrm{N}(nl_1m)]^2 \\
&\quad + 2\mathrm{C}(0, l_1, l_2, m)\int_0^\infty \mathrm{R}''_0(a)\,a^2[\mathrm{A}(0, l_1, l_2, 0)+\mathrm{A}(0, l_1, l_2, a) \\
&\qquad\qquad\qquad\qquad\qquad\qquad -2\mathrm{A}(0, l_1, l_2, \mathrm{D})]\,da \\
&\quad + 2\left\{\sum_{r=1}^{(l_1+l_2)/2}\mathrm{C}(2r, l_1, l_2, m)\Big[-2\mathrm{A}(2r, l_1, l_2, \mathrm{D})\right. \\
&\qquad\qquad \left. +\int_0^\infty \mathrm{R}''_{2r}(a)\,\mathrm{A}(2r, l_1, l_2, a)\Big]a^2\,da\right\}\begin{matrix}\times 1 & l_1+l_2>2, \\ \times 0 & l_1+l_2<2,\end{matrix}
\end{aligned}
$$

where we have used the symbols:

$$\mathrm{R}''_{2r}(a) = \int_{-1}^{1} 2\pi\,[\mathrm{M}_+(a)]^2\,\mathrm{P}_{2r}(\mu_a)\,d\mu_a$$

$$\mathrm{A}(2r, l_1, l_2, x) = \int_0^\infty (nl_1|a)_0\,(nl_2|a)_0\,a^2\begin{Bmatrix}a^{2r}/x^{2r+1} \\ x^{2r}/a^{2r+1}\end{Bmatrix}da \quad \begin{matrix}a<x, \\ a\geqslant x,\end{matrix}$$

$$\mathrm{C}(2r, l_1, l_2, m) = \int_{-1}^{1}\mathrm{P}_{2r}(\mu)\,\mathrm{P}_{l_1}^{m}(\mu)\,\mathrm{P}_{l_2}^{m}(\mu)\,d\mu = \mathrm{C}(2r, l_2, l_1, m).$$

"Exchange term":

$$
\begin{aligned}
(nl_1m|\mathrm{H}+\mathrm{E}|nl_2m)_2 &= \Big\{\mathrm{I}(l_2)\Big[\varepsilon_{nlm}\mathrm{I}(l_1) \\
&\quad + \int_0^\infty\int_{-1}^{1}(2\pi)^{\frac{1}{2}}\,\mathrm{P}_{l_1}(\mu_a)\,(nl_1|a)_0\,[\mathrm{H}_a+\mathrm{E}_+]\,\mathrm{M}_+(a)\,a^2\,da\,d\mu_a\Big] \\
&\quad + 2\int_0^\infty[\mathrm{B}(0, l_2, l_2, 0)+\mathrm{B}(0, l_2, l_2, a)-2\mathrm{B}(0, l_2, l_2, \mathrm{D})]\,\mathrm{R}'_{l_1}(a)\,(nl_1|a)_0\,a^2\,da \\
&\qquad\qquad\qquad\qquad -2\mathrm{I}(l_1)\,\mathrm{F}(l_2, \mathrm{D})\Big\}\,\delta(m, 0)\,\delta(\text{even } l\text{'s}) \\
&\quad + 2\left\{\sum_{s_1=0}^{\infty}\sum_{s_2=0}^{\infty}\sum_{t>0}\tfrac{1}{2}\int_0^\infty(4s_1+1)(4s_2+1)\,\mathrm{C}(2s_1, l_1, t, m)\,\mathrm{C}(2s_2, l_2, t, m)\right. \\
&\qquad\qquad \left.\frac{[t-|m|]!}{[t+|m|]!}\,\mathrm{R}'_{2s_1}(a)\,\mathrm{B}(t, 2s_2, l_2, a)\,(nl_1|a)_0\,a^2\,da\right\},
\end{aligned}
$$

where we have used the symbols:

$$
\begin{aligned}
\mathrm{I}(l) &= \int_0^\infty\int_{-1}^{1}(2\pi)^{\frac{1}{2}}\mathrm{M}_+(a)\,(nl|a)_0\,\mathrm{P}_l(\mu_a)\,a^2\,d\mu_a\,da \\
&= \int_0^\infty (nl|b)_0\,\mathrm{R}'_l(b)\,b^2\,db
\end{aligned}
$$

$$\mathrm{F}(l, \mathrm{D}) = \int_0^\infty\int_{-1}^{1}[\mathrm{V}_a-2/\mathrm{G}]\,(2\pi)^{\frac{1}{2}}\,\mathrm{M}_+(a)\,(nl|a)_0\,\mathrm{P}_l|\mu_a)\,a^2\,d\mu_a\,da$$

$$\mathrm{B}(t, 2s, l, x) = \int_0^\infty (nl|a)_0\,\mathrm{R}'_{2s}(a)\,a^2\begin{Bmatrix}a^t/x^{t+1} \\ x^t/a^{t+1}\end{Bmatrix}da \quad \begin{matrix}a\leqslant x, \\ a>x,\end{matrix}$$

"t" is summed over even or odd integers between the greatest of unity, $|m|$, $|l_1 - 2s_1|$ and $|l_2 - 2s_2|$ to the lesser of $l_1 + 2s_1$ and $l_2 + 2s_2$, according as l_1 and l_2 are even or odd.

§ 3. *Notes on the Calculations.*—It will be noted that we have used the $(nlm\,|a)$ functions expressed in spherical co-ordinates while $M_+(a)$ is in spheroidals. With far separated nuclei one may consider an electron as attached to either nucleus, in which case the obvious co-ordinate system is the latter for both electrons. However, as the nuclei approach each other this picture becomes meaningless since the "inner electron" becomes $H^+{}_2$-like, the outer electron moving in a nearly central field. For our purposes it would be very convenient *to have $M_+(a)$ expressed in a simple polar form.* No suitable expressions in such form have been found, so in order to avoid questionable expansions of the spheroidal functions in terms of sphericals, it has been found best to use graphical methods for obtaining such expressions as $R'(a)$, $R''(a)$, $B(t, 2s, l, x)$, $F(l, D)$ and integrals containing these expressions. Much of the graphical integration is multiple and therefore extremely tedious. Over 500 graphs were measured in the present work, any "personal errors" showing themselves immediately by the presence of irregular points. The functions $A(2r, l_1, l_2, x)$ and $C(2r, l_1, l_2, m)$* were calculated from their analytical formulæ.

The "Coulomb" terms were comparatively simple to calculate, but the "interchange" contributions presented great complications. For the latter the "s_1" and "s_2" summations were limited to the numbers 0, 1, and 2, the approximation being justified in selected cases by a rather complicated bounding analysis, apparent numerical convergence of all cases being rapid. The terms involving $(H_a + E_+)$ should vanish for a true $H^+{}_2$ function or one formed by a variation process involving a series of $(nlm\,|a)_{m=0}$ functions. The Guillemin and Zener $M_+(a)$ was found in fact to give negligible contributions in this type of term.

It will be noted that in the integrals involving the quantity $(V_b + V_{ab} + 1/b)$ we have collected the $(1/b)$ with the first term of each of the polar expansions for (V_b) and (V_{ab}). This procedure was made necessary by the fact that otherwise the results would, in certain cases, cancel within the accuracy obtainable in the graphical integration unless the terms were kept together throughout the work.

Values of ϵ_{nlm} in Units of $-Rh$.

$2s$	$^1\Sigma$	$-0{\cdot}080$	$3s$	$^1\Sigma$	$-0{\cdot}023$	$3d$	$^1\Sigma$	$+0{\cdot}0025$
	$^3\Sigma$	$-0{\cdot}016$		$^3\Sigma$	$-0{\cdot}005$		$^3\Sigma$	$+0{\cdot}0023$
$2p$	$^1\Sigma$	$+0{\cdot}010$	$3p$	$^1\Sigma$	$+0{\cdot}004$	$3d$	$^1\Pi$	$+0{\cdot}0008$
	$^3\Sigma$	$+0{\cdot}092$		$^3\Sigma$	$+0{\cdot}026$		$^3\Pi$	$+0{\cdot}0013$
$2p$	$^1\Pi$	$-0{\cdot}038$	$3p$	$^1\Pi$	$-0{\cdot}011$	$3d$	$^1\Delta$	$-0{\cdot}0023$
	$^3\Pi$	$+0{\cdot}005$		$^3\Pi$	$+0{\cdot}002$		$^3\Delta$	$-0{\cdot}0019$

* 'Phil. Trans.,' A, vol. 228, p. 151 (1929).

In the case of the pairs $3s\Sigma$, $3d\Sigma$ it is found that the constants C_{300} and C_{320} are such that

$$(C_{300}/C_{320}) \sim \begin{matrix} 10^{6} & \text{for } 3s\Sigma \\ 10^{-6} & \text{for } 3d\Sigma \end{matrix}$$

and therefore the states may be considered "pure" as regards non-singular integrations. The values of the C_{nlm}'s required to normalise the functions are given by

$$C_{nlm} = [2(1 \pm S_{nlm})]^{-\frac{1}{2}},$$

where $S_{200} \sim 0{\cdot}006$, $S_{300} \sim 0{\cdot}001$, $S_{320} \sim 0{\cdot}0001$, and zero in all others.

§ 4. *Correlation of Theoretical and Experimental Energies.*—The writer wishes to express his indebtedness to Dr. P. M. Davidson for data and suggestions concerning the connection between the theoretical and the experimental data. Following the procedure described by Kronig,* and using atomic units as before, the total energy (E_t) (Kronig's $W^0 = -RhE_t$) of the molecule is determined to a good degree of accuracy in most cases by the following "vibration equation":

$$\left\{\frac{1}{\mu\rho^2}\frac{d}{d\rho}\left(\rho^2\frac{d}{d\rho}\right) - E_t + E(\rho) - \frac{K(K+1)}{\mu\rho^2} - G(\rho)\right\} P(\rho) = 0.$$

Here (ρ) is the inter-nuclear separation distance, 2μ is the mass of the proton (in terms of the electron), K is the rotation quantum number such that $K \geqslant |m|$, $l \geqslant |m|$ ((l) and (m) being as in the first part of this paper). Also

$$G(\rho) = \frac{1}{\mu\rho^2}\int [\bar{\psi}(M^2 - 2m^2)\psi - \rho^2\bar{\psi}\frac{d^2}{d\rho^2}\psi]\, d\tau \quad d\tau \equiv \text{electron space},$$

where $E(\rho)$ and ψ refer to the "fixed-nucleus" problem, and M is the angular momentum operator for the electrons.

The experimental values of the energies are based on the Fues solution† of the vibration equation, using the expansion

$$\begin{aligned} E(\rho) - G(\rho) &= E_0 - U(\rho) \\ U(\rho) &= k(1 - \rho_0/\rho)^2 + \sum_{n>2} c_n (\rho/\rho_0 - 1)^n, \end{aligned}$$

where (ρ_0) is the equilibrium (ρ), and E_0, k and c_n are constants. From the band structure the values of the intervals may be determined between the $[E_0 - U(\rho)]$ values for all the known singlets, and for all the triplets except $d\,^3\Sigma$, Π, Δ and $2p\,^3\Pi$ which form a separate system of bands. To fix the actual values of individual E_0's it is necessary to employ rather drastic extrapolations which may introduce an error of 0·1 volt.

---

* Kronig, "Band Spectra and Molecular Structure," p. 16, Camb. Univ. Press (1930).

† 'Ann. Physik,' vol. 80, p. 367 (1926).

Using the ψ wave functions developed in this paper, the values of $G(\rho)_{\rho=2}$ are found to be given by

$$G(2) = (4 \times 1846/2)^{-1}[l(l+1) - 2m^2 + 2\cdot55] \text{ units of } + Rh$$

correct to 5 per cent., having values ranging between 0·03 to 0·001 volts.

We may therefore compare the experimental $\Delta[E_0 - U(\rho)]_{\rho=2}$ intervals with their theoretical equivalents $\Delta[E(\rho) - G(\rho)]_{\rho=2}$. This comparison is shown in the diagram, fig. 1. To make the intervals comparable the energy values associated with theory and experiment have been aligned at the $3^{1,3}d\Pi$, $3^3p\Pi$ levels in which the perturbation terms are found to be smallest. The diagram is based on the following data.* Note that comparative data can *only* be seen in the *diagram* and *not* in the table.

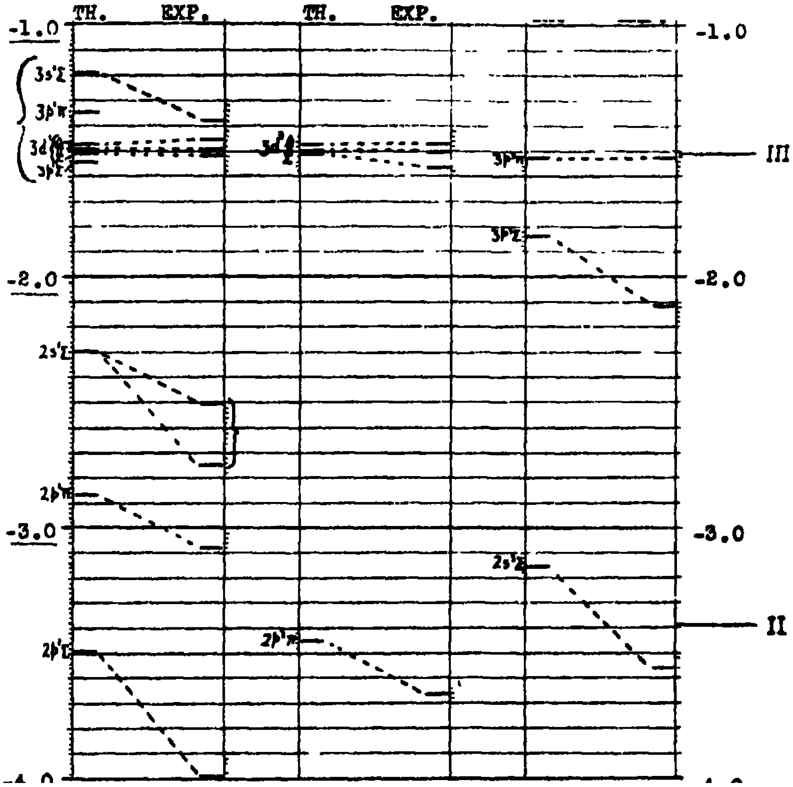

FIG. 1.—Electron Energies in Volts below Normal H^+_2.

---

* 'Proc. Roy. Soc.,' A, vol. 125, p. 23 (1929) and vol. 131, p. 658 (1931), and data interpreted in terms of wave mechanics formulæ privately communicated by Dr. P. M. Davidson.

State.		Exp. state.	Transition.	ΔE_0 (cm.$^{-1}$) (volts).		U(2) (volts).	$\Delta\,[E_0 - U(2)]$ (volts) (Exp.).	$[-E(2)+G(2)+E_t(2)]$ (volts) (Theor.).
2*s*	$^1\Sigma$	Inf. red	→ 2$p\,^1\Sigma$	13070	1·613*		1·485‡	$-2{\cdot}29_5$
	$^3\Sigma$	2 ^{3}S				0·035		$-3{\cdot}15_5$
2*p*	$^1\Sigma$	B				0·128		$-3{\cdot}49_6$
	$^3\Sigma$	—						−4·620
2*p*	$^1\Pi$	C	→ 2$p\,^1\Sigma$	8363	1·032	0·005	0·909	$-2{\cdot}86_5$
	$^3\Pi$	2 ^{3}P				0 004		$-3{\cdot}45_6$
3*s*	$^1\Sigma$	3 ^{1}O	→ 2$p\,^1\Sigma$	22190	2·738		2·610‡	$-1{\cdot}18_5$
	$^3\Sigma$	—						−1·423
3*p*	$^1\Sigma$	—						$-1{\cdot}54_2$
	$^3\Sigma$	$np\,^3\Sigma$	→ 2$s\,^3\Sigma$	11838	1·461	0·01	1·44	$-1{\cdot}84_6$
3*p*	$^1\Pi$	—						$-1{\cdot}34_5$
	$^3\Pi$	3 ^{3}P	→ 2$s\,^3\Sigma$	16768	2 069	0·0014	2·036	$-1{\cdot}52_3$
3*d*	$^1\Sigma$	3 ^{1}C	→ 2$p\,^1\Sigma$	21070	2·600†		2·472‡	−1·508
	$^3\Sigma$	3$d\,^3\Sigma$	→ 2$p\,^3\Pi$	17055	2·105		2·101‡	−1·505
3*d*	$^1\Pi$	3 ^{1}A, B	→ 2$p\,^1\Sigma$	21272	2·626†		2·497‡	−1·492
	$^3\Pi$	3$d\,^3\Pi_{ab}$	→ 2$p\,^3\Pi$	17575	2·169		2·165‡	−1·500
3*d*	$^1\Delta$	"New"§	→ 2$p\,^1\Sigma$	21575	2·663†		2·535‡	−1·472
	$^3\Delta$	3$d\,^3\Delta_{ab}$	→ 2$p\,^3\Pi$	17805	2·198		2·194‡	−1·477

* This assumes that the band at frequency 13400 has vibration number $v = 0$. If it is actually $v = 1$ then $\Delta E_0 = 1{\cdot}366$ volts.

† These singlet "D-levels" have been corrected approximately for uncoupling by a theory (to be published later) similar to that of Kronig and Fujioka ('Z. Physik,' vol. 63, p. 158 (1930)) for He_2. The d^3-levels are not so well established experimentally as are the singlets and the uncoupling correction has not been made for them.

‡ These data assume that the U(2)'s for the initial states are negligible (probably true except possibly for 2$s\,^1\Sigma$ and 3$s\,^1\Sigma$).

§ This "new" level refers to unpublished material kindly supplied by Dr. P. M. Davidson. The bands were known before they were used in connection with the present theory.

§ 5. *Discussion of Results.*—Upon examining the diagram, fig. 1, it will be seen that where the theoretical and the experimental levels corresponding to the same states are not in line with one another the theoretical values lie above the experimental positions. This strongly supports the interpretation of the experimental material since variation energies are greater than or equal to the correct theoretical eigenwerte. The figure and Table also show that where the perturbation energy is small the agreement is good. With the exception of the state $2s\,{}^3\Sigma$ the displacements from the unperturbed 2- and 3-quantum positions, indicated in the figure by the lines II and III respectively, are in the same direction as those given by the experimental data. As one might expect from the nature of the theory the perturbations and the discrepancies are greatest for the states with low values of the quantum numbers n, l, m. For these states there is strong interaction between the electrons. According to Hund* the $2p\,{}^3\Sigma$ is connected adiabatically with two unexcited atoms infinitely separated. The present theory supports this view, the displacement of the level being great in the downward direction (below the range of the diagram). The levels $3p\,{}^1\Sigma$ and $3p\,{}^1\Pi$ have not been established yet experimentally. Possibly they are represented by two of the extra levels near $n = 3$ mentioned by Richardson (*loc. cit.*). In the diagram it is assumed that the $3\,{}^1$O system is $3s\,{}^1\Sigma$. The stronger system $3\,{}^1$N would give better agreement with theory if its ρ_0 is near 2 atomic units.

Summary.—Using a variation method based on H^+_2 and atomic H functions, the electron energies for 2- and 3-quantum levels in H_2 are calculated. Graphical integrations for a nuclear separation $\rho = 2$ atomic units are employed in order to avoid unjustified series expansions for certain quantities. Perturbations involving the electron angular momentum and the ρ-variation of the wave functions are evaluated as a necessary process in correlating theoretical and experimental data. The sequence of the levels is the same as that found experimentally and the numerical values of the intervals between combining levels agree quite well with the present interpretation of the experimental material.

The writer wishes to express his great indebtedness to his wife for aid in the numerical and graphical calculations, and to Dr. P. M. Davidson and Professor O. W. Richardson for valuable information concerning the experimental data. The author is pleased to acknowledge the supervision of Professor R. H. Fowler. The research was made possible through the renewal of an 1851 Exhibition Scholarship and an Emmanuel College Research Studentship.

---

* 'Z. Physik,' vol. 63, p. 740 (1930).

The Reproducibility and Rate of Coagulation of Stearic Acid Smokes.

By H. S. PATTERSON and W. CAWOOD.

(Communicated by R. Whytlaw-Gray, F.R.S.—Received January 21, 1932.)

In a previous communication* the validity of the equation

$$\sigma = \sigma_0 + Kt$$

as a general expression for the coagulation of smokes was discussed. In this equation σ is the particulate volume of the smoke at time t, and σ_0 that at zero time. It was shown, however, that the value of the constant K varied with the weight of material dispersed, the rate of coagulation, and hence K, being greater, the smaller the weight concentration. This was found to be in general accordance with the theory of Smoluchowski when applied to smokes. At that time, however, a smoke of a given weight concentration could not be accurately reproduced, and consequently it was not possible to estimate how far the agreement with theory was qualitative rather than quantitative. In the same paper preliminary experiments were described which indicated that by blowing a stream of air over the material during dispersal, not only was it easier to reproduce a smoke of a given weight concentration, but also the uniformity of size of the particles composing the smoke was increased considerably. This method of producing smokes has now been worked out in detail and it has been found possible to obtain data enabling a quantitative comparison with theory to be made.

Method.

The material was dispersed from a boat, a drawing of which is shown in fig. 1. A is a basket made of fine silver gauze and screwed on to a narrow brass rim B, which is again screwed on to a keel-shaped piece of brass C. C is so shaped that it rests during dispersal on two parallel quartz tubes ⅜ inch in diameter, containing nickel chromium wire which can be heated electrically.

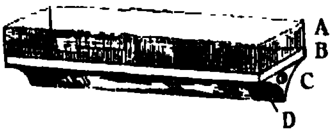

FIG. 1.

---

* 'Proc. Roy. Soc.,' A, vol. 124, p. 502 (1929).

At the end of the boat is a hole D into which a thermocouple can be inserted in order to obtain some idea of the temperature of dispersal. The boat and quartz tubes are contained in a brass box E (fig. 2) which is clamped and ground on to a brass tube F. The other end of F is wound with nickel chromium wire G which is heated during dispersal and assists in the production of a uniform size of particle. The action is probably to be attributed to a partial evaporation of the particles, followed, as the smoke cools, by a recondensation. This latter will take place much more rapidly on the smaller particles and should lead to an increase of uniformity. The air stream, which is carefully filtered to remove dust, passes through an anemometer and thence enters the heater at H. The volume or velocity of the air passing over the boat can thus be estimated.

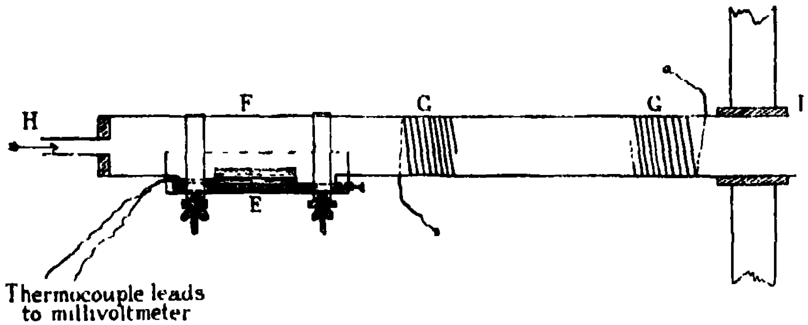

FIG. 2.

To disperse a smoke, a weighed amount of the material is melted on to the horizontal surface of the silver gauze and the boat is put into the heater. The air stream is then turned on and a suitable current passed through the nickel chromium wire in the quartz tubes, so that the material is gradually dispersed. The heating must not be too slow or the material is merely dissipated as vapour, whilst if it is too rapid there will be a loss of uniformity of size of particle. During dispersal a current is also passed through the spiral G. This again must not be too great or the smoke is volatilised, whilst if too small no homogenising action occurs. The limits of temperature for both heaters are, however, wide, comparatively large variations producing little effect on the smoke. No attempt is made to disperse the smoke at a constant temperature, a slow but gradual rise taking place all the time. The dispersal as a rule takes about a minute.

The smoke is carried by the air stream through the end L of the heater into a chamber of either 1 or 3·3 cubic metres capacity, where it is thoroughly mixed with the chamber air by an electric fan. The pressure in the chamber does not, of course, rise appreciably during dispersal, as part of the contents of the chamber is pushed out by the incoming air stream. In order to ensure that the smoke is evenly distributed throughout the chamber it is necessary to continue fanning for a minute or two after dispersal has ceased and the air stream has been turned off.

The number of particles per cubic centimetre of the smoke at any time is now found by counting in the special ultramicroscope cell previously described.

Mass Concentration of the Smokes.

It is obvious that when a smoke is produced in the above way all the material volatilised from the boat cannot appear as particulate matter in the chamber, as some is displaced by the air stream. A good estimate of the mass of material remaining in the chamber after dispersal may, however, be made, provided we know the volume of air entering the chamber in unit time and the time of dispersal. Thus, suppose that the volume of air entering the chamber in unit time is v and that this carries with it a mass of dispersed material b, then if V is the volume of the chamber, the rate of increase of mass of dispersed material remaining in the chamber is given by

$$\frac{dm}{dt} = b - \frac{vm}{\mathrm{V}} = b - am,$$

where m is the mass of material present in the chamber at any time, and $a = v/\mathrm{V}$. On integration we obtain

$$\log_e \frac{b}{b - am} = at,$$

or

$$m = \frac{b}{a}(1 - e^{-at}).$$

From this equation we obtain the amount of material remaining in the chamber, when the rate of dispersal is b and time of dispersal t. For example, in many of our experiments the volume of air entering the chamber was 213 litres per minute and the time of dispersal was about 1·5 minutes. Accordingly, if 15 mgm. of material were dispersed into a cubic metre chamber, the mass of smoke in the chamber after dispersal would be

$$m = \frac{10}{0 \cdot 213}(1 - e^{-0 \cdot 319}) = 12 \cdot 8 \text{ mgm.}$$

In deducing this equation it is assumed that the rate of dispersal is uniform and that perfect mixing of the smoke with the air of the chamber takes place at each instant during dispersal. Actually neither of these assumptions is correct, but as the velocity of coagulation is not greatly affected by small changes of mass at these concentrations, it appears unlikely that any significant error is introduced.

Experimental Results.

The greater number of our data have been obtained with smokes of stearic acid. This material was chosen since it can readily be dispersed at a comparatively low temperature, and without appreciable decomposition. A few experiments have also been made with oleic acid, a material which disperses in a very similar way and has the advantage of forming liquid rather than solid particles which will accordingly coalesce on coagulation and not form aggregates.

In order to find how far a given smoke was reproducible a number of experiments were made by dispersing either 15 mgm. of stearic acid into the 1 cubic metre chamber or 50 mgm. into the 3·3 cubic metre chamber. The amounts of dispersed material calculated by the above equation are 12·8 and 14·2 mgm. per cubic metre respectively. The coagulation graphs obtained by plotting particulate volume against time approximate closely to straight lines, so that no appreciable error is made by assuming that the slope is constant. The initial number of particles found by extrapolating these graphs to zero time is in all cases of the order of 10 million per cubic centimetre. The velocity coefficients of coagulation obtained from the slopes of the curves are given in the following table :—

Stearic acid. Velocity coefficient of coagulation. K $\text{cm.}^3/\text{min.} \times 10^7$.

For concentrations 12·8 mgm. per cubic metre in 1 cubic metre chamber.	For concentrations 14·2 mgm. per cubic metre in 3·3 cubic metre chamber.
0·32	0·32
0·32	0·31
0·31	0·30
0·31	0·31
0·31	0·31
0·31	0·32
0·31	0·31
0·30	0·31
0·31	0·30
0·32	0·32
0·32	0·30
0·32	0·31
0·32	0·31
0·32	—
Average 0·314 ± 0·004	Average 0·310 ± 0·005

It will be seen that the deviation of the velocity coefficients from the mean values is small and may confidently be attributed to chance errors in counting. The smokes may therefore be said to be reproducible within the limits of error of our experimental methods. Also, the average velocity coefficient in the case of the smokes of lower concentration is slightly greater than for the others. This, of course, would be anticipated since the average particle is smaller and this, as we have previously shown (*loc. cit.*), leads to more rapid coagulation. The difference between the two averages lies almost within the limit of experimental error, though actually, as will be seen later, it is the amount which would be anticipated theoretically. It may be noted that a very strict control of the conditions of dispersal does not appear to be necessary in order to reproduce a smoke of this type. Thus, the velocity of the air stream, the exact temperature of the heaters, etc., may be varied within moderately wide limits, without appreciably altering the smoke. This appears to us to furnish strong evidence that the method of dispersal which we have used is effective in producing a comparatively homogeneous system, since it seems unlikely that various changes in the conditions would always give a smoke of a constant degree of heterogeneity. This is borne out by the apparent uniformity of size of the smoke particles in the early stages, as seen in the ultramicroscope cell.

In the case of oleic acid the type of system produced is closely similar, the extrapolated initial number and velocity coefficient of coagulation being the same within the limits of error of experiment.

Theoretical Considerations.

It remains to consider whether the velocity coefficient of coagulation which we have found can be deduced theoretically by assuming that the smokes are homogeneous in the early stages. It has already been shown (*loc. cit.*, p. 520) the value of the coefficient for a homogeneous smoke is given by the equation

$$K = \tfrac{2}{3} \frac{RT}{\eta N} (1 + A\lambda/r)\, s,$$

in which R is the gas constant, T the absolute temperature, η the viscosity of the medium, N the Avogadro number, A a constant determined experimentally by Millikan, λ the mean free path in air, r the radius of the average particle, and s the ratio of the radius of the sphere of influence of a particle to its actual radius, which for particles that coagulate only on touching is equal to 2. It will be seen that the rate of coagulation depends upon *r*, the radius of the average particle, that is the weighted mean radius taking account of size and number. Practically it has been assumed that *r* can be found to a sufficient degree of approximation by calculation from the average mass of a particle, obtained by dividing mass per unit volume by number. This, of course, is equivalent to assuming that the smoke is homogeneous at each stage of coagulation and is similar to the assumption made by Smoluchowski for coagulating sols.

This equation will now be used to find the mean value of the velocity coefficient of the stearic acid smokes of concentrations 12·8 mgm. per cubic metre and 14·2 mgm. per cubic metre. In order to do this the velocity coefficient at various equidistant stages of coagulation covering the range over which the experiments were made, must be calculated and a mean value taken. A time-particulate volume curve typical of these reproducible stearic acid smokes is shown in fig. 3. The curves for these smokes, as already stated, are almost straight lines, the slope of which determines the velocity coefficient. The coagulation was generally studied from a few minutes after dispersal for rather more than 1 hour, that is from the time that the particulate volume was about $0\cdot2 \times 10^{-6}$ c.c. until it became rather over $2\cdot0 \times 10^{-6}$ c.c. If then we calculate the velocity coefficient at particulate volumes, $0\cdot5 \times 10^{-6}$ c.c., $1\cdot0 \times 10^{-6}$ c.c., $1\cdot5 \times 10^{-6}$ c.c., $2\cdot0 \times 10^{-6}$ c.c. corresponding to numbers of particles per cubic centimetre of 2×10^6, 1×10^6, $0\cdot67 \times 10^6$, $0\cdot5 \times 10^6$, and take the arithmetic mean, it is clear that a good average value for the coefficient should be obtained. We have previously shown that for our experiments

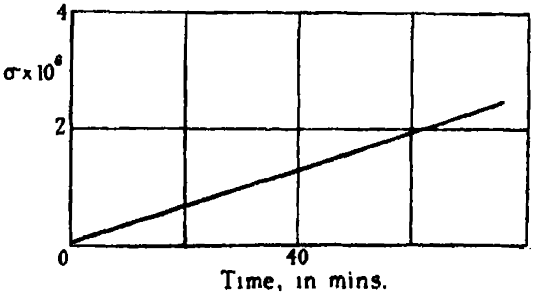

FIG. 3.

$$\frac{4}{3}\frac{RTs}{\eta N} = 1\cdot76 \times 10^{-8} \text{ cm.}^3/\text{min.}$$

$$A\lambda = 9\cdot10^{-6}.$$

Using these figures the results for the two smokes are given in the following table :—

Particulate volume $\times 10^6$.	Velocity coefficient of coagulation (cm.^{3} per min. $\times 10^7$).	
	For concentration 12·8 mgm. per cubic metre.	For concentration 14·8 mgm. per cubic metre.
0·5	0·300	0·304
1·0	0·282	0·278
1 5	0·268	0·265
2 0	0·260	0·257
Average .	0·280	0·276

It will be seen that the average calculated velocity coefficients are far slower than those measured experimentally ($0·314 \times 10^{-7}$ and $0·310 \times 10^{-7}$ cm.^{3} per minute respectively). The difference between the two rates $0·004 \times 10^{-7}$ is, however, the same.

If now we consider the cause of this divergence, it becomes clear that the above method of calculation must give too slow a velocity of coagulation. It is assumed that at each stage the smoke is of perfectly uniform texture. This is not the case, as owing to coagulation there is present a greater or less range of size, many of the particles being well below the average and a number above it. In consequence of this the velocity of coagulation will be greater than that calculated, partly owing to the greatly augmented rate of coagulation of the small particles, but chiefly perhaps owing to the fact that particles of different sizes coagulate much more rapidly than those of an average size, especially when they are fine (*loc. cit.*, p. 516). If now we could find the size distribution at any time, we should be able to take these factors into account and thus obtain an accurate value for the velocity coefficient of coagulation at any time.

Experimentally we have not been able to find any satisfactory way of determining the size distribution of our stearic acid smokes. On the theoretical side Smoluchowski* has worked out the numbers of the different sizes which should occur in a sol originally homogeneous which has coagulated for a definite time. To obtain a solution of the problem, however, he found it necessary to assume that the collision frequency of different sized particles is the same as that for particles of the same size. This, as stated above, is quite incorrect, especially if the divergence of size is great and will result in our calculating too great a number of fine particles and too small a number of large. In the case of smokes the error is accentuated as the coagulation velocity depends upon actual as well as relative size, increasing with decrease of radius. The velocity coefficients of coagulation worked out from distributions found in this way should, therefore, be greater than the experimental values, owing to the presence of too many fine particles and too few large. Since, however, there appears to be no other way of obtaining an estimate of the size distribution, we have calculated the distribution for a system initially homogeneous, when the numbers have decreased to definite fractions of those initially present using the Smoluchowski distribution equations in the form,

---

* 'Z. phys. Chem.,' vol. 92, p. 129 (1918).

$$n_1 = \frac{n^2}{n_0},$$

$$n_2 = \frac{n^2 (n_0 - n)}{n_0^2},$$

$$n_3 = \frac{n^2 (n_0 - n)^2}{n_0^3},$$

$$n_r = \frac{n^2 (n_0 - n)^{r-1}}{n_0^r}.$$

Here n_1, n_2, n_3, ..., are the numbers of units, doublets, triplets, ..., present when the number of particles has decreased to n from an initial number n_0. In order to find the velocity coefficient of coagulation, we require to know the fractional number of particles of various radii which are present. Now Smoluchowski's units, doublets, triplets, etc., are not, of course, equivalent to radii 1, 2, 3, ..., since, for example, the radius of a doublet formed by the coalescence of two units is $2^{\frac{1}{3}} = 1 \cdot 26$ and not 2. Accordingly particles of radius 2 are formed from 8 units and those of radius 3 from 27 units. We may, therefore, consider particles of radius 1 to consist of sizes 1 to 3, those of radius 2 of sizes 4 to 16, those of radius 3 of sizes 17 to 43 and so on. In the following table we have calculated the percentage of particles of the various radii which are present according to this theory, for a system initially homogeneous, when the total number becomes reduced by coagulation to 0·5, 0·25, 0·167, 0·125 of those originally present.

Fraction of initial number of particles.	Percentage radius distribution.			
	Radius 1.	Radius 2.	Radius 3.	Radius 4.
1·0	100·0	0·0	0·0	0·0
0·5	87·5	12·5	0·0	0·0
0·25	57·8	41·4	0·8	0·0
0·167	42·1	52·5	5·4	0·0
0·125	33·0	55·2	11·5	0·3

We will now make use of this distribution to find the average value of the velocity coefficient of coagulation for a stearic acid smoke of concentration 12·8 mgm. per cubic metre. This will be assumed to be homogeneous when 4×10^6 particles per cubic centimetre are present, as we think it likely that, at about this stage, the smoke attains to its maximum degree of uniformity. In this case $r_1 = 0{\cdot}93 \times 10^{-5}$ cm., $r_2 = 1{\cdot}86 \times 10^{-5}$ cm., $r_3 = 2{\cdot}79 \times 10^{-5}$ cm., $r_4 = 3{\cdot}72 \times 10^{-5}$ cm.

Suppose now, for example, that at any time the relative numbers of particles of radii r_1, r_2, r_3 are n_{r_1}, n_{r_2}, n_{r_3}. Then the relative numbers of collisions of the various types involved are

$$\tfrac{1}{2}K_{1\,1} . n_{r_1}^2, \quad \tfrac{1}{2}K_{2\cdot 2} . n_{r_2}^2, \quad \tfrac{1}{2}K_{3\cdot 3} . n_{r_3}^2, \quad K_{1\cdot 2} . n_{r_1}n_{r_2}, \quad K_{1\cdot 3} . n_{r_1}n_{r_3}, \quad K_{2\,3} . n_{r_2}n_{r_3},$$

and the average value of the velocity coefficient is

$$\frac{\tfrac{1}{2}K_{1\cdot 1} . n_{r_1}^2 + \tfrac{1}{2}K_{2\cdot 2} . n_{r_2}^2 + \tfrac{1}{2}K_{3\cdot 3} . n_{r_3}^2 + K_{1\cdot 2} . n_{r_1}n_{r_2} + K_{1\cdot 3} . n_{r_1}n_{r_3} + K_{2\cdot 3} . n_{r_2}n_{r_3}}{\tfrac{1}{2}n_{r_1}^2 + \tfrac{1}{2}n_{r_2}^2 + \tfrac{1}{2}n_{r_3}^2 + n_{r_1}n_{r_2} + n_{r_1}n_{r_3} + n_{r_2}n_{r_3}}.$$

where $K_{1\cdot 1}$ is the velocity coefficient for the collision of two particles of radius r_1, $K_{2\cdot 2}$ that for the collision of two particles of radius r_2, and so on.

We have already shown how the value of the velocity coefficient for the collision of particles of equal size may be calculated. For particles of unequal size this coefficient is given by (*loc. cit.*, pp. 513, 514):

$$K_{1\cdot 2} = 2\pi (D_1 + D_2)\left(\frac{\quad + S_1}{2} \right.$$

$$= 2\pi \frac{RT}{6\pi\eta N} \left\{ \frac{1 + A\frac{\lambda}{r_1}}{r_1} + \frac{1 + A\frac{\lambda}{r_2}}{r_2} \right\} \frac{(r_1 + r_2) S}{2}$$

$$= \frac{RT}{6\eta N} \left[\frac{1 + A\frac{\lambda}{r_1}}{r_1} + \frac{1 + A\frac{\lambda}{r_2}}{r_2} \right. \quad (r_1 + r_2) S,$$

where D_1, D_2 and S_1, S_2, are the respective diffusion constants and radii of the spheres of influence of the two colliding particles of radii r_1 and r_2, and the other constants have the same significance and numerical values as given above.

The numerical results for the average values of the velocity coefficient at particulate volumes $0{\cdot}5 \times 10^{-6}$, $1{\cdot}0 \times 10^{-6}$, $1{\cdot}5 \times 10^{-6}$, $2{\cdot}0 \times 10^{-6}$, assuming the smoke to be homogeneous at particulate volume $0 \cdot 25 \times 10^{-6}$, are given in the following table :—

Particulate volume $\times 10^6$.	Velocity coefficient of coagulation cm.^{3} per minute $\times 10^7$ concentration 12·8 mgm. per cubic metre.
0·5	0·345
1·0	0·336
1·5	0·325
2·0	0·317
Average . .	0·331

In this case the calculated rate is faster than that found experimentally ($0 \cdot 314 \times 10^{-7}$ cm.^{3} per minute). This is not surprising when it is remembered that the theory predicts far too many of the smaller particles. For it must be borne in mind that not only is the rate of coagulation of the smallest particles of radius r_1 high ($K_{1 \cdot 1} = 0 \cdot 344 \times 10^{-7}$), but also that the rate of coagulation of the particles of radius r_1 with those of radius r_2 is even greater ($K_{1 \cdot 2} = 0 \cdot 357 \times 10^{-7}$) owing to the effect of the divergence in size. It will be noticed, however, that the average velocity coefficient calculated in this way, and thus making an approximate allowance for heterogeneity, is in much closer agreement with experiment than that found by assuming that the smoke is uniform at each stage.

We have, therefore, arrived at the result, that whereas the experimental velocity coefficient of coagulation of reproducible stearic acid smokes of concentration 12·8 mgm. per cubic metre is $0 \cdot 314 \times 10^{-7}$ cm.^{3} per minute, a theoretical calculation which must give rather too high a velocity yields the value $0 \cdot 331 \times 10^{-7}$ cm.^{3} per minute, whilst one which must give too low a rate yields $0 \cdot 280 \times 10^{-7}$ cm.^{3} per minute. As the correct theoretical velocity lies between these calculated values and is probably nearer the higher, the disparity between theory and experiment cannot be great. There appears to be considerable evidence, therefore, that the velocity coefficient that we have measured for smokes which we believe to be nearly homogeneous in the early stages, would be in close accordance with the coagulation theory previously given (*loc. cit.*, p. 513), if accurate account could be taken of the heterogeneity produced by coagulation.

In conclusion, it may be mentioned that we have assumed throughout that the particles, whether unitary or complex, are spherical and of normal density. Actually microscopic examination of stearic acid particles shows that the larger are generally irregularly spherical complexes, the density of which must be less than normal. Now the experiments of Millikan* show that such irregularities of shape cause little difference to the mobility of particles. On the other hand, the average radii of the complexes will be somewhat greater than we calculated, assuming they were solid spheres. This will give rather too small a value for the velocity coefficient owing to the diminution in the term $(1 + A\,\lambda/r)$. At the same time the coefficient will tend to be increased, as the divergence of size between the smallest particles and the complexes will be greater than calculated. It appears likely that these two effects will to a great extent cancel out. This is confirmed by our experiments with oleic acid, a liquid having almost the same density in bulk as stearic acid. In this case coalescence rather than aggregation of the particles will occur so that these errors cannot arise. The velocity coefficient of coagulation is, however, the same as that of stearic acid within the limit of error of experiment.

An apparatus is described by means of which it is possible to reproduce closely smokes volatilised at a low temperature. When this apparatus is used in a suitable way, the smokes obtained exhibit initially a high degree of uniformity. A number of experimental results obtained with stearic acid smokes of the same weight concentration are given, and it is shown that the velocity of coagulation is constant within small limits.

The experimental velocities of coagulation are compared with values deduced from the Smoluchowski theory of coagulation as modified to apply to smokes. When the usual assumption is made that the smoke remains homogeneous during coagulation, the divergence between theory and experiment is large. If, however, account is taken of the fact that a smoke which is initially homogeneous must become heterogeneous owing to coagulation, the agreement between theory and experiment is good. The experiments are considered to show that the modified Smoluchowski theory represents to a close approximation the rate of coagulation of a smoke.

---

* 'Phys. Rev.,' vol. 22, p. 1 (1923)

The Motion of Electrons in the Static Fields of Hydrogen and Helium.

By J. McDougall, B.A., Pembroke College, Cambridge.

(Communicated by R. H. Fowler, F.R.S.—Received January 30, 1932.)

1. The scattering of electrons by atoms was first investigated by Born,* who adopted a method similar to that used by Huyghens and Kirchoff for the scattering of light by obstacles. Physically, Born's approximation represents the integral of the amplitude of the secondary wavelets scattered from the incident plane wave only, and neglects the distortion of the plane wave by the atom. The perturbation of the incident wave will be smaller the larger the energy of the wave, so one would expect Born's theory to be valid for high velocity impacts. Criteria for its validity have been given by Mott† and Möller.‡ The Born theory certainly breaks down for sufficiently low velocities as the cross-section curves obtained fall uniformly with increase of velocity of the incident electron beam, whereas the rare gas and alkali metal cross-sections (obtained from experiments) exhibit maxima and minima.

At an impact there are present the incident waves and those scattered, both elastically and inelastically, and all these will interact. Born's first approximation neglects the effect of the scattered waves and the next approximation is obtained by neglecting only the inelastically scattered waves, and calculating exactly the elastic scattering of the electrons by the static field. This is done by the method of partial cross-sections which was developed by Faxen and Holtsmark§ and applied to the rare gases. The method consists in resolving the incident electrons into beams with different angular momenta, $\sqrt{\{l(l+1)\}}\,h/2\pi$, and a numerical solution of the wave equation is found which gives asymptotically the sum of an incident plane wave and a scattered spherical wave. The analysis is similar to that used by Rayleigh for the scattering of sound waves by obstacles. The incident electrons with $l = 0$ make head-on collisions, and these are most important for slow electrons and weak fields. For strong fields and fast particles, the main contribution to the scattering may come from large values of l, when the calculation of scattered intensities by this method is not so convenient. In these cases the Born approximation is usually satisfactory. The agreement between Holtsmark's calculations and experiment is reasonably good, showing that the distortion of the wave is of fundamental importance in the scattering of slow electrons.

---

* 'Z. Physik,' vol. 38, p. 803 (1926).

† 'Proc. Camb. Phil. Soc.,' vol. 25, p. 304 (1928).

‡ 'Z. Physik,' vol. 62, p. 54 (1930).

§ 'Z. Physik,' vol. 45, p. 307 (1927).

The numerical work involved in Faxen and Holtsmark's method is somewhat tedious, and recently Allis and Morse* have used a simple atomic model, using a potential field

$$V = Ze^2\left(\frac{1}{r} - \frac{1}{r_0}\right), \qquad r < r_0,$$
$$V = 0, \qquad r > r_0.$$

Z and r_0 are chosen to make the field approximate as closely as possible to that of an actual atom. The solution of the wave equation with this form of potential may be carried out in terms of Whittaker functions. This method has been successful in explaining the cross sections of the rare gases and the alkalis.

It appears that for the scattering of slow electrons by heavy atoms the distortion of the incident wave by the atom predominates, but the scattering curves for helium and hydrogen show minima for low voltages and do not agree with the Allis and Morse theory, although one would expect the agreement to be very good for low voltages. The non-static nature of the atomic field must be considered in order to explain the helium and hydrogen results, and such investigations are discussed by Massey and Mohr.† Their method has been applied to atoms with a simple electronic structure because of the complexity of the calculations, and the work on hydrogen and helium given in this paper has been carried out as a preliminary to their extension.

2. *The Method of Partial Cross-sections.*—The equation for the motion of electrons in a field of force V (r) is

$$\nabla^2\psi + \frac{8\pi^2 m}{h^2}(E - V)\psi = 0. \tag{1}$$

ψ is expanded in a series of zonal harmonics

$$\psi = \sum_l L_l(r)\, P_l(\cos\theta), \tag{2}$$

and the problem reduces to the solution of

$$\frac{d^2}{dr^2}(rL_l) + \left\{\frac{8\pi^2 m}{h^2}(E - V) - \frac{l(l+1)}{r^2}\right\}(rL_l) = 0. \tag{3}$$

---

* 'Z. Physik,' vol. 70, p. 567 (1931).

† 'Proc. Roy. Soc.,' A., vol. 136, p. 289 (1932).

We assume $r^2\text{V} \to 0$ as r increases, and the solution for large r becomes that of the equation

$$\frac{d^2}{dr^2}(r\text{L}_l) + \left\{\frac{8\pi^2 m}{h^2}\text{E} - \frac{l(l+1)}{r^2}\right\}(r\text{L}_l) = 0. \tag{4}$$

The solutions are

$$r\text{L}_l = r^{\frac{1}{2}}\text{J}_{l+\frac{1}{2}}(kr) \quad \text{and} \quad r\text{L}_l = r^{\frac{1}{2}}\text{J}_{-l-\frac{1}{2}}(kr),$$

where $k^2 = \dfrac{8\pi^2 m\text{E}}{h^2}$.

Now

$$\left.\begin{aligned} &\text{J}_{l+\frac{1}{2}}(kr) \sim \frac{\text{C}}{\sqrt{(kr)}}\sin(kr - \tfrac{1}{2}l\pi) \\ \text{and}\quad &\text{J}_{-l-\frac{1}{2}}(kr) \sim (-1)^l \frac{\text{C}}{\sqrt{(kr)}}\cos(kr - \tfrac{1}{2}l\pi) \end{aligned}\right\}. \tag{5}$$

Hence the asymptotic form of the solution is

$$r\text{L}_l = \text{A}_l\text{J}_{l+\frac{1}{2}}(kr)\,r^{\frac{1}{2}} + \text{B}_l\text{J}_{-l-\frac{1}{2}}(kr)\,r^{\frac{1}{2}}, \tag{6}$$

$$= \text{C}_l \sin(kr - \tfrac{1}{2}l\pi + \delta_l), \tag{7}$$

where

$$\sin\delta_l = \frac{(-1)^l\,\text{B}_l}{\sqrt{(\text{A}_l^2 + \text{B}_l^2)}}.$$

δ_l is a phase constant depending on l, $\text{V}(r)$, and k.

The asymptotic form of ψ is

$$\psi \sim \sum_l \frac{\text{C}_l}{r}\sin\left(kr - \frac{l\pi}{2} + \delta_l\right)\text{P}_l(\cos\theta). \tag{8}$$

Faxen and Holtsmark (*loc. cit.*) break up the form (8) for ψ into the sum of an incident plane wave and a scattered spherical wave and express the scattered intensity in the form

$$\begin{aligned} \text{Q} &= \Sigma\text{Q}_l, \\ &= \frac{4\pi}{k^2}\sum_l (2l+1)\sin^2\delta_l \\ &= \frac{4\pi}{k^2}\sum_l (2l+1)\frac{\text{B}_l^2(\infty)}{[\text{A}_l^2(\infty) + \text{B}_l^2(\infty)]}. \end{aligned} \tag{9}$$

This expression has the dimensions of an area and represents the cross-section exposed to the incident beam by the scattering system.

3. In the present work, equation (3) is solved by numerical methods and the calculation continued until the field V has effectively vanished. By comparing the solutions beyond the field with the form (6) the ratio of the constants A_l, B_l, is found and hence the phase δ_l. Atomic units are used, and as V is negative for an attractive field, it is convenient to write $V = -v$. Then equation (3) may be written

$$P'' + \left[2v + k^2 - \frac{l(l+1)}{r^2}\right] P = 0, \qquad (10)$$

where $P = rL_l$. The method of solution is that given by Hartree* in the determination of self-consistent fields. For helium the field given by Hartree (*loc. cit.*) was used. This is given in Table I, Z being the "effective nuclear charge." In the calculations Z_p the "effective nuclear charge for potential" is required. This has been calculated and is included in the table. The relation between Z and Z_p is

$$dZ \qquad Z - Z \qquad (11)$$

Table I.—Field of Neutral Helium.

r.	Z.	Z_p.	r.	Z.	Z_p.
0	2·000	2·000	1·6	0·239	0·048
0·1	1·988	1·668	1·8	0·159	0·029
0·2	1·932	1·366	2·0	0·105	0·018
0·3	1·826	1·104	2·2	0·068	0·010
0·4	1·682	0·885	2·4	0·044	0·006
0·6	1·344	0·558	2·6	0·028	0·004
0·8	1·013	0·346	2·8	0·018	0·002
1·0	0·733	0·212	3·0	0·011	0·001
1·2	0·515	0·130	3·5	0·003	0
1·4	0·354	0·079	4·0	0·001	0

For hydrogen, the potential v is $e^{-2r}\left(1 + \frac{1}{r}\right)$, so that

$$Z_p = rv = e^{-2r}(1 + r).$$

For helium, $Z_p < 0 \cdot 001$ at $r = 3 \cdot 2$, *i.e.*, $r = r_0$, and beyond this point the solution obtained is an exact solution of (4) with the boundary value $P(r_0)$ at $r = r_0$, where $P(r_0) = r_0 L_l(r_0)$ is a solution of (3). When fitting the P curves on to those given by (6) the zeros are compared in order to avoid arbitrary constants.

---

* 'Proc. Camb. Phil. Soc.,' vol. 24, p. 89 (1928).

$l = 0$ *Calculations.*—Beyond the field, the P curves are sine curves and the distance between consecutive zeros is π/k. The calculations were continued outwards so as to give three or four zeros (found by interpolation) and their distance apart compared with π/k. They were found to agree to within 1 in 5000. The intervals of integration were varied with the value of k, viz., $k = 1$, 13·5 volts, interval in r of 0·2 giving 16 intervals between consecutive zeros; $k = 2$, 54·1 volts, interval in r of 0·1; and $k = 4$, 216·6 volts, intervals of 0·5. For the smaller intervals it was necessary to interpolate to find the field for normal helium. The phase is given by the equation

$$k\rho = p\pi - \delta, \tag{12}$$

for a zero at $r = \rho$; p is an integer.

In fig. 1 are drawn the P curves for helium and the corresponding curves for plane waves (which are sine curves) for 1, 10, 25, 50 and 216·6 volt electrons. The curves show clearly the distortion of the waves by the atom, and how the radius of the sphere in which the field is effective varies with the velocity of the electrons. The Allis and Morse value $r_0 = 0{\cdot}55$ is much too small for

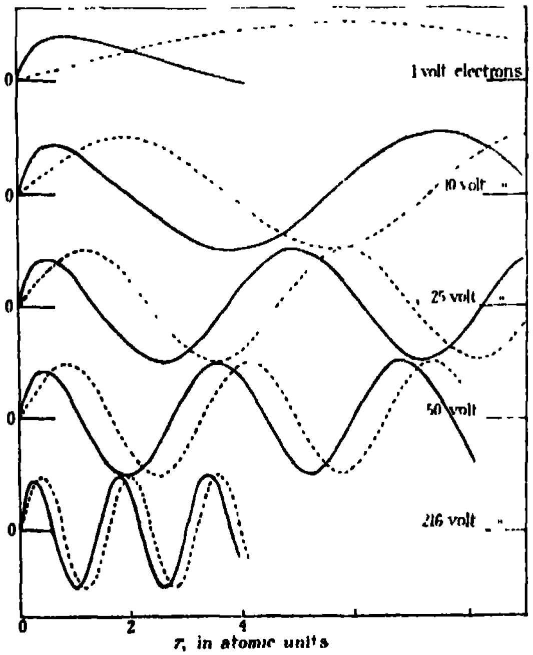

FIG. 1.—Illustrating wave functions of electrons with zero angular momentum in the static field of the helium atom. The full line curve gives r times this wave function, the broken curves the corresponding plane wave functions $\sin kr$, for comparison.

slow electrons. Table II gives the phases found and these are plotted in fig. 2.

Table II.—Phases. Helium and Hydrogen.

Helium.					Hydrogen.		
Volts.	k.	δ_0.	δ_1.	δ_2.	Volts.	k.	
¼	0·136	2·570	0	0	$\frac{1}{16}$	0·068	0·557
1	0·272	2·108	0	0	¼	0·136	0·847
5	0·608	1·659	0·020	0	1	0·272	1·034
10	0·859	1·481	0	0	2	0·384	1·060
15	1·053	1·360	0·070	0·006	5	0·608	1·007
25	1·359	1·256	0	0	13·54	1	0·905
50	1·922	1·093	0·186	0·041	54·15	2	0·694
121·8	3	0·898	0·272	0·095	121·8	3	0·569
216·6	4	0·784	0·301	0·130	216·6	4	0·490
338·5	5	0·696	0·308	0·152	338·5	5	0·432

$l = 1, 2$ *Calculations.*—Beyond the field, the P curves are of the form

$$r^{\frac{1}{2}}\left[\mathrm{A}_l \mathrm{J}_{l+\frac{1}{2}}(kr) + \mathrm{B}_l \mathrm{J}_{-l-\frac{1}{2}}(kr)\right], \tag{13}$$

and the zeros of P are the zeros of the bracket. The distance between zeros is of the order of π/k, and the intervals were taken as in the $l = 0$ calculations. The zeros of the P curves were found by interpolation, and the phases given by

$$\tan \delta_l = (-1)^l \frac{\mathrm{B}_l}{\mathrm{A}_l} = (-1)^{l+1} \frac{\mathrm{J}_{l+\frac{1}{2}}(k\rho)}{\mathrm{J}_{-l-\frac{1}{2}}(k\rho)}, \tag{14}$$

where $r = \rho$ is a zero of P. It was necessary to calculate the Bessel functions for each value of $k\rho$ as tables* do not give them at sufficiently small intervals. The values of $\mathrm{J}_{l+\frac{1}{2}}(k\rho)$ are small as this function is close to a zero, and those of $\mathrm{J}_{-l-\frac{1}{2}}(k\rho)$ are numerically large (near a maximum or minimum) and it is essential to find $k\rho$ and $\mathrm{J}_{l+\frac{1}{2}}(k\rho)$ as accurately as possible. Two or three phases beyond the field were found and the tan δ_l values were in very close agreement. The phases found are given in Table II and fig. 2. As the helium results showed that the $l = 1, 2$ contributions were unimportant except for high velocity impacts, these calculations were not made for hydrogen.

4. *Discussion.*—The behaviour of the phases δ_0 for hydrogen and helium differ greatly (fig. 2). The helium curve rises to π and the hydrogen falls to 0 for zero velocity. This corresponds to the much greater disturbance of the

---

* *E.g.*, Hayashi, "Tafeln der Besselschen etc. Funktionen," Springer (1930).

incident waves by the field in the case of helium. The phase value will always be an integral multiple of π for zero velocity, and for atoms in which this harmonic predominates minima will be obtained in the cross-section curves at the velocities for which the phase is π, 2π, etc.

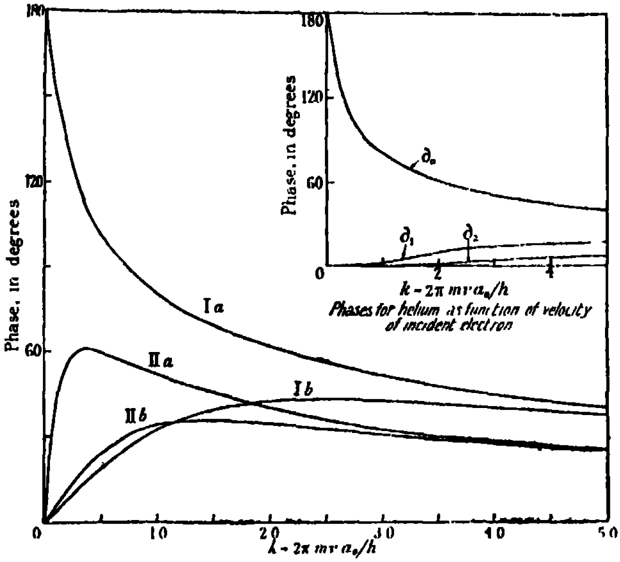

FIG. 2.—Illustrating phase changes for helium and hydrogen and comparison with approximate formula. I*a*, exact δ_0 phases for helium; I*b*, approximate δ_0 phases for helium given by Born formula; II*a*, exact δ_0 phases for hydrogen; II*b*, approximate δ_0 phases for hydrogen.

It is of interest to compare the phases with those given by the first Born approximation. Mott* has shown that these phases are

$$\delta_l = \frac{8\pi^2 m}{kh^2} \int_0^\infty V(r) \, [\chi_l^0(r)]^2 \, dr, \tag{15}$$

where

$$\chi_l^0 = \sqrt{\frac{\pi r k}{2}} \, J_{l+\frac{1}{2}}(kr). \tag{16}$$

These have been calculated and are compared with the values found by the methods of this paper in Table III. The corresponding curves are found in fig. 2.

For hydrogen the δ_0 phases agree within 5 per cent. for electrons over 125 volts. The δ_0 phases for helium are not in such good agreement: at $k = 5$ (338·5 volts) the difference is 3° in 40°. This is better than Mott's criterion

---

* 'Proc. Camb. Phil. Soc.,' vol. 25, p. 304 (1929).

Table III.—Comparison of Phases with Born-Mott Values.

k.	Helium.						Hydrogen.	
	$l = 0$.		$l = 1$.		$l = 2$.		$l = 0$.	
	Exact.	Born.	Exact.	Born.	Exact.	Born.	Exact.	Born.
0	3·14	0	0	0	0	0	0	0
1	1·40	0·57	0·07	0·04	0·006	0·005	0·91	0·60
2	1·07	0·74	0·19	0·15	0·041	0 033	0·69	0·60
3	0·90	0·75	0·27	0·24	0·095	0·077	0·57	0·54
4	0·78	0·70	0·30	0·27	0·130	0·113	0·49	0·47
5	0·69	0·64	0·31	0·29	0·152	0·138	0·43	0·42

indicates, since he shows that Born's first approximation is sufficient only when the phase is small ($\delta \ll 1$). The $l = 1$, 2 phase-velocity curves rise slowly to a maximum and fall to zero again with increase of velocity of incident electrons. On the low velocity side of the maximum the agreement with the Born values is not very satisfactory. The reason for this is found by considering the correct form

$$\delta_l = \frac{4\pi^3 m}{h^2} \int_0^\infty \mathrm{V}(r) \,.\, \mathrm{P}^2 \, dr, \tag{17}$$

which replaces formula (15). P is the wave function given by equation (10) and differs only slightly from $r^{\frac{1}{2}} \mathrm{J}_{l+\frac{1}{2}}(kr)$ for large values of k. Hence the phases given by the Born formula should be correct for sufficiently large k. For small values of k the main contribution to the integral (17) comes from small values of r where P and $r^{\frac{1}{2}} \mathrm{J}_{l+\frac{1}{2}}(kr)$ are both small but may have a high percentage difference. Consequently the phases given by (15) and (17) will both be small, but the difference may be a large proportion of the correct value. As the agreement between the δ_0's is good when δ is as high as $\frac{1}{2}$, a good approximation to the scattering formula can be obtained by using the Born-Mott formula (15) to calculate the phases, and substituting these values in the Faxen and Holtsmark expression

$$f(\theta) = \frac{1}{2ik} \sum_{l=0}^{\infty} (e^{2i\delta_l} - 1)(2l + 1) \mathrm{P}_l(\cos\theta), \tag{18}$$

for the scattering function. The experiments of Dymond and Watson with 210 volt electrons agreed well with the Born scattering curve and the phase found in this paper differs by about 5½° from the Born value 39½° at 210 volts.

The cross-section curve for helium has been drawn in terms of the experimental absorption coefficient α (for 0° C. and a pressure of 1 mm. of mercury), and are compared in fig. 3 with the Allis and Morse and experimental curves. If the cross-section Q (equation (9)) is measured in units of the square of the first Bohr hydrogen radius, the relation between Q and α is $Q = 1 \cdot 02\alpha$. The curve III shows values greater than the experimental curve II, but the consideration of exchange effects reduces the curve III values greatly for low velocities. The Allis and Morse curve is below curve III since they ignore the scattering by the field outside the radius r_0 at which their assumed field vanishes. This scattering is very large for low velocity impacts. The agreement between the Allis and Morse and experimental curves is better than could be expected and appears to be due to the cancellation of scattering due to the outer field and the exchange effects.

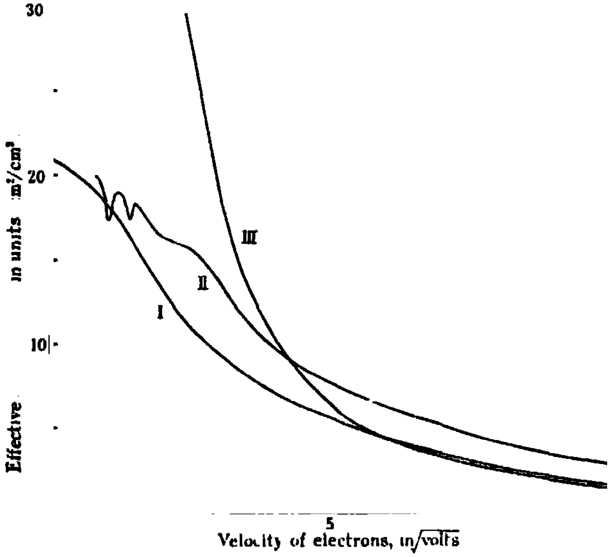

Fig. 3.—Comparison of observed and calculated cross-section curves for helium. I, calculated for approximate atomic field (Allis and Morse); II, observed; III, calculated for correct atomic field.

The consideration of the scattering of electrons by a static field does not represent the complete solution of the problem of the scattering of electrons by the atom, but by use of the wave functions calculated above it is possible to obtain further approximations. This is done in an accompanying paper by Massey and Mohr, who investigate the effect of exchange phenomena.

The wave equation for the motion of an electron in the static fields of hydrogen and helium is solved by numerical methods for electrons of energy up to 340 volts. The phase-velocity relations for the zero order harmonic for hydrogen, and the first three harmonics for helium, are compared with the Born-Mott curves. A comparison of helium cross-section curves is made. The wave functions found in the static field may be used as first approximations in calculations which take account of the actual non-static nature of the field.

The writer wishes to express his thanks to Messrs. H. S. W. Massey and C. B. O. Mohr for their interest in the work, which was made possible by a grant from the Department of Scientific and Industrial Research.

Electron Polarisation.

By G. O. Langstroth, Ph.D., 1851 Exhibition Scholar, King's College, London.

(Communicated by O. W. Richardson, F.R.S.—Received February 5, 1932.)

Dirac's modified wave equation which successfully accounts for many of the phenomena interpreted as due to the spin of orbital electrons, also predicts that the free electron should have a spin. On this basis each electron wave is characterised by a definite direction other than that of propagation, and an electron beam should be capable of exhibiting polarisation. A method for the production and detection of a polarised electron beam is suggested by the double scattering experiments for the production and detection of polarised X-rays, especially in view of the similarity between diffraction phenomena for electrons and electromagnetic waves.

Double scattering experiments have been performed by a number of investigators and it has been well established that no observable effect is found with electrons having energies in the neighbourhood of 100 volts.* With very much higher energies, however, an asymmetry in the intensity distribution of the secondary scattering appears to exist, although the evidence is somewhat contradictory and incomplete. This paper gives an account of a double scattering experiment in which electrons were successively reflected at approximately 90° from thick polycrystalline tungsten targets. The results* extend the region in which the asymmetry in the secondary scattering is known to be less than 1 per cent. to electron energies of 10 kilovolts.

---

* Davisson and Germer, 'Nature,' vol. 122, p. 809 (1928); 'Phys. Rev.,' vol. 33, p. 118 (1929), vol. 33, p. 760 (1929); 'Bell. Syst. Tech. J.,' vol. 8, p. 466 (1929).

Theoretically, it has been shown† that when a beam of electrons is twice scattered by single stripped nuclei, the intensity distribution of the secondary scattering should be asymmetric about the direction of incidence of the secondary beam. The asymmetry is of observable magnitude‡ only when large scattering angles, high velocity electrons, and nuclei of high atomic number are used. It has a periodicity of 2π, and the maximum and minimum intensity occur at 0° and 180° of the azimuth, *i.e.*, in the plane of the primary and secondary beams. In the 90°-270° azimuthal plane the predicted scattering is symmetrical.

There is some difficulty in applying these results to the actual double scattering experiment, for one is concerned in practice not with single nuclei, but with aggregations of nuclei. They may be expected to describe the phenomenon accurately only if no electrons which have undergone multiple or plural scattering in a target enter the measurements, if the polarisation effects due to single scattering centres are additive, and if electronic scattering is negligible.

An investigation of the polarisation relations for small angle scattering (" regular reflection "), in which the targets were treated as two-dimensional gratings, gave a result qualitatively different from that for isolated nuclei.§ The value of the calculation in practice depends upon the nature of the mechanism of reflection at the target's surface, of which little is known, and in any event the results cannot be extrapolated to large angles.

Experimentally, asymmetric distributions have been observed with fast electrons both for small and large scattering angles. The reported effects are of quite different kinds, varying apparently with the method of production. With small angle scattering from solid targets an effect has been reported‖ which is not found when the scattering occurs through foils.¶ Moreover, a still different effect is observed when a combination of solid target and foil is used.* An additional type of asymmetry (in the 90°–270° plane) was first observed by Cox, McIlwraith, and Kurrelmeyer,† but was later attributed to instrumental causes.‡ More recently,§ however, Chase has reported that this type of asymmetry does exist. Finally, a small asymmetry (about 2 per cent.) of the type predicted by the specialised theory has been observed by Dymond‖ in electron scattering at large angles from thin foils.

---

* Indicated in 'Nature,' vol. 127, p. 891 (1931).

† Mott, 'Proc. Roy. Soc.,' A vol. 124, p. 425 (1929).

‡ Mott, 'Nature,' vol. 128, p. 454 (1931). Calculations of reference 3 corrected and extended.

§ Halpern, 'Z. Physik,' vol. 67, p. 320 (1931).

‖ Rupp, 'Z. Physik,' vol. 53, p. 548 (1929), vol. 61, p. 158 (1930); 'Naturwiss,' vol. 18, p. 207 (1930).

¶ Thomson, 'Nature,' vol. 126, p. 842 (1930); Kirchner, 'Phys. Z.,' vol. 31, p. 772 (1930).

Several methods other than the double scattering experiment have been suggested for the production and detection of polarised electron beams,¶ but they do not yield themselves readily to experimental investigation. Other methods which have been tried have had inconclusive results.**

Experimental.

In this experiment a beam of electrons was twice scattered from tungsten targets, and the intensity of the secondary scattering at 0° and 180° of the azimuth was determined.

In most types of apparatus one target is rotated through 180° between measurements of the intensity scattered at 0° and 180° of the azimuth. This rotation may introduce an asymmetry which is a property of the tube and not of the electrons. The writer's apparatus was constructed so that the intensity scattered at 0° and 180° of the azimuth could be measured without altering the relative position of the polarising and analysing targets. By rotating the polarising target through an angle of 180° and the use of a second filament, an additional set of measurements could be made, in which the spin asymmetry should have been reversed in direction, and so have appeared doubly magnified in the results.

The tube design is shown schematically in fig. 1. A beam of electrons from a tungsten filament (F or F′) was accelerated through a system of slits (A or A′) and impinged at 45° on a tungsten target P. The specularly reflected beam passed through two slits (S, S′) and impinged at normal incidence on a tungsten target B. The electrons scattered from this target at an angle of slightly more than 90° in the plane of the primary and secondary beam passed through slits D and D′ and through a retarding field to the Faraday cylinders C and C′. The polarising target P could be magnetically rotated through 180° so that either filament could be used. Once properly set the angle of rotation was assured by the stops L and L′.

---

* Rupp, 'Naturwiss.,' vol. 19, p. 109 (1931); Rupp and Szilard, 'Naturwiss.,' vol. 19, p. 422 (1931).

† 'Proc. Nat. Acad. Sci.,' vol. 14, p. 544 (1928).

‡ Chase, 'Phys. Rev.,' vol. 34, p. 1069 (1929).

§ 'Phys. Rev.,' vol. 36, p. 1060 (1930).

‖ "Nature," vol. 128, p. 149 (1931).

¶ Mott, 'Proc. Roy. Soc.,' A, vol. 125, p. 222 (1929); Fues and Helmann, 'Phys. Z.,' vol. 31, p. 465 (1930); Pauli, 'Report to the Solvay Congress,' October, 1930.

** Wolf, 'Z. Physik,' vol. 52, p. 314 (1928); Meyers and Cox, 'Phys. Rev.,' vol. 34, p. 1067 (1929).

Since the slit system was enclosed, with the exception of the slits A, A′, D and D′, by brass walls 3 mm. thick kept at a constant potential, the electrons were scattered in an approximately field free space. The slits defining the secondary beam were circular and were 5 mm. in diameter. The slits D and D′ were rectangular slits 1·5 mm. wide and 5 mm. long. With the procedure used accurate symmetry in the size of the slits and the capacities of the collecting systems was not essential, although an effort was made to have the apparatus as symmetrical as possible.

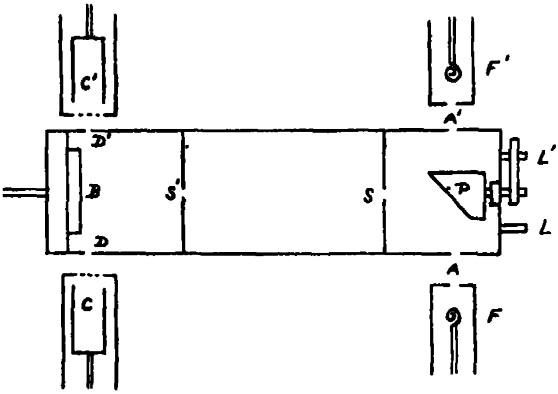

FIG. 1.—Experimental Tube.

The containing tube was made of pyrex glass, and the metal-glass joints were made vacuum tight with sealing wax.

Each Faraday cylinder was surrounded by an earthed metal protecting cylinder, and the opening through which the electrons entered was covered with a gauze which formed one terminal of the retarding field. The protecting cylinder was adjusted so that the distance between the gauze and the walls of the slit system was small. Accordingly, only those electrons which had a large velocity component in the direction of the axis of the cylinder could reach the collector against the retarding field. This prevented the large number of electrons scattered from various parts of the apparatus and having paths outside the walls of the slit system from interfering with the measurements.

The insulation and support of the Faraday cylinders was a long pyrex tube into which the tungsten electrometer lead was sealed. Each cylinder was connected permanently to one set of quadrants of a Dolazalek electrometer, and each system was provided with an earthing key. The electrometer was used heterostatically. The sensitivity of the measuring system as used in most cases was $2 \cdot 5 \times 10^{-13}$ amperes per millimetre per second.

The filaments were surrounded by cylindrical brass caps which were supported on pyrex tubes for the sake of thermal insulation from the wax joints. Electrical connection was made by means of a fine tungsten wire. The electrons passed through a circular slit in the cap, and could be focussed by moving the cap in the direction of its axis. The correct position for focussing on the polarising target was found from preliminary experiments, and was taken as that in which no discolouration of the sides of the slit (A, A′) occurred. The accelerating potential was applied between the cap (and the filament) and the walls of the slit system.

Because of the proximity of the filaments at high potential, the shielding of the collecting systems and of the electrometer had to be very complete. A small lead shield immediately about the tube was used to absorb any X-radiation which might have penetrated the walls of the slit system. An earthed metal shield enclosed as completely as possible the collecting systems, the electrometer leads, and the electrometer itself. An additional earthed metal sheet was placed between the shield and the filaments. With this arrangement no motion of the electrometer needle occurred on running a well-evacuated tube with a cold filament.

The high potential was obtained from the terminals of an oil condenser which were connected through a point plane rectifying tube to the secondary terminals of a large induction coil. This apparatus furnished a rectified potential of from 8·5 to 10 kilovolts. Since the positive condenser plate was earthed and the walls of the slit system were kept at 1·7 kilovolts positive to earth by means of accumulators, an accelerating potential of from 10·2 to 11·7 kilovolts was obtained. In the following discussion this will be referred to as 10 kilovolts. The condenser voltage was measured by means of a spark gap composed of two balls 4 cm. in diameter.*

Potentials of 2 kilovolts were obtained from an Evershed direct current generator, and were measured by means of an electrostatic voltmeter. Voltages of 1·7 kilovolts and less were obtained from a bank of accumulators.

---

* Kaye and Laby, "Physical and Chemical Constants," 6th ed., p. 97.

The pumping system was composed of a two-stage Volmer mercury diffusion pump, backed through a $CaCl_2$ drying tube by a Hyvac oil pump. Charcoal and liquid air was used to clean up the residual vapours in the later stages of evacuation. Pressures were indicated by a MacLeod gauge.

Procedure.

Before the metal parts were assembled in the pyrex tube they were baked out at about 300° C. until a pressure of 10^{-6} mm. of mercury was obtained at this temperature. After they had been placed in the tube and it had been evacuated, the slit system and the targets were again degassed by means of a furnace which fitted over the end of the tube. The electron guns were baked out with a gas flame.

The tube was baked out thoroughly before each series of measurements, and in addition the targets were bombarded with 10 kilovolt electrons for at least half an hour before taking readings. During a run the pressure was always less than 10^{-6} mm. of mercury, and in general a good sticking vacuum was maintained. With these pressures no drift of the electrometer occurred when the back of the polarising target was bombarded with 10 kilovolt electrons and an accelerating potential (for positive ions) of 1·7 kilovolts was applied between the gauze and the slit walls.

A milliammeter in the filament circuit, and a voltmeter connected directly across the filament served as an indication of the steadiness of electron emission, but the ability to repeat electrometer readings was taken as the final criterion.

The magnitudes of the retarding fields were fixed by the following considerations :—

(*a*) The fields had to be large enough to prevent electrons, which had paths outside the walls of the slit system, from reaching the collectors. This condition was considered as fulfilled when on bombarding the back of the polarising target no electrons reached the Faraday cylinders.

(*b*) The considerations which fix the lower limit of the retarding field arise from the results of investigations on the scattering of fast electrons from metallic surfaces.* The scattered beam is composed of two groups, a relatively large one of low velocity electrons, and a small one of fast electrons, the majority of which have nearly the primary energy. When gold is used as a scatterer the maximum in the energy distribution curve for the fast group lies at approximately 0·94 of the primary energy, Wagner (*loc. cit.*). Only the fast group must be allowed to reach the collectors.

---

* Farnsworth, 'Phys. Rev.,' vol. 20, p. 358 (1922); Baltruschat and Starke, 'Phys. Z.,' vol. 23, p. 403 (1922); Chylinsky, 'Phys. Rev.,' vol. 28, p. 429 (1926); Becker, 'Ann. Physik,' vol. 78, p. 228 (1925); Wagner, 'Phys. Rev.,' vol. 35, p. 98 (1930); Stehberger, 'Ann. Physik,' vol. 86, p. 825 (1928); Schonland, 'Proc. Roy. Soc.,' A, vol. 108, p. 187 (1925); Webster, Clark and Hansen, 'Phys. Rev.,' vol. 37, p. 115 (1931).

The arrangement of the fields is given in the following table.

Table I.

Arrangement.	Accelerating potential.	Retarding potential.
	volts.	volts
1	10000	1700
2	2000	284
3	1100	100

A complete set of measurements consisted of four distinct parts. The rate of drift of the electrometer needle was determined for each collector system using (*a*) 10 kilovolt electrons from filament F, (*b*) 1 kilovolt electrons from filament F, (*c*) 10 kilovolt electrons from filament F′, (*d*) 1 kilovolt electrons from filament F′. The readings for the two collector systems were taken alternately so that any change in the electron emission might not pass unnoticed. The ratio of the rates of drift for the two collector systems was taken as a measure of the secondary electron scattering at 0° and 180° of the azimuth.

The reversal of the polarising target should have reversed the spin asymmetry but left the tube asymmetry in the same direction. In this way any asymmetry, such as that due to a diffraction effect in the analyser, which might tend to mask a real or indicate a false spin asymmetry, was apparent.

The tube current and the collector current were respectively of the order of 10^{-4} and 10^{-13} amperes in this experiment.

Results.

The experimental ratios for the rates of drift for the collectors C and C′ (0° and 180° of the azimuth) with 10, 2 and 1 kilovolt electrons are given in Table II. These values have not been corrected for the asymmetry inherent in the apparatus, the magnitude of which is given, very nearly, by the values for the slow electrons. The same parts were used in tubes 1, 2 and 3, but they were entirely dismantled and reassembled so that all adjustments were made anew for each series of measurements.

Table II.—Experimental Ratios of the Intensities Scattered at 0° and 180° of the Azimuth.

Tube.	Filament.	1 kv.	2 kv.	10 kv.
1	F	1·06	—	1·06
	F′	1·06	—	1·07
2	F	—	1·10	1·10
	F′	—	1·12	1·14
3*	F	1·24	—	1·24
	F′	1·45	—	1·45

* Tube 3 was a preliminary tube. On taking it down after a series of readings it was found that the polarising target was not correctly set and that the metal cylinder which surrounded the filament, and which in this tube was brought out through a wax joint, had become warm, softened the wax, and caused a distortion of the electron guns. This fault in design was rectified in later tubes as previously described. In this tube the ratios obtained with the reversal of the target were quite different. It is probable that had the slits used to define the secondary beam been smaller this effect would not have appeared.

Altogether 160 determinations of the ratio of the scattered intensity at 0° and 180° of the azimuth were made. The calculated error of reading in a single observation was 3·2 per cent., and a sufficient number of readings were made with each tube under each set of conditions to give the mean values in Table II an accuracy of 1 per cent. Only two of the determined ratios showed deviations from the mean greater than the calculated error, which could not be definitely accounted for. These two values were included in calculating the averages given in Table II. It is probable that they were due to vibrations which affected the electrometer needle.

Discussion.

The results given in Table II show that for 10 kilovolt electrons scattered twice through angles of 90° from thick tungsten targets, the asymmetry in the 0°–180° azimuthal plane (if any) is less than 1 per cent.† The scattering in the 90°–270° plane was not investigated.

It is of interest to examine the various types of asymmetry which have been reported to exist under different experimental conditions. When the electron velocities are very high the following types have been observed.

(*a*) Asymmetry. Cox and co-workers; Chase (*loc. cit.*).—A large asymmetry in the 90°–270° and a smaller asymmetry in the 0°–180° azimuthal plane.

Experimental Method.—Fast particles (velocity of from 0·7 to 0·95 the velocity of light) were successively scattered at 90° from thick lead targets.

---

† The asymmetry given by the corrected calculations for isolated tungsten nuclei is less than 1 per cent. for electrons of 10 kilovolts energy.

(*b*) Asymmetry. Rupp (*loc. cit.*).—A 12 per cent. asymmetry in the 0°–180° azimuthal plane, the scattered intensity being greatest at $\phi = 0°$. Symmetrical scattering in the 90°–270° plane.

Experimental Method.—80 kilovolt electrons were twice scattered at grazing incidence from thick targets of gold.

(*c*) Asymmetry. Thomson (and Kirchner) (*loc. cit.*).—Less than 1 per cent. in any direction.

Experimental Method.—High velocity electrons (about 65 kilovolts) were twice scattered by passage through thin foils. A portion of the first diffraction pattern was screened off, and the intensity of opposite sides of the rings in the second pattern compared.

(*d*) Asymmetry. Rupp, and Rupp and Szilard (*loc. cit.*).—A large asymmetry in the 0°–180° plane, the scattered intensity being largest at $\phi = 180°$. Symmetrical scattering in the 90°–270° plane. This asymmetry could be rotated about the azimuth by application of a suitable magnetic field to the secondary beam.

Experimental Method.—220 kilovolt electrons scattered at 90° from a thick gold target were passed through a thin gold foil, and the intensity of opposite sides of the diffraction rings compared.

(*e*) Asymmetry. Dymond (*loc. cit.*).—A small (about 2 per cent.) asymmetry in the 0°–180° azimuthal plane, the scattered intensity being greatest at $\phi = 0°$.

Experimental Method.—70 kilovolt electrons were twice scattered at 90° from gold foils.

These experiments indicate a wide variety in the nature of the effect obtained under different conditions of scattering. The results of (*c*), (*d*) and (*e*) seem least liable to contain an effect which is not due to a property of the electron itself. While (*c*) and (*e*) may be considered to follow in general the predictions of the theory, there is apparently no reason to expect the result of (*d*).

In view of the fact that practical conditions may be immensely more complicated than those of the Mott theory, it is not surprising that it does not furnish a guide, even in a qualitative way, to all the above experiments. This may be due to (*a*) the fact that a large proportion of the beam scattered from a thick target consists of electrons which have undergone more than one collision, (*b*) the insufficiency of the theoretical model, (*c*) the inclusion of extraneous effects in the experimental results.

(*a*) One would expect that a large proportion of these electrons in a beam would cause depolarisation and so lead to negative results. It is difficult to see how it could possibly account for the observed effects. Multiple scattering was largely eliminated in Dymond's experiment and his results for the 0°–180° azimuthal plane are qualitatively in accord with the theory, but are too low by a factor of five. It is also practically negligible in those experiments in which the scattering is produced by the diffraction of electrons in thin films. For the small angles obtainable by this method, however, the predicted effect is not of observable magnitude.

(*b*) In order to apply the Mott theory to a practical case, it is necessary to assume that effects due to single scattering nuclei are additive. Polarisation effects of observable magnitude have been obtained in the diffraction type of experiment, and at first sight this might be attributed to the fact that the electron wave makes a collision with a crystal as a whole, and so the above assumption breaks down. Intensity measurements of the ordinary electron diffraction rings indicate that at small angles at least the scattering follows the Rutherford law if due account be taken of the effect of the atomic charge cloud.* Since the addition of single effects is valid here it might be expected to apply also in the case of polarisation.

On the other hand, Halpern† has investigated the polarisation asymmetry for the double scattering experiment at small angles, by making use of the experimental fact that a beam of electrons impinging on a target at nearly grazing incidence, is for the most part specularly reflected without loss of energy. The targets were represented by two-dimensional gratings and the polarisation relations differ qualitatively from those calculated for isolated nuclei. They cannot be obtained by a superposition of single effects and are expressed in terms of unknown quantities, the force fields in the gratings. For large angles this treatment is not valid.

Simpler theoretical models for the targets, such as a vacuum at a different electrical potential than the surrounding vacuum, lead to negative results for the double scattering experiment.‡

The electronic scattering should, on theoretical grounds,§ be negligible in comparison with the total scattering and the work of Mark and Wierl (*loc. cit.*) indicates that its effect vanishes at angles of the order of 10°.

---

* Mark and Wierl, 'Z. Physik,' vol. 60, p. 741 (1930).

† 'Z. Physik,' vol. 67, p. 320 (1931).

‡ Frenkel, 'C. R. Acad. Sci. Paris,' vol. 188, p. 153 (1929); Alexandrow, 'Z. Physik,' vol. 60, p. 387 (1930).

§ Wolfe, 'Phys. Rev.,' vol. 37, p. 591 (1931).

I wish to express my thanks to Professor O. W. Richardson for the suggestion of the problem and for helpful discussion, and to the Royal Commission for the Exhibition of 1851, whose award made this work possible.

Summary.

A description is given of a type of experimental tube in which electrons are scattered twice at approximately 90° from thick tungsten targets. The intensities of the secondary scattering in the plane of the primary and secondary beams (0° and 180° of the azimuth) can be determined without altering the relative position of the polarising and analysing targets.

The experimental results obtained with this tube indicate that the intensities scattered at 0° and 180° of the azimuth do not differ by more than the experimental error (1 per cent.) for primary electron energies up to 10 kilovolts.

A short summary of the positive results obtained by various investigators for very fast electrons is given, and their connection with the specialised theory developed by Mott is briefly discussed.

Ionic Diamagnetic Susceptibilities.

By W. Rogie Angus, Sir William Ramsay Laboratories of Inorganic and Physical Chemistry, University College, London.

(Communicated by F. G. Donnan, F.R.S.—Received February 3, 1932.)

1. *Introduction.*

Various attempts have been made to evaluate ionic diamagnetic susceptibilities. The two chief methods of attack have been (1) by the evaluation of formulæ connecting the diamagnetic susceptibility with the charge distribution of a symmetrical atom or ion, and (2) from a consideration of experimental data. In this paper ionic diamagnetic susceptibilities are calculated from Slater's formula† introducing a slight modification in the method of evaluating the effective nuclear charge.

2. *Methods of Calculating Diamagnetic Susceptibility.*

The classical formula‡ for the diamagnetic susceptibility of a symmetrical atom or ion is

$$\chi = -\frac{e^2}{6mc^2}\Sigma\bar{r}^2, \tag{1}$$

where $\bar{r}^2$ is the time average of r^2, the distance of the electron from the nucleus. The summation is extended over all the circumnuclear electrons. In quantum mechanics this formula also holds, but the value of $\bar{r}^2$ is different. Van Vleck§ and Pauling,‖ independently, have calculated the value of $\bar{r}^2$ as

$$\bar{r}^2 = a_0{}^2\frac{n^4}{(\mathrm{Z}-s)^2}\left[1+\tfrac{3}{2}\left\{1-\frac{l(l+1)-\frac{1}{3}}{n^2}\right\}\right], \tag{2}$$

where $(\mathrm{Z}-s)$ is the effective nuclear charge, a_0 the radius of the one quantum orbit of hydrogen ($a_0 = 0\cdot532\times10^{-8}$ cm.), and n and l the total and serial quantum numbers. Substituting this value of $\bar{r}^2$ in equation (1) and introducing numerical values for the physical constants the diamagnetic susceptibility of a gram atom is given by

$$\chi = -2\cdot010\times10^{-6}\,\Sigma\frac{n^4}{(\mathrm{Z}-s)^2}\left\{1-\frac{3l(l+1)-1}{5n^2}\right\}. \tag{3}$$

---

† 'Phys. Rev.,' vol. 36, p. 57 (1930).

‡ Stoner, "Magnetism and Atomic Structure," 1926.

§ 'Proc. Nat. Acad. Sci.,' vol. 12, p. 662 (1926).

‖ 'Proc. Roy. Soc.,' A, vol. 114, p. 181 (1927).

The screening constant, s, was estimated by Pauling for different electron groups and a number of susceptibilities for ions and atoms were calculated by him (see Table II). In general these susceptibilities were much higher than the experimental values. An extension of Pauling's work has been made by Gray and Farquharson[†] who, in order to explain their results on halides, halogenates and perhalogenates, calculated the susceptibilities of ions like I^{+5}, Br^{+3}, Cl^{+1} by evaluating equation (3) using screening constants, interpolated from Pauling's constants, for the halogen *plus* one electron and the halogen *minus* six electrons. Using the ionic susceptibilities thus obtained Gray and his collaborators[†] find that the theoretical values are considerably larger than the experimental results and attribute the differences to "bond magnetism."

Stoner[‡] has calculated a number of ionic susceptibilities using Hartree's[§] space charge distribution method. The radial charge density in electron units per unit radial distance is (dZ/dr). The total number of electrons in the atom is given by the total charge $\int_0^\infty (dZ/dr)dr$, and

$$\bar{r}^2 = \frac{\int_0^\infty r^2 (dZ/dr)\, dr}{\int_0^\infty (dZ/dr)\, dr}. \tag{4}$$

Therefore the ionic susceptibility is

$$\chi = -\,0{\cdot}807 \times 10^{-6} \int_0^\infty r^2 (dZ/dr)\, dr. \tag{5}$$

Again theoretical values are much higher than experimental results, and Brindley[||] gives a table comparing ionic susceptibilities obtained in this way with experimental results.

Zener[¶] has shown that the nodes in a wave function are unimportant. Slater (*loc. cit.*) has made use of this to show how wave functions of atoms and ions may be calculated conveniently by neglecting the nodes and taking as the radial part of the wave function of one electron in a symmetrical atom

$$\psi = r^{(n^*-1)}\, e^{-\left(\frac{Z-s}{n^* r}\right)} \tag{6}$$

[†] 'Phil. Mag.,' vol. 10, p. 191 (1930); 'Phil. Mag.,' vol. 11, p. 81 (1931).

[‡] 'Proc. Leeds Phil. Soc.,' vol. 1, p. 484 (1929).

[§] 'Proc. Camb. Phil. Soc.,' vol. 24, p. 89 and p. 111 (1928).

[||] 'Phil. Mag.,' vol. 11, p. 786 (1931).

[¶] 'Phys. Rev.,' vol. 36, p. 51 (1930).

where n^* is the effective quantum number, and $(Z - s)$ the effective nuclear charge, *i.e.*, the difference between the nuclear charge, Z, and the screening constant, s. Rules are given by Slater for the evaluation of n^* and s for any electron group. He divides the electrons into the following groups, each of which has a different screening constant :—1*s* ; 2*s*, *p* ; 3*s*, *p* ; 3*d* ; 4*s*, *p* ; 4*d* ; 4*f* ; 5*s*, *p* ; etc. For any n the s and p electrons are grouped together.

By integration of the wave functions the value of $\bar{r}^2$ is obtained as

$$\bar{r}^2 = \frac{(n^*)^2 (n^* + \tfrac{1}{2}) (n^* + 1)}{(Z - s)^2}, \tag{7}$$

and therefore the diamagnetic susceptibility of each electron in the group is

$$\chi = \frac{-0{\cdot}807 \times 10^{-6} (n^*)^2 (n^* + \tfrac{1}{2}) (n^* + 1)}{(Z - s)^2}. \tag{8}$$

Brindley (*loc. cit.*) has shown that ionic susceptibilities calculated by this formula are in better agreement with the experimental results than those of Pauling or Stoner.

3. *Present Method of Calculating Ionic Susceptibilities.*

In the calculation of effective nuclear charges and ionic susceptibilities neither Slater nor Brindley make any distinction between the s and p electrons having the same quantum number. Consider, for example, Cl^{-1} consisting of two 1*s*, two 2*s*, six 2*p*, two 3*s*, and six 3*p* electrons. Applying Slater's screening rule to find the effective nuclear charge we have for each quantum level :—

		$(Z - s)$
1*s*	$17 - (1 \times 0{\cdot}30)$	$= 16{\cdot}7$
2*s*, *p*	$17 - (7 \times 0{\cdot}35) - (2 \times 0{\cdot}85)$	$= 12{\cdot}85$
3*s*, *p*	$17 - (7 \times 0{\cdot}35) - (8 \times 0{\cdot}85) - (2 \times 1{\cdot}00)$	$= 5{\cdot}75$

But if we consider the s and p groups separately and work out the effective nuclear charges we obtain :—

		$(Z - s)$
1*s*	$17 - (1 \times 0{\cdot}30)$	$= 16{\cdot}7$
2*s*	$17 - (1 \times 0{\cdot}35) - (2 \times 0{\cdot}85)$	$= 14{\cdot}95$
2*p*	$17 - (7 \times 0{\cdot}35) - (2 \times 0{\cdot}85)$	$= 12{\cdot}85$
3*s*	$17 - (1 \times 0{\cdot}35) - (8 \times 0{\cdot}85) - (2 \times 1{\cdot}00)$	$= 7{\cdot}85$
3*p*	$17 - (7 \times 0{\cdot}35) - (8 \times 0{\cdot}85) - (2 \times 1{\cdot}00)$	$= 5{\cdot}75$

The values of the ionic susceptibilities obtained by this method of evaluating the effective nuclear charges are slightly lower than those obtained by Slater's method. This is shown in Table I where the effective nuclear charges and ionic susceptibilities of O^{-2}, Br^{-1}, and Cs^{+1} are given in detail. The nuclear charge of the ion is given in column 2; in the third column the electron group and, in brackets, the number of electrons in the group; the next two columns give the values of the effective nuclear charge using both the methods just mentioned; the sixth and seventh show the diamagnetic increments for each electron group; whilst the last three columns give the ionic susceptibilities calculated by the present method and by the methods of Slater and Pauling.

Table I.—Ionic Susceptibilities of O^{-2}, Br^{-1}, and Cs^{+1}.

Ion.	Z.	Electron	$(Z - s)$.		$-\Delta\chi_A \times 10^6$.		$-\chi_A \times 10^6$.		
			W.R.A.	J.C.S.	W.R.A.	J.C.S.	W.R.A.	J.C.S.	L.P.
O^{-2}	8	1*s* (2)	7·7	7·7	0·08	0·08			
		2*s* (2)	5·95	3·85	1·37	3·28			
		2*p* (6)	3·85	3·85	9·80	9·80	11·25	13·15	12·6
Br^{-1}	35	1*s* (2)	34·7	34·7	—	—			
		2*s* (2)	32·95	30·85	0·04	0·05			
		2*p* (6)	30·85	30·85	0·15	0·15			
		3*s* (2)	25·85	23·75	0·30	0·36			
		3*p* (6)	23·75	23·75	1·08	1·08			
		3*d* (10)	13·85	13·85	5·3	5·3			
		4*s* (2)	9·35	7·25	4·98	8·27			
		4*p* (6)	7·25	7·25	24·8	24·8	36·65	40·01	54
Cs^{+1}	55	1*s* (2)	54·7	54·7	—	—			
		2*s* (2)	52·95	50·85	0·02	0·02			
		2*p* (6)	50·85	50·85	0·06	0·06			
		3*s* (2)	45·85	43·75	0·10	0·11			
		3*p* (6)	43·75	43·75	0·32	0·32			
		3*d* (10)	33·85	33·85	0·89	0·89			
		4*s* (2)	29·35	27·25	0·51	0·59			
		4*p* (6)	27·25	27·25	1·76	1·76			
		4*d* (10)	15·85	15·85	8·67	8·67			
		5*s* (2)	11·35	9·25	4·52	6·79			
		5*p* (6)	9·25	9·25	20·36	20·36	37·21	39·57	55

In this way the ionic susceptibilities of a large number of ions have been calculated and the results are collected in Table II.

4. *Comparison of Susceptibilities of Atoms and Ions Calculated by Different Methods.*

Table II gives the values obtained by Pauling and values calculated by the author using both the original and the modified forms of Slater's scheme.

The different completed groups are separated by a line drawn across the table; all ions having the same electronic configuration are in the same group.

Table II.—Comparison of Calculated Susceptibilities.

Ion.	$-\chi_A \times 10^6$.		
	L.P.	J.C.S.	W.R.A.
H^{0}	2·415	2·421	2·421
He^{+1}	0·604	0·605	0·605
Li^{+2}	0·268	0·27	0·27
H^{-1}	8	9·87	9·87
He	1·54	1·68	1·68
Li^{+1}	0·63	0·665	0·665
Be^{+2}	0·34	0·35	0·35
B^{+3}	0·21	0·22	0·22
C^{+4}	0·15	0·15	0·15
N^{+5}	0·11	0·11	0·11
O^{+6}	—	0·08	0·08
F^{+7}	—	0·06	0·06
C^{-4}	50	56·65	45·65
N^{-3}	22	23·94	19·96
O^{-2}	12·6	13·15	11·25
F^{-1}	8·1	8·30	7·25
Ne	5·7	5·72	5·07
Na^{+1}	4·2	4·17	3·74
Mg^{+2}	3·2	3·18	2·89
Al^{+3}	2·5	2·50	2·28
Si^{+4}	2·1	2·03	1·87
P^{+5}	1·7	1·66	1·54
S^{+6}	1·4	1·41	1·31
Cl^{+7}	1·2	1·19	1·12
Si^{-4}	110	109·5	91·11
P^{-3}	65	59·39	50·78
S^{-2}	40	37·41	32·63
Cl^{-1}	29	25·79	22·86
A	21·5	18·87	16·95
K^{+1}	16·7	14·40	13·06
Ca^{+2}	13·3	11·38	10·42
Sc^{+3}	10·9	9·22	8·48
Ti^{+4}	9·0	7·65	7·09
V^{+5}	7·7	6·45	6·01
Cr^{+6}	6·6	5·50	5·15
Mn^{+7}	5·7	4·73	4·45
Cu^{+1}	13	19·40	19·26
Zn^{+2}	11	15·57	15·45
Ga^{+3}	9·5	12·84	12·73
Ge^{+4}	8·5	10·78	10·69
As^{+5}	7·5	9·19	9·11
Se^{+6}	6·5	7·94	7·88
Br^{+7}	6·0	6·94	6·87
Ge^{-4}	140	107·18	93·79
As^{-3}	95	72·46	64·62
Se^{-2}	70	52·54	47·58
Br^{-1}	54	40·01	36·65
Kr	42	31·73	29·33
Rb^{+1}	35	25·81	24·05
Sr^{+2}	28	21·53	20·19
Y^{+3}	24	18·16	17·14
Zr^{+4}	20	15·63	14·79
Nb^{+5}	17	13·58	12·91
Mo^{+6}	15	11·92	11·38
Ag^{+1}	44	42·37	42·11
Cd^{+2}	37	34·16	33·94
In^{+3}	32	28·26	28·08
Sn^{+4}	28	23·88	23·71
Sb^{+5}	24	20·51	20·36
Te^{+6}	20	17·80	17·68
I^{+7}	17	15·63	15·52
Sn^{-4}	180	152·54	134·61
Sb^{-3}	130	105·67	94·40
Te^{-2}	105	77·27	70·62
I^{-1}	80	59·83	55·32
Xe	66	48·00	44·78
Cs^{+1}	55	39·57	37·21
Ba^{+2}	46	33·30	31·59
La^{+3}	38	28·50	27·09
Ce^{+4}	33	24·71	23·59
Au^{+1}	65	58·62	58·38
Hg^{+2}	55	47·77	47·57
Tl^{+3}	48	39·86	39·68
Pb^{+4}	42	33·97	33·81
Bi^{+5}	37	20·36	29·22
Rn	—	61·26	57·43

In Table III are collected the values of the diamagnetic susceptibilities of ions in some of which the groups and sub-groups are not completed. The second column gives the values obtained by Gray and Farquharson.[*] Values calculated by the author using Slater's method and the modified method of Slater are given in columns 3 and 4.

---

[*] 'Phil. Mag.,' vol. 10, p. 191 (1930).

Table III.—Diamagnetic Susceptibilities of "Incomplete" Ions.

Ion.	$-\chi_A \times 10^6$.			Ion.	$-\chi_A \times 10^6$.		
	G. & F.	J.C.S.	W.R.A.		G. & F.	J.C.S.	W.R.A.
C^{+4}	0·15	0·15	0·15	F^{+7}	0·063	0·06	0·06
C^{+2}	4·83	3·25	3·25	F^{+5}	1·52	1·07	1·07
C^{0}	10·32	9·31	7·83	F^{+3}	2·95	2 54	2·31
C^{-2}	21·00	22·50	18·15	F^{+1}	4·98	4·77	4·21
C^{-4}	50	56·65	45·65	F^{-1}	8·10	8·30	7·25
N^{+5}	0·11	0·11	0·11	Cl^{+7}	1·20	1·19	1·12
N^{+3}	3·04	2·09	2·09	Cl^{+5}	5·71	4·48	4·41
N^{+1}	6·19	5 47	4·77	Cl^{+3}	10·92	9·15	8·39
N^{-1}	11·46	11·63	9·77	Cl^{+1}	18 19	15·86	14·19
N^{-3}	22	23·94	19·96	Cl^{-1}	29·0	25·79	22·86
O^{+6}	0·08	0·08	0·08	Br^{+7}	6·00	6·94	6·87
O^{+4}	2·09	1·45	1·45	Br^{+5}	13·74	11·91	11·84
O^{+2}	4·09	3·60	3·21	Br^{+3}	23·09	18·58	17·67
O^{0}	7·19	7·10	6·13	Br^{+1}	35·81	27·55	25·59
O^{-2}	12 6	13·15	11 25	Br^{-1}	54·00	40·01	36·65
S^{+6}	1·4	1·41	1·31	I^{+7}	17·00	15·63	15·52
S^{+4}	—	5·73	5·63	I^{+5}	27·68	22·28	22·17
S^{+2}	—	12·13	10·99	I^{+3}	40·53	31·15	29·93
S^{0}	—	21·95	19·32	I^{+1}	57·27	43·03	40·52
S^{-2}	40	37·41	32·63	I^{-1}	80·00	59·83	55·32

An examination of Tables II and III will show that the modification introduced into Slater's method has the effect of lowering the susceptibility considerably. Practically all the values given in Table II are lower than Pauling's values. As will be shown in a later section, the calculated values obtained by the present method agree much better with experimental data than either Pauling's or Slater's values.

5. *Deduction of Atomic and Ionic Susceptibilities from the Experimental Results for Salts.*

Pascal* has measured the diamagnetic susceptibilities of a large number of organic substances and has deduced a set of atomic susceptibilities. These are for atoms in combination and are found to be fairly reliable for use in interpreting the results of molecules containing organic radicals.

Ionic susceptibilities have been deduced from measurements on salts either in solution or in the crystalline state by comparing the susceptibilities obtained by measurements on a large number of substances containing the same anion or cation. This procedure was adopted by Joos* in considering the measurements of Königsberger. Pauling (*loc. cit.*) applied the method to Pascal's† experimental results on salts of the alkali and alkaline earth metals. For the ionic susceptibilities of Na^{+1} and K^{+1} he chose the values $-5 \cdot 2$ and $-14 \cdot 5 \times 10^{-6}$ respectively (in each instance 4·0 less than the values chosen by Pascal). From this starting point, which appears to be unjustifiable, he deduced the susceptibilities of a number of ions. The agreement between the values obtained in this way and the values predicted by equation (3) was good for simple ions but with more complicated ions Pauling's predicted values were much too high. Such a procedure, although unjustifiable, led to values which were approximately correct. It is shown, too, in Table II that Pauling's values for the more complicated ions are much too high.

---

* 'C. R. Acad. Sci. Paris,' vol. 158, p. 1895 (1914).

Ikenmeyer‡ has deduced values for halogen, alkali, and alkaline earth ions from his measurements on aqueous solutions of halides by starting with CsI and assuming that the ionic susceptibilities are proportional to the squares of the nuclear charges. Brindley has modified this by taking the susceptibilities as being proportional to the squares of the effective nuclear charges.

Quite recently Weiss§ has pointed out that diamagnetic susceptibilities of aqueous solutions of salts may be influenced by the action of charged ions on the water molecules in the same way as optical refractivity is influenced. He estimated the magnitude of this effect and found it greatest for small ions and negligible for large ions. Then starting with the observed value for HCl he estimated a number of ionic susceptibilities from the measurements of Hocart, Reicheneder, and Pascal.

Although, admittedly, the values of the ionic susceptibilities deduced from experimental results give an approximate value which agrees with experimental data, the agreement is obtained only by an arbitrary choice of the susceptibilities of the ions from which other susceptibilities are deduced.

6. *Comparison of the Ionic Susceptibilities Calculated by the Present Method with Experimental Data.*

A disappointing feature of diamagnetic measurements is the lack of agreement between the results obtained by different investigators who have measured the same substance. The results, collected in the International Critical Tables (1929), have been tested with the values calculated. Unquestionably many of these results are inaccurate and the measurements should be repeated, but in practically every case where an *accurate* experimental figure has been tested it is found that the values calculated by the author agree with the experimental values better than those predicted by the methods of Pauling or Slater.

---

* 'Z. Physik,' vol. 19, p. 347 (1923), and vol. 32, p. 835 (1925).

† 'C. R. Acad. Sci. Paris,' vol. 158, p. 37 (1914), vol. 159, p. 429, and vol. 173, p. 144 (1921).

‡ 'Ann. Physik,' vol. 1, p. 169 (1929).

§ 'J. Physique,' vol. 1, p. 185 (1930).

The rare gases were measured by Wills and Hector* with an accuracy claimed to be 2 per cent. The experimental values are given in column 2 of Table IV and compared with the theoretical values of Pauling and those calculated by the author using Slater's method and the modification discussed.

Table IV.

	Experimental.	Calculated.		
		Pauling.	Slater.	Angus.
He	1·88	1·54	1·68	1·68
Ne	6·66	5·7	5·7	5·07
A	18·1	21·5	18·87	16·95

It is possible that the experimental value for neon is too large since it is considerably higher than all calculated values.

The values predicted by the present method give very good agreement with the observed values for the halogens, Table V. In computing the calculated value for a halogen molecule it was assumed to be formed by the union of two halogen atoms, one carrying a charge of +1 and the other a charge of −1, and the calculated susceptibility is the sum of the appropriate ionic susceptibilities, Table III.

Table V.

	Experimental.	Calculated.		
		Pauling.	Slater.	Angus.
Cl_2 .	40·05	47·19	41·65	37·05
Br_2	62·4	89·81	67·56	62·24
I_2	91·5	137·27	102·86	95·84

---

* 'Phys. Rev.,' vol. 23, p. 209 (1924); 'Phys. Rev.,' vol. 24, p. 418 (1924).

In Table VII Ikenmeyer's experimental results (column 2) are compared with the values calculated by nine different methods; in the next five columns are values deduced from experimental results by Ikenmeyer (I), Joos (J), Weiss (W), Brindley (B), and Pauling (P_P) (from Pascal's experimental data) respectively; and in the last four columns are the values calculated by Pauling (P_C), from equation (3), from Hartree's formula (4) (H), and by the author from equation (8) using Slater's method of evaluating the effective nuclear charge (S), and the modification discussed previously (A).

Table VI.

Salt.	Experimental.	I.	J.	W.	B.	P_P.	P_C.	H.	S.	A.
†LiCl	26·8	24·4	—	—	24·7	24·3	29·63	41·1	26·45	23·53
LiBr	37·3	38·8	—	—	42·2	34·8	54·63	—	40·67	37·32
LiI	55·6	53·25	—	—	56·4	48·8	80·63	—	60·49	55·99
†NaCl	30·0	30·8	26·0	31·1	29·2	29·3	33·2	46·14	29·96	26·60
†NaBr	43·2	45·2	46·0	42·1	42·7	39·8	58·2	—	44·18	40·39
NaI	60·4	59·65	67·0	58·2	60·9	52·8	84·2	—	64·0	59·06
KCl	36·2	37·3	34·0	39·3	37·5	38·6	45·7	58·0	40·21	35·92
†KBr	52·6	51·7	54·0	50·3	51·0	49·1	70·7	—	54·43	49·71
KI	67·8	66·1	75·0	66·4	69·2	63·1	96·7	—	74·25	68·38
†RbBr	65·5	51·7	—	58·4	61·5	57·8	89·0	—	65·82	60·70
CsI	92·5	95·0	—	88·2	92·5	85·6	135·0	—	99·40	92·53
*$MgCl_2$	47·9	45·3	48·0	—	51·8	51·5	61·2	85·1	54·76	48·61
$MgBr_2$	72·2	71·1	88·0	—	78·5	72·5	111·2	—	83·20	76·19
MgI_2	111·4	103·0	130·0	—	115·2	100·5	163·2	—	122·84	113·53
‡$CaCl_2$	51·2	51·8	48·0	57·6	58·8	56·0	71·3	94·2	63·96	56·14
‡$SrCl_2$	61·6	66·2	63·0	65·9	67·5	64·7	86·0	—	73·11	65·91
‡$SrBr_2$	85·3	95·0	103·0	87·9	94·5	85·7	136·0	—	101·55	93·49
SrI_2	131·1	123·9	145·0	120·1	130·9	113·7	188·0	—	141·20	130·83
$BaCl_2$	74·0	80·7	82·0	—	78·0	78·0	104·0	—	84·88	77·31
$BaBr_2$	103·6	109·5	122·0	—	105·0	99·0	154·0	—	113·32	104·89

* The experimental value is misprinted in the original paper as 49·7.

The values calculated by the present method are in more consistent agreement with experimental data than any of the other calculated values. The experimental value for the salts marked † is too high and a value closer to the calculated is reported in the literature; whilst with those marked ‡ Ikenmeyer's experimental values are lower than those predicted, and others, which give better agreement, are available. Since the experimentally determined values are not consistently too high or too low it may be assumed that values calculated by the present method, assuming additivity, are in complete accord with experimental results.

Not only is this good agreement obtained with halides but it holds also for simple compounds of many different kinds, some of which are given in Table VII.

Table VII.

	Experimental.	Calculated.		
		Pauling.	Slater.	Angus.
$BaI_2 . 2H_2O$	163	231·2	179·26	164·73
$CsCl$	61	84	64·36	60·07
H_3BO_3	32·3	38·01	39·67	33·97
KF	20·85	24·8	22·7	20·31
K_2SO_4	73·1	85·2	82·81	72·43
HCl	23·05	29·0	25·79	22·86
ZnO	26·75	23·6	28·72	26·70
$SnCl_4$	115·3	144	127·04	115·15

It seems therefore that the addition of calculated ionic susceptibilities (Table II) gives values which are in good agreement, for simple compounds, with experimental results. These results are used in the next paper in the interpretation of the diamagnetic susceptibilities of some compounds of beryllium.

8. *Summary.*

The different methods of calculating ionic diamagnetic susceptibilities are reviewed briefly. The ionic or atomic susceptibilities of 76 atoms or ions having completed groups and sub-groups have been evaluated by Slater's method and by a modification of Slater's method which is discussed. Values for the ionic susceptibilities of 24 ions with incomplete groups or sub-groups have also been calculated by both methods. The modified Slater's method gives values which are in very good agreement with experimental results. Methods of deducing ionic susceptibilities from measurements on salts in solution or in the crystalline state are criticised.

My thanks are due, in the first place, to Professor F. G. Donnan, F.R.S., for his kind interest and encouragement; to Dr. John Farquharson, University College, London, for friendly criticism; and to the Ramsay Memorial Fellowships Trustees for a British Fellowship.

The Diamagnetic Susceptibilities of some Beryllium Compounds.

By W. Rogie Angus and John Farquharson, Sir William Ramsay Laboratories of Inorganic and Physical Chemistry, University College, London.

(Communicated by F. G. Donnan, F.R.S.—Received February 3, 1932.)

1. *Introduction.*

The investigation of the molecular structure of organic beryllium compounds is being studied by one of us (W.R.A.) from the standpoint of their infra-red absorption spectra. During a mechanical defect in the infra-red apparatus the diamagnetic susceptibilities of basic beryllium acetate, propionate, and pivalate, and of beryllium acetylacetonate were measured in order to obtain further physical data on the structure of these molecules. The susceptibilities were measured on a Curie-Chéneveau magnetic torsion balance by the method previously described by Farquharson.* Measurements were made at 18° C.

The compounds were finely powdered in an agate mortar and packed tightly into a small graduated glass tube of very slight susceptibility. Packing of solids is most important in diamagnetic susceptibility measurements. Inefficient packing leads to values of the specific susceptibility much lower than the *true* value. This diminution results from the fact that the volume of solid is virtually diminished by air spaces and a volume correction should be applied.

The results are all given relative to the usual standard ($\chi_{H_2O} \times 10^6 = -0 \cdot 72$).

Small amounts of each of these compounds were very kindly supplied by Professor G. T. Morgan, F.R.S., and Dr. Sugden, and the authors welcome this opportunity of recording their thanks to them.

2. *Diamagnetic Susceptibilities of Beryllium Salts.*

The diamagnetic susceptibilities of only a very few beryllium salts have been measured. These are collected in Table I and will be discussed later in the light of the theoretical considerations of the next two sections.

3. *Pascal's Measurements on Organic Substances.*

Pascal has made an extensive series of diamagnetic susceptibility measurements on organic compounds and has deduced values† for atoms in com-

---

* 'Phil. Mag.,' vol. 12, p. 283 (1931).

† Stoner, 'Magnetism and Atomic Structure," 1926.

Table I.—Diamagnetic Susceptibilities of Beryllium Salts.

Salt.	− Mol. suscept. × 10^6.
*BeO	0
†$Be(OH)_2$	23·1
*$BeCl_2$	47·94
*$BeSO_4$	48·3
*$BeSO_4 . 4H_2O$	90·3
*$BeCO_3 . 2BeO$	40·46

* Meyer, 'Ann. Physik,' vol. 69, p. 236 (1899).
† 'Internat. Crit. Tables,' vol. 6, p. 354 (1929).

bination in an organic molecule and for constitutive correcting factors (ring formation, double bonds, etc.). His original results were vitiated by referring them to water as $-0{\cdot}75 \times 10^{-6}$ instead of $-0{\cdot}72 \times 10^{-6}$. Table II gives the values (corrected for $\chi_{H_2O} = -0{\cdot}72 \times 10^{-6}$) required for the interpretation of the experimental results on the beryllium compounds.

Table II.—Pascal's Atomic Susceptibilities and Constitutive Correcting Constants.

——	$-\chi_A \times 10^6$.
C	5·95
H	2·9
O	4·6
COO	13·85
C=C bond	−5·5
C=O bond	−1·73

Since these figures are obtained from a large number of measurements their use as standards appears justifiable.

4. *Calculation of Screening Constants and Ionic Diamagnetic Susceptibilities.*

Screening constants and ionic diamagnetic susceptibilities have been evaluated by the method discussed in another paper.‡ For the evaluation of the theoretical diamagnetic susceptibilities of the basic beryllium compounds only Be^{+2} and O^{-2} were required; these are given in Table III along with C^{+4}, S^{+6} and Cl^{-1}, so that the theoretical values for previously measured beryllium salts could be compared with the experimental results.

---

‡ Angus, 'Proc. Roy. Soc.,' A, vol. 136, p. 569 (1932).

Table III.—Ionic Diamagnetic Susceptibilities.

Ion.	$-\chi_A \times 10^6$.
Be^{+2}	0·35
O^{-2}	11·25
S^{+6}	1·31
C^{+4}	0·45
Cl^{-1}	22·86

5. *Comparison of Calculated and Experimental Values.*

Gray and his co-workers* found that the calculated values were very much larger than the experimental results because their calculated values were worked out from Pauling's† formula, using, where necessary, interpolated screening numbers. The differences they attributed to bond diamagnetism or paramagnetism. Following this procedure with the basic beryllium complexes would be very difficult. These molecules contain a large number of bonds (more than 50) so that a reliable estimate of the bond magnetism could not be expected. For the organic part of the molecules, therefore, Pascal's values have been used and they take bond magnetism into account.

It is assumed that the ionic diamagnetic susceptibility of H^{+1} is zero.

The results are given in Table IV. The ions in column 1 neutralise each other to give the molecule (column 2); whilst in columns 3 and 4 are given the calculated and experimental values. The method of arriving at the calculated values may be illustrated by basic beryllium acetate. This molecule, $Be_4O(CH_3COO)_6$, is formed by the neutralisation of $4Be^{+2} + O^{-2} + 6(CH_3COO)^{-1}$ and the sum of the appropriate susceptibilities from Tables II and III gives the calculated value, *thus*:

—	$-\Delta\chi_A \times 10^6$.	$-\chi_A \times 10^6$.
$4Be^{+2}$	0·35	1·40
O^{-2}	11·25	11·25
6C	5·95	35·70
18H	2·9	52·20
6COO	13·85	83·10

$$\Sigma(-\chi_A \times 10^6) = -\chi_M \times 10^6 = 183{\cdot}65$$

---

* Gray and Farquharson, 'Phil. Mag.,' vol. 10, p. 191 (1930); Gray and Dakers, 'Phil. Mag.,' vol. 11, p. 114 (1931).

† 'Proc. Roy. Soc.,' A, vol. 114, p. 181 (1927).

Table IV.—Diamagnetic Susceptibilities of Beryllium Compounds.

Ions.	Molecule.	$-\chi_M \times 10^6$.	
		Calc.	Exptl.
$4Be^{+2} + O^{-2} + 6(CH_3COO)^{-1}$	$Be_4O(CH_3COO)_6$	183·65	182·19 ±0·2
$4Be^{+2} + O^{-2} + 6(C_2H_5COO)^{-1}$	$Be_4O(C_2H_5COO)_6$	254·15	252·78 ±5·1
$4Be^{+2} + O^{-2} + 6\{C(CH_3)_3COO\}^{-1}$	$Be_4O\{C(CH_3)_3COO\}_6$	395·15	396·65 ±2·7
$Be^{+2} + 2(C_5H_7O_2)^{-1}$	$Be(C_5H_7O_2)_2$	104·39	107·9 ±0·6
* $Be^{+2} + O^{-2}$	BeO	11·60	0
† $Be^{+2} + 2O^{-2} + 2H^{+1}$	$Be(OH)_2$	22·85	23·1
* $Be^{+2} + 2Cl^{-1}$	$BeCl_2$	46·08	47·94
* $Be^{+2} + S^{+6} + 4O^{-2}$	$BeSO_4$	46·64	48·3
* $Be^{+2} + S^{+6} + 4O^{-2} + 4(2H^{+1} + O^{-2})$	$BeSO_4 . 4H_2O$	91·66	90·3
* $Be^{+2} + C^{+4} + 3O^{-2} + 2Be^{+2} + 2O^{-2}$	$BeCO_3 2BeO$	57·45	40·46

* See Table I. † See Table I.

Except for the oxide and the basic carbonate the agreement between the calculated and the experimental values is very good. There seems no obvious reason for a zero susceptibility in beryllium oxide, especially since the oxides of the other alkaline earths are all diamagnetic. This measurement, like many of the older ones, should be repeated. The specific susceptibility of the basic carbonate appears to be much too low when compared with the specific susceptibilities of the other simple salts ($-0·34 \times 10^{-6}$ compared with $-0·46$ to $-0·60 \times 10^{-6}$). The exact composition of the basic carbonate is by no means definitely established. There are some six or seven formulæ recorded in the literature and preliminary experiments by one of us (W.R.A.) indicates that the formula is $BeCO_3 . 3Be(OH)_2 . H_2O$.

6. *The Structure of Basic Beryllium Complexes.*

The crystal structure of the basic beryllium complexes ($Be_4O(RCOO)_6$, where R is an alkyl group) has been determined by Bragg and Morgan* and is discussed in detail by Morgan and Astbury.† They found that these molecules had a symmetrical structure; that the four beryllium atoms were situated at the corners of a regular tetrahedron with the unique oxygen at the centre and the six acyl groups symmetrically disposed on the six edges. Recently Sugden‡ has determined the parachor of basic beryllium propionate and interprets his results on the basis of a formula in which he uses only "singlet" (one electron) and "triplet" (three electron) linkages. This configuration and the more usual one, using single (two electron) and double (four electron) bonds, are shown in fig. 1 (*a*) and (*b*) respectively. Only one of the six interlocking six-membered rings of the tetrahedron is shown in detail and each line between atoms in this ring represents a one-electron linkage.

---

* 'Proc. Roy. Soc.,' A, vol. 104, p. 437 (1923).

† 'Proc. Roy. Soc.,' A, vol. 112, p. 441 (1926).

‡ "The Parachor and Valency," p. 145 (1930); 'J. Chem. Soc.,' p. 318 (1929).

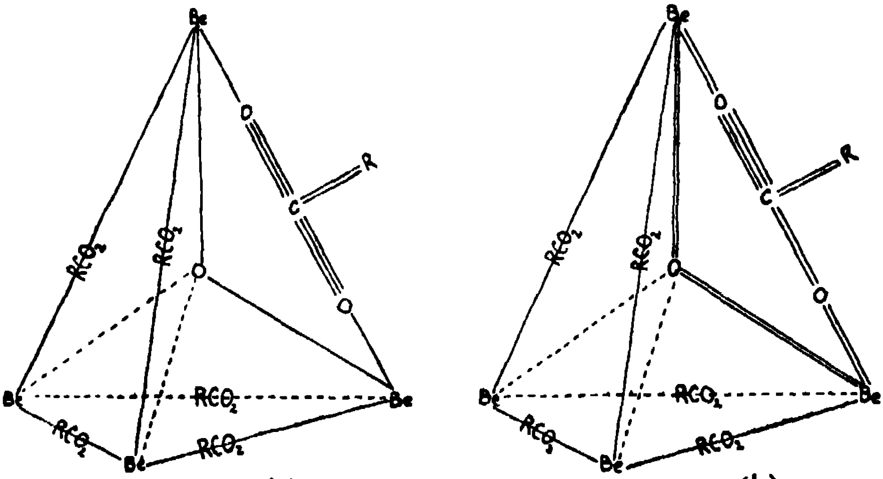

(a) (b)

Fig. 1. (*a*) and (*b*).

The theoretical values for the diamagnetic susceptibilities of these basic complexes indicate that the structure is that shown in fig. 1 (*b*). Pascal's values for the COO group were used and the presence of a double bond between carbon and one of the oxygen atoms allowed for. Pauling[*] has recently discussed the conditions under which odd electron bonds are formed and has shown that they exist in only a few compounds.

7. *The Structure of Beryllium Acetylacetonate.*

Again, with this compound two alternative formulæ are obtained, one with single and triple electron linkages (*c*), and the other with single and double bonds (*d*). Lines joining atoms have the same significance as in the last section.

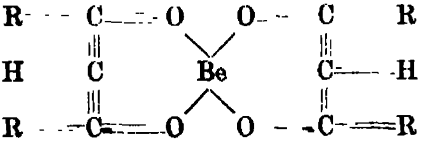

(*c*)

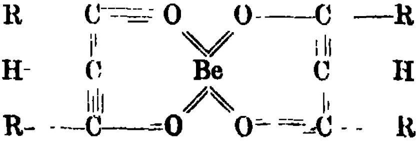

(*d*)

---

[*] 'J. Amer. Chem. Soc.,' vol. 53, p. 3225 (1931).

Here also diamagnetic measurements favour the second structure. In the computation of the theoretical susceptibility allowance was made for two $C=O$ and two $C=C$ double bonds and the agreement between theoretical and experimental values is very good. From the fact that the experimental value is slightly higher than the theoretical it may be supposed that all the linkages are satisfied.

8. *Summary.*

The diamagnetic susceptibilities of basic beryllium acetate, propionate, and pivalate and of beryllium acetylacetonate are given. For the ions theoretical susceptibilities are calculated by Angus's modification of Slater's method; whilst for the organic groups Pascal's data are used. Theoretical and experimental values are in good agreement. Existing data on simple salts are discussed. The structure of the organic derivatives is considered and Sugden's configurations using odd electron linkages are criticised.

In conclusion, our best thanks are due to Professor F. G. Donnan, F.R.S., for his kind interest and advice during the course of this investigation. W.R.A. desires to record his gratitude to the Ramsay Trustees for the award of a British Fellowship; and J.F. to the Royal Commissioners of the 1851 Exhibition for a Senior Studentship.

Fine Structure in the Arc Spectra of Bromine and Iodine.

By S. TOLANSKY, B.Sc., Ph.D., Earl Grey Memorial Fellow, Armstrong College, Newcastle-upon-Tyne.

(Communicated by O. W. Richardson, F.R.S.—Received February 3, 1932.)

[PLATE 10.]

Introduction.

The fine structures of a number of bromine arc and spark lines have been previously reported by Hori,* who examined the emission lines given by a spark discharge through a capillary tube, a small transmission echelon being employed to observe the structures. He found that four of the strongest lines in the red region had similar structures, each showing four components degrading in intensity and interval to the short wave-length side. The intervals in the four lines, though not identical, were fairly close to one another. De Bruin† assumed that these four lines, which come to the $5s\,.\,{}^4P_{5/2}$ term, have identical structures which are characteristic of that term. Since the lines are quartet, he suggested that the nuclear spin is $\frac{3}{2}$. As supporting evidence he took the mean value of the four line structures as being the term structure and pointed out that the interval ratios corresponded to this value of the spin.

An account is given here of further observations in the bromine arc lines, the structures being considerably extended by the use of a high frequency electrodeless discharge in pure bromine vapour and a Fabry-Perot interferometer of variable plate separation. Although it is shown that de Bruin's assumption as to the equality of these four structures is incorrect, the spin of $\frac{3}{2}$ is confirmed. It is further shown that the two isotopes of bromine (79, 81) have the same nuclear spin.

No fine structures have been previously observed in the iodine arc lines. Wood and Kimura‡ examined the emission from a Geissler tube containing iodine, the structures being observed with a transmission echelon. Many spark lines were found to be complex, but the authors state that in no case did any arc line show fine structure. Since the spark spectrum of iodine has not been analysed, very little can be concluded from the spark fine structures as to the value of the nuclear spin. As stated in a preliminary note,* structure has been observed here in the arc lines (region λλ 4700–8000) by using essentially similar apparatus as for bromine. The fine structures are very similar to the bromine structures, but the individual components are generally broader. A nuclear spin of $\frac{9}{2}$ has been deduced, but the value is not so certain as that found for bromine, since the full multiplicity with such a large spin is not attained and thus the value is decided by the interval ratios.

---

* 'Mem. Coll. Sci. Kyoto,' vol. 9, p. 307 (1926).

† 'Nature,' vol. 125, p. 414 (1930).

‡ 'Astrophys. J.,' vol. 48, p. 181 (1917).

Theoretical.

The following discussion on bromine holds in detail for all the halogens. The analysis of the gross structure of the bromine arc spectrum has been made in a very complete manner by Kiess and de Bruin.† All the important terms predicted by Hund's theory‡ have been found. The theoretical term scheme expected is shown in Table I. Since the lines involving the $4s^2 . 4p^5 . {}^2P$ terms lie in the ultra-violet, they will not be considered here at all. Of the remaining terms those based on the $4s^2 . 4p^4 . 5s$ and $4s^2 . 4p^4 . 5p$ configurations are the most prominent.

Table I.—Terms of Br I.

Electron configuration.	Basic ion terms of Br II.		
	${}^3P$.	${}^1D$.	${}^1S$.
$4s^2 . 4p^5$	${}^2P$		
$4s^2 . 4p^4 . 5s$	${}^2P$ ${}^4P$	${}^2D$	${}^2S$
$4s^2 . 4p^4 . 5p$	${}^2(SPD)$ ${}^4(SPD)$	${}^2(PDF)$	${}^2P$
$4s^2 . 4p^4 . 4d$			

A graphical vector method of predicting the fine structures in the terms of a complex electron system has been described by White and Ritschl,§ and successfully applied to the explanation of the Mn I structures. It is assumed that the nucleus has a magnetic moment associated with a mechanical moment $I \frac{h}{2\pi}$, I being defined as the nuclear spin quantum number. It is the coupling of I with J which produces the fine structure of a term of given J value, the number of the fine structure levels being $2I + 1$ or $2J + 1$ according to which is the smaller. Each level is determined by a fine structure quantum number F, the vectors I and J compounding to various F values and precessing about this resultant. Transitions between levels are governed by the selection principle $\Delta F = \pm 1$ or 0 ($0 \rightarrow 0$ excluded) and the ordinary interval and intensity rules of gross multiplets will hold good if the coupling between I and J is proportional to cos (IJ). The theoretical treatments of Hargreaves,* Pauling and Goudsmit,† Goudsmit‡ all show that the coupling energy is of the form

---

* 'Nature,' vol. 127, p. 855 (1931).

† 'Bur. Stand. J. Res.,' vol. 4, p. 666 (1930).

‡ 'Z. Physik,' vol. 52, p. 601 (1928).

§ 'Phys. Rev.,' vol. 35, p. 1146 (1930).

$$E = AIJ \, . \cos (IJ) = \frac{AIJ}{2IJ} \, . \{F(F + 1) - I(I + 1) - J(J + 1)\}$$

which is the normal interval rule, where A is the interval factor, the separation between the two states $F + 1$ and F being $A(F + 1)$.§ The above energy relationship holds for the case of a single *s* electron, where the value of A depends primarily upon the degree of penetration and the actual $g(I)$ factor. More strictly the *s* electron coupling is proportional to cos (IS) where S is the resultant spin vector.

It was assumed by White and Ritschl that a complex electron group will also couple with the nuclear spin so as to obey the interval rule, but that the actual interval factor is determined by the electron coupling associated with the terms in question. The most prominent configurations in Br which are considered here are those of $4s^2 . 4p^4 . 5s$ and $4s^2 . 4p^4 . 5p$. As in the gross structure, the completed sub-group $4s^2$ will have no effect. In the first case the $4p^4$ electrons are considered as a group coupled to the $5s$ electron and as the latter is penetrating wide fine structures appear in the terms arising from this configuration. In the second case the $4p^4$ group couples to the $5p$ electron and, as there is no marked penetration in these, it is to be expected that the resulting structures will be very small and in general not observable. The method of coupling the $5s$ to the $4p^4$ electrons will now be considered. Any given gross structure term splits into a group of fine structure components and the total width of this group is mA where $m = \Sigma F$ (minus the smallest F value). The relative value of A is given by the particular value that cos (IS) has when cos (IJ) $= 1$, that is to say, the nuclear spin vector I is coupled so as to be parallel to the vector J (*i.e.*, cos (IJ) $= 1$). Having thus fixed the direction of I the resulting value of cos (IS) determines the relative value of A. Since from the properties of vectors cos (IS) = cos (IJ) cos (JS) and as cos (IJ) = 1, then cos (IS) = cos (JS). If then for the particular term in question cos (JS) is positive, the fine structures will be normal, and if negative, they will be inverted. In order to obtain the relative values of cos (JS) the term scheme must be built up from the parent ion electron configuration, in this case Br II.

---

* 'Proc. Roy. Soc.,' A, vol. 124, p. 568 (1929).

† "Structure of Line Spectra" (1930).

‡ 'Phys. Rev.,' vol. 37, p. 663 (1931).

§ Goudsmit and Bacher, 'Phys. Rev.,' vol. 34, p. 1501 (1929).

The vector method of coupling (following White and Ritschl) as applied in detail to the $4s^2 . 4p^4 . 5s$ configuration of Br I is shown in fig. 1. The left of the diagram A shows the three ^3P terms of Br II based on the $4s^2 . 4p^4$ configuration. For each term the vector couplings are shown to the right. The two $4s$ electrons forming a closed group have no influence on gross or fine structures. The resultant S of the four $4p$ electrons is shown by a thick arrow, the resultant L by a dotted arrow, and the J direction by a thin arrow. The ^2P and ^4P terms of Br I, shown at B, are obtained when the $5s$ electron, shown by a thick hollow arrow, is added to the $4s^2 . 4p^4$ group. The result of coupling a nuclear spin $I = \frac{3}{2}$ is shown at C, only the initial placing of I (in the direction of cos (IJ) = 1) is shown, the curved arrow indicating that I and J are to be compounded to various F values. To the right of C is shown the angle made between I and the s electron spin, *i.e.*, cos (IS), and, as shown, this determines the relative total spread of each group. So far it has been assumed that the electron coupling is of the (LS) type only. The final result, omitting intermediate steps, is shown for (JJ) coupling at D at the extreme right. Identical methods can be applied to $4s^2 . 4p^4 . 5p$ terms and since there is no unpaired s electron here, much smaller structures will be expected. This is largely true, but experimental deviations occur. Since there is very little agreement, if any, between observations and predictions, the predicted intervals for the $5p$ electrons are not reproduced.

The narrowness of the p electron structures, together with the intensity distribution greatly simplify the appearance of the resulting fine structure multiplets. The rules for calculating the intensities have been given by Hill.* The intensity of each component can be obtained, the sum of the intensities of all the lines to a given F level being proportional to 2F + 1, the transition $F = 0 \rightarrow 0$ being of zero intensity.

The intensity formulæ are simple to apply when I and J are known for all the lines. A very powerful method of analysing complex structures, using these calculated intensities, has been given by Fisher and Goudsmit.* This is of very great value when both upper and lower levels have appreciable structures resulting in a complex pattern which can only be partially resolved. The method is as follows. The interval factors for both upper and lower terms are made equal and the resulting line structure plotted. The upper term is then inverted, the interval factor remaining unchanged, and the resulting line structure plotted below these. The lines involving identical F transitions are joined by a straight line, the thickness of which is roughly proportional to the intensity. At the upper limit the pattern is that given when the interval factor ratio in the two terms is + 1 and the lower limit pattern that given when it is —1. At the centre the pattern is that given when the upper term has a zero interval factor. Hence the line structure is completely determined for any ratio of interval factors by drawing a horizontal line at the point corresponding to that ratio. The result is that even if a pattern is only poorly resolved the ratio of the interval factors can be calculated with a fair amount of certainty. Only when there is no structure in one of the terms

---

* 'Proc. Nat. Acad. Sci.,' vol. 15, p. 779 (1929).

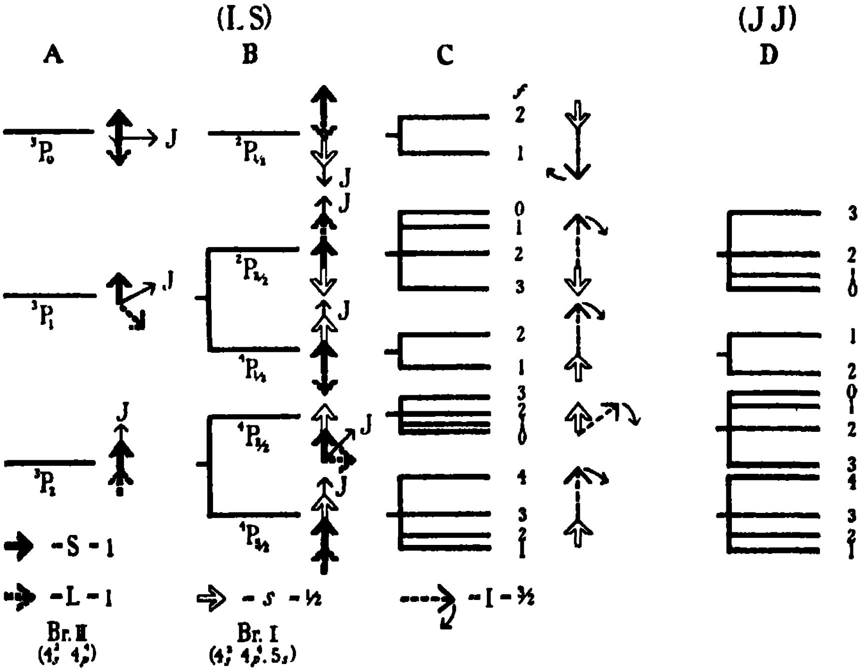

FIG. 1.—Vector Scheme for Bromine Fine Structures.

---

* 'Phys. Rev.,' vol. 37, p. 1059 (1931).

will the interval rule hold exactly within the line complex itself, and for this reason the inferences of de Bruin (*loc. cit.*) as to the interval rule support for a spin of $\frac{3}{2}$ are unsound.

The graphs applicable to all the lines investigated in Br I are shown in fig. 2, these being later applied to the explanation of the observed structures. A number of apparent anomalies are completely accounted for and it will be shown to what extent the simple graphical method of White and Ritschl, for determining the relative order of the interval factors, is verified.

Experimental Procedure.

A very simple form of tube was employed, made of Pyrex glass, 40 cm. long and 2·5 cm. bore. It was evacuated by means of a mercury pump and charcoal cooled in liquid air. Pure bromine was distilled into a side limb and from there back and forth into another side limb during the time of pumping. The tube, containing about 1 c.c. of liquid bromine, was then sealed off from the pump. A 20-metre high frequency electrodeless discharge was used to excite the vapour, and two 250-watt valves using 7 amps. through the filament and 2500 volts on the anode were employed, the circuit being that given by Smith-Rose and McPetrie.* By immersing the side limb of the discharge tube in a mixture of solid CO_2 and alcohol, the vapour pressure in the tube was maintained at about 0·2 mm., at which pressure the high frequency excitation gave a brilliant discharge of practically pure arc. The tube remained fairly cold, so that the Doppler broadening of the lines was not very appreciable. The lines were examined for fine structure with a Hilger N.71 silvered Fabry-Perot interferometer crossed by a Hilger E.1 spectrograph, and the plates used were Ilford Soft Gradation Panchromatic, Ilford Monarch and Kodak Extreme Red. The region observed was λλ 7500–4400, the separations of the interferometer plates varying from 5 to 100 mm. and the exposure times from 1 minute to 2 hours. Only in a few cases were the structures completely resolved.

Experimental Observations.

Measurements were carried out on 27 lines of the arc spectrum. The structure of eight of these has been given by Hori (*loc. cit.*), but since he only used a small transmission echelon grating, and as his source was certainly inferior to the one employed here it follows that his resolution was much less than the present one. For this reason agreement is only expected with the coarser structures. There are small discrepancies even in the widest lines, and since the present observations are considered more reliable both on the score of better source and better resolving power, only these will be considered.

---

* 'Exp. Wireless,' vol. 6, p. 532 (1929).

The complete list of the structures measured is given in Table II. They are classified A, B, C, D, according to the reliability of the measurements. In A the probable error is about ± 1 (all measurements are given in thousandths of a wave number), in B it is ± 3, in C it is ± 6, whilst in the worst D cases it is ± 10. Most of the structures are in the form of quartets degrading to the violet. Where there has been no resolution, the first and second members are resolved, but not the last two. In these cases the tail end of the structure has been measured. This is difficult to do and the biggest errors lie here, the class being decided by this. It is thus seen that the separations of the first pair are generally in the previous class.

Column 1 gives the allocations of the lines as given by Kiess and de Bruin (*loc. cit.*), column 2 the wave-lengths, column 3 the class, column 4 the structure, all the lines forming a degraded series are marked with an asterisk, whilst in

Table II.—Fine Structures of Bromine Arc Lines.

Allocation.	Wave-length.	Class.	Structure.					Width.
$5s\,.\,{}^4P_{5/2}-5p\,.\,{}^4D_{7/2}$	7513·0*	A	0	83	147	205	228	228
$5s\,.\,{}^4P_{3/2}-5p\,.\,{}^2D_{3/2}$	7348·6*	C	0	54	⟶	103		103
$5s\,.\,{}^4P_{1/2}-5p\,.\,{}^2D_{3/2}$	6631·6*	A	0	196	330	402		402
$5p\,.\,{}^4P_{1/2}-4d\,.\,{}^4D_{1/2}$	6582·2*	D	0	50	⟶	96		96
$5s\,.\,{}^4P_{5/2}-5p\,.\,{}^4S_{3/2}$	6559·8*	A	0	199	336	417		417
$5p\,.\,{}^4P_{5/2}-4d\,.\,{}^4D_{7/2}$	6544·6*	D	0	46	⟶	106		106
$5s\,.\,{}^4P_{3/2}-5p\,.\,{}^2P_{3/2}$	6350·7*	A	0	205	349	442		442
$5p\,.\,{}^4D_{5/2}-5d\,.\,{}^4F_{7/2}$	6177·4	A			Single			
$5s\,.\,{}^4P_{3/2}-5p\,.\,{}^2D_{5/2}$	6148·6*	A	0	194	324	417		417
$5p\,.\,{}^4D_{7/2}-5d\,.\,{}^4F_{9/2}$	6122·1	A			Single			
$5p\,.\,{}^4P_{5/2}-5d\,.\,{}^4D_{7/2}$	5852·1	A			Single			
$5p\,.\,{}^4P_{3/2}-5d\,.\,{}^4D_{5/2}$	5833·4	A			Single			
?	5783·3	A			Single			
$5s\,.\,{}^2P_{1/2}-6p\,.\,{}^2P_{3/2}$	5466·2†	B	0	295				295
$5s\,.\,{}^2P_{1/2}-6p\,.\,{}^2P_{1/2}$	4979·8	D			Complex			
$5s\,.\,{}^4P_{3/2}-6p\,.\,{}^4P_{5/2}$	4785·2	D			Complex			
$5s\,.\,{}^4P_{5/2}-6p\,.\,{}^4D_{7/2}$	4780·3*	D	0	56	⟶	118		118
$5s\,.\,{}^2P_{1/2}-5p\,.\,{}^2P_{3/2}$	4775·2	B	0	76	163			163
$5s\,.\,{}^4P_{5/2}-6p\,.\,{}^4D_{5/2}$	4752·3*	C	0	118	⟶	193		193
$5s\,.\,{}^4P_{3/2}-6p\,.\,{}^4D_{5/2}$	4643·5*	C	0	103	⟶	165		165
$5s\,.\,{}^2P_{3/2}-6p\,.\,{}^2D_{5/2}$	4614·6*	C	0	100	⟶	160		160
$5s\,.\,{}^2P_{1/2}-6p\,.\,{}^2D_{3/2}$	4575·8*	D	0	89	⟶	142		142
$5s\,.\,{}^4P_{5/2}-6p\,.\,{}^4S_{3/2}$	4529·8	A			Single			
$5s\,.\,{}^4P_{3/2}-6p\,.\,{}^4P_{3/2}$	4525·6*	C	0	99	⟶	198		198
$5s\,.\,{}^4P_{5/2}-6p\,.\,{}^4P_{5/2}$	4513·4*	C	0	53	⟶	169		169
$5s\,.\,{}^4P_{1/2}-6p\,.\,{}^2S_{1/2}$	4490·4	A			Single			
$5s\,.\,{}^4P_{3/2}-6p\,.\,{}^4D_{1/2}$	4477·8*	D	0	78	⟶	137		137
$5s\,.\,{}^4P_{5/2}-6p\,.\,{}^4P_{3/2}$	4472·6	D			Complex			
$5s\,.\,{}^4P_{3/2}-6p\,.\,{}^4D_{3/2}$	4441·7	D			Complex			

† Doubtful.

column 5 the total widths of the structures are given. The lines given as single are extremely narrow, showing no evidence of structure even with the high resolving power given by a 60-mm. gap (the line λ 6122·1 shows an isotope effect, however, which will be referred to later). Some lines are very complex indeed, being fairly broad but showing no evidence of individual components. This is undoubtedly due to the fact that the structure in the upper and lower terms is of the same order, resulting in a complex pattern which is quite impossible to resolve. Such lines are recorded as complex.

In all cases except λ 4775·2, the intensities and intervals degrade together to the violet. With this line the intensities are in the ratio 1 : 1·5 : 1 (visual estimate) and further there is no resemblance to a degraded series. The two infra-red lines λ 7513·0 and λ 7348·6 were taken on Kodak extreme red sensitive plates. With a 10-mm. gap, the line λ 7513·0 showed a degraded series, but the last component was too strong. By using 17·5 mm. and a small stop before the first plate of the interferometer, this last component was found to be double, so that the line has five components although $I = \frac{1}{2}$. This will be completely explained later. λ 5466·2 is a sharp doublet, intensities 3 : 2, the violet component being stronger.

This line is very doubtful since it was very weak and only appeared on one plate. In addition there is a line close to it. If it is genuine then the interval factor deduced from it is abnormally large. Since there is reason to doubt the structure recorded, it will be neglected in the calculations.

Analysis of Structures.

The lines coming to a common level are grouped together in Table III, the intervals between adjacent components being given. It is seen that lines coming to the same lower *s* term have generally quite different structures, due to the fact that the interval factors for the upper levels are appreciable. The four lines $5s\,.\,{}^4P_{\frac{5}{2}}-5p\,.\,{}^2D_{\frac{5}{2}}$, $5s\,.\,{}^4P_{\frac{5}{2}}-5p\,.\,{}^4S_{\frac{3}{2}}$, $5s\,.\,{}^4P_{\frac{5}{2}}-5p\,.\,{}^2P_{\frac{3}{2}}$, $5s\,.\,{}^4P_{\frac{5}{2}}-5p\,.\,{}^2D_{\frac{3}{2}}$, are completely resolved and show only a quartet structure, the structures being so similar as to have originated obviously in the $5s\,.\,{}^4P_{\frac{5}{2}}$ term. This is in accordance with theoretical predictions, since only in this term, amongst those involved, is there an unpaired *s* electron. These four structures can all be fitted almost perfectly into their respective graphs in fig. 2 if I is taken as $\frac{3}{2}$ and for no other value. Also since the lower term has a J value of $\frac{5}{2}$ the quartet can only arise out of an $I = \frac{3}{2}$, this value also being borne out by the interval ratios in the structures. The differences in the

Tolansky. *Proc. Roy. Soc.*, *A*, *vol.* 136, *Pl.* 10.

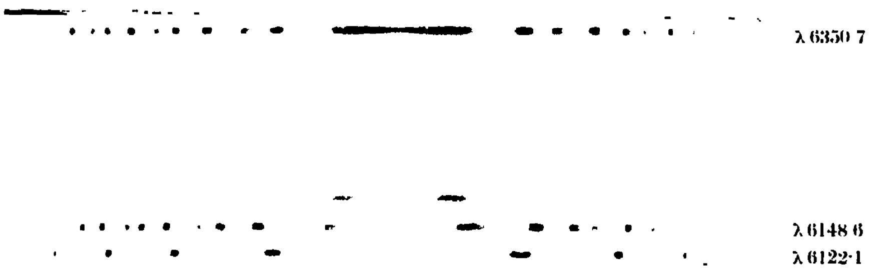

A. Fabry-Perot fringes in Bromine. Plate separation 9·5 mm.

B. - Fabry-Perot fringes of λ 6122 ($5p\,^4D_{7/2} - 5d\,^4F_{9/2}$) Plate separation 50 mm.

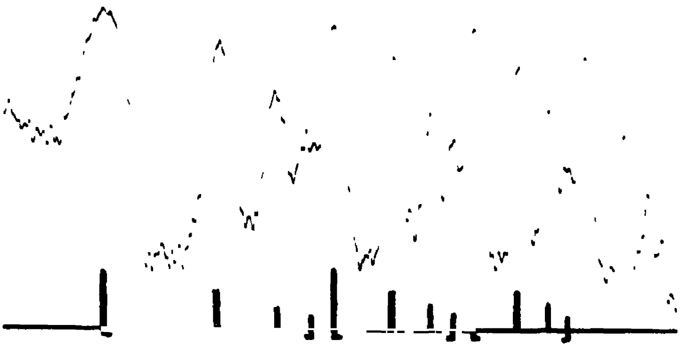

C.—Microphotometer trace of Fabry-Perot fringes of λ 6350·7 (Br.), 9·5 mm. gap.

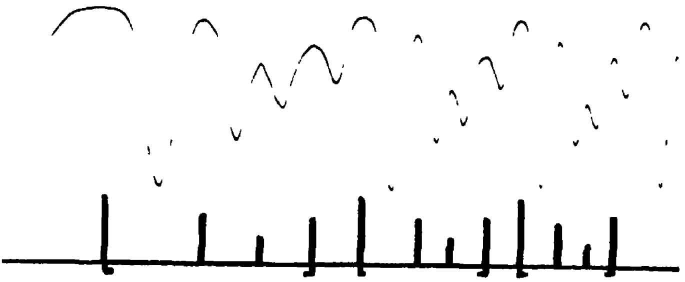

D.—Microphotometer trace of Fabry-Perot fringes of λ 7513·0 (Br.), 17·5 mm. gap.

(*Facing p.* 593.)

Table III.—Structures of Bromine Lines involving Common Levels.

Lower term.	Upper terms.							
$5s\,.\,{}^4P_{5/2}$	$5p\,.\,{}^2P_{3/2}$	$5p\,.\,{}^2D_{5/2}$	$5p\,.\,{}^2D_{3/2}$	$5p\,.\,{}^4S_{3/2}$	$5p\,.\,{}^4D_{7/2}$	$6p\,.\,{}^4P_{5/2}$	$6p\,.\,{}^4P_{3/2}$	$6p\,.\,{}^4D_{7/2}$.
	205	194	196	199	83	53	99	79
	144	130	134	137	64	↓	↓	↓
	93	93	72	81	58	116	99	58
					· 23			
Total . .	442	417	402	417	228	169	198	137
$5s\,.\,{}^4P_{3/2}$	$5p\,.\,{}^2D_{5/2}$	$6p\,.\,{}^4D_{1/2}$	$6p\,.\,{}^4D_{3/2}$	$6p\,.\,{}^4D_{5/2}$				
	54	103	118	56				
	↓	↓	↓	↓				
	49	62	75	62				
Total . . .	103	165	193	118				
$5s\,.\,{}^2P_{3/2}$	$6p\,.\,{}^2D_{5/2}$	$6p\,.\,{}^2D_{3/2}$						
	100	89						
	↓	↓						
	60	53						
Total ...	160	142						
$5s\,.\,{}^2P_{1/2}$	$5p\,.\,{}^2P_{1/2}$ $({}^1S)$							
	76							
	87							
Total	163							
$5s\,.\,{}^4P_{1/2}$	$6p\,.\,{}^2S_{1/2}$ Single	$6p\,.\,{}^4S_{3/2}$. Single						
$5p\,.\,{}^4P_{1/2}$	$5d\,.\,{}^4D_{3/2}$ Single	$5d\,.\,{}^4D_{1/2}$. Single						

appearance of the lines arise from the different J values and different interval factors in the upper terms, and since the graphs are only fitted at one position, the absolute values of the interval factors of both upper and lower terms can be calculated. The above four lines all fit their respective curves close to the zero line resulting in quartets degrading to the violet. Two of these lines are shown in Plate 10, the microphotometer record of one of them also being shown. The line λ 6350·7 has the sharpest components and actually fits its graph very close to the zero line. It will be observed that the lines are not to be expected to be identical as was assumed by de Bruin from Hori's measurements, and that, further, the interval rule should only hold closely in the line with upper interval factor small. This is shown by the consideration of the folowing two cases, the calculated interval factor being :—

A	....	51	48	47	$(5s\,.\,{}^4P_{5/2}—5p\,.\,{}^2P_{3/2})$
B	....	49	44	36	$(5s\,.\,{}^4P_{3/2}—5p\,.\,{}^2D_{5/2})$

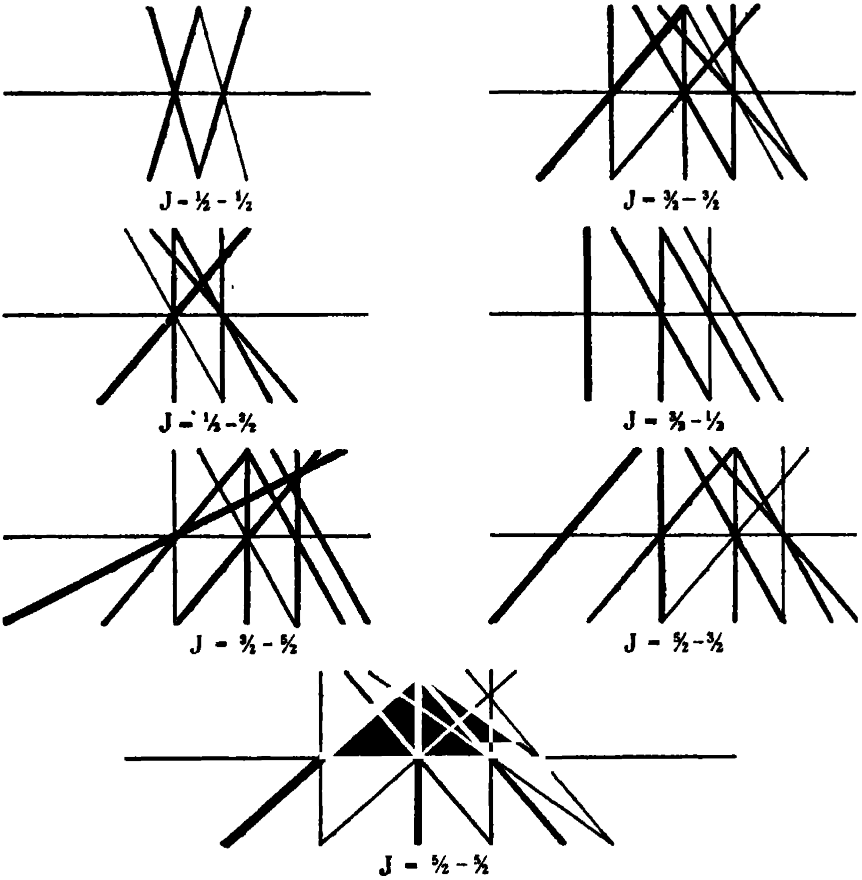

J = ½ - ½ J = 3/2 - 3/2

J = ½ - 3/2 J = 3/2 - ½

J = 3/2 - 5/2 J = 5/2 - 3/2

J = 5/2 - 5/2

FIG. 2.—Fine Structure Line Complexes in Bromine.

In A the interval factor in the line itself is nearly constant, and in this case the ratio of lower to upper term interval factor is 12 : 1. In B the term interval ratio is 5 : 1 and the deviations are apparent.

There seems little reason to doubt the allocation of the lines involving the $5s\,.\,{}^4P_{5/2}$ level, since they are the strongest lines in the spectrum and their gross structure differences are very exact. The fact that the structures involving this term vary from 137 to 442 units, can be completely accounted for by the graphical method. Of particular interest is the line λ 7513·0, since it shows five components, thus appearing to violate the conclusion that $I = 3/2$. However, the structure is altogether different from that of the four previously mentioned lines Firstly, with smaller resolution four components are seen, but the fourth is far too strong. This is shown very well in Plate 10. This record, which is that of the line as observed with a plate separation of 17·5 mm., can be compared with that of λ 6350·7 at 9·5 mm., from which it is seen that the structure is also on a much smaller scale although involving the same *s* term. It is found that this structure fits its graph almost exactly at the point corresponding to a ratio of lower to upper interval factors of 5 : 4, the observed and calculated separations together with the theoretical intensities of the five resulting components at this ratio being :—

Intervals	Observed	0	83	147	205	228
	Calculated	0	82	148	204	230
Intensities—Calculated		360	224	126	116	124

Since with lower resolution the last two components are not resolved the intensities will be 360, 224, 126, 240, that is, the last component is much stronger than the third. If there were no separation of these last two, then the compound one would be stronger even than the second, but since there is a partial resolution on the photometer trace resulting in a broadening, then this effectively lowers the intensity somewhat, and it is seen to be actually less than the second, although much stronger than the third. The appearance of five components is thus completely accounted for both qualitatively and quantitatively, the I value of $\frac{5}{2}$ remaining good.

It is possible to calculate the interval factors of all the terms involving the lines which have been measured. In all cases there is much greater uncertainty in determining the small upper value than the large lower value. Thus the factors are classed into three groups, A, those which are expected to be reliable, B, reasonably reliable but mostly calculated as small upper term values, C, which are definitely doubtful as regards numerical value but give an indication of the order. The values are all positive and are given in Table IV in thousandths of a wave-number.

The results show that all the terms involving an unpaired *s* electron, except $5s\,.\,{}^4P_{\frac{1}{2}}$ which will be discussed later, have large interval factors as predicted. Of the remaining 19*p* terms, 14 are small and a number of interesting comparisons may be made between the 5*p* and 6*p* terms. It is seen from Table II that only two lines involving a lower *p* level, namely, the two faint lines $5p\,.\,{}^4P_{\frac{5}{2}}-4d\,.\,{}^4D_{\frac{7}{2}}$ and $5p\,.\,{}^4P_{\frac{3}{2}}-4d\,.\,{}^4D_{\frac{5}{2}}$ show any visible structure.

Comparison will now be made with the *s* electron structures predicted by the method of White and Ritschl, fig. 1. Both (LS) and (JJ) coupling require

Table IV.—Term Interval Factors in Bromine.

	Term.	Interval factor.	Class.	
5s.	$^2P_{1/2}$	43	A	
	$^2P_{3/2}$	35	A	
	$^4P_{1/2}$	Small	A	
	$^4P_{3/2}$	42	A	
	$^4P_{5/2}$	55	A	
5p.	$^2P_{3/2}$	7	B	
	$^4P_{3/2}$	12	C	
	$^4P_{1/2}$	Small	B	
	$^2D_{5/2}$	11	B	
	$^2D_{3/2}$	11	B	(= 16 C)
	$^4S_{3/2}$	11	B	
	$^4D_{7/2}$	44	B	
	$^4D_{1/2}$	Small	B	
	$^4D_{5/2}$	Small	B	
6p.	$^2P_{1/2}$	2	C	
	$^4P_{5/2}$	55	C	
	$^4P_{1/2}$	28	C	
	$^2D_{3/2}$	4	C	
	$^4D_{5/2}$	22	C	
	$^4D_{3/2}$	15	C	
	$^2S_{1/2}$	Small	C	
	$^4S_{1/2}$	Small	C	
5d.	$^4D_{5/2}$	Small	B	
	$^4D_{7/2}$	Small	B	

that the $^4P_{5/2}$ term should be normal, and have the widest of all the structures, and this is actually observed, the interval factor being taken as the criterion. The $^4P_{3/2}$ term is as predicted, somewhat less, and as it is normal, a tendency to (LS) coupling is indicated. However, the $^4P_{1/2}$ term is of interest since it quite definitely shows no signs of structure. It is seen that (LS) coupling produces a wide normal doublet, and (JJ) coupling a wide inverted doublet. There is a great deal of evidence from the gross structure analysis, that there is a change from (LS) type to (JJ) type coupling in the halogens proceeding from the lightest to the heaviest. Hence an intermediate coupling exists for bromine and this may account for the structure of the *5s*. $^4P_{1/2}$ term which, lying as it does between a wide normal, and a wide inverted doublet, will be expected to be very small. The *5s*. $^2P_{1/2}$ level is wide and normal, indicating a (JJ) tendency, the *5s*. $^2P_{3/2}$ term is wide and normal, also indicative of a (JJ) coupling tendency. Hence it may be concluded that, on the whole, if the coupling is considered as intermediate but biassed towards JJ type, that the predictions for the *5s* terms are fitted fairly reasonably by the observations.

As regards *p* electron terms, the first point of interest is that in some cases the structures are as wide as those in the *s* electron terms, due to the coupling of the *p* electrons all being additive. There is no experimental evidence of inverted terms, although the detection of these is difficult when occurring as small upper term factors of the B and C class. There is no general agreement with the (LS) predictions, and the (JJ) predictions are often indeterminate. Further, the experimental data are not very convincing in a number of cases. It may therefore be concluded that the vector method of prediction is sound when applied to an *s* electron, but no safe conclusion as to its applicability to *p* electrons can be drawn. Certain points of comparison between similar terms arising respectively from 5*p* and 6*p* electrons may be noted. In $^2P_{\frac{1}{2}}$ and in $^2D_{\frac{5}{2}}$ the interval factor is small for the 5*p* term decreasing for the 6*p*. The factor for 5*p* . $^4P_{\frac{3}{2}}$ is 12 C, but for 6*p* . $^4P_{\frac{1}{2}}$ it is 55 C (a high value for the latter is certain since another line involving this term is recorded as complex). There is thus an increase in going from 5*p* to 6*p*. The same is true for the $^4P_{\frac{5}{2}}$ and $^4D_{\frac{5}{2}}$ terms. Finally the term 5*p* . $^4D_{\frac{3}{2}}$ has a very large factor, whilst 6*p* . $^4D_{\frac{3}{2}}$ is involved in a complex line, also therefore having a large factor. No general rule as to behaviour with increasing current quantum number can therefore be deduced.

Isotope Effect.

A number of independent isotope effects have been observed in hyperfine structure. The first observed was a simple mass effect. Due to the varying masses of the different isotopes, the Rydberg constants of the series produced differ slightly, resulting in a small bodily displacement of the structures of one isotope relative to the other, the intensities of the respective structures, otherwise identical, being proportional to the abundance ratios of the isotopes. This effect was first definitely observed in neon by Hansen,* being verified later by Nagaoka and Mishima,† and by Thomas and Evans.‡ The latter observed that the displacements were a little greater than those required by the simple Bohr theory, but of the same order, and were in addition constant for the lines in a series. The intensity ratio was also found to be of the right order.

The second type was that first observed by Schüler and Brück in cadmium.§ This arises from the fact that in a mixed group of isotopes, those with even atomic weight have zero nuclear spin. Hence the odd isotopes form a fine structure multiplet—the mass displacement is generally much too small to be observed—and at the optical centre of gravity of the multiplet lies an undisplaced single line arising from all the even isotopes. This type of isotope effect has been verified in a number of cases.

---

* 'Naturwiss.,' vol. 15, p. 163 (1927).

† 'Sci. Pap. Inst. Phys. Chem. Res. Tokyo,' vol. 13, p. 293 (1930).

‡ 'Phil. Mag.,' vol. 60, p. 128 (1930).

§ 'Z. Physik,' vol. 55, p. 575 (1929).

The third type was observed by Schüler and Keyston* in thallium and in mercury. In some terms in thallium there is both a large displacement of isotope lines, far greater than the calculated mass effect, and also a slight alteration of the scale of the structures. Schüler and Keyston consider that the effect is due to a variation of nuclear electric field, being quite independent of nuclear magnetic moment. In addition to this effect, mercury shows a further complication, in that the even isotopes each contribute a line to the structure, each line being displaced.

Bromine is very suitable for examination for isotope effect, since there are only two isotopes of equal abundances, masses 79 and 81. The only line which shows any effect is λ 6122·1 since it is strong, very narrow and in a very good region for a silvered interferometer. The line does not show its true structure even with such large plate separations as 50 mm., see Plate 10, remaining quite single. The allocation is $5p\,.\,{}^4D_{7/2}$—$5d\,.\,{}^4F_{9/2}$, so that there are nine components to the line and as the F values are large, the interval factors must be very small indeed. It is of interest that a graph shows that if the interval factors are of the same order, the resulting pattern is a single strong line with wings on either side, as observed. By using a small stop before the first plate of the interferometer and a plate separation of 100 mm. the line was resolved. At this plate separation the line is broad, due to the fact that the true structure is beginning to show. However, it can be just clearly resolved into two patches of equal intensity, the separation being $0\cdot007 \pm 0\cdot003$ cm.$^{-1}$. The Rydberg mass displacement, when calculated from the simple Bohr theory is $0\cdot0036$ cm.$^{-1}$. The discrepancy is not necessarily significant when the extreme difficulty of the observation is considered. Since the structure is absolutely different from that expected if there were no isotope effect, and as it is a doublet of equal intensity, the isotope abundance ratio being known to be unity, it may be concluded with certainty that the observed effect is the simple mass isotope displacement. That this displacement is small was previously inferred from the sharpness of the components of some of the lines observed. There is no evidence of any other isotope effect. It is therefore obvious that the two bromine isotopes have the same nuclear spin, namely $\frac{3}{2}$.

---

* 'Z. Physik,' vol. 70, p. 1 (1931); 'Naturwiss.,' vol. 19, p. 676 (1931).

IODINE.

Experimental Procedure.

As previously stated, no fine structures have been observed by other workers in the arc lines of iodine, due presumably to the difficulty of securing a suitable source and to the employment of insufficient resolving power. The same form of discharge was employed as for bromine, and as a source a simple tube 25 cm. long and 2·5 cm. bore. After careful evacuation pure iodine was distilled into the tube which was then sealed off from the pump. The discharge drove iodine into the walls making them opaque, but the window was kept clear by using a " cap " electrode as previously employed with mercury.* At room temperature the tube emitted a mixture of iodine bands and arc lines, and since the temperature of the tube when running was about 40° C. the iodine distilled to the projecting, sealed end which was cooler. Since the electrodes were somewhat hotter than the rest of the tube, the temperature of the cold end, and so the vapour pressure in the tube, could be conveniently controlled by moving an electrode near to it. This control was found to be very critical and when the vapour pressure was about 0·2 mm. strong arc lines appeared, spark lines developing when the pressure was raised. The tube was always adjusted for arc lines only. The same interferometer, etc., was employed as for bromine, similar exposure times being used. The region observed was λ 8000–λ 4700.

Experimental Observations.

Measurements were carried out on 16 lines of the arc spectrum. These are mostly quartets and sextets forming series which degrade to the violet, being very similar in nature to the bromine structures. One line is a doublet, and the rest are quite single with diffuse tails degrading to the red, the doublet line also degrading to the red. The lines are altogether much broader and much more difficult to measure than those of bromine, although there is only one isotope, and the Doppler width is less. The graphical method of analysis shows that this effect is produced when the I value is large, for then the off diagonal components are of a similar order of intensity to the main diagonal lines, with the result that the lines are effectively broadened even when the ratio of lower to upper interval factor is fairly large. A partial analysis of the gross multiplet structure of the iodine arc spectrum has been made by S. F. Evans,† and the line allocations given by him will be employed. The lower *s* electron terms are well established, but only the J values are known for most of the *p* electron terms. The gross structure is very similar to that of the other halogens, only there is the indication that the coupling is more nearly (JJ) type. The list of observed structures is given in Table V. All the lines, except those marked as single, and λ 5119·3, are series degrading to the violet. Three lines are given as sextets although only five components could be resolved. In these cases, however, the fifth tail-end component was obviously too broad and therefore considered as double. Bigger plate separations to achieve resolution could not be used owing to the overlapping of orders. The same accuracy classification is used as for bromine.

---

* 'Proc. Roy. Soc.,' A, vol. 130, p. 558 (1931).

† 'Proc. Roy. Soc.,' A, vol. 133, p. 417 (1931).

Table V.—Fine Structures in the Iodine Arc Lines.

Allocation.	Wave-length.	Class.	Structure.	Width.
$6s\,.\,{}^4P_{5/2}$ -- $6p\,.\,b_{3/2}$†	8043·7*	B	0 105 213 300 380 426	426
$6p\,.\,6 - 5d\,.\,3$	7469·0	A	Single	
$6p\,.\,6 - 5d\,.\,5$	7402·1	A	Single	
$6p\,.\,4 - 5d\,.\,9$	6619·7	A	Single	
$6p\,.\,1 - 5d\,.\,6$	6213·2	A	Single	
$6p\,.\,1 - 5d\,.\,7$	6192·0	A	Single	
$6s\,.\,{}^4P_{3/2} - 7p\,.\,h_{5/2}$	6082·5*	B	0 88 170 230	230
$6s\,.\,{}^4P_{5/2} - 7p\,.\,g_{3/2}$	5894·1*	B	0 60 116 159	159
$6s\,.\,{}^4P_{5/2} - 7p\,.\,i_{3/2}$	5764·4*	B	0 213 404 571 ⟶ 671	671
$6s\,.\,{}^4P_{5/2} - 7p\,.\,h_{7/2}$	5586·7*	B	0 250 485 635 ⟶ 845	845
$6s\,.\,{}^4P_{5/2} - 7p\,.\,g_{7/2}$	5427·1*	B	0 213 409 565 ⟶ 676	676
$6s\,.\,{}^4P_{1/2} - 7p\,.\,b_{3/2}$	5119·3	A	0 116	116
$6s\,.\,{}^4P_{5/2} - 7p\,.\,{}^4D_{7/2}$	4917·0*	B	0 119 212 297 372 433	433
$6s\,.\,{}^4P_{5/2} - 7p\,.\,e_{3/2}$	4896·8*	C	0 85 183 ⟶ 310	310
$6s\,.\,{}^4P_{3/2} - 7p\,.\,a_{5/2}$	4862·4*	A	0 123 226 309	309
$6s\,.\,{}^4P_{5/2} - 7p\,.\,b_{5/2}$	4763·4*	C	0 100 208 303 371 440	440

† Doubtful. Faint, structure uncertain.

Analysis of Structures.

The lines coming to the same levels are arranged in Table VI, frequency differences being given. As in the case of bromine, these are not identical, the reason being the same. The lines involving the $6s\,.\,{}^4P_{5/2}$ term are all sextets, hence I must be at least equal to $\frac{5}{2}$ since the multiplicity is determined by 2I + 1 or 2J + 1 according to which is the smaller. Structure only appears in lines involving an unpaired *s* electron term. Two factors indicate that I should have a high value, firstly, the width of the components; secondly, the complete absence of any visible alternating intensities in the rotation lines of the I_2 band spectrum. After various values had been tried, the structures were found to fit an I value of $\frac{5}{2}$ quite well. The sharpest line is the quartet

Table VI.—Fine Structures of Iodine Lines involving Common Levels.

Lower term.	Upper terms.						
	$6p.b_{5/2}$	$7p\ ^4D_{7/2}$	$7p.b_{5/2}$	$7p.e_{3/2}$	$7p.g_{5/2}$	$7p.h_{7/2}$	$7p.i_{7/2}$.
$6s.^4P_{5/2}$	105 108 87 80 46	119 93 85 75 61	100 108 95 68 69	85 98 – ↓ 127	213 204 156 ↓ 112	250 235 150 ↓ 210	213 191 167 ↓ 100
Total	426	433	410	310	670	845	671
	$7p.a_{1/2}$	$7p.b_{1/2}$	$7p.g_{5/2}$	$7p.h_{3/2}$.			
$6s.^4P_{3/2}$	123 103 83	116	60 56 43	88 82 60			
Total . ..	309	116	159	230			
$6p.6$	$5d.3$. Single	$5d.5$. Single					
$6p.1$	$5d.6$. Single	$5d.7$. Single					

$6s.^4P_{3/2}—7p.a_{1/2}$, the sharpness indicating a very large ratio of lower to upper interval factor. The intervals in this particular case are 123, 103, 83, *i.e.*, 6 × 20·5, 5 × 20·6, 4 × 20·7 being thus in the exact ratio 6 : 5 : 4, and since the structures obviously come from the *s* term with J value $\frac{3}{2}$ it follows that to fit these intervals I must be $\frac{5}{2}$. Graphs were therefore constructed with this value for I and the rest of the structures were found to fit these graphs extremely well. The following two examples shown below illustrate the extent of agreement in the best cases :—

Line.			Intervals.		
$6s.^4P_{3/2}—7p.h_{3/2}$	Calculated ..	0	90	169	228
	Observed ..	0	88	170	230
$6s.^4P_{3/2}—7p.h_{5/2}$	Calculated ..	0	60	115	165
	Observed ..	0	60	116	159

Resolution was not completely achieved with the tail end of the second line, therefore the last interval is a little less than the calculated value. The other lines mostly fit their graphs almost as well, so that the $\frac{5}{2}$ is a reasonably justified value. It is of interest that an interval factor ratio of 10 : 7 for λ 5119·3 results in a doublet, the violet component being about twice as strong as the red, the calculated interval being about 120. The observed interval is 116, the intensities are those required by the graph.

The two lines involving the $6p$. 6 term as the lower level, are both single and of about the same width, whilst the two lines coming to the $6p$. 1 term, although also single are both broader, indicating that the $6p$. 6 term is narrower than the $6p$. 1 term, both being small however. All the lines involving $5d$ electron configuration terms show no structure at all.

The calculated interval factors are shown in Table VII. Three of these have each been deduced from two lines, so that two columns are given and the best mean taken. The value of 27·0 for $7p$. $b_{3/2}$ is unreliable since the line from which it is calculated lies within the strong iodine continuous band, and, further, the region is also not very suitable. There is satisfactory agreement between the different values calculated for both $7p$. $g_{3/2}$ and $7p$. $h_{5/2}$. Since L values are unknown little can be deduced, except that the $7p$ terms seem to show wider structures than the $6p$ terms, but the evidence is not conclusive. It is interesting to note that, as in bromine, the interval factors for some p terms are quite as large as those of s terms. In agreement with the predictions of the method of White and Ritschl the $5s$. $^4P_{3/2}$ term is wider than the $5s$. $^4P_{5/2}$ term, the actual ratio being 1·9 : 1.

Table VII.—Term Interval Factors in Iodine.

Term.	Interval factor.	Class.	Interval factor.	Class.	Best mean.	Class.
$5s$. $^4P_{5/2}$	20·5	A	—	—	20·5	A
$5s$. $^4P_{3/2}$	39·5	A	—	—	39·5	A
$6p$. $b_{3/2}$	29†	B	—	—	29	B
$6p$. 1	Small	B	—	—	Small	B
$6p$. 6	Small	A	—	—	Small	A
$6p$. 4	Small	B	—	—	Small	B
$7p$. $a_{1/2}$	Small	B	—	—	Small	B
$7p$. $b_{3/2}$	27	C	16	B	20	C
$7p$. $e_{1/2}$	32	C	—	—	32	C
$7p$. $g_{3/2}$	10	B	14	B	12	B
$7p$. $h_{5/2}$	4·1	B	4·0	B	4·0	B
$7p$. $i_{3/2}$	14	B	—	—	14	B
$7p$. $^4D_{1/2}$	28	C	—	—	28	C
$5d$. 3, 5, 6, 7, 9	Small	B	—	—	Small	B

† Uncertain.

Comparison of the Halogens.

The experimental observations for iodine are not as reliable as those for bromine, largely due to the high I value which causes an effective broadening of the lines. In general the interval factors in bromine appear to be on a larger scale than those in iodine, particularly for the *s* electron terms. The type of structure is very similar in both, generally wide in *s* electron terms, occasionally wide in *p* electron terms and apparently narrow in the case of *d* electrons.

A comparison of the most probable values of the nuclear spins of all the halogens is given below :—

Halogen :	Fluorine.	Chlorine.	Bromine.	Iodine.
Protons	19	35, 37, 39	79, 81	127
Spin	$\frac{1}{2}$	$\frac{5}{2}$ — —	$\frac{3}{2}$ $\frac{3}{2}$	$\frac{9}{2}$

The value for fluorine was obtained by Gale and Monk* from the band spectrum of F_2, the value appearing to be very reliable. The spin for Cl_{35} is the result of extensive intensity measurements carried out on the Cl_{35-35} absorption bands by Elliot,† who was unable to measure the Cl_{37-37} bands owing to their faintness. In bromine both the isotopes have the same spin of $\frac{3}{2}$. The value given for iodine is fairly reliable, but for such a large value confirmatory evidence by Zeeman effect observations are desirable. Support for the high value is given by Mulliken,‡ who states that $I > \frac{5}{2}$. No apparent regularity exists in the table, the only point of interest, which may easily be accidental, is that the large and small spin values are both associated with single isotopes. All the atomic weights are odd and all the spins half integral, so that it is easy to arrange a table such as that given below, which may have very little significance, if any at all. Since, however, Barton§ successfully predicts the spins of a number of lighter elements by this means, the table is included.

Halogen :	F.	Cl.	Br.		I.
Protons	19	35	79	81	127
α-particles	4	7	19	19	29
Paired protons	2	2	—	2	2
Spin protons	1	5	3	3	9

---

* 'Astrophys. J.,' vol. 69, p. 77 (1929).

† 'Proc. Roy. Soc.,' A, vol. 127, p. 638 (1930).

‡ 'Trans. Faraday Soc.,' vol. 25, p. 634 (1929).

§ 'Phys. Rev.,' vol. 37, p. 326 (1931).

Attention may be directed to the nuclear spin of chlorine. Elliot's observations on the Cl_{35-35} bands make it quite certain that the Cl_{35} atom possesses a nuclear spin. The author* has examined lines involving *s* terms in the Cl^+ spectrum, with a hollow cathode tube cooled in liquid air. No trace of a nuclear spin fine structure was observed, but the lines due to the isotopes 35 and 37 were displaced by an amount about twice that calculated from the simple Bohr theory. It was concluded that the absence of fine structure could only be explained by assuming that the $g(I)$ factor, and therefore the magnetic coupling, is small. The author has since obtained evidence that the $g(I)$ factors of the atoms 27, 31, 35, 37 and 39 are all very small. This is an indication that the magnetic coupling in the nucleus may possibly be compounded of proton spin and something akin to orbital motion. If these two processes oppose then the resultant $g(I)$ factor will be small. Full details of this are being published elsewhere.†

The hyperfine structure of a number of the arc lines of the bromine and iodine spectra are recorded as a source of high frequency, electrodeless discharge in the pure vapours was employed, and a Fabry-Perot interferometer used to observe the lines. Twenty-nine bromine lines and sixteen iodine lines were examined. In most cases the structures were not completely resolved, and a graphical method was used to analyse them. The nuclear spin found for bromine is $\frac{3}{2}$, both the isotopes having the same spin. A simple mass isotope displacement was observed in bromine of the same order as that calculated. The nuclear spin determined for iodine is $\frac{9}{2}$. The fine structure interval factors for 24 terms in bromine and 17 terms in iodine have been calculated, although the approximate order only is known in about one-third of these. There is evidence that the simple cosine method for predicting fine structures works reasonably well with *s* electron terms, but no conclusions can be drawn about *p* terms. A table of nuclear spins for all the halogens is given.

I wish to express my deepest thanks to Professor W. E. Curtis, of Armstrong College, for his kind help and constant advice during the progress of this work, and for the very full experimental facilities granted me. I also wish to record my appreciation of the discussions held with Mr. S. F. Evans, and for the use of his then unpublished data on iodine.

---

* 'Z. Physik,' vol. 73, p. 470 (1931).

† 'Z. Physik,' vol. 74 (1932).

The Anomalous Scattering of α-Particles by Hydrogen and Helium.[*]

By H. M. Taylor, Clare College, Cambridge.

(Communicated by R. H. Fowler, F.R.S.—Received February 12, 1932.)

§ 1. In a previous paper,[†] the author has shown that the anomalous scattering of α-particles in helium can be accounted for, if one postulates the validity of the wave mechanics to describe the phenomenon, and assumes a simple spherically symmetrical form for the field between the two colliding particles. The solutions obtained were exact, no approximate methods being used, but only the scattering at large angles, 34° and 45°, was considered. The purpose of this paper is threefold. Firstly, these results are extended to the case of the scattering of α-particles by hydrogen, and good agreement with experiment is obtained. Secondly, it is shown that the scattering at small angles both in hydrogen and in helium can be explained by the *same* field as is used to explain the scattering at large angles. It is therefore no longer necessary to assume a "plate-like" form for the α-particle, in order to explain the scattering at small angles, as formerly according to the classical mechanics. Thirdly, a discussion is given of the extent to which the explanation here advanced for the experimental results is dependent on the particular form assumed for the potential energy of the one particle in the field of the other. It is found that, provided we assume that the potential energy, V (r), is Coulombian for distances greater than about 5×10^{-13} cm., then *whatever the form of the potential for smaller distances*, the ratio, R, of the scattering to that to be expected from a purely Coulombian field is given by the formula

$$\mathrm{R} = | e^{-i/ak \,.\, \log \cos^2 \chi} + iak \cos^2 \chi \, (e^{2i\mathrm{K}_0} - 1) |^2,$$

where the scattering is in hydrogen, χ is the angle of scattering,[‡] and $ak = hv/4\pi\varepsilon^2$. A similar formula is found for the scattering in helium. The formula contains only one parameter, K_0, which depends on the velocity of the incident α-particles, v, and also on the field assumed, but is independent of the angle of scattering, χ. Thus we may determine K_0 from the observed scattering for a given value of v and of χ, and deduce the scattering at other angles for the same value of the velocity. The agreement obtained with experiment is then quite independent of any special choice of a potential energy function. In order to calculate K_0 and its variation with v, we should have to assume a particular form for V (r). Conversely, from the values of K_0 determined by the experimental values of R, we may calculate V (r) as in the previous paper for the case of two α-particles.

---

[*] A preliminary notice of part of this work appeared in 'Nature,' vol. 129, p. 56 (1932).

[†] Taylor, 'Proc. Roy. Soc.,' A, vol. 134, p. 103 (1931).

[‡] See the precise definition of χ at the beginning of § 2.

§ 2. *The Scattering Formula for Hydrogen.*—In the experiments[†] on the scattering by hydrogen, it is found convenient to count the scintillations due to the hydrogen nuclei projected forward by the collision rather than those due to the deflected α-particles themselves, and therefore in this portion of the paper we shall denote by R the ratio of the number of protons found experimentally to be projected in a given direction, to the number predicted by the Rutherford law. The fact that R refers to the particles struck on from rest makes a considerable simplification in the collision relations, for if we consider the collision of two particles of mass m_1 and m_2, of which m_1 is initially at rest, and if we denote by χ the angle made by the final direction of motion of this particle with the incident direction of m_2, and by θ the angle through which either particle is deflected, measured in a frame of reference moving with the velocity of the centre of gravity of the two particles, then

$$\chi = \tfrac{1}{2}(\pi - \theta), \tag{1}$$

independently of the ratio m_1/m_2. The relation between the angle θ and the angle ϕ, through which the incident particle m_2 is deflected, is on the other hand dependent on the relative masses of the particles.

On the wave theory, as on the classical theory, the problem of the collision of two interacting particles can be reduced to the problem of the collision between a single particle and a fixed field of force (Taylor, *loc. cit.* p. 105). Let v be the velocity of the incident α-particle, and V (r) the potential energy of the two colliding particles when at a distance r apart. We wish to calculate the ratio R of the number of protons knocked on in the direction making an angle χ with the direction of the incident α-particles, to the number to be expected with a Coulombian interaction potential. The one-body problem to which this may be reduced is the following. A particle of mass M^*, where

$$M^* = m_1 m_2/(m_1 + m_2),$$

moving with velocity v, collides with a field of force whose potential is V (r). The ratio R above is equal to the ratio of the two probabilities that this particle will be scattered through an angle θ, first when V (r) is non-Coulombian and second when it is Coulombian. The angle θ is, of course, related to the angle χ by the equation (1).

[†] Chadwick and Bieler, 'Phil. Mag.,' vol. 42, p. 923 (1921).

To determine this ratio, we must solve the wave equation for this corresponding one-body problem,

$$\nabla^2\Psi + \frac{8\pi^2 M^*}{h^2}(E_r - V(r))\,\Psi = 0, \tag{2}$$

in which the energy E_r has the value $\frac{1}{2}M^* v^2$. We shall denote by Ψ^c that special solution of this equation which, for the ordinary Coulombian value of $V(r)$, namely, $V^c = ZZ'\varepsilon^2/r$, represents an incident plane wave of unit amplitude together with the corresponding scattered wave. Similarly by Ψ^s we shall denote that special solution which, for the value of V given by the equations (3) below, represents a unit incident wave and its corresponding scattered wave.

The scattered part of the wave function Ψ^c is well known to yield the ordinary Rutherford law,† and to account for anomalous scattering we assume an interaction energy of the type suggested by Gamow, namely

$$\left.\begin{array}{ll} V^s = f(r) & r < r_0 \\ V^s = ZZ'\varepsilon^2/r & r > r_0 \end{array}\right\}, \tag{3}$$

where the function $f(r)$ is at present left completely arbitrary. By analogy with the case of the interaction of two α-particles, we may, however, expect that r_0 will be a length somewhat less than 5×10^{-13} cm.

Now the general solution of the equation (2) which possesses axial symmetry may be written

$$\Psi = \sum_{n=0}^{\infty} A_n P_n(\cos\theta)\, L_n(r), \tag{4}$$

where the A_n are arbitrary constants, and the L_n are solutions of

$$\frac{d^2 L_n}{dr^2} + \frac{2}{r}\cdot\frac{dL_n}{dr} + \left\{\frac{8\pi^2 M^*}{h^2}(E_r - V) - \frac{n(n+1)}{r^2}\right\} L_n = 0. \tag{5}$$

We now denote by A_n^c and $L_n^c(r)$ the special values of A_n and $L_n(r)$ which yield the solution Ψ^c, and similarly by A_n^s and $L_n^s(r)$ those that yield the solution Ψ^s. In the equation (5) we must, of course, write V^c for V in order to obtain the equation of which $L_n^c(r)$ is a solution, and similarly V^s for V to obtain the equation of which $L_n^s(r)$ is a solution.

---

† *Cf.* Gordon, 'Z. Physik,' vol. 48, p. 180 (1928).

But Gordon (*loc. cit.*) has shown that

$$A_n^c = i^n/k\,.\,(2n+1)\exp(i\sigma_n)$$

and

$$L_n^c(r) \sim r^{-1}\cos\{kr-(n+1)\pi/2-1/ak\,.\,\log 2kr+\sigma_n\}, \tag{6}$$

where

$$k = 2\pi\,(2M^*E_r)^{\frac{1}{2}}/h = 2\pi M^* v/h,$$

$$1/a = 4\pi^2 M^* Z Z' \varepsilon^2/h^2,$$

and

$$\sigma_n = \arg\Gamma\,(i/ak+n+1).$$

Now in the region $r > r_0$, where V^s and V^c have the same value, L_n^s and L_n^c therefore both satisfy the same differential equation (5), and therefore differ only in being combinations in different proportions of the two independent solutions of this equation. Gordon shows that these two independent solutions have the asymptotic values

$$r^{-1}\exp\{\pm i\,(kr-(n+1)\pi/2-1/ak\,.\,\log 2kr+\sigma_n)\},$$

and therefore we obtain

$$L_n^s(r) \sim r^{-1}\cos\{kr-(n+1)\pi/2-1/ak\,.\,\log 2kr+\sigma_n+K_n\}, \tag{7}$$

where K_n is an arbitrary phase parameter, and where we have not introduced any arbitrary constant factor multiplying the cosine term, since the constant A_n^s is at present undetermined.

But the wave functions Ψ^s and Ψ^c both represent the same incident wave together with the appropriate scattered wave, and therefore their difference must represent a scattered wave only. This condition determines A_n^s, for it implies that $A_n^s L_n^s(r) - A_n^c L_n^c(r)$ is a function of e^{ikr} alone, which, on insertion of the values from (6) and (7), gives

$$A_n^s = A_n^c\exp(iK_n) = i^n/k\,.\,(2n+1)\exp\{i(K_n+\sigma_n)\} \tag{8}$$

Now when the de Broglie wave associated with a particle of mass M^* is scattered by a field of potential $V(xyz)$, each volume element $dx\,dy\,dz$ of the field scatters a wavelet, and the amplitude of this wavelet, measured at a distance R from the volume element, is†

$$\frac{2\pi M^*}{h^2}\,V(xyz)\,\psi(xyz)\,dx\,dy\,dz/R.$$

Further, the wave functions Ψ^s and Ψ^c differ only by the wave scattered by the potential field $V^s - V^c$, and this field is zero except in the region $r < r_0$. This enables us, with the help of a simple physical analogy, to infer that the difference $\Psi^s - \Psi^c$ should be a spherically symmetrical function. For, when a wave is scattered by an obstacle small compared with the wave-length, the scattered wave is well known to be spherically symmetrical. But the wave-length to be associated here with an α-particle incident with velocity v is h/M^*v, where M^* is one-fifth of the mass of an α-particle, and so the shortest wave-length used in practice (that for α-particles from RaC) is about 26×10^{-13} cm., whereas the region in which $V^s - V^c$ differs from zero is probably somewhat less in extent than 5×10^{-13} cm. Thus we should expect that, to a first approximation, $\Psi^s - \Psi^c$ should be spherically symmetrical. In terms of the phase parameter K_n, this means that only the first, namely K_0, should be different from zero, as may be seen by considering that, in the expansion of Ψ^s according to (4), only the term for which $n = 0$ must differ from the corresponding term in the expansion of Ψ^c.

---

† Mott, 'Proc. Roy. Soc.,' A, vol. 127, p. 658 (1930).

This physical argument may be put on a rigorous basis as follows.† The physical argument suggests that $L_n^s(r)$ should differ very little from $L_n^c(r)$ except for the one case when n is zero; we therefore proceed to evaluate $L_n^s(r)$ by a perturbation method. Let us write

$$y_c = rL_n^c(r) \quad , \quad y_s = rL_n^s(r)$$

and

$$y_s = y_c + f, \tag{9}$$

where f is the small quantity which we wish to evaluate. The differential equation (5) transforms into

$$y''_s + \frac{8\pi^2M^*}{h^2}\left\{E_r - V^s(r) - \frac{n(n+1)}{r^2}\right\} y_s = 0,$$

where dashes denote differentiation with respect to r. Substituting from the equation (9), we obtain

$$f'' + \frac{8\pi^2M^*}{h^2}\left\{E_r - V^c(r) - \frac{n(n+1)}{r^2}\right\} f = \frac{8\pi^2M^*}{h^2}\{V^s(r) - V^c(r)\}y_c, \tag{10}$$

in which we have neglected the product of the perturbation f and the perturbing potential $V^s - V^c$. If we now write $f = y_cZ$, the equation (10) yields

$$y_cZ'' + 2y_c'Z' = \frac{8\pi^2M^*}{h^2}\{V^s - V^c\}y_c,$$

or

$$\frac{d}{dr}(y_c^2Z') = \frac{8\pi^2M^*}{h^2}\{V^s - V^c\}y_c^2.$$

---

† This method was suggested to me by Mr. Mott.

Hence we obtain

$$y_c{}^2 Z' = \frac{8\pi^2 M^*}{h^2} \int_0^r \{V^s - V^c\} y_c{}^2 \, dr, \tag{11}$$

where the lower limit of the integral has the value zero in order that the right-hand side of the equation may vanish when r is zero, as is seen to be necessary since $y_c{}^2 Z'$ is zero when r is zero. But $V^s - V^c = 0$ for all values of r greater than r_0, and so in the equation (11) we may, in considering the left-hand side for large values of r, replace the upper limit of integration by r_0. Therefore, for large r,

$$y_c{}^2 Z' = \frac{8\pi^2 M^*}{h^2} \int_0^{r_0} \{V^s - V^c\} \, y_c{}^2 \, dr$$

$$= A_n. \tag{12}$$

In this equation let us substitute the asymptotic value for y_c from equation (6). We therefore obtain

$$Z' \sim \sec^2 (kr + \lambda) \, . \, A_n,$$

where λ denotes $\sigma_n - (n + 1)\pi/2 - 1/ak \, . \log 2kr$. Integrating this equation and neglecting the variation of the logarithmic term in λ, we obtain

$$Z \sim A_n/k \, . \tan (kr + \lambda) + \delta,$$

where δ is a constant. Thus

$$f \sim A_n/k \, . \sin (kr + \lambda) + \delta \cos (kr + \lambda)$$

and therefore

$$y_s \sim (1 + \delta) \cos (kr + \lambda) + A_n/k \, . \sin (kr + \lambda).$$

But y_s differs only slightly from y_c, and so both δ and A_n/k should be small, and the above equation can therefore be written

$$y_s \sim (1 + \delta) \cos (kr + \lambda - A_n/k),$$

which shows that we may identify $-A_n/k$ with our phase parameter K_n. We therefore may evaluate the parameters by this method and see whether they are in fact small.

To evaluate the integral of equation (12), we use the value of y_c given by Gordon (*loc. cit.*), namely,

$$y_c = kr \, . \, e^{-\pi/2ak} \frac{|\Gamma (n + 1 + i/ak)|}{(2n + 1)\,!} (2kr)^n \, e^{ikr} \, F\, (i/ak + n + 1, \, 2n + 2, \, -2ikr),$$

and we find that in the region $r < 5 \times 10^{-13}$ cm., the function

$$e^{ikr} \, F\, (i/ak + n + 1, \, 2n + 2, \, - 2ikr)$$

is adequately represented by the first two terms of its expansion as a power series. By analogy with the case of two α-particles discussed in the author's previous paper, we may expect that V^s will not attain negative values much greater than -10^7 electron volts, and that, for values of r greater than 5×10^{-13} cm., V^s will have the ordinary Coulombian value V^c. Let us therefore, in (12), choose for V^s the constant value -2×10^7 electron volts, and for r_0 the value 5×10^{-13} cm. Then *any* field which differs from the Coulombian field only in the region $r < 5 \times 10^{-13}$ cm. and which does not reach potentials lower than -20×10^6 electron volts will yield smaller values of K_n than we calculate with this field. Taking the value of k corresponding to the α-particles from RaC, we obtain for K_1 the value 0·05, and K_2 is roughly 100 times smaller. The corresponding value for K_0 is about 0·7, but, of course, the approximations of the perturbation method are no longer valid in this case.

Hence we see that for any field which becomes Coulombian at a distance of about 5×10^{-13} cm. the wave function Ψ^s will differ from the Coulombian function Ψ^c only by the first term of the expansion (4). Therefore

$$\Psi^s = \Psi^c - A_0{}^c L_0{}^c(r) + A_0{}^s L_0{}^s(r),$$

which, on substitution from (6), (7) and (8), yields

$$\Psi^s - \Psi^c \sim (e^{2iK_0} - 1)\exp\{i(kr - 1/ak \,.\, \log 2kr + 2\sigma_0)\}/2ikr.$$

But Gordon finds for Ψ^c the value

$$\Psi^c \sim I + f^c(\theta) \,.\, S,$$

where I is the incident wave of unit amplitude, and $f^c(\theta) \,.\, S$ the scattered wave, given by

$$f^c(\theta) = \exp\{-i/ak \,.\, \log \sin^2 \tfrac{1}{2}\theta + i\pi\} \,.\, \operatorname{cosec}^2 \tfrac{1}{2}\theta,$$

and

$$S = \exp\{i(kr - 1/ak \,.\, \log 2kr + 2\sigma_0)\}/2k^2ar.$$

We therefore at once obtain

$$\Psi^s \sim I + f^s(\theta) \,.\, S,$$

where

$$f^s(\theta) = -\{\operatorname{cosec}^2 \tfrac{1}{2}\theta \,.\, e^{-i/ak \,.\, \log \sin^2 \frac{1}{2}\theta} + iak(e^{2iK_0} - 1)\}.$$

But the ratio, R, of the probability that with the non-Coulombian field the particle will be deflected through the angle θ to the similar probability for the Coulombian field is given by

$$R = |f^s(0)|^2/|f^c(\theta)|^2, \qquad (13)$$

and therefore the scattering ratio of the two-body problem is obtained from (13) by substituting $\frac{1}{2}\theta = \frac{1}{2}\pi - \chi$ from equation (1).

Hence we at once obtain

$$\begin{aligned} R &= \left|\sec^2\chi \,.\, e^{-i/ak\,.\,\log\cos^2\chi} + iak\,(e^{2iK_0} - 1)\right|^2/\sec^4\chi \\ &= \left|e^{-i/ak\,.\,\log\cos^2\chi} + iak\cos^2\chi\,(e^{2iK_0} - 1)\right|^2. \end{aligned} \tag{14}$$

In this formula, K_0 is a parameter whose value depends on the velocity v, the precise form of the dependence being determined by the nature of the function $f(r)$ of equation (3), but it is important to notice that the derivation of the formula (14) is quite independent of the form of this function.

§ 3. *Application of the Scattering Formula.*—Let us consider first the angular distribution of the protons projected by a homogeneous beam of α-particles of velocity v. The experimentally determined value of R for *one* value of χ serves to determine the value of K_0 *for the particular velocity in question*, and the formula (14) will then predict R at all other angles, for that one velocity. Table I shows the result of such a determination. The value of K_0 was calculated from the scattering in the range of angles 21·4° to 31·2°, the mean value 27° being used for substitution in the formula (14), since this value divides the range into two parts in which an equal number of particles would be expected according to the Rutherford law. The prediction of an angle-variation over such a wide range as is included in this table provides a severe test of the theory, and the good agreement obtained is a very satisfactory confirmation.

Table I.—Scattering in Hydrogen. $v = 1 \cdot 84 \times 10^9$ cm./sec.

Angle χ:	0°–10°.	10°–15°.	15°–20°.	21·4°–31·2°.	30°–40°.	40°–50°.	50°–60°.
R (observed)†	44	50	48	29	13	7	1·4
R (calculated)	44	43	39	29	17	7·8	2·4

† Chadwick and Bieler, *loc. cit.*

In fig. 1, these results are shown graphically together with similar results for other velocities of the incident α-particles. The velocity $1 \cdot 84 \times 10^9$ cm./sec. is the only one for which the scattering has been determined over such a wide range of angles and it therefore provides the best test of the theory, but the distributions for the other velocities provide additional confirmation. In each case the scattering for the range of angles between 21·4° and 31·2° was used to calculate the appropriate value of K_0.

§ 4. *The Determination of a Nuclear Model.*—If the variation of K_0 with v is calculated from equation (14), using the experimentally determined values of R, the results may be used to determine a model for the potential field, as has already been done for the interaction of two α-particles (Taylor, *loc. cit.*).

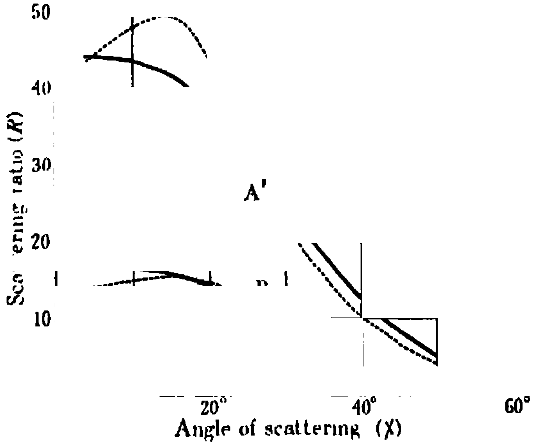

Fig. 1.—Angular distribution of the knocked-on protons, for scattering in hydrogen. Dotted lines, experimental values; full lines, calculated values. The calculated values were fitted to the experimental values at the points marked by a cross (+). Curve A, 6·6 cm. α-particles; curve B, 4·3 cm. α-particles; curve C, 2·9 cm. α-particles.

We must now make some simplifying assumption about the function $f(r)$ of equation (3), and if we choose as our potential

$$\left.\begin{aligned} V &= f(r) = -d \qquad & r &< r_0 \\ V &= ZZ'\varepsilon^2/r \qquad & r &> r_0 \end{aligned}\right\},$$

the calculation of the wave functions and the determination of r_0 and d follow in precisely the same manner as for the case of the two α-particles. It is found that the values of r_0 and d which give the best agreement with the experimental results are

$$r_0 = 4\cdot5 \times 10^{-13} \text{ cms.},$$

and

$$d = 6 \times 10^6 \text{ electron volts.}$$

In fig. 2 the potential field so determined is shown, and, on the same diagram, the wave functions $rL_0{}^s(r)$ are shown for three different values of the incident velocity. These wave functions are all normalised so that $rL_0{}^s(r)$ has unit amplitude at infinity. The three horizontal lines show the energies

($E_r = \frac{1}{2}M^*v^2$) for incident α-particles with these three velocities, and the dotted ordinates show the corresponding distances of closest classical approach.

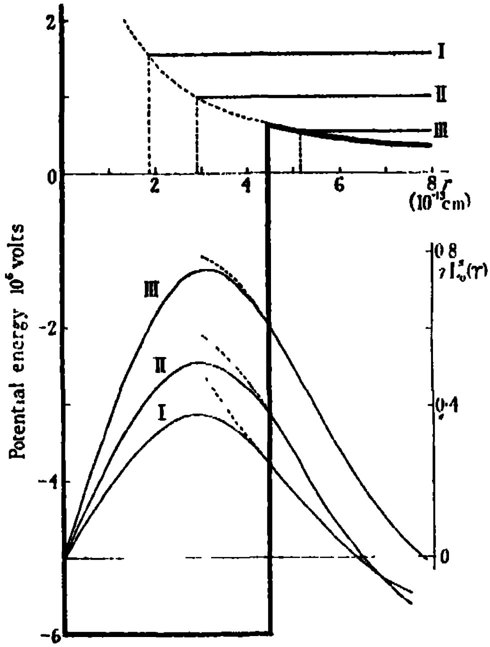

FIG. 2.—The mutual potential energy of a proton and an α-particle. I, $v/v_0 = 1 \cdot 0$ II, $v/v_0 = 0 \cdot 8$; III, $v/v_0 = 0 \cdot 6$. $v_0 = 1 \cdot 922 \times 10^9$ cm./sec.

The existence of a stable energy level for this potential field has been investigated, and it is found that an α-particle and a proton could coalesce to form a nucleus of mass number 5 with a liberation of energy of amount about $0 \cdot 8 \times 10^6$ electron volts. This result is somewhat difficult to discuss, firstly because an element of mass number 5 does not occur in the table of known isotopes, and secondly because all known nuclei contain at least twice as many electrons as protons, while the nucleus formed from an α-particle and a proton would violate this rule. We may perhaps say this much, that the binding energy is in accord with what one would expect for such a nucleus if it did exist, by analogy with the binding energies of other nuclei of mass number $4n + 1$ as shown in Table II.

Table II.

Nucleus.	α-particle + proton.	C_{13}.	Cl_{37}.
Binding energy (in 10^6 volts)	(calculated) 0·8	(experimental)† 10·7	44

† *Cf.* Gamow, "Atomic Nuclei and Radioactivity," p. 6.

§ 5. *The Scattering Formula for Helium.*—The problem of the scattering by helium differs from the hydrogen problem in two ways. In the first place M^* is now one half of the mass of an α-particle instead of one fifth, and therefore the wave-length to be associated with the α-particles from RaC is, in this case, $10 \cdot 3 \times 10^{-13}$ cm. Thus the physical analogy of § 2 would no longer suggest that the wave scattered by the region of non-Coulombian field should be spherically symmetrical. As the wave-length is still somewhat larger than the region of probable divergence from the Coulomb law, we shall assume, however, that only the terms for which n has the values 0 and 1 in the expansion (4) are changed from their Coulombian values. It is difficult to apply the method developed in § 2 to test the legitimacy of this assumption, for the function

$$F\,(i/ak + n + 1,\ 2n + 2,\ -2ikr),$$

required for the evaluation of the integral (12), is in this case not quickly convergent, and hence it is not possible to calculate K_2 conveniently.

The second point of difference from the hydrogen problem is the identity of the two particles concerned in the collision, and the fact that they obey the Einstein-Bose statistics. From this it follows (Taylor, *loc. cit.*, p. 110), that the wave function that describes the collision contains only the even harmonics of the expansion (4), and that, as a consequence of the above assumption that only the harmonics $n = 0$ and $n = 1$ differ from their Coulombian value, therefore the wave function Ψ^s differs from Ψ^c only by a spherically symmetrical term in this case also.

Taking into account the fact that the wave function must be symmetrical in the co-ordinates of the two particles, we may now deduce precisely as was done in § 2 that the ratio of the number of observed particles to the number predicted by the Rutherford law is given by†

$$R = \frac{\left|\operatorname{cosec}^2\phi \,.\, e^{-i/ak\,.\,\log\sin^2\phi} + \sec^2\phi \,.\, e^{-i/ak\,.\,\log\cos^2\phi} + 2iak\,(e^{2iK_0} - 1)\right|^2}{\operatorname{cosec}^4\phi + \sec^4\phi}, \quad (15)$$

where ϕ denotes the angle between the directions of the incident α-particles and of the scattered particles, and where the scattered particles are, of course, made up of deflected α-particles and knocked-on helium nuclei.

The application of this formula to the angular distribution of the scattering has already been to some extent tested in the author's previous paper, where the values of K_0 for fig. 4 were calculated from the observed values of R for the two different scattering angles $\phi = 34°$ and $\phi = 45°$. The two different sets of values of K_0 showed satisfactory agreement, indicating that the formula (15) predicts the correct variation of R with angle, for angles in the neighbourhood of 45°.

---

† This formula was given in the author's previous paper (equations (3) and (11)), but the derivation there given appeared to depend on the special field chosen, whereas the present method shows that this is not the case.

A more severe test has now been applied to the formula (15). Taking the value of K_0 as obtained for each velocity, from the scattering at 45°, the variation of the scattering with velocity, at 10°, has been calculated from the formula. The results are shown in fig. 3, together with the experimental value of the scattering ratio as recently re-determined in the Cavendish laboratory by Mr. P. Wright. I am indebted to Mr. Wright for permission to use these results before a complete account of the experiments has been published.

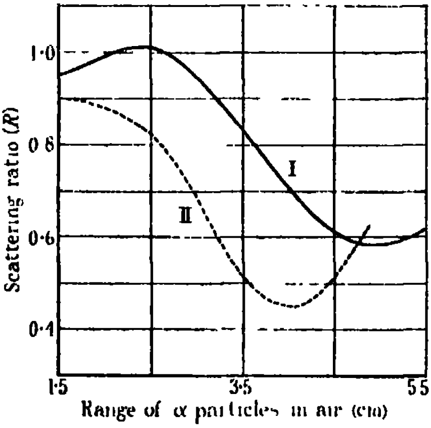

Fig. 3.—Scattering in Helium at 10°. Curve I, calculated; curve II, experimental.

The agreement between the two curves shows that the formula (15) forms a good first approximation to the law of scattering, but there is sufficient discrepancy to show that the phase change K_2 is not in this case altogether negligible. By taking into account as many of the phase changes K_2, K_4, etc., as may be necessary, instead of assuming that only K_0 is appreciable, we may develop a formula analogous to (15), and with such a formula it should be possible to make the agreement of fig. 3 exact. It is probable that K_2 would be the only other phase parameter appreciably different from zero, and, since $P_2(\cos\theta)$ is zero for $\theta = 54° 47'$, the scattering at 27° would serve to determine an accurate value of K_0, and then taking this value of K_0, we could calculate K_2 from the scattering at, say, 45°. The experimental results are, however, scarcely sufficiently reliable at present to enable such a calculation to be undertaken.

§ 6. *The Scattering at Small Angles.*—On the classical theory, the fact that the scattering is found to be anomalous at small angles involves the difficulty of assuming that in a small angle collision the non-Coulombian forces extend a much greater distance than in a large angle collision. For, on the classical theory, if two α-particles of the same energy are scattered by a nucleus, the one through a large angle and the other through a small angle, then the first must approach much more closely to the nucleus than the second. But the scattering is anomalous only when the α-particle enters the region of non-Coulombian interaction, and it is found that the smallest velocity for which the scattering is appreciably anomalous is virtually independent of the angle of scattering. Hence it becomes necessary to assume that for particles scattered through small angles the interaction ceases to be Coulombian at greater distance from the nucleus than in the case of particles scattered through large angles.

As soon as it is admitted that the scattering is a wave phenomenon, this difficulty disappears. The wave function describing the scattering enables us to determine the probability that α-particles will approach within a given distance of the nucleus and also the probability that they will be scattered through given angles, but it gives no correlation between the closeness of approach and the angle of scattering. Thus the above argument ceases to be valid. On the other hand, the formulæ (14) and (15) deduced from the spherically symmetrical field of the equations (3) do give an accurate account of the anomalies in the scattering even at small angles.

§ 7. *Applicability of this Method to Heavier Elements.*—The methods of this paper are convenient only when it is possible to assume that the actual scattered wave differs from the Coulombian one by a spherically symmetrical wave alone. A formula analogous to (14) may be developed for the case where phase changes other than K_0 have to be introduced, but the calculation of the parameters would be tedious, and in the case where m parameters had been introduced, the scattering at m different angles would be required in order to determine the parameters. The next two elements for which the anomalous scattering has been observed are beryllium and boron, and, for the case of the scattering with these elements, the wave-length to be associated with the α-particles from RaC is about 7×10^{-13} cm., so that considerably more terms of the expansion (4) would be affected in this case than in the scattering by helium. Further, there would not be the simplification which occurs in the helium problem due to the disappearance of all the odd harmonics of the expansion (4). Hence the methods of this paper cannot conveniently be applied to any elements other than hydrogen and helium.

Summary.

(1) The methods of a previous paper on the scattering by helium are extended to apply to the scattering by hydrogen. Good agreement with experiment is obtained.

(2) It is shown that the scattering at small angles, both in hydrogen and in helium can be explained by the same field as that which explains the scattering at large angles.

(3) These results are shown to be quite independent of the particular form of the potential energy curve assumed for the one particle in the field of the other, provided only that the energy becomes Coulombian for distances greater than about 5×10^{-13} cm.

It is a pleasure here to acknowledge my indebtedness to Mr. N. F. Mott for much assistance and advice given to me throughout the course of this work. A grant from the Department of Scientific and Industrial Research has made possible the undertaking of the problem.

Experiments with High Velocity Positive Ions.—(I) *Further Developments in the method of obtaining High Velocity Positive Ions.*

By J. D. Cockcroft, Ph.D., Fellow of St. John's College, Cambridge, and E. T. S. Walton, Ph.D.

(Communicated by Lord Rutherford, O.M., F.R.S.—Received February 23, 1932.)

[Plate 11.]

Introduction.

In a previous communication* we described the development of a method of obtaining positive ions of hydrogen with energies up to 300 kilovolts. A system of rectifiers was built which allowed steady potentials of this order to be obtained, and the methods necessary for the acceleration of positive ions from a hydrogen discharge tube were worked out.

With this apparatus, investigations were made to determine whether any X-radiations or γ-radiations of appreciable intensity were produced by the impact of protons and molecular ions of hydrogen on matter. It was found, when all secondary effects were excluded, that if any such radiation is produced its intensity was comparable with the limits of error of the experiment, and was certainly not greater in intensity than one-millionth of the intensity of the continuous X-radiation which would have been produced by an equal electron source of the same energy. Since the intensity of any radiation would be expected to increase rapidly with the energy of the ions it became apparent that to obtain results of interest it would be necessary to extend the field of the work to higher voltages. The method used in the present experiments is an extension of that described in the previous paper. A source of high voltage has been developed, using thermionic rectifiers and condensers, which is capable of producing 800,000 volts steady potential. This potential is applied to an experimental tube down the axis of which protons from a hydrogen canal ray tube are accelerated. The protons can be transmitted through a mica window into an experimental chamber. Up to the present we have been able to produce and carry out experiments with protons having energies up to 710 kilovolts, and there seems no reason to doubt that the method will allow of this range being extended considerably.

---

* 'Proc. Roy. Soc.,' A, vol. 129, p. 477 (1930).

The Method of Generating the High Potential.

In the previous paper we gave reasons why we considered it advantageous to work with steady potentials rather than with impulse voltages, Tesla coil voltages or alternating currents. Our experiments at the lower voltages confirmed this view, and we therefore decided to construct a system of rectifiers which would enable a steady potential of 800 KV. to be obtained.

In order to be able to carry out this plan at a reasonable cost, and within the limits of ordinary laboratory accommodation, it became evident that it would be very necessary to use some form of voltage multiplying circuit

The general principle underlying the method adopted is illustrated by fig. 1.

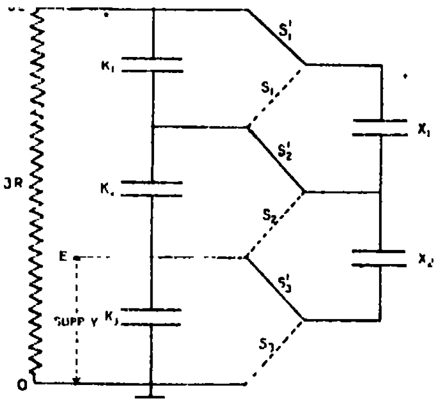

FIG. 1.

Three condensers, K_1, K_2 and K_3, each of capacity C, are connected in series and condenser K_3 is connected to a source of steady potential E. If now two other condensers, X_1, X_2, are connected to condensers K_1, K_2, K_3, first as shown by the dotted lines S_1, S_2, S_3, and then as shown by the full lines S_1', S_2', S_3', then in the first cycle when X_1 and X_2 are connected to K_2 and K_3, condenser X_2 will be charged to voltage E. When the switches are moved over to the upper position, condenser X_2 will share its charge with condenser K_2 and both will be charged to E/2 if they have equal capacity. In the next reversal of the switches, condensers K_2 and X_1 will be connected and take up potentials E/4 whilst condenser X_2 will be recharged to potential E. It is thus evident that charge will gradually be transferred to all the condensers until, in the absence of loss, a potential 3E will be developed across the condensers K_1, K_2, K_3 in series.

The principle is evidently capable of extension, and by adding more condensers any multiple of a given steady voltage may be obtained. It is further clear that the principle is reversible and that if the terminals 3E and O are connected to a source of potential 3E, then current may be drawn off at potential E between the terminals E and O.

Various methods of carrying out the switching process other than mechanical means can be devised. Two of the switches may be replaced by controlled grid triodes and the remainder by diodes. Thus in fig. 2, switches S_3 and S_3' of fig. 1 are replaced by two triodes or thyratrons T_1 and T_2, whose grid potentials are varied cyclically and in opposite phase so that they conduct in alternate half cycles. Switches S_1 and S_1', S_2 and S_2', are replaced by diodes D_1, D_1', D_2, D_2'. Now, when valve T_2 is conducting, if E has a positive potential the condenser X_2 is charged through diode D_2 and triode T_2 to potential E. Thus when valve T_1 becomes conducting, the potential of t_3 will rise to the potential E and the potential of t_2 will rise to a potential 2E, and condenser X_2 will therefore charge condenser K_2 through diode D_2' and triode T_1. It is further clear that in successive cycles when T_1 is conducting, condenser X_1 will charge condenser K_1 through diode D_1', and will be charged through diode D_1 when T_2 is conducting. Thus we have exactly the same process as in the switching circuit of fig. 1.

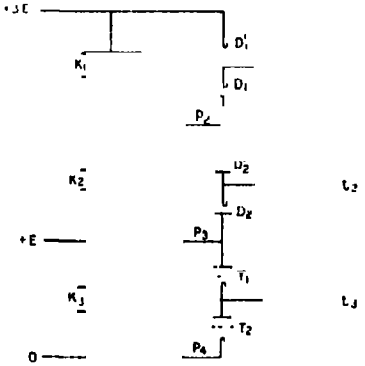

FIG. 2.

The difficulty in applying this method to obtain potentials of the order of 800 KV. lies in the development of triodes which will stand potentials of the order of 200–400 KV. Fortunately, however, it is possible to perform the same operations when relatively small outputs are required, by more simple means.

It has been shown that the triodes operate by causing the potential of t_3 to assume alternately the potentials of p_3 and p_4. If now we replace triodes T_1 and T_2 by diodes D_3 and D_3', and connect the high tension winding of a transformer giving a potential E/2 in series with a condenser across the diode D_3', then power will be delivered from the transformer and condenser X_3 is charged through diode D_3' to potential E/2 at the negative peak of the transformer wave. The potential of t_3 will therefore alternate between zero and E. Now when t_3 approaches potential E, condenser K_3 will be charged through diode D_3 instead of receiving power from a D.C. source as in the previous circuit. As the potential of t_3 falls again, the potential of t_2 falls below the potential of p_3 and hence condenser X_2 is charged through diode D_2' exactly as in the earlier circuit. Thus an equilibrium state is reached when each of condensers K_1, K_2, K_3, X_1 and X_2 is charged approximately to voltage E.

If now a load of resistance 3R is connected across the system, then in the equilibrium state the condenser K_1 will lose charge $Q = E\tau/R$ during a cycle of period τ. It will therefore receive charge Q over a small fraction of the half cycle when the transformer voltage is a maximum. The charging period is represented in fig. 3 (*a*). At the same time, condenser K_2 receives charge 2Q to replenish the charge lost to the load in the cycle and the charge transferred to X_1 in the transfer half cycle. Condenser K_3 will at the same time receive charge 3Q making up charge Q lost in the load and charge 2Q lost in the transfer cycle. The transformer will at the same time supply power 3Q . E/2.

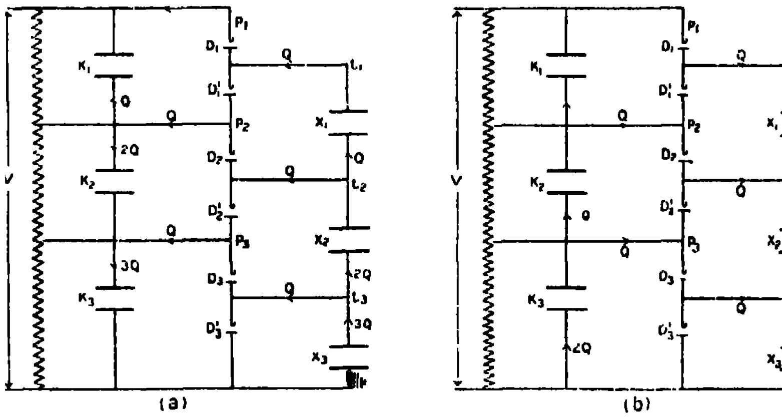

(a) (b)

FIG. 3.

The transfer half cycle is illustrated by fig. 3 (*b*). When the transformer potential is near the negative peak value, diodes D_1', D_2', D_3' become conducting; condenser K_2 transfers to condenser X_1 the charge lost to K_1 in the previous transfer, condenser K_3 transfers charge 2Q and the transformer passes charge 3Q.

Thus for an *n* stage circuit (2*n* voltage multiplication) the total voltage fluctuation across the load will be given by the voltage charge during the charging period,

$$\delta V = \frac{Q}{C} + \frac{2Q}{C} + \dots \frac{nQ}{C} = \frac{n \, . \, n+1}{2} \, . \, \frac{E\tau}{CR} \, .$$

Thus the percentage voltage fluctuation will be

$$\frac{\delta V}{V} = \frac{n+1}{2}\,\frac{\tau}{CR}. \tag{1}$$

Thus if $n = 2$, $R = 10^9$, $C = 0\cdot001\ \mu F$ and $\tau = 10^{-2}$ seconds, the percentage fluctuation will be 1·5 corresponding to a load current of 0·4 milliamps. at 800 KV. We have assumed, of course, that the filament emission does not limit the transference of charge. The emission has to be adequate to transfer the charge during a small fraction of a cycle. Should this not be the case, then the full theoretical voltage multiplication will not be obtained. The absolute value of the ripple will be unaltered, but its value as a percentage of the mean output voltage will be increased. To obtain a fluctuation of less than 2 per cent. with full voltage multiplication, the emission must be at least 30 times the load current.

The efficiency of the system will clearly depend on the voltage characteristics of the diodes, and on the voltage difference across the valves when they become conducting. It may be shown that if space charge be neglected the efficiency of transfer is of the order of $1 - \delta V/V$.

The amount of power which can be transformed by the system depends on the size of the condensers used and can never be great by reason of the low switching frequency attainable. If a transformation system is required for large powers it will be necessary to use the method of fig. 2 where the switching frequency could be made very high and a square wave form used. It is also interesting to note that this system could be reversed by interchanging triodes T_1, T_2 with diodes D_1, D_1'. It would be possible therefore by some such arrangement to transform D.C. power from a high voltage to a low voltage should this be required.

For our work, however, where the load current is determined solely by corona loss and is of the order of milliamperes, the circuit of fig. 3 has the great advantage of simplicity. Each rectifier and condenser has to stand twice the voltage of the transformer and the number of stages is therefore determined by the maximum voltage for which rectifiers can be constructed. From our previous experience it appeared probable that rectifiers could be built to stand a voltage of 400 KV. without difficulty. We therefore decided to use a double stage circuit giving fourfold voltage multiplication, using four rectifiers and four condensers.

The circuit finally adopted, differs in the arrangement of condensers from a circuit suggested by Schenkel,* which also allowed voltage multiplication to any extent, but required some of the condensers used to withstand the full voltage of the output circuit.

---

* 'Elektrotech Z.,' vol. 40, p. 333 (1919).

The Rectifiers.

In our previous rectifiers we used 12-inch diameter glass bulbs with an overall length of 36 inches and stem diameters of 2 inches and 3 inches respectively. Our experience with these rectifiers showed that when a voltage greater than 300 KV. was applied they tended to puncture near the neck of the bulb on the side of the smaller diameter stem, this being the positive side. Experiments were therefore carried out which showed that it was possible to eliminate this trouble by using, instead of bulbs, cylinders of approximately 14 inch diameter and length 3 feet.

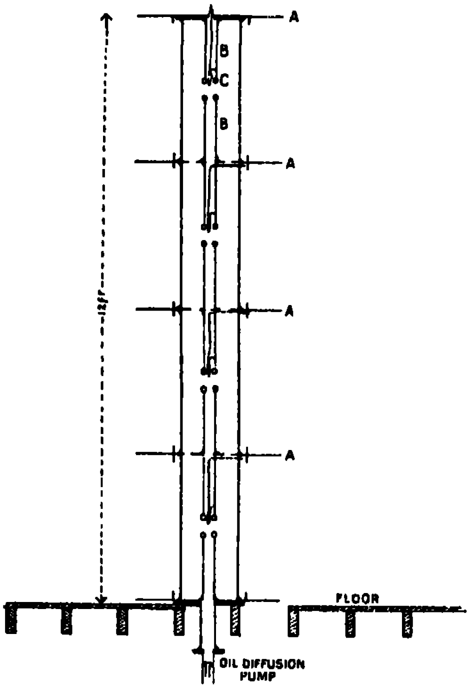

Fig. 4.

We therefore decided on the rectifier system illustrated in fig. 4. Four glass cylinders of these dimensions were erected in the form of a tower, and pieces of tinned sheet iron, A, 3 feet square, were placed between adjacent cylinders, The electrodes, B, were attached to these and they also served the purpose of giving a fairly uniform potential gradient down the length of the cylinders. The top and bottom of the tower were closed by thick metal plates. All the joints were made airtight by means of "plasticene" placed on the outside.

When this is worked in tightly with the fingers, quite a good vacuum can be obtained. The surface is then rubbed over with tap grease to seal up any minute holes such as might occur along the surface between the glass or metal and the plasticene. This method of making joints has been found to be very reliable. The ease with which the joint may be made and broken again make it a very convenient type of vacuum joint. The two surfaces to be joined require only a very rough preparation. Thus a good joint between a flat plate and a 3-inch brass tube can easily be made even if the end of the latter has merely been sawn off roughly with a hacksaw and considerable gaps have to be bridged by the plasticene. In some preliminary experiments on the large glass cylinders, ordinary commercial plasticene was employed and found to be quite satisfactory. In the final tower of rectifiers, a special putty like sealing compound was used, which had been made from low vapour pressure products.*

The electrodes were made from thin walled steel tube and the ends were fitted with thick rings, C, made from ¾-inch diameter steel to prevent auto-electronic emission. Before insertion in the apparatus, these rings were outgassed in a vacuum furnace. Each filament consisted of about 3 cm. of 0·25 mm. tungsten wire bent to the form of a V and supported in the middle as well as at the ends. They projected slightly beyond the ends of the steel electrodes. One end of each filament was connected to one of the tinned sheets and the lead to the other end was brought out of the apparatus through a small hole drilled near the end of each cylinder. These holes were then sealed up with plasticene. The filaments were heated from 6-volt accumulators which were kept in rounded metal boxes, these being placed on the tops of the various condensers. The rectifiers were evacuated by a three-stage oil diffusion pump of the type described in the previous paper and this was backed by a hyvac. In order to save head room, the pumps were placed under the floor and they were connected to the tower of rectifiers by a short length of 3-inch brass tubing. The condensers employed had each a capacity of 0·001 microfarads with bakelite insulation. Three of these would each stand up to 400 KV., while the fourth was rated at 300 KV. Three of the condensers required insulation from earth and were supported on bakelite cylinders.

Most of the current drawn from the rectifiers was in the form of corona discharge, and at the higher voltages this was slightly over half a milliampere as measured by a D.C. instrument placed on the earthed side of the transformer secondary. We should therefore expect a ripple of the order of 1·5 per cent. The wave form has been measured using a cathode ray oscillograph in conjunction with a potential divider and the ripple has been found to be of this order. At the lower voltages the apparatus gave very nearly a fourfold multiplication of the transformer voltage, provided the filaments of the rectifiers were kept sufficiently bright. The emission from the filaments was not sufficiently large to give a fourfold multiplication of voltage at the higher potentials on account of the larger corona losses. The factor varied between three and four and it did not seem worth while dismantling the apparatus to put in filaments which would give the necessary emission. The voltage was measured by sparkover between the 75 cm. diameter aluminium spheres shown in the photograph, Plate 11. The gap was adjusted by raising or lowering the upper sphere.

---

* We are indebted to Messrs. Metropolitan-Vickers Electrical Co., Ltd., for the supply of a quantity of this before it had been placed on the market.

The Experimental Tube.

The experimental tube consisted of two glass tubes similar to those used in the tower of rectifiers, and is shown in fig. 5. A steel plate, A, was placed between the cylinders, and this formed the support for the electrodes, B. The thin sheets of metal used in the rectifiers would not have been sufficiently rigid to give the accurate alignment of the electrodes which is necessary in this case to direct the beam of ions down the axis of the tube. This metal plate had a 3 feet square piece of sheet metal, C, attached externally which acts as a stress distributor and which is maintained at half the total potential by a connection to the middle point of the tower of rectifiers. Protons were generated in a hydrogen discharge tube, D, placed above the apparatus. The discharge tube was of the Wien type described in the previous paper. The potential applied across the discharge tube was obtained from a 60 KV. transformer, E, fig. 6, the primary of this being supplied with alternating current at low potential. It was found that a much better proton current could be obtained from the discharge tube when the current sent through it was rectified by placing a small kenetron between it and the transformer.

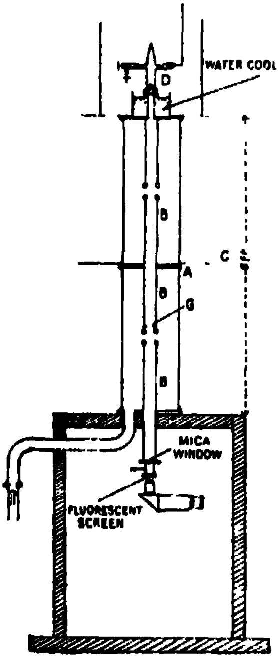

Fig. 5.

The usual voltage required on the discharge tube was 40 KV. To supply the exciting current from the mains would have required an insulation transformer to stand 800 KV. between primary and secondary windings, and this would have been bulky and expensive. Its use can, however, be avoided by exciting the transformer from a small alternator which is placed at high potential, the alternator being driven by an insulating belt, F, from a motor at earth potential, as shown in fig. 6. The belt used was a cotton rope, the join being made by splicing. A distance of 8 feet between the motor and the alternator gave ample insulation. The method has been found to be very satisfactory and could be used for still higher voltages.

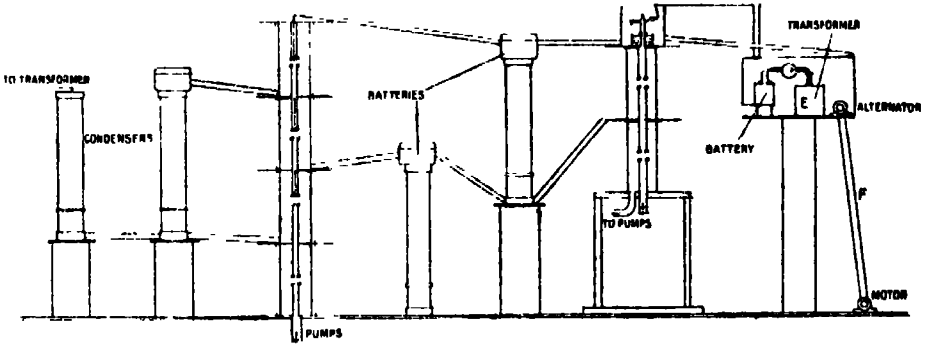

FIG. 6.

The protons passed through a canal in the cathode, passed down the axis of the tube and were accelerated in the space between the electrodes. In the upper cylinder a focussing of the ions was produced in the way described in the previous paper. In the lower cylinder there is less focussing action since the ions are then travelling fast and they are not deviated much by any radial components of the field. This meant that a considerable number of ions struck the ring on the end of the lower electrode and there liberated secondary electrons. Some of these were accelerated towards the upper electrode and there gave rise to X-rays. Some of them struck the wall of the glass tube and the charges built up caused puncture of the glass at comparatively low voltage. Both of these troubles were satisfactorily eliminated by inserting a diaphragm as shown in fig. 5 at G, which prevented the ions from striking the electrodes except at places well inside it, where there was no appreciable field. The tube was evacuated by a fast oil diffusion pump, the connection to the pump being made through 3-inch steam piping. Experiments could be carried out on the protons by attaching a suitable apparatus at the bottom of the tube.

The Operation of the Apparatus.

When the apparatus is first connected to the transformer it is found that considerable quantities of gas are evolved from the walls. The voltage has to be increased slowly with intervals of a few seconds between the different evolutions of gas to allow the pumps to clear the tubes. Thus it may take a whole day's operation before the full voltage can be applied to the apparatus. After this outgassing process is complete, however, full voltage can usually be obtained within 30 minutes of starting the pumps and within a few minutes of first applying the potential. The tube will then run continuously without trouble.

Up to the present we have been prevented from proceeding to the full voltage for which the apparatus was designed by the voltage limitation on one condenser. We have, however, been able to apply voltages up to 690 KV. to our experimental tube, giving a total proton energy of about 710 KV. At this voltage we punctured the lower glass cylinder of the experimental tube. Although we were able to continue work by stopping the hole with plasticene, we were never able to go beyond this limiting voltage again since we invariably found that a spark would find its way through the plasticene at about the same limiting voltage. We therefore propose to increase the length of our experimental cylinders by 6 inches, and expect that this will enable us to obtain the full 800 KV. It is probable that the puncture of the lower cylinder arose from charging of the walls resulting from secondary electron emission from the electrodes under positive ion bombardment, and that a smaller diaphragm placed in the path of the ions will eliminate the trouble.

Should higher voltages be required in future it would be quite feasible to add another unit to our rectifiers and experimental tube did space allow. It might then be expected that voltages of over a million volts could be used. It would in this case be necessary to take much greater precautions against corona loss than have been necessary in our present apparatus, or to use filaments having much larger emissions.

Experimental Work.

After passing down the axis of the cylindrical electrodes of the tube, the protons emerge through a 3-inch diameter brass tube at the base of the apparatus, into a chamber well shielded by lead and screened from electrostatic fields. Here any apparatus for experimental work can be attached using a flat joint and a plasticene seal. Proton currents of the order of 10 microamperes can be obtained in this chamber.

When it is desired to carry out experiments at atmospheric pressure the protons can be passed through a thin mica window into the experimental chamber. In the first series of experiments on the range of protons in different gases only a very narrow beam is required. It was therefore a very simple matter to find a piece of mica to act as a window with the necessary small stopping power. A pin hole in a sheet of foil was covered with mica having a weight of 220 micrograms per square centimetre. It was found that protons could be first observed outside at accelerating voltages of the order of 80 KV. After the window had been bombarded for some time it was found that the protons first appeared at accelerating voltages as low as 50 KV. It would appear that the mica is being slowly sputtered away, but it is evidently possible to work for many hours with one window. When the observation chamber is made quite dark it is easily possible to observe luminescence in the gas due to the pencil of protons. By allowing the protons to strike a fluorescent screen, measurements of their range in different gases have been made ; these experiments will be described in Part II.

Summary.

In order to obtain high steady potentials for the acceleration of protons, a method has been developed by which the voltage of a transformer can be rectified and multiplied several times by an arrangement of valves and condensers. A rectifier system has been built consisting of four glass cylinders placed end to end, and arranged in the form of a tower 12 feet high, the cylinders containing suitable electrodes and hot filaments and being evacuated continuously. With this apparatus and four condensers, a potential of over 700 KV. has been obtained, which is steady to within a few per cent. The method used is a special case of a more general method of transforming steady potentials from low to high voltages and in the reverse direction.

The voltage of the rectifier is applied to an experimental tube which is built to allow positive ions to be accelerated by the full voltage available. Positive ions of hydrogen are directed down the axis of two glass cylinders and focussed by suitable electrodes, current of the order of 10 microamperes being obtained. Protons having energies up to 710 KV. have been produced and have been

transmitted through a mica window into an experimental chamber at atmospheric pressure where their ranges are measured.

The equipment of the laboratory has been made possible by a special grant from the University.

We wish to express our gratitude to Professor Lord Rutherford for his constant encouragement and support in this work. One of us (E.T.S.W.) is indebted to the Department of Scientific and Industrial Research for a Senior Research award.

On some Close Collisions of Fast β-Particles with Electrons, Photographed by the Expansion Method.

By F. C. Champion, Cavendish Laboratory, Cambridge.

(Communicated by Lord Rutherford, O M , F.R.S.—Received February 23, 1932.)

[Plates 12 and 13.]

1. *Introduction.*

The present paper gives an account of measurements on some close collisions of fast β-particles with electrons, photographed by the Wilson cloud method. These measurements afford a direct test of the applicability of the principles of the conservation of momentum and energy and the principles of relativistic mechanics to individual atomic phenomena.

On the basis of Newtonian mechanics, if one particle collides with another which is initially at rest and the two particles are of equal mass, the angle between the directions of motion of the two particles after collision is equal to 90° for all angles of scattering of the incident particle. On relativistic mechanics, however, this angle becomes a function of the angle of scattering and the velocity of the incident particle, and in particular, it becomes smaller and smaller as this velocity approaches that of light. Qualitative evidence has already been given by Wilson,* Bothe† and others that this angle is less than 90° for the collisions of fast β-particles with electrons, but up to the present no quantitative study has been made of the general relation between the whole angle after collision, the angle of scattering, and the velocity of the incident particle. Assuming that momentum and energy are conserved in the collision the following calculation may be made.

---

* 'Proc. Roy. Soc.,' A, vol. 104, p. 1 (1923).

† 'Z. Physik,' vol. 12, p. 117 (1922).

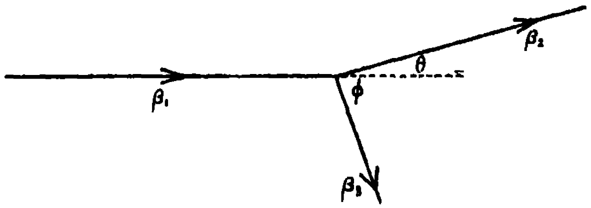

Fig. 1.

Consider the incident electron to have a velocity v_1 with respect to the observer and the stationary electron and let $\beta_1 = v_1/c$. Let the final directions of motion of the two electrons be inclined at θ and ϕ to the initial direction of motion of the incident electron and the velocities in these two directions correspond to β_2 and β_3 respectively. Then from the relativistic momentum and energy relations :—

$$\beta_1\gamma_1 = \beta_2\gamma_2 \cos\theta + \beta_3\gamma_3 \cos\phi \tag{1}$$

$$\beta_2\gamma_2 \sin\theta = \beta_3\gamma_3 \sin\phi \tag{2}$$

$$\gamma_1 + 1 = \gamma_2 + \gamma_3, \tag{3}$$

where

$$\gamma = \frac{1}{(1-\beta^2)^{\frac{1}{2}}}.$$

From these we obtain

$$\beta_2 = \frac{\beta_1 \sin\phi}{\{\beta_1^2 \sin^2\phi + \sin^2(\phi+\theta)/\gamma_1^2\}^{\frac{1}{2}}} \tag{4}$$

$$\beta_3 = \frac{\beta_1 \sin\theta}{\{\beta_1^2 \sin^2\theta + \sin^2(\phi+\theta)/\gamma_1^2\}^{\frac{1}{2}}}, \tag{5}$$

and*

$$\cos(\phi+\theta) = \frac{(\gamma_1 - 1)\sin\theta\cos\theta}{\{(\gamma_1+1)^2\sin^2\theta + 4\cos^2\theta\}^{\frac{1}{2}}}. \tag{6}$$

For the symmetrical case in which $\phi = \theta$ and $\beta_2 = \beta_3$, (7) reduces to the simple form

$$\cos\theta = \frac{\beta_1}{(2/\gamma_1 + 3\beta_1^2 - 2)^{\frac{1}{2}}}, \tag{7}$$

a result obtained by Bothe.†

---

* Wolfe, 'Phys. Rev.,' vol. 137, p. 591 (1931).

† *Loc. cit.*

2. *Experimental Method.*

The experimental arrangement of the automatic expansion chamber has been described in a previous paper*; it utilises the disposition of two cameras with their axes mutually at right angles. The application of the expansion chamber method to the present problem becomes possible only when there is available a large number of photographs of fast β-ray tracks, for the chance of a close collision with an atomic electron is certainly very small. A fork which is being used for the investigation must obey the following conditions for the value of $(\theta + \phi)$ to depart most from 90°. The collision must be as nearly as possible a symmetrical one. This type of collision is very infrequent. Again, the velocity of the incident electron must be as large as possible. The source of particles used in the present experiment was radium E; the velocities of these particles range up to about $\beta_1 = 0 \cdot 94$, but the fraction with β_1 greater than $0 \cdot 90$ is only a few per cent. of the total number of particles emitted. Even with a source of considerable strength, therefore, a large number of photographs is required before one of those shows a very high speed particle making a close collision.

The velocities of the incident particles were determined from the curvatures of the tracks in a magnetic field which was perpendicular to the plane of the chamber, Champion, *loc. cit.* Artificial tracks of known curvature were placed in the position of the natural tracks in the plane of the chamber and the photographs so obtained were fitted to those of the natural tracks by process of trial and error. For the maximum accuracy in the determination of v_1 the curvature should be as large as possible, but this decreases the accuracy of measurement of ϕ and θ, for which purpose the arms of the fork should have as little curvature as possible. Some balance has therefore to be struck concerning the value of the magnetic field. The value used in the earlier experiments was about 180 gauss, but the curvature produced in the fastest tracks was insufficient for accurate work and in all the later experiments this value was raised to about 250 gauss. With the latter field a particle with $\beta_1 = 0 \cdot 90$ has on the relativity calculation a path of radius of curvature $\rho = 14$ cm. For accurate determination of this curvature (say to 2 per cent.) it is necessary to have about 9 cm. of the track of the incident electron free from nuclear bends. This will again be of rare occurrence, and the adherence to this criterion necessitated the rejection of several otherwise technically good collisions. Further, a collision suitable for accurate measurement, should have the individual drops deposited as evenly

---

* Champion, 'Proc. Roy. Soc.,' A, vol. 134, p. 672 (1932).

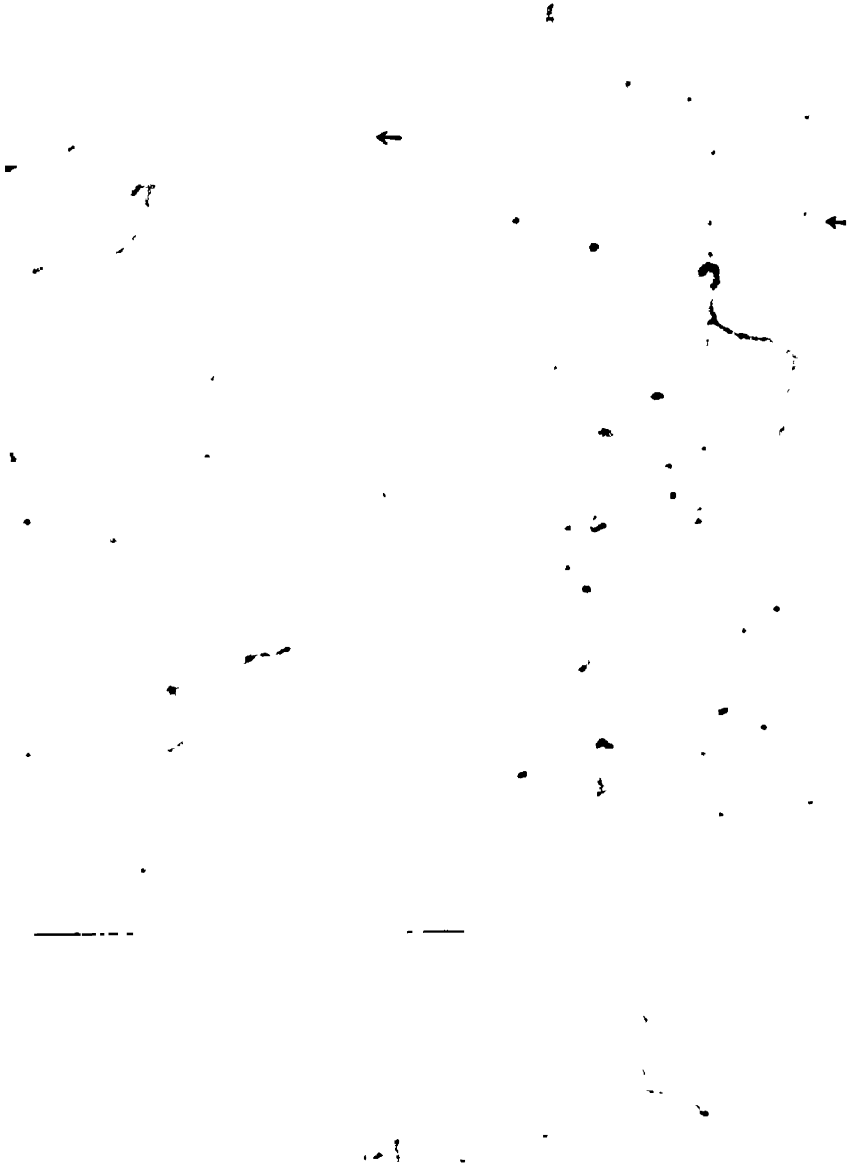

1 (*a*)

1 (*b*)

2 (*a*)

2 (*b*)

as possible along the three branches of the fork; sporadic dense clumps of ions separated by blank spaces of no ionisation render the angle determinations less accurate especially when the curvature of the tracks is taken into account. It is very rare indeed that all these criteria are satisfied simultaneously; the collisions quoted quantitatively here satisfy all the more important criteria. The close collision in Plate 12 satisfies nearly all the required conditions, and in addition it occurs almost exactly in the plane of one of the cameras so that the correction for the true spatial angle is very small and the apparent angle on the left-hand photograph is almost the true value of $(\theta + \phi)$.*

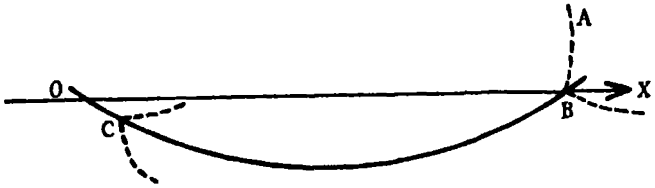

Fig. 2.

4. *Results and Discussion.*

Some 30,000 tracks of fast β-particles in nitrogen and about 5000 in oxygen have been investigated. About 50 close collisions with electrons were observed, and in all cases the measured angles agreed approximately with the values predicted theoretically from relativity considerations. Measurements on 14 of these collisions which satisfy best the more important criteria for accurate quantitative investigation are shown in Table I. In the first column is given the measured value of β_1, the second column giving the corresponding value of the energy of the incident electron in electron volts. In the third column is given the measured value of θ, while the fourth column contains the observed

---

* Let OX represent the mean direction of the incident β-particle which actually traverses a curved path such as OCB. Then owing to the optical arrangement, the errors involved in the calculation of the true spatial angle of any fork from the angles measured on the photograph become very large if either arm of the fork approaches a direction perpendicular to OX such as at BA. The angle between one of the arms and OX cannot be much less than 45° in the collision of particles of equal mass, and if the collision occurs at B or C where the main stem is itself inclined at a considerable angle to OX, one of the arms of the fork must approach this perpendicular direction. It was necessary to reject all collisions of this type and in actual practice this involved the rejection of several otherwise technically good collisions. The collisions in Table I were all such that these analytical errors were small.

To check the velocities of the particles after collision, that is to determine the values of β_2 and β_3 for comparison with the values calculated from (4) and (5), the curvatures of the

Table I.

No.	β_1.	E.	$\theta \pm 0\cdot5°$.	$(\theta + \phi)°$.			$\psi°$.
				Obs.	Calc.	Diff.	
1	0·85 ±1 per cent.	457,100	20·0	83·6 ±1·0	82·7 ±1·0	−1·1	2·6
2	0·83 ±1 per cent.	403,400	26·6	81·2 ±1·0	81·7 ±1·0	+0·5	0·0
3	0·83 ±1 per cent.	403,400	31·4	81·0 ±1·0	81·0 ±1·0	0·0	1·0
4	0·82 ±1 per cent.	380,200	22·0	84·1 ±1·0	83·2 ±1·0	0·9	0·0
5	0·85 ±1 per cent.	457,100	22·2	82·2 ±1·0	81·7 ±1·0	−0·5	1·0
6	0·83 ±1 per cent.	403,400	22·4	82·1 ±1·0	82·3 ±1·0	+0·2	0·0
7	0·84 ±1 per cent.	428,900	23·4	82·7 ±1·0	81·7 ±1·0	−1·0	0·0
8	0·90 ±2 per cent.	658,500	24·5	79·6 ±1·0	77·4 ±1·5	−2·2	3·7
9	0·88 ±1 per cent.	562,400	35·4	76·8 ±0·5	77·3 ±1·0	+0·5	1·1
10	0·85 ±1 per cent.	457,100	21·1	82·7 ±1·0	81·8 ±1·0	−0·9	0·0
11	0·91 ±2 per cent.	700,000	36·9	75·2 ±0·5	75·2 ±1·5	0·0	1·9
12	0·93 ±2 per cent.	885,000	29·6	72·5 ±0·5	72·6 ±1·5	+0·1	3·1
13	0·85 ±1 per cent.	457,100	21·8	82·4 ±1·0	81·4 ±1·0	−1·0	2·5
14	0·82 ±1 per cent.	380,000	36·9	80·6 ±0·5	81·0 ±1·0	+0·4	1·8
15	0·87 ±2 per cent.	523,000	24·7	83·6 ±1·0	79·6 ±2·0	−4·0	9·7

values of $(\theta + \phi)$ and the values calculated from (6). The last column contains the value of the angle between the plane of the arms of the fork and the main stem. The first two collisions were in oxygen, the remainder in nitrogen.

The agreement between the theoretical and the observed values of $(\theta + \phi)$ is seen to be excellent.* The maximum departure of $(\theta + \phi)$ from a right angle occurs in collision 12 where the deviation is as much as 17·5°; in this instance the mass of the incident electron is nearly three times its rest mass.

---

arms of the fork must be measured. It is clearly impossible to use the same method as that used for determining the curvature of the main stem unless the collision occurs in the plane of the chamber. Further, if the arms are inclined at any appreciable angle to the plane of the chamber, they rapidly pass out of focus of the cameras. for it is necessary to use an aperture *f*/5·6 to secure adequate intensity of the photographic image, and this aperture gives a depth of focus of only about ⅛ cm. The arms also pass out of the illuminating beam. There is thus rarely sufficient length of arm to make any accurate quantitative determination of the curvature. Even when the three arms lie approximately in the plane of the chamber it is very rare that none of them exhibits a nuclear bend over the distance necessary for any accurate measurement. However, rough measurements have been made for those collisions where the three arms lie in the plane of the chamber and the values of β_2 and β_3, as might be expected from the agreement of the angle relationships in Table I, were found to agree within experimental error with the values calculated from (4) and (5).

* The concept of the Abraham rigid electron ('Ann. Physik,' vol. 10, p. 105 (1903)) has been applied to the present results for the special case where the energy of the electrons is shared equally after collision. Collision 11 in Table I approximates to this special case and it is found on inserting the Abraham formula for the mass in the momentum and energy equations that $(\theta + \phi)$ is 58°; actually $(\theta + \phi)$ equals 75·2° in excellent agreement with the value calculated from the relativity expression.

With regard to the errors of measurement, the error in β_1 depends upon the errors in the curvature ρ and the field H. Combining the expression $m = m_0/(1 - \beta_1^2)^{\frac{1}{2}}$ with the expression $mv^2/\rho = Hev$, we find for the total random error

$$(\Delta\beta_1)^2 = \frac{a^2}{(1-a)^3}\left[\left(\frac{\Delta H}{H}\right)^2 + \left(\frac{\Delta\rho}{\rho}\right)^2\right], \tag{8}$$

where

$$a = \left(\frac{m_0 c}{e} \cdot \frac{1}{H\rho}\right)^2.$$

The error in ρ ranges from 2–4 per cent. over the range of curvatures measured and the error in H is not more than 2 per cent. From (8) the error in the determination of β_1 is therefore not greater than 2 per cent. The determination of the error in the theoretical calculation of $(\theta + \phi)$ from (6) is lengthy, but it may be shown that using the value of $\Delta\beta_1$ from (8) and the value of $\Delta\theta$ as estimated from measurement as $\pm 0{\cdot}5^\circ$, $\Delta(\theta + \phi)$ varies from $\pm 1{\cdot}0^\circ$ to $\pm 1{\cdot}5^\circ$ over the range of β_1 considered.

The validity of the theoretical results has depended entirely on the assumption that there has been no loss of momentum or energy in the form, for example, of electro-magnetic radiation, when the electrons collide. It may be shown that if the energy radiated is comparable with that of the incident electron, the momenta of the radiation and the electron are also comparable. No calculation seems to have been made of the radiation to be expected during the collision of two electrons either on classical or quantum theories. Suppose the energy was radiated as a single quantum in the direction in which the incident electron was travelling immediately before collision. Then consideration of the momentum and energy equations for the symmetrical case shows that with $\beta_1 = 0{\cdot}90$ it would be necessary for the incident electron to lose as much as 30 per cent. of its energy before the angle between the two arms of the fork departed from that calculated from (7) by 2°. Assuming, however, that the radiation could be emitted in any direction, the most favourable test would be the resultant general departure of the arms of the fork from coplanarity. It would be necessary in the most favourable case for the incident electron to lose only about 15 per cent. of its energy for the arms of the fork to depart from coplanarity by 5°. This is about twice the average estimated experimental error and such a deviation would therefore be easily detectable. The foregoing estimate assumes both electrons to share the momentum reaction of the departing radiation. If, however, it was confined to one electron, the least detectable radiation loss would be reduced approximately by one-half.

The last collision in Table I is observed to depart from coplanarity by about 10°. This collision is reproduced in Plate 13.

Another possible explanation of the non-coplanarity of the tracks in this case is that immediately after the collision one of the electrons passed close to a nucleus and underwent a nuclear bend which is not resolved on the photograph. It may be remarked, however, that nuclear bends are usually accompanied by an increase in the number of drops in the neighbourhood of the bend, due probably to the absorption of liberated radiation, and there is no evidence of this in the collision under discussion. Considering the total number of collisions measured, it would appear that if any considerable amount of energy is lost by radiation during close encounters, the number of such inelastic collisions is not greater than a few per cent. of the total number of collisions.

It is of interest to observe that Gray,* using β-particles from radium E has reported the excitation of γ-rays when the β-particles impinge on solid matter. In this case the collision is presumably with the comparatively massive nucleus and Skobelzyn,† using the expansion method, has obtained photographs of inelastic collisions of β-particles with nuclei. Several examples of this type of collision were observed in the present photographs. There is theoretical evidence‡ that a few per cent. of the total number of nuclear collisions are likely to be inelastic. However, the probability of radiation in an electron-electron collision is almost certainly less than in a nuclear collision, for the centre of mass of the system coincides with its electrical centre and there is thus no quantity analogous to a dipole moment. It is conceivable therefore that, in general, the system may be perfectly coupled, all the energy being used to accelerate the initially stationary electron.

Summary.

(1) An automatic expansion chamber was used to investigate the close collisions of fast β-particles with electrons.

(2) In all the cases examined, except one, momentum and energy were found to be conserved and the relations predicted by the restricted principle of relativity, found to hold accurately.

---

* 'Proc. Roy. Soc.,' A, vol. 85, p. 131 (1911); 'Proc. Roy. Soc.,' A, vol. 86, p. 513 (1912).

† 'Z. Physik,' vol. 43, p. 354 (1927).

‡ Kramers, 'Phil. Mag.,' vol. 46, p. 836 (1923); Gaunt, 'Phil. Trans.,' vol. 229, p. 163 (1930); Mott, 'Proc. Camb. Phil. Soc.,' vol. 27, p. 255 (1931).

(3) If any considerable amount of energy is lost as radiation during the encounters, it is estimated that it occurs in not more than a few per cent. of the total number of collisions.

The writer wishes to thank Lord Rutherford for his interest in the work and Mr. P. M. S. Blackett for constant encouragement and advice.

DESCRIPTION OF PHOTOGRAPHS.

PLATE 12.

The lower photograph shows a slow electron-electron collision; the angle between the two branches is observed to be about 90°.

The two upper photographs are paired photographs of a collision the measurements of which are given in No. 11, Table I. The angle in the left-hand photograph is almost the actual spatial angle and is observed to be much less than 90°.

PLATE 13.

Nos. 1*a* and 1*b* are paired photographs of two collisions which happened to occur on the same photograph, a very rare occurrence. The measurements for the left-hand collision are given in No. 9, Table I. The coplanarity of the three arms of the right-hand collision is strikingly shown in the left-hand photograph.

Nos. 2*a* and 2*b* show the collision the three arms of which are not coplanar.

On the Polarisation of Electrons by Scattering.

By E. G. DYMOND, M.A.

(Communicated by Lord Rutherford, O.M., F.R.S.—Received March 3, 1932.)

The possibility of demonstrating the spin of the electron directly has been discussed since the first growth of wave mechanical conceptions, and the ascription of a magnetic moment to the electron to explain doubling of spectral lines. Bohr has shown, however, that any experiment designed to do this by deflection in a magnetic field, in any manner similar to that used by Gerlach and Stern to measure the magnetic moment of atoms, must fail owing to the operation of the Uncertainty Principle. It does not seem, however, that this will hinder us from demonstrating an asymmetry in the electron by means of scattering experiments; the method is closely analogous to the asymmetric scattering of polarised light, and was in fact used by Barkla to show the polarisation of X-rays.

The earlier experiments which were carried out on the polarisation of electrons by Wolf,* by Joffé and Arsenieva† and by Davisson and Germer‡ all led to negative results. The very careful work of Davisson and Germer should be specially mentioned, in that they reflected electrons from the faces of single crystals at angles corresponding to coherent scattering of the waves. Working up to a velocity of 120 volts they found no asymmetry in the scattering more than ½ per cent., which was within the limit of error of the apparatus. Darwin§ has shown, however, that no polarisation is to be expected in this type of experiment.

The conditions under which a polarisation may be expected to be observed have been investigated by Mott,|| who, using the Dirac relativistic wave equation for the motion of the electron, calculated the intensity of scattering when an electron is deflected in turn by the fields of two nuclei. He finds that the number scattered by the second nucleus will vary with the angle which the plane of scattering makes with the initial direction of motion when :—

(*a*) the velocity of the electrons is comparable with the velocity of light;
(*b*) the angles of scattering at both nuclei are large;
(*c*) the atomic numbers of the scattering nuclei are large.

* 'Z. Physik,' vol. 52, p. 314 (1928).

† 'C. R. Acad. Sci. Paris.,' vol. 188, p. 152 (1929).

‡ 'Phys. Rev.,' vol. 33, p. 760 (1929).

§ 'Proc. Roy. Soc.,' A, vol. 120, p. 631 (1928).

|| 'Proc. Roy. Soc.,' A, vol. 124, p. 425 (1929).

Unless all these conditions are carried out, together with the implicit one that the scattering occurs only at the two nuclei and at no others, no polarisation is to be expected. An experimental arrangement to demonstrate the effect is shown diagrammatically in fig. 1.

Fast electrons strike a thin foil A of material of high atomic number, and a beam scattered through 90° is selected. The foil must be sufficiently thin to ensure that "multiple" scattering at this angle does not take place. The selected beam is again scattered through 90° at a second similar foil at B, and the twice scattered beam is measured.

If now the foil B and measuring apparatus be rotated about the line AB to the position shown by dotted lines, a change of intensity should be observed. Due to the use of approximations this change can only be calculated from Mott's paper (which contains misprints in the final result on p. 439) for elements of small atomic number, such as aluminium. The polarisation in this case is far too small to be measurable. Mott*, however, has recently given numerical values for the polarisation due to scattering in gold, and shows that the maximum change in intensity of 15 per cent. is to be expected at a velocity of the electron in the neighbourhood of 130 kilovolts.

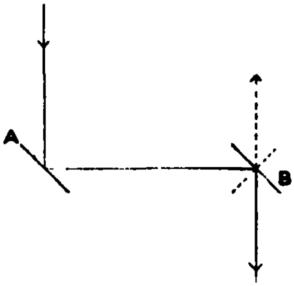

FIG. 1.

Chase† has carried out experiments with electrons of somewhat higher velocities (β rays), but finds no significant polarisation. But he scattered from solid targets where the deflections should be expected to be due to multiple scattering within the target, and the conditions laid down by Mott were not satisfied. Still less so were they in the work of Rupp, to be discussed later.

In the experiments to be described, these conditions have been observed as closely as possible, in order to provide a fair test of the theory, and as will be seen a polarisation has been observed—although this should still be accepted with some reserve—but the amount is markedly less than that predicted by Mott. A preliminary account of this work has already appeared.‡

General Description of Method.

It will be seen immediately that the necessity for the metal foils to be thin enough to ensure single nuclear scattering results in an exceedingly feeble final beam. If we calculate the intensity of this beam when twice scattered through 90° by commercial gold leaf, of thickness $< 10^{-5}$ cm., by means of the Rutherford formula, we find that for electrons of 100 KV. energy, the intensity must be about 10^{-12} of the initial beam, in the apparatus to be described. The Rutherford formula for scattering by an inverse square law field of force is not accurate in this region of velocity, but it has been shown by Mott (*loc. cit.*) to be correct as far as order of magnitude.

---

* 'Proc. Roy. Soc.,' A, vol. 135, p. 429 (1932).

† 'Phys. Rev.,' vol. 36, p. 1060 (1930).

‡ Dymond, 'Nature,' vol. 128, p. 149 (1931).

It is evident therefore that great precautions must be taken to eliminate stray effects due to X-rays, positive ions from residual gas, and secondary electrons removed by bombardment of the metal parts, as any of these may easily be of the same magnitude, or greater than the effect to be measured. The means whereby these disturbances were guarded against will be considered in detail later.

Apparatus.

Source of Electrons.—Electrons from a tungsten filament were accelerated to the required velocity in a tube of special design, developed in the Cavendish Laboratory, to withstand high voltages. It was very similar to that used by Cockcroft and Walton* as a rectifier. It was originally designed to withstand very much higher voltages than were actually used, and proved a source of considerable trouble.

The filament was mounted at one end of a long steel tube, partly surrounded by a larger tube which acted as anode. The lower ends of the tubes are shown in the drawing, fig. 2.

Due to the great length of the tube, the exact position of the filament could not be held constant, as the applied fields were sufficient to deflect the tube appreciably if it was not exactly central in the outer tube; also thermal expansion caused the filament to move slightly. As the placing of the filament inside the tube to protect it from the full field caused a focussing effect of the electron beam, a very small movement of the filament caused a larger movement of the focal spot, and therefore an alteration in intensity of the beam passing through the fine hole A. In the earlier part of this experiment mechanical vibrations were also a source of inconstancy in the beam, but these were eliminated later.

Scattering Chamber.—The beam was collimated by the two fine holes A and B, in aluminium. The large amount of heat liberated at the focal spot in the neighbourhood of the upper hole A was removed by water cooling ducts drilled in the large steel disc C. The two discs were ground flat, and could be moved relatively to each other to adjust the hole A under the focal spot.

---

* 'Proc. Roy. Soc.,' A, vol. 129, p. 477 (1930).

The gold foil D, cut from the thinnest commercial gold leaf, was of thickness 9×10^{-6} cm. and was mounted at 45° on an aluminium tube. The beam scattered through nearly 90° was allowed to pass out through a hole in a slightly larger tube to the second foil E. Two lead diaphragms F, 1 cm. thick, served to limit the beam and to absorb stray X-rays and secondary electrons. The second scattered beam passed through a hole G 1 mm. diameter in an aluminium disc to the Faraday cylinder H. The whole of the steel tube containing the second foil E and Faraday cylinder could be rotated about the axis DE, the tube working in a ground cone joint J, enabling the scattering in different azimuths relative to the initial beam to be examined. The position shown in the diagram is called henceforth the 180° azimuth.

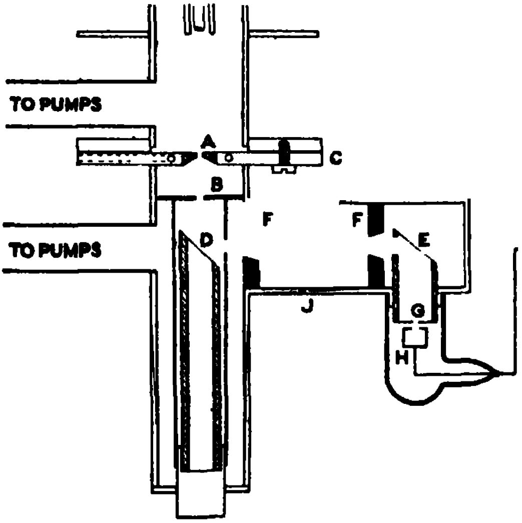

FIG. 2.

As a protection against slow secondary electrons and drifting positive ions reaching the Faraday cylinder, a thin aluminium foil, as free from holes as possible, was mounted immediately in front of the cylinder. Its thickness was 7×10^{-5} cm.; it was practically transparent to 70 KV. electrons, the fastest used, and only partly absorbed the slowest (20 KV.), while no slow electrons or positive ions were allowed to pass.

Electrical Measurements.

A Compton electrometer was used to measure the intensity of the scattered beams. In order to reduce the capacity of the leads, the electrometer was brought as close as possible to the rest of the apparatus. The situation on the second floor was subject to considerable vibration from a rotary converter in the neighbourhood and the passing traffic of the laboratory, so the electrometer was mounted on an antivibration support of the type designed by Müller.* It differs from the usual type of Julius suspension in that the supports are thin rods in compression, loaded nearly to the point of instability. It has the great advantage over the suspension type of support of great compactness and portability, and was found to behave satisfactorily in most exacting conditions. The electrometer was housed in a box sheathed with 3 mm. of lead to shield it from stray X-rays produced by the tube. The lead was extended to protect the whole of the leads and Faraday cylinder.

In order to measure the very small currents, high sensitivity of the electrometer was required; its potential sensitivity was between 6,000 and 20,000 divisions per volt.

Miscellaneous.

The pumping system for evacuation of the tube consisted of a fast diffusion pump filled with Burch oil† rendering the use of a liquid-air trap unnecessary, and a "Megavac" rotary oil backing pump.

The high-tension supply was drawn from a transformer and rectifier, smoothed by a condenser. The "ripple" of the rectified direct current amounted to 1 per cent. of the full voltage with a load of 1 milliampere. Voltage was measured with a "peak" voltmeter, which records the charging current of a condenser, one of whose plates is connected to the high tension side of the transformer. The rectified voltage will be less than that measured by an amount equal to the voltage drop, which was always small, in the valve. No great accuracy in the absolute voltage measurements was aimed at, as it was required rather to maintain constancy in the voltage than to know exactly what its value might be. Frequent calibration of the voltmeter against a sphere spark gap was made, and it is not expected that the measured voltages were in error by more than 2 per cent.

---

* 'Ann. Physik.,' vol. 1, p. 613 (1929).

† 'Proc. Roy. Soc.,' A, vol. 123, p. 271 (1929).

Possible Sources of Error.

It is obvious that with an apparatus of the type described, stray effects may be present to vitiate the experiment, owing to the very small asymmetry to be expected from polarisation of the beam; these effects must be examined carefully.

1. *Secondary Electrons.*—These are produced by bombardment of the various slits and limiting diaphragms. Their quantity was reduced as much as possible by placing aluminium at all points where such bombardment was likely. It is well known that by far the greater number of such electrons have quite small energies, and will fail to penetrate the aluminium window in front of the Faraday cylinder.

2. *Scattering of fast electrons* from other parts of the apparatus than the foils. Under this head are included the "secondary" electrons of large energy which can penetrate the aluminium window. The current reaching the electrometer from these was examined by removing successively the two foils D and E, and comparing with the currents when they were present. When D is broken, but E is in place, the current is less than 1 per cent. of the normal scattered current. When E is broken but D is in place, the amount was somewhat greater, of the order of 10 per cent. of the normal. The first experiment assures us that no part of the main electron beam reaches the electrometer, except after scattering from the first foil; the second, that the stray scattering from the surroundings of the second foil E, is not more than 10 per cent. of that due to the foil itself. It is of course not possible to estimate by this method the stray effect due to secondary emission from the beam from the first foil being scattered by the second foil. It is not likely, however, that the fast components of this secondary scattering, *i.e.*, the only part which can reach the Faraday cylinder, will be of the same order of magnitude as the beam which produces it.

3. *X-rays Produced at various Points of the Apparatus.*—These may liberate photoelectrons at any point along the scattered beams. Their effect was studied by interposing thin sheets of aluminium (thickness 0·03 cm.) in various parts of the beam. They will stop all electrons, but will allow X-rays, if present, to pass freely.

A sheet was first placed immediately in front of the Faraday cylinder. No deflection of the electrometer was observed even with the largest values of electron emission from the filament. Hence no X-rays were reaching the neighbourhood of the Faraday cylinder in measurable quantity. The aluminium was then placed between the two gold foils D and E, and was again found to cut down the electrometer deflection to zero.

It was concluded therefore that X-rays produced no measurable effects.

4. *Faulty geometry of the apparatus* produces a spurious asymmetry in the scattered beams.

It is impossible to ensure the exact symmetry of all the various diaphragms and foils in the path of the beam. Reliance was placed on accurate machining of the steel parts to cause the main beam, defined by the holes A and B, to strike the first foil D at a point on the axis of rotation of the ground joint J. This confidence proved misplaced. The natural asymmetry in the scattering was undesirably large, as will be seen in the results to be discussed. However, when the machining error had been discovered and rectified—unfortunately towards the close of the experiments—the natural asymmetry was very much reduced, but the polarisation effect was not altered. It should be noted that even with the most careful adjustment of the positions of the various diaphragms it is not possible to ensure perfect symmetry in the scattered beam, owing to the inhomogeneities of the gold foils. When examined under a low-power microscope, their thickness is found to vary considerably within small areas, due to the nature of the beating process in producing the foils. The thicker portions will scatter more strongly than the thinner ones, and if one of these thicker parts lies somewhat off the centre of the main beam from A and B, it will cause the scattered beam to lie somewhat off the true axis. By using many foils this effect should disappear in taking the mean values of the asymmetry over all the foils.

As the polarisation effect depends on the velocity of the electron, and was expected to be vanishingly small at 20 KV., any asymmetry in the scattered beams in the two azimuths 0° and 180° at that velocity may be assumed to be due to the apparatus, and the difference between this asymmetry and that found at 70 KV. may be taken as the amount due to polarisation. The extreme range of the natural asymmetry (20 KV.) was from 1·1 to 10·0 per cent., but it is difficult to see any correlation between the natural and the polarisation effects. It can be assumed, therefore, that the natural asymmetry can be compensated for completely by the method of combining observations.

5. *Fluctuations in the Intensity of the Original Beam.*—These fluctuations were a serious embarrassment, and could only be compensated by taking a very large number of readings. They were caused partly by the motion of the filament, as has been mentioned above, and partly by variation in the voltage of the supply mains. According to the Rutherford formula, the twice scattered

intensity is proportional to $1/V^4$ where V is the voltage. Consequently fluctuations in the supply voltage seriously affect the measurements. The electrometer was also responsible for some unsteadiness. The high sensitivity required to measure the small currents entails a loss of stability, which is more serious the less the current to be measured. The method of taking observations and combining them was as follows. The second foil and Faraday cylinder were set in the 0° azimuth, and, say, six readings of the time of charging of the electrometer between definite limits were taken, the electron velocity being 20 KV. The mean of the six readings was taken together with its probable error, calculated from the deviation of the readings. The process was repeated at 180° azimuth, and again at 0°. The azimuth was changed from 8 to 10 times, and then a fresh series at 70 KV. was taken. A further series at 20 KV. and again at 70 KV. was taken until the first foil D was punctured by the electron bombardment. The entire set of readings with one foil at the two velocities was called a group. The weighted mean of all the readings at 0° azimuth and 20 KV. was calculated, the weighting factors being the reciprocals of the squares of the probable errors; similarly the means for 180° at 20 KV. and for 0° and for 180° at 70 KV. were worked out. The mean asymmetry is the difference, expressed as a percentage, between the means at 0° and 180°, and its probable error is calculated by least squares from the deviation of the individual differences. The difference of the asymmetry at 20 KV. and 70 KV. gave the polarisation effect. The polarisation values of the various groups were combined in a similar manner, each value being weighted with its appropriate factor proportional to the reciprocal of the squared probable error.

This method of weighting the results is completely objective, and seems to be as little objectionable as any. Due to the great variation in the errors of the individual readings from day to day, some method of weighting the results was necessary. The standard methods of combining observations are necessarily arbitrary unless the number of readings dealt with is very large, a condition that rarely occurs in physical measurements, but no better methods are available. Perhaps the best that can be said in favour of this method of weighting is that in over 700 cases there was only one value obviously in discordance with the rest which was accorded a high weight. This particular value was discarded. Further, at the end of the analysis it was found that the unweighted mean did not differ from the weighted mean by more than twice the probable error of the latter. It is accordingly safe to assume that the order of magnitude of the effect found has not been influenced by the method of combining observations.

Table I.

Group.	20 K.V.	70 K.V.	Difference (= polarisation).
			per cent.
A	4·50 ± 0·57	6·10 ± 0·55	1·60 ± 0·79
B	6·76 ± 0·36	9·34 ± 0·64	2·58 ± 0·73
C	7·76 ± 0·51	11·42 ± 0·94	3·66 ± 1·07
(D	9·56 ± 0·18	18·92 ± 0·88	9·36 ± 0·90)
E	10·00 ± 0·40	10·53 ± 0·48	0·53 ± 0·62
F	5·41 ± 0·57	9·34 ± 0·30	3·93 ± 0·64
G	5·91 ± 0·09	7·22 ± 0·36	1·31 ± 0·37
	6·47 ± 0·32	7·22 ± 0·36	0·75 ± 0·48
H	4·59 ± 0·23	6·96 ± 0·48	1·37 ± 0·53
J	6·20 ± 0·21	10·69 ± 1·21	4·49 ± 1·23
O	3·58 ± 0·17	5·67 ± 0·39	2·09 ± 0·43
Q	6·60 ± 0·46	10·80 ± 0·48	4·20 ± 0·66
X	2·63 ± 0·14	3·28 ± 0·35	0·65 ± 0·38
Aa	1·07 ± 0·77	2·98 ± 0·83	1·91 ± 1·13
		Weighted mean	1·70 ± 0·33

The results are given in Table I. The first column gives the group letter. Each group, as mentioned above, corresponds to a replacement of one or both of the scattering foils or of the filament, and entails a partial dismounting of the diaphragm system. Errors consequent upon a possible orientation of crystals in the foils, it is reasonable to expect, have been eliminated by the use of a dozen foils. It should be noted that group D shows a result very discordant with all the others, and has not been included in deriving the final mean. The second column gives the values of the asymmetries at 20 KV. with their respective probable errors. It is assumed that these values are the natural asymmetries. The third column gives similar values for 70 KV., while the fourth, which gives the difference of the second and third, represents the actual polarisation.

It should be noted that in all cases the 0° azimuth has the greatest intensity. This direction is the same as that demanded by theory.

In order to provide a check on the truth of the above results experiments were made with the scattering foils of aluminium instead of gold. All asymmetries arising from geometry should not be changed by the use of aluminium, but Mott's work shows that the polarisation effect should be proportional to Z^2 where Z is the atomic number of the scattering nucleus. The intensity of scattering, however, varies as $1/Z^2$ (for double scattering), and it was not found possible to work with two aluminium foils. Accordingly only the second was aluminium (thickness 7×10^{-5} cm.). The results are shown in

Table II. The expected asymmetry is then in the ratio Z(Al)/Z(gold) (*i.e.*, 0·16) to that found for gold, and should be far too small to be measurable. The mean effect is less than the probable error, and it is therefore clear that there is no polarisation with aluminium as one of the scattered foils.

Table II.

Group.	20 K.V.	70 K.V.	Difference.
			per cent.
L	1·85 ± 0·61	2·50 ± 0·81	0·65 ± 1·01
M	3·91 ± 0·79	3·70 ± 0·56	−0·21 ± 0·97
N	9·61 ± 0·13	9·70 ± 0·34	+0·09 ± 0·36
U	11·08 ± 0·23	11·16 ± 0·57	+0·08 ± 0·61
		Weighted mean	0·11 ± 0·10

The results with aluminium lend strong support to the view that a real effect in the case of gold has been observed. In order to check this further, measurements were also made at the two azimuths 90° and 270°, which should give, apart from geometric effects, exactly equal beams for all velocities. This, however, proved not to be the case. Readings were taken at the two azimuths 90° and 270° successively in exactly the same way as with the previous azimuths 0° and 180°. An asymmetry in the two positions was found, of the same order of magnitude as that previously described. The actual values are shown in Table III.

It will be seen that there is a marked difference in character of the results. The sign of the effect is not constant. With some foils the 90° beam is the most intense, in others less so, while the effect of varying the velocity also is in opposite directions in different foils.

Table III.

Group.	20 K.V.	70 K.V.	Difference
			per cent.
P	− 1·33 ± 0·18	− 4·76 ± 0·30	− 3·43 ± 0·35
R	− 0·72 ± 0·20	− 1·89 ± 0·39	− 1·17 ± 0·44
S	− 0·45 ± 0·30	− 3·54 ± 0·51	− 3·09 ± 0·59
Y	+ 0·22 ± 0·24	+ 2·36 ± 0·80	+ 2·14 ± 0·84
Z	+ 1·85 ± 0·30	+ 3·36 ± 0·53	+ 1·51 ± 0·61
		Weighted mean	− 1·75 ± 0·98

A similar series of readings when one foil is aluminium is shown in Table IV. The convention in sign used is that an asymmetry is reckoned positive when the 90° beam is the stronger.

Table IV.

Group.	20 K.V.	70 K.V.	Difference.
			per cent.
T	− 2·04 ± 0·18	− 1·74 ± 0·48	+ 0·30 ± 0·51
V	− 1·50 ± 0·09	− 0·30 ± 0·38	1·20 ± 0·39
W	− 3·14 ± 0·43	− 0·13 ± 0·87	3·01 ± 0·97
		Weighted mean .	+ 1·97 ± 0·84

As will be seen from Table III, the mean difference is only slightly larger than the probable error, while the asymmetry when one foil is aluminium is twice the probable error. The results shown in Tables III and IV alone would emphatically lead to the conclusion that there is no real asymmetry between the two azimuths, in accordance with the theoretical predictions. The very much greater concordance of the results in the 0°–180° plane, where there is no single instance of a reversed sign, leads one to believe that here the asymmetry has a real significance. Nevertheless the behaviour of the apparatus in the 90°–270° is disturbing, as no reason can be given for the results found.

In order to explain an aymmetry in a plane at right angles to the direction of the initial beam of electrons, there must be some asymmetric influence on the electrons which is a function of their velocity, and whose sign is capable of reversal on dismantling and reassembling the apparatus. A stray magnetic field might cause such an effect, and its presence was not impossible in view of the fact that the whole body of the apparatus was constructed of steel.

However, at the end of the measurements a careful survey was made with a search coil and ballistic galvanometer of all the steel parts. The maximum flux in the neighbourhood of any of the steel parts was only of the order of 1 gauss, while within the tubes it was very much less, as might be expected from the shielding effect on the earth's field. No evidence, therefore, of permanent magnetism was found, and the very small fields that do exist can hardly influence electrons of the velocities used.

Discussion of Results.

The experimental value of the difference in the polarisation at 20 KV. and at 70 KV. is 1 · 70 per cent. As mentioned above, the results cannot be directly calculated from Mott's first paper, owing to a breaking down of approximations for scatterers of high atomic number. The numerical values which Mott* has calculated for this particular case of scattering by gold nuclei through 90° are shown in Table V.

Table V.

Velocity in kilovolts	10·5	25	45	79	127	204
Per cent. Polarisation	0·5	0·2	3·0	11·5	15·5	14

The interpolated difference in polarisations at 20 KV. and 70 KV. is 10 per cent. This is six times the experimental value. Certain factors influencing the experimental result should cause it to be too low rather than too high.† The most important is the effect of the inhomogeneity of the gold foils. As was mentioned above, these were commercial beaten leaves, and were by no means uniform in thickness, even over very small areas. Now it is necessary for the application of Mott's results that the scattering should be single, *i.e.*, that only one nucleus in each foil should be implicated. The use of Wenzel's‡ criterion for single scattering showed that the foils used—if of uniform thickness—were sufficiently thin to fulfil this condition, although no great reliance can be placed upon it. The margin of thickness was not very great, however, and it is highly probable that plural scattering can occur in the thicker portions. As the polarisation increases rapidly with scattering angle, plural scattering, in which the electron is deflected on the average through several smaller angles in succession, should give rise to little or no polarisation. Consequently the plurally scattered electrons should show no asymmetry, and tend to dilute the effect of the single scattered electrons. If other secondary effects have not been sufficiently compensated for, a similar result would ensue Although it is not possible to estimate the influence of plural scattering, it does not seem likely that it can be called upon to bridge the gulf between the experimental and theoretical values. The experiments, however, are being continued with foils of uniform thickness produced by the sputtering process, and it is hoped they will clear up the ambiguity of the results. On the theoretical side, no hopes are entertained that a lower value may be the correct one. Mott points out that the Dirac relativistic wave equation leads to the correct solution of the energy states in a Coulomb field, and it is not likely to fail in the problem under discussion.

---

* 'Proc. Roy. Soc.,' A, vol. 135, p. 429 (1932).

† It may be mentioned here that the unweighted mean of the results shown in Table I is 2·24 per cent.

‡ 'Ann. Physik.' vol. 69, p. 335 (1922).

Mention must also be made of the experiments of Rupp* and of Rupp and Szilard.† Their method consisted of scattering electrons of 220 KV. energy through 90° at a solid target of gold (not a thin foil), and then causing the beam to pass through a very thin foil arranged normally to the scattered beam. The diffraction rings due to interference in the second foil were observed photographically, and were found to have marked differences in intensity round their circumference. Due to the photographic method no quantitative measure of the asymmetry is given, but it is necessarily much greater than that found in the work described here. An exhaustive comparison of the two methods cannot be made here, partly in view of the fact that no detailed description of Rupp's experiments, with the precautions used to obviate stray effects, has yet appeared. It should, however, be mentioned, firstly, that the theoretical work of Mott is obviously not relevant in this case, as the second scattering angle is very small; and secondly, that while the "polariser" of Rupp is similar to that here used, the "analyser" is different. G. P. Thomson‡ and Kirchner§ have carried out experiments in which both "polariser" and "analyser" were similar to Rupp's, *i.e.*, thin films from which the small angle coherent scattering is utilised. Neither worker found any asymmetry in the diffraction rings which could be assigned to a polarisation phenomenon. As their work was carried out at lower velocities (65 KV.), agreement between the various experimental results can only be made by postulating a rapid rise in the polarisation after a velocity of 70 KV. or so. As will be seen from a reference to Table V, such a rise is not expected, and the final conclusion on the present evidence is that there is no concordance with theoretical expectations. The polarisation found by Rupp is many orders of magnitude greater, while that found in the work here described is some six times smaller than the value which we are led to expect from theoretical considerations.

Summary.

A direct experimental test of the conclusions reached by Mott on the scattering of fast electrons by single nuclei has been made. Electrons of a maximum velocity of 70 KV. are scattered successively through 90° by thin gold foils, and a change in the intensity is looked for as the azimuth of the second scattered beam is altered. As the change looked for is very small, precautions must be taken to eliminate all stray effects due to X-rays, secondary electrons, and faulty alignment of the apparatus. These precautions are discussed in detail.

---

* 'Naturwiss.,' vol. 19, p. 109 (1931).

† 'Naturwiss.,' vol. 19, p. 423 (1931).

‡ 'Nature,' vol. 126, p. 842 (1930).

§ 'Phys. Z.,' vol. 31, p. 772 (1930).

The polarisation effect found is $1 \cdot 7 \pm 0 \cdot 3$ per cent. That predicted by Mott is 10 per cent. The polarisation when a light scatterer (aluminium) is substituted for gold is shown to be negligible, confirming the view that the effect found is a true one. Reasons are given to show that the experimental value is likely to be too low rather than too high, but it is not anticipated that it can be so high as 10 per cent.

An unexplained asymmetry in the direction at right angles to the initial beam is also found, but its magnitude and direction are not constant, and it is doubtful whether it has real significance.

On the Photographic Action of Slow Electrons.

By R. Whiddington, F.R.S., and J. E. Taylor, B.Sc., University of Leeds.

(Received March 2, 1932.)

[Plate 14.]

Introduction.

The fact that fast moving electrons have a blackening effect on photographic emulsion has been known for a quarter of a century and many investigators have utilised this important property in their researches.

In the important fields of β-ray and X-ray electron investigation, for example, electron spectra have been recorded photographically, Innes* leading the way in 1907, followed amongst others, by Robinson and Rawlinson,† de Broglie‡ and Whiddington.§ Within the last year or two, G. P. Thomson and Reid‖ have also used this method for the recording of electron diffraction patterns.

---

* 'Proc. Roy. Soc.,' A, vol. 79, p. 442 (1907).

† 'Phil. Mag.,' vol. 28, p. 277 (1914).

‡ 'J. Physique,' vol. 2, p. 265 (1921).

§ 'Phil. Mag.,' vol. 43, p. 1116 (1922).

‖ 'Nature,' vol. 119, p. 890 (1927).

In 1922 one of us (R.W.) in the course of some experiments on low speed electrons found it necessary to increase the sensitiveness of photographic films to electrons of about "50 volts velocity." This led to a qualitative investigation by Brett,[*] in this laboratory, of the sensitising effect of a superimposed film of oil, and the working out of a suitable technique for its application.

This method where applicable is preferable, in our experience, to that of Schumann[†] as used, for example, by Duclaux and Jeantet[‡] in which, by the use of acid, the gelatin of the film is partially removed, as in this latter method the technique is so troublesome and the results inconsistent.

Brett's results showed that in the neighbourhood of 60 volts a great increase in sensitiveness of the plate resulted from the use of a thin coating of some fluorescent grease, such as vaseline.

Cole's[§] qualitative experiments confirmed these results and in addition brought out the not surprising point that, as with light, different plates have different sensitivenesses to a definite current of electrons of given speed.

Carr[||] continued Cole's qualitative work using electrons generated at less than 35 volts and extended the work in a specially interesting direction. He found that it was possible to use a gold or silver plate instead of a photographic film, developing the image by means of an atmosphere of mercury vapour. One of the advantages of such a method is that the metal plate has high conductivity and there is therefore no possibility of the incident electrons diffusing over the plate as a result of electrostatic charges on its surface. This effect certainly occurs in a very disturbing manner with ordinary photographic films and plates when large electron current densities are used.

Little experimental work appears to have been carried out on the law of blackening of photographic plates by slow electrons along lines similar to the well investigated case of light blackening, although Seitz and Harig[¶] investigated the photographic blackening produced by electrons generated at 1500 to 18,500 volts and found that for low current densities the photographic density was proportional to log It, where I was the electron current and t the time of exposure.

There seems to be little information available for low velocity electrons in the region of 100 volts and the present experiments were carried out in order to obtain data within a comparatively narrow range of electron velocity and for a particular type of photographic film which is being used in this laboratory for certain electron recording experiments.

---

[*] 'Proc. Leeds Phil. Lit. Soc.,' vol. 1, p. 1 (1925).

[†] 'Ann. Physik,' vol. 5, p. 349 (1901).

[‡] 'J. Physique,' vol. 2, p. 156 (1921).

[§] 'Phys. Rev.,' vol. 28, p. 781 (1926).

[||] 'Rev. Sci. Inst.,' vol. 1, p. 711 (1930).

[¶] 'Phys. Z.,' vol. 30, p. 758 (1929).

This investigation, therefore, does not aim at completeness, but adequate information has been obtained for the purpose in view and it seems to be of sufficient general interest to place on record.

The Apparatus.

The apparatus is arranged to produce an electron beam of uniform and measurable current density which can be directed at will on selected parts of a photographic film. These two main parts of the apparatus termed the gun and the camera respectively are shown diagrammatically in fig. 1.

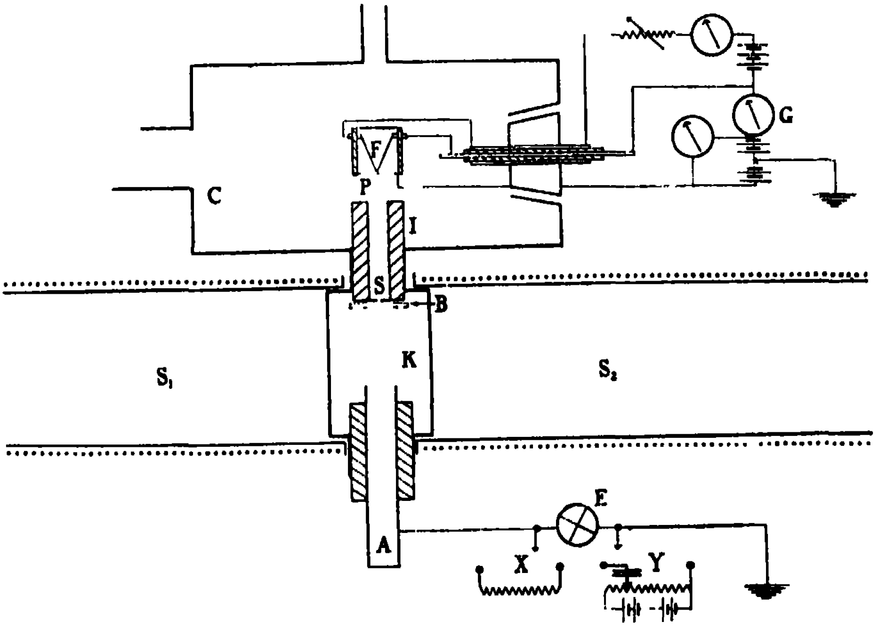

Fig. 1.

The electron beam itself is produced from a heated filament F placed very near a wire grid P, maintained at a suitable potential. An insulating quartz cylinder 1 cm. in diameter and 1·5 cm. long forms the mechanical base. This brass gun is mounted on a brass ground joint which permits orientation in the vacuum within the containing cylinder C.

The electron beam is directed along the axis of the iron cylinder I which carried a correctly aligned slit S at its far end. The camera, K, is just a rectangular box of substantially the same construction and size as that previously described by one of us (R.W.),* but in this case used in conjunction with a long split solenoid S_1 S_2 which gives a substantially uniform magnetic field over the greater part of the camera.

The current in this solenoid could be adjusted (by means not shown in the diagram) so as to deflect the electron beam emerging from the slit S on to a photographic film placed in the guides B which must be understood to run at right angles to the plane of the diagram. Under such circumstances the marks which appear on the film are due only to deflected electrons and are not caused by any light emerging from the slit, which will be collected by the cylinder A.

The cylinder A fulfilled another purpose, which is mentioned later, as it was insulated and connected to an electrometer in order to act as a Faraday collecter.

A high vacuum was produced in the gun-camera system by means of a Pfeiffer oil pump and a mercury vapour diffusion pump. A pressure less than 0·0001 mm. mercury was readily and rapidly attained after degassing of the metal parts of the apparatus had been carried out. "Apiezon" low vapour pressure grease was used for the joints.

The electrical circuits were of the simplest character and are sufficiently indicated by fig. 1. They comprised (1) the filament heating circuit; (2) the anode circuit, in which an accelerating potential up to 300 volts produces an emission current of strength measured by the galvanometer G; and (3) the Faraday cylinder A which, connected to one of the two alternative sub-circuits X or Y, could measure "beam currents" over a sufficiently large range down to 10^{-13} amperes, using a frequently calibrated Lindemann electrometer.

Preliminary Investigations.

It was soon found that there was no easily discoverable relation between the emission current measured by G and the beam current entering A† (zero field in S_1 S_2) and measured by E. This was not unexpected, although for obvious reasons there was still some advantage accruing from including G in the circuit.

---

* Jones and Whiddington, 'Phil. Mag.,' vol. 6, p. 889 (1928).

† Previous close investigation by Dr. Seddon in this laboratory had shown that for this purpose the right dimensions for this cylinder were 8 cm. long and 0·7 cm. diameter.

It was, therefore, necessary always to use the A circuit for measuring the beam current, thereafter switching it round by the magnetic field of S_1 S_2 on to the film F for the required time of exposure.

The kind of photograph obtained is shown in fig. 2, Plate 14. This spectrum clearly shows that, while at the expected position (1) there is a sharply defined slit image due to electrons which have a speed corresponding to the accelerating voltage between F and P, yet there is in addition another, less well marked band (2) in a lower velocity position on the film. This is a well-known effect due to the emission of secondary electrons by the primary ones at various points along their paths. It is clear, then, that these electrons will also be included in the reading of A when the magnetic field is zero, although they cannot contribute to the density of the line (1) in the photograph.

This matter was set right by applying a sufficiently large retarding potential on A to turn back these lower speed electrons, the high speed flight only being registered in this case by E.

The necessary minimum value of this retarding potential was obtained from a curve of the type shown in fig. 3. Here, beam current in arbitrary units, is plotted against retarding potential in volts. It is clear that in the case of an accelerating voltage (F to P) of about 193 volts, about 100 volts retarding potential on A is necessary in order to ensure a correct reading in E.

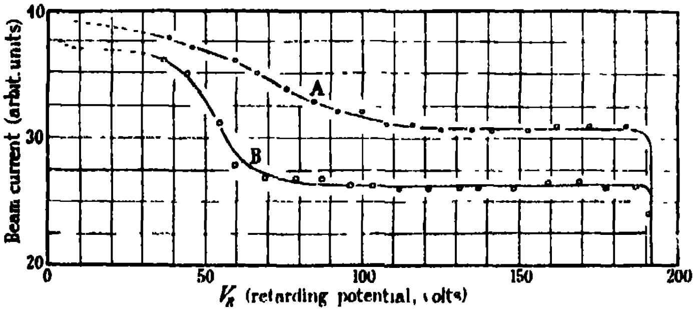

FIG. 3.

In fig. 3 the upper curve (A) was taken with the edges of S clean and bright—in the lower curve (B) the same slit was covered with a soot deposit. The curve (B) is clearly representative of a better velocity distribution, in that the long horizontal part of the curve means an entire absence of unwanted electrons within the range 70 to 193 volts. Soot covered slits were therefore always used. This procedure never completely prevented the production of low velocity secondaries, but they were not troublesome, being recorded on the film at some distance from the important area (1) of fig. 2, Plate 14.

It was found convenient to remove the retarding potential on A when the photographic exposure was in operation.

Method of Experiment.

Broadly speaking, the method of experiment was to measure first the beam current I in the manner described, then to turn on a steady magnetic field for a time t, which produced on development a line of density D as measured by the photometer. It is the relation between D, t and I which is sought.

It is necessary now to give a brief summary of the precautions taken in regard to development and photometry.

The technique previously worked out by many investigators for ordinary light photography was closely followed.*

Development was carried out for a fixed time in a vigorously stirred vertical tube placed in a large thermostatically controlled bath kept at 20° ± 0·1° C.†

The following metol quinol developer was employed :—

Metol................	0·7 gm.	Pot. Brom.	0·2 gm.
Hydroquinone	1·4 gm.	Sod. Carb.	10·0 gm.
Sod. Sulph.	10·0 gm.	Water up to	1200 c.c.

Fixing and lengthy washing were carried out in the usual way.

The photometry presented some initial difficulties. But the final arrangement comprised a half watt lamp run at about two-thirds its normal voltage, in train with a good optical condensing system, a narrow slit, a photoelectric cell and Lindemann electrometer.

The light absorption in the film was recorded by the electrometer and D was evaluated from the formula

$$D = \log_{10} C_0/C,$$

where

C_0 = electrometer current when the clear part of the film was in the path of the light.

C = electrometer current when the exposed part of the film was in path of the light.

In the measurement of C, care was taken to ensure a linear relation between electrometer reading and current. Densities were also checked by the use of an optical wedge.

---

* Dobson, Griffith and Harrison, "Photographic Photometry."

† We are indebted to Mr. Hume, of the Chemical Department, for valuable help in setting up this thermostat.

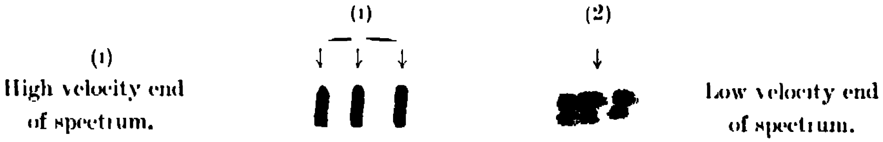

(i) Three separate exposures of equal intensity with different magnetic fields. Note: Clear-cut broad lines and low velocity band at (2).

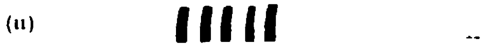

(ii) Slit sooted, well-defined lines of different electron intensity with different magnetic fields. Very little low velocity band.

FIG. 2.

In order to test the working of the whole apparatus, a set of lines was produced on the film, fig. 2, (i), Plate 14, the position of each exposure on the film being altered by varying the magnetic field slightly. The values of I and t were kept constant.

A typical case gave the following values :—

$$D = 0{\cdot}34\,;\ 0{\cdot}35\,;\ 0{\cdot}35$$

for three exposures on the one film close together.

Experiments of this sort showed that it was definitely possible to ensure repetition on the same film of identical exposures so as to yield substantially the same values of D.

Similar experiments comparing densities on different strips cut from the same sheet showed somewhat larger variations of D up to about 8 per cent.—but it was observed that when films cut from different film batches were tried, there were much larger variations.

It was very soon found that the well-known empirical light law connecting D, I and t held with some accuracy.

This law states that

$$D = \gamma \,.\, \log It^{p} - i,^{*}$$

where

D is the density or blackening, measured photometrically and expressed by $\log_{10} \dfrac{\text{incident light}}{\text{transmitted light}}$.

γ is a constant if the method of development and the nature of the light do not vary.

I is the intensity of the light incident on the film.

t is the time of exposure.

p is "Schwarzchild's constant."

i is the "inertia" of the plate or film.

In the case of electron blackening of the film, it is only necessary to replace I by electron beam current and D by $\log_{10} C_0/C$ and the formula holds but, of course, with different values for the constants p, i and γ.

The evaluation of the constants was not difficult from the experimental results and the following procedure was followed.

Observations were first taken keeping I constant, varying only t. From the

---

[*] Dobson, Griffiths and Harrison (*loc. cit.*).

values of D emerging, a curve was drawn showing D against $\log t$. It was a straight line. The above formula therefore holds if I is constant.

But if on a film giving the result just described with intensity (I_A) constant, another line be placed with a different intensity (I_B) which, with an exposure t_B gives a density D_B within the range of observation, then it is possible to choose a point on the curve just described for which there is an equal density corresponding to time t_A and intensity I_A. In which case clearly

$$\log I_A t_A^{\,p} = \log I_B t_B^{\,p},$$

and therefore

$$p = \frac{\log I_A - \log I_B}{\log t_B - \log t_A}.$$

The value of γ was obtained by investigating the relation between D and $\log I$, keeping t constant. This curve was also found to be linear, and γ was obtained at once from the slope of the curve, since

$$D = \gamma \,.\, \log I + \gamma p \log t - i,$$

and the last two terms in this equation are constant. Moreover, if $D = 0$; $i = \gamma \log I + \gamma p \log t$, where $\log I$ is the intercept and t the constant value of the exposure in the experiments.

The following table gives the results obtained using "Imperial Duoplex" film, the probable mean error also being indicated. In fig. 4 is exhibited in graphical form some of the results incorporated in the table, the smooth curve being that calculated for the formula $D = 0{\cdot}31 \log It^{0\cdot88} - 0{\cdot}47$.

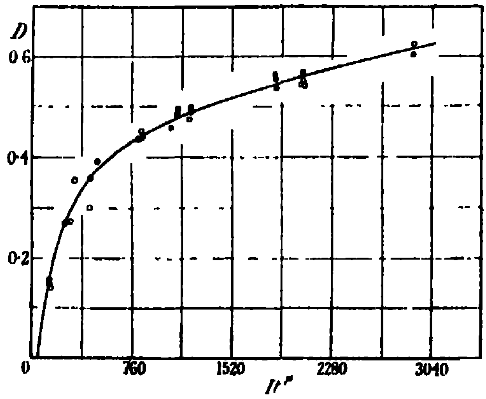

FIG. 4.—Continuous curve represents $D = 0{\cdot}31 \log It^{0\cdot88} - 0{\cdot}47$.

p.	i.	γ.	
0·88 ± 0·01	0·47 ± 0·03	0·31 + 0·01	Electrons—Film untreated.
0·90 ± 0·02	0·17 ± 0·01	0·27 ± 0·01	Electrons—Film oiled.
0·86	—	0·41	Li

It is to be noted that γ and p are ratios and independent of the units of I and t. In the case of i, however, which here has the value of 0·47, the units of I and t are respectively ampères per square centimetre $\times 10^{-8}$ and seconds.

It is to be noted that the range of D was sevenfold, and that the relations hold over more than a hundredfold variation of I and of t.

Examination of the above table of results brings out that the value of the constants p and γ do not change much for electrons striking an oiled or an untreated film. The increased sensitiveness for the oiled film being expressed in the formula by a large reduction in i—the so-called "inertia" of the film. To give a numerical idea of this increased sensitiveness; a certain I for exposure time 60 seconds gave a certain D on an untreated film; an oiled film would give the same D for the same I in only 5 seconds.

It is of interest finally, to record the important fact that whether oiled or untreated films be used, there is no observable change in D with the velocity of the electron beam at any rate between 60 and 300 volts. On the view that the increased sensitiveness of an oiled film is due to fluorescence of the oil, this result is readily understood. The investigations of Harrison and Leighton* show that when fluorescence is evoked by incident light of varying frequency, the number of quanta emitted is proportional only to the number incident and independent of the frequency. In the present case, assuming the electron energy to be far in excess of the excitation value, the number of quanta emitted by the oil (fluorescent light intensity) will be proportional only to the number of incident electrons and not on their energy—the result observed—thus the film is to be regarded as "panchromatic" within the above-mentioned range.

Comparison of Photographic Action of Electrons of Different Velocities.

It may not be out of place to compare now the photographic effects of electrons over the whole range of energy so far examined by different investigators. This can however only be done in a very general way, since the effects depend to some extent on the nature of the photographic emulsion.

---

* 'Phys. Rev.,' vol. 38, p. 899 (1931).

The earlier attempts at accurate measurement in the case of electrons were confined to the β-rays from radioactive preparations and Bothe* examining heterogeneous β-rays found the Reciprocity Law held, namely that $D = f(It)$ which furnished a linear characteristic curve up to values of 0·5 for D.

This result was not entirely confirmed by Salbach† or by Ellis and Wooster,‡ the latter, however, found that the Reciprocity Law held, suggesting the formula

$$D = C \log (It/\tau + 1)$$

as expressing closely enough the characteristic curve which, under the conditions of their experiments was linear up to $D = 0{\cdot}3$, the form of the curve being independent of the velocity.

This latter point was investigated in further detail by Ellis and G. H. Aston§ who found a very rapid change of photographic action with electron velocity.

The results of the present experiments show that within the region of electron velocity, between 60 and 300 volts, the simple reciprocity law does not hold, but that a law of the Schwarzchild type $D = f(It^p)$ must be employed, as in the case of light.

The value of p is sufficiently far from unity to make the difference between the Reciprocity and Schwarzchild relations very marked.

A further difference between the slow electrons and the faster β-rays lies in the fact that within the region considered there is no change in photographic action with velocity. This no doubt depends on the fact that in the case of the faster particles, owing to their high penetrating power, only part of the available energy is used within the film, whereas the slower particles used in our experiment are wholly absorbed and of the whole energy of the slower particles again, only a definite amount, in the case of each particle, is employed in photographic action.

If it be supposed further that this definite energy acts in a secondary manner on the emulsion viâ fluorescence excitation, it can be understood that a relation of the Schwarzchild type might be required to explain the facts.

Acknowledgments.

It is a pleasure to record the fact that one of us (J.E.T.) is in receipt of a maintenance grant for a student in training from the Department of Scientific

---

* 'Z. Physik,' vol. 2, p. 243 (1922).

† 'Z. Physik,' vol. 2, p. 107 (1922).

‡ 'Proc. Roy. Soc.,' A, vol. 114, p. 266 (1927).

§ 'Proc. Roy. Soc.,' A, vol. 119, p. 645 (1928).

and Industrial Research and that some of the apparatus was purchased out of a grant from the Royal Society.

Summary.

The photographic action of electrons (60–300 volts) has been experimentally investigated in the case of " Imperial Duoplex " films.

The considerable increase in sensitiveness previously discovered on oiling the film surfaces has been found to be associated mainly with a diminution of the value of i in the formula

$$D = \gamma \, . \log It^{p} - i,$$

where

D is the density or blackening, measured photometrically and expressed by $\log_{10} \frac{\text{incident light}}{\text{transmitted light.}}$

I is the intensity of the light incident on the film.

t is the time of exposure.

p is " Shwarzchild's constant."

i is the " inertia " of the plate or film.

The constants have the following values :—

p.	i.	γ.	
0·88 ± 0·01	0·47 ± 0·03	0·31 ± 0·01	Electrons—Film untreated.
0·90 ± 0·02	0·17 ± 0·01	0·27 ± 0·01	Electrons—Film oiled.
0·86	—	0·41	Light.

The results in this table are based on the units, seconds and ampères per square centimetre × 10^{-8} for t and I respectively.

It has been found that these constants are independent of the velocity of the electrons within the range considered.

The evidence in favour of the sensitising effect of the oil being due to fluorescence is mentioned.

A preliminary account of this work was published in 1931 in the ' Proceedings of the Leeds Philosophical Society.'[*]

---

[*] Whiddington and Taylor, ' Proc. Leeds Phil. Lit. Soc.,' vol. 2, p. 264 (1931).

[*Note added.*—Since writing the preceding we have seen a paper by Herr Valentin Weidner, of Heidelberg, entitled "die photographische Wirkung langsamer Kathodenstrahlen," 'Ann. Physik.,' vol. 12, p. 239 (1932).

This author has investigated in some detail the photographic action of electrons of speeds between 30 and 1100 volts. The plates he used were not the same as ours and he finds a simple reciprocity law of blackening instead of the more complicated form which we find necessary. This difference may be due to the different emulsion, but it is rather difficult to see how the agreement that between 60 and 300 volts the blackening is independent of electron energy, fits in with this supposition.]

The Nature of the Interaction between Gamma-Radiation and the Atomic Nucleus.

By L. H. Gray, Ph.D., Fellow of Trinity College, Cambridge, and
G. T. P. Tarrant, M.A., Pembroke College, Cambridge.

(Communicated by Lord Rutherford, O.M., F.R.S.—Received April 14, 1932.)

§ 1. *Introduction.*

A number of independent investigations by Chao,* Meitner and Hupfeld,† and Tarrant,‡ have shown that the absorption of strongly filtered thorium C″ γ-rays, both in magnitude and in the manner of its variation with the atomic number of the absorbing element, was in definite disaccord with what was independently known concerning the absorption of γ-rays by extra-nuclear electronic systems. The additional absorption was attributed to interaction with the nuclei of the atoms concerned. In the case of quantum energies as high as 2½ million electron-volts, interaction with a heavy nucleus is quite important. In lead, for example, it accounts for 20 per cent. of the total absorbing power of the atom. The amount of energy absorbed by a nucleus is roughly proportional to the square of its atomic number, and from the investigations of Jacobson* and Tarrant,† it appears that the absorption increases regularly from element to element.

---

* 'Proc. Nat. Acad. Sci. Wash.,' vol. 16, p. 431 (1930).

† 'Z. Physik,' vol. 67, p. 147 (1930).

‡ 'Proc. Roy. Soc.,' A, vol. 128, p. 345 (1930).

The object of the present investigation was to discover something of the nature of this interaction between the quantum and the nucleus. It was evident that the whole of the absorbed energy was not re-radiated without change of wave-length, since no certain difference was observed‡ between the intensity of the secondary radiations from heavy and light elements within the angular range 10° to 30°, although the conditions were such that if a third of the energy absorbed by the nucleus had been re-radiated with uniform angular distribution and without change of wave-length it could have been detected with certainty.

If any part of the energy is emitted as a quantum radiation it will clearly be most easily detected in the backward direction, where there is least chance of confusion with Compton scattered radiation. The secondary γ-ray emission in the backward direction has often been investigated, but until recently the conditions have never been such as to favour the detection of any secondary emission of nuclear origin—either because the element irradiated was of low atomic number, or because the absorption coefficient of the secondary radiation was measured with insufficient filtering to eliminate the Compton scattered radiation. The *first definite evidence for the emission of secondary radiation* of nuclear origin was obtained by Chao,§ who investigated the relative intensity, and the hardness of the secondary emission from aluminium and lead over a wide range of angles. He found that in addition to Compton scattered radiation, there was present, in the case of lead, a radiation of wave-length $\lambda \sim 22$ X.U. emitted in roughly the same intensity in all directions. Meitner and Hupfeld,‖ on the other hand, from a study of the absorption in copper of the secondary emission from lead and aluminium, were led to conclude that, if the absorption curve could be followed to sufficiently great thicknesses, the radiation emitted at 90° might be found to consist of a mixture of Compton radiation and radiation of primary hardness.

The starting point of our own investigation (commenced before the publication of Chao's results) was a careful study of the secondary radiation emitted by lead at angles of 125° and 145° with the primary radiation.

---

* 'Z. Physik,' vol. 70, p. 145 (1931).

† 'Proc. Roy. Soc.,' A, vol. 135, p. 223 (1932).

‡ L. H. Gray, 'Proc. Roy. Soc.,' A, vol. 130, p. 524 (1931).

§ 'Phys. Rev.,' vol. 36, p. 1519 (1930).

‖ 'Naturwiss.,' vol. 19, p. 775 (1931). See, however, the footnote on p. 667.

§ 2. *Study of the Secondary Radiation from Lead at* 125° *and* 145°.

The problem which confronts us in the study of the abnormal secondary radiation from lead and other elements is that of investigating a radiation which is only part of the total secondary γ-ray emission, and which is itself very weak, if thorium C″ γ-rays are used to excite the nucleus, on account of the weak radiothorium sources available for experiment. Confusion with the ordinary scattered radiation is almost entirely eliminated by examining the secondary radiation at large angles, since not only is the Compton radiation relatively very much weaker, but there is the additional advantage that, having suffered a large increase in wave-length, it is comparatively soft, and is easily absorbed in the radiator itself or in a very small thickness of absorber.

The minimum dimensions of the apparatus are fixed ultimately by the necessity of shielding the measuring apparatus from the direct radiation from the source. This can only be done adequately by the interposition of some 30 cm. of lead. For the investigation of the secondary radiation within a limited angular range, the most advantageous and practicable arrangement of apparatus seems to be that in which the radiator is cylindrical, and the source and ionisation chamber are situated on the axis of the cylinder, being separated by a cone of lead as shown in fig. 1, which is a scale diagram of the apparatus employed for the investigation at 125°.

The cylindrical form of the radiator made it possible to meet the difficulty of the intrinsic smallness of the effects by the use of a large mass of the material (100–200 kilos.) to be investigated. Even so, the initial intensity of the secondary radiation from lead was only such as to give rise to an ionisation in the chamber of about 100 ions per cubic centimetre per second at atmospheric pressure. This was augmented some 50 times by the use of a steel ionisation chamber containing nitrogen at 100 atmospheres pressure.* Since the smallest currents measured, viz., 20J* were only about a fifth of the ionisation due to penetrating radiation, it was sometimes necessary to allow for the variation of the intensity of this radiation with barometic pressure. Any possible diurnal variation was eliminated by taking measurements with and without the radiator in position, in inverse order on successive days. The source was situated in the position shown, at the base of a lead cone 30 cm. high, which reduced the radiation passing direct to the chamber to a negligible

---

* A large inner electrode was used so as to produce a reasonably large field (from 30 to 210 volts per centimetre) with a potential difference of 400 volts between the electrode and the walls, since it is exceedingly difficult even to approach "saturation currents" in ionisation chambers containing gas at very high pressures. The detailed mechanism of the production and collection of ions in these chambers is at present very imperfectly understood. Specific tests were made to ascertain whether the ionisation is proportional to the intensity of the incident radiation, by comparing the ionisation produced by two sources together with the sum of their separate intensities. The results agree with those of Broxon ('Phys. Rev.,' vol. 37, p. 1320 (1931)) in showing that, for the voltage employed in the experiment, the ionisation produced in these chambers is a reliable measure of the intensity of the radiation, which is all that is required for the present investigation.

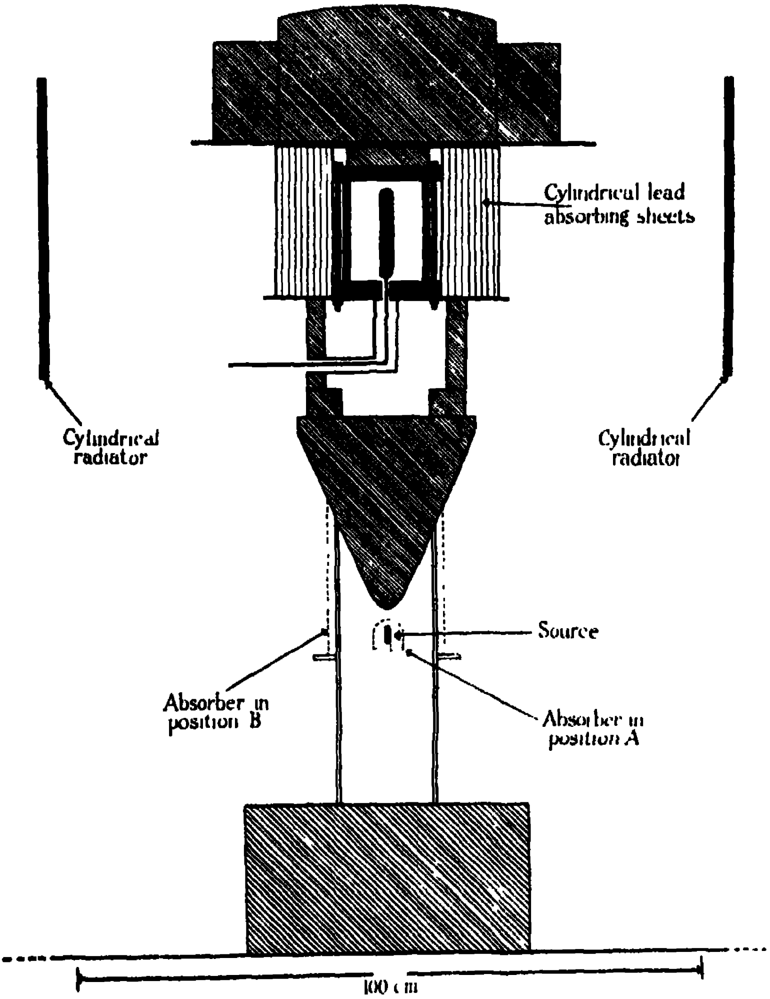

FIG. 1.

---

* Throughout this paper ionisation currents will be expressed in terms of the unit "J," which is the rate of production of 1 ion per cubic centimetre per second at the pressure existing in the chamber, viz., about 100 atmospheres.

intensity. The secondary radiation reaching the chamber proceeded from the radiator* in a direction making an angle 125° ± 15° with that of the primary radiation from the source. The absorption of the secondary radiation was always studied in lead, which was in the form of sheets 0·15 cm. thick, placed immediately round the chamber. As is well known, the apparent absorption coefficient of hard γ-radiation measured by placing the absorber close to the ionisation chamber is markedly smaller than the true absorption coefficient, on account of the fact that a considerable proportion of the energy scattered by the absorber enters the chamber. On the other hand, the absorption observed with our particular experimental disposition will be greater than that corresponding to the (radial) thickness of the absorber, both on account of the cylindrical form of the chamber and absorbers, and because the radiation entering the chamber is in general inclined at a small angle to the horizontal. These points have been carefully considered, both theoretically and experimentally, and appropriate corrections have been deduced.

The lead was irradiated by the unfiltered γ-rays from a radiothorium source (30 mgm. activity), kindly lent by Dr. C. D. Ellis. The ionisation was measured† as the thickness of the absorber was increased in steps up to 4·5 cm. of lead, with the results shown in curve 1, fig. 2.

It happens that, in the case of the lead radiator, the fully corrected and the uncorrected curves are nearly identical. Since we are not, at present, concerned with the absolute values of the absorption coefficients, the present discussion is based on the uncorrected curves.

It is evident, in the first place, that the radiation is not monochromatic. The absorption curve corresponds roughly with that of a mixture of the two radiations of absorption coefficients 0·85 cm.$^{-1}$ and 1·9 cm.$^{-1}$ in the proportion (by energy) of 1 : 2. The corresponding wave-lengths and energies‡ are

---

* In the earlier measurements which were concerned chiefly with the secondary radiation from lead, the material, in the form of sheets of "old lead," was bolted on to an iron frame-work which always remained in position supported by four brick pillars. In the later measurements, the radiator was lowered into position by means of a block and tackle, thus obviating the necessity for the brick supports. This procedure has the great advantage that measurements with and without the radiator in position could be made in quick succession.

† We are indebted to Dr. Feather and Mr. Lea for assisting us with some of the measurements.

‡ The absorption coefficients have been interpreted by means of the empirical photoelectric law given by L. H. Gray, 'Proc. Camb. Phil. Soc.,' vol. 27, p. 103 (1931). The experimental evidence upon which this law is based has not altered since the time of publication. The absorption coefficients of hard X-rays in lead, for quantum energies up

13·5 X.U. or $h\nu = 0\cdot92$ million e-volts, and 27 X.U., or $h\nu = 0\cdot47$ million volts × 10^6 e-volts.* A unique analysis is, of course, not possible, and at this stage it might be considered that the radiation had a continuous spectrum, though it will be seen later that this is very unlikely.

It will be observed that the quantum energies of the two components of characteristic radiation are of the same order as the softer components of the natural thorium C″ spectrum, so that the question arises as to whether the

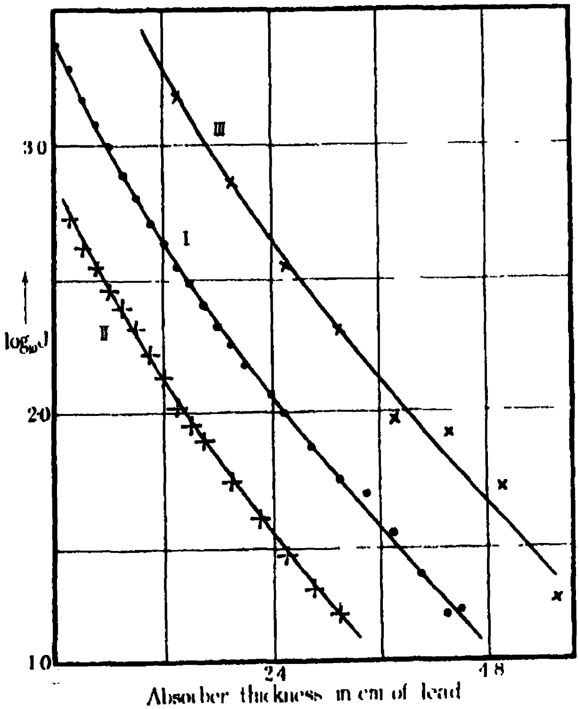

Fig. 2.—I, Thorium C″ γ-rays, emission at 125°. II, Thorium C″ γ-rays, emission at 145°. III, Radium (B + C) γ-rays, emission at 125°.

---

to half a million volts, have been measured by Hermann and Jaeger ('Z. tech. Phys.,' vol. 41, p. 461 (1930)), who find values considerably larger than those given by the empirical law. The method of "end-filtering" was used, and the observed absorption coefficient at the greatest filter thickness was assumed to correspond to radiation of quantum energy equal to the voltage on the tube. Since at most 0·6 cm. of filter was employed, the radiation was, in fact, far from homogeneous; making a rough allowance for this inhomogeneity, the values of the corrected absorption coefficients are found to be in reasonably good agreement with the empirical law.

* The wave-length of the soft component is thus equal to that of hard Ra C γ radiation scattered through about 90°, and, therefore, could not have been detected by the experimental arrangement employed by Meitner and Hupfeld (*loc. cit.*), p. 663.

secondary radiation which we have been observing might not be due to nuclear resonance, or to classical scattering of the soft components by the extranuclear electrons of the radiator. Calculation (based on the theory of unmodified X-ray scattering), however, indicated that this radiation must be 100 times smaller than that observed; further, the possibility can be entirely eliminated on experimental grounds, both in the case of lead and other elements, since the values of the apparent absorption coefficient of the primary radiation recorded in Table V show that the secondary emission cannot in any way depend on the soft components of the radiation emitted by the source which have a mean absorption coefficient of the order of 2·3 cm.$^{-1}$.

By arranging the lead sheets on a wooden platform, approximately in the form of a cylinder, at 100 cm. from the source, it was possible to study the absorption of the secondary radiation emitted within the angular range 145° ± 5°. The logarithmic absorption curve is shown in curve II, which runs approximately parallel to curve I. This fact is rather remarkable, for though the mean angle of emission has not changed greatly (125° to 145°) between this and the previous experiment, yet it implies that over this limited angular range there is clearly no appreciable difference in the character of the secondary radiation. In particular, it is clear that at neither angle is there any appreciable proportion of radiation scattered by the extranuclear electrons, since (owing to the Compton change of wave-length) the absorption coefficient of such a radiation would change from 4·5 cm.$^{-1}$ to 6·0 cm.$^{-1}$, and the presence of such a radiation, the hardness of which varied in this manner, would produce a very marked change in the absorption curve. This result is in accordance with expectation, since the intensity of the Compton scattered radiation should be initially only about one-fifth of that which we have been observing, and will be very rapidly reduced by the first few millimetres of absorber.

§ 3. *Nuclear Excitation by the γ-Rays of Radium (B + C).*

Although it is only in the case of the hard Th C″ γ-rays that direct absorption measurements have given definite indication of the participation of the nucleus in the absorption process, it has been pointed out[*] that the Ra (B + C) absorption data strongly suggest that some of these γ-rays also are capable of nuclear interaction. It therefore seemed of special interest to study the radiation re-emitted when lead was irradiated with Ra (B + C) γ-rays, for this radiation has a wide spectral distribution, extending to 3 . 10^6 e-volts, and the experiment should yield information concerning the dependence of the hardness and intensity of the nuclear radiation on the wave-length of the incident radiation.

---

[*] L. H. Gray, 'Proc. Camb. Phil. Soc.,' vol. 27, p. 103 (1931).

The lead radiator was set up, as in the first experiment, for studying the secondary emission at 125°. The primary radiation was the unfiltered γ-radiation from Ra (B + C) in equilibrium with 350 mgm. radon.

From fig. 2 it will be seen that the experimental points are satisfactorily represented by curve III, which has the same gradient at each absorber thickness as curve I, representing the absorption of the secondary radiation excited by the Th C″ γ-rays. Unfortunately, owing to certain technical defects,* the experimental accuracy of the radium measurements was less than that of the previous thorium measurements, so that a somewhat different curve might be drawn through the points, and it is not possible to insist on the exact identity of the secondary radiation excited in the two cases. Nevertheless, remembering that a 10 per cent. change in gradient corresponds to a change of only 5 per cent. in the corresponding quantum energy of the radiation, any difference that may exist between the quantum energies of the secondary radiations is certainly small compared with the energy differences of the exciting radiations.

Thus it appears that the absorption of the primary radiation in some way leaves the nucleus in an "excited state," and the radiation which we have been observing is a "characteristic" radiation emitted when the nucleus returns to the normal state.

§ 4. *The Minimum Energy of Quanta capable of exciting the Nucleus.*

If the secondary radiation is excited in the manner suggested, we should expect that there will be a certain threshold frequency at which interaction commences, though this will not necessarily be equal to the energy of the nucleus in the excited state since there must evidently be some mechanism for disposing of the difference between this energy and that of the absorbed quantum, and this mechanism may itself involve the expenditure of energy as in the case of the absorption and emission of characteristic X-rays.

The mean energy of the Ra (B + C) quanta capable of exciting the lead nucleus has been estimated by placing a hemispherical lead absorber 1·6 cm. thick round the source in the position shown, fig. 1. The observed absorption coefficient of the effective primary rays from Ra (B + C) is given in the following table for three different thicknesses of absorber round the ionisation chamber.

---

* The measurements are in the course of repetition, since the identity of the two curves is a matter of great significa

Table I.

Thickness of lead round the ionisation chamber in cm.	1·35	2·55	4·35
Apparent absorption coefficient of the primary rays in cm.^{-1}	0·46	0·44	0·47

The three values are equal within the limits of error, and are very different from the absorption coefficient $1 \cdot 0$ cm.^{-1} of unfiltered Ra (B + C) γ-rays, showing clearly that the Ra B and the softer Ra C γ-rays do not give rise to the emission of secondary nuclear γ-radiation. In fact, the mean quantum energy of the interacting radiation appears to lie between 2 and $2 \cdot 5 \times 10^6$ e-volts.

It is to be noted that essentially the same value of the absorption coefficient of the primary rays was obtained, although the thicknesses of absorber around the ionisation chamber varied widely. This is a fact of some importance, for with 1·35 cm. of lead round the chamber 30 per cent. of the ionisation is due to soft components, whereas for a thickness 4·35 cm. this component has been completely absorbed, so that the two component radiations evidently have the same threshold, and are therefore presumably excited by a single process, and not independently.

We cannot infer the position of the threshold from these results without making some hypothesis as to the way in which the nuclear absorption coefficient (*i.e.*, the probability of excitation) varies with wave-length. If, following the X-ray analogy, we assume that it is zero on the long wave-length side of the threshold, and decreases with the wave-length between $\lambda = \lambda_e$ and $\lambda = 0$, then, taking into consideration the distribution of energy in the Ra C spectrum, we estimate $\lambda_e = 7$ X.U. ($1 \cdot 8 \times 10^6$ e-volts).

This method of fixing the quantum energy of the threshold is very much more sensitive than would appear at first sight owing to the large intensity of radiation in the Ra (B + C) spectrum in the region of $1 \cdot 8 \times 10^6$ e-volts and on account of the relatively rapid change in absorption coefficient with wave-length. It is interesting to note that this estimate of the threshold agrees with that found by Chao,* who, by making use of the Compton change of wave-length, was able to measure the absorption coefficient in lead and other elements of roughly monochromatic γ-rays of various wave-lengths between 4·7 and 9·3 X.U. The difference between the absorption coefficients per electron in lead and light elements, which is due in part to nuclear absorption and in part to photoelectric absorption (so that $\Delta\mu_e = \kappa_e + \tau_e$), fell sharply between

---

* 'Proc. Roy. Soc.,' A, vol. 135, p. 206 (1932).

5·9 and 6·6 X.U. to about the estimated value of τ alone. It would appear, therefore, that nuclear interaction commences fairly suddenly in the neighbourhood of 6 X.U. in fair agreement with the above estimate of λ_0.

There is still another independent method of estimating the threshold wavelength. We have found that the nuclear γ-radiation excited by Th C″ γ-rays is 2·2 times as intense as that excited by a Ra (B + C) source of the same γ-ray activity, measured through 5 mm. of lead.

The following table shows the absolute number of quanta of γ-radiation

Table II.

Thorium C″.			Radium C.					
			Skobelzyn.			Ellis.		
A. Quantum energy $\times 10^{-6}$ ϵ-volts.	B. Number of quanta per mgm. $\times 10^{-7}$.	C.	A. Quantum energy $\times 10^{-6}$ ϵ-volts.	B. Number of quanta per mgm. $\times 10^{-7}$.	C.	A. Quantum energy $\times 10^{-6}$ ϵ-volts.	B. Number of quanta per mgm. $\times 10^{-7}$.	C.
2·65	1·43	**1·43**	2·65	0·161	**0·161**			
			2·21	0·251	**0·412**	2·219	0·271	**0·271**
2·05	0·28	**1·71**	1·93	0·100	**0·512**			
			1·78	0·758	**1·270**	1·788	0·944	**1·215**
1·65	0·28	**1·99**	1·61	0·089	**1·359**			
			1·42	0·641	**2·000**	1·426	---	**1·215**
						1·389	0·234	**1·449**
						1·248	0·230	**1·679**
			1·13	1·178	**3·178**	1·130	0·754	**2·483**
						0·941	0·245	**2·678**
<0·79	3·46	**5·45**				0·773	0·238	**2·916**
			0·608	2·120	**5·298**	6·12	2·410	**5·326**
Total	... .	**5·45**	Total	... . .	**5·30**	Total . .	..	**5·33**

The estimates of the Th C″ γ-ray intensities given in the table have been obtained by the method outlined by Rutherford, Chadwick and Ellis (‘Radiations from Radioactive Substances,’ p. 500), and were based ultimately on an experimental value (1·45) for the total number of quanta emitted per disintegration by Ra C, and on a comparison, by Shenstone and Schlundt (‘Phil. Mag.,’ vol. 43, p. 1039 (1922)) of the ratio of the γ-ray emission of Ra C and Th C″, and the α-particle emission of Ra C′ and Th C′ in equilibrium with these bodies. It will be observed that two lines having quantum energies of 2·05 and 1·65 . 10⁶ ε-volts have been included in the Th C″ spectrum which have not so far been observed by the method of the β-ray magnetic spectrum. We are indebted to Mr. Skobelzyn for communicating to us privately the fact that he has observed recoil electrons corresponding to these lines by the Wilson chamber method. From the circumstances of the observation it is not yet quite certain that the lines are of primary origin and belong to the Th C″ spectrum. The existence of these lines has, however, been taken as genuine, since it would appear from the absolute intensity estimates that, if these lines do not exist, 40 per cent. of the atoms disintegrating must emit two quanta of exactly 2·65 . 10⁶ ε-volts energy, which on general grounds seems very unlikely.

emitted per second by Th C″ and Ra C of 1 mg. equivalent activity. The Ra C data are given in duplicate, since different estimates as derived from the recoil electron statistics of Skobelzyn and the excited spectrum data of Ellis. Column C in each case gives the total number of quanta of energy greater than the value shown in column A. Since the soft components of the Th C″ γ-rays certainly do not take part in the nuclear interaction, not more than a third of the Th C″ quanta are giving rise to the excitation of the characteristic radiation. This radiation, however, is 2·2 times as intense as that excited by a Ra C source of the same activity, so that if all quanta have the same efficiency, not more than a seventh of the Ra C quanta are taking part in the interaction. Glancing down column C it is evident (whichever spectral distribution we consider) that this sets the threshold energy at about $1 \cdot 8 \times 10^6$ e-volts. A careful consideration of all the relevant factors leads to the conclusion that if κ changes discontinuously with λ, then $\lambda_0 = 7$ X.U. ($1 \cdot 8 \times 10^6$ e-volts).

The minimum quantum energy necessary for the excitation of tin has also been estimated from the intensity measurements with the Ra (B + C) and the Th C″ γ-radiations. The value obtained is, as nearly as can be judged, identical with that found above for lead.

It is of interest to note that essentially the same value of the threshold wavelength is obtained whether we study the absorption (Chao's method), or the re-emission of characteristic radiation.

In order to facilitate a quantative discussion of the position of the threshold frequency we have assumed that the nuclear absorption coefficient varies discontinuously with wave-length, changing from zero to its maximum value at a certain value of the wave-length λ_0. This hypothesis has led to the conclusion that while the quantum energy of the characteristic radiations are of the order of half a million and 1 million volts respectively, the nucleus is not excited in such a manner as to emit these radiations till the energy of the primary quanta exceeds about 2 million volts. Moreover, as will be shown later, the total energy of the characteristic radiations is only 1·5 million volts, thus leaving half a million volts energy to be accounted for in some other way. If κ does not vary discontinuously, however, we cannot fix λ_0 with any exactness, by any of the methods described above, on the basis of the existing experimental data. Since the total energy re-radiated as characteristic radiation is $1 \cdot 5 \,.\, 10^6$ e-volts, this may be taken as the lower limit of the threshold energy. We know also that at $2 \cdot 65 \,.\, 10^6$ e-volts the nuclear absorption coefficient ${}_N\kappa \sim 2 \cdot 9 \,.\, 10^{-24}$. Between these two points the form of the variation of κ with λ can only be conjectured; the three lines of experimental evidence which we have already discussed agree, however, in setting the following approximate limits :—

(1) At 2·0 . 10^6 e-volts κ is not likely to be less than half, or more than 50 per cent. greater than the value at 2·65 . 10^6 e-volts.

(2) It seems fairly certain that at 1·8 . 10^6 e-volts κ cannot be more than a third of the value given above, since Ra C emits fairly intense γ-rays of about this energy, and their contribution to the secondary emission could not easily be overlooked if they were participating to an appreciable extent in the nuclear interaction.

§ 5. *The Magnitude of the Total Nuclear Re-emission from Lead.*

In order to decide whether both hard and soft quanta are emitted as the result of each nuclear excitation, or whether they are alternative modes of de-excitation, we have to estimate the total energy re-radiated by the nucleus. By measuring the ionisation produced in our chamber by the direct radiation from the radiothorium source filtered through 5 cm. of lead (under appropriate conditions), the ionisation due to the hard Th C'' γ-rays at this filter thickness was obtained, and hence, knowing the absorption coefficient of the radiation, the unfiltered intensity of the hard radiation could be calculated.* The intensity of the characteristic radiation emitted at 125° could thus be expressed as a fraction of that of the primary radiation falling on the radiator.

If, further, we assume that the radiation is emitted isotropically, we can calculate a coefficient ${}_{\mathrm{N}}\kappa_{\gamma}$, which is the integrated energy re-emitted in the form of γ-radiation by a single nucleus, expressed as a fraction of the intensity of the primary γ-radiation absorbed by the same nucleus.

Writing ${}_{\mathrm{N}}\kappa$ for the absorption coefficient per nucleus of the primary γ-radiation in question, ${}_{\mathrm{N}}\kappa_{\gamma}/{}_{\mathrm{N}}\kappa$ is the fraction of the energy absorbed by the nucleus, which is re-emitted as characteristic radiation. The measurements with lead already described lead to the value ${}_{\mathrm{N}}\kappa_{\gamma}/{}_{\mathrm{N}}\kappa = 0{\cdot}52$. Since the energy of the absorbed quantum is $2{\cdot}65 \times 10^6$ e-volts, the total energy re-radiated is $0{\cdot}52 \times 2{\cdot}65 \times 10^6 = 1{\cdot}4 \times 10^6$ e-volts, which is just equal to the sum of the quantum energies of the two components of characteristic radiation.

---

* Due regard must be given, of course, to the "ionisation function" of the chamber, *i.e.*, the relative ionisation produced by quanta of different energy. Apart from absorption in the walls of the chamber, this is clearly proportional to the γ-ray energy absorbed by the gas, viz., $h\nu \cdot \sigma_a$ per quantum of primary radiation. The allowance for the absorption in the walls is complicated by the fact that part of the scattered radiation enters the chamber, and has a different ionising power from that of the primary radiation.

Each excitation is therefore followed by the emission of one quantum of each component radiation, or three quanta of the softer component.*

This conclusion has been reached on the assumption that the secondary radiation is spacially isotropic. The two measurements at 125° and 145° naturally do not afford a very stringent test of this assumption, though they are consistent with it. Certain measurements which we have made on the radiation emitted between 2° and 17°, and other experiments† within the angular range 10°–30° show that the intensity of the characteristic radiation emitted in the forward direction cannot be more than 50 per cent. greater than that in the backward direction. From the theoretical standpoint an isotropic, or possibly a Thomson distribution $I \alpha (1 + \cos^2 \theta)$ seems most likely, and since it happens that the ratio of the intensity at 125° to the total integrated intensity emitted by the nucleus is the same for both distributions, it is immaterial for our calculation which one is assumed.

§ 6. *Characteristic Radiations of Tin, Iron, and Water.*

Experiments of the same kind as those already described were also made, using tin, iron, and water as radiators. The geometrical arrangement in the case of tin and iron was the same as in the investigation of the secondary emission from lead at 125°. The water was contained in glass vessels, arranged on a platform so as to have approximately the same geometry as the other elements.

The experimental data, together with all necessary corrections, are contained for one typical element in Table III.

Corresponding to each thickness of absorber round the chamber (column A), the increase in ionisation after correcting for barometric change, leak of the chamber, and decay of the source, is shown in column C. These values must be corrected to an extent shown under D for the change in natural leak (B) owing to the absorption by the radiator of secondary γ-radiation from the walls of the room; this correction was calculated by assuming that the radiation from the walls of the room fell isotropically on the chamber. With increasing absorber thickness an increasing proportion of this ionisation was produced by the radiation incident more or less normally on the chamber, owing to the greater absorption of the radiation travelling obliquely through the absorbers.

---

* The fact that the quantum energy of the high component is just double that of the soft, suggests that the two quanta of the latter may sometimes be emitted instead of one of the former (*see infra*, p. 683).

† L. H. Gray, 'Proc. Roy. Soc.,' A, vol. 130, p. 524 (1931).

Table III.—Tin Radiator.

Pressure ~ 87·5 atmospheres.

Standardisation J = 628·1.

Source = 61·6 mgs. radiothorium.

Thickness of tin = 1·54 cm.

Radius of tin = 48·0 cm.

Height above centre of chamber—

Top + 15·1 cm.

Bottom − 15·1 cm.

A.	B.	C.	D.	E.	F.	G.	H.	I.	K.	L.	M.	N.	P.
Absorber thickness in centimetres.	Natural leak J_0.	Apparent J due to radiator.	Correction for scattering from walls of room.	Compton scattering of hard component.	Compton scattering of soft component.	$(\alpha+\beta)$ correction for hard component.	$(\alpha+\beta)$ correction for soft component.	Ionisation due to framework.	Scattering correction.	Final corrected values of J due to nuclear radiation.	$\log_{10}$ J.	$\log_{10}$ J with absorber round source.	Absorption coefficient of radiation responsible.
0·15	586·4	2188	+152	−519	−125	+55·2	+93·5	−336	−67	1442	3·159	—	—
0·15*	452·7	976·3	67·8	271	10·9	24·6	41·6	163	28·3	637·0	—	2·804	0·491 ± 0·044
0·45	237·7	1048·7	42·4	135·4	5·8	53·9	72·0	125·8	98·0	852	2·930	—	—
0·45*	210·3	505·5	20·5	70·5	0·5	26 0	34·7	66·1	46 6	403·0	—	2·605	0·449 ± 0 016
0·9	140·6	464·5	15·5	18·9	0	46·6	39·0	48·0	81·7	417 0	2·620	—	—
0·9*	129·9	225·5	7·5	9·8	—	22·7	19·0	26·1	38·8	200·0	—	2·301	0·441 ± 0·016
1·35	101·2	217·6	7·5	2·7	—	38 0	18·1	19·6	55·1	203·8	2·309	—	—
1·95	83·9	94·5	3·4	0	-	27·2	6·2	8·9	32·6	89·8	1·953	—	—
2·55	73·7	48·3	2·2	—	—	18·5	1·6	4·1	20·5	46·0	1·663	—	—
2·55*	80·9	21·3	1·0	—	—	8·2	0·7	2·2	8·9	20·1	—	1·303	0·497 ± 0·040
3·15	70·0	26·6	1·7	—	—	12·4	0	2·0	13·3	25·4	1·405	—	—
3·75	68·1	15·7	1·3	—	—	8·1	—	0·9	9·1	15 1	1·179	—	—

Measurements taken with the lead absorber (position B, fig. 1, effective thickness 1·67 cm.) round the source are denoted *.

It may be mentioned in passing that the major portion of this secondary radiation from the walls of the room was undoubtedly of nuclear origin since it had approximately the same absorption curve as that found for the other radiators, lead, tin, iron, and water.

The calculated intensity of the Compton scattered radiation from all the components of the Th C″ spectrum is given in columns E and F. The ionisation due to nuclear radiation is thus

$$J = C + D - E - F.$$

In order to derive an absorption curve which has a real physical significance, J must be corrected for the obliquity of the radiation in passing through the absorbers; this correction takes account not merely of the increased absorption of the radiation in passing obliquely through the absorbers, but also of the effect due to the spatial disposition of the various portions of the radiator as well as the fact that each portion of the radiator contributes differently to the total observed ionisation. The need for this correction can be seen from the following table where the effective contribution of each part of the radiator is expressed as a fraction of that due to the central portion.

Table IV.

Height of portion of scatterer above centre of chamber, in cm.	25	20	15	10	5	0	−5	−10	−15	−20	−25	Mean value.
Filter thickness, 0 cm.	0·452	0·542	0·654	0·777	0·888	1·0	1·092	1·142	1·200	1·210	1·092	0·914
Filter thickness, 5 cm.	0·165	0·279	0·448	0·656	0·852	1·0	1·048	0·976	0·822	0·624	0·431	0·482

A comparison with the mean values given in the last column shows that, although the correction is only 10 per cent. when there is no absorber round the chamber, yet at 5 cm. of lead absorber, owing to the large absorption of the rays travelling obliquely into the chamber, the correction is as large as 110 per cent.

A further correction is necessary to take into account the greater thickness of absorber encountered, because of the cylindrical form of the chamber and absorbers, by radiation which traverses a chord rather than a diameter of the chamber. Both of these corrections vary with absorber thickness and with absorption coefficient, and were evaluated separately for the two components of the nuclear radiation. They are referred to in Table III as $(\alpha + \beta)$ correction.

In order to derive an absorption curve which has a real physical significance, J must also be corrected for the close proximity of the absorbers and the chamber, which results in some of the scattered radiation entering the chamber. This correction (column K) is of opposite sign to the two corrections already discussed, and is nearly equal in magnitude to their sum. A new method of calculating this correction has been devised* which was tested experimentally with the hard component of Th C″ γ-radiation with satisfactory results.

---

* This method of calculation (and also the ionisation function) will be published shortly in 'Proc. Camb. Phil. Soc.'

The experimental results for all four elements are shown in Table V and in fig. 3. In each case the ordinate is the logarithm of the observed ionisation, fully corrected in the manner described. The abscissæ, giving the radial

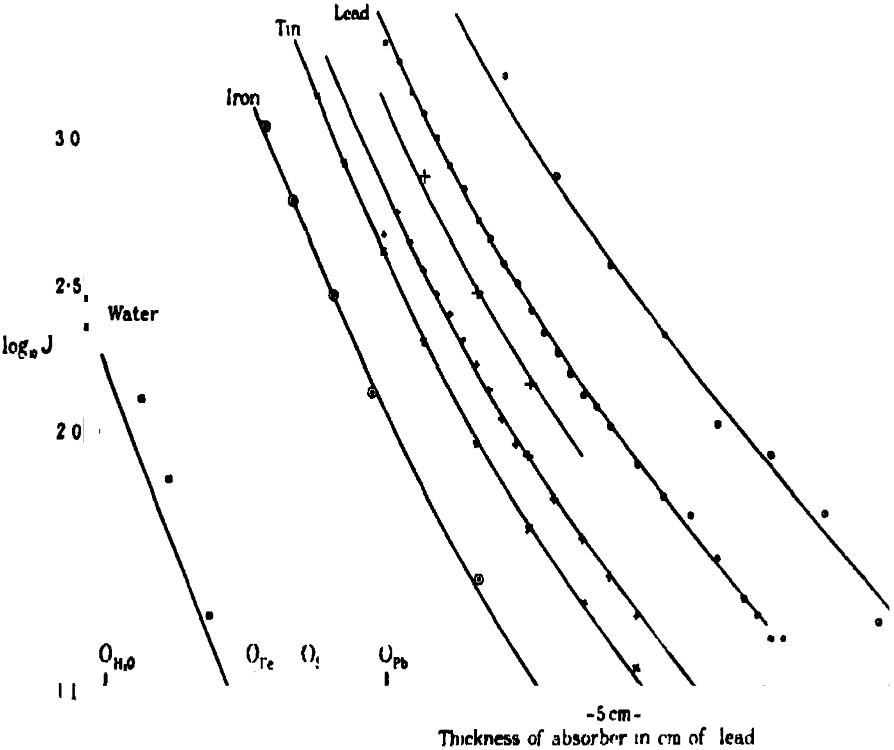

FIG. 3.

● Lead with Ra (B + C) γ-rays at 125°.

• Lead with Th C″ γ-rays at 125°.

-|- Tin with Ra (B + C) γ-rays at 125°.

+ Lead with Th C″ γ-rays at 145°.

× Tin with Th C″ γ-rays at 125°.

◉ Iron with Th C″ γ-rays at 125°.

■ Water with Th C″ γ-rays at 125°.

thickness of the lead absorber round the ionisation chamber, have the same scale for each element, but the origin (zero thickness of absorber) is displaced to the position shown for reasons which will be evident later.

Table V.

Lead at the Smaller Angle.

Analysis of the absorption curve—

Hard component $\mu_H = 0·85$ cm.$^{-1}$; $J_H = 820$ J.
Soft component $\mu_S = 1·9$ cm.$^{-1}$; $J_S = 1530$ J.

Pressure ~ 98 atmospheres.
Standardisation J = 679.
Radiothorium source = 38·1 mgm. Ra equiv.
Thickness of lead = 0·925 cm.

Radius of lead = 48 cm.
Height above centre of chamber—
Top + 23·5 cm.
Bottom − 23·5 cm.

Absorber thickness in cm.	0	0·15	0·30	0·45	0·60	0·75	0·90	1·05	1·2	1·35	1·5	1·65	1·80
Corrected value of ionisation per c.c. per sec.	2143	1880	1459	1235	1024	818	677	537	457	375·1	323·4	269·8	219·3

Absorber thickness in cm. . .	1·95	2·10	2·25	2·4	2·55	2·85	3·15	3·45	3·75	4·05	4·20	4·35	4·50
Corrected value of ionisation per c.c. per sec.	189·2	159·1	133·9	122·0	103·6	76·2	58·0	51·0	36·3	26·0	23·2	19·4	19·1

Lead at the Larger Angle.

Pressure ~ 98 atmospheres.
Standardisation J = 678.
Radiothorium source = 38·0 mgm. Ra equiv.
Thickness of lead = 0·703 cm.

Radius of lead = 95 cm.
Height above centre of chamber—
Top + 23·5 cm.
Bottom − 23·5 cm.

Absorber thickness in cm. ...	0	0·15	0·30	0·45	0·60	0·75	0·90	1·05	1·20
Corrected value of ionisation per c.c. per sec.	468·1	557·9	441·0	370·4	296·5	251·4	206·2	169·4	137·3

Absorber thickness in cm. .	1·35	1·50	1·65	1·95	2·25	2·55	2·85	3·15	
Corrected value of ionisation per c.c. per sec. .	107·5	80·2	81·1	57·4	41·9	30·8	22·5	18·0	

Lead at the Smaller Angle.

Pressure ~ 91 atmospheres.
Standardisation J = 634.
Radon source = 342 mgm. Ra equiv.
Thickness of lead = 0·925 cm.

Radius of lead = 48 cm.
Height above centre of chamber—
Top + 23·5 cm.
Bottom − 23·5 cm.

Absorber thickness in cm.	1·35	1·35*	1·95	2·55	2·55*	3·15	3·75	4·35	4·35*	4·95	5·55
Corrected value of ionisation per c.c. per sec. .	1676	837*	762	377	195*	215·5	106·3	83·1	42·4*	52·1	21·8
Absorption coefficient of radiation responsible, cm.$^{-1}$ lead	0·434 ± 0·04		—	0·412 ± 0·041		—		0·422 ± 0·042		—	

Measurements denoted * were taken with an absorber round the source, in position A (fig. 1) in the case of the lead radiator, and in position B for all other measurements.

Table V—(continued).

Tin.

Pressure ~ 87·5 atmospheres.
Standardisation J = 628·1.
Radiothorium source = 61·6 mgm. Ra equiv.
Thickness of tin = 1·54 cm.

Radius of tin = 48·0 cm.
Height above centre of chamber—
Top + 15·1 cm.
Bottom − 15·1 cm.

Absorber thickness in cm.	0·15	0·15*	0·45	0·45*	0·9	0·9*	1·35	1·95	2·55	2·55*	3·15	3·75
Corrected value of ionisation per c.c. per sec.	1442	637*	852	403*	417	200*	203·8	80·8	46·0	20·1*	25·4	15·1
Absorption coefficient of radiation responsible, cm.$^{-1}$ lead	0·491 ±0·044		0·449 ±0·016		0·441 ±0·016		—		0·497 ±0·040		—	

Tin.

Pressure ~ 91 atmospheres.
Standardisation J = 634.
Radon source = 342 mgm. Ra equiv.
Thickness of tin = 1·54 cm.

Radius of tin = 48·0 cm.
Height above centre of chamber—
Top + 15·1 cm.
Bottom − 15·1 cm.

Absorber thickness in cm.	1·35	1·95	2·55
Corrected value of ionisation per c.c. per sec.	754·0	208·5	144·6

Iron.

Pressure ~ 87·5 atmospheres.
Standardisation J = 628·1.
Radiothorium source = 61·6 mgm. Ra equiv.
Thickness of iron = 1·42 cm.

Radius of iron = 54 cm.
Height above centre of chamber—
Top + 23·7 cm.
Bottom − 23·7 cm.

Absorber thickness in cm.	0·15	0·15*	0·45	0·45*	0·9	0·9*	1·35	1·35*	2·55	2·55*
Corrected value of ionisation per c.c. per sec.	1103	583*	618	324*	292·5	158·5*	134·6	67·6*	30·7	13·1*
Absorption coefficient of radiation responsible, cm.$^{-1}$	0·415 ±0·040		0·423 ±0·015		0·416 ±0·015		0·449 ±0·02		0·56 ±0·06	

Water.

Pressure ~ 61 atmospheres.
Standardisation J = 544.
Radiothorium source = 27·3 mgm. Ra equiv.

Contained in glass cells of varying height, radius, and thickness.

Absorber thickness in cm.	0	0·15	0·45	0·75	1·2
Corrected value of ionisation per c.c. per sec.	985·0	412·0	127·8	67·4	23·1

Measurements denoted * were taken with an absorber round the source, in position A (fig. 1) in the case of the lead radiator, and in position B for all other measurements.

§ 7. *The Analysis of the Absorption Curves.*

It is at once apparent that the absorption curve of the characteristic radiation changes very little from element to element, and this impression is confirmed by the figures given in the following table, which are the result of careful and independent analyses of the absorption curves of tin and lead. The limiting values given in the case of tin take account of the probable error of the experimental measurements.

Table VI.

Element.	Quantum energy of hard component, e-volts × 10^{-6}.	Quantum energy of soft component, e-volts × 10^{-6}.
Lead	0·92	0·47
Tin ..	0·86—0·93	0·477—0·488

Considering the wide variation in atomic number between lead and tin, the possible difference in energy of the characteristic radiations is so small (at most 6 per cent.) that we must, at least as a first approximation, consider that the same radiations are emitted by both nuclei—though in different proportions. The following simple considerations show that if this hypothesis is correct, the absorption curves of the secondary radiations from each element will have the same gradient at any given abscissa value, if plotted with respect to displaced origins.

The absorption curve for one element can be represented by

$$J_1 = I_1\, e^{-\mu x} + f_1 I_1\, e^{-\mu' x} = I_1\, e^{-\mu x}\{1 + f_1\, e^{-(\mu'-\mu)x}\}$$

and the displaced curve for the second element will similarly be

$$J_2 = I_2\, e^{-\mu(x+\delta)} + f_2 I_2\, e^{-\mu'(x+\delta)} = I_2\, e^{-\mu(x+\delta)}\{1 + f_2\, e^{-(\mu'-\mu)(x+\delta)}\}.$$

Then clearly

$$\frac{J_1}{J_2} = \frac{I_1}{I_2}\, e^{\mu\delta} = \text{constant},$$

for all values of x if $f_1/f_2 = e^{-(\mu'-\mu)\delta}$, so that the logarithmic curves will have the same gradients at all absorber thicknesses.

The full curves, fig. 3, have all been drawn with the same stencil, and show that all the experimental results except those of water are compatible with the suggested hypothesis. The fact that the experimental results for water do not fall into line, is not of serious consequence, since in this case only a third of the ionisation at zero filter thickness is due to nuclear radiation. The remainder is due to Compton scattered radiation, the intensity of which is rather uncertain.*

At larger filter thicknesses the experimental points appear to be tending to the full curve, which is the absorption curve for the soft component ($h\nu = 0 \cdot 5 \,.\, 10^6$ e-volts) alone, so that oxygen may be considered as constituting the limiting case when all the energy is radiated in the form of the soft component. It is noteworthy also that the characteristic radiation of tin, like that of lead, is independent of the quantum energy of the radiation which excites the nucleus. This is shown by the fact that curve V, fig. 3, representing the absorption of the secondary radiation from tin excited by Ra C γ-rays is parallel to the tin-Th C″ curve II. Moreover, the threshold quantum energy in the case of tin is approximately the same as that for lead, judged both from the absorption coefficient of the primary Ra C γ-rays giving rise to secondary emission (estimated by placing lead round the source as described on p. 669) and from the relative intensity of the secondary radiations excited by Ra C and Th C″ γ-rays.

§ 8. *The Total Energy Re-radiated by the Nucleus.*

The integrated intensity of the two component radiations expressed as coefficients ${}_{\text{N}}\kappa_{\text{H}}$ and ${}_{\text{N}}\kappa_{\text{S}}$, calculated as already described in the case of lead (p. 673) are given in the following table.

Table VII.

Element.	Lead.	Tin.	Iron.
${}_{\text{N}}\kappa_{\text{H}} \times 10^{27}$	374	55·9	8·25
${}_{\text{N}}\kappa_{\text{S}} \times 10^{27}$	1131	403	122·6
Ratio ${}_{\text{N}}\kappa_{\text{H}}/{}_{\text{N}}\kappa_{\text{S}}$	0·332	0·139	0·067
Sum ${}_{\text{N}}\kappa_{\gamma} = ({}_{\text{N}}\kappa_{\text{H}} + {}_{\text{N}}\kappa_{\text{S}}) \times 10^{27}$	1505	489	131
${}_{\text{N}}\kappa_{\gamma}/Z^2 \times 10^{27}$	0·225	0·195	0·196

For reasons already explained, the intensity of the characteristic radiation emitted by water cannot be estimated with sufficient accuracy to be included in the table. We notice, however, from the last line, that very approximately,

---

* Our results appear to indicate a larger amount of scattered (quantum) radiation than is predicted by the Klein-Nishina formula. This is in agreement with the observations of Skobelzyn, who finds, both in the case of Ra (B + C) γ-rays ('Z. Physik,' vol. 65, p. 773 (1930)) and Th C″ γ-rays (private communication), that the number of recoil electrons ejected within the first 10° is about 50 per cent. greater than the theoretical value.

${}_N\kappa_\gamma$ is proportional to Z^2, and that the proportion of the hard component decreases rapidly with atomic number. If we extrapolate to $Z = 8$, we obtain an estimate of the intensity of this nuclear radiation to be expected from water, which is shown by the full curve, fig. 3, which, at large absorber thicknesses, appears to be in very satisfactory agreement with the experimental results. There can be no doubt, therefore, that the Th C″ γ-rays are absorbed by the oxygen nucleus, and it appears that the quantum energy of the characteristic radiation which is thereby excited is of the same order as that emitted by other nuclei. The observed intensity provides, moreover, a rough confirmation of the extrapolation of the Z^2 law. The ionisation observed at small thicknesses of filter is greater than can be ascribed to the nuclear effect. This excess may be due to faulty corrections for the effect of the glass cells or to errors in the estimate of the wall-scattered radiation, but is much more likely to be due, as has already been suggested, to the fact that the magnitude of the Compton scattering has been very considerably under-estimated.

Table VIII.

	Lead.	Tin.	Iron.	Oxygen (water.)
Atomic number Z .	82	50	28	8
Absorption coefficient for $h\nu = 2 \cdot 65 \,.\, 10^6$ e-volts, per nucleus $\times 10^{27}$	2880	860	260	21
${}_N\kappa_\gamma = ({}_N\kappa_H + {}_N\kappa_S) \times 10^{27}$	1505	459	131	10·8
Ratio ${}_N\kappa_\gamma / {}_N\kappa$	0·523	0·534	0·504	0·515
Number of hard quanta produced by one incident quantum	0·373	0·188	0·091	0
Number of soft quanta produced by one incident quantum	2·23	2·65	2·68	2·95
Relative probability of dual transitions, r	0·605	0·228	0·108	~0
$\frac{2}{3}$H + $\frac{1}{3}$S	0·992	1·005	0·953	0·983

Table VIII shows, besides the values of ${}_N\kappa_\gamma$ found above, the values of the nuclear absorption coefficient obtained from direct absorption measurements,* and the ratio of these two coefficients, which is the fraction of the incident energy re-emitted as characteristic radiation. Since the quantum energy of the two component radiations are the same for each element, the constancy of this ratio leads to a generalisation of the result already reached in the case of lead (p. 673), viz., that in every case, the absorption of a quantum of $2 \cdot 65 \,.\, 10^6$ e-volts energy excites the nucleus, which subsequently emits quanta of total energy $1 \cdot 4 \,.\, 10^6$ e-volts. Since, however, the proportion of the two components varies greatly from element to element the emission of two soft quanta of energy $0 \cdot 47 \,.\, 10^6$ e-volts or one quantum of $0 \cdot 94 \,.\, 10^6$ e-volts must obviously be alternative modes of de-excitation. The excitation process may therefore be represented quite generally by the energy level diagram, fig. 4.

---

* G. T. P. Tarrant (*loc. cit.*). The total absorption coefficient (extrapolated to infinite filter thickness) $\mu = \sigma + \tau + \kappa$. Since ${}_e\sigma$ (the scattering per electron) is independent of the atomic number Z, ${}_e\mu_Z - {}_e\mu_{Z \to 0} = {}_e\tau + {}_e\kappa$. To obtain the nuclear coefficient ${}_e\kappa$ we have to subtract ${}_e\tau$. The value assumed for Pb (*cf.* the photoelectric law given by L. H. Gray, *loc. cit.*) is ${}_e\tau = 9 \cdot 3 \,.\, 10^{-27}$. The value of ${}_e\mu_{Z \to 0}$ ($= {}_e\sigma$) was chosen so that in the case of water ${}_e\mu - {}_e\mu_{Z \to 0}$ ($= {}_e\kappa$) leads to the same value of the ratio ${}_N\kappa_\gamma / {}_N\kappa$ as is found for the other three elements. This value of ${}_e\sigma$, viz., $125 \cdot 3 \,.\, 10^{-27}$ is slightly higher than the theoretical Klein-Nishina value $123 \cdot 5 \,.\, 10^{-27}$. The choice of these particular values of ${}_e\tau$ and ${}_e\sigma$ will be discussed elsewhere.

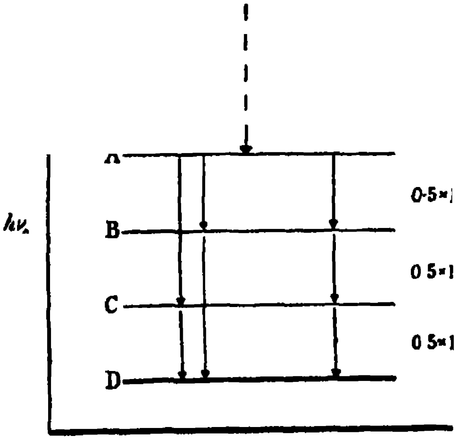

FIG. 4.

The virtual level, shown by a dotted line, is at a height above ground equal to the energy of the incident quantum. The level A is presumably at a height above ground equal to the minimum quantum energy capable of exciting the nucleus. Transitions A → B, B → C and C → D will give rise to soft quanta, while A → C and B → D correspond to the emission of hard quanta.

The conclusion has previously been reached that, if the nuclear absorption coefficient varies discontinuously with wave-length, being greatest at the long wave-length limit, as in X-ray absorption, the minimum quantum energy for excitation must be of the order of 2 million volts. In this case, a nucleus in the state D still has half a million volts in excess of its normal energy. Nothing is yet known of the manner in which the nucleus disposes of this energy. It is just possible that a fourth quantum is emitted, but which, owing to strong selective absorption in lead, does not escape from the radiator with sufficient intensity to be detected.*

Similarly it is not yet known by what mechanism the nucleus passes from the virtual state to the state A, except to say that unless the angular distribution of the radiation is rather peculiar (three-quarters of the energy being emitted between 30° and 90°), it is unlikely that the energy is emitted in the form of quantum radiation.

Since the presence of any γ-radiation of unchanged wave-length in the secondary emission would be of considerable theoretical interest, this point was investigated by an entirely different experimental arrangement which was specially sensitive to the presence of any radiation of primary hardness, but without a positive result.† Having regard to the sensitivity of the arrangement, it is estimated that any unmodified scattering of the hard Th C″ γ-rays by lead, in the backward direction, does not amount to as much as 2 per cent. of the secondary radiation emitted by the nucleus, or 0·2 per cent. of the total energy absorbed by the atom.

§ 9. *Interpretation of the Level System.*

In conclusion, we may note a possible interpretation of the energy level system, fig. 4, which leads to certain conclusions of interest concerning the wider problem of nuclear structure.

If we follow the analogy of electronic transitions in the outer atom, we shall interpret the level system as indicating the transition of a single particle between a number of different quantum states, excitation being possible only for transitions to the highest energy state A. Such an interpretation, however, besides raising the question as to why the nucleus cannot be raised to the state B, C or D, encounters certain difficulties, since it is not easy to see why the relative frequency of transitions between non-adjacent states, which give rise to the emission of hard quanta, should vary so greatly between different nuclei, while at the same time the difference in energy between the various levels is very nearly the same in nuclei of such widely different structure as lead, tin, iron, and oxygen. The essential identity of the characteristic radiation of all four elements—and these presumably may be regarded as typical of nuclei in general, since the nuclear absorption coefficient varies regularly with atomic number—receives a natural explanation if we assume that it is not the nucleus as a whole which is excited, but an oscillating unit common to all nuclei. Since the absorbing power of an aggregate of n oscillators for radiation of wavelength long compared with its distance apart, is proportional to n^2, and we have found that the intensity of the characteristic radiation is roughly proportional to Z^2, it appears that the number of oscillators present in a nucleus is roughly proportional to Z. Since, moreover, the characteristic radiation from the nuclei of iron and oxygen, both of which are predominantly of the $4n$ type, do not show any abnormality either with respect to quality or intensity, we are led to the conclusion that the oscillating unit is the α-particle.

---

* *Cf.* Kuhn, 'Phil. Mag.,' vol. 8, p. 625 (1929).

† This experiment is described in the Appendix.

We may develop this hypothesis a little further by supposing, as has been suggested by Rutherford and Ellis in the case of the Ra C energy levels, that the energy level diagram of fig. 4 represents, not the excitation of a single particle in different quantum states, but the excitation of different numbers of particles to the same state. According to this hypothesis an oscillator in the state A contains three (or four) particles in the excited state. The transition of each particle separately to the ground state gives rise to the emission of a quantum of half a million volts energy, while the simultaneous transition of two particles results in the emission of a quantum of 1 million volts, which is the hard component of the characteristic radiation. From the relative intensity of the two components we can calculate the relative probability of dual and simple transitions. This ratio "r" is given in Table VIII. It is evident that the simultaneous transition of three particles will be of such rare occurrence that we should not have expected to have observed any radiation of 1½ million volts energy.

The association of three, or four, particles in the excitation process directs our attention at once to the possibility that the four protons in the α-particle are the individual oscillators, and from this standpoint it is perhaps easier to understand why the excitation must always be to the state A, since in this case the α-particle as a whole is excited.

It is not immediately obvious why the probability of the simultaneous transition of two protons within the same α-particle should depend to such a considerable extent on the complexity of the nucleus of which the α-particle forms a part, but if we try to explain the 1 million volt radiation as due to the simultaneous transition of protons in different α-particles, we encounter the much more serious difficulty of accounting for the fact that interaction of γ-radiation with the nucleus always leads to the excitation of at least three particles.

The balance of evidence thus appears to us to indicate that when γ-radiation of 2 to 3 million volts energy is absorbed by atomic nuclei, the interaction is not with the nucleus as a whole, but with a small group of protons and electrons —such as the α-particle—which is present as a structural unit in all nuclei. The radiation which is subsequently emitted is the characteristic radiation of the group, and in the case of the α-particle might be the result of the independent or simultaneous transition of the four protons to the ground state.

The characteristic radiations which we have been studying fall within the same energy range as the radioactive γ-rays which, in some cases, appear to be the characteristic radiations of the nucleus, left in an excited state by the previous α- or β-disintegration. Gamma rays of about half a million volts and 1 million volts do indeed occur in nearly all the radioactive spectra, but there is no evidence of the simplicity which characterises the radiation of the non-radioactive nuclei. This, of course, may be due to the fact that, apart from Th C″ and Po, in the case of the radioactive nucleus the characteristic radiation is always that of an unstable nucleus. Though the spectrum of the radiation attributed to the Th C nucleus is not at all simple, it is noteworthy that the γ-rays of Ra G (following the disintegration of Po) were found by Webster[*] to consist of two components of approximately the same energy as the characteristic radiations of the non-radioactive nuclei which we have been studying.

Summary.

When lead, tin, iron, and water are irradiated by hard γ-rays, a secondary radiation of nuclear origin is observed. The quality of this secondary radiation from any one element has been found to be independent of the angle of emission, and also of the quantum energy of the primary radiation. The emission is approximately isotropic. It appears, therefore, that the primary radiation excites the nucleus, which subsequently emits a characteristic radiation. The characteristic radiation of all four elements appears to consist of the same two components, viz. :-

Hard component	$\mu_{Pb} = 0 \cdot 85$ cm.$^{-1}$	$h\nu = 0 \cdot 92 . 10^6$ *e*-volts $\lambda = 13 \cdot 5$ X.U.
Soft component	$\mu_{Pb} = 1 \cdot 9$ cm.$^{-1}$	$h\nu = 0 \cdot 47 . 10^6$ *e*-volts $\lambda = 27$ X.U.

emitted in different proportions. In the case of lead, not more than 2 per cent. of the nuclear radiation could have consisted of quanta of unchanged wavelength.

---

[*] 'Proc. Roy. Soc.,' A, vol. 136, p. 451 (1932).

The energy of quanta capable of exciting the nucleus has been investigated by two independent methods. The return of the nucleus to the normal state results, in each case, in the emission of 1½ million volts energy, either as one quantum of hard radiation and one of soft, or as three quanta of soft radiation.

It is suggested that the observed secondary radiation is the characteristic radiation of a structural unit such as the α-particle, which is present in all nuclei.

We gratefully acknowledge a grant of £250 from the Rouse Ball Research Fund, which covered the cost of the radiothorium source, and some of the apparatus employed in these investigations.

We wish to express our thanks also to Lord Rutherford and Dr. Chadwick for their helpful advice throughout the investigation.

One of us (G.T.P.T.) desires also to express his indebtedness to the Department of Scientific and Industrial Research and to the Goldsmiths Company for the opportunity to carry out this research.

APPENDIX.

The Possible Existence of Unmodified γ-Radiation in the Secondary Emission from Lead.

Apart from the possibility of classical scattering by the outer electrons, or re-radiation without change of wave-length by nuclei in general, there is special reason to look for the presence of unmodified radiation in the secondary emission from lead, since ordinary lead contains about 50 per cent. of "thorium lead," and it is in the re-adjustment of this nucleus immediately after its formation from thorium C″ that the so-called thorium C″ γ-rays are emitted. There therefore arises the possibility of resonance between these γ-rays and the lead nucleus.

Although the absorption coefficient of the hardest component of the characteristic nuclear radiation observed in the experiments already described is almost double that of the incident γ-radiation, it is not possible to say from an analysis of the curve alone that as much as 30 per cent. of unmodified radiation might not be present. In fact, from the results of similar experiments, Meitner and Hupfeld* have suggested that the secondary emission may consist merely of an unmodified γ-radiation mixed with a considerable intensity of Compton scattered radiation.

---

* 'Naturwiss.,' vol. 19, p. 775 (1931).

The following experiment was therefore designed to test whether any radiation of the same hardness as the primary radiation is emitted in the backward direction when lead is irradiated with thorium C″ γ-rays.

Let the intensity of the primary radiation from a source S, situated on the axis of a cylindrical hole in a lead block at the point P, fig. 5, be

$$\frac{\mathrm{I}}{r^2} e^{-\mu(r - d \operatorname{cosec} \theta)},$$

where d is the radius of the hole in the lead.

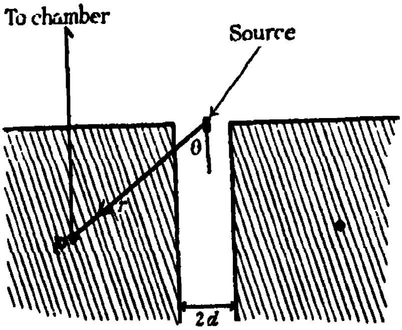

FIG. 5.

The number of atoms in the volume ($r\,d\theta\,dr\,2\pi r \sin\theta$) of the annular ring through P, will be

$$\frac{\mathrm{N}}{\mathrm{Z}}(r\,d\theta\,dr\,2\pi r \sin\theta),$$

and if ψ_{N} represent the fraction of the incident energy scattered by each nucleus with unchanged wave-length, the ionisation produced in the chamber, fig. 6, due to the annular ring is

$$\frac{\mathrm{I}_0\chi}{r^2} e^{-\mu(r - d \operatorname{cosec} \theta)} \left(\frac{\mathrm{N}}{\mathrm{Z}} 2\pi r \sin\theta r\,d\theta\,dr\right) \frac{\psi_{\mathrm{N}}\mathrm{A}}{4\pi} e^{-\mu r \cos\theta},$$

where χ is the ionisation function, A the solid angle subtended by the chamber at the source, and where $e^{-\mu r \cos\theta}$ is the factor which takes into account the absorption of the radiation in emerging perpendicularly from the lead radiator.

The total ionisation produced by the radiator is obtained by integrating with respect to r and θ, and may be shown to be

$$\mathrm{S} = \frac{0 \cdot 693}{2} \mathrm{I}_0 \mathrm{A}\chi \frac{\left(\psi_{\mathrm{N}} \overline{\mathrm{Z}}\right)}{\mu} e^{-\mu d}.$$

The ratio of the ionisations produced by the scattered and the direct radiations is then

$$\frac{S}{D} = \frac{0\cdot693}{2}\frac{\psi_N}{\mu_N}e^{-\mu d}.$$

On introducing a suitable lead block at the back of the source an increase in ionisation should occur in the chamber, and that increase should always be the same fractional part of the ionisation produced by the direct radiation whatever may be the filter thickness employed, since the primary and secondary radiations are assumed to have the same absorption coefficients.

In the experimental arrangement, which is shown in fig. 6, geometrically similar blocks were constructed of lead and of iron. The ionisation due to the direct effect alone was always measured with the iron block in position, and very great care was taken to ensure that the change from iron to lead did not alter the ionisation due to radiation scattered from the walls of the room. The accuracy with which the intensity of the secondary radiation can be measured may obviously be increased by introducing the lead cone, which reduces the direct radiation reaching the chamber without altering the intensity of the secondary radiation.

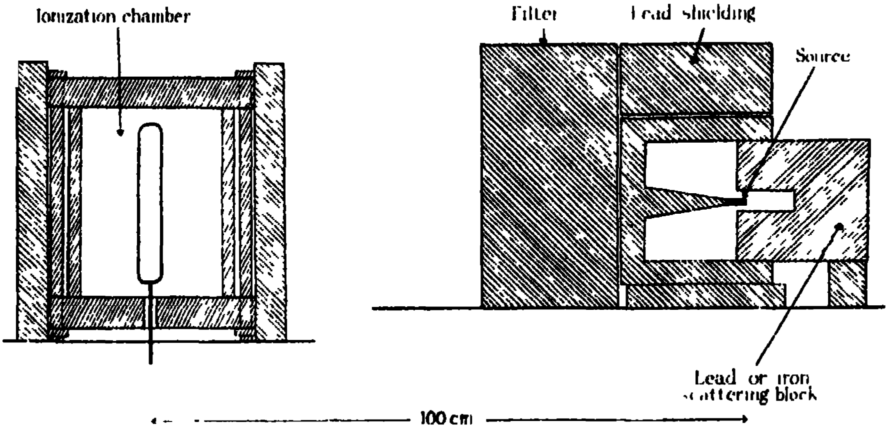

Fig. 6.

With a lead filter 16·5 cm. thick, the observed increase in ionisation was very small, namely 0·07 ± 0·14 per cent., so that the fraction of the incident energy re-radiated per electron without change of wave-length is $0\cdot1 \pm 0\cdot3 \times 10^{-27}$. At the large filter thicknesses employed the characteristic nuclear radiations already discussed in the paper make no appreciable contribution to the ionisation and a numerical evaluation of the formula (based on the wave-mechanics) for the ratio of incoherent to coherent scattering for X-rays show that the classical scattering for the orbital electrons would be expected to be very much smaller than the above figures, viz., $1 \cdot 5 \times 10^{-32}$.

The value of ψ_N found from the above results is $12 \cdot 5 \pm 27 \cdot 0 \times 10^{-27}$, so that not more than 2 per cent. of the secondary radiation emitted by the nucleus (or $0 \cdot 2$ per cent. of the total energy absorbed by the nucleus and its orbital electrons) is of unchanged wave-length.

This result may now be examined in connection with the calculations of Kuhn.* The natural half-width of the hard component of the thorium C″ radiation should be $\nu' = 10^{15}$ sec.$^{-1}$, if it is produced by the oscillation of an α-particle inside a heavy nucleus. The broadening of the emission line caused by temperature vibrations and the displacement consequent on the γ-ray recoil should be very small relative to the natural half-width, being $1 \cdot 5 \times 10^{14}$ sec.$^{-1}$ and 2×10^{13} sec.$^{-1}$ respectively. Thus nearly the whole of the energy of this γ-ray should lie exactly within the absorption line, so that the absorption coefficient in pure thorium lead should be about 12 cm.$^{-1}$, or 6 cm.$^{-1}$ in ordinary lead. Such absorption coefficients are certainly not observed.

If, however, the emission of the γ-radiation occurs while the atom of thorium lead is still recoiling as a result of the β-particle disintegration of thorium C″, the γ-ray line will be broadened to a half-width $\nu = 1 \cdot 5 \times 10^{15}$ sec.$^{-1}$. One-third of the γ-ray only would then lie in the absorption band, and the mean absorption coefficient would be about 2 cm.$^{-1}$, or, per electron, 730×10^{-27}, which is 2000 times larger than the limit set by the above experiment.

The disagreement would be even greater if the radiation was produced by an electron or a proton, so that it appears necessary to conclude either that the theoretical calculations are incorrect, or, as is highly probable, that the resonance cannot occur because the lower energy level of the transition emitting this radiation ($2 \cdot 65 \times 10^6$ e-volts) is not the general ground level of the atom.

Summary.

A number of independent investigations have shown that γ-radiation of 2 to 3 million volts quantum energy is much more strongly absorbed than would be expected, in elements of high atomic number. The additional absorption has been attributed provisionally to interaction with the nucleus.

---

* 'Phil. Mag.,' vol. 8, p. 625 (1929).

This conclusion receives further support from the experiments described in this paper, which show that in the case of the hard γ-rays of Th C″ and Ra C the absorption is associated with the emission of a secondary γ-radiation quite unlike the radiation scattered by the electronic system of the outer atom, in that the wave-length of this radiation is neither the same as that of the primary radiation, nor varies with angle in accordance with the Compton equations. Moreover, the quantum energy of the secondary radiation appears to be independent of that of the primary radiation, provided this exceeds a certain threshold value, which by two independent methods, has been found to lie between 1·5 and 2·0 million volts. These results suggest that the absorption process consists in the excitation of the nucleus, which subsequently emits "characteristic radiations."

The absorption curves of the characteristic radiations of lead, tin, iron, and oxygen have been found to be very similar. A unique determination of wave-length is not possible by absorption methods, but the simplest interpretation of the curve is that all four elements emit the same two radiations (having quantum energies of 0·5 and 1·0 million volts) but in different proportions, leading to the view that the radiations are characteristic of some unit of nuclear structure present in all nuclei.

The Existence of a Neutron.

By J. Chadwick, F.R.S.

(Received May 10, 1932.)

§ 1. It was shown by Bothe and Becker* that some light elements when bombarded by α-particles of polonium emit radiations which appear to be of the γ-ray type. The element beryllium gave a particularly marked effect of this kind, and later observations by Bothe, by Mme. Curie-Joliot† and by Webster‡ showed that the radiation excited in beryllium possessed a penetrating power distinctly greater than that of any γ-radiation yet found from the radioactive elements. In Webster's experiments the intensity of the radiation was measured both by means of the Geiger-Müller tube counter and in a high pressure ionisation chamber. He found that the beryllium radiation had an absorption coefficient in lead of about $0 \cdot 22$ cm.$^{-1}$ as measured under his experimental conditions. Making the necessary corrections for these conditions, and using the results of Gray and Tarrant to estimate the relative contributions of scattering, photoelectric absorption, and nuclear absorption in the absorption of such penetrating radiation, Webster concluded that the radiation had a quantum energy of about 7×10^6 electron volts. Similarly he found that the radiation from boron bombarded by α-particles of polonium consisted in part of a radiation rather more penetrating than that from beryllium, and he estimated the quantum energy of this component as about 10×10^6 electron volts. These conclusions agree quite well with the supposition that the radiations arise by the capture of the α-particle into the beryllium (or boron) nucleus and the emission of the surplus energy as a quantum of radiation.

The radiations showed, however, certain peculiarities, and at my request the beryllium radiation was passed into an expansion chamber and several photographs were taken. No unexpected phenomena were observed though, as will be seen later, similar experiments have now revealed some rather striking events. The failure of these early experiments was partly due to the weakness of the available source of polonium, and partly to the experimental arrangement, which, as it now appears, was not very suitable.

---

* 'Z. Physik,' vol. 66, p. 289 (1930).

† I. Curie, 'C. R. Acad. Sci. Paris,' vol. 193, p. 1412 (1931).

‡ 'Proc. Roy. Soc.,' A, vol. 136, p. 428 (1932).

Quite recently, Mme. Curie-Joliot and M. Joliot* made the very striking observation that these radiations from beryllium and from boron were able to eject protons with considerable velocities from matter containing hydrogen. In their experiments the radiation from beryllium was passed through a thin window into an ionisation vessel containing air at room pressure. When paraffin wax, or other matter containing hydrogen, was placed in front of the window, the ionisation in the vessel was increased, in some cases as much as doubled. The effect appeared to be due to the ejection of protons, and from further experiment they showed that the protons had ranges in air up to about 26 cm., corresponding to a velocity of nearly 3×10^9 cm. per second. They suggested that energy was transferred from the beryllium radiation to the proton by a process similar to the Compton effect with electrons, and they estimated that the beryllium radiation had a quantum energy of about 50×10^6 electron volts. The range of the protons ejected by the boron radiation was estimated to be about 8 cm. in air, giving on a Compton process an energy of about 35×10^6 electron volts for the effective quantum.†

There are two grave difficulties in such an explanation of this phenomenon. Firstly, it is now well established that the frequency of scattering of high energy quanta by electrons is given with fair accuracy by the Klein-Nishina formula, and this formula should also apply to the scattering of quanta by a proton. The observed frequency of the proton scattering is, however, many thousand times greater than that predicted by this formula. Secondly, it is difficult to account for the production of a quantum of 50×10^6 electron volts from the interaction of a beryllium nucleus and an α-particle of kinetic energy of 5×10^6 electron volts. The process which will give the greatest amount of energy available for radiation is the capture of the α-particle by the beryllium nucleus, Be^9, and its incorporation in the nuclear structure to form a carbon nucleus C^{13}. The mass defect of the C^{13} nucleus is known both from data supplied by measurements of the artificial disintegration of boron B^{10} and from observations of the band spectrum of carbon; it is about 10×10^6 electron volts. The mass defect of Be^9 is not known, but the assumption that it is zero will give a maximum value for the possible change of energy in the reaction $Be^9 + \alpha \rightarrow C^{13}$ + quantum. On this assumption it follows that the energy of the quantum emitted in such a reaction cannot be greater than about 14×10^6 electron volts. It must, of course, be admitted that this argument from mass defects is based on the hypothesis that the nuclei are made as far as possible of α-particles; that the Be^9 nucleus consists of 2 α-particles + 1 proton + 1 electron and the C^{13} nucleus of 3 α-particles + 1 proton + 1 electron. So far as the lighter nuclei are concerned, this assumption is supported by the evidence from experiments on artificial disintegration, but there is no general proof.

---

* Curie and Joliot, 'C. R. Acad. Sci. Paris,' vol. 194, p. 273 (1932).

† Many of the arguments of the subsequent discussion apply equally to both radiations, and the term "beryllium radiation" may often be taken to include the boron radiation.

Accordingly, I made further experiments to examine the properties of the radiation excited in beryllium. It was found that the radiation ejects particles not only from hydrogen but from all other light elements which were examined. The experimental results were very difficult to explain on the hypothesis that the beryllium radiation was a quantum radiation, but followed immediately if it were supposed that the radiation consisted of particles of mass nearly equal to that of a proton and with no net charge, or neutrons. A short statement of some of these observations was published in 'Nature.'* This paper contains a fuller description of the experiments, which suggest the existence of neutrons and from which some of the properties of these particles can be inferred. In the succeeding paper Dr. Feather will give an account of some observations by means of the expansion chamber of the collisions between the beryllium radiation and nitrogen nuclei, and this is followed by an account by Mr. Dee of experiments to observe the collisions with electrons.

§ 2. *Observations of Recoil Atoms.*—The properties of the beryllium radiation were first examined by means of the valve counter used in the work† on the artificial disintegration by α-particles and described fully there. Briefly, it consists of a small ionisation chamber connected to a valve amplifier. The sudden production of ions in the chamber by the entry of an ionising particle is detected by means of an oscillograph connected in the output circuit of the amplifier. The deflections of the oscillograph were recorded photographically on a film of bromide paper.

The source of polonium was prepared from a solution of radium (D+E+F)‡ by deposition on a disc of silver. The disc had a diameter of 1 cm. and was placed close to a disc of pure beryllium of 2 cm. diameter, and both were enclosed in a small vessel which could be evacuated, fig. 1. The first ionisation chamber used had an opening of 13 mm. covered with aluminium foil of 4·5 cm. air equivalent, and a depth of 15 mm. This chamber had a very low natural effect, giving on the average only about 7 deflections per hour.

---

* 'Nature,' vol. 129, p. 312 (1932).

† Chadwick, Constable and Pollard, 'Proc. Roy. Soc.,' A, vol. 130, p. 463 (1931).

‡ The radium D was obtained from old radon tubes generously presented by Dr. C. F. Burnam and Dr. F. West, of the Kelly Hospital, Baltimore.

When the source vessel was placed in front of the ionisation chamber, the number of deflections immediately increased. For a distance of 3 cm. between the beryllium and the counter the number of deflections was nearly 4 per minute. Since the number of deflections remained sensibly the same when thick metal sheets, even as much as 2 cm. of lead, were interposed between the source vessel and the counter, it was clear that these deflections were due to a penetrating radiation emitted from the beryllium. It will be shown later that the deflections were due to atoms of nitrogen set in motion by the impact of the beryllium radiation.

When a sheet of paraffin wax about 2 mm. thick was interposed in the path of the radiation just in front of the counter, the number of deflections recorded by the oscillograph increased markedly. This increase was due to particles ejected from the paraffin wax so as to pass into the counter. By placing absorbing screens of aluminium between the wax and the counter the absorption curve shown in fig. 2, curve A, was obtained. From this curve it appears that the particles have a maximum range of just over 40 cm. of air, assuming that an Al foil of 1·64 mg. per square centimetre is equivalent to 1 cm. of air By comparing the sizes of the deflections (proportional to the number of ions produced in the chamber) due to these particles with those due to protons of about the same range it was obvious that the particles were protons. From the range-velocity curve for protons we deduce therefore that the maximum velocity imparted to a proton by the beryllium radiation is about $3 \cdot 3 \times 10^9$ cm. per second, corresponding to an energy of about $5 \cdot 7 \times 10^6$ electron volts.

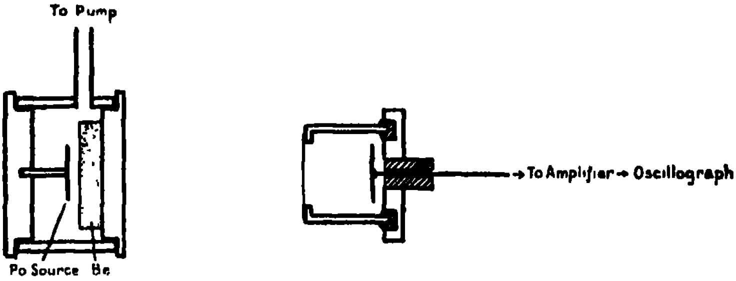

FIG. 1.

The effect of exposing other elements to the beryllium radiation was then investigated. An ionisation chamber was used with an opening covered with a gold foil of 0·5 mm. air equivalent. The element to be examined was fixed on a clean brass plate and placed very close to the counter opening. In this way lithium, beryllium, boron, carbon and nitrogen, as paracyanogen, were tested. In each case the number of deflections observed in the counter increased when the element was bombarded by the beryllium radiation. The ranges of the particles ejected from these elements were quite short, of the order of some millimetres in air. The deflections produced by them were of different sizes, but many of them were large compared with the deflection produced even by a slow proton. The particles therefore have a large ionising power and are probably in each case recoil atoms of the elements. Gases were investigated by filling the ionisation chamber with the required gas by circulation for several minutes. Hydrogen, helium, nitrogen, oxygen, and argon were examined in this way. Again, in each case deflections were observed which were attributed to the production of recoil atoms in the different gases. For a given position of the beryllium source relative to the counter, the number of recoil atoms was roughly the same for each gas. This point will be referred to later. It appears then that the beryllium radiation can impart energy to the atoms of matter through which it passes and that the chance of an energy transfer does not vary widely from one element to another.

It has been shown that protons are ejected from paraffin wax with energies up to a maximum of about $5 \cdot 7 \times 10^6$ electron volts. If the ejection be ascribed to a Compton recoil from a quantum of radiation, then the energy of the quantum must be about 55×10^6 electron volts, for the maximum energy which can be given to a mass m by a quantum $h\nu$ is $\frac{2}{2 + mc^2/h\nu} \cdot h\nu$. The energies of the recoil atoms produced by this radiation by the same process in other elements can be readily calculated. For example, the nitrogen recoil atoms should have energies up to a maximum of 450,000 electron volts. Taking the energy necessary to form a pair of ions in air as 35 electron volts, the recoil atoms of nitrogen should produce not more than about 13,000 pairs of ions. Many of the deflections observed with nitrogen, however, corresponded to far more ions than this; some of the recoil atoms produced from 30,000 to 40,000 ion pairs. In the case of the other elements a similar discrepancy was noted between the observed energies and ranges of the recoil atoms and the values calculated on the assumption that the atoms were set in motion by recoil from a quantum of 55×10^6 electron volts. The energies of the recoil atoms were estimated from the number of ions produced in the counter, as given by the size of the oscillograph deflections. A sufficiently good measurement of the ranges could be made either by varying the distance between the element and the counter or by interposing thin screens of gold between the element and the counter.

The nitrogen recoil atoms were also examined, in collaboration with Dr. N. Feather, by means of the expansion chamber. The source vessel was placed immediately above an expansion chamber of the Shimizu type, so that a large proportion of the beryllium radiation traversed the chamber. A large number of recoil tracks was observed in the course of a few hours. Their range, estimated by eye, was sometimes as much as 5 or 6 mm. in the chamber, or, correcting for the expansion, about 3 mm. in standard air. These visual estimates were confirmed by a preliminary series of experiments by Dr. Feather with a large automatic expansion chamber, in which photographs of the recoil tracks in nitrogen were obtained. Now the ranges of recoil atoms of nitrogen of different velocities have been measured by Blackett and Lees. Using their results we find that the nitrogen recoil atoms produced by the beryllium radiation may have a velocity of at least 4×10^8 cm. per second, corresponding to an energy of about $1 \cdot 2 \times 10^6$ electron volts. In order that the nitrogen nucleus should acquire such an energy in a collision with a quantum of radiation, it is necessary to assume that the energy of the quantum should be about 90×10^6 electron volts, if energy and momentum are conserved in the collision. It has been shown that a quantum of 55×10^6 electron volts is sufficient to explain the hydrogen collisions. In general, the experimental results show that if the recoil atoms are to be explained by collision with a quantum, we must assume a larger and larger energy for the quantum as the mass of the struck atom increases.

§ 3. *The Neutron Hypothesis.*—It is evident that we must either relinquish the application of the conservation of energy and momentum in these collisions or adopt another hypothesis about the nature of the radiation. If we suppose that the radiation is not a quantum radiation, but consists of particles of mass very nearly equal to that of the proton, all the difficulties connected with the collisions disappear, both with regard to their frequency and to the energy transfer to different masses. In order to explain the great penetrating power of the radiation we must further assume that the particle has no net charge. We may suppose it to consist of a proton and an electron in close combination, the " neutron " discussed by Rutherford* in his Bakerian Lecture of 1920.

When such neutrons pass through matter they suffer occasionally close collisions with the atomic nuclei and so give rise to the recoil atoms which are observed. Since the mass of the neutron is equal to that of the proton, the recoil atoms produced when the neutrons pass through matter containing hydrogen will have all velocities up to a maximum which is the same as the maximum velocity of the neutrons. The experiments showed that the maximum velocity of the protons ejected from paraffin wax was about $3\cdot3 \times 10^9$ cm. per second. This is therefore the maximum velocity of the neutrons emitted from beryllium bombarded by α-particles of polonium. From this we can now calculate the maximum energy which can be given by a colliding neutron to other atoms, and we find that the results are in fair agreement with the energies observed in the experiments. For example, a nitrogen atom will acquire in a head-on collision with the neutron of mass 1 and velocity $3\cdot3 \times 10^9$ cm. per second a velocity of $4\cdot4 \times 10^8$ cm. per second, corresponding to an energy of $1\cdot4 \times 10^6$ electron volts, a range of about 3·3 mm. in air, and a production of ions of about 40,000 pairs. Similarly, an argon atom may acquire an energy of $0\cdot54 \times 10^6$ electron volts, and produce about 15,000 ion pairs. Both these values are in good accord with experiment.*

---

* Rutherford, 'Proc. Roy. Soc.,' A, vol. 97, p. 374 (1920). Experiments to detect the formation of neutrons in a hydrogen discharge tube were made by J. L. Glasson, 'Phil. Mag.,' vol. 42, p. 596 (1921), and by J. K. Roberts, 'Proc. Roy. Soc.,' A, vol. 102, p. 72 (1922). Since 1920 many experiments in search of these neutrons have been made in this laboratory.

It is possible to prove that the mass of the neutron is roughly equal to that of the proton, by combining the evidence from the hydrogen collisions with that from the nitrogen collisions. In the succeeding paper, Feather records experiments in which about 100 tracks of nitrogen recoil atoms have been photographed in the expansion chamber. The measurement of the tracks shows that the maximum range of the recoil atoms is 3·5 mm. in air at 15° C. and 760 mm. pressure, corresponding to a velocity of $4\cdot7 \times 10^8$ cm. per second according to Blackett and Lees. If M, V be the mass and velocity of the neutron then the maximum velocity given to a hydrogen atom is

$$u_p = \frac{2M}{M+1} \cdot V,$$

and the maximum velocity given to a nitrogen atom is

$$u_n = \frac{2M}{M+14} \cdot V,$$

whence

$$\frac{M+14}{M+1} = \frac{u_p}{u_n} = \frac{3\cdot3 \times 10^9}{4\cdot7 \times 10^8},$$

---

* It was noted that a few of the nitrogen recoil atoms produced about 50 to 60,000 ion pairs. These probably correspond to the cases of disintegration found by Feather and described in his paper.

and

$$M = 1 \cdot 15.$$

The total error in the estimation of the velocity of the nitrogen recoil atom may easily be about 10 per cent., and it is legitimate to conclude that the mass of the neutron is very nearly the same as the mass of the proton.

We have now to consider the production of the neutrons from beryllium by the bombardment of the α-particles. We must suppose that an α-particle is captured by a Be^9 nucleus with the formation of a carbon C^{12} nucleus and the emission of a neutron. The process is analogous to the well-known artificial disintegrations, but a neutron is emitted instead of a proton. The energy relations of this process cannot be exactly deduced, for the masses of the Be^9 nucleus and the neutron are not known accurately. It is, however, easy to show that such a process fits the experimental facts. We have

$$\begin{aligned} &Be^9 + He^4 + \text{kinetic energy of } \alpha \\ &\qquad = C^{12} + n^1 + \text{kinetic energy of } C^{12} + \text{kinetic energy of } n^1. \end{aligned}$$

If we assume that the beryllium nucleus consists of two α-particles and a neutron, then its mass cannot be greater than the sum of the masses of these particles, for the binding energy corresponds to a defect of mass. The energy equation becomes

$$\begin{aligned} (8 \cdot 00212 + n^1) + 4 \cdot 00106 + \text{K.E. of } \alpha > 12 \cdot 0003 + n^1 \\ + \text{K.E. of } C^{12} + \text{K.E. of } n^1 \end{aligned}$$

or

$$\text{K.E. of } n^1 < \text{K.E. of } \alpha + 0 \cdot 003 - \text{K.E. of } C^{12}.$$

Since the kinetic energy of the α-particle of polonium is $5 \cdot 25 \times 10^6$ electron volts, it follows that the energy of emission of the neutron cannot be greater than about 8×10^6 electron volts. The velocity of the neutron must therefore be less than $3 \cdot 9 \times 10^9$ cm. per second. We have seen that the actual maximum velocity of the neutron is about $3 \cdot 3 \times 10^9$ cm. per second, so that the proposed disintegration process is compatible with observation.

A further test of the neutron hypothesis was obtained by examining the radiation emitted from beryllium in the opposite direction to the bombarding α-particles. The source vessel, fig. 1, was reversed so that a sheet of paraffin wax in front of the counter was exposed to the "backward" radiation from the beryllium. The maximum range of the protons ejected from the wax was determined as before, by counting the numbers of protons observed through different thicknesses of aluminium interposed between the wax and the counter.

The absorption curve obtained is shown in curve B, fig. 2. The maximum range of the protons was about 22 cm. in air, corresponding to a velocity of about $2 \cdot 74 \times 10^9$ cm. per second. Since the polonium source was only about 2 mm. away from the beryllium, this velocity should be compared with that of the neutrons emitted not at 180° but at an angle not much greater than 90° to the direction of the incident α-particles. A simple calculation shows that the velocity of the neutron emitted at 90° when an α-particle of full range is captured by a beryllium nucleus should be $2 \cdot 77 \times 10^9$ cm. per second, taking the velocity of the neutron emitted at 0° in the same process as $3 \cdot 3 \times 10^9$ cm. per second. The velocity found in the above experiment should be less than this, for the angle of emission is slightly greater than 90°. The agreement with calculation is as good as can be expected from such measurements.

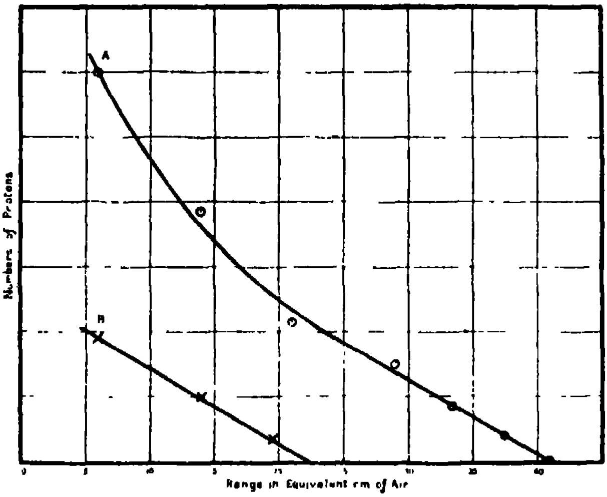

Fig. 2.

§ 4. *The Nature of the Neutron.*—It has been shown that the origin of the radiation from beryllium bombarded by α-particles and the behaviour of the radiation, so far as its interaction with atomic nuclei is concerned, receive a simple explanation on the assumption that the radiation consists of particles of mass nearly equal to that of the proton which have no charge. The simplest hypothesis one can make about the nature of the particle is to suppose that it consists of a proton and an electron in close combination, giving a net charge 0 and a mass which should be slightly less than the mass of the hydrogen atom. This hypothesis is supported by an examination of the evidence which can be obtained about the mass of the neutron.

As we have seen, a rough estimate of the mass of the neutron was obtained from measurements of its collisions with hydrogen and nitrogen atoms, but such measurements cannot be made with sufficient accuracy for the present purpose. We must turn to a consideration of the energy relations in a process in which a neutron is liberated from an atomic nucleus; if the masses of the atomic nuclei concerned in the process are accurately known, a good estimate of the mass of the neutron can be deduced. The mass of the beryllium nucleus has, however, not yet been measured, and, as was shown in § 3, only general conclusions can be drawn from this reaction. Fortunately, there remains the case of boron. It was stated in § 1 that boron bombarded by α-particles of polonium also emits a radiation which ejects protons from materials containing hydrogen. Further examination showed that this radiation behaves in all respects like that from beryllium, and it must therefore be assumed to consist of neutrons. It is probable that the neutrons are emitted from the isotope B^{11}, for we know that the isotope B^{10} disintegrates with the emission of a proton.[*] The process of disintegration will then be

$$B^{11} + He^4 \rightarrow N^{14} + n^1.$$

The masses of B^{11} and N^{14} are known from Aston's measurements, and the further data required for the deduction of the mass of the neutron can be obtained by experiment.

In the source vessel of fig. 1 the beryllium was replaced by a target of powdered boron, deposited on a graphite plate. The range of the protons ejected by the boron radiation was measured in the same way as with the beryllium radiation. The effects observed were much smaller than with beryllium, and it was difficult to measure the range of the protons accurately. The maximum range was about 16 cm. in air, corresponding to a velocity of $2 \cdot 5 \times 10^9$ cm. per second. This then is the maximum velocity of the neutron liberated from boron by an α-particle of polonium of velocity $1 \cdot 59 \times 10^9$ cm. per second. Assuming that momentum is conserved in the collision, the velocity of the recoiling N^{14} nucleus can be calculated, and we then know the kinetic energies of all the particles concerned in the disintegration process. The energy equation of the process is

$$\begin{aligned}\text{Mass of } B^{11} &+ \text{mass of } He^4 + \text{K.E. of } He^4 \\ &= \text{mass of } N^{14} + \text{mass of } n^1 + \text{K.E. of } N^{14} + \text{K.E. of } n^1.\end{aligned}$$

---

[*] Chadwick, Constable and Pollard, *loc. cit.*

The masses are $B^{11} = 11 \cdot 00825 \pm 0 \cdot 0016$; $He^4 = 4 \cdot 00106 \pm 0 \cdot 0006$; $N^{14} = 14 \cdot 0042 \pm 0 \cdot 0028$. The kinetic energies in mass units are α-particle = 0·00565; neutron = 0·0035; and nitrogen nucleus = 0·00061. We find therefore that the mass of the neutron is 1·0067. The errors quoted for the mass measurements are those given by Aston. They are the maximum errors which can be allowed in his measurements, and the probable error may be taken as about one-quarter of these.* Allowing for the errors in the mass measurements it appears that the mass of the neutron cannot be less than 1·003, and that it probably lies between 1·005 and 1·008.

Such a value for the mass of the neutron is to be expected if the neutron consists of a proton and an electron, and it lends strong support to this view. Since the sum of the masses of the proton and electron is 1·0078, the binding energy, or mass defect, of the neutron is about 1 to 2 million electron volts. This is quite a reasonable value. We may suppose that the proton and electron form a small dipole, or we may take the more attractive picture of a proton embedded in an electron. On either view, we may expect the "radius" of the neutron to be a few times 10^{-13} cm.

§ 5. *The Passage of the Neutron through Matter.*—The electrical field of a neutron of this kind will clearly be extremely small except at very small distances of the order of 10^{-12} cm. In its passage through matter the neutron will not be deflected unless it suffers an intimate collision with a nucleus. The potential of a neutron in the field of a nucleus may be represented roughly by fig. 3. The radius of the collision area for sensible deflection of the neutron will be little greater than the radius of the nucleus. Further, the neutron should be able to penetrate the nucleus easily, and it may be that the scattering of the neutrons will be largely due to the internal field of the nucleus, or, in other words, that the scattered neutrons are mainly those which have penetrated

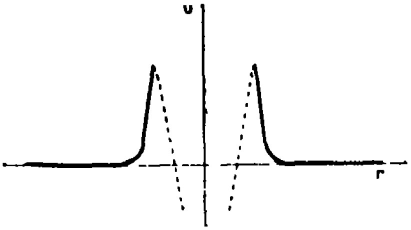

Fig. 3.

---

* The mass of B^{11} relative to B^{10} has been checked by optical methods by Jenkins and McKellar ('Phys. Rev.,' vol. 39, p. 549 (1932)). Their value agrees with Aston's to 1 part in 10^5. This suggests that great confidence may be put in Aston's measurements.

the potential barrier. On these views we should expect the collisions of a neutron with a nucleus to occur very seldom, and that the scattering will be roughly equal in all directions, at least as compared with the Coulomb scattering of a charged particle.

These conclusions were confirmed in the following way. The source vessel, with Be target, was placed rather more than 1 inch from the face of a closed counter filled with air, fig. 1. The number of deflections, or the number of nitrogen recoil atoms produced in the chamber, was observed for a certain time. The number observed was 190 per hour, after allowing for the natural effect. A block of lead 1 inch thick was then introduced between the source vessel and the counter. The number of deflections fell to 166 per hour. Since the number of recoil atoms produced must be proportional to the number of neutrons passing through the counter, these observations show that 13 per cent. of the neutrons had been absorbed or scattered in passing through 1 inch of lead.

Suppose that a neutron which passes within a distance p from the centre of the lead nucleus is scattered and removed from the beam. Then the fraction removed from the beam in passing through a thickness t of lead will be $\pi p^2 nt$, where n is the number of lead atoms per unit volume. Hence $\pi p^2 nt = 0 \cdot 13$, and $p = 7 \times 10^{-13}$ cm. This value for the collision radius with lead seems perhaps rather small, but it is not unreasonable. We may compare it with the radii of the radioactive nuclei calculated from the disintegration constants by Gamow and Houtermans,* viz., about 7×10^{-13} cm.

Similar experiments were made in which the neutron radiation was passed through blocks of brass and carbon. The values of p deduced in the same way were 6×10^{-13} cm. and $3 \cdot 5 \times 10^{-13}$ cm. respectively.

The target areas for collision for some light elements were compared by another method. The second ionisation chamber was used, which could be filled with different gases by circulation. The position of the source vessel was kept fixed relative to the counter, and the number of deflections was observed when the counter was filled in turn with hydrogen, nitrogen, oxygen, and argon. Since the number of neutrons passing through the counter was the same in each case, the number of deflections should be proportional to the target area for collision, neglecting the effect of the material of the counter, and allowing for the fact that argon is monatomic. It was found that nitrogen, oxygen, and argon gave about the same number of deflections; the target areas of nitrogen and oxygen are thus roughly equal, and the target area of argon is nearly twice that of these. With hydrogen the measurements were very difficult, for many of the deflections were very small owing to the low ionising power of the proton and the low density of the gas. It seems probable from the results that the target area of hydrogen is about two-thirds that of nitrogen or oxygen, but it may be rather greater than this.

---

* 'Z. Physik.' vol. 52, p. 453 (1928).

There is as yet little information about the angular distribution of the scattered neutrons. In some experiments kindly made for me by Dr. Gray and Mr. Lea, the scattering by lead was compared in the backward and forward directions, using the ionisation in a high pressure chamber to measure the neutrons. They found that the amount of scattering was about that to be expected from the measurements quoted above, and that the intensity per unit solid angle was about the same between 30° to 90° in the forward direction as between 90° to 150° in the backward direction. The scattering by lead is therefore not markedly anisotropic.

Two types of collision may prove to be of peculiar interest, the collision of a neutron with a proton and the collision with an electron. A detailed study of these collisions with an elementary particle is of special interest, for it should provide information about the structure and field of the neutron, whereas the other collisions will depend mainly on the structure of the atomic nuclei. Some preliminary experiments by Mr. Lea, using the pressure chamber to measure the scattering of neutrons by paraffin wax and by liquid hydrogen, suggest that the collision with a proton is more frequent than with other light atoms. This is not in accord with the experiments described above, but the results are at present indecisive. These collisions can be more directly investigated by means of the expansion chamber or by counting methods, and it is hoped to do so shortly.

The collision of a neutron with an electron has been examined in two ways, by the expansion chamber and by the counter. An account of the expansion chamber experiments is given by Mr. Dee in the third paper of this series. Mr. Dee has looked for the general ionisation produced by a large number of neutrons in passing through the expansion chamber, and also for the short electron tracks which should be the result of a very close collision between a neutron and an electron. His results show that collisions with electrons are extremely rare compared even with those with nitrogen nuclei, and he estimates that a neutron can produce on the average not more than 1 ion pair in passing through 3 metres of air.

In the counter experiments a beam of neutrons was passed through a block of brass, 1 inch thick, and the maximum range of the protons ejected from paraffin wax by the emergent beam was measured. From this range the maximum velocity of the neutrons after travelling through the brass is obtained and it can be compared with the maximum velocity in the incident beam. No change in the velocity of the neutrons due to their passage through the brass could be detected. The accuracy of the experiment is not high, for the estimation of the end of the range of the protons was rather difficult. The results show that the loss of energy of a neutron in passing through 1 inch of brass is not more than about $0 \cdot 4 \times 10^6$ electron volts. A path of 1 inch in brass corresponds as regards electron collisions to a path of nearly 2×10^4 cm. of air, so that this result would suggest that a neutron loses less than 20 volts per centimetre path in air in electron collisions. This experiment thus lends general support to those with the expansion chamber, though it is of far inferior accuracy. We conclude that the transfer of energy from the neutron to electrons is of very rare occurrence. This is not unexpected. Bohr* has shown on quite general ideas that collisions of a neutron with an electron should be very few compared with nuclear collisions. Massey,† on plausible assumptions about the field of the neutron, has made a detailed calculation of the loss of energy to electrons, and finds also that it should be small, not more than 1 ion pair per metre in air.

General Remarks.

It is of interest to examine whether other elements, besides beryllium and boron, emit neutrons when bombarded by α-particles. So far as experiments have been made, no case comparable with these two has been found. Some evidence was obtained of the emission of neutrons from fluorine and magnesium, but the effects were very small, rather less than 1 per cent. of the effect obtained from beryllium under the same conditions. There is also the possibility that some elements may emit neutrons spontaneously, *e.g.*, potassium, which is known to emit a nuclear β-radiation accompanied by a more penetrating radiation. Again no evidence was found of the presence of neutrons, and it seems fairly certain that the penetrating type is, as has been assumed, a γ-radiation.

Although there is certain evidence for the emission of neutrons only in two cases of nuclear transformations, we must nevertheless suppose that the neutron is a common constituent of atomic nuclei. We may then proceed to build up nuclei out of α-particles, neutrons and protons, and we are able to avoid the presence of uncombined electrons in a nucleus. This has certain advantages for, as is well known, the electrons in a nucleus have lost some of the properties which they have outside, *e.g.*, their spin and magnetic moment. If the α-particle, the neutron, and the proton are the only units of nuclear structure, we can proceed to calculate the mass defect or binding energy of a nucleus as the difference between the mass of the nucleus and the sum of the masses of the constituent particles. It is, however, by no means certain that the α-particle and the neutron are the only complex particles in the nuclear structure, and therefore the mass defects calculated in this way may not be the true binding energies of the nuclei. In this connection it may be noted that the examples of disintegration discussed by Dr. Feather in the next paper are not all of one type, and he suggests that in some cases a particle of mass 2 and charge 1, the hydrogen isotope recently reported by Urey, Brickwedde and Murphy, may be emitted. It is indeed possible that this particle also occurs as a unit of nuclear structure.

---

* Bohr, Copenhagen discussions, unpublished.

† Massey, 'Nature,' vol. 129, p. 469, corrected p. 691 (1932).

It has so far been assumed that the neutron is a complex particle consisting of a proton and an electron. This is the simplest assumption and it is supported by the evidence that the mass of the neutron is about 1·006, just a little less than the sum of the masses of a proton and an electron. Such a neutron would appear to be the first step in the combination of the elementary particles towards the formation of a nucleus. It is obvious that this neutron may help us to visualise the building up of more complex structures, but the discussion of these matters will not be pursued further for such speculations, though not idle, are not at the moment very fruitful. It is, of course, possible to suppose that the neutron may be an elementary particle. This view has little to recommend it at present, except the possibility of explaining the statistics of such nuclei as N^{14}.

There remains to discuss the transformations which take place when an α-particle is captured by a beryllium nucleus, Be^9. The evidence given here indicates that the main type of transformation is the formation of a C^{12} nucleus and the emission of a neutron. The experiments of Curie-Joliot and Joliot,* of Auger,† and of Dee show quite definitely that there is some radiation emitted by beryllium which is able to eject fast electrons in passing through matter. I have made experiments using the Geiger point counter to investigate this radiation and the results suggest that the electrons are produced by a

---

* 'C. R. Acad. Sci. Paris,' vol. 194, p. 708 and p. 876 (1932).

† 'C. R. Acad. Sci. Paris,' vol. 194, p. 877 (1932).

γ-radiation. There are two distinct processes which may give rise to such a radiation. In the first place, we may suppose that the transformation of Be^9 to C^{12} takes place sometimes with the formation of an excited C^{12} nucleus which goes to the ground state with the emission of γ-radiation. This is similar to the transformations which are supposed to occur in some cases of disintegration with proton emission, *e.g.*, B^{10}, F^{19}, Al^{27}; the majority of transformations occur with the formation of an excited nucleus, only in about one-quarter is the final state of the residual nucleus reached in one step. We should then have two groups of neutrons of different energies and a γ-radiation of quantum energy equal to the difference in energy of the neutron groups. The quantum energy of this radiation must be less than the maximum energy of the neutrons emitted, about $5 \cdot 7 \times 10^6$ electron volts. In the second place, we may suppose that occasionally the beryllium nucleus changes to a C^{12} nucleus and that all the surplus energy is emitted as radiation. In this case the quantum energy of the radiation may be about 10×10^6 electron volts.

It is of interest to note that Webster has observed a soft radiation from beryllium bombarded by polonium α-particles, of energy about 5×10^5 electron volts. This radiation may well be ascribed to the first of the two processes just discussed, and its intensity is of the right order. On the other hand, some of the electrons observed by Curie-Joliot and Joliot had energies of the order of 2 to 10×10^6 volts, and Auger recorded one example of an electron of energy about $6 \cdot 5 \times 10^6$ volts. These electrons may be due to a hard γ-radiation produced by the second type of transformation.*

It may be remarked that no electrons of greater energy than the above appear to be present. This is confirmed by an experiment† made in this laboratory by Dr. Occhialini. Two tube counters were placed in a horizontal plane and the number of coincidences recorded by them was observed by means of the method devised by Rossi. The beryllium source was then brought up in the plane of the counters so that the radiation passed through both counters in turn. No increase in the number of coincidences could be detected. It follows that there are few, if any, β-rays produced with energies sufficient to pass through the walls of both counters, a total of 4 mm. brass; that is, with energies greater than about 6×10^6 volts. This experiment further shows that the neutrons very rarely produce coincidences in tube counters under the usual conditions of experiment.

---

* Although the presence of fast electrons can be easily explained in this way, the possibility that some may be due to secondary effects of the neutrons must not be lost sight of.

† *Cf.* also Rasetti, 'Naturwiss.,' vol. 20, p. 252 (1932).

In conclusion, I may restate briefly the case for supposing that the radiation the effects of which have been examined in this paper consists of neutral particles rather than of radiation quanta. Firstly, there is no evidence from electron collisions of the presence of a radiation of such a quantum energy as is necessary to account for the nuclear collisions. Secondly, the quantum hypothesis can be sustained only by relinquishing the conservation of energy and momentum. On the other hand, the neutron hypothesis gives an immediate and simple explanation of the experimental facts; it is consistent in itself and it throws new light on the problem of nuclear structure.

Summary.

The properties of the penetrating radiation emitted from beryllium (and boron) when bombarded by the α-particles of polonium have been examined. It is concluded that the radiation consists, not of quanta as hitherto supposed, but of neutrons, particles of mass 1, and charge 0. Evidence is given to show that the mass of the neutron is probably between 1·005 and 1·008. This suggests that the neutron consists of a proton and an electron in close combination, the binding energy being about 1 to 2×10^6 electron volts. From experiments on the passage of the neutrons through matter the frequency of their collisions with atomic nuclei and with electrons is discussed.

I wish to express my thanks to Mr. H. Nutt for his help in carrying out the experiments.

The Collisions of Neutrons with Nitrogen Nuclei.

By N. FEATHER, Ph.D., Fellow of Trinity College, Cambridge.

(Communicated by J. Chadwick, F.R.S.—Received May 10, 1932.)

[PLATES 15 AND 16.]

Introduction.

Elsewhere in these 'Proceedings'* experiments are described in which the radiations excited in certain light elements under α-particle bombardment are examined in great detail by means of the valve counter. On the basis of such experiments in the case of beryllium Chadwick† was first led to suggest that the radiation, previously believed to be of the γ-ray type, in fact consisted of particles of zero resultant charge and unit mass. In the present paper a study of this radiation is described, in which the expansion chamber is employed.

Initially visual observations were made with a Shimizu chamber and the production in air of recoil atoms demonstrated.† A more detailed investigation has now been completed in which the usual photographic methods‡ have been employed. Curie and Joliot§ likewise used an expansion chamber in preliminary experiments to establish the ejection of protons from paraffin under the influence of the radiation from beryllium, and later published photographs|| of recoil tracks both of protons and helium nuclei. Similar photographs were published by Rasetti,¶ whilst Auger** has also given examples of the tracks of protons produced in this way. Kirsch and Rieder†† have made more extensive experiments, using visual methods throughout. In certain cases electron tracks also were reported. This aspect of the problem is dealt with by Dee‡‡ in the paper next after this.

---

* Chadwick, 'Proc. Roy. Soc.,' A, vol. 136, p. 692 (1932).

† 'Nature,' vol. 129, p. 312 (1932).

‡ Photographs were taken with a source of polonium and beryllium in the centre of an expansion chamber by Holoubek in 1927 ('Z. Physik,' vol. 42, p. 704 (1927)) and, with a different arrangement employing smaller solid angles, by Champion in 1931 (see Webster, 'Proc. Roy. Soc.,' A, vol. 136, p. 428 (1932)), but as far as is known no recoil track was observed in either case to originate in the gas.

§ 'C. R. Acad. Sci. Paris,' vol. 194, p. 708 (1932).

|| 'C. R. Acad. Sci. Paris,' vol. 194, p. 876 (1932).

¶ 'Naturwiss.,' vol. 20, p. 252 (1932).

** 'C. R. Acad. Sci. Paris,' vol. 194, p. 877 (1932).

†† 'SitzBer. Akad. Wiss. Wien.' (*in course of publication*). Communication No. 288 (*a*) from the Radium Research Institute of Vienna.

‡‡ 'Proc. Roy. Soc.,' A, vol. 136, p. 727 (1932).

In the experiments to be described the gas chiefly used was nitrogen, and the general results may be stated at once. Recoil tracks of maximum length about 3·5 mm. under standard conditions were obtained with considerable frequency and almost as frequently an entirely new phenomenon was observed, namely, examples of paired tracks having a common origin. These are regarded as evidence for the disintegration of the nitrogen nucleus by the incident radiation[*]; so interpreted they provide further support for the hypothesis of its neutron (particular) nature. It is of interest to remark that the first evidence for artificial disintegration by α-particles also was obtained in the case of nitrogen,[†] whilst the only disintegration photographs hitherto published[‡] have reference to the same gas. Detailed analysis in the present case shows that when disintegration occurs with capture of the neutron an α-particle is expelled (capture of an α-particle results normally in the expulsion of a proton), but it also suggests that other types of non-capture disintegration occur, in some of which, at least, it is more probable that a proton is emitted. It will be seen, then, that the results are both novel and also of considerable complexity. Further investigation will obviously be required before a complete statement can be made.

General Experimental Arrangement.

The apparatus employed in the present experiment is the same, except for small modifications, as that which the writer has been using during the past 6 months for α-particle track photography, in an attempt to observe certain cases of artificial disintegration. A more detailed description of the automatic expansion chamber and stereoscopic camera system may be reserved until the results of the above-mentioned work are published. It suffices here to give a brief description. The expansion chamber had an internal diameter of 17 cm. and a maximum depth of 5·9 cm. It was illuminated by light from two horizontal quartz mercury lamps placed behind suitably arranged[§] cylindrical lenses, and a condenser of 1/20 mfd. charged to about 30 kv. was discharged through the two lamps in parallel immediately after each full expansion.

---

[*] Photographs were first taken on February 16 and this general conclusion reached during the following week. A preliminary announcement was made on March 18 by Lord Rutherford in the course of a lecture before the Royal Institution, an abstract of which lecture has since appeared in 'Nature,' vol. 129, p. 457 (1932).

[†] Rutherford, 'Phil. Mag.,' vol. 37, p. 581 (1919).

[‡] Blackett, 'Proc. Roy. Soc.,' A, vol. 107, p. 349 (1925); Harkins and Shadduck, 'Proc. Nat. Acad. Sci.,' vol. 12, p. 707 (1926); Harkins and Schuh, 'Phys. Rev.,' vol. 35, p. 809 (1930); Blackett and Lees, 'Proc. Roy. Soc.,' A, vol. 136, p. 325 (1932).

[§] Only the lower three-fifths of the chamber was directly illuminated.

The axes of the two lenses of the camera were equally inclined to the vertical, and included a stereoscopic angle of 8° 54′, the magnification of the photographs, taken on a single length of standard ciné negative and each occupying the full width of the film, being about 0·17. In order to increase the effective solid angle of irradiation a circular hole 2 cm. in diameter was made centrally in the glass roof of the chamber and the metal source container inserted as shown to scale in fig. 1. The cylindrical walls of the source container introduced an absorption of 0·75 gm. per square centimetre of brass in the path of the radiation and an additional absorber of lead to the extent of 2·74 gm. per square centimetre was disposed as indicated. The lower end of the source container was closed by a plug of brass 1 cm. thick. In this way it was ensured that any characteristic X-radiation produced by α-particle excitation in the metal parts of the interior of the container (or soft γ-rays if a small amount of radium D were present in the source) should be reduced to a completely negligible intensity in the chamber itself. This precaution was necessary on account of the comparatively large number of short electron tracks produced by such a radiation. Under the experimental conditions some of these tracks would almost certainly have been mistaken for the tracks of recoil atoms produced at too late a stage for the best photography. Furthermore, absorbers of the total thickness used are known to have practically no effect on the nuclear radiation from beryllium. A piece of beryllium of 5·7 mm. maximum thickness and freshly cut upper surface 1·7 sq. cm. in area* rested at the bottom of the source container and the polonium source (that used in Dr. Chadwick's experiments) was

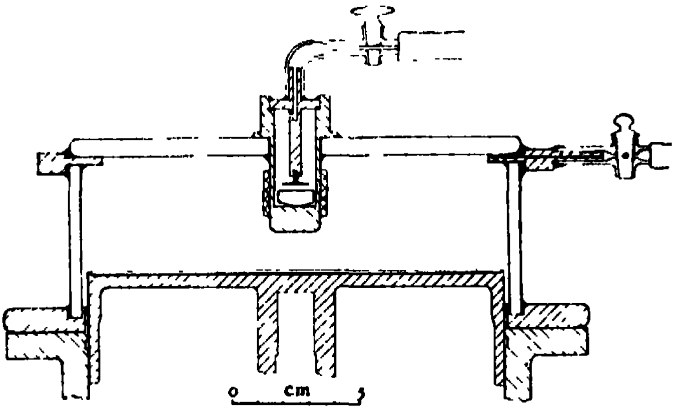

FIG. 1.

---

* I am indebted to Professor Kapitza for this material.

supported 2–3 mm. above. Throughout the experiments the pressure of air in the source container was maintained at 1–2 cm. of mercury, to prevent both undue oxidation of the silver-polonium surface and also needless reduction in velocity of the α-particles incident on the beryllium.

Measurement of the photographs was effected by the method of Nuttall and Williams.* In this method† the film is replaced in the camera, the real image of any track is reconstructed by stereoscopic re-projection and explored by means of pins carried on a revolving table and capable of a wide range of adjustment. A second projection system then allows of the measurement of lengths and angles on a screen, approximately at a fourfold magnification. Angles were not measured directly on the screen, but the latter was covered with a large sheet of squared paper so that the observation of pairs of two-dimensional co-ordinates sufficed. Since in no case does a track appear on the photographs proceeding from the source to the place of nuclear collision, it is obviously impossible to know the direction of incidence of the responsible radiation. This may, however, be fixed within limits, so far as the scattering by the source container and the walls of the chamber will allow, and for this purpose it was arranged that one of the pins on the revolving table could be brought into coincidence with the point in the re-projected image corresponding to the centre of the upper surface of the beryllium in the chamber itself. A knowledge of the distance of this point from the point of collision in any case fixes the corresponding maximum uncertainty in the initial direction.

Altogether 1740 pairs of photographs were taken, the rate of working being generally maintained at about two photographs per minute.

Preliminary Experiments.

The original valve counter experiments of Chadwick showed that under the influence of the nuclear radiation from beryllium sudden bursts of ionisation, many of them representing the production of 3–4 . 10^4 pairs of ions, occurred in a small volume of air, of about 2 cm. maximum linear dimension, at atmospheric pressure. Observations with the Shimizu expansion chamber afforded strong confirmation of the view that these electrical effects, which on any hypothesis pointed to the transformation of 1–1·5 . 10^6 electron volts of energy in a single process, were in fact due to the production of recoil atoms of nitrogen or oxygen with about this amount of energy. If this energy were in any way transferred to the atoms of the gas any other hypothesis would have been untenable almost from the beginning. It was the object of the detailed investigations with the larger chamber to examine the agreement above mentioned on a more definitely quantitative basis and generally to explore other possible types of nuclear interaction which the new type of radiation might show.

---

* 'Proc. Phys. Soc.,' vol. 42, p. 212 (1930).

† The apparatus used was that constructed by Williams and Terroux, 'Proc. Roy. Soc.,' A, vol. 126, p. 289 (1930), and employed in subsequent researches in the Cavendish Laboratory by Terroux, 'Proc. Roy. Soc.,' A, vol. 131, p. 90 (1931); Richardson, 'Proc. Roy. Soc.,' A, vol. 133, p. 367 (1931); and Terroux and Alexander, 'Proc. Camb. Phil. Soc.,' vol. 28, p. 115 (1932).

To this end four short runs, each covering about 70 pairs of photographs, were taken with air initially at atmospheric pressure in the chamber. Two hundred and eighty pairs of photographs* contained 12 examples of recoil tracks, the longest of which was 3·22 mm. in length.† Four tracks showed the projection of particles from the surface of the source container. It is most probable that these particles were protons, since a film of water was generally found to be condensed on the metal surface. One track in the gas more than 5 mm. long and making an angle of 76° with the line joining the centre of the upper surface of the beryllium to the point of collision was with considerable probability ascribed to a proton projected from a molecule of water vapour present in the gas. In addition to these recoil tracks five cases of paired tracks were found. These were regarded as evidence of a new type of artificial disintegration, as has already been indicated. It therefore became highly desirable to replace the air in the chamber by some single gas and so concentrate attention upon a more definite investigation.‡

The Experiments with Nitrogen.

Air was removed from the expansion chamber and nitrogen, from a cylinder, admitted until the composition by volume of the permanent gases present was roughly nitrogen 96 per cent., oxygen 4 per cent. (the residual argon amounted to 0·15 per cent.). This small amount of oxygen was retained for the purpose of ensuring more sharply defined tracks than it is possible to obtain in nitrogen of a higher degree of purity.*

---

* The photographic film, four lengths of about 10 feet each, was developed in the laboratory. One of these afterwards proved useless for measurement owing to a shrinkage of about 0·2 per cent., caused by too long a period of washing.

† The lengths of all tracks are expressed in terms of standard air, *i.e.*, dry air at 760 mm. pressure and 15° C.

‡ Above no mention is made of tracks due to α-particle contamination. This occurred throughout the experiments to the extent of about 19 tracks in 200 expansions, but of these at least half appeared to originate in a highly localised spot of radioactive material on the walls of the chamber. Except for the possibility of some of the tracks from the source container being due to this cause it was not difficult to eliminate contamination effects entirely from the final results.

Two 100-feet lengths of film were exposed with the chamber so filled, and the films, which together contained 1460 pairs of photographs were developed by Messrs. Kodak, Ltd., Kingsway, London. On examination it was found that there had been registered more than a hundred recoil tracks, about thirty paired disintegration tracks and fifty tracks of particles, probably protons, projected from the surface of the source container. These ratios are in general agreement with those found in the preliminary work, which latter were subject to a much greater statistical error. Electron tracks were found on some of the photographs, but the conditions of photography were not sufficiently good nor the expansion conditions the most suitable for their full investigation. For that reason they were left out of account altogether.†

Measurements were made of the lengths of the recoil tracks and, in addition, whenever it was possible with any degree of accuracy, of the angle between the initial direction of motion of the recoiling nucleus and the most probable direction of incidence of the responsible radiation. The maximum angular uncertainty in this latter direction due to the finite size of the effective source was also determined in each case by the method already described. In the case of the paired disintegration tracks the lengths of the tracks were measured, or a lower limit fixed, in case one or other of the particles was not completely absorbed in the chamber, and the following angles were also determined, namely, ω, the angle between the two visible tracks; γ, the angle between the plane of the visible fork and the most probable direction of incidence of the effective radiation; θ, the angle between this most probable direction and the initial direction of motion of the new nucleus; ϕ, the angle between the most probable direction of incidence and the initial direction of motion of the disintegration particle, and Δ, the angle subtended at the point of collision by half the diameter of the effective source. Then, if there is no error in the measurement of the angles so defined, must

$$\omega = \cos^{-1}\left(\frac{\cos\theta}{\cos\gamma}\right) + \cos^{-1}\left(\frac{\cos\phi}{\cos\gamma}\right),$$

---

* Blackett, 'Proc. Roy. Soc.,' A, vol. 107, p. 349 (1925).

† In the course of measurement a few of the "recoil" tracks were rejected on the more probable supposition that they were in fact due to slow electrons, being produced either by the δ particles observed by Dee or as branches to fast β-particle tracks which themselves had escaped detection under the poor conditions obtaining.

and this relation* may be used as a test of the accuracy in actual practice attained.

Analysis of the Results.

Recoil Tracks.—Ranges were measured of 109 recoil tracks starting in the gas.† Of these two had lengths greater than could be measured and for two others values of 5·11 and 11·87 mm. were obtained. The distribution with range of the remaining 105 tracks is shown in fig. 2. Fig. 2, *a* gives the direct distribution, and fig. 2, *b*, the integrated curve, providing a rough comparison with absorption measurements. From either diagram a maximum range of about 3·5 mm. in standard air may be derived. According to the determination of Blackett and Lees‡ this corresponds to a velocity of recoil of 4·72 . 10^8 cm. per second. As has been pointed out elsewhere this value, taken in conjunction with the corresponding maximum velocity of recoil for hydrogen

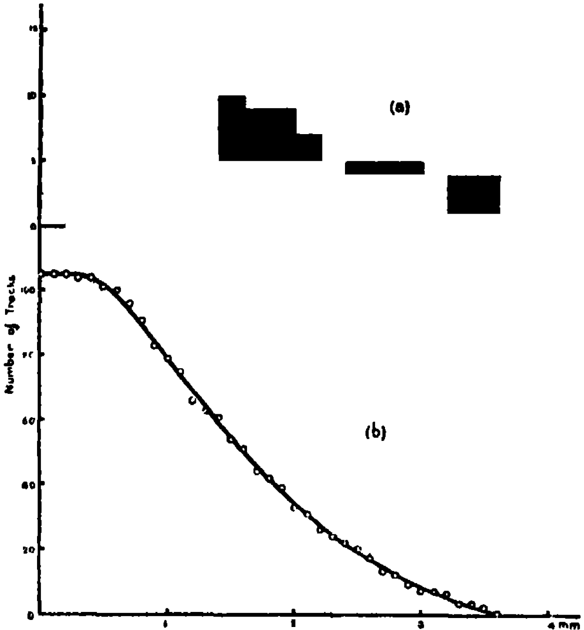

Fig. 2.

---

* When γ is small we have, approximately, if all angles be measured in degrees,

$$\omega = \theta + \phi - \frac{\gamma^2}{114 \cdot 6} (\cot \theta + \cot \phi).$$

† This includes nine tracks obtained in the preliminary experiment with air in the chamber.

‡ 'Proc. Roy. Soc.,' A, vol. 134, p. 658 (1932).

nuclei as determined by Chadwick, and assuming only the conservation of energy and momentum, provides one important test of any hypothesis concerning the nature of the radiation effective in the collisions. If that radiation consisted of quanta of energy small compared with the proper energy of the nuclei concerned then recoil velocities should to a first approximation be inversely as the masses of the recoiling particles. Nitrogen nuclei of range 3·5 mm. in standard air would correspond to protons of about 4 metres range under similar conditions. The maximum range found by Chadwick is about one-tenth of this. The hypothesis of a particle radiation, on the other hand, is in good accord with the facts if particles of mass unity be assumed. The absence of primary tracks due to these particles shows that they possess no resultant charge.

The data obtained from the recoil tracks may be analysed in greater detail than this. Nuclei projected at an angle θ with the direction of incidence by neutrons of a definite initial velocity have, if the collision be perfectly elastic, velocities v_θ given by

$$v_\theta = v_0 \cos \theta,$$

where v_0 is the velocity attained in a head-on collision. By means of the experimental curve of Blackett and Lees this relation may be transformed into one connecting range with angle of projection. In fig. 3 the curves *a*, *b* and *c*, relate *r* and (1 — cos θ) for nitrogen nuclei for the three cases in which v_0=4·5,

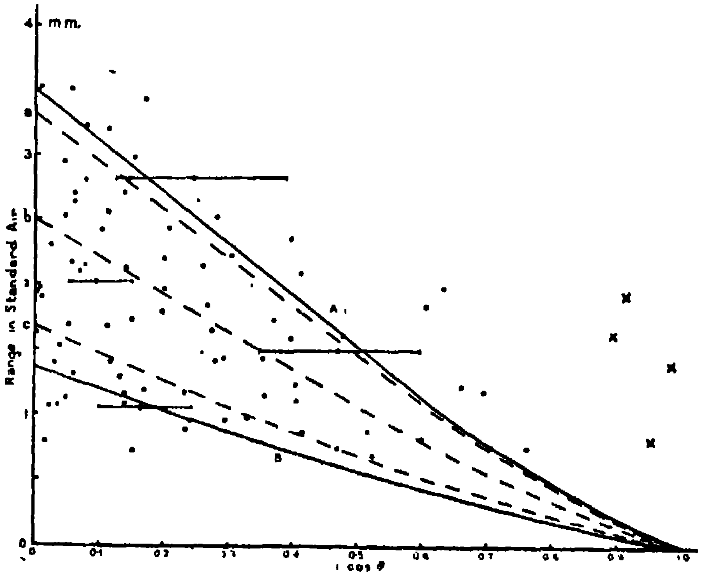

Fig. 3.

3·5 and 2·5 . 10^8 cm. per second, respectively. The points represent measured values of r and θ for 84 of the recoil tracks included in the distributions of fig. 2. The maximum uncertainty in θ due to the finite size of the effective neutron source is indicated by a horizontal line in a number of representative cases. It is obvious at once that, if elastic collisions be assumed, the incident radiation is not homogeneous. An upper limit of v_0 of 4·7 . 10^8 cm. per second and a lower limit not greater than 2·1 . 10^8 cm. per second* appears to be indicated, curves A and B. The probable range of neutron velocities is therefore seen to extend from 3·5 to about 1·6 . 10^9 cm. per second.

Four of the points marked by crosses at the right-hand side of fig. 3 appear to lie beyond the limits of experimental error. The tracks to which they refer, as well as the four longer tracks already excluded from the distribution of fig. 2, were probably produced by protons ejected from the water vapour in the chamber.† Hydrogen atoms contained in the water vapour constitute about 2 per cent. of the total number of gas atoms present; it seems not unreasonable, therefore, that 8 tracks in 109 should be ascribed to protons since the shortest nitrogen recoil tracks no doubt fail to be detected whilst the longer proton tracks are not similarly overlooked.

Figs. 4 to 11, Plate 15, show nitrogen recoil tracks of progressively smaller apparent length, numbers 14 and 16 the tracks of protons ejected from the water condensed on the source container.‡ On number 14 the tracks of long δ-rays are easily visible, number 16 has a length of about 1 cm. in the gas. Amongst the recoil tracks photographed three showed measurable spurs; two of these cases are here reproduced, figs. 12 and 13, Plate 15. Measurement showed, within the limits of error, that the angle between the forward branches of the fork in these cases was 90°, additional evidence, if that were required, that the recoil tracks themselves were produced by nitrogen nuclei. Finally, photograph number 15 is only of interest from the fact that on one occasion three recoil tracks were obtained at a single expansion.§

---

* This lower limit might well have been further reduced if measurement of θ had been possible for all the recoil tracks observed. In general the shorter tracks were excluded from the distribution of fig. 3.

† On this assumption, from the measured values of θ for the tracks of length 5·11 and 11·87 mm. above mentioned, neutron velocities of 3·12 and 2·14 . 10^9 cm. per second, respectively, may be deduced.

‡ In all cases the photographs are so arranged that the source is towards the bottom of the picture; on numbers 7, 10 and 16 part of the upper rim of the source container is visible as a circular arc.

§ The third track at the left-hand bottom corner is, however, very faint on this photograph.

The photographs reproduced appear at a magnification of about eight times from the original film; the magnification from the conditions of standard air is about 1·9.

Disintegration Tracks.—Measurements were made on 32 examples (including certain border-line cases) of paired disintegration tracks photographed in the course of the experiments.* On 12 occasions both the new nucleus and the disintegration particle had been completely absorbed in the chamber, in the 20 remaining cases it was impossible to do more than fix a lower limit to the length of one or other of the tracks. The immediate data which the measurements provided showed fairly conclusively that more than one type of disintegration was in fact being observed. In less than one-half of the cases did the plane of the visible fork contain a possible direction of incidence of the primary (unscattered) radiation. This condition of coplanarity, which is impossible unless $\gamma < \Delta$ (p. 714), must necessarily be fulfilled if disintegration takes place with capture of the incident particle. The remaining cases for which $\gamma > \Delta$ obviously represent nuclear disintegration without capture of the neutron. In these latter cases, as will appear, it is much more difficult from the measurements alone to determine with certainty the exact details of the process involved.

As regards the (presumably) capture cases the following possibilities were numerically explored† :—

(i) $N^{14} + n^1 \rightarrow C^{14} + H^1$.
(ii) $N^{14} + n^1 \rightarrow C^{13} + H^2$.
(iii) $N^{14} + n^1 \rightarrow B^{11} + He^4$.

From the range-velocity curve of Blackett and Lees (*loc. cit.*) for nitrogen recoil atoms similar curves were constructed for the recoil atoms B^{10} (this curve will be employed later), B^{11} and C^{12} (which are indistinguishable for the purpose in hand; that for C^{12} will be employed later), C^{13} (this curve is practically identical with that for N^{14}) and C^{14}. The empirical relation

$$r = kmz^{-\frac{1}{2}} f(v),$$

first suggested by Blackett,‡ was here used. Range velocity curves for protons and α-particles were taken from the latest results of Blackett* in the one case and from those of Briggs† and of Blackett and Lees in the other. Finally, the curve for the recoil atoms H^2 was obtained from the proton curve by the use of the empirical formula above quoted. Using these curves, and assuming in turn each of the possibilities (i) to (iii) mentioned above, the momenta of the new nucleus and the disintegration particle, respectively, were evaluated (where this was possible) for each case. In this way, from the different pairs of possible values, employing the measured value of ω, the resultant final momentum was determined in magnitude and direction. A consistent interpretation of any case was regarded as having been reached only when two conditions had been fulfilled. It was necessary that the magnitude of the resultant momentum should be a possible one for the momentum of the incident neutron—the permissible range of values had already been deduced from the recoil track measurements—and the direction of that resultant an admissible direction of incidence. When it was found impossible in any case to fulfil these conditions on the basis of one or other of the three possibilities, that case was included for consideration with the remaining cases more obviously incapable of explanation on the assumption of artificial disintegration with capture. On the other hand, when these conditions had been fulfilled, not only the general features of the process, but also the energy changes involved could be determined from the measurements. For, initial and final momenta and the masses of the particles being known, it becomes a simple matter to calculate the amount of energy released in the disintegration.

---

* In this number are included four cases occurring in the preliminary work with air in the chamber. A fifth such case, fig. 17, Plate 16, was found on the short length of film which had to be rejected (*vide sup.*).

† The symbol n^1 has been employed to represent a neutron of unit mass.

‡ 'Proc. Roy. Soc.,' A, vol. 107, p. 349 (1925).

Twelve cases of capture were recognised with a fair degree of certainty. It proved possible to explain them all on the assumption that the disintegration particle was an α-particle and the new nucleus so formed a boron nucleus of mass 11. Whilst this explanation covered all the cases, one or other of the remaining possibilities appeared as a considerably less probable alternative in a small fraction of them. As an example of the general method of numerical investigation the following case may be cited.

Serial number XI 531 (ii), fig. 25, Plate 16. Length of track of new nucleus: 1·93 mm. in standard air. Length of track of disintegration particle: 7·32 mm. ω, 128·0°, γ, 4·4°, θ, 63·5°, $\phi = 65{\cdot}4°$, Δ, 7·9°. Test of accuracy of measurement of angles

$$\cos^{-1}\left(\frac{\cos\theta}{\cos\gamma}\right) + \cos^{-1}\left(\frac{\cos\phi}{\cos\gamma}\right) = 128{\cdot}7°.$$

---

* 'Proc. Roy. Soc.,' A, vol. 135, p. 132 (1932).

† 'Proc. Roy. Soc.,' A, vol. 114, p. 341 (1927).

(*a*) On assumption (i) above—

Velocity of new nucleus, C^{14} : $2 \cdot 62 \,.\, 10^8$ cm. per second.

Velocity of disintegration particle, H^1 : $8 \cdot 76 \,.\, 10^8$ cm. per second.

Velocity of incident neutron (calculated) : $3 \cdot 21 \,.\, 10^9$ cm. per second—possible.

Calculated value of θ : 12·4°—quite impossible.

(*b*) On assumption (ii) above—

Calculated value of θ : 20·4°—equally impossible.

(*c*) On assumption (iii) above—

Velocity of new nucleus, B^{11} : $2 \cdot 98 \,.\, 10^8$ cm. per second.

Velocity of disintegration particle, He^4 : $7 \cdot 84 \,.\, 10^8$ cm. per second.

Velocity of incident neutron (calculated) : $2 \cdot 82 \,.\, 10^9$ cm. per second—possible.

Calculated value of θ : 61·3°—possible.

Possibility (iii) being assumed correct—

Energy of incident neutron : $4 \cdot 13 \,.\, 10^6$ electron volts.

Energy of new nucleus : $0 \cdot 51 \,.\, 10^6$ electron volts.

Energy of disintegration particle : $1 \cdot 28 \,.\, 10^6$ electron volts.*

Kinetic energy absorbed in the disintegration process $2 \cdot 34 \,.\, 10^6$ electron volts.

The energy change was found not to be constant from one case to another. Table I exhibits this aspect of the results. The velocity of the incident neutron, V, in units of 10^9 cm. per second, and the absorption of energy W, in units of 10^6 electron volts, are given for the 12 capture cases found.

Table I.

No.	1	2	3	4	5	6	7	8	9	10	11	12
V	2·82	3·26	3·60	3·14	3·45	3·45	2·23	>2·7	2·38	8·49	3·22	~3·5
W	2·34	1·40	2·41	0·63	2·57	0·65	~0·1	~1·0	1·13	3·7	4·5	~ 0

In numbers 1 to 3 both tracks appeared complete, so that the measurements are to that extent the more trustworthy, for the rest one or other particle was not observed over the full length of its path. Results 4 to 7, however, are regarded as entirely satisfactory; only to the figures given in the last five cases does any real suspicion attach, and even in those the values given for V are entirely possible ones.

---

* It may be pointed out that this value for the energy of the disintegration particle is much less than that corresponding to the peak of the potential barrier of B^{11} as against α-particles, > $3 \cdot 10^6$ electron volts, *cf.* Riezler, 'Proc. Roy. Soc.,' A, vol. 134, p. 154 (1931).

For the apparently non-capture cases it was assumed that one or other of the following possibilities must apply :—

(iv) $N^{14} + n^1 \rightarrow C^{13} + H^1 + n^1$.
(v) $N^{14} + n^1 \rightarrow C^{12} + H^2 + n^1$.
(vi) $N^{14} + n^1 \rightarrow B^{10} + He^4 + n^1$.

These were explored, as numbers (i) to (iii) had been, employing the experimental data and the appropriate range velocity curves already referred to.

To reach a decision here, however, was much more difficult than in the former case, for it was no longer possible, employing each assumption in turn, to calculate the momentum of the incident neutron from the data obtained. It became necessary to rely entirely upon the limiting values of the energy change, deduced on the assumption of neutrons of maximum energy, and in many cases rendered still more uncertain on account of a lack of complete knowledge of the energy of the disintegration particle involved. The final conclusion was that no statement could justifiably be made concerning many examples of non-capture disintegration, except that they did not appear to fall in a single class with the rest. The latter, amounting to 6 cases out of 16, are satisfactorily explained on assumption (iv) above, upper limits to the amount of energy absorbed in the process ranging from 3·5 to 0·8 million electron volts, but, if process (vi) is assumed there is a spread of about 10^7 electron volts in the calculated values. We shall assume, therefore, that process (iv) does in fact take place and leave open the possibility that other types of disintegration also occur.

Amongst the 32 cases listed for measurement as presumable examples of disintegration forks there were, in addition to those falling within the broad divisions above made, two cases in each of which the aggregate length of the two components of the visible fork was less than the maximum length found amongst the nitrogen recoil tracks observed. The angles of the forks, however, precluded the possibility that either represented a close collision such as is shown by figs. 12 and 13 of Plate 15, otherwise a branch track would also have been visible. Two possibilities arise: either a recoil atom of nitrogen has made close collision with an atom of argon present in small amount in the gas, or the tracks are due to protons from the water vapour and these have suffered appreciable deflection by the heavier nitrogen nuclei without the production of a visible fork in either case. As a remotely possible alternative to the recoil track explanation is the suggestion that these forks represent a more drastic disintegration process, the production from N^{14} of the two nuclei Be^8 and Li^6, for example, or perhaps more probably, by capture, from N^{15} of Be^8 and Li^7. At this stage, however, it would be unprofitable to pursue further such a suggestion as this.

Examples of the photographs of paired disintegration tracks are collected in Plate 16. The conditions of magnification and the orientation of the photographs are the same as those adopted for the recoil track photographs of Plate 15. Figs. 18, 21 and 25, also showing a recoil track on the same photograph, have been interpreted as due to disintegration with capture, and figs. 19, 22, 24 and 26 as non-capture forks. Figs. 22 and 24 form a stereoscopic pair; mere inspection in this case is sufficient to show that the plane of the fork cannot pass through the source, situated towards the bottom of the photograph. Fig. 17 probably represents non-capture, also, but a final decision in this case was impossible as the length of film on which it occurred had to be rejected.* Fig. 20 is also indefinite, since the fork occurred in a portion of the chamber visible through one of the camera lenses only.

Discussion.

Before entering upon a general discussion of the results of the numerical analysis it will be useful to consider certain features of the experimental method which have a direct bearing upon the interpretation. In the first place this depends to a large extent upon the measurement of angles, but the angles deduced from the photographs will be of value only if they are the true angles involved in the primary collisions. This will not in general be the case if a collision has occurred before the completion of the expansion, and since no mechanical shutter was employed a certain number of "early" tracks were only to be expected. In the extreme cases a very diffuse cloud indicated that the ions had been widely separated by the applied field, cut off just before the end of the expansion, and by diffusion. A few intermediate cases were also detected and excluded from consideration. Nevertheless, other less noticeable cases may well have been overlooked and their inclusion may to some slight extent be responsible for the apparent diversity of explanation which the results require.

In the second place there is the uncertainty caused by the absence of an

---

* Footnote, p. 713.

4

5

6

7

8

9

10

11

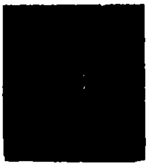

12

13

14

16

15

(*Facing p.* 722.)

17

18

19

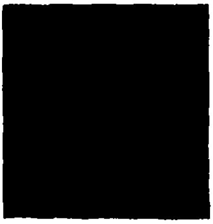

20

21

22

23

24

25

26

easily detectable track due to the neutron itself. One aspect of this uncertainty has already been discussed, but its extent is not entirely defined merely by considering the upper surface of the beryllium as the effective neutron source. Small angle deflections in nearly 3 mm. of lead might not be very uncommon, whilst particles scattered by surrounding matter and traversing the chamber in random directions cannot altogether be neglected. General considerations indicate that backwards scattering is likely to be most effective from the floor of the chamber, but it is extremely difficult to form a reasonable estimate of the extent to which it might occur. Having mentioned these two difficulties, therefore, we shall proceed on the assumption that the complexity of the results is not chiefly to be attributed to either of them.

Finally, there is the question of the accuracy attained in the measurement of angles, entirely apart from their identification. In a recent paper Blackett and Lees* have discussed this question in detail and conclude that in the case of disintegration forks, examined by the method of right-angle photography, a probable error of 1° in θ and 0·5° in ϕ is a reasonable assumption. In the present method somewhat greater errors are to be expected; moreover it is likely that the error in θ is increased more than is the error in ϕ. Probable errors of 3° in the former case and 1° in the latter may be tentatively assumed. Whilst these will not in general make decision between alternative modes of capture disintegration impossible, they will obviously lead to considerable uncertainty in the energy change in any specified case. A probable error of about 0·2 mm. in measured lengths must also be considered.

About 130 cases of interaction between a neutron and a nitrogen nucleus have been observed; of these about 30 resulted in disintegration, more than half of the latter without capture of the neutron. This is very different from the results obtained under α-particle bombardment, where elastic collisions, resulting in measurable spurs in an expansion chamber, outnumber inelastic (disintegration) collisions by a factor of the order of 1000 : 1. Moreover, although the possibility of non-capture disintegration by α-particles has frequently been considered,† unexceptionable evidence for its occurrence has yet to be obtained. The former of these points of difference is certainly to be ascribed to the different extent of the external fields of the two particles, that of the neutron falling off very rapidly to become already inappreciable at a few diameters distance; it is quite possible that further investigation will exhibit the latter difference, also, as a direct result of the same circumstances.‡

---

* 'Proc. Roy. Soc.,' A, vol. 136, p. 338 (1932).

† Chadwick and Gamow, 'Nature,' vol. 126, p. 54 (1930).

‡ It would hardly arise in this way on the basis of the detailed mechanism suggested by Pollard, 'Proc. Leeds Phil. Soc.,' vol. 2, p. 206 (1931).

A study of the angular distribution of recoil tracks must obviously lead to important data for any theory of the field of the neutron, but hydrogen collisions are so much more suited to this study, owing to the greatly simplified conditions, that this aspect of the problem must be left until the experimental data are available. For the present the distribution shown in fig. 3 may be discussed from another point of view, namely, the process in which neutrons are liberated.

The experiments of Webster[*] and of Kirsch and Rieder (*loc. cit.*) have shown that whilst the effects observed with beryllium are produced for the most part by α-particles of more than 4 million electron volts energy, yet in some part they are to be attributed to particles of lower energy. They do not become inappreciable until the energy of the incident particles is reduced to about 2·6 million electron volts. Now if neutrons of $6 \cdot 4 \,.\, 10^6$ electron volts energy, corresponding to the upper limit of velocity $3 \cdot 5 \,.\, 10^9$ cm. per second, are ejected in the forward direction when α-particles of $5 \cdot 3 \,.\, 10^6$ electron volts energy are captured, and if the energy released in this process is constant, then when α-particles of $2 \cdot 6 \,.\, 10^6$ electron volts are captured the neutrons emitted in the backward direction will have an energy of $2 \cdot 2 \,.\, 10^6$ electron volts. Almost all directions of emission are represented in the data of fig. 3 and a lower limit of $1 \cdot 3 \,.\, 10^6$ electron volts has been deduced ($v_{\text{min.}} = 1 \cdot 6 \,.\, 10^9$ cm. per second) from that distribution. The discrepancy is not outside the limits of error; and if it be divided, and mutually consistent limits, 5·8 and $1 \cdot 7 \,.\, 10^6$ electron volts, be assumed, the internal agreement may be regarded as quite satisfactory, whilst the agreement between the upper limit here deduced and that adopted by Chadwick is greatly improved. It may be that the energy change is not constant, the C^{12} nucleus in some cases being left in an excited state, but more extensive and more accurate data than the present would certainly be required in order to establish this result from energy considerations alone.

From the disintegration phenomena, on the other hand, we have more definite proof of a state of higher energy in the case of the boron nucleus B^{11}, the energy of excitation being of the order of $1 \cdot 5 \,.\, 10^6$ electron volts.[†] The capture disintegration here observed is of interest from another point of view also. Curie and Joliot and Chadwick have shown that the anomalous effects found with beryllium are obtained with boron also under α-particle bombardment. If the α-particle is captured in this case, as in the former, when the neutron is liberated it is most probable that the nucleus B^{11} is effective, for otherwise the final result would be N^{13}, hitherto unknown. On the assumption of capture, therefore, we have observed the nuclear reaction

---

[*] 'Proc. Roy. Soc.,' A, vol. 136, p. 428 (1932).

[†] This excess energy is doubtless emitted in the form of γ-radiation in a time negligible compared with the time of description of the recoil track of the new nucleus. The observed direction of the latter will differ from the original direction on this account, but the difference is well within the limits of acuracy of measurement.

$$B^{11} + He^{4} \rightleftarrows N^{14} + n^{1}$$

to take place both in the forward and reverse directions. In the reverse direction the maximum release of energy found is almost certainly negative, $1 \cdot 5 \,.\, 10^{5}$ electron volts. In the forward direction, likewise, no release of energy greater than about $-1 \cdot 5 \,.\, 10^{6}$ electron volts has as yet been detected. There is a discrepancy here which may be due either to the restricted data of Table I or to the difficulty of absorption measurements in the case of a weak proton radiation markedly inhomogeneous in velocity, but at least it indicates that in one case or the other, or in both, capture of the incident particle into the ground level of the final nucleus is a relatively infrequent occurrence.*

So far we have been considering the balance of energy without reference to its wider implications. It becomes necessary now to investigate the bearing of the present results upon the general question of the mass defects of the lighter nuclei. These have generally been calculated on the assumption of a nuclear structure composed of α-particles, protons and electrons in which the number of α-particles is as large as possible. Then Aston's† results lead to the values $(16 \cdot 7 \pm 1 \cdot 6) \,.\, 10^{-3}$ and $(14 \cdot 0 \pm 2 \cdot 8) \,.\, 10^{-3}$ mass units for B^{11} and N^{14}, respectively. This corresponds to a liberation of energy, $2 \cdot 5 \,.\, 10^{6}$ electron volts in probable amount, in the transition $N^{14} \rightarrow B^{11}$. If the net result is, in fact, the liberation of energy, considerably less than this amount is involved. The discrepancy is not entirely beyond the limits of error in the direct determinations of mass, but it may be pointed out that it would be greatly reduced if a structure composed of α-particles, protons and neutrons were adopted, the binding energy of the neutron being assumed to be of the order of $1\text{–}1 \cdot 5 \,.\, 10^{6}$ electron volts.

It is much more difficult to explain the non-capture results on the basis of the general assumptions hitherto accepted. The mass defect of C^{12}, calculated from the α-particle disintegration experiments with boron, is probably $4 \cdot 2 . 10^{-3}$ mass units less than that of N^{14}, so that the absorption of $3 \cdot 9 . 10^6$ electron volts of energy* should be necessary to effect the non-capture disintegration $N^{14} \rightarrow C^{13} + H^1$, presumed to occur. Actually about $1 \cdot 5 . 10^6$ electron volts appear to be required. Moreover, the present suggestion of the α-particle-proton-neutron structure does little to remove the difficulty. For the nuclei B^{10}, N^{14} are similar in type; the difference in mass defect of the two, and therefore the difference $C^{13} \rightarrow N^{14}$, would not be greatly influenced by the change. Finally, if release of energy in certain cases is eventually established it may be necessary to assume, following Gamow,† that the number of α-particles in the nuclear structure is not the maximum possible on merely arithmetical grounds—and it may even be the case that certain of the non-capture disintegrations observed are really of the type $N^{14} \rightarrow C^{12} + H^2$, though this assumption would require the further structural unit H^2 with the consequent additional complication of the problem of the mass defects of nuclei.

---

* This is also found in the capture (resonance) disintegration of boron, fluorine and aluminium by α-particles, Chadwick and Constable, 'Proc. Roy. Soc.,' A, vol. 135, p. 48 (1932).

† 'Proc. Roy. Soc.,' A, vol. 115, p. 487 (1927).

At present more extensive data are urgently required. It is the writer's hope to be able to undertake, in the near future, the necessary investigations which will enable us to study as many cases as possible of the artificial disintegration of nuclei under neutron bombardment. The expansion chamber is indispensable for such investigations and it is of interest to point out that the speed with which data may be obtained is limited only by the strength of source available, since the absence of a track due to the neutron itself does not impose any restriction upon the number of particles admitted to the chamber at each expansion. In the present experiments that number was probably of the order of a few thousand.

Summary.

Tracks have been observed in an expansion chamber resulting from elastic and inelastic collisions between neutrons of mass 1 and nitrogen nuclei. The neutrons were obtained from beryllium under α-particle bombardment. They are shown to be emitted with energies distributed over a wide range.

Inelastic collisions resulting in disintegration were found to be of two main types, in the first the neutron is captured and an α-particle liberated, in the second the neutron is not captured. It is probable that a proton is liberated in the second type of collision, although certain indications are found of a further subdivision of this class corresponding to the possible occurrence of

---

* This figure may be reduced to $3 . 10^6$ electron volts if optical data be adopted.

† "Atomic Nuclei and Radioactivity," p. 112 (1931).

non-capture disintegrations with emission of α-particles or H^2 nuclei, also. The emission of γ-radiation in cases of artificial disintegration appears as a general phenomenon.

A general consideration of the energy changes involved in the various nuclear processes has been undertaken.

The investigations above described would have been altogether impossible but for a generous gift of old radon tubes from Dr. C. F. Burnam and Dr. F. West of the Kelly Hospital, Baltimore, to whom my best thanks are due. I wish to thank Dr. Chadwick, also, for preparing the polonium source from this material and for his continual help and encouragement throughout the course of the experiment. I wish, further, to acknowledge many helpful discussions with Professor Lord Rutherford and, finally, to express my gratitude to the Council of Trinity College for a grant from the Rouse Ball Research Fund towards the cost of the apparatus.

Attempts to Detect the Interaction of Neutrons with Electrons.

By P. I. Dee, M.A., Pembroke College, Cambridge.

(Communicated by J. Chadwick, F.R.S.- -Received May 10, 1932.)

[Plates 17–19.]

§ 1. *Introduction.*

The present paper contains an account of investigations made with a Wilson chamber on the penetrating radiation emitted by beryllium when the latter is bombarded by the α-particles of polonium. Dr. Chadwick[*] has suggested that this radiation consists of a stream of neutrons of unit mass and maximum velocity $3 \cdot 3 \times 10^9$ cm. per second. The neutrons in their passage through matter collide occasionally with the atomic nuclei and produce recoil atoms of short range and great ionising power. The recoil atoms of nitrogen have been studied in detail by Dr. Feather,[†] using an automatic expansion chamber, and the lengths of the recoil tracks are in agreement with the neutron hypothesis. It is of special interest to examine the interaction of the neutrons with electrons.

[*] 'Nature,' vol. 129, p. 312 (1932).

[†] 'Proc. Roy. Soc.,' A, vol. 136, p. 709 (1932).

The impact of a similar neutron of the same velocity with an electron might be expected to communicate to the latter velocities up to a maximum of $6 \cdot 6 \times 10^9$ cm. per second, that is, twice the velocity of the neutron for a direct collision, corresponding to a maximum energy of the recoil electron of approximately 13,000 electron volts. According to the data of Nuttall and Williams* such an electron has a range of recoil of 3·4 mm. As, however, the total ionisation in this length of track would be only 350 ion pairs the valve counter and automatic expansion chamber are unsuitable for its detection. Further, as will be shown later, it is impossible to detect with certainty the occurrence of such recoil electrons produced by neutrons unless the individual water drops produced in the expansion chamber are clearly photographed. For such experiments, and to a still greater degree for the experiments described in § 4, it is also necessary that there shall be no appreciable background of drops in the chamber. Even in the absence of ionisation such a general distribution of drops is usually produced unless special precautions are taken. The detection of individual ions by the condensation on them of water vapour and the photography of the individual drops thus produced, while avoiding the presence of water drops which are not associated with ions, has been a special study of the writer working under the supervision of Professor C. T. R. Wilson.

The existence of short electron recoil tracks produced by beryllium radiation is of special interest on account of the great difference to be expected on the two views concerning the nature of this radiation. On the quantum hypothesis the range of the recoil electron, even for the lowest quantum energy compatible with the absorption coefficient, is of the order of metres of air. To account for the recoil atoms of nitrogen, etc., observed by Dr. Chadwick higher quantum energies have to be assumed which would correspond to even greater ranges of recoil electrons. Thus the observation of short electron recoil tracks of length less than 3·4 mm. would afford a powerful test of the neutron hypothesis and one which is quite independent of the evidence described in the two previous papers.

§ 2. *Experimental Procedure.*

For the present purpose it will be sufficient to give only a brief description of the expansion apparatus. The main features are similar to those described by Professor Wilson in earlier papers.† The glass chamber was 8 cm. deep and 16 cm. in diameter, but a central volume of 100 c.c. only is illuminated. The roof of the chamber was a brass disc 4 mm. thick which, for the greater part of the work, was covered inside the chamber by a glass plate of 3 mm. thickness. The function of the glass plate was to reduce the amount of any characteristic X-radiations from the metal roof, which on absorption in the gas might have produced electron tracks of about the range sought. An electric field of the order of 50 volts per centimetre was maintained between the roof and floor of the chamber, the roof being positively charged. This field was, in many of the experiments, cut off at the instant of expansion.

---

* 'Phil. Mag.,' vol. 2, p. 1109 (1926).

† 'Proc. Roy. Soc.,' A, vol. 87, p. 277 (1912), and vol. 104, p. 1 (1923).

Air was used in the chamber at a final pressure of about 40 cm. of mercury. After each expansion all residual nuclei were removed by a succession of small expansions, the pressure adjusted for the following expansion, and then sufficient time was allowed to elapse before taking the next photograph in order to allow the temperature to reach its equilibrium value. Trial exposed plates were developed at frequent intervals to keep a careful check on the working conditions, suitable adjustments being made as seemed necessary. These requirements greatly slow up the rate at which photographs can be taken but in general it is found more satisfactory to work under these conditions than to take a long run without frequent control experiments. Imperial process plates were used and Beck Iso-stigmar lenses at an aperture of *f*/16.

The polonium preparation and beryllium target enclosed in an evacuated metal box as described by Dr. Chadwick,* and kindly lent by him for these experiments, was mounted, with its axis vertical, above the illuminated part of the chamber.

§ 3. *Results of Search for Short Electron Recoil Tracks.*

The first attempt to detect the presence of short electron tracks was made with a chamber which had a gelatine coating on the lower surface of the brass roof.

The production of recoil protons from the gelatine layer by the beryllium radiation was at once observed, as well as the presence in the chamber of fast β-rays.†

Fig. 1, Plate 17, shows one of these fast protons passing from roof to floor of the chamber. Fig. 2 is an enlargement of another proton track showing a recoil electron track of length 2·5 mm. in standard air, the initial velocity of this electron would be 6×10^9 cm. per second corresponding to a minimum velocity of the proton of 3×10^9 cm. per second. This short electron track is therefore typical of the type of track which might be expected to occur separately, that is, not as a branch track, if the neutron itself produced no appreciable continuous ionisation along its path.

---

* 'Proc. Roy. Soc.,' A, vol. 136, p. 692 (1932).

† Curie and Joliot, 'C. R. Acad. Sci. Paris,' vol. 194, p. 876 (1932); Auger, 'C. R. Acad. Sci. Paris,' vol. 194, p. 877 (1932); Rasetti, 'Naturwiss.,' vol. 20, p. 252 (1932).

Fig. 6, Plate 18, illustrates the main difficulty of these experiments. A fast β-ray, slightly out of focus, has produced a short branch electron track of about the range sought. Such a track in worse focus would result in the disappearance of the fast track leaving the observation of the heavily ionised branch little affected, and thus lead to possible interpretation of the branch as a separately occurring short electron track. Also the background of drops due to the intense production and diffusion of ions in the gas before the expansion by the protons ejected from the roof tends to conceal the faint straight track without relative concealment of the branch. For these reasons it was necessary to prevent the proton production and to reduce the number of fast β-rays present.

The main run for the electron recoils was therefore made with the gelatine layer replaced by a glass plate and with an increased voltage applied to the chamber to reduce the time interval before the expansion during which ions may be produced and yet not completely removed by the electric field. The number of fast β-rays present was partly reduced by increasing the thickness of absorber in the path of the beryllium radiation.

A further great improvement results from these alterations in that the supersaturation does not change appreciably in the interval between the expansion of the gas and illumination of the tracks. In the presence of a *heavy* background of drops the supersaturation falls rapidly in this interval so that only few of the ions produced by the radiations which enter late after the expansion are caught and form visible drops. This effect again would result in the misinterpretation of branch tracks as separately occurring short electron tracks, the sparsely ionised straight track disappearing much more rapidly with reduction of the number of ions caught than the more densely ionised branch. For this main run, however, the background effect, due to uncharged nuclei, was not rigorously eliminated as could be done by a reduction of expansion ratio, as such a reduction brings the expansion ratio so near to the critical limits required to catch the ions that the effective interval during which capture of all the ions occurs is again reduced. A suitable compromise was made to give the best conditions for the detection of fast β-rays with as great a permissible interval of effective supersaturation. The actual number of stray drops in this run was in general only of the order of 5 per cubic centimetre.

Fig. 5, Plate 18, is typical of the improved conditions; 383 stereoscopic pairs were exposed, of which 351 were quite suitable for the detection of the recoiling electrons.

On these plates 29 recoil nitrogen atoms were recorded, and it was immediately obvious that the ionisation along a neutron track was less than 3 ion pairs per centimetre. Often the intense ionisation in these recoils produced a general haze of drops round the track preventing the fixing of the above ionisation to a lower limit.

No electron tracks of ranges near 3·4 mm. were observed. A search was made for all shorter ranges, no short track being accepted unless it was sharply in focus to ensure detection of any fast track of which it may have been a branch.

Two short tracks only were observed which rigidly satisfied this condition, they are reproduced in figs. 7, 8, Plate 18.

Fig. 3, Plate 17, shows one of the nitrogen recoils together with an electron track of range 0·4 mm. This latter track is not added to the two above as it was not in the best possible focus.

The reduced ranges of the two electron tracks above were 0·47 mm. and 0·30 mm. It is difficult to estimate the initial energies of these electrons, the experiments of Nuttall and Williams (*loc. cit.*) on the ranges of electrons barely extending to such low energies. The range given, however, for a 4800-volt electron in hydrogen being 0·36 cm. it is probable that the range in air would be approximately 0·5 mm. for the same energy, so that the longer of the two cases quoted would seem to correspond approximately to an energy of 4800 volts, the shorter being due possibly to the absorption of a quantum of argon K-radiation. The fact, however, of the occurrence of the electron track of range 0·4 mm., fig. 3, Plate 17, in the immediate neighbourhood of the densely ionised nitrogen recoil track would suggest that this electron was due to the absorption of a quantum of argon K-radiation generated in the nitrogen track. In the absence of satisfactory data on the ranges of such slow electrons, as well as the great uncertainty in the actual range, when scattering must play so great a part, it is clear that neither electron can be quoted with certainty as the product of neutron-electron interaction.

The main conclusion to be drawn therefore from these experiments is that the production of electron recoils by neutrons is a rare occurrence compared with the production of recoil nitrogen atoms. Had these two probabilities been equal one would have obtained approximately $7 \times 29 = 203$ recoil electron tracks. It may safely be concluded therefore that the probability of interaction of a neutron with an electron is not much greater than 1 per cent. of the probability of interaction of a neutron with a nitrogen nucleus.

§ 4. *Ionisation along the Path of a Neutron.*

The nitrogen recoils observed in § 3 fixed an upper limit to the ionisation along a neutron track of 3 pairs per centimetre.

Experiments were now made to determine this limit with greater accuracy. Rigorous precautions were taken to ensure cleanliness of operation and in one set of experiments an expansion ratio was used for which, in the absence of the source, the total number of drops recorded was of the order of 10 in the whole illuminated part of the chamber. Alternate expansions were made with and without the source present, and counts made of the total number of drops photographed in the chamber.

It was concluded that the number of drops per plate in the presence of the source, excluding those along β tracks, did not exceed the number in its absence by more than five.

A similar run with a slightly increased expansion ratio and with rather more background gave approximately the same result. Fig. 10, Plate 19, is a typical photograph obtained with the higher expansion. Fig. 9, Plate 19, was obtained with a smaller value of the electric field, giving increased probability of collecting tracks entering before the expansion, and shows a slow β-ray separated into its positive and negative ions. These photographs offer strong confirmation of the efficiency of this method for recording total ionisation.

Now let N = the number of neutrons passing through the chamber per expansion, r cm. = the effective radius for a neutron-nitrogen collision, x cm. = the average length of a neutron track in the chamber.

Then the probability of recording a nitrogen recoil per expansion $= p = 5\cdot4 \times 10^{19} \times \pi r^2 \times \mathrm{N} \times x$. If I ion pairs per centimetre be the ionisation along a neutron track the above experimental result states that $2\mathrm{IN}x < 5$. Whence $\mathrm{I} < \dfrac{27 \times 10^{19} \times \pi \times r^2}{2p}$. Now p is known from the frequency of observation of nitrogen recoils in § 3, and equals $\dfrac{1}{30}$,* and if, as seems probable, r is of the order 5×10^{-13} cm., we obtain that $\mathrm{I} < 3 \times 10^{-3}$ ion pairs per centimetre, or of the order of one ion pair per 3 metres of air. Should r, however, be as great as 5×10^{-12} cm. the ionisation may be one pair per

---

* The value of p used here is not 29/351 (see § 3), correction having been made for the different conditions of experiment here employed. This correction was made by comparison of the number of fast β-rays per plate observed in this run with the number observed in § 3 for the same screening.

3 cm., and for greater values of r the experiment does not apply as $N < 1$. Subsequent research should give the value of r with fair accuracy when the maximum possible ionisation per centimetre will be calculable from the above data. For the present the value of 1 ion pair per 3 metres would seem to be a reasonable upper limit. It should be noticed that the above measurements give upper limits only to the ionisation per centimetre, some of the ions observed being possibly stray ions from the β-radiation also present.

§ 5. *General Effects of the Beryllium Radiation.*

Owing to the slow rate of photography necessitated for the above experiments only few of the events described by Feather (*loc. cit.*) were recorded. It is of interest to note, however, that of the 30 nitrogen recoils obtained 7 had a reduced range of less than 0·6 mm. Feather records 5 recoils in the same interval of range out of a total of 105. The shorter recoil tracks would be recorded much more readily in these experiments than those of Feather and the above result would seem to indicate that the deficiency of such ranges in his experiments was instrumental and not a real phenomenon.

One clear case of disintegration was photographed and is reproduced in fig. 4, Plate 17. The most probable interpretation of this event is disintegration of a nitrogen atom with the ejection of an α-particle, the short branch representing the recoil of a B^{11} nucleus.

The total number of fast β-rays observed on the plates mentioned in § 3 was 656—these tracks were all approximately straight and 96 per cent. of them appeared to originate in the matter beneath the source. One hundred and seventy-eight β-rays of energy of about 50 kilovolts or less were observed. Thus the ratio of the number of fast β-rays to the number of nitrogen recoils is about 23 after the beryllium radiation has traversed approximately 2 cm. of brass. It was verified that more than 80 per cent. of these β-rays were associated with the bombardment of the beryllium, the remainder being due to the γ-rays of polonium.

Summary.

Experiments have been made with the Wilson cloud track chamber to investigate the interaction of beryllium radiation with electrons in air. It is concluded (*a*) that the probability of interaction of a neutron with an electron with the production of a recoil electron track is less than 1 per cent. of the probability of similar interaction with a nitrogen nucleus, and (*b*) that if the effective radius for interaction of a neutron with a nitrogen nucleus with production of

a recoil nitrogen atom is of the order 5×10^{-13}c m., then the ionisation along the path of the neutron is less than 1 ion pair per 3 metres of air.

I wish to express my gratitude to Dr. J. Chadwick and Professor C. T. R. Wilson for their advice and assistance during the course of the work. This research was carried out with the apparatus of Professor C. T. R. Wilson at the Solar Physics Observatory. My thanks are due to Professor F. J. M. Stratton for placing the facilities of his laboratory at my disposal, and to Mr. W. H. Manning for help with the photographic work.

DESCRIPTION OF PLATES.

The magnification given beneath each photograph is the ratio of the size of the reproduction to the size of the image in the chamber at the final pressure projected normally upon a plane perpendicular to the axis of one of the camera lenses.

The source would be at the top of each picture with the exception of fig. 10, where it would be on the left-hand side.

Plate 17.

Fig. 1.—Fast proton.

Fig. 2.—One proton showing production of a recoil electron track. Had this been a direct collision the velocity of the proton would be 3×10^9 cm. per second.

Fig. 3.—A recoil nitrogen atom, which has suffered an early deflection. Also a short electron track.

Fig. 4.—The disintegration of a nitrogen atom, the long branch probably being an α-ray emitted and the short branch the recoil of the residual atom. The two dense spots on the left are due to the positive and negative ions of a nitrogen recoil atom, produced before the expansion.

Plate 18.

Fig. 5.—Two fast electron tracks starting from the roof and the negative ions of a track which entered before the expansion.

Fig. 6.—A fast β-ray, in poor focus, has produced a recoil electron of short range.

Figs. 7 and 8.—Short electron tracks produced in the chamber, not branches of a straight track.

Plate 19.

Fig. 9.—The two parallel tracks are the positive and negative ions of a slow β-ray entering before the expansion. Note also the sparsely ionised fast track and the two slower tracks in poorer focus.

Fig. 10.—Two fast electrons ejected from the roof. On the extreme left is a similar track separated into its positive and negative ions.

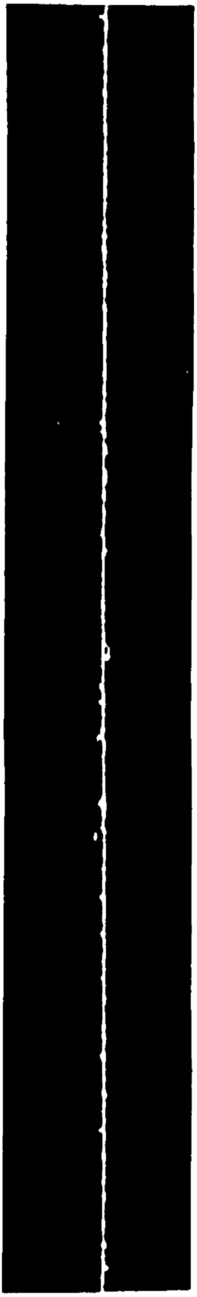

1

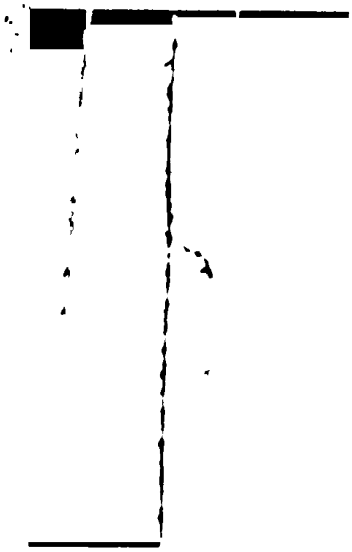

2

3

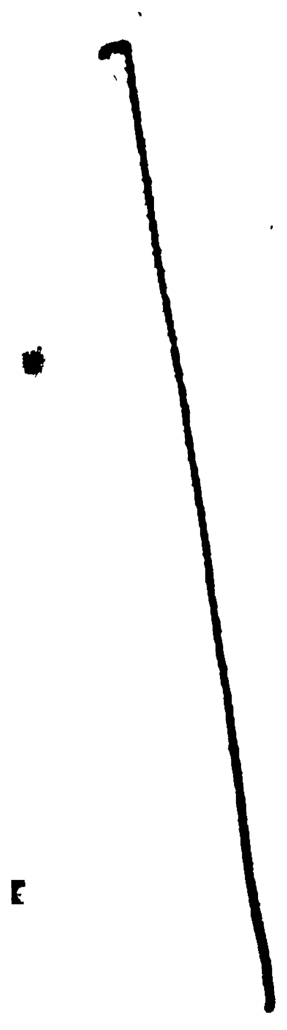

4

No. 1, ×2, No. 2, ×3·5; No. 3, ×7; No. 4, ×4.

5

7

8

6

No. 5, ×4; No. 6, ×5; Nos. 7 and 8, ×8.

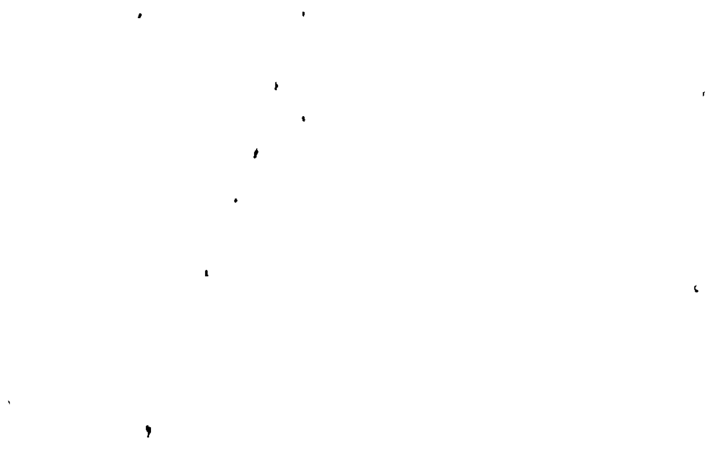

9

10

Nos. 9 and 10. × 3

Discussion on the Structure of Atomic Nuclei.

OPENING ADDRESS.

By Lord Rutherford, O.M., F.R.S.

(April 28, 1932.)

Lord Rutherford: In my address to-day, I shall briefly review some of the main lines of advance in our knowledge of atomic nuclei since the last discussion* which I had the honour to open. In the interval, there has been substantial progress in many directions, and new and promising methods of attack on this formidable problem have been opened up. I can only refer in passing to the valuable data obtained by Aston and others on the isotopic constitution of the elements and the relative abundance of the isotopes of many of the elements. This has made it possible to determine the chemical atomic weight of many elements with considerable accuracy by the use of the mass spectrograph. A number of new experiments have been made to determine with accuracy the relative quantities of the isotopes of lead, and in particular of lead obtained from pure uranium and thorium minerals of great geological age. Data of this kind are of much interest and importance, not only from the point of view of radioactivity but also with regard to the fixation of an accurate time scale in geology. It seems certain that the end product of the actinium series—actinium lead—has an atomic mass 207 and that actinium is derived from the transformation of an isotope of uranium. From the relative abundance of actinium-lead and uranium-lead derived from old radioactive minerals, it is possible to deduce the average life of this uranium isotope. I pointed out some time ago in 'Nature,' that important inferences could be drawn with regard to the production of elements in the sun from a consideration of the average life of the two uranium isotopes.

Optical Methods.—One of the most interesting developments in recent years has been the application of optical methods to determine the presence of isotopes and to throw light on the movements of the nucleus. The study of the band-spectra of the molecules of the lighter elements had disclosed the presence of isotopes existing in small quantity compared with the main isotope. It has been shown that oxygen consists of three isotopes of masses 16, 17, 18, carbon 12, 13, beryllium 8, 9, boron 11, 10, while recent observations of Urey, Brickwedde and Murphy are believed to indicate the presence in small quantity in hydrogen of a new isotope of mass 2. Attempts are in progress to concentrate the new isotope by fractional distillation of liquid hydrogen.

---

* 'Proc. Roy. Soc.,' A, vol. 123, p. 373 (1929).

In addition to identifying lines due to new isotopes, considerable attention has been directed to the relative intensities of the lines in the band spectra. Not only does this yield information about the spin of the nucleus but it also provides a method of attack on one of the most fundamental points of nuclear physics, namely whether the members of a given isotopic system are identical.

During the last few years, there have been many researches to determine the hyperfine structure in optical spectra. This gives another line of attack on the difficult problem of spin of the nucleus. I shall leave to Professor R. H. Fowler the task of discussing the data obtained and the conclusions that can be drawn.

Application of Wave-mechanics.—In the last discussion reference was made to the application by Gamow and by Gurney and Condon of the then new wave-mechanical ideas to certain nuclear problems, and in particular to the explanation of the well-known Geiger-Nuttall rule connecting the velocity of escape of an α-particle from a radioactive substance and its transformation constant. On this theory it was supposed that the nucleus was surrounded by a high positive potential barrier, and that the α-particles and other nuclear constituents within this barrier were held in equilibrium by strong but unknown types of attractive forces. On such a model, there is a finite probability that the α-particle in the nucleus can escape through the barrier without loss of energy, the probability increasing rapidly with increase of the energy of the α-particle. This general conception of the nucleus has proved very valuable in a number of directions and has been a very useful working guide to the experimenter. Unfortunately it has not so far been found possible on the theory to give any detailed picture of the structure of a nucleus. It is generally supposed that the nucleus of a heavy element consists mainly of α-particles with an admixture of a few free protons and electrons, but the exact division between these constituents is unknown. On the theory, there is a great difficulty in including within the minute nucleus particles of such widely different masses as the α-particles and electron. In addition, the nucleus is such a concentrated structure, and the constituent particles are so close together, that the theory of the action of one particle on another, applicable under ordinary conditions, cannot be safely applied for such minute distances.

It appears as if the electron within the nucleus behaves quite differently from the electron in the outer atom. This difficulty may be of our own creation for it seems to me more likely that an electron cannot exist in the free state in a stable nucleus, but must always be associated with a proton or other possible massive units. The indication of the existence of the neutron in certain nuclei is significant in this connection. The observation of Beck, that in the building up of heavier elements from the lighter, electrons are added in pairs, is of much interest and suggests that it is essential to neutralise the large magnetic moment of the electron by the addition of another for the formation of a stable nucleus. It may be that uncharged units of mass 2 as well as the neutron of mass 1 may be secondary units in the structure of nuclei.

While no definite theory of the nucleus seems at present feasible, yet much progress can be made by the use of suitable analogies based on the general model of the nucleus previously outlined. For example, Gamow has drawn important inferences with regard to the mass defect of the lighter atoms composed of α-particles, *i.e.*, of elements of the type $4n$, on the analogy that the forces in the nucleus resemble in a general way those acting in a minute drop of water. In addition he has discussed in an illuminating way the conditions to be fulfilled for the formation of stable nuclei of high atomic number. Unfortunately, the masses of the isotopes of many of the elements require to be known with much greater accuracy before much further progress can be made in this problem along these lines.

In another direction, too, it has been found fruitful to apply to the nucleus many of the general ideas of energy levels which have proved so useful in discussing the electronic structure of the outer atom. It has long been supposed that the quantum laws hold within the nucleus, and the correctness of this assumption has been abundantly verified in recent years. It will be seen that the conceptions of energy levels and of excitation of nuclei have proved of great utility in much recent work on the difficult problem of the origin of the γ-rays, and in understanding the observations obtained in the study of the artificial disintegration of the elements.

Origin of the γ-rays.—It has long been recognised that the γ-rays originate in the nucleus and represent in a sense the characteristic modes of vibration of the nuclear structure. The interpretation of the complicated γ-ray spectra shown by the radioactive elements has, however, been rendered difficult by our ignorance of the origin of this radiation—whether it arises from the constituent electron, proton or α-particle, or from the nucleus acting as a single entity. During the last few years, there has been a vigorous attack on this problem, and it now seems clear that the nuclear γ-rays are due to the transition of an α-particle between energy levels in an excited nucleus. Two different lines of attack have been developed depending on—

(1) a study of the long range α-particles from radium C and thorium C;

(2) the fine structure shown in the α-particles emission from certain radioactive substances.

It may be supposed that the emission of a β-particle during a transformation causes a violent disturbance in the resulting nucleus, some of the constituent α-particles being raised to a much higher level of energy than the normal. These α-particles are unstable, and after a very short interval fall back to the normal level, emitting their surplus energy in the form of a γ-ray of definite frequency, defined by the quantum relation. In this short interval, there is a small chance that some of the α-particles in the higher levels may escape through the potential barrier of the nucleus. On this point of view, the escaping α-particles from the different levels represent the groups of long range α-particles observed. The energy of the escaping α-particle gives the value of the energy level occupied by the α-particle before its release in the excited nucleus.

To test this hypothesis, the long range α-particles from radium C have been carefully analysed, using the new counting methods, by a group of workers, Wynn Williams, Ward, Lewis and the writer, and found to consist of at least nine distinct groups. The difference of energy between the various groups was found to be closely connected with the energies of some of the most prominent γ-rays, and in general the experiments gave strong evidence that the γ-rays had their origin in the transitions of one or more α-particles in an excited nucleus. At the same time, the experiments gave us direct information of the magnitude of a number of the possible energy levels in this particular nucleus.

In the great majority of cases, the α-particles in a radioactive transformation are expelled with identical speed. Rosenblum, however, showed that the element thorium C emitted not one but five distinct groups of α-particles, and evidence of a fine structure in the α-rays has since been obtained for other radioactive bodies. Gamow pointed out that γ-rays should arise in all cases where such a fine structure in the α-rays was present. Owing to certain technical difficulties in the case of thorium C, it has been difficult to give clear-cut evidence of the correctness of this point of view. Ellis and also Rosenblum conclude that Gamow's view is correct, but Meitner reached an opposite conclusion.

I can only refer in passing to some recent experiments of Mr. Bowden and myself for the proof of the emission of γ-rays from the actinium emanation, which Lewis and Wynn Williams found emitted two distinct groups of γ-rays. The results seem to me to support the general correctness of the theory that a fine structure in the emission of α-rays is always accompanied by the appearance of γ-rays. I shall leave to a later speaker, Dr. Ellis, the task of dealing more adequately with the present situation of this important problem.

When once the origin of the γ-rays is definitely settled there is a reasonable prospect of attacking successfully the whole question of the interpretation of γ-ray spectra in general, in which so far only a beginning has been made. It is obvious that a closer understanding of this problem may be expected to throw much light on the detailed structure of the nucleus. It is of great importance for this purpose to determine the spectrum of the γ-rays with the greatest possible precision, and this will entail many years of work.

Before leaving this part of the subject, I should like to emphasise the remarkable difference between the emission of an α-particle and a β-particle in disturbing a nucleus. Strange to say, the escape of an α-particle either does not excite a nucleus at all, or only raises one more of the constituent α-particles to a comparatively low level of energy above the normal. In many cases, however, the escape of a β-particle causes a violent excitation of the residual nucleus, some of the α-particles being raised to a very high level of energy and with the emission of high energy γ-rays. This difference between the effects of the two types of particle is very striking and may be intimately connected with the processes which cause the emission of a β-particle from a radioactive element.

Whenever we have to deal with the behaviour of the electron in the nucleus, we find grave difficulty in applying our theoretical ideas. The most striking instance is perhaps that radioactive nuclei of the β-ray type emit electrons with a wide range of energy, and that there appears to be no compensating process which would permit of that definite energy balance to be expected on quantum dynamics. This is undoubtedly one of the most fundamental problems to-day, but it is unlikely that we shall have sufficient time to discuss its theoretical implications.

Excitation of Nuclei by γ-rays.—Until recently, it had been generally supposed that the absorption of X-rays and γ-rays was due entirely to the interaction of the radiation with the extra nuclear electrons, and that the nucleus itself took no part in the process. It is now clear that if the quantum energy of the γ-rays exceeds about 2 million volts, an additional type of absorption appears with ordinary nuclei, accompanied by the emission of characteristic radiations of different frequencies from the primary. This effect of the nucleus on the absorption has been brought out by the work of Chao, Meitner, Hupfield, Tarrant and others using the penetrating γ-radiation from thorium C of energy about $2 \cdot 65 \times 10^6$ electron-volts. In a paper now in course of publication by this Society, Gray and Tarrant* give the results of a detailed examination of this nuclear excitation by different elements. Not only γ-rays from thorium C have been used, but also the high frequency components in the radiation from radium C. They conclude that this nuclear excitation is a general property of the elements at any rate between oxygen and lead. Characteristic radiations of similar type appear to be emitted by all the elements, the intensity of the radiation from different elements varying approximately as the square of the atomic number. These characteristic radiations from the nucleus which appear to be emitted uniformly in all directions, can be resolved into two components of quantum energy about 500,000 and 1,000,000 electron volts. In explanation they suggest that the γ-radiation does not excite the nucleus as a whole, but some constituent like the α-particle which is common to all the elements. It may be that the characteristic radiations observed represent some of the modes of vibration of the α-particle structure itself. It will be of much interest to pursue these important investigations further, but progress is hindered by the difficulty of obtaining strong sources of high frequency radiation over a wide range of quantum energy. The excitation of the nucleus by high frequency radiation is no doubt intimately connected with the processes which give rise to the γ-rays from a radioactive nucleus, and may help to throw further light on this problem.

Artificial Transmutation.—In the last few years there has been a rapid increase of our knowledge of the artificial transmutation of light elements by bombardment with α-particles. This has been largely due to the development of new electrical methods of counting α-particles and protons in place of the useful but trying scintillation method. Pose first showed that some of the protons ejected from aluminium appeared in groups of definite velocities. Our knowledge has been extended by the work of Pose, Meitner, Bothe, de Broglie and Ringuet and Chadwick and Constable. For example, Chadwick and Constable have resolved the protons liberated from aluminium by the α-particles of polonium into eight distinct groups connected in pairs. In explanation it is supposed that the protons or α-particles in the bombarded nucleus occupy definite energy levels. It is supposed, following the suggestion of Gurney, that there is a much greater chance of entering the potential barrier of the nucleus owing to resonance if the bombarding α-particle has about the same energy as that of the proton or α-particle in the nuclear level. For a given energy of α-particle, two groups of proton are emitted corresponding, it is believed, to two distinct processes of capture of the α-particle by the nucleus. Similar results have been observed in fluorine and other light elements. It has been found that these resonance levels for privileged capture of the α-particle are fairly broad, corresponding to about 5 per cent. of the energy level. The results as far as they have gone have yielded important information on the values of the energy levels of light nuclei, and with the use of still swifter particles than those from polonium we may expect to extend our knowledge of these levels still further.

---

* 'Proc. Roy. Soc.,' A, vol. 136, p. 662.

In interpretation of these experiments, it has been implicitly assumed that the laws of the conservation of energy and momentum apply. In this way it has been possible to calculate with considerable accuracy the atomic mass of the element resulting from the capture of the α-particle and the emission of the proton.

When two groups of protons of different speeds are connected with a single resonance level, it is found that γ-rays appear of quantum energy corresponding approximately to the difference of energy of the protons in the two groups. The study of the γ-radiations emitted during artificial transmutation has in the last few months led to new and interesting developments. Bothe and Becker in 1930 found that the element beryllium when bombarded by α-particles did not emit protons but gave rise to what appeared to be a γ-radiation of penetrating power greater than the γ-rays from radium C′.

The absorption of this radiation by matter was examined by Mme. Curie-Joliot and M. Joliot, and also by Webster. This year Mme. Curie-Joliot and M. Joliot observed by the ionisation method that this radiation emitted protons of high velocity from hydrogen material. It was at first suggested that the swift protons might be due to an interaction between the γ-ray quantum and the proton, but this required the quantum energy of the radiation to be very high, of the order of 50 million volts. As a result of further experiments by electrical methods of counting, Chadwick found that a similar recoil effect could be observed for all light atoms, and concluded that the effects might be explained on the assumption that a stream of swift neutrons were liberated from the beryllium nucleus. It is not easy to distinguish between these two suggestions, but sufficient evidence has been accumulated to show that this new type of radiation has surprising properties and is able to produce disintegration in nitrogen, probably in a novel way.

I shall leave to Dr. Chadwick to give you a fuller account of the work on artificial transmutation and on the properties of this new type of radiation.

The idea of the possible existence of "neutrons," that is, of a close combination of a proton and an electron to form a unit of mass nearly 1 and zero charge is not new. In the Bakerian Lecture before this Society in 1920, I discussed the probable properties of the neutron, while the late Dr. Glasson and J. K. Roberts in the Cavendish Laboratory made experiments to detect the formation of neutrons in a strong electric discharge through hydrogen but without success. If the neutron hypothesis be confirmed by experiment, it will obviously much influence our conception of the formation and constitution of nuclei. Many years ago in a lecture before the Royal Institution, I discussed the possibility of the formation of heavy nuclei from hydrogen through the intermediary of the neutron. It seems not unlikely that the neutrons, owing to their mutual attraction, may collect in massive aggregates which in course of time by the processes of disintegration and association, re-arrange themselves to form the nuclei of the stable elements. I merely throw out this old idea as one possibly worthy of further consideration in the light of later knowledge.

Scattering of α-particles.—In previous discussions attention has been directed to the anomalous scattering of α-particles by light elements, and the difficulty of interpretation of the results obtained. Many of these difficulties have been removed by the application of the wave-mechanical ideas to these problems. For example, H. M. Taylor has been able to account in considerable detail for the anomalous scattering of α-particles observed both in hydrogen and helium, by simple considerations based on the wave-mechanics. Mott drew attention to the anomalies to be expected in the scattering of low velocity α-particles by helium, and his conclusions have been amply confirmed by the work of Chadwick and Blackett and Champion. On the theory of Mott, similar anomalies are to be expected in collisions between two identical nuclei of any kind.

General.—I have endeavoured in the above review to bring to your attention what appear to me the most important lines of experimental attack on the problem of the structure of atomic nuclei. I have not entered into speculative questions like the possibility of the annihilation of matter and its conversion into radiation, nor have I referred to the guesses, which we may hope will prove inspired, of the numerical relation between the unit of charge and Planck's constant h or of the relation between the masses of the electron and proton; nor have I entered, except in an incidental way, upon the difficult question on which much has been written of the formation and transformation of nuclei, under the influence of conditions existing in hot stars.

In making this review, I have been struck by the comparatively rapid progress that has been made since our last discussion on the attack on this central problem of Physics. Progress would be much hastened if we could obtain in the laboratory powerful but controllable sources of high-speed atoms and high-frequency radiations to bombard matter. By the experiments of Tuve, Hafsted and Dahl, in the Department of Terrestrial Magnetism, Washington, and by Cockcroft and Walton in the Cavendish Laboratory, it has been found possible by the use of high potentials to produce a stream of protons artificially with an individual energy of about 1 million electron volts and to examine their properties. A number of other methods of producing high-speed atoms are under trial by other investigators, and I would especially refer to the ingenious method developed by Lawrence and Livingston, of the University of California, where, by using multiple accelerations, protons have been obtained of an energy corresponding to about 1 million volts. In a recent paper they conclude that it should be possible by this method to obtain a stream of high-speed atoms of a much higher energy. There is thus a hopeful prospect that we may be able in the near future to obtain useful sources of high-speed atoms and high frequency radiation, and thereby extend our knowledge of the structure of the nucleus.

Addendum.

Since this statement has been circulated to the Fellows of the Society, some interesting new experiments have been made by J. D. Cockcroft and E. T. S. Walton in the Cavendish Laboratory. An apparatus has been designed to give a steady potential of 600–800 thousand volts. By means of an auxiliary discharge tube, protons are produced and then accelerated by a high potential in a vacuum tube. In this way a steady stream of swift protons of energies up to 600 thousand volts can be produced and used to bombard a number of elements. The material to be bombarded by these swift ions was placed inside the tube at 45° to the direction of the beam. A thin mica window was sealed on to the side of the tube, and the existence of swift particles was investigated by the scintillation method outside the tube.

The first element examined was lithium, when a few bright scintillations were observed at an accelerating potential of about 125 thousand volts. The number increased rapidly with increase of voltage up to 400 thousand volts, when many hundreds of scintillations per minute were observed for a proton current of a few micro-amperes. These particles had a maximum range of about 8 cm. in air. The brightness of the particles indicated that they were probably α-particles, and this was confirmed by observations of the tracks produced by these particles in an expansion chamber. It seems clear that some of the lithium nuclei have been disintegrated. The simplest assumption to make is that the lithium nucleus of mass 7 captures a proton, and the resulting nucleus of mass 8 breaks up into two α-particles. On this view the energy emitted corresponds to about 16 million electron volts, a value in good accord with the conservation of energy when we take into account the difference between the initial and final masses of the nuclei. If this view proves correct, a disintegrating nucleus of lithium should give rise to α-particles projected in opposite directions, and it is proposed to try experiments to test this. For about 200 thousand volts it can be estimated that the number of disintegrations is about 1 for 10^9 protons.

Experiments have been made with a number of other elements. Boron, fluorine and aluminium all give rise to particles, resembling α-particles, of a characteristic range for each element. A number of scintillations, some bright and others faint, were also observed from beryllium and carbon, and there is also an indication that nitrogen gives a few very bright scintillations. Oxygen and copper gave no scintillations for protons of energy up to 400 thousand volts.

It is obvious that a great amount of work will be required to examine all the elements by this method and to determine the nature of the swift particles which may be emitted. In some cases they appear to be α-particles, but we must always bear in mind the possibility of emission of particles of different types and masses.

It is not difficult to make suggestions as to the possible modes of disintegration of some of the elements mentioned consistent with the conservation of energy. For example, it may be possible that the nucleus of fluorine of mass 19, after capturing a proton, breaks up into an α-particle and the oxygen nucleus. Similarly, aluminium may be transformed into magnesium. We must, however, await further evidence before any definite decision can be reached on such questions. It is clear that the successful application of these new methods opens up a new and wide field of research where the effect of bombarding matter by swift ions of different kinds can be examined. Dr. Cockcroft and Dr. Walton are to be congratulated on their success in these new experiments which have taken several years of hard work in preparation.

J. Chadwick, F.R.S.: Experiments in which elements are bombarded by α-particles have proved particularly fruitful in providing information about the structure of nuclei. The advances since the last discussion have been partly due to improved technique in the experiments and partly to the application of the new mechanics to these problems. To show how this increased knowledge has been obtained I shall take as an example the case of the aluminium nucleus.

When a beam of α-particles falls on a thin foil of aluminium some of the particles are scattered by collisions with the aluminium nuclei. If the incident α-particles are slow, the scattering is completely described by the Rutherford theory of scattering, and we conclude that the force between the α-particle and the nucleus is given by Coulomb's law. As the velocity of the incident particles is increased, the scattering begins to depart from the normal laws; the amount of the scattering at 135°, for example, first decreases below the normal and then rapidly increases as the velocity of the α-particle is further increased. This anomalous scattering is difficult to explain by means of classical mechanics, but is easily accounted for on the wave mechanics. Suppose a particle makes a very close collision with the nucleus and comes to a point on the potential barrier where the thickness of the barrier is of the same order of magnitude as the wave-length of the α-particle. There is then a certain probability that the α-particle will penetrate the barrier. The scattered wave which represents such a particle will have a certain deviation in phase and will disturb the classical distribution of the scattered particles. The experiments of Riezler show that the scattering becomes anomalous when the α-particles come within a distance of 6×10^{-13} cm. of the Al nucleus. On certain plausible assumptions it follows that the radius of the top of the potential barrier must lie between 3 and 6×10^{-13} cm. Taking a mean of $4{\cdot}5 \times 10^{-13}$ cm. the height of the barrier of Al (against an α-particle) is about 8×10^{6} electron volts.

I turn now to observations of the *artificial disintegration* of aluminium. When aluminium is bombarded by α-particles we observe, in addition to the scattered α-particles, an emission of protons of high energies which is roughly equal in all directions. An α-particle which penetrates into the nucleus of Al^{27} may be captured; a proton is emitted and a nucleus Si^{30} is formed. We assume that the α-particles and the protons in a nucleus are in definite energy levels. The captured α-particle of kinetic energy W, falls into a level E_a, say, and a proton is emitted from a level E_p (both below ground level). The kinetic energy of the ejected proton will be $W + E_a - E_p$, neglecting the small energy of the residual nucleus. On this view, a homogeneous beam of α-particles incident on a very thin Al foil should give rise to the emission of protons of the same energy (in a given direction). The observations show, however, that in such a case two groups of protons are emitted. This is explained by supposing that in some cases (the majority) the final Si^{30} nucleus is formed in two steps; the α-particle is captured (perhaps into an intermediate level) and a proton emitted with the formation of an excited Si^{30} nucleus, which passes into the ground state with the emission of a quantum of radiation. This explanation is supported by the observation that Al bombarded by α-particles does actually emit a γ-radiation of about the appropriate energy.

Observations of the protons emitted from a thick foil of Al exposed to polonium α-particles show that the protons consist of eight groups associated in pairs. Although collisions are taking place between Al nuclei and α-particles of all velocities from zero up to the initial velocity of the polonium α-particle, yet the disintegrations appear to be due only to α-particles of certain specified velocities. Such a possibility was first pointed out by Gurney, who suggested that there may be a resonance effect between the incident α-particle and the atomic nucleus. If the α-particle has exactly the energy corresponding to a resonance level of the nucleus its chance of penetrating the potential barrier will be very much greater than if its energy is more or less than this. The first evidence for this resonance effect was found by Pose in the disintegration of aluminium. The later observations just mentioned show that there are four resonance levels of the aluminium nucleus between about 4 and $5 \cdot 3 \times 10^6$ electron volts. The levels are not very sharp but have a width of about 250,000 volts. Penetration of the α-particle through each level and its capture gives rise to the emission of a pair of proton groups.

There is still a large region of the potential barrier of aluminium which has not been investigated in this way. It may be that further experiment will discover certain relations between the levels of the same element and correspondences between the levels of one element and those of another.

Particular interest has recently been shown in the disintegration of the elements beryllium and boron. It was found by Bothe and Becker that these elements emitted a penetrating radiation, apparently of the γ type, when bombarded by polonium α-particles. A few months ago, Mme. Curie-Joliot and M. Joliot made the very striking observation that these radiations have the property of ejecting protons with high speeds from matter containing hydrogen. They found that the protons ejected by the beryllium radiation had velocities up to nearly 3×10^9 cm. per second. They supposed that the ejection of the protons occurred by a process analogous to the Compton effect, and concluded that the beryllium radiation had a quantum energy of about 50×10^6 electron volts. Two serious difficulties arise if this explanation be adopted. Firstly, it is known that the scattering of a quantum by an electron is well described by the

Klein-Nishina formula, and there is no reason to suppose that a similar relation should not be true for scattering by protons. The observed scattering is, however, very much too great. Secondly, it is difficult to account for the emission of a quantum of such high energy from the transformation $Be^9 + He^4 \rightarrow C^{13}$ + quantum. I therefore examined the properties of this radiation, using the valve counter. It was found that the radiation ejects particles not only from hydrogen but from helium, lithium, beryllium, etc., and presumably from all elements. In each case the particles appear to be recoil atoms of the elements. It seemed impossible to ascribe the ejection of these particles to a recoil from a quantum of radiation, if energy and momentum are to be conserved in the collisions.

A satisfactory explanation of the experimental results was obtained by supposing that the radiation consists not of quanta but of particles of mass 1 and charge 0, or neutrons.

In the case of two elements, hydrogen and nitrogen, the ranges of the recoil atoms have been measured with fair accuracy, and from these their maximum velocities were deduced. They are $3{\cdot}3 \times 10^9$ cm. per second and $4{\cdot}7 \times 10^8$ cm. per second, respectively. Let M_1V be the mass and maximum velocity of the particles of which the radiation consists. Then the maximum velocity which can be given to a hydrogen nucleus in a collision is

$$u_H = \frac{2M}{M+1} . V,$$

and to a nitrogen nucleus

$$u_N = \frac{2M}{M+14} . V.$$

Hence

$$\frac{M+14}{M+1} = \frac{u_H}{u_N} = \frac{3{\cdot}3 \times 10^9}{4{\cdot}7 \times 10^8},$$

and

$$M = 1{\cdot}15.$$

Within the error of experiment M may be taken as 1, and therefore

$$V = 3{\cdot}3 \times 10^9 \text{ cm. per second.}$$

Since the radiation is extremely penetrating the particle must have a charge very small compared with that of an electron. It is assumed that the charge is 0, and we may suppose that the neutron consists of a proton and an electron in close combination.

The available evidence strongly supports the neutron hypothesis. In the case of beryllium, the transformation process which results in the emission of a neutron is $Be^9 + He^4 \rightarrow C^{12} +$ neutron. It can be shown that the observations are compatible with the energy relations of this process. In the case of boron, the transformation is probably $B^{11} + He^4 \rightarrow N^{14} + n'$. In this case, the masses of B^{11}, He^4, and N^{14} are known from Aston's measurements, the kinetic energies of the particles can be found by experiment, and it is therefore possible to obtain a much closer estimate of the mass of the neutron. The mass so deduced is 1·0067. Taking the errors of the mass measurements into account, it appears that the mass of the neutron probably lies between 1·005 and 1·008. Such a value supports the view that the neutron is a combination of proton and electron, and gives for the binding energy of the particles about 1 to 2×10^6 electron volts.

The neutron may be pictured as a small dipole, or perhaps better, as a proton embedded in an electron. On either view the "radius" of the neutron will be between 10^{-13} cm. and 10^{-12} cm. The field of the neutron must be very small except at close distances, and the neutrons in their passage through matter will be unaffected except when they make a direct hit on an atomic nucleus. Measurements made on the passage of neutrons through matter give results in general agreement with these views. The collisions of neutrons with nitrogen nuclei have been studied by Dr. Feather, using an automatic expansion chamber. He has found that, in addition to the normal tracks of nitrogen recoil atoms, there are a number of branched tracks. These are due to disintegration of the nitrogen nucleus. In some cases the neutron is captured and an α-particle is emitted, a nucleus of B^{11} being formed. In other cases the mechanism is not yet known with certainty.

C. D. Ellis, F.R.S.: It has been known for many years that the γ-rays form the characteristic spectra of the radioactive nuclei, but it is only quite recently that evidence has been obtained which gives any indication of their mode of origin. They were at first attributed to the electrons in the nucleus, but this point of view, so natural from our experience of the extra nuclear structure, began gradually to be open to suspicion as information accumulated that nuclear electrons behave very differently to those outside. The rapid progress in our knowledge of the α-particles, both experimental and theoretical, has provided a satisfactory escape from this difficulty, and it is now generally believed that the γ-rays are associated with transitions between α-particle stationary states in the nucleus. This conclusion is of far-reaching importance to the subject, both stimulating, and giving point to the further investigation of the γ-rays and suggesting the possibility of obtaining minute and accurate information about the α-particles. But in proportion to the interest of the line of work that is opened up, is the importance of examining carefully the validity of this conclusion.

Lord Rutherford has already mentioned that recent work has brought to light a complexity in the emission of α-rays which had not been noticed in the early experiments. There is, firstly, the phenomenon of the long range particles, the most typical example of which is furnished by radium C. In the disintegration of this body, out of 1,000,000 atoms, about 999,978 emit α-particles whose energy is $7 \cdot 8 \times 10^6$ volts, whereas the remaining 22 emit particles of greater energy distributed among at least nine groups. The fastest of these groups has an excess energy of about 3,000,000 volts, covering just the range of the known γ-rays. Closer examination shows that the difference of energy between the faster groups and the main $7 \cdot 8 \times 10^6$ volts group, corresponds with $h\nu$ of the γ-rays. Further, while the number of particles in these groups is extremely small, the aggregate number of γ-ray quanta amount to about 1 per atom. Both the approximate agreement of the frequencies with the energies and the relative intensities of the long range α-particles and the number of quanta are compatible with the view that the radium C nucleus is initially formed in an excited state. There are then two possibilities open to the nucleus by which it can get rid of its energy. The first, and by far the least probable, is for it to disintegrate at once, the α-particle carrying away the whole of the energy of excitation. Such an α-particle would form one of the high energy groups. The other possibility is that the nucleus will first emit part of its energy of excitation in the form of a γ-ray, and then will be left with just enough to emit a normal α-particle of $7 \cdot 8 \times 10^6$ volts. This explanation has been considered in detail by Lord Rutherford and the writer,* and also subsequently by Gamow and Delbruck,† and, while the available data are at the moment not sufficient to test it in complete detail, it can at least be said that the energy relations and the intensity relations are compatible with this view.

The body thorium C also shows a series of α-ray groups which are distributed according to another scheme. These are usually referred to as the fine structure α-particle groups, chiefly because the energy differences in this case only amount to about 300,000 volts. There is another difference, in that the less intense groups are in this case those of lowest energy. It is at once clear that the explanation given for radium C cannot be applied in this case, but a simple point of view which appears to meet the case has been suggested by Gamow. His view is that the thorium C nuclei, left, of course, with the potentialities of disintegration, are all initially in the same state. Each nucleus has a certain available amount of energy to get rid of. It may do this, either by emitting an α-particle with this total energy, or it may emit the α-particle in one of a series of groups of lower energy, the energy left over remaining in the nucleus as a state of excitation. The essential difference in this suggestion for associating the α-particles and γ-rays is that the emission of a γ-ray is a sequent process to the emission of an α-particle in a certain group as compared to an alternative one in the first scheme. This difference in the outlook is determined unambiguously by the relative intensities in this case of the γ-rays and α-particles in the groups. It will be noticed that it is assumed that the emission of α-rays occurs after disintegration, whereas it would be just as easy as regards energy relations to assume that the α-particle in the normal state first made a transition to a lower energy state by emitting γ-rays and then from this level emerged from the nucleus. A view of this character would give, however, the extreme difficulty that whereas we have a convincing explanation for the long time which a radioactive atom can exist, but yet possess the potentiality of disintegration, all other evidence goes to show that any system which has the potentiality of emitting radiation can never exist as such for more than a minute fraction of a second. Now the period of thorium C for α-disintegration is about 3 hours, and any alternative to Gamow's view would involve a radiation process of a half-period of 3 hours, which is clearly an impossibility. I have endeavoured to investigate the applicability of Gamow's theory to this body, thorium C. The details about the fine structure of the α-particles have been found by Rosenblum from his experiments with the large Paris magnet, and the first point was to show that thorium C did in point of fact also emit γ-rays. This was never thought to be the case until it was suggested by Gamow. Actually the γ-rays are investigated by means of their β-ray spectra, and I have measured the β-ray spectra of both the joint emission of thorium C + C″ and also that due to thorium C″ alone. The experiments are described in detail in a paper in the course of publication, but the result is that certain groups which are found in the joint spectrum definitely do not occur in the spectrum of thorium C″ alone. The next point in the argument is to show that the γ-rays responsible for these groups do agree approximately with the energy differences of the α-particle groups found by Rosenblum. This appears to be the case within the rather large uncertainties of the data.

---

* Rutherford and Ellis, 'Proc. Roy. Soc.,' A, vol. 132, p. 667 (1931).

† Gamow and Delbruck, 'Z. Physik,' vol. 72, p. 492 (1931).

The last point is to consider the relative intensities in order to show that the relative number of α-particles in the different sub-groups which show a certain degree of excitation correspond with the relative number of quanta as deduced from the γ-ray spectrum. It is not possible to give a definite answer to this question. All that can be said is that the relative intensities are compatible with the view. Since writing the paper referred to above I have carried out some further experiments. While I have not been able to obtain any fresh evidence, I have confirmed these conclusions using a different apparatus.

This question deserves further investigation, particularly in the direction of seeing whether the $h\nu$'s of the γ-rays do agree exactly or not with the energy differences of the α-particle groups, but this will need greater accuracy in both sets of measurements. At the moment, however, it can safely be said that there is strong suggestive evidence in favour of the general association of the α-particles and γ-rays and it appears to be a reasonable hypothesis to follow.

It is then relevant to consider exactly what this hypothesis means, and, to put it in its simplest form, it is that the principle of the conservation of energy applies to the nucleus, or better, to that part of the nucleus which is associated with the emission of α-particles and the emission of γ-rays. It will be noticed that in both these cases, what has been established is the equivalence of the total amount of energy emitted when this energy can be divided in two ways. Either an α-particle carries away all the available energy, or if it takes only part, the remainder is emitted in the form of γ-rays. The nucleus is a small system, and contains a great number of particles, and it is doubtful whether it is justifiable to talk about any one of these separately. It is, therefore, questionable whether it has any meaning to state that the γ-rays are emitted by α-particles. It would scarcely have any meaning if the conservation of energy applied to the nucleus as a whole, but actually, as we know from the phenomenon of the continuous β-ray spectrum, this is not the case. We have seen that this present evidence does show that the conservation of energy applies both to the emission of α-particles and the emission of γ-rays, whereas from other evidence it definitely does not appear to hold for the emission of the β-particles. To this extent, then, it seems justifiable to make a distinction between the α-particles in the nucleus and the electrons, and to the extent of the validity of this distinction we can say that the γ-rays are associated with the α-particle portion of the nucleus. It must not be forgotten that there are other particles in the nucleus besides α-particles and electrons. Fowler has suggested that the presence of protons may be responsible for certain peculiarities of the spectrum, and recent work shows that we may even have to consider neutrons of one or more kinds.

The examination of the detailed connection of the γ-rays with the α-particles and protons and possibly other bodies is a problem for the future, but at present purely as a working hypothesis it is convenient to take the narrower view that the γ-rays are associated with α-particle states in the nucleus in the same kind of way as the X-rays and optical spectra are associated with the electronic structure.

The investigation of these α-particle states of the radioactive nuclei will need the co-operation of at least two lines of research, on the one hand the direct investigation of the energies and intensities of the different α-particle groups, on the other the measurement of the γ-ray spectra. Of the former there is no need to speak, but an appreciation of the importance of the latter will lead naturally to a point I wish specially to emphasise. This is the urgent need for an improvement both in the accuracy and in the extent of our knowledge of γ-ray spectra.

There are several methods of investigating γ-ray spectra—the crystal method, the absorption method, the method of observing recoil tracks by the cloud-chamber—but, indispensable as these are for settling certain points, it is clear that at present we must look to the study of β-ray spectra for the most accurate and detailed information. The first point I would urge is the recognition of the type of work which is needed. We have left behind us the pioneer stage of the subject when an investigation of the β-ray spectrum of a certain body aimed at giving a general survey of the lines. We are now in need of accurate and detailed investigation. Most of the spectra are so rich in lines that publication would be unduly delayed if any one investigator attempted to cover the whole of one spectrum with this care, and I hope to see careful investigation of small groups of lines or even the homogeneity of a single line considered as a sufficient subject for a research.

The second point is the need for increased accuracy. There is no fundamental difficulty in obtaining the ratio of the $H\rho$'s, that is, momenta, of the β-rays in two lines, to an accuracy of at least one in three thousand, but it will need considerably more attention to the mechanical construction of the apparatus than has been given in the past. But, since the results of the measurements need to be compared with those from a different field—the α-rays—relative measurements by themselves are of little use and we need absolute measurements. Here the position is far from satisfactory, and the whole scale of β-ray measurements is uncertain, although possibly not inaccurate, to half a per cent. Determinations by independent observers of the absolute energies of certain standard lines spread throughout the spectrum are urgently needed.

An accuracy of one in five hundred should be attainable with our present technique, but any further considerable advances seem to demand a reconsideration of the whole problem and possibly the adoption of new methods.

It might well be thought that deeds are more forceful than words, and that to follow these precepts oneself would be the best recommendation for others to adopt them. But it is only within the last year that the position in relation to the γ-rays has become clear and with it the need and justification for this type of research. There is much to be done, and if reliable results are to be reached in a reasonable time it will need the comparison of the results of several independent experimenters.

R. H. Fowler, F.R.S.: There are two main lines of evidence which tell us more or less unambiguously what must be the value of the nuclear spin. These are both fairly familiar and can be shortly recapitulated. The first and best is the evidence of alternating intensities in the band spectra of diatomic molecules in which the two atoms are identical—for example, the molecule $H - H$, $N_{14} - N_{14}$ or $O_{16} - O_{16}$ (but not $O_{16} - O_{17}$, etc.). Linear molecules such as acetylene $H - C_{12} = C_{12} - H$ also yield evidence of the same type, but, of course, we get nothing new here, only further evidence for the spin of the proton. If the spin of the nuclei in such molecules is $n(h/2\pi)$ then the intensities of the band lines alternate in the ratio $(n+1)/n$. We find in this way with certainty the following spins (the list is not exhaustive):—

$$H\ \tfrac{1}{2}\,;\ He\ 0\,;\ N_{14}\ 1\,;\ C_{12}\ 0\,;\ O_{16}\ 0.$$

We find, too, in this way the most unambiguous evidence for the type of statistics satisfied by the nuclei, in particular that N_{14} has the Einstein-Bose statistics which forces us (along with other evidence) to the deep and disturbing conclusion that the electrons in the nucleus no longer contribute to the spin or the statistical type.

The second main type of evidence is from the details of the hyperfine structure of atomic spectra. Here we are concerned with all the perturbation which a nucleus can exert on the optical spectrum, and it is not always easy to separate spin effects from others such as isotope effects, which must all be observed together. Nevertheless, it has been possible, especially by the use of the Zeeman effect as modified by the Paschen-Back effect for the hyperfine structure, to determine the spin with certainty for some atomic species, notably Bi, 9/2. This determination uses only qualitative evidence. By using quantitative evidence from the width of the hyperfine structure one ought to be able to determine the magnitude of the nuclear *magnetic moment* associated with the nuclear spin. It has been shown in this way that nuclear magnetic moments are of the order of the *protonic Bohr magneton*, *i.e.*, of the order of 1/2000 the ordinary Bohr magneton. But there are still great difficulties in a more exact determination.

A subsidiary line of spectroscopic evidence, which may prove very useful in future, is derived from a study of the depolarisation of resonance radiation in the manner of Ellett.

While these are the main ways in which the nuclear spin must be determined, they are not closely relevant to radioactive nuclei, and we have at present little hope of a direct determination for such nuclei by optical methods. But the spin may none the less be very relevant, as has been shown recently by Gamow in a letter to 'Nature.'* He there compares the regular sequences of radii for the uranium-radium and thorium families of radioactive elements, calculated from his theory from the observed rates of decay, with the irregular radii deduced for the actinium series. He suggests that this may be due to changes of spin of the nuclei of the actinium series. If the spin changes the α-particle must carry away the corresponding angular momentum, and the formula for the life of the nucleus is modified. The observed irregularities are accounted for if changes of the order of 3 units of spin can occur in the actinium series (atomic weights $4n + 3$), whereas they do not occur in the other series (weights $4n$ and $4n + 2$). This seems quite possible, but of course is purely speculative at present.

J. C. McLennan, F.R.S.: Data derivable from a study of the fine structure of spectral lines are now available for a number of elements. These enable us to evaluate mechanical moments and the corresponding $g(\mathrm{I})$ factors—ratio of magnetic to mechanical moment—for certain of the atomic nuclei.

Up to the present the observed "I" values (spin quantum numbers) for nuclei have been explained consistently by assuming that only the protons within atomic nuclei contribute, by their spin, to the resultant nuclear moment. The simple assumption by which each proton contributes $\frac{1}{2}(h/2\pi)$ to the resultant moment has until recently been considered sufficient to explain the known facts.

Some anomalies, however, have of late been brought to light. For example, it is known that while the relative separations of the hyperfine structure components of homologous spectral lines in the spectra of Tl II and $\mathrm{Pb}_{(207)}$ III are similar, the actual magnitudes of the separations involved in the structure of the $Pb_{(207)}$ III spectral lines are much smaller than those obtained with the corresponding lines of Tl II. The values of the separations involved enable us to make comparisons directly and it appears that the $g(I)$ factor for the Tl nucleus is about four times that of the nucleus of $Pb_{(207)}$. This result is especially significant, for on the simple theory enunciated above the resultant moments of the nuclei of Tl and $Pb_{(207)}$ atoms, for both of which $I = \frac{1}{2}$, would be due to one unneutralised spinning proton. The $g(I)$ factors of the two nuclei, then, would be expected to be the same, for there is no evidence to indicate why different spinning protons with the same mechanical moments should have widely different magnetic moments.

---

* 'Nature,' vol. 129, p. 470 (1932).

The obvious conclusion is that the moment of at least one of the nuclei is composite and not due simply to a spinning proton. This conclusion would invalidate the simple rule that each proton contributes $\pm \frac{1}{2}(h/2\pi)$ to the resultant moment. Moreover, it would require us to endow at least one proton with some property in addition to spin in either one or both of the Tl and $Pb_{(207)}$ nuclei. Further evidence for this conclusion is obtainable from the ratio of the $g(I)$ factors for thallium and bismuth. Although the "I" value for Bi nuclei is 9/2 the $g(I)$ value should be the same as that for Tl if the resultant moments of both nuclei be due to spinning protons only. The observed ratio, however, is about 4 to 1. This approximate equality of the $g(I)$ factors for $Pb_{(207)}$ and Bi indicates that the resultant moment of the Tl nucleus is more complex in its origin than it has hitherto been thought to be. Although the evidence does not definitely indicate what this additional property should be, McLennan, McLay and Crawford* and also Bartlett† suggested orbital motions of the protons within nuclei as a possibility. This idea has been developed by White‡ and by Bryden,§ but it would appear to be quite inadmissible to assign orbital motions indiscriminately, as they have done, to all the protons within atomic nuclei.

Again, I may add, it has been known for some time that the mathematical theory available for calculating the interaction of an electron, other than one of the *s* type, with the nuclear spin, was not correct.

This was shown by the experiments of Wulff‖, by those of Fisher and

---

* 'Proc. Roy. Soc.,' A, vol. 133, p. 652 (1931).

† 'Phys. Rev.,' vol. 37, p. 327 (1931).

‡ 'Phys. Rev.,' vol. 38, p. 2078 (1931).

§ 'Phys. Rev.,' vol. 38, p. 1989 (1931).

‖ 'Z. Physik,' vol. 69, p. 70 (1931)

Goudsmit,[*] and by those of McLennan, McLay and Crawford (*loc. cit.*). Recently the theory was extended by Breit,[†] who introduced a correction in the term $(1/\gamma^3)$ due to the relativistic variation in mass of the interacting electron. This correction, which varies in value with the different states of the doublet arising from the interaction of a single non-*s* electron with a nucleus, is such as to give a better agreement between theory and experiment. However, the theory even with this improvement is not satisfactory. For instance, the older theory predicts in the case of Tl

$$A_{(\mathrm{I},\,1/2)}\,{}^2P_{1/2}/A_{(\mathrm{I},\,3/2)}\,{}^2P_{3/2} = 5/1,$$

where $A_{(ij)}$ is the binding constant in the energy equation

$$E_{(ij)} = A_{(ij)},\ IJ\cos(IJ).$$

The observed ratio was about 30/1. The relativistic correction which varies in value from element to element gives for heavy elements a predicted ratio of about 10/1. This shows that even with this improvement in the theory the observed values differ from the theoretical ones by a factor of two or three. Racah[‡] has given a treatment similar to that of Breit and has applied it also to observations on the Tl spectrum. His comparisons again show that the theory is not as yet satisfactory.

Recently a test of hyperfine structure theory was made by Bacher and Campbell.[§] The total hyperfine structure separations of the two members of the doublet arising from the single 5*p* electron were found by a study of the resonance spectral lines of indium I. Difficulties experienced in a study of thallium spectral lines due to isotope displacement with resulting complexity in the line structure pattern were not met with in the case of indium, for this element is simple and has but one type of nucleus. Bacher and Campbell found in the case of indium lines that the spectral separation $\Delta\,{}^2P_{\frac{1}{2}}$ was $0\cdot390$ cm.$^{-1}$ while that represented by $\Delta\,{}^2P_{1\frac{1}{2}}$ was $0\cdot133$ cm.$^{-1}$, giving a ratio of 2·9/1. This, it is clear, is not in agreement with the non-relativistic theoretical value of the ratio 1·67. It is, however, in better agreement with 2·05, the value corrected according to Racah, and in still better agreement with 2·7, the corrected value as given by Breit.

---

[*] 'Phys. Rev.,' vol. 37, p. 1057 (1931).

[†] 'Phys. Rev.,' vol. 37, p. 1182 (1931); vol. 38, p. 463 (1931).

[‡] 'Z. Physik,' vol. 71, p. 431 (1931).

[§] 'Bull. Amer. Phys. Soc.,' April 28, 1932.

F. A. LINDEMANN, F.R.S.: Attention has been drawn to the irregular behaviour of the nuclear electrons. It would seem clear that one cannot expect them to behave so simply as the α-particles. According to Gamow's scheme, which has been referred to so frequently, the α-particles are confined in a potential barrier surrounding or defining the nucleus. This provides a picture which enables one to construct a relation between the energy with which they escape and the half-life period of the atom. For if the α-particle climbs over the barrier or percolates through it, then of course it is expelled by the field and attains a considerable velocity by the time it has reached distances great compared with the radius of the potential barrier. It is as though we had boulders in the crater of a volcano. If they are pushed through the wall of the crater or over the edge they will run down the hill and arrive at the bottom with an amount of energy depending upon the difference of level.

It is clear that such a model leads to serious difficulties when applied to electrons. A field repelling an α-particle must attract an electron. In the terms of our analogy the electrons would be represented by balloons in the crater of the volcano. Obviously there would be no force or reason to keep them there; they would tend to climb to the edge and festoon the ridge.

In my opinion it is impossible to maintain the individuality of electrons inside the nucleus. If they existed as individual particles, one would expect evidence of their magnetic spin moments to appear in the hyperfine structure of the spectra. As was emphasised by D. A. Jackson some 3 or 4 years ago, no trace of this is to be found. The separations of the spectral lines imply magnetic moments corresponding to massive particles, to protons rather than to electrons.

Again, it has been frequently pointed out that an electron whose position in space could be stated with an accuracy of the order 10^{-12} cm., *i.e.*, an electron inside a nucleus, would possess momentum of the order $6 \cdot 5 \, . \, 10^{-15}$ g. cm. per second which corresponds to an energy enormously greater than its own intrinsic energy. Its contribution to the mass of the nucleus would be large, which does not seem to be borne out by experiment. Even on the Classical Theory the energy in the field would far exceed that of the electron itself. Since the Nullpunktsenergie varies inversely with the mass this difficulty scarcely arises with the more massive protons or α-particles.

If we must have some form of model, the only picture that would seem at all possible is a sort of inversion of the atomic model proposed by J. J. Thomson some 25 years ago. If one refrains from endeavouring to assign positions to the negative electrons one can treat them as though they formed a sphere of more or less uniform volume electrification. In such a field the protons would tend towards the centre, possibly collected in groups of four, repelling one another electrostatically, but attracting one another magnetically. The field opposing the escape of a positive charge from such a sphere of negative electricity would increase up to the boundary, which might thus be identified with the potential barrier which is presupposed in Gamow's theory.

Though mental images of this sort may be attractive, I am convinced that attempts to represent the nucleus in spatio-temporal terms can at best be figures of speech. We know quite well that it is meaningless to endeavour to assign a position to the electron in the normal hydrogen atom. If this mode of representation fails completely in such a comparatively simple case, there is very little justification for trying to describe in a space-time frame-work the conditions inside the nucleus.

I was much impressed by the accuracy with which Dr. Chadwick claims to have determined the mass of the neutron. To obtain results accurate to within ½ per cent. for the mass, the velocities of the neutron on the Classical Theory must be the same to within about 0·2 per cent. If their velocity depends upon the velocity of the primary α-particles, a very curious circumstance which I gather has been established, one would scarcely expect to find such definite figures.

The difficulty of representing these phenomena in terms of space and time is peculiarly noticeable in the case of such neutrons. Presumably, they would interact with the nuclei only over very short distances. According to the principle of indeterminacy, one would therefore expect to find very great uncertainties in the momenta transferred. If the momentum relations are accurate, then one must assume, as in the case of monochromatic light, that the region of interaction is ill-defined. This is what one has to do, of course, in the case of protons and is an example of the difficulty of describing such phenomena in terms of space and time. It becomes much more acute when we have to apply the same methods to particles whose rest mass is presumably of the order of the mass of a hydrogen atom. With α-particles, whose region of interaction, owing to their charge, would naturally be expected to be very much greater, the difficulty is much less serious.

If we are definitely precluded from regarding the beryllium radiation as protons, a situation to which I am not yet altogether resigned, we must examine how the neutron fits into the scheme of modern physics. From the point of view of the classical quantum theory, it is difficult to see how it can exist. The hydrogen atom would seem to represent the smallest system containing a

---

"*Discussion on the Structure of Atomic Nuclei*," Proceedings A, vol. 136, 1 June, 1932, p. 758:

Line 28 *from the top*, "protons" *should read* "photons."
Line 35 *from the top*, "protons" *should read* "photons."

proton and an electron. If one is content, of course, with a purely formal mathematical expression one can obtain dimensions of the right order of magnitude. The Schrödinger equation for the hydrogen atom is found by considering an electron moving in a Coulomb field of force. For unit charge this leads to a mean separation of the order $5 . 10^{-9}$ cm. between the charges. If one writes down the Schrödinger equation for a proton moving in the same field of opposite sign, one obtains similar solutions with linear dimensions reduced by a factor of 1850. A system of this type might have the properties required for the neutron, but the derivation implies that instead of the electron rotating or oscillating about the proton, the proton rotates or oscillates about the electron. Even though we admit the spatio-temporal description fails and that words like rotating or oscillating have little meaning in this connection, it would seem difficult to accept a formula, even though it does give the right answer, whose space-time interpretation is so much at variance with our ordinary physical ideas.

N. F. Mott: The application of quantum mechanics to the problem of the anomalous scattering of α-particles has led to the explanation of certain experimental results, and to the prediction of some new phenomena. So long as the law of force between an α-particle and a nucleus is assumed to be that of the inverse square, classical mechanics and quantum mechanics* lead in general to the same scattering formula, namely, in the case of infinitely heavy nuclei to the formula $(2Ze^2/2mv^2)^2 \operatorname{cosec}^4 \frac{1}{2}\theta$ for the number of particles scattered per unit solid angle through an angle θ. The only case in which classical and quantum mechanics make different predictions is that in which the struck particle is of the same kind as the incident particle, as for instance when α-particles are scattered by helium.† The number of particles scattered then depends on the statistics obeyed by the particle, and the number of spin quanta which it possesses. The scattering at 45°, for instance, is greater than that predicted by the classical theory by a factor

$2(s+1)/(2s+1)$	Einstein-Bose statistics
$2s/(2s+1)$	Fermi-Dirac statistics,

where $s + h/2\pi$ is the "spin" angular momentum of the particle. The spin and the statistics may be determined from the band spectrum of a diatomic molecule of which the particles in question form the nuclei.* The scattering thus forms a method of verifying the results obtained from the band spectrum.

---

* Gordon, 'Z. Physik,' vol. 48, p. 180 (1928).

† Mott, 'Proc. Roy. Soc.,' vol. 126, p. 259 (1930).

Evidence from the band spectra of He_2 shows that α-particles have no spin and obey the Einstein-Bose statistics. One would therefore expect that the scattering at 45° in helium would be twice that given by the classical theory. This has been verified experimentally by Chadwick†, and other results of the theory have been verified by Blackett and Champion‡. Slow α-particles (velocities $1–8 \cdot 5 \times 10^8$ cm. per second) were used, to avoid the effects due to the failure of the inverse square law forces at close distances.

In order to explain the anomalous scattering of fast particles in hydrogen and helium, and also the anomalous scattering by such elements as Al, Mg, B, one must assume that the inverse square law of force breaks down for distances less than a certain distance r. It is natural to assume that for smaller distances the force becomes attractive. One therefore takes for the potential energy of an α-particle in the field of a nucleus a function of the form shown in fig. 1. The scattering to be expected from such a field will now be discussed.

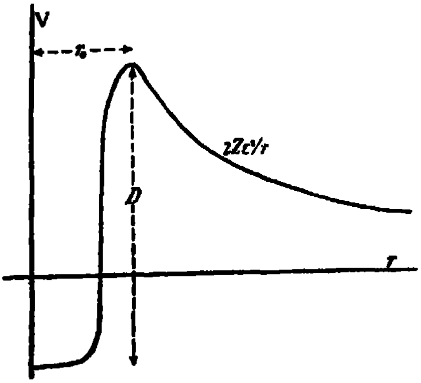

Fig. 1.

If the classical distance of closest approach for a head-on collision, namely, $2Ze^2/\frac{1}{2}mv^2$, is greater than r, the deviations from classical scattering will, in general, be very small. It is, however, possible that there will exist ranges of energy of breadth $\frac{1}{2} \times 10^6$ electron volts or less (resonance levels) such that an α-particle with these energies can penetrate easily through the potential barrier. For such energies the scattering would be anomalous, and artificial disintegration could take place. The existence and position of the resonance levels depends on the shape of the field within the nucleus; their breadth depends on the thickness of the potential barrier. The possibility of their existence according to the wave mechanics was first pointed out by Gurney,* and they have been discussed in several theoretical papers.†

---

* *Cf.* Kronig, "Band Spectra and Molecular Structure," Cambridge, p. 94 (1930).

† 'Proc. Roy. Soc.,' A, vol. 128, p. 114 (1930).

‡ 'Proc. Roy. Soc.,' A, vol. 130, p. 380 (1931).

If the classical distance of closest approach is less than r, deviations will occur from the classical formula, even at angles for which the classical particle moves only in the Coulomb field. It is therefore no longer necessary to postulate a non-spherical nucleus to explain the fact that anomalous scattering in helium begins at roughly the same energy for large and for small angles.

If the field for $r_0 < r$ is attractive, the ratio of observed to classical scattering should first decrease and then increase, as the energy is increased.

From the observed scattering‡ one may make an estimate of the field for $r_0 < r$. This has been done by Taylor§ for hydrogen and helium. In the case of helium, if one makes the assumption that r is less than about 4×10^{-23} cm., the scattering formula deduced from a field such as shown in fig. 1 is

$$\mathrm{R} = 2 \quad 1 + \frac{1}{2\alpha} e^{i[\frac{1}{2}\pi - \alpha \log 2]} (e^{2i\kappa} - 1) \qquad \alpha = \frac{2\pi e^2}{hv}$$

where R is the ratio of the scattering to that predicted with inverse square law fields. The parameter κ depends on the field, and is a function of the energy but not of the angle. It is not therefore the case that any observed scattering can be explained by the choice of a suitable field; for from the observed scattering at a given angle and energy one can deduce K, and hence calculate the scattering at all other angles for the same energy. Good agreement with experiment is obtained, showing that the problem is one which may be treated by quantum mechanics. Similar results are obtained for hydrogen.

From the observed value of K, and its variation with the energy, the depth D of the potential hole may be estimated. It has not, however, been found possible to use this value of D to make predictions about any other phenomenon; for instance, the attractive force between two α-particles found from the scattering is larger than is required to explain their binding energies in the nucleus.

Dr. Aston then exhibited some results of neon-spectrum analysis of leads from different sources. A full account of these experiments will appear in due course.

---

* 'Nature,' vol. 123, p. 568 (1929).

† Atkinson, 'Z. Physik,' vol. 64, p. 507 (1930); Beck, 'Z. Physik,' vol. 64, p. 32 (1930); Mott, 'Proc. Roy. Soc.,' A, vol. 133, p. 228 (1931).

‡ Rutherford and Chadwick, 'Phil. Mag.,' vol. 4, p. 605 (1927).

§ 'Proc. Roy. Soc.,' A, vol. 134, p. 103 (1931), and vol. 136, p. 605 (1932).

In the ensuing discussion one of the speakers said that with regard to the remarks made about the collisions of neutrons with atoms there was really no difficulty because the quantum mechanics would allow the neutrons to be represented by a train of waves of unlimited length, and therefore having an energy defined with any desired degree of accuracy. The fact that the field of the neutron extended through only a very small space was beside the point; it did not in any way prevent the supposition of a very long train of waves. There was no more trouble in the case of the neutron than in the case of the light quantum.

The question was raised as to the accuracy of the estimate of the mass of the neutron, given as 1·005 to 1·008. In reply it was stated that this estimate depended on the mass measurements of B^{11} and N^{14} by Aston. The ratio of the masses of B^{11} and B^{10} has been checked by optical methods, and the result agrees with Aston's to 1 part in 10^6. The mass of N^{14} is more doubtful, but there is no reason to suspect that it is much in error.

In conclusion, Lord Rutherford stated that the new experiments involving the use of high potentials to produce fast particles for the bombardment of elements were but the beginning of a very wide investigation. The whole range of elements had to be examined, and it could not be foretold what would happen in these collisions.

INDEX TO VOL. CXXXVI. (A.)

Aerials, frame, action of tuned rectangular, when receiving short waves (Palmer), 193.

Air speeds, measurement of low (Ower and Johansen), 153.

Alpha particles, anomalous scattering by Hydrogen and Helium (Taylor), 605.

Aluminium alloys, formation of superlattices (Bradley and Jay), 210.

Angus (W. R.) Ionic Diamagnetic Susceptibilities, 569.

Angus (W. R.) and Farquharson (J.) The Diamagnetic Susceptibilities of some Beryllium Compounds, 579.

Argon, mobility of positive alkali ions in (Tyndall and Powell), 145.

Bakker (C. J.) *See* Fowler and Bakker.

Beryllium compounds, diamagnetic susceptibilities (Angus and Farquharson), 579.

Beta-particles, collisions with electrons, photographed by the expansion method (Champion), 630.

Bismuth, atomic heat at higher temperatures (Carpenter and Harle), 243.

Blackett (P. M. S.) and Lees (D. S.) Investigations with a Wilson Chamber, I, III, 325, 338.

Bowden (B. V.) *See* Rutherford and Bowden.

Bradley (A. J.) and Hope (R. A. H.) The Atomic Scattering Power of Iron for Various X-ray Wave-lengths, 272.

Bradley (A. J.) and Jay (A. H.) The Formation of Superlattices in Alloys of Iron and Aluminium, 210.

Bromine, arc spectrum (Tolansky), 585.

Burton (A. C.) *See* McLennan and others.

Carpenter (L. G.) and Harle (T. F.) The Atomic Heat of Bismuth at Higher Temperatures, 243.

Caspari (W. A.) Crystallography of the Simpler Quinones, 82.

Cawood (W.) *See* Patterson and Cawood.

Chadwick (J.) The Existence of a Neutron, 692.

Champion (F. C.) On some Collisions of Fast β-particles with Electrons, Photographed by the Expansion Method, 630.

Cockcroft (J. D.) and Walton (E. T. S.) Experiments with High Velocity Positive Ions. I—Further Developments in the method of obtaining High Velocity Positive Ions, 619.

Darwin (C. G.) Notes on the Theory of Radiation, 36.

Dee (P. I.) Attempts to Detect the Interaction of Neutrons with Electrons, 727.

Desai (M. S.) The Determination of the Heat of Dissociation of Fluorine and of the Latent Heat of Vaporisation of Lithium, 76.

Diamagnetic Susceptibilities, Ionic (Angus), 569.

Diamagnetic Susceptibilities of some Beryllium Compounds (Angus and Farquharson), 579.

Dipole moments and molecular structure (Smith), 251, 256.

Dirac (P. A. M.) Relativistic Quantum Mechanics, 453.

Discussion on the Structure of Atomic Nuclei (Rutherford), 735.

Dissociation, mechanism and molecular statistics (Topley), 413.
Duncan (W. J.) On the Torsion of Cylinders of Symmetrical Section, 95.
Dymond (E. G.) On the Polarisation of Electrons by Scattering, 638.

Eckersley (T. L.) Radio Transmission Problems treated by Phase Integral Methods, 499.
Electrochemistry, quantum mechanics (Gurney), 378.
Electrons, collision with fast β-particles (Champion), 630.
Electrons, interaction with neutrons (Dee), 727.
Electrons, motion in static fields of Hydrogen and Helium (McDougall), 549.
Electron Polarisation (Langstroth), 558.
Electron Polarisation by Scattering (Dymond), 638.
Electrons, slow, collision with atoms (Massey and Mohr), 289.
Electrons, slow, photographic action of (Whiddington and Taylor), 651.
Electron-levels in H_2 (MacDonald), 528.
Ellis (C. D.) The Association of γ-rays with the α-particle groups of Thorium C, 396.
Ethane and ethylene, influence of Hydrogen on pyrolysis (Travers and Hockin), 1.

Farquharson (J.) *See* Angus and Farquharson.
Feather (N.) The Collisions of Neutrons with Nitrogen Nuclei, 709.
Fluorine, determination of heat of dissociation (Desai), 76.
Foster (A. G.) *See* Lambert and Foster.
Fowler (A.) and Bakker (C. J.) The Band Spectrum of Nitrogen Sulphide (NS), 28.

Gamma-rays, association with α-particle groups of Thorium C (Ellis), 396.
Gamma-rays from actinium emanation (Rutherford and Bowden), 407.
Gamma-radiation and the atomic nucleus (Gray and Tarrant), 662.
Gamma-radiation, nuclear, artificial production (Webster), 428.
Gas-solid equilibria (Lambert and Foster), 363.
Gravitational fields, equations of axially symmetric (Lewis), 176.
Gray (L. H.) and Tarrant (G. T. P.) The Nature of the Interaction between Gamma-radiation and the Atomic Nucleus, 662.
Gurney (R. W.) The Quantum Mechanics of Electrochemistry, II. Appendix by R. H. Fowler, 378.

Harle (T. F.) *See* Carpenter and Harle.
Havelock (T. H.) Ship Waves: their Variation with Certain Systematic Changes, 465,
Heat, atomic, of Bismuth (Carpenter and Harle), 243.
Helium, mobility of positive alkali ions in (Tyndall and Powell), 145.
Henderson (S. T.) *See* Lowry and Henderson.
Hockin (L. E.) *See* Travers and Hockin.
Hope (R. A. H.) *See* Bradley and Hope.
Hydrogen influence on pyrolysis of ethane and ethylene (Travers and Hockin), 1.

Iodine, arc spectrum (Tolansky), 585.
Ionic Diamagnetic Susceptibilities (Angus), 569.
Ions, method of obtaining high velocity positive (Cockcroft and Walton), 619.
Iron alloys, formation of superlattices (Bradley and Jay), 210.

Jay (A. H.) *See* Bradley and Jay.
Johansen (F. C.) *See* Ower and Johansen.

Lambert (B.) and Foster (A. G.) Studies of Gas-solid Equilibria, IV, 363.
Langstroth (G. O.) Electron Polarisation, 558.
Lees (D. S.) *See* Blackett and Lees.
Lewis (T.) Some Special Solutions of the Equations of Axially Symmetric Gravitational Fields, 176.
Lithium, determination of latent heat of vaporisation (Desai), 76.
Lowry (T. M.) and Henderson (S. T.) Molecular Structure and Physical Properties of Prussic Acid. I—Refractive Dispersion of Prussic Acid and its Homologues, 471.

MacDonald (J. K. L.) A Theory of some Electron-levels in H_2, 528.
McDougall (J.) The Motion of Electrons in the Static Fields of Hydrogen and Helium 549.
McLennan (J. C.), Burton (A. C.), Pitt (A.) and Wilhelm (J. O.) The Phenomena of Superconductivity with Alternating Currents of High Frequency, 52.
Massey (H. S. W.) and Mohr (C. B. O.) The Collision of Slow Electrons with Atoms, I, 289.
Mohr (C. B. O.) *See* Massey and Mohr.

Naudé (S. M.) Quantum Analysis of the Rotational Structure of the First Positive Bands of Nitrogen (N_2), 114.
Neon, mobility of positive alkali ions in (Tyndall and Powell), 145.
Neutrons, collision with Nitrogen nuclei (Feather), 709.
Neutron, existence of (Chadwick), 692.
Neutrons, interaction with electrons (Dee), 727.
Nitrogen, rotational structure of first positive bands (Naudé), 114.
Nitrogen sulphide, band spectrum (Fowler and Bakker), 28.
Nuclei, atomic, discussion, 735.
Nuclei, collision of Nitrogen, with neutrons (Feather), 709.
Nucleus, atomic, interaction with γ-radiation (Gray and Tarrant), 662.

Ower (E.) and Johansen (F. C.) On a Determination of the Pitot-Static Tube Factor at Low Reynolds Numbers, with Special Reference to the Measurement of Low Air Speeds, 153.

Palmer, L. S.) On the Action of Tuned Rectangular Frame Aerials when receiving Short Waves, 193.
Patterson (H. S.) and Cawood (W.) The Reproducibility and Rate of Coagulation of Stearic Acid Smokes, 538.
Pitot-static tube factor, determination at Low Reynolds numbers (Ower and Johansen), 153.
Pitt (A.) *See* McLennan and others.
Powell (C. F.) *See* Tyndall and Powell.
Price (W. C.) Theoretical Intensities in the Spectrum of H_2, 264.
Prussic Acid, molecular structure and physical properties, I (Lowry and Henderson), 471.

Quantum mechanics, relativistic (Dirac), 453.
Quinones, crystallography (Caspari), 82.

Radiation, notes on the theory (Darwin), 36.
Radio transmission problems treated by phase integral methods (Eckersley), 499.
Rectification, a note on theory of (Wilson), 487.

Rutherford (Lord) Opening Address on the Structure of Atomic Nuclei, 735.
Rutherford (Lord) and Bowden (B. V.) The γ-rays from Actinium Emanation and their Origin, 407.

Scattering, atomic, of iron at X-ray wave-lengths (Bradley and Hope), 272.
Scattering of α-particles, anomalous (Taylor), 605.
Ship waves: Variation with Systematic Changes (Havelock), 465.
Smith (J. W.) Dipole Moments and Molecular Structure, I, II, 251, 256.
Smokes, Stearic acid, reproducibility and rate of coagulation (Patterson and Cawood), 538.
Spectra, arc of Bromine and Iodine (Tolansky), 585.
Spectrum, band, of nitrogen sulphide (Fowler and Bakker), 28.
Spectrum of H_2, theoretical intensities (Price), 264.
Spectrum of nitrogen, first positive bands (Naudé), 114.
Superconductivity phenomena (McLennan and others), 52.
Superlattices, formation in iron and aluminium alloys (Bradley and Jay), 210.

Tarrant (G. T. P.) *See* Gray and Tarrant.
Taylor (H. M.) The Anomalous Scattering of α-Particles by Hydrogen and Helium, 605.
Taylor (J. E.) *See* Whiddington and Taylor.
Thyratron automatic counter (Wynn-Williams), 312.
Tolansky (S.) Fine Structure in the Arc Spectrum of Bromine and Iodine, 585.
Topley (B.) The Mechanism and Molecular Statistics of the Reaction $CuSO_4 . 5H_2O = CuSO_4 . H_2O + 4H_2O$, 413.
Torsion of cylinders of symmetrical section (Duncan), 95.
Travers (M. W.) and Hockin (L. E.) On the Influence of Hydrogen on the Pyrolysis of Ethane and Ethylene near 600°, I, 1.
Tyndall (A. M.) and Powell (C. F.) Mobility of Positive Alkali Ions in Argon, Neon and Helium, 145.

Walton (E. T. S.) *See* Cockcroft and Walton.
Wasastjerna (J. A.) On the Nature of X-rays, 233.
Webster (H. C.) The Artificial Production of Nuclear γ-radiation, 428.
Whiddington (R.) and Taylor (J. E.) On the Photographic Action of Slow Electrons,
Wilhelm (J. O.) *See* McLennan and others.
Wilson (A. H.) A Note on the Theory of Rectification, 487.
Wilson chamber investigations (Blackett and Lees), 325, 338.
Wynn-Williams (C. E.) A Thyration "Scale of Two" Automatic Counter, 312.

X-rays, nature (Wasastjerna), 233.
X-ray wave-lengths, atomic scattering power of iron (Bradley and Hope), 272.

END OF THE ONE HUNDRED AND THIRTY-SIXTH VOLUME (SERIES A).

I. A. R. I. 75

IMPERIAL AGRICULTURAL RESEARCH
INSTITUTE LIBRARY
NEW DELHI.

Date of issue.	Date of issue.	Date of issue.

I. A. R. I. 75

IMPERIAL AGRICULTURAL RESEARCH
INSTITUTE LIBRARY
NEW DELHI

Date of issue.	Date of issue.	Date of issue.